

EUROPEAN COMMISSION



**Atlas of Geothermal
Resources in Europe**

EUROPEAN COMMISSION

Research Directorate-General

Atlas of Geothermal Resources in Europe

**Editors: Suzanne Hurter
Ralph Haenel**

**Leibniz Institute for Applied Geosciences (GGA);
Stilleweg 2, D-30655, Hannover, Germany**

Publication No. EUR 17811 of the European Commission.
Office for Official Publications of the European Communities,
L-2985 Luxembourg

© European Communities, 2002

Legal Notice

Neither the European Commission nor any person acting on behalf of the Commission is responsible for the use which might be made of the following information.

All Rights Reserved

No part of the material protected by this copyright notice may be reproduced or utilized in any form or by any means, electronic or mechanical, including photocopying, recording or by any information storage and retrieval system, without written permission from the copyright owner.

Cartography by
Lovell Johns Limited, 10 Hanborough Business Park,
Long Hanborough, Witney, Oxfordshire. OX29 8RU.

CONTRIBUTORS

Contributors are presented in order of first appearance in the contribution of each country.

ALBANIA

A. Frasheri
Polytechnic University
Faculty of Geology and Mining
Rruga Durrësit
Pall.7, Ap.6
AL-Tirana

V. Čermák
Geophysical Institute
Czech Academy of Sciences
Bocní II/1a
CZ-141 31 Praha 4, Czech Republic

D. Doracaj
Polytechnic University
Faculty of Geology and Mining
Rruga Durrësit
Pall.7, Ap.6
AL-Tirana

N. Kapedani
Polytechnic University
Faculty of Geology and Mining
Rruga Durrësit
Pall.7, Ap.6
AL-Tirana

R. Liço
Polytechnic University
Faculty of Geology and Mining
Rruga Durrësit
Pall.7, Ap.6
AL-Tirana

R. Bakalli
Polytechnic University
Faculty of Geology and Mining
Rruga Durrësit
Pall.7, Ap.6
AL-Tirana

H. Halimi
Polytechnic University
Faculty of Geology and Mining
Rruga Durrësit
Pall.7, Ap.6
AL-Tirana

M. Krešl
Geophysical Institute
Czech Academy of Sciences
Bocní II/1a
CZ-141 31 Praha 4, Czech Republic

E. Vokopola
Polytechnic University
Faculty of Geology and Mining
Rruga Durrësit
Pall.7, Ap.6
AL-Tirana

E. Jareci
Polytechnic University
Faculty of Geology and Mining
Rruga Durrësit
Pall.7, Ap.6
AL-Tirana

B. Çanga
Polytechnic University
Faculty of Geology and Mining
Rruga Durrësit
Pall.7, Ap.6
AL-Tirana

L. Kučerova,
Geophysical Institute
Czech Academy of Sciences
Bocní II/1a
CZ-141 31 Praha 4, Czech Republic

E. Malasi
Polytechnic University
Faculty of Geology and Mining
Rruga Durrësit
Pall.7, Ap.6
AL-Tirana

J. Šafanda
Geophysical Institute
Czech Academy of Sciences
Bocní II/1a
CZ-141 31 Praha 4, Czech Republic

BELARUS

(heat-flow density and temperature data)

V. I. Zui
Institute of Geological Sciences
Kuprievich 7
220141 Minsk

BELGIUM

N. Vandenberghe
Historische Geologie - Allgemeine Aardkunde
Katholieke Universiteit Leuven
Redingenstraat 16
B-3000 Leuven

BOSNIA-HERZEGOWINA

(temperature data)

N. Miosic
Geological Survey
Danila Dokika 19
Sarajevo

BULGARIA

K. Shterev
AQUATER
Ground Waters and Thermal Mineral Waters
Consulting & Engineering
Buxton Blvd
Bl.201-A, Vh.A, Ap.5
BG-1618 Sofia

I. Zagorchev
Geological Institute,
Bulgarian Academy of Sciences
BG-1113 Sofia

P. Petrov
Geological Institute,
Bulgarian Academy of Sciences
BG-1113 Sofia

K. Bojadgieva
Geology and Geophysics Corp.
23, Sitnyakovo Str.
BG-1505 Sofia

S. Gasharov
Geological Institute,
Bulgarian Academy of Sciences
BG-1113 Sofia

P. Bokov
Geology and Geophysics Corp.
23, Sitnyakovo Str.
BG-1505 Sofia

D. Shterev
BULGARGAZ-EAD
Geology, Production & Storage Dept.
66, Filipovsko Shosse
Ljulin 2, P.O.Box.3
BG-1336 Sofia

N. Kostova
Geology and Geophysics Corp.
23, Sitnyakovo Str.
BG-1505 Sofia

M. Vakarelska
Geology and Geophysics Corp.
23, Sitnyakovo Str.
BG-1505 Sofia

I. Stefanov
Committee of Geology and Mineral Resources
22, Maria-Louisa Blvd.
BG-1000 Sofia

M. Galabov
University of Mining and Geology
Department of Hydrogeology and Engineering Geology
BG-1100 Sofia

I. Stefanov
Committee of Geology and Mineral Resources
22, Maria-Louisa Blvd.
BG-1000 Sofia

R. Ivanov
BULGARGAZ-EAD
Geology, Production & Storage Dept.
66, Filipovsko Shosse
Ljulin 2, P.O.Box.3
BG-1336 Sofia

CROATIA
(temperature data)

S. Čubrić
INA Oil Industry
Šubićeva 29
10000 Zagreb

K. Jelić
Faculty of Mining, Geology and Petroleum Engineering
Pierottijeva 6
10000 Zagreb

CZECH REPUBLIC

V. Myslík
GEOMEDIA Ltd.
Společná 35
CZ-182 00 Praha 8

J. Burda
Czech Geological Survey
Klárov 3/131
CZ-118 21 Praha

J. Francu
Czech Geological Survey
Leitnerova ul 22
CZ-65869 Brno

M. Stibitz
GEOMEDIA Ltd.
Společná 35
CZ-182 00 Praha 8

DENMARK

N. Balling
Geofysisk Afdeling
Aarhus Universitet
Finlandsgade 8
DK-8200 Aarhus N

J. M. Hvid
Geofysisk Afdeling
Aarhus Universitet
Finlandsgade 8
DK-8200 Aarhus N

A. Mahler
Dansk Olie- & Naturgas A/S
Agern Allé 24-26
DK-2970 Hørsholm

J. J. Møller
Danmarks og Grønlands Geologiske Undersøgelse
Thoravej 8
DK-2400 København NV

A. Mathiesen
Danmarks og Grønlands Geologiske Undersøgelse
Thoravej 8
DK-2400 København NV

T. Bidstrup
Danmarks og Grønlands Geologiske Undersøgelse
Thoravej 8
DK-2400 København NV

L. H. Nielsen
Danmarks og Grønlands Geologiske Undersøgelse
Thoravej 8
DK-2400 København NV

ESTONIA

A. Jõelett
Institute of Geology
University of Tartu
Vanemuise 46
EE-2400, Tartu

FINLAND

I. Kukkonen
Department of Geophysics
Geological Survey of Finland
Betonimiehenkuja 4
FIN-02150 Espoo

FRANCE

F. Jaudin
French Geological Survey
(BRGM)
P.B. 6009
F-45060 Orléans, Cedex 2

I. Ignatiadis
French Geological Survey
(BRGM)
P.B. 6009
F-45060 Orléans, Cedex 2

A. Menjoz
French Geological Survey
(BRGM)
P.B. 6009
F-45060 Orléans, Cedex 2

J. Lemale
Agency for Environment and Energy Management
(Ademe)
27 Rue Louis Vicat
F-75737 Paris 15

A. Gérard
SOCOMINE
European Deep Geothermal
Energy Research Programme
B.P. 39
F-67250 Soultz-sous-Forêts

GERMANY

R. Schellschmidt
Joint Geoscientific Research Institute
(GGA)
Stilleweg 2
D-30655 Hannover

S. Hurter (now at*)
Joint Geoscientific Research Institute
(GGA)
Stilleweg 2
D-30655 Hannover

*GeoForschungsZentrum Potsdam
Telegrafenberg
D-14473 Potsdam

A. Förster
GeoForschungsZentrum Potsdam
Telegrafenberg
D-14473 Potsdam

E. Huenges
GeoForschungsZentrum Potsdam
Telegrafenberg
D-14473 Potsdam

H. Karg
Wintershall AG
D-49406 Barnstorf

C. Bücker
RWE-DEA AG
Ueberseering 40
D-22297 Hamburg

C. Fitzer
University of Gießen
Diezstr. 15
D-35390 Gießen

S. Fluhrer
University of Gießen
Diezstr. 15
D-35390 Gießen

B. Sanner
University of Gießen
Diezstr. 15
D-35390 Gießen

GREECE

V. Karkoulas
Kapa Systems
6 Navarinou
Pefki
GR-151 21 Athens

M. Fytikas
Department of Geology
Aristotle University
GR-540 06 Thessaloniki

P. Dalambakis
OMEGA European Consulting
20 Anatolikos Thrakis St
Papagou
GR-156 69 Athens

D. Mendrinou
OMEGA European Consulting
20 Anatolikos Thrakis St
Papagou
GR-156 69 Athens

HUNGARY

P. Dövényi
GEOMEGA
Mester-u. 4 I/2
H-1095 Budapest

F. Horváth
GEOMEGA
Mester-u. 4 I/2
H-1095 Budapest

D. Drahos
GEOMEGA
Mester-u. 4 I/2
H-1095 Budapest

ICELAND

(heat-flow density data)

O.G. Flovenz
Orkustofnun
Grensasvegi 9
108 Reykjavik

IRELAND

(heat-flow density and temperature)

A. Brock
Applied Geophysics Unit
University College Galway
IRL-Galway

ITALY

P. Baldi
ENEL SpA
Via Andrea Pisano 120
I-56122 Pisa

E. Barbier
International Institute for Geothermal Research (CNR)
Piazza Solferino 2
I-56126 Pisa

G. Buonasorte
ENEL SpA
Via Andrea Pisano 120
I-56122 Pisa

C. Calore
International Institute for Geothermal Research (CNR)
Piazza Solferino 2
I-56126 Pisa

G. Dialuce
Ministry of Industry Direction General of Mines (MICA)
Via Molise 2,
I-00100 Rome

R. Ghezzi
GETAS - PETROGEO Srl
Piazza San Giorgio 6
I-56126 Pisa

A. Martini
Ministry of Industry Direction General of Mines (MICA)
Via Molise 2,
I-00100 Rome

P. Squarci
International Institute for Geothermal Research (CNR)
Piazza Solferino 2
I-56126 Pisa

L. Taffi
International Institute for Geothermal Research (CNR)
Piazza Solferino 2
I-56126 Pisa

G. Ghezzi
GETAS - PETROGEO Srl
Piazza San Giorgio 6
I-56126 Pisa

S. Bellani
International Institute for Geothermal Research (CNR)
Piazza Solferino 2
I-56126 Pisa

G. Bertini
ENEL SpA
Via Andrea Pisano 120
I-56122 Pisa

G. M. Cameli
ENEL SpA
Via Andrea Pisano 120
I-56122 Pisa

A. Ceccarelli
ENEL SpA
Via Andrea Pisano 120
I-56122 Pisa

A. Fiordelisi
ENEL SpA
Via Andrea Pisano 120
I-56122 Pisa

G. Cappetti
ENEL SpA
Via Andrea Pisano 120
I-56122 Pisa

I. Dini
ENEL SpA
Via Andrea Pisano 120
I-56122 Pisa

A. Ridolfi
ENEL SpA
Via Andrea Pisano 120
I-56122 Pisa

G. Stefani
ENEL SpA
Via Andrea Pisano 120
I-56122 Pisa

S. Grassi
International Institute for Geothermal Research (CNR)
Piazza Solferino 2
I-56126 Pisa

LATVIA

A. Freimanis
Geotherma of Latvia
State Company
2 Perses Str.
LV-1442 Riga

E. Eihmanis
Geotherma of Latvia
State Company
2 Perses Str.
LV-1442 Riga

M. Morozova
Geotherma of Latvia
State Company
2 Perses Str.
LV-1442 Riga

V. Drikis
Geotherma of Latvia
State Company
2 Perses Str.
LV-1442 Riga

J. Proks
Geotherma of Latvia
State Company
2 Perses Str.
LV-1442 Riga

A. Zazimko
Geotherma of Latvia
State Company
2 Perses Str.
LV-1442 Riga

L. Sokurenko
Geotherma of Latvia
State Company
2 Perses Str.
LV-1442 Riga

LITHUANIA

B. Radeckas
GEOTERMA
Lithuanian State Power System
13, A. Juozapavičiaus
LT-2205 Vilnius - 5

J. Vaceliunas
GEOTERMA
Lithuanian State Power System
13, A. Juozapavičiaus
LT-2205 Vilnius - 5

B. Krasnevic
GEOTERMA
Lithuanian State Power System
13, A. Juozapavičiaus
LT-2205 Vilnius - 5

V. Rasteniene
GEOTERMA
Lithuanian State Power System
13, A. Juozapavičiaus
LT-2205 Vilnius - 5

THE NETHERLANDS

Th. H. M. van Doorn
Netherlands Institute of Applied Geoscience TNO
Richard Holdake 10
NL-2000 AD Haarlem

R.H.B. Rijkers
Netherlands Institute of Applied Geoscience TNO
Richard Holdake 10
NL-2000 AD Haarlem

POLAND

W. Górecki
Akademiagórniczno-Hutniczaw Krakowie
Gmach Główny A-0
al. Mickiewicza 30
PL-30-059 Kraków

T. Kozdra
Akademiagórniczno-Hutniczaw Krakowie
Gmach Główny A-0
al. Mickiewicza 30
PL-30-059 Kraków

T. Kuźniak
Akademiagórniczno-Hutniczaw Krakowie
Gmach Główny A-0
al. Mickiewicza 30
PL-30-059 Kraków

B. Bruszezwska
Państwowy Instytut Geologiczny w Warszawie
ul. Rakowiecka 4
PL-00-950 Warszawa

J. Sokołowski
Polish Academy of Sciences
ul. J. Wybickiego 7
PL-31261 Kraków

J. Sokołowska
Polish Academy of Sciences
ul. J. Wybickiego 7
PL-31261 Kraków

S. Plewa
Polish Academy of Sciences
ul. J. Wybickiego 7
PL-31261 Kraków

M. Krokoszyska
Polish Academy of Sciences
ul. J. Wybickiego 7
PL-31261 Kraków

U. Krzysiek
Polish Academy of Sciences
ul. J. Wybickiego 7
PL-31261 Kraków

PORTUGAL

A. Correia
Departamento de Física
Universidade de Évora
Largo dos Colegiais, 2
P-7000 Évora

E.C. Ramalho
Instituto Geológico e Mineiro
Estrada da Portela, Zambujal
Apartado 7586
P-2720 Alfragide

A.M. Rodrigues da Silva
Gabinete para a Pesquisa e Exploração do Petróleo
Rua do Vale de Pereiro, 4
P-1250 Lisboa

L. A. Mendes-Victor
Centro de Geofísica da Universidade de Lisboa
Departamento de Física da U.L.
Rua da Escola Politécnica, 58
P-1200 Lisboa

M.R.A. Duque
Departamento de Física
Universidade de Évora
Largo dos Colegiais, 2
P-7000 Évora

L. Aires-Barros
J. M. Marque
Laboratório de Mineralogia do IST
Av. Rovisco Pais
P-1096 Lisboa Codex

F. M. Santos
Centro de Geofísica da Universidade de Lisboa
Departamento de Física da U.L.
Rua da Escola Politécnica, 58
P-1200 Lisboa

F. Aumento
3R Research
Necessidades 101
Livramento
P-9500 Ponta Delgada
Acores

ROMANIA

D. Panu
FORADEX S.A.
5 Milcov str.
RO-78344 Bucuresti

H. Mitrofan
FORADEX S.A.
5 Milcov str.
RO-78344 Bucuresti

L. Codrescu
FORADEX S.A.
5 Milcov str.
RO-78344 Bucuresti

O. Militaru
FORADEX S.A.
5 Milcov str.
RO-78344 Bucuresti

M. Preda
FORADEX S.A.
5 Milcov str.
RO-78344 Bucuresti

C. Radu
FORADEX S.A.
5 Milcov str.
RO-78344 Bucuresti

M. Stoia
FORADEX S.A.
5 Milcov str.
RO-78344 Bucuresti

F. Serban
FORADEX S.A.
5 Milcov str.
RO-78344 Bucuresti

RUSSIA

G. S. Vartanyan
All-Russian Research Institute of
Hydrogeology and Engineering Geology
(VSEINGEO)
Zeleny Village
Noginsk District
RUS-Moskow Region

V. A. Komyagina
All-Russian Research Institute of
Hydrogeology and Engineering Geology
(VSEINGEO)
Zeleny Village
Noginsk District
RUS-Moskow Region

A. A. Shpak
All-Russian Research Institute of
Hydrogeology and Engineering Geology
(VSEINGEO)
Zeleny Village
Noginsk District
RUS-Moskow Region

SLOVAKIA

A. Remsík
Geological Survey of Slovak Republic
Mlynská dolina 1
SK-817 04 Bratislava

M. Fendek
Geological Survey of Slovak Republic
Mlynská dolina 1
SK-817 04 Bratislava

J. Mello
Geological Survey of Slovak Republic
Mlynská dolina 1
SK-817 04 Bratislava

M. Král
THERMEX
Svätoplukova 12
SK-902 01 Pezinok

SLOVENIA

D. Rajver
Institute of Geology, Geotechnics and Geophysics
Geological Survey Ljubljana
Dimiceva 14
SI-61109 Ljubljana

D. Ravnik
Institute of Geology, Geotechnics and Geophysics
Geological Survey Ljubljana
Dimiceva 14
SI-61109 Ljubljana

U. Premru
Institute of Geology, Geotechnics and Geophysics
Geological Survey Ljubljana
Dimiceva 14
SI-61109 Ljubljana

P. Mio
Institute of Geology, Geotechnics and Geophysics
Geological Survey Ljubljana
Dimiceva 14
SI-61109 Ljubljana

P. Kralj
Institute of Geology, Geotechnics and Geophysics
Geological Survey Ljubljana
Dimiceva 14
SI-61109 Ljubljana

SPAIN

M. Fernández
Institut de Ciències de la Terra
'Jaume Almera' (ICT-CSCIC)
Martí i Franques
E-08028 Barcelona

C. García de la Noceda
Instituto Tecnológico
GeoMinero de España (ITGE)
Ríos Rosas, 23
E-28003 Madrid

I. Marzán
Institut de Ciències de la Terra
'Jaume Almera' (ICT-CSCIC)
Martí i Franques
E-08028 Barcelona

J. Sánchez-Guzmán
Tecnología y Recursos de la Terra (TRT)
Plaza Castilla 3-20D1
E-28046 Madrid

SWEDEN

M. Lehtmetts
Swedish Geotechnical Institute
S-581 93 Linköping

P-G. Alm
Lund Institute of Technology
Department of Engineering Geology
S-221 00 Lund

R. Olsson
Chalmers University of Technology
Department of Geotechnical Engineering
S-412 96 Gothenburg

SWITZERLAND

F. Medici
Institute of Geophysics
ETH Hoenggerberg
CH-8093 Zurich

L. Rybach
Institute of Geophysics
ETH Hoenggerberg
CH-8093 Zurich

UKRAINE

R.I.Kutas
Institute of Geophysics
National Academy of the Ukraine
Palladina 32
252142 Kiev

E.E. Sobolevsky
State Committee of the Ukraine for
Geology and Use of Interior
Derzhkomgeologia of the Ukraine
Kiev

G.I. Veliky
State Committee of the Ukraine for
Geology and Use of Interior
Derzhkomgeologia of the Ukraine
Kiev

E.A. Yakovlev
State Committee of the Ukraine for
Geology and Use of Interior
Derzhkomgeologia of the Ukraine
Kiev

UNITED KINGDOM

K. Rollin
British Geological Survey
Regional Geophysics Group
Keyworth
Nottingham, NG12 5GG

G.A. Kirby
British Geological Survey
Regional Geophysics Group
Keyworth
Nottingham, NG12 5GG

W.J. Rowley
British Geological Survey
Regional Geophysics Group
Keyworth
Nottingham, NG12 5GG

D.K Buckley
British Geological Survey
Regional Geophysics Group
Keyworth
Nottingham, NG12 5GG

EUROPEAN COMMISSION

J. Garnish
European Commission
Rue de la Loi 200
B-1049 Brussels
Belgium

PREFACE

THE ATLAS OF GEOTHERMAL RESOURCES IN EUROPE

Foreword

It is a real pleasure to have the opportunity to write the foreword to this update of the Atlas of Geothermal Resources of Europe. The Atlas of Geothermal Resources in the European Community was first published in 1988 and provided a compilation and assessment of geothermal resources in the member states with those in Austria and Switzerland. It represented the results from work in many countries over several years and has been fundamental to the ongoing development of geothermal resources in Europe.

This exciting new atlas follows closely the structure of the previous edition but contains updated information for all the states and has been augmented by data from 14 additional countries. It now presents an overview of the geothermal resources in practically the whole European continent from Portugal to Russia and is the most authoritative reference source of its kind.

Clear and informative presentations allow immediate assessment and comparison of regions and locations that have accessible geothermal resources. As each country and region develops energy strategies for the future, the atlas provides the data to support the development of this most important energy source.

Europe has already installed approximately 998 megawatts of geothermal electrical generation capacity as well as using more than 8000 megawatts of thermal power from direct use and heat pump technologies. Plans are underway to increase these capacities, reduce the temperature at which useful exploitation can take place and expand power production to non volcanic regions. Without reliance on wind or sunlight, geothermal power plants have high availability and load factors and are a particularly effective means of reducing emissions and fossil fuel use. The atlas allows a first order assessment of the geothermal resource availability in regions with high emission reduction priority, opening up the prospect of reducing dependence on some of the poorer fuels and systems in current use.

Publication of the atlas comes at a time when the promotion of sustainable development and the limitation of negative environmental impacts are high on the agenda of all European governments, local government officials and most businesses. This new atlas provides the means to understand the Europe-wide distribution of geothermal resources and will help to ensure that geothermal energy plays a significant role in our sustainable future.

The Atlas of Geothermal Resources in Europe is a wonderful achievement and I am sure it will provide valuable support to future geothermal development throughout Europe.

Eur Ing Dr Tony Batchelor
International Geothermal Association Board Member
Managing Director of GeoScience Ltd., UK

CONTENTS

Text

	Page
Introduction	15
1 Definitions and assessment of resources	17
2 European geothermal resources	19
3 National geothermal resource assessments	21
Albania	21
Belgium	23
Bulgaria	24
Czech Republic	26
Denmark	27
Estonia	28
Finland	29
France	30
Germany	32
Greece	35
Hungary	36
Italy	39
Latvia	42
Lithuania	43
The Netherlands	44
Poland	46
Portugal	47
Romania	50
Russia	51
Slovakia	53
Slovenia	54
Spain	56
Sweden	57
Switzerland	59
Ukraine	61
United Kingdom	61
4 Abbreviations and symbols	64
5 Tables	
Springs and geothermal installations	65
Heat-flow density	76
General Legend	93

Maps

	Plate
European scale:	
Geodynamics and geothermal perspectives	1
Heat-flow density	2
Temperature at 1000 m depth	3
Temperature at 2000 m depth	4
Geothermal resources	4
National scale:	
Albania	5
Belgium	7
Bulgaria	10
Czech Republic	13
Denmark	15
Estonia	17
Finland	18
France	19
Germany	20
Greece	25
Hungary	29
Italy	36
Latvia	41
Lithuania	44
The Netherlands	51
Poland	55
Portugal	59
Romania	61
Russia	64
Slovakia	70
Slovenia	74
Spain	77
Sweden	79
Switzerland	81
United Kingdom	83
Local aquifer names in relation to the Geological Time Scale	88

INTRODUCTION

Geothermal energy can be extracted with a variety of technologies and will generally involve drilling and pumping geothermal water from depth. The temperature and permeability of the geothermal reservoir, as well as the chemical composition of the fluid contained in its pores dictate the extraction method to be used as well as the kind of application that may be installed. Rigorously, one would need an assessment procedure for each kind of application (doublet, heat pump, electric power generation, etc.) and each type of reservoir (e.g. porous or fractured, fluid or steam). Such an approach would render gaining an overview of geothermal resources at a large scale more difficult. Geothermal energy feeds a great diversity of applications, alone or in combination with other sources of energy. This fact in addition to the wide range of temperature and geological conditions in geothermal reservoirs contribute to the difficulty of representing adequately geothermal resources. At the same time, one of the strengths of geothermal energy is its capacity to offer various options tailored to supply specific needs and consumers.

During the last decade many new, mostly low enthalpy, applications were developed that can be installed in regions considered earlier to not have enough resource concentration to be of interest. Therefore, it is necessary to estimate the resources in such a way as not to constrain perspectives on new applications or technologies. Furthermore, a single procedure for assessing geothermal resources allows comparison between regions and regional planning of investments in every kind of geothermal application. This is the goal of this atlas.

This work is a companion volume to the Atlas of Geothermal Resources in the European Community, Austria and Switzerland published in 1988. It contains updated information on geothermal resources from the participants of the previous atlas and adds information of another 13 countries. It is not a new edition of updated material because presently valid information from the previous atlas is not repeated here. The information for Austria given in the first atlas is still valid, so no additional material is shown. Norway does not possess geothermal resources as defined here atlas (pers. commun. E. Sundvor University of Bergen, Norway). Updated information for Ireland has been incorporated in the heat-flow density and temperature maps at the European scale. Together the two atlases display specific information on geothermal resources for the following countries: Albania, Austria, Belgium, Bulgaria, Czech Republic, Denmark, Estonia, France, Germany, Greece, Hungary, Ireland, Italy, Latvia, Lithuania, the Netherlands, Poland, Portugal, Romania, Russia, Slovakia, Slovenia, Spain, Sweden, Switzerland, and the United Kingdom. Updated information is included at a European scale also for Belarus, Bosnia-Herzegovina, Croatia, Iceland and the Ukraine. Participants of the Atlas of Geothermal Resources in the European Community, Austria and Switzerland (1988) were: Austria, Belgium, Denmark, France, Germany, Great Britain, Greece, Ireland, Italy, the Netherlands, Portugal, Spain and Switzerland.

Although the basis for resources assessment remained the doublet (or singlet) model of geothermal energy exploitation, the atlas does furnish enough information to assess the possibilities of low enthalpy applications such as heat pumps. As an example, Switzerland has one of the world-wide largest densities of heat pumps.

France prepared one of the largest contributions in the previous atlas and supports a very successful geothermal energy exploitation programme. It becomes clear the present contribution of France, that after assessing resources, most of the action towards an economically successful exploitation is at the surface and not at depth. Careful and detailed monitoring of the system allows the adjustments necessary to develop further known resources. With the proper data, modelling and management tools, efficiency is much increased and more energy is extracted without increasing the number of boreholes. This is an important achievement, as the drilling still causes most costs.

Resources assessment for potential Hot Dry Rock (HDR) or Enhanced Geothermal Systems (EGS) technology is not specifically addressed here. In the understanding of the editors, this technology, although promising, is not yet fully evolved. At present the most successful project is taking place in the extensional rift environment of the Rhine Graben in France. There are well-grounded hopes that this technology will be applicable in other tectonic environments as well. The discussion on what procedures to follow to quantify resources for HDR/EGS type applications is in progress.

This atlas is not a tool to determine drilling sites for geothermal installations. Rather, it is a tool for delineating areas of interest for further exploration and indicating possibilities of which kind of

geothermal application that could be installed. It also facilitates identifying potential partners for international joint ventures (as encouraged by the European Commission) in regions of similar geologic conditions. The information contained here does not replace the need for detailed local studies, although the maps presented herein permit a first order evaluation of the geothermal potential in terms of technical and economic viability. The assessment procedure applied uniformly to all countries and regions permits comparisons and serves as a guide for setting priorities and planning geothermal development.

Lastly, both atlases present a selection of material. Format constraints and financial limitations mandated a choice, so that the material included here does not exhaust all knowledge on geothermal potential areas in Europe. Despite this restriction, this work shows that countries with no geothermal application are rather the exception in Europe.

Acknowledgements

Dr. John Garnish (European Commission) was always available when needed. His encouragement accompanied this project through difficult times until its successful completion. Erika Staroste (European Commission) put much energy into getting the project started and took care especially of the PECO (Pays de l'Europe Central et d' Ouest) partners. She took her retreat before seeing the completion of this project. Dr. Andrew Green from Camborne School of Mines Ltd. (presently ABB) was responsible for the financial management of the partners under the PECO program. Special gratitude is owed to Dieter Schmidtman for his meticulous financial management of the project in Hannover. In the face of many currencies and fluctuating exchange rates, this was truly a Herculean piece of work.

Within the Joint Geoscientific Research Institute (GGA), the organisation that hosted the co-ordinator, many gave freely of their time. Dr. Christoph Clauser, head of the Geothermics and Hydraulic section, is thanked for his unflagging support. Juliane Herrman was instrumental in putting together some of the European maps and helping out with the layout. Rüdiger Schellschmidt supported this project well beyond his duties.

The European Commission provided funds for the preparation and printing of the maps for all countries. It also supported the work of members of the European Union at the time of project commencement (Belgium, Denmark, France, Germany, Greece, Ireland, Italy, the Netherlands, Portugal, Spain) and the PECO countries (Albania, Bulgaria, Czech Republic, Estonia, Hungary, Latvia, Lithuania, Poland, Slovakia, Slovenia and Romania). Special mention is made of those partners funded by their own countries: Finland, Russia and Switzerland. Another group (Belarus, Croatia and the Ukraine) provided information freely, which is much appreciated. The effort of K. Dimitrov. (St. Cyril & Methodius University, Skopje, Macedonia, FYROM), M. Milivojevic, University of Belgrade, Serbia) and Z. Demirel (MTA- General Directorate of Mineral Research and Exploration, Ankara, Turkey) in attempting to secure support in their own countries is acknowledged here.

1 Definitions and assessment of resources

Geothermal resources are that part of the geothermal energy which can be extracted economically and legally in the near future. The reserves, which are part of the resources, can be exploited at present and have been demonstrated by drilling or geochemical, geological and geophysical data. Potential geothermal areas are those regions, which appear to be adequate for geothermal exploitation, but for which the data are currently inadequate to permit a quantitative assessment of resources. Additional details are given in the previous atlas (Haenel and Staroste, 1988).

To quantify these resources, the amount of heat available in the rock and the fluids contained therein (geothermal reservoir) as well as the characteristics of the reservoir which affect extraction of heat need to be determined. There are numerous methods and models for the quantification of geothermal resources. This work is based on a volumetric heat content model for porous reservoirs assuming exploitation of geothermal energy by a doublet (production and injection boreholes) or a singlet (one production borehole only) system is the basis of the calculation (Muffler and Cataldi, 1976).

The resource H_1 (in J), is given by

$$H_1 = H_0 \cdot R_0 \quad (1)$$

H_0 represents the heat in place (in J) contained by the reservoir assuming a volume model of heat extraction. It takes into account the heat stored in the rock matrix (m) and in the water occupying the pores (w):

$$H_0 = [(1 - P) \cdot \rho_m \cdot c_m + P \cdot \rho_w \cdot c_w] \cdot [T_t - T_0] \cdot A \cdot \Delta z \quad (2)$$

where:

ρ_m, ρ_w	density of the rock matrix and water, respectively, kg/m^3 ,
c_m, c_w	specific heat capacity of the rock matrix and water, respectively, $\text{J}/(\text{kg K})$,
P	effective porosity, unit less,
T_t	temperature at the top of the aquifer, $^\circ\text{C}$,
T_0	temperature at the surface, $^\circ\text{C}$,
A	surface area under consideration, m^2 ,
Δz	net aquifer thickness, m.

The fraction of this heat capable of being extracted is R_0 , a recovery factor that depends on the extraction technology used. If exploitation is made with a doublet system, i.e. with a production borehole and an injection borehole used to re-inject the fluid after use, it can be shown that (Lavigne, 1978):

$$R_0 = 0.33 \frac{(T_t - T_r)}{(T_t - T_0)} \quad (3a)$$

where T_r is the re-injection temperature. Re-injection avoids a pressure decline in the aquifer during exploitation or prevents environmental degradation of surficial water and soil due to the disposal of highly saline geothermal water. The expert group of the European Commission recommends a value of $T_r = 25^\circ\text{C}$. This restriction cannot be applied to countries in which the mean annual temperature is low (e.g. Sweden). The same temperature difference ($T_t - T_r$), albeit with much lower reservoir and re-injection temperature may produce comparable resource and exploitation possibilities as in countries of warmer climate and higher reservoir temperatures. Here the recommended value is taken unless where stated otherwise.

If the extraction of geothermal energy is planned with one production borehole only, a singlet, the recovery factor reduces to (Gringarten, 1979):

$$R_0 \approx 0.1 \quad (3b)$$

The data needed for this assessment consist of generally available information (stratigraphy, porosity from cores or geophysical logging, temperature measurements) and geophysical and geological surveys to determine structures (faults) and the spatial distribution of reservoir formations. In the procedure presented above, the resources are based on the effective porosity of the aquifer. Generally, fluid extraction is governed by hydraulic conductivity or transmissivity. This information is also displayed in the maps where available. The knowledge of these parameters requires expensive pumping tests, an investment more often undertaken in local studies for a specific location rather than for the overall characterisation of an aquifer. Information on the chemistry (salinity) of the geothermal fluid is important for evaluating the extraction technology and long-term behaviour of the system. The need to re-inject spent fluid can be evaluated and measures planned for preventing scaling or corrosion. Wherever possible, these data have been incorporated into maps. Although these additional data are

essential, they are often not available. Porosity determinations (on cores in the laboratory or during geophysical logging) are easier to secure.

The resources evaluation procedure used for compiling the present atlas is simple. Because of that, it does not consider all critical conditions needed for successful energy extraction. Exploitation of geothermal resources is practically determined by the permeability of the aquifer, which constrains production rates. Permeability data and pumping test results are only available for few areas. It would not be possible to obtain assessments for most of Europe based only on such data. Furthermore, permeability may vary over several orders of magnitude within short distances with almost unpredictable consequences for exploitation. Even if the resources assessment were to include permeability and more sophisticated models, it would still not allow localized predictions about the geothermal system. The atlas does not explicitly account for the availability of consumers for the resources presented. However, background information on the maps, such as cities, provides an indication of potential consumers. Maps of depth, thickness, temperature and resources characterize the geothermal reservoir in this atlas. First order assessments are also possible in regions of very limited data coverage, because of the small number of parameters used in the present resource evaluation method.

2 European geothermal resources

An overview of the relevant geothermal aspects of Europe is presented in the following maps at an European scale: Heat-Flow Density, Temperature at 1000 m and 2000 m depth and European Geothermal Resources.

Heat Flow Density (Plate 1)

S. Hurter and R. Schellschmidt

Terrestrial heat-flow density is given by Fourier's law that describes the vertical transport of heat by conduction in the Earth's crust:

$$q = \lambda \cdot \text{grad}T \quad (4)$$

where q is heat-flow density (in W/m^2), λ is the thermal conductivity of the rocks (in $\text{W m}^{-1}\text{K}^{-1}$) measured on core samples or drill cuttings and $\text{grad}T$ is the geothermal gradient (in K/m) obtained from temperature logging in boreholes. HAENEL et al (1988) offer detailed guidelines and recommendations for the determination of heat-flow density.

The Table of Heat-Flow Densities (page 78) lists the heat-flow density data provided by the project partners. Data for Bosnia-Herzegovina, Macedonia (FYRM), Montenegro, The Netherlands, North Africa, Russia, Serbia, and Turkey were taken from HURTIG et. al. (1990). Uniform criteria apply for the all data sources: no paleoclimatic correction was made and topographic correction was applied where needed (e.g. Alpine regions). Compared to the previous atlas, the data coverage is much improved, especially for The Netherlands and Spain.

The heat-flow density values were processed with the Geographic Mapping Tools software (WESSEL and SMITH, 1998). The cubic spline under tension algorithm was applied for gridding according to SMITH and WESSEL (1990). A grid size of 0.1° was chosen under a tension factor of 0.0025. No geological criteria were used to aid isoline tracing. Major tectonic units are reflected in the map, where data density is sufficient, while regions of sparse data coverage are not well characterized.

Higher heat-flow density characterizes regions in Europe with active volcanic and shallower igneous activity such as Iceland, parts of Italy and Greece. The Rhine Graben exhibits also high values of heat-flow density. Additionally, other areas of enhanced heat-flow density are related to sedimentary basins such as the Pannonian and the Paris basins.

Temperature at 1000 m and 2000 m depth (Plate 2 and 3)

The temperature maps in 1000 m and 2000 m depth are composed of three sources of information. National maps produced by individual countries were juxtaposed with parts of the previous atlas (France and Austria), which were not updated, because the increase in data would not cause significant changes in isoline pattern. Other parts (mostly Macedonia, Montenegro, Russia, Serbia) were incorporated from the Geothermal Atlas (HURTIG et al., 1992). Thirdly, heat-flow density values were used to extrapolate (downward continuation) temperatures at greater depth (Norway, Estonia).

If the thermal effects of fluid motion in the subsurface are negligible or can be removed with appropriate corrections, the heat-flow density can be used to infer the temperature at depth (z):

$$T_z = T_0 + \frac{q}{\lambda}z - H \frac{z^2}{2\lambda} \quad (5)$$

T_0 is the temperature at the surface ($z = 0$) and H is the radiogenic heat production rate of the rocks produced by the decay of minute concentrations of uranium (^{235}U), thorium (^{232}Th) and potassium (^{40}K) occurring naturally in certain minerals making up the rock. The mean radiogenic heat production rate of the continental crust is about $1 \mu\text{W}/\text{m}^3$.

Other factors and processes influence heat flow at the surface: topography, sedimentation, erosion and, climatic variations (e.g. glaciations). Details on how to evaluate the magnitude of these effects and remove them from heat-flow density measurements are given in HAENEL et al. (1988).

Ideally raw temperature data for all Europe should be collected and processed uniformly so that the data are interpolated to yield temperature values at the depths of interest. Appropriate gridding and contouring algorithms would produce consistent temperature maps over all of Europe. Unfortunately, raw data is not easily available, because most of these data are confidential or the property of industry.

The approach taken here was a collage of individual maps. Each partner produced national temperature maps, which then were assembled, i.e. pasted together to yield European maps of temperature. Even though neighbouring partners worked together to adjust their data and maps at the common borders, inconsistencies remained. The sources of these inconsistencies are manifold. On the one hand, isolines from one country to the next may cross tectonic units which are not or very poorly surveyed with temperature data (e.g. Alps or other mountain ranges). On the other hand, different kinds and quality of data on both sides of the border make it difficult to weigh the data consistently.

The adjustment of the isolines across such areas was accomplished manually, although care was taken not to use geologic information to dictate the tracing so the map does not include a geologic bias. It is not certain that all individual maps pieces consistently avoided a geologic bias. Otherwise, where the maps reflect geologic features, this may be interpreted as a thermal contrast between provinces when data density is adequate to capture the fundamental characteristics of the thermal field in each unit. Although these temperature maps are flawed by uncertainties, they are at the most updated European scale view of subsurface temperature.

Geothermal Resources

(Plate 4)

This map highlights the areas in which an assessment of geothermal resources has been made according to the procedure adopted in the previous atlas. Areas of resource assessment presented in the previous atlas have been included here, so a complete European overview can be shown. Sites of geothermal installations listed in the Table of Springs, Geothermal Installations (page 65) are located on the map. Outside the shaded areas shown in the map, no resource assessment has been made according to the criteria, not implying the non-existence of such resources. HUTTRER (2000) as well as LUND and FREESTON (2000) discuss the worldwide status of geothermal power generation and direct uses, respectively. Many additional articles for most countries in Europe can be found in IGLESIAS, et al., (2000).

It can be seen that practically all European sedimentary basins have low enthalpy geothermal resources that could be utilised in some form and moreover, countries with no geothermal application are rather the exception in Europe. The higher enthalpy areas (with electric power generation) coincide with tectonically or volcanically active regions such as the Mediterranean region (Italy, Greece) and Iceland.

Supplementary Information

Local aquifer names in relation to the Geological Time Scale (Plates 88 and 89)

The aquifers presented in each country are displayed with respect to their geologic age. The geologic time scale was taken from HARLAND (1990).

References

Gringarten, A.C., 1978: Reservoir lifetime and heat recovery factor in geothermal aquifers used for urban heating. - *Pageoph*, 117, 297-308.

Haenel, R. and Staroste, E., (Eds.), 1988: Atlas of geothermal resources in the European Community, Austria and Switzerland. - Th. Schäfer, Hannover, Germany, 74 p., 110 plates.

Haenel, R., Rybach, L. and Stegena, L., (Eds.), 1988: Handbook of terrestrial heat-flow density determination with guidelines and recommendations of the International Heat Flow Commission. - Kluwer Academic Publishers, Dordrecht/ Boston/ London, 486 pp.

Harland, W.B., 1990: A geological time scale 1989. - Cambridge University Press, Cambridge, 262 pp.

Hurtig, E., Čermák, V., Haenel, R. and Zui, V., (Eds.), 1992: Geothermal Atlas of Europe. - Hermann Haak Verlagsgesellschaft mbH, Germany.

Huttrer, G.W., 2000: The status of world geothermal power generation 1995-2000. - In: Proc. World Geothermal Congress 2000 (Eds: Iglesias, E., Blackwell, D., Hunt, T., Lund, J., Tamanyu, S., and Kimbara, K), Kyushu-Tohoku, Japan, May 28-June 10, 23 - 37.

Iglesias, E., Blackwell, D., Hunt, T., Lund, J., Tamanyu, S., and Kimbara, K., 2000: Proc. World Geothermal Congress 2000, Kyushu-Tohoku, Japan, May 28-June 10.

Lavigne, J., 1978: Les ressources géothermiques françaises - possibilités de mise en valeur. - Ann. des Mines, avril, 16 p.

Lund, J.W. and Freeston, D.H., 2000: World-wide direct uses of geothermal energy 2000. In: Proc. World Geothermal Congress 2000 (Eds: Iglesias, E., Blackwell, D., Hunt, T., Lund, J., Tamanyu, S., and Kimbara, K), Kyushu-Tohoku, Japan, May 28-June 10, 1- 21.

Lund, J.W., 2000: World status of geothermal energy use overview 1995-2000. - In: Proc. World Geothermal Congress 2000 (Eds: Iglesias, E., Blackwell, D., Hunt, T., Lund, J., Tamanyu, S., and Kimbara, K), Kyushu-Tohoku, Japan, May 28-June 10, 4105-4111.

Muffler, P. and Cataldi, R., 1978: Methods for regional assessment of geothermal resources. - Geothermics, 7, 53-89.

Smith, W.H.F. and Wessel, P., 1990: Gridding with continuous curvature splines in tension. - Geophysics, 55, 3, 293-305.

Wessel, P. and Smith, W.H.F., 1998: New, improved version of Generic Mapping Tools released. - EOS Trans. Amer. Geophys. U., 79, 47, 441, p. 579.

3 National geothermal resource assessments

The geothermal resources of a geothermal aquifer is displayed with a set of four maps:

1. The map of the depth to the top of the aquifer shows the range of depth variation of the reservoir. Depth is a critical parameter for evaluating the order of magnitude of the investment needed to develop the available geothermal potential, as drilling costs still make up the major part of this investment.
2. The map of aquifer thickness is an indication of the size of the resource. Experience in geothermal energy applications in northern Germany, e.g., suggests that aquifers of net thickness less than 20 m rarely are capable of supporting the required production rates.
3. The temperature at the top of the aquifer provides a lower bound on the range of temperatures in the aquifer, indicating what type of application may be installed.
4. The distribution of the resources over a region is shown with a map of isolines representing the resources per unit area (H_1/A , in GJ/m^2). Here the effects of all parameters in equations 2 and 3 are lumped together. It is possible to display resources information that includes confidential data (e.g. porosity of certain aquifers) without explicitly revealing this data.

Other parameters may be presented in the maps where available. Piezometric level, pressure and the distribution of boreholes is shown on the depth map. Porosity, permeability and transmissivity are found on the map of reservoir (net) thickness. Salinity is superposed on the temperature map. The General Legend explains all symbols commonly used in the maps. Deviations from the definitions given earlier (e.g. re-injection temperature T_r) or in the General Legend are marked on the maps, e.g. temperature in the map referring to the mid-depth in the aquifer instead of the top.

ALBANIA

A. Frasher, V. Čermák, D. Doracaj, N. Kapedani, R. Liço, R. Bakalli, H. Halimi, M. Krešl, E. Vokopola, E. Jareci, B. Çanga, L. Kučerová, E. Malasi and J. Šafanda

Geothermal thematic map (Plate 5)

The Albanides are the main geological feature in the territory of Albania. This orogenic belt is located between the Dinarids in the N and the Helenids in the S, forming the Dinaric branch of the Mediterranean Alpine Belt. The Albanide rocks range from Ordovician-Quaternary in age and were formed in the Triassic over a Hercynian substrate. The structures are typically Alpine, running SSE/NNW with asymmetric W vergence, sometimes with recumbent, overthrust and overtwisted features. The western flanks are affected by rifting. The internal branch, or Inner Albanides, comprises the Korabi and Mirdita (ophiolite belt) tectonic zones, while the Krasta-Cukali, Kruja and Ionian tectonic zones make up the external branch (Outer Albanides). Folding and deformation migrated from E to W, culminating with the overthrusting of the Inner Albanides over the external zones. Late Jurassic oceanic crust is found in the ophiolite belt running along the western border of the Mirdita zone. The Pre-Adriatic Depression lies in the Outer Albanides, extending into the shelf area of the Adriatic Sea. Up to 17 km of Miocene and Pliocene sediments fill this molassic basin. Deep longitudinal and transverse faults cutting through the entire crust intercept the Albanides.

Although some thermal springs in Albania are isolated geothermal manifestations, most are concentrated in three geothermal areas: Kruja, Ardenica and Peshkopia (FRASHERI et al., 1996). Flow rates are greater than 10 l/s, reaching 40 l/s. The geothermal waters in Albania have been and are still exclusively used for medical purposes.

Temperatures (Plate 5)

Temperature measurements were carried out in 145 boreholes. Data from 8 thermal springs or groups of springs and 8 geothermal boreholes

were included as well. In general, temperature was measured in wells filled with mud or water and in the steady state thermal regime. When this was not possible, DRURY's (1994) method was used to obtain an undisturbed temperature. The data were processed by using trend analysis of the first and second order. Topographic corrections were applied where needed. Temperature data in the Peri-Adriatic Depression are affected by sedimentation of Serravalian age. This effect amounts to about 25 % of the measured geothermal gradient. The lowest temperatures are observed in mountainous regions, where there is pervasive circulation of cold underground waters. Further details on the thermal structure and heat-flow density in Albania, including measurement techniques and data treatment, can be found in FRASHERI (1992), FRASHERI et al. (1996) and ČERMÁK et al., (1996) and the literature cited therein.

Potential geothermal reservoirs

The *Ardenica* geothermal area is situated 40 km N of Vlora within the Peri-Adriatic Depression. It comprises the molassic Neogene brachyanticline Ardenica, the Semani anticline, the northern periclinal Patos-Verbasi carbonate structure and the overlying Neogene molasses. The Ardenica geothermal area is intercepted by the Vlora-Elbasan-Dibra transversal fault (FRASHERI et al, 1995; SHTETO, 1995). The aquifer section comprises alternating layers of sandstone, clay and siltstone. At the surface, the boreholes discharge at temperatures of 32 - 35 °C.

The *Kruja* geothermal area concentrates most geothermal resources in Albania. This area extends from the Adriatic coast in the Ishmi region (N of Tirana) to the SE, penetrating into Greece, along a total length of 180 km and a width of 4 - 5 km. Two subzones are recognized: the Tirana-Elbasani (north) and the Galigati (south) zones. In the first, geothermal resources are estimated to be of the order of 0.59×10^{18} - 5.1×10^{18} J, while geothermal resources of the Galigati zone are of the order of 0.65×10^{18} J. The Kruja region consists of a series of anticline structures with Cretaceous-Eocene carbonate cores of neritic limestones, dolomitic limestones and dolomites covered with Eocene to Oligocene flysch deposits. In some of the structures, Tortonian molasse transgressively overlies the carbonate rocks, while in other structures, the Burdigalian marlstone transgresses over the flysch section (GEOLOGICAL MAP OF ALBANIA, 1984). The flysch and limestone strata plunge down to 10 km, where they are underlain by the Permian-Triassic evaporitic formations (DIAMANTI et al., 1995). The geothermal aquifer consists of karstified carbonate formations which allow water to penetrate to great depths (150 - 200 °C). The cataclastic rocks of the tectonized zone provide pathways for the hot water to move up and fill the carbonate reservoirs. Various geothermometers indicate reservoir temperatures to be of the order of 145 - 250 °C. This suggests that at least part of the thermal water in the reservoir came from deeper zones.

The *Peshkopia* geothermal area is located in the NE of Albania, the Korabi hydrogeologic zone (FRASHERI et al., 1996; EFTIMI et al., 1989). At a distance of 2 km east of Peshkopia, water at 43.5 °C flows out of a group of thermal springs on a river slope composed of flysch deposits. Some of the springs yield flow rates up to 14 l/s. Different geothermometers indicate the reservoir temperatures are 144 - 270 °C. The occurrence of these springs is associated with a deep fault at the periphery of a gypsum diapir of Permian-Triassic age. This diapir extends vertically over 3 - 4 km (KODRA et al., 1993) and comprises the main aquifer of this geothermal system. Considering the regional geothermal gradient, temperatures of 220 °C would be found at depth of 8 - 12 km. However, the gypsum diapir represents a high thermal conductivity body focusing heat from its surroundings. Therefore, water could become warmer at shallower depths than suggested by the geothermal gradient. Where the gypsum formation plunges underneath the free circulation zone, the presence of H_2S can be detected in the water. The thermal waters are of $Ca-SO_4$ type, with a mineralization of up to 4.4 g/l, containing 50 mg/l H_2S . The geothermal potential of the Peshkopia system is estimated to be of the same order of that of the Tirana-Elbasani area.

Ardenica (Plate 6)

The Ardenica geothermal reservoir comprises sandstone sections of Serravalian, Tortonian and Pliocene age. These sandstone layers are composed of coarse, medium and fine grains. Hot water discharges from the boreholes Ardenica-3 (Ar3) and Ardenica-12 (Ar12), both situated in the Ardenica brachyanticline, Semani-1 (Se1) in the anticlinal structure

of the same name, the Verbasi-2 (Ver2) drilled in the Patosi monocline and the Bubullima-5 (Bub5) borehole that intercepts the carbonatic section of the Patos-Verbasi structure. Water flows into these boreholes at depth intervals of 1200 - 1700 m (Ar3), 1935 - 1955 m (Ar12), 2250 - 2275 m (Se1), 875 - 1035 m (Ver2) and 2385 - 2425 m (Bub5).

Electrical resistivity and SP logs in the Ardenica and Semani-1 boreholes show that the sandstone section has a thickness of 445 - 1165 m. As an example, these geophysical logs for the Ardenica-12 borehole are shown together with the temperature log and a lithologic column. It is clearly demonstrated that the aquifer temperatures are higher in sandstone layers than above or beneath them. At the well-head, temperatures are 32 °C for Ardenica-12, 35 °C for Semani-1 and 38 °C for Ardenica-3. However, the temperature in the aquifer at depths of 1935 - 1955 m is 45.8 °C.

Effective porosity of the aquifer is about 15.5 % and permeability reaches 283 mD. Hydraulic conductivity is 4.98 m/s and transmissivity has a value of $8.9 \times 10^{-5} \text{ m}^2/\text{s}$. These reservoir properties translate into an output of 5 - 18 l/s. This Ca-Cl thermal water contains 21.2 mg/l iodide, 110 mg/l bromide and 71 mg/l boric acid.

Ardenica reservoir has $0.82 \times 10^{18} \text{ J}$ heat in place (H_0) and identified resources (H_1) of $8.19 \times 10^{18} \text{ J}$. Resources density varies from 0.25 - 0.39 GJ/m².

Unfortunately all boreholes have been abandoned and await renewed investment into geothermal exploitation.

Kruja (Plate 6)

Three boreholes produce hot and mineralized water: Ishmi-1/b (Ishmi-1/b), Kozani-8 (Ko8) and Galigati 2 (Ga2). The thermal springs of the Llixha Elbasani spa are located about 12 km S of Elbasani. There are 7 groups of springs distributed along an arcuate belt associated with the main regional thrust of the Kruja tectonic zone. The reservoir lies within the Llixha limestone structure.

The Ishmi-1/b is the northernmost borehole of the Kruja geothermal field, about 20 km NW of Tirana. It was drilled in the upper part of the fissured and karstified limestone. The borehole intercepts the limestone section at 1300 m depth and continues through more than 1000 m of carbonatic strata. Effective porosity is less than 1 % and the permeability ranges from 0.05 - 3.5 mD. The hydraulic conductivity of the limestone section varies between 8.6×10^{-10} - $8.8 \times 10^{-8} \text{ m/s}$ and the transmissivity ranges from 8.6×10^{-7} - $8.5 \times 10^{-5} \text{ m}^2/\text{s}$ (FRASHERI et al., 1996).

Kozani-8 borehole is located on hills 26 km SE of Tirana. It encounters limestone strata at 1819 m depth, penetrating 10 m into the section. Hot water has continuously discharged from the Ishmi-1/b and the Kozani-8 boreholes at rates of 3.5 l/s and 10.3 l/s, respectively, since the end of drilling operations (1964 and 1988, respectively).

Galigati-2 borehole is located on a hill, about 50 km SE of Tirana. At a depth of 2800 m, it discloses a 85 m thick limestone section.

The Langarica river thermal springs and the Sarandaporo springs can be found in the S of the Kruja geothermal area. Thermal water flows out from the contact between Eocene fissured and karstified limestone and the flysch section.

Well-head temperatures in the Tirana-Elbasani zone vary from 60 - 65.5 °C. The temperature at the top of the aquifer reaches 80 °C in the Kozani-8 hole. According to the temperature logs in Ishmi-1/b and Galigati 2, temperatures at depth in the carbonatic section are 42.2 °C and 52.8 °C, respectively. The difference between the temperature of thermal water discharging at the surface and of the limestone section at depth shows that a mixture of waters from different depths and temperatures has occurred.

The Elbasani Llixha springs and Ishmi-1/b and Kozani-8 boreholes have exhibited constant yields with stable temperatures for decades. The springs have been discharging at a rate of 3.5 l/s during the last 50 years, while the boreholes have maintained an output of 15 l/s for 10 years. Hot water has a salinity of 4.6 - 19.3 g/l. Elbasani Llixha water contains Ca, Na, Cl, SO₄, and H₂S (AVGUSTINSKY et al., 1957) while in the Tirana-Elbasani, thermal waters are of Mg-Cl type. They contain the cations Ca, Mg, Na and K, as well as the anions Cl, SO₄ and HCO₃ with pH of 6.7 - 8 and density of 1.001 - 1.006 g/cm³.

The southern spring waters at Langarica river are much different. They do not contain H₂S, CO₂ and are a factor of 7 - 9 times less mineralized than waters from the Tirana-Elbasani zone.

For the Tirana-Elbasani subzone heat in place (H_0) is 5.87×10^{18} - $50.8 \times 10^{18} \text{ J}$, identified resources (H_1) are 0.59×10^{18} - $5.08 \times 10^{18} \text{ J}$, while specific reserves ranges between values of 38.5 - 39.6 GJ/m². The second subzone, Galigati, has lower concentration of resources 20.63 GJ/m², while geothermal resources amount to $0.65 \times 10^{18} \text{ J}$. These reserves have been extrapolated for this whole subzone up to the Albanian-Greek border. As both subzones are geologically and hydrogeologically similar and geothermal resources of Galigati are of the same order as those of Llixha, equivalent geothermal reserves are expected to be found in the less well known southern part of the Kruja geothermal area.

Present status and future perspective of the use of geothermal energy

The geothermal resources in Albania constitute a potential for low enthalpy energy exploitation. In addition to the traditional balneology, greenhouses and other industrial applications could be implemented.

The Peshkopia, Llixha Elbasani and Langarica Permeti springs and Ishmi 1/b borehole are used for medical treatment. In Elbasani Llixha, there is a medical center with about 200 beds for the treatment of rheumatism and skin diseases. Thermal waters of the Langarica springs are used as potable water in their natural state to treat digestion diseases.

Thermal waters of the Elbasani Llixha and Peshkopia springs and the Ishmi-1/b and Kozani-8 wells are in good technical condition and close to an area with a high level of social-economic development. They could be put into use practically immediately. The proper equipment installed on the Ishmi-1/b and Kozani-8 boreholes, would permit their hot waters to be used for medical, green-houses and industrial applications.

At the sites of the Elbasani Llixha and Peshkopia springs, shallow boreholes need to be drilled to capture water at depth, in order to increase the water yield and the heat output.

In Peri-Adriatic Depression geothermal gradients of 18 - 20 °C/km have been measured. Here, abandoned oil and gas wells could be used as single or double Vertical Linear Heat Probes.

References

- Avgustinsky V. L., Astashkina A. A. and Shukevič L. I., 1957: Mineral Springs and Health Centers in Albania. - Ministry of Health, Tirana, Albania.
- Čermák V., Krešl M., Kučerová L., Šafanda, J., Frasher A., Kapedani L., Liço R. and Cano D., 1996: Heat flow in Albania. - *Geothermics*, 25, p. 91-102.
- Diamanti F., Sadikaj Y., Zajmi L., Tusha I., Gjoka M., Prifti I. and Murataj B., 1995: Hydrocarbon potential of Albania. - Symposium Alb-Petrol 95, Fieri.
- Drury, M.J., 1989: On the possible source of error in extracting equilibrium formation temperatures from borehole BHT data. - *Geothermics*, 13, p.175-180.
- Eftimi R., Tafilaj I. and Bisha G., 1989: Hydrogeologic Division of Albanides. Bulletin of Geological Studies, 4, p. 303-315 (in Albanian, English summary).
- Frasher A. 1992: Albania. - In: Geothermal Atlas of Europe. (Eds.: Hurtig, E., Čermák, V., Haenel, R. and Zui, V.), Hermann Haack Verlagsgesellschaft, Gotha, Germany, p. 13.
- Frasher A., Čermák V., Kapedani N., Liço R., Krešl M., Jareci E. and Čanga B. 1995: Geothermal Atlas of Albania. - Polytechnic University of Tirana, Faculty of Geology and Mining, Tirana, Albania and Geophysical Institute of Academy of Sciences of Czech Republic, Prague.
- Frasher A., Čermák V., Doracaj M., V., Kapedani N., Liço R., Bakalli F., Krešl M., Jareci E., Halimi H., Čanga B. and Malasi E., 1996: Geothermal Resource Atlas of Albania. - Polytechnic University of Tirana, Faculty of Geology and Mining, Tirana, Albania.
- Geological Map of Republic of Albania, 1:200000, 1984: Institute of Geological Studies of Tirana, Faculty of Geology and Mining of Polytechnic University of Tirana, Geological Institute of Oil and Gas, Fier.
- Kodra A., Gjata K. and Bakalli F., 1993: Les principales etapes de l'évolution paleo-geo graphique et geodynamique des Albanides Internes au cours du Mesozoique. - Bull. Soc. Geol. France, p. 69-77.
- Shteto K., 1995: Thrust tectonics in the Tragjasi and Sazani tectonic units. - Doc. Thesis, Polytechnic University of Tirana, Faculty of Geology and Mining.

BELGIUM

N. Vandenberghe

Geothermal thematic map (Plate 7)

In the previous edition of this atlas, complete sets of maps depicting geothermal resources were presented for the Neeroeteren Sandstones. Other potential areas such as the Tufaceous Chalk, the Dinantian within the Campine Basin and the Hainaut Basin were characterised by depth and temperature maps and salinity information. In the present edition geothermal resource assessments for these potential areas are presented. The reader is referred to the previous edition of this atlas for information on the geothermal resources of the Neeroeteren Sandstones.

The main part of NW Belgium is made up by the eastern part of the London-Brabant Caledonian Massif. It consists of hard clastic rocks and is overlain by a thin Late Cretaceous chalk and Tertiary soft clastic cover. Around the Caledonian Massif, the flanks of the Brabant Massif are covered by Hercynian rocks, starting with clastics and carbonates of Middle and Late Devonian age. These are overlain by Dinantian carbonates, including an important anhydrite sequence in the Hainaut province, and subsequently by the coal-bearing Late Carboniferous clastics.

The Hainaut, Namur, and Liège basins were tectonically influenced by the prograding Variscan overthrust front, whilst the Campine Basin, N of the Brabant Massif, is affected by block faulting partly related to the Mesozoic and Cenozoic activity of the Roermond graben. The top of the Palaeozoic in the Campine Basin is covered by almost 1000 m of Late Cretaceous chalk and Tertiary clastics. The waters of aquifers in Tertiary rocks are cooler than 30°C and will therefore not be discussed further.

The region S of the Midi-Condros-Eifel overthrust (N Variscan thrust front) is dominated by Devonian and Early Carboniferous folded rocks. Carbonate rocks occur in the Middle Devonian, in part of the Late Devonian and in the Dinantian. The extent of the Dinantian is limited to relatively shallow synclines in the Condros area and to the E of Liège.

Compared to the geothermal thematic map in the previous edition of the atlas further tectonic details in the Campine area have been added. All operating geothermal installations presented before continue to operate, although the building heating with energy from the Turnhout borehole had to be stopped because of clogging. This borehole, however, continues operating for heating a swimming pool. The boreholes presently in use tap the Dinantian reservoirs or the Tuffeau chalk reservoir. The Merkplas geothermal plant construction under way at the time of the preparation of the previous edition was never completed. The table of geothermal springs and installations has been updated accordingly.

The SO₄ rich thermal water from boreholes in the Hainaut area have temperatures ranging from 53 - 73 °C. In the boreholes in the Campine Basin, CO₂ type water occurs with temperatures of 27 - 36°C.

Temperatures (Plate 7)

The subsurface temperature data for Belgium were first listed by LEGRAND (1975). These data have been revised and all data collected since 1975 by the Belgian Geological Survey are incorporated in the present review. All data are kept in the archives of the Belgian Geological Survey.

The temperatures have been measured mainly in research drillings, partly for the purpose of geothermal energy development. The differences between the previous and present temperature maps are the result of the application of temperature correction procedures and the use of new geostatistical data treatment and interpolation techniques, rather than large changes in data quantity or distribution produced by new data. The measured temperatures corrected to approach true formation temperatures using an empirical correlation. Geostatistical estimates of the temperature values at the nodes of a three dimensional grid were made for preparing the temperature maps and for the calculation of the resources, in combination with digitised depths and thickness data. Additional details are found in the previous atlas and VANDENBERGHE (1991).

The temperature distribution on all maps reflects the main structural elements of Belgium. Lower temperatures prevail in the Caledonian Brabant Massif and the Hercynian Condros-Ardenne area separated by the Mons, Namur, Liège coal bearing synclinal structures that exhibit

higher temperatures. Local shallow temperature anomalies can be explained by convective heat transport in porous rocks, clastic sediments or karstic reservoirs. Examples are the warm anomalies in the Hainaut basin, the Maastricht border area with the Netherlands and the relatively cool temperatures to the east of Chaudfontaine.

VERKEYN (1995) discusses the heat-flow density pattern for Belgium.

Potential geothermal reservoirs

The youngest and shallowest potential reservoir is the top of the Late Cretaceous, and also the Palaeocene tufaceous chalk arenite, in N Belgium. Another potential geothermal reservoir in the NE of the Campine Basin comprises the porous Permo-Triassic sandstones that overlay the Westphalian. Here the Neeroeteren sandstone (top of the Westphalian) is also a small potential reservoir, described in the previous edition of this atlas. The main low enthalpy geothermal reservoirs, however, are within the Dinantian limestones around the Brabant Massif. The Dinantian limestones in the Liège area have a limited potential due to the small area of occurrence and the shallow depth. Therefore more detailed maps were not prepared.

Resources were calculated for all the reservoirs considered using a maximum aquifer depth of 2500 m, a minimum reservoir temperature of 25 °C and a recovery factor of 0.33. Resource values for each reservoir were calculated per 1 km² area and mapped.

Dinantian in the Hainaut Basin (Plate 8)

The St. Ghislain borehole has shown the presence of karstic levels in mainly anhydrite rocks. The porous and permeable Late Visean collapse breccia further up dip are contemporary with the karstic anhydrites. The dissolution is due to a circulation system of meteoric water infiltrating in the E outcrop zone and resurging in the lower lying W Hainaut Basin. The high permeability of the karstic and breccia reservoirs allow heat to be redistributed by fluid flow such that the reservoir to the E is relatively cold compared to the reservoir in the W. The latter is demonstrated by the presence of warm springs in the W Hainaut area. The Hainaut boreholes have artesian flow rates between 95 - 100 m³/h and temperatures of about 70°C. The equilibrium of the reservoir water with anhydrite leads to an almost fresh SO₄ water.

Although the depth and temperature maps have not changed significantly, here a complete set of maps has been included to characterise the geothermal resources.

Tufaceous chalk in the Cretaceous Campine (Plate 8)

This chalk arenite has porosities between 20 - 40 %. The maximum measured permeabilities in N Belgium are about 300 mD, but values as low as 25 mD are also measured. This confined aquifer has artesian water, but the specific flow rate reduces to 0.5 (m³/h)/m (Turnhout, Dessel) and even to almost 0.1 (m³/h)/m (Loenhout, Meer) during pumping. The water is saline. In the outcrop zone of the reservoir chalks (though of no geothermal value) the water is fresh, permeabilities are as high as several darcies and specific flow rates can exceed 10 (m³/h)/m.

Buntsandstein in the Campine Basin (Plate 8)

The reservoir consists of quartzitic red-stained sandstones of Triassic age. They have thicknesses of several hundred metres as shown by seismic interpretations and confirmed by boreholes. An approximately 200 m thick sandstone assemblage at the bottom of the Middle Buntsandstein, with an effective porosity of 10 %, has a good potential. One reservoir test yielded an injectivity of 1.3 (m³/h)/bar.

Dinantian in the Campine Basin (Plate 9)

Experience of drilling deeply in N Belgium has shown (through increased drilling rates and mud losses) that, except in a few boreholes very near the Dinantian subcrop, the top of the Dinantian limestone is porous and highly permeable. The thickness of the karstified top varies between 5 - 60 m.

Test results from several boreholes are consistent with a reservoir permeability of several darcies and about 4 % average porosity, locally exceeding 20 %. The reservoir water is very saline (> 100 g/l). Interference tests show that the reservoir extends continuously over distances of at least 10 km. Borehole seismics, oriented fracture logs and cores have shown that the reservoir consists mostly of steep fractures

widened by dissolution. The fractured reservoir seems to be the result of the dissolution by meteoric water of tension fractures caused by tectonic uplift at the end of the Early Carboniferous. The karstification resulted in a pronounced morphology at the top of the Dinantian limestones below the Namurian shales.

Present status and future perspective of the use of geothermal energy

In the Hainaut basin, the St. Ghislain borehole produces geothermal energy for space and greenhouse heating and for the stimulation of gas generation from sludge in a water treatment plant. Geothermal water at a rate of about 650 000 m³/yr is used in a single borehole operation (singlet).

In Douvrain, geothermal water at a rate of 75 000 m³/yr (singlet) is used for air conditioning in a hospital. The use of the Ghlin borehole is still under study.

At Baudour, Dinantian water at about 50 °C, resurging through faults in an inclined shaft driven in Namurian shales, was used early in this century for heating the buildings of the "Radio Institut de Baudour". The Institute used the water for therapeutic purposes, but exists no longer.

In the Campine area, at Merksplas-Beerse, a doublet exploitation was planned with the aim of production from the Dinantian and reinjection into the shallower chalk. However, due to the low energy prices, the project has been stopped. The doublet exists.

At Turnhout a swimming pool and its building are heated geothermally, while at Herentals an open-air swimming pool is served in the summer. Near Dessel a small fish farm is in operation. The use of the Meerborehole is technically possible but no project has been implemented yet.

The Oostende and Gent boreholes have tapped an artesian aquifer at the top of the fissured Caledonian Brabant Massif overlain by Late Cretaceous chalks.

Summary of geothermal resources

Location	Area (km ²)	Geothermal Resources (H ₁ in 10 ¹⁸ J)
Dinantian (Hainaut)	373	2,9
Dinantian (Campine)	2096	4,45
Dinantian (Liège)	113	0,0185
Triassic Buntsandstein (Campine)	530	5,08
Tuffeau Chalk (Campine)	2155	1,77
Neeroeteren Sandstone (Campine)	52	0,123

The results presented here are based on investigations of VANDENBERGHE and FOCK (1989) and VANDENBERGHE (1991).

Under the present energy prices, the only development in the use of geothermal energy are large capacity heat pumps for industrial purposes rather than for domestic heating. Energy prices will need to increase substantially before new installations are considered

Acknowledgments

The help of the staff of the Belgian Geological Survey in collecting the data is greatly acknowledged. The author also thanks the Directors of the Belgian Geological Survey for permission to publish the data.

References

- Belgische Geologische Dienst, Ministerie Economische Zaken, Brussel, Archieven.
- Legrand, R., 1975: Jalons géothermiques. - Mém. Expl. Cartes Géol. et Minières de la Belgique, n 16, 46 p., 3 figures and 9 plates.
- Vandenberghe, N., 1991: Belgium. - In: Geothermal Atlas of Europe (Eds.: Hurtig, E., Cermák, V., Haenel, R. and Zui, V.), Hermann Haack Verlagsgesellschaft, Gotha, Germany, p. 14-15.
- Vandenberghe, N. and Fock, W., 1989: Temperature data in the subsurface of Belgium. - Tectonophysics, 164 (1989), p. 237-250.
- Verkeyn, M., 1995: Bepaling van de warmtestroomdichtheid in België. Een verkenning naar de mogelijkheden en de beperkingen - Diploma-Thesis, Katholieke Universiteit Leuven, Leuven, Belgium.

BULGARIA

Geothermal thematic map (Plate 10)

K. Shterev and I. Zagortchev

The territory of Bulgaria is a geological mosaic of pre-Alpine tectonic units included in the Alpine orogen at the southern margin of the Eurasian plate. The pre-Alpine and Alpine tectonic units are made up of features of Late Triassic, Middle Cretaceous, Late Cretaceous, Palaeogene and earliest Neogene age. They exhibit considerable lithologic, magmatic and geodynamic contrasts. The southern margin of Eurasia (BOYANOV et al., 1989) includes from N to S: the southern half of the Moesian platform; the Fore-Balkan Zone and the Balkan (Stara-Planina) fold belt (both with dominant Palaeogene and early Neogene deformations); the Srednogorie Zone (a Late Cretaceous volcanic island arc with associated troughs, in some stages considered also as a rift zone); the Morava-Rhodope Zone comprising the Middle Cretaceous autochthonous to para-autochthonous Rhodope Superunit (Massif), the Struma (Tran-Vlahina) Superunit, the allochthonous Morava (Penkyovtsi-Eleshnitsa) Superunit and the Ograzhden Unit (Serbo-Macedonian Massif). During the Palaeogene, the Srednogorie and the Morava-Rhodope zones were deeply affected by orogeny and intense igneous activity. In Middle-Late Neogene and Quaternary times, rifting occurred along fault belts and the crests of neotectonic swells. Thick Neogene terrigenous deposits filled the resulting graben structures.

More than 100 structures bearing thermal waters have been found in southern and partly northern Bulgaria (Galabov and Shterev, 1990). These aquifers host meteoric thermal waters with a low content of dissolved solids (0.1 - 1.5 g/l) and temperatures ranging from 25 - 30 °C up to 100 - 120 °C. The total output of these reservoirs is estimated to be 13 - 14 m³/s containing 1500 MW_t to 1800 MW_t of thermal energy.

Generally, each of about 150 geothermal systems is situated in one of the following settings:

- 1) Regional artesian aquifers developed in the deeper stratigraphic levels of the Moesian platform and the Fore-Balkan.
- 2) Restricted layered reservoirs in fragmentary Mesozoic carbonate bodies in the Balkan (Stara-planina) belt and the Srednogorie Zone, and subordinately, in the Precambrian Rhodopian marbles.
- 3) Fault and joint hosted geothermal systems in granitoid and metamorphic terrains of the Srednogorie Zone and the Rhodope.
- 4) Geothermal systems developed in joints and dykes in Late Cretaceous (Srednogorie) and Palaeogene (Rhodope) volcano-tectonic structures.
- 5) Tertiary (usually Neogene - Quaternary) grabens with terrigenous geothermal reservoirs superposed to structures of the previous four types. These geothermal systems usually are made up of several levels, the uppermost Tertiary layered reservoirs often being recipients of thermal waters originated in the granitoid-metamorphic, volcanogenic, or carbonate basement of the grabens.

The geothermal resources of North Bulgaria (Moesian platform and Fore-Balkan) are represented mainly by saline thermal waters and brines with reservoir temperatures between 30 - 40 °C and 130 - 140 °C. The principal geothermal reservoirs comprise three regional carbonate aquifers of Devonian-Carboniferous, Triassic and Malm-Valanginian ages, respectively (SHTEREV and PENEV, 1991).

Temperatures (Plate 10)

P. Petrov, K. Bojadgieva and S. Gasharov

The temperature maps (500 m, 1000 m and 2000 m) published by BOJADGIEVA et al. (1991) have been updated for the present publication. Most temperature data were obtained from exploration drilling for oil, gas, coal, ore and water. Measurements were made in about 450 boreholes. Temperatures in 500 m depth increase from the NE to the S and SW.

Potential geothermal reservoirs

K. Shterev, P. Bokov, I. Zagortchev, D. Shterev and R. Ivaviov

Regional reservoirs in carbonate aquifers of the Moesian platform and the Fore-Balkan

Devonian-Carboniferous (Givetian-Tournaisian) aquifer

This is the deepest and least studied geothermal reservoir in the Moesian platform. It extends probably over the most of the platform, yet its great depth (2500 - 6000 m) excludes it for the time being from

commercialisation. It consists of a thick (up to 1500 - 1800 m) sequence of limestones and dolomites probably permeable at some levels due to secondary dolomitization and karstification. Drilling on the banks of the Danube at the village of Gomotartsi (NW of Vidin) and near Shumen reached permeable and productive levels. Both these findings and lithostratigraphic regularities suggest this aquifer accumulates large volumes of hot saline waters and brines with temperatures of 50 °C up to 140 - 150 °C.

Middle - Late Triassic aquifer

This carbonate complex is widespread and well studied with respect to areal distribution, lithostratigraphy and structural features. However, the hydrologic and geothermal characteristics are less well known. Limestones and dolomites of Anisian to Carnian age (Doyrentsi Formation) form a potential reservoir of thermal brines with temperatures between 40 °C and 130 - 140 °C. This aquifer is situated at depths between 1500 m and 4000 - 5000 m. Its thickness varies between 100 - 200 m and 500 - 800 m. Although the reservoir extends over 12 000 km², the region fulfilling commercial requirements is by far more restricted.

Malm-Valanginian aquifer.

The Malm-Valanginian aquifer is, at present, the best studied and most important geothermal reservoir in Bulgaria. The productive area of the reservoir extends over 11 000 km² at depths between 800 m and 2500 - 3000 m. Geothermal resources of the order of 74×10^{18} J are distributed over five regions (Vidin, Vratsa, Pleven and the Black Sea coast). Along the Black Sea coast and the southwestern slope of the North-Bulgarian Swell, the aquifer contains low-mineralised meteoric water with temperatures of 25 - 65 °C at constant recharge and production rates. In the western Moesian platform and the Fore-Balkan, three areas with saline thermal waters and temperatures between 40 °C and 90 - 100 °C are outlined.

Geothermal systems of meteoric thermal waters in South Bulgaria

The geothermal systems of this group are found, identified, or inferred exclusively in South Bulgaria and in some structures of the Stara-Planina (Balkan) fold belt. They occur in the settings 2, 3, 4 and 5 described above.

Fracture hosted (faults, joints or dikes) aquifer systems in granitic-metamorphic or volcanic terrains are important geothermal reservoirs in Bulgaria. In these regions, geothermal gradients of 35 - 40 °C/km and heat-flow density of 60 - 90 mW/m² were measured. These fracture hosted geothermal systems occur in the Rhodope Massif and the Srednogorie Zone (SHTEREV, 1988). They occupy an area of tens to hundreds of square kilometres reaching depths of 500 m to 3000 - 3500 m below the erosional baseline. An area of 1 km² of such a system produces at depth between 0.1 l/s and 0.3 - 0.4 l/s thermal water with 20 - 70 kW_t geothermal energy. The geothermal water output of the system at the surface is distributed among unconnected discharge zones with flow rates of 5 - 10 l/s up to 80 - 100 l/s.

Geothermal System of the Struma Rift Valley

The Struma geothermal system (SHTEREV et al., 1995) embraces the granitic-metamorphic basement and the Neogene filling of a NW - SE trending rift valley (Struma rift valley or Struma graben complex) that continues further S into Greece (ZAGORCHEV, 1992). Extensive movements in Neogene and Quaternary times with large vertical displacements (up to 3.5 km) stimulated deep mobilisation and circulation of meteoric water charged at depth with geothermal energy. About 235 l/s are captured by natural springs and boreholes, the highest temperatures reaching 80 - 100 °C. The geothermal potential in the Bulgarian part of the valley is supposedly distributed among 40 hydrogeothermal occurrences. Only half of them are characterized by chemical thermometry, geochemical and geostructural information. The total geothermal production of all exposed or potential occurrences in the basement and borders of the valley are estimated at 950 l/s thermal water and 236 MW_t thermal energy. Most of the reservoirs are hosted in fault/joint systems. Porous reservoirs of thermal waters were drilled in the Neogene deposits of the southernmost (Sandanski) graben. Some of these reservoirs are secondary recipients of thermal waters ascending from the basement.

Sofia Geothermal Basin (Plate 10)

K. Shterev and I. Zagorchev

The Sofia basin lies on the Mesozoic and pre-Mesozoic basement of the Sofia Neogene graben within the basal sandstone and gravel formation

(aquifer) of Miocene age. Thermal water is extracted from a Late Cretaceous volcanogenic-sedimentary formation as well as from fragmentary bodies of Triassic and Late Jurassic limestones and dolomites. Vertical movement of thermal water across different stratigraphic levels and reservoirs is associated with active (neotectonic) fault structures, lithofacies windows and volcanic and intrusive igneous bodies. This convective effect can be observed on the temperature field.

The geothermal activity in the Sofia basin is expressed by a multitude of natural springs and drilled thermal sources, some of them in the central part of Sofia. Most of thermal water is meteoric with very low contents of dissolved solids. The depth of circulation controls the temperature ranging from 30 - 40 °C up to 60 - 80 °C. A considerable area in the N of the basin contains thermal water with greater HCO₃ and SO₄ mineralization (2 - 5 g/l).

At present estimates of the geothermal potential of the basin are very approximate. It yields 360 l/s thermal water and 45 MW_t thermal energy. Possibilities for doublet exploitation of some Triassic carbonate reservoirs and of the Neogene aquifer are soon to be explored and evaluated.

Malm-Valanginian (Danube) (Plate 11)

K. Shterev, P. Bokov, N. Kostova, K. Bojadgieva, M. Vakarelska and D. Shterev

This part of the reservoir consists of three geothermal areas well specified both in area, facies and stratigraphy: Pleven, Vidin and Vratsa.

The Pleven area (NE) is the largest and most important Bulgarian geothermal project in the next decade. It is situated between the Danube, the Stara-Planina range, between 24° E and 26° E, extending further E, as can be seen on the national map of geothermal resources (Plate 10). The reservoir has a total thickness of 800 - 1200 m. Temperature and salinity increase uniformly from NE - SW, reflecting the increase in depth and thickness along this direction. In the NE fresh waters recharge the aquifer. Data on temperature, porosity and permeability of the reservoir are still insufficient and qualitative. The great yield of many tested boreholes indicate a high permeability for almost all lithostratigraphic levels of the reservoir that contain cavernous secondary dolomites and dolomitic limestones. The Drinovo Formation (up to 600 m thick) is particularly favourable. According to preliminary estimations, a doublet in the Pleven area may produce between 40 - 80 l/s and 140 - 190 l/s thermal water and 10 MW_t to 20 - 30 MW_t thermal energy. The piezometric level of the reservoir reaches and even exceeds ground level near the Danube riverbank. In the higher southern areas, it is at 50 m to 150 - 200 m beneath the surface. The geothermal resources add up to 59×10^{18} J in this region.

The Vidin area (NW) is poorly known. The estimations and characteristics presented on the maps are approximate and based mainly on suppositions and prognoses. The depth to the aquifer is estimated to vary from 300 - 1300 m from N - S, with a thickness of about 900 m. The highest temperatures are expected to be about 60 °C. Extraction and use of geothermal energy along the Danube riverbank would have to deal with the technical problems caused by high salinity (up to 60 g/l) and high HS content. The piezometric level of the reservoir along the Danube riverbank is between 5 - 15 m (a.g.l.). The estimate of geothermal resources here is 5.9×10^{18} J. Projects with balneological and geothermal purposes are in preparation.

The Vratsa area (S) is almost unstudied. The geothermal resources are quite large (4.7×10^{18} J) considering the size of the region. However, the reservoir is situated at a great depth (1000 - 2100 m), has high temperatures (50 - 90 °C), but other features are unknown. Its continuation to the E is also unclear.

Malm-Valanginian (Black Sea - Varna) (Plate 12)

K. Shterev, I. Stefanov, M. Galabov, P. Bokov and D. Shterev

The Black Sea portion of the Malm-Valanginian reservoir is part of an artesian basin with very active hydrodynamics. The transmissivity of the aquifer increases from S - N from 0.02 - 0.14 m²/s (representing a transmissibility of 1300 - 10 500 Dm). With the exception of a coastal area around Shabla-Tyulenovo, the aquifer contains fresh cold and thermal water of constant yield. The total artesian flow in the thermal and coastal part of the basin is estimated at about 3.45 m³/s, with 1.2 m³/s being captured in flowing boreholes at depths of 800 - 1800 m. Despite the great depth of the reservoir, temperatures are not high (< 65 °C) due to convective cooling and heat transport to natural discharge areas into the Black Sea. This cooling explains the low geothermal gradient as well as the inaccuracies in the determination of the unperturbed (conductive) heat-flow density in this area. As a

consequence geothermal resources are low, adding up to 2.9×10^{18} J.

In addition to assessing the geothermal resources based upon a doublet heat extraction model, as presented in the resources map, an estimate of the thermal energy output was made using the natural artesian flow rate. This estimation given in the table on the resources map assumes the artesian flow is captured by a linear system of wells along the littoral section, where temperatures are highest. Such an exploitation model respects the natural recharge regime of the system. This method is applied to several operating geothermal installations in Varna and the coastal tourist centres N of this town.

Present status and future perspective of the use of geothermal energy

K. Shterev

The use of thermal water for heating mineral baths and public buildings is known in Bulgaria since the Greco-Roman epoch. Today, geothermal energy is used for local heating, hot-water supply, swimming pools and other applications in about 30 balneological and tourist centres, towns, industrial and greenhouse enterprises (BOJADGIEVA et al, 1995). The total power of the presently operating heating systems is 140 MW_t. Approximately the same power is planned for forthcoming projects. Even after the completion of these projects, the geothermal energy in use will represent only a small fraction of the geothermal potential of the areas studied, as shown in the next tables.

Geothermal resources in Bulgaria (doublet model)

Aquifer	Surface (km ²)	ARB ₃ (x 10 ¹⁸ J)	Heat in Place H ₀ (x 10 ¹⁸ J)	Resources H ₁ (x 10 ¹⁸ J)
Malm-Valanginian				
A. Danube				
Pleven area	7 000	1 800	245	59.15
East prolongation	600	136	11	1.50
Vidin area	1 290	333	24	5.90
Vratsa area	478	128	20	4.74
B. Black Sea (Varna)	1 222	269	21	2.86
Total	10 590	2 666	321	74.15

Available thermal power of other potential areas

Basin	Mean water temperature (°C)	Yield (l/s)	Thermal power (MW _t)
Varna	35	3450	289
Sofia	46	360	45
Struma rift valley	73	1010	243
Total		4820	577

The low prices of crude oil inhibited for a long time the use of geothermal energy in Bulgaria. In spite of investment and technology difficulties, the exploration of the geothermal potential of this country continued with the completion of a few important drilling projects.

As soon as the difficulties associated with the transition to market economy, the establishment of free enterprise, and the restitution of private property are overcome, high commercial interest is expected in the hydrogeothermal potential of the Black Sea and Danube (Pleven) areas of the Malm-Valanginian reservoir. In the Black Sea area, the priority will belong to geothermal projects for heating and air-conditioning of tourist centres and buildings (hotels etc.). In the Danube region, large-scale projects for geothermal greenhouses in combination with aquaculture farms and enterprises for dried fruits and vegetables will be initiated. The large occurrences of thermal waters in the Rhodope region (Velinograd, Dolna Banya, Razlog area) will cover the needs of balneological and tourist centres.

References

- Bojadgieva, K., Hristov, H. and Hristov, V., 1995: Geothermal energy utilization in Bulgaria within the period 1990-1994. - Proc. World Geothermal Congress 1995, Florence, Italy, 18-31 May 1995, vol 1, p. 57-61.
- Bojadgieva, K., Petrov, P., Gasharov, S. and Velinov, T., 1991: Bulgaria. - In: Geothermal Atlas of Europe (Eds.: Hurtig, E., Čermák, V., Haenel, R. and Zui, V.), Hermann Haack Verlagsgesellschaft, Gotha, Germany, p. 16-17.
- Boyanov, I., Dabovski, C., Gocev, P., Kostadinov, V., Tzankov, Tz. and Zagorchev, I., 1989: A new view on the Alpine evolution of Bulgaria. - Geologica Rhodopica (Sofia), 1, p. 107-121.
- Shterev, K. 1988: Captage moderne et exploitation flexible des gisements hydrothermaux en terrains granitiques et metamorphiques. Actes du XXI^{ème} Congrès International des Techniques Hydrothermales, Evian; p. 17-33.
- Shterev, K. and Penev, I. 1991: Overview of geothermal resources and activities in Bulgaria. - Geothermics, 20; p. 91-98.
- Shterev, K., Zagorchev, I. and Shterev, D. 1995: Geothermal resources and systems in the Struma (Strymon) rift valley (Bulgaria and Greece). - Proc. World Geothermal Congress 1995, Florence, Italy, 18-31 May 1995, vol 2, p. 1185-1191.

Zagorchev, I. 1992: Neotectonics of the central parts of the Balkan Peninsula: basic features and concepts. - Geologische Rundschau, 81, 3; p. 635-654.

CZECH REPUBLIC

V. Myslíl, J. Burda, J. Franců and M. Stibitz

Geothermal thematic map (Plate 13)

The Bohemian Massif and the Carpathian System are the two main tectonic units in the Czech territory.

The Bohemian Massif is an old consolidated basement formed by Proterozoic and Paleozoic crystalline rocks that occupies most of the country. These rocks have been affected by the Variscan, Hercinian and Alpine orogenies, which caused extensive block faulting and folding. This basement is overlain by several sedimentary basins of Paleozoic, Cretaceous and Neogene age.

In the N, the elongate Cretaceous Basin overlies the Bohemian Massif. It is filled with Permo-Carboniferous and Mesozoic sediments. In the NW, the Krušné Hory rift is filled with Neogene deposits. Here is situated the North Bohemian Basin, one of the largest Tertiary basins in the rift.

In the SW, the West Carpathians are part of the Alpine-Carpathian orogen. They consist of nappes containing rocks of Precambrian - Tertiary age and can be divided into several elongate zones, one of which is of interest here: the Carpathian Foredeep. This structure is filled with sediments a few 100 m to > 6000 m thick. The depth of the basin increases to the SW, towards the Vienna Basin. The Tertiary sedimentary deposits overlie a basement made up of Devonian carbonates and granitic rocks.

Thermal springs have traditionally been used for balneological purposes. The warmest spring, in Karlovy Vary, has a temperature of 72 °C. It is situated in the Krušné Hory rift. The 12 hot springs occur at the intersection of 3 fault systems and yield together 40 l/s with a salinity of 6 g/l. The mineral water is Na-HCO₃-SO₄-Cl type. Other spas are also situated in this rift: Teplice (25 l/s) and Jáchymov. The spring of Jánské Lázně lies on the S border of the Krkonoše granite massif. The springs of Teplice nad Bečvou (16 l/s), Velké Losiny (15 l/s) and Bludov Lázně (7 l/s) are located in Moravia.

Temperatures (Plate 13)

Temperature measurements exist in 498 boreholes. Heat-flow density values have been determined at 200 sites. The heat-flow density and subsurface temperatures are lower in the Bohemian Massif than in the Cretaceous Basin, the Krušné Hory rift (North Bohemian Basin) and the Carpathian Foredeep. This fact is related to differences in crustal thickness (ČERMÁK et al., 1991).

Potential geothermal areas

For the assessment of geothermal resources in the Czech territory, a reinjection temperature of 10 °C was used.

North Bohemian Tertiary Basin (Plate 13)

This basin extends between the Krušné Hory and České Středoohoří mountains. Rifting of the metamorphic and granitic basement led to the formation of several basins. The North Bohemian one is the largest Tertiary basin with an area of about 800 km² and a major axis directed roughly SW-NE. Its greatest depth occurs between Teplice and Most, where the Tertiary deposits are 200 - 250 m thick. These deposits are made of basal sands followed by coal seams and impermeable clays containing layers of fine sandstone of variable thickness. Some of these sandy layers form confined aquifers of up to 50 m thickness. The salinity of the water is up to 2 g/l and specific flow rates vary from 1- 10 (m³/h)/m.

Bohemian Cretaceous Basin (Plate 14)

The Bohemian Cretaceous Basin is filled with Permo-Carboniferous and Cretaceous sediments. At the base, fine sandstones and small lenses

of clays and coal were laid down in the Cenomanian. Thereupon, Lower Turonian marls, Middle Turonian sandstones and Senonian fine clayey sandstones followed. The Turonian and Cenomanian sandstones form a confined aquifer with a mean thickness of 100 m. The deepest strata are found to the W of the basin's axis. The E part of the basin is of less geothermal interest. Two zones of geothermal interest were identified in the basin: Ústí-Děčín, where the sediments attain their maximum thickness, and Mělník-Saný, located on the junction of three regional fault systems. The aquifer fluid has a temperature from 32 - 42 °C and low salinity (up to 2 g/l). In Ústí-Děčín, an output of 200 l/s is predicted to be possible, while at Mělník-Saný conditions are not so favorable because of a reduced thickness and lower permeability.

Carpathian Foredeep, Neogene (Plate 14)

The W Carpathian nappe structure is part of the Alpine orogen that borders the SE part of the Bohemian Massif. On the boundary between these two tectonic units a narrow foredeep basin developed. This basin is connected to the S with the Vienna Basin extending into Austria. The high heat-flow density measured in this area is associated to a thinner crust underneath the contact zone of the Carpathians and the Bohemian Massif.

The main aquifer is confined and is situated at the base of the Tertiary sediments and in Devonian limestones and conglomerates. Hydrogeological information is limited as the main focus of the studies in this region is related to petroleum and gas exploration. The porosity of the Tertiary deposits is < 15 % and artesian conditions cause an outflow of 10 l/s at some boreholes. Salinity is > 30 g/l.

Present status and future perspective of the use of geothermal energy

In addition to balneologic use, low enthalpy applications comprise domestic and swimming pool heating and the use in industrial processes in small companies. More than 1000 heat pumps are installed at present. Recently, 100 heat pumps with a capacity of 2 MW were put in place.

The energy output of geothermal installations used for domestic heating is < 20 kW, while for hotels, swimming pools and small businesses, the output ranges 20 - 100 kW. Three water treatment plants use heat pumps with a capacity of > 100 kW each. A heat pump of 1 MW operates in the Prokop mine in the Příbram ore mining district. Here, warm water (28°C) is pumped up at a rate of 10 l/s. At a temperature gradient of 10 °C, the heat pump increases the water temperature to 65 °C. Heat pumps of smaller capacities are also in use in Krasna Hora and Zadni Chodov and the possibility of installing geothermal heat pumps for the mines of Ostrava and Chomutov is being investigated. Thermal water from the Cretaceous aquifer is used for heating a swimming pool in Strekov and in soap factories in Ústí nad Labem. A prefeasibility study has been completed for district heating in the town of Breclav using 15 MW heat pumps. The integrated use of geothermal energy for spas, domestic heating, swimming pools and greenhouses is a project for Mušov and Písek (close to Jáchymov)

Summary of geothermal resources in the Czech Republic.

Region	Area (km ²)	Heat in Place H ₀ (x 10 ¹⁸ J)	Resources H ₁ (x 10 ¹⁸ J)
Bohemian Cretaceous Basin	12 062	107.60	33.9
N Bohemian Basin	787	4.14	1.3
W Carpathian Foredeep	6676	79.80	25.4
Total Czech Republic	79 530	177.30	55.20

References

Čermák, V., Král, M., Šafanda, J., Krešl, M., Kučerová, L., Kubik, J., Jánčí, J., Lizon, I., Marusiak, I. and Franko, O., 1991: Czechoslovakia - In: Geothermal Atlas of Europe (Eds.: Hurtig, E., Čermák, V., Haenel, R. and Zui, V.), Hermann Haack Verlagsgesellschaft, Gotha, Germany, p. 21-24.

DENMARK

B. Balling, J.M. Hvid, A. Mahler, J. J. Møller, A. Mathiesen, T. Bidstrup and L.H. Nielsen

Geothermal thematic map (Plate 15)

In the previous edition of the atlas, five reservoirs covering most part of the Danish onshore area were described. The updated maps on the three following reservoirs are presented: *Frederikshavn Member*, *Haldager Sand* and *Gassum Formation*. Maps of the *Skagerrak* and the *Bunter Sandstone* Formations are not included in this edition because the previous information and evaluation is still valid and their economic potential has been downgraded due to hypersaline conditions.

The reservoir properties have been derived from oil and gas well data and a few geothermal boreholes. Porosity and permeability evaluations are taken from well production tests, core analysis, and logs. Temperatures have been estimated from well measurements and thermal modeling. The mapping of the reservoirs is based on seismic and well data. Only reservoirs with temperatures of 25 °C and depths of 3000 m have been considered.

The subsurface structural framework of relevance for geothermal resources may be subdivided in the following major elements:

The Skagerrak - Kattegat Platform, which forms the SW part of the stable Precambrian and Palaeozoic Fennoscandian Craton.

The Sorgenfrei - Tornquist Zone, which forms a complex faulted border zone between the Fennoscandian Craton and the Danish Basin. The Danish Basin is the E part of the Norwegian-Danish Basin bounded to the S by the Ringkøbing-Fyn High.

The Ringkøbing-Fyn High is a Hercynian WE trending high. This system of highs separates the Danish Basin from the North German Basin to the south. This configuration is documented to exist since the Early Permian.

Additional information can be found in MICHELSEN and NIELSEN (1993) and the literature cited therein.

The borehole Thisted-2 is still the only geothermal installation in operation in Denmark today.

Temperatures (Plate 15)

Temperatures have been estimated from borehole measurements and thermal modeling. The one-dimensional steady state heat equation for a layered earth model is solved using a constant surface temperature of 8 °C and an uniform background heat-flow density of 67 mW/m² for the whole area. Each layer is assumed to have a constant thermal conductivity, and heat production rate is the same for all layers. Further information on the thermal regime in Denmark is presented in BALLING (1991) and NIELSEN et al. (1993).

Potential geothermal reservoirs

The geothermal resources of the three reservoirs mentioned above are assessed in the present atlas. All units occur in the Upper Triassic - Lower Cretaceous section of the Danish Basin including the Sorgenfrei-Tornquist Zone and the Skagerrak-Kattegat Platform. The rocks contain sandstones of sufficient thickness and quality to be regarded as reservoirs. Of these units only the *Gassum Formation* is present S of the Ringkøbing-Fyn High.

Frederikshavn Member (Plate 15)

The *Frederikshavn Member* was deposited in Volgian-Valanginian times. It shows large variation in thickness (75 - 225 m) and depth (500 - 1800 m) partly controlled by local faults and salt-structures.

In the northern and easternmost parts of Jylland the formation consists primarily of marine siltstones and mudstones interbedded with shallow marine sandstones with good reservoir qualities. Here temperatures are 35 - 45 °C, and net sand thickness reaches up to 70 m. Transmissibilities are unknown but may be relatively high due to the shallow burial depth.

Toward the W and S, the number and thickness of sandstone layers

rapidly decreases. Here, the formation becomes dominated by offshore mudstones, and is not regarded as a potential geothermal reservoir.

Haldager Sand (Plate 16)

The Haldager Sand was formed in Aalenian-Callovian times, and consists of sandstones interbedded with thin mudstones. The thickness of the formation is strongly influenced by contemporaneous movements on faults and salt-structures. In the Sorgenfrei-Tornquist Zone at depths of 1500 m the net thickness generally is between 25 - 50 m with a maximum of 150 m N of the city of Ålborg. In this area temperatures are calculated to be 40 - 60 °C, and transmissibilities may be in the order of 10 - 20 Dm.

Gassum Formation (Plate 16)

The Gassum Formation was deposited during Rhaetian - Early Sinemurian times and shows a stepwise younging toward the NE. The formation is dominated by interbedded shallow marine shoreface sandstones, offshore marine and lagoonal heteroliths and mudstones, and lacustrine claystones and coal seams. Maximum net thickness of > 100 m is found in the Sorgenfrei-Tornquist Zone in the area around the city of Ålborg. In this area the formation is shallower than 2000 m. Transmissibilities of up to 100 Dm and temperatures between 40 - 70 °C may be found. Similar conditions exist over mid-Sjælland (Zealand) and in areas above salt structures in the Danish Basin. Below 2000 m, the permeability decreases rapidly, and in the central part of the Danish Basin transmissibilities of 0.5 - 5 Dm are expected. This reservoir feeds the Thirsted geothermal installation.

Present status and future perspective of the use of geothermal energy

Geothermal reservoirs of interest in Denmark cluster along the Sorgenfrei-Tornquist Zone. Neither volcanic activity nor hot springs occur. However warm geothermal water has a potential for district heating. The geothermal resources exceed the energy needed for heating in Denmark for hundreds of years. The ongoing establishment of large combined heat and power plants in Danish towns does however reduce the demand for heat and thus delay further geothermal development.

At present only one geothermal pilot plant is operating in Denmark. The plant is installed at Thisted, and has now been running for 12 years. It has a capacity of 3 MW, extracted from 46 °C, 15 % saline geothermal water. The geothermal water is produced from the Gassum Formation with a transmissibility of 100 Dm and is later reinjected back into the same formation at a depth of 1200 m. The production has been limited to between 35 000 - 48 000 GJ/a due to the reduced heat demand as a consequence of the existing heat and power plant in the town.

References

- Balling, N., 1991: Denmark. - In: Geothermal Atlas of Europe (Eds.: Hurtig E., Čermák, V., Haenel, R., and Zui, V.), Hermann Haack Verlagsgesellschaft mbH, Geographisch-Kartographische Anstalt Gotha, Germany, p. 25-28.
- Michelsen, O. and Nielsen, L.H. 1993: Structural development of the Fennoscandian Border Zone, offshore Denmark. - *Marine and Petroleum Geology*, Vol. 10, p. 124-134.
- Nielsen, S. B., Balling, N. and Christiansen, H. S., 1993: Formation temperatures determined from stochastic inversion of borehole observations. - *Geophys. J. Int.*, 101, p. 581-590.

ESTONIA

A. Jõeht

Geothermal thematic map (Plate 17)

Estonia is situated on the southern slope of the Baltic Shield, which displays generally low heat-flow density (URBAN et al., 1991; JÕELEHT and KUKKONEN, 1996), such as the Baltic shield itself (BALLING, 1995; ČERMÁK et al., 1993). The thickness of the Phanerozoic sedimentary rocks that cover the Early Proterozoic basement, increases from 150 m in the N to 600 - 700 m in the S (see map of temperature at the top of the basement). This sedimentary cover is made up of rocks of Vendian, Cambrian, Ordovician, Silurian and Devonian age. Aquifers in Cambrian and Vendian sandstones are the most interesting for geothermal energy applications. Due to the low heat-flow density from the Precambrian basement and the small thickness of sedimentary rocks, the groundwater temperature in the Phanerozoic aquifers is 15 °C. Such conditions imply diminute geothermal resources precluding the use of classical geothermal applications (e.g. doublet systems). However, these formations are adequate for producing geothermal energy for space heating with heat exchangers.

Temperatures and heat-flow density (Plate 17)

The temperature maps are based upon data from JURIMA and ERG (1984) as well as JÕELEHT and KUKKONEN (1996). Only data from boreholes that are deeper than 67 % of the reference depth of the map were included.

In northern Estonia, the higher temperatures at depths of 250 m and 500 m (11 °C and 14 °C, respectively) are attributed to the thermal blanketing effect caused by the low thermal conductivity of the Lower Cambrian clays (about 1.3 W/(m.k), which are about 100 m thick. In southern Estonia, the increased temperatures at the top of the basement correlate with greater depth to the basement. Here the basement lies deeper than in northern Estonia.

The heat-flow density data was assembled from URBAN et al. (1991) and JÕELEHT and KUKKONEN (1996). URBAN et al. (1991) do not report details on the corrections applied to their data. This data is included as apparent heat-flow density. The heat-flow density in Estonia ranges from 22 - 62 mW/m², with a mean value of 35 mW/m².

Palaeoclimatic corrections to the geothermal gradient were calculated using homogeneous half-space models. The ground surface temperature history applied to the corrections is described in detail in JÕELEHT and KUKKONEN (1996). The greatest temperature perturbations (up to 3 °C) occurring at depths of 1500 m are the thermal signal of past glaciations. The heat-flow density corrected for palaeoclimatic effects ranges between 28 - 68 mW/m² with a mean value of 42 mW/m². While the magnitude of the correction is significant, the geographic pattern of heat-flow density is not much affected.

Radiogenic heat production rate (Plate 17)

The Estonian Precambrian basement consists of metamorphic rocks of amphibolite and granulite facies (HÖLTTÄ and KLEIN, 1991). In general, the mean radiogenic heat production rate decreases with increasing metamorphic grade from 3.23 µW/m³ (amphibolite facies) to 1.26 µW/m³ (granulite facies). Granulite facies rocks that suffered retrograde overprint under amphibolite facies conditions have intermediate values with a mean of 2.09 µW/m³ (KUKKONEN and JÕELEHT, 1996; JÕELEHT and KUKKONEN, 1998).

Geothermal potential and hydrological conditions

In earlier investigations, temperature measurements were taken in boreholes 250 - 350 m deep. At depths > 150 m, readings were made at 50 m intervals. This procedure does not necessarily allow hydrologic disturbances to the temperature log to be identified. However, numerical fluid and heat transfer simulations indicate that heat transfer by groundwater flow is not significant, although small disturbances at shallow depths may exist (KUKKONEN and JÕELEHT, 1996). These

disturbances affect heat-flow density by up to 10 mW/m² and are due to the high hydraulic permeability of the sedimentary rocks (up to 5 x 10⁻¹² m²). However, this hydrologic effect is constrained to depths of 200 m. In southern Estonia, the hydraulic gradient is greater (up to 0.02 km/m) because of greater topographic variations, possibly affecting heat-flow density to a greater degree. Therefore, in the heat-flow density maps only data from boreholes deeper than 200 m were used.

URBAN et al. (1991) reported a low heat-flow density area (< 10 mW/m²) in central Estonia. It was based on measurements made in boreholes, which are located in the vicinity of major fracture zones striking NE-SW and NW-SE. These fracture zones are up to 10 km wide and consist, in detail, of many smaller fractures zones. The increased permeability creates local groundwater recharge systems and downward flowing water may produce heat-flow density minima at these shallow depths (down to 250 m). Moreover, some of the boreholes for which heat-flow density values have been reported, are visibly disturbed by water flow within the borehole itself.

The small thickness of the sediment cover associated with the low heat-flow density are responsible for the lack of aquifers appropriate to geothermal energy applications. Space heating with shallow heat exchangers is possible in the Palaeozoic sedimentary formations. Geothermal energy is used for local heating in one installation near Tallinn, northern Estonia.

In NE Estonia, temperatures of about 30 °C are expected at depths of the order of 1 km. The origin of the increased heat-flow density in this region is not yet well understood. Since there is no thermally important regional groundwater flow system, this anomaly is more likely attributed to crustal heat sources in the basement. The Hot-Dry-Rock (HDR) technique for electric power generation is also not a viable option in Estonia. One could envision using the same principle as in HDR (i.e. drilling and enhancing permeability and reservoir capacity at depth with hydraulic stimulation) to create a fractured reservoir in the basement in order to obtain higher temperatures required for certain industrial and agricultural applications.

References

- Balling, N., 1995: Heat flow and thermal structure of the lithosphere across the Baltic Shield and northern Tornquist Zone. - *Tectonophysics*, 244, p. 13-50.
- Čermák, V., Balling, N., Kukkonen, I. and Zui, V., 1993: Heat flow in the Baltic shield - results of the lithospheric geothermal modelling. - *Precambrian Res.*, 64, p. 53-65.
- Hölttä, P. and Klein, V., 1991: PT-development of granulite facies rocks in southern Estonia. - *Geological Survey of Finland, Special Paper 12*, p. 37-47.
- Jöeleht, A., and Kukkonen, I., 1996: Heat flow in Estonia - Assessment of palaeoclimatic and hydrological effects. - *Geophysica*, 32, 3, p. 291-317.
- Jöeleht, A., and Kukkonen, I., 1998: Thermal properties of granulite facies rocks in the Precambrian basement of Finland and Estonia. - *Tectonophysics*, 291, p. 195-203.
- Jurima, M. and Erg, K., 1984: Geotemperaturnoe pole Estonia na melko mastanyh kartah. - *Geological Fund of Estonia, unpublished report in Russian, Tallinn*, 44 p.
- Kukkonen, I. and Jöeleht, A., 1996: Geothermal modelling of the lithosphere in the central Baltic Shield and its southern slope. - *Tectonophysics*, 255, p. 25-45.
- Urban, G., Tsybulia, L., Cozel, V. and Schmid, A., 1991: A geothermal characterization of the northern part of the Baltic Syncline. - *Proc. of the Estonian Academy of Sciences, Geology*, 40, p. 112-121 (in Russian).

FINLAND

I. Kukkonen

Geothermal thematic map (Plate 18)

Finland is a part of the Fennoscandian (or Baltic) Shield. The bedrock is of Archaean or Proterozoic age, and it is covered by a thin, usually 5 m thick layer of Quaternary glacial sediments. The lithosphere is cool and thick (150 - 200 km) and characterized by heat-flow density mostly below continental average (< 65 mW/m²). Topography is subdued and does not easily produce advective redistribution of geothermal heat by groundwater flow in the bedrock. Porosity of crystalline bedrock is low (< 1 %) and thus the water content is low as well. Prospects for producing electricity from hot dry or wet formations in Finland are not favorable. However, direct use of geothermal energy for heating purposes in family houses, agriculture and industry is a possibility.

Over 1000 vertical heat exchangers (VHE) have been installed in shallow boreholes all over the country. Most of these applications

produce space heating for single-family houses, but they include also space heating systems of small industrial buildings.

Accessible Resource Base

Because of the geological characteristics of Finland just described above, geothermal resources in a general sense, are represented as the Accessible Resource Base down to 7 km depth (ARB₇). The extraction of this heat will depend on the existence of fracture networks providing permeability and a reservoir large enough to permit exploitation during decades. Natural fractures are ubiquitous in crystalline rocks and their hydraulic performance can be enhanced by artificial hydraulic stimulation. In the case of insufficient fluid supply in the fractured reservoir, surficial water could be injected into the rock by one borehole and recuperated by another, as in the Hot Dry Rock (HDR) concept.

To the present there are no adequate procedures to evaluate geothermal resources for crystalline rock formations. Temperature and heat-flow density maps are still the main source of information. In addition to such maps, it is useful to show the depth at which a certain temperature threshold for a certain geothermal energy application is encountered in the subsurface.

Temperatures and heat-flow density

The values have been either taken directly from temperature logs or calculated by linear extrapolation. The extrapolated values were included in the maps only if the extrapolation depth did not exceed 50 % of the borehole depth. Extrapolated values are shown in brackets on the maps, and for sites with several boreholes the temperature range is given. Temperatures vary spatially in a similar fashion as heat-flow density, with the highest values generally in southern Finland. This can partly be attributed to the higher heat flow but also to higher mean annual temperatures in southern Finland. Mean annual ground surface temperatures vary from 6.0 - 2.0 °C from S across to N Finland.

Heat-flow density values are based on KUKKONEN and JÄRVIMÄKI (1991), references mentioned therein and unpublished data by the present author. The data set comprises temperature measurements in boreholes which range in depth from 125 - 1100 m, and thermal conductivity measurements of the corresponding core samples taken with the divided bar method. No palaeoclimatic correction was applied to the heat-flow density. If this correction were included, heat-flow density would increase by a few mW/m² only (KUKKONEN, 1987). Topographic corrections are not necessary. Heat-flow density correlates with the tectonic age, heat production and lithology of the sites. The lowest values are encountered in the Archaean and Early Proterozoic areas in eastern and northern Finland in granite gneiss areas and greenstone belts (13 - 30 mW/m²), whereas the higher values are related to Early Proterozoic late-kinematic and anorogenic granitoids in southern Finland (40 - 70 mW/m²) and Middle Proterozoic sedimentary formations on the Bothnian Bay coast (44 - 50 mW/m²). Arithmetic mean of heat-flow density is 37.0 mW/m² (46 sites, standard deviation 11.2 mW/m²).

Radiogenic heat production rate

Radiogenic heat production rate at the bedrock surface is based on uranium, thorium and potassium analyses of 1054 samples of glacial till, the basal Quaternary sediment cover on top of the Precambrian. Till is a mechanical disintegration product of the bedrock and its geochemistry is a reasonably good estimator of bedrock concentrations. The data and map preparation have been discussed in detail in the literature (KUKKONEN, 1989a, 1989b, 1993). A correlation exists between heat production rate and heat-flow density (KUKKONEN, 1989b; 1993):

$$Q = D \cdot A + Q_R$$

where Q is the measured heat flow density (mW/m²), A is heat production rate (mW/m³), D = 10.8 ± 2.6 km and Q_R = 15.8 ± 4.9 mW/m².

Depth to 40 °C and to 100 °C

In order to auxiliary geothermal resource assessment in crystalline rocks, it is useful to represent the depth at which certain temperatures can be reached, as the choice of geothermal energy applications is often constrained by a certain temperature range. The decision to invest in a specific geothermal application depends on economic considerations. The drilling represents a significant portion of the investment in a geothermal application, therefore, the depth to be drilled gives a first order estimate of the investment costs.

The depth to 40 °C varies from 2 - 3 km in Finland. The temperature of 100 °C is encountered at depths between 6 - 8 km.

Muhos formation (Plate 18)

One site which has anomalous temperatures at shallow depths is the unmetamorphosed Middle Proterozoic *Muhos* sedimentary formation in northern Finland, near the city of Oulu. The low conductivity sediments form an heat insulating layer, so that temperatures are 5 - 10 °C higher in the sedimentary rocks in comparison to the surrounding crystalline basement. The temperatures shown on the cross-section are based on a numerical conductive thermal model calibrated with temperature and conductivity measurements in a 1 km deep borehole (at Liminka) and gravity models of the basin structure. The *Muhos formation* may have potential for applications using the HDR concept, i.e. drilling and applying hydraulic stimulation in order to enhance the reservoir permeability.

Present status and future perspective of the use geothermal energy

In Finland temperatures are slightly above, but usually below 20 °C at 1 km depth. For conventional geothermal applications, the temperatures should preferably be higher than 40 °C at depths of 1 - 1.5 km. Prospecting for such temperatures should be directed to the high heat production granitoids in southern Finland. Here, thermal models suggest that 40 °C temperatures would be encountered at depths between 2 - 3 km. In order to exploit this potential in such fractured systems, it is probable that HDR technology would be needed.

Small-scale direct use of geothermal heat, such as VHE, is the most promising application for geothermal energy utilization in the conditions prevailing in Finland. Borehole depths range from 120 - 200 m, and heat power output is typically of the order of 50 W/m (power output per drilled metre). The total number of VHE applications in use is not known exactly, but it is estimated to be between 50 - 100. The applicability of VHE technology is mainly controlled by the shallow subsurface temperatures, and these are highest in southern Finland.

References

- Kukkonen, I., 1987: Vertical variation of apparent and palaeoclimatically corrected heat flow densities in the central Baltic Shield. - *J. Geodynamics*, 8, p. 33-53.
- Kukkonen, I., 1989a: Terrestrial heat flow in Finland, the central Fennoscandian Shield. - Geological Survey of Finland, Nuclear Waste Disposal Research, Report YST-68, 99 p.
- Kukkonen, I., 1989b: Terrestrial heat flow and radiogenic heat production in Finland, the central Baltic Shield. - In: V. Cermák, L. Rybach and E.R. Decker (Eds.), *Heat Flow and Lithosphere Structure*. - *Tectonophysics*, 164, p. 219-230.
- Kukkonen, I.T., 1993: Heat flow map of northern and central parts of the Fennoscandian Shield based on geochemical surveys of heat producing elements. - *Tectonophysics*, 225, p. 3-13.
- Kukkonen, I.T. and Järvinmäki, P., 1991: Finland. - In: *Geothermal Atlas of Europe* (Eds.: Hurtig, E., Čermák V., Haenel, R. and Zui, V.), Hermann Haack, Gotha, p. 29.

FRANCE

F. Jaudin, I. Ignatiadis, A. Menjoz, J. Lemale and A. Gerard

Geothermal thematic map (Plate 19)

The surveys carried out and boreholes drilled since the previous atlas have provided only local modifications of the information presented in the previous atlas. Hence, a revised edition of the maps is not justified. This explanatory text summarizes and updates the information on the uses of geothermal energy in the Aquitaine and Paris basins and describes in more detail the recent experience in managing the geothermal resources of the Paris Basin. Information on general geothermal aspects of France can be found in LUCAZEAU et al. (1991) and the references therein.

The low-enthalpy resources of France are contained in aquifers of the major sedimentary basins, i.e. the Northern Basin, Paris Basin, Upper Rhine Graben, Aquitaine Basin, the Limagne and Bresse regions, the Rhone Corridor and the Mediterranean region. These resources are shown in the previous atlas where 25 exploited or potential geothermal reservoirs are described.

In 1995, France counted > 60 active geothermal energy operations: 41 in the Paris Basin (38 doublets), 14 in the Aquitaine Basin, 7 in other regions. Geothermal operations now provide heating for > 200 000 dwellings in France. Although most geothermal heat is fed to urban heating networks, it is also used for agriculture (greenhouses) and fish farming. It represents an overall saving of more than 230 000 TOE/a and comprises a total installed power of > 400 MW_{th}.

The conditions for extraction of geothermal energy in the Paris and Aquitaine basins are different.

Aquitaine Basin

The geothermal energy of the Aquitaine Basin is extracted mainly by single boreholes. The static water levels of the aquifers vary from < 100 m depth (negative head) to a positive artesian head of about 30 m. All types of pumping systems are applied: surface pumps for artesian exploitation and submersible pumps driven either by surface or submerged motors (constant or variable speed).

The largest geothermal installations tap the Cretaceous aquifer (Plates 58 - 59 of the previous atlas). Two plants tap the Lower and Middle Eocene aquifers (Plate 57 of the previous atlas), which are normally reserved for providing drinking water. The first supplies hot water for a swimming pool. The second, running since 1982, services an air-conditioning system with relative heat and 'cold' from the aquifer using a geothermal doublet. The water extracted is completely reinjected to the aquifer.

The other geothermal reservoirs shown in the previous atlas have not yet been exploited. A few shallow aquifers (at 15 - 40 m depth) are exploited with individual heat pumps (a few m³/h of water with temperatures between 10 - 15 °C).

None of the installations in the Aquitaine Basin have shown serious corrosion even after several years of operation. The heat distribution networks are varied: single pipe systems with no initial heat exchanger; double pipe systems with an initial exchanger; three pipe systems with heat exchangers. Some networks are equipped with hot water storage systems either using natural reservoirs (subsurface storage) or thermally insulated steel tanks. The choice depends on whether the operator is aiming at minimum investment, user flexibility, and/or maximum discharge of geothermal heat.

The technologies in use are mainly control systems that favour cold returns and thermodynamic cascades: aerotherms, radiators, convection heaters, floor heating, swimming pools, ice rinks, heat pumps (electric or natural-gas motors with heat recovery).

The high quality of the geothermal water is responsible for the low operating costs of geothermal operations in the Aquitaine Basin. The water is generally potable and can safely be returned to the environment and no problems arise from reinjecting the water back into the original aquifer, so that very few restrictions have to be met by the operation of these plants. Moreover, numerical simulation showed that 10 of the 14 geothermal operations in the Aquitaine Basin do not need to reinject fluids to maintain aquifer pressure.

Paris Basin

Two plants tap the Albian aquifer (Plates 44 - 45, in the previous atlas) covering air conditioning demands in Paris. The first, operating since 1963, supplies the heating/cooling system of the Maison de la Radio. It consists of a single 600 m deep borehole, which produces fresh water at 27 °C with a maximum discharge of 200 m³/h. The second one, constructed in 1980, feeds the air conditioning system of two large office blocks; it operates on the doublet principle with alternating interseasonal storage of heat and cold in the ground, associated with a heat pump.

A third plant in the vicinity of Paris, at Bruyère-le-Chatel, supplies heat and industrial water. It taps the Neocomian (aquifer with similar characteristics to the Albian, but slightly deeper) and produces water at a temperature of 33 °C with a discharge of 130 m³/h. Further projects are planned for the Neocomian.

The Albian and Neocomian aquifers are little exploited because access is highly controlled. The Albian, in particular, is a strategic drinking water reserve for Paris in the event of accidental pollution of the surface waters that supply 95% of the Paris region.

European Hot Dry Rock project in Soultz-sous-Forêts

A European Hot Dry Rock (HDR) project is taking place in Soultz-sous-Forêts (Alsace), at the western edge of the Rhine Graben, 50 km N of Strasbourg. Circulation tests between two boreholes (3600 m and 3900 m deep, respectively) showed that hydraulic stimulation was able to successfully enhance the permeability of the natural fracture system and increase the performance of the geothermal boreholes. Stable production rates of 20 l/s water at > 140 °C were achieved with a circulation experiment of over 4 months. This HDR system was deepened to 5020 m (202 °C). More information on this venture is given in BAUMGÄRTNER et al. (1998).

Geothermal exploitation of the Dogger of the Paris Basin

Location of installations, water temperatures and flow rates (Plate 19)

The Dogger of the Paris Basin is the most exploited geothermal aquifer in France. The high salt (between 15 - 35 g/l) and high sulphide content causes high costs of access to this resource. Because the artesian production of the Dogger aquifer of the Paris Basin is insufficient to meet the demand, 87 % of the operating geothermal doublets are fitted with pumps. The 38 doublet installations feed urban heating networks that supply > 150 000 dwellings. This is possible because the resource characteristics (temperature, flow rate) at depth match the demand of the users at the surface (apartments connected to urban heating networks). A plant tapping the Dogger can only be considered economical for a warranted clientele of > 2000 dwellings (see graph: Dwellings heated with geothermal energy).

The oldest plant at Melun l'Almont in the Paris Basin uses since 1995 a triplet borehole technique. Except for this plant that started operating as a doublet in 1969, all other plants were commissioned at the end of the 1980s. Technical maintenance and management teams for these operations have had to adapt very rapidly, along with suitable support structures. The high density of operations in certain parts of the Paris suburbs made it necessary to develop simulation and prediction models in order to be able to dimension properly additional sets of doublets avoiding interference from neighboring doublets.

The difficulties likely to be encountered during exploitation are of three types: (1) Shutdown of the installation, due to a breakdown of pumps or ancillary equipment, because of the highly corrosive environment. (2) Decreased well productivity commonly caused by restriction or clogging of the production or injection boreholes. (3) Damage to the borehole, endangering the whole installation. This happens when the steel casing of the borehole is corroded. Curative and preventive measures are discussed in DEMANGE et al. (1995).

Sulphide concentrations (Plate 19)

The geothermal installations exploiting the Dogger aquifer in the Paris Basin have suffered from corrosion of the carbon-steel borehole casings, as well as scaling and clogging, due to the corrosivity of the geothermal fluids (AMALHAY et al., 1994a,b). The fluids form an anaerobic medium characterized mainly by the presence of Cl, H₂S, SO₄ and HCO₃. These compounds have been present since the aquifer was first exploited.

High dissolved sulphide concentrations are always observed in areas where significant clogging occurs (FOUILLAC et al., 1990). The sulphide content in the fluids increases at certain production well-heads (IGNATIADIS et al., 1991). The investigation of sulphide concentrations throughout the Dogger aquifer revealed two distinct sulphide zones (high sulphide and low sulphide) and variation of concentrations at the regional as well as at the local scale. A zone of high initial sulphide concentration (25 - 100 mg/l) lies to the N and W of Paris where the concentrations do not vary significantly with time nor with flow rate. Lower initial sulphide concentrations S and E of Paris are found to vary both with time and with flow rate at the well-head. Variation of sulphide concentrations by several orders of magnitude has been detected between certain boreholes to the S and E and at few sites to the N and W (regional variation), even though the total dissolved solids (TDS) vary only by a factor of 5 - 6 (5.8 - 35 g/l) over all the geothermal boreholes. No general correlation has been found between sulphide concentration and fluid temperature and/or TDS. Locally, sulphide concentrations are not stable over time in the low sulphide zones (IGNATIADIS, 1994).

The map of sulphide concentrations is based on sulphide content data

obtained in 1994 and on older, but validated, data for certain boreholes which are no longer operational.

Monitoring the ratio of sulfur ³⁴S to ³²S isotopes in the fluid showed that the increase in sulphide concentration occurring when the well flow rate decreases, is related to current and increasing bacterial activity (sulphate-reducing type).

Present status and future perspective of the use of geothermal energy

The development of geothermal energy in France is concentrated in two major sedimentary basins (Aquitaine and Paris basins) which have the double advantage of an abundant available resource and a sufficient concentration of potential users. It has also benefited, as a result of the 1970s energy crisis, from the government's incentive to develop this energy source. The system of geological risk insurance linked to drilling, development, and exploitation of geothermal boreholes; the formation of a Technical Committee to ensure the quality of the projects; the creation of a scientific centre dedicated to geothermal energy, operating for a decade; as well as various aid and financing schemes contributed significantly to stabilize and mature the French geothermal industry.

The activities of the past few years have mostly been devoted to combating corrosion and scaling, optimising heating networks. In addition to increasing the knowledge of the reservoir over the last decade, the techniques for exploiting and managing the resource itself, and the equipment and the installations optimizing the use of this resource were improved. As a result, the amount of energy extracted with a certain geothermal discharge exploited at given temperature, increased, augmenting the global energy output of most installations. The usable quantity of geothermal energy was increased without any investment in new boreholes. This made it possible to connect new users to existing operations and increase availability of operations and the percentage of geothermal energy added to the network from a doublet. In this manner, it is estimated that more than 30 000 new housing units can be hooked up to existing heat networks in the next decade.

Successful long term operation of doublet and multiple borehole installations depends on knowledge of the thermal recovery time and practical life time of the system. To achieve this goal, advantage will be taken from the network for remote measuring and transmission of geothermal data installed in 1987 at 40 geothermal sites in the Paris region. It provides continuous and detailed measurements of 10 parameters. Custom-designed software is used for filtering, visualizing, storing and processing the data, which are available to operators and serve to draw up exploitation statistics for the Dogger aquifer. In the presence of exploitation anomalies, it is possible to take into account local causes resulting from the specific functioning of a doublet (e.g. decrease in flowrate, scaling in the casing, etc.), as well as more regional causes related to the amplitude of interaction between systems (e.g. pressure interference and modifications in the functioning of neighbouring doublets). This data base associated to numerical modelling of the reservoir behaviour will provide the tools needed to predict the short and long-term needs for further geothermal development.

References

- Baumgärtner, J., Gérard, A., Baria, R., Jung, R., Tran-Viet, T., Gandy, T., Aquilina, L. and Garnish J., 1998: Circulating the HDR reservoir at Soultz: maintaining production and injection flow in complete balance- initial results of the 1997 circulation experiment. - Proc. Twenty-Third Workshop on Geothermal Reservoir Engineering, Stanford University, Stanford, California, January, 26-28, 1998, p.11-20.
- Amalhay M., Abou Akar A. and Ignatiadis I. (1994a): Study of the deposition phenomena in geothermal wells in the Paris Basin. In: Proceedings of the International Symposium, Geothermics 94 in Europe, from Research to Development, BRGM (ed), Orléans France, 8-9 February 1994, pp. 223-232.
- Amalhay M., Gauthier B. and Ignatiadis I. (1994b): Influence of some physico-chemical parameters and exploitation conditions on corrosion and scaling in geothermal wells in the Paris basin. In: Proceedings of the International Symposium, Geothermics 94 in Europe, from Research to Development, BRGM (ed), Orléans France, 8-9 February 1994, pp. 233-240.
- Demange, J., Jaudin, F., Lemale, J. and Munjoz, A., 1995: The use of low-enthalpy geothermal energy in France. - Proc. World Geothermal Congress 1995 (Eds: Barbier, E., Frye, E., Iglesias, E. and Palmason, G.), vol 1, 105-109.
- Fouillac C., Fouillac A.M. and Criaud A., (1990): Sulfur and oxygen isotopes of dissolved sulfur species in formation waters from the Dogger geothermal aquifer, Paris Basin, France. Applied Geochemistry, Vol. 5, N°4, pp. 414-427.

Ignatiadis I., Cheradame J.-M., Brach M., Castagne S., Guezennec J. (1990): Reduction by biocide treatment of hydrogen sulfide concentration in a geothermal brine. Proceedings of the International Congress on Microbially Influenced Corrosion Knoxville USA 7-12 October 1990, section 8, pp. 33-36.

Ignatiadis I., Cheradame J.M., Lafforgue M. and Castagne S. (1991): Evolution des teneurs en sulfures dissous dans les fluides géothermaux. Rapport BRGM n°R33518 IRG SGN 91, 160 p.

Ignatiadis I. (1994): Origins of the increased sulfide concentrations noted in geothermal fluids at production wellheads in the south and east of the Paris basin. In: Proceedings of the International Symposium, Geothermics 94 in Europe, from Research to Development, BRGM (ed), Orléans France, 8-9 February 1994, pp. 241-248.

Lucazeau, F., Cautru, J.P., Maget, P. and Vasseur, G., 1991: France. - In: Geothermal Atlas of Europe (Eds.: Hurtig, E., Čermák, V., Haenel, R. and Zui, V.), Hermann Haack Verlagsgesellschaft, Gotha, Germany, p.30-33.

GERMANY

R. Schellschmidt, S. Hurter, A. Förster and E. Huenges

Geothermal thematic map (Plate 20)

Geothermal resources for the following aquifers in Western Germany were published in the previous atlas: Bentheimer Sandstein and Valendis-Sandstein in the North German Basin; Upper Muschelkalk, Early Triassic (Buntsandstein) and Hauptrogenstein in the Upper Rhine Graben; Aquitan-Sande, Chatt-Sande, Baustein-Schichten, Late Jurassic (Malm) and Trigonodusdolomit (Upper Muschelkalk) in the W Molasse Basin; Burdigal-Sande, Aquitan-Sande, Chatt-Sande, Baustein-Schichten, Ampfinger Schichten and Priabon-Basissandstein, Cenoman-Sandstein and Gault-Sandstein, as well as Late Jurassic in the E Molasse Basin. A reassessment of geothermal resources and update of the maps is not justified on the basis of new information.

At present 22 geothermal installations for the direct use of geothermal heat are in operation in Germany, each with an installed capacity > 100 kW. Most of these plants are located in the North German sedimentary basin and in the Molasse Basin in S Germany. The remaining installations are concentrated along the Rhine Graben. Additional information and a recent review of the status of geothermal energy utilisation in Germany can be found in SCHELLSCHMIDT et al., (2000). These installations comprise district heating systems, thermal spas combined with space heating and, in some cases, greenhouses and large installations of vertical heat exchangers used for space heating or cooling.

In addition to these large-scale plants, there are 50 000 - 90 000 small units (earth-coupled heat pumps and groundwater heat pumps).

Temperatures (Plate 21)

Temperature maps are based on temperature measurements taken with various methods: equilibrium logs, non-equilibrium logs (temperatures affected by drilling disturbances), formation temperatures obtained during borehole tests (production test, drill stem tests) and Bottom Hole Temperatures (SCHULZ and SCHELLSCHMIDT, 1991). Data statistics are shown on the pie charts.

Software facilities of the Temperature Data Bank of the Joint Geoscientific Research Institute (GGA) were used to prepare the maps. The data base received the addition of a large compilation of data from the eastern part of the North German Basin. For the disturbed logs in this area no corrections were applied because an appropriate correction methodology still has to be devised for this unique type of data. The characteristics of this compilation are discussed in detail in FÖRSTER (1997). The temperature corrections are automatically chosen and applied according to data type (SCHULZ et al., 1992). Linear interpolation was applied to determine the temperatures at the specific depth of the map. No extrapolation to depth greater than measurement depth was permitted. The data are gridded using a minimum curvature algorithm (WESSEL and SMITH, 1991), including a tension parameter.

In the North German Basin, the isotherm pattern seems to be related to the shape of the subsurface salt bodies. Salt pillows in the E part are rounded almost equidimensional features in map view, while in the W part, salt structures are made up of very long roughly NS trending salt domes in the N that change to more circular forms in the S.

The Molasse Basin in S Germany shows generally EW striking isotherms, in agreement with the direction of the basin axis. There seems to be an increase in temperature from S to N. The depth to the

basement of this asymmetric basin increases in the opposite direction, i.e. from N to S.

The order of magnitude of the temperature is similar in both basins, although isoline structure is quite different, with shorter wavelength in the North German Basin.

The Upper Rhine Graben shows clearly elevated temperatures compared to the Molasse and North German Basins. This pronounced temperature and heat flow density anomaly is associated with a regional redistribution of heat driven by groundwater circulation (PRIBNOW and SCHELLSCHMIDT, 2000).

Potential geothermal reservoirs

Areas for which geothermal resources were determined in the previous atlas are shown along with the new assessments of this atlas. At this large scale, practically all areas of interest in the country have been surveyed.

A large potential exists in the North German Basin. However, detailed local studies are needed, because this basin has been subjected to intense tectonic overprint with large scale salt migration, as is shown on the cross-section (HAUPT, 1996). As a consequence, geometry and properties of geothermal aquifers may vary significantly over small distances.

An intensive and systematic program of geothermal resource evaluation in the German Democratic Republic produced maps at a scale of 1 : 200 000 covering that whole country. The present assessment for the aquifers of the E North German Basin have strongly drawn from the work of DIENER and WORMBS (1988-1990) as well as DIENER and WORMBS (1990-1992).

Aachen Area (Plate 21)

H. Karg and C. Bucker

This area lies at the boundary between the tectonic blocks of Erft and Rur. The potential reservoir comprises the Grafenberg sand at the base of the Tertiary sequence (KARG et al., 1998), deposited in a shallow marine and estuarine environment. The depth and thickness of the Grafenberg sands echoes the palaeogeography and tectonic pattern of the Lower Rhine Embayment during the Oligocene.

The highest temperatures are observed in the vicinity of Liège and Maastrich in Belgium, and along the Rur boundary fault. Regions with elevated temperatures are associated with ascending groundwater from deeper levels of the Lower Rhine Basin. The centres of the tectonic blocks in the Lower Rhine Embayment appear as low temperature regions due to descending cold meteoric waters. These large areas show relatively uniform subsurface temperature distribution unrelated to tectonic structure. Temperature increases steadily towards the NE, with increasing depth. The elevated temperatures in the depocentre are overprinted by the effects of forced convection of heated groundwaters associated with the Erft boundary fault system. In this region, maximum temperatures above 44 °C are expected at the top of the aquifer. This is much higher than the mean temperature of about 28 °C resulting from averaging all thermal data for the Grafenberg aquifer. Additionally, gravity-driven groundwater flow directed towards the NE, i.e. towards the centre of the basin, affects the temperature field. Thus the shape of the 28 °C and the 32 °C isotherms E of Jülich indicate the direction of flow resulting from a slope in the regional groundwater table.

An estimated mean porosity of 25 % was used to calculate the geothermal resources within the Grafenberg reservoir.

The resources map shows a similar pattern to the temperature map. Geothermal resources increase towards the NE, where the greatest depth and temperatures are reached.

Eastern North German Basin

The North German Basin is the central part of the Central European Basin. The present-day sediment thickness in the North German Basin ranges from 2 - 10 km. Halokinetic movements of the Zechstein layers are responsible for the intense and complex deformation of Mesozoic and Cenozoic formations (DEKORP-BASIN Research Group, 1998; FRANKE et al., 1996). This tectonic disturbance strongly affects the local conditions of the geothermal reservoirs. Because of the salt tectonics, great variations of depth (locally > 1000 m) and thickness occur along short distances. Therefore, the temperature and resource maps are strongly influenced by the depth range of the respective aquifer.

The Mesozoic deposits of the North German Basin are made up of sandstones, claystones and carbonates, with evaporite intercalations. Four Jurassic and Triassic sandstone aquifers are of interest for direct use of geothermal energy: (1) Aalen, (2) Lias and Rhät, (3) Schilfsandstein, and (4) Buntsandstein.

Generally, salinity of the formation water increases with depth: as a rule, for each depth interval of 100 m, salinity augments by 10 g/l. The fresh/salt water interface (1 g/l) is at 50 - 300 m depth, after which, salinity increases strongly. Highly concentrated Na-Cl-brines of 150 - 280 g/l and greater can be found in the sandstone aquifers of this basin. Many salt water outlets at the surface have been detected and, in some regions, the infiltration of meteoric waters dilutes the formation waters. Corrosion is potentially more important than precipitation, as these waters are rich in chloride therefore re-injection is compulsory for any geothermal application.

Porosity data from measurements on cores and from geophysical logs were used for the calculation of resources. Porosities obtained from geophysical logs were averaged and weighted according to the depth interval of measurement. Porosities from borehole cores were averaged. Mean porosities from geophysical logs and laboratory measurements were combined to a mean aquifer value for each borehole.

The local discontinuities due to faults are not considered explicitly for isoline tracing. Therefore, the isolines on the maps are a smoothed expression of regional geologic structure based on borehole data. Consequently, local studies are necessary in order to better constrain the geometry and dimensions of the aquifers and its engineering characteristics.

Aalen (Plate 22)

The Aalen sandstone is the basal unit of the Dogger formation. It is intruded frequently by salt structures, over which it has been eroded (N and W Brandenburg and parts of Mecklenburg). The sand proportion of the Aalen sediments decreases from N to S and from E to W.

These deposits comprise medium to fine sandstones with clayey portions. The lower part of the aquifer consists of alternating grey to dark grey sandstones and siltstones of variable clay content. Locally, the clay intercalations contain pyrite concretions. The upper part of the aquifer comprises fairly clean sandstones and silty interlayers. Sometimes the low cohesiveness of these rocks prevents cores being recovered (in this case porosities measured in the laboratory are biased towards lower values). The aquifer is confined by a claystone layer. Although the sandstones are poorly cemented, local variations in reservoir properties due to cementation occur.

The mean porosity determined on core samples is 25 %. Mean permeability is 1000 mD, although values up to 3000 mD have been measured.

Lias and Rhät (Plate 22)

This aquifer complex extends over the whole North German Basin with exception of regions above salt domes where these deposits were eroded off. Depth to the bottom of this aquifer varies laterally from 500 m to > 2000 m. As a function of the salt structures, the thickness of the aquifer is also highly variable.

The lithology and thickness of the Lias-Rhät sequence is affected by synsedimentary tectonic activity (including salt kinetics). The Rhät sandstone is heterogeneous, 50 - 100 m thick. At the base, two alluvial fans make up the sandy facies. The remaining region is covered by sandy-clayey deposits overlain by 20 - 30 m thick sandstones, with locally significant shaly intercalations. The Lias is separated from the Rhät aquifer by a predominantly shaly layer (Triletes). Sometimes this separation is missing. Therefore, the Lias is treated together with the Rhät as one single hydrologic unit. The Lias aquifer units comprise principally the Hettang and Lower Sinemur sandstones, but may, in some places, include sandstone horizons from the Domer.

Porosity ranges from 10 - 35 %, with a mean of 25 %. The permeability ranges from 250 - 2000 mD.

Schilfsandstein (Plate 23)

The Schilfsandstein consists of fluvial delta deposits, that are observed extending from Scandinavia to southern Germany. In some places, these sediments have been eroded above salt domes. Rapid vertical and lateral lithologic variations are a result of the depositional environment. Lateral

depth variations of the bottom of the aquifer of up to 1800 m occur, depth being shallower above salt bodies. Fine to medium grained grey to grey-green sandstones make up these deposits. They are sometimes coarser toward the bottom and exhibit distinctive cross-bedding. Alternating layers of silt and clay containing carbonaceous material may occur at the bottom and at the top of the sandstones. In some places, the pores are filled with gypsum and anhydrite cement.

Porosity data are mostly from geophysical logs with few measurements on cores. Values range 10 - 35 % with a mean of 22 %. Permeability is about 10 mD, from limited data. Salinity increases with depth and ranges from 86 - 215 g/l.

Buntsandstein (Plate 23)

The Middle Buntsandstein was deposited during the main subsidence episode of the basin. The deposits exhibit uniform lithologies and thickness over large distances. The uplifted regions to the N and to the S are the source areas of the clastic material. Coarser sandstones were deposited along the margins and finer grained sediments in the central part of the basin. Posterior salt kinetics has significantly affected the depth to these formations, causing lateral variations of the order of a few thousand metres.

The deepest aquifer complex is the Middle Buntsandstein comprising 4 units, representing each a cycle of fining upward: (1) Solling, (2) Hardegsen, (3) Detfurth, and (4) Volpriehausen. Each unit begins with a coarse sandstone at the base overlain by alternating sandy-silty strata.

Porosity ranges from 10 - 35 %, with a mean of 22 %.

Northern Upper Rhine Graben

C. Fitzer, S. Fluhrer and B. Sanner

In the N part of the Upper Rhine Graben the vertical temperature gradient in the sediments averages 60 mK/m, twice the mean value for Germany. In this area two stratigraphic units are useful from the geothermal perspective: the Rotliegend layers (Permian) and the Hydrobien layers (Tertiary).

Hydrobien (Plate 24)

Hydrobien layers consist of clayey-marly sediments and dip towards the S down to a depth of 800 m. These layers reach thicknesses of about 800 m in the S and thin out towards NE. Minimum thickness of 100 m is observed in the NE, E of Frankfurt. A porosity of 20 % was assumed for the resources calculation. The maximum resources occur in the NE of Worms.

Rotliegend (Plate 24)

The Rotliegend crops out in the Frankfurt area and dips towards the W down to a depth of 2300 m W of Mainz. The aquifer extends over a thickness of more than 2200 m in the NW and thins out towards the E. The temperature at top of the Rotliegend is between 90 - 130 °C. The resources increase from E to W as a result of the great depth and thickness of this formation.

Present status and future perspective of the use of geothermal energy.

A conservative estimate of the total thermal power installed at present yields roughly 323 MW_t. About 12 % is provided by large installations. Currently 14 new centralised plants are planned. Additionally, > 20 potential sites have been identified for direct use of geothermal heat in Germany. By the year 2000, the increase in both types of applications, centralised and decentralised units, is estimated to boost the total installed thermal power in Germany to about 467 MW_t (CLAUSER, 1997).

Most plants are located in the North German Basin, in the Molasse Basin in S Germany, or along the Rhine Graben. The three largest geothermal plants - Waren (Müritz), Neubrandenburg, and Neustadt-Glewe - are located in the eastern North German Basin and operate since 1984, 1988, and 1995, respectively. The total installed power of these major installations is about 22 MW_t.

Resources and probable reserves of Germany

Reg.	Aquifer	A km ²	T _i °C	Resources 10 ¹⁸ J	A' GJ/m ²	Probable reserves 10 ¹⁸ J	P GJ/m ²	MW _e	
A	Valendis Sst.	143*	50	0.11	0.79	96	0.023	0.24	24
	Bentheimer Sst.	361*	54	0.28	0.78	158	0.078	0.49	82
B	Aalen	66250	43	80.83	1.22				
	Lias and Rhät	68125	38	102.87	1.51				
	Schilfsandstein	63125	48	37.88	0.60				
	Buntsandstein	67500	49	70.88	1.05				
C	Garfenberg-Schicht	597	28	0.29	0.48				
D	Hydrobien-Schicht	2117	30	5.72	2.70				
	Ob. Muschelkalk	2060	137	3.17	1.53	1880	0.210	0.11	222
	Buntsandstein	2746*	137	45.72	16.65	2574	1.830	0.71	1937
	Rotliegendes	2117	110	89.79	42.41				
E	Hauptrogenstein	332	79	0.49	1.47	236	0.019	0.08	20
	Ob. Muschelkalk	1616	75	1.11	0.69	764	0.033	0.04	35
	Buntsandstein	1688*	85	9.78	5.80	6.28	0.220	0.35	233
F	Aquitain-Sande	3776	48	6.79	1.80				
	Chatt-Sande	2564	72	9.05	3.53	944	1.050	1.11	1111
	Baustein-Schichten	880	45	0.36	0.41				
	Malm	7740*	69	11.79	1.52	6568	0.570	0.09	603
G	Ob. Muschelkalk	3728	67	1.29	0.34	140	0.001	0.01	1
	Burdigal-Sande	268	45	0.22	0.82				
	Aquitain-Sande	763	45	1.33	1.82	124	0.100	0.80	106
	Chatt-Sande	3348	53	10.48	3.13	2044	1.850	0.90	1958
	Baustein-Schichten	304	42	0.14	0.47				
	Ampf., Priabon	436	79	0.39	0.89	156	0.040	0.25	42
	Gault/Cenoman	6112	77	4.61	0.75	1040	0.230	0.27	243
Malm	8790*	78	17.05	1.94	6444	0.630	0.10	667	

T _i = mean temperature at top of aquifer	Reg.:	A = W North German Basin
A = areal extent of potential area		B = E North German Basin
A' = areal extent of probable reserves		C = Lower Rhine Graben
P = thermal power (= reserves/30 years)		D = N Upper Rhine Graben
		E = S Upper Rhine Graben
		F = W Molasse Basin
		G = E Molasse Basin

* These values correspond to the largest surface of an aquifer for particular regions. They are summarised in Table 2 of the previous atlas.

Current research funded by the German government involves two approaches. In the first, the behaviour of a geothermal reservoir under long term exploitation conditions is examined. In the second, the optimization of geothermal applications for the various kinds of reservoir are analyzed from economic and technological points of view.

The project *Hydraulic, thermal and mechanical behaviour of geothermal aquifers under exploitation*, is a joint collaboration of the GGA Institute, the Mecklenburg-Vorpommern Geological Survey, the University of Bonn, the Technical University Hamburg-Harburg, among others. Numerical modelling is conducted to predict the hydraulic and thermal long term behaviour (30 - 50 yrs) of high salinity aquifers and attempt to quantify the associated changes in reservoir properties. Numerical tools capable of dealing with coupled simulation of flow, heat and mass transport as well as the chemical interaction of fluid and rock matrix are being developed (BARTELS., 1998; KÜHN et al., 1999). Model parameters are derived from large petrophysical data sets collected from various sandstone aquifers in NE-Germany. Additionally, an experimental approach completes the research concept: high-pressure and high-temperature permeability experiments are carried out under aquifer conditions to determine the permeability-porosity relationship for precipitation and dissolution, in particular for carbonates.

The project *Evaluation of Geologic and Economic Conditions for Utilizing Low-Enthalpy Hydrogeothermal Resources* was conducted by the GeoForschungsZentrum Potsdam (GFZ Potsdam) and involved several institutes. The complex interactions of geological, economical, technological, and ecological conditions for successful use of geothermal energy were examined, considering especially the technology developed and used in Germany over the past 20 years. An exploration strategy was conceived considering different kinds of reservoir conditions with the purpose to minimize the risk of drilling geothermal wells. The results of this project provide a basis for political decisions in the process of promoting and installing geothermal heating plants. An expert system (ERBAS et al., 1996) was created that is capable of quantifying the effect on the final energy costs of various choices in the technologies and components used for building a geothermal installation. It includes a comprehensive energy balance and confronts the geothermal potential with consumer demand. This analysis helps to conceive geothermal systems that are competitive when compared to other energy sources (EHRlich et al., 1998; KAYSER, 1999). Special attention is given to the concept of geothermal water as part of a multi-user system, designed, for example, for the heating of buildings in conjunction with a balneologic utilization, which

optimizes the exploitation of geothermal energy. The possibility of such combined systems has to be introduced to the public and certainly will help to convince communities to invest in geothermal heating plants.

At present no electrical power is produced from geothermal resources in Germany. The lack of appropriate high-enthalpy steam reservoirs implies that only binary or Organic Rankine Cycle (ORC) power plants can be used for electrical power generation. A successful development of the Hot Dry Rock (HDR) technology would change this situation fundamentally. An European scientific HDR pilot plant is established in the Upper Rhine Graben in France. First circulation experiments conducted in 1997, exceeded expectations. In 1998 a large circulation system was created at 5000 m depth with a temperature of 200 °C and a thermal power of 30 MW_e. The price for HDR-generated electrical power is expected to be in the range of present electricity costs by taking advantage of the local conditions of this site (JUNG et al., 1997; BAUMGÄRTNER et al., 1998).

Acknowledgements

Katja Glies helped with data input and digitizing. In addition to digitizing, Juliane Herrman helped with the graphical layout. Colleagues of the Section Geothermics and Groundwater Hydraulics gave freely of their time, especially to deal with reticent computers and convoluted programs: Fred Haegedorn, Georg Kosakowski, Hans Herrman.

Temperature data for E Germany were kindly made available by Dr. S. Schretzenmayr (Erdöl-Erdgas Gommern GmbH) and Dr. S. Fricke (BLM GmbH, Gommern). J. Haupt of the Mecklenburg-Vorpommern Geological Survey provided the cross-section of the E North German Basin. Wolfgang Bauer and Prof. Dr. Udluft (University Würzburg) kindly supplied details on the chemical composition of some geothermal springs.

References

- Bartels, J., 1998: Long term behaviour of geothermally used aquifers. The joint research project: overview. - Proc. of 5 Geothermische Fachtagung, 12-15 Mai, Schaubj, Germany, p.292-296.
- Baumgärtner, J., Gérard, A., Baria, R., Jung, R., Tran-Viet, T., Gandy, T., Aquilina, L. and Garnish J., 1998: Circulating the HDR reservoir at Soultz: maintaining production and injection flow in complete balance- initial results of the 1997 circulation experiment. - Proc. Twenty-Third Workshop on Geothermal Reservoir Engineering, Stanford University, Stanford, California, January, 26-28, 1998, p.11-20.
- DEKORP-BASIN Research Group, 1998. Survey provides seismic insights into an old suture zone. - EOS, Transactions, American Geophysical Union, vol 79, 12, p. 151, 159.
- Diener, I., Wormbs, J. and the geothermal group, 1988-1990: Geothermische Ressourcen im Nordteil der DDR. - Kartenwerk Geothermie 1 : 200 000, ZGI, Berlin.
- Diener, I., Wormbs, J. and the geothermal group, 1990-1992: Geologische Grundlagen für die Geothermienutzung in Nordost-Deutschland. - UWG, Berlin.
- Ehrlich, H., Erbas, K. and Huenges, E. (Eds.), 1998. Geothermie Report 98-1: Angebotspotential der Erdwärme sowie rechtliche und wirtschaftliche Aspekte der Nutzung hydrothermaler Ressourcen, Scientific Technical Report STR98/09, 95 p.
- Erbas, K., Hoth, P., Huenges, E., Schallenberg, K. and Seibt, A., 1996: Evaluierung geowissenschaftlicher und wirtschaftlicher Bedingungen für die Nutzung hydrogeothermaler Ressourcen. - In: Geothermie - Energie der Zukunft, 4. Geothermische Fachtagung, Tagungsband (Proceedings) 18 - 20.09.1996, Konstanz, p. 112-119.
- Förster, A., 1997. Bewertung der geothermischen Bedingungen im Nordostdeutschen Becken. - In: Geothermie Report 97-1: Geowissenschaftliche Bewertungsgrundlagen zur Nutzung hydrothermaler Ressourcen in Norddeutschland (Eds.: Hoth, P., Seibt, A., Kellner, T. and Huenges, E.), Scientific Technical Report STR97/15, GeoForschungsZentrum Potsdam, 20-41.
- Franke, D., Hoffmann, N. and Lindert, W., 1996. The Variscan deformation front in east Germany. Part 2: tectonic interpretation. - Z. angew. Geologie, B. 42, H. 1, p. 44-56.
- Haupt, J., 1996: SW-NE verlaufender Vertikalschnitt von Mecklenburg-Vorpommern. - In: Geologische Karte von Mecklenburg-Vorpommern, Verbreitung der unter Quartär anstehenden Bildungen mit Tiefenlage der Quartärbasis (Ed. Geologisches Landesamt Mecklenburg-Vorpommern). - Schwerin.
- Jung, R., Baumgärtner, J., Kappelmeyer, O., Rummel, F. and Tenzer, H., 1997: HDR-Technology - geothermische Energiegewinnung der Zukunft. - Geowissenschaften, vol 15 (8), p. 259-263.
- Karg, H., Bücken, C., Wohlenberg, J. and Schellschmidt, R. (1998): New investigations on the present-day subsurface temperature field and geothermal reservoir studies in the northern Rhenish Massif and the Tertiary Lower Rhine Basin (West Germany). - submitted to Geothermics.
- Kayser, M., 1999: Energetische Nutzung hydrothermaler Erdwärmeverkommen in Deutschland - eine energiewirtschaftliche Analyse. - Doctoral diss. Technical University Berlin, Germany, pp.166.
- Kühn, M., Bartels, J., Pape, H., Schneider, W. and Clauser, C., 1999. Simulation of permeability changes in aquifers caused by chemical reactions. - European Union of Geosciences conference 10, March, 28 - April, 1, Strasbourg, France, J. Conf. Abs. 4, 585.
- Pribnow, D. & Schellschmidt, R., 2000: Thermal Tracking of Upper Crustal Fluid

Schellschmidt, R., Clauser, C. & Sanner, S., 2000: Geothermal Energy Use in Germany at the Turn of the Millennium. - In: Iglesias, E., Blackwell, D., Hunt, T., Lund, J. & Tamanyu, S. (eds): Proceedings of the World Geothermal Congress 2000, Kyushu - Tohoku, Japan, May 28 -June 10, 2000, 427-432: Auckland (IGA).

Schulz, R., Haenel, R. and Kockel, F., 1992: Federal Republic of Germany - West federal states. - In: Geothermal Atlas of Europe (Eds.: Hurtig, E., Čermák, V., Haenel, R. and Zui, V.). - Hermann Haak Verlagsgesellschaft mbH Geographisch-Kartographische Anstalt, Gotha, p. 34-37.

Schulz, R. and Schellschmidt, R., 1991: Das Temperaturfeld in südlichen Oberrheingraben. - Geol. Jb., E48, p. 153-165.

Wessel, P. and Smith, W.H.F., 1991: Free software helps map and display data. - EOS Trans., Amer. Geophys. V., vol 72, pp.441, 445-446.

GREECE

V. Karkoulas, M. Fytikas, P. Dalambakis and D. Mendrinou

Geothermal thematic map (Plate 25)

Areas belonging to the active S Aegean volcanic arc, are privileged with high enthalpy ($T > 150$ °C) geothermal fields such as the islands of Milos and Nisyros. Low enthalpy geothermal fields ($T < 150$ °C) are more common within Greek territory. General information on thermal aspects of Greece are also described by TAKITOS (1991).

In the previous edition of this atlas detailed maps of the Thessaloniki area were presented and will not be repeated here.

During the last five years a series of low enthalpy projects were completed in N and central Greece (FYTIKAS. et al., 1995). The depth of the investigated reservoirs varies between 100 - 500 m, although 3 boreholes, with depths exceeding 1000 m, intercepted deep permeable formations. Production tests and reservoir engineering studies performed in some well known fields yielded a few hundreds to 1000 m³/h of hot water of 40 - 80 °C with salinity varying between 0.8 - 49 g/l.

The high enthalpy projects of Milos and Nisyros islands have been suspended. The estimated geothermal resources of these two fields may support over 200 MW_e of installed power for a time period exceeding 20 years.

Temperatures (Plate 25)

In comparison with the temperature maps presented in the previous edition, this map exhibits significant changes in isoline pattern mostly in the NW of the county.

Eratino-Chrysoupolis

This geothermal field lies in the Delta Nestos basin. The 14 exploratory boreholes drilled in this geothermal field identified a permeable zone at 600 - 800 m depth covering an area > 20 km². The temperatures of the geothermal fluid ranges 70 - 90 °C and the salinity is 6 - 8 g/l. No production data are available.

Lesvos

Shallow drilling has indicated the existence of several geothermal fields on the island with a considerable geothermal potential. The characteristics of these fields are summarized in the table below.

Geothermal field	Area (km ²)	*Number of boreholes	Depth range (m)	Temperature (°C)	Yield (m ³ /h)	Water Type	TDS (g/l)
Polinichtos	10	25 / 8	50-150	67 - 92	400	Na-Cl	12
Lisvori	-	2 / (1)	-	68	20	Na-Cl	11
Stipsi-Napi	10	3	50-150	42 - 67	30	Na-Cl	1 - 5
Argenos	4	3	10-180	86	800	Na-Cl	12
Kalloni	10	6	50-200	25 - 30	300	Cl-CO ₃	0.5
Therma of Yeras	2	5 / 1	20-80	40	150	Cl-CO ₃	1 - 2
Thermi	10	2 / (1)	10-50	60	200	Na-C	35
Petra-Mythimna	10	4	100-200	35 - 60	100	Cl-CO ₃	1
Mytilene	10	15	50-150	60	500	1	2

* borehole/production well, () hot spring

DOTSIKA et al. (1995) provide details on geothermal exploration in the Mytilene area.

Potential geothermal reservoirs

The geothermal resources correspond to the heat stored in the permeable zone only at each field, as indicated by production or exploratory boreholes.

Mygdonia Basin (Plate 26)

Three geothermal fields, Langadas, Nymfopetra and Nea Apollonia, are located in the vicinity of the lakes Koronia and Volvi. In the eighties, 19 exploratory boreholes were drilled. The geothermal potential of the area was further examined in the early nineties, by the drilling of an additional borehole and the performance of production tests in 5 productive boreholes. As a result of these investigations, the geothermal field was defined over an area of 10 km².

The *Langadas* aquifer top lies at 210 m depth extending over an area of 6 km². Existing wells can produce 300 m³/h of Na - SO₄ - CO₃ water with salinity > 1 g/l. In *Nymfopetra*, the aquifer extends in the depths range of 60 - 100 m covering an area of 2 km². An output of 200 m³/h of water can be achieved with similar chemical properties as in Langadas, but with higher CO₂ content. In *Nea Apollonia*, the aquifer extends over 2 km². Here, 400 m³/h of fluid are drawn from the aquifer at depths of 50 - 110 m. The chemical properties of the fluid resemble the ones of Nymfopetra.

Nea Kessani - Xanthi (Plate 26)

This is presently the most important low enthalpy system in Greece. The main reservoir is located within the clastic Palaeogene sediments. The fluid is of Na - Cl - CO₃ type with high CO₂ content and salinity around 5 - 6 g/l. The 34 boreholes drilled in this field have delineated an area of 15 km² of geothermal potential. Reservoir porosity is 20 %.

The optimum production rate for 20 years of exploitation is estimated at 250 m³/h, based upon tests on 4 production boreholes. The rate of energy extracted corresponds to 1.2 m³/h of conventional fuel. A shallow production borehole has been scheduled for reinjection. Another 200 m deep borehole yields 160 m³/h artesian flow at 80 °C. In addition, a deep borehole of 1000 m has intercepted various productive aquifers from 300 m to bottom hole (basement). No production tests have been carried out at this well.

Milos (Plate 27)

The island is part of the active Aegean volcanic arc. The geothermal reservoir is liquid dominated and contains high salinity fluid (45 g/l Cl and 75 g/l TDS). It is located in fractured schists of the the metamorphic basement. The maximum measured temperature is 323 °C and the pressure is 110 bar at 1100 m b.s.l. The upflow zone of the system is situated underneath the Zefyria plain where the top of the geothermal zone is at a depth of 750 - 900 m. A caprock about 250 m thick, probably created by mineral deposition, confines the upflow zone. Sea water (21 g/l Cl) recharges the system offshore and is enriched in Cl due to boiling and steam loss.

A steam heated CO₂ rich (bicarbonate) fluid of low salinity lies on the top of the high salinity geothermal fluid. It is originated by mixing meteoric waters with sea water near the coast. In some areas, acid fluids cause intense argillic alteration near the surface. These two types of fluids supply the hot springs, fumaroles and hot grounds at the surface. The flow rates are extremely low, indicating very low permeabilities. The conductive heat loss over the E of the island, where the geothermal anomaly has greater magnitude, has been estimated at 50 MW_{th}.

In 1985, a pilot plant of 2 MW_e was installed in Milos. However, this installation was shut down in 1988, because the inhabitants and local organisations of the island opposed strongly its operation, quoting environmental concerns.

Strymon Basin

Nigrita (Plate 27)

The geothermal field of Nigrita occupies an area of 16 km² at the western margin of the Strymon Basin, S of Serres. The geothermal anomaly is associated with two deep fault systems striking NNE-SSW (normal) and NW-SE (strike slip). The reservoir is hosted in basal conglomerates of Neogene age. In the nineties, 5 productive boreholes were added to the existing 9 exploratory and 1 productive boreholes

drilled in 1983. The average discharge of each borehole is 70 m³/h. All are used for greenhouse heating purposes. The fluid type is Na - Ca - CO₃ with a high CO₂ content. The flow rate of the existing boreholes exceeds 400 m³/h.

Sidirokastro (Plate 27)

Two distinct aquifer zones have been identified in the geothermal field of Sidirokastro extending to an area of about 10 km². The shallow one is located at 20 - 50 m depth and the deep one at 250 - 400 m. Both contain Na - CO₃ fluid with salinity of 1.3 - 2 g/l. The flow rate that existing boreholes can yield from the deeper aquifer has been estimated at 150 m³/h.

Neo Erasnio-Xanthi (Plate 28)

The geothermal field of Magana lies at the E edge of the Delta Nestos basin. At present, 21 exploratory and 3 production boreholes define a low enthalpy reservoir extending over 15 km². This reservoir is made up of sandstones and conglomerates from the base of the post Alpine sedimentary sequence including the top of the metamorphic basement (gneiss, granite). Two types of fluid have been identified: Na-Cl rich fluids with TDS between 7 - 12 g/l and Na-HCO₃ rich fluids with TDS up to 1 g/l.

Production tests carried out in the three recently drilled boreholes, indicate that an optimal flow rate of 400 m³/h of water at 63 °C can be achieved. The total reserves are estimated to amount to 30 MW_{th}. Additionally, sufficient reserves of fresh water and the proximity of the sea makes the field of Magana most promising for investments in agriculture and fish farming.

Other areas

Nisyros

Nisyros is a complex volcano of Pleistocene-Holocene age with hydrothermal activity in its caldera. A reservoir at depths of 1500 - 1800 m provides geothermal fluids with temperatures > 250 °C. However the geothermal fluid has a high salinity and corrosion capacity. Production and injection tests performed in boreholes N2 and N1 indicated that, while N1 cannot be used for reinjection because of self-sealing, N2 can produce 8 t/h steam and 11 t/h brine at 17 bar. There were plans to drill 5 additional boreholes and build a power plant. However high enthalpy geothermal development on the island has been postponed, due to objections of the local population, influenced by the events of Milos island, where a power plant was shut down because of environmental concerns.

Aristino

This area is located at the W margin of the Alexandropulos sedimentary basin, extending into Turkey. Two main fault systems, NNW-SSE and NNE-SSW, controlled the spatial evolution of sedimentation and volcanism, which started in the middle Eocene. Altered volcanic formations of high secondary permeability form the reservoir. Six shallow (110 - 210 m) boreholes drilled during 1994 identified two aquifers. The temperature range of 40 - 55 °C and a salinity of up to 5 g/l is recorded in the upper aquifer zone (40 - 150 m deep), while the lower one (110 - 250 m) has a temperature around 92 °C and salinity exceeding 10 g/l. Until now surface and subsurface surveys cover only part of the area of geothermal potential, which may well be > 50 km².

Soussaki

Soussaki geothermal field is located at the NW margin of the active volcanic Aegean arc, near the Corinth canal. Drilling exploration revealed three main permeable formations: one in Neogene sediments (60 - 80 °C), another within the Upper Cretaceous ophiolitic thrust (60 - 67 °C), and a third deeper aquifer in limestones (Lias) and the dolomitised limestones (Lower Jurassic-Triassic) with temperatures of 50 - 63 °C. Production rates of 50 - 90 m³/h were achieved with the aid of a lineshaft pump in the shallow boreholes (> 200 m). The 900 m deep borehole S1 produces at a rate of 160 m³/h, and borehole S3, 1080 m deep, produces 100 m³/h. Experiments with a Downhole Heat Exchanger in a shallow production borehole resulted in 31 °C inlet and 41.5 °C outlet temperatures for a flow rate of 17.5 m³/h.

Present status and future perspective of the use of geothermal energy

Balneology and greenhouse heating are the main geothermal energy applications in Greece. Electric power generation has been deactivated; the 2 MWe power plant on Milos island was shut down in 1988, due environmental concerns.

Traditional balneology applications abound in Greece. Spas are sited in Sterea Hellas (Loutraki, Thermopyles, Kamena Vourla, Ypati and Platystomo), in Evia (Aidhipsos and Gialtra), in Macedonia (Thermie or Anthemountas, Sidirokastro, Nigrita, Agistro, Aridea, Langadas, Nea Appolonia, Agia Paraskevi and Eleftheres Kavallas), in Thrace (Nea Kessani, Trianoupolis and Echinis), in Peloponnissos (Methana, Kaiafa and Kyllini), in Ipiros (Prevaza, Kavassila and Amarantos Konitsa), in Thessalia (Smokovo), as well as on the Aegean islands (Lesvos, Limnos, Nisyros, Ikaria, Samos, Kithnos, Kos, Santorini and Samothraki). Kamena Vourla has one large indoor pool and 250 baths at two therapeutic centers and one hotel. Methana offers 136 pools and baths. Langadas has two large pools and 6 baths in operation, and a mud-bathing center under construction. Sidirokastro, with two large pools and 20 baths, is the only balneology center in Greece open during the winter.

Geothermally heated greenhouses operate in Sidirokastro, Nigrita, Nea Appolonia, Langadas and the islands of Lesvos and Milos. They cover an overall area of 6.9 x 10⁵ m², including 4.8 x 10⁴ m² of greenhouses not operating presently. In particular, 18 % of this area lies in Sidirokastro, 33 % in Nigrita, 19 % in Nea Appolonia, 7 % in Langadas, 12 % on Lesvos island and 4 % on Milos island, respectively. The main products are tomatoes, cucumbers and roses. The heating system used in most cases is made up of spiral polypropylene pipes, combined occasionally with air-water heaters. Load factors vary between 10 - 28 %.

Geothermal installations in Greece tend to be poorly engineered systems. In Aidhipsos, heat exchangers cool the hot water before using it for bathing. Early systems in Lesvos included steel pipes, which corroded rapidly, as standard corrosion prevention practices were not applied. Desired indoor temperatures in the Lisvori greenhouses could not be maintained, so that water air-heaters had to be added recently to the system. Geothermal greenhouses, covered by double polyethylene sheets used to be heated by spraying them with low-temperature geothermal water. However, they now operate as conventional greenhouses, because of interior lightning problems. Improvement of the design of geothermal installations will increase the efficiency of these systems.

References

- Dotsika, E., Fytikas, M., Mountrakis, D., Papageorgiou, F. and Zouros, N., 1995: Geothermal exploration in Mytilene area (Lesvos island, Greece). - Proc. World Geothermal Congress 1995, Florence, Italy, May 18-31, (Eds: Barbier, E., Frye, E., Iglesias, E. and Palmason, G.), vol 1, p. 989-994.
- Fytikas, M., Dalambakis, P., Karkoulias, V. and Mendrinis, D., 1995: Geothermal exploration and development activities in Greece during 1990-1994. - Proc. World Geothermal Congress 1995, Florence, Italy, May 18-31, (Eds: Barbier, E., Frye, E., Iglesias, E. and Palmason, G.), vol 1, p. 119-127.
- Takitos, S., 1991. Greece. - In: Geothermal atlas of Europe. (Eds.: Hurtig, E., Cermák, V., Haenel, R. and Zui, V.), Hermann Haack Verlagsgesellschaft, Gotha, Germany p. 41-43.

HUNGARY

P. Dövényi, F. Horváth and D. Drahos

Geothermal thematic map (Plate 29)

Intensive lithospheric extension, mainly during the Miocene, created the geological conditions that determine the geothermal energy potential of Hungary. The result of this rapid extension is a complex basin system, called the Pannonian basin, which is filled up mostly with clastic sedimentary rocks. The thickness of this Early Miocene - Quaternary basin fill is 2000 - 2500 m on average, but locally, it can attain 7000 m. As a consequence of lithospheric extension a large asthenospheric dome developed causing the high geothermal gradient and heat-flow density in the Pannonian basin. Extensive calc-alkaline volcanism occurred contemporaneously with the culmination of this rifting event (Middle - Late Miocene). Alkaline basalt erupted during a second phase of volcanic activity from the latest Miocene - Early Quaternary.

The basement is the continuation of the surrounding orogenic terranes (Alps, Carpathians and Dinarides) and consists of similar Mesozoic and Palaeozoic rocks. The pre-Tertiary rocks crop out mostly along the Transdanubian Central Range, in some places of northern Hungary (Bükk Mts.) and in southern Transdanubia (Mecsek and Villány Mts).

In Hungary, geothermal water ($> 30\text{ }^{\circ}\text{C}$) is found over $> 70\%$ of the country's territory. There are two principal aquifer systems of regional extent, which feed most of the 1200 geothermal boreholes and a few thermal springs. One is the fractured and/or karstified Mesozoic basement, and the other is the clastic Late Miocene - Quaternary fill of the Pannonian basin. There are some thermal water occurrences deriving from other layers (i.e. Palaeozoic metamorphic basement, Devonian, Eocene and Middle Miocene limestones, fractured Oligocene marls, etc.), but they are of only minor importance for the total geothermal resources.

There are 777 geothermal boreholes with installations in Hungary. It is impossible to plot all these boreholes on the map at the given scale in this atlas. Instead, groups of boreholes in close proximity are shown at the geometric center of their positions. The color of each symbol corresponds to the maximum temperature of the outflowing water within each group. The chemical composition bars encompass the information on the individual boreholes within each group.

The salinity of the thermal water varies between 0.5 - 25 g/l. Generally, it increases with the depth and temperature. The main constituent dissolved in the water is HCO_3 . A minor amount of Cl and exceptionally SO_4 are also present. In some boreholes the thermal water contains dissolved CH_4 gas or even liquid hydrocarbons.

Temperatures (Plate 29)

A detailed description of the thermal database can be found in (HORVÁTH and DÖVÉNYI, 1991). At present, it contains more than 12 000 temperature records distributed in 4666 boreholes. Whenever necessary, the temperature measurements have been corrected for drilling disturbances (Bottom-Hole temperatures). Data from 3192 boreholes were selected according to certain quality criteria for the construction of the temperature map at 500 m depth. Map construction was fully automatic. The vertical and horizontal interpolation of temperature data is based on thermal conductivity estimations of the layers penetrated by the borehole. Additionally, weighting factors were applied as a function of the reliability and the distances of temperature measurements relative to the reference level (500 m). The geographic pattern of the thermal field at a depth of 500 m can be followed at greater depths. For instance, at 500 m depth, the low temperature in the NW (in the Transdanubian Central Range) can still be identified at a depth of 2000 m.

Surface heat-flow density (uncorrected for palaeoclimatic effects) for most of Hungary is greater than the average for continental areas (65 mW/m^2), being between $80 - 110\text{ mW/m}^2$. An exception is a low heat-flow density anomaly ($< 50\text{ mW/m}^2$) in the Transdanubian Central Range also identified on the temperature maps. Generally the heat-flow density pattern seems to echo the temperature field. The high geothermal gradient and heat-flow density are a consequence of lithospheric extension that created the Pannonian basin system in the Miocene.

Potential geothermal reservoirs

The national resource map shows the sum of the resources calculated for the two main aquifer systems in Hungary. Areas of high geothermal resource ($> 40\text{ GJ/m}^2$) lie in the SE and W. The potential medium to high enthalpy areas (vertically hatched zones on the map) consist of Mesozoic basement at a depth of 3000 - 4000 m (i.e. at $150 - 200\text{ }^{\circ}\text{C}$) located in the vicinity of major fault (shear) zones. Two such aquifers have been drilled and yielded hot steam with remarkable overpressure (HORVÁTH and DÖVÉNYI, 1991).

Quaternary

Great Plain (Plate 30)

Quaternary terrigenous sediments dominated by sands and loess overlay unconformably the Upper Pannonian (Pontian-Pliocene) complex. This section is rarely $> 50\text{ m}$ thick in Transdanubia, but is $> 600\text{ m}$ in the southern part of the Great Plain. The Quaternary forms an integral part of the Upper Pannonian aquifer system with almost no geothermal resource due to the low temperatures of near-surface layers. The few

exceptions are localized in the deepest part of the basin. These thermal anomalies form in regions of ascending hot water. Details on the procedure for resource calculation are described in the next section dedicated to the Pontian-Pliocene aquifer. An effective thickness of 70% of the formation section was used for the geothermal resource assessment.

The waters hosted in the Quaternary layers are characterized by low salinity ($\leq 1\text{ g/l}$).

Pontian-Pliocene (Plates 30 and 31)

Great Plain

Most part of the country is covered by Pontian-Pliocene basin fill, which is called Upper Pannonian strata in the traditional Hungarian stratigraphic terminology. These layers are made up of a delta-plain sequence with frequent alternation of sands, sandstones, siltstones and clayey-marly layers. The average thickness of this complex is $500 - 1000\text{ m}$, although it can be $> 2500\text{ m}$ in the deep Neogene troughs.

The effective porosity strongly decreases with depth, but the sandy members retain remarkable porosity even at depths of $2500 - 3000\text{ m}$. The decrease in porosity is not so sharp above the deep troughs as above the shallower parts of the basin. The permeability exhibits similar trends. Horizontal permeability in the sandstone layers is $400 - 500\text{ mD}$ on average, with extreme values of 100 mD and 800 mD , at a depth of 2500 m and close to the surface, respectively. Also in this depth interval, the vertical permeability changes from $30 - 300\text{ mD}$. The permeability of marls and shales are an order of magnitude lower, but still large enough to connect hydraulically separate sandstone layers. Evidence for subvertical fluid flow (upward or downward) of a few m/yr is found in a few places of the basin (e.g. Tizsakécske geothermal maximum).

The compact marls are practically impermeable at greater depth, so that the turbiditic sandstones of the Lower Pannonian delta-slope and prodelta sequences are hydraulically isolated. Furthermore, the evaluation of many well-log profiles shows that the marl/sandstone ratio of this sequence is significantly higher ($2.3 - 1.5$) than that of the Upper Pannonian ($0.7 - 0.6$). Therefore, pre-Upper Pannonian sediments were not included in the geothermal resource assessment.

It is not possible to divide the Upper Pannonian aquifer system into discrete aquifers of definite thickness and horizontal extent. Therefore, resources are calculated for the aquifer system as a whole using the temperature halfway between the top and bottom of the aquifer. The porosity estimation was based on porosity-depth curves. An effective thickness of 60% of the total section was assumed based on the marl/sandstone ratio mentioned above.

The chemical composition of Upper Pannonian thermal water is dominated by alkaline-hydrocarbonates. The TDS is between $1 - 3\text{ g/l}$. In deep, isolated parts of the aquifer this value can be $> 10\text{ g/l}$, often with higher Cl content.

Mesozoic (Plate 32)

The Mesozoic carbonate aquifer system can be divided into two parts. A first part is at the surface of the Hungarian mountains. It forms the recharge zone for the meteoric water that feeds the aquifer. The second and largest part is underneath the Neogene basin fill. Discharge may occur at some hot springs on the foothills of karstic aquifers (Hévíz, Budapest, Eger) or at depth where the hot water enters into the overlying clastic sedimentary rocks of Neogene age. Some parts of the Mesozoic aquifer system, for example in southwestern Transdanubia, are isolated and have no direct connection to the open karstic areas.

The lithology of the basement is composed predominantly of Late Triassic dolomites and limestones, Cretaceous epicontinental sediments and various Jurassic rocks of minor importance. The thickness of this Mesozoic complex is often uncertain but reaches a few 1000 m in many places. Both the depth to the Mesozoic basement aquifer and the temperature at its top are rather well-known due to the great number of seismic sections and drillholes that often reach the Mesozoic complex even at large depth (5 km), but rarely penetrate it more than a few 10 m . In the upper 100 m , porosity and permeability are high enough to form an aquifer. The resource maps are based upon estimates of effective porosity of $1 - 3\%$ and effective thickness of $100 - 500\text{ m}$. A few permeability data for the karstified and fractured Mesozoic basement can be derived from flow rate measurements during borehole tests. The yield can exceed $60\text{ m}^3/\text{h}$, from which a permeability of up to 100 mD can be calculated. The salt content of the water in the basement aquifer is mostly Mg - and Ca - HCO_3 , and its amount depends mainly on the flow velocity and water temperature.

West Hungary (Plate 33)

In the vicinity of outcropping Mesozoic rocks in the Transdanubian Central Range, the main part of the aquifer is made up of karstified *Triassic Hauptdolomit and Dachstein Limestone*. In the NW, S of the Little Hungarian Plain, and in the SE, along Lake Balaton, faults border the aquifer. In addition to this fault bounded aquifer system, the Paleozoic crystalline basement with low porosity and permeability may locally act as an aquifer (Bük, Sárvár).

The relatively low salinity of the Hévíz thermal water (< 1 g/l) suggests high flow velocity in this region.

For resource calculations, the thickness and porosity estimated in the Transdanubian Central Range were 300 m and 2 % (N), 500 m and 2.5 % (NE) as well as 300 m and 1.5 % (SW), respectively.

In the S and SW of Transdanubia, a more or less independent aquifer system exists (with outcrops in Croatia). The high Cl content of this Zalakaros karstic thermal water (~ 5 g/l) is probably the consequence of mixing with Miocene water. The whole aquifer can be characterized by an average thickness and porosity of 100 m and 1 %, respectively.

The Mesozoic aquifer in the neighbourhood of the Mecsek and Villány inselbergs in S Hungary has a different lithology than in the Transdanubian Range, but the porosity conditions and aquifer thickness are similar: 1.5 - 3 % and 200 m, respectively. The salinity in this region is < 1 g/l.

Central Hungary (Plate 34)

Large portions of these aquifers are the continuations of the West Hungarian aquifers. The thickness and porosity estimates for the resource calculation are 200 m and 2.5 % to the N of, and 300 m and 2 % to the E of Budapest. In the NE corner of the maps for this region, the characteristic thickness and porosity are 100 m and 1 %, respectively.

In some places, the Mesozoic basement and the younger overlying rocks (i.e. the Eocene limestones S of the Pest plain, E of Budapest) form together a hydrodynamically interconnected aquifer system.

The salinity of the Budapest thermal water is 1 - 2 mg/l with remarkable content of Cl and SO₄.

Northeast Hungary (Plate 35)

This entire region can be characterized by an average aquifer thickness of 100 m and an average porosity of 1 %, containing thermal water of relatively low salinity. In the S, the sharp aquifer boundary is a fault zone separating the Mesozoic and Paleozoic basement. In those parts where the thick Neogene volcanic complex is present, the resource assessment is uncertain.

South Hungary (Plate 35)

The aquifers are the continuations of the SE part of the West Hungarian maps. Estimated thickness and porosity values are: 200 m and 3 % in the vicinity of the Mecsek Mts; 200 m and 2.5 % SE of the Villány Mts; and 100 m and 1 % in the NE edge of the map. The water salinity is low (< 1 g/l).

Present status and future perspective of the use of geothermal energy

M. Árpási

Three kinds of reservoirs are tapped in Hungary producing water with outflow temperatures > 30 °C:

- The Upper Pannonian (Pontian-Pliocene) system consists mostly of porous sandstones making up a reservoir with an estimated volume of 3800 km³. The average water temperature at the well-head is 68 °C. This aquifer provides 87 % of the total thermal water production;
- the Mesozoic reservoir system formed by fractured and karstic carbonate rocks occupies an estimated volume of 200 km³. The water tapped from this reservoir by boreholes and a few natural springs amounts to 13 % of the total production, and;
- geopressed reservoirs have been found in the course of oil and gas exploration in the deep basement of the Pannonian basin.

Considering a temperature difference (utilization step) of 55 °C for the exploitation of geothermal energy (without reinjection), 2300 km³ of the available volume of the geothermal reservoirs are capable of providing it. This corresponds to a heat content of 570 x 10¹⁸ J.

When an utilization step of only 40 °C is considered, the available geothermal resources permit an extraction of 0.26 km³/a at a heat content of 43.5 x 10¹⁵ J without reinjection, or 0.38 km³/a at 63.5 x 10¹⁵ J with reinjection.

The total volume of underground thermal water extracted in Hungary from 1950 - 1993 amounts to 9.05 km³. This production is distributed among 777 boreholes according to the tables below.

Geothermal water production according to outflow temperature (01.01.95)

Outflow Temperature [°C]	Number of boreholes	Percentage of boreholes [%]	Cumulative yield [m ³ /min.]	Percentage of yield [%]
30-40	334	47	84.6	37
40-50	153	20	49.3	21
50-60	82	10	18.2	11
60-70	76	9	24.2	10
70-80	54	6	12.3	8
80-90	38	4	8.3	7
90-100	38	4	16.1	6
>100	2	-	2.6	-
Total	777	100	215.3	100

Status of geothermal energy use (01.01.95)

Kind of utilization	Percentage [%]
Drinking water supply	29.9
Balneology	35.7
Agriculture	19.6
Industrial	11.4
Space heating and communal hot water supply	3.4
Total	100.0

Most geothermal water comes out of the Upper Pannonian reservoir system. The high production rates and the absence of reinjection have led to a general drop of the well-head pressure of the originally artesian boreholes. Balneology and drinking water supply are the most important applications of geothermal water (65 %) in Hungary. No generation of electricity takes place. The direct heat use (space heating of buildings and greenhouses) has a seasonal character covering only 160 - 180 d/a. The temperature decrease during utilization is very low, 20 - 30 °C. Heat pumps are not used for increasing the efficiency of geothermal heat utilization. The total amount of geothermal energy used in 1994 was 2.96 x 10¹⁵ J, which corresponds to 0.24 % of the total energy consumption in Hungary. The number of thermal boreholes shut down increased significantly in the period of 1989 - 1994. Thus, 138 boreholes were closed in 1990 and 315 by the end of 1994, respectively. More information on the present status of geothermal energy exploitation can be found in ÁRPÁSI (1995 a, b) and SZITA (1995).

New geothermal projects are being prepared based on results of earlier studies and recent well tests carried out in cooperation with foreign companies. These studies have indicated some potential sites for electric energy generation, where abandoned hydrocarbon exploration boreholes can be used as a source of geothermal brine. There are plans for the nearby disposal of cooled water by reinjection into the reservoir. The possibility of producing electrical energy is discussed by e.g. ANDRISTYÁK et al. (1995). The geothermal energy would be used for electricity generation and for agricultural as well as district heating in an integrated energy cascade system. Such a system would be the first complex geothermal project in the country.

References

- Andrityák, A., Lajer, L. and Pota, G., 1995: Possibilities for electrical energy generation from geothermal energy in Hungary. - Proc. World Geothermal Congress 1995, Florence, Italy, May 18-31, (Eds: Barbier, E., Frye, E., Iglesias, E. and Pálmason, G.), vol 3, p. 2097-2101.
- Árpási, M., 1995a: Country update for Hungary. - Proc. World Geothermal Congress 1995, Florence, Italy, May 18-31, (Eds: Barbier, E., Frye, E., Iglesias, E. and Pálmason, G.), vol 1, p. 141-143.
- Árpási, M., 1995b: Geothermal activity in Hungary, prospects and future. - Proc. World Geothermal Congress 1995, Florence, Italy, May 18-31, (Eds: Barbier, E., Frye, E., Iglesias, E. and Pálmason, G.), vol 1, p. 511-513.
- Horváth, F. and P. Dövényi, 1991: Hungary. - In: Geothermal atlas of Europe. (Eds.: Hurlig, E., Čermák, V., Haenel, R. and Zui, V.), Hermann Haack Verlagsgesellschaft, Gotha, Germany p. 45-47.
- Szita, G., 1995: The situation of harnessing geothermal energy in Hungary. - Proc. World Geothermal Congress 1995, Florence, Italy, May 18-31, (Eds: Barbier, E., Frye, E., Iglesias, E. and Pálmason, G.), vol 1, p. 515-518.

Geothermal thematic map and potential geothermal areas (Plate 36)

P. Baldi, E. Barbier, G. Buonasorte, C. Calore, G. Dialuce, R. Ghezzi, A. Martini, P. Squarci and L. Taffi

The geological structure of Italy is extremely complex and the existing geothermal information differs widely from region to region, so that it is difficult to define overall criteria on which to base the evaluation of the national geothermal resources.

The central Mediterranean area and, in particular, the Italian territory have been affected by the Alpine orogeny and subsequent geodynamic events, starting from the Late Miocene. During the Alpine orogeny (starting in the Cretaceous) the collision between the African and European plates gave rise to the formation of the Alpine and Apennine chain. In the Late Miocene the compressional front shifted E to the outer margin of the Apennine chain, resulting in the formation of foredeep basins along the E margin of Italy. The inner W Apennines were affected by extension lasting up to the Pleistocene. This led to the opening of the Tyrrhenian basin, and to a significant crustal thinning associated to uplift of the mantle along most of the W Italian belt. Intensive intrusive and effusive magmatic activity occurred (Miocene - Quaternary) along the Tyrrhenian belt, in the Tyrrhenian Sea itself, in Ischia island, in E Sicily (including the Aeolian and Pantelleria islands) and in Sardinia (Campidano graben). Volcanic activity still occurs in some areas of southern Italy, such as the Vesuvius-Phlegrean Fields, the Etna volcano, the Aeolian and Pantelleria islands.

Geothermal areas of greatest interest are located in the central-southern Tyrrhenian belt, in the domain of recent acid magmatism related to extensional tectonics and crustal thinning. The Italian territory can be divided into various sectors of geothermal interest according to the existence (or absence) of large aquifers down to a depth limit of 2000 m and the maximum temperature expected in these aquifers. Additional information on the evaluation of geothermal resources in Italy can be found in BARBIER et al. (1995) and CATALDI et al. (1995).

Potential geothermal reservoirs

Since the previous edition of the atlas, 500 new boreholes were drilled and recent assessments of geothermal resources of local or regional interest were carried out. In the Tuscany-Latium geothermal region, 150 new exploration/production boreholes cover a greater depth range than in the previous assessment.

New maps are presented for the Larderello, Travale and Amiata geothermal fields. The maps of the previous edition of the atlas still adequately represent the geothermal conditions in the other regions, such as Phlegrean Fields, Aeolian islands, Torre Alfina, as well as Cesano and Latera fields.

Po River plain (Plate 37 and 38)

C. Calore, G. Ghezzi, R. Ghezzi, P. Squarci and L. Taffi

The Po River plain is located in a foredeep basin area of low geothermal gradients and rather uniform temperatures. It is a national priority target for the exploitation of low-enthalpy geothermal resources. The high concentration of possible users for various types of applications is especially favorable for a multiple utilization concept of geothermal energy, also in combination with conventional sources. The evaluation of geothermal resources covers the underground to a depth of 1000 m and included data from 2000 hydrocarbon (AGIP) and water boreholes (GETAS, 1989).

The lithostratigraphy of this foreland basin is quite complex. Various depositional environments, tectonic evolution and different rates of subsidence caused lateral and vertical heterogeneity. Deposition on the Mesozoic - Eocene carbonate substratum took place during two main sedimentary cycles: pre-evaporitic and evaporitic Oligo-Miocene cycle and the post-evaporitic Late Messinian-Pleistocene cycle.

The 26 units forming the sedimentary sequence have been subdivided into 6 aquicludes and 20 aquifer units. The formations considered impervious are those showing < 20 % of porous layers on the electric logs. The rock sequence was assessed with data from 500 hydrocarbon and 300 water boreholes.

Two main hydrogeological systems can be identified in the subsurface. The *Discontinuous Aquifer System* includes the carbonate sequence, with a pronounced fracture permeability. These carbonates occur within the depth of 1000 m only at the foot-hills of the Alps in Lombardia and Veneto, in the area surrounding the Euganei-Berici hills and in the easternmost Friuli plain. The *Continuous Aquifer System* comprises the permeable formations of the post-Eocene sedimentary cycles. These form mainly porous aquifers, although in some cases fracture permeability may be present.

The shallowest aquifer is the multilayer complex of the Continental Quaternary, its thickness ranging from a few metres to > 500 m. It generally rests on the Plio-Pleistocene Asti sand aquifer. The Early Pliocene-Messinian aquifer (Caviaga and Cortemaggiore Formations, Sergnano Formation and its lateral equivalents) is separated from the Asti Formation by a thick aquiclude (Santerno clay Formation). Only over anticline tops and in the northern belt of the Pedalpine homocline is this aquifer found at depths shallower than 1000 m. The underlying aquifers belong to the Oligocene-Tortonian units (Gonfolite, Ottobiano, Sevravalle and Marnoso-Arenacea Formations): they seldom occur above 1000 m depth and often show low permeability and pass laterally into the Gallare marl pelitic unit. The latter serves as the basal aquiclude, separating the *Continuous Aquifer System* from the underlying carbonate sequence.

Temperatures

Subsurface temperature information derives from measurements in 450 hydrocarbon boreholes. The few values from water boreholes were used to define temperature at shallow depths (300 - 500 m) as data from hydrocarbon boreholes are very scarce for depths < 800 m. When shallow data are not available, temperatures at 300, 500 and 1000 m have been estimated by assuming a steady-state vertical conductive heat transfer from the measured values. Reliable shallow data from water boreholes were corrected to account for convective effects due to cold water flow at shallow depths. The resulting temperatures are generally lower (3 °C) than those expected from conductive interpolation between deep data and the surface.

The maps of temperature reveal the existence of wide zones with relatively low, uniform temperatures separated by smaller well defined zones with higher temperatures (positive thermal anomalies). The position and the distribution of most positive thermal anomalies appear to be tied to the structural elevations of the pre-Pliocene substratum, and associated to the uprising of the fresh water-salt water interface. This suggests relatively fast upflow of thermal and mineralized water facilitated by faults and fractures. Convective heat transfer is stopped at the base of the Pliocene Santerno clay Formation. The most significant anomalies are associated to shallow depths of the fractured carbonate substratum (Ferrara, Vicenza, Euganei-Berici hills, Tagliamento River and Grado). Smaller anomalies, as those on the southern margin of the Po plain and in the central part of the plain between Pavia and Cremona, appear to correlate with structural highs of Miocene formations in the Apennine folds. These anomalies are probably linked to faulting on anticline hinges. On the other hand, a widespread cooling is observed in areas where the Plio-Quaternary sequence reaches its maximum thickness.

Geothermal Potential Areas

Insufficient information on the effective porosity of the reservoirs preclude a quantitative large scale assessment of geothermal resources.

For 10 out of the 20 aquifer units of the *Continuous Aquifer System*, permeability values were supplied by core analyses or production tests. Permeability near the minimum of the measured ranges was combined with estimates of aquifer thickness in order to obtain transmissibility. The thickness was evaluated from resistivity and SP logs. Mean net thickness expressed as percentage of the formation thickness was extended to areas where the values appeared to be fairly uniform.

Such a quantitative evaluation could not be undertaken for the *Discontinuous Aquifer System* (main aquifer). Instead, its occurrence down to the depth of 1000 m is indicated qualitatively with *possible existence of conspicuous potential*. Detailed small scale investigations are needed to ascertain this potential.

Fresh water - salt water interface

The interface between saline and fresh water separates the deep static water and the overlying flowing water. It also separates areas to be reserved for fresh water exploitation for civil, agricultural and industrial use from those that can be exploited for geothermal utilization. The level of 2 g/l salinity is conventionally taken to define this interface. The depth of the fresh water-salt water interface increases with increasing hydrostatic head. This is particularly pronounced in the alluvial fans rimming the foot of the Alps where the interface appears to be deeper than 1000 m. Along the foot of the Apennines this lowering is not observable, except in the largest alluvial fans (rivers Trebbia, Taro, Secchia). In the central part of the plain, the piezometric surface is flat, varying gently. Here, the elevation of the interface is directly proportional to the structural elevation. The interface is deeper in the larger and deeper basins. It is shallower over the top of the anticlines in all the folded arcs and where the upflow of the deep brines is facilitated by faults, such as the extensional faults along the crest of the anticlines, the reverse faults at the edge of the overthrusts and the transversal faults. The Emilia-Romagna and Veneto coastal plain is affected by lens-shaped sea water intrusions with shapes affected by the rate of exploitation of the fresh water.

Prospective Zones

The most promising areas are located where higher temperatures coincide with favourable reservoir characteristics. Errors for the temperature distribution (3 °C) and the depth of the fresh water-salt water interface (100 m) are small, but may be large for the transmissibility. However, the qualitative evaluation is consistent with subsurface geology.

Tuscany-Latium geothermal area (Plate 39)

P. Baldi, S. Bellani, G. Bertini, G. Buonasorte, G. M. Cameli, A. Ceccarelli, A. Fiordelisi, P. Squarci and L. Taffi

Tuscany and Latium belong to the Apennine orogenic system, which began to develop in the Cretaceous. This system is a compressional folded thrust belt which later, in the Late Miocene–Quaternary, underwent tensional tectonics on a large scale. Tensional tectonics and crustal thinning to less than 20 km are the main cause for the magmatic and volcanic activity in both regions. Crustal thinning gave rise to the regional geothermal anomaly, while large magmatic stocks and associated volcanic phenomena caused more intense local anomalies, such as in Larderello-Travale, Mount Amiata, and the lakes of Bolsena, Vico and Bracciano.

Geophysical surveys in Tuscany identified partly melted magma bodies at depths of 6 - 8 km that correspond to the geothermal anomalies of Larderello–Travale and Mount Amiata. Some parts of Tuscany are characterized by the presence of a strong, seismic continuous reflecting horizon (K-horizon) at depths of 4 km (Larderello–Travale and Amiata) to > 7 km. One interpretation of this seismic zone is a highly fractured horizon, possibly containing geopressured fluids, linked to the emplacement of a granite body. Another possibility is that this horizon represents the brittle/ductile transition of rocks of contrasting rheological behaviour.

In addition to alluvial and detrital deposits, the stratigraphic sequence throughout the Tuscany-Latium region, from top to bottom, is described below:

(1) Post-orogenic deposits consist of magmatic and volcanic rocks as well as sedimentary formations. The volcanic and magmatic rocks (Pliocene - Quaternary) are prevalently acid in Tuscany (sporadic outcrops) and chiefly alkali-potassic in northern Latium.

(2) Clays, conglomerates and sands (Late Miocene–Pliocene) which filled lacustrine, lagoonal and marine sedimentary basins, make up the sedimentary rocks.

(3) The Allochthonous Flysch Facies Complex (Liguridi Units) is composed of argillaceous and subordinately calcareous and arenaceous formations (Cretaceous - Early Miocene). Together with the post-orogenic deposits, it serves as an aquiclude capping the geothermal reservoirs.

(4) Anhydritic-dolomitic formations make up the underlying Tuscan or Umbrian Series. Carbonate formations predominate in the lower part, while terrigenous formations in the upper part (Late Trias - Early Miocene). This unit has been removed by tectonic processes in Tuscany.

(5) The Tectonic Wedge Complex includes phyllites, quartzites, anhydrites and dolomitic limestones.

(6) The regional metamorphic basement (Precambrian - Paleozoic), consists of phyllites, micaschists and gneisses.

The last two units do not outcrop and have never been intercepted by boreholes in Latium. Therefore, the regional basement there lies at depths greater than 6000 m.

In both Tuscany and Latium, the main geothermal reservoir is composed of carbonate and anhydritic formations of the Tuscan-Umbrian Series, and in Tuscany, also by the underlying metamorphic formations of the Tectonic Wedge Complex and the regional metamorphic basement. The most localized thermal anomalies, with temperatures of 200 - 250 °C at 500 - 1000 m depth, are connected to shallow circulation of fluids in the reservoir.

Tuscan geothermal fields

G. Bertini, G. Buonasorte, G. Cappetti, A. Ceccarelli, I. Dini, A. Ridolfi and G. Stefani

Italy's most important producing geothermal fields are located in Tuscany (BALDI et al., 1995): the fields of Larderello and Travale-Radicondoli (vapour-dominated) and the fields of Mount Amiata (Bagnore and Piancastagnaio, vapour-dominated in the shallow part and water-dominated in the deep one). In the Tuscan fields, zones with steam production from deep horizons have been encountered beneath aquifers connected to near-surface circulation. Productive fractures have been discovered in metamorphic rocks at considerable depth (> 3500 m), so that the exploited areas were enlarged.

Mount Amiata geothermal field (Plate 39)

The Mount Amiata geothermal area, 70 km SE of Larderello, includes a Quaternary volcanic edifice bordered by Neogene basins. This uplifted geologic structure trends N-S and is made up by the Allochthonous Flysch Facies Complex, the Tuscan Series and the regional metamorphic basement. The geothermal fields of Bagnore and Piancastagnaio are 10 km apart, situated at the southern edge of the volcanic edifice.

The top of the reservoir is found in elevated structures of the Triassic calcareous-anhydritic formation of the Tuscan Series. The maximum temperature and the initial pressure in the gas cap (reservoir top), were about 170 °C and 2.2 MPa at Bagnore, and 220 °C and 4.2 MPa at Piancastagnaio, respectively. After 20 years of exploitation, the temperature and pressure are: 150 °C and 0.4 MPa at Bagnore, and 200 °C and 2 MPa at Piancastagnaio, respectively.

A second reservoir under hydrostatic pressure is situated at depths of 2500 - 3000 m in the metamorphic basement. In spite of the low permeability layers that separate it from the shallower reservoir, both reservoirs are hydraulically connected. Temperature and pressure of the fluid in this second deeper reservoir range between 300 - 350 °C and 19 - 25 MPa, respectively.

Further exploitation of the deep reservoir will include the drilling of a few tens of boreholes and the construction of a few 20 MW geothermal power stations (BERTINI et al., 1995).

Larderello and Travale-Radicondoli geothermal fields (Plate 40)

Larderello and *Travale-Radicondoli* geothermal fields are located on a structural high of the Tuscan Series and of the Tectonic Wedge Complex that form the main reservoir (CAMELI et al., 1993).

The Tuscan Series and the Tectonic Wedge Complex overlie the metamorphic basement with variable thickness. Discontinuous permeable layers alternate with very thick low-permeability strata. The top of the reservoir is characterized by a series of structural highs and lows trending NNW-SSE or N-S. The intensely fractured and brecciated Triassic evaporitic formation of the Tuscan Series is most often found at the top of the reservoir. This reservoir exhibits high secondary permeability in the top part, at the contact with the Allochthonous Flysch Facies Complex (Liguridi Units).

Maximum temperatures (> 250 °C) occur in the most permeable, structurally highest zones of the reservoir. The *Larderello* and *Travale-Radicondoli* geothermal fields are separated by a shallow low-

temperature area due to the penetration of cold meteoric waters into the reservoir through permeable outcrops. The temperature distribution at depths of 2000 m and 3000 m is more uniform and shows that at depth the two fields constitute a single geothermal system covering about 400 km². The pattern of the isotherms reflects permeability variations with depth inside the reservoir: they are farther apart where heat transfer occurs by fluid flow and closer together where it occurs by conduction in the less permeable zones.

The fluid pressure at the reservoir top is strongly correlated with the permeability distribution and affected by decades of intense exploitation with boreholes feeding from the upper part of the reservoir. The maximum reservoir pressure is 7 MPa, the same for the two zones at the E and W borders of the *Larderello-Travale* geothermal system. The increase of pressure with depth is ascribed to the weak hydraulic connection between the various productive layers, which prevents the drainage effects caused by fluid production from the shallow layers from spreading at depth. In the central area of Larderello (Valle Secolo), high permeability has caused the effect of drainage to extend down to a depth of 3 km (BARELLI et al., 1995).

The geothermal system is vapour-dominated everywhere, with superheating of about 50 °C in the deep layers. A liquid phase is present only at the southern boundary of the field where meteoric waters seep into the reservoir through the permeable outcrops. Thus, the *Travale-Radicondoli* field, previously considered an independent geothermal field, is in fact the E margin of a larger homogeneous geothermal area which includes the *Larderello* field.

In order to sustain productivity at *Larderello*, steam is drawn from deeper, undrained or only partially drained levels. New steam is produced by reinjecting water into the most permeable and most exploited areas of the field. The average gas content in the fluid has decreased, because this steam contains no gas. Electrical energy saved by not having to remove the gas from the condensers improved the performance of the power plants. Geothermal power stations in the Larderello-Travale fields are being renewed in order to reduce the steam consumption.

Pantelleria island (Plate 40)

S. Bellani, C. Calore, S. Grassi and P. Squarci

Pantelleria is a volcanic island located in the Sicily Channel in the median part of the continental rift system between Sicily and Tunisia. The surface geothermal manifestation consists of fumaroles, mofettes and hot springs with temperatures up to 98 °C.

The oldest rocks on the island date back to 300 ka. Six main silicic eruptive cycles occurred in the last 45 - 50 ka, indicating the presence of a deep and still active magma chamber which gives origin to and feeds the geothermal anomaly. The most significant volcanic episodes (50 - 10 ka) have produced two nested calderas. These calderas, affected by regional and local tectonism as well as by recent volcanic events, have different shapes. The older caldera La Vecchia, is elliptic while the younger one, named Cinque Denti or Monastero, is sub-circular. Recent volcanism (about 4 ka) began with basaltic composition and has shifted towards felsic differentiates, up to peralkaline rhyolites.

A geothermal program, promoted by the Mining Board of Sicily (EMS) and sponsored by the European Union, was launched by CESEN (Center for Energy Studies) in 1990. Thermal surveys were carried out in 1991-1993 in water boreholes and in geothermal exploration boreholes. In 1992, four shallow exploratory boreholes (PT1, PT2, PT3, PT4) were drilled within the old caldera. Thermal surveys in these boreholes indicate that the central-S zone of the island is the most promising for the recovery of medium-to-high temperature fluids. In 1993, two deep (1200 m) exploratory boreholes, PPT1 and PPT2, were drilled. Stabilized temperatures in the range 250 - 265 °C were recorded in PPT1, between 750 - 1000 m depth. Productive zones with temperature > 200 °C are inferred below 500 m depth. Subsequent borehole stimulation led to the production of a two-phase mixture of H₂O, NaCl and non-condensable gases, mainly CO₂ (CHIERICI et al., 1995).

Present status and future perspective of the use of geothermal energy

High-temperature geothermal resources for electricity generation, are present only in Tuscany, Latium and Campania and in the islands of Ischia, Aeolian and Pantelleria. In the remaining Italian territory, geothermal resources occur in some areas for direct heat production

(ALLEGRIINI et al, 1995).

Electricity generation

All the geothermal plants for electricity generation are located in Tuscany (status of January, 1995). These plants are concentrated in the areas of Larderello, Travale-Radicondoli and Mount Amiata and supply a total installed capacity of 622 MW, with generation of 3417 GWh in the year 1994.

Power plants are under construction or planned for Larderello and Mount Amiata fields and in the areas of Latera - Torre Alfina and Marta (Latium). It is foreseen that the construction of additional units will increase the installed capacity to > 850 MW within the year 2002. This value could be higher depending on the results of exploration surveys in progress in Tuscany, aimed at extending the productive zones beyond the current boundaries of the fields.

The exploration programs in Latium and Campania as well as on the Aeolian islands revealed several unfavourable conditions for exploration or the environment: low permeability of the aquifers, high salinity and incrustating properties of the fluids. Significant development of research and exploration activity is not expected in these areas.

Direct heat production

Direct heat uses correspond to a peak capacity of 308 MW_t and to a total energy use of about 3600 TJ/a. Operative plants, or under construction, for heating and industrial purposes are also concentrated in Tuscany-Latium area. Applications include: district heating, swimming pool heating, industrial processes, greenhouses, fish-farming and CO₂ supply plants. Further installations for such applications and food processing as well as salt extraction are planned. Few more plants exist in the rest of Italy, confined to direct heat production for district heating or industrial purposes.

The geothermal potential in Italy is greatly under-utilized, and the development of direct uses has been very slow. This is mainly due to the high mining risk and the higher initial costs of geothermal direct uses compared to conventional sources. Further developments require financial incentives and promotion of indigenous environmentally benign energy sources.

References

- Allegrini G., Cappetti G. and Sabatelli, F., 1995: Geothermal development in Italy: country update report. - Proc. World Geothermal Congress 1995, Florence, Italy, May 18-31, (Eds: Barbier, E., Frye, E., Iglesias, E. and Pálmason, G.), Vol. 1, p. 201-208.
- Baldi, P., Bellani, S., Ceccarelli, A., Fiordelisi, A., Rocchi, G., Squarci, P. and Taffi, L., 1995: Geothermal anomalies and structural features of Southern Tuscany. - Proc. World Geothermal Congress 1995, Florence, Italy, May 18-31, (Eds: Barbier, E., Frye, E., Iglesias, E. and Pálmason, G.), Vol. 2, p. 1287-1291.
- Barbier, E., Buonasorte, G., Dialuce, G., Martini, A. and Squarci, P., 1995: The Italian geothermal inventory: a valid tool for energy strategy. - Proc. World Geothermal Congress 1995, Florence, Italy, May 18-31, (Eds: Barbier, E., Frye, E., Iglesias, E. and Pálmason, G.), v. 1, p. 537-542.
- Barelli, A., Cappetti, G. and Stefani, G., 1995: Results of deep drilling in the Larderello/Travale - Radicondoli geothermal area. - Proc. World Geothermal Congress 1995, Florence, Italy, May 18-31, (Eds: Barbier, E., Frye, E., Iglesias, E. and Pálmason, G.), Vol. 2, p. 1275-1278.
- Bertini, G., Cappetti, G. and Lovari, F., 1995: Deep drilling results and updating of geothermal knowledge on the Mount Amiata area. - Proc. World Geothermal Congress 1995, Florence, Italy, May 18-31, (Eds: Barbier, E., Frye, E., Iglesias, E. and Pálmason, G.), Vol. 2, p. 1283-1286.
- Cameli, G.M., Dini, I. and Liotta, D., 1993: Upper crustal structure of the Larderello geothermal field as a feature of post-collisional extensional tectonics (Southern Tuscany, Italy). - *Tectonophysics*, 224, p. 413-423.
- Cataldi, R., Mongelli, F., Squarci, P., Taffi, L., Zito, G. and Calore, C., 1995: Geothermal ranking of Italian territory. - *Geothermics*, 24/1, p. 115-129.
- Chierici, R., Grassi, S., La Rosa, N., Nannini, R., Squarci, P. and Zurlo, R., 1995: Geothermal exploration in Pantelleria Island (Sicily Channel): first results. - Proc. World Geothermal Congress 1995, Florence, Italy, May 18-31, (Eds: Barbier, E., Frye, E., Iglesias, E. and Pálmason, G.), Vol. 2, p. 697-702.
- GETAS (Geologia e Ingegneria, Tecnologia, Assistenza Servizi), 1989: Assessment of the low-enthalpy geothermal resources. Po Valley - Italy. - Report to EC Commission, Contract EN.3G.0031.I (S).

LATVIA

A. Freimanis, E. Eihmanis, M. Morozova, V. Drikis, J. Prols, A. Zazimko and L. Sokurenko

Geothermal thematic map (Plate 41)

Latvia is situated on the NW part of the Precambrian East European Platform, where large tectonic structures are separated by faults. The western half of the country is dominated by the Baltic Syncline. The Latvian Saddle occupies most of eastern Latvia. The southern slope of the Baltic shield extends over the remaining central northern region of the country. Two geological environments can be distinguished in Latvia: the crystalline basement and the sedimentary cover.

The crystalline basement is composed of magmatic and metamorphic rocks of Archean - Proterozoic age: Archean shales, gneisses, quartzites and Proterozoic granite and gneisses (E Latvia), large intrusions (W Latvia), shales and meta-andesites (central Latvia). The crystalline basement underneath the Baltic Syncline is found at 600 - 1950 m depth. The depth increases towards SW and W.

The sedimentary cover is 300 - 1800 m thick and is made up of terrigenous, carbonaceous-terrigenous and carbonaceous rocks of Palaeozoic age, although also Mesozoic deposits exist in the SW. The sedimentary section in Latvia has been affected by tectonic activity of the basement related to the Baikalian, Caledonian, Hercynian and Alpine orogenic events.

The Baikalian complex includes strata of Vendian and Early Cambrian (Lontovian formation) ages and defines the top of the basement. Sediments attributed to the Caledonian complex were deposited during part of the Early to Late Cambrian, Ordovician, Silurian and also partly during the Early Devonian (Gargzdai unit). Both Baikalian and Caledonian rocks are cut by EW and NE trending faults imposing a typical block structure for these sequences. The Hercynian strata comprise Devonian (Kemeru formation), Carboniferous and partly Early Permian deposits. This sequence dips gradually towards S and SW. The sediments are practically unaffected by faulting. The Alpine sequence has only local expression being restricted to the SE, where Late Permian deposits occur.

Part of the crystalline basement rocks and sedimentary sections of Vendian, Cambrian, Ordovician, Silurian and Early and Middle Devonian age are of interest for the extraction of geothermal water. The Vendian and Cambrian rocks are very similar so they can be considered jointly as a single aquifer. The faults can form significant hydrogeological borders limiting lateral water migration within the Cambrian-Vendian aquifer.

The Cambrian-Vendian brines and Early-Middle Devonian mineral waters are used broadly for balneological purposes. Presently no other kind of application of geothermal heat is used.

The database compiled for this contribution contains information from 391 boreholes drilled for different purposes: exploration, ore prospecting, waste disposal, gas storage monitoring, stratigraphic reconnaissance and research. The isolines on the maps presented here were produced using kriging and minimum curvature interpolation algorithms.

Temperatures (Plate 41)

The map of temperature at 500 m and 1000 m is based on temperature measurements taken in boreholes. Temperature at depth > 1000 m was calculated using heat-flow density for downward continuation of the temperature at the top of the basement.

Potential geothermal reservoirs

There are two main areas for which enough information exist for a complete geothermal resource assessment: SW and central Latvia. Here, only aquifers with temperatures greater than 25 °C and minimum transmissibilities of 6 Dm are considered. The Cambrian aquifer fulfills these conditions.

Vendian-Cambrian

In eastern Latvia, the *Vendian* comprises the following formations: Kraslava, Gdovsk, Kotlin and Voronka. They are composed of gravels, conglomerates, tuff-gravelstones, sandstones, tuffstones, tuffaceous siltstones, siltstones and clays. In western Latvia, this system is represented by the small area of the Zuras formation made up of tuffaceous and terrigenous sediments.

The Cambrian in western Latvia comprises the *Ovishi*, *Ventava* and *Tebra* formations, in addition to the extensive Deimena formation. In eastern and central Latvia, the Lontava (clays interlayered with sandstones and siltstones) and the Cirma (siltstones and sandstones with thin layers of clay) compose the Cambrian section.

Generally, the rocks with good permeability are sandstones, gravelstones and conglomerates. Sandstones occupy mostly the upper part of the Cambrian section. They are fine to medium grained and with a strong variation in their degree of cementation. Porosity ranges from 13 - 26 % and gas permeability from 200 - 1000 mD, respectively. In zones of quartz cementation, porosity is reduced to 4 - 5 % or even less. However, gas permeabilities reach 1mD. Porosity and permeability decrease with increasing depth.

The salinity of the water ranges from 100 - 120 g/l. It is of Na-Cl type with a bromide contribution of the order of 250 mg/l. The gas saturation in these aquifers is very low, less than 0.025 m³/m³.

Ovishi-Ventava-Tebra (Plate 42)

The Early-Middle Cambrian deposits of the *Ovishi*, *Ventava* and *Tebra* formations include siltstones, sandstones, clays and argillite with ferruginous oolites. The depth of this complex may vary locally significantly due to faulting. It generally increases from N to S. The information on transmissibility is restricted to the eastern region of occurrence. The temperature is a function of depth and attains more than 50 °C. Geothermal resources were calculated only for the western section where the greatest resource is 1 GJ/m².

Deimena (Plate 42)

The Middle Cambrian *Deimena* formation is made up of sandstones and siltstones with thin intercallations of clay. The depth distribution of this formation is similar to the *Ovishi-Ventava-Tebra* complex as it is affected by the same faulting pattern. Geothermal resources are limited by the 30 °C isoline, and are slightly larger in the SW than in the SE.

Devonian

The Early Devonian system comprises 3 units: the *Gargzdai* series and the *Kemeru* and *Rezekne* formations.

The *Gargzdai* series occurs in W and E Latvia and is composed of variegated marl, clay, siltstone and sandstone with dolomite interlayers. The *Kemeru* formation is more widespread and is made up of sandstone (mainly in central Latvia), clay and sand (W of 23° E longitude) and siltstone. In the central part of Latvia, 80 % of the Devonian section is composed of sandstone, while the sandstone fraction is only 40 % in the W. The mean transmissibility is 110 Dm, and the salinity of the water ranges from 4 - 40 g/l, with values occasionally up to 100 g/l.

Kemeru (Plate 43)

The *Kemeru* formation is much less affected by faulting than the previously described Cambrian units. Its depth increases from W to E. However, the temperature distribution does not always reflect the depth distribution. Maximum temperatures of about 25 °C occur at 550 m depth in the southern central part and deeper in the SE (800 m). The formation thickness increases from N to S.

Gargzdai (Plate 43)

The *Gargzdai* unit extends mostly over eastern Latvia. However, a patch of this formation is also found in the NW. Here, thickness is generally greater than 10 m with two small regions more than 20 m thick. In the second area of occurrence, in E Latvia, the depth increases from W to E and the formation thickness increases from the edges to the central part.

Present status and future perspective of the use of geothermal energy

Basically, there are two potential geothermal areas in Latvia: the central part of Latvia (known as Eleja) and the SW, in proximity to the coastal town of Liepaja. The following table summarizes the status of known geothermal resources.

Summary of geothermal resources in Latvia

Area	Formation	Heat in Place		Resources		
		Surface km ²	ARB ₃ x 10 ¹⁸ J	H ₀ x 10 ¹⁸ J	Surface km ²	H ₁ x 10 ¹⁸ J
Liepaja	Deimena		494.30	11.01	1745.0	1.99
	Ovishi-Venta-Tebra	1764.0	24.46			
Eleja	Deimena			7.45	4357.5	1.02
	Ovishi-Venta-Tebra	4807.5	1520.00	27.54	4807.5	2.75
Latvia		65 771.5	2014.30	70.46		5.76

In Latvia only low enthalpy geothermal energy is available. Possible applications would be space heating, balneology, agriculture (greenhouses) and fishery. Further information is given in EIHMANIS (1994) and the references therein. Geothermal energy projects are at the stage of feasibility studies. The present financial difficulties prevent the development and implementation of specific projects.

References

Eihmanis, E., 1994: Information about the geothermal energy investigation and usage projects in Latvia (update report 94). - Proc. World Geothermal Congress 1995, Florence, Italy, vol 1, p. 223 - 225.

LITHUANIA

B. Radeckas, J. Vačeliūnas, B. Krasnevič and V. Rasteniene

Geothermal thematic map (Plate 44)

The territory of Lithuania is situated on the Precambrian East European Platform. It is defined by large tectonic structures: the Baltic Syncline, the Mosurian-Belarusian Antecline and the Latvian Saddle.

The geological section comprises two stages: the lower stage consists of crystalline rocks of Pre-Riphean age and the upper stage is composed of sedimentary rocks of Vendian - Quaternary age. The most complete and thickest sedimentary section has been found in western Lithuania, while it is thin and incomplete to the SE. Sedimentary formations overlie Archean and Proterozoic crystalline rocks.

The crystalline basement is made up of Caledonian and Hercynian structures. These structures consist of terrigenous, carbonate and, in the upper part, sulphurous rocks. Faults that intersect the basement affect the temperature field.

Temperatures (Plate 44)

Both Bottom-Hole Temperatures and conventional temperature logs were used for preparing the temperature maps. Temperatures in the basement at a depth of 2000 m were calculated from the heat-flow density. Data distribution is better in the W than E of the country. General studies containing geothermal aspects of Lithuania are found in SMIRNOV et al. (1991).

Potential geothermal reservoirs

Information on the aquifer properties presented herein was derived mainly from boreholes drilled for oil prospecting and other research boreholes or from results of geophysical investigations. Because of the non-uniform distribution of the boreholes, mapping is mainly based on interpolations between these boreholes. Porosity and permeability evaluations are from logs, analysis of core material and borehole production tests. Only aquifers with temperatures > 25 °C and transmissibilities > 5 Dm are included here.

In the sedimentary cover of Lithuania, hot water from the Cambrian and warm water from the Early Devonian aquifers are the potential geothermal energy reservoirs. The Cambrian aquifer lies at depths of

200 - 2200 m and consists of Middle Cambrian Deimena and Lower-Middle Cambrian Aischaian deposits. The Early Devonian aquifer extends from depths of 200 - 1200 m and is made up of strata from the Gargzdai, Kemeris and Parnu formations.

Geothermal water is highly mineralised, containing mainly chloride. The formation water of the Cambrian aquifer is more saline than that of the shallower Devonian aquifer (Plate 50). Salinity generally increases from E to W and with increasing depth. The water is neutral or slightly acidic with a pH of 6.8 - 7.1 in the Devonian aquifer and 5.2 - 7.4 in the Cambrian, respectively. However, higher acidity (pH of 3.0 - 4.5) is recorded in some Cambrian aquifers. The amount of dissolved gases in the Devonian and Cambrian brines is about 0.1 m³/m³ and 0.1-1.0 m³/m³, respectively. There is no hydrogen sulphide in both types of water.

Aischaian, Cambrian (Plate 45)

The Aischaian formation includes the Early Cambrian Geges and Vjrbaliai suites, as well as the Middle Cambrian Kybartai suite. The rocks comprise argillites, aleurolites and sandstones.

The top surface descends in steps from the N to the S following a E-W fault system. Borehole testing has confirmed the existence of a fault of approximate NS direction in the western part.

In the central and eastern part it is useful to add the Deimena sediments to the Aischaian sandstones, as well as the Vend sandstones and gravels with good reservoir properties.

In western Lithuania, the temperature at the top of the Aischaian aquifer is > 70 °C, although the transmissibility in this region is < 5 Dm. The reservoir properties of the Aischaian rocks are better in the eastern part. The region with transmissibility > 5 Dm extends over 10 000 km². The usable resources amount to 2.29 X 10¹⁸ J.

Deimena, Middle Cambrian (Plate 46)

The Middle Cambrian Deimena rocks are represented mainly by sandstones and to a lesser degree by clayey rocks. This formation is the most important oil reservoir of the Lithuanian Republic. It consists of pure quartz arenite of marine origin, well consolidated and with reduced permeabilities at greater depths due to compaction and quartz cementation. The reservoir transmissibility is < 5 Dm. In shallower areas along the borders of the basin, the Cambrian aquifer rock characteristics improve, with permeabilities of 1 D and porosities up to 25 %.

The boreholes are mostly non-artesian. The static water level has been measured at 25 - 70 m. The water is a highly saline brine. The productivity varies from 1.2 m³/(d bar) up to 6 - 10 m³/(d bar).

Gargzdai, Early Devonian (Plate 47)

Gargzdai series rocks occur only in western Lithuania. The EW Telsiai and NS Gargzdai faults intercept these deposits. In spite of rather high average net thicknesses and temperatures up to 45 °C, the well head resources are rather low, because of the low permeability of this layer. The transmissibility is > 5 Dm over only 254 km² of south-western Lithuania. However, the Gargzdai series can usefully and effectively enlarge the Kemeris aquifer, described below.

Kemeris, Early Devonian (Plate 48)

The Kemeris formation is separated from the Gargzdai by a significant unconformity and intercepted by the EW Telsiai fault. The top of the formation dips from E to W.

The aquifer consists of sandstones with intercalations of clay. Net thicknesses of sandstones attain 90 m in some places. In the W and SW of Lithuania, thicknesses of some layers amount to 20 m with thin clayey interbeds of 1 - 5 m. The porosity reaches 20 - 30 %, and very often, the transmissibility is > 100 Dm. Transmissibility > 5 Dm occurs over an area of 11 753 km².

A productivity of 51.1 m³/(h bar) was measured in boreholes Vilkyciai-3 and Vilkyciai-5. The great abundance of water is the reason why Kemeris series strata are considered to be the main aquifer.

The Middle Devonian Parnu suite exhibits similar structure as the Kemeru formation. However, it has a larger extent. The Parnu horizon forms together with the Kemeru a single hydrologic system. It is overlain by regionally impermeable Narva strata.

The effective thickness of the Parnu strata may attain 15 m. Sandstone layers, as a rule, are not thicker than 1 - 3 m. In the SW and in the NE, effective thickness amounts to 10 m.

Present status and future perspective of the use of geothermal energy

Geothermal reservoirs of interest are present in Lithuania. However, only low enthalpy geothermal resources are found in the Baltic Syncline. The geothermal energy stored in the reservoirs in the depth interval of 500 - 3000 m is $6\,000 \times 10^{18}$ J. Geothermal resources are also discussed by SUVEIZDIS et al. (1995).

Assuming an exploitation with doublets and heat pumps, the estimated well-head resources are 15.34×10^{18} J (see table).

Summary of geothermal resources for Lithuania

Formation	Surface (km ²)	ARB ₃ (10 ¹⁸ J)	Heat in Place H ₀ (10 ¹⁸ J)	Resources H ₁ (10 ¹⁸ J)
Aischyaian	9945		9.95	2.29
Deimena	9518		36.55	8.37
Gargzdai	254		1.71	0.18
Kemeru	11753		53.87	4.50
Lithuania	29025	6000	112.03	15.34

The most promising aquifer for the geothermal energy utilisation for heating purposes is the Lower Devonian Kemeru aquifer lying at depths of 700 - 1000 m.

At present no use of geothermal energy is made in Lithuania. However two low-enthalpy geothermal plants are planned. A geothermal installation is planned in Klaipėda. Warm water (42 °C) will be exploited from the Kemeru-Gargzdai aquifer. The plant will consist of a doublet combined with absorption heat pumps. Near Palanga, in the village of Vidmantai, two geothermal boreholes tap the Middle Cambrian Deimena strata at 2 km depth. The hydrodynamical tests in both boreholes show that aquifer properties determined by them are more favorable than those measured on core samples in the laboratory. Temperature of 73.3 °C and a salinity of 164 g/l were encountered. Flow rates of 32 m³/d caused a pressure decline of 1 bar. It is planned to use this resource for greenhouse heating (SUVEIZDIS and RASTENIENĖ, 1993).

The investigations carried out for the Baltic Geothermal Energy Project show that geothermal energy is economically justified only where a large heat demand exists all the year round. This is the case for only few areas situated outside larger cities where production of district heating with geothermal heat is of interest. Therefore, only a small part of the total heat demand is realistically expected to be supplied from geothermal plants.

References

- Smirnov, Ya. B., Kutas, R. I. and Zui, V., 1991. Union of the Socialist Republics (USSR). - In: Geothermal Atlas of Europe, (Eds: Hurtig, E., Čermák, V., Haenel, R., and Zui, V.), Hermann Haack Verlagsgesellschaft mbH, Geographisch-Kartographische Anstalt Gotha, p. 91-101.
- Suveizdis, P. and Rasteniene, V., 1993. The geothermal resources in Lithuania. - Geol. Soc. of Lithuania, Scientific Papers, 4, 26 p.
- Suveizdis, P., Rasteniene, V. and Zinevicius, F., 1995. Geothermal energy possibilities of Lithuania. - Proc. World Geothermal Congress 1995, Florence, Italy, May 18-31, (Eds: Barbier, E., Frye, E., Iglesias, E. and Palmason, G.), vol 1, p. 227-232.

THE NETHERLANDS

Th. H. M. van Doorn and R. H. B. Rijkers

Geothermal thematic map (Plate 51)

Here, the principal structural elements and relevant stratigraphical units of the subsurface of the Netherlands are summarized. Additional information is found in VAN ADRICHEM BOOGAERT and KOUWE (1993), RIJKS GEOLOGISCHE DIENST (1995) and ZIEGLER (1990).

During the deposition of the Upper Rotliegend Sandstone in the Permian, the structural architecture of the Netherlands was dominated by the Southern Permian Basin, extending from eastern England to western Poland. Within this basin, a number of smaller (sub)basins developed. To the S it was bordered by the London-Brabant Massif and to the N by the Mid North Sea/Rinköbing-Fyn High. The basin configuration changed slightly during the Triassic and thick successions of sandstones accumulated in the Ems Low and the Roer Valley Graben/West Netherlands Basin (GELUK et al., 1996).

The Permian - Middle Jurassic sediments of the Netherlands form an apparently conformable sequence, in most areas bounded at the base by the Saalian and at the top by the Mid - Late Kimmerian unconformities. Locally, the Early Triassic Hardegsen (Base Solling) and Late Triassic Early Kimmerian unconformities strongly affect the sequence.

During the Late Jurassic, normal faulting intensified and heat-flow density increased, accompanied by igneous activity. Rifting prograded from the present North Sea to the Dutch onshore area. High sedimentation rates and significant facies changes characterize the Middle and Late Jurassic. After Late Jurassic - Early Cretaceous extensional faulting ceased, high areas were gradually transgressed. During this transgression, Lower Cretaceous sands were deposited in the Vlieland Basin, the West Netherlands Basin and the Lower Saxony Basin.

Subsidence patterns were completely reorganized during the Late Cretaceous (Conician-Santonian). The previously stable high areas subsided rapidly, in which thick sequences of chalk accumulated. Following this period of strong basin subsidence, tectonic inversion affected the Late Jurassic - Early Cretaceous rift basins throughout the Late Cretaceous and Early Tertiary. Finally, deposition of sands and clays occurred during the Cenozoic. The total thickness of this section varies from a few metres in the S of the Netherlands to more than 3500 m in the central North Sea.

Most of the data used for this study are owned by the oil and gas industry, but are made available for the RIJKS GEOLOGISCHE DIENST (1995) and HAILE et al. (1987). Borehole and seismic data were used to map the depth and the thickness of the aquifers presented in the following.

Temperatures (Plate 51)

Temperature at depths of 500 m, 1000 m, and 2000 m are based on data compilation of 464 boreholes situated onshore as well as offshore of the Netherlands. Measurements in disturbed temperature fields (bottom hole temperature or BHT) and from drill stem tests (DST) have been used in order to obtain consistent isotherm contours on the maps (HURTIG et al., 1991).

The geothermal gradient decreases from 26 °C/km in the S of the Netherlands to about 4 °C/km in the Broad Fourteens Basin, Vlieland Basin, Central Netherlands Basin and the NW of the Dutch offshore area (Cleaver Bank High). Temperature anomalies correlate with structural units of Late Jurassic - Early Cretaceous age. High regions and platform areas are generally characterized by anomalously low temperatures, while higher temperatures are observed in the basinal environment. An exception to this rule is the Cenozoic Roer Valley Graben in the southern Netherlands, where the low temperatures are not yet explained. A striking anomaly is the so-called Zuidwal volcano in the northern Netherlands with temperatures > 125 °C at 3000 m depth.

Potential geothermal reservoirs

Two aquifers have been investigated: the Triassic Sandstone covering the whole Dutch territory and the Early Cretaceous Sandstone in the eastern part of the Netherlands (Lower Saxony Basin). Information on the geothermal resources of the Early Permian *Slochteren Sandstone*

were presented in the previous edition of the atlas and will not be repeated here.

Early Cretaceous Sandstone Formation

Early Cretaceous sandstones occur in three different basins, the West Netherlands Basin, the Lower Saxony Basin and the Vlieland Basin. In the West Netherlands Basin, the geothermal resources for thick successions of the Rijswijk Sandstone Member, Berkel Sandstone Member, IJsselmonde Sandstone Member and De Lier Member were described in the previous atlas and in HEEDERIK et al. (1995). Early Cretaceous Sandstones in the Vlieland Basin (Friesland Sandstone) are partly situated below the Waddenzee. In the Vlieland Basin and on the Friesland Platform, these sandstones often contain gas (Riiks Geologische Dienst, 1991b, 1993b). For this reason, this area is not considered suitable for geothermal applications.

The Early Cretaceous section in the Lower Saxony Basin consists of a succession of sandstones and claystones deposited during the Valanginian and the Hauterivian in a shallow marine environment (coastal barrier system). Intensive salt tectonics during the Late Jurassic - Early Cretaceous, and inversion tectonics during the Late Cretaceous - Early Tertiary affected the *Early Cretaceous Sandstone* in the Lower Saxony Basin (shown on cross-sections). A complete overview of Early Cretaceous lithostratigraphy is given in VAN ADRICHEM BOOGAERT and KOUWE (1993).

Geothermal resources of the *Bentheimer Sandstone Member* are represented here. Other sandstones in this basin, such as the Gildehaus Sandstone Member, have very low porosity caused by mineral cementation, so that no geothermal resources assessment was carried out.

Bentheimer Sandstone Member (Plate 52)

The *Bentheimer Sandstone* is a thick sequence of massive and slightly calcareous sandstones, with abundant shell fragments, lignite particles and glauconite grains. Grain sizes range predominantly from fine to medium. The thickness at the edge of the basin is 3 m and increases to > 65 m towards the centre. The *Bentheimer Sandstone* is characterized by a funnel-shaped gamma-ray log pattern and can locally be described as a transgressive depositional system. Porosity is high and ranging from 15 to > 30 %. The permeability ranges from 220 - 500 mD in the depocentre.

Early Triassic sandstone (Plates 53 and 54)

Triassic sandstones in the Netherlands occur in a rather complicated stratigraphic framework. The sequence displays a cyclic alternation of (sub)arkosic sandstones and clayey siltstones. The sandstones and siltstones have been deposited in aeolian, fluvial and lacustrine environments (AMES and FARFAN, 1996; GELUK et al., 1996). The most important sandstones of the Triassic occur in the *Main Buntsandstein Subgroup* (Scythian) and the *Röt Formation* (Early Anisian).

For geothermal mapping only the thickest sandstone members of the Triassic have been considered: the *Early Volpriehausen Sandstone*, *Late Volpriehausen Sandstone*, *Early Detfurth Sandstone*, *Late Detfurth Sandstone*, *Hardeggen Formation* and the *Röt Fringe Sandstone*. The stratigraphic subdivision is illustrated in well-correlation panels and a litho-chronostratigraphic section.

Main Buntsandstein Subgroup

The Main Buntsandstein Subgroup displays good aquifer characteristics. On the high areas surrounding the Roer Valley Graben and in the West Netherlands Basin, this section is very thick and entirely developed in sandy facies. Towards the N they grade into clayey siltstones. In the Ems Low, only the *Early Volpriehausen Sandstone Member* and the *Early Detfurth Sandstone Member* form good reservoir units.

Early and Late Volpriehausen Sandstone Member

The *Early Volpriehausen Sandstone* is a clean sandstone and has a blocky appearance on wire-line logs. The *Late Volpriehausen Sandstone* contains several claystone layers. The total thickness of the sandstones in the West Netherlands Basin is locally 150 m, while in the Roer Valley Graben their thickness reaches 250 m and up to 40 m in the Ems Low. Quartz percentages are slightly below 50 % and the fraction of calcite and dolomite cement is high in the lower parts. The average porosity of sandstones of the *Volpriehausen Formation* in the West Netherlands

Basin/Roer Valley Graben is 9 %. Scarce porosity measurements in the Ems Low indicate high values of 15 %. Permeability varies from 2 - 200 mD in the West Netherlands Basin/Roer Valley Graben and from 250 - 2000 mD in the Ems Low. The *Early Buntsandstein* is very coarse in the Roer Valley Graben and on the bordering high areas.

Early and Late Detfurth Sandstone Member

The *Early Detfurth Sandstone* is characterized by low gamma-ray readings and low transit times. Thickness in the West Netherlands Basin/Roer Valley Graben varies from 20 - 70 m. In the Ems Low the thickness reaches 47 m. This unit consists of up to 60 % of quartz. Its cement is also made up by quartz. Porosities in the West Netherlands Basin/Roer Valley Graben vary from 13 - 19 %. In the Ems Low, the mean porosity is 20 %. Permeability ranges from 3 - 500 mD in the West Netherlands Basin, while such data are not yet available for the Roer Valley Graben and the Ems Low.

Hardeggen Formation Member

A rapid alternation of sandstones and claystones characterizes the *Hardeggen Formation*. In the S part of the Netherlands, sandstones are more massive. The thickness of the Hardeggen Formation varies strongly as result of erosion at the top (Solling unconformity) attaining a maximum of about 70 m. The porosity varies from 8 - 10 % in the Roer Valley Graben to 19 % in the West Netherlands Basin. The average permeability in the West Netherlands Basin is 400 mD.

Röt Fringe Sandstone Member

The *Röt Fringe Sandstone* is a member of the *Röt Formation*. It is limited to the Roer Valley Graben and the West Netherlands Basin. The maximum thickness is 70 m. Towards the N the sands grade rapidly into siltstones, accompanied by increasing cementation. Porosity in the West Netherlands Basin and Roer Valley Graben varies from 8 - 15 %. Permeabilities range from 30 - 1000 mD.

Present status and future perspective of the use of geothermal energy

In the Netherlands four geothermal boreholes have been drilled into Tertiary and Dinantian aquifers (Arcen, Nieuweschans, Nijmegen and Valkenburg). Presently, these boreholes produce warm water (30 - 45 °C). Only two boreholes tap a pre-Tertiary aquifer: Arcen and Valkenburg. Additionally, two low-enthalpy geothermal projects are planned for Ameland and De Lier. All geothermal boreholes in the Netherlands exploit geothermal energy for direct use in greenhouses and balneology.

Many aquifers at depths of 2000 - 3000 m are of interest for direct use of geothermal energy. Aquifer performance and feasibility studies of deeper aquifers (Slochteren, Triassic and Lower Cretaceous) were carried out during the last decade, targeting temperatures > 75 °C. However, very low energy prices (gas and oil) and high drilling costs inhibit geothermal projects in the Netherlands (WALTER, 1995).

Summary of geothermal resources

Aquifer	Heat in Place (H ₀) or Resources (H ₁) (x 10 ¹⁸ J)
Lower Cretaceous Sandstone	
West Netherlands Basin*	H ₀ = 3.0
Lower Saxony Basin	H ₁ = 0.4
Triassic Sandstone	
West Netherlands Basin and Roer Valley Graben	H ₁ = 30.0
Lower Saxony Basin	H ₁ = 3.0
Other areas	H ₁ = 4.0
Triassic total	
Slochteren Sandstone (Lower Rotliegend)	H ₀ = 50.0

*data from HAENEL and STAROSTE (1988).

Interest of public utility companies in geothermal energy has strongly increased during the last years, because the Dutch government offers subsidies for energy (or electricity) producing methods that reduce CO₂ emissions. This incentive increases the feasibility of geothermal projects, as an environmentally friendly energy source.

References

- Ames R. and Farfan, P. F., 1996: The environment of deposition of the Triassic Main Buntsandstein Formation in the P and Q quadrants, offshore Netherlands. - In: Geology of Gas and Oil und the Netherlands, (Eds: Rondeel, H. E., Batjes, D. A. J. and Nieuwenhuijs, W. H.), p. 167-178.
- Geluk, M. G., Plomp, A. and van Doorn, Th. H. M., 1996: Development of the Permo-Triassic sequence in the basin fringe area, southern Netherlands. - In: Geology of Gas and Oil und the Netherlands, (Eds: Rondeel, H. E., Batjes, D. A. J. and Nieuwenhuijs, W. H.), p. 57-78.
- Haenel, R. and Staroste, E., 1988: Geothermal Resources in the European Community, Austria and Switzerland. - Verlag Th. Schaefer, Hannover, Germany, 69 p., 110 plates.

Haile, N.S., Flavell, W.S. and Gorst, M., 1987: Geothermal database North Sea. - Robertson Research International Ltd.

Heederik, J. P.; van der Meer, M. and van der Straten, R., 1995: Demonstration project geothermal exploitation De Lier: exploration and evaluation of geothermal resources in the western Netherlands. - Proc. World Geothermal Congress 1995 (Eds: Barbier, E., Frye, E., Iglesias, E. and Pálmason, G.), Florence, Italy, May 18-31, vol 3, 2263-2268.

Hurtig, E., Čermák, V., Haenel, R. and Zui, V., 1991: Geothermal atlas of Europe. - Hermann Haack Verlagsgesellschaft mbH, Geographisch-Kartographische Anstalt Gotha, 74 p., 110 plates.

Rijks Geologische Dienst, 1995: Internal report on EG-Geothermal project - update 1995. Geothermal Resources in Europe, contribution of the Geological Survey of The Netherlands. - Report nr.: 95KAR09.

Van Adrichem Boogaert, H. A. and Kouwe, W. P. F., 1993: Stratigraphic nomenclature of the Netherlands, revision and update by RGD and NOGEP. - Meded. Rijks Geologische Dienst, vol. 50.

Walter, F., 1995: The status of geothermal energy in the Netherlands. - Proc. World Geothermal Congress 1995 (Eds: Barbier, E., Frye, E., Iglesias, E. and Pálmason, G.), Florence, Italy, May 18-31, vol 1, 279-281.

Ziegler, P.A., 1990: Geological Atlas of Western and Central Europe. - Second and completely revised edition. Shell International Petroleum Maatschappij BV, 239 p., 56 encl.

POLAND

W. Górecki, T. Kozdra, T. Kuźniak and B. Bruszezwska

Geothermal thematic map (Plate 55)

Poland extends over parts of three major tectonic provinces: the East European Platform in the NE, the Mid-European Platform in the SW and the Variscan fold belt in the W.

Northeastern Poland (E of the Tornquist-Teisseyre Lineament) lies on the Precambrian East European Platform, which is divided into several structural units: Leba Elevation, Peri-Baltic Syncline, Mazury-Suwalki Elevation, Podlasie Depression and Podlasie-Lublin Elevation. The Paleozoic and Meso-Cenozoic cover of the East European Craton is of no economic interest for geothermal exploration because of the very low heat-flow density.

SW Poland is flanked by the Sudetes Paleozoic structure consisting of a mosaic of tectonic units with complex geological history and origin. The existence of isolated potential geothermal reservoirs in the Sudetes is indicated by hot springs with temperature of 62 °C, and a temperature gradient ranging from 28 - 34 °C/km. Further studies are needed to define geothermal reservoir dimensions and characteristics (SOKOLOWSKI, 1995).

In the S, the Carpathians are of little interest for geothermal energy utilization, except for the Podhale Trough, a Paleogene Basin located between Tatra Mountains and Pieniny Klippen Belt. Here the well-head temperature from a borehole of a pilot geothermal installation is 72 - 86 °C. It is being exploited at a flow rate of 60 m³/h (SOKOLOWSKI et al., 1995). The geothermal water comes from Eocene limestones and Middle Triassic dolomites that are covered with impermeable flysh.

The most important geothermal reservoirs lie in central and NW Poland. The Polish Trough, extending over the central and northern Polish Lowlands, is filled with Permo-Mesozoic sediments. The basin suffered tectonic inversion during Late Cretaceous / Early Triassic age leading to the development of Middle Polish Anticlinorium and marginal furrows of which the Mogilno-Łódź basin has a potential for geothermal exploitation. In general, aquifers hosted in the Early Jurassic and Early Cretaceous section have the greatest geothermal potential in the Mesozoic cover. However, detailed investigations of other geological units may reveal additional potential.

Assessment of the geothermal reservoir properties is derived mainly from the data obtained from oil and gas boreholes, water wells, laboratory measurements and geophysical surveys.

Temperatures (Plate 55)

Maps of temperatures are based on the interpolation of the data from 298 wells, although the number of available data decrease with depth. Temperature anomalies are predominantly caused by the presence of salt diapirs. Other studies on geothermal aspects of Poland are found in PLEWA et al. (1991).

Potential geothermal reservoirs

Polish Lowlands

Early Cretaceous (Plate 56)

The aquifers in the Early Cretaceous succession are made up of sandstones and arenaceous and arenaceous-carbonaceous rocks with minor arenaceous mudstones. Poorly permeable and impermeable intercalations are formed by claystones and mudstones. The most important aquifers are Barremian-Early Albian, Middle Valanginian and Late Hauterivian strata with total thickness of up to 500 m. Mean effective porosity and permeability is 17 % and 300 mD, respectively. General groundwater flow is from SE to NW.

Early Jurassic (Plate 57)

The Early Jurassic section exhibits high lithological variability. In the western part the rocks are of marine origin becoming partly continental towards the E. The most important aquifers are Hettangian, Late Sinemurian, Domerian and Late Toarcian sandstones with total thickness reaching 750 - 1200 m. These are separated by low permeability to practically impermeable discontinuous layers of fine-grained sandstones, mudstones and claystones.

The Late Toarcian unit has the most uniform, arenaceous character in the whole Polish Trough fill. Early Toarcian (clays) and Late Sinemurian (sandstones locally interbedded with claystones and mudstones) successions also exhibit similar homogeneity.

An effective porosity of 18 % and mean permeability of 280 mD has been used for resources assessment. General direction of groundwater flow is from SE to NW such as in Early Cretaceous strata, with discharge into the Baltic Sea.

Reservoir properties

J. Sokołowski, J. Sokolowska, S. Plewa, S. Nagy, M. Krokoszyńska and U. Krzysiek

Reservoir properties of Early Cretaceous and Jurassic formations are based on information drawn from laboratory data of core samples and borehole geophysical logs. Porosity and permeability are determined qualitatively and can sometimes be quantified using the analysis of intrinsic resistivity and gamma logs. Both kinds of data form the basis for the following maps.

Early Cretaceous (Plate 58)

Porosity of Early Cretaceous formations range from 10 % in the central part of the basin to about 32 % at the margin and the central part of the Mogilno - Łódź basin and in the central part of the Pomeranian-Warsaw basin. Permeabilities range from 2 - 2100 mD.

Malm, Late Jurassic (Plate 58)

In the central and southeastern part of Poland, the Malm formation is composed of calcareous and marly rocks. However, in the western part, clastic formations are also present such as in the Early (Oxford) and Late (Portland) part of Szczecin - Wągrowiec basin. Only the location of the most important boreholes is shown on this map. Porosity ranges from 1 - 31 % and permeability from 1 - 2140 mD.

Dogger, Middle Jurassic (Plate 58)

In Poland, the Dogger formation is made up mainly by sandstones, mudstones and shales that occur in different proportions at different places. Minimum porosities (> 5 %) have been recorded in the central part of the basin, the Middle - Polish anticlinorium. Along the margins of the Pomeranian, Warsaw and Szczecin - Łódź basins, the average porosities reach 25 - 30 %. Permeabilities overall range from

0 - 424 mD. Optimum reservoir conditions in the Dogger exist in the SW of Szczecin - Łódź and in the NE of Grudziądz - Warsaw basin.

Lias, Early Jurassic (Plate 58)

The Lias formation consists mostly of epicontinental clastic deposits and marine clays. Porosities range from several to 15 % in the central part of the basin, where Lias strata are thickest. At the periphery, i.e. Szczecin - Łódź and Pomeranian - Warsaw synclinorium, the average porosities reach 26 %. The higher values are found within local structures associated to salt tectonics. Permeabilities range from several 100 to < 1500 mD.

Present status and future perspective of the use of geothermal energy

Only low-enthalpy geothermal resources are found in Poland. Total geothermal energy resources of the Polish Lowlands (Early Cretaceous and Early Jurassic), which can be economically exploited at the industrial scale, are 2.1×10^{18} J/a (GÓRECKI et al., 1995a, GÓRECKI et al., 1995b). This corresponds to the equivalent of 4.8×10^7 toe/a.

Interest in geothermal energy utilization in Poland increased in the second half of the 1980's. At present, geothermal energy is exploited at two installations and feasibility studies for another eight were performed. It is estimated that within 25 years Poland can utilize 0.5 % of the reserves which will be about 2 % of the heat production coming from the centralized sources.

Over the last decades, the natural environment in Poland has suffered the consequences of the coal-based energy production. The use of geothermal energy would contribute to the mitigation of this problem.

References

- Górecki, W., Kuźniak, T., Lapinkiewicz, A. P., Mackowski, T., Strzetelski, W. and Szklarczyk, T., 1995a: Atlas zasobów energii geotermalnej na Niziu Polskim (Atlas of geothermal energy resources in the Polish Lowlands). - , Towarzystwo Geosynoptyków GEOS, Kraków, 28 plates, 37pp (Polish with English summary and map captions).
- Górecki, W., Kuzniak, T., Strzetelski, W., Szklarczyk, T., Ney, R. and Myśko, A., 1995b: Evaluation of geothermal resources in the Polish Lowlands., - Proc. World Geothermal Congress 1995, Florence, Italy, May 18-31, (Eds: Barbier, E., Frye, E., Iglesias, E. and Pálmason, G.), vol 1, p. 593-597.
- Plewa, M., Plewa, S., Poprava, D. and Tomás, A., 1991: Poland. - In: Geothermal atlas of Europe, (Eds: Hurlig, E., Cermák, V., Haenel, R., Zui, V.), Hermann Haack Verlagsgesellschaft mbH, Geographisch-Kartographische Anstalt Gotha, p. 67-69.
- Sokolowski, J., 1995: Country update report from Poland. - Proc. World Geothermal Congress 1995, Florence, Italy, May 18-31, (Eds: Barbier, E., Frye, E., Iglesias, E. and Pálmason, G.), vol 1, p. 293-300.
- Sokolowski, J., Sokolowska, J. and Piwinski, P., 1995: The effects of reinjection of geothermal water in Poland. - Proc. World Geothermal Congress 1995, Florence, Italy, May 18-31, (Eds: Barbier, E., Frye, E., Iglesias, E. and Pálmason, G.), vol 3, p. 2001-2004.

PORTUGAL

A. Correia and E. Ramalho

Geothermal thematic map (Plate 59)

Portugal is dominated by the Hesperian massif (Variscan fold belt). The opening of the Atlantic and Tethys (Permian-Tertiary) created the passive margin accomodating the Lusitanian and the Algarve basins. The convergence of the Eurasian and African plates caused rifting during the Oligocene that gave rise to the Basin of Tejo and Sado. Hercynian faults extend over most of the country and were active during several episodes up to recent times.

The most favourable low-enthalpy geothermal areas are located in the northern part of the country in Palaeozoic granites and schists. Most of the hot springs are associated with deep circulation in regional NW or NNW faults; other hot springs are related to faults in Jurassic diapiric structures (CALADO, 1991).

Geothermal manifestations in the Azores are known from six of the nine islands which make up the Archipelago (São Miguel, Terceira, Graciosa, Pico, Faial and Flores).

Temperatures (Plate 59)

Information obtained in oil boreholes as well as in mining and water boreholes were used to produce subsurface maps of temperature. Some of the borehole data used in the previous atlas had to be rejected because they show evidence of fluid flow. This re-evaluation of the data revealed that the conspicuous southern anomaly appearing in the temperature maps of the previous atlas reflects shallow fluid flow. In this contribution, data from 47 boreholes were included.

Recent work on geothermal aspects of Portugal is described in MENDES-VICTOR et al. (1991), DUQUE and MENDES-VICTOR (1993), and FERNÁNDEZ et al. (1995).

Potential geothermal reservoirs

Mesozoic margin

Tejo Basin, Aptian-Albian aquifer (Plate 59)

The Aptian-Albian formation (*Grés de Almagem*) comprises mostly siliceous sandstones. In the previous atlas, a conservative porosity of 15 % (rock sample porosity varies from 15 - 25 %) was assumed for this aquifer, so that the identified resources (H_1) for a basin area of 290 km² amounted to 0.5×10^{18} J (1.7 GJ/m²). These calculations were based on data from the borehole Monsanto-1, in the N of the Tejo River. Since then, borehole AC1-BALUM was drilled and reaches this aquifer at depths of 1200 - 1450 m, cutting through basaltic sills and veins of Palaeogene age. A transmissivity of 2 m²/d was estimated from continuous pumping tests of 80 days. The temperature at the bottom of the hole and at well-head was 52 °C and 50 °C, respectively. The temperature profile is affected by flow of warmer water in the aquifer. The geothermal fluid exhibits TDS of 440 mg/l and is suitable for human consumption. The inclusion of the information from this borehole does not cause the former estimate of geothermal resources to change significantly.

Tejo Basin, Valanginian aquifer (Plate 59)

No boreholes drilled for geothermal purposes reach this aquifer. The conservative assessment made in the previous atlas based on oil exploration data is still valid.

Hesperic Massif

Caldas de Aregos (Plate 59)

Aregos springs are used for balneotherapy since the 12th century. Small local discontinuous aquifers in these formations may be of geothermal interest. The thermal springs emerge at depths of 43 - 49 m at the intersection of the NW Aregos fault with N and NNE fault systems that cut granodiorites as well as grey biotitic fine and medium equigranular granites.

The reservoir volume is difficult to estimate because of the lack of geophysical surveys. Geothermometric studies indicate a reservoir temperature of 107 °C (AIRES-BARROS, 1981). Three artesian boreholes show interference, although Aregos collects its water from only two of them (AC1 and AC3), with depths of < 65 m. Pumping rates are 9 and 5 l/s, respectively. The specific water flow is 1l/(m s) and the transmissivity 50 - 100 m²/d (CARVALHO, 1993). This water is hyperthermal (61 °C), sodic sulphureous with a salinity of 300 mg/l, pH of 9.3, electrical conductivity of 400 mS/cm and high fluoride content of 19 mg/l (IGM, 1994).

São Pedro do Sul (Plate 59)

São Pedro do Sul lies on Hercynian syntectonic granites, strongly affected by the NNE Verin-Penacova regional fault system (locally, the Ribamá Fault) and the NE Termas Fault. These fault systems control the occurrence of thermal springs. Meteoric water penetrates the superficially highly fractured granites. At depth, the granite has lower permeability, acting as an aquiclude (HAVEN et al., 1985). Part of the water appears to be transported a large distance and depth through the Ribamá Fault and flows to the surface through the Termas Fault. Another transverse fault system (N70°W) enhances the secondary porosity and facilitates the upflow. Reservoir temperatures estimated with geothermometers are 102 - 130 °C (MOITINHO DE ALMEIDA, 1982) or even higher. Oxygen isotopic studies indicate that reservoir water mixes with cold meteoric waters.

The São Pedro do Sul area can be divided in three sections with favourable prospects for geothermal exploitation: Termas, Vau and Varzea. In the *Termas* section, spring water flows at a rate of 10 l/s and is used for balneotherapy since Roman times. As a result of geophysical surveys, two boreholes were drilled in the *Vau* section (SDV1 and SDV2). The artesian flow amounts to 3 l/s with a temperature of 69 °C and the system allows a sustainable pumped flow of 10 l/s. A 72 h pumping test indicated a transmissivity of 107 m²/d and a storage coefficient of 4×10^{-5} (CARVALHO, 1993). The borehole drilled at *Varzea* was not productive because the permeability was too low.

Considering the effect of radioactive heat production rate of the São Pedro do Sul granite (31.5 mW/m³), the temperature at 1 km and 7 km depth is calculated to be 73 °C and 231 °C, respectively. Assuming an area of 2.5 km², the accessible resource base (ARB) amounts to 4.2×10^{12} J (LEMOS et al., 1992).

Acknowledgements

The authors wish to thank Dr. Vítor Oliveira, Dr. João de Matos, Dr. Carlos Galvão, Dr. Acúrsio Parra, Dr^a Margarida Vairinho and Eng^o Silva Lopes (from Instituto Geológico e Mineiro), Dr. Pedro Carvalho and Dr. Álvaro Beliz (from Somincor), Dr. Manuel Marques da Silva (from University of Aveiro), Eng^o Mário Pinho and Dr. André Rodrigues (from Beralit Tin and Wolfram Portuguesa) and Dr. João Carlos Sousa (from Sociedade Mineira do Rio Artezia) for their kindness and co-operation.

Chaves (Plate 60)

L. A. Mendes-Victor, M. R. Duque, L. Aires-Barros and F. Monteiro Santos

The Chaves hydrothermal system has been used for medicinal purposes since Roman times. Today, this thermal water is tapped by springs as well as by two boreholes 98 m and 147 m deep, respectively, that are used for hydrotherapy and heating swimming pools.

The Chaves graben is 7 km x 3 km and lies at an altitude of 350 m. The E boundary of this graben is the fault escarpment of Padrela Mountain rising 400 m above the graben ground. The W boundary is composed of horsts and grabens that step up to Heights of Barroso at an elevation of 900 m. Northwards, the depression extends into the Verin Basin (Galiza-Spain) which is similar to the Chaves basin. The most recent deposits are variable thicknesses of Miocene - Pleistocene detritic sediments deposited in lacustrine, alluvial and colluvial environment (UTAD, 1992). The NNE-SSW Chaves-Verin fault and a set of ENE-WSW sinistral faults control the graben structure. The hydrothermal system formed as a consequence of extensive tectonic activity accompanying the Alpine orogeny.

The Chaves thermal water is hosted in granitic rocks. The recharge of the system is situated on the highest (intensely fractured) topography where rainfall is important (Padrela outcrop, E Chaves). The fluid percolates at great depth and then discharges on the Chaves plain. The precipitation at low elevations flows into a superficial aquifer on top of the thermal aquifer. The thermal water has TDS of 2.5 g/l. It is neutral (pH = 7) and is typical of water circulating within granitic rocks (Na-CO₂-type). Stable isotopic composition indicates the thermal water is of meteoric origin and has not been subjected to surface evaporation (AIRES-BARROS et al, 1993). Tritium values indicate circulation times > 150 a. Outflow temperature ranges 55 - 76 °C. Reservoir temperature estimates from chemical geothermometry and hydrogeochemical modelling (MARQUES et al, 1993) are 89 - 204 °C. Geothermometric interpretations of the chemical composition of the thermal water show it has experienced a temperature of 120 °C. The maximum temperature measured in the aquifer is 100 °C. Using the geothermal gradient for the region (32 - 65 °C/km), a maximum depth of 4 km is estimated for this system.

The accessible resource base (ARB) down to a depth of 7 km (ARB) is 14.23×10^{18} J, assuming a geothermal gradient of 32 °C/km and a mean rock density of 2650 kg/m³. The heat in place (H₀) contained in the aquifer was obtained assuming an effective porosity of 15 %, a mean thickness of 1200 m, 30 °C for the temperature at the top of the aquifer, a heat capacity of 800 J/(kg K) as well as a rock density of 2350 kg/m³. The mean surficial temperature in the region is 13 °C. The value obtained for the heat in place is 0.39×10^{18} J considering an area of 8.56 km².

Acknowledgements

We would like to thank to Prof. Andrade Afonso for his comments and geoelectric data. Geological work in Chaves Region was conducted by Prof. Portugal Ferreira.

Azores

F. Aumento

The Azores archipelago lies on the triple junction between the Mid-Atlantic Ridge and the Azores-Gibraltar Ridge. To the W lies the North American Plate and to the E the Euroasian and African Plates. The nine major islands, comprising a surface of 2.33 km², extend over an elongated submarine platform running WNW-ESE which extends over 615 km from Santa Maria in the E to Corvo in the W. Only the westernmost islands of Corvo and Flores lie on the North American Plate, to the W of the Mid-Atlantic Ridge (HIRN et al., 1993).

São Miguel (Plate 60)

São Miguel straddles the Terceira Ridge. The oldest part of the island (3 Ma) is at Nordeste. From E to W, Furnas, Agua de Pau and Sete Cidades are three active volcanic systems. Most spectacular are the geothermal manifestations of Furnas: hot grounds, steaming vents, fumaroles, hot bubbling mud pools, and hot springs. In Agua de Pau, commercial geothermal development has taken place, and there are several emissions of hot waters (HENNEBERGER and ROSA NUNES, 1991). Sete Cidades has the least impressive manifestations.

The *Agua de Pau* system is a 947 m high strato-volcano with abundant geothermal manifestations on the northern slopes of the volcano, from Lagoa do Fogo down to Ribeira Grande. The *Ribeira Grande* geothermal field lies on the northern flanks of this large volcanic complex. There are also minor fumaroles within the northern rim of the caldera, and to the S of the volcano, in the sea off Ribeira Cha, and more recently just inland from the town of Vila Franca do Campo.

Linear radon anomalies form sub-parallel NW-SE and NE-SW zones indicating areas of higher permeabilities. The main upwelling limb of the geothermal system ascends along NE-SW faults within the oceanic lava series, at the northern caldera rim. A second, sub-parallel upwelling limb ascends at the southern rim. Geothermal fluids disperse from these fractures flowing down to the sea along permeable horizons or systems of NW-SE fractures. The pillow lava sequence is less permeable than the overlying pyroclastics and lavas. Downslope geothermal fluid flow probably follows the lowest subaerial pyroclastic and the aereal/marine transitional horizon. Vertical fluid flow is facilitated by the more competent basaltic lava flows, which retain open fissures more readily than the overlying poorly consolidated material.

In 1980, an atmospheric discharge turbogenerator fed by borehole PV-1 began working at Pico Vermelho. This small station is still in operation, but is plagued by scaling. Reaming out is undertaken periodically. In 1989, geothermal production borehole CL-1 was sited a considerable distance uphill, towards Lagoa do Fogo. Borehole CL-2 was drilled in 1992. The first commercial geothermal power station went on line in 1994, producing 5 MW_e from the Ribeira Grande Geothermal field.

In the N area bounded by Riberinha, Pico da Trindade, Cerrado Novo and Caldeiras do Ribeira Grande, exploitation would have several advantages. There would be no interference with current exploitations upslope. The terrain is stable and of easy access. Competent lithologies and lower hydrostatic heads offer easier drilling conditions and water supply aquifers would not suffer contamination.

The scarcity of manifestations on the southern slopes may be due to reduced faulting activity or to a more deeply buried geothermal system. Preliminary rare gas exploration and geoelectric prospecting indicate that conditions are similar to those on the northern slopes.

The geothermal manifestations in *Furnas* include hot, highly mineralized springs, some with gas and steam emissions and temperatures at the boiling point. Most of the Furnas water is meteoric, heated by hot volcanic gases rising from the depths. The high CO₂/Rn ratios are indicative of low permeabilities or of very limited geothermal activity at depth. Furnas is a protected natural area and touristic zone and probably no geothermal development will be permitted in the near future. There are other geothermal manifestations outside the protected area, which may offer an alternative: on the coast at Ribeira Quente and in the valley of Ribeira dos Tambores. Neither have been investigated in detail yet.

Terceira (Plate 60)

Terceira island was built up through successive, sometimes contemporaneous eruptions of predominantly oceanic alkali basalts. Activity commenced with the formation of a large basaltic shield 300 ka with subsequent collapses along NNW-SSE. Four volcanic massifs then

built up the visible part of Terceira: *Cinco Picos*, *Guilherme Moniz*, *Pico Alto*, *Santa Barbara* and the *Central Rift* (SELF, 1986). The latest eruptions occurred in 1761.

Current hydrothermal activity is to be found only within the Furnas do Enxofre area at the intersection of NNE-SSW, NW-SE and E-W faults. Although sulphur occurs around some of the vents, there is no hot or mineralized water. Linear radon anomalies trend NW-SE and NE-SW, delineating active fault zones. Anomalies are an order of magnitude higher than those found over the Ribeira Grande geothermal field on São Miguel.

A magnetotelluric survey suggests that geothermal activity is more intense in the S-SE part of the *Pico Alto* area, and is controlled by active NE-SW faults. In spite of geophysical evidence for a geothermal field (ANDERSON et al., 1983), there is not much visible present-day hydrothermal. Yet, exploratory boreholes record 150 °C at depths of only 150 m near Furnas de Enxofre. The geothermal aquifer consists of a thin tabular body with area and volume of 57 km² and 28 km³, respectively. It is thin and close to the surface at the S of the Pico Alto area. It dips to the NW, thickening and dropping below sea level as it reaches the coast. Pico Alto has a probable energy potential of 25 MW_e. The southern region is the most promising for a feasibility study for commercial exploitation (AUMENTO, 1994).

Graciosa (Plate 60)

The island of Graciosa differs from other islands of the central part of the Archipelago: it is the only one without historic volcanism. Lying at the W end of the Terceira Rift, it comprises several *en echelon* basins separated by various horsts and massifs. Faults with major topographic expression follow NW-SE, dipping NE and SW, and show evidence of right-lateral slip. Of secondary importance are N-S normal faults, dipping E and W. Gas emissions occur along NE-SW.

The island can be divided into four zones: *Serra das Fontes*, with the oldest rocks outcropping on the island (620 ka; FERRAUD et al., 1980); *South-Central Massif* (270 ka) composed of trachytic domes and pyroclastics covered by recent basaltic lava flows and scoria; the *Caldeira Massif*, on the SE end of the island, an important central volcano with basaltic lava flows interlayered with pyroclastics and lahars, with a small caldera originated at 12.7 ka; and the *NW Platform*, a flat area of *pahoehoe* and *aa* lava flows. Continuing subterranean volcanic activity is indicated by gas emissions at Furna do Enxofre and the thermal springs (Carapacho and Baía dos Homiziados) associated with the central volcano.

Recent surveys revealed important linear radon anomalies concordant with the visible tectonic lineaments and a younger NE-SW trend. These anomalies have magnitudes of the order of those on Terceira, suggesting the existence of geothermal activity in open fractures.

Faial (Plate 60)

Faial, closest island to the axis of the Mid-Atlantic Ridge, is characterized by the NW step-faulted Flamings Graben, with active volcanic centres. A NE-SW fracture system, such as found on other Azores islands, is superimposed onto these regional faults.

In 1957, a submarine volcano appeared 1 km off the western tip of Faial, at Capelas. Several islands were formed and eventually, by 1958, had grown sufficiently in size so as to attach themselves to Faial, forming the Capelinhos peninsula. Recent (1993) submarine activity offshore to the NW shows that this activity continues periodically, extending the Flamings Graben lineament (now a series of 15 cones aligned NW-SE) westwards into the sea. The most recent eruption, at the W end of the island, has yet to establish a working hydrothermal system. However, tectonic activity opened up new fractures to the E, some with fumarolic activity and emanations of rare gases. Upwellings occur along NE-SW fractures, and flows downslope along NW-SE fractures and faults (DEMANGE et al., 1982).

The size of the island, the population density and its political and economic development provide a favourable scenario for the development geothermal energy sources.

Present status and future perspective of the use of geothermal energy

Thermal springs have been used for baths and medical treatments since Roman times. In recent years, several low-enthalpy geothermal

installations have been built, and private companies are showing a growing interest in geothermal development. Although there are good prospects for fish farming, the geothermal resources of the Hesperic Massif are applied in urban heating complexes only, such as swimming-pools, hotels and spas, and greenhouses for growing tropical fruits; other uses include the production of warm sanitary water (50 °C) and the heating of a hospital in Lisbon, from a borehole reaching Aptian-Albian sandstones in the Lisbon basin (CARVALHO and CARDOSO, 1994).

On some of the Azores islands there is considerable need for geothermal energy (São Miguel and Terceira), others (e.g., Flores) are of a size, and with a population density insufficient to warrant the exploration and exploitation costs. This situation may change if the transmission of electricity via underwater cables proves more cost effective. In São Miguel, a small turbogenerator fed by a single borehole with a capacity of 500 - 700 KW_e operated for more than a decade. A 5.4 MW_e Rankine cycle power station went on line in 1994.

References

- Airões-Barros, C.A.R., 1981 : Sobre as potencialidades em geocalor de alguns pólos geotérmicos do continente português. - Boletim de Minas, n18, mº2, p.1-8.
- Aires-Barros, L., Marques, J. M. and Graça, R. C., 1993: O papel da geoquímica isotópica na avaliação dos recursos geotérmicos da região de Chaves. - Recursos Hídricos, Rev. da Associação Portuguesa dos Recursos Hídricos / APRH, vol. 14, nº 2 e 3, p 73-80.
- Anderson, E., Ussher, G. and Tearney, K., 1983: Geophysical Survey of the Pico Alto Geothermal Prospect, Terceira Island, Azores. - Geotherm. Res. Council, Trans., p. 385-390.
- Aumento, F., 1994: TERGEOTER: Terceira Geothermal Project. - Commission of the European Communities D.G. XII Non Nuclear Energy Programme 1991-94 (Joule II); Contract # J0U2-CT92-114. Final Report.
- Calado, C., 1991: Carta de Nascentes Minerais 1:1.000.000. Portugal. - Atlas do Ambiente. Ministério do Ambiente e Recursos Naturais. Direcção-Geral de Recursos Naturais.
- Carvalho, J. M., 1993: Mineral and thermal water resources development in the portuguese hercynian massif. - Memoires of the XXIVth Congress of IAH, ÅS, Oslo, p. 548-561.
- Carvalho, J. M. and Cardoso, A. A. T., 1994: The Air Force Hospital geothermal project in Lisbon. - Geothermics'94 in Europe, document BRGM nº 230, Éditions BRGM, Orléans, p. 441-448.
- Demange, J., Fabriol, R., Gerard, A. and Iundt, F., 1982: Prospection Géothermique Iles de Faial et de Pico (Açores). Rapport Géologique, Géochimique et Gravimétrique. BRGM nº 82, N 003 GTH.
- Duque, M. R. And Mendes-Victor, L. A., 1993: Heat flow and deep temperature in South Portugal. Studia Geoph. et Geod., 37, p.279-292.
- Ferraud, G., Kaneokola, I., Allegre, G.J., 1980: K/Ar ages and stress pattern in the Azores: Geodynamic implications. - Earth and Planet. Sci. Lett., 46, p. 275-286.
- Fernández, M., Almeida, C. and Cabal, J., 1995: Heat flow and heat production in Western Iberia. - Proc. World Geothermal Congress 1995, Florence, Italy, May 18-31, (Eds: Barbier, E., Frye, E., Iglesias, E. and Pálmason, G.), v. 2, p. 745-749.
- Haven, H. L. T., Konings, R., Schoonen, M., Jansen, J. B. H., Vriend, S. P. Van Der Weijden, C. H., and Buitenkamp, J., 1985: Geochemical studies in the drainage basin of the Rio Vouga (Portugal) - II. A Model for the origin of hydrothermal water in the Vouzela Region. - Chemical Geology, v. 51, p. 225-238.
- Henneberger, R. C. and Rosa Nunes, J., 1991: A new discovery well in the upper Agua de Pau Geothermal System, São Miguel Island, Azores: Results of drilling and Testing. - Geotherm. Res. Council, Trans., p. 1-6.
- Hirn, A., Lápine, J.-C., and Sapin, M., 1993: Triple Junction and Ridge Hotspots: Earthquakes, Faults, and Volcanism in Afar, the Azores, and Iceland. - J. Geophys. Res., 98, B7, p. 11995-12000.
- Instituto Geológico e Mineiro (IGM), 1994: Análise físico-química completa dos furos AC1 e AC3 das Caldas de Aregos. - Report, 16 p.
- Lemos, L. S., Moreira, A. D., Nolasco Silva, M. C., Pires, M. R. and Sousa, P. O., 1992: Contribuição para a investigação do campo geotérmico de S. Pedro do Sul. - Estudos, Notas e Trabalhos, D.G.G.M., t. 34, p.107-138.
- Marques, J. M., Aires-Barros, L. and Graça, R. C., 1993: Sobre a aplicação da modelação matemática à hidrogeoquímica das águas termais de Chaves. - Recursos Hídricos, Rev. Associação Portuguesa dos Recursos Hídricos / APRH, Vol. 14, N° 2/3, p 89-93.
- Mendes-Victor, L. A., Duque, R. M., Correia, A. and Espírito Santo, T. R., 1991: Portugal. - In: Geothermal atlas of Europe, (Eds.: Hurtig, E., Cermák, V., Haenel, R. and Zui, V.), Hermann Haack Verlagsgesellschaft, Gotha, Germany, p.70-71.
- Moitinho de Almeida, F., 1982: Novos dados geotermométricos sobre as águas de Chaves e S. Pedro do Sul. - Com. serv. Geol. Portugal, t. 68, fasc. 2, p. 179-190.
- Self, F., 1986: The recent volcanology of Terceira, Azores. J. Geol., London, 32, p. 645-666.
- UTAD (Universidade de Trás-os-Montes e Alto Douro), 1992: Evaluation of geothermal resources between Lamego and Vila Verde da Raia. - Geological final report, Programme JOULE/ECE-JOUG-0009-C.

ROMANIA

D. Panu, H. Mitrofan, L. Codrescu, O. Militaru, M. Preda, C. Radu, M. Stoia and F. Serban

Geothermal thematic map (Plate 61)

Romania extends over a variety of tectonic units. The Pannonian Basin is bounded to the W by the Western Carpathians and to the S by the Southern Carpathians. The Transylvanian Basin is surrounded by the Western, Eastern and Southern Carpathians. In the S and E, the Getic and Pericarpethian Fordeeps separate the Southern and Eastern Carpathians from the Moesian and Moldavian platforms, respectively.

Extensive geothermal resources have been identified so far in sedimentary basins situated to the W (Pannonian Depression) and to the S (Moesian Platform). Additional geothermal resources in the Getic Foredeep and in the Neogene volcanics of the Eastern Carpathians are essentially isolated occurrences and not suitable for isoline representation.

Geothermal installations are preferentially situated in the NW of the country, the Pannonian Basin. A few have been installed in the Getic Foredeep and the Moesian Platform. Applications include: balneology, space heating, domestic hot water, greenhouses and industrial uses such as milk pasteurization and timber drying.

Information on the aquifers presented here derives from boreholes drilled for geothermal exploration, and, to a lesser extent, from oil and gas boreholes. Reservoir mapping relied largely on reflection seismics. Most of the data used in the preparation of this work are detained by the oil company FORADEx S.A. Additional data and cartographic information were incorporated from ORASEANU (1994) and IORDACHE et al., (1994). Other sources of information on geothermal aspects of Romania are the publications by COHUT (1994), MITROFAN et al. (1992), DEMETRESCU et al. (1991) as well as VELICIU and VISARION (1984).

Temperatures (Plate 61)

The geographic distribution of subsurface temperature data and heat-flow density (VELICIU, 1994) is rather irregular, most of them being concentrated in the center and E of the Transylvanian Basin, in the Neogene volcanic ridge of the Eastern Carpathians, in the Moesian Platform and in the Carpathian Foredeep. Observations are scarce in the Southern Carpathians, in the Moldavian Platform, in the S of the Moesian Platform and in the W of the Transylvanian Basin. The coverage is also poor in the Western Carpathians and on the E border of the Pannonian Basin. Temperature at 500 m depth increases from E to W, being more elevated in the Pannonian Basin, the centre of the Transylvanian Basin and the Moesian Platform. This temperature pattern is also observed at greater depths.

Potential geothermal reservoirs

In addition to the extense region of the Moesian platform, several smaller regions, in parts of the Pannonian Basin in the NW, have been evaluated and are shown on the resources map at the national scale. Geothermal resources per unit area of these regions range from 1 - 30 GJ/m², while much larger values are computed for the Moesian Platform.

Moesian Platform

Late Jurassic-Early Cretaceous (Plate 61 and 62)

The reservoir consists essentially of an E-W striking carbonate slab, of variable dip. Vigorous fluid flow generates thermal maxima and minima, alternating every 2 - 3 km along the general strike of the reservoir. As a result, temperature contrasts of 20 - 40 °C at similar depths of the top of the reservoir may occur, even within restricted areas. At the scale of the maps presented here, it is virtually impossible to draw in detail the corresponding isotherms. Moreover, temperature distribution affected by fluid flow within the reservoir is difficult to predict. Under these circumstances, the maximum temperature expected at the top of the reservoir in selected favorable areas was considered for resource evaluation.

Recorded piezometric levels are > 25 m a.s.l. As a consequence, most boreholes have their static water level several 10 m below ground, so that withdrawal by pumping is compulsory. The large reservoir thickness (up to 1300 m) favours radial spherical flow toward restricted pay zones tapped by production boreholes. As a result, the aquifer undergoes virtually no pressure decline during exploitation. The values of 1 % and 120 mD derived for porosity and permeability, respectively, are probably characteristic of highly fractured reservoir sections. Corresponding bottomhole specific yields are 10 - 40 l/(s bar) compared to 1 - 6 l/(s bar), recorded in the more compact sections.

Pannonian Depression

Middle Triassic (Plate 62)

Triassic carbonate rocks occur in the basement of the Pannonian Depression as an isolated body, that extends 10 - 20 km in the vicinity of the city of Oradea. A major fracture zone, situated W of Oradea, separates two distinct reservoir compartments.

In the thinner, western compartment, permeable areas form linear fluid pathways, with net thicknesses of a few 10 m. An 'instantaneous' bottomhole specific yield of 2 l/(s bar) was estimated. In addition, the reservoir pressure, initially 4 - 15 bar above hydrostatic, undergoes severe decline as a result of exploitation. The geothermal fluid has 5 - 15 g/l TDS, with 1 Nm³/m³ and 4 Nm³/m³ of dissolved CO₂ and CH₄, respectively. Maximum well-head temperatures reach 125 - 130 °C.

In the eastern compartment, the temperature and salinity distribution is controlled by regional fluid flow: hot upflow of rather low salinity fluid (< 2 g/l) takes place along the major fracture zone W of Oradea, cools and becomes more dilute while flowing eastward and eventually discharges through the natural thermal springs at Felix spa. Reservoir pressures vary accordingly, from 7 bar above hydrostatic W of Oradea, to hydrostatic near the spring at Felix. The large (600 - 1200 m) reservoir thickness favours radial spherical flow toward restricted pay zones tapped by production boreholes, so that there is virtually no pressure decline in the reservoir during exploitation. The reservoir has low overall porosity (1 %) and permeability (0.3 - 25 mD), yet, since productivity is controlled by local, highly permeable fractures incidentally intercepted by boreholes, bottomhole specific yields of 4 - 11 l/(s bar) are normally encountered.

Another deeply buried and thick reservoir compartment exists N of Biharia, but no productivity information is available for it.

North and South Pliocene (Plate 63)

The entire Pliocene section (ALEXANDRESCU et al., 1984) includes reservoir rocks consisting of slightly consolidated sandstones. Only those reservoir sections tapped by most of the productive geothermal boreholes, have been designated as the 'Main Aquifer'. They occur in several distinct, not always synchronous depositional sequences, occupying roughly the median part of the Pliocene section.

Pliocene sandstones occur as linear interconnected bodies (probably old channel fills and bars, surrounded by shaly interchannel and levee deposits). According to spinner surveys, the net pay zone within the Main Aquifer is usually a few 10 m thick. Porosities between 20 - 35 %, and core permeabilities of 0.2 - 2.6 D have been measured. Since well tests indicate that values of 10³ - 10⁶ D m² (permeability x throughflow-area) are characteristic for the linear aquifer bodies, the lateral extent of the throughflow-areas should range between a few 10 m and a few km. Bottomhole specific yield of individual wells are generally 3 - 6 l/(s bar), exceptionally 25 l/(s bar). Reservoir pressures were initially several bars above hydrostatic, but nowadays the water level has declined down to 5 - 45 m below ground in most of the exploited fields. As a general rule, 1 - 2 Nm³/m³ of CH₄ is dissolved in the geothermal water of the reservoir.

The maximum artesian discharge was assessed by numerical simulation, for those boreholes for which the required parameters were available. If necessary, interference between boreholes belonging to the same field was taken into account. Seasonal withdrawal was considered under declining reservoir pressure conditions. As a result, an artesian lifetime of 5 years starting from 1995, was predicted.

Present status and future perspective of the use of geothermal energy

Geothermal resources (H_1) have been calculated for each aquifer assuming exploitation with singlets, which proved operational during almost two decades. For the Pliocene reservoir, resources have been calculated for few distinct areas, where necessary data is available. For the Late Jurassic - Early Cretaceous reservoir, a 2/3 reduction was applied, in order to account for the fact that resource computations had used the maximum temperature, expected in selected favorable areas only. For the three considered reservoirs, the resources, H_1 , are:

Middle Triassic:	12 x 10 ¹⁸ J
Pliocene:	1 x 10 ¹⁸ J
Late Jurassic - Early Cretaceous:	160 x 10 ¹⁸ J

During 1974 - 1989, geothermal heating installations funded by government development programmes (PANU, 1995) started operating in 18 sites in the Pannonian Depression, in 2 sites in the Moesian Platform, and in 2 sites in the Getic Foredeep. A new heating installation to be located in the Getic Foredeep has been commissioned in 1994.

Most geothermal installations provide space heating and domestic hot water to small towns and villages (Tasnad, Marghita, Curtici, Nadlac, Sânnicolau Mare, Jimbolia, Calimanesti, etc.), but also to the city of Oradea. Geothermally heated greenhouses are operating at Acâs, Sacuieni, Bors, Oradea, Ciurmeghi, Salonta, Curtici, Macea, Dorobanti and Tomnatic. Industrial uses include milk pasteurization and timber drying, in factories at Oradea and Sacuieni. Many of the direct-use installations supply geothermal water also to balneological resorts.

References

- Alexandrescu, M., Burghina, V., Gheorghiu, G., Graf, C., Lungu, A. and Popescu, M., 1984: Sinteza lucrărilor de prospectiune și explorare pentru ape geotermale din Câmpia de Vest. - Raport IPGG XV/6.
- Cohut, I., 1994: Utilisation of geothermal resources in Romania - Course text-book, International summer school on direct application of geothermal energy, Oradea, p.45-50.
- Demetrescu, C., Veliciu, S. and Burst, A. D., 1991: Romania. - In: Geothermal atlas of Europe, (Eds: Hurtig, E., Cermák, V., Haenel, R., Zui, V.), Hermann Haack Verlagsgesellschaft mbH, Geographisch-Kartographische Anstalt Gotha, p. 72-73.
- Iordache, S., Margaritescu, C., Popa, Gh. and Vacarescu, Gh., 1994: Moesian Platform, Late Jurassic-Early Cretaceous structural maps and additional hydrogeothermal informations. - PETROM R.A., 103 Toamnei str., 72152 Bucuresti.
- Mitrofan, H., Cohut, I., Tudor, M. and Sarbulescu, M., 1992: La geothermie en Roumanie. - Reseaux & chaleur, 16, p. 21-27.
- Oraseanu, N., 1994: Harta surselor geotermale din România. - Raport "Prospectiuni S.A." 100/1993, Prospektiuni S.A., 1 Caransebes str., 78344 Bucuresti.
- Panu, D., 1995: Geothermal resources in Romania - Results and prospects. - Proc. World Geothermal Congress 1995, Florence, Italy, May 18-31, vol1, p. 301-308.
- Veliciu, S., 1994: Geographic distribution of the geothermal field on Romania's territory. - Raport IGR 112/93-94, Geological Institute of Romania, 1 Caransebes str., 78344 Bucuresti.
- Veliciu, S. and Visarion, M., 1984: Geothermal model for the East Carpathians. - Tectonophysics, 103, p.157-165.

RUSSIA

G. S. Vartanyan, V. A. Komyagina and A. A. Shpak

Geothermal thematic map (Plate 64)

In the European part of Russia, the geothermal resources are found in the artesian basins of the Epipaleozoic *Scythian Platform* to the N of the Alpine folded Caucasus and also, in the large artesian basins of the Pre-Cambrian *East-European Platform*.

The artesian basins on the *East-European Platform* extend over most of western Russia. These deposits consist mostly of Palaeozoic rocks containing brines. In this area, heat-flow density varies from 38 - 67 mW/m² and the average geothermal gradient in Palaeozoic sedimentary rocks is close to 17 °C/km. The NE of the Moscow Artesian Basin (Roskovskoye Syncline) is the most promising region for geothermal water. The heat-flow density of the Moskovskaya Syncline is 46 mW/m². The geothermal gradient varies from 16 - 25 °C/km. This variation is caused mainly by differences in the lithological composition of the sedimentary cover.

The sediments covering the *Scythian Platform* are younger than the sedimentary cover of the East-European Platform. It is made up of Meso-Cenozoic sedimentary rocks including salt-bearing sediments that contain fresh water and brines. The permeability of these Meso-Cenozoic rocks is much higher than that of Palaeozoic sediments in the Pre-Cambrian Platform, because of lower degrees of compaction and diagenesis. The Scythian Platform is characterized by heat-flow density of 54 - 92 mW/m². The geothermal gradient in the Meso-Cenozoic strata varies from 30 - 40 °C/km. In zones of discharge of thermal water, along faults or erosive discontinuities, it increases to 50 - 60 °C/km. Two large geothermal potential regions can be defined in the Scythian Artesian Basin: N Caucasus on the territory of Russia and the Crimea Plain that extends beyond Russia into the Ukraine. The N Caucasus hosts a complex confined aquifer system consisting of large artesian basins interconnected with each other: the Azov-Kubansky and the East-For-Caucasian basins, separated by the Stavropolskoye dome. About 9 aquifers can be distinguished in the the Meso-Cenozoic sediments. The most promising for thermal water exploration are the Middle Miocene (Karagan-Chokraksky) and Lower Cretaceous aquifers.

More information on geothermal resources in Russia can be found in DYADKIN and VAINBLAT (1991), KULIKOV and MAVRITSKY (1984), MAVRITSKY and SHPAK (1983), SHPAK (1980), SHPAK and ANTONENKO (1994). Some of the methodical approaches used in Russia are described in BONDARENKO and VARTANYAN (1986), SEKEI and SHPAK (1986).

Potential geothermal reservoirs

Moscow Basin (Moskovskaya Syncline)

The main thermal aquifers are *Middle Devonian* and *Middle Cambrian* formations. The thermal fluid contained in these confined aquifers are of Na-Ca-Cl-CH₄ composition with a salinity of 150 - 300 g/l. The main recharge areas are the S and W borders of the Moscow Artesian basin. The pressures are highest in the central and NE areas of the basin. Practically all information derives from exploration boreholes for oil and gas. Only one borehole was specially drilled for thermal water within the Medyaginskaya area.

The largest geothermal resources of the Middle Devonian and Middle Cambrian aquifers are found in the eastern and deepest part of the Moskovskaya Syncline. Geothermal resources are greater in the lower Middle Cambrian than in the Middle Devonian above it, because of higher ground water temperatures, although the hydrologic properties are less favorable.

The accumulated geothermal resources for both aquifers add up to an energy density of 2 - 3.6 GJ/m², except for areas where only one (Middle Devonian) water-bearing complex is present and not more than 1 GJ/m² is estimated to be available. The total geothermal resources of Moskovskaya Syncline are estimated at 1.33 x 10¹¹ GJ. This is equivalent to 4.5 x 10⁹ t of conventional fuel. A (t.c.f.) ton of conventional fuel is an unit widely used in Russia. It attempts to furnish the order of magnitude of possible amounts of fuel that can be saved; 1 t.c.f. is equal to 29.4 GJ.

Middle Cambrian (Plates 65 and 67)

The Middle Cambrian aquifer is situated in the northern part of the Moskovskaya Syncline. It is composed of quartz sandstone with subordinated interbeds of siltstone, mudstone and clay. The total thickness of the section is about 250 m, while the net thickness ranges from 12 - 97 m. The permeability varies from 0.05 - 1500 mD and porosity from 5 - 17 %. The depth to top of the aquifer increases from W to E. The formation temperature increases with depth.

Summary of geothermal resources for the Middle Cambrian aquifer

Num-ber	Name of Area	Formation Temperature (°C)	Effective Thickness (m)	Effective Porosity (%)	Total Heat (GJ/m ²)	Geothermal Resources (GJ/m ²)
7	Soligalichskaya	51	2	10	0.2	0.02
13	Pestovskaya	25	81	15	2.8	0.06
14	Lyubinskaya	54	80	10	8.3	1.80
15	Buiskaya	57	41	10	4.6	1.03
16	Galichskaya	57	40	10	4.4	0.97
17	Bukalovskaya	62	50	10	6.2	1.40
18	Danilovskaya	58	65	10	7.4	1.70
23	Rybinskaya	55	60	10	6.3	1.40
25	Tolbukhinskaya	63	70	10	8.8	2.10
26	Sudislavskaya	52	60	10	5.9	1.20
30	Medyaginskaya	53	75	10	7.6	1.60
31	Nekrasovskaya	51	97	10	9.3	1.90
37	Iliyinskaya	32	12	15	0.6	0.06
39	Pereslavskaya	34	21	15	1.2	0.15

*see map on Plates 64 and 67

The areas in Tolbukhinskaya, Nekrasovskaya and Lyubimskaya concentrate geothermal resources of 2.1, 1.9 and 1.8 GJ/m², respectively.

Middle Devonian (Plates 66 and 67)

The Middle Devonian aquifer extends throughout the Moskovskaya Syncline and comprises interbedded sand, sandstone, clay and siltstone. The total thickness of the complex ranges from 200 - 270 m, increasing in the near-axis zone of the Syncline to 400 - 450 m. The net thickness of the water-bearing layers is 60 - 120 m and the permeability varies from 0.1 - 2500 mD. Porosity is 10 - 20 %. The top of the aquifer dips from W to E.

The greatest accumulation of geothermal resources in the Middle-Devonian reservoir is found in Danilovskaya, Lyubimskaya and Galichskaya with 1.9, 1.7 and 1.6 GJ/m², respectively.

Summary of geothermal resources for the Middle Devonian aquifer

Num-ber	Name of Area	Formation Temperature (°C)	Effective Thickness (m)	Effective Porosity (%)	Total Heat (GJ/m ²)	Geothermal Resources (GJ/m ²)
3	Gagarinskaya	32	70	10	3.6	0.4
7	Soligalichskaya	37	76	10	4.6	0.7
14	Lyubimskaya	44	117	10	9.1	1.7
15	Buiskaya	50	80	10	7.3	1.5
16	Galichskaya	51	76	10	7.3	1.6
17	Bukalovskaya	44	80	10	5.4	1.0
18	Danilovskaya	53	92	10	9.2	1.9
19	Neiskaya	39	82	10	5.4	0.9
23	Rybinskaya	40	58	10	3.9	0.6
25	Tolbukhinskaya	46	75	10	6.2	1.2
26	Sudislavskaya	38	95	10	6.0	0.9
30	Medyaginskaya	36	54	10	3.2	0.4
31	Nekrasovskaya	39	90	10	5.9	0.9
37	Iliyinskaya	26	80	15	3.0	0.06
39	Pereslavl'skaya	28	65	15	2.7	0.15

Azov-Kubansky Basin

(Early Cretaceous) (Plates 67 and 68)

The geothermal aquifer in the Azov-Kubanian Artesian Basin is the Early Cretaceous section at depths generally greater than 2000 m. It consists of conglomerates, clay, sandstone and siltstone 190 - 300 m thick. The net thickness of water-bearing layers is 40 - 150 m. This aquifer contains mostly saline water and brines of Na-Cl-CH₄ composition.

Among the potential areas associated to the Early Cretaceous aquifer, those located in the SE margin of the basin (such as Mostovskaya, Voznesenskaya, Kazminskaya, Labinskaya and others) are of high economic interest. The favourable conditions can be related to an extensive area with low-salinity water (1.2 - 3 g/l) and increased permeability due to the rather broad zone weakened by crustal extension. In cross-section, 3 - 4 productive sandstone layers 65 - 120 m thick can be defined. As the aquifer deepens, formation temperatures increase from 70 - 140 °C. Piezometric head varies from 25 - 170 m. An artesian borehole yields 2000 - 3000 m³/d.

At present, 20 fields of thermal water are exploited within the Azov-Kubanian Basin (Krasnodarsky and Stavropolsky Regions, the Adygei Autonomous Republic). Maximum concentration of geothermal resources is found around Voznesenskaya, Labinskaya and Maikopskaya (7.9, 6.0 and 5.4 GJ/m², respectively), because of high temperatures and favorable hydrological properties of the rocks. The total geothermal resources of the Early Cretaceous are estimated at 8.6 x 10¹⁹ J, a rather impressive value (the averaged density of resources is 5.1 GJ/m²) for its relatively small size (16.9 x 10³ km²).

Summary of geothermal resources of the Azov-Kubanian Basin (N Caucasus)

Num-ber	Name of Area	Formation Temperature (°C)	Effective Thickness (m)	Effective Porosity (%)	Total Heat (GJ/m ²)	Geothermal Resources (GJ/m ²)
49	Ust-Labinskaya	140	70	10	18.8	6.0
50	Armavirskaya	123	40	10	8.4	2.6
52	Novo-Yaroslavskaya	95	80	15	12.6	3.9
53	Labinskaya	106	101	15	19.2	6.0
54	Uliyanovskaya	85	77	15	10.7	3.3
55	Mostovskaya	77	152	15	18.0	5.4
56	Voznesenskaya	120	118	15	25.5	7.9
57	Kaz'minskaya	133	40	10	9.5	2.8
58	Voskresenskaya	124	53	15	12.3	3.8
59	Otradnenskaya	110				
60	Maikopskaya	95	107	15	17.2	5.4
61	Cherkesskaya	70	101	10	10.0	2.9

Additionally, four areas in the North Caucasus also explore thermal water contained in the *Pliocene* formations.

East Fore-Caucasian Basin

Middle Miocene (Plates 67 and 69)

In the East Fore-Caucasian Artesian Basin, the Middle Miocene (Karagan-Chokrak) aquifer is of geothermal interest and especially the Sunzhenskaya anticlinal zone of the Tersko-Sunzhensky Basin (Hankalskaya and Goitinskaya). It is composed of marine terrigenous and sometimes carbonate formations, including clay, sandstone, sand, siltstone with interbeds of limestone and marl. The total thickness varies from 100 - 900 m, with net aquifer thickness at 24 - 260 m. The water is of Na-HCO₃-CH₄-NO₃ type.

In the Sunzhenskaya anticlinal zone, 24 sandy layers intercalated by clays can be distinguished. A geothermal anomaly is associated with intensive heat transport by fluid flow from beneath. The piezometric head is about 55 - 130 m, and artesian wells yield 1500 - 3500 m³/d. Here, the water is fresh (0.9 - 2.1 g/l) and of Na-HCO₃ type. In the 1970's, two productive aquifers were exploited in Hankalskaya using a doublet system. This was the first installation of this kind in Russia.

The potential geothermal resources are estimated to be 16.4 GJ/m² and 13.5 GJ/m², for Hankal and Goit, respectively. In spite of high temperatures of ground water (65 - 100 °C), geothermal resources in the remaining areas are much lower (1.4 - 5.0 GJ/m²), chiefly because of a decrease in the aquifer thickness and its effective porosity.

The East Fore-Caucasian Basin has 29 thermal-water fields under exploration with temperature of 40 - 106 °C (the Republics of Dagestan, Chechnya, Kabardino-Balkariya). Twenty four fields are currently being exploited at a rate of 18.9 x 10⁶ m³/a of geothermal fluid, saving of the order of 206.8 x 10³ t/a of conventional fuel.

The total geothermal resources of the region amount to (1-32) x 10¹¹ GJ, of the same order as those of the Moskovskaya Syncline. However, the area of the East Fore-Caucasian Basin is a factor of 2.6 smaller than the area of the Syncline.

Summary of geothermal resources for the East-Fore-Caucasian Basin

Num-ber	Name of Area	Formation Temperature (°C)	Effective Thickness (m)	Effective Porosity (%)	Total Heat (GJ/m ²)	Geothermal Resources (GJ/m ²)
63	Kayasula	82	89	10	9.9	3.0
64	Georgiyevskaya	65	92	10	7.4	2.2
65	Chervlenye Buruny	92	37	15	4.4	1.4
66	Tereklynskaya	93	24	15	3.4	4.0
67	Tarumovskaya	99	58	15	9.1	2.8
68	Kizlyar	110	35	15	8.0	2.5
70	Nalchikskaya	41	32	10	1.1	0.3
71	Chervlenskaya	93	107	15	16.3	5.0
72	Gunyushki	75	109	15	10.7	3.2
73	Goity	101	210	20	43.6	13.5
74	Kankala	102	263	25	53.0	16.4
75	Groznenskaya	103				
76	Gudermes	70	171	15	15.9	4.7
77	Novogroznenskaya	82				
78	Makhachkalinskaya	103	70	20	12.8	4.0
79	Izberbash	64	59	15	4.7	1.4
80	Kayakent	64	39	15	3.0	0.9

Present status and future perspective of the use of geothermal energy

At the present time, geothermal resources are widely used in the North-Caucasian Region for heating greenhouses, in municipal households, for balneological and other purposes.

The low potential (20 - 63°C) of the highly saline water and brines of the Moscow Basin may be of importance for exploitation using doublet technology associated to high efficiency heat-pumps.

Geothermal installations operate in three areas of the East Fore-Caucasian Basin with the re-injection of the exploited water into a productive layer. In the Azov-Kubanian Basin, such an installation is under construction.

The scale at which geothermal energy is used is expected to increase with the introduction of intensive doublet technology.

Summary of geothermal resources

Region	Surface (km ²)	ARB ₁ (x10 ¹⁸ J)	Heat in Place Resources H ₀ (x10 ¹⁸ J)	H ₁ (x10 ¹⁸ J)
North Caucasus	58.275	17.890	702	218
Azov-Kubanian Basin	16.875	5.470	245	86
East Fore-Caucasian Basin	41.400	12.420	457	132
Moskovskaya Syncline	108.675	19.560	769	133
Russia	166.950	37.450	1.471	351

References

- Bondarenko, S. S. and Vartanyan, G. S. (Eds.), 1986: Methods of study and estimation of deep groundwater resources. - Nedra, 479 pp.
- Dyadkin, Yu. D. and Vainblat, A. B., 1991: The Map of Geothermal Heat Supply Resources of the USSR Territory, Scale 1:10.000.000, Explanatory Note, Leningrad, 28 pp.
- Kulikov, G. V. and Mavritsky, B. F. (Eds), 1984: Atlas of geothermal resources in the USSR, Leningrad, VSEGEI.
- Mavritsky, B.F. and Shpak, A. A., 1983: Explanatory notes to atlas of maps on thermal resources in the USSR, VSEGINGEO, 113 pp.
- Sekei, F. and Shpak, A. A. (Eds.), 1986: Methodical recommendations on prospecting, exploration, estimation and mapping of hydrothermal resources (experience of the countries - COMECOM members and Yugoslavia), COMECOM, 130 pp.
- Shpak, A. A., 1980: Regional estimation of thermal water yield. - Soviet Geology, 9, p. 110-116.
- Shpak, A. A. and Antonenko, G. K., 1994: Hydrothermal Resources in the European Part of the Former USSR. - Hydrogeothermics, Vol. 15, Hannover, Heise, pp 57-85.

SLOVAKIA

A. Remšík, M. Fendek, M. Král and J. Mello

Geothermal thematic map (Plate 70)

The West Carpathians in Slovakia consist of an Alpine folded mountain system and Tertiary basins. The mountain system is divided lengthwise by the Clippen Belt into the Outer and Inner West Carpathians. The Outer West Carpathians comprise the Flysch Belt and Palaeogene sedimentary rocks. The Inner West Carpathians are characterized by abundant pre-Upper Carboniferous crystalline schists, Variscan granitoids, Late Palaeozoic sediments and volcanics, Mesozoic carbonates and pre-Senonian nappe structures. The region was affected by Alpine metamorphism and the formation and emplacement of granitoids. Post-Cretaceous vertical movements modified centres of deposition. Further tectonic activity caused the elevation of mountains and the creation of depressions that were filled with widespread Palaeogene and Neogene sedimentary and volcanic formations.

Geothermal water has been tapped by 76 boreholes drilled to depths extending from several 10 m to 2605 m. Natural outflow rates of these boreholes are 5 - 40 l/s and water temperatures at the well-head range from 20 - 92 °C. As far as the chemistry is concerned, the water is largely of Na-HCO₃-Cl, Ca-Mg-HCO₃-SO₄ and Na-Cl type. The salinity (TDS) is 0.7 - 20.0 g/l.

Temperatures (Plate 70)

A compilation of 376 temperature logs from deep boreholes forms the database for the temperature maps. These data sample all major structural-tectonic units of the West Carpathians. Both the vertical and geographic distribution of temperatures reveals major differences between the individual units.

The West Carpathians can be divided into two regions according to their subsurface temperature. Fairly low temperatures are characteristic of the core mountains in the central and northern Inner West Carpathians and of the western Outer Flysch Belt. In contrast, high subsurface temperatures typically occur in Neogene basins and volcanic mountains with adjacent intramontane basins.

Potential geothermal reservoirs

Geothermal resources occur S of the Clippen Belt (Inner West Carpathians). Here, 26 potential areas with geothermal energy have been defined. These are outlined on the map and include mostly Tertiary basins and intramontane depressions. The combined surface area of these 26 hydrogeothermal areas amounts to 27 % of Slovakia's territory. Geothermal water in these structures is bound largely to Triassic dolomites and limestones of the Krížna and Choč nappes (Fatricum and Hronicum), less frequently to Neogene sands, sandstones and conglomerates (Danube Basin central depression, Horné Strháre - Trenč graben, Dubník depression) and to Neogene andesites and related pyroclastics (Beša-Cičarovce structure). These geothermal aquifers are found at depths of 200 - 5000 m (outside spring areas) and contain geothermal water of 20 - 240 °C.

Low-temperature geothermal resources (T < 100 °C) prevail over medium- (100 - 150 °C) and high-temperature (T > 150 °C) resources. The heat content in individual hydrogeothermal areas ranges from 1 - 1317 MW_t. In total, these 26 hydrogeothermal systems contain 6608 MW_t.

Additional information is given in FRANKO et al. (1989), REMŠÍK et al. (1990), FRANKO (1995) and REMŠÍK and FENDEK (1995), as well as in the literature cited therein.

Liptov Basin

The Liptov Basin lies roughly between the Nízke (Low) and Západné Tatry Mountains. It is elongated in the E-W direction and covers an area of 611 km². This intramontane depression in the Inner West Carpathians is filled with Palaeogene sediments (claystones and sandstones), 100 - 1700 m thick (borehole ZGL-1 and Liptovská Mara, respectively). The pre-Palaeogene basement is rugged and its morphology is determined by the Choč and Krížna nappes.

Geothermal water in the Liptov Basin is discharged through springs and boreholes. One, two and possibly three aquifers might overlie one another below the Palaeogene, in the deep nappe structure of the basin. Geothermal waters of 20 - 140 °C occur at depths of 500 - 5000 m underneath the Palaeogene section. Four boreholes, 1987 - 2500 m deep, discharge geothermal water at rates of 6 - 31 l/s with a temperature of 32 - 62 °C.

Triassic of the Choč nappe (Plate 71)

The Choč nappe underlies Palaeogene sediments. This nappe consists almost exclusively of Middle and Upper Triassic dolomites and limestones interlayered with shales 100 - 200 m thick (Lunz Member - Carnian). At a regional scale, the Choč nappe is a complex of geothermal aquifers. Triassic dolomites and limestones of this nappe are widespread in elevated and sunken morphological features of the pre-Palaeogene basement in the central to eastern and westernmost sectors of the basin. These rocks form fairly large bodies, but occur also as small isolated portions. The mean porosity ranges from 15 - 25 % and the effective porosity, however, is < 5 %.

The geothermal resources per unit area reflect temperature patterns and aquifer thicknesses and rise from 0.5 GJ/m² at the edge of the basin to 6.0 GJ/m² in the centres of depressions.

Triassic of the Krížna nappe (Plate 71)

The Krížna nappe underlies the Choč nappe or, locally, lies directly underneath the Palaeogene sediments. This faulted unit presumably underlies the whole basin and forms elevations and depressions of more or less complicated shapes. Geothermal aquifers include Middle and Late Triassic dolomites and limestones. The Late Triassic to Early Cretaceous rocks (shales, limestones, sandstones, marls, marly limestones) make up a fairly impermeable complex and act as an aquiclude at a regional scale. Aquifer transmissibilities exceed those in the Choč aquifers. Mean porosity decreases with depth from 30 - 5 %, whereas effective porosity attains 2 - 5 %.

In this region, the distribution of geothermal resources displays a pattern similar to that in the Choč nappe and ranges from 0.6 GJ/m² to 6.5 GJ/m².

Danube Basin (central depression)

The central depression of the Danube Basin is situated between Bratislava and Komárno. It is filled with Quaternary and Rumanian gravels and sands as well as with Dacian, Pontian and Pannonian sediments (clays and sandy clays alternating with sands and sandstones). This depression evolved from the Pannonian to the Pliocene. It forms a brachysynclinal structure with its maximum depth in the Gabčíkovo area (borehole FGGa-1).

On the flanks and at the bottom, the reservoir is confined by relatively impermeable clay layers that dip from all directions towards the centre reaching a depth of 3400 m (borehole FGGa-1). The main geothermal aquifer consists of *Pannonian* and *Pontian* sands and sandstones. In the centre of the depression, it is made up of Dacian sands and sandstones. Intercalated clay layers form aquicludes. At a depth of 1000 m, the reservoir extends up to 75 km from NW - SE and 60 km from the NE - SW. It attains a maximum thickness of 2400 m in the centre. At the margin of the depression, the aquifer layers make up 50 % of the section. This percentage decreases to 20 % in the centre. However, as a result of the increasing thickness of the reservoir towards the centre, the total volume of aquifer increases along this direction.

Five hydrogeologic complexes have been distinguished in the reservoir with regard to lithology. Each is characterized by a certain ratio of aquifer to aquiclude layers. The lateral and vertical extent does not depend on the stratigraphy of the Neogene. The complexes are described on cross section II-II'.

The natural discharge of 34 geothermal boreholes drilled in the Central depression ranges from 3 - 25 l/s. These boreholes were drilled to depths between 500 - 2800 m tapping geothermal waters of 24 - 92 °C.

Pontian (Plate 72)

The *Pontian* encompasses the hydrogeologic complexes 2, 3, 4, and locally also 5 (cross section II-II'). The depth and thickness of the *Pontian* as well as the temperature at its top increase from the margins of the depression towards its centre due to the bowl-like shape of the structure. The permeability of the *Pontian* aquifer diminishes from the W and NW to the E and SE.

The geothermal resources per unit area increase concentrically from the edge of the depression towards its centre.

Pannonian - Pontian (Plate 73)

Hydrogeologic complex 3 is widespread in the upper section of the *Pannonian* and in the lower part of the *Pontian*. It locally underlies or is laterally adjacent to hydrogeologic complex 2 (cross section II-II'). Regardless of stratigraphy, both complexes together make up a single unit in the depression in which the aquifers attain 50 % or more of the section. These complexes are missing in the vicinity of borehole FGČ-1 and between boreholes FGT-1 and FGV-1. The minimum thicknesses are largely near the edge of the depression, while the maximum ones are in the centre (borehole FGGa-1).

On average, aquifer permeability here is lower than in the *Pontian* and it diminishes with depth. The permeability generally decreases from the NW - SE, and reaches maximum values in the N of the depression. The piezometric head exhibits a similar trend to that of the *Pontian*.

The geothermal resources (per unit area) reflect the thickness variations of hydrogeologic complexes 2 and 3 and increase from 1.0 GJ/m² at the edge of the depression to 15.0 GJ/m² in its centre.

Present status and future perspective of the use of geothermal energy

In Slovakia, geothermal water (except thermal mineral waters used for medical purposes in spas) is an auxiliary energy source. Given the lack of energy, rising energy prices, and necessity to protect the environment (especially the atmosphere), geothermal energy may be successfully and effectively exploited as a local source of heat or even electricity.

Slovakia is particularly rich in low-temperature geothermal resources (T < 100 °C). At present, the extent and technology of geothermal energy exploitation are inadequate. The recovery rate of the currently exploited geothermal resources is only about 20 %.

Geothermal water is used for space heating, recreation and swimming pools in 35 localities. Their combined discharge is 601 l/s and recoverable thermal power 83 MW_t. Buildings in three towns are partly heated in this way, and so are greenhouses covering 20 000 m² in ten localities. About 80 thermal pools exceeding a total area of 50 000 m² serve for swimming and recreation. Thermal spas and swimming pools can admit 75 000 visitors a day. Most exploited sources of geothermal energy are situated in southern Slovakia, primarily in the central depression of the Danube Basin. At Vrbov in the Vysoké Tatry area, geothermal water is used not only for recreation but also for fish farming. In the Liptov Basin, it is used for recreational swimming in one thermal spa (Bešeňová).

Essential conditions for geothermal energy exploitation have already been created in Slovakia. A project to heat 1300 flats, town hospital and a pensionist hostel in the town of Galanta in the Danube Basin is under preparation. The goal of another project is the construction of a reinjection station at Podhájska (to heat greenhouses and buildings with heatpumps and swimming pools). Geothermal water will also be used to heat 500 flats and an indoor swimming pool in the town of Poprad (Vysoké Tatry area).

Approximately 800 MW_t of geothermal resources will presumably be exploited by 2005. At a recovery rate of 45 %, it implies 360 MW_t of thermal power or 2160 GWh of energy. Geothermal energy will be used

for space heating, greenhouses, water for households, for drying, fish farming and in recreational as well as balneologic facilities. It could be harnessed to generate electricity in the Košice Basin.

References

- Franko, O., 1995: Geothermal energy exploration in Slovakia. - Proc. World Geothermal Congress 1995, Florence, Italy, May 18-31, (Eds: Barbier, E., Frye, E., Iglesias, E. and Pálmason, G.), vol 1, p. 619 - 624.
- Franko, O., Bodiš, D., Fendek, M., Remšík, A., Jančí, J. and Král, M., 1989: Methods of research and evaluation of geothermal resources in pore environment of Pannonian Basin. - Západné Karpaty, sér. hydrogeológia a inz. geol. 8, Geol. úst. D. Štúra, Bratislava, p. 165-192.
- Remšík, A., Franko, O., Fendek, M. and Bodiš, D., 1990: Geotermálne vody podunajskej a viedenskej panvy. - Mineralia slovacica, 3, 22, Bratislava, p. 241-250.
- Remšík, A. and Fendek, M., 1995: Geothermal country update for Slovakia. - Proc. World Geothermal Congress 1995, Florence, Italy, May 18-31, (Eds: Barbier, E., Frye, E., Iglesias, E. and Pálmason, G.), vol 1, p. 315-320.

SLOVENIA

D. Rajver, D. Ravnik, U. Premru, P. Mio and P. Kralj

Geothermal thematic map (Plate 74)

Slovenia extends over several tectonic units: the Pannonian Basin in the NE and the Eastern Alps, the Southern Alps as well as the Dinarides, which are part of the Adriatic microplate. Here numerous deep fracture zones enable thermal water from depths of several kilometres to reach the surface, providing they are permeable enough.

The Pannonian basin is filled with Tertiary marine and fresh water sediments that attain thicknesses from a few 100 m to > 5000 m in the E. Clays and marls predominate in shallow layers with intercalations of sands, while the deeper layers consist of claystones and marls with intercalations of porous sandstones, where mineral, thermomineral and thermal waters reside. The basement of the Tertiary section comprises mainly Paleozoic metamorphic rocks and locally also Mesozoic dolomites, limestones and shales. The Mesozoic carbonates, overlying the metamorphic basement, are several 10 m to a few 100 m thick. At depths > 4000 m, temperatures of > 200 °C and have been recorded.

Other areas of geothermal interest include: the Krško depression filled with Mesozoic carbonates, the Rogatec area comprising Tertiary andesites, depressions and synclines associated to the Sava folds as well as the Eastern Karavanken area filled with Tertiary clays, sands, and at deeper levels marls and sandstones.

The Eastern Alps consist mostly of Palaeozoic metamorphic rocks. Only zones that have been more intensely tectonized, such that deep reaching fracture networks were formed, are of geothermal interest.

In the Southern Alps, especially in the eastern part of the Sava folds, Tertiary depressions and synclines form deep (1500 m) narrow wedges in the Palaeozoic and Mesozoic layers along the faults. Andesitic tuffs are also present here (Rogatec area). The basement consists of Paleozoic and Mesozoic carbonate and clastic sediments, where thermal water with temperatures of 20 - 48 °C are hosted. The thermal springs in these areas yield up to 50 kg/s.

Further information on geological aspects of Slovenia can be found in RAVNIK et al. (1995) and the references therein.

The 16 thermal springs depicted on the map have constant temperature of at least 20 °C. Their chemical composition is taken from ŽLEBNÍK (1979) and recent works. Most thermal springs seem to be associated to deep circulation of groundwater in steeply dipping faults (RAVNIK et al., 1992). The water in the coastal area and around Nova Gorica reside in Cretaceous limestones underlying flysch sediments and are probably < 40 °C. The Dinarides are devoid of thermal springs as a result of karstification. In this environment, descending surface water cools the rocks far below the surface.

Temperatures (Plate 74)

Temperature data from 197 boreholes were used to trace the isotherms at 500 m depth. The isotherms at 1000 m and at 2000 m depth are based on data from 188 and 165 boreholes, respectively. In 46 oil wells only few multiple BHT measurements or even only a single BHT value from each borehole were available. These boreholes were drilled in the NE

part of Slovenia and their data were considered with caution.

At 500 m depth the temperature increases from N to NE and SE. At 1000 m depth, temperatures gradually increase from the W to the NE. This pattern can be observed even at greater depths. Heat-flow density is low in western Slovenia and increases progressively to the Pannonian Basin. RAVNIK et al. (1992) and RAVNIK et al. (1995) provide more detailed information on temperatures and heat-flow density for Slovenia.

Potential geothermal reservoirs

The data for most geothermal areas in Slovenia derive from boreholes drilled principally for water. Additional data from the oil company Nafta Lendava was also made available. Geothermal resources in the Pannonian Basin and the Krško depression are presented later, while here a brief description of the remaining potential areas is given.

Tertiary formations

It is possible to tap thermal water from other *Tertiary* formations such as the Mura formation as well as from layers of the Lendava (Late Pannonian to Early Pontian) and Murska Sobota (Eggenburgian to Lower Pannonian) formations. Thermal water of higher temperatures is expected in deeper layers, although with much lower permeabilities than in the Mura formation. Mineralization is much stronger, leading to scaling and corrosion during exploitation.

Pre-Tertiary basement

The *pre-Tertiary* basement is composed of many different lithologies, as evidenced by numerous oil wells. Seismic reflection surveys show that it lies at depths of less than 400 m to > 5000 m. In the Radgona and Ptuj-Ljutomer depressions, the basement consists of Mesozoic rocks: limestones, dolomites, locally also limey marls and breccias. During the Tertiary and Quaternary, the basement was fractured and thrust in many phases, leaving fractures that were widened by dissolution in some places. The occurrence of Mesozoic carbonate rocks was confirmed during exploration for oil and underground gas storage. In some places their thickness is only a few 10 m, in others a few 100 m. Permeabilities of a few 100 mD were determined in some boreholes. The resources in the Mesozoic aquifers, covering an area of about 1880 km², amount roughly to 6.3×10^{18} J, with an average resource density of 3.4 GJ/m² and a maximum of 15.4 GJ/m².

Sava folds region

Celje depression: The reservoirs are located probably at depths < 500 m to 1600 m with temperatures of up to 60 °C. They consist of Mesozoic limestones, in some places also of dolomites. Their extent has not yet been determined.

Lasko-Zagorje syncline: This structure is narrow but deep, stretching from Podčetrtek in the E to Medijske Toplice in the W. The main geothermal aquifer is the Triassic dolomite at depths of up to 1500 m, where temperatures between 22 - 45 °C exist.

Ljubljana depression: Here the geothermal reservoir consists of carbonate rocks at depths of > 500 m to 1000 m. They underlie Tertiary marls in the area around and NW of Kranj. At the SW borders of the depression, warm springs with temperatures 20 °C exist, while in the NE (Vaseno) a warm spring yields water at 30 °C. Around Ljubljana, thermal water (70 °C) is expected in presumably carbonate rocks below Carboniferous sandy claystones and shales. These carbonates are believed to lie at < 1000 m to > 2000 m depth. S of Ljubljana, below thin Quaternary sediments, warm water is found in shallow Triassic carbonates with temperatures of 20 - 25 °C.

Rogatec area

Drilling has revealed thermal aquifers in Tertiary andesitic tuffs below Miocene sediments and also in Triassic dolomites at a depth of 1400 m. Temperatures of 70 °C are expected.

Eastern Karawanken area

Velenje depression: Warm springs with temperatures of 35 °C are located mostly at the border of the Velenje depression, along fault zones. The geothermal reservoir consists of carbonate rocks underneath Tertiary sandy marls, sandstones and andesitic tuffs. Its depth can reach > 1000 m.

Coastal area

Here many wells were drilled for water and some of them tapped water with temperatures of 28 °C. The main reservoir is composed of Upper Cretaceous limestones that outcrop E and S of this area.

Nova Gorica area

A few shallow boreholes and one deep borehole were drilled for water exploration. A temperature of 32 °C at a depth of 1560 m was measured in Paleogene limestone. More geophysical exploration is to be done in search for the Mesozoic carbonates that otherwise outcrop towards the N and the S.

Pannonian basin

Pliocene and/or Late Miocene sands (Plate 75)

This extensive aquifer is hosted in the Mura formation. It has an effective maximum thickness of 60 m, dipping from the surface down to depths of 1500 m. The thermal waters have temperatures of up to 80 °C. Each of the wells drilled yields 5 - 35 kg/s. Mineralization (1 - 7 g/l) is strongly dependant on CO₂ content. The maximum measured permeabilities are about 2700 mD, but values as low as 16 mD were recorded during hydrocarbon exploration. In the area of about 1850 km² the geothermal resources amount to 0.84×10^{15} J with a maximum resource per unit area of 2.25 GJ/m² in the E part of the aquifer and an average of 0.62 GJ/m².

Krško depression (Plate 76)

The main reservoir is a Triassic dolomite covered in some places by Cretaceous marly limestone, marl and flysch. On top of this section, marly and clayey Miocene sediments with intercalations of sand and limestone were deposited. Tectonic activity was followed by erosion and later the deposition of Pliocene-Quaternary sediments. Borehole data and geophysical surveys confirm a total thickness of the Tertiary deposits of a few 100 m to 1600 m. Permeabilities of the Triassic dolomite reach a few darcies, and temperatures are close to 70 °C.

The geothermal resources for Triassic (occasionally also Jurassic) carbonates were evaluated for a smaller region (112 km²) in the eastern Krško depression. These geothermal resources amount to 0.47×10^{18} J, with an resource per unit area of 4.14 GJ/m² and a maximum of 11.20 GJ/m², based on a conservative assessment of net aquifer thickness (400 m). On the border of the Krško depression many warm springs are located with total maximum yield of 136 kg/s and temperatures between 23 - 35 °C.

Present status and future perspective of the use of geothermal energy

At present the total maximum possible flow rate of all thermal springs and boreholes with a temperature of at least 20 °C is 1100 kg/s corresponding to a thermal power of 64 MW_t considering 25 °C as the outflow temperature, which is an ideal case.

The installed thermal power at 21 locations amounted to 37 MW_t in 1994 for direct heat applications (RAJVER et al., 1995; KRALJ et al., 1993). In that same year, the total geothermal energy consumption at 21 locations (18 locations are represented by the geothermal installation symbol on the geothermal thematic map) reached about 762 TJ, or 17,880 TOE, considering the total annual average flow rate of 327 kg/s. Thermal spas and recreation centres are the main consumers (50.3 %). Hot water is used also for space heating (26.9 %), greenhouse heating (9.4 %) and heat pumps (8.4 %) as well as to a lesser extent for industrial processes (1.7 %) and air conditioning (3.3 %). More than 400 heat pumps are in use, contributing an additional 40 TJ (940 TOE) of thermal energy.

Geothermal investigations over the last 5 years resulted in 32 boreholes being drilled representing a total drilled length of about 24.4 km. Most of them (26) were intended for further exploration of already known resources for increasing their capacities or for tapping new aquifers. The remaining boreholes were drilled for exploitation purposes.

The extraction of geothermal energy (heat mining) has been limited to the use of exploitation boreholes (singlets) only. Doublet schemes are not yet in use. The users and the state authorities are aware of the necessity for reinjection of used thermal water for maintaining an optimal and long-term utilization. Shallow geothermics is also being

promoted, but at a slow pace.

The most favorable areas for geothermal energy exploitation are the NE part of Slovenia and those depressions close enough to potential users. In the remaining parts of Slovenia, more geophysical and geological investigations are needed to locate and characterize potential geothermal reservoirs.

Acknowledgements

The help of the staff of the Geological Survey Ljubljana in collecting the data and drawing the maps is greatly acknowledged. Many thanks are also due to L. Žlebnič and F. Drobne from the Geological Survey for useful comments and suggestions.

References

- Kralj, P., Rajver, D., Žlebnič, L. and Drobne, F., 1993: Present status of geothermal energy exploration and exploitation in Slovenia.- In: Geothermal energy for greenhouses and aquaculture in Central and East European Countries, K. Dimitrov (Ed.), Proceedings Intern. Workshop, Bansko (Bulgaria), Printed in Macedonia, p. 1-12.
- Rajver, D., Ravnik, D., Žlebnič, L. and Čebulj, A., 1995: Utilization of geothermal energy in Slovenia. - Proc. World Geothermal Congress 1995, Florence, Italy, May 18-31, (Eds: Barbier, E., Frye, E., Iglesias, E. and Palmason, G.), vol 1, p. 321-326.
- Ravnik, D., Kolbah, S., Jelič, K., Milivojević, M., Miošić, N., Tonic, S. and Rajver, D., 1992: Yugoslavia. - In: Geothermal Atlas of Europe (Eds: Hurtig, E., Cermák, V., Haenel, R. and Zui, V.), Hermann Haack Verlagsgesellschaft, Gotha, p. 102-105.
- Ravnik, D., Rajver, D., Poljak, M. and Živčić, M., 1995: Overview of the geothermal field of Slovenia in the area between the Alps, the Dinarides and the Pannonian basin. - Tectonophysics 250, p. 135-149.
- Žlebnič, L., 1979: Map of thermal and mineral waters of Slovenia with an explanation guide (in Slovenian). - Unpublished report, Geological Survey Ljubljana, p. 78.

SPAIN

M. Fernández, C. García-Noceda, I. Marzán and J. Sánchez-Guzmán

Geothermal thematic map (Plate 77)

The Variscan Iberian Massif extends over the western half of Spain and is made up mainly of metasediments and granitic rocks. The regions to the E and S comprise three Alpine chains (Pyrenees, Betic and Iberian chain) and Tertiary basins (Duero, Tajo, Ebro and Guadalquivir). Extension in the Mesozoic and the Neogene formed the Atlantic and Mediterranean margins, respectively. Neogene extension was accompanied by a significant amount of volcanism.

Deep seismic data recently acquired in the northern and southern Variscan Massif (FERNÁNDEZ-VIEJO, 1997; GONZÁLEZ et al., 1996) constrain the crustal and lithospheric structure in these regions. The regional thermal regime in the eastern part of Spain is clearly affected by lithospheric thickness variations related to the Alpine and Neogene tectonic events (e.g. ZEYEN and FERNÁNDEZ, 1994) as can be seen on the heat-flow density map.

This geothermal thematic map of Spain includes a thorough and extended compilation of thermal springs. Most of these thermal springs are associated with faults and rough topography at mountain ranges or basin flanks. Groundwater is driven by lateral hydraulic gradients and the faults serve as ascent conduits (FERNÁNDEZ and BANDA, 1990). Physicochemical data for 202 thermal springs with temperatures > 20 °C were assembled for the present map.

Temperatures (Plate 77)

Generally, water and mining exploration boreholes are not more than 300 m deep, providing information only on the shallow temperature field. Therefore, temperature maps were based mainly on the deeper oil borehole data. Where needed, temperatures were extrapolated down to a depth exceeding up to 250 m the measurement depth. Because of the scarcity of deep exploration boreholes in the Variscan Massif, most of the data are restricted to the eastern half of Spain.

Local thermal anomalies can be observed on the temperature maps in the southwestern Valencia trough and Ebro platform, eastern Betics (Almería), northern Ebro basin, and the Basc-Cantabrian basin. These anomalies can be traced down to 2000 m depth.

Surface heat-flow density determinations exist in a total of 562 sites: 84 measurements were obtained from water and mining exploration boreholes (ITGE, 1990; ITGE, 1993; MARZÁN et al., 1996), 199 in oil boreholes (NEGREDO et al., 1994). The remaining 279 values are

seafloor measurements.

Potential geothermal reservoirs

In the previous edition of the atlas, maps of resources for the Subijana Limestone (Vitoria-Treviño area in the Pyrenees' foreland), the Cretaceous of the Duero Basin and the Detritic Tertiary of Madrid were presented. These areas are also shown on the updated map. The present contribution includes resource assessments for some of the regions designated as potential areas in the earlier atlas. They are: the Cartagena Basin and the Mula Basin (both situated in the Betic Cordillera), the Ebro Basin (in the foreland of the Pyrenees), and the Guadalquivir Basin.

The Jurassic limestone is the main geothermal reservoir in the *Vega de Granada* basin. The available information includes data from a few geothermal and oil boreholes, many groundwater boreholes and a few geophysical surveys. The reservoir extends from 500 - 1000 m depth, being 200 - 250 m thick. The limestone has a porosity of the order of 5 - 8 %. The temperature of the aquifer is between 35 - 45 °C and the salinity of the fluid is of the order of 3 - 4 g/l. No maps are presented for this region at this time.

Information on the remaining potential areas given in the previous edition of the atlas will not be repeated here.

Campo de Cartagena Basin (Plate 77)

Both the middle Miocene calcarenite and the Jurassic limestone, are the geothermal reservoirs in this area. The Campo de Cartagena basin is a structural graben in which several connected aquifers are present. The available data was acquired from hydrogeological and geophysical surveys and numerous groundwater boreholes. The Jurassic limestone extends from the surface to > 1000 m depth and is 100 - 150 m thick. Salinity is 2 - 3 g/l and the porosity ranges between 6 - 9 %. The temperature in the aquifer is 25 - 50 °C.

Ebro Basin (Jaca-Sabiñánigo Area) (Plate 78)

In this area S of the Pyrenees, gas prospecting boreholes located an important geothermal reservoir in carbonate levels of Palaeocene-Early Eocene age. In addition to the data from these gas boreholes, geophysical surveys characterize the aquifer. This formation is found at a depth of 2800 - 3600 m and exhibits a thickness of 500 - 600 m. The calcareous deposits at the top of the reservoir grade into dolomites towards the bottom. The reservoir rocks have a porosity of 5 - 8 % filled with fluids of a salinity of 2 g/l. The temperature varies between 150 - 180 °C.

Mula Basin (Plate 78)

In the Mula basin, the middle Miocene calcarenite and the Jurassic limestone are connected hydraulically forming a single geothermal reservoir in this area. The characteristics of this reservoir were defined by data from geothermal boreholes and geophysical surveys. The depth of the reservoir is variable, extending from 100 - 1000 m. Total thickness ranges from 100 - 300 m in a few places. The rocks possess a porosity of 10 % filled with fluids of 1 mg/l salinity. The temperature ranges from 30 - 70 °C.

Guadalquivir Basin (Plate 78)

This Jurassic limestone geothermal reservoir is well mapped by oil and salt exploration boreholes. The depth of the formation is variable ranging from depths of 300 - 3000 m. Total formation thickness exhibits also great variation: 250 m - 1000 m. The porosity is about 16 - 19 % and the temperature lies between 50 - 75 °C.

Present status and future perspective of the use of geothermal energy

Exploitation of low temperature geothermal energy at present is limited to greenhouses heating in the Mediterranean area (Murcia- Alicante and Tarragona). A few projects in Galicia and Lérida use geothermal energy for domestic heating (ITGE, 1991; BANDA et al., 1991).

Other projects associated with thermal springs and balneological

applications were not shown on the maps or tables. The geothermal energy is mainly used to heat spa buildings. The total amount of conventional energy substituted by geothermal energy is about 5000 - 7000 TOE/a.

There are still several geothermal areas in which research projects will allow important geothermal projects not only for greenhouse heating purposes, but also for industrial, fish-farming, and other uses. It is foreseeable that several small geothermal projects with shallow wells and low salinity water will be developed in the next years.

References

- Banda, E., Albert-Bertram, J. F., Fernández, M. and García de la Noceda, C., 1991: Spain. - In: Geothermal atlas of Europe. (Eds.: Hurtig, E., Cermák, V., Haenel, R. and Zui, V.), Hermann Haack Verlagsgesellschaft, Gotha, Germany, p. 75-77.
- Fernández, M. and Banda, E., 1990: Geothermal anomalies in the Vallés-Penedés graben master fault: Convection through the horst as a possible mechanism. - J. Geophys. Res., 95, p. 4887-4894.
- Fernández-Viejo, G. 1997: Estructura cortical de la Cordillera Cantábrica y su transición a la Cuenca del Duero a partir de datos de sísmica de refracción/reflexión de gran ángulo. - Ph.D Thesis, University of Barcelona, 316 p.
- González, A., Torné, M., Córdoba, D., Vidal, N., Matías, L.M. and Díaz, J., 1996: Crustal thinning in the southwestern Iberia margin. - Geophys. Res. Lett., 23, p. 3477-2480.
- ITGE, 1990: Trabajos de medición e inventario de datos de flujo de calor en áreas seleccionadas del Macizo Ibérico Español. - Instituto Tecnológico Geominero de España, Madrid, 53 p.
- ITGE, 1991: Análisis de la utilización de recursos geotérmicos en España. Situación actual. - Instituto Tecnológico Geominero de España, Madrid, 111 p.
- ITGE, 1993: Trabajos de medición e inventario de datos de flujo de calor en España: Cordilleras Béticas y Suroeste Peninsular. - Instituto Tecnológico Geominero de España, Madrid, 64 p.
- Marzán, I., Fernández, M. and Cabal, J., 1996: Estudio geotérmico en la mitad Occidental de España. - Geogaceta, 20, p. 745-748.
- Negredo, A.M., Fernández, M. and Jurado, M.J., 1994. Determinación del flujo de calor a partir de sondeos petroleros en la Cuenca Catalano-Balear. - Acta Geol. Hispánica, 29, p. 27-40 (Pub. 1996).
- Zeyen, H. and Fernández, M., 1994: Integrated lithospheric modeling combining thermal, gravity, and local isostasy analysis: Application to the NE Spanish Geotranssect. - J. Geophys. Res., 99, p. 18089-18102.

SWEDEN

M. Lehmets, P.-G. Alm and R. Olsson

Geothermal thematic map (Plate 79)

The bedrock in Sweden consists mainly of Precambrian igneous and metamorphic rocks with minor areas of Phanerozoic sedimentary platform cover in the S and SE. In the NW, on the other hand, the Precambrian basement is concealed under Caledonian allochthonous nappes consisting of late Precambrian to Palaeozoic sedimentary and igneous rocks together with large portions of disconnected slices of Precambrian basement. The areal distribution of the major geological provinces (the Precambrian, the Caledonian and the Phanerozoic sedimentary platform cover) and the location of thrusts and faults presented on the simplified geological map are principally taken from LUNDQVIST and BYGGHAMMAR (1994) and STEPHENS et al. (1994).

The exposed Precambrian basement is a part of the Fennoscandian Shield (Baltic Shield), which was formed mainly between 3500 - 1500 Ma (e.g. GAAL and GORBATSCHEV, 1987). The shield features a regular geochronological zonation with the oldest rocks in the NE and the youngest rocks in the SW. The roughly NW-SE trending Tornquist-line/Transeuropean fault system is generally considered to represent the boundary between the East European Platform and Central Europe with its Phanerozoic mobile belts and platform cover.

In the southernmost part of Sweden, the Precambrian crystalline basement is faulted along lines trending NW-SE. The basement to the SW of these faults is covered by an up to 2.5 km thick sequence of Phanerozoic sedimentary rocks. Palaeozoic rocks also occur as undisturbed platform cover deposits resting on the Precambrian basement. Examples are found on the islands of Öland and Gotland in the Baltic Sea. Thin sequences of sedimentary rocks, generally < 100 m thick, also occur as residual hills in the SW of Sweden and in down-

faulted basins in the central part of southern Sweden. The amount of igneous rock in these Phanerozoic sequences is very small and generally restricted to fairly thin basaltic sills.

The information on the geothermal resources of Sweden has mainly been derived from data from mining fields, oil-gas wells, geothermal boreholes and boreholes for radioactive waste prospecting.

Temperatures (Plate 79)

The temperature data has been updated from the Geothermal Atlas of Europe (ELIASSON et al, 1991). A few new boreholes have been added. The temperatures were estimated from logs and maximum borehole temperature records. Extrapolation of temperature was only made down to an additional 50 % of the total borehole depth.

Except for two 6.6 km deep boreholes in the district of lake Siljan in Central Sweden, there are no deep wells in the Precambrian bedrock in Sweden. Reliable and representative temperature data from one of these wells is presented (BALLING et al., 1990). The temperature profile is smooth, except for a small kink at 2.2 km. A temperature gradient of 16.1 °C/km was estimated. A number of relatively deep boreholes (depth up to 2.6 km) are located in the Phanerozoic sedimentary rock formations in southern Sweden. The present work includes geothermal data from 120 boreholes with maximum depths generally ranging from 100 - 2500 m.

Potential geothermal reservoirs

The potential geothermal reservoirs are located in the district of Scania. Additionally, one formation on the island of Gotland may be utilised for geothermal purposes.

In order to make the data from all countries comparable for calculation of the identified resource the EU expert group recommends a value of 25 °C for the reinjected water temperature (T_r). This recommendation is disadvantageous for the identified Swedish resources. In Sweden there is a commercial geothermal plant in operation with $T_r = 4$ °C. However, only aquifers with a temperature of more than 25 °C have been considered in this presentation.

Scania

The six possible reservoirs in Scania are the Early Triassic *Ljunghusen sandstone*, the Early Triassic *Bunter sandstone*, the Late Triassic *Kågeröd arkose* and *Keuper sandstones*, the *Jurassic sandstone*, the *Cenomanian* and *Early Cretaceous sandstones* as well as the Late Cretaceous *Campanian sandstone*. Tectonic activity in Scania caused vertical displacements along faults running mainly NW-SE, sectioning Scania into nine major tectonic blocks in which the geothermal reservoirs are found. The results presented regarding the geothermal potential in sedimentary rocks are mainly based on the research work of BJELM et al. (1980), BJELM and PERSSON (1981) as well as ALM and BJELM (1995).

Campanian sandstone (Plate 80)

The *Campanian sandstone* consists of well sorted, fine to coarse grained quartz sand, occasionally unconsolidated or poorly consolidated. Its porosity is high, about 25 %. The *Campanian sandstone* has a mean thickness of 25 m, but can exceed 200 m in some locations.

Kågeröd arkose and Keuper sandstones (Plate 80)

The *Kågeröd arkose* and *Keuper formation* is a porous sandstone interbedded with clay and shale layers. Hydraulic contact between the sandstone layers may exist due to fractures created during the intense tectonic activity during and following the Triassic. The formation thickness increases towards the S and the W of the Vellinge fault. The mean thickness of the formation is 60 m. The temperature varies between 45 - 85 °C.

Bunter sandstone (Plate 80)

The Early Triassic *Bunter formation* is also found in the SW of Sweden. The formation becomes thinner towards the Malmö fault, but locally it

extends across the fault in the NE direction. In the E, the formation boundary runs along the Svedala fault, except in the southern part, where sedimentation occurs also E of the fault. The depth to the top of the formation varies locally between 1.75 - 2.5 km and its mean thickness is 150 m. The temperature in the formation ranges between 55 - 75 °C. A porosity of 20 % has been estimated from borehole logs. Permeability tests on cores yield a permeability of 20 mD while pump tests in boreholes suggest values as high as 200 mD.

Jurassic sandstone (Plate 80)

The *Jurassic formation* dips towards the Romele fault in the N and the E. The formation thickness is between 50 - 70 m. The depth to the top of the formation varies locally from 800 - 1950 m. The temperature ranges from 30 - 65 °C. Tests on cores from the SW of Scania indicate permeability values of 20 - 700 mD.

Cenomanian and Early Cretaceous sandstones (Plate 80)

The sediment thickness of the Early Cretaceous increases towards the Romele fault, but is greatest towards the E. The thickness of the formation varies between 30 - 40 m. These *Cenomanian* and *Early Cretaceous sandstones* are encountered at depths of 1.2 - 1.85 km. The temperature range is 42- 60 °C.

Ljunghusen sandstone (Plate 80)

The Early Triassic *Ljunghusen sandstone* (Early Bunter) is unconsolidated, homogeneous, and medium to coarse grained. The formation can only be found in the SW of the Falsterbo peninsula. It dips towards W-SW with the formation thickness also increasing along the direction of dip. The average thickness is 50 m. The top of the formation is located 1.95 - 2.4 km below the ground surface. The temperature range within the formation is 63 - 80 °C and the porosity is about 20 %.

När sandstone, Gotland (Plate 80)

The basement of Gotland is covered with Cambrian - Silurian sedimentary deposits. Within the Cambrian sediments five different sandstone layers can be discerned. Among these sandstone layers, the *När sandstone* has proved to have the best potential for geothermal utilisation.

The *När sandstone* formation dips in a S-SE direction. The total thickness of the Cambrian-Silurian section varies between 400 - 800 m, while the thickness of the *När sandstone* is at most 25 - 40 m. Several boreholes on the island have provided temperature measurements in the *När sandstone* of 20 - 25 °C. (KARLQVIST et al., 1982).

Present status and future perspective of the use of geothermal energy

As stated above, the major part of Sweden consists of Precambrian igneous and metamorphic rocks of low natural permeability and porosity. In contrast, the younger sedimentary sequences containing horizons of porous and permeable rocks, tentatively suitable for extraction of geothermal energy are principally restricted to the southernmost part of Sweden (Scania) and to the island of Gotland. The small areas with remnants of the Phanerozoic sedimentary cover in the inland of Sweden are too thin or shallow to be considered as useful for geothermal energy production.

The generally low surface heat-flow density in Sweden implies that only low enthalpy geothermal resources will be found (see table below). Consequently, heat pumps are the only feasible application for the use of naturally occurring geothermally heated groundwater for heating purposes.

The main geothermal resources and heat in place.

Formation	Area km ²	Depth m	Thick- ness m	T C	Porosity %	Sali- nity TDS %	HIP (H ₀) x10 ¹⁸ J	Resource (H ₁) x10 ¹⁸ J	Resources per unit area GJ/m ²
Ljunghusen sandstone	45	2100	50	70	20	19	0.374	0.090	2.00
Bunter sandstone	45 360 25	1900 1900 1650	150 100 75	63 63 55	20 15 15	19 19 19	0.995 5.074 0.226	0.227 1.157 0.048	5.04 3.21 1.92
Kågeröd arkose	45 360	1600 1700	50 50	53 56	18 18	17 17	0.319 2.724	0.066 0.581	1.47 1.06
Keuper sandstones	460 73	2100 1450	50 50	70 49	18 18	17 17	3.739 0.393	0.896 0.076	1.95 1.04
Jurassic sandstone	45 360 460 790 500	1400 1500 1950 1500 800	75 75 50 50 75	48 50 65 50 30	20 20 15 20 15	16 16 15 13 4	0.360 3.025 3.190 4.395 2.076	0.068 0.594 0.808 0.863 0.156	1.51 1.65 1.76 1.09 0.31
Cenomanian / Lower Creta- ceous sandstones	45 360 460 790	1200 1300 1850 1400	30 35 40 30	42 45 61 48	30 22 20 20	12 12 15 16	0.131 1.249 2.589 2.523	0.022 0.223 0.580 0.479	0.49 0.62 1.26 0.61
Campanian sandstone	460 790	700 700	25 25	27 27	20 20	2 2	0.571 0.980	0.020 0.034	0.04 0.04

The main resources and probable reserves in Sweden are located in the Phanerozoic sedimentary rocks of Scania. However, the assessment of the magnitudes of these resources contains uncertainties. Exact information about aquifers and water yield can only be gained by additional drilling and long term pumping tests.

The 47 MW geothermal heat plant in Lund has been in operation since the beginning of 1985 and produces about 45 % of the total annual heat demand (750 MWh/a) in Lund. The heat plant operates with two heat pumps with a maximum output capacity of 20 MW and 27 MW, respectively. The temperature in the most promising part of the reservoir is 22 - 23 °C. (ALM and BJELM, 1995). Today, the geothermal system includes four production boreholes and six re-injection boreholes. The distance between the centre of the production and the re-injection area is approximately 2.0 km. The geothermal reservoir is the *Campanian sandstone* which, at this location, occurs at a depth of 500 - 800 m. The depth of the boreholes is 700 m. The total production rate from the boreholes is 1600 m³/h. Additional information can be found in BJELM and LINDEBERG (1995).

The plant on Gotland is located in the village of Klintehamn and has been in use since the end of 1985. It operates with four heat pumps having a total output capacity of 800 kW. The heat pumps are divided in two parallel supply systems. The geothermal water is taken from the *När Sandstone* at a depth of 500 m. Only one production borehole is used in the system, and after the heat extraction, the water is disposed of in the Baltic sea. The production rate of the borehole is 25 m³/h and the water temperature is 18 °C.

Research and development are carried out with the goal of geothermal energy extraction from crystalline rocks with Hot Dry Rock (HDR) technology (WALLROTH et al., 1994; ELIASSON et al., 1988, LANDSTRÖM et al., 1980). Field experiments, including circulation tests in a 0.5 km deep reservoir, have been accomplished in the Bohus granite on the Swedish W coast. The objective of the Swedish HDR programme is to investigate the viability and future potential for heat pump based HDR heating systems. The technology is, however, not considered economically competitive at present.

References

- Alm, P.G. and Bjelm, L., 1995: Geothermal Energy in Scania. A summary of research activities and results within the national program for geothermal energy in sedimentary rocks 1977-1994. - Department of Engineering Geology, Lund Institute of Technology, Lund University. ISRN: LUTVDG/TVTG--3042-SE.
- Balling, N., Lind, G., Landström, O., Eriksson, K. G. and Malmqvist, D., 1990: Thermal measurements from the deep Gravberg-1 well. - R & D-report, no. TE30. Vattenfall, Vällingby.
- Bjelm, L. and Lindeberg, L., 1995: Long-term experience from a heatpump plant in Lund, Sweden, using a low-temperature geothermal aquifer. - Proc. World Geothermal Congress 1995 (Eds: Barbier, E., Frye, G., Iglesias, E., Palmason, G.), Florence, Italy, May 18-31, vol 3, p. 2173-2176.
- Bjelm, L. and the Working-group for Geothermal Energy, 1980: Geotermisk energiutvinning i Skåne. Delrapport 4. Förutsättningarna för utvinning i Skåne. Lagring i geotermalförformationer (in Swedish). - Tekniska Högskolan i Lund. LUTVDG/(TVGL-3009)/1-15/(1980).

- Bjelm, L. and Persson, P.G. and the Working-group for Geothermal Energy, 1981: Geotermisk energiutvinning i Skåne. Slutrapport 4. Del 1: Förutsättningarna för utvinning i Skåne. Lagring i geotermalformationer. Del 2: Provbörning vid Landskrona. - Tekniska Högskolan i Lund (in Swedish). LUTVDG/(TVGL-3013)/1-52/(1981).
- Eliasson, T., Lindblom, U., Slunga, R., Sundquist, U. and Wallroth, T., 1988: The Swedish Hot-Dry-Rock Project: Some preliminary Achievements. In: Exploration of Deep Continental Crust, Vol. 2, Deep Drilling in Crystalline Bedrock, (Eds: Boden, A. and Eriksson, K. G.), Springer Verlag, Berlin, p. 391-400.
- Eliasson, T., Eriksson, K.G., Malmqvist, D., Lindqvist, G. and Parasnis, D., 1991: Sweden. - In: Geothermal Atlas of Europe, (Eds: Hurtig, E., Čermák, V., Haenel, R., and Zui, V.), Hermann Haack Verlagsgesellschaft mbH, Geographisch-Kartographische Anstalt Gotha, p. 78, 100 plates.
- Gaal, G. and Gorbatshev, R., 1987: An outline of the Precambrian Evolution of the Baltic Shield. - *Precambrian Res.*, 35, p. 15-52.
- Karlqvist, L., Fogdestam, B. and Engqvist, P., 1982: Description and Appendices to the Hydrogeological Map of Gotland County. - Swedish Geological Survey, SGU, ser. Ah Nr. 3, Uppsala, Sweden ISBN 91-7158-259-2.
- Landström, O., Larson, S.Å., Lind, G. and Malmqvist, D., 1980: Geothermal investigations in the Bohus Granite area in Southwestern Sweden. - *Tectonophysics*, 64, p. 131-162.
- Lundqvist, T. and Bygghammar, B., 1994: The bedrock. - In: National Atlas of Sweden (Ed: Fredén, K.).
- Stephens, M., Wahlgren, C.-H. and Weihed, P., 1994: Geological map of Sweden. Scale 1:3 million. - SGU Series Ba no. 52.
- Wallroth, T., Eliasson, T. and Sundquist, U., 1994: Status of the Fjällbacka HDR research project, Sweden. - Proc. Int. Symp. Geothermics 94 in Europe, Orleans, France, 8-9 Feb. 1994, p. 115-122.

SWITZERLAND

F. Medici and L. Rybach

Geothermal thematic map (Plate 81)

This contribution updates the previous atlas, benefiting mainly from an extended data base and especially from the thorough revision of the Geothermal Map of Switzerland (Heat-Flow Density) by MEDICI and RYBACH (1995). More detailed information can be found in RYBACH and HAUBER (1990) and RYBACH and GORHAN (1995).

Since the previous atlas, various endeavours and projects led to drilling activities which in turn supplied new data. These were in particular:

- oil and gas exploration (Thun; with 5 952 m the deepest borehole in Switzerland),
- geothermal energy exploration and development in Elgg, Kreuzlingen, Krone ZH, Otelfingen, Payerne, Reinach, Riehen, St. Moritz and Uster,
- radioactive waste disposal feasibility studies in Böttstein, Kaisten, Leuggern, Riniken, Schafisheim, Siblingen, Weiach and Wellenberg,
- tunnels of Gotthard, Lötschberg and Tujetsch,
- investigations in Campo Vallemaggia, Delemont and Eptingen.

Geothermal installations and thermal springs are spread out over the entire country with some concentration in the eastern Jura and the Rhône river. The location of Borehole Heat Exchanger (BHE) systems in Switzerland is also shown separately. A BHE heating system consists of a borehole heat exchanger (plastic tube installed in a backfilled drillhole, typically about 100 m long), a heat pump and low-temperature underfloor heating. With > 10 000 heating units, the areal density (number of BHE's per country area) is highest world-wide; the distribution corresponds roughly to that of the population density.

Temperature (Plate 81)

The temperature and heat-flow density maps were based on 340 data points; 150 in Switzerland and 190 in the surroundings. Heat-flow density in the Molasse Basin is between 70 - 120 mW/m², decreasing southwards to 60 mW/m² in the Alps (MEDICI and RYBACH, 1995).

Potential geothermal reservoirs

In the course of the drilling and exploratory activities, several aquifers were identified which might be of interest for geothermal energy development. They are either related to fracture systems (in the Alps and in the Jura, the two main geologic units of the country) or to stratiform, porous formations (in the Tertiary Molasse basin, the third main unit). The Molasse basin, located between the Jura and the Alps, is the most densely populated area in Switzerland.

Molasse Basin

It is striking that there are no thermal springs in the Swiss Molasse basin (the 25 °C thermal water produced at Yverdon is pumped from Mesozoic (Malm) strata underlying the Molasse sediments). The absence of thermal springs indicates that vertical permeability (which is needed for recharge and descent as well as ascent and discharge in deep-reaching circulation) of the Molasse sediments is generally low.

Obere Meeresmolasse (Miocene) (Plate 81)

The Miocene *Obere Meeresmolasse* (OMM, Upper Marine Molasse) formation in the region between the lakes of Zurich and Constance is suitable for geothermal development. Hydrocarbon and geothermal exploration data have characterised the aquifer reasonably well. Much is known about depth, thickness, lithology, porosity, and permeability of the sediments as well as about the physical and chemical characteristics of the formation fluid (temperature, mineralisation). Several boreholes have established that the basal section of the OMM, consisting of porous and permeable sandstones, is a regional aquifer of geothermal interest in the areas of Basersdorf, Kloten, Kreuzlingen and Tiefenbrunnen. In Fehraltorf near Zurich, drilling failed because the borehole turned out to be dry. The mineralisation of the geothermal fluid is rather low (usually < 5 g/l) which permits surface disposal and thus enables the use of singlet systems.

Five new data points with respect to previous atlas, cause the isolines of depth, thickness, temperature, porosity, permeability and transmissivity to change slightly. The top of the OMM, in the region of interest, extends from the surface down to 800 m, where temperature reaches up to 40 °C. Formation thickness increases from 50 m to > 800 m from N to S, while porosity decreases in that direction. New is the information on salinity. It increases from NW to SE. The resources map was redrawn to accommodate these new data assuming a singlet utilization.

A summary of the borehole data for this aquifer comprises elevation, depth, thickness, porosity, temperature and salinity. The letter codes serve to identify the sites on the map:

Site	La. (N)	Long. (E)	Elev. (m)	Depth (m)	Thickn. (m)	Por. (%)	Temp. (°C)	Sal. (g/l)	Code in map
Aqui 1	47 21 35	8 31 30	417	300	—	>10	24	1.052	f
Berlingen 2	47 40 10	9 01 50	538	500	—	—	—	—	a
Kreuzlingen 2	47 38 55	9 10 40	417	436	197	—	—	—	b
Fehraltorf	47 23 10	8 44 25	522	404	472	7	20	3.9	c
Kloten	47 27 00	8 35 25	444	125	257	15	19	0.921	d
Otelfingen	47 27 20	8 23 45	460	37	66	15	12	0.347	e
Tiefenbrunnen/ Zürich	47 21 10	8 33 10	408	326	389	>10	25	3.72	g

Although not represented in maps, a few comments are given on other potential aquifers of currently limited interest for geothermal energy exploitation: the *Malm* and the *Obere Muschelkalk* formations.

Malm

The base of the Tertiary Molasse sediments also has geothermal potential. The carbonatic *Cretaceous* or *Malm* formation can exhibit significant permeability due to karstification. However, the karstic cavities are often filled and sealed by fine-grained Eocene clays causing a reduction in permeability (RYBACH, 1992). Exploration risk, in absence of geophysical methods capable of providing permeability information from surface measurements, is rather high. Mineralisation is expected to be moderate (< 10 g/l).

Obere Muschelkalk

The Triassic *Obere Muschelkalk* is also present below the Molasse basin, but is expected to have unfavourable aquifer characteristics (low permeability, high salinity and H₂S content).

Oberer Muschelkalk (Middle Triassic) (Plate 82)

The *Obere Muschelkalk* (OMK) is a fractured and often karstified Middle Triassic dolomite formation. Thermal springs or shallow drillholes yield thermal water for balneological applications and for space heating (e.g. in Baden). The salinity of the geothermal fluid can reach several 10 g/l and fluid temperature is < 60 °C.

With respect to the information used to construct the maps in the previous atlas, numerous new data have been collected in the northern part. Therefore, the isoline pattern changes in the northern part, remaining relatively unchanged in the southern part.

This formation extends from the surface to depths > 4 km. For the purpose of geothermal resource assessment, only the region above 3 km was included in the computations. A temperature of 65 °C is found at a depth of 1500 m. The formation thickness ranges from 50 - 100 m. The porosity and permeability data show no spatial trend, as is common for karstified reservoirs. The resources isolines were computed assuming doublet system of exploitation.

In the table below, a summary of the data includes (from left to right) information on elevation, depth, thickness, porosity, temperature, salinity, transmissivity and permeability. The letter codes identify these sites on the maps.

Site	Lat. (N)	Long. (E)	Elev. (m)	Depth (m)	Thickn. (m)	Por. (%)	Temp. (°C)	Sal. (g/l)	Trans. (D m)	Perm. (mD)	Code in map
Altishofen	47 10 07	7 58 25	478	—	—	—	—	—	—	—	c
Berlingen1	47 39 40	9 02 55	593	—	—	—	—	—	—	—	k
Birmenstorf											
BT4	47 27 50	8 14 10	344	132	95	5-20	22	—	43.68	406	s
Böttstein	47 43 00	8 13 10	348	122	75	< 30	20	6.2	24.96	312	q
Courtion 1	46 51 25	7 04 35	599	—	—	—	—	—	—	—	a
Eptingen 1	47 23 40	7 49 00	540	470	50	—	—	—	—	—	d
Frenkendorf	47 30 40	7 43 05	308	—	—	—	—	—	—	—	x
Hausen HH1	47 27 35	8 12 20	380	280	100	5-15	—	—	0.73	6	u
Kaiseraugst											
WB5	47 32 00	7 44 25	300	—	—	—	—	—	—	—	y
Kreuzlingen 1	47 37 25	9 09 30	539	—	—	—	—	—	—	—	i
Leuggern	47 35 25	8 12 10	359	49	40	> 20	12	1.0	5.93	364	p
Lindau	47 26 25	8 40 10	516	—	—	—	—	—	—	—	g
Lostorf Bad 3	47 23 35	7 56 00	549	291	106	—	—	—	—	—	e
Mülligen BT2	47 27 50	8 13 40	355	1	67	—	—	—	15.18	312	t
Pfaffnau 1	47 14 10	7 52 10	500	—	—	—	—	—	—	—	b
Pratteln 41J8	47 31 55	7 43 55	270	—	—	—	—	—	—	—	z
Riehen 1	47 35 05	7 41 05	276	1444	92	—	65	17.1	1.04	36	bb
Riehen 2	47 35 00	7 39 00	285	1123	100	—	51	14.2	0.20	6	aa
Riniken	47 30 25	8 11 30	385	616	72	—	46	14.3	6.97	73	r
Schafisheim	47 22 10	8 09 00	421	1228	60	—	59	15.1	0.46	10	f
Schinznach S2	47 26 45	8 10 00	342	72	> 53	—	40	—	520.00	10400	v
Siblingen	47 43 40	8 30 25	574	177	57	< 30	20	1.2	0.09	156	m
Weiach	47 33 50	8 27 30	369	819	69	—	50	3.2	4.37	—	n
Zurzach 3	47 35 30	8 17 10	346	—	—	—	—	—	—	—	o

Thermal water is being produced also from the crystalline basement at Zurzach.

Alps

This geologically complex domain has no extended, stratiform aquifers. The naturally issuing thermal springs in the Alpine region are evidence of deep-reaching fracture zones and their association with favourable hydraulic conditions (pronounced relief of the water table; minima in hydraulic potential at discharge points). At several places the thermal water is used, in addition to balneological applications, for space heating (Bad Ragaz, Brigerbad, Lavey-les-Bains, Leukerbad). It is expected that further deep-reaching fracture zones could be of local geothermal interest. GEOTHERMOVAL, a detailed exploration program operating since 1987 (RYBACH and GORHAN, 1995), has led to the selection of several drilling targets in the Rhone valley (Saillon, Sion, St. Maurice).

Present status and future perspective of the use of geothermal energy**Aquifers**

The Federal Government offers a guarantee for the risk of geothermal drilling amounting to 15 million Swiss francs to cover activities from 1987 - 1997 (RYBACH and HAUBER, 1990). Thanks to this programme, several drilling projects have been initiated, on the basis of intensive, small-scale local exploration for localising adequate drillsites. In the late eighties, several drilling projects were successful (Kloten/ZH, Kreuzlingen/TG, Riehen 1&2/BS; see RYBACH and HAUBER, 1990). In fact, the first Swiss geothermal doublet (geothermal capacity 4.7 MW_g, total heating power 15.2 MW_h) started its operation successfully in 1993

(BOISSAVY and HAUBER, 1994; BÖHI and HUSER, 1994). Unfortunately, the activities in the early nineties were less successful. In a number of deep drillholes (Bulle, St. Moritz, Thonex, Weissbad) the flow rate was much less than expected and definitely too low for utilisation.

Borehole Heat Exchangers (BHE)

The early nineties mark a turning point in Swiss geothermal development. The relatively modest success of the deep drilling projects, albeit encouraged by a governmental risk coverage system, gave momentum to countrywide borehole heat exchanger (BHE) installations. Subsequently Switzerland became world leader in the application of this small-scale heat pump-coupled system, well suited to supply heat to decentral objects.

BHE's are ideal to use the omni-present, shallow geothermal resources. The most popular BHE heating system with one or more boreholes (typically 50 - 150 m deep) is a decentral, closed-circuit, heat pump-coupled system, ideally suited to supply heat to smaller objects like single family or multi-family dwellings. They can be installed in nearly all kinds of geologic media (except in materials with low thermal conductivity like dry gravel). The environmental awareness of developers and recent governmental and cantonal subsidy led as incentives to a BHE boom in Switzerland. To date there are over 10 000 such systems installed, with a total of 1500 km BHE length. Areal density (number of BHE's per country area) is highest world-wide. This remarkable development and the considerable BHE potential not yet tapped leads to research and development activities for new concepts such as multiple BHE's, combined heat extraction/storage, "energy piles" (foundation piles equipped with heat exchanger tubes) and deep BHE's. For more detailed information see RYBACH and HOPKIRK (1995).

Deep Borehole Heat Exchangers

Deep BHE's can provide whole residential areas with heating energy. These could be installed either in specially drilled holes, or alternatively in abandoned "dry" deep drillholes. There exist many deep boreholes, otherwise unused, which would apparently lend themselves to development as borehole heat exchangers and consequently as a new type of heat source for space heating. At present, two pilot and demonstration plants of this type are subsidised by the Bundesamt für Energiewirtschaft.

Tunnel Waters

Several deep tunnels crosscut considerable sections of the Swiss Alps which drain, especially in permeable fracture zones, large amounts of warm water. Utilisation for space heating of such waters, flowing under gravity to the portals, is already underway. The outflow from the 16 km long Furka railway tunnel feeds a local distribution system to heat part of the village of Oberwald (canton Wallis). The new NEAT project aims at two deep tunnels (Gotthard, 56 km; Lötschberg, 39 km). A preliminary potential assessment, based on predicted rock/water temperatures and inflow rates, yields several 10 MW_{th} for both planned tunnels. Nearby potential consumers have already been identified. For more detailed information see RYBACH and WILHELM (1995).

Deep Heat Mining (DHM)

Since 1996 the Federal Office of Energy (OFEN) is supporting the Deep Heat Mining (DHM) project with the goal to produce electrical power and heat from a deep enhanced geothermal system, generated by hydraulic stimulation. Presently an exploration hole is being drilled in Basel.

Annual Energy Use

The following figures were compiled for December 1994:

Aquifers	23.9 TJ/a
BHE's (shallow and deep)	821.0 TJ/a
Tunnel waters	32.0 TJ/a

For comparison: Switzerland used a total of 346 PJ/a for space heating in 1993 (RYBACH and GORHAN, 1995).

Acknowledgements

We thank the Bundesamt für Energiewirtschaft (BEW) for continuous support and Mr. B. Bucher for compilational help.

References

- Böhi, H. and Huser M., 1994: "Wärmeverbund Riehen" - Geothermic utilization in a district heating system. - In: Proc. Int. Symp. "Geothermics 94 in Europe - From research to development". Document BRGM no. 230, p. 461-466.
- Boissavy, C. and Hauber, L., 1994: Results of the geothermal boreholes Riehen 1 and 2 (Basel, Switzerland). - In: Proc. Int. Symp. "Geothermics 94 in Europe - From research to development". Document BRGM no. 230, p. 453-460.
- Medici, F. and Rybach, L., 1995: Geothermal map of Switzerland 1 : 500 000 (Heat-Flow Density). - Beitr. Geol. Schweiz. Ser. Geophys. Nr. 30.
- Rybach L. and Hauber L., 1990: Swiss Geothermal Energy Update 1985 - 1990. - In: Proc. International Symposium on Geothermal Energy, Hawaii, Vol. 1, p. 239-246.
- Rybach, L., 1992: Geothermal potential of the Swiss Molasse basin. - *Eclogae geol. Helv.* 85, p. 733-744.
- Rybach, L., and Gorhan, H., 1995: Swiss Geothermal Energy Update 1990-1995. - In: Proc. World Geothermal Congress 1995, Florence, Italy, May 18-31, (Eds: Barbier, E., Frye, E., Iglesias, E. and Pálmason, G.), v. 1, p. 329-337.
- Rybach, L., and Hopkirk, R., 1995: Shallow and deep borehole heat exchangers - achievements and prospects. Proc. World Geothermal Congress 1995, Florence, Italy, May 18-31, (Eds: Barbier, E., Frye, E., Iglesias, E. and Pálmason, G.), v. 3, p. 2133-2139.
- Rybach, L., and Wilhelm, J., 1995: Potential and use of warm waters from deep Alpine tunnels. - In: Proc. World Geothermal Congress 95, Florence, Italy, May 18-31, (Eds: Barbier, E., Frye, E., Iglesias, E. and Pálmason, G.), v. 3, p. 2199-2203.

UKRAINE (Plates 1, 2 and 3)

R.I. Kutas, E.E. Sobolevsky, G.I. Veliky and E.A. Yakovlev

The most suitable conditions for the exploration of geothermal water in the Ukraine exist in the Crimean Plain and in the Trans-Carpathian trough.

Crimean Plain

The Crimean Plain is part of the Paleozoic Scythian platform. It is covered by Meso-Cenozoic terrigenous and carbonate sediments whose thickness varies from a few hundreds of metres to 5000 m. Heat-flow density in Crimea ranges from 50 to 110 mW/m². Values greater than 70 mW/m² are observed in the central part of the Crimean Plain (Novoselivka and Tarhankut). Temperature is 44 - 68 °C at 1000 m depth and 70 - 88 °C at 2000 m.

The most promising aquifers for geothermal applications are formations of Lower Cretaceous (Neocomian-Aptian) and Danian-Palaeocene ages that occur at depths of 3000 m. The Neocomian-Aptian aquifer consists of fractured limestones and conglomerates. Temperature at its top ranges from 70 - 120 °C. Salinity does not exceed 35 g/l and the productivity of the boreholes is greater than 2 - 3 l/s. The Danian-Palaeocene aquifer is composed of fractured limestones and marls. Water temperature is > 70 °C and salinity is less than 25 g/l.

Trans-Carpathian Trough

The Trans-Carpathian trough is filled with Neogenic molassic sediments whose thickness varies from 500 m in the NE to 3000 m in the SW. Mafic and silicious volcanic rocks of Neogene age are widespread. The basement is highly deformed and fractured. Heat-flow density varies from 75 - 105 mW/m². Temperature ranges from 50 - 68 °C and 92 - 160 °C in 1000 m and 2000 m, respectively. Maximum temperature of 206 °C was registered in the Chop-Mukachivo depression.

The best geothermal reservoirs are volcanic rocks and terrigenous sediments of Helvetian, Tortonian and Levantin age. Their temperature varies from 40 - 50 °C with salinity < 35 g/l. Production rates of 10-20 l/s are expected.

UNITED KINGDOM

K. Rollin, G. A. Kirby, W. J. Rowley and D. K. Buckley

Geothermal thematic map (Plate 83)

The Marchwood borehole near Southampton is the first drilling for geothermal purpose in Great Britain. It taps a geothermal reservoir in the Triassic Sherwood Sandstone Group at a depth of about 1700 m producing water at 72 °C. At a flow rate of 30 l/s the pressure reduces by 3.7 MPa. The thermal yield at 20 l/s was about 3 MW_t.

A second geothermal borehole in Southampton penetrates the geothermal reservoir at 1700 m. Test results were disappointing (at 20 l/s the pressure reduces by 3.0 MPa) and a smaller revised scheme for district geothermal heating was proposed. The geothermal brine enters the heat station at the surface at 75 °C and is filtered before entering the 2000 kW plate heat exchanger. The heat is transferred to freshwater and the heated freshwater is circulated in insulated piping to more than 15 major customers in the city centre. The exploited heating water is returned at 28 °C. The geothermal energy is supplemented by waste heat from Combined Heat and Power (CHP) generators and by high efficiency boilers to meet seasonal demand and provide a connected load of 24.4 MW. The performance of the geothermal aquifer and the geochemistry of the production fluid is monitored against a reservoir model that has been successful in predicting the observed water level variations. Geochemical changes have not been significant. At present, this is the only geothermal installation operating in the UK.

Temperatures (Plate 84)

Maximum temperatures recorded during logging are the main kind of new sub-surface temperature information. About 50 new boreholes were added to the UK Geothermal Catalogue (ROLLIN, 1987) which now contains subsurface temperature data for 1216 sites. Of a total of 3057 temperature values, 70 % are Bottom Hole Temperatures (BHT). There are 567 wells deeper than 1000 m, of which 94 % have a summary geological log allowing the thermal resistance profile to be determined. Temperatures at 878 boreholes with data at or below 500 m depth were interpolated to the 500 m level. Data distribution is uneven and no new data are available in the northern part. Temperatures at 1000 m depth are interpolations of measurements in 501 boreholes.

Potential geothermal reservoirs

The previous UK geothermal resource assessment (DOWNING and GRAY, 1986; HAENEL and STAROSTE, 1988) identified five Mesozoic basins which contain low enthalpy geothermal resources with temperatures > 40 °C: East Yorkshire, Lincolnshire (Eastern England), Cheshire, Worcester, Wessex and North Ireland. The first four basins are reappraised on the basis of new geological, porosity and temperature data available from seismic surveys and new drilling.

Potential areas for geothermal energy extraction have in the past been defined by transmissivity minimum of 10 Dm or 5 Dm. Under these criteria, the reservoir feeding the Southampton geothermal installation would barely be considered as a geothermal potential. Here, transmissivity has not been considered as a limiting function alone. The effective reservoir thickness was attributed to that percentage of the section with porosity exceeding 15 - 20 % (from geophysical logs). Unless stated otherwise, resources refer to areas of aquifer temperatures > 40 °C. The revised models of the structure and thickness of the main aquifers include now the effects of vertical and inclined faults. Porosity analysis of geophysical logs from about 35 boreholes led to better identification of the size and position of the main reservoirs.

Additional temperature data or improved analysis of the previous data also exist for all four basins. The temperature field in the reservoir of the Eastern England basin has been derived directly from the observed data alone. Because of the scarce data coverage in the other three basins, subsurface temperatures were computed from the observed heat-flow density, the structural model of the basin and the thermal conductivity and radiogenic heat production rate of the rocks.

Eastern England Basin, Sherwood Sandstone (Plate 84)

This basin is the onshore extension of the southern North Sea Basin, which during Permo-Triassic times was a thermal sag type basin with little associated faulting except perhaps for the Vale of Pickering-

Flamborough Head fault zone running E-W across the northern part of the basin. The small sub-basin in the NE is interpreted as being 100 m deeper than shown in the previous atlas.

The main reservoir is composed of the Triassic Sherwood Sandstone Group (SSG). In the SW, this Group is conglomeratic and in the NE, shaley and finer-grained. At depth, the Sherwood Sandstone Group is fluvial, red to purplish brown, uniform, medium-grained, occasionally micaceous and firm to friable. It comprises layers approximately 3 m thick. The sandstone is generally lightly-cemented although certain thin horizons are extensively cemented. The cement is made up of anhydrite or dolomite with minor amounts of calcium carbonate.

The temperature measurements selected in 250 boreholes were interpolated to obtain the temperature at the mid-level of the reservoir. This surface was taken as the depth to the aquifer. Geothermal resources were calculated using a reservoir fraction of 0.70 of the aquifer thickness.

Geophysical logs indicate a mean porosity for the full formation thickness of 21 % (13 - 28 %) with higher porosity in the lower section. Mean porosity is 23.6 % when measured on cores and mean permeability is 2166 mD. The porosity decreases to the N and with depth: it is 30 % at outcrop in the S, while it is reduced to 20 - 24 % at depths of about 1500 m. Permeability also decreases from outcrop values to 400 - 1000 mD at depth. The decrease in porosity and permeability downdip into the basin is due to increasing degree of cementation and presence of fibrous illite in the pores.

Transmissivities measured on cores are similar to those estimated from a porosity-permeability regression (35 Dm). Gas-lift tests result in values a factor of 2 higher (57 - 62 Dm). The use of the correlation between porosity and gas permeability (DOWNING et al., 1985) result in values an order of magnitude greater (220 D m). This overestimate is probably caused by drying of the core samples prior to measurement (MILODOWSKI et al., 1987).

A previous estimate of geothermal heat in place (H_0) of the Sherwood Sandstone Group was 99×10^{18} J with an identified resource (H_1) of 10.6×10^{18} J ($R_0 = 0.25$, $T_r = 30$ °C). In the present reappraisal, the total (H_0) are 122×10^{18} J. This is substantially more than the previous assessment even though a much more restricted reservoir is considered. The total identified resource (H_1) has practically doubled to 20×10^{18} J.

Cheshire Basin, Permo-Triassic Sandstone (Plate 85)

The Cheshire Basin is roughly elliptical in plan with its long axis trending NE-SW. It is markedly asymmetrical in cross-section and has the form of a faulted half-graben, deepest in the SE. The Bridgemere - Red Rock Fault System forms the SE margin of the basin, with a present-day cumulative throw in places approaching 4000 m. In contrast, the W margin of the basin is relatively unfaulted, forming a feather-edge characterised by depositional onlap. The internal structure of the basin is complex and, for the most part, heavily faulted. This causes considerable lateral thickness variations of the geothermal reservoir. Faults with a trace length of less than 3 km have been omitted from the maps presented here. The larger faults subdivide the basin into a system of tilt-blocks and sub-basins. The Cheshire basin is the deepest onshore UK Mesozoic basin. The deepest parts are found in the Wem-Audlem and Sandbach-Knutsford sub-basins where the base of the Permo-Triassic basin-fill lies at depths > 4000 m.

The Permo-Triassic and Jurassic deposits (EVANS et al., 1993) form a dominantly arenaceous sequence (*Collyhurst Sandstone Formation* and *Sherwood Sandstone Group*) overlain by a largely argillaceous sequence with evaporites (Mercia Mudstone Group). Locally in the N and central parts of the basin, the Permian Collyhurst Sandstone is separated from the Sherwood Sandstone Group by the Manchester Marl Formation, an argillaceous aquiclude.

The aeolian *Permo-Triassic Collyhurst Sandstone* is 565 m and 472 m thick at the Knutsford (in the N) and Prees (in the S) boreholes, respectively. It is made up of aeolian sands consisting of millet seed grains and large scale dune beds. The section has a mean porosity of 14 %. Several depth intervals exhibit maximum porosities > 25 % and it seems that a suitable reservoir would be available at depth. Interpreted porosities from the density logs indicate a general increase in porosity with depth.

The *Sherwood Sandstone Group* (SSG) is divided into five formations from the bottom to the top of the section: (1) The Kinnerton Sandstone Formation is largely aeolian and reaches a maximum recorded thickness of 110 m. The mean porosity is 11 %. (2) The overlying Chester Pebble Beds Formation consists of conglomerates, pebbly sandstones and cross-bedded red sandstones, with the proportion of pebbles decreasing

towards the NW. These deposits represent a reworked alluvial fan and are thinner to the NW. At outcrop they have a porosity of 20 - 30 % and a permeability of 80 - 8000 mD (SKINNER, 1977). Geophysical logs show mean porosities of 12 - 18 % below 600 m depth. Where the Pebble Beds are silicified, permeability can reduce to 4 - 8 %. (3) Above it, the Wilmslow Sandstone Formation has a maximum recorded thickness of 920 m and is composed of fine-grained argillaceous and cross-bedded sandstones of fluvial and lacustrine origin. At shallow depths, reported porosities varying from 13 - 30 % and permeability ranging from <10 mD to >10 000 mD due to varying degrees of cementation and clay mineral content. Partial silicification at depth causes the porosity of the Wilmslow Sandstone to decrease. (4) The Bulkeley Hill Sandstone Formation is a massive, well-bedded, fairly coarse brown sandstone with interbedded flaggy sandstones, soft millet-seed sandstones and red-brown mudstones. It accumulated up to 220 m thickness in the depocentre. An unconformity, correlated with the Hardegson unconformity, divides the aeolian and fluvial (5) Helsby Sandstone (up to 200 m thick) at the top from the underlying succession. This formation is a mixture of aeolian and fluvial sandstones including pebbly sandstones. The mean porosity of the Helsby Sandstone at shallow depth is 28 - 30 % reducing to 21% at 753 m - 874 m depth (Knutsford borehole in the N) and about 11 % below 1900 m (Prees borehole in the S).

The first estimate of the geothermal heat in place (H_0) of the basin (GALE et al., 1984) suggested about 17×10^{18} J in the *Triassic Sherwood Sandstone Group* and about 28×10^{18} J in the underlying *Permian* and *Triassic* sandstones. Identified resources (H_1 , $T_r = 30$ °C and $R_0 = 0.25$) were about 2.1×10^{18} J and 3.8×10^{18} J, respectively.

In this contribution, temperature calculated at the mid-depth of the formation was taken for the resources calculation. Geothermal resources have been estimated assuming that reservoir sandstones make up approximately 0.25 and 0.30 of the Permian sandstone and SSG section, respectively. Total H_0 of the Permo-Triassic and SSG reservoirs have been recalculated to 38×10^{18} J and 36×10^{18} J, and the identified resources (H_1) to 9.1×10^{18} J and 7.6×10^{18} J, respectively. This is a significant increase on the previous estimates. The resources are concentrated in the SE of the basin against the main bounding fault and centred on Crewe.

Worcester Basin (Plate 86)

The Worcester Basin is a roughly symmetrical graben system, bounded to the W and E by major NS trending normal faults and extending from Droitwich in the N to Cirencester in the S. The sedimentary rocks of the basin rest upon Precambrian and Palaeozoic basement. Maximum present-day sediment thicknesses are found in the central and eastern parts of the basin and may locally be > 3000 m. Mercia Mudstone and younger rocks crop out over much of this basin, and are underlain by very substantial thicknesses of the *Sherwood Sandstone Group* and the *Permian Bridgnorth Sandstone Formation*.

The W boundary of the basin (and the aquifer) is the NS trending E Malvern Fault which dips to the E at approximately 45° and has a throw of > 2500 m. The E margin of the Worcester Basin is marked by several large normal faults which have sub-planar fault surfaces dipping to the W at about 50°. The most important of these, the Inkberrow Fault, has a present-day throw which decreases upwards from over 1000 m at the base Permo-Triassic to only 100 - 200 m at the base of the Jurassic. This indicates more than 800 m syndepositional Permo-Triassic displacement occurred. Within the basin itself, several smaller normal faults are present, again with dominantly NS trends showing evidence of syndepositional movement.

The hydraulic properties of the Bridgnorth, Wildmoor and Bromsgrove sandstones were assessed. TDS of the Permian sandstone at Kempsey and the Triassic Wildmoor Sandstone are 25 g/l and 6 g/l, respectively. At Kempsey the Triassic sandstones over a section with average porosity of 23 % have an average permeability of 690 mD. A drill stem test yielded a field permeability of about 300 mD. Laboratory permeability of 450 mD was determined on samples from the same zone.

Sherwood Sandstone Group

Isopach contours for the Triassic sandstones have been derived from fault controlled gridding of the digitised seismic interval. New interpretation of the fault-bounded block between Evesham and Worcester suggests a local graben with the Sherwood Sandstone Group surface at depths of over 1000 m. The Kidderminster Formation, at the base of the Sherwood Sandstone Group, consists of coarse, cross-bedded pebbly sandstones up to 175 m thick. The Wildmoor Sandstone

Formation oversteps the Kidderminster Formation and is thought to be of fluvial origin. The Bromsgrove Sandstone rests unconformably on the Wildmoor Sandstone Formation and consists of upward fining fluvial cycles (made up of conglomerates, sandstones, siltstones and mudstones). These deposits were laid down in alluvial fan, braided river and meandering river plain environments. They are on average 500 m thick and pass gradationally up into the overlying Mercia Mudstone Formation. The geophysical logs show it contains clayey marl bands. In the S of the basin, this formation passes laterally and distally into a mudstone facies. Mean porosity is 19 % ranging from 11 - 25 %. At outcrop it has permeability of 780 - 7800 mD (SKINNER, 1977). A drill stem test of the Wildmoor sandstone over part of a cored interval gave a permeability of 290 mD compared to the permeability measured on core of 450 mD. The Wildmoor Sandstone and Bromsgrove Sandstone are considered as one hydrogeological unit.

The heat in place of the Triassic sandstones were recalculated using a reservoir fraction of 0.40 of the total section. The H_0 of the Triassic sandstones are estimated at 8×10^{18} J. The total identified resources (H_1) are estimated as 13×10^{18} J compared with 1.4×10^{18} J in the previous assessment.

Permo-Triassic

The *Permian Bridgnorth Sandstone* is a red aeolian sandstone consisting of rounded wind-polished grains that are only lightly cemented with iron oxide. Large scale cross-beds and thin marl bands are present. It reaches a maximum recorded thickness of 938 m in the Kempsey borehole although seismic data suggest it is > 1400 m E of Worcester. Locally basal breccias occur several 10 m thick.

At outcrop the porosity is typically 25 - 30 % and at 1364 - 2296 m depth the mean porosity in the Kempsey borehole is 25 %. Measurements on core from Kempsey borehole (1476 - 1484 m) show a mean porosity of 19.7 % and mean permeability of 22 mD, although values as high as 3000 mD have been measured these cores. A drill stem test in this formation gave 126 - 150 mD.

Observed temperatures at the base of the Permian at depths in excess of 2000 m are limited to two boreholes: Kempsey (60 °C) and Guiting Power 1 (55°C). The maximum calculated temperatures are about 70 °C. The calculated temperature at Kempsey is about 55 °C underestimating the measured temperature of 61 °C. At Guiting Power calculated and observed temperatures agree closely.

A net reservoir thickness of 0.75 of the total formation thickness was taken for the calculation of H_0 . This results in $H_0 = 60 \times 10^{18}$ J, a factor of 6 greater than the previous estimate.

Wessex Basin (Plate 87)

The Wessex Basin overlies a basement of Cambrian - Carboniferous age (SMITH, 1985) deformed by thrust-related structures during the Variscan Orogeny. The Permian - Cretaceous tectonic evolution of the Wessex Basin was controlled by extensional reactivation of these thrusts giving rise to rapid subsidence of fault-bounded basins and the erosion of adjacent upfaulted blocks. Syn-depositional faulting during Permo-Triassic times was largely restricted to the W part of the Wessex Basin where extensional reactivation of the Variscan Front and Wardour thrusts produced the Vale of Pewsey, Mere, Cranborne and Winterborne Kingston faults (CHADWICK, 1986). The southerly downthrowing Vale of Pewsey fault delineates the N basin margin separating it from the London Platform to the N. Within the basin, growth faults split the basin into structural provinces. The Portsdown-Middleton and Mere faults define the N edge of a half-graben including the Hampshire-Dieppe and Cranborne-Fordingbridge highs. The Cranborne fault defines the N margin of the Winterborne Kingston trough and Dorset Basin.

Very coarse-grained basal Permian deposits outcrop in the W and are overlain by the siltstones and mudstones of the Aylesbeare Group (SMITH et al., 1974). These are succeeded by the coarsely arenaceous *Sherwood Sandstone Group*. It consists of breccias and conglomerates of the Budleigh Salterton Pebble Beds overlain by a series of cyclically deposited sandstones of the Otter Sandstone Formation (HOLLOWAY et al., 1989). The Sherwood Sandstone Group is covered by the argillaceous Mercia Mudstone Group.

The principal geothermal aquifer is the Sherwood Sandstone Group. The depth to the top of this sandstone increases steadily from the outcrop towards the E. It is deeper than 1000 m over most of the basin and reaches a maximum depth greater than 2300 m in the Winterborne Kingston Trough. The aquifer attains depths greater than 2200 m just to the S of the Pewsey Fault, although here the Group is thin and probably not a viable geothermal aquifer. Several major fault zones intercept the aquifer, generally trending E-W and defining a series of highs and lows.

The main depocentre lies in SW Dorset where the thickness is greater than 300 m. Thickness variations are smooth with no evidence of substantial fault control.

Mean porosity ranges mostly from 11 - 19 % but may reach 24 %. The porosity measured on cores is similar to geophysical log derived porosities. Generally thin high porosity fluvial sandstone layers contribute the overwhelming bulk of brine production. The fluid produced during testing was brine (> 100 g/l NaCl) at a downhole temperature of 75 °C. The lower part of the aquifer is heavily cemented with CaCO₃ and some dolomite. Core permeabilities range 100 - 5600 mD.

Hydraulic testing of the Sherwood Sandstone at Marchwood included 4 drill-stem tests (DST), a gas-lift well test, and a 30-day constant rate production test. The tests yield transmissivities of 3.5 - 10 D m. (PRICE and ALLEN, 1982). The transmissivity of the Sherwood Sandstone increases from about 5 Dm S of Salisbury to 50 Dm towards the W. The initial distribution and subsequent dissolution of the cements and the distribution and sorting of medium- and coarse-grained sands are key factors in controlling the geothermal aquifer porosity and permeability (MILODOWSKI et al, 1986).

The previous assessment of the geothermal resources of Sherwood Sandstone Group of the Wessex Basin (ALLEN and HOLLOWAY, 1984) indicated a H_0 of about 23×10^{18} J and of 3.2×10^{18} J. Much of the identified resource was located in the Dorset sub-basin west of Bournemouth.

In this contribution, the geothermal resources of the Wessex basin have been calculated using the temperature field at the base of the Sherwood Sandstone. This emphasises the fact that the reservoir is concentrated in the lower part of this unit and is generally less than 300 m thick. Reservoir fraction in the Wessex basin was taken as 0.33 of the thickness of the Sherwood Sandstone Group. This corresponds to the fraction of the unit with estimated porosities of over 18 %. A minimum aquifer thickness of 50 m was applied.

The total heat in place (H_0) of the reservoir are estimated at 27×10^{18} J with maxima locally of about 20 GJ/m². The value has increased by over 10 % from the previous calculation with a new zone of resources north of Salisbury. The total identified resources (H_1) are estimated at about 7×10^{18} J.

Present status and future perspective of the use of geothermal energy

The reassessment of the total heat in place UK above 40°C for the four basins studied resulted in an increase by about a factor of 1.6, from about 180×10^{18} to 290×10^{18} J. Revised models of the basin structure, based on seismic data have significantly changed the aquifer-reservoir models and extended the geothermal resource estimates.

The table below summarises the main results of the revised resource calculation in comparison with the estimates of 1988. The largest changes are in the Worcester and Cheshire basin with increases by factors of 5.6 and 1.6, respectively.

Summary of Heat Low Enthalpy Geothermal Resources Place H_0 (in 10^{18} J)

Basin	Aquifer	1988		1995	
		H_0	Area km ²	H_0	H_1
East England	SSG Triassic	99	4827	122.2	24.6
Wessex	SSG Triassic	23	4188	27.2	6.5
Worcester	SSG Triassic	12	500	8.2	1.5
	BNS Permian	-	1173	60.3	11.8
Cheshire	SSG Triassic	17	677	36.2	7.6
	CS Permian	28	1266	38.5	9.1
Total		179		292.6	61.1

Heat in Place (H_0) above 40 °C.
Identified Resources (H_1) $T_r = 25$ °C. $R_0 = 0.33$.
SSG Sherwood Sandstone Group
BNS Bridgnorth Sandstone
CS Collyhurst Sandstone

References

- Allen, D. J and Holloway, S., 1984: The Wessex Basin. - Investigation of the Geothermal Potential of the UK, British Geological Survey, 80 p.
- Chadwick, R. A., 1986: Extensional tectonics in the Wessex Basin, southern England. - J. Geol. Soc. London. 143, p. 465-488.
- Downing, R. A. and Gray, D. A., 1986: (editors) Geothermal Energy: the potential in the United Kingdom. - HMSO. 187 p.

- Downing, R. A., Allen, D. J., Bird, M. J., Gale, I. N., Kay R. L. F. and Smith, I. F., 1985: Cleethorpes No 1 Geothermal Well - a preliminary assessment of the resource, Investigation of the Geothermal Potential of the UK.. - British Geological Survey, 67 p.
- Evans, D. J., Rees, J. G. and Holloway, S., 1993: The Permian to Jurassic stratigraphy and structural evolution of the central Cheshire Basin.. - Journal Geological Society London. 150, p. 857-870.
- Gale, I. N., Evans, C. J., Evans, R. B., Smith, I. F., Houghton, M. T. and Burgess, W. G., 1984: The Permo-Triassic aquifers of the Cheshire and West Lancashire basins. Investigation of the Geothermal Potential of the UK.. - British Geological Survey, 39 p.
- Haenel, R. and Staroste, E. (eds), 1988: Atlas of Geothermal Resources in the European Community.. - Publication No EUR 11026 of the Commission of the European Communities, Brussels.
- Holloway, S, Milodowski, A. E., Strong, G. E. & Warrington, G., 1989: The Sherwood Sandstone Group (Triassic) of the Wessex Basin, southern England. - Proceedings of the Geologists Association, 100, p. 383-394.
- Milodowski, A. E., Strong, G. E., Wilson, K. S., Holloway, S. and Bath, A. H., 1987: Diagenetic influences on the aquifer properties of the Permo-Triassic sandstones in the East Yorkshire and Lincolnshire Basin, Investigation of the Geothermal Potential of the UK.. - British Geological Survey, 36 p.
- Price, M. and Allen, D. J., 1982: The production test and resource assessment of the Marchwood Geothermal borehole, Investigation of the Geothermal Potential of the UK.. - British Geological Survey, 34 p.
- Ramingwong, T., 1974: Hydrogeology of the Keuper Sandstone in the Droitwich syncline area, Worcestershire. - PhD Thesis, University of Birmingham, (unpublished).
- Rollin, K. E., 1987: Catalogue of Geothermal data for the land area of the United Kingdom. Third Revision: April 1987, Investigation of the Geothermal Potential of the UK.. - British Geological Survey. 16 p.
- Skinner, A. C., 1977: Groundwater in the regional water supply of the British Midlands. - Memoirs of the International Association of Hydrogeologists, 13, p. A1-A12.
- Smith, D. B., Brunstrom, R. G. W., Manning, P. I., Simpson, S., and Shotton, F. W., 1974: A correlation of Permian rocks in the British Isles. *Special Report of the Geological Society of London*, 5, 45 p.
- Smith, N. J. P., 1985: The pre-Permian Geology of the United Kingdom (South). - British Geological Survey 150th Anniversary Publication.

4 Abbreviations and symbols

b.g.l.	=	below ground level
EC	=	European Community
GJ	=	Gigajoule
GWy	=	Gigawatt year
ha	=	hectare
Ma	=	million years
MW _e	=	Megawatt electric
MW _t	=	Megawatt thermal
ppm	=	parts per million
TDS	=	Total Dissolved Solids
toe	=	tonnes of oil equivalent
mtoe	=	million tonnes of oil equivalent
toe/a	=	tonnes of oil equivalent per year
g/l	=	gram per litre
l/s	=	litre per second
m/s	=	metre per second
m ³ /h	=	cubic metre per hour
t/h	=	tonnes per hour
>	=	greater than
<	=	smaller than
≥	=	greater than or equal to
≤	=	smaller than or equal to
≈	=	approximately equal to

5 Tables of springs, geothermal installations and heat-flow density

Springs and geothermal installations

The serial number in the table identifies the spring or geothermal installation on the national geothermal thematic map. The cross following the serial number indicates that a geothermal installation is in operation and a cross in brackets indicates that a geothermal installation is under construction.

Albania

No.	Location	Co-ordinates		Temp. °C
		Lat. (N)	Long. (E)	
1	Peshkopi	41 41 06	20 27 18	44
2	Mamurras	41 35 12	19 42 48	21
3	Shupal	41 26 54	19 55 48	30
4	Llixha Elbasan	41 01 36	20 05 00	60
5	Perroi i Holtes, Gramsh	40 55 30	20 13 12	24
6	Ura e Kadiut, Langarice, Permet	40 14 42	20 26 12	30
7	Sarandoporo, Leskovik	40 05 54	20 40 06	27
8	Finiq, Sarande	39 52 54	20 03 00	34
9	Kozani-8	41 07 18	20 01 06	66
10	Ishmi 1b	41 29 48	19 40 36	60
11	Galigati 2	40 57 12	20 09 18	45-50
12	Bubullima 5	40 45 42	19 39 48	48-50
13	Ardenica 3	40 48 48	19 35 36	38
14	Semani 1	40 50 00	19 25 00	35
15	Ardenica 12	40 48 42	19 35 42	32
16	Verbasi 2	40 41 36	19 36 36	29

Belgium

No.	Location	Co-ordinates		Temp. °C
		Lat. (N)	Long. (E)	
1	Meer	51 26 43	04 45 50	35
2+	Merksplas*	51 20 32	04 49 42	72
3+	Turnhout	51 19 24	04 57 06	36
4	Oostende	51 13 39	02 54 04	20
5+	Dessel	51 13 38	05 04 02	31
6+	Herentals	51 11 17	04 49 44	27
7	Chaudfontaine	50 35 06	05 38 48	36
8	Baudour	50 29 08	03 50 10	53
9+	Douvrain	50 28 20	03 51 27	66
10	Ghlin	50 27 52	03 54 50	71
11+	St. Ghislain	50 26 50	03 49 47	73

* not in operation, see text.

Bulgaria

No.	Location	Co-ordinates		Temp. °C
		Lat. (N)	Long. (E)	
1	Gomotartsi	43 05	22 57	67
2	Slanotran	44 02	22 59	43
3	Kutovo-Antimovo	44 01	22 56	44
4	Vidin	44 00	22 54	45
5	Dalgodeltsi	43 35	23 18	90
6	Zamfirovo	43 17	23 14	50
7+	Dolni Lukovit	43 31	24 13	71
8+	Dolni Dabnik	43 23	24 28	67
9(+)	Pleven	43 23	24 39	67
10	Shipkovo	42 52	24 32	24-37
11(+)	Chiflik	42 49	24 34	51
12(+)	Krushuna	43 14	25 01	59
13	Slavianovo	43 27	24 53	55
14	Belene	43 38	25 09	48
15	Svishtov - W	43 37	25 19	49
16	Svishtov - E	43 37	25 23	42
17	Ovcha mogila	43 27	25 17	52
18	Obedinenie	43 20	25 29	47
19+	Resen	43 11	25 34	55
20	Polski Trambesh	43 22	25 40	44-48
21	Voditsa	43 21	23 03	42
22	Razgrad	43 31	26 32	27
23	Targovishte	43 15	26 33	46
24+	Marash (Shumen)	43 12	26 57	67
25	Ignatievo	43 15	27 42	32
26	Ezerovo-Beloslav	43 11	27 45	31-33
27(+)	Zvezditsa (Chayka)	43 11	27 50	55
28(+)	Varna - g	43 14	27 49	44
29	Aksakovo	43 15	27 49	39
30	Oreshak	43 17	27 54	35
31+	Varna - d	43 13	27 54	50
32	Varna - e	43 12	27 51	48
33	Varna - c	43 11	27 54	50-55
34	Bliznatsi	43 05	27 54	63
35+	Varna - b	43 12	27 55	51-55
36+	Varna - a	43 11	27 56	51
37+	Sv. Konstantin +Evksinovgrad	43 10	28 00	40-49
38	Chayka-Journalist	43 15	28 01	39

No.	Location	Co-ordinates		Temp. °C
		Lat. (N)	Long. (E)	
39+	Zlatni Pyasatsi resort	43 20	28 03	32-37
40	Kranevo	43 20	28 03	30
41	Albena	43 22	28 04	28-30
42	Balchik	43 24	28 09	24
43	Topola-Tuzla	43 24	28 15	34
44	Kavarna	43 25	28 21	29
45	Rusalka	43 25	28 31	32
46	Shabla	43 33	28 33	35-40
47	Barzia	43 11	23 10	32
48	Slatina	43 13	23 14	27
49	Spanchevtsi	43 10	23 15	32
50	Varshets	43 12	23 16	36-40
51	Elenov dol	43 03	23 28	27
52	Kostinbrod	42 50	23 12	23-31
53	Novi Iskar	42 48	23 20	42
54	Iliantsi-Trebich	42 45	23 20	52
55+	Nadezhda	42 44	23 18	49-52
56	Svetovrachene	42 47	23 24	48
57	Chepintsi	42 45	23 25	50
58	Dolni Bogrov	42 42	23 30	46
59	Ravno pole	42 40	23 31	50-59
60+	Kazichene	42 40	23 28	62-80
61	Pancharevo	42 36	23 24	43-48
62	Sofia - Lozenets	42 41	23 19	30-48
63	Sofia - centre	42 42	23 19	47
64	Ovcha koupel	42 41	23 16	32
65	Knyazhevo	42 40	23 14	23-37
66	Gorna banya	42 41	23 15	33-42
67	Bankya	42 43	23 09	36-38
68	Rudartsi	42 36	23 10	28
69	Dolni Rakovets	42 28	23 01	21-31
70	Zhelezuitsa	42 33	23 24	21-32
71	Belchinski bani	42 22	23 28	41
72	Iskar	42 28	23 33	25
73	Poibrene	42 30	24 00	33-42
74	Banya, Panagyursko	42 28	24 08	37-43
75	Panagyurushte	42 30	24 14	44
76	Strelcha	42 31	24 19	43-56
77+	Krasnovo	42 28	24 29	54
78	Staro Zhelezare	42 27	24 39	20-29
79+	Hisarya	42 31	24 43	36-52
80	Pesnopoy	42 28	24 48	30-43
81+	Banya, Karlovo	42 33	24 50	35-54
82	Kliment	42 36	24 42	30
83	Stoletovo	42 42	24 34	33
84	Klisura	42 42	24 27	21
85	Voyvodino	42 13	24 48	32
86	Chirpan	42 12	25 18	36
87	Merichleri	42 09	25 30	30-45
88(+)	Simeonovgrad	42 02	25 53	51-54
89	Topolyane	42 18	25 52	33
90	Starozagorski bani	42 27	25 30	36-44
91+	Pavel banya	42 38	25 19	43-61
92+	Ovoshtnik	42 37	25 24	41-78
93	Yagoda	42 32	25 35	44-53
94+	Banya, Korten	42 36	26 00	42-58
96	Slivenski bani	42 36	26 14	42-50
97	Straldzha	42 37	26 41	44-77
98	Stefan Karadzhovo	42 13	26 50	21
99	Polyanovo	42 42	27 12	49
100	Aytos	42 42	27 17	18-44
101	Sadievo	42 40	27 19	20-30
102	Burgaski bani	42 37	27 24	41
103	Medovo	42 42	27 31	29-39
104	Slanchev bryag	42 40	27 44	29-31
105+	Kyustendil	42 18	22 42	76
106	Nevestino	42 16	22 49	24-30
107+	Sapareva banya	42 17	23 15	83-101
108	Rila	42 06	23 09	37
109	Blagoevgrad	42 02	23 06	55
110(+)	Zeleni dol	42 00	23 04	63
111	Dolno Osenovo	41 57	23 14	36-59
112+	Simitli	41 54	23 14	54-63
113	Gorna Breznitsa	41 44	23 05	26-40
114	Oshlava	41 48	23 13	40-56
115	G. Gradshnitsa	41 42	23 14	45-67
116+	Sandanski	41 35	23 17	63-83
117	Spatovo	41 31	23 19	38
118	Hotovo	41 30	23 20	37
119+	Levounovo	41 29	23 18	73-87
120	Rupite (Kozhuh)	41 28	23 15	73-76
121	Kromidovo	41 27	23 23	47
122+	Marikostinovo	41 26	23 19	42-62
123	Mousomishita	41 35	23 46	21-22
124+	Ognyanovo+Garmen	41 37	23 49	25-43
125	Dobrinishte	41 49	23 34	31-43
126+	Eleshnitsa-Mesta	41 52	23 36	39-56
127	Eleshnitsa-Zlataritsa	41 54	23 39	26-38
128+	Banya, Razlog	41 53	23 32	28-58
129	Bachevo	41 56	23 26	21-26
130	Yakorouda	41 59	23 41	36-42
131	Kostenets	42 16	23 50	47
132(+)	Dolna banya	42 18	23 46	56-64
133 +	Pchelinski bani	42 22	23 46	72

No.	Location	Co-ordinates		Temp. C
		Lat. (N)	Long. (E)	
134+	Momin prohod	42 20	25 53	65
135+	Chepino-Velingrad	41 59	23 58	36-48
136+	Ladzane-Velingrad	42 02	23 59	33-63
137+	Kamenitsa-Velingrad	42 03	23 59	85-91
138+	Draginovo	42 03	24 00	59-95
139	Rakitovo	42 00	24 05	31-50
140	Malko Belovo	42 12	24 03	20-25
141+	Varvara	42 08	24 07	36-91
142	Krichim	41 59	24 28	28-30
143	Mihalkovo	41 51	24 26	26
144	Devin	41 45	24 23	42-44
145	Bedenski bani	41 42	24 30	76
146	Narechenski bani	41 54	24 44	20-31
147	Kuklen	42 02	27 28	32
148	Asenovgrad	41 58	24 54	25-44
149	Topolovo	41 37	25 00	60
150	Lenovo	41 57	25 08	47
151	Bryagovo	41 59	25 10	22-27
152	Novakovo	41 53	25 05	22
153	Banite	41 38	25 00	43
154(+)	Erma reka	41 24	24 58	87-100
155	Dzhebel	41 31	25 17	33
156	Kirkovo	41 19	25 20	22
157+	Mineralni bani	41 56	25 21	54-58

Czech Republic

No.	Location	Co-ordinates		Temp. °C
		Lat. (N)	Long. (E)	
1	Soos	50 06 00	12 24 36	18
2	Karlovy Vary	50 12 36	12 49 48	72
3	Jehlicna	50 12 36	12 43 12	21
4	Jáchymov	50 21 00	12 55 48	32
5	Teplice Spa	50 38 24	13 50 24	42-46
6	Jánske Lázně	50 36 00	15 55 12	28-32
7	Bohdanec	50 04 12	15 40 48	21
8	Velké Losiny	50 02 24	17 02 24	33
9	Bludov	49 39 00	16 55 48	24
10	Teplice nad Bečvou	49 31 48	17 45 00	23

Denmark

No.	Location	Co-ordinates		Temp. °C
		Lat. (N)	Long. (E)	
1+	Thisted-2	56 57 56	08 42 57	46

Estonia

No springs above 20 °C.

Finland

No springs above 20 °C. Exact amount and localization of heat pumps are not known. There are over 1000 vertical heat exchangers all over the country.

France

For geothermal springs see previous atlas. Only geothermal installations are listed below.

No.	Location	Co-ordinates		Temp. °C
		Lat. (N)	Long. (E)	
*d	Alfortville	48 46 39	2 25 42	74
*d	Aulnay-sous-Bois	48 57 13	2 30 45	67
*d	Bonneuil-sur-Marne	48 46 05	2 29 05	79
*d	Bruyère le Chatel	48 35 33	2 11 12	33
*d	Cachan-Nord	48 47 20	2 19 49	70
*d	Cachan-Sud	48 47 20	2 19 49	70
*d	Champigny-sur-Marne	48 48 00	2 33 50	78
*d	Châtenay-Malabry	48 46 02	2 15 25	68
*d	Chelles	48 52 07	2 35 49	68
*d	Chevilly-Larue	48 46 13	2 22 01	73
*d	L'Hay-les-Roses	48 46 20	2 20 41	70
*d	Clichy-sous-Bois	48 54 47	2 32 46	71
*d	Coulommiers	48 49 24	3 05 56	83
*d	Créteil	48 46 17	2 27 55	74
*d	Epinay-sous-Sénart	48 41 45	2 30 57	74
*d	Evry	48 37 45	2 24 52	72
*d	Fresnes	48 45 22	2 19 54	72
*d	La Courneuve-Nord	48 55 49	2 24 10	58
*d	La Courneuve-Sud	48 55 40	2 23 04	56
*d	Le-Blanc-Mesnil	48 57 02	2 27 22	67
*d	Le-Mée-sur-Seine	48 32 39	2 37 59	72
*d	Maisons-Alfort-I	48 48 06	2 26 27	72

No.	Location	Co-ordinates		Temp. C
		Lat. (N)	Long. (E)	
*d	Maisons-Alfort-II	48 47 15	2 26 03	73
*d	Meaux-Beauval 1	48 56 52	2 55 15	78
*d	Meaux-Beauval 2	48 56 53	2 55 16	78
*d	Meaux-Collinet	48 56 28	2 54 05	78
*d	Meaux-Hôpital	48 58 07	2 53 33	78
*d	Melun-L'Almont	48 32 26	2 40 53	71
*d	Montgeron	48 41 54	2 26 39	72
*d	Orly-I	48 45 00	2 25 09	75
*d	Orly-II	48 44 30	2 24 25	75
*	Paris-Maison de la Radio	48 51 40	2 16 40	26
*ds	Paris-AGF	48 51 39	2 16 00	27
*d	Ris-Orangis	48 38 36	2 24 06	70
*d	Sucy-en-Brie	48 46 19	2 31 20	78
*d	Thiais	48 45 28	2 23 36	76
*d	Tremblay-les-Gonnesse	48 56 50	2 34 35	73
*d	Vaux-le-Penil	48 31 57	2 41 33	71
*d	Vigneux-sur-Seine	48 42 35	2 24 51	74
*d	Villeneuve-Saint-Georges	48 44 33	2 27 22	76
*ds	Villiers-le-Bel	49 00 21	2 25 09	66
	Begles	44 48 22	0 33 42 W	21
	Bordeaux Benauges	44 50 33	0 32 39 W	44
	Bordeaux Meriadeck	44 50 13	0 35 17 W	54
	Pessac Saige Formanoir	44 47 36	0 37 32 W	48
	Pessac Stadium	44 48 10	0 36 40 W	34
	Mérignac BA 106	44 49 05	0 42 40 W	55
	Mios-le-Teich	44 36 25	0 58 28 W	73
	Dax	43 42 21	1 05 32 W	47
	Hagetmau	43 39 03	0 35 28 W	33
	Mont de Marsan 1	43 54 19	0 29 54 W	60
	Mont de Marsan 2	43 54 13	0 27 51 W	56
	Saint Paul les Dax	43 43 34	1 03 03 W	65
	Blagnac	43 38 16	1 23 01	58
	Libourne	44 53 43	0 13 06 W	23
	Châteauze	46 48 04	1 42 17	30
	Lamazère	43 33 29	0 26 43	57
	Casteljaloux	44 18 41	0 05 14	43
	Nogaro	43 45 22	0 13 52 W	50
	Jonzac	45 25 57	0 25 36 W	61
	Dieuze	48 50 08	6 34 42	31
	Montagnac	43 26 09	3 32 05	26

*Paris area

d:doublet (installation with 2 wells)

ds:Doublet with heat storage

Germany

The serial numbers of springs and installations are the same as in the previous atlas. New installations are identified with a new serial number and those installations that have been shut down have not been replaced, i.e. the installation and its serial number is missing from the table and the map.

No.	Location	Co-ordinates		Temp. °C
		Lat. (N)	Long. (E)	
1	Bad Bevensen	53 05 27	10 39 05	23
2	Bad Nenndorf	52 20 11	09 24 43	22
3	Bad Oeynhausen	52 12 49	08 49 34	36
4	Bad Salzuflen	52 05 34	08 45 03	37
5	Bielefeld-Heepen	52 05 00	08 37 01	26
6	Salzgitter Bad	52 02 38	10 22 23	20
7	Bad Bodenwerder	51 58 51	09 31 23	22
8	Bad Harzburg	51 54 22	10 33 30	26
9	Bad Lippspringe	51 47 15	08 48 52	28
10	Paderborn	51 45 00	08 42 52	23
11	Bad Waldliesborn	51 42 52	08 20 30	37
12	Hamm	51 41 18	07 50 49	31
13	Bad Westernkotten	51 38 10	08 21 23	23
14	Wanne-Eickel	51 30 56	07 10 29	40
15	Bad Raffelberg	51 26 00	06 49 00	25
16	Kassel-Wilhelmshöhe	51 18 26	09 30 00	25
17	Köln	50 58 52	06 59 00	20
18+	Bad Aachen	50 48 38	06 05 00	68
19	Bad Bodendorf	50 35 15	07 14 59	28
20	Bad Neuenahr	50 33 00	07 08 00	54
21	Bad Honningen	50 30 55	07 19 00	28
22	Rheinbrohl	50 30 16	07 19 35	21
23	Bad Breisig	50 30 10	07 18 15	34
24+	Bad Ems	50 23 13	07 42 50	43
25	Bad Nauheim	50 21 44	08 44 15	33
27	Lahnstein	50 18 19	07 36 40	31
28	Rhens	50 16 52	07 38 55	23
29	Bad Kissingen	50 13 57	10 03 20	21
30	Bad Soden a.T.	50 08 26	08 30 00	32
31+	Staffelstein	50 06 06	10 58 05	54
32	Offenbach	50 06 00	08 45 26	21
33	Schlangenbad	50 05 44	08 06 06	31
34+	Wiesbaden	50 05 12	08 14 00	69
35	Bad Bertrich	50 04 28	07 02 13	33
36	Mürsbach I, 3-6	50 03 06	10 53 00	50
37	Kriedrich	50 02 42	08 03 26	24
38	Assmannshausen	50 00 00	07 52 18	31
39	Bad Wildstein	49 55 31	07 07 12	33
40	Bad Münster a.St.	49 48 52	07 50 40	29
41	Bad König	49 44 34	09 02 00	21
42	Fürth	49 28 13	11 01 52	22
43	Heidelberg	49 24 45	08 42 05	24

No.	Location	Co-ordinates		Temp. °C
		Lat. (N)	Long. (E)	
44	Wiebelskirchen	49 22 32	07 11 20	37
45	Bad Friedrichshall	49 14 06	09 11 45	20
46	Bad Schönborn	49 12 50	08 39 43	46
47	Velsen	49 12 49	06 49 45	24
49	Bad Langenbrücken	49 07 12	08 22 48	26
50	Bad Bergzabern	49 06 00	08 00 00	22
51	Bad Rotenfels	48 50 11	08 17 00	21
52	Aalen	48 50 00	10 07 00	36
53	Bad Gögging	48 49 44	11 47 00	24
54	Bad Cannstatt	48 48 26	09 13 50	20
55	Bad Herrenalb	48 48 00	08 26 40	25
56	Bad Liebenzell	48 46 40	08 44 00	27
57+	Baden-Baden	48 45 30	08 14 40	70
58	Wildbad	48 45 02	08 33 09	40
59	Reichenbach/Fils	48 42 42	09 28 32	28
60	Ottersweier	48 42 00	08 01 40	36
61	Bad Boll	48 38 50	09 32 17	49
62	Gingen	48 37 30	10 14 30	21
64	Beuren, Krs. Nürtingen	48 36 32	09 14 16	48
65	Lautenbach-Sulzbach	48 35 52	08 10 00	21
66	Bad Ditzgenbach	48 35 24	09 42 10	45
67	Obersasbach	48 34 55	08 00 00	21
68+	Bad Urach	48 30 30	09 22 30	58
69+	Griesbach i.R.	48 27 00	13 11 05	60
70+	Birnbach	48 26 42	13 05 46	70
71+	Bad Füssing	48 21 33	13 18 38	56
72(+)	Erding I	48 17 26	11 53 16	65
73	Gölldorf	48 09 44	08 39 28	20
74+	Jordanbad, Biberach	48 05 36	09 49 12	49
75	Waldkirch	48 04 23	07 57 51	24
76+	Bad Buchau	48 03 07	09 38 02	48
77	Oberbergen	48 02 11	07 37 49	21
79	Freiburg	48 00 00	07 50 00	29
80(+)	Endorf	47 55 02	12 17 08	65-70
81	Bad Krozingen	47 55 00	07 42 11	41
82+	Bad Waldsee	47 55 00	09 45 00	30
83	Ravensburg	47 49 00	09 38 05	29
84	Badenweiler	47 48 06	07 40 29	26
85	SteinStadt	47 46 10	07 33 19	34
87	Bad Bellingen	47 44 00	07 33 16	38
88	Bad Wiessee	47 43 05	11 43 26	21
89+	Konstanz	47 39 54	09 12 54	29
90	Lottstetten	47 37 00	08 34 00	23
91	Stein	47 34 48	10 14 18	38
92	Säckingen	47 33 31	07 56 48	30
93(+)	Göhren-Lebbin	54 19 48	13 43 48	
94+	Neubrandenburg	53 33 36	13 16 12	54
95+	Waren (Müritz)	53 31 12	12 40 48	60
96+	Neustadt-Glewe	53 22 12	11 34 48	95
97+	Prenzlau	53 19 12	13 52 12	108
98(+)	Rheinsberg	53 06 00	12 52 48	60-65
99(+)	Meppen	52 42 00	07 18 00	60
100+	Gladbeck	51 34 12	06 58 48	
101+	Düsseldorf	51 13 48	06 47 24	
102	Bad Sulza	51 05 26	11 37 17	22
103	Bad Liebenstein	50 48 51	10 20 57	19
104(+)	Ehrenfriedersdorf	50 37 48	12 58 12	11-14
105	Birkenhügel	50 26 07	11 42 45	28
106(+)	Lobenstein	50 25 48	11 37 48	50
107	Bad Collberg	50 16 38	10 48 06	39
108+	Frankfurt-Höchst	50 07 12	08 33 00	
109(+)	Bayreuth	49 56 24	11 34 48	31
110+	Weiden	49 40 48	12 09 36	26
111(+)	Marktschwaben	48 52 12	11 51 00	80-85
112(+)	Straubing	48 52 12	12 34 48	38
113(+)	Neufahrn	48 19 12	11 40 12	80-85
114(+)	Simbach am Inn	48 16 12	13 01 12	90-100
115(+)	Altötting	48 13 48	12 40 48	90-100
116(+)	Krumbach	48 12 00	10 24 00	55
117+	Kochel am See	47 39 00	11 13 12	

Greece

Geothermal springs

No.	Location	Co-ordinates		Temp. °C
		Lat. (N)	Long. (E)	
1	Loutra Agistrou Serres	41 21 16	23 32 51	41
2	Therme Schinou, Xanthis	41 20 11	24 57 51	52
3	Therma Drama	41 19 05	24 32 08	52
4	Ag. Barbara Gefyra Sidirokastrou	41 12 32	23 25 00	44
5	Promachi Arideas, Edessa	41 01 38	22 00 00	26
6	Potamia Kessanis, Xanthis	41 01 38	25 02 51	53
7	Loutra Arideas, Edessa	40 58 54	21 56 20	36
8	Loutra Therme Nigritas, Serres	40 55 05	23 31 25	56
9	Traianoupolis Alexandroupoli	40 53 27	26 07 51	50
10	Pigi Dexamenis, Lagadas	40 43 38	23 06 21	39
11	Nea Apollonia Eleftheron Kavala	40 43 38	24 05 43	41
12	Xyno Nero Florinis Pigi Loutron Neas Apollonias,	40 41 27	21 37 25	Gas
13	Langadas Therme Anthemountos Sedes	40 38 11	23 27 31	49
14	Thessaloniki	40 30 32	23 04 14	38
15	Therma Samothrakis B. Samothr.	40 29 27	25 33 10	49
16	Therma Samothrakis A. Samothr. Pyxaria-Bithoulki - Ag. Barbara.	40 28 54	25 33 10	54
17	Konitsa	40 12 00	20 44 17	32

No.	Location	Co-ordinates		Temp. °C
		Lat. (N)	Long. (E)	
18	Kavassila, Konitsa Ag. Paraskevi,	40 02 11	20 40 43	30
19	Ag. Nikolaos Kasandras	39 57 16	23 35 17	39
20	Iphestos Therma, Limnos	39 55 38	25 06 21	44
21	Eftalou, Lesvos	39 21 48	26 15 20	45
22	Psarotherma Argenou, Lesvos	39 21 48	26 18 08	80
23	Petra, Lesvos	39 19 38	26 14 39	30
24	Sfagia Kallonis, Lesvos	39 14 43	26 14 39	27
25	Pigi Pileos Smokovo, Karditsa	39 12 00	22 02 05	36
26	Gerakari Kallonis, Lesvos	39 12 00	26 11 52	25
27	Pigi Alexandrou Smokovo, Karditsa	39 10 54	22 00 41	40
28	Pigi Irakleous Smokovo, Karditsa	39 10 54	22 02 47	40
29	Loutra Thermis, Lesvos	39 09 48	26 30 41	47
30	Kourtzi, Lesvos	39 07 38	26 29 18	36
31	Loutra Kolpou Geras, Lesvos	39 07 05	26 27 54	39
32	Loutra Ag. Ioanni Lisvoriou	39 06 30	26 14 39	67
33	Loutra Polychnitou Loutra Kryffi Panagia	39 04 54	26 12 33	82
34	Plomariou Lesvos	39 01 05	26 16 44	44
35	Pigi Loutron Platistomou, Lamia	39 00 32	22 06 58	34
36	Paleosaraga Preveza	38 58 54	20 43 57	21
37	Ypati, Lamia	38 58 54	22 17 26	34
38	Gialtra, Evia	38 51 16	22 59 18	43
39	Piges Damarion Edipsos, Evia	38 50 43	23 05 35	71
40	Piges Ano Synikias Edipsos, Evia	38 50 43	23 07 40	57
41	Piges Thermopylon, Lamia	38 45 49	22 32 05	41
42	Piges Kallidromou, Lamia Piges Dexamenon	38 45 49	22 34 00	34
43	Kam. Vouria, Lamia Pigi Koniavitou	38 45 49	22 49 32	35
44	Kam. Vouria, Lamia	38 45 49	22 50 56	33
45	Agiasmata-Keramou, Chios	38 34 22	25 56 31	68
46	Psanis Nafpactos	38 23 27	21 51 08	21
47	Kounoupeli, Ilia	38 05 27	21 22 04	28
48	Piges E.O.T., Loutraki	37 57 49	23 00 00	31
49	Piges Dimos, Loutraki	37 56 43	22 59 19	30
50	Sousaki	37 55 38	22 04 08	Gas
51	Kyllini, Ilia	37 51 16	21 08 10	25
52	Eyryali Glyfada, Attiki	37 51 16	23 47 02	32
53	Piges Spileou Vouliagmenis, Atti.	37 48 00	23 48 50	25
54	Potami Karlovassio, Samos	37 48 00	26 53 47	40
55	Souvala Vatheos, Aegina	37 43 38	23 27 57	24
56	Irea, Arcadia	37 42 32	21 56 35	20
57	Perdiki-Ag. Kyriakis, Ikaria	37 40 54	26 20 00	37
58	Frasinias Pyrgos, Ilia	37 39 49	21 21 49	29
59	Kaki Skala Pyrgou, Tinos	37 39 16	25 02 03	24
60	Lefkada-Ag. Kirykou, Ikaria	37 36 00	26 15 10	58
61	Piges Bromolimnis, Methana	37 35 27	23 23 52	34
62	Athanato Nero, Ikaria	37 35 27	26 13 47	22
63	Pigi Ag. Nicolaou, Methana	37 33 49	23 21 49	41
64	Pigi Spileou Kaiafas, Ilia	37 27 49	21 37 30	36
65	Loutra Ag. Anargyri, Kythnos	37 27 16	24 24 32	38
66	Loutra Kakavos, Kythnos	37 26 43	24 25 13	52
67	Ag. Anargyri-Naussas, Paros	37 08 11	25 16 22	25
68	Therma, Kalymnos	36 57 16	27 00 00	37
69	Ag. Soulas, Kos	36 51 48	27 15 00	32
70	Ag. Fokas, Kos	36 51 12	27 16 22	42
71.1	Agioclima, Kimolos	36 49 38	24 32 03	55
71.2	Paralia, Prasson, Kimolos Kardamena-Monastiraki-Ag.	36 49 05	24 34 46	47
71.3	Irinis, Kos	36 49 38	27 13 38	46
72	Kimolos Kapro	36 48 32	24 32 03	48
73	Kos	36 45 49	27 00 00	Gas
74.1	Adamas Charou Bania, Milos	36 44 43	24 25 13	26
74.2	Schinopi Adamanda, Milos	36 43 38	24 25 54	41
74.3	Adamos, Milos	36 43 38	24 27 57	28
75.1	Vapour Milos	36 43 38	24 29 19	Gas
75.2	Paralia Komia, Milos	36 43 38	24 32 02	24
75.3	Kannava Adamanda, Milos	36 42 00	24 27 57	50
75.4	Milos	36 41 27	24 32 02	Gas
76.1	Loutra Mandrakiou, Nisyros	36 37 38	27 10 13	46
76.2	Palli-Emporiou, Nisyros	36 36 00	27 08 52	40
76.3	Nisyros	36 35 27	27 12 08	Gas
76.4	Nikia-Avlaki, Nisyros	36 34 54	27 11 35	57
76.5	Vapour Nisyros	36 34 22	27 09 32	Gas
77	Plaka Megalochoriou, Santorini	36 23 27	25 26 17	34
78	Vagia-Anafi, Kyclades	36 21 48	25 45 50	26
79	Santorini	36 21 16	25 24 40	Gas
80	Emporio-Blychada, Santorini	36 21 16	25 26 17	32
81	Aristino	49 09 18	25 54 37	79
82	Nea Kessani	41 01 38	25 02 51	83
83	Nigrita	40 54 00	23 24 00	60
84	Sidirokastrou	41 16 30	23 25 00	67
85	Iraklia	41 11 08	23 25 00	62
86	Nimfopetra	40 41 40	23 21 35	45
87	Langadas	40 43 20	23 04 50	40
88	Nea Apollonia	40 39 10	23 25 00	51
89	Athemountas	40 30 32	23 04 14	40
90	Eleochoria	40 21 40	23 14 11	42
91	Aidipsos	38 50 43	23 05 35	81
92	Kalloni-Stipsi	39 16 50	26 13 08	67
93	Mytilini town	39 06 25	26 32 57	35
94	Polichnitos	39 04 54	26 12 33	92
95	Nenita	38 12 41	26 04 13	30
96	Soussaki	37 56 06	23 05 25	79
97	Andravida	37 47 07	21 22 06	26
98	Milos, Zefyria	36 42 13	24 30 06	323
99	Nysiros, Volcano	36 34 22	27 09 32	350
100	Magana	40 56 00	24 50 00	65
101	Eratino	40 57 00	24 38 00	90

No.	Location	Co-ordinates		Temp. C
		Lat. (N)	Long. (E)	
102	Lilantio	38 26 12	23 51 26	32
103	Cape Agrivia	38 12 41	26 04 13	gas. 52

Geothermal installations

No.	Location	Co-ordinates		Temp. °C
		Lat. (N)	Long. (E)	
1(+)	Nea Kessani (Xanthi)	41 04	24 59	
2+	Nigrita	40 52	23 27	
3+	Langadas	40 41	23 03	
4+	Nea Apollonia	40 37	23 29	
5+	Polichnitos	39 05	26 15	
6+	Aidipsos	38 52	23 05	
8+	Sidirokastron	41 12	23 25	
9(+)	Sousaki	37 56	23 05	

Hungary

No.	Location	Co-ordinates		Temp. °C
		Lat. (N)	Long. (E)	
1.1	Sárospatak	48 19 39	21 35 06	45
1.2	Sárospatak	48 19 48	21 34 57	49
2	Encs	48 19 58	21 06 47	37
3.1	Kisvárdá	48 13 53	22 04 15	43
3.2	Kisvárdá	48 13 57	22 04 12	47
3.3	Kisvárdá	48 13 54	22 04 16	49
4	Gemzse	48 08 05	22 11 21	52
5	Vásárosnamény	48 07 32	22 20 59	57
6	Nagyhalász	48 07 53	21 44 43	38
7	Taktaszada	48 06 51	21 10 38	31
8.1	Miskolc	48 06 09	20 49 31	45
8.2	Miskolc	48 06 07	20 48 28	43
8.3	Miskolc	48 06 03	20 48 29	45
8.4	Miskolc	48 06 07	20 46 40	46
9	Fehérgyarmat	47 59 44	22 31 00	46
10	Baktalórántháza	47 59 00	22 04 26	45
11.1	Nyíregyháza	47 57 02	21 42 08	35
11.2	Nyíregyháza	48 00 26	21 43 47	51
11.3	Nyíregyháza	48 00 24	21 43 47	50
11.4	Nyíregyháza	47 57 11	21 42 30	48
11.5	Nyíregyháza	47 58 23	21 42 45	48
11.6	Nyíregyháza	47 57 06	21 43 46	48
11.7	Nyíregyháza	48 00 01	21 43 52	38
11.8	Nyíregyháza	48 00 25	21 43 19	50
11.9	Nyíregyháza	48 00 22	21 43 34	49
12.1	Bükkszék	47 59 41	20 10 30	39
12.2	Bükkszék	47 59 42	20 10 29	38
13	Mátészalka	47 56 58	22 19 44	58
14.1	Sajóhídvég	47 59 49	20 59 18	90
14.2	Leninváros	47 56 01	21 03 13	62
15	Tiszavasvári	47 56 35	21 21 51	67
16	Recsk	47 56 45	20 04 43	39
17	Pásztó	47 55 47	19 41 43	30
18.1	Bogács	47 54 30	20 31 47	73
18.2	Bogács	47 54 33	20 31 55	69
19	Nagykálló	47 52 31	21 51 20	46
20	Polgár	47 52 57	21 06 48	42
21	Mosonmagyaróvár	47 52 35	17 16 42	75
22.1	Andornaktálya	47 50 19	20 25 04	38
22.2	Eger	47 53 54	20 22 55	32
22.3	Eger	47 53 51	20 22 55	32
22.4	Eger	47 51 58	20 23 23	50
22.5	Eger	47 53 48	20 22 50	32
22.6	Egerszalók	47 51 11	20 20 08	66
23.1	Lipót	47 51 24	17 27 49	61
23.2	Lipót	47 51 42	17 27 26	64
24.1	Hajdúdorog	47 49 43	21 30 01	62
24.2	Hajdúnánás	47 49 54	21 25 09	67
24.3	Hajdúnánás	47 51 26	21 22 23	73
24.4	Hajdúnánás	47 49 44	21 25 15	59
25	Domoszló	47 49 40	20 07 14	30
26.1	Mezőkövesd	47 47 33	20 31 16	68
26.2	Mezőkövesd	47 47 33	20 31 14	48
26.3	Mezőkövesd	47 47 44	20 31 25	44
27	Gyöngyös	47 46 27	19 55 21	31
28	Visegrád	47 45 53	18 57 22	38
29	Lőrinci	47 44 50	19 40 31	32
30.1	Lébénymiklós	47 43 40	17 24 59	85
30.2	Lébénymiklós	47 43 42	17 24 05	76
31	Komárom	47 44 06	18 06 24	60
32.1	Tiszacsege	47 44 20	21 00 17	51
32.2	Tiszacsege	47 42 22	20 57 54	72
33.1	Hajdúböszörmény	47 41 06	21 29 59	49
33.2	Hajdúböszörmény	47 41 13	21 30 05	48
33.3	Hajdúböszörmény	47 41 09	21 29 59	62
34	Ács	47 42 20	17 55 54	70
35.1	Leányfalu	47 43 08	19 04 57	56
35.2	Szentendre	47 40 53	19 05 02	35
36.1	Abda	47 40 46	17 34 13	65
36.2	Győr	47 41 56	17 37 34	68
36.3	Győr	47 41 08	17 37 00	69
36.4	Győr	47 40 40	17 35 50	68

No.	Location	Co-ordinates		Temp. C
		Lat. (N)	Long. (E)	
37	Hort	47 41 18	19 47 58	32
38	Poroszló	47 38 50	20 39 10	33
39	Veresegyház	47 39 12	19 16 49	63
40.1	Csorna	47 37 44	17 15 08	69
40.2	Csorna	47 37 43	17 15 07	60
41	Hegykői	47 37 10	16 47 14	57
42.1	Balmazújváros	47 36 52	21 20 22	61
42.2	Balmazújváros	47 36 48	21 20 51	38
43.1	Tiszafüred	47 37 01	20 46 34	48
43.2	Tiszafüred	47 37 25	20 44 58	49
44.1	Hatvan	47 39 05	19 39 39	40
44.2	Tura	47 36 42	19 34 31	95
45.1	Adács	47 41 28	19 58 49	30
45.2	Vámosgyörk	47 40 56	19 55 48	32
45.3	Visznek	47 38 20	20 01 15	33
45.4	Tarnaörs	47 35 58	20 03 28	32
45.5	Jászdózsa	47 33 32	20 01 53	30
45.6	Jászárokszállás	47 36 59	19 57 59	32
45.7	Jászárokszállás	47 38 10	19 59 50	52
45.8	Jászdózsa	47 33 32	20 01 53	33
45.9	Jászdózsa	47 33 53	20 00 57	32
46	Nyírbátor	47 34 40	22 05 51	52
47	Bábolna	47 36 36	17 59 09	32
48.1	Kapuvár	47 35 57	17 02 25	66
48.2	Kapuvár	47 35 46	17 03 09	62
49	Petiháza	47 35 41	16 53 29	45
50	Hortobágy	47 34 45	21 08 55	61
51.1	Kömlő	47 35 54	20 25 44	38
51.2	Tiszanána	47 33 23	20 30 01	54
51.3	Kömlő	47 36 51	20 26 16	35
51.4	Tarnaszentmiklós	47 31 34	20 22 54	30
51.5	Hevesvezekény	47 33 31	20 21 39	36
52.1	Boconád	47 38 18	20 10 59	36
52.2	Boconád	47 38 38	20 13 16	33
52.3	Heves	47 36 24	20 17 03	35
52.4	Heves	47 36 31	20 17 34	37
52.5	Eger	47 35 54	20 16 04	48
52.6	Heves	47 35 24	20 17 16	47
52.7	Heves	47 36 07	20 17 23	35
52.8	Heves	47 38 59	20 15 50	40
52.9	Jászivány	47 31 35	20 14 43	37
52.10	Jászszeptandrá	47 34 53	20 10 16	42
52.11	Pély	47 30 38	20 20 28	48
52.12	Jászszeptandrá	47 35 09	20 10 14	35
52.13	Tarnasádnány	47 40 40	20 09 38	30
52.14	Tarnaméra	47 39 11	20 09 29	39
52.15	Jászapáti	47 31 11	20 08 57	42
52.16	Jászapáti	47 31 53	20 08 39	34
52.17	Jászapáti	47 31 20	20 07 58	46
52.18	Jászapáti	47 30 47	20 09 21	31
52.19	Jászapáti	47 31 07	20 08 54	35
52.20	Jászapáti	47 31 54	20 08 51	33
52.21	Jászapáti	47 29 20	20 10 35	35
52.22	Jászapáti	47 29 19	20 10 35	37
52.23	Jászapáti	47 29 56	20 10 12	37
53	Győrsemere	47 33 43	17 34 14	45
54.1	Debrecen	47 33 00	21 39 39	62
54.2	Debrecen	47 33 29	21 38 03	64
54.3	Debrecen	47 30 23	21 36 11	69
54.4	Debrecen	47 31 16	21 38 44	65
54.5	Debrecen	47 33 31	21 38 05	50
54.6	Debrecen	47 33 46	21 40 30	47
54.7	Debrecen	47 30 28	21 38 16	42
54.8	Debrecen	47 33 48	21 40 34	60
54.9	Debrecen	47 32 47	21 38 37	61
54.10	Debrecen	47 31 04	21 39 22	49
55	Tóalmás	47 31 00	19 40 02	48
56.1	Jászapáti	47 30 12	20 06 24	42
56.2	Jászfákóhalma	47 30 50	20 01 39	40
56.3	Jászfákóhalma	47 30 54	19 59 42	30
56.4	Jásztelek	47 29 01	20 00 31	31
56.5	Jászapáti	47 30 04	20 06 23	32
57	Nagyiván	47 29 28	20 55 51	32
58.1	Jászberény	47 29 53	19 52 50	45
58.2	Jászberény	47 30 11	19 54 37	45
59	Biatorbágy	47 29 47	18 45 04	37
60.1	Tiszaörs	47 28 33	20 49 29	47
60.2	Tiszaörs	47 28 18	20 49 30	51
61.1	Érd	47 21 17	18 56 19	40
61.2	Törökbálint	47 26 36	18 56 28	33
61.3	Budapest XI kerület	47 27 20	19 00 51	62
61.4	Budapest XI kerület	47 29 15	19 02 57	44
61.5	Budapest II kerület	47 31 04	19 02 21	49
61.6	Budapest II kerület	47 31 10	19 02 18	63
61.7	Budapest IX kerület	47 28 55	19 03 52	44
61.8	Budapest IX kerület	47 27 49	19 04 13	48
61.9	Budapest XI kerület	47 29 19	19 02 49	44
61.10	Budapest XIII kerület	47 31 08	19 02 39	72
61.11	Budapest XIII kerület	47 32 03	19 03 36	45
61.12	Budapest XX kerület	47 26 03	19 05 29	46
61.13	Budapest XXI kerület	47 24 26	19 06 07	45
61.14	Budapest XII kerület	47 24 32	19 01 23	52
61.15	Budapest I kerület	47 29 23	19 02 54	47
61.16	Budapest I kerület	47 29 24	19 02 55	47
61.17	Budapest I kerület	47 29 22	19 02 54	43
61.18	Budapest XX kerület	47 31 07	19 02 21	58
61.19	Budapest II kerület	47 31 04	19 02 22	63
61.20	Budapest XI kerület	47 28 09	19 02 12	49

No.	Location	Co-ordinates		Temp. °C
		Lat. (N)	Long. (E)	
61.21	Budapest XI kerület	47 29 03	19 03 18	42
61.22	Budapest XI kerület	47 29 10	19 03 07	43
61.23	Budapest XIII kerület	47 32 04	19 03 16	42
61.24	Budapest XIII kerület	47 32 05	19 03 11	38
61.25	Budapest XIII kerület	47 32 25	19 03 43	37
61.26	Budapest XIV kerület	47 30 55	19 04 44	74
61.27	Budapest XIV kerület	47 31 07	19 05 06	77
61.28	Budapest XIV kerület	47 31 14	19 07 55	70
62.1	Hajdúszoboszló	47 27 01	21 24 24	70
62.2	Hajdúszoboszló	47 25 50	21 24 30	70
62.3	Hajdúszoboszló	47 27 01	21 24 28	70
62.4	Hajdúszoboszló	47 26 23	21 25 28	35
62.5	Hajdúszoboszló	47 27 29	21 23 57	48
62.6	Hajdúszoboszló	47 27 47	21 24 42	34
62.7	Hajdúszoboszló	47 26 56	21 24 30	58
62.8	Hajdúszoboszló	47 27 04	21 24 24	36
62.9	Hajdúszoboszló	47 27 24	21 23 46	36
62.10	Hajdúszoboszló	47 28 25	21 21 31	32
62.11	Hajdúszoboszló	47 27 02	21 24 22	65
63.1	Nádudvar	47 25 52	21 09 40	39
63.2	Nádudvar	47 25 51	21 09 38	38
63.3	Nádudvar	47 26 01	21 09 49	43
64.1	Besenyszög	47 18 35	20 16 15	60
64.2	Besenyszög	47 14 51	20 13 35	55
64.3	Jászládány	47 21 54	20 12 34	51
64.4	Jászládány	47 21 31	20 09 58	56
64.5	Jászládány	47 22 20	20 08 36	30
64.6	Jászkisér	47 24 01	20 10 21	34
64.7	Jászkisér	47 26 03	20 11 48	42
64.8	Jászkisér	47 26 11	20 12 12	48
64.9	Jászkisér	47 27 28	20 12 13	52
64.10	Jászkisér	47 28 11	20 11 23	46
64.11	Jászkisér	47 27 47	20 14 01	69
64.12	Jászkisér	47 27 31	20 13 13	48
64.13	Jászkisér	47 27 31	20 13 13	43
64.14	Jászkisér	47 26 09	20 12 25	70
64.15	Jászládány	47 24 01	20 10 21	51
64.16	Jászládány	47 21 00	20 08 55	50
65.1	Bük	47 22 49	16 47 13	58
65.2	Bük	47 22 25	16 46 38	58
65.3	Bük	47 22 47	16 46 56	42
66	Kunhegyes	47 22 11	20 38 33	58
67.1	Nagykátá	47 24 18	19 44 39	57
67.2	Tápiószentmárton	47 20 13	19 45 49	54
68.1	Tápiógyörgye	47 20 09	19 56 37	30
68.2	Tápiógyörgye	47 20 04	19 56 54	34
68.3	Tápiószéle	47 19 39	19 53 05	30
68.4	Tápiógyörgye	47 19 18	19 56 43	31
68.5	Jászboldogháza	47 21 48	19 59 56	38
68.6	Jászboldogháza	47 21 48	19 59 33	42
68.7	Alattyan	47 25 27	20 02 19	42
68.8	Jánoshida	47 22 58	20 03 08	54
68.9	Alattyan	47 25 05	20 03 38	45
68.10	Jászsalsószentgyörgy	47 23 00	20 04 19	46
68.11	Jászsalsószentgyörgy	47 23 24	20 05 10	49
68.12	Szászberek	47 19 04	20 05 13	45
68.13	Jászsalsószentgyörgy	47 21 08	20 05 53	39
69.1	Bucsa	47 14 55	20 58 18	32
69.2	Karcag	47 19 44	20 54 24	40
69.3	Karcag	47 20 14	20 53 08	40
69.4	Karcag	47 22 56	20 50 27	43
69.5	Karcag	47 23 17	20 50 54	57
69.6	Karcag	47 23 16	20 50 45	54
70.1	Földes	47 17 50	21 21 17	66
70.2	Kaba	47 21 17	21 16 39	48
71	Pápa	47 20 06	17 29 11	42
72.1	Püspökladány	47 19 18	21 06 15	45
72.2	Püspökladány	47 19 14	21 06 10	47
72.3	Karcag	47 19 15	21 01 01	75
73	Kötelek	47 19 42	20 24 45	62
74.1	Bénye	47 21 19	19 32 25	31
74.2	Monor	47 18 45	19 30 13	38
75	Szászberek	47 16 27	20 08 41	48
76.1	Sárvár	47 15 08	16 56 26	48
76.2	Sárvár	47 14 47	16 56 52	44
76.3	Sárvár	47 16 55	16 56 03	74
76.4	Sárvár	47 14 42	16 56 58	44
77.1	Hencida	47 15 01	21 41 58	35
77.2	Szentpéterszeg	47 14 19	21 37 09	30
78.1	Kismarja	47 14 04	21 48 29	31
78.2	Kismarja	47 14 31	21 49 27	32
79.1	Szombathely	47 13 50	16 36 18	37
79.2	Szombathely	47 14 00	16 36 17	37
79.3	Szombathely	47 13 48	16 36 32	36
80.1	Bakonyszeg	47 11 29	21 26 19	30
80.2	Berettyóújfalu	47 13 50	21 27 08	30
80.3	Berettyóújfalu	47 13 42	21 30 29	32
80.4	Berettyóújfalu	47 12 00	21 32 17	35
80.5	Berettyóújfalu	47 11 44	21 32 12	32
80.6	Berettyóújfalu	47 13 18	21 32 11	34
80.7	Berettyóújfalu	47 14 17	21 31 45	36
80.8	Berettyóújfalu	47 13 22	21 32 33	63
80.9	Furta	47 07 44	21 27 30	35
81.1	Cegléd	47 10 40	19 40 45	41
81.2	Albertirsa	47 15 01	19 36 57	32
81.3	Albertirsa	47 15 00	19 37 04	42
82.1	Kisújszállás	47 12 20	20 45 50	36
82.2	Kisújszállás	47 13 18	20 45 26	50

No.	Location	Co-ordinates		Temp. °C
		Lat. (N)	Long. (E)	
83.1	Nagyrabé	47 11 47	21 19 22	46
83.2	Biharnagybajom	47 11 48	21 14 18	49
84.1	Borgáta	47 09 48	17 05 53	47
84.2	Mesteri	47 13 08	17 05 39	64
85.1	Cegléd	47 13 24	19 49 47	67
85.2	Cegléd	47 12 11	19 48 17	30
85.3	Cegléd	47 10 41	19 49 14	36
85.4	Cegléd	47 11 10	19 53 23	34
85.5	Cegléd	47 12 44	19 48 44	30
85.6	Cegléd	47 10 32	19 48 23	32
85.7	Cegléd	47 10 33	19 48 16	64
85.8	Cegléd	47 12 15	19 47 02	68
86.1	Abony	47 11 09	20 00 30	45
86.2	Abony	47 11 09	20 02 35	36
86.3	Abony	47 12 30	20 01 18	38
86.4	Abony	47 10 21	20 01 26	41
86.5	Abony	47 11 08	20 02 09	42
86.6	Törtel	47 06 34	19 56 02	45
86.7	Zagyvarékas	47 14 32	20 05 40	41
86.8	Zagyvarékas	47 15 07	20 06 39	48
87	Gárdony	47 11 01	18 38 12	50
88	Ráckeve	47 10 49	18 56 42	42
89.1	Szolnok	47 10 22	20 12 00	62
89.2	Szolnok	47 11 08	20 10 17	63
89.3	Szolnok	47 08 51	20 07 40	35
89.4	Szolnok	47 09 57	20 11 34	54
89.5	Szolnok	47 10 40	20 12 12	46
89.6	Szolnok	47 10 06	20 11 13	52
89.7	Szolnok	47 10 37	20 08 27	56
89.8	Szolnok	47 11 22	20 09 20	32
89.9	Szolnok	47 09 35	20 08 40	55
89.10	Szolnok	47 09 23	20 09 33	60
89.11	Szolnok	47 09 38	20 08 50	49
89.12	Szolnok	47 09 08	20 09 42	31
89.13	Szolnok	47 10 13	20 10 12	56
89.14	Szolnok	47 08 06	20 08 35	58
89.15	Szolnok	47 10 18	20 11 48	54
90	Bojt	47 08 17	21 43 54	31
91.1	Tiszatenyő	47 08 08	20 22 36	30
91.2	Törökszentmiklós	47 11 21	20 25 08	64
91.3	Törökszentmiklós	47 06 41	20 27 40	30
91.4	Törökszentmiklós	47 11 23	20 25 23	60
92.1	Szeghalom	47 06 14	21 04 39	30
92.2	Szeghalom	47 06 10	21 04 49	32
93.1	Túrkeve	47 05 58	20 40 37	32
93.2	Túrkeve	47 05 54	20 45 05	80
94	Vasvár	47 04 03	16 48 26	72
95.1	Füzesgyarmat	47 06 37	21 12 04	31
95.2	Füzesgyarmat	47 05 42	21 12 18	35
95.3	Szeghalom	47 02 06	21 11 04	36
95.4	Szeghalom	47 00 11	21 13 25	30
95.5	Szeghalom	47 03 01	21 11 14	37
95.6	Szeghalom	47 03 01	21 11 13	32
95.7	Füzesgyarmat	47 06 29	21 12 43	36
95.8	Füzesgyarmat	47 04 54	21 11 26	36
95.9	Füzesgyarmat	47 05 43	21 12 16	62
95.10	Füzesgyarmat	47 05 13	21 11 37	38
95.11	Szeghalom	47 00 47	21 10 16	35
95.12	Szeghalom	47 01 35	21 11 28	30
95.13	Szeghalom	47 00 59	21 09 25	36
96	Nagykirós	47 02 19	19 47 05	48
97.1	Sümege	46 58 57	17 16 11	32
97.2	Ukk	47 02 46	17 13 51	31
97.3	Zalagyömör	47 01 17	17 14 11	32
98.1	Martf	47 01 14	20 17 12	64
98.2	Martf	47 00 52	20 17 43	30
98.3	Tiszaföldvár	46 59 51	20 15 10	30
98.4	Tiszaföldvár	46 59 19	20 15 23	71
98.5	Martf	47 01 13	20 16 27	62
99.1	Dévaványa	47 01 48	20 56 50	41
99.2	Dévaványa	47 01 50	20 56 50	65
99.3	Dévaványa	47 00 16	20 59 27	30
99.4	Dévaványa	47 01 57	20 58 33	35
99.5	Kirösladány	46 59 28	21 02 16	31
99.6	Kirösladány	46 57 24	21 03 27	30
99.7	Szeghalom	47 02 33	21 04 53	31
99.8	Kirösladány	46 58 01	21 05 13	31
99.9	Kirösladány	46 55 32	21 04 53	30
99.10	Kirösladány	46 59 46	21 03 21	31
99.11	Kiröstarcsa	46 54 16	21 02 42	31
99.12	Szeghalom	47 04 12	21 06 09	31
100.1	Újiráz	46 59 16	21 21 45	31
100.2	Újiráz	46 59 17	21 21 49	36
101.1	Mezőtúr	46 58 45	20 37 15	37
101.2	Mezőtúr	46 58 45	20 37 15	35
101.3	Mezőtúr	46 58 43	20 37 15	30
101.4	Mezőtúr	47 00 14	20 37 49	33
101.5	Mezőtúr	47 00 56	20 36 59	32
101.6	Mezőtúr	47 00 40	20 36 44	33
101.7	Mezőtúr	46 59 23	20 36 23	34
101.8	Mezőtúr	47 00 24	20 36 43	46
101.9	Mezőtúr	47 00 24	20 36 54	74
102.1	Biharugra	46 57 58	21 36 24	56
102.2	Gádosos	46 57 59	21 36 22	31
103	Szentgotthárd	46 57 16	16 16 42	32
104.1	Zsádány	46 55 29	21 29 51	36
104.2	Komádi	46 58 39	21 30 0	56
104.3	Komádi	46 58 39	21 30 0	50

No.	Location	Co-ordinates		Temp. C	No.	Location	Co-ordinates		Temp. C
		Lat. (N)	Long. (E)				Lat. (N)	Long. (E)	
105.1	Mesterszállás	46 56 29	20 26 16	33	123.12	Murony	46 45 37	21 02 03	35
105.2	Mezihék	47 01 16	20 24 05	30	123.13	Murony	46 45 27	21 00 38	42
105.3	Mezihék	46 59 49	20 23 42	30	124.1	Kardos	46 47 40	20 43 01	32
105.4	Mezihék	46 59 50	20 23 16	30	124.2	Kondoros	46 45 31	20 47 43	36
105.5	Mesterszállás	46 57 25	20 26 00	33	124.3	Kondoros	46 45 12	20 47 48	34
105.6	Mezihék	47 01 26	20 23 20	31	124.4	Kondoros	46 46 18	20 45 42	31
105.7	Öcsöd	46 54 12	20 24 06	40	124.5	Kondoros	46 46 14	20 46 07	32
106	Endrőd	46 57 03	20 43 41	85	125.1	Solt	46 45 14	18 59 46	30
107.1	Gyoma	46 56 24	20 49 59	64	125.2	Dunaföldvár	46 48 31	18 55 50	35
107.2	Gyoma	46 56 51	20 50 54	37	126.1	Csongrád	46 45 19	20 03 03	63
108.1	Vésztő	46 55 37	21 14 41	40	126.2	Csongrád-Bokros	46 45 34	20 02 33	57
108.2	Bélmegyer	46 52 22	21 11 10	37	126.3	Csongrád-Bokros	46 46 02	20 02 06	69
108.3	Tarhos	46 48 56	21 12 46	40	127.1	Igar	46 46 34	18 31 02	30
108.4	Vésztő	46 53 34	21 14 58	36	127.2	Simontornya	46 45 07	18 32 52	33
108.5	Vésztő	46 54 36	21 16 40	36	127.3	Simontornya	46 45 23	18 33 58	37
108.6	Vésztő	46 55 44	21 14 25	32	127.4	Simontornya	46 44 57	18 32 01	31
108.7	Vésztő	46 55 49	21 11 54	30	127.5	Simontornya	46 45 09	18 33 00	39
108.8	Vésztő	46 55 33	21 15 38	33	127.6	Simontornya	46 45 07	18 33 37	34
109.1	Okány	46 53 40	21 21 04	34	127.7	Simontornya	46 45 10	18 33 48	36
109.2	Kirösújfalú	46 57 44	21 24 52	32	128.1	Sarkad	46 44 36	21 23 00	30
109.3	Mezgyán	46 51 34	21 25 54	30	128.2	Sarkad	46 43 10	21 23 24	44
109.4	Sarkadkeresztúr	46 49 53	21 25 09	32	129.1	Vajta	46 43 25	18 39 41	40
109.5	Sarkadkeresztúr	46 50 25	21 21 13	32	129.2	Vajta	46 43 01	18 39 02	39
109.6	Vésztő	46 56 06	21 18 35	38	130	Kiskunfélegyháza	46 42 34	19 50 18	51
110	Szarvas	46 54 14	19 51 20	97	131	Buzsák	46 41 04	17 33 41	41
111.1	Lakitelek	46 53 43	19 58 01	34	132.1	Fábiánsebestyén	46 40 41	20 24 26	96
111.2	Lakitelek	46 53 27	20 02 02	32	132.2	Szentes	46 39 58	20 22 14	96
111.3	Lakitelek	46 53 08	20 00 46	30	132.3	Szentes	46 39 25	20 22 50	98
111.4	Lakitelek	46 51 37	19 59 39	42	132.4	Cserebökény	46 45 34	20 23 30	100
111.5	Lakitelek-Tiszakécske	46 53 27	20 02 12	57	132.5	Szentes	46 39 58	20 22 11	87
111.6	Tiszakécske	46 54 02	20 02 50	42	133.1	Gyula	46 38 33	21 17 29	32
111.7	Tiszakécske	46 54 01	20 03 45	63	133.2	Gyula	46 38 40	21 17 16	72
111.8	Tiszakécske	46 55 03	20 04 37	58	133.3	Gyula	46 38 40	21 17 20	44
111.9	Tiszakécske	46 56 06	20 06 41	53	133.4	Gyula	46 38 17	21 15 34	59
111.10	Tiszakécske	46 55 51	20 07 47	52	133.5	Gyula	46 38 48	21 17 54	91
112.1	Kecskemét	46 53 58	19 40 01	46	134.1	Csanytelek	46 35 04	20 05 57	68
112.2	Kecskemét	46 54 03	19 40 33	47	134.2	Felgy	46 39 53	20 09 29	84
113	Tapolca	46 53 18	17 25 04	34	134.3	Csongrád	46 42 16	20 09 58	60
114.1	Kirőstarcsa	46 52 47	21 01 09	34	134.4	Szentes	46 39 03	20 13 25	83
114.2	Kirőstarcsa	46 52 49	21 01 09	35	134.5	Szegvár	46 34 45	20 14 41	37
115.1	Cserkeszilő	46 51 59	20 12 12	69	134.6	Szegvár	46 34 48	20 15 40	69
115.2	Cserkeszilő	46 51 59	20 12 13	42	134.7	Szegvár	46 34 47	20 16 17	90
115.3	Tiszainoka	46 54 12	20 09 30	30	134.8	Mindszent	46 31 48	20 13 32	78
115.4	Cserkeszilő	46 52 03	20 11 45	83	134.9	Szentes	46 39 16	20 16 21	30
115.5	Kunszentmárton	46 50 33	20 16 11	42	134.10	Szentes	46 38 53	20 16 52	92
116.1	Szarvas	46 51 12	20 34 53	39	134.11	Szegvár	46 35 04	20 15 40	87
116.2	Szarvas	46 52 47	20 32 54	38	134.12	Szegvár	46 34 59	20 14 46	95
116.3	Szarvas	46 51 34	20 37 09	92	134.13	Szegvár	46 35 12	20 15 17	92
116.4	Szarvas	46 50 59	20 35 15	94	134.14	Szegvár	46 35 26	20 16 18	82
116.5	Szarvas	46 51 46	20 31 56	97	134.15	Szentes	46 39 50	20 15 02	77
116.6	Szarvas	46 50 46	20 34 26	37	134.16	Szentes	46 41 42	20 19 32	94
116.7	Szarvas	46 50 45	20 34 26	31	134.17	Szentes	46 42 35	20 19 07	74
116.8	Békésszentandrás	46 52 12	20 28 59	41	134.18	Szentes	46 42 33	20 19 07	88
116.9	Csabacsüd	46 47 10	20 37 01	34	134.19	Szentes	46 41 42	20 19 41	84
116.10	Csabacsüd	46 47 10	20 37 01	30	134.20	Szentes	46 42 37	20 19 06	80
116.11	Szarvas	46 49 48	20 31 30	35	134.21	Szentes	46 40 59	20 19 21	90
116.12	Szarvas	46 50 11	20 38 24	30	134.22	Szentes	46 38 55	20 14 14	86
116.13	Szarvas	46 51 34	20 31 22	43	134.23	Szentes	46 39 48	20 20 09	98
116.14	Szarvas	46 51 44	20 33 10	40	134.24	Szentes	46 39 45	20 14 24	78
116.15	Szarvas	46 49 02	20 31 31	30	134.25	Szentes	46 39 01	20 14 47	78
116.16	Szarvas	46 51 45	20 33 06	38	134.26	Szentes	46 42 14	20 14 35	91
116.17	Szarvas	46 51 25	20 34 30	40	134.27	Szentes	46 39 50	20 19 56	84
116.18	Szarvas	46 49 45	20 34 52	30	134.28	Szentes	46 37 25	20 16 09	86
116.19	Szarvas	46 51 17	20 36 42	82	134.29	Szentes	46 40 57	20 20 09	81
116.20	Szarvas	46 53 46	20 35 23	36	134.30	Szentes	46 41 18	20 21 20	98
116.21	Szarvas	46 52 21	20 34 06	37	134.31	Szentes	46 41 47	20 21 21	86
116.22	Szarvas	46 50 05	20 36 21	98	134.32	Szentes	46 40 22	20 18 34	84
116.23	Mezitúr	46 56 31	20 32 55	30	134.33	Szentes	46 39 01	20 12 22	99
116.24	Mezitúr	46 56 34	20 33 01	32	134.34	Szentes	46 41 56	20 15 16	96
117	Kunszentmárton	46 50 37	20 17 57	34	134.35	Szentes	46 40 51	20 19 10	96
118	Lajoskomárom	46 50 02	18 19 43	34	134.36	Szentes	46 39 53	20 15 09	63
119.1	Hévíz	46 47 33	17 11 21	37	134.37	Szentes	46 39 10	20 16 29	72
119.2	Hévíz	46 47 16	17 11 16	41	134.38	Szentes	46 41 16	20 17 25	76
119.3	Hévíz	46 46 49	17 11 12	37	134.39	Szentes	46 37 44	20 15 59	30
119.4	Hévíz	46 47 35	17 11 22	37	134.40	Szentes	46 39 53	20 15 10	56
119.5	Kehidakustány	46 50 01	17 06 25	38	135.1	Árpádhalom	46 37 25	20 31 50	32
119.6	Zalacsány	46 48 39	17 05 36	32	135.2	Árpádhalom	46 36 59	20 33 00	36
119.7	Hévíz	46 46 50	17 11 15	41	135.3	Eperjes	46 42 34	20 33 51	30
119.8	Hévíz	46 47 22	17 11 05	42	135.4	Nagyágocs	46 35 45	20 30 49	96
119.9	Hévíz	46 47 15	17 11 30	41	135.5	Nagyágocs	46 36 50	20 27 02	31
119.10	Hévíz	46 47 14	17 11 28	41	135.6	Fábiánsebestyén	46 40 08	20 26 44	31
119.11	Hévíz	46 47 17	17 11 23	41	135.7	Nagyágocs	46 35 21	20 28 24	52
119.12	Rezi	46 49 26	17 13 36	36	135.8	Árpádhalom	46 37 04	20 33 23	33
120	Izsák	46 48 17	19 20 26	34	135.9	Eperjes	46 40 59	20 34 27	42
121.1	Nagyberény	46 46 54	18 09 28	60	135.10	Eperjes	46 41 10	20 34 12	43
121.2	Nagyberény	46 48 09	18 09 43	40	135.11	Fábiánsebestyén	46 40 33	20 27 31	30
122	Ormándlak	46 45 43	16 45 17	44	135.12	Nagyágocs	46 34 48	20 29 20	30
123.1	Békéscsaba	46 40 35	21 06 14	41	135.13	Cserebökény	46 43 24	20 27 41	35
123.2	Békés	46 45 49	21 08 45	43	135.14	Fábiánsebestyén	46 40 33	20 25 15	96
123.3	Meziberény	46 48 25	21 02 53	32	135.15	Fábiánsebestyén	46 41 04	20 24 52	94
123.4	Meziberény	46 49 27	21 02 35	33	135.16	Székkutas	46 33 25	20 32 35	31
123.5	Békés	46 46 21	21 08 01	33	136.1	Lenti	46 37 12	16 32 08	35
123.6	Békés	46 46 03	21 08 32	53	136.2	Lenti	46 36 59	16 28 54	56
123.7	Békéscsaba	46 40 33	21 06 15	76	137.1	Tamási	46 38 03	18 17 52	33
123.8	Békéscsaba	46 41 40	21 05 34	41	137.2	Tamási	46 37 31	18 17 10	45
123.9	Meziberény	46 49 40	21 02 15	50	137.3	Tamási	46 37 25	18 17 02	53
123.10	Meziberény	46 48 34	21 03 09	50	138	Újkígyós	46 35 40	21 01 07	32
123.11	Meziberény	46 49 09	21 02 02	33	139.1	Marcali	46 35 35	17 24 15	44

No.	Location	Co-ordinates		Temp. °C
		Lat. (N)	Long. (E)	
139.2	Nagyatád	46 35 33	17 24 15	32
140.1	Kecel	46 32 05	19 15 00	43
140.2	Kiskörös	46 37 20	19 16 24	58
140.3	Kiskörös	46 37 21	19 16 29	58
141.1	Nagyszénás	46 40 11	20 40 22	85
141.2	Orosháza	46 35 57	20 36 45	35
141.3	Orosháza	46 33 57	20 40 02	36
141.4	Orosháza	46 34 21	20 37 34	40
141.5	Orosháza	46 33 32	20 40 55	38
141.6	Orosháza	46 34 02	20 42 31	37
141.7	Orosháza	46 34 21	20 41 42	95
141.8	Orosháza	46 33 56	20 37 36	46
141.9	Orosháza	46 34 29	20 37 16	95
141.10	Székkutas	46 32 24	20 35 18	100
142.1	Zalakaros	46 33 04	17 07 43	47
142.2	Zalakaros	46 32 34	17 07 42	53
142.3	Zalakaros	46 33 11	17 07 48	99
142.4	Zalakaros	46 32 39	17 07 40	91
143.1	Igal	46 32 29	17 56 42	71
143.2	Igal	46 32 29	17 56 41	51
144	Kalocsa	46 32 03	18 59 26	32
145.1	Csengele	46 33 28	19 51 38	77
145.2	Csengele	46 30 08	19 52 58	74
146.1	Kiskunmajsa	46 31 53	19 45 44	74
146.2	Kiskunmajsa	46 31 49	19 45 08	72
146.3	Kiskunmajsa	46 31 49	19 45 08	74
147	Mindszent	46 30 38	20 11 56	98
148.1	Székkutas	46 30 22	20 32 23	35
148.2	Hódmezivásárhely	46 27 03	20 31 23	30
148.3	Székkutas	46 32 03	20 33 20	36
149.1	Baks	46 32 18	20 06 21	70
149.2	Ópusztaszer	46 27 57	20 02 46	70
150	Hígyész	46 30 01	18 23 43	54
151	Nagykanizsa	46 26 57	16 59 40	46
152.1	Mezőkovácsháza	46 24 08	20 55 21	63
152.2	Nagybánhegyes	46 27 16	20 53 45	72
152.3	Vétegyháza	46 24 29	20 52 24	70
153.1	Kiskunhalas	46 25 56	19 28 17	46
153.2	Kiskunhalas	46 25 56	19 28 09	46
154	Nagybajom	46 24 01	17 29 12	43
155.1	Hódmezivásárhely	46 24 02	20 17 53	30
155.2	Hódmezivásárhely	46 24 17	20 17 36	31
155.3	Hódmezivásárhely	46 24 37	20 19 07	43
155.4	Hódmezivásárhely	46 21 26	20 13 28	33
155.5	Hódmezivásárhely	46 24 45	20 22 26	70
155.6	Hódmezivásárhely	46 24 11	20 22 25	32
155.7	Hódmezivásárhely	46 24 43	20 19 09	76
155.8	Hódmezivásárhely	46 24 51	20 22 09	80
155.9	Hódmezivásárhely	46 24 43	20 17 31	30
155.10	Hódmezivásárhely	46 24 29	20 17 53	30
156	Lengyel	46 22 46	18 21 06	34
157.1	Kaposvár	46 22 44	17 46 52	31
157.2	Kaposvár	46 22 31	17 49 15	30
157.3	Kaposvár	46 21 02	17 48 09	53
157.4	Kaposvár	46 23 11	17 48 22	32
157.5	Kaposvár	46 22 22	17 47 53	32
157.6	Kaposvár	46 21 04	17 47 56	50
157.7	Kaposvár	46 21 03	17 48 18	34
158.1	Kaposszekcső	46 21 39	18 07 43	33
158.2	Igal	46 17 01	18 12 00	48
158.3	Dombóvár	46 24 05	18 10 43	45
158.4	Dombóvár	46 24 02	18 09 35	54
158.5	Dombóvár	46 24 06	18 10 39	50
158.6	Dombóvár	46 21 59	18 08 33	36
158.7	Dombóvár	46 22 11	18 08 07	32
159.1	Kaposkeresztúr	46 20 47	17 56 49	30
159.2	Taszár	46 22 57	17 54 16	38
159.3	Taszár	46 22 35	17 54 06	36
159.4	Kaposhomok	46 21 41	17 56 02	30
159.5	Kaposkeresztúr	46 21 26	17 56 43	32
159.6	Kaposkeresztúr	46 21 03	17 57 54	32
159.7	Nagyberki	46 20 23	18 00 10	31
160.1	Tótkomlós	46 24 43	20 44 06	42
160.2	Mezőhegyes	46 19 02	20 48 19	32
160.3	Mezőhegyes	46 17 33	20 46 28	30
160.4	Mezőhegyes	46 18 56	20 48 17	33
160.5	Mezőhegyes	46 18 11	20 48 57	35
160.6	Mezőhegyes	46 18 34	20 49 30	36
160.7	Tótkomlós	46 24 40	20 43 58	31
160.8	Tótkomlós	46 25 21	20 42 48	86
160.9	Tótkomlós	46 25 11	20 45 33	80
160.10	Pitvaros	46 19 48	20 44 22	40
160.11	Pitvaros	46 19 39	20 43 39	74
160.12	Csanádalberti	46 19 41	20 41 36	32
160.13	Csanádpalota	46 15 45	20 44 05	35
160.14	Nagyér	46 22 11	20 43 44	43
161.1	Forráskút	46 21 31	19 55 56	87
161.2	Forráskút	46 21 06	19 56 47	81
161.3	Forráskút	46 21 20	19 54 54	82
161.4	Forráskút	46 20 58	19 54 21	76
161.5	Üllés	46 20 23	19 52 52	76
162.1	Szekszárd	46 20 42	18 45 22	32
162.2	Szekszárd	46 20 31	18 44 46	32
162.3	Szekszárd	46 21 00	18 42 37	31
162.4	Szekszárd	46 20 48	18 44 58	32
163.1	Ruzsa	46 18 28	19 46 29	60
163.2	Üllés	46 20 41	19 48 34	64
164	Battonya	46 16 40	21 01 25	49

No.	Location	Co-ordinates		Temp. °C
		Lat. (N)	Long. (E)	
165	Királyhegyes	46 15 57	20 36 33	30
166.1	Domaszék	46 14 29	20 01 33	80
166.2	Domaszék	46 15 04	20 03 44	77
166.3	Domaszék	46 13 22	20 03 22	85
166.4	Domaszék	46 14 02	20 02 20	80
166.5	Domaszék	46 14 11	20 04 12	82
166.6	Röszke	46 11 46	20 02 31	77
166.7	Algyi	46 15 46	20 07 30	54
166.8	Szeged	46 15 21	20 08 58	51
166.9	Szeged	46 15 09	20 09 31	32
166.10	Szeged	46 15 12	20 09 36	36
166.11	Algyi	46 15 50	20 07 35	57
166.12	Szeged	46 13 26	20 04 30	85
166.13	Szeged	46 16 13	20 06 18	36
166.14	Szeged	46 15 54	20 05 47	30
166.15	Szeged	46 16 21	20 07 11	80
166.16	Szeged	46 15 05	20 09 24	44
166.17	Szeged	46 13 56	20 07 23	31
166.18	Szeged	46 13 49	20 07 49	34
166.19	Szeged	46 14 19	20 07 00	31
166.20	Szeged	46 14 39	20 06 50	32
166.21	Szeged	46 17 58	20 10 09	72
166.22	Szeged	46 17 56	20 10 11	64
166.23	Szeged	46 12 58	20 04 17	84
166.24	Szeged	46 17 16	20 10 15	73
166.25	Szeged	46 17 19	20 10 19	69
166.26	Szeged	46 14 36	20 11 27	53
166.27	Szeged	46 18 11	20 10 45	53
166.28	Szeged	46 13 59	20 08 29	31
166.29	Szeged	46 15 17	20 08 16	31
166.30	Szeged	46 14 52	20 09 40	90
166.31	Szeged	46 14 26	20 07 28	33
166.32	Szeged	46 16 12	20 08 51	31
166.33	Szeged	46 14 35	20 08 45	32
166.34	Szeged	46 16 19	20 08 08	31
166.35	Szeged	46 16 11	20 08 52	33
166.36	Szeged	46 15 23	20 07 16	89
166.37	Szeged	46 16 15	20 09 23	32
166.38	Szeged	46 16 23	20 06 55	86
166.39	Szeged	46 14 17	20 11 45	82
166.40	Szeged	46 15 50	20 06 29	30
166.41	Szeged	46 15 50	20 06 29	32
166.42	Algyi	46 17 02	20 10 38	74
166.43	Szeged	46 14 22	20 08 48	37
166.44	Szeged	46 15 46	20 07 44	38
166.45	Szőreg	46 11 51	20 11 47	84
166.46	Szeged	46 13 58	20 10 42	90
166.47	Szeged	46 15 51	20 05 52	30
166.48	Szeged	46 15 59	20 08 40	30
166.49	Szeged	46 15 34	20 06 01	30
166.50	Szeged	46 13 57	20 07 21	34
166.51	Szeged	46 14 17	20 07 05	31
166.52	Algyi	46 19 01	20 12 14	57
166.53	Szeged	46 15 05	20 09 23	31
166.54	Tápe	46 16 00	20 12 15	30
166.55	Szeged	46 14 38	20 06 51	31
166.56	Szeged	46 17 02	20 10 38	32
166.57	Szeged	46 19 12	20 09 34	73
166.58	Szeged	46 18 02	20 09 30	56
166.59	Szeged	46 18 29	20 09 28	66
166.60	Szeged	46 18 43	20 09 25	56
166.61	Tiszasziget	46 10 37	20 10 21	80
166.62	Tiszasziget	46 10 04	20 10 53	90
166.63	Tiszasziget	46 10 04	20 10 53	31
167	Gálosfa	46 15 12	17 54 19	68
168.1	Földeák	46 18 50	20 30 07	31
168.2	Földeák	46 18 08	20 28 44	87
168.3	Makó	46 12 55	20 28 27	41
168.4	Magyarcsanak	46 12 01	20 33 24	92
168.5	Makó	46 13 02	20 27 48	91
168.6	Makó	46 13 02	20 27 52	76
168.7	Makó	46 12 32	20 27 39	90
168.8	Makó	46 12 41	20 29 28	94
169	Mórahalom	46 13 00	19 53 19	39
170	Deszk	46 12 41	20 14 26	76
171	Hencse	46 12 19	17 37 29	43
172.1	Nagylak	46 11 41	20 43 22	37
172.2	Nagylak	46 11 44	20 43 27	46
173.1	Csokonyavisonta	46 06 53	17 26 36	71
173.2	Nagyatád	46 11 46	17 21 14	30
173.3	Nagyatád	46 14 19	17 22 15	30
173.4	Nagyatád	46 13 44	17 21 52	50
173.5	Tarany	46 10 29	17 18 14	33
173.6	Csokonyavisonta	46 06 26	17 26 08	69
173.7	Nagyatád	46 14 18	17 22 01	59
173.8	Tarany	46 11 36	17 25 49	65
174.1	Magyarhertelend	46 11.29	18.08 23	64
174.2	Magyarszék	46 11 17	18 12 04	38
174.3	Komló	46 11 39	18 15 16	56
174.4	Komló	46 10 37	18 13 15	36
174.5	Magyarhertelend	46 11 30	18 08 18	38
175.1	Ásotthalom	46 09 41	19 47 11	30
175.2	Ásotthalom	46 09 34	19 47 29	70
176	Hímesháza	46 04 35	18 34 40	49
177.1	Szigetvár	46 03 41	17 47 36	60
177.2	Szigetvár	46 03 15	17 47 42	62
178.1	Babocsa	46 02 16	17 21 00	65
178.2	Babocsa	46 02 25	17 21 08	55

No.	Location	Co-ordinates		Temp. °C
		Lat. (N)	Long. (E)	
179	Magyarsarlós	46 02 51	18 20 03	34
180.1	Szentlőrinc	46 02 11	17 59 54	35
180.2	Szentlőrinc	46 02 53	17 59 07	33
180.3	Szentlőrinc	46 02 40	17 59 55	32
180.4	Szentlőrinc	46 02 53	17 58 57	33
181	Szulok	46 02 15	17 32 37	56
182.1	Dávod	46 00 17	18 53 53	38
182.2	Dávod	46 00 06	18 53 39	37
182.3	Nagybaracska	46 02 14	18 54 08	34
183	Barcs	45 57 36	17 27 10	34
184.1	Újpetre	45 56 41	18 21 54	40
184.2	Újpetre	45 55 28	18 20 54	31
185	Bogdása	45 52 57	17 48 29	48
186.1	Márok	45 52 25	18 30 36	33
186.2	Majs	45 53 15	18 35 33	33
187.1	Harkány	45 51 00	18 14 19	62
187.2	Harkány	45 51 04	18 14 19	61
187.3	Harkány	45 51 01	18 14 19	62
187.4	Harkány	45 51 03	18 14 17	61

Italy

For geothermal springs see previous atlas. Only geothermal installations (non-electrical) are listed below.

Geothermal installations
(Non electrical utilization)

No.	Location	Co-ordinates		Temp. °C
		Lat. (N)	Long. (E)	
+	Vicenza	45 33 53	11 33 04	65
+	Rodigo	45 13 44	10 38 40	57
+	Abano (Eugenei Hills)	45 20 11	11 47 14	78
+	Montegrotto (Eugenei Hills)	45 19 50	11 46 46	75
+	Battaglia (Eugenei Hills)	45 16 10	11 47 05	64
+	Calzigniano (Eugenei Hills)	45 18 26	11 45 32	86
+	Acqui Terme	44 40 31	08 28 10	70
+,(+)	Ferrara	44 52 42	11 38 17	95
(+)	Bagnore (Mt. Amiata)	42 50 42	11 35 30	-
+	Bagno di Romagna	43 49 06	11 57 38	43
1-5+	Larderello	43 13 21	10 52 35	78-200
6+	Bulera (Larderello)	43 17 27	10 51 51	120
7-10+	Castelnuovo	43 11 36	10 53 48	105-160
11+	Canalino	43 11 36	10 53 48	70
12-13+	Castelnuovo	43 11 36	10 53 48	70-105
14+	Monterotondo (Larderello)	43 09 10	10 50 20	95
15+	Lago Boracifero	43 10 05	10 45 20	125
16+	Radicondoli	43 11 05	11 02 25	120
17+	Orbetello	42 27 00	11 10 34	22-25
18+	Piancastagnaio (Mt. Amiata)	42 49 18	11 43 12	97
19+	Torre Alfina	42 46 18	11 56 52	-
20+	Pantani	42 08 38	11 45 27	50
21(+)	Montecerboli	43 15 21	10 52 20	200
22(+)	Bulera	43 17 27	10 51 51	148
23(+)	Sasso Pisano (Larderello)	43 10 00	10 51 39	105
24(+)	Serrazzano (Larderello)	43 12 08	10 48 21	180
25(+)	Lustignano (Larderello)	43 10 45	10 48 14	180
26(+)	Carboli (Larderello)	43 05 50	10 45 15	180
27(+)	Radicondoli	43 11 05	11 02 25	-
28(+)	Roselle	42 48 20	11 09 51	42
29(+)	Piancastagnaio	42 49 18	11 43 12	95
30(+)	San Casciano dei Bagni (Mt. Amiata)	42 52 15	11 52 19	40
31(+)	Castelgiorgio	42 42 36	11 58 58	80
32(+)	Latera	42 38 48	11 48 53	85
33(+)	Cesano	42 05 00	12 26 08	-

Latvia

No springs above 20 °C.

Lithuania

No.	Location	Co-ordinates		Temp. °C
		Lat. (N)	Long. (E)	
1(+)	Klapeida Geothermal Demonstration Plant	55 41 01	21 12 10	42

No springs above 20° C

The Netherlands

No.	Location	Co-ordinates		Temp. °C
		Lat. (N)	Long. (E)	
1(+)	Ameland, (Aqua Plaza)	53 27 14	5 46 47	37*
2	Arcen, (Klein Vink)	51 29 55	6 11 08	42
3(-)	Asten	51 22 51	5 46 32	60*

No.	Location	Co-ordinates		Temp. °C
		Lat. (N)	Long. (E)	
4(-)	Delfland	51 56 57	4 13 20	89*
5(+)	De Lier	51 57 00	4 15 00	86*
6	Nieuweschans, (Fontana)	53 12 02	7 10 55	28
7	Nijmegen, (Sanadome)	51 49 12	5 50 02	23
8	Utrecht, (De Uithof)	52 05 10	5 10 09	90#
9	Valkenburg, (Thermae 2000)	50 52 15	5 49 22	32

No springs with temperature above 20 °C.

(-) suspended project

* temperature prediction for operation

temperature of injected water

Poland

No.	Location	Co-ordinates		Temp. °C
		Lat. (N)	Long. (E)	
1	Ciechocinek T14	52 52 15	18 47 48	28
2	Ciechocinek T16	52 52 42	18 48 06	35
3	Pyrzyce GT 1	53 09 01	14 54 40	61
4	Pyrzyce GT 2	53 09 47	14 55 14	57
5	Pyrzyce GT 3	53 08 58	14 54 51	56
6	Pyrzyce GT 4	53 09 21	14 56 05	58
7	Skierniewice GT 1	51 58 20	20 10 57	55
8	Uniejów IGH 1	51 59 50	18 46 27	68
9	Uniejów PIG/AGH 1	51 59 27	18 46 52	70
10	Bañska IG-1	49 24 00	20 01 00	70
11	Ciechocinek	18 48 00	52 52 00	31
12	Konstancin	21 07 00	52 06 00	31
13	Trzebnica	17 04 00	51 19 00	37
14	Cieplice	15 41 00	50 52 00	62
15	Lądek-Zdrój	16 52 00	50 21 00	28
16	Jaztrzębie/Zdrój	18 35 00	49 57 00	21
17	Ustroń	18 49 00	49 44 00	28
18	Iwonicz-Zdrój	21 47 00	49 35 00	24
+	Banska	49 23 00	20 02 00	70
+	Pyrzyce	53 09 00	14 52 00	64
(+)	Stargard Szczeciński	53 21 00	15 02 00	
(+)	Skierniewice	51 57 00	20 09 00	
(+)	Żyrardów	51 03 00	20 26 00	
(+)	Mszczonów	51 58 00	20 30 00	
(+)	Podębice	51 54 00	18 56 00	
(+)	Koło	52 12 00	18 37 00	
(+)	Czarnków	52 54 00	16 35 00	
(+)	Uniejów	51 59 00	18 46 00	

Portugal

No.	Location	Co-ordinates		Temp. °C
		Lat. (N)	Long. (W)	
1	Monção	42 04 39	8 28 22	50
2+	Chaves	41 44 12	7 28 15	76
3	Gerês	41 43 44	8 09 37	47
4	Carvalhelhos	41 41 39	7 43 43	22
5	Caldelas	41 39 59	8 22 05	33
6	Eirogo	41 33 54	8 35 26	25
7+	Taipas	41 29 05	8 20 28	32
8	São Miguel das Aves	41 22 45	8 24 09	22
9	Vizela	41 22 44	8 18 25	62
10	Saúde	41 22 12	8 28 15	30
11	Carlão	41 19 41	7 22 16	29
12	São Lourenço	41 17 27	7 22 11	30
13	Canavezes	41 11 42	8 09 09	35
14	Moledo	41 09 13	7 50 00	45
15+	Fonte Sta. do Seixo	41 09 39	7 17 38	21
16	Aregos	41 06 08	8 00 33	62
17	Longroiva	40 57 50	7 12 29	34
18	São Jorge	40 57 19	8 29 17	23
19	Carvalhal	40 51 06	7 55 52	41
20	Cavaca	40 46 18	7 34 42	29
21+	São Pedro do Sul	40 44 15	8 05 34	69
22	Alcafache	40 36 16	7 52 05	51
23	São Gemil	40 31 26	7 58 01	50
24	Cró	40 26 42	7 02 30	23
25	Felgueira	40 29 13	7 51 47	36
26	Manteigas	40 23 00	7 32 27	48
27	Luso	40 22 57	8 22 38	27
28	São Paulo	40 19 31	7 50 30	23
29	Unhais da Serra	40 15 45	7 37 48	37
30	Amieira	40 05 22	8 44 41	27
31	Bicanho	40 05 03	8 44 22	28
32	Azenha	40 04 47	8 44 15	29
33	Monfortinho	40 00 05	6 52 25	28
34	Fonte Quente	39 44 47	8 47 58	24
35	Salgadas	39 38 25	8 48 54	23
36	Envendos	39 36 24	7 51 36	22
37	Piedade	39 34 13	9 00 00	27
38	Salir	39 30 45	9 08 29	20
39	Caldas da Rainha	39 24 19	9 08 09	36
40	Arrábidos	39 22 14	9 08 05	29
41	Vimeiro	39 11 03	9 19 22	26
42	Cucos	39 05 36	9 14 28	40
43+	Alcaçarias	38 42 32	9 08 20	30
44	Estoril	38 42 20	9 23 12	35

No.	Location	Co-ordinates		Temp. °C
		Lat. (N)	Long. (W)	
45	Santa Comba	38 08 40	7 27 01	22
46	Malhada Quente	37 20 08	8 31 09	28
47	Alferce	37 17 49	8 29 42	27
48	Monchique	37 17 11	8 33 08	32
49	Santo António Ribeira, São Miguel Island (Açores)	37 07 12	7 38 51	25

Romania

Geothermal springs

No.	Location	Co-ordinates		Temp. °C
		Lat. (N)	Long. (E)	
1	Mangalia	43 48 47	28 34 48	27
2	Capidava	44 29 48	28 05 09	23
3	Topalu	44 33 04	28 02 29	26
4	Ghindaresti	44 39 20	28 00 50	25
5	Harsova	44 41 16	27 57 00	42
6	Baile Herculane	44 53 12	22 25 57	62
7	Bala	44 53 46	22 48 42	32
8	Minis	45 01 38	21 52 33	21
9	Siriu	45 31 27	26 12 08	59
10	Sanmihaiu German	45 42 36	21 02 27	66
11	Timisoara	45 44 55	21 13 08	34 - 52
12	Calan	45 45 36	23 00 29	29
13	Rapoltel	45 54 22	23 03 36	25
14	Bobalna	45 54 28	23 06 28	24
15	Geoagiu	45 56 19	23 09 05	28
16	Calacea	45 56 33	21 06 32	42
17	Cheile Cibului	46 02 30	23 10 20	23
18	Tusnad	46 08 35	25 51 30	63
19	Arad	46 12 10	21 17 06	29 - 39
20	Sofronea	46 16 40	21 19 05	50
21	Miercurea Ciuc	46 21 00	25 47 34	22
22	Carand	46 26 39	22 05 36	26
23	Moneasa	46 26 53	22 15 00	32
24	Danesti	46 31 09	25 44 40	22
25	Rabagani	46 44 09	22 14 30	27
26	Tinca	46 46 23	21 57 04	34
27	Madaras	46 50 06	21 40 37	51
28	Toplita	46 55 38	25 21 10	27
29	Lunca Bradului	46 57 18	25 02 50	25
30	Felix-I Mai	47 00 22	22 00 00	49
31	Alesd	47 03 20	22 23 58	44
32	Mihai Bravu	47 15 43	21 56 47	69
33	Satu Mare	47 47 09	22 53 51	55 - 65

Geothermal installations

No.	Location	Co-ordinates		Temp. °C
		Lat. (N)	Long. (E)	
	Acãs	47 33	22 48	69 - 70
	Tãsnad	47 28	22 34	70
	Marghita	47 21	22 20	65 - 73
	Sãcuieni	47 21	22 06	81 - 90
	Bors	47 06	21 05	124 - 130
	Oradea	47 03	21 57	71 - 107
	Livada	47 02	21 48	90
	Salonta	46 48	21 39	86
	Ciumeghiu	46 44	21 35	96 - 104
	Curtici	46 20	21 18	62 - 72
	Nãdlac	46 10	20 46	79
	Sãnnicolau Mare	46 04	20 37	78 - 84
	Saravale	46 04	20 45	85
	Tomnatec	45 59	20 39	82 - 84
	Lovrin	45 58	20 45	76 - 82
	Jimbolia	45 47	20 43	79 - 82
	Cãciulata	45 16	24 20	92
	Otopeni	44 34	26 04	62
	Bãneasa	44 29	26 04	42

Russia

Geothermal installations

No.	Location	Co-ordinates		Temp. °C
		Lat. (N)	Long. (E)	
57(+)	Kozminskaya, Azov-Kuban basin	44 35	41 33	133
67+	Tarumovskaya, East-Fore Causasian basin	44 03	46 30	99
68+	Kizlyar, East-Fore Caucasian basin	43 50	46 40	110
74+	Khankala, East-Fore Caucasian basin	43 16	45 48	102

* approximate co-ordinates from the map

Slovakia

No.	Location	Co-ordinates		Temp. °C
		Lat. (N)	Long. (E)	
1	Vyšné Ružbachy	49 18 00	20 34 00	24
2(+)	Oravice	49 17 46	19 44 50	56
3	Belusske Slatiny	49 02 35	18 20 21	22
4	Stranavy	49 10 32	18 49 59	24
5	Rajecke Teplice	49 08 00	18 41 00	39
6(+)	Kamenna Poruba	49 06 11	18 41 20	38
7	Rájec	49 05 41	18 38 06	27
8	Kúpele Lúčky	49 08 00	19 24 00	33
9	Besenova	49 06 05	19 26 44	62
10(+)	Liptovský Trnovec	49 06 20	19 34 20	61
11(+)	Liptovská Kokava	49 05 27	19 48 20	44
12(+)	Pavčina Lehota	49 02 13	19 33 51	32
13	Liptovský Ján	49 02 43	19 41 07	29
14+	Vrbov	49 05 03	20 25 16	59
15(+)	Poprad	49 03 45	20 18 24	48
16(+)	Ganovce	49 01 35	20 19 03	25
17(+)	Arnutovce	48 58 21	20 25 02	31
18(+)	Šaštín	48 38 59	17 08 42	73
19(+)	Lakšárska Nová Ves	48 34 07	17 12 41	77
20	Kúpele Piešťany	48 37 00	17 50 00	68
21	Koplotovce	48 28 20	17 48 34	24
22	Trenčianske Teplice	48 55 00	18 10 00	40
23	Mošovce	48 54 29	18 53 33	23
24	Turčianske Teplice	48 51 00	18 52 00	45
25	Kúpele Bojnice	48 46 06	18 26 14	46
26(+)	Kos	48 43 41	18 34 23	67
27	Kremnica	48 42 43	18 54 37	48
28	Bánovce nad Bebravou	48 42 54	18 14 45	46
29	Chalmovec	48 40 40	18 29 49	39
30	Male Bielice	48 37 22	18 20 29	39
31(+)	Topoľčany	48 34 07	18 08 33	55
32	Sklené Teplice	48 31 43	19 06 08	52
33	Vyhne	48 29 51	18 48 17	35
34	Kúpele Brusno	48 49 00	19 37 00	20
35	Banská Bystrica	48 44 08	19 08 16	20
36	Kúpele Kovacova	48 36 30	19 06 08	48
37	Kúpele Sliach	48 36 53	19 09 58	33
38(+)	Tahanovce	48 45 09	21 15 13	26
39	Kúpele Sobrance	48 45 32	22 08 20	20
40(+)	Stretava	48 34 58	22 03 15	80
41	Bysta	48 31 41	21 34 07	15
42	Borša	48 23 51	21 43 32	32
43	Kralík	48 24 39	20 14 37	17
44	Dolná Strehová	48 15 42	19 28 27	36
45(+)	Chorvatsky Grob	48 13 52	17 16 22	48
46	Kráľova pri Senci	48 12 02	17 26 07	52
47+	Galanta	48 11 29	17 42 51	77
48(+)	Eliasovce	48 07 34	17 29 00	65
49	Diakovce	48 08 05	17 47 01	68
50(+)	Čilistov	48 01 03	17 18 27	52
51+	Horná Potoň	48 02 41	17 29 12	68
52+	Dunajský Klatov	48 01 46	17 42 03	75
53+	Vlčany	48 02 02	17 54 55	68
54+	Dunajská Streda	47 59 08	17 37 04	92
55+	Topolníky	47 58 37	17 47 27	74
56	Polný Kesov	48 10 10	18 03 54	50
57	Komjatice	48 09 15	18 08 34	78
58+	Tvrdošovce	48 05 02	18 04 51	70
59+	Podhajska	48 06 28	18 21 37	80
60	Nové Zámky	47 59 59	18 11 02	59
61(+)	Zeliezovce	48 02 54	18 40 09	52
62	Kalinciakovo	48 10 28	18 40 03	25
63	Santovka	48 08 52	18 45 30	26
64	Kúpele Dudince	48 10 00	18 53 00	27
65	Gabčíkovo	47 53 22	17 35 50	52
66+	Čalovo	47 50 48	17 45 50	78
67+	Cilizska Radvan	47 49 38	17 41 35	82
68(+)	Zemianska Olca	47 49 16	17 52 01	74
69(+)	Ontopa	47 46 03	17 56 41	51
70(+)	Bruty	47 55 07	18 35 03	75
71(+)	Dolný Peter	47 49 19	18 11 25	32
72(+)	Marcelov	47 48 15	18 17 09	56
73	Komárno	47 45 28	18 08 17	49
74	Patince	47 44 52	18 18 35	27
75(+)	Kravany	47 45 36	18 30 20	20
76	Štúrov	47 47 49	18 43 34	40

Slovenia

No.	Location	Co-ordinates		Temp. °C
		Lat. (N)	Long. (E)	
1	Zatolmin	46 12 06	13 44 48	22
2	Nova Gorica	45 55 19	13 38 14	20
3	Portoroz	45 30 25	13 36 12	23
4	Bled	46 22 02	14 06 46	22
5+	Vrhnika	45 57 31	14 18 07	22
6	Hotavlje	46 07 10	14 05 32	21
7	Curnovec	46 01 12	14 27 57	23
8(+)	Vaseno - Snovik	46 13 10	14 42 16	29
9+	Medijske Toplice	46 09 24	14 55 58	24
10	Trbovlje	46 07 48	15 02 24	25
11+	Rimske Toplice	46 07 13	15 12 35	38
12+	Laško	46 09 33	15 14 14	34
13+	Dolenjske Toplice	45 45 30	15 03 44	35

No.	Location	Co-ordinates		Temp. C
		Lat. (N)	Long. (E)	
14+	Šmarješke Toplice	45 51 57	15 14 34	32
15	Klevevz	45 54 24	15 14 15	25
16	Kostanjevica	45 51 03	15 24 46	23
17	Kostanjevica - Sajevece	45 51 58	15 25 58	35
18	Buseca vas	45 52 12	15 31 23	26
19+	Čatež	45 53 30	15 37 53	62
20+	Podčetrtek	46 09 56	15 36 37	41
21(+)	Rogaska Slatina	46 13 44	15 38 31	62
22	Podplat	46 14 55	15 35 41	27
23+	Zreče	46 21 31	15 24 10	28
24+	Dobrna	46 20 21	15 13 42	36
25+	Topolšica	46 24 16	15 01 19	32
26	Lajse	46 24 14	15 02 47	48
27	Podlog pri Zalcu	46 16 34	15 08 19	20
28+	Ptuj	46 25 22	15 51 32	39
29	Maribor	46 32 27	15 40 53	45
30	Gabrnik	46 28 49	15 57 09	<40
31	Moravci pri Buckovcih	46 30 54	16 03 26	35
32+	Banovci	46 34 22	16 10 32	58
33	Benedikt	46 36 38	15 53 07	>20
34+	Radenci	46 38 28	16 03 18	<40
35+	Lendava	46 32 20	16 28 24	65
36+	Murska Sobota	46 39 34	16 10 13	50
37+	Moravci	46 40 58	16 13 36	66
38	Cerkno	46 07 41	13 59 34	30

Spain

Geothermal springs

No.	Location	Co-ordinates		Temp. °C
		Lat. (N)	Long. (W)	
1	Carballo	43 12 56	08 41 22	37
2	Caldas de Reyes	42 36 11	08 38 26	48
3	Cuntis	42 37 54	08 33 50	58
4	El Grove	42 29 05	08 50 46	42
5	Tuy	42 03 10	08 34 20	47
6	Arteijo	43 18 12	08 30 27	42
7	Fontao-Silleda	42 45 25	08 14 18	20
8	Cotobad	42 31 10	08 30 45	25
9	Boboras	42 26 33	08 09 20	27
10	Carballino	42 25 51	08 04 45	27
11	Carballino	42 24 30	08 04 04	35
12	Leiro	42 20 43	08 08 20	28
13	Maside	42 25 00	08 01 10	21
14	Punxín	42 22 17	07 59 42	27
15	Punxín	42 22 15	07 59 42	20
16	Punxín	42 22 11	07 59 43	26
17	Cenlle	42 20 02	08 00 50	42
18	Canedo-Orense	42 20 48	07 55 07	63
19	Canedo-Orense	42 20 49	07 55 01	64
20	Canedo-Orense	42 21 06	07 54 30	65
21	Orense	42 20 56	07 52 40	47
22	Las Caldas-Orense	42 20 48	07 52 21	64
23	Orense	42 20 09	07 51 48	68
24	Cenlle	42 19 37	08 01 46	50
25	Prexigueiro-Melón	42 15 16	08 09 28	39
26	Cortegada	42 12 04	08 10 15	33
27	Lovios	41 51 42	08 06 50	67
28	Lugo	43 00 05	07 33 30	45
29	Orense	42 20 48	07 50 21	30
30	Junquera de Ambía	42 12 45	07 44 12	24
31	Banos de Molgas	42 14 37	07 40 15	50
32	Banos de Molgas	42 14 37	07 40 15	48
33	Verín	41 56 17	07 25 41	20
34	Pedralba de la Pradería	41 57 53	06 43 48	26
35	Ceclavín	39 50 25	06 48 20	30
36	Retortillo	40 47 40	06 24 48	48
37	Ciudad Rodrigo	40 37 46	06 29 48	24
38	Ciudad Rodrigo	40 35 22	06 26 27	27
39	Alange	38 47 02	06 14 43	26
40	Oviedo	43 19 56	05 55 20	42
41	Ledesma	41 03 38	06 03 45	29
42	Ledesma	41 04 15	05 54 00	48
43	Banos	40 19 04	05 51 25	40
44	Vegaquemada	42 50 30	05 18 15	29
45	Bonar	42 52 30	05 19 00	22
46	Algodonales	36 52 00	05 30 30	30
47	Manilva	36 23 50	05 15 40	22
48	Tolox	36 40 50	04 54 34	20
49	Tolox	36 41 23	04 54 35	20
50	Penamellera Baja	43 19 05	04 36 20	26
51	Tresviso	43 15 09	04 36 17	51
52	Ardales	36 53 00	04 50 40	20
53	Cartama	36 45 10	04 37 04	21
54	Cartama	36 46 38	04 36 39	20
55	Almogía	36 49 00	04 31 44	20
56	Alhaurín el Grande	36 35 55	04 43 28	24
57	Piedrabuena	39 02 30	04 13 17	20
58	Fuencaliente	38 24 15	04 18 13	32
59	Montoro	38 03 38	04 24 38	23
60	Montoro	38 03 38	04 24 38	23
61	Periana	36 57 08	04 12 17	21
62	Corrales de Buelna	43 17 54	04 04 21	36
63	Puente Viesgo	43 17 55	03 57 52	34
64	Santiurde de Toranzo	43 11 53	03 55 19	25
65	Santiurde de Toranzo	43 11 52	03 55 02	25

No.	Location	Co-ordinates		Temp. C
		Lat. (N)	Long. (W)	
66	Poblete	38 56 06	04 01 07	20
67	Villar del Pozo	38 50 33	03 57 58	24
68	Villanueva de San Carlos	38 37 57	03 55 21	20
69	Andújar	38 02 40	03 56 42	25
70	Martos	37 41 20	03 52 36	21
71	Martos	37 41 21	03 52 36	21
72	Alhama de Granada	37 01 10	03 58 55	49
73	Alhama de Granada	37 01 20	03 58 45	40
74	Entrambasaguas	43 23 40	03 42 00	21
75	Entrambasaguas	43 23 45	03 42 09	23
76	Aldea del Rey	38 45 34	03 51 01	21
77	Jaén	37 44 22	03 48 59	24
78	Atarfe	37 23 50	03 43 19	34
79	Malá	37 06 18	03 43 30	30
80	Dúrcal	36 58 54	03 35 09	24
81	Dúrcal	37 59 00	03 35 08	24
82	Dúrcal	36 58 52	03 34 50	25
83	Dúrcal	36 58 42	03 34 48	25
84	Drcal	36 58 30	03 34 55	24
85	Lección	36 55 53	03 33 40	24
86	Melegís	36 55 55	03 34 02	24
87	Melegís	36 55 50	03 34 08	22
88	Canena	38 02 55	03 29 15	20
89	Diezma	37 18 08	03 19 14	32
90	Cortes y Graena	37 18 18	03 12 14	40
91	Lanjarón	36 55 36	03 29 30	28
92	Lanjarón	36 55 36	03 29 30	24
93	Lanjarón	36 55 19	03 28 06	21
94	Albunol	36 48 00	03 13 00	23
95	Albunol	36 47 42	03 12 29	28
96	Albunol	36 47 40	03 12 35	28
97	Albunol	36 48 28	03 12 22	22
98	Albunol	36 48 30	03 12 14	23
99	Albunol	36 47 50	03 11 22	27
100	Albunol	36 47 52	03 11 32	27
101	Villanueva de las Torres	37 30 35	03 06 20	34
102	Paterna del Río	37 00 28	02 56 32	20
103	Berja	36 49 53	03 01 00	26
104	Torrejón de Cameros	42 15 35	02 36 32	24
105	Castrill	37 49 08	02 46 00	24
106	Huésca	37 48 12	02 31 13	20
107	Galera	37 43 10	02 31 50	20
108	Galera	37 43 04	02 32 18	20
109	Cortes de Baza	37 39 26	02 49 52	21
110	Zújar	37 35 53	02 48 48	37
111	Baza	37 36 08	02 48 20	26
112	Zújar	37 35 45	02 48 52	28
113	Caniles	37 28 10	02 40 15	28
114	Serón	37 21 25	02 33 43	25
115	Serón	37 21 23	02 33 25	24
116	Serón	37 21 20	02 33 10	26
117	Serón	37 21 30	02 32 55	26
118	Canjajar	36 59 32	02 43 28	22
119	Alhama de Almería	36 57 30	02 34 20	45
120	Alicún	36 58 05	02 36 00	30
121	Bentarique	36 59 09	02 37 32	20
122	Dalías	36 42 10	02 50 42	28
123	Arnedillo	42 12 26	02 14 24	52
124	Orce	37 43 44	02 30 08	21
125	Orce	37 43 38	02 30 03	21
126	Orce	37 43 45	02 29 59	22
127	Orce	37 43 45	02 29 59	21
128	Lúcar	37 24 00	02 25 58	23
129	Lúcar	37 24 12	02 25 22	23
130	Lúcar	37 22 25	02 26 45	28
131	Pechina	36 57 48	02 23 50	57
132	Rioja	36 59 13	02 27 28	21
133	Fitero	42 03 25	01 54 15	50
134	Embid de Ariza	41 23 18	01 58 34	29
135	Alhama de Aragón	41 18 03	01 54 17	30
136	Alhama de Aragón	41 17 47	01 53 55	32
137	Alhama de Aragón	41 17 38	01 53 47	30
138	Jaraba	41 11 26	01 52 06	23
139	Jaraba	41 11 26	01 52 14	27
140	Jaraba	41 11 21	01 52 37	33
141	Jaraba	41 11 18	01 52 43	34
142	Jaraba	41 11 15	01 53 10	32
143	Jaraba	41 10 57	01 53 17	29
144	Jaraba	41 10 50	01 53 20	22
145	Lorca	37 47 25	01 56 43	24
146	Vélez Blanco	37 41 30	02 05 35	20
147	Lorca	37 42 58	01 57 33	22
148	Lorca	37 43 15	01 59 38	23
149	Bullas	38 01 20	01 41 50	21
150	Bullas	38 01 14	01 41 00	20
151	Lorca	37 53 05	01 42 32	21
152	Totana	37 49 30	01 36 04	20
153	Aledo	37 47 53	01 34 42	20
154	Lorca	37 40 56	01 43 52	21
155	Lorca	37 43 45	01 35 01	24
156	Archena	38 07 42	01 18 10	40
157	Mula	38 02 20	01 25 25	37
158	Mula	38 04 19	01 26 42	22
159	Sigüera Assoveral	42 36 50	00 55 35	26
160	Segura de los Banos	40 57 27	00 56 48	24
161	Teruel	40 22 45	01 05 47	22
162	Domeno	39 42 35	00 54 30	22
163	Chulilla	39 37 38	00 52 18	23

No.	Location	Co-ordinates		Temp. °C
		Lat. (N)	Long. (W)	
164	Siete Aguas	39 28 19	00 54 55	23
165	Cortes de Pallás	39 14 10	00 59 03	22
166	Fortuna	38 12 35	01 06 35	44
167	Fortuna	38 12 35	01 06 48	44
168	Orihuela	38 05 40	00 56 28	25
169	Mediana de Aragón	41 27 26	00 44 34	24
170	Arino	41 02 45	00 35 22	22
171	Montanejos	40 04 27	00 31 52	24
172	Novelda	38 26 10	00 46 55	20
173	Novelda	38 26 08	00 46 40	20
174	San Javier	37 48 57	00 48 55	34
175	Panticosa	42 45 45	00 13 49	52
176	Panticosa	42 45 48	00 14 08	24
177	Panticosa	42 44 27	00 15 03	21
178	Puértolas Puyarruego	42 31 01	00 06 12 (E)	28
179	Fiscal Liguerra de Ara	42 28 12	00 04 53	20
180	Alquezar	42 10 05	00 01 49 (E)	21
181	Aínsa Sobrarbe	42 24 40	00 13 35 (E)	22
182	Gandesa	41 00 10	00 25 47 (E)	28
183	Lés	42 48 20	00 42 50 (E)	30
184	Benasque	42 39 37	00 35 08 (E)	36
185	Alto Arán (Arties)	42 41 53	00 51 50 (E)	40
186	Alto Arán (Tredós)	42 39 30	00 55 50 (E)	38
187	Barruera (Bohí)	42 33 50	00 50 35 (E)	56
188	Espot	42 34 00	01 04 35 (E)	28
189	Aristot-Toloriu	42 21 50	01 34 40 (E)	35
190	Aristot-Toloriu	42 22 05	01 35 45 (E)	38
191	Llés	42 22 15	01 40 45 (E)	30
192	Santa Eulalia del Río	39 01 06	05 14 27 (E)	23
193	Esparreguera	41 34 11	01 52 08 (E)	28
194	Ribes de Freser	42 16 15	02 09 42 (E)	24
195	La Garriga	41 41 00	02 17 20 (E)	60
196	Caldes de Montbuí	41 37 55	02 09 55 (E)	70
197	Santa Coloma de Farners	41 50 45	02 40 32 (E)	42
198	Caldes de Malavella	41 50 15	02 48 30 (E)	60
199	Caldes de Estrach	41 34 15	02 31 48 (E)	39
200	Campmany	42 22 00	02 53 50 (E)	20
201	San Climent Sescebes	42 22 00	02 58 50 (E)	28
202	Campos del Puerto	39 21 03	03 00 49 (E)	37

Geothermal installations

No.	Location	Co-ordinates		Temp. °C
		Lat. (N)	Long. (W)	
1	Quintela	42 21 26	7 53 45	67
2	Orense	42 19 55	7 51 53	70
3(+)	Gaztelu	42 47 18	2 38 14	55
4(+)	Villalonguéjar	42 21 47	3 46 13	78
5(+)	Santa Fé	37 17 07	3 45 11	41
6 -	Mazarrón - 1	37 45 53	1 38 44	38
7(+)	Mazarrón - 2	37 39 32	1 20 39	51
8	Fuente Alamo - 1	37 46 12	1 06 33	40
9	Fuente Alamo - 2	37 46 13	1 06 32	40
10	Gea y Truyols	37 52 51	1 01 18	36
11	Orihuela	37 53 41	0 50 18	30
12	San Javier - 1	37 46 44	0 49 02	39
13	San Javier - 2	37 51 12	0 49 22	30
14	San Javier - 3	37 49 41	0 50 14	30
15	Pilar de la Horadada - 1	37 51 59	0 49 42	30
16	Pilar de la Horadada - 2	37 51 17	0 51 17	38
17	Pilar de la Horadada - 3	37 51 27	0 49 03	30
18	Pilar de la Horadada - 4	37 52 31	0 48 55	30
19	Lérida	41 37 37	0 37 59 (E)	57
20	Montbrió	41 07 35	0 59 06 (E)	60

- out of operation at present

Sweden

No.	Location	Co-ordinates		Temp. °C
		Lat. (N)	Long. (E)	
1	Lund	55 42 10	13 09 06	22
2	Klintehamn	57 23 00	18 11 40	18

Switzerland

No.	Location	Co-ordinates		Temp. °C
		Lat. (N)	Long. (E)	
1+	Bad Lostorf 3	47 23 36	7 56 00	27
2+	Bad Ragaz	46 58 06	9 29 12	37
3+	Bad Schinznach	47 26 54	8 10 06	32
4+	Baden	47 29 00	8 18 00	48
5+	Bassersdorf	46 26 24	8 38 12	22
6+	Brigerbad	46 19 00	7 55 00	53
7+	Kloten	47 27 00	8 35 24	18
8+	Kreuzlingen 2	47 38 54	9 10 42	30
9+	Lavey-les-Bains	46 12 06	7 01 24	62
10+	Leukerbad	46 22 48	7 37 30	51
11+	Oberwald	46 32 00	8 21 18	16
12+	Riehen	47 35 00	7 39 00	65

No.	Location	Co-ordinates		Temp. °C
		Lat. (N)	Long. (E)	
13+	Saillon	46 11 00	7 11 06	24
14+	Saxon 1	46 08 48	7 10 12	25
15+	Saxon 2	46 08 42	7 10 00	26
16+	Weggis	47 02 00	8 25 30	40
17+	Yverdon/Belair	46 47 00	6 54 00	25
18+	Zurzach 3	47 35 24	8 17 18	42
19s	Acquarossa	46 26 00	8 57 00	25
20s	Bovernier	46 05 00	7 09 00	21
21s	Combioula	46 12 00	7 26 00	28
22s	Hauensteintunnel	47 22 48	7 54 36	28
23s	Simplontunnel	46 17 30	8 03 48	<49
24s	Tiefenbrunnen/Zürich	47 21 12	8 33 12	32
25s	Vals	46 38 00	9 11 00	25
26s	Weissenburg	46 40 36	7 28 00	27

Temperature = Production temperature

+ Geothermal installation used for balneology, space heating or both

s unused spring or borehole

Note: there are over 10 000 Borehole Heat Exchangers installed.

United Kingdom

No.	Location	Co-ordinates		Temp. °C
		Lat. (N)	Long. (W)	
1	Buxton Spa	53 15 29	01 54 52	28
2	Matlock Bath	53 07 02	01 33 44	20
3	Taff's Well	51 32 45	03 16 14	20
4	Bristol	51 27 11	02 37 34	24
5	Bath	51 22 49	02 21 39	47
6+	Southampton (SU96)	50 54 20	01 24 32	72

Heat-Flow Density

Only new and updated list of heat-flow density are included in this table. For further information on this data, see text.

Albania

No. Location	Co-ordinates		Heat-Flow density mW/m ² without palaeo-cor.
	Lat. (N)	Long. (E)	
1 RE-308	40 30	20 37	66
2 GJE-2	42 07	20 31	13
3 VL-1127	42 13	20 29	45
4 TH-547	41 20	20 16	21
5 KE-839	42 03	20 15	67
6 BUL-4	41 27	20 13	35
7 NO-1	40 09	20 12	3
8 KAL-3	39 49	20 10	2
9 PR-1	40 32	20 09	33
10 DEL-4	39 56	20 08	13
11 GAL-2	40 57	20 08	27
12 ER-2	40 08	20 07	-3
13 VU-14	39 53	20 05	25
14 ME-2	40 21	20 05	21
15 BUT-1	39 42	20 04	35
16 VU-30	39 53	20 04	5
17 VU-57	39 54	20 03	32
18 VA-2	39 55	20 03	25
19 GOR-1	40 47	20 00	28
20 GR-4	40 53	20 00	56
21 PA-1	41 02	20 00	56
22 PER-589	41 43	20 00	28
23 KUC-8	40 49	19 59	36
24 SA-1	39 59	19 54	28
25 LA-2	41 20	19 53	21
26 BALL-27	40 34	19 48	28
27 PE-30	40 59	19 48	30
28 RU-M	41 46	19 46	29
29 KOM-967	42 05	19 46	31
30 AMA-1	40 21	19 45	28
31 AM-8	40 24	19 45	25
32 VE-1	42 34	19 45	9
33 MO-31	40 33	19 44	31
34 CA-17	40 35	19 44	31
35 CA-12	40 35	19 43	32
36 HY-1	40 24	19 42	23
37 KM-1	40 52	19 42	34
38 ISH-1b	41 30	19 41	27
39 SEL-4	40 32	19 40	30
40 MA-1	40 43	19 40	32
41 KO-10	40 45	19 40	40
42 GER-6	40 26	19 39	28
43 BUB-6	40 46	19 39	32
44 AR-18	40 48	19 38	24
45 DIV-11	40 58	19 37	37
46 DIV-265	40 57	19 36	38
47 DIV-33	40 58	19 36	34
48 VL-9	40 27	19 33	13
49 BALL-50	41 04	19 33	24
50 FR-44	40 38	19 32	35
51 KR-18	41 07	19 32	32
52 KR-10	41 09	19 31	32
53 TAR-1	42 02	19 28	6
54 SEM-1	40 50	19 26	31
55 ZV-3	40 32	19 24	28
56 PO-3	40 42	19 24	22
57 DU-15	41 19	19 21	38

Belgium

No. Location	Co-ordinates		Heat-Flow density mW/m ² without palaeo-cor.
	Lat. (N)	Long. (E)	
1 Meer	51 26 43	04 45 50	86
2 Peer	51 03 08	05 15 20	92
3 St. Ghislain	50 26 50	03 49 47	81
4 Soumagne	50 21 43	05 27 14	64
5 Grand-Halleux	50 11 04	05 32 33	59
6 Havelange	50 10 50	05 08 44	69

Bulgaria

No. Location	Co-ordinates		Heat-Flow density mW/m ² without palaeo-cor.
	Lat. (N)	Long. (E)	
1 Makresh	43 48	22 37	46
2 Bjalo pole	43 41	22 54	73
3 Orsoja	43 47	23 10	70
4 Kovatchitza	43 46	23 24	75
5 Kozlodui	43 42	23 37	62
6 Rasovo	43 42	23 13	79
7 Komostitza	43 41	23 21	75

No. Location	Co-ordinates		Heat-Flow density mW/m ² without palaeo-cor.
	Lat. (N)	Long. (E)	
8 Dalgodeltsy	43 35	23 18	66
9 Hajredin	43 34	23 42	79
10 Sofronievo	43 34	23 49	71
11 B.Geran	43 31	23 38	72
12 Dobrolevo	43 29	23 52	77
13 Blagovo	43 22	23 13	67
14 Tchiren	43 20	23 38	82
15 Borovtzy	43 17	23 11	75
16 Zamfirivo	43 17	23 14	79
17 Glavatsy	43 16	23 22	70
18 B.Izvor	43 15	23 31	78
19 Ponora	43 17	23 35	79
20 Vesletz	43 13	23 43	79
21 G.Pestene	43 18	23 45	82
22 Drashan	43 13	23 55	74
23 Orjahovo	43 30	24 01	70
24 Brest	43 48	24 36	65
25 Galovo	43 38	24 04	65
26 D.Lukovit	43 31	24 13	71
27 Trastenik	43 31	24 28	53
28 D.Dabnik	43 23	24 28	87
29 Kneja	43 30	24 05	77
30 Pelovo	43 25	24 17	79
31 Grivitsa	43 23	24 46	74
32 Glava	43 24	24 12	82
33 Pisarovo	43 20	24 23	74
34 Tutchenitsa	43 22	24 39	77
35 Begledg	43 14	24 32	70
36 Devetaky	43 12	24 53	84
37 Umarevtsy	43 09	24 49	86
38 Stejerovo	43 30	25 08	58
39 G.Slivovo	43 13	25 09	89
40 G.Oriahovitsa	43 05	25 45	86
41 V. Tarnovo	43 05	25 37	73
42 Sevlievo	43 02	25 10	90
43 Tchereshovo	43 53	26 22	48
44 Kavlak	43 13	26 03	89
45 Bukak	43 01	26 12	70
46 Omurtag	43 07	26 25	63
47 Straja	43 07	26 35	60
48 Zlatar	43 08	26 54	86
49 Marash	43 09	27 19	72
50 Preslav	43 09	26 20	60
51 Vetrino	43 18	27 31	43
52 Mirovo	43 06	27 28	67
53 Sultantsy	43 07	27 32	77
54 Junak	43 02	27 39	60
55 Bozvely	43 03	27 29	72
56 Komunary	42 58	27 19	62
57 Shabla	43 33	28 35	49
58 Gorun	43 30	28 30	50
59 Balgarevo	43 24	28 35	54
60 Balsha	42 51	23 13	88
61 Dobroslavtsy	42 48	23 15	95
62 Kremikovtsy	42 47	23 22	79
63 Sofia	42 42	23 19	75
64 Elin Pelin	42 40	23 36	69
65 Kosatsha	42 53	22 50	50
66 Bobov dol	42 21	23 01	55
67 St. Dimitrov	42 15	23 06	69
68 Krainitsy	42 18	23 18	99
69 Jakoruda	41 59	23 41	92
70 Rila	42 06	23 09	77
71 Sr. kolo	42 13	22 39	64
72 Elatzite	42 44	24 03	46
73 Tchelopetch	42 40	24 08	69
74 Toplika	42 28	24 12	60
75 Pesovets	42 26	24 16	66
76 Starosel	42 27	24 33	65
77 Tserovo	42 20	24 04	54
78 Elshitsa	42 22	24 14	54
79 Radka	42 23	24 20	53
80 M. Tcherdak	42 19	24 38	47
81 Voivodinovo	42 13	24 48	56
82 Bratsigovo	42 02	24 25	52
83 D. Voden	42 03	24 53	66
84 Asenovgrad	42 00	24 54	81
85 Elena	42 57	25 52	63
86 Skobelovo	42 41	25 12	53
87 Koprinka	42 38	25 26	55
88 Kazanlak	42 37	25 24	50
89 Maglig	42 35	25 34	55
90 Nikolaevo	42 37	25 48	45
91 O. Kirilovo	42 22	24 59	36
92 Rajena	42 31	25 34	47
93 Maritsa	42 02	25 50	89
94 Dimitrovgrad	42 02	25 37	63
95 Svirkovo	42 00	25 59	65
96 Borov dol	42 43	26 06	67
97 Sliven	42 40	26 20	78
98 Karnobat	42 36	27 28	68
99 Nova Zagora	42 30	26 02	42
100 Jambol	42 27	26 32	71
101 Bakadgik	42 22	26 43	53
102 Kovatchevo	42 10	26 05	52
103 Drjanovo	42 05	25 55	50
104 Alexandrovo	42 17	26 54	61

No. Location	Co-ordinates		Heat-Flow density mW/m ² without palaeo-cor.
	Lat. (N)	Long. (E)	
105 Ustrem	42 01	26 29	61
106 Solník	42 55	27 38	48
107 Samotino	42 56	27 53	62
108 Aitos	42 42	27 17	80
109 Sl. Brjag	42 20	27 44	70
110 Pomorie	42 43	27 38	44
111 Aheloy	42 37	27 39	57
112 Rosen	42 23	27 35	54
113 Zidarovo	42 20	27 24	60
114 Primorsko	42 16	27 47	55
115 Gramatikovo	42 02	27 39	53
116 M. Tarnovo	41 58	27 32	55
117 Oranovo	41 53	23 07	83
118 Belitsa	41 56	23 34	84
119 Gara Pirin	41 43	23 11	84
120 Laskarevo	41 42	23 19	94
121 Melnik	41 31	23 23	75
122 Tchereshnitsa	41 30	23 28	40
123 Kromidovo	41 27	23 23	86
124 Grantcharitza	41 56	23 56	43
125 Hvojna	41 49	24 47	76
126 Laky	41 48	24 54	95
127 Davidkovo	41 40	24 58	85
128 Smolian	41 35	24 42	91
129 Mugla	41 34	24 30	50
130 D. Vlahovo	41 33	24 38	90
131 Lozen	41 46	26 04	80
132 Madgarovo	41 35	25 55	78
133 Zvezdel	41 23	25 33	90
134 Ptsheljad	41 22	25 33	74
135 Djebel	41 24	25 21	93
136 Ardino	41 30	25 09	81
137 Lenovo	41 57	25 08	92
138 Ivailovgrad	41 30	26 08	83
139 Mandritsa	41 23	26 08	49
140 G. Likovo	41 21	26 04	59
141 Lesovo	41 55	26 35	65

Czech Republic

No. Location	Co-ordinates		Heat-Flow density mW/m ²	
	Lat. (N)	Long. (E)	without palaeo-cor.	incl. palaeo-cor.
1 Lesná	50 52 00	14 35 00	58	
2 Cínovec	50 44 00	13 46 00	84	
3 Benešov	50 44 00	14 19 00	60	
4 Křižany	50 44 00	14 52 00	68	
5 Cínovec	50 43 36	13 45 54	77	
6 Cínovec	50 43 00	13 45 54	68	
7 Dubí	50 41 30	13 46 54	105	
8 Roztoky	50 41 00	14 12 00	61	
9 Teplice	50 38 36	13 49 18	158	
10 Teplice	50 38 24	13 49 42	86	
11 Teplice	50 38 00	13 50 54	185	
12 Lochočic	50 37 42	13 57 00	68	
13 Rydec	50 36 54	14 10 18	72	
14 Libkovic	50 35 00	13 41 00	98	
15 Horní Rokytá	50 34 18	14 51 24	63	
16 Košťálov	50 34 00	15 24 00	79	
17 Libštát	50 33 30	15 25 18	81	
18 Svatoňov	50 32 30	16 03 18	67	
19 Strážkov	50 32 24	16 03 48	60	
20 Strážkov	50 31 36	16 05 18	64	
21 Z. Zdírní	50 31 00	15 40 00	70	
22 Rokytník	50 30 36	16 08 54	61	
23 Bystré	50 30 30	16 07 48	69	
24 Bystré	50 30 12	16 07 48	66	
25 Bohdašín	50 30 00	16 07 48	64	
26 Brňany	50 29 12	14 09 00	80	
27 Trebívli	50 27 00	13 54 00	59	
28 Stranká	50 25 30	14 39 12	72	
29 Zlatý Kopec	50 25 00	12 54 00	97	
30 Košnice	50 24 54	13 57 24	52	
31 Bechlín	50 24 54	14 21 54	70	
32 Sřemy	50 23 06	14 32 54	79	
33 Pernink	50 22 30	12 46 30	59	
34 Hled'sebe	50 21 36	14 32 54	63	
35 Jenichov	50 21 36	14 34 42	81	
36 Skuhrov	50 20 12	13 34 48	90	
37 Vysoka Liben	50 20 12	14 31 00	60	
38 Peruc	50 19 42	13 58 54	74	
39 Chotělice	50 19 06	15 28 12	63	
40 Luštěnice	50 19 00	14 54 42	67	
41 Benátky	50 17 36	14 48 24	80	
42 Oploty	50 17 06	13 26 36	53	
43 Dřínov	50 16 36	14 05 42	62	
44 Běřovice	50 16 30	14 07 48	62	
45 Kostelní Hlavno	50 16 18	14 42 42	96	
46 Zlovědice	50 16 00	13 23 42	54	
47 Bakov	50 16 00	14 06 00	55	
48 Běřovice	50 16 00	14 08 00	60	
49 Hlušice	50 16 00	15 24 42	62	
50 Luníkov	50 15 24	14 08 54	62	
51 Otruby	50 15 18	14 05 24	62	
52 Byseň	50 15 00	14 04 00	59	

No. Location	Co-ordinates		Heat-Flow density mW/m ²	
	Lat. (N)	Long. (E)	without palaeo-cor.	incl. palaeo-cor.
53 Slaný	50 15 00	14 06 00	81	
54 Slaný	50 13 24	14 05 06	63	
55 Heřmanov	50 11 03	17 24 00	32	
56 Týniště	50 10 06	16 05 36	96	
57 Dlouhupolsko	50 09 42	15 19 24	69	
58 Krásná	50 07 30	12 48 00	92	
59 Čistá	50 07 00	12 44 00	45	
60 Odava	50 06 24	12 24 48	71	
61 Čistá	50 05 54	12 42 48	81	
62 Sokoleč	50 05 18	15 06 48	62	
63 Božkov	50 05 00	16 43 00	49	
64 Roblín	49 57 24	14 15 36	62	
65 Skřečůň	49 54 36	18 22 30	78	68
66 Zadní Chodov	49 53 00	12 39 00	55	
67 Planá	49 53 00	12 42 00	70	
68 Stokov	49 51 06	12 38 06	51	
69 Detrichov	49 49 06	17 23 00	55	
70 Vítkov	49 49 00	12 39 48	56	
71 Stonava	49 48 24	18 31 42	99	79
72 Vítkov	49 48 00	12 40 00	55	
73 Louky	49 47 36	18 35 00	76	62
74 Pernolec	49 46 18	12 40 30	59	
75 Tachov	49 46 12	12 41 42	56	
76 Hlinné	49 45 00	12 46 00	54	
77 Vendolí	49 45 00	16 25 00	40	
78 Lom Str.	49 44 00	12 53 00	61	
79 Květná	49 44 00	16 22 00	21	
80 Květná	49 43 00	14 03 00	48	
81 Stare Ransko	49 43 00	15 51 00	71	
82 Pomezí	49 43 00	16 20 00	22	
83 Příbram	49 41 12	13 59 48	57	
84 Plavý	49 39 12	14 05 12	31	
85 Lešetice	49 39 00	14 01 00	62	
86 Bystrice	49 38 00	18 44 00	64	70
87 Kozlovic	49 36 06	18 15 12	86	70
88 Milín	49 36 00	14 04 00	34	
89 Kozlovic	49 35 42	18 16 54	78	79
90 Malenovice	49 35 00	18 24 36	85	79
91 Pstruží	49 34 24	18 19 48	87	73
92 Tichá	49 34 06	18 14 54	73	72
93 Choryně	49 34 00	17 53 00	71	72
94 Kozlovic	49 33 54	18 17 12	112	77
95 Šebřov	49 33 30	14 49 42	56	
96 Ostravice	49 33 30	18 22 54	92	71
97 Předboří	49 33 06	14 15 18	54	
98 Tichá	49 33 00	18 14 24	75	69
99 Kunčice	49 32 48	18 16 30	77	62
100 Čeladná	49 32 36	18 18 18	80	72
101 Kunčice	49 32 24	18 15 12	104	92
102 Polná	49 32 12	15 44 00	43	
103 Kunčice	49 32 06	18 17 06	91	69
104 Frenštát	49 31 54	18 14 06	76	66
105 Krasná	49 31 54	18 31 06	60	62
106 Trojanov	49 31 42	18 11 18	83	71
107 Trojanov	49 31 42	18 15 24	71	68
108 Kunčice	49 31 36	18 18 36	120	79
109 Věřovice	49 31 30	18 08 24	82	73
110 Trojanov	49 31 24	18 10 30	90	68
111 Trojanov	49 31 24	18 13 24	124	74
112 Trojanov	49 31 18	18 12 00	45	59
113 Trojanov	49 31 06	18 14 00	61	47
114 Trojanov	49 31 00	18 12 30	84	72
115 Trojanov	49 30 48	18 15 18	86	74
116 Rožnov	49 30 36	18 09 30	63	55
117 Trojanov	49 30 36	18 12 00	82	65
118 Čeladná	49 30 30	18 20 24	83	73
119 Trojanov	49 30 24	18 14 06	104	72
120 Trojanov	49 30 12	18 11 24	89	70
121 Novotník	49 29 00	13 32 00	72	
122 Rožínka	49 28 00	16 12 00	31	
123 St. Hamry	49 27 36	18 25 30	76	64
124 Strážek	49 27 24	16 11 48	39	
125 Bor u Tachova	49 24 00	12 47 00	53	
126 T. N. Ves	49 24 00	16 18 00	24	
127 Nova Res	49 23 06	14 47 42	47	
128 Jablunca	49 23 00	17 57 00	85	68
129 Rusava	49 20 24	17 41 18	65	65
130 Tučapy	49 18 42	14 58 54	61	
131 Rataje	49 16 18	17 19 48	51	
132 Lubná-2	49 13 06	17 23 12	54	
133 Lidečko	49 13 06	18 03 06	75	
134 Lubná-6	49 12 18	17 19 48	63	
135 Vizovice	49 12 00	17 52 00	71	
136 Lubná-8	49 10 48	17 22 18	76	
137 Slavkov	49 09 36	16 51 48	55	
138 Bučovice	49 08 42	16 59 36	58	
139 Újezd	49 06 54	16 45 12	48	
140 Nesvačil	49 05 36	16 44 30	54	
141 Žarosi-2	49 04 18	16 56 36	45	
142 Ždánice	49 04 00	17 02 00	51	
143 Žarosi-1	49 03 06	16 57 48	46	
144 Ježov-2	49 02 30	17 08 42	42	
145 Nikolč-4	49 01 18	16 43 54	44	
146 Nicolč-6	48 59 42	16 46 00	51	
147 Nikolč-1	48 59 12	16 46 06	64	
148 Vranovic	48 58 06	16 40 42	60	
149 Kobylí	48 55 30	16 54 24	63	
150 Holubov	48 53 42	14 19 06	47	

No. Location	Co-ordinates		Heat-Flow density mW/m ² without palaeo-cor.
	Lat. (N)	Long. (E)	
151 Müso	48 53 30	16 36 42	49
152 Dunaj 11	48 51 12	16 36 18	46
153 Dunaj 13	48 50 00	16 34 00	72
154 Mikulov	48 48 24	16 35 54	42
155 Hrušk-10	48 47 06	16 58 18	53

Denmark

No. Location	Co-ordinates		Heat-Flow density mW/m ² without palaeo-cor.
	Lat. (N)	Long. (E)	
1 Hyllebjerg-1	56 48 53	09 20 54	71
2 Års-1	56 47 44	09 30 34	71
3 Farsø-1	56 46 53	09 21 50	76
4 Rødding-1	56 38 49	08 48 18	71
5 Skive-1	56 37 38	09 00 11	78
6 Oddesund-1	56 33 37	08 34 10	68
7 Kvols-1	56 31 41	09 17 56	78
8 Voldum-1	56 23 02	10 16 01	75
9 Rønde-1	56 18 14	10 26 06	66
10 Nøvling-1	56 10 09	08 48 36	64
11 Grondalseng	55 41 19	12 30 40	56
12 Logumkloster	55 02 33	08 57 04	76
13 Varnaes 1	55 02 13	09 35 32	78
14 Ørslev	54 46 55	11 59 02	82

Estonia

No. Location	Co-ordinates		Heat-Flow density mW/m ²	
	Lat. (N)	Long. (E)	without palaeo-cor.	incl. palaeo-cor.
1 Loksa	59 35	25 44	36	45
2 Saviranna	59 30	25 03	40 - 43	48 - 51
3 Maardu	59 28	25 06	41	48
4 Jöelähtme	59 27	25 10	34	40
5 Meriküla	59 26	28 00	61 - 62	67 - 68
6 Keila-Joa	59 24	24 19	37	42
7 Vintse	59 17	23 53	31	41
8 Lasila	59 16	26 16	38	43
9 Nabala	59 15	24 53	28	32
10 Nõmme	59 09	23 45	32	40
11 Lohu	59 08	24 47	26	32
12 Ramma	59 03	26 05	34	39
13 Tudulinna	59 03	27 09	35	39
14 Förby	59 00	23 09	38	46
15 Kärdla	58 59	22 40	34	42
16 Taebla	58 58	23 47	37	47
17 Haapsalu	58 57	23 35	27	37
18 Maidla	58 57	24 11	29 - 31	37 - 38
19 Koluvvere	58 55	24 10	25	35
20 Tooma	58 53	26 19	32	37
21 Jõgeva	58 41	26 27	33	40
22 Are	58 33	24 38	31	40
23 Pärnu	58 21	24 40	45	54
24 Ramsi	58 19	25 36	34	40
25 Pärnu	58 16	24 44	28	36
26 Võru	57 52	27 03	22	28

Finland

No. Location	Co-ordinates		Heat-Flow density mW/m ²	
	Lat. (N)	Long. (E)	without palaeo-cor.	incl. palaeo-cor.
1 Sokli	67 49	29 20	42	
2 Sodankylä	67 42	26 59	25	
3 Sodankylä-2	67 40	26 16	13	
4 Sodankylä-3	67 40	26 17	17	
5 Sodankylä-1	67 38	26 15	13	
6 Sodankylä-4	67 37	25 53	19	
7 Sodankylä-5	67 36	25 52	24	
8 Kolari-198	67 34	23 56	29	
9 Kolari-197	67 33	23 56	27	
10 Kolari-162	67 33	23 56	34	
11 Ranua	66 06	26 10	25	
12 Liminka	64 51	25 26	44	
13 Hyrynsalmi	64 35	29 19	37	
14 Vihanti	64 23	25 05	32	
15 Kuhmo	64 13	29 56	24	
16 Honkamäki	64 08	26 54	32	
17 Otanmäki	64 07	27 06	32	
18 Ylivieska	64 02	24 08	34	
19 Nivala	63 51	25 03	34	
20 Sievi	63 43	24 51	44	
21 Pyhäjärvi	63 40	26 05	38	
22 Keitele	63 17	26 22	41	
23 Pielavesi	63 12	26 40	34	
24 Siilinjärvi-157	63 07	27 44	15	
25 Siilinjärvi-112	63 07	27 44	22	
26 Siilinjärvi-171	63 06	27 44	19	

No. Location	Co-ordinates		Heat-Flow density mW/m ² without palaeo-cor.
	Lat. (N)	Long. (E)	
27 Ylistaro	62 57	22 32	49
28 Luikonlahti	62 57	28 42	31
29 Ilomantsi	62 52	30 45	31
30 Konginkangas	62 49	25 42	35
31 Outokumpu-740	62 47	29 13	36
32 Outokumpu-737	62 47	29 13	33
33 Outokumpu-741	62 47	29 13	32
34 Outokumpu-290	62 43	29 01	33
35 Kotalahti	62 34	27 37	37
36 Hammaslahti	62 27	30 01	39
37 Virtasalmi	62 04	27 34	27
38 Kangasniemi	62 02	26 35	38
39 Kerimäki	62 01	28 57	35
40 Lavia	61 39	22 41	46
41 Parikkala	61 35	29 41	28
42 Pori	61 27	21 45	53
43 Sääksjärvi	61 27	22 45	44
44 Heinola	61 15	26 22	45
45 Eurajoki	61 14	21 29	32
46 Mäntsälä	60 37	25 11	69
47 Elimäki	60 37	26 29	34
48 Nummi-Pusula	60 28	26 46	55
49 Loviisa	60 22	26 18	57
50 Lohja	60 16	24 05	38
51 Kisko	60 14	23 31	68
52 Parainen	60 11	22 19	38
53 Espoo	60 11	24 50	48

Germany

No. Location	Co-ordinates		Heat-Flow density mW/m ²	
	Lat. (N)	Long. (E)	without palaeo-cor.	incl. palaeo-cor.
1	54 38 06	13 21 06	71	
2	54 37 48	13 20 18	65	
3	54 37 42	13 13 30	76	
4	54 36 00	13 08 00	35	
5	54 35 54	13 17 36	60	
6	54 35 30	13 14 00	65	
7	54 33 47	13 19 00	68	
8	54 33 00	13 20 48	71	
9	54 31 18	13 15 30	71	
10	54 31 00	13 33 30	43	
11	54 28 00	12 30 12	55	
12	54 26 48	13 17 06	47	
13	54 25 54	12 40 30	57	
14	54 25 00	13 01 00	72	
15	54 23 30	12 29 36	65	
16	54 23 18	12 29 00	90	
17	54 22 48	13 18 24	64	
18	54 22 30	13 39 00	40	
19	54 20 30	13 13 30	69	
20	54 20 12	12 59 54	68	
21	54 19 12	12 32 42	63	
22	54 19 00	12 22 30	82	
23	54 18 12	13 42 42	60	
24	54 17 12	12 35 00	66	
25	54 15 54	12 55 48	63	
26	54 14 30	13 23 42	59	
27	54 13 42	12 50 06	64	
28	54 13 36	13 16 48	59	
29	54 12 24	12 41 48	70	
30	54 11 12	13 10 36	64	
31	54 10 54	13 10 42	67	
32	54 10 24	13 03 48	60	
33	54 10 12	13 09 30	65	
34	54 10 00	13 13 24	55	
35	54 09 18	13 02 30	65	
36	54 08 18	13 24 42	62	
37	54 07 36	13 33 00	83	
38	54 07 30	13 32 00	63	
39	54 06 12	12 46 00	59	
40	54 04 30	13 41 30	80	
41	54 02 18	13 43 00	50	
42	54 02 06	13 53 48	70	
43	54 01 06	12 14 18	78	
44	54 00 18	13 35 42	73	
45	53 59 54	13 36 54	71	
46	53 56 36	11 09 48	53	
47	53 56 30	12 06 24	97	
48	53 54 54	14 01 00	70	
49	53 52 30	13 32 30	78	
50 Rehna-Rüting 1	53 48 00	11 03 00	62	
51	53 47 00	13 31 30	75	
52	53 46 18	12 39 48	78	
53	53 46 00	13 16 00	88	
54 Fahrenhorst	53 45 59	10 05 46	47	54
55 Langenhorn	53 39 47	10 01 19	49	56
56	53 39 24	11 55 24	52	
57 Appen	53 39 18	09 43 49	52	59
58	53 36 30	12 40 18	103	
59	53 34 00	11 21 12	49	
60	53 33 30	11 18 18	40	
61	53 31 36	12 41 06	59	

No. Location	Co-ordinates		Heat-Flow density		No. Location	Co-ordinates		Heat-Flow density	
	Lat. (N)	Long. (E)	without palaeo-cor.	incl. palaeo-cor.		Lat. (N)	Long. (E)	without palaeo-cor.	incl. palaeo-cor.
62	53 31 36	12 41 12	53		159	52 40 00	11 17 36	96	
63	53 31 06	13 56 00	63		160	52 39 06	13 09 42	52	
64	53 31 00	12 57 36	77		161	52 39 00	10 58 42	74	
65	53 29 06	11 42 00	74		162	52 39 00	11 43 00	90	
66	53 26 48	11 47 54	51		163	52 38 12	11 11 06	63	
67	53 26 30	10 40 00	70		164	52 38 12	13 19 36	77	
68	53 22 24	12 15 00	70		165	52 38 00	10 56 00	48	
69	53 22 12	12 12 48	60		166 Altmark-15	52 37 30	11 53 30	70	
70	53 19 54	11 65 06	65		167	52 37 24	12 27 30	77	
71	53 19 54	11 57 48	103		168	52 37 00	11 54 24	90	
72	53 19 06	14 15 00	71		169	52 36 12	12 32 12	75	
73	53 19 06	14 15 06	63		170	52 35 12	11 05 42	69	
74	53 18 48	10 39 00	81		171	52 35 00	12 28 12	85	
75	53 17 36	11 20 48	48		172	52 33 48	11 09 06	64	
76	53 17 30	12 29 00	99		173 Altmark-14	52 33 36	11 39 30	50	
77	53 17 12	11 39 42	52		174 Calvoerde-5	52 33 18	11 10 30	74	
78	53 16 30	13 57 54	72		175	52 33 12	14 32 00	95	
79	53 16 24	13 13 00	82		176	52 33 00	12 43 00	90	
80	53 16 18	12 58 00	96		177 Calvoerde-6	52 32 24	11 13 30	67	
81	53 15 42	11 38 00	56		178	52 32 24	11 43 12	72	
82	53 15 30	11 42 12	71		179'	52 32 00	11 43 30	62	
83	53 15 12	11 41 00	79		180	52 31 18	11 13 24	60	
84	53 13 48	14 02 30	70		181 Calvoerde-7	52 30 36	11 15 00	58	
85	53 13 36	12 33 12	54		182	52 29 54	13 51 00	81	
86	53 13 24	11 51 00	42		183	52 29 48	12 09 30	77	
87	53 12 54	13 17 18	72		184	52 29 30	11 06 06	47	
88	53 12 42	12 28 00	52		185 Calvoerde-8	52 29 24	11 24 00	64	
89 Prignitz-27	53 10 48	11 37 00	54		186	52 29 12	13 50 48	82	
90	53 10 24	11 17 00	75		187	52 27 54	11 26 12	55	
91	53 10 24	11 37 30	75		188	52 27 54	11 49 12	87	
92	53 10 18	11 50 30	67		189	52 27 48	13 48 18	87	
93	53 10 12	13 48 30	91		190	52 27 36	11 19 24	54	
94	53 10 06	14 20 42	81		191	52 26 48	11 27 48	56	
95	53 09 36	14 00 24	74		192	52 26 30	11 24 12	61	
96	53 08 42	11 14 48	70		193	52 26 24	11 17 30	72	
97 Prignitz-26	53 08 24	12 24 30	65		194	52 26 06	11 17 36	69	
98	53 08 00	12 58 00	67		195 Oebisfelde	52 26 00	10 59 00	48	
99	53 07 42	12 19 18	79		196	52 26 00	11 15 30	68	
100	53 06 36	12 18 36	77		197	52 25 42	12 15 18	95	
101 Prignitz-25	53 05 06	12 18 30	59		198	52 25 24	11 18 36	62	
102	53 04 54	11 39 48	88		199 Bramsche	52 24 36	07 57 44	45	59
103	53 04 48	11 27 48	103		200	52 23 48	11 42 12	69	
104	53 04 18	12 18 12	63		201 Calvoerde-10	52 23 24	11 25 30	64	
105	53 04 00	11 45 30	84		202 Calvoerde-9	52 23 00	11 23 00	60	
106	53 02 42	11 37 48	52		203	52 22 00	11 41 36	87	
107	53 02 36	11 44 48	83		204	52 21 30	11 27 30	60	
108 Prignitz-24	53 02 24	12 12 30	58		205	52 21 18	12 32 24	66	
109	53 01 54	12 56 24	78		206 Meerdorf	52 21 18	10 19 48	89	89
110	53 01 48	14 03 30	91		207	52 21 00	13 35 30	41	
111	53 01 42	12 13 12	60		208	52 20 48	11 27 54	61	
112	53 01 30	13 24 06	105		209 Höver	52 20 42	09 53 36	55	68
113	53 01 00	13 17 30	74		210	52 19 48	12 31 54	87	
114	53 00 24	12 11 18	65		211	52 19 00	11 26 54	62	
115 Prignitz-23	52 59 24	12 10 00	64		212	52 18 24	11 36 18	67	
116	52 57 30	11 45 30	55		213 Calvoerde-13	52 18 00	11 46 30	96	
117	52 56 24	13 17 00	74		214 Calvoerde-12	52 17 30	11 35 30	67	
118	52 55 42	12 32 18	60		215	52 17 30	11 39 48	49	
119	52 55 30	13 49 00	88		216	52 17 30	13 29 54	45	
120	52 54 12	12 18 18	62		217	52 17 30	13 31 30	62	
121	52 54 00	11 04 00	75		218	52 17 12	11 37 54	60	
122	52 53 36	12 59 00	50		219 Calvoerde-11	52 16 00	11 34 30	68	
123	52 53 06	11 31 18	57		220	52 15 06	11 46 18	97	
124 Altmark-21	52 52 30	11 36 00	78		221	52 11 30	14 36 00	135	
125	52 51 30	11 17 36	71		222	52 11 24	14 38 30	48	
126 Altmark-18	52 51 00	11 19 30	85		223 Konrad	52 11 06	10 24 18	71	74
127	52 50 48	13 11 12	64		224 Subherzyn-4	52 10 12	11 09 30	62	
128	52 50 00	11 18 36	85		225	52 08 36	13 39 36	65	
129	52 50 00	12 44 36	74		226	52 07 30	13 21 06	22	
130	52 49 48	11 20 00	81		227	52 07 18	11 07 42	61	
131	52 49 06	11 13 30	81		228	52 05 48	12 51 00	50	
132	52 49 00	10 58 06	117		229 Subherzyn-3	52 05 24	11 04 00	64	
133	52 48 48	11 00 24	83		230	52 04 06	14 24 30	71	
134	52 48 30	11 44 06	90		231	52 03 54	11 27 54	65	
135 Altmark-17	52 48 00	11 29 30	100		232	52 03 48	14 08 54	52	
136	52 47 54	11 26 00	51		233	52 03 36	14 08 24	75	
137	52 47 65	12 34 42	58		234	52 03 18	14 09 06	70	
138 Prignitz-22	52 47 00	12 20 00	65		235	52 03 06	13 35 54	52	
139	52 46 54	10 47 30	59		236	52 02 54	13 13 06	63	
140	52 46 42	11 10 30	108		237 Subherzyn-2	52 01 30	10 42 00	68	
141	52 46 36	13 45 00	86		238	52 01 30	13 58 36	73	
142	52 46 24	10 48 24	60		239 Münsterland	52 00 35	07 20 32	58	76
143	52 46 24	10 48 12	59		240	52 00 06	10 44 12	75	
144	52 46 18	10 50 48	62		241	51 59 12	10 43 42	76	
145 Altmark-19	52 46 12	10 51 00	91		242	51 59 06	13 58 36	60	
146	52 46 00	13 50 00	90		243	51 59 06	14 41 30	70	
147	52 45 36	12 19 42	64		244	51 57 42	14 40 42	57	
148	52 45 24	14 13 54	68		245	51 57 42	14 41 54	47	
149	52 44 48	11 27 30	63		246	51 56 48	13 52 54	74	
150	52 44 30	11 03 30	87		247	51 56 06	13 50 30	47	
151	52 44 30	13 00 00	68		248	51 55 36	13 51 36	82	
152 Altmark-16	52 44 24	11 26 30	75		249	51 55 00	10 55 00	62	
153	52 43 30	12 24 36	90		250	51 54 54	14 41 54	63	
154	52 42 00	11 01 18	60		251	51 54 48	14 39 00	49	
155	52 41 36	11 01 00	89		252	51 54 42	11 07 24	72	
156 Altmark-20	52 40 12	10 55 00	101		253	51 53 24	14 26 30	70	
157	52 40 06	10 53 30	85		254	51 52 54	14 18 48	85	
158	52 40 06	11 58 30	42		255	51 52 48	14 17 48	68	

No. Location	Co-ordinates		Heat-Flow density		No. Location	Co-ordinates		Heat-Flow density	
	Lat. (N)	Long. (E)	without palaeo-cor.	incl. palaeo-cor.		Lat. (N)	Long. (E)	without palaeo-cor.	incl. palaeo-cor.
256	51 51 36	11 06 42	62		353	51 08 00	11 26 36	69	
257 Subherzyn-1	51 51 00	11 08 00	53		354 Langensalza-10	51 07 36	10 41 00	92	
258 Staßfurt	51 50 30	11 37 30	70		355 Langensalza-22	51 07 00	10 42 00	70	
259	51 49 24	14 34 54	51		356 Spröttau-3	51 06 00	11 12 00	57	
260	51 48 30	14 06 00	58		357	51 06 00	11 19 00	78	
261	51 47 48	14 12 24	47		358	51 05 54	11 22 30	63	
262	51 47 42	14 08 18	79		359	51 05 48	11 15 00	61	
263	51 47 00	14 07 06	47		360	51 05 30	11 15 48	50	
264	51 46 12	14 11 12	58		361 Hainich-Mihla-1	51 04 00	10 25 00	93	
265	51 45 06	14 09 54	53		362 Fahner Höhe-10	51 04 00	10 46 00	72	
266	51 43 30	14 23 12	42		363	51 03 36	11 15 48	69	
267	51 41 30	11 39 00	39		364 Wiegleben-1	51 03 00	10 36 00	67	
268	51 41 06	14 28 18	52		365 Fahner Hone-17	51 03 00	10 44 00	61	
269	51 39 24	14 30 12	64		366 Hainich-Berka-103	51 02 30	10 25 00	85	
270 Juessee	51 39 18	10 20 36	59	64	367 Hainich-Berka-107	51 02 30	10 30 30	72	
271	51 39 12	14 41 36	67		368 Fahner Hohe-3	51 02 24	10 48 30	83	
272	51 38 30	14 14 18	48		369 Jena-Z 105	51 02 24	11 37 00	64	
273	51 38 12	11 12 24	59		370 Jackerather Horst	51 02 10	06 25 54	60	68
274	51 38 12	14 38 42	60		371 Behringen-5	51 02 00	10 32 00	70	
275	51 38 06	14 35 24	68		372 Behringen-9	51 01 48	10 32 30	64	
276	51 37 42	14 39 36	84		373 Ettersberg-4	51 01 30	11 13 30	44	
277	51 37 12	14 37 36	57		374 Hainich-Berka-102	51 01 00	10 27 00	98	
278	51 37 12	14 39 42	60		375 Behringen-4	51 01 00	10 30 30	80	
279 Königshall	51 36 30	10 00 30	56	67	376	51 00 36	13 18 30	58	
280 Straßberg	51 36 00	11 03 00	65		377 Behringen-13	51 00 30	10 38 00	75	
281	51 36 00	14 20 00	64		378	50 59 00	13 22 00	41	
282	51 35 54	14 29 00	55		379 Freital	50 59 00	13 38 30	25	
283	51 35 54	14 44 18	60		380 Krahnberg-12	50 58 30	10 39 00	80	
284	51 35 00	14 21 00	61		381	50 58 12	13 17 06	39	
285	51 33 36	14 31 06	121		382 Mechterstädt-5	50 58 00	10 31 00	75	
286	51 33 30	14 27 00	60		383	50 58 00	10 31 00	70	
287	51 32 54	14 31 24	130		384 Krahnberg-17	50 58 00	10 36 00	66	
288	51 32 30	14 24 48	84		385	50 58 00	10 39 00	65	
289	51 29 00	10 38 00	23		386 Krahnberg-16	50 58 00	10 40 30	67	
290 Bleicherode	51 27 00	10 35 00	44		387 Krahnberg-4	50 57 48	10 41 30	67	
291	51 26 54	11 48 00	34		388	50 57 06	10 38 00	46	
292	51 26 00	11 50 18	36		389 Mechterstädt-2	50 57 00	10 31 30	65	
293	51 25 48	10 40 00	56		390 Neudietendorf-1	50 57 00	10 51 30	44	
294	51 25 00	11 44 54	63		391	50 56 00	13 11 48	20	
295	51 19 36	10 55 48	42		392	50 54 30	10 45 00	101	
296	51 19 30	10 30 24	90		393 Freiberg	50 54 30	13 20 30	71	
297	51 19 30	10 42 30	71		394	50 54 00	11 09 00	45	
298 Wattesattel 1	51 19 00	10 32 30	78		395 Deuz	50 53 32	08 07 31	55	86
299	51 18 30	11 36 48	63		396	50 53 30	10 41 30	85	
300 Sollstedt 2	51 18 00	10 27 30	63		397	50 52 30	12 15 00	44	
301	51 18 00	10 26 30	54		398 Branderbisdorf	50 52 00	13 19 00	85	
302	51 17 54	10 25 00	49		399 Dormdorf	50 51 30	10 06 00	63	
303	51 17 30	10 30 18	112		400 Ohrdruf	50 51 30	10 46 00	94	
304	51 17 30	10 21 24	52		401	50 50 00	11 10 48	57	
305	51 17 30	10 28 00	54		402	50 50 00	14 44 30	44	
306	51 17 24	10 27 18	59		403	50 49 18	13 44 36	65	
307	51 17 00	10 20 12	109		404	50 48 30	12 39 00	63	
308 Schwarzbachtal	51 16 57	06 53 16	54	68	405 Wehrhausen	50 48 26	09 52 41	72	79
309	51 16 30	10 24 06	81		406 Helpenstell	50 47 32	07 35 28	76	104
310	51 16 30	10 25 18	73		407	50 47 18	10 04 30	59	
311	51 16 12	10 24 00	90		408 Buchenau	50 47 10	09 44 58	69	78
312	51 16 00	10 23 00	91		409	50 47 00	09 59 30	53	
313	51 16 00	10 26 30	81		410	50 46 18	10 04 00	75	
314	51 16 00	10 30 30	116		411	50 46 00	09 57 00	42	
315	51 15 54	10 23 00	81		412 Altenberg	50 46 00	13 42 30	92	
316	51 15 30	10 20 00	108		413 Füssenberg	50 45 30	07 56 48	58	64
317	51 15 30	10 21 12	117		414 Zwickau	50 44 30	12 34 30	55	
318	51 15 30	10 43 00	58		415	50 43 30	10 04 00	63	
319	51 15 00	10 21 06	45		416	50 40 00	10 55 30	71	
320 Mühlhausen-25	51 15 00	10 32 00	56		417	50 39 30	13 05 00	72	
321	51 14 06	10 27 18	79		418	50 39 30	13 05 00	35	
322 Allmenhausen-4	51 14 00	10 43 00	60		419	50 39 24	10 56 00	66	
323	51 13 42	11 07 06	63		420	50 39 18	12 54 42	82	
324	51 13 36	10 25 00	98		421 Fleischbach	50 38 33	08 18 09	66	92
325	51 13 12	10 41 30	52		422	50 37 54	12 52 30	95	
326 Hainich-Eigenrieden 4	51 13 00	10 16 00	91		423	50 37 54	13 11 48	68	
327 Hainich-Eigenrieden 2	51 13 00	10 17 30	108		424	50 37 48	13 11 30	64	
328 Mühlhausen-19	51 13 00	10 28 30	60		425	50 37 12	12 43 30	105	
329 Mühlhausen-4	51 13 00	10 32 00	39		426	50 37 06	12 49 24	31	
330 Allmenhausen-8	51 13 00	10 42 00	54		427	50 36 42	13 02 48	54	
331	51 13 00	10 42 30	54		428 Rheinbach	50 36 31	06 56 42	59	89
332 Kirchheilingen-20	51 12 30	10 38 00	46		429 Pechtelsgrün	50 35 30	12 24 30	60	
333	51 12 30	10 42 30	63		430 Georg	50 34 12	07 31 05	58	65
334 Griefstedt T 1	51 12 30	11 06 30	60		431	50 34 12	11 47 06	47	
335	51 12 18	10 40 00	63		432 Dreiborn	50 32 37	06 24 21	32	61
336 Mühlhausen-22	51 12 07	10 33 00	45		433 Schmiedefeld	50 32 30	11 13 00	52	
337	51 12 06	10 39 18	67		434	50 31 00	13 11 54	77	
338 Hainich-Eigenrieden 3	51 12 00	10 18 30	88		435	50 30 18	11 14 36	117	
339 Kirchheilingen-20	51 12 00	10 40 00	63		436	50 29 30	10 34 24	67	
340 Kirchheilingen-31	51 12 00	10 39 00	64		437	50 27 36	10 31 30	66	
341	51 11 30	10 43 30	58		438	50 25 54	12 06 48	75	
342 Kirchheilingen-34	51 10 30	10 42 30	82		439	50 25 54	12 29 30	65	
343 Hainich-Heyerode-1	51 10 00	10 20 00	67		440 Montabaur	50 25 52	07 50 43	52	81
344 Straußfurt-T2	51 09 30	10 58 00	67		441	50 25 48	12 07 00	50	
345 Altengottern-1	51 09 00	10 34 00	56		442	50 25 42	12 07 00	80	
346 Langensalza-18	51 09 00	10 38 30	79		443	50 25 30	12 06 00	87	
347 Roldisleben-1	51 09 00	11 18 00	33		444	50 25 30	12 39 06	92	
348	51 08 36	11 23 18	56		445 Schmidtheim	50 25 21	06 33 35	51	76
349	51 08 24	10 39 42	74		446	50 25 12	12 05 12	56	
350	51 08 24	11 13 42	57		447	50 25 06	12 05 24	82	
351	51 08 12	11 33 36	59		448	50 25 00	12 05 30	80	
352 Altengottern-2	51 08 00	10 34 30	51		449	50 25 00	12 06 30	86	

No. Location	Co-ordinates		Heat-Flow density	
	Lat. (N)	Long. (E)	without palaeo-cor.	incl. palaeo-cor.
450	50 24 54	12 05 18	57	
451 Laacher See	50 24 48	07 16 18	73	76
452	50 24 30	12 05 00	70	
453	50 24 30	12 07 30	80	
454	50 24 06	11 45 18	35	
455	50 24 06	12 06 00	70	
456 Hirzenhain	50 23 27	09 07 49	70	81
457	50 23 00	12 27 54	97	
458 Böß-Gesäß	50 22 42	09 16 06	73	84
459	50 22 00	12 28 24	76	
460 Ochtendung	50 21 33	07 22 09	62	68
461	50 21 18	12 29 00	57	
462 Wehrheim	50 18 18	08 35 16	31	56
463 Hillesheim	50 17 21	06 42 22	56	81
464	50 16 00	10 48 54	100	
465 Gemünder Maar	50 10 60	06 49 60	61	65
466 Weinfelder Maar	50 10 36	06 51 30	60	64
467 Bleidenstadt	50 08 34	08 08 46	47	70
468 Pulvermaar	50 08 00	06 55 30	61	66
469 Wießenstein	50 07 50	11 41 23	57	67
470 Wießenstadt	50 05 19	11 54 24	69	
471 Wülfersreuth	50 03 31	11 45 37	62	
472 Röthenbach	50 03 19	12 08 58	45	
473 Alexandersbad	50 00 43	12 00 55	59	77
474 Rheinböllen	49 59 56	07 40 30	64	96
475 Hardeck	49 58 18	12 26 24	76	
476 Neusorg	49 57 28	11 59 47	74	
477 Poppenreuth	49 55 00	12 27 19	58	
478 Wäldern	49 52 42	12 02 42	64	87
479 Griesbach	49 51 56	12 29 57	72	
480 Falkenberg	49 51 35	12 12 02	78	92
481 Kylltal	49 50 36	06 38 30	64	78
482 Morbach	49 48 48	07 06 27	54	85
483 Püllersreuth	49 47 15	12 08 04	58	
484 Hähnlein	49 46 24	08 34 12	69	72
485 Remmelbelg	49 40 20	12 16 07	63	
486 Eschenfelden	49 35 18	11 37 50	62	75
487 Nabburg	49 26 12	12 06 43	66	78
488 Marienschacht	49 24 30	12 10 54	72	85
489 Jungenwald	49 20 18	07 04 00	66	72
490 Netzbach	49 18 48	06 59 36	68	75
491 Landau 1	49 15 30	08 08 12	111	110
492 Landau 3	49 14 06	08 08 18	116	118
493 Landau 2	49 13 48	08 08 24	139	140
494 Maybach	49 10 00	07 04 60	59	65
495 Bruchsal GB2	49 07 35	08 34 06	110	110
496 Heuchelberg	49 06 48	09 04 53	102	115
497 Dinkelsbühl	49 02 10	10 22 42	82	93
498 Riedenburg	48 57 46	11 41 28	75	87
499 Nördlingen	48 53 27	10 30 42	73	78
500 Grafenau	48 51 18	13 23 52	76	86
501 Wörnitzostheim	48 50 07	10 38 20	81	101
502 Lorch	48 47 54	09 40 30	80	93
503 Oberreichenbach	48 43 48	08 40 00	70	84
504 Bühl 1	48 41 43	08 07 33	116	112
505 Wildbad T2	48 41 20	08 29 35	88	
506 Bad Teinach	48 40 54	08 39 36	72	96
507 Sachsenhausen	48 36 25	10 18 08	82	96
508 Urach 3	48 30 28	09 22 27	86	85
509 Missismühle	48 29 09	10 08 17	71	83
510 Griesbach	48 27 09	08 14 22	96	
511 Perterstal B1	48 26 06	08 12 54	105	
512 Tiefental	48 25 42	09 41 54	71	86
513 Berghaupten	48 24 53	07 58 45	89	
514 Gundershofen	48 22 30	09 37 12	78	95
515 Silberberg	48 20 11	08 20 32	103	
516 Donaustetten	48 20 01	09 56 02	88	97
517 Riegelsberg	48 17 43	09 13 46	89	
518 Hechtsberg	48 16 53	08 08 02	89	
519 Vulkan	48 15 54	08 06 51	82	
520 Schönmat	48 14 54	08 07 56	81	
521 Moosgrund	48 14 03	08 16 41	88	
522 Geschahse	48 12 32	08 05 45	77	
523 Bäratal	48 05 48	08 54 24	67	76
524 Waldkirch	48 05 10	07 56 34	72	
525 Hausen im Tal	48 04 54	09 02 06	70	88
526 Ettersbach	48 04 41	08 03 05	92	
527 Kunklerwald	48 01 38	07 59 16	71	
528 Saulgau	48 01 00	09 28 43	88	95
529 Ammersee	47 59 36	11 07 24	72	76
530 Kirchzarten	47 58 36	07 58 36	72	81
531 Stanberger See N.	47 57 12	11 20 42	97	101
532 Stanberger See M.	47 54 24	11 18 48	82	91
533 Feldsee	47 52 24	08 01 60	65	69
534 Buggingen	47 51 36	07 38 18	70	79
535 Starnberger See S.	47 51 06	11 19 30	82	87
536 Hegau	47 47 24	08 46 23	64	70
537 Peißenberg	47 47 24	11 03 24	79	79
538 Singen	47 45 01	08 49 34	69	80
539 Überlinger See	47 45 00	09 10 18	69	74
540 Schliersee	47 43 42	11 51 48	64	68
541 Bodensee 1	47 40 28	09 12 59	64	68
542 Bodensee 2	47 39 42	09 15 60	65	70
543 Bodensee 3	47 37 36	09 23 24	80	85
544 Walchensee	47 35 12	11 21 18	76	80
545 Aplssee	47 33 03	10 43 30	88	92
546 Bodensee 4	47 31 30	09 27 60	79	84

No. Location	Co-ordinates		Heat-Flow density	
	Lat. (N)	Long. (E)	without palaeo-cor.	incl. palaeo-cor.
547 Koenigssee	47 31 30	12 57 30	76	81
548 Bodensee 5	47 30 00	09 31 60	77	82
549 Bodensee 6	47 28 00	09 37 60	57	60

Greece

No. Location	Co-ordinates		Heat-Flow density	
	Lat. (N)	Long. (E)	without palaeo-cor.	incl. palaeo-cor.
1 Orestias 3	41 35 39	26 30 11	85	
2 Komotini 1	41 03 11	25 12 15	85	
3 Strimon 1	40 57 53	23 40 14	88	
4 Nestos 3	40 52 37	24 38 56	101	
5 Delta Evros 3	40 49 11	36 09 14	92	
6 Alexandria 1	40 41 29	22 06 09	65	
7 Agriosikia 1	40 40 52	22 18 40	65	
8 Aiginion 1	40 29 32	22 32 15	63	
9 Epanomi 2	40 23 37	22 57 25	84	
10 Neapolis 2	40 18 35	21 21 11	69	
11 Aegean Sea	40 15 08	25 16 04	90	
12 Aegean Sea	40 13 05	24 41 02	69	
13 Cassandra 2	40 06 25	23 33 56	81	
14 Loudias 1	40 04 54	22 34 48	81	
15 Posidi 1	39 58 17	23 23 09	92	
16 Aegean Sea	39 50 07	24 27 05	104	
17 Lavdani 2	39 49 42	20 29 42	50	
18 Dragopso 1	39 37 12	20 41 30	40	
19 Filiates 1	39 36 12	20 14 12	103	
20 Aegean Sea	39 35 04	23 53 00	65	
21 Agnatero 2	39 27 48	21 50 09	75	
22 Aegean Sea	39 24 02	23 32 00	52	
23 Almadar 4	39 20 54	22 12 06	196	
24 Anemorahi 2	39 18 06	26 06 54	58	
25 Archangelos 3	39 04 00	21 50 54	100	
26 Aegean Sea	38 56 03	25 27 02	75	
27 Astakos 1	38 36 30	21 07 36	70	
28 Aitolikon 1	38 30 12	21 22 54	59	
29 Aegean Sea	38 24 08	25 27 02	110	
30 LG-5 P. Rafti	37 51 12	24 01 18	59	
31 KG-8 Vari	37 50 12	23 50 00	158	
32 Alykes 1	37 50 00	20 46 30	73	
33 Peristeri 1	37 49 07	21 31 03	80	
34 Myrtia 1	37 42 10	21 21 32	84	
35 G-25 Samos	37 41 48	26 46 12	61	
36 Myrtoan Sea	37 06 00	23 49 07	114	
37 Ionian Sea	36 52 00	19 39 00	31	
38 M-2 Milos	36 42 45	24 30 07	625	
39 West Milos	36 41 00	24 24 00	150	
40 N-2 Nisiros	36 35 12	27 10 06	497	
41 Sea of Crete	35 56 07	25 06 07	77	
42 Mediterranean Sea	35 31 00	28 12 00	31	
43 K-3 Gravoussa	35 29 30	23 36 18	51	
44 EGM-7 Miloniana, Crete	35 27 48	23 56 42	52	
45 Mediterranean Sea	34 30 00	23 25 00	51	
46 Ionian Sea	34 29 00	20 04 00	33	
47 Mediterranean Sea	34 22 00	22 32 00	33	
48 Mediterranean Sea	34 19 00	27 11 00	10	
49 Mediterranean Sea	34 15 00	25 01 00	26	

High values from individual geothermal fields (e.g. Milos) are based on data from shallow boreholes.

Hungary

No. Location	Co-ordinates		Heat-Flow density	
	Lat. (N)	Long. (E)	without palaeo-cor.	incl. palaeo-cor.
1 Hidasnémeti-I	48 30 36	21 14 11	102	
2 Edelény (E-475)	48 18 00	20 46 00	131	
3 Recsk (Rm-8,Rm-15)	47 56 00	20 07 00	109	
4 Tiszapalkonya-1	47 51 59	21 03 13	114	
5 Szirák-2/a	47 48 29	19 33 21	84	
6 Detk-1	47 44 35	20 07 26	118	
7 B sárkány (B s-1)	47 41 41	17 15 41	83	
8 Szentendre (Sze-2)	47 40 56	19 05 00	84	
9 Hajdúszoboszló (Hsz-6)	47 32 12	21 21 47	108	
10 Kaba (K-É-1)	47 30 29	21 14 09	97	
11 Budapest (Népliget)	47 27 00	19 10 00	52	
12 Mikepércs-1	47 26 49	21 41 13	107	
13 Vál (Vál-3)	47 22 09	18 39 44	108	
14 Derecske-I	47 16 59	21 41 16	102	
15 Szombathely-II	47 13 00	16 36 14	108	
16 Kerkáskápolna-I	46 47 09	16 25 37	90	
17 Nagylengyel (NI-47,NI-62)	46 45 45	16 45 26	84	
18 Fábiansbestyén (Fáb-4)	46 41 39	20 27 15	97	
19 Bárszentmihályfa (Bm-I)	46 39 51	16 35 54	92	
20 Tótkomlós (T-I)	46 26 44	20 45 24	106	
21 Sándorfalva (S-I)	46 24 40	20 00 06	113	
22 Kiskunhalas (Kiha-4)	46 22 30	19 28 23	91	
23 Iharosberény-I	46 22 25	17 08 47	106	
24 Hódmez vásárhely (Hód-I)	46 21 16	20 25 46	82	
25 Komló-Zobák (mine-shaft)	46 11 00	18 14 00	138	

No. Location	Co-ordinates		Heat-Flow density mW/m ² without palaeo-cor.
	Lat. (N)	Long. (E)	
26 Hosszúhetény (mine-shaft)	46 10 00	18 22 00	104
27 K vágótöltés (MÉV-5065)	46 07 17	18 04 13	108
28 Bakonya (MÉV--2142/a)	46 06 00	18 04 00	103

Ireland

No. Location	Co-ordinates		Heat-Flow density mW/m ²	
	Lat. (N)	Long. (E)	without palaeo-cor.	incl. palaeo-cor.
1 Portmore	55 13	06 19	80	
2 Larne	54 51	05 49	59	
3 Ballymacilroy	54 47	06 20	59	
4 Barnesmore	54 43	07 57		69
5 Ballyshannon	54 34	08 06		75
6 Killary Glebe	54 33	06 41	60	
7 Annalong valley	54 09	05 45		87
8 Seefin quarry	54 08	05 55		84
9 Ballina	54 02	09 19	45	
10 Boyle	53 58	08 15		62
11 Navan	53 39	06 44	75	
12 Ballinalack	53 38	07 28	75	
13 Moate	53 27	07 41	70	
14 Clifden	53 27	10 01		59
15 Castlejordan	53 24	07 07	72	
16 Camus	53 22	09 35		65
17 Ros-a-Mhil	53 16	09 32		77
18 Eyrecourt	53 13	08 08	60	
19 Killimore	53 12	08 21	66	
20 Sally Gap	53 09	06 20		74
21 Tynagh	53 08	08 23	61	
22 Avoca	52 52	06 13	65	
23 Slieve Allaun	52 50	09 13	70	
24 Carlow	52 48	06 55		64
25 Sixmilebridge	52 46	08 48	57	
26 Courtbrown	52 38	08 59	58	
27 Rathkeale	52 30	09 00	52	

Latvia

No. Location	Co-ordinates		Heat-Flow density mW/m ² without palaeo-cor.
	Lat. (N)	Long. (E)	
1 1	56 24 05	23 46 03	81
2 3	56 13 13	25 35 12	32
3 4	56 32 53	25 26 08	37
4 6	56 59 09	21 21 33	26
5 11	56 57 12	21 42 25	16
6 45	56 38 34	21 02 44	22
7 48	56 39 00	21 17 02	10
8 53	56 25 53	21 00 06	66
9 57	56 22 09	21 05 29	75
10 63	56 17 22	20 59 25	66
11 66	56 38 30	21 24 56	41
12 68	56 14 01	21 06 47	77
13 100	56 25 37	21 50 25	42
14 111	56 25 21	22 19 54	18
15 115	56 36 53	23 03 51	26
16 126	56 48 20	23 23 04	42
17 130	56 52 59	23 04 52	24
18 142	57 35 25	21 53 49	16
19 150	57 22 08	22 36 57	25
20 151	57 22 45	22 35 45	23
21 152	56 57 44	26 26 54	28
22 156	57 27 11	22 53 36	21
23 160	57 15 11	25 10 06	67
24 161	57 25 21	21 35 12	20
25 162	57 25 20	21 35 43	23
26 163	57 25 25	21 35 19	27
27 166	56 49 46	23 56 08	48
28 170	56 49 13	23 55 48	47
29 172	56 49 34	23 56 16	47
30 177	56 47 32	23 54 34	46
31 197	56 28 47	21 11 28	53
32 198	56 22 23	20 58 41	65
33 202	56 58 16	23 33 37	43
34 204	56 56 32	23 30 21	44
35 206	56 58 44	23 49 03	59
36 208	56 57 40	23 47 16	58
37 211	56 52 41	23 37 08	47
38 214	57 00 55	23 29 55	38
39 216	57 44 55	24 24 21	30
40 217	57 34 12	24 26 08	27
41 219	57 49 59	24 44 34	22
42 220	57 08 04	24 16 24	39
43 221	57 05 20	24 13 39	42
44 236	57 50 12	24 43 56	26
45 238	56 19 45	21 18 40	64
46 245	57 14 34	24 39 31	55
47 268	57 24 27	26 53 52	35
48 269	57 12 10	25 38 48	40
49 270	56 39 24	25 07 21	57
50 275	56 27 29	26 03 13	53

No. Location	Co-ordinates		Heat-Flow density mW/m ² without palaeo-cor.
	Lat. (N)	Long. (E)	
51 279	56 33 42	27 45 09	28
52 282	57 00 51	25 28 10	40
53 298	56 32 41	26 23 31	27
54 312	56 56 44	27 43 29	42
55 349	57 37 30	22 23 46	20
56 371	56 30 27	20 59 47	53
57 372	56 41 05	22 30 58	29
58 380	56 35 12	21 51 23	30
59 383	56 28 53	23 10 46	53
60 385	56 29 54	24 05 01	64
61 390	56 31 34	22 55 06	31
62 391	56 48 14	23 36 11	59
63 392	56 24 45	24 15 04	55
64 393	56 33 04	23 47 14	71

Lithuania

No. Location	Co-ordinates		Heat-Flow density mW/m ² without palaeo-cor.
	Lat. (N)	Long. (E)	
1 Žemytė-1	56 10 39	21 19 36	72
2 Salantai-3	56 03 04	21 30 10	81
3 Pabalvė-1	56 00 46	22 36 12	65
4 Žutautai-1	55 49 31	21 32 03	69
5 Mamiai-1	55 54 42	21 37 31	72
6 Velaičiai-3	55 54 28	21 27 29	62
7 Šatrija-1	55 50 35	22 32 04	64
8 Kuliai-1	55 49 05	21 44 35	55
9 Laužai-1	55 48 22	21 58 55	54
10 Klaipėda-1	55 44 25	21 11 32	74
11 Drukšai-1	55 39 38	26 32 45	38
12 Gargždai-8	55 37 55	21 29 00	83
13 Baubliai-3	55 36 48	22 07 36	77
14 Gargždai-12	55 34 06	21 28 15	80
15 Pociiai-1	55 30 10	21 30 13	87
16 Šilalė-1	55 30 00	21 48 10	86
17 Maldūnai-1	55 29 06	22 33 16	75
18 Žviliai-1	55 29 03	22 12 42	93
19 Pajūris-1	55 27 28	22 06 53	94
20 Lašai-2	55 27 39	21 31 31	82
21 Gorainiai-1	55 24 56	21 57 40	88
22 Vainutas-1	55 21 44	21 57 54	83
23 Žalgiriai-1	55 18 42	21 25 30	76
24 Aukštupiai-149	55 17 32	22 03 56	90
25 Balninkai-1	55 17 00	25 17 00	40
26 Rusnė-1	55 16 12	21 18 24	67
27 Pramedžiuva-97	55 15 52	23 12 42	53
28 Pasaltuonis-94	55 15 40	22 37 03	56
29 Bebirva-111	55 14 53	22 50 53	56
30 Geluva-99	55 14 35	23 30 23	47
31 Graužai-105	55 13 00	23 52 08	40
32 Lauksargiai-1	55 09 20	22 07 08	65
33 Vepriai-1	55 07 00	24 41 00	32
34 Vepriai-2	55 06 00	24 32 00	32
35 Jurbarkas-36	55 05 35	22 46 00	70
36 Sutkai-86	55 00 58	23 20 34	53
37 Šakiai-42	54 55 18	22 47 40	46
38 Vilkaviškis-127	54 43 19	22 57 08	56
39 Vilnius-1	54 41 26	25 17 40	40
40 Marcinkonis-2	53 58 16	24 13 49	43

Poland

No. Location	Co-ordinates		Heat-Flow density mW/m ² without palaeo-cor.
	Lat. (N)	Long. (E)	
1 Zarnowiec IG-1	54 47	18 05	47
2 Bytów IG-1	54 17	17 36	33
3 Bartoszyce IG-1	54 14	20 57	34
4 Krzemionka-20	54 13	22 53	34
5 Udryń-4	54 13	22 57	34
6 Ustronie Morskie IG-1	54 11	15 46	52
7 Kętrzyn IG-1	54 10	21 03	24
8 Gościno IG-1	54 07	15 40	65
9 Grzybnica IG-1	54 03	16 31	41
10 Wolin IG-1	53 55	14 27	69
11 Olsztyn IG-1	53 52	20 00	40
12 Prabuty IG-1	53 47	19 13	41
13 Rokita IG-1	53 46	15 03	46
14 Oświno IG-1	53 45	15 24	54
15 Połczyn IG-1	53 45	16 05	51
16 Człuchów IG-1	53 43	17 20	45
17 Goleniów IG-1	53 41	14 30	73
18 Olszyny IG-1	53 33	21 05	28
19 Grudziądz IG-1	53 26	18 50	42
20 Nidzica IG-1	53 22	20 16	35
21 Zambrów IG-1	52 57	22 15	38
22 Wagrowice IG-1	52 47	17 12	45
23 Konary IG-1	52 44	18 27	91
24 Cykowo IG-1	52 38	18 21	85
25 Płońsk IG-2	52 35	20 27	41

No. Location	Co-ordinates		Heat-Flow density mW/m ² without palaeo-cor.
	Lat. (N)	Long. (W)	
26 Lochów IG-1	52 34	21 42	52
27 Wrotnów IG-1	52 30	22 08	41
28 Stadniki IG-1	52 29	22 44	48
29 Ośno IG-1	52 27	14 43	81
30 Siekierki Wielkie	52 22	17 09	49
31 Okuniew IG-1	52 17	21 18	90
32 Nadarzyn IG-1	52 05	20 51	64
33 Koło IG-4	52 01	19 02	69
34 Kock-5	51 56	22 24	51
35 Mszczonów IG-2	51 56	20 27	60
36 Wschowa-1	51 49	16 11	72
37 Izdebnó IG-1	51 46	21 34	37
38 Warka IG-1	51 43	21 03	45
39 Kock-7	51 37	22 20	50
40 Tyszowice IG-1	51 36	23 43	79
41 Dęblin-7	51 33	22 00	61
42 Kock-12	51 33	22 29	31
43 Ursynów-1	51 33	21 22	46
44 Lisów-1	51 31	21 10	62
45 Lubartów-1	51 26	22 40	45
46 Abramów-3	51 25	22 19	44
47 Abramów-5	51 25	22 30	38
48 Ostrzeszów 1	51 24	17 54	56
49 Abramów-8	51 22	22 31	54
50 Abramów-1	51 21	22 16	80
51 Lubin S 200	51 21	16 10	63
52 Łęczna-20	51 21	22 49	55
53 Bachus-1	51 20	23 17	79
54 Dorohucza IG-1	51 18	22 42	58
55 Łęczna IG-9	51 18	22 53	75
56 Ciepeliów IG-1	51 16	21 38	37
57 Świdniki-7	51 15	22 37	44
58 Minkowice-1	51 14	22 43	58
59 Zemborzyce-5	51 14	22 19	49
60 Polski 1	51 12	21 15	39
61 Zemborzyce-3	51 12	22 31	42
62 Więcki IG-1	51 05	18 53	66
63 Dankowice IG-1	50 25	18 48	49
64 Tomaszów Lub. IG-1	50 25	23 35	57
65 Zólcza 1	50 22	20 59	46
66 Łądec Zdrój	50 21	16 53	71
67 Sosnowiec IG-1	50 16	19 08	54
68 Orzesze 37	50 11	18 43	65
69 Zory 25	50 03	18 38	55
70 Leszczyna 3	50 01	20 23	60
71 Bzie-Dębina 3	49 56	18 40	74
72 Goczałkowice IG-1	49 56	18 58	58
73 Głogoczków IG-1	49 53	19 49	71
74 Siekierczyzna IG-1	49 46	20 52	65
75 Sucha Beskidzka 1	49 44	19 31	67
76 Łodygowice IG-	49 43	19 08	42
77 Cisowa IG-1	49 41	22 33	27
78 Jordanów IG-1	49 41	19 49	59
79 Kuźmina-1	49 36	22 26	54
80 Obidowa IG-1	49 33	19 59	54
81 Paszowa-1	49 32	22 25	56
82 Maruszyna IG-1	49 25	20 00	51
83 Bańska IG-1	49 24	20 01	60
84 Zakopane IG-1	49 18	19 58	56
85 Suche Rzeki IG-1	49 16	22 30	43

Portugal

No. Location	Co-ordinates		Heat-Flow density mW/m ² without palaeo-cor.
	Lat. (N)	Long. (W)	
1 S4A (m)	41 38 30	6 36 22	86
2 Cavala-4 (o)	41 30 51	9 05 18	77
3 5 A-1 (o)	41 08 02	9 07 45	71
4 ACCP5 (w)	40 44 57	8 39 54	42
5 ACCP4 (w)	40 44 40	8 39 57	42
6 Dourada-1 (o)	40 19 44	9 06 23	83
7 MP (m)	40 10 09	7 44 55	54
8 S7 (m)	40 09 48	8 05 38	85
9 S13 (m)	40 09 19	8 03 51	69
10 CP6 (m)	40 09 19	7 45 22	59
11 CP7 (m)	40 08 51	7 45 13	74
12 13 C-1 (o)	40 01 35	9 08 01	106
13 14 C-1A (o)	39 58 07	9 24 03	90
14 Faneca-1 (o)	39 54 00	9 15 52	78
15 16 A-1 (o)	39 43 01	9 18 09	79
16 17 C-1 (o)	39 25 00	9 22 00	83
17 Campelos-1 (o)	39 12 22	9 14 57	73
18 Benfeito-1 (o)	39 07 57	9 07 11	73
19 Sobral-1 (o)	38 57 28	9 11 39	87
20 Barreiro-4 (o)	38 39 00	9 02 44	73
21 TI54 (m)	38 33 56	8 04 21	53
22 TI14 (m)	38 31 54	8 04 19	64
23 Golfinho-1 (o)	38 20 35	8 57 12	90
24 C.D.1 (m)	38 08 48	8 32 54	75
25 Pescada -1 (o)	38 08 07	9 02 09	65
26 SDM10 (m)	38 07 42	7 26 03	56
27 SDM5 (m)	38 07 31	7 25 56	53
28 SDM8 (m)	38 07 26	7 25 47	52
29 SDSA2 (m)	37 59 10	7 09 45	80

No. Location	Co-ordinates		Heat-Flow density mW/m ² without palaeo-cor.
	Lat. (N)	Long. (W)	
30 SDSA3 (m)	37 59 09	7 09 53	77
31 FS26 (m)	37 52 15	8 08 27	66
32 FS25 (m)	37 51 25	8 09 13	73
33 CHI (m)	37 42 24	7 27 05	94
34 Castro Verde (m)	37 42 18	8 07 30	91
35 OT1 (m)	37 38 21	8 11 55	115
36 AL1 (m)	37 36 49	8 11 56	82
37 NG1 (m)	37 36 47	7 58 36	91
38 NE26 (m)	37 35 00	7 57 48	72
39 NE6 (m)	37 34 48	7 58 26	97
40 NE4 (m)	37 34 47	7 58 30	92
41 CVH1 (m)	37 33 08	7 53 24	80
42 VCI (m)	37 31 22	7 36 07	72
43 PN2 (m)	37 30 18	7 42 41	79
44 CST1 (o)	37 22 47	7 32 02	77
45 Algarve-1 (o)	36 59 04	7 33 59	73
46 Ruivo-1 (o)	36 53 11	8 11 29	63

m mining borehole
o oil borehole
w water borehole
,

Romania

No. Location	Co-ordinates		Heat-Flow density mW/m ² without palaeo-cor.	
	Lat. (N)	Long. (E)	without palaeo-cor.	incl. palaeo-cor.
1 Camirzana	48 08	23 24	126	101
2 14-CAM	48 01	23 21	104	82
3 601-NER	47 59	23 35	103	82
4 602-GHI	47 53	23 34	132	103
5 607-VBR	47 50	23 42	127	101
6 508-BSP	47 41	23 45	123	101
7 Mogosa	47 40	24 44	85	65
8 125-VRO	47 39	23 55	119	100
9 Cavnic	47 38	23 49	90	65
10 19-Rot	47 37	23 59	72	52
11 126-Rot	47 37	23 59	78	53
12 1F14	47 28	26 05	39	39
13 506-RAZ	47 26	23 49	74	53
14 111-RAZ	47 22	24 00	68	68
15 6-BRO	47 15	25 42	45	45
16 3F16	47 13	22 13	94	53
17 4135-BIS	47 08	24 30	58	58
18 4F12	47 08	26 25	43	43
19 531-BOR	47 07	21 49	70	50
20 532-BOR	47 07	21 49	61	50
21 4141-BEU	47 04	24 10	33	33
22 7F13	47 03	26 25	58	52
23 Zebrac	47 02	25 20	82	60
24 16-FIN	46 56	24 17	45	45
25 2-REMET	46 54	25 26	75	50
26 1-OCN	46 51	24 29	33	33
27 9-F15	46 49	27 09	39	39
28 10-SIL	46 47	24 18	30	30
29 1-CHI	46 41	24 53	33	33
30 281-BAL	46 40	25 47	57	57
31 12F10	46 37	26 29	47	47
32 2-FIE	46 36	25 30	77	50
33 1-MAG	46 34	24 55	39	39
34 15F19	46 31	24 45	74	50
35 16F11	46 30	26 40	54	54
36 1-NIC	46 29	24 33	29	29
37 21-ACA	46 29	24 38	31	31
38 39-SIN	46 25	24 51	50	50
39 30-IVO	46 24	25 26	113	100
40 2-VLA	46 21	25 31	104	100
41 MONEAS	46 20	22 09	75	50
42 33-SIN	46 18	25 44	73	50
43 18-PRO	46 16	24 39	30	30
44 20F18	46 15	25 44	83	50
45 1-DUM	46 13	24 35	26	26
46 21F21	46 12	21 20	85	85
47 22F20	46 09	22 53	79	50
48 1-H-Tus	46 09	25 52	118	100
49 16-AXS	46 07	24 10	41	41
50 347-VAR	46 01	20 58	65	65
51 10-BAR	46 00	24 55	46	46
52 11-BAR	46 00	24 55	46	46
53 50-SAN	45 56	20 54	64	64
54 519-SAN	45 55	20 54	65	65
55 1-TIM	45 45	21 14	50	50
56 Jitia	45 36	26 46	46	46
57 9-STIP	45 19	29 14	71	50
58 69012-STOE	45 18	25 15	47	47
59 7-LET	45 18	29 24	53	53
60 Izvoarele	45 17	26 01	59	59
61 Stipoc	45 16	29 11	75	75
62 11-C-A-R	45 15	29 30	66	66
63 Barbuncesti	45 13	26 38	39	39
64 24F02	45 11	26 19	48	39
65 61488-SOM	45 10	28 37	65	65
66 626-CIM	45 07	25 44	39	39
67 117-PAC	45 07	26 06	30	30
68 6-L-R	45 07	29 38	58	58

No. Location	Co-ordinates		Heat-Flow density	
	Lat. (N)	Long. (E)	without palaeo-cor.	incl. palaeo-cor.
98 Galanta, FGG-1	48 12 21	17 40 34	77	79
99 Kráľova pri Senci, FGS-1A	48 12 02	17 26 07	77	81
100 Kráľova pri Senci, VMK-1	48 12 02	17 26 08	77	84
101 Galanta, FGG-2	48 11 53	17 43 26	80	81
102 Galanta, FGG-3	48 11 29	17 42 51	79	81
103 Polny Kesov, BPK-1	48 10 10	18 03 53	70	77
104 Polny Kesov, BPK-2	48 10 10	18 03 54	70	77
105 Šal'a, HTS-1	48 09 39	17 52 10	74	80
106 Diakovce, D-1	48 08 06	17 47 07	77	79
107 Eliasovce, VZK-10	48 07 34	17 29 00	79	81
108 Podhajska, GRP-1	48 06 37	18 21 37	94	94
109 Tvrdošovce, FGTv-1	48 05 02	18 04 51	80	81
110 Rusovce, HGB-1	48 03 26	17 09 28	61	66
111 Zelizovce, HGZ-3	48 02 54	18 40 09	99	101
112 Lehnice, BL-1	48 02 52	17 27 25	79	82
113 Horná Potoň, FGHP-1	48 02 41	17 29 12	80	81
114 Horná Potoň, VHP-12-R	48 02 41	17 29 44	80	82
115 Vlčany, FGV-1	48 02 02	17 54 55	82	82
116 Dunajský Klatov, VDK-15	48 01 46	17 42 03	82	82
117 Cilistov, FGC-1	48 01 03	17 18 27	69	70
118 Nové Zámky, GNZ-1	47 59 59	18 11 02	81	84
119 Dvory nad Žitavou, FGDZ-1	47 59 40	18 15 22	83	83
120 Dunajská Streda, DS-1	47 59 08	17 37 04	83	84
121 Dunajská Streda, DS-2	47 59 06	17 36 43	84	86
122 Topolníky, FGT-1	47 58 37	17 47 27	90	90
123 Kolrovo, K-2	47 55 40	18 02 21	87	87
124 Bohelov, GPB-1	47 55 27	17 42 29	92	93
125 Svodín-Bruty, VTB-1	47 55 07	18 35 03	77	79
126 Gabčíkovo, FGGa-1	47 53 22	17 35 50	92	93
127 Topolovec, VTP-11	47 50 56	17 37 49	92	93
128 Čalovo, C-1	47 50 48	17 45 50	85	85
129 Modřany, MO-1	47 50 45	18 21 53	64	67
130 Cilizska Radvan, CR-1	47 49 38	17 41 35	86	86
131 Cilizska Radvan, VCR-16	47 49 38	17 41 05	88	89
132 Doln. Peter, PGT-11	47 49 19	18 11 25	73	75
133 Zemianska Olca, VZO-14	47 49 16	17 52 01	79	80
134 Marcelov, GTM-1	47 48 15	18 17 09	68	70
135 Ontopa, VZO-13	47 46 03	17 56 41	70	72
136 Komárno, FGK-1	47 45 45	18 04 19	67	70
137 Komárno, M-3	47 45 28	18 08 17	65	70

Slovenia

No. Location	Co-ordinates		Heat-Flow density	
	Lat. (N)	Long. (E)	without palaeo-cor.	incl. palaeo-cor.
1 Sredisce	46 46 04	16 19 44	107	109
2 Dankovci	46 45 17	16 10 59	150	158
3 Pecarovci	46 44 26	16 08 28	107	108
4 Podgorje-Cmurek	46 42 19	15 50 16	84	92
5 Moravci	46 40 59	16 13 36	100	108
6 Moravci	46 40 51	16 13 40	122	131
7 Sv. Martin	46 39 39	16 23 18	85	86
8 Murska Sobota	46 39 36	16 09 58	127	134
9 Murska Sobota	46 39 34	16 10 13	95	100
10 Somat	46 38 37	15 45 50	109	116
11 Benedikt	46 36 38	15 53 07	145	155
12 Hrastje-Mota	46 36 09	16 04 42	106	112
13 Doklezovje	46 35 44	16 11 10	107	107
14 Maribor	46 32 29	15 40 31	112	124
15 Petisovci	46 32 16	16 29 24	132	129
16 Maribor	46 32 09	15 41 25	112	115
17 Petisovci	46 31 56	16 27 45	87	85
18 Ljutomer	46 30 52	16 11 41	116	113
19 Murski gozd	46 29 56	16 31 36	93	93
20 Slovenj Gradec	46 29 41	15 05 03	89	97
21 Gabrnik	46 28 49	15 57 09	79	87
22 Karavanke Tunnel	46 28 05	14 00 05	30	43
23 Druzmirje	46 23 06	15 04 29	45	48
24 Druzmirje-Velenje	46 22 49	15 04 19	56	61
25 Zrece	46 22 22	15 23 11	67	79
26 Zrece	46 21 56	15 24 11	68	80
27 Zrece	46 21 18	15 24 40	83	94
28 Statenberg	46 19 23	15 40 47	50	67
29 Brdo pri Kranju	46 17 22	14 24 17	48	63
30 Zalec	46 15 23	15 09 48	56	64
31 Rogaska Slatina	46 14 55	15 35 41	67	77
32 Celje	46 14 31	15 13 41	45	55
33 Rogaska Slatina	46 13 44	15 38 31	68	72
34 Rogaska Slatina	46 13 26	15 38 52	85	100
35 Skofja Loka	46 10 30	14 17 06	75	103
36 Podcetrtek	46 09 56	15 36 37	138	147
37 Cerklje	46 07 41	13 59 34	48	52
38 Nadgorica-Ljubljana	46 05 21	14 34 04	87	94
39 Sentjakob-Ljubljana	46 05 16	14 35 30	82	100
40 Zirovski vrh,U.mine	46 04 34	14 09 14	34	44
41 Zirovski vrh,U.mine	46 04 33	14 09 12	27	37
42 Zirovski vrh	46 03 47	14 09 40	31	47
43 Prelesje	46 01 42	13 36 01	32	41
44 Brezovica	46 01 41	14 26 13	84	108
45 Curnovec	46 01 13	14 28 05	95	105
46 Curnovec	46 01 12	14 27 57	100	120
47 Debeli hrib Tunnel	46 00 34	14 34 14	37	50
48 Sv. Marko-Sempeter	45 55 45	13 39 29	44	54
49 Sempeter	45 55 19	13 38 14	28	35

No. Location	Co-ordinates		Heat-Flow density	
	Lat. (N)	Long. (E)	without palaeo-cor.	incl. palaeo-cor.
50 Drnovo	45 54 51	15 30 38	34	39
51 Catez - Mostec	45 53 57	15 37 54	182	184
52 Catez - Mostec	45 53 31	15 36 02	63	71
53 Kostanjevica	45 52 01	15 24 15	81	92
54 Sajevece	45 51 58	15 25 58	69	77
55 Kostanjevica	45 51 19	15 25 04	72	77
56 Sec-Kocevje	45 45 09	14 51 30	22	32
57 Osp	45 34 24	13 51 28	32	41
58 Kanizarica	45 32 59	15 10 43	21	30
59 Praproce	45 32 02	13 55 16	25	37
60 Rizana	45 31 44	13 53 19	31	41
61 Hrastovlje	45 31 07	13 54 18	42	47
62 Portoroz-Lucija	45 30 25	13 36 12	38	42
63 Dragonja	45 26 51	13 41 09	34	49
64 Dragonja	45 26 41	13 41 03	39	49

Spain

No. Location	Co-ordinates		Heat-Flow density	
	Lat. (N)	Long. (W)	without palaeo-cor.	incl. palaeo-cor.
1 Asturias D-2b	43 51 12	05 31 49	64	
2 Galicia B-2	43 42 58	06 33 11	63	
3 Mar Cantabrico C-5	43 40 29	05 02 59	77	
4 Vizcaya B-2	43 33 41	02 52 20	67	
5 Golfo de Vizcaya-1	43 31 55	01 55 30	60	
6 Mar Cantabrico E-1	43 30 07	04 26 28	51	
7 Caldones-1	43 28 45	05 37 44	63	
8 Ajo-1	43 27 14	03 34 37	48	
9 Liermo-1	43 26 12	03 37 48	64	
10 Vizcaya C-2	43 25 26	02 33 01	72	
11 Ancillo-1	43 15 04	03 30 18	63	
12 Vivanco	43 05 40	03 22 16	60	
13 La Eñana	43 04 56	03 44 25	66	
14 Espinosa CB-1	43 03 03	03 33 24	51	
15 Ribero-1	43 01 59	03 28 59	65	
16 Ribero-2	43 01 51	03 29 01	79	
17 Rozas-2	43 01 48	03 43 54	76	
18 Espinosa CB-2	43 01 28	03 34 03	69	
19 Arco Iris-1	43 00 56	03 42 50	157	
20 Arija Sur-1	42 58 36	03 57 37	67	
21 Navajo-1	42 57 00	03 43 26	66	
22 Mazanedo-1	42 54 20	03 37 42	72	
23 Boveda-1 bis	42 54 14	03 12 34	62	
24 La Hoz-2	42 53 45	03 14 36	68	
25 Osmo-1	42 53 34	03 04 00	76	
26 Marinda-1	42 52 25	02 56 06	68	
27 Pamplona-6	42 50 55	01 36 48	55	
28 Aoiz-1	42 50 45	01 24 47	72	
29 Castillo-3	42 49 08	02 40 43	68	
30 Castillo-5	42 48 14	02 43 45	65	
31 Polientes-2	42 48 13	03 49 21	63	
32 Polientes-1	42 47 56	03 49 26	67	
33 Pamplona-5	42 47 36	01 40 27	78	
34 Roncal	42 46 40	00 57 47	55	
35 Escalada-1	42 46 38	03 47 46	59	
36 Astrain-1	42 46 31	01 44 17	55	
37 Huidobro-1	42 46 06	03 41 16	94	
38 Peña-1	42 46 00	04 31 21	41	
39 Treviño-4	42 44 32	02 43 27	73	
40 Rioja-3	42 43 27	02 41 12	59	
41 Tozo-4	42 41 58	03 57 11	74	
42 Valle de Allin-1	42 41 56	02 05 23	97	
43 Tozo-1	42 41 52	03 57 10	75	
44 Tozo-5	42 41 43	03 37 26	70	
45 Sal-2	42 40 00	03 33 40	60	
46 Sal-1	42 40 00	03 35 11	62	
47 Urbel-1	42 39 44	03 54 30	56	
48 Lagran-1	42 38 44	02 34 16	53	
49 Alcozar-1	42 37 52	03 21 19	59	
50 Pino-1	42 37 42	03 49 39	67	
51 Vilanovilla	42 37 00	00 29 14	71	
52 Castillo-4	42 36 52	02 38 41	45	
53 Broto-1	42 35 37	00 07 31	140	
54 Hontomin-2	42 35 08	03 38 36	67	
55 Rojas NE-1	42 34 03	03 25 13	57	
56 Rojas-1	42 33 16	03 27 03	58	
57 Valdearnedo-1	42 33 11	03 33 16	69	
58 Hontomin S -1	42 32 45	03 42 33	80	
59 Hontomin S -2	42 32 29	03 42 17	79	
60 Villameriel-1	42 31 05	04 26 53	63	
61 Rioja-4	42 24 56	02 40 60	58	
62 Rioja-1	42 24 06	02 50 13	68	
63 Rioja-2	42 23 37	02 51 08	65	
64 Campanue-1	42 21 38	00 20 55	59	
65 Villalonquejar	42 21 38	03 45 56	69	
66 Marcilla-1	42 20 21	01 42 32	79	
67 Demanda-1	42 18 43	02 55 45	57	
68 Erinyá -1	42 17 39	00 56 21	68	
69 Centenera-2	42 17 37	00 23 32	57	
70 Centenera-1	42 17 16	00 24 31	46	
71 Tamurcia-1	42 16 46	00 45 18	65	
72 Cajigar-1	42 16 08	00 36 56	61	
73 Graus-1	42 14 24	00 20 59	69	

No. Location	Co-ordinates		Heat-Flow density mW/m ² without palaeo-cor.	No. Location	Co-ordinates		Heat-Flow density mW/m ² without palaeo-cor.
	Lat. (N)	Long. (W)			Lat. (N)	Long. (W)	
74 Santa Creu-1	42 14 20	00 26 57	59	171 Palancares-1	37 19 13	06 12 21	87
75 Pontevedra B-1	42 12 55	09 17 25	60	172 Marismas C-1	37 18 19	06 11 19	62
76 Sant Corneli-1	42 12 06	01 00 36	46	173 Almonte-1	37 15 50	06 28 20	50
77 Arnedo-1	42 12 02	02 03 36	69	174 Villamanrique-1	37 14 02	06 18 31	69
78 Riudaura-2	42 11 30	02 23 37	67	175 Casa Nieves-1	37 11 35	06 19 08	63
79 Boixols-1	42 11 07	01 08 04	44	176 Huelva-1	37 10 42	06 46 59	92
80 Ebro-3	42 11 03	00 03 05	57	177 Isla Mayor-1	37 09 33	06 08 49	60
81 Riudaura-1	42 10 55	02 23 47	79	178 Moguer-1	37 09 21	06 48 03	59
82 Huesca-1	42 08 08	00 06 57	53	179 Marisma A-1	37 05 30	06 34 21	62
83 Isona-1 bis	42 07 52	01 09 33	51	180 Asperillo-1	37 04 43	06 38 51	59
84 Valpalmas-1	42 07 26	00 54 22	70	181 Sapó-1	37 03 53	06 12 31	37
85 Ejea-1	42 07 15	01 15 03	85	182 Betica 14-1	37 01 19	06 08 14	60
86 Tolva-1	42 06 40	00 31 24	71	183 Atlantida	36 59 25	07 11 56	37
87 Beranbarre-1	42 06 16	00 26 42	64	184 Cadiz C-5	36 58 42	07 01 56	54
88 Jabali-1	42 03 51	01 52 50	67	185 Bornos-1	36 50 13	05 45 09	59
89 Rio Franco-1	41 59 07	04 03 07	59	186 Golfo de Cadiz 6-X	36 50 02	07 12 33	53
90 Tauste Este 1	41 58 23	01 03 27	74	187 Betica 18-1	36 46 47	06 00 03	51
91 Castilfrio	41 56 42	02 18 18	60	188 Cabo de Gata-1	36 45 49	02 12 21	84
92 Monzon-1	41 53 44	00 13 15	57	189 Golfo de Cadiz 6-Y 1	36 42 23	07 03 39	55
93 Zuera-1	41 49 46	00 51 18	79	190 Roquetas-1	36 41 16	02 43 54	65
94 Don Juan-1	41 49 09	04 04 45	53	191 Cadiz G-1	36 38 29	06 39 44	45
95 Magallon-1	41 48 07	01 28 22	43	192 Alboran A-1	36 37 56	04 12 31	63
96 Sariñera-1	41 47 29	00 05 22	71	193 Andalucía A-1	36 36 04	02 44 04	92
97 Rosas 2-1	41 47 28	03 11 45	71	194 Neptuno-2	36 28 45	06 26 21	49
98 Esplus-1	41 47 22	00 18 31	65	195 Andalucía G-1	36 23 48	04 45 09	37
99 Aldehuela-1	41 46 10	02 43 39	60	196 Cerro Gordo-2	36 22 10	05 23 21	35
100 La Cuenca-1	41 44 34	02 44 40	97	197 Cerro Gordo-1	36 21 20	05 21 30	31
101 Ucero-1	41 43 16	02 59 29	263	198 Cerro Gordo-3	36 21 15	05 19 59	45
102 Lerida-1	41 39 49	00 36 52	54	199 Almarchal	36 08 45	05 48 11	33
103 Quintana Redonda-1	41 39 01	02 33 14	74	200 Iberian Massif	43 27 04	06 50 07	42
104 Ebro-2	41 38 39	00 06 24	74	201	43 24 28	05 50 17	35
105 Mayals-1	41 30 17	00 32 19	84	202	43 18 38	04 35 27	36
106 Martorell-1	41 29 48	01 50 37	63	203	43 14 50	05 53 08	47
107 Gormaz-1	41 29 22	03 03 05	30	204	43 12 00	05 59 18	47
108 Calella C-1	41 26 34	02 22 25 (E)	82	205	42 51 43	05 36 22	48
109 Ebro-1	41 22 56	00 10 18	77	206	42 14 15	08 27 41	81
110 El Gredal-1	41 22 21	02 29 37	84	207	42 13 45	08 28 07	151
111 Lopin-1	41 21 00	00 34 44	88	208	42 13 45	08 28 07	146
112 Barcelona M-A1	41 12 38	02 20 02	80	209	40 37 43	06 37 14	44
113 Caspe-1	41 10 29	00 06 36	69	210	40 37 42	06 37 25	44
114 Garraf-2	41 09 58	01 50 08	50	211	40 37 38	06 37 25	62
115 Barcelona G-1	41 07 10	02 11 50 (E)	93	212	40 37 29	06 37 42	55
116 Reus-1	41 06 58	01 05 39	43	213	37 46 49	06 50 50	75
117 Baidés-1	40 59 48	02 48 56	95	214	37 46 43	06 57 48	58
118 Tarragona D-2	40 59 37	01 32 51	74	215	37 41 25	07 19 48	72
119 Tarragona C-2	40 55 06	01 02 33 (E)	69	216	37 40 25	05 49 50	66
120 Tarragona E-8	40 52 44	01 19 25	37	217	37 36 28	06 50 14	69
121 Santa Barbara-A	40 49 41	02 47 12	73	218	37 34 16	06 01 48	47
122 Delta del Ebro-1	40 43 52	00 48 35	90	219	37 33 31	06 46 32	65
123 Pulpo-1	40 43 30	01 15 53	84	220	37 32 39	06 51 06	93
124 Casablanca-2	40 42 18	01 22 17	81	221	37 31 26	06 13 23	106
125 Sardina-1	40 41 21	01 07 11	91	222	37 25 07	06 37 16	77
126 Montanazo D-3	40 40 58	01 29 06	71	223 Tertiary Galicia basin	43 24 59	07 52 00	72
127 San Carlos-1	40 40 49	00 40 14	69	224	43 23 43	07 54 51	86
128 Amposta-1	40 39 26	00 46 31	87	225	43 23 36	07 53 35	97
129 Mirambell	40 36 50	00 26 33	66	226	43 22 45	07 51 23	94
130 Tres Cantos	40 35 06	03 42 21	78	227	43 22 28	07 51 39	124
131 Pradillo-1	40 34 24	03 35 12	88	228	42 08 07	07 40 48	146
132 San Sebastian de L. R.	40 33 34	03 37 24	70	229	42 05 13	07 43 54	154
133 Alcanar-1A	40 32 44	00 44 45	64	230 Mesoz.-Tert. Asturian	43 25 60	05 44 45	48
134 Delta E-3	40 27 54	00 45 54 (E)	79	231	43 25 29	05 48 22	48
135 Maestrazgo-1	40 27 24	00 20 14	52	232	43 23 23	05 43 14	67
136 Vinaroz-3	40 24 20	00 33 20	59	233	43 23 10	05 45 49	70
137 Maestrazgo-2	40 24 05	00 27 43	65	234 Duero basin	42 27 52	04 58 25	41
138 Salsadella-1	40 23 08	00 10 19	92	235	42 25 12	05 42 24	80
139 Castellon D-2	40 21 40	00 56 23	83	236	42 23 03	05 07 25	79
140 Rapita-1	40 21 14	01 21 02	56	237	42 21 49	05 08 39	42
141 Castellon-3	40 18 57	00 39 08	75	238	41 07 06	04 01 11	57
142 Torralba-1	40 18 19	02 15 52	64	239	41 01 00	04 22 25	103
143 Tielmes-1	40 14 58	03 18 07	62	240 Guadalquivir basin	37 31 52	06 08 35	29
144 Castellon G-1	40 13 01	00 50 38	88	241	37 31 40	05 58 42	88
145 Benicarlo C-1	40 05 04	01 05 37	72	242	37 30 41	06 07 28	126
146 Castellon L-1	39 53 41	00 23 55	75	243	37 29 20	06 05 20	29
147 San Lorenzo de la P.	39 51 50	02 21 28	62	244	37 24 33	06 32 24	171
148 Columbretes A-1	39 39 21	00 34 49	76	245	37 01 12	06 08 30	81
149 Cabriel B2-A	39 34 24	01 11 01	96	246 Osona	42 02 31	02 06 52 (E)	83
150 Valencia 3-1	39 28 08	00 06 34	79	247	42 01 58	02 17 16 (E)	81
151 Perenchiza-1	39 26 32	00 34 12	74	248	42 00 40	02 18 07 (E)	65
152 Ledaña-1	39 19 32	01 43 13	69	249	41 59 47	02 17 05 (E)	92
153 Ibiza Marino AN-1	39 11 35	00 48 07	104	250	41 59 34	02 18 19 (E)	100
154 Carcelen-1	39 05 16	01 18 12	68	251	41 57 06	02 09 07 (E)	110
155 Jaraco-1	39 01 37	00 14 25	89	252	41 57 03	02 19 06 (E)	59
156 Denia-1	39 00 18	00 04 37	54	253	41 56 12	02 16 11 (E)	137
157 Tribaldos-1	38 58 29	02 56 45	68	254	41 55 46	02 16 04 (E)	122
158 Salobral-1	38 52 10	01 42 11	72	255	41 55 36	02 18 53 (E)	109
159 Javea-1	38 42 08	00 21 24	61	256	41 54 30	02 13 29 (E)	65
160 Alicante A-1	38 27 40	00 13 08	66	257	41 54 27	02 18 03 (E)	143
161 Alicante MU-1	38 26 59	00 19 34	80	258	41 54 25	02 12 50 (E)	60
162 Sierra Larga-1	38 22 38	01 22 01	60	259	41 54 18	02 15 07 (E)	87
163 Socovos-2	38 17 53	02 01 17	71	260	41 54 05	02 19 29 (E)	70
164 San Miguel-2	37 58 27	00 47 22	72	261	41 51 57	02 16 07 (E)	265
165 Fuensanta-1	37 40 15	03 52 49	50	262	41 51 57	02 16 10 (E)	42
166 Nueva Carteya-1	37 35 57	04 23 37	53	263	41 50 25	02 12 07 (E)	95
167 Cordoba A-3	37 35 03	05 26 56	110	264	41 50 24	02 12 23 (E)	95
168 Sevilla-3	37 30 29	05 39 11	119	265	41 48 01	02 13 14 (E)	94
169 Sevilla-1	37 29 54	05 43 09	91	266 Balearic islands	39 58 12	04 08 19 (E)	46
170 Castilleja de la C.	37 23 20	06 03 43	70	267	39 57 49	03 51 00 (E)	92

No. Location	Co-ordinates		Heat-Flow density	No. Location	Co-ordinates		Heat-Flow density
	Lat. (N)	Long. (W)	mW/m ² without palaeo-cor.		Lat. (N)	Long. (W)	mW/m ² without palaeo-cor.
268	39 57 41	04 03 34 (E)	65	365	39 31 35	00 33 36 (E)	84
269	39 56 33	03 50 02 (E)	80	366	39 31 14	00 34 02 (E)	83
270	39 50 48	04 16 57 (E)	74	367	39 30 57	00 34 11 (E)	85
271	39 46 26	02 59 09 (E)	32	368	39 30 33	00 34 26 (E)	85
272	39 42 45	03 02 59 (E)	24	369	39 29 58	00 34 52 (E)	89
273	39 42 02	02 58 36 (E)	24	370	39 29 26	00 35 18 (E)	90
274	39 41 52	02 54 52 (E)	51	371	39 29 10	00 35 33 (E)	91
275	39 41 41	03 12 02 (E)	35	372	39 28 58	00 36 10 (E)	91
276	39 41 24	03 11 39 (E)	34	373	39 28 17	00 36 40 (E)	93
277	39 38 46	02 42 26 (E)	77	374	39 28 10	00 36 47 (E)	93
278	39 35 05	02 45 23 (E)	83	375	39 27 41	00 36 40 (E)	95
279	39 34 35	02 47 08 (E)	88	376	39 27 19	00 37 00 (E)	94
280	39 34 16	02 49 01 (E)	82	377	39 26 54	00 37 26 (E)	94
281	39 30 55	03 07 50 (E)	44	378	39 22 19	00 41 32 (E)	86
282	39 26 58	02 51 46 (E)	78	379	39 21 57	00 41 42 (E)	84
283	39 23 10	03 00 35 (E)	66	380	39 21 32	00 42 10 (E)	82
284 Valencia trough	41 16 35	04 20 05 (E)	73	381	39 20 47	00 42 32 (E)	86
285	41 14 56	03 31 55 (E)	66	382	39 20 33	00 42 40 (E)	86
286	41 12 18	03 31 55 (E)	66	383	39 20 23	00 43 04 (E)	86
287	41 10 01	03 31 36 (E)	68	384	39 19 49	00 43 29 (E)	88
288	41 08 00	03 31 25 (E)	66	385	39 19 21	00 43 54 (E)	88
289	41 06 30	03 31 32 (E)	68	386	39 12 17	00 49 21 (E)	77
290	41 04 35	03 31 14 (E)	64	387	39 11 09	00 50 25 (E)	79
291	41 04 30	02 17 04 (E)	63	388	39 10 26	00 50 51 (E)	78
292	41 03 14	02 15 51 (E)	73	389	39 09 26	00 51 29 (E)	77
293	41 01 59	02 14 29 (E)	79	390	39 08 36	00 52 05 (E)	78
294	41 00 43	02 13 36 (E)	80	391	39 07 52	00 52 41 (E)	77
295	41 00 10	03 31 01 (E)	67	392	39 07 00	00 53 17 (E)	68
296	40 59 10	02 12 12 (E)	104	393	39 06 01	00 53 55 (E)	62
297	40 58 17	02 12 23 (E)	90	394 Alboran Sea	36 31 30	03 14 42	80
298	40 57 21	03 31 10 (E)	76	395	36 27 54	03 15 47	113
299	40 56 47	02 12 34 (E)	82	396	36 25 23	04 26 49	42
300	40 55 32	03 31 07 (E)	60	397	36 24 18	03 16 59	130
301	40 55 28	02 12 38 (E)	79	398	36 23 24	03 18 18	120
302	40 53 51	02 13 02 (E)	79	399	36 22 59	04 25 19	46
303	40 52 20	02 13 12 (E)	72	400	36 20 49	04 23 42	40
304	40 51 12	02 14 00 (E)	71	401	36 19 37	03 18 07	130
305	40 50 16	02 14 16 (E)	69	402	36 18 25	04 20 35	59
306	40 49 58	03 30 35 (E)	64	403	36 18 11	01 45 36	137
307	40 48 48	02 14 41 (E)	64	404	36 18 07	01 19 41	104
308	40 47 11	02 14 50 (E)	64	405	36 18 07	02 02 24	115
309	40 46 59	03 30 19 (E)	63	406	36 17 60	01 25 55	111
310	40 45 48	02 15 23 (E)	69	407	36 17 60	01 32 49	120
311	40 43 39	03 29 54 (E)	61	408	36 17 60	01 59 06	121
312	40 42 49	02 16 02 (E)	73	409	36 17 53	01 52 19	128
313	40 42 13	02 16 60 (E)	76	410	36 17 49	01 06 00	129
314	40 42 01	03 30 02 (E)	51	411	36 17 49	01 29 17	121
315	40 40 57	02 18 08 (E)	78	412	36 17 49	01 39 11	120
316	40 40 54	02 18 13 (E)	88	413	36 17 49	01 55 48	124
317	40 40 42	02 18 21 (E)	78	414	36 17 31	01 11 24	115
318	40 40 31	02 18 32 (E)	85	415	36 16 12	04 19 30	72
319	40 40 21	02 18 49 (E)	96	416	36 16 05	04 53 13	31
320	40 40 20	02 16 07 (E)	114	417	36 15 00	04 18 54	81
321	40 40 05	02 18 52 (E)	105	418	36 14 53	02 04 05	112
322	40 39 53	02 19 18 (E)	101	419	36 14 49	02 23 24	124
323	40 39 41	02 18 59 (E)	87	420	36 14 31	04 52 37	34
324	40 39 28	03 29 58 (E)	37	421	36 14 17	04 19 37	84
325	40 39 27	02 19 21 (E)	87	422	36 13 30	02 30 00	110
326	40 39 14	02 19 22 (E)	93	423	36 13 30	03 20 35	208
327	40 39 02	02 19 33 (E)	86	424	36 13 23	02 02 31	105
328	40 38 48	02 19 45 (E)	86	425	36 12 29	04 19 19	103
329	40 38 36	02 20 02 (E)	83	426	36 12 18	02 36 11	133
330	40 38 33	02 20 21 (E)	72	427	36 12 11	04 51 11	33
331	40 38 30	02 20 17 (E)	75	428	36 12 07	02 01 23	97
332	40 37 08	02 21 45 (E)	71	429	36 11 42	03 20 53	254
333	40 37 01	03 30 03 (E)	17	430	36 11 35	04 20 60	92
334	40 35 54	02 22 50 (E)	82	431	36 11 31	02 39 18	123
335	40 34 46	02 23 39 (E)	83	432	36 10 55	04 19 01	123
336	40 34 19	03 29 43 (E)	-2	433	36 10 48	04 16 59	106
337	40 34 12	03 29 49 (E)	-1	434	36 10 41	02 42 43	119
338	40 31 37	03 30 06 (E)	-4	435	36 09 47	04 49 55	38
339	40 25 46	02 23 25 (E)	80	436	36 09 11	04 18 29	104
340	40 25 10	02 23 17 (E)	72	437	36 07 12	04 48 11	38
341	40 24 43	02 23 03 (E)	69	438	36 06 29	04 19 30	78
342	40 24 32	02 22 47 (E)	71	439	36 04 23	03 58 30	100
343	40 24 18	02 22 54 (E)	72	440	36 04 19	04 01 23	97
344	40 23 09	02 23 37 (E)	62	441	36 04 19	04 47 24	37
345	40 21 37	02 24 14 (E)	57	442	36 04 01	04 04 19	92
346	40 20 06	02 24 41 (E)	54	443	36 04 01	04 07 59	90
347	40 18 38	02 25 08 (E)	77	444	36 04 01	04 44 53	52
348	40 17 32	02 25 10 (E)	76	445	36 03 47	04 10 59	89
349	40 17 21	02 25 49 (E)	48	446	36 03 43	03 55 12	116
350	40 16 25	02 26 03 (E)	63	447	36 03 43	04 21 07	92
351	40 15 39	02 26 17 (E)	71	448	36 03 43	04 27 43	79
352	40 14 18	02 26 59 (E)	73	449	36 03 43	04 31 12	63
353	40 13 21	02 27 13 (E)	70	450	36 03 43	04 41 06	50
354	40 12 31	02 27 50 (E)	49	451	36 03 36	04 14 13	73
355	40 11 32	02 28 12 (E)	48	452	36 03 36	04 17 42	79
356	40 10 36	02 28 36 (E)	44	453	36 03 25	04 34 23	59
357	40 09 26	02 28 57 (E)	58	454	36 03 25	04 38 06	54
358	40 03 13	01 36 55 (E)	78	455	36 03 25	04 48 36	39
359	40 01 34	01 37 45 (E)	72	456	36 03 18	04 23 42	95
360	39 59 54	01 39 03	69	457	36 02 31	04 20 35	98
361	39 58 09	01 40 18	68	458	36 00 54	02 37 55	110
362	39 56 05	01 41 33	77	459	36 00 29	04 20 24	97
363	39 54 50	01 42 12	73	460	35 58 55	02 40 05	126
364	39 52 43	01 45 14	104	461	35 58 41	04 37 55	53

No. Location	Co-ordinates		Heat-Flow density mW/m ² without palaeo-cor.
	Lat. (N)	Long. (W)	
462	35 57 36	04 20 53	76
463	35 57 29	02 42 47	124
464	35 57 11	04 40 30	53
465	35 55 59	02 45 29	108
466	35 55 55	04 43 05	51
467	35 54 43	04 20 60	79
468	35 54 29	04 46 05	48
469	35 53 13	02 45 47	113
470	35 52 59	01 59 53	116
471	35 52 48	04 48 43	54
472	35 52 23	01 55 59	115
473	35 52 12	04 20 60	78
474	35 51 00	04 51 36	43
475	35 50 17	02 45 29	120
476	35 49 30	04 21 29	71
477	35 49 23	04 54 47	45
478	35 48 11	04 57 25	51
479	35 47 13	04 21 11	74
480	35 46 19	05 00 25	63
481	35 44 06	04 21 07	71
482	35 43 01	03 12 11	118
483	35 42 00	03 16 37	140
484	35 41 42	04 20 60	70
485	35 40 59	03 21 11	125
486	35 40 37	03 19 12	119
487	35 38 60	04 21 18	69
488	35 38 31	03 22 59	114
489	35 37 12	03 25 30	111
490	35 34 59	03 19 01	117
491	35 32 60	03 19 01	153
492 Atlantic margin	42 10 12	12 05 36	37
493	42 09 42	12 50 12	40
494	42 09 36	12 39 00	38
495	42 08 60	13 33 00	43
496	42 08 54	12 08 12	48
497	42 08 54	12 18 00	35
498	42 08 48	12 24 06	36
499	42 08 48	12 42 48	42
500	42 08 42	12 04 54	39
501	42 08 42	12 10 12	72
502	42 08 42	13 08 42	48
503	42 08 30	13 18 42	40
504	42 08 24	11 55 30	32
505	42 08 06	12 31 12	45
506	42 07 54	11 58 00	30
507	42 07 42	13 02 06	46
508	40 59 43	13 10 25	72
509	40 59 11	13 10 43	61
510	40 59 08	13 06 49	46
511	40 59 03	13 09 09	69
512	40 57 48	12 53 20	48
513	40 50 45	12 24 13	52
514	40 50 20	12 28 26	53
515	40 41 39	11 17 41	55
516	40 41 28	11 48 13	52
517	40 41 11	11 46 13	50
518	40 41 06	11 40 25	51
519	40 41 06	12 07 26	49
520	40 41 05	11 44 17	37
521	40 41 01	11 35 54	56
522	40 40 60	10 45 00	45
523	40 40 60	11 36 16	59
524	40 40 59	11 41 60	50
525	40 40 56	11 36 53	69
526	40 40 56	11 50 01	54
527	40 40 54	11 31 53	57
528	40 40 43	11 52 11	48
529	40 40 39	11 03 13	46
530	40 40 35	11 04 32	60
531	40 40 34	11 16 52	46
532	40 40 29	11 12 39	44
533	40 40 29	11 15 35	48
534	40 40 27	11 03 35	39
535	40 40 26	11 06 05	49
536	40 40 25	11 07 11	40
537	40 40 22	11 10 09	42
538	40 40 21	11 08 52	41
539	40 40 18	11 14 31	45
540	40 40 16	11 11 28	41
541	39 36 00	12 13 00	44
542	36 38 60	17 21 00	48
543	35 58 60	09 58 60	36
544	35 38 60	13 43 00	58
545	35 38 30	13 42 30	58
546	35 27 06	12 59 54	62
547	35 19 36	14 03 18	50
548	34 06 00	14 24 00	39
549	34 00 00	15 50 60	24
550 Balearic basin	40 05 48	04 51 48 (E)	98
551	40 04 36	04 51 24 (E)	117
552	40 03 48	04 51 30 (E)	116
553	40 03 36	04 58 48 (E)	79
554	40 02 54	05 00 42 (E)	97
555	40 02 48	04 52 06 (E)	110
556	40 02 36	04 54 54 (E)	82
557	40 02 36	04 57 42 (E)	79
558	40 02 30	04 56 06 (E)	85

No. Location	Co-ordinates		Heat-Flow density mW/m ² without palaeo-cor.
	Lat. (N)	Long. (W)	
559	40 02 24	04 52 54 (E)	82
560	40 01 36	04 53 36 (E)	82
561	40 00 24	04 54 00 (E)	86
562 DSDP372	40 01 53	04 46 52 (E)	102

Sweden

No. Location	Co-ordinates		Heat-Flow density mW/m ² without palaeo-cor.
	Lat. (N)	Long. (E)	
1 Smygehuk 1	55 18 16	13 02 58	52
2 Trelleborg 1	55 22 12	13 11 32	55
3 Hammarlöv 1	55 22 52	13 05 31	56
4 Maglarp 1	55 23 14	13 03 51	62
5 Hammar 1	55 23 37	14 02 49	116
6 Ljunghusen 1	55 23 37	12 54 48	84
7 Höllviksnäs	55 24 32	12 56 23	64
8 Kungstorp 1	55 26 16	12 58 59	52
9 Häslöv 1	55 26 33	13 03 11	68
10 Köpingsberg 1	55 26 50	13 58 18	57
11 Köpingsberg 3	55 27 00	13 58 37	38
12 Eskiltorp 1	55 28 57	13 02 05	59
13 Svedala 1	55 30 35	13 13 59	53
14 Mossheddinge 1	55 36 54	13 18 21	34
15 Kyrkheddinge 3	55 38 34	13 15 30	49
16 Kyrkheddinge 1	55 39 09	13 16 00	47
17 Kyrkheddinge 2	55 39 34	13 15 57	45
18 Flackarp 1	55 41 10	13 10 10	48
19 Värpinge 1	55 42 10	13 09 06	49
20 Skälsåker 1	55 42 30	13 07 40	44
21 Barsebäck 1	55 44 40	12 55 31	56
22 Norrevång 1	55 46 45	13 01 27	51
23 Nyhem	55 53 46	13 51 49	43
24 Karlshamn	56 09 00	14 51 00	40
25 Klipperåsen	56 48 00	15 41 00	53
26 Laxemar (klx 02)/a1*	57 24	16 38	52
27 Ävrö	57 25	16 41	48
28 Kråkemåla	57 28	16 38	49
29 Solstad	57 35	16 34	95
30 Göteborg/a1	57 41	11 59	41
31 Bersbo	58 16	16 03	63
32 Jordfall	58 20	11 35	40
33 Lyse	58 20	11 26	51
34 Statraf 6	58 20	11 26	54
35 Statraf 9	58 20	11 26	50
36 Ormestad	58 22	11 37	36
37 Hamburgsund	58 32	11 17	72
38 Bön	58 35	11 40	40
39 Rabbelshede	58 35	11 29	47
40 Fjällbacka	58 36	11 19	85
41 Fjällbacka (Fjb1)/a2*	58 36	11 18	63
42 Fjällveden 1	58 40	16 55	48
43 Fjällveden 2	58 40	16 55	46
44 Rimseröd	58 45	11 36	43
45 Lur	58 47	11 21	47
46 Raftötången	58 47	11 12	68
47 Zinkgruvan	58 48	15 05	56
48 Lervik	59 04	11 11	69
49 Stripa	59 42	15 05	60
50 Grimsö	59 45	15 28	46
51 Stråssa	59 45	15 12	63
52 Gammelbo	59 47	15 27	62
53 Rallso	59 48	15 06	51
54 Värmlandsberg	59 50	14 09	54
55 Malingsbol	59 52	15 37	75
56 Sandvret-Gruv	59 53	15 08	55
57 Koppar	59 53	15 03	64
58 Klotten	59 54	15 18	60
59 Alingsbol	59 55	15 08	66
60 Rudgruvan	60 01	15 46	54
61 Dannemora	60 02	17 51	60
62 Blötberget	60 07	15 03	61
63 Intrånget	60 20	16 09	44
64 Finnsjön	60 22	17 55	45
65 Solberga/a1	60 59	15 13	43
66 Hättberg/a1	61 04	14 50	43
67 Stajsås/a1	61 07	14 50	47
68 Gravberg/a1	61 08	14 15	52
69 Guttusjön(9holes)	61 59	12 24	53
70 Myrv-Orrviken	63 00	14 24	72
71 Häggenas	63 22	14 53	68
72 Gideå (9holes)	63 29	19 05	44
73 Rörmrberget (9 holes)	64 20	19 51	40
74 Långsele 588	64 51	20 17	48
75 Långsele 594	64 51	20 17	60
76 Långsele 597	64 51	20 17	58
77 Boliden 679	64 51	20 20	33
78 Boliden 678	64 52	20 22	36
79 Långsele	64 52	20 19	55
80 Strömfors-Nyholm	64 52	20 27	41
81 Boliden-Strömfors-Nyholm	64 52	20 27	41
82 Strömfors 6	64 53	20 26	41
83 Renström	64 55	20 06	39
84 Norrliden	65 01	19 36	40

No. Location	Co-ordinates		Heat-Flow density	
	Lat. (N)	Long. (E)	without palaeo-cor.	incl. palaeo-cor.
85 Kristineberg	65 04	18 33	34	
86 Gunarsjön (3 holes)	65 09	17 15	65	
87 Svärträsk 77006	65 10	17 15	57	
88 Svärträsk 78001	65 10	17 15	60	
89 Storuman	65 12	16 53	97	
90 Adak	65 22	18 38	40	
91 Stravsträsk	65 35	20 46	40	
92 Luleå	65 37	22 09	43	
93 Djupträsk	65 38	20 41	18	
94 Kamlunge (7 holes)	66 03	22 55	39	
95 Laisvall (7 holes)	66 08	17 08	33	
96 Tekelvar 74002	66 44	19 00	48	
97 Tekelvar 75002	66 44	19 00	42	
98 Saggat	66 54	17 48	51	
99 Aitik	67 05	20 57	45	
100 Aitik 250	67 05	20 57	49	
101 Aitik 251	67 05	20 57	43	
102 Aitik 523	67 05	20 57	48	
103 Aitik 535	67 05	20 57	48	
104 Malmberget	67 10	20 40	45	
105 Malmberget 4000	67 10	20 40	48	
106 Malmberget 4092	67 10	20 40	44	
107 Malmberget 3946	67 10	20 41	43	
108 Patok	67 36	19 38	42	
109 Kiruna 2997	67 51	20 14	44	
110 Kiruna 3226	67 52	20 08	45	
111 Kiruna 2210	67 52	20 09	48	
112 Kiruna 3215	67 52	20 09	48	
113 Viscaria	67 52	20 09	46	
114 Kiruna (Lapp)	67 53	20 16	54	
115 Taavinunanan	68 01	20 59	32	

*a1, thermal conductivity assumed to be 3.24 W/mK

*a2, thermal conductivity assumed to be 3.6 W/mK

Switzerland

No. Location	Co-ordinates		Heat-Flow density	
	Lat. (N)	Long. (E)	without palaeo-cor.	incl. palaeo-cor.
1 Wellenberg SB1	47 53 20	8 25 00	58	
2 Wellenberg SB3	47 53 20	8 23 25	63	129
3 Hermrigen 1	47 05 10	7 14 05	77	95
4 Siblingen	47 43 40	8 30 25	87	116
5 Böttstein	47 43 00	8 13 10	192	
6 Berlingen 2	47 40 10	9 01 50	116	79
7 Berlingen 1	47 39 40	9 02 55	91	92
8 Steckborn	47 39 20	9 01 25	125	
9 Homburg 1	47 39 00	9 01 35	115	135
10 Kreuzlingen 2	47 38 55	9 10 40	113	80
11 Bodensee 3 B *	47 38 00	9 20 00	109	
12 Kreuzlingen 1	47 37 25	9 09 30	105	
13 Bodensee 2 B *	47 37 00	9 23 00	103	
14 Herdern 1	47 36 50	8 55 10	109	
15 Bodensee 1 B *	47 36 00	9 25 00	104	
16 Klingnau 3	47 35 50	8 15 40	148	
17 Klingnau 1	47 35 35	8 15 25	127	
18 Klingnau 2	47 35 35	8 15 25	111	90
19 Zurzach 3	47 35 30	8 17 10	127	192
20 Leuggern	47 35 25	8 12 10	159	
21 Riehen 2	47 35 00	7 39 00	94	35
22 Eglisau 2	47 34 30	8 30 50	120	110
23 Weiach	47 33 50	8 27 30	133	101
24 Allschwil 1	47 33 25	7 32 40	114	100
25 Riburg 2	47 33 20	7 49 35	80	93
26 Beznau KKW	47 33 10	8 13 50	117	50
27 Ruckfeld	47 32 40	8 16 00	124	70
28 Allschwil 2	47 32 30	7 31 05	117	110
29 Kaisten	47 32 25	8 02 00	118	92
30 Kaiseraugst WB5	47 32 00	7 44 25	69	
31 Pratteln 41J8	47 31 55	7 43 55	76	87
32 Frenkendorf	47 30 40	7 43 05	176	
33 Reinach 1	47 30 40	7 36 25	97	92
34 Riniken	47 30 25	8 11 30	113	89
35 Bodensee 4 B *	47 29 55	9 24 40	105	113
36 Bronschhofen	47 28 55	9 01 30	97	105
37 Elgg	47 28 40	8 51 25	75	110
38 Buix	47 28 35	7 01 25	109	201
39 Thal Büchberg	47 28 30	9 33 30	62	94
40 Birmo AG	47 28 05	8 14 25	155	
41 Otelfingen	47 28 00	8 23 15	93	
42 Birmenstorf BT 4	47 27 50	8 14 10	163	
43 Mörschwil Steinach	47 27 50	9 24 20	100	
44 Mülligen BT2	47 27 50	8 13 40	179	
45 Habsburg 5556.19	47 27 35	8 10 10	184	
46 Hausen HH1	47 27 35	8 12 20	168	
47 Schinznach 5256.26	47 27 35	8 08 00	90	
48 Oberbüren Sonnental	47 27 25	9 08 50	93	89
49 Furttal 709	47 27 06	8 26 50	122	89
50 Furttal 706	47 27 00	8 25 30	79	131
51 Kloten	47 27 00	8 35 25	101	144
52 Schinznach QN 83	47 26 55	8 09 10	91	87
53 Densbüren	47 26 45	8 03 20	120	
54 Grellingen	47 26 25	7 34 40	110	

No. Location	Co-ordinates		Heat-Flow density	
	Lat. (N)	Long. (E)	without palaeo-cor.	incl. palaeo-cor.
55 Lindau	47 26 25	8 40 10	107	190
56 Gubrist	47 25 20	8 27 50	101	118
57 Oberuzwil Bichwil	47 25 10	9 08 50	85	80
58 Gossau Silthang	47 24 54	9 16 50	187	51
59 Gossau Niederdorf	47 24 42	9 13 50	134	
60 Eptingen 1	47 23 40	7 49 00	98	72
61 Lostorf Bad 3	47 23 35	7 56 00	96	70
62 Fehraltorf	47 23 10	8 44 25	93	118
63 Krone / Zürich	47 22 55	8 32 55	85	147
64 Hauenstein °	47 22 50	7 54 35	85	
65 Schafisheim	47 22 10	8 09 00	119	
66 Greifensee 1 *	47 21 42	8 40 00	89	119
67 Aquil 1	47 21 35	8 31 30	94	106
68 Tiefenbrunnen/Zürich	47 21 10	8 33 10	97	132
69 Delemont 1	47 21 00	7 20 40	72	101
70 Greifensee 2 *	47 21 00	8 40 55	89	72
71 Hölzlisberg	47 20 40	9 31 05	50	
72 Uster 401	47 20 40	8 43 30	91	
73 Brunnadern	47 19 40	9 08 25	34	
74 Küsnacht	47 19 05	8 37 10	71	
75 Boswil 1	47 17 05	8 17 50	82	
76 Zürichsee 1 *	47 16 00	8 36 00	97	
77 Zürichsee 2 *	47 16 00	8 36 00	103	
78 La Foule	47 15 50	7 21 30	46	
79 Pfaffnau 1	47 14 10	7 52 10	91	
80 Altshofen	47 12 10	7 58 25	87	
81 Pfaffnau Süd 1	47 12 00	7 54 00	80	
82 Tuggen	47 12 00	8 57 10	103	47
83 Baldeggersee *	47 11 50	8 15 50	103	159
84 Menzingen	47 11 10	8 36 20	44	109
85 Hünenberg 1	47 10 05	8 26 05	70	62
86 Sevelen 14	47 07 55	9 28 50	69	98
87 Sevelen 13	47 07 50	9 29 10	46	
88 Bielersee *	47 07 00	7 11 00	47	67
89 Zugersee *	47 06 00	8 30 00	92	104
90 Zugersee *	47 06 00	8 30 00	98	
91 Ruppoldsried	47 05 30	7 26 55	93	61
92 Balzers	47 03 30	9 30 20	78	52
93 Tschugg 1	47 01 20	7 04 40	105	
94 Vierwaldstättersee 1 *	47 01 00	8 26 00	105	
95 Vierwaldstättersee 2 *	46 59 00	8 29 00	104	
96 Vierwaldstättersee 3 *	46 59 00	8 31 00	94	
97 Martel Dernier	46 58 55	6 42 55	60	124
98 Entlebuch 1	46 58 30	8 06 40	88	
99 Lago di Lugano 5 *	46 57 30	8 53 40	68	
100 Lac de Neuchâtel 1 *	46 57 00	6 54 00	68	84
101 Lac de Neuchâtel 2 *	46 54 00	6 50 00	70	92
102 Courtion 1	46 51 25	7 04 35	69	
103 Linden	46 50 55	7 40 20	61	87
104 Vereina	46 49 35	9 58 20	49	106
105 Payerne	46 49 00	6 56 40	66	109
106 Treykovagnes 1	46 46 20	6 36 10	85	108
107 Yverdon/Belair	46 46 15	6 39 00	96	113
108 Cuarny	46 46 10	6 42 55	103	79
109 Lavin 1	46 45 50	10 06 35	46	
110 Thun 1	46 45 30	7 42 20	83	56
111 Essertines	46 42 35	6 39 05	105	88
112 Tujetsch SB1	46 40 55	8 45 30	29	
113 Tujetsch SB2	46 40 55	8 45 30	29	76
114 Tavanasa °	46 40 50	9 00 00	58	119
115 Rueras 2	46 40 20	8 45 55	72	
116 Chapelle 1	46 39 55	6 45 00	92	
117 Eclepens 1	46 39 50	6 34 00	86	
118 Romanens 1	46 39 30	6 58 20	86	
119 Gotthardstrassentunnel °	46 38 42	8 35 55	69	87
120 Bulle	46 37 50	7 03 00	85	
121 Gotthard SBB 1 °	46 37 30	8 35 40	51	
122 Guspispach (Schacht)	46 35 40	8 34 55	86	78
123 Sta. Maria	46 35 25	8 48 00	56	31
124 Gotthard 2a Strass. °	46 34 54	8 34 06	60	
125 Gotthard 2b strass. °	46 34 48	8 34 10	43	
126 Gotthard SBB 3 °	46 33 06	8 36 00	50	
127 Savigny 1	46 32 50	6 44 20	86	85
128 San Bernardino °	46 29 25	9 10 50	79	97
129 Lötschberg SB6	46 29 10	7 39 50	57	77
130 St. Moritz	46 28 35	9 50 05	65	98
131 Chiggiogna	46 28 10	8 49 20	49	112
132 Lötschberg SB7	46 27 25	7 41 10	86	50
133 Lac Lemman 1 *	46 27 00	6 37 00	76	59
134 Lac Lemman 2 *	46 27 00	6 34 00	70	107
135 Lac Lemman 3 *	46 26 00	6 28 00	82	
136 Malvaglia	46 25 35	9 01 30	57	
137 Biaschina	46 25 20	8 51 40	79	28
138 Lötschberg °	46 25 10	7 43 20	62	
139 Campo Vallemaggia	46 17 20	8 29 20	81	
140 Simplon N (2) °	46 16 20	8 05 50	75	
141 Palagnedra 3 °	46 15 40	8 38 35	80	133
142 Simplon S (1) °	46 15 40	8 06 35	48	84
143 Palagnedra 1 °	46 10 50	8 38 10	48	74
144 Verbano 2	46 09 10	8 40 40	28	100
145 Verbano 1	46 08 55	8 41 35	48	
146 Lago di Lugano 2 *	46 01 00	9 02 20	59	
147 Lago di Lugano 1 *	46 00 30	9 01 30	59	
148 Lago di Lugano 3 *	45 56 30	8 57 10	68	
149 Lago di Lugano 4 *	45 55 50	8 53 50	81	

* Measurements in lakes

° Measurements in tunnels and shafts

United Kingdom

No. Location	Co-ordinates		Heat-Flow density	
	Lat. (N)	Long. (W)	without palaeo-cor.	incl. palaeo-cor.
1 Warbeth	58 57 38	3 19 49	46	
2 Houstrie of Dunn	58 28 22	3 21 60	45	
3 Achanarras	58 28 19	3 27 02	42	
4 Altnabreac A	58 23 06	3 42 44	43	
5 Yarrow	58 23 02	3 10 48	52	
6 Altnabreac B	58 21 08	3 40 10	53	
7 Tilleydesk	57 25 55	2 04 18	29	
8 Loch Ness 9	57 20 46	4 23 36	43	
9 Loch Ness 8	57 18 56	4 25 52	43	
10 Loch Ness 7	57 17 24	4 27 33	55	
11 Bennachie	57 16 43	2 32 57	76	
12 Loch Ness 6	57 16 20	4 29 11	67	
13 Loch Ness 5	57 16 01	4 29 15	82	
14 Loch Ness 4	57 15 10	4 30 59	57	
15 Loch Ness 3	57 13 50	4 32 47	62	
16 Loch Ness 2	57 11 40	4 36 07	64	
17 Loch Ness 1	57 09 24	4 39 08	73	
18 Cairngorm	57 08 09	3 40 14	70	
19 Ballater	57 04 29	2 59 17	71	
20 Mount Battock	57 00 13	2 45 15	59	
21 Montrose	56 44 04	2 27 22	46	
22 Ballachulish	56 39 29	5 12 29	53	
23 Glenrothes	56 12 54	3 11 58	56	
24 Balfour	56 11 26	3 05 28	36	
25 Boreland	56 08 08	3 07 12	40	
26 Clachie Bridge	56 01 37	4 10 30	55	
27 Edinburgh	55 58 16	3 08 56	53	
28 Kipperoch	55 57 43	4 36 24	54	
29 Barnhill	55 56 55	4 31 15	60	
30 South Balgray	55 56 41	4 24 08	64	
31 Meall Mhor	55 54 53	5 27 53	57	
32 Livingston	55 54 18	3 34 15	66	
33 Maryhill	55 53 20	4 17 02	63	
34 Blythswood	55 53 02	4 23 52	52	
35 Hurler	55 49 15	4 23 34	60	
36 Marshall Meadows	55 48 18	2 01 57	51	
37 Selkirk	55 32 30	2 49 30	60	
38 Port More	55 13 43	6 19 13	80	
39 Longhorsley	55 13 39	1 46 22	92	
40 Becklees	55 02 05	3 00 50	43	
41 Rowlands Gill	54 55 04	1 44 25	99	
42 Sillioth No2	54 52 39	3 21 39	55	
43 Castle Douglas	54 52 24	3 59 59	61	
44 Larne No.2	54 50 54	5 48 33	59	
45 South Hetton	54 48 04	1 24 21	58	
46 Ballymacilroy	54 47 15	6 19 50	59	
47 Rookhope	54 46 47	2 05 49	95	
48 Skiddaw	54 40 22	3 03 50	101	
49 Nebiggin	54 39 11	2 32 43	85	
50 Woodland	54 38 42	1 51 32	96	
51 Dufton	54 37 10	2 29 15	85	
52 Kirkleatham 1	54 34 59	1 05 25	48	
53 Killary Glebe	54 33 21	6 41 10	60	
54 Boulby	54 33 18	0 49 24	47	
55 Tocketts 1	54 33 15	1 01 25	49	
56 Shap	54 28 18	2 40 50	78	
57 Lake Windermere 3	54 24 02	2 57 07	74	
58 Lake Windermere 2	54 23 49	2 57 07	69	
59 Lake Windermere 1	54 22 22	2 55 59	69	
60 Raydale	54 15 29	2 08 58	65	
61 Beckermonds Scar	54 13 01	2 12 34	69	
62 Annalong Valley	54 09 03	5 56 38	69	87
63 Seefin Quarry	54 08 13	5 54 60	70	84
64 Wray	54 05 08	2 33 48	40	
65 Farnham	54 02 05	1 28 12	40	
66 Towthorpe	54 01 25	1 03 23	56	
67 Shipton	54 01 13	1 10 08	56	57
68 Swinden No1	53 57 04	2 12 48	66	
69 Clitheroe MHD2	53 54 43	2 28 40	84	
70 Harewood	53 53 29	1 30 38	65	
71 Thornton Cleveley	53 53 19	3 01 05	52	
72 Clitheroe No 2	53 51 50	2 22 19	40	
73 Skipwith Bridge	53 51 29	1 00 20	59	
74 Approach Farm	53 50 29	1 02 44	54	
75 Skipwith	53 49 33	0 59 28	54	
76 Weeton Camp	53 48 56	2 55 41	52	
77 North Duffield	53 48 31	0 57 01	60	
78 Market Weighton	53 48 10	0 41 41	57	
79 Kirkham	53 47 07	2 51 42	71	
80 Booth Ferry	53 43 23	0 52 48	57	
81 Marsden	53 36 12	1 55 28	50	
82 Rosebridge Coll	53 32 52	2 38 13	43	
83 Cleethorpes No 1	53 32 39	0 02 03	73	
84 Nettleton Bottom	53 28 06	0 18 18	67	
85 Misson	53 27 15	0 57 12	85	
86 Corringham	53 25 53	0 38 48	63	
87 Scaftworth	53 25 02	0 58 57	75	
88 Parys Mountain	53 23 20	4 20 40	59	
89 Ranby Hall	53 20 02	1 01 33	77	
90 Holford	53 19 60	2 30 00	31	38
91 Grove No3	53 19 22	0 51 16	54	
92 Donnington on Bain	53 19 09	0 08 18	75	
93 Ranby Camp	53 19 09	1 00 12	83	
94 Bradley Mill	53 17 06	2 42 13	59	
95 Eyam	53 16 50	1 41 08	17	
96 Welton No.1	53 16 40	0 26 45	65	

No. Location	Co-ordinates		Heat-Flow density	
	Lat. (N)	Long. (W)	without palaeo-cor.	incl. palaeo-cor.
97 Organsdale	53 12 34	2 40 21	25	
98 Priors Heyes	53 11 32	2 43 50	34	
99 Clotton	53 10 02	2 42 22	33	
100 Eakring 6	53 08 43	0 59 52	115	
101 Eakring 5	53 08 33	0 59 14	114	
102 Caunton 11	53 08 04	0 54 04	70	
103 Eakring 141	53 07 32	0 58 45	120	
104 Eakring 64	53 07 32	0 59 53	82	
105 Kelham Hills 1	53 06 36	0 51 56	62	
106 Cree	53 05 11	2 28 24	57	
107 Papplewick	53 03 48	1 11 02	71	
108 Goosedale	53 02 20	1 09 33	64	
109 Long Bennington	53 00 15	0 47 55	88	
110 Burton Lodge	52 58 48	0 20 25	58	
111 Eady's Farm	52 55 31	0 48 58	54	
112 Woodlands Farm	52 52 53	0 51 26	51	
113 Bryn Teg	52 52 14	3 55 58	41	
114 Trunch	52 51 31	1 24 27 (E)	63	
115 Rhiw	52 50 0	4 37 46	45	65
116 Coed-y-Brenin	52 48 53	3 51 34	42	
117 Mochras	52 48 40	4 08 48	57	
118 Welby Church	52 46 48	0 55 43	47	
119 Morley Quarry	52 45 22	1 17 38	54	
120 Tydd St Mary	52 44 09	0 07 11 (E)	57	
121 Bardon Hill	52 42 49	1 19 43	46	56
122 Twycross	52 38 50	1 29 58	41	
123 Leicester Forest	52 37 14	1 13 32	53	
124 Croft Quarry	52 33 46	1 14 35	37	
125 Thorpe-by-Water	52 33 31	0 41 36	56	
126 Church Stretton	52 33 10	2 51 17	46	63
127 Glanfred	52 28 24	4 00 59	59	
128 Home Farm	52 21 14	1 21 56	36	
129 Huntingdon	52 19 36	0 11 05	38	
130 Stowlangtoft	52 16 57	0 51 17 (E)	35	
131 Worcester	52 12 58	2 12 07	41	
132 Cambridge	52 12 53	0 05 45	54	
133 Malvern Gasworks	52 08 25	2 18 35	34	
134 Llanwrtyd Wells	52 07 46	3 38 33	54	
135 Wyche	52 05 39	2 20 09	43	60
136 Withycombe Farm	52 03 28	1 22 12	60	
137 Steeple Aston	51 55 44	1 19 06	46	
138 Treffgarne No3	51 52 54	4 59 20	43	
139 Treffgarne No2	51 52 26	5 00 21	39	
140 Betws	51 44 39	3 56 59	34	
141 Gelli Fawr	51 42 53	4 11 29	50	
142 Carn Caglau	51 41 18	3 39 02	36	
143 Chalgrove	51 39 40	1 03 16	48	
144 Harwell No3	51 34 15	1 19 13	44	
145 Newtown	51 33 14	3 20 32	48	57
146 St. Fagans	51 29 41	3 16 20	50	
147 Fair Cross	51 21 48	0 59 54	59	
148 Vernhamsdean	51 18 22	1 30 28	25	
149 West Lavington	51 18 20	2 00 53	42	
150 Fetcham Mill	51 17 43	0 20 20	53	
151 Humbly Grove No1	51 11 51	0 58 51	51	
152 Barton Stacey	51 10 56	1 22 29	42	
153 Shrewton	51 10 36	1 57 18	51	
154 Cannington Park	51 09 17	3 04 32	40	45
155 Currypool Farm	51 08 31	3 06 18	54	61
156 Honeymead 2	51 08 25	3 43 01	54	
157 Godley Bridge No1	51 07 13	0 38 23	54	
158 South Molton	51 04 31	3 49 23	55	
159 Bunkers Hill	50 55 59	1 34 03	60	
160 Southampton No1	50 54 20	1 24 32	71	
161 Marchwood	50 53 54	1 25 57	61	
162 Clumphil	50 51 23	1 54 22	67	
163 Chard	50 51 14	2 56 01	51	
164 Ramnor Inclosure	50 50 29	1 33 25	61	
165 Hankham Colliery	50 49 17	0 18 01 (E)	30	
166 Winterborne	50 46 48	2 13 01	70	
167 Venn Ottery	50 42 42	3 19 05	56	
168 Meldon	50 42 40	4 01 45	104	114
169 Winter Tor	50 42 23	3 57 59	79	107
170 Wilsey Don	50 40 14	4 34 35	67	
171 Blackingstone	50 39 35	3 43 09	85	105
172 Withycombe Raleigh	50 38 52	3 22 04	50	
173 Seabarn Farm	50 37 22	2 31 42	56	
174 Bray Down	50 36 25	4 33 26	89	113
175 Soussons Wood	50 36 05	3 52 30	123	132
176 Bovey Tracey	50 36 03	3 39 27	79	95
177 Blackhill	50 34 29	4 33 57	97	119
178 Laughter Tor	50 33 47	3 53 51	90	114
179 Foggin Tor	50 32 30	4 01 25	89	111
180 Pinnockshill	50 32 30	4 33 21	103	121
181 Brownnelly	50 31 24	4 33 01	87	108
182 Gt. Hammet Farm	50 29 60	4 33 17	98	119
183 Callywith Farm	50 28 43	4 41 40	91	101
184 Lanivet	50 26 35	4 47 12	79	93
185 Belowda Beacon	50 25 38	4 50 46	78	85
186 Hemerdon	50 24 30	4 00 29	93	108
187 Tregarden Farm	50 24 08	4 44 13	106	126
188 Gaverigan	50 23 43	4 54 38	97	98
189 Colcerrow Farm	50 23 10	4 43 06	103	127
190 Newlyn East	50 20 38	5 04 19	91	105
191 Wheal Jane P	50 15 07	5 06 32	126	
192 Wheal Jane O	50 15 00	5 06 42	113	
193 Merrose Farm	50 14 40	5 17 17	72	79

No. Location	Co-ordinates		Heat-Flow density	
	Lat. (N)	Long. (W)	without palaeo-cor.	incl. palaeo-cor.
194 Wheal Jane E	50 14 22	5 08 25	136	
195 South Crofty	50 13 30	5 16 20	129	
196 Grillis Farm	50 11 60	5 15 07	92	113
197 Polgear Beacon	50 11 03	5 13 57	101	122
198 Troon	50 11 02	5 16 57	109	123
199 Longdowns	50 10 03	5 10 12	105	112
200 Rosemanowes D	50 10 03	5 10 18	103	106
201 Rosemanowes RH 11	50 10 03	5 10 19	115	
202 Rosemanowes RH 12	50 10 03	5 10 19	118	
203 Rosemanowes A	50 10 02	5 10 18	103	106
204 Medlyn Farm	50 09 41	5 12 33	99	114
205 Newmill	50 09 15	5 33 19	103	124
206 Geevor Mine	50 09 15	5 40 20	129	
207 Treaghan Farm	50 07 45	5 10 09	95	113
208 Trevease Farm	50 07 45	5 10 09	92	112
209 Kestle Wartha	50 05 21	5 08 29	82	96
210 Bunker's Hill	50 05 17	5 37 56	105	124
211 Kennack Sands	50 00 16	5 09 53	68	73
212 Predannack	50 00 06	5 13 26	60	61

GENERAL LEGEND

Special symbols, and deviations from this general legend are noted on individual maps where they occur.

- Solid isolines indicate reliable data and/or good data distribution
- Broken isolines indicate uncertain data and/or an inadequate density of data

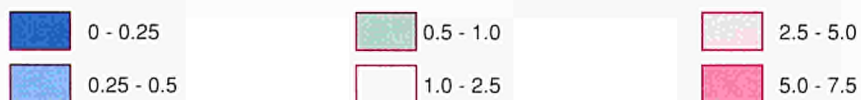
Geothermal symbols

- Borehole location
- Geothermal installation
- Geothermal installation under construction
- Depth of top of the aquifer relative to mean sea level, isohypses in metres, m; or depth of top of the aquifer below ground level, isobaths in metres, m
- Pressure in bar; or piezometric level relative to sea level in metres, m
- Net thickness or thickness of aquifer, isopachytes in metres, m
- Porosity in per cent, %
- Permeability in millidarcies, mD
1 D (darcy) = 1000 mD = 10⁻¹² m² = 10⁻⁸ cm²
- Transmissibility in darcy metres, Dm
1 Dm = 10⁻¹² m³
- Temperature at top of the aquifer either relative to sea level or below ground level, isotherms in degrees Celsius, °C
- Temperature at depth below ground level, isotherms in degrees Celsius, °C
- Salinity as NaCl content or as Na Cl equivalent

Geological symbols:

- Volcanic area
- Outcrop of aquifer
- Limit of aquifer
- Shale boundary
- Fault
- Normal fault
- Thrust fault or reverse fault
- Transgression
- Cross-section
- Borehole
- Aquifer within a cross section
- s.l. Sea level
- Fault within a cross section
- Horizontal or vertical displacement
- Crystalline rock
- Limestone, karst, karst region
- Sand, sandstone
- Clay, claystone

Geothermal resources or geothermal potential areas in gigajoule per square metre, GJ/m²



Hydrogeological symbols:

Origin of data:

- Spring
- Springs
- Borehole
- Boreholes, or boreholes and springs
- Spa, Balneology

Temperature:

- 20°C ≤ T < 40°C

Chemical composition:

- Uncertain, Inconnue, Unbekannt, Sconosciuto
- Steam, Vapeur, Dampf, Vapore

Other symbols:

- City, less than one million inhabitants
- City, more than one million inhabitants

LEGENDE GENERALE

Les symboles spéciales et les modifications de cette légende générale sont signalées sur les planches intéressées

- Lignes d'isovaleur de bonne à assez bonne fiabilité - bonne densité d'information
- Lignes d'isovaleur de fiabilité médiocre - faible densité d'information

Symboles géothermiques:

- Emplacement du sondage
- Installation géothermale
- Installation géothermale en construction
- Cote du toit du réservoir par rapport au niveau moyen de la mer; isohypses en mètres, m, ou profondeur du toit du réservoir par rapport au sol, isobathes en mètres, m
- Pression en bar; ou niveau piézométrique par rapport au niveau de la mer
- Épaisseur de l'aquifère, ou épaisseur utile; isopaches en mètres, m
- Porosité en pour cent, %
- Perméabilité intrinsèque en millidarcies, mD
1 D (darcy) = 1000 mD = 10⁻¹² m² = 10⁻⁸ cm²
- Transmissibilité en darcy mètres, Dm
1 Dm = 10⁻¹² m³
- Température au toit du réservoir ou par rapport au niveau de la mer ou par rapport au sol, isothermes en degrés Celsius, °C
- Température de profondeur par rapport au sol, isothermes en degrés Celsius °C
- Salinité, teneur en NaCl, en équivalent NaCl

Symboles géologiques:

- Zone volcanique
- Affleurement du niveau considéré
- Limite d'existence du niveau considéré
- Limite d'argilosité
- Faïlle
- Faïlle normale
- Faïlle inverse, chevauchement
- Discordance
- Coupe
- Forage
- Aquifère sur une coupe
- Niveau de la mer
- Faïlle sur une coupe
- Rejet horizontal ou vertical
- Roche cristalline
- Calcaire, karst, région karstique
- Sable, grès
- Argile, marne

Ressources géothermales ou zones géothermiques potentielles en gigajoule par mètre carré, GJ/ m²



Symboles hydrogéologiques:

Origine des données:

- Source
- Groupe de sources
- Forage
- Groupe de forages, ou forages et sources
- Station thermale

Température:

- 40°C ≤ T < 60°C

Chimisme:

- Ca, Mg
- Na, K
- Cl
- SO₄

Autres symboles:

- Ville, moins d'un million d'habitants
- Ville, plus d'un million d'habitants

GENERAL LEGENDE

Sofern Sonderzeichen und Abweichungen von der General Legende in den Karten auftreten, sind diese dort vermerkt.

- Ausgezogene Linien weisen auf verlässliche Daten und/oder auf eine gute Datenverteilung hin
- Unterbrochene Linien weisen auf unsichere Daten und/oder auf eine unzulängliche Datendichte hin

Geothermische Symbole:

- Bohrloch - Lokation
- Anlage zur Nutzung geothermischer Energie
- Anlage zur Nutzung geothermischer Energie im Bau
- Tiefe der Aquiferoberkante auf mittlere Meereshöhe bezogen, Isohypsen in Metern, m; oder Tiefe der Aquiferoberkante auf Erdoberfläche bezogen, isobathen in Metern, m
- Druck in bar; oder piezometrisches Niveau auf Meereshöhe bezogen in Metern, m
- Nettomächtigkeit oder Mächtigkeit des Aquifers, Isopachen in Metern, m
- Porosität in Prozent, %
- Permeabilität in Millidarcies, mD
1 D (darcy) = 1000 mD = 10⁻¹² m² = 10⁻⁸ cm²
- Transmissibilität in Darcy Metern, Dm
1 Dm = 10⁻¹² m³
- Temperatur an Aquiferoberkante bezogen auf Meereshöhe oder auf Erdoberfläche, Isothermen in Grad Celsius, °C
- Temperatur in der Tiefe bezogen auf Erdoberfläche, Isothermen in Grad Celsius °C
- Salinität als NaCl - Gehalt oder in NaCl - Äquivalent

Geologische Symbole:

- Vulkangebiet
- Ausbiß des Aquifers
- Verbreitungsgrenze des Aquifers
- Vertonungslinie, Vertonungsgrenze
- Störung
- Normale Störung, Abschiebung
- Überschiebung
- Transgression
- Profilschnitt
- Bohrung
- Aquifer innerhalb eines Profilschnittes
- Meeresniveau
- Störung innerhalb eines Profilschnittes
- Horizontale oder vertikale Verschiebung
- Kristallines Gestein
- Kalkstein, Karst, Karstgebiet
- Sand, Sandstein
- Ton, Tonstein

Geothermische Ressourcen, oder potentielle geothermische Gebiete in Gigajoule pro Quadratmeter, GJ/ m²



Hydrogeologische Symbole:

Herkunft der Daten:

- Quelle
- Quellen
- Bohrung
- Bohrungen oder Bohrungen und Quellen
- Kurbad, Balneologie

Temperatur:

- 60°C ≤ T < 80°C

Chemismus:

- HCO₃
- H₂S

Andere Symbole:

- Stadt, weniger als eine Million Einwohner
- Stadt, mehr als eine Million Einwohner

LEGENDA GENERALE

I simboli speciali e quelli non compresi nella Legenda Generale sono indicati nelle singole carte interessate.

- Isolinee costruite con dati attendibili e ben distribuiti
- Isolinee costruite con dati incerti e/o con inadeguata distribuzione

Simboli geotermici:

- Postazione del sondaggio
- Impianto geotermico
- Impianto geotermico in costruzione
- Profondità del tetto dell'acquifero rispetto al livello medio del mare, isopse in metri, m; oppure profondità del tetto dell'acquifero dal piano campagna, isobate in metri, m
- Pressione in bar; o livello piezometrico rispetto al livello del mare in metri, m
- Spessore dell'acquifero oppure spessore utile; isopache in metri, m
- Porosità in per cento, %
- Permeabilità in millidarcies, mD
1 D (darcy) = 1000 mD = 10⁻¹² m² = 10⁻⁸ cm²
- Transmissibilità in darcy metri, Dm
1 Dm = 10⁻¹² m³
- Temperatura al tetto dell'acquifero o rispetto al livello del mare o dal piano campagna, isoterme in gradi centigradi, °C
- Temperatura a profondità rispetto al piano campagna, isoterme in gradi centigradi, °C
- Salinità, contenuto in NaCl oppure in NaCl equivalente

Simboli geologici:

- Zona vulcanica
- Affioramento dell'acquifero
- Limite dell'acquifero
- Limite delle argille
- Faglia
- Faglia normale
- Faglia inversa, accavallamento
- Discordanza
- Sezione
- Sondaggio
- Acquifero in sezione
- Livello del mare
- Faglia in sezione
- Rigetto orizzontale o verticale
- Roccia cristallina
- Calcareo, carsismo, zona carsica
- Sabbia, arenaria
- Argilla

Risorse geotermiche o zone geotermiche potenziale in gigajoule per metro quadrato, GJ/ m²



Simboli idrogeologici:

Origine dei dati:

- Sorgente
- Gruppo di sorgenti
- Sondaggio
- Gruppo di sondaggi oppure sondaggi e sorgenti
- Terme

Temperatura:

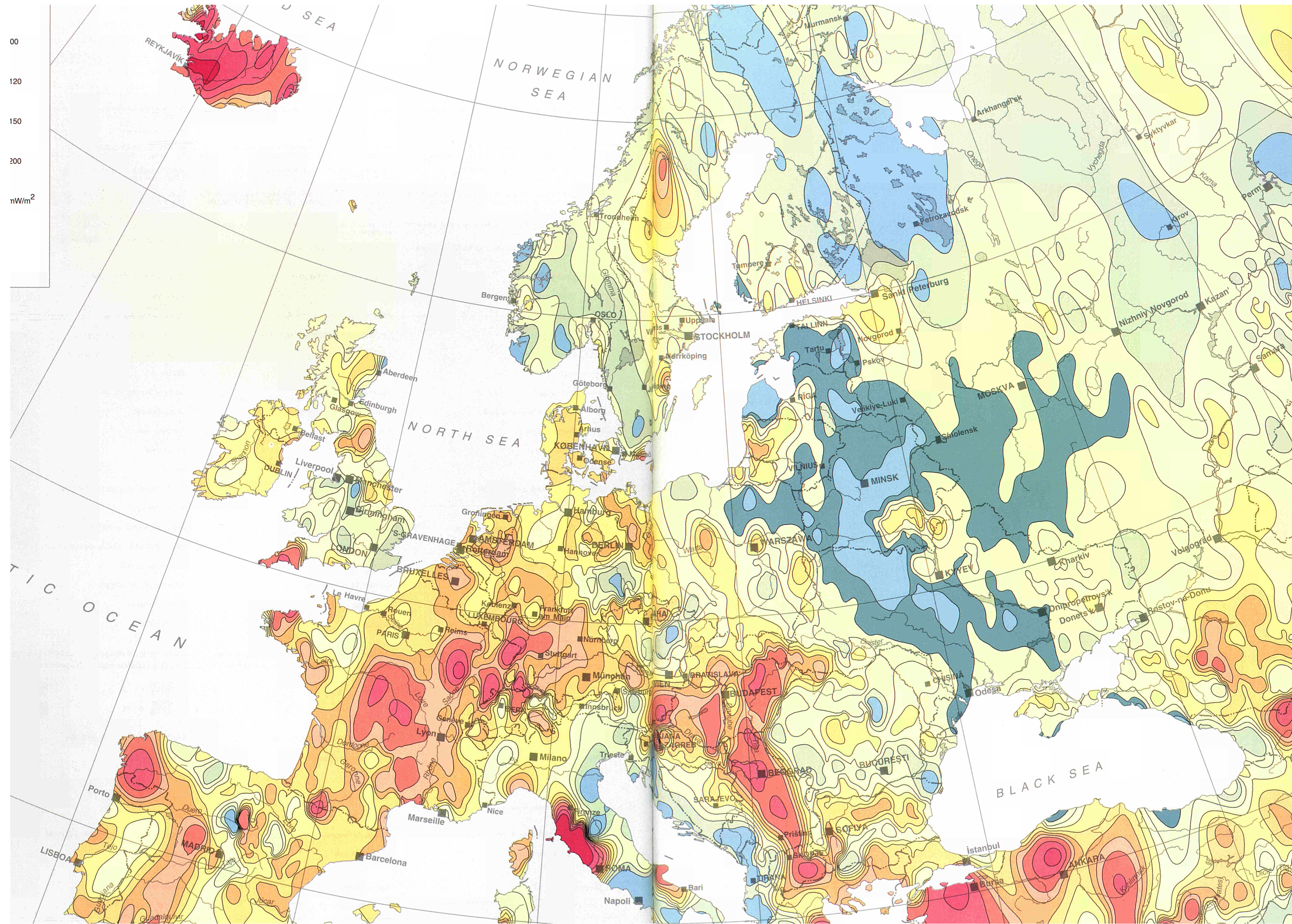
- 80°C < T

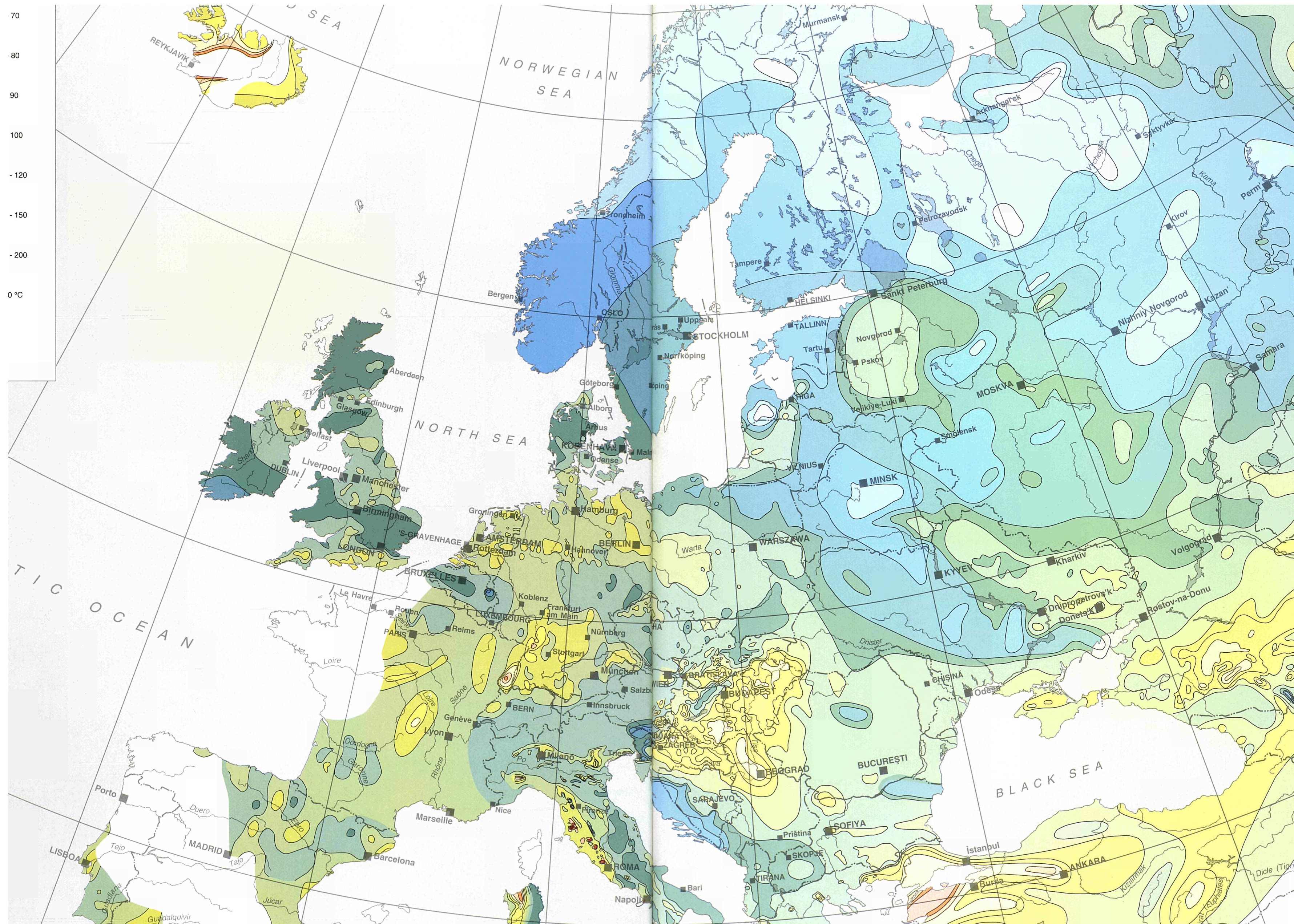
Chimismo:

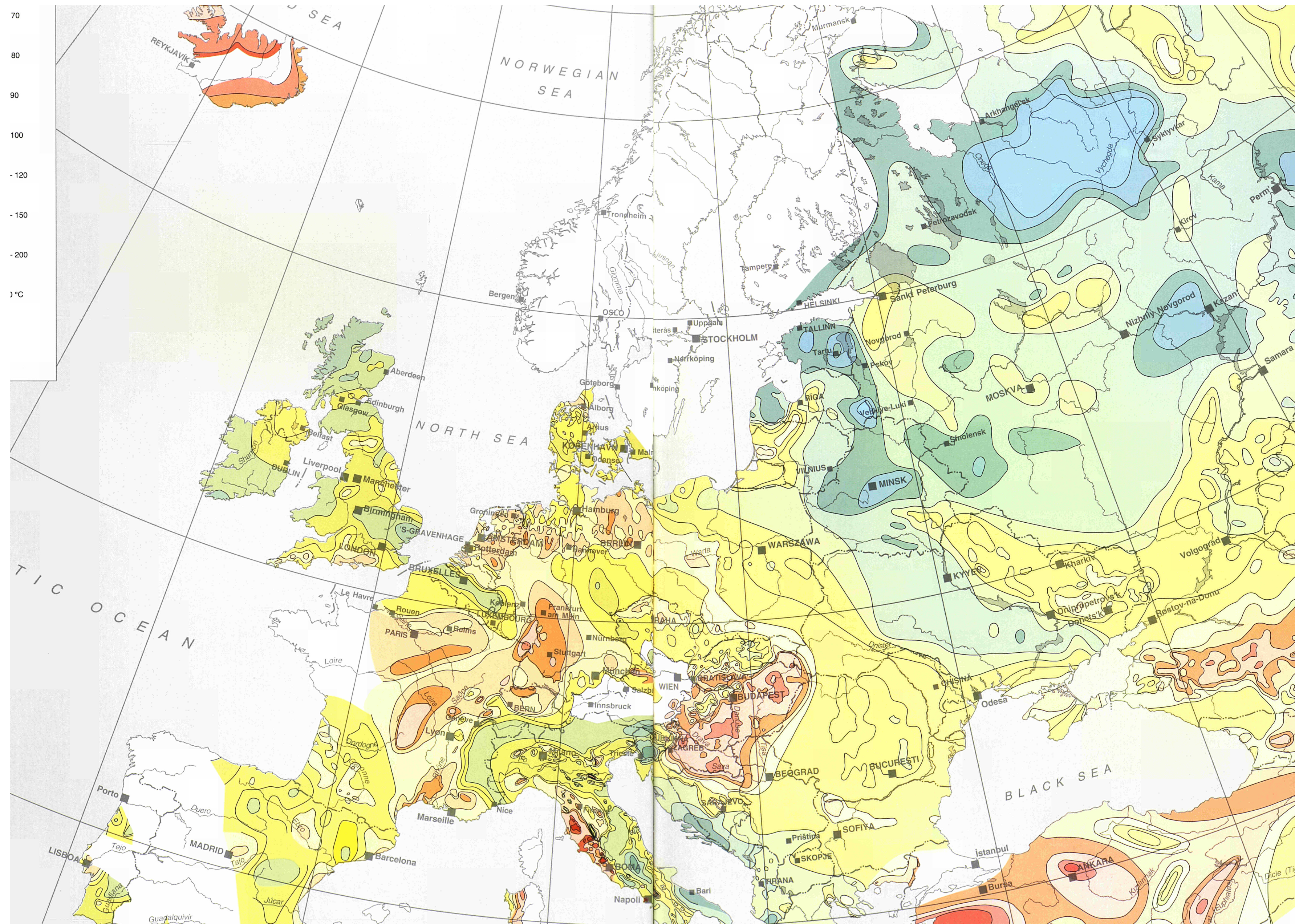
- CO₂ (250 mg/kg)

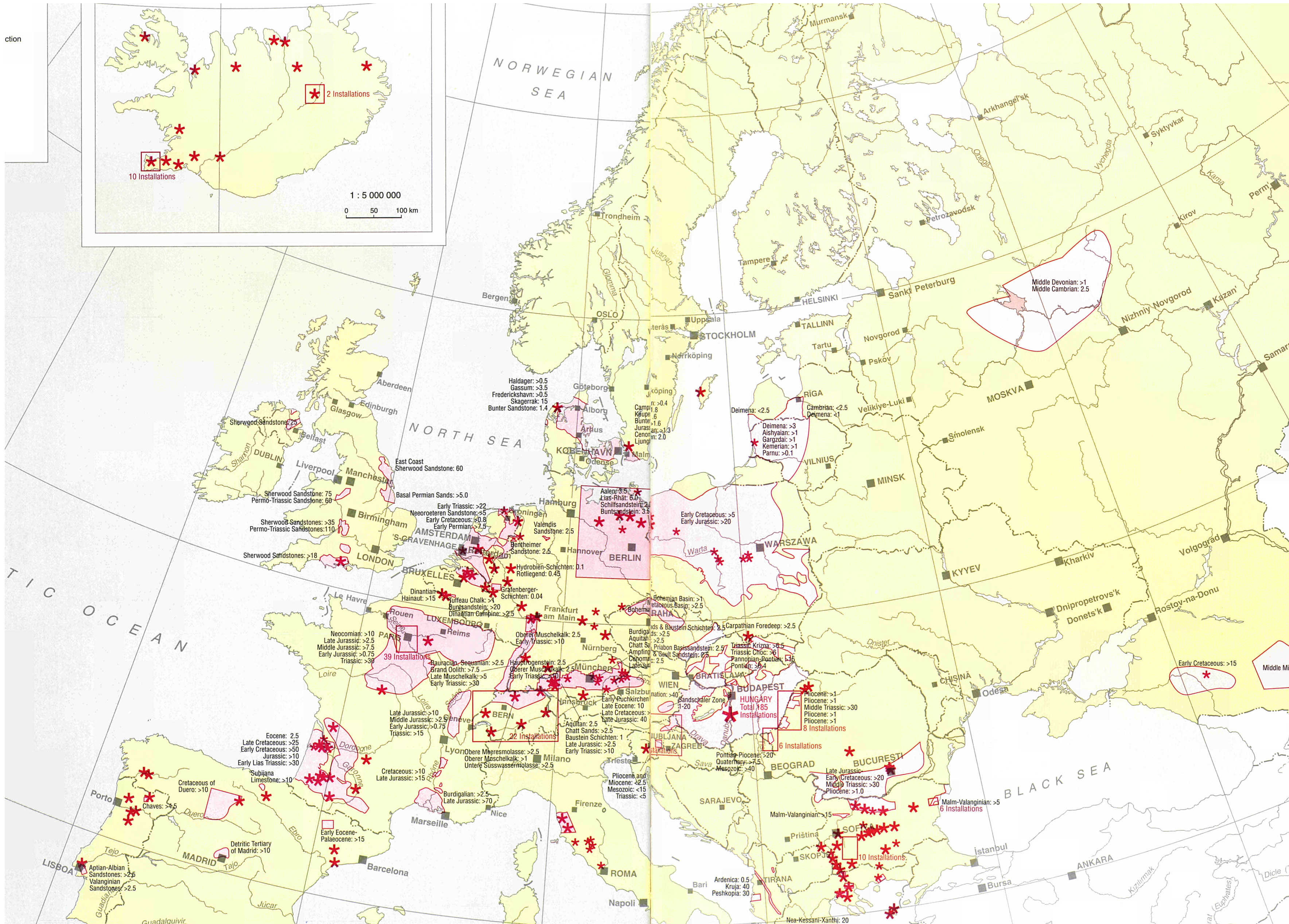
Altri simboli:

- Città, meno di un milione d'abitante
- Città, più di un milione d'abitante

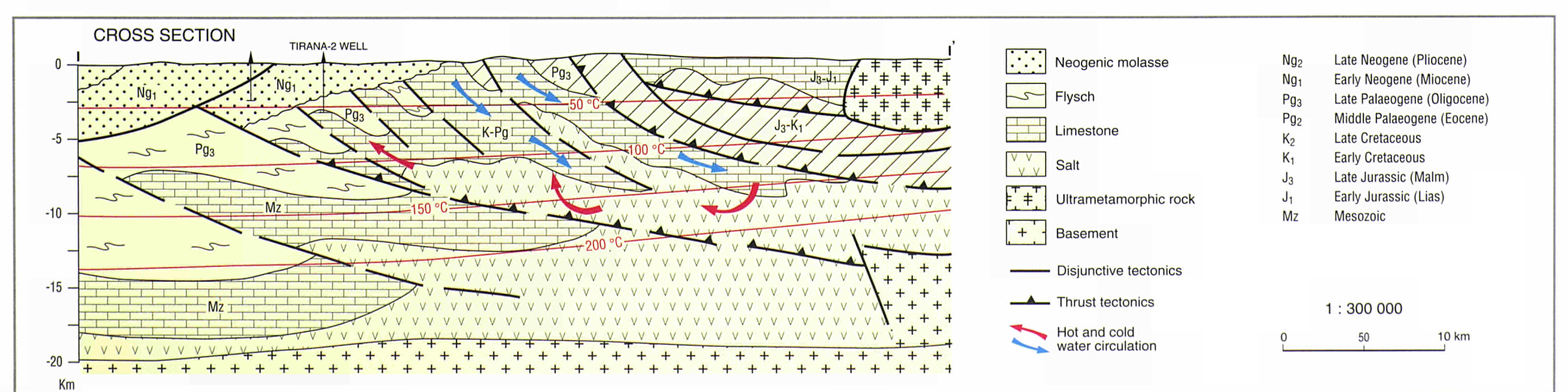
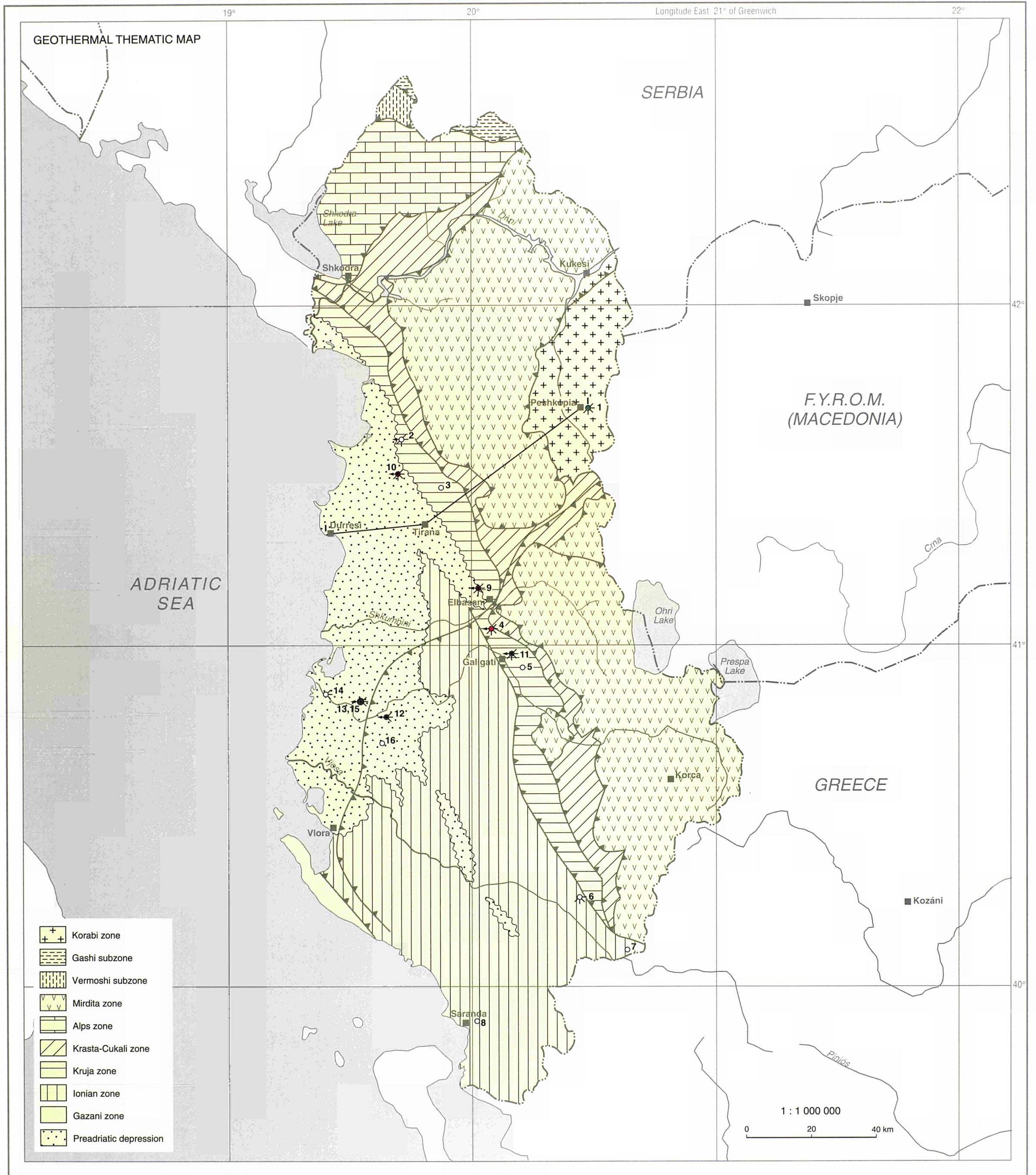


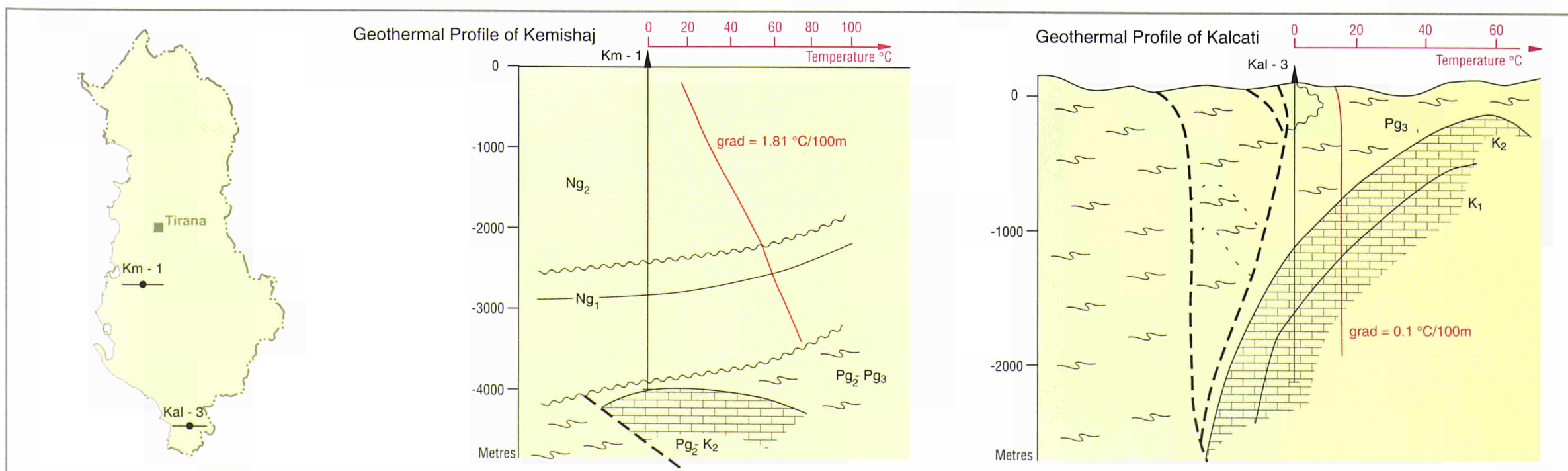
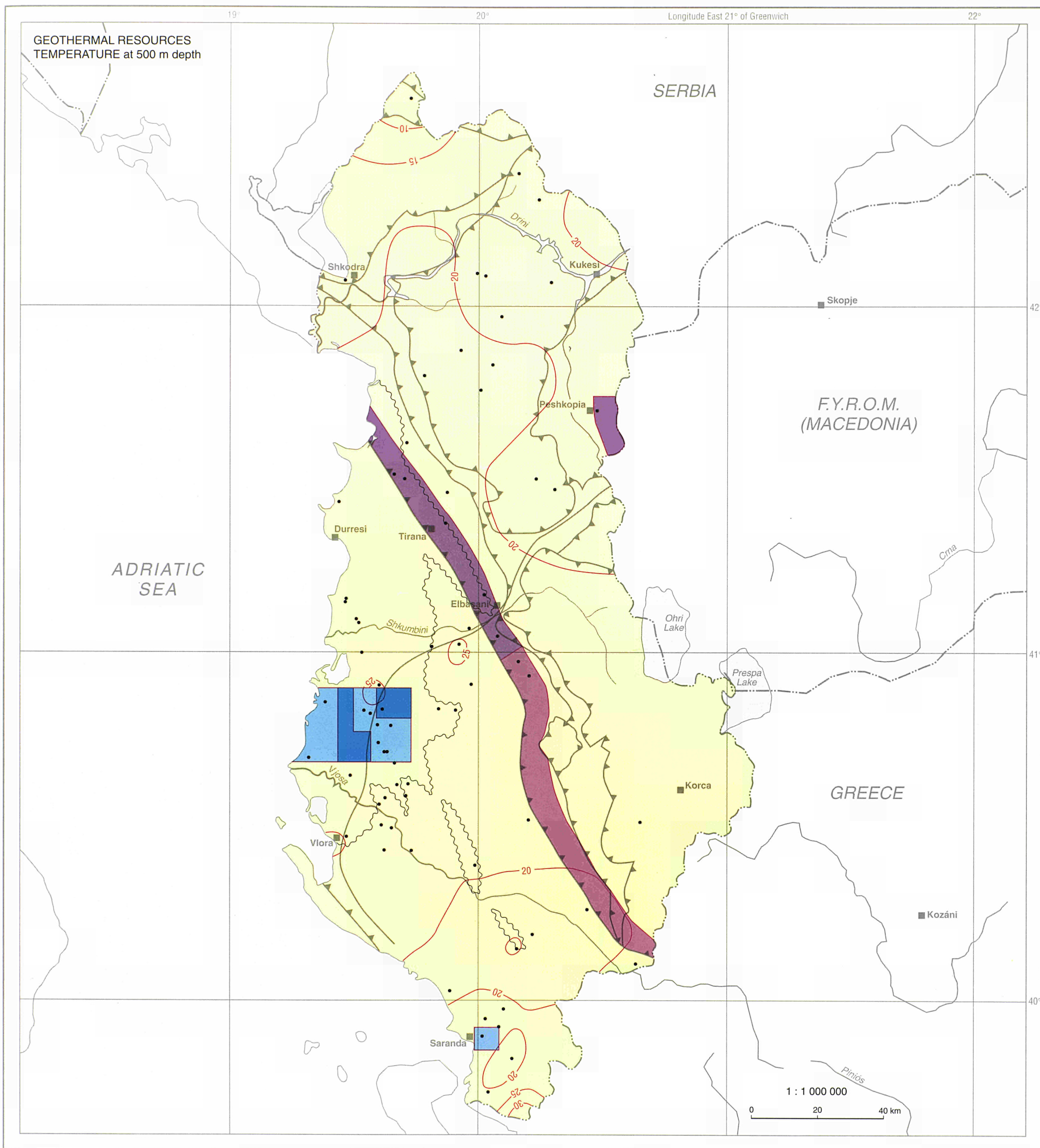






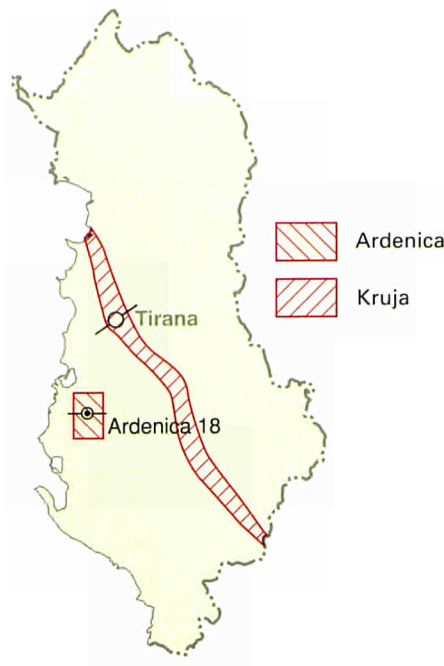
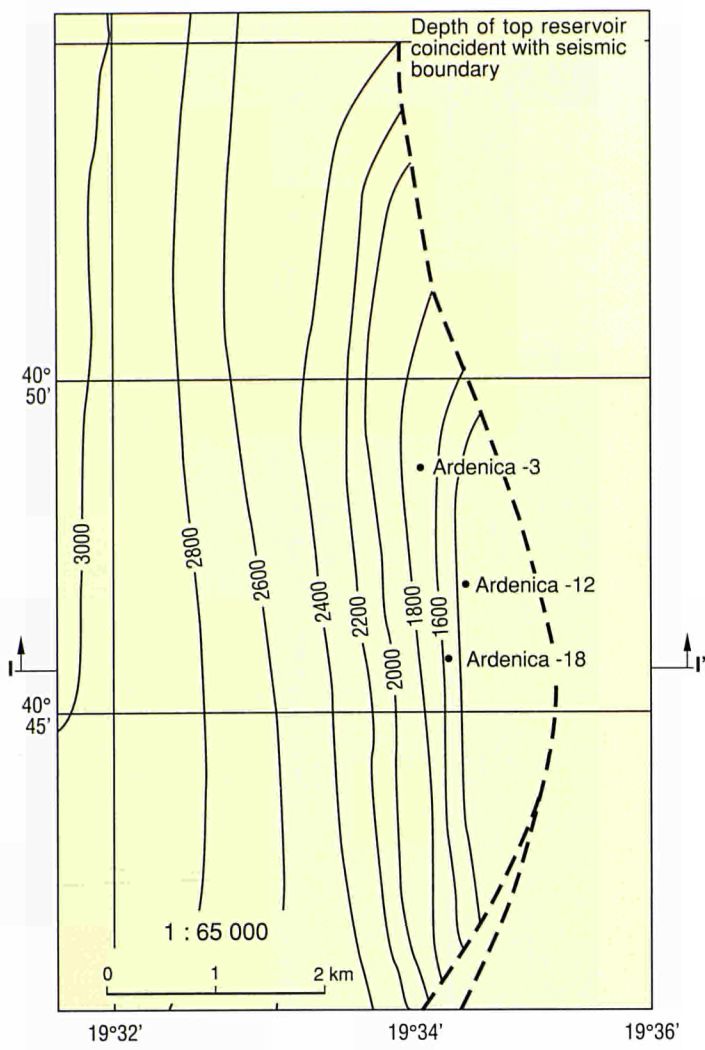
ALBANIA





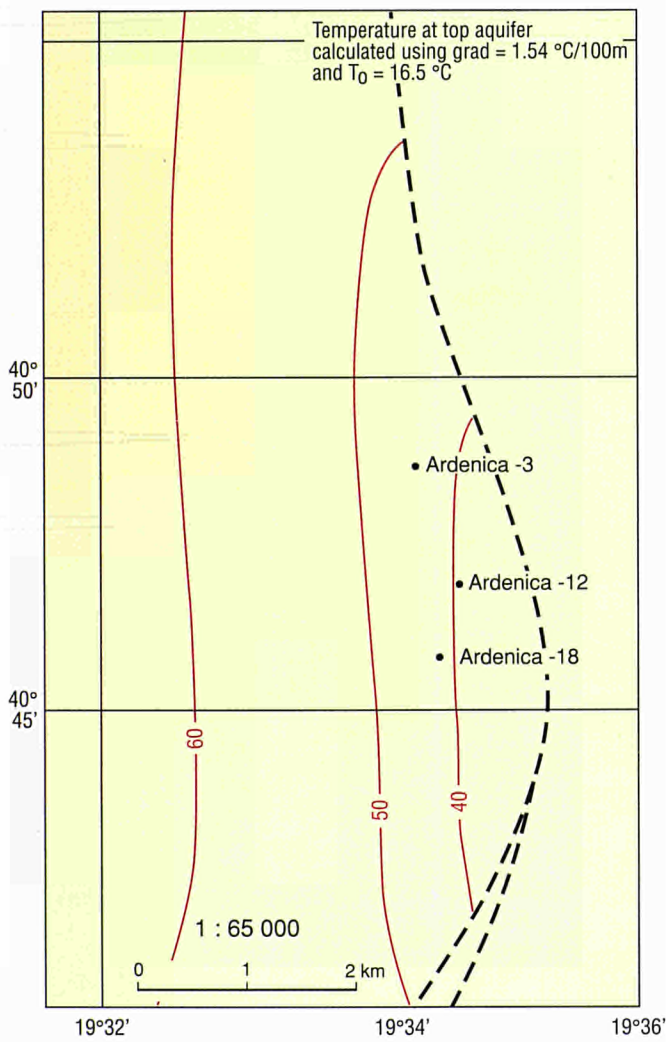
ALBANIA, Ardenica

DEPTH

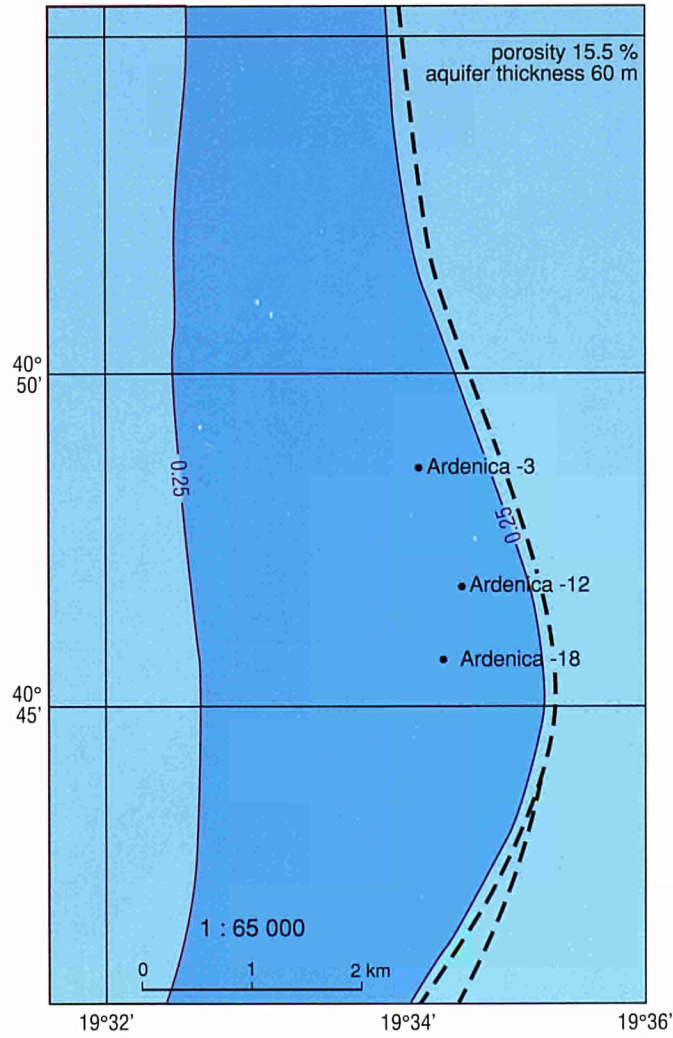


- Clay
- Hot water inflow
- Geological age boundary
- Seismic boundary
- Disjunctive tectonics
- Molasse
- Flyshoid
- Flysh
- Limestones
- Sandstones

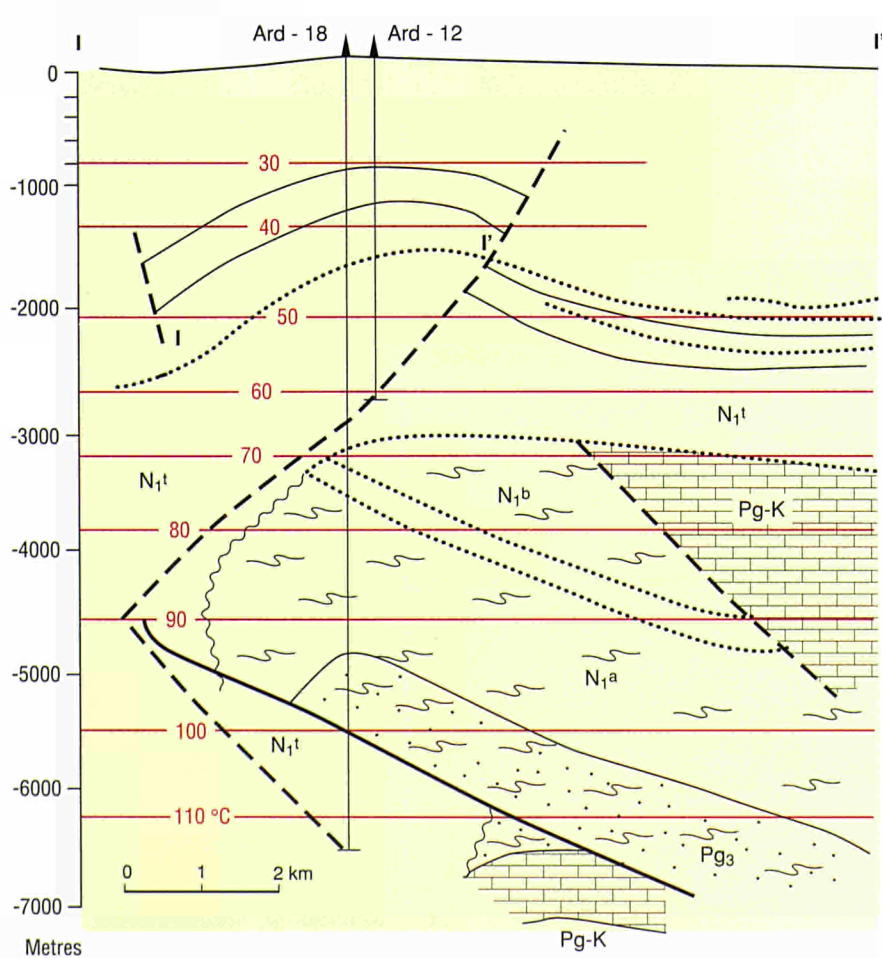
TEMPERATURE



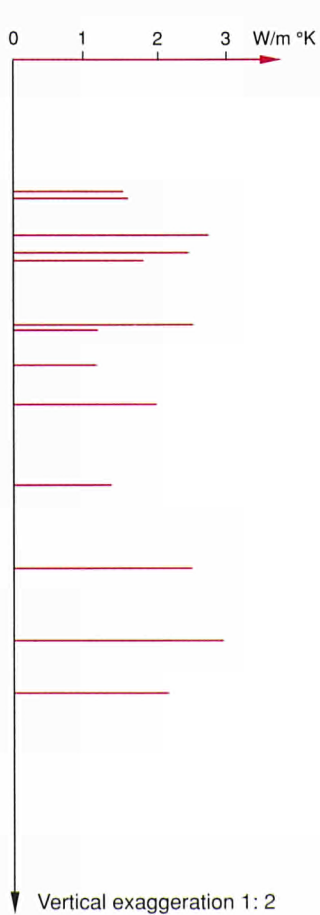
RESOURCES



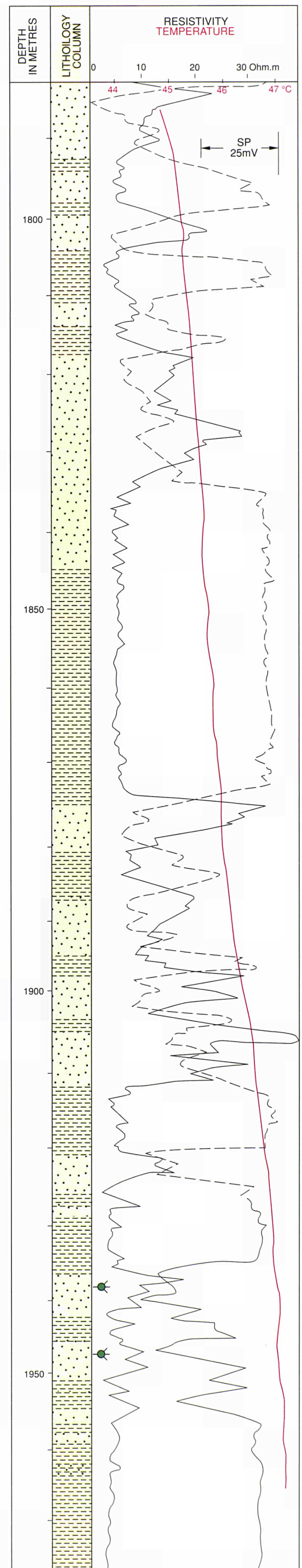
CROSS SECTION



THERMAL CONDUCTIVITY

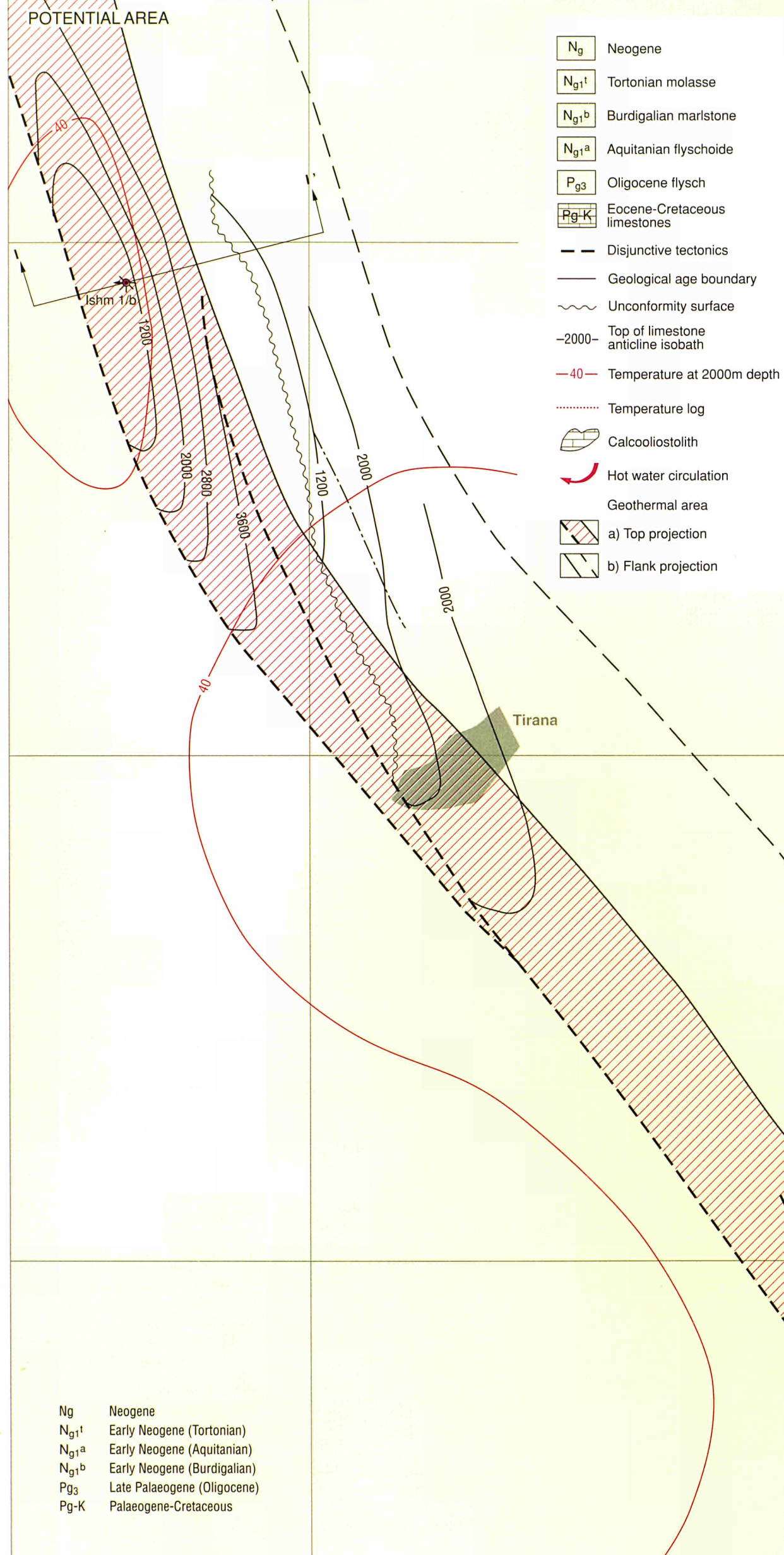
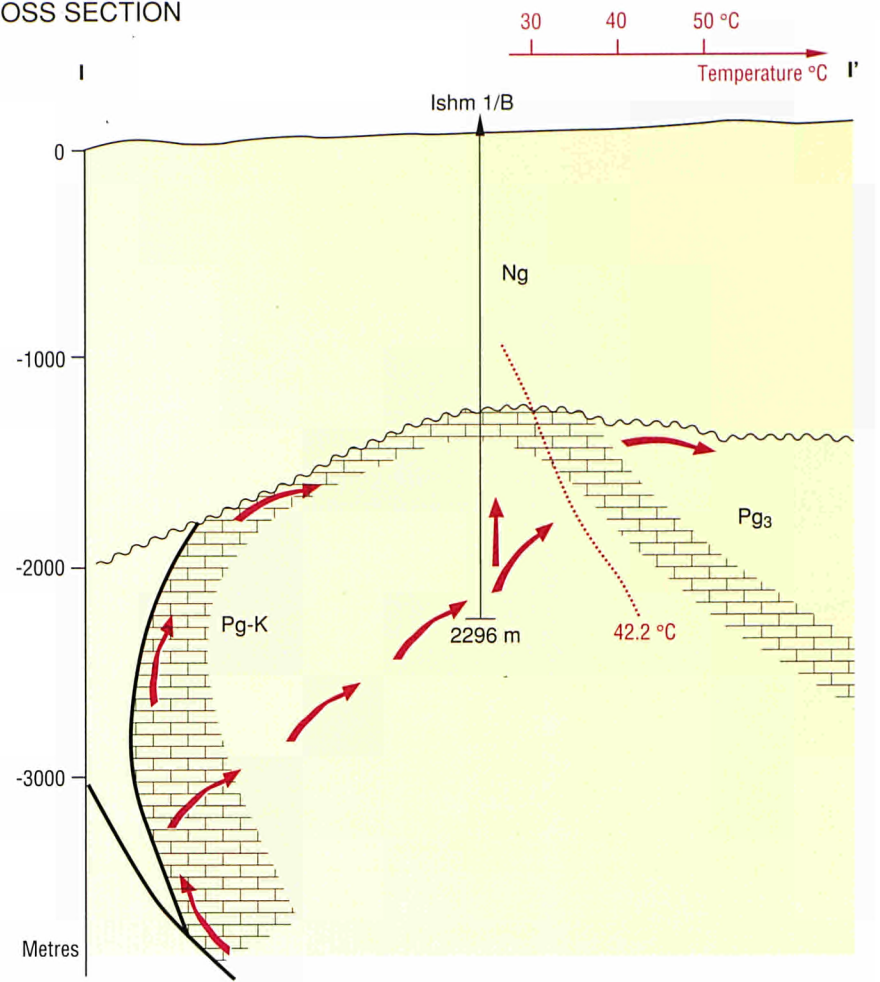


GEOPHYSICAL SECTION OF BOREHOLE ARDENICA -12



Longitude East 19°45' of Greenwich

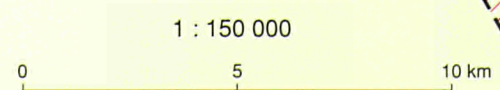
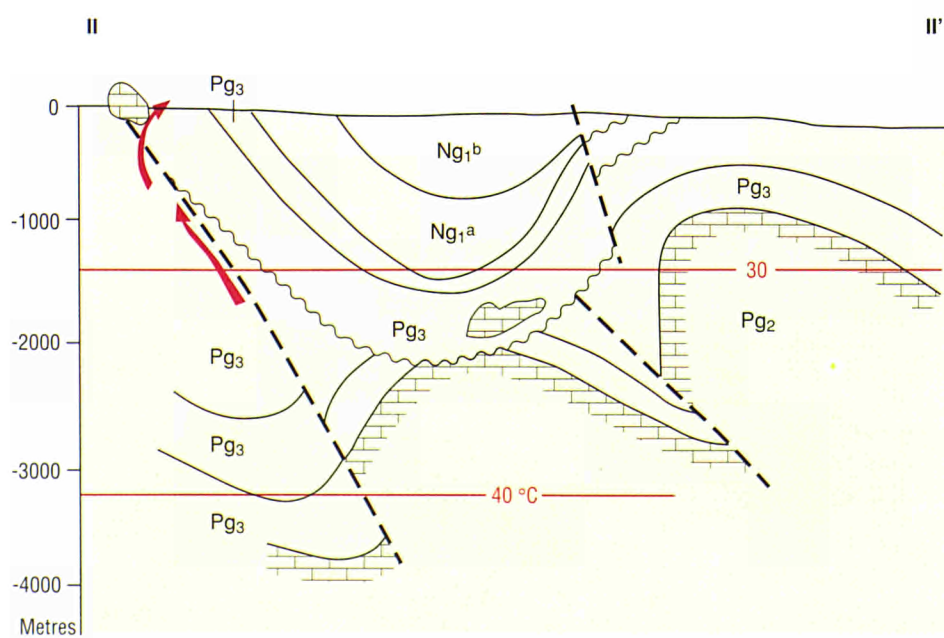
CROSS SECTION



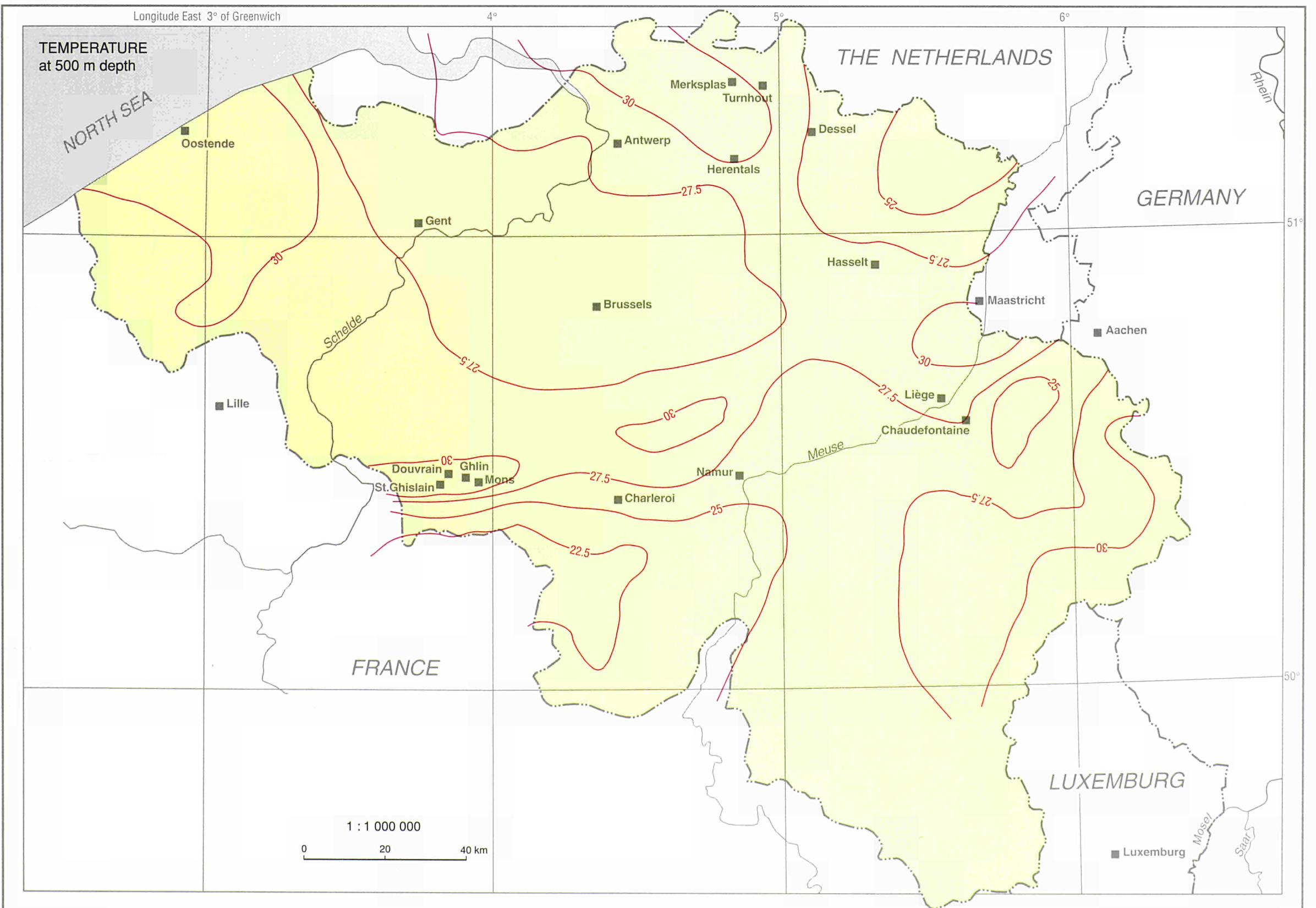
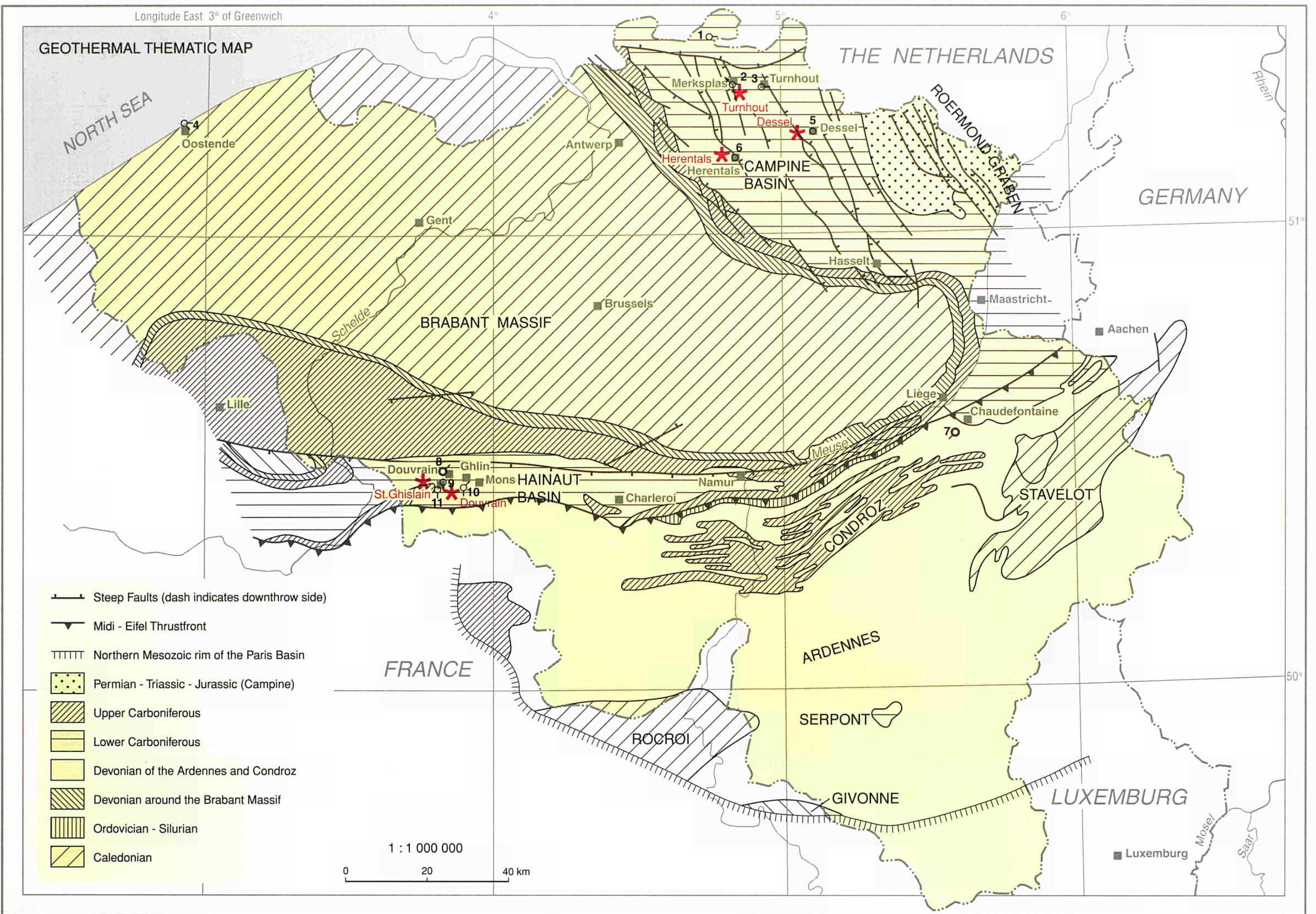
- Ng Neogene
- Ng₁^t Tortonian molasse
- Ng₁^b Burdigalian marlstone
- Ng₁^a Aquitanian flyschoides
- Pg₃ Oligocene flysch
- Pg-K Eocene-Cretaceous limestones
- Disjunctive tectonics
- Geological age boundary
- ~ Unconformity surface
- 2000- Top of limestone anticline isobath
- 40- Temperature at 2000m depth
- Temperature log
- Calcooliolith
- Hot water circulation
- Geothermal area
- a) Top projection
- b) Flank projection

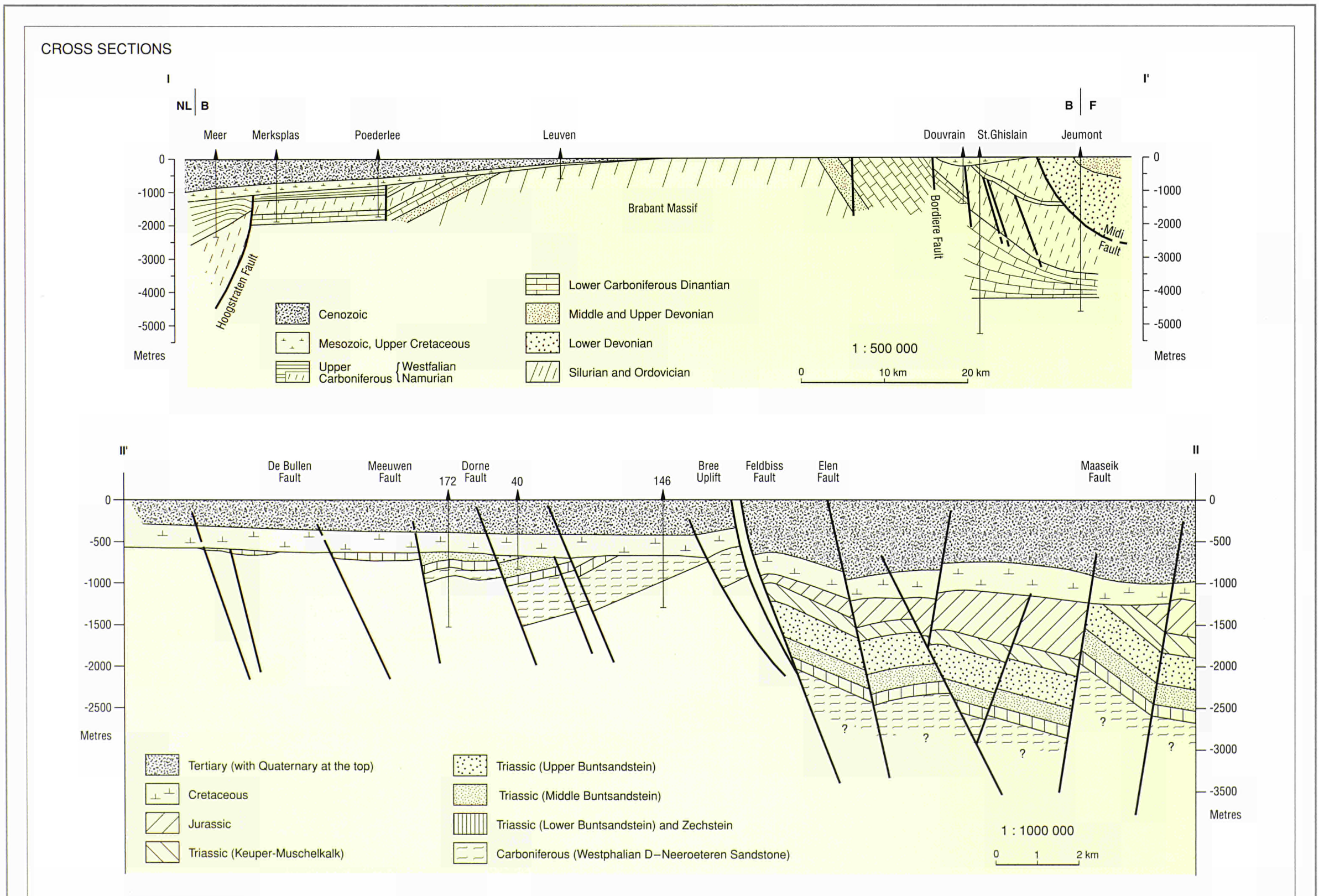
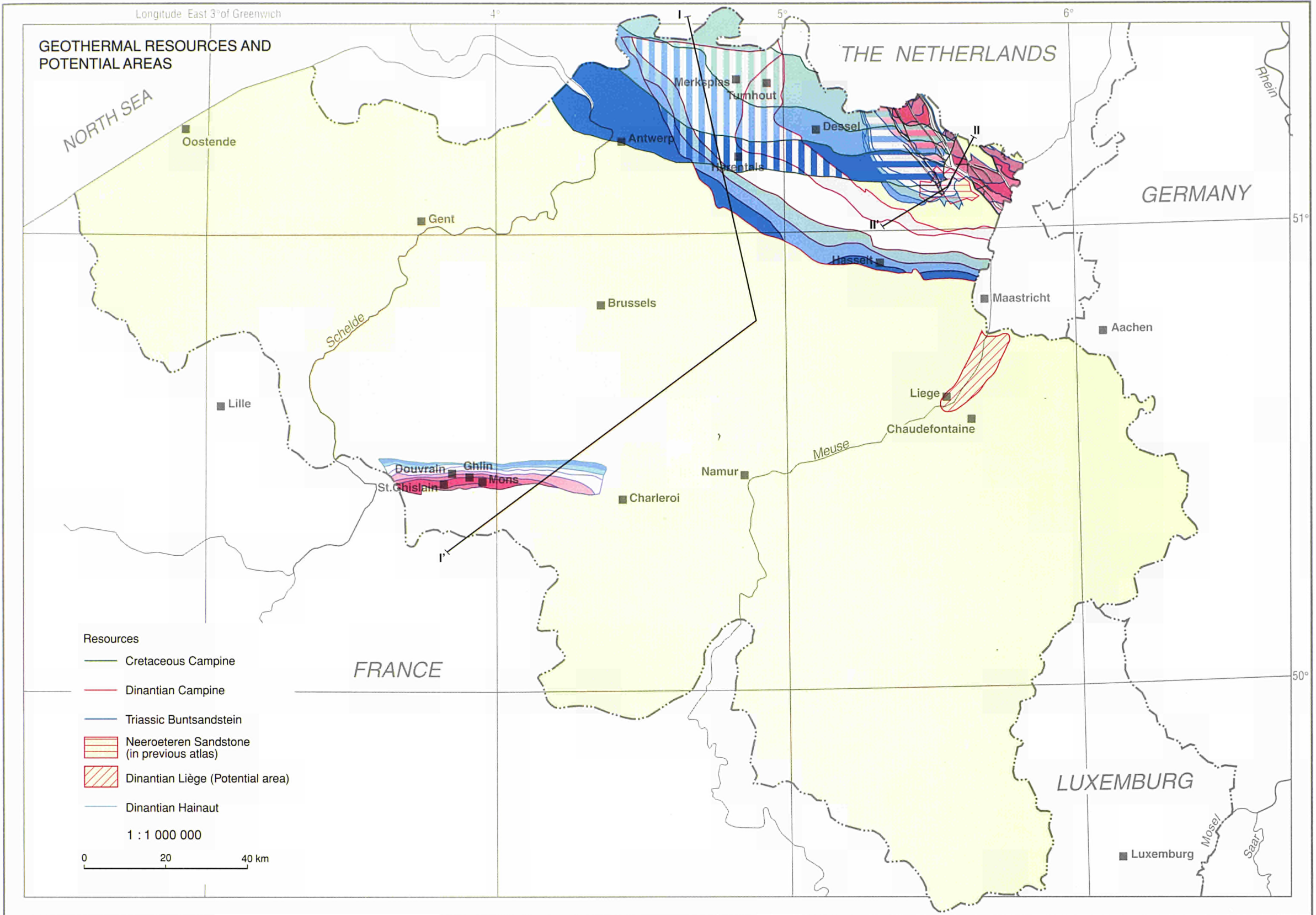
- Ng Neogene
- Ng₁^t Early Neogene (Tortonian)
- Ng₁^a Early Neogene (Aquitanian)
- Ng₁^b Early Neogene (Burdigalian)
- Pg₃ Late Palaeogene (Oligocene)
- Pg-K Palaeogene-Cretaceous

CROSS SECTION

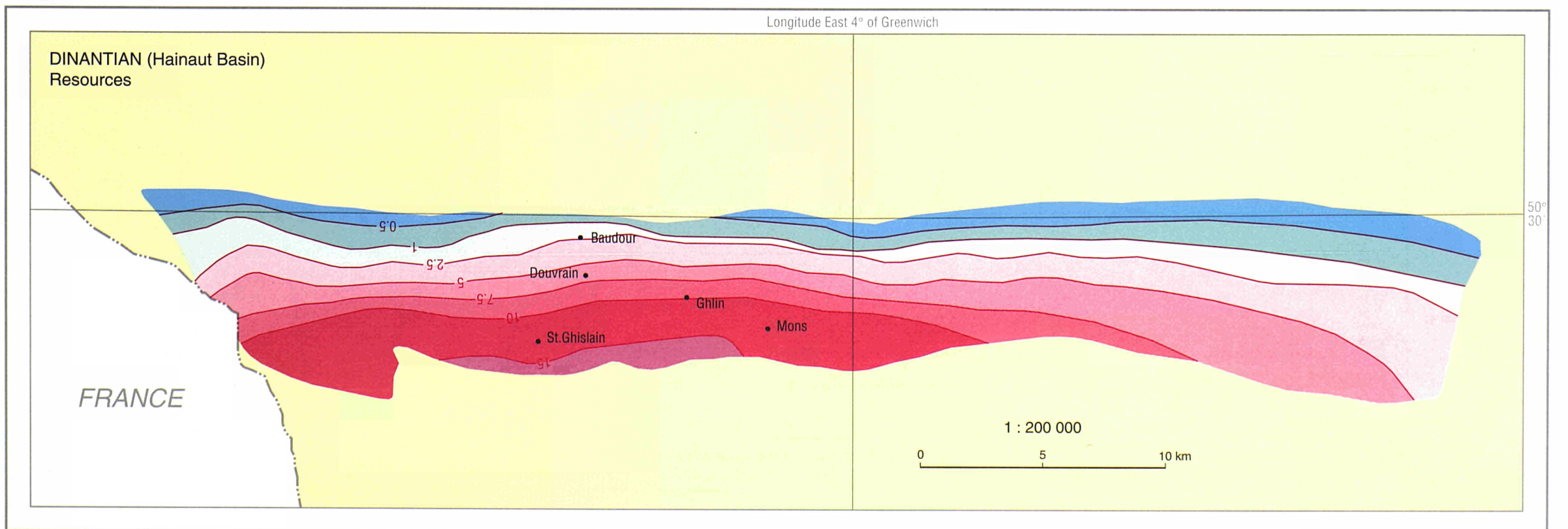
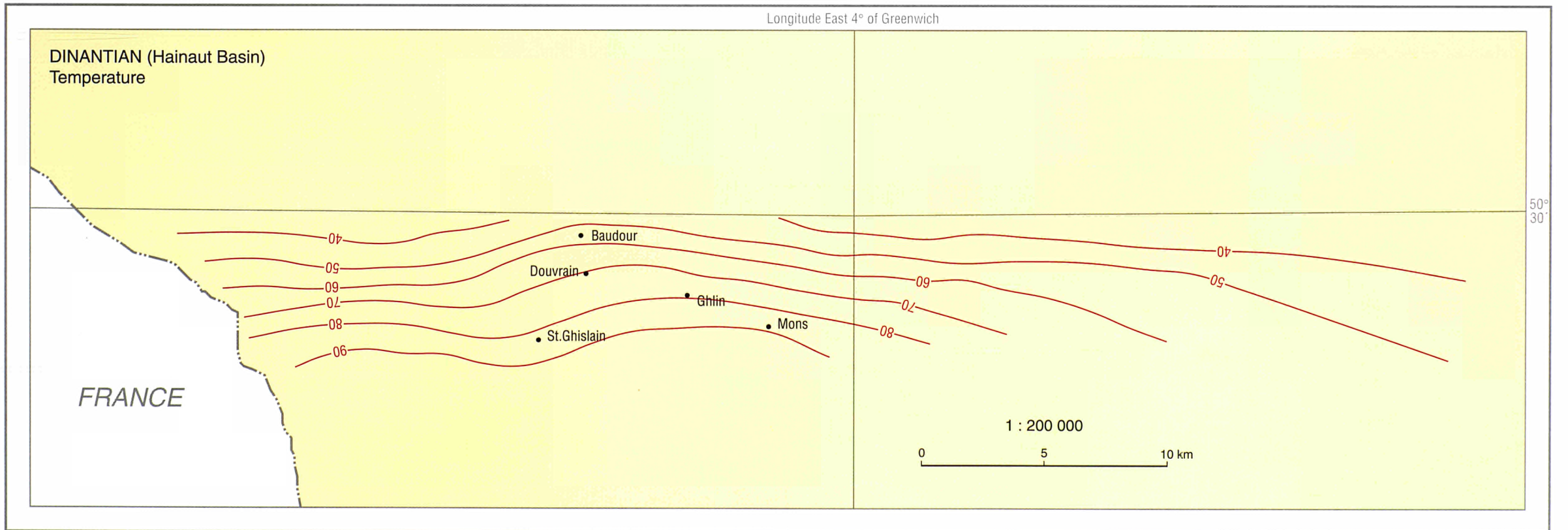
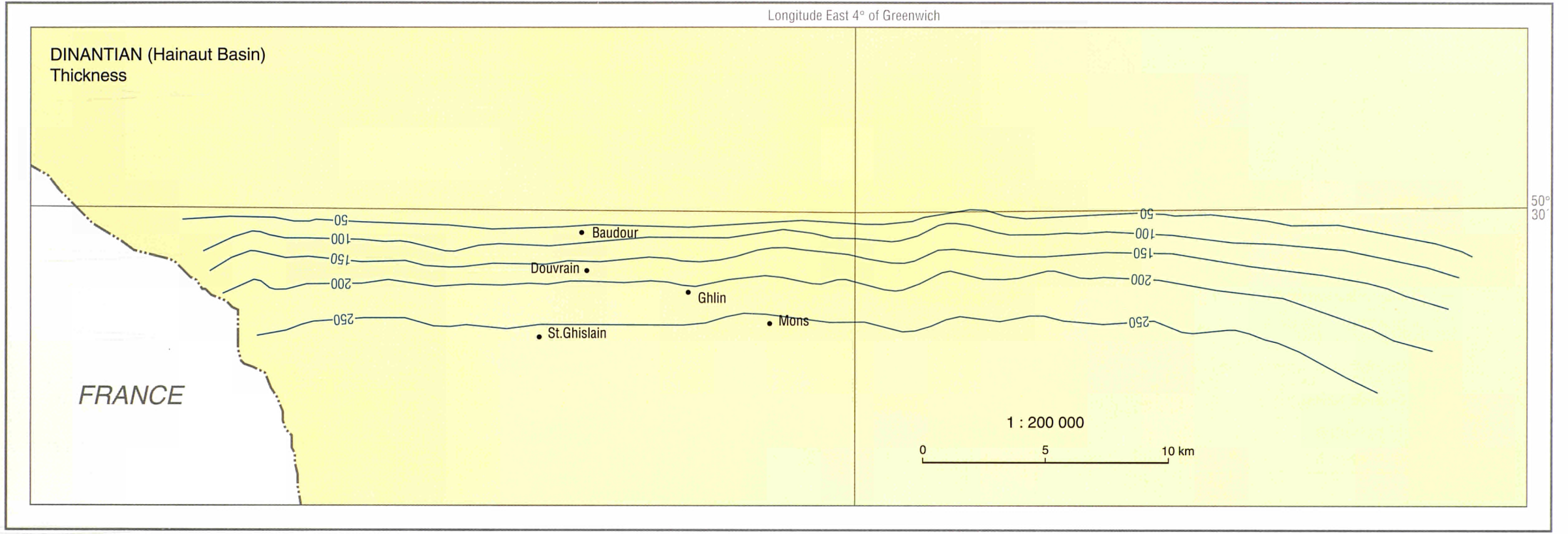
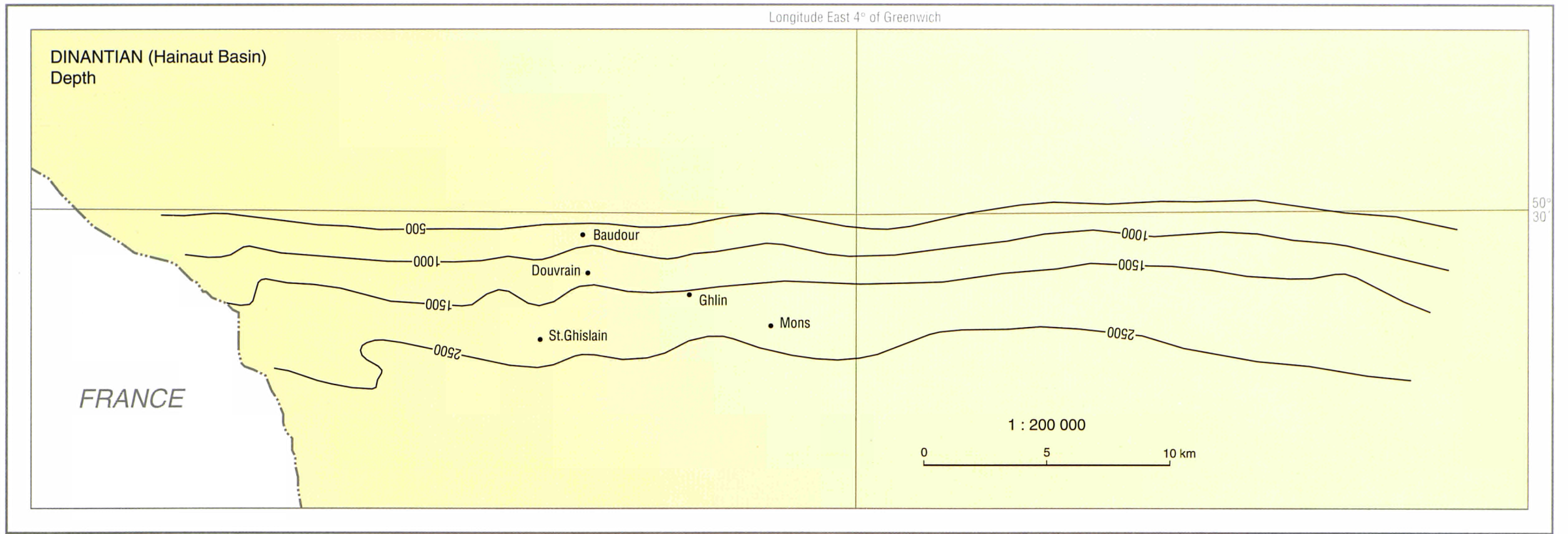


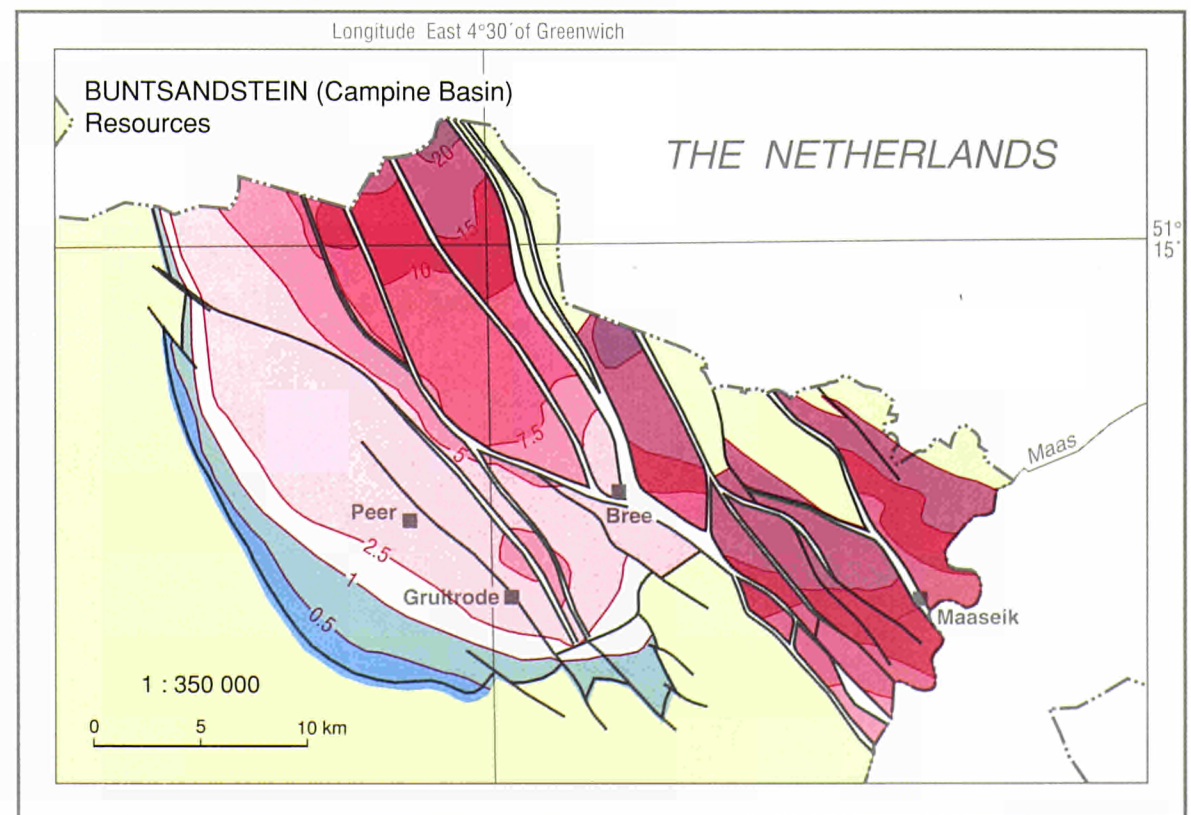
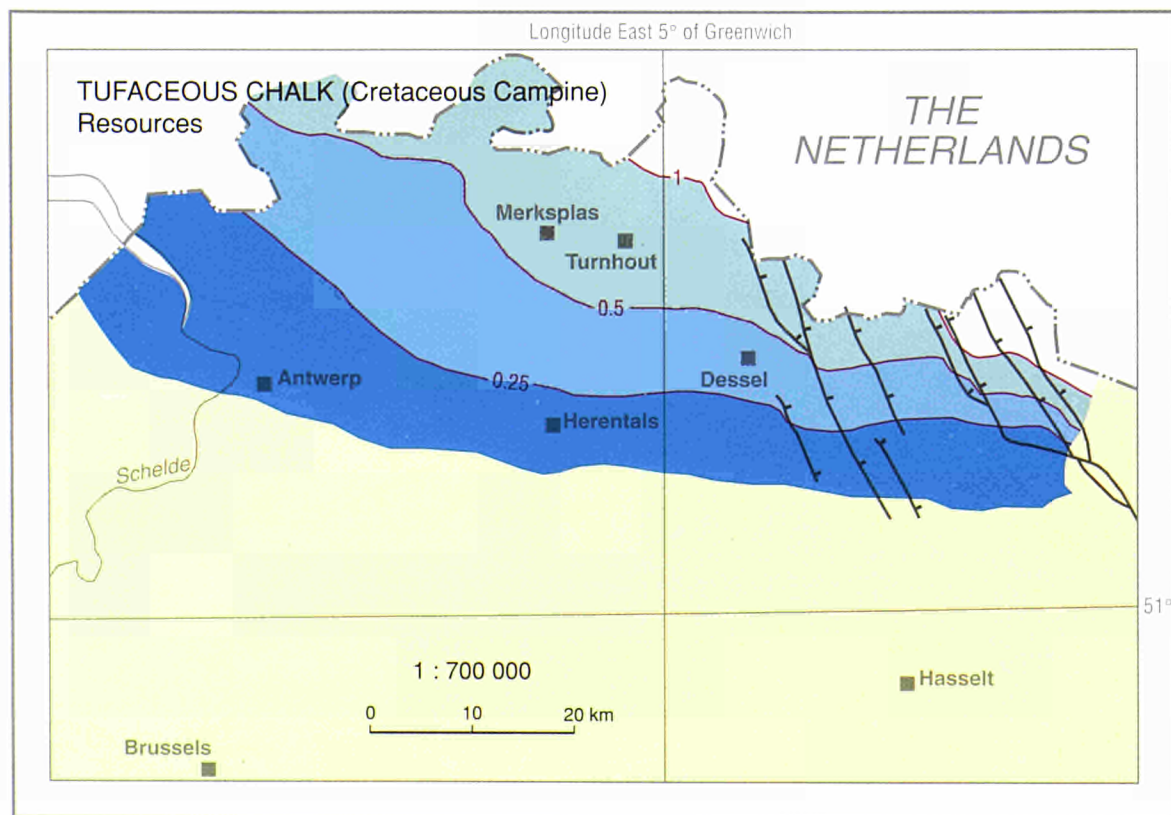
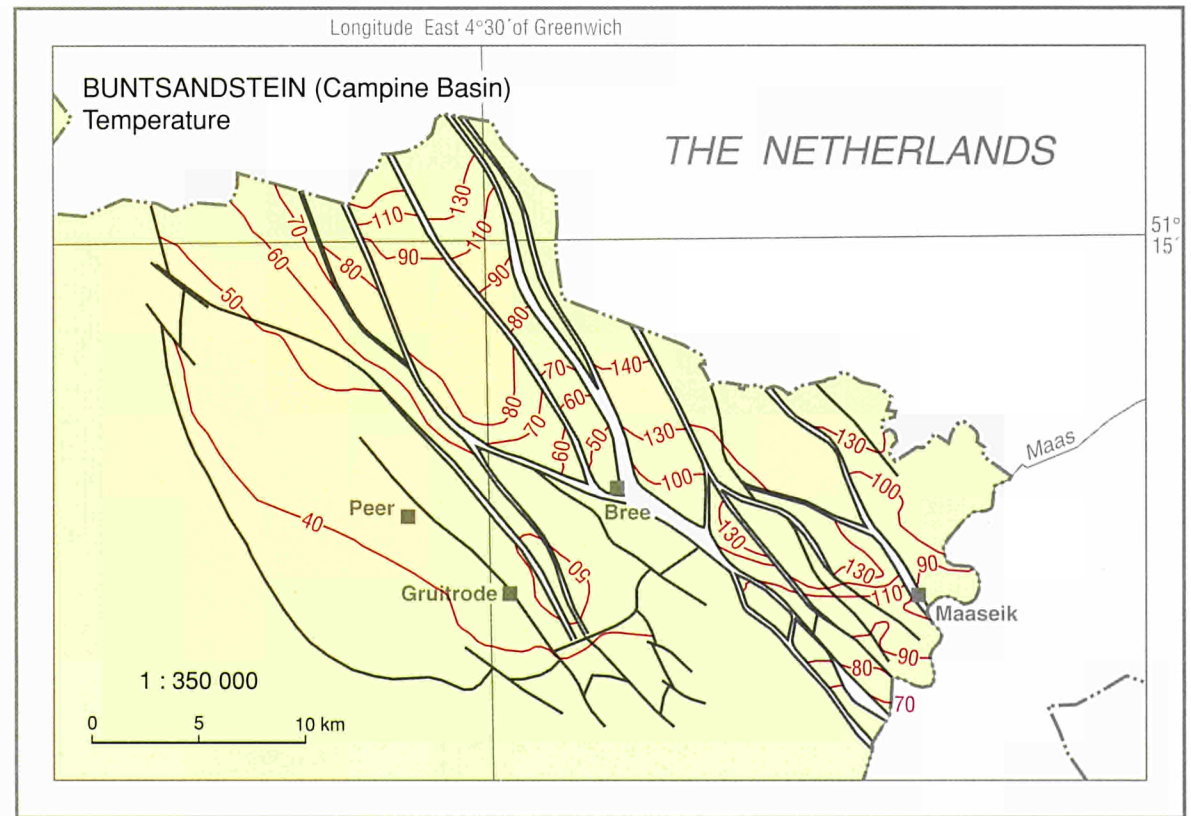
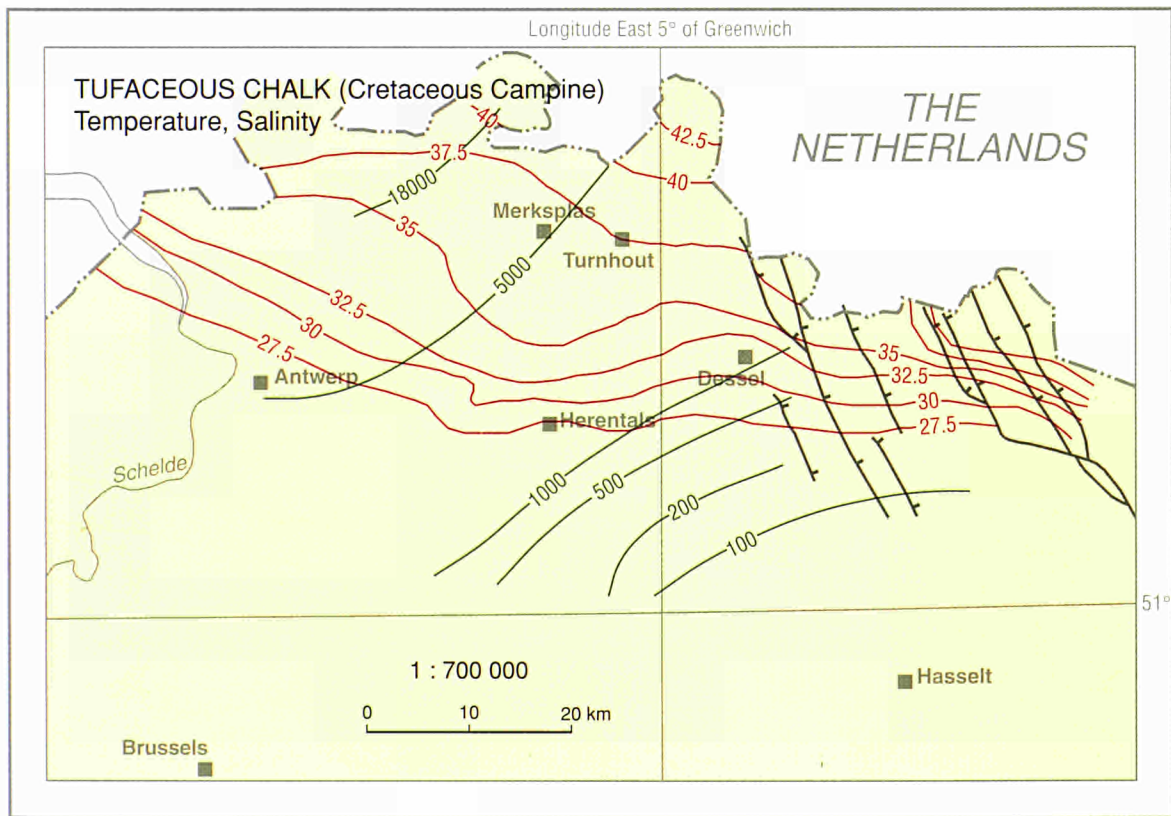
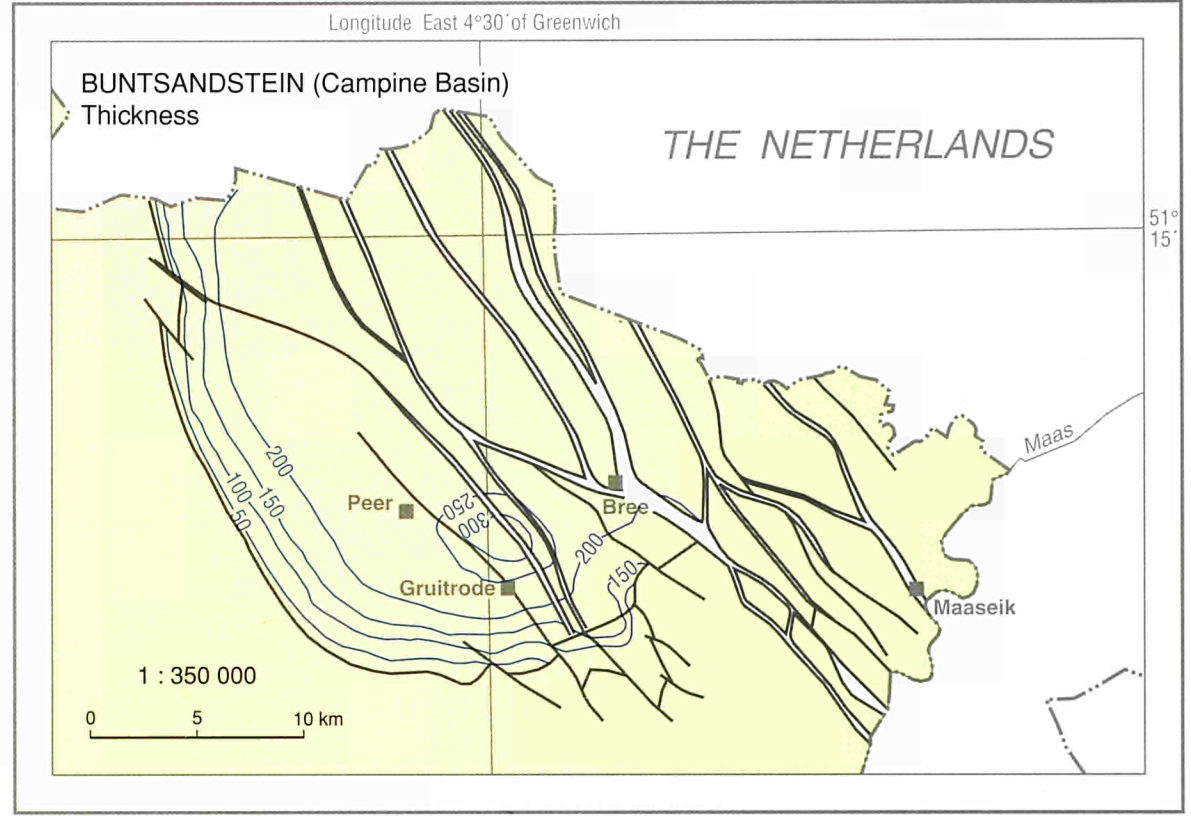
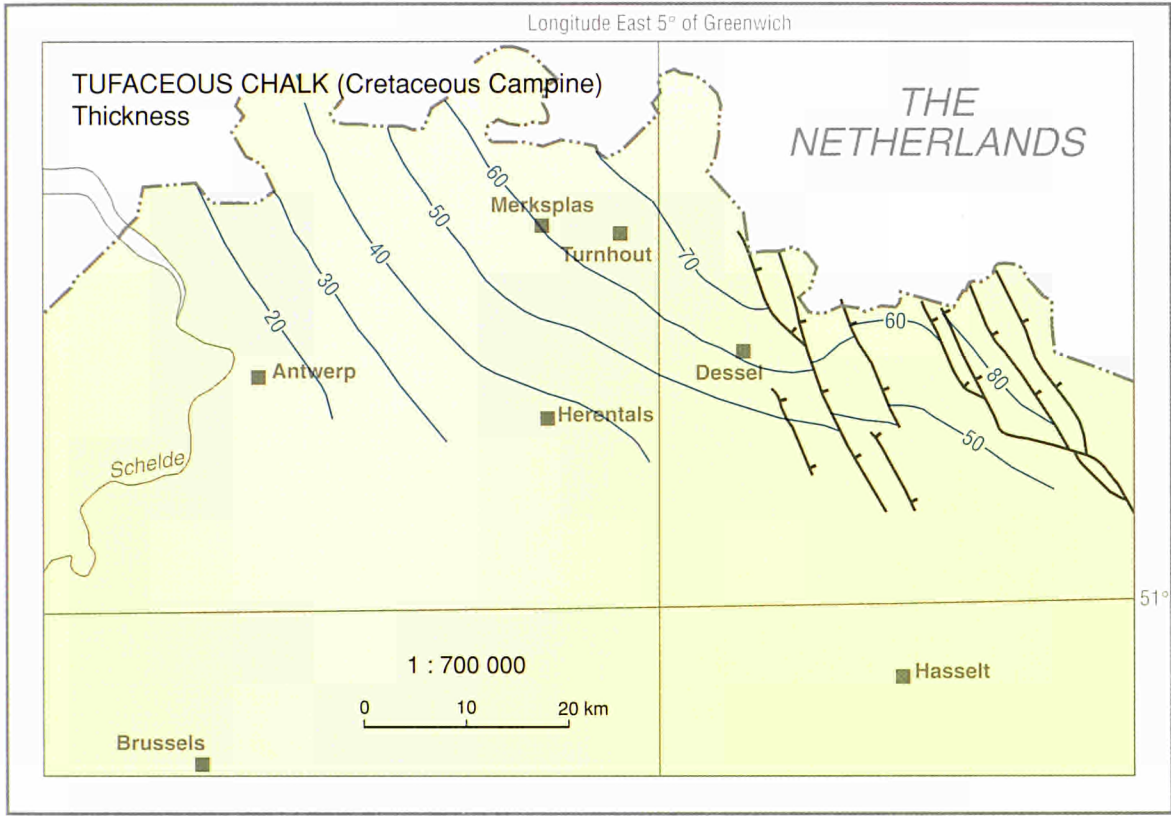
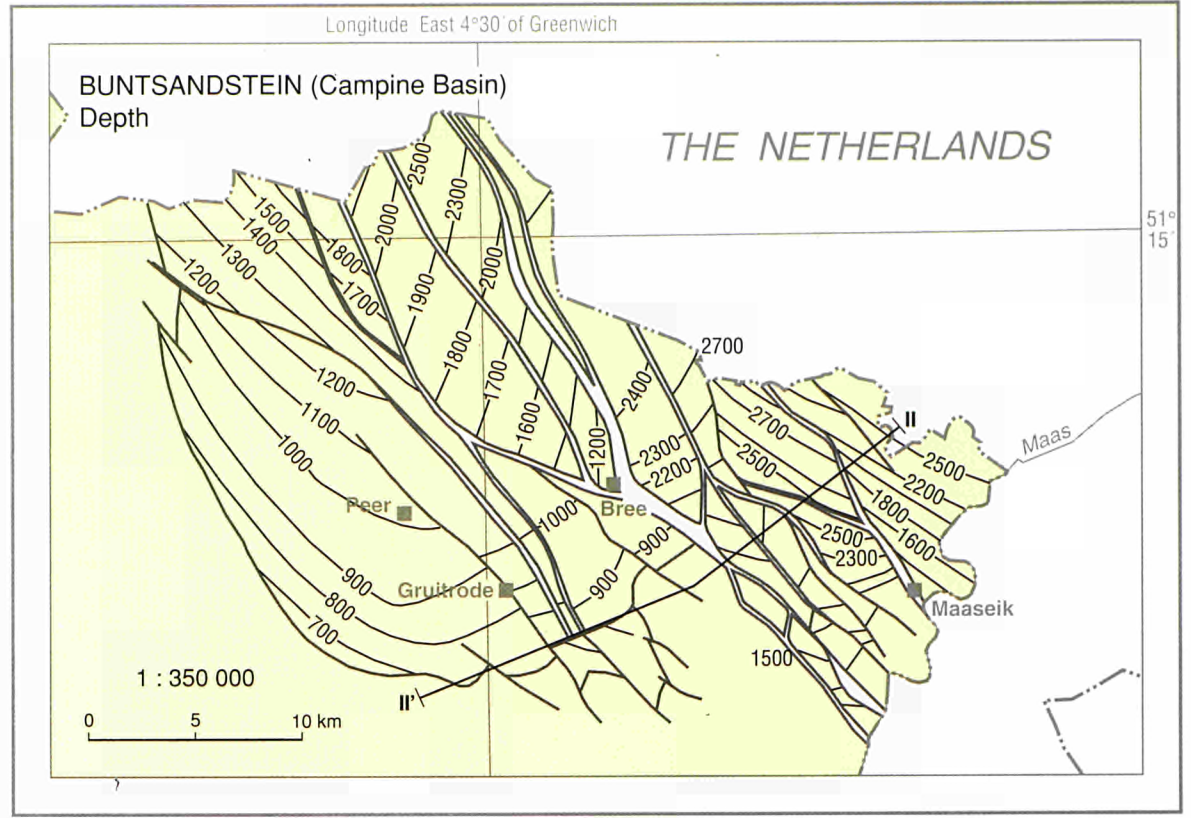
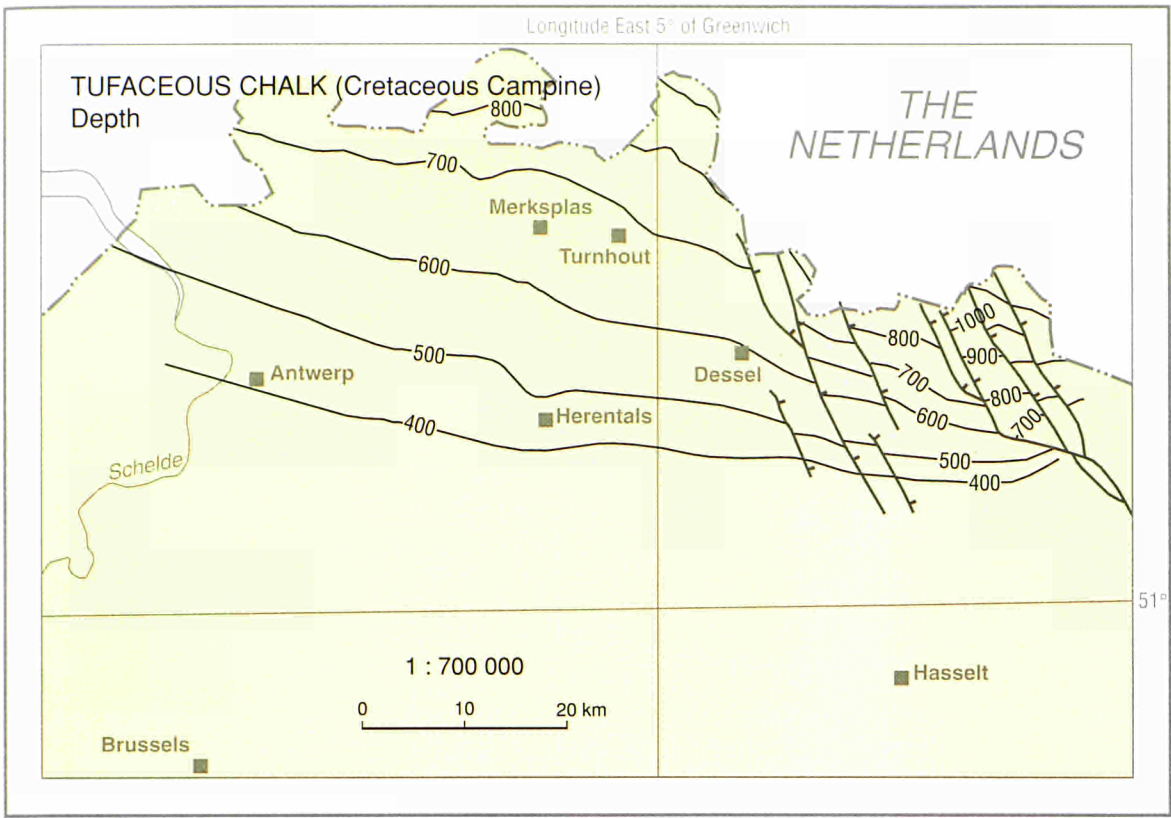
BELGIUM



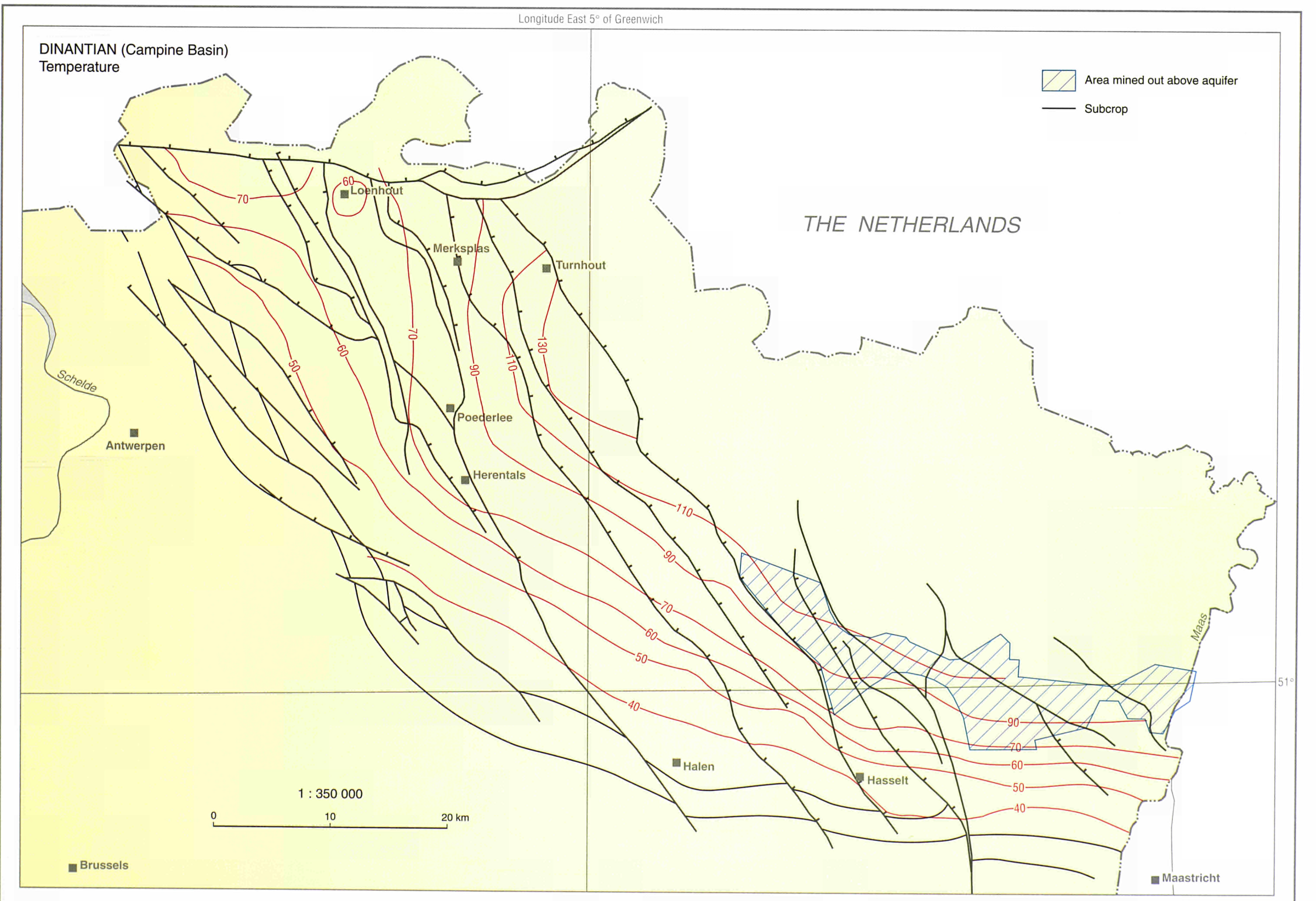
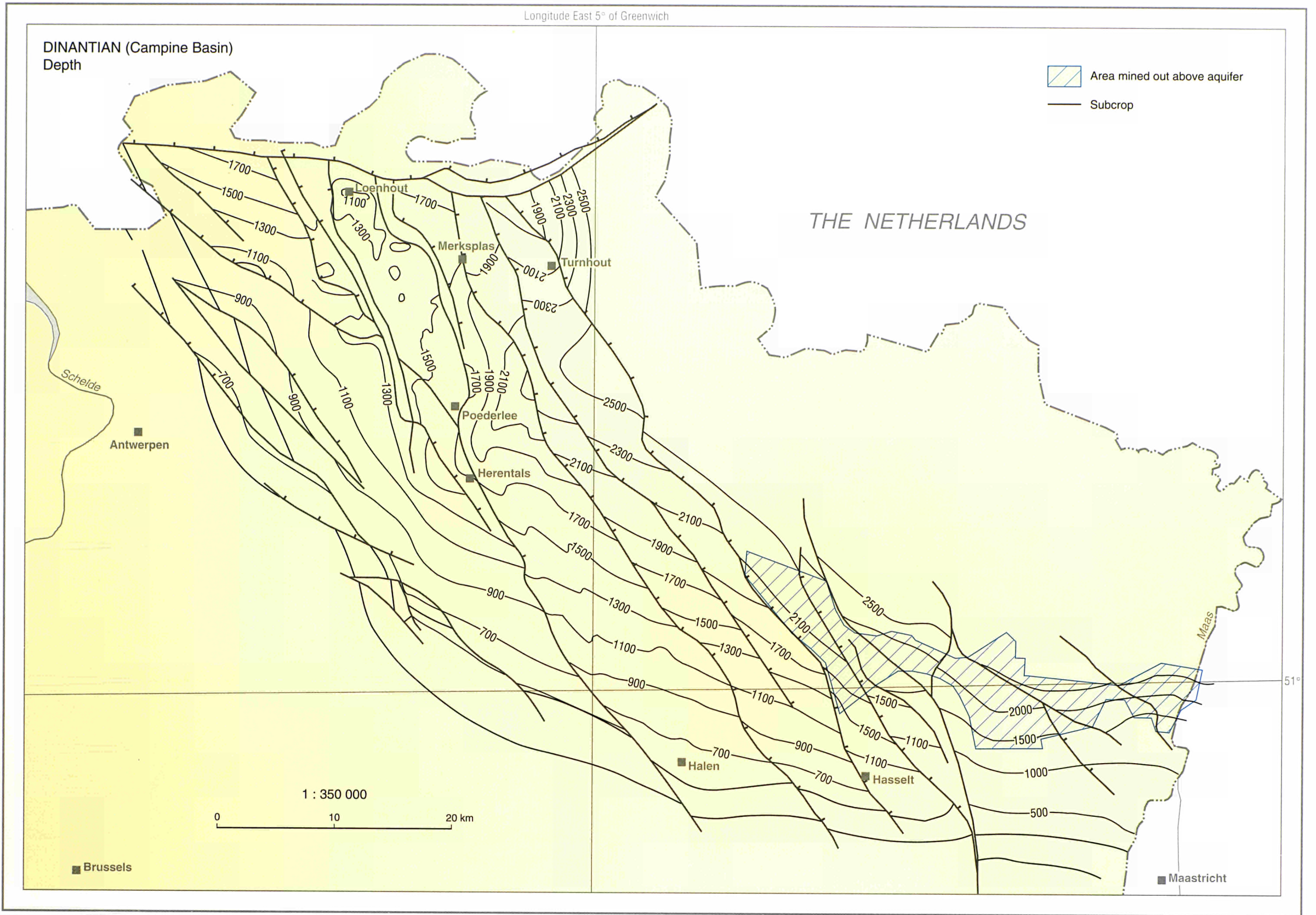


BELGIUM



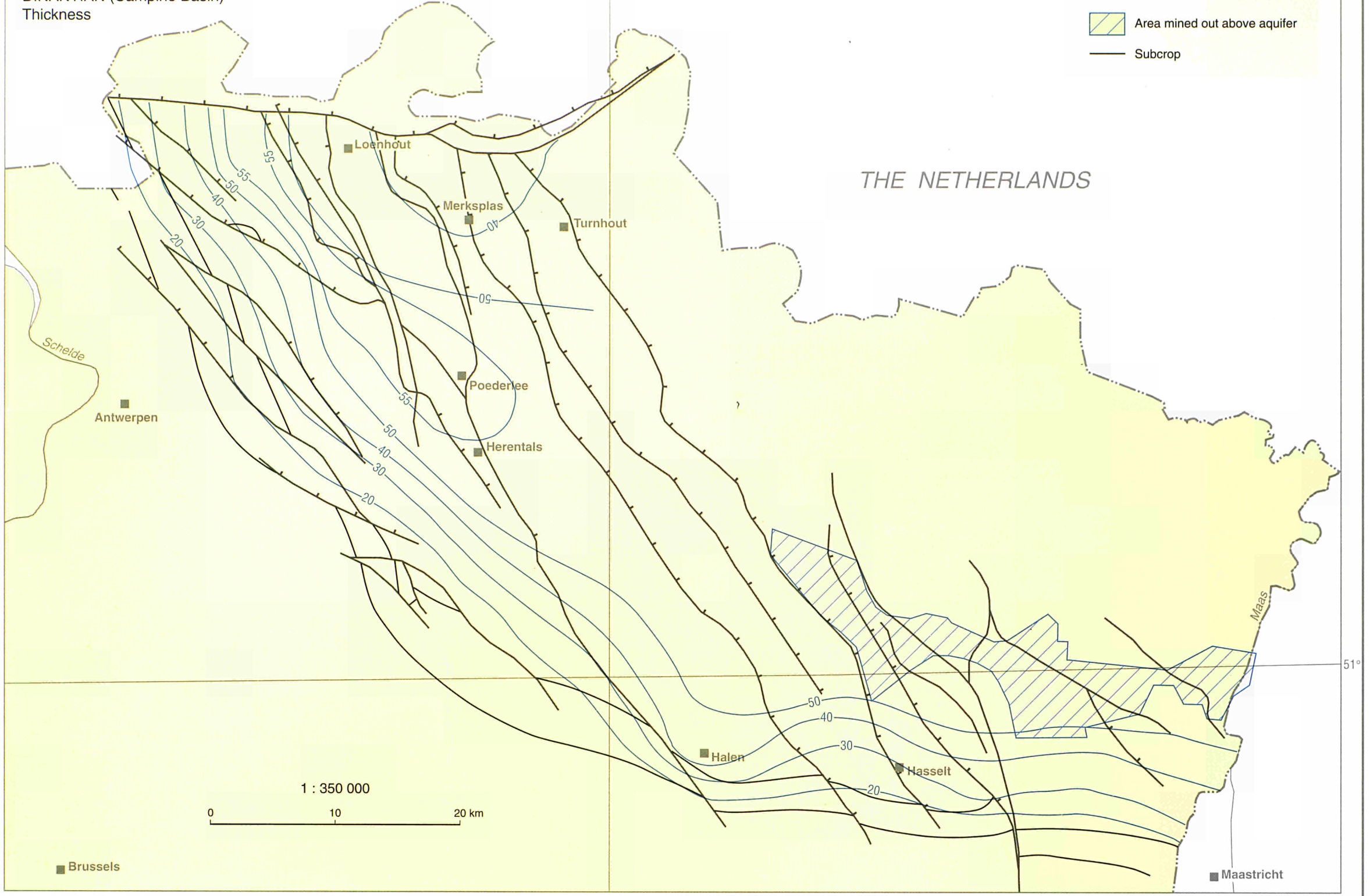


BELGIUM



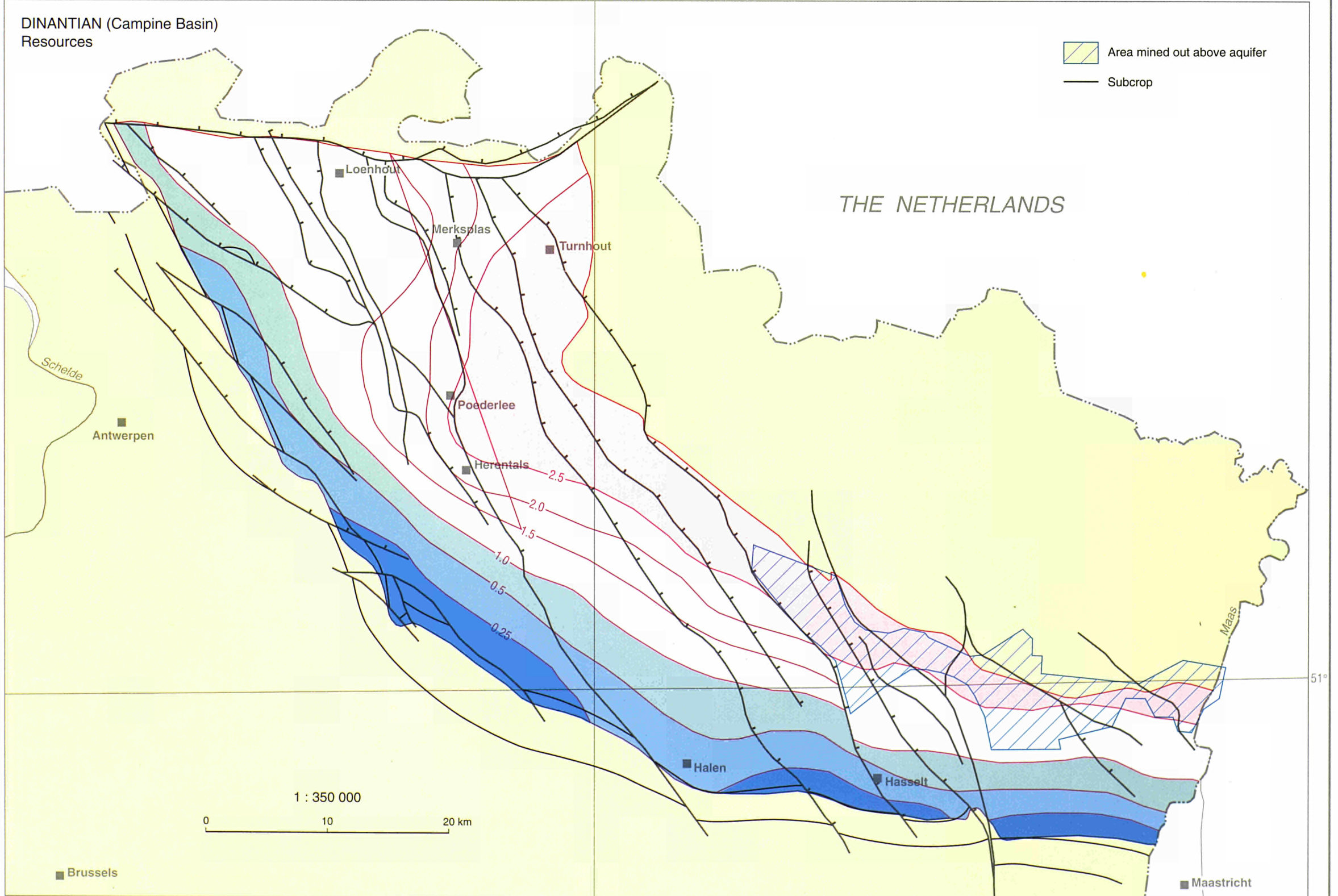
Longitude East 5° of Greenwich

**DINANTIAN (Campine Basin)
Thickness**

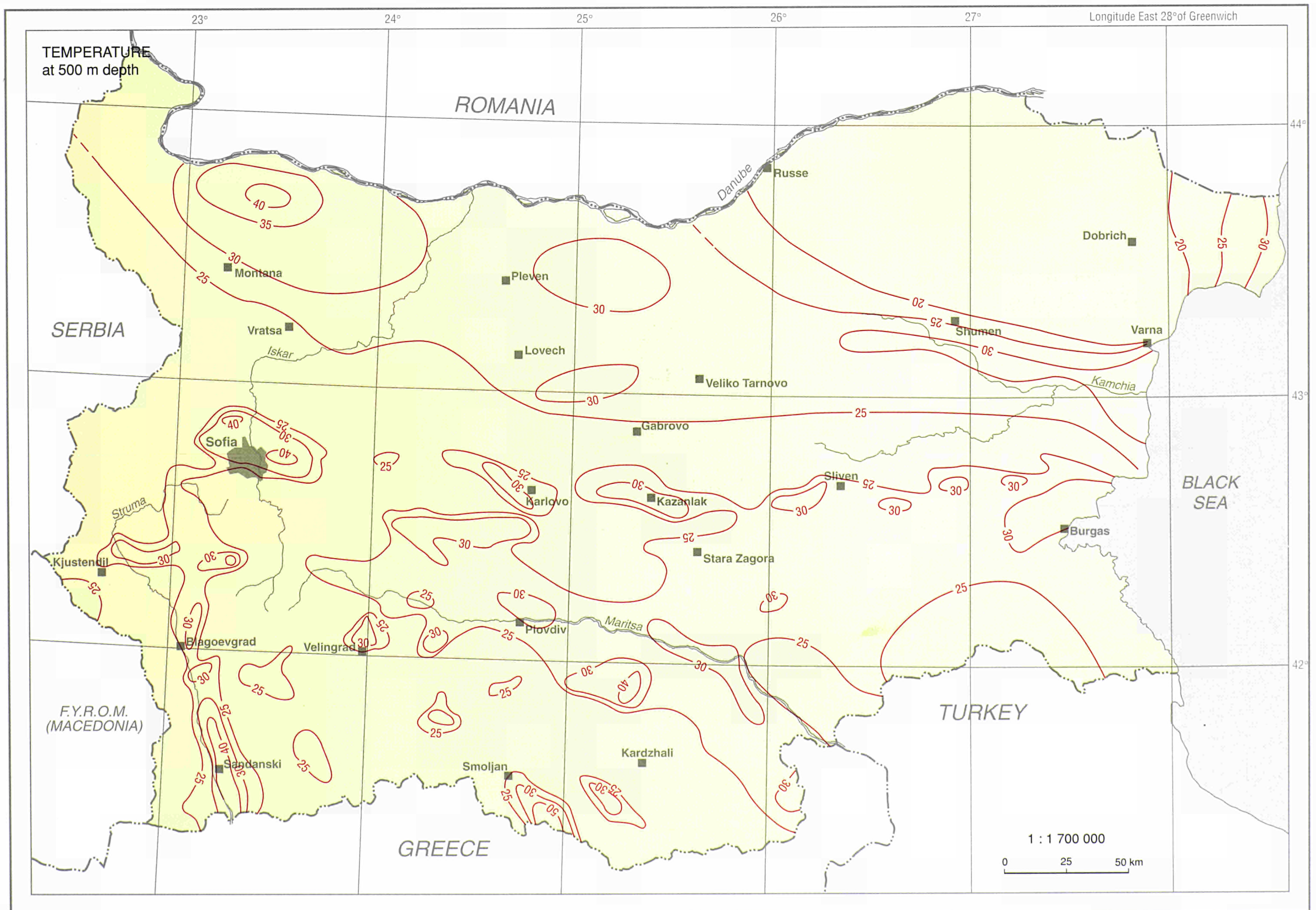
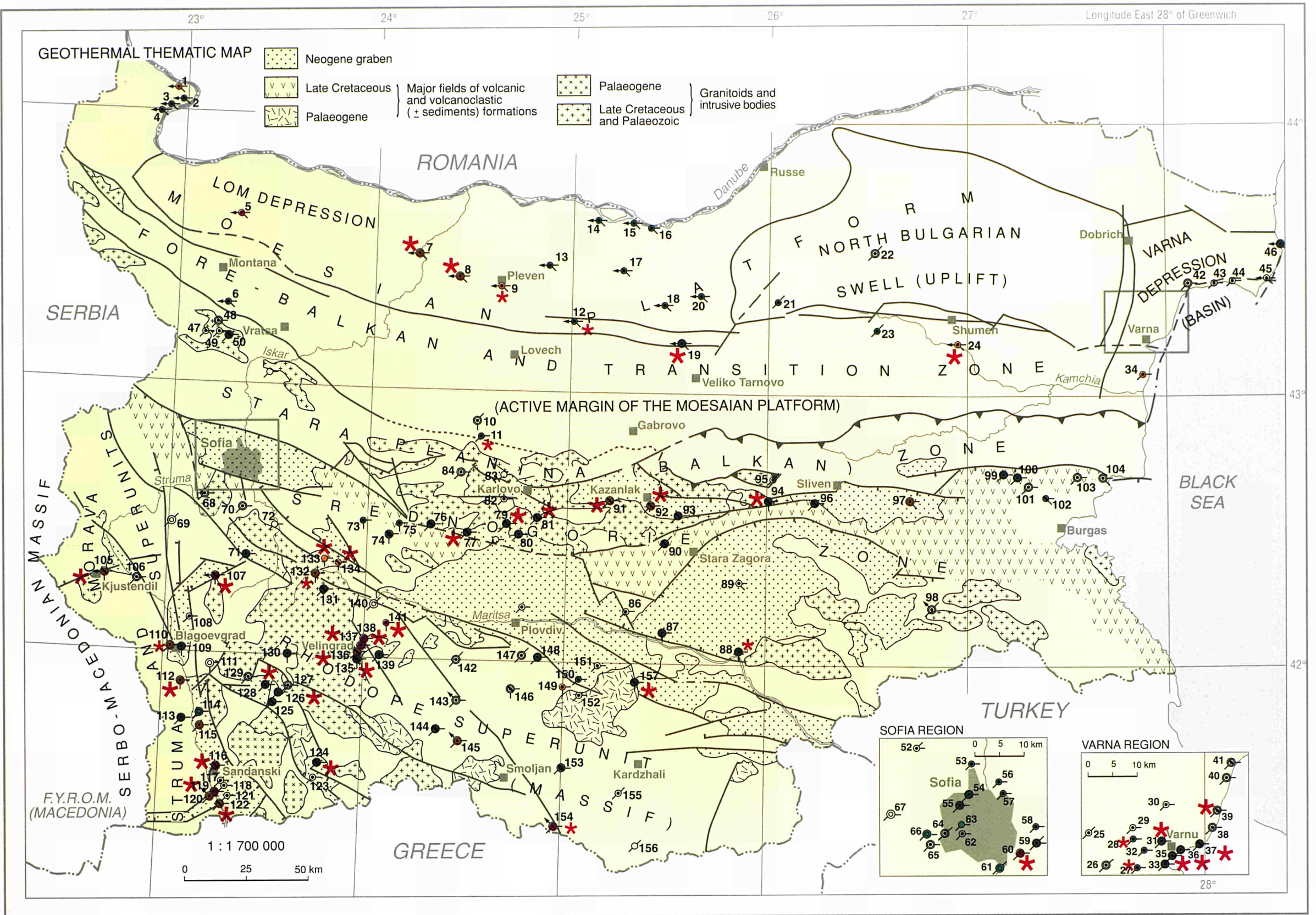


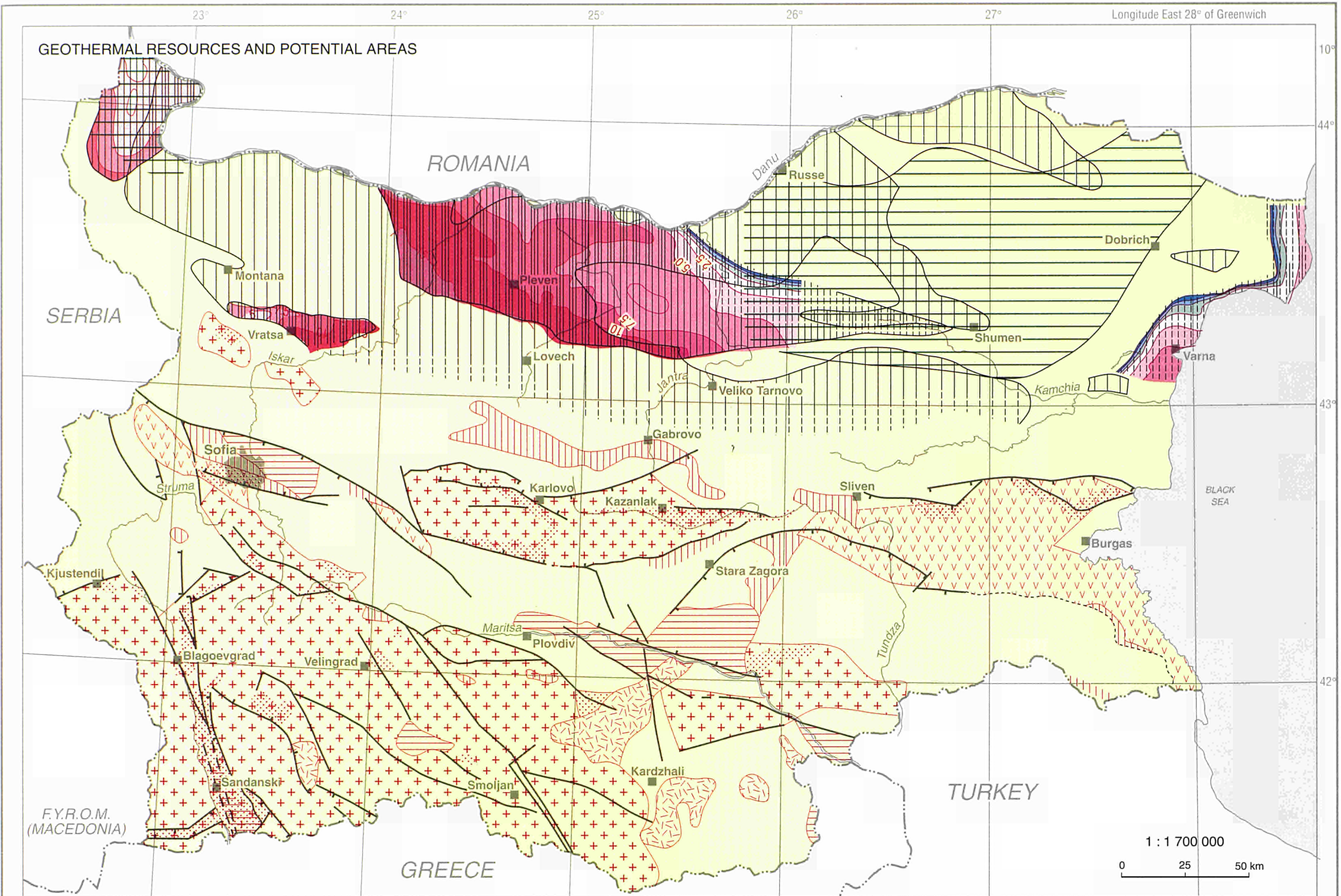
Longitude East 5° of Greenwich

**DINANTIAN (Campine Basin)
Resources**



BULGARIA



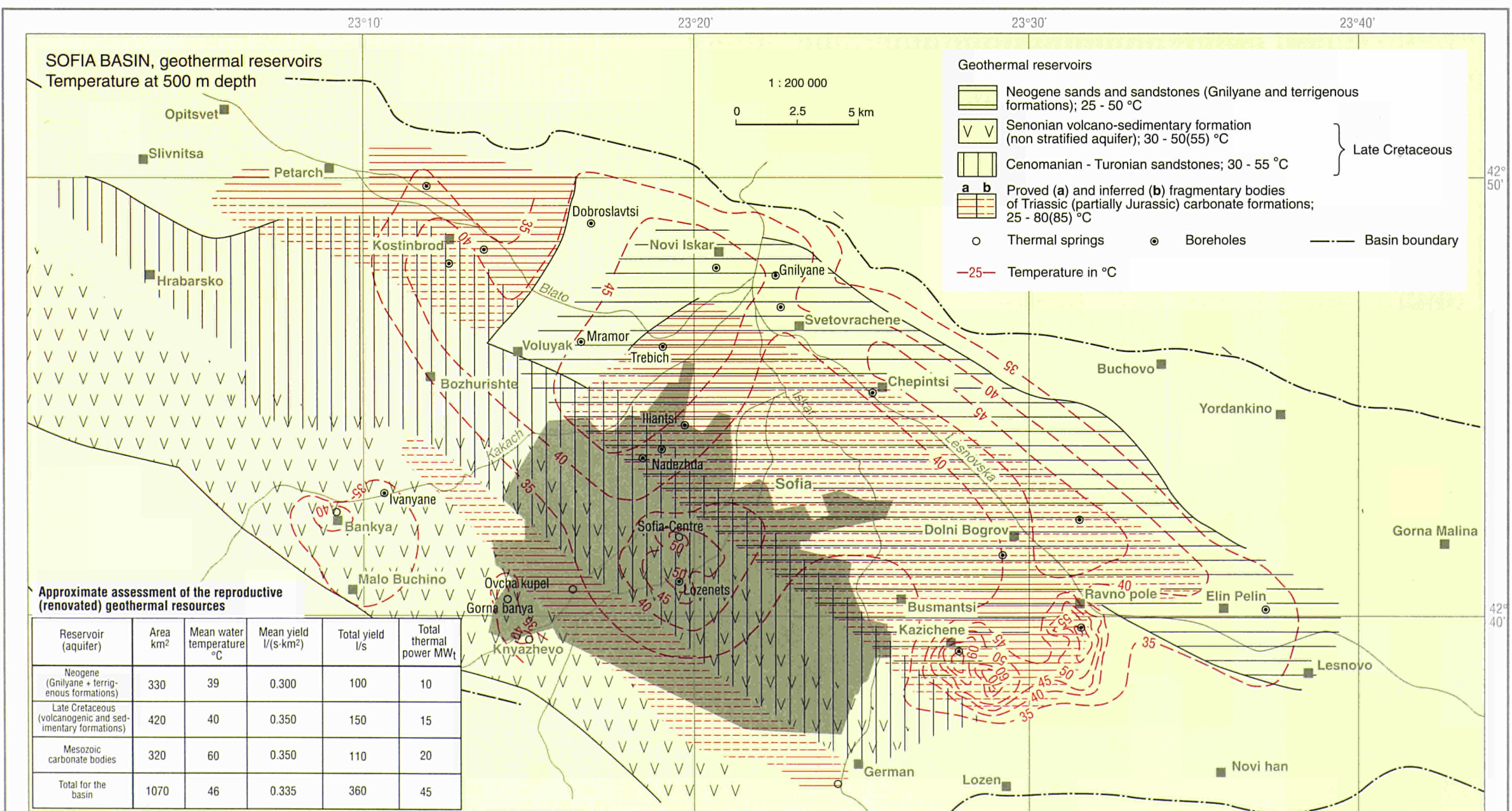


Regional geothermal reservoirs in carbonate formations (aquifers)

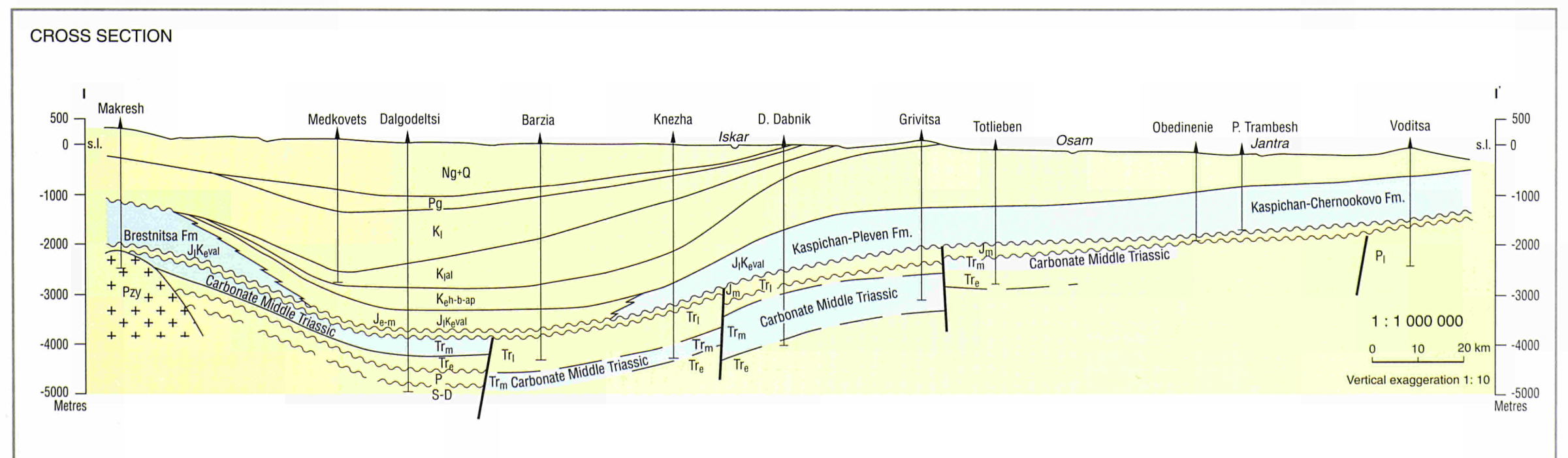
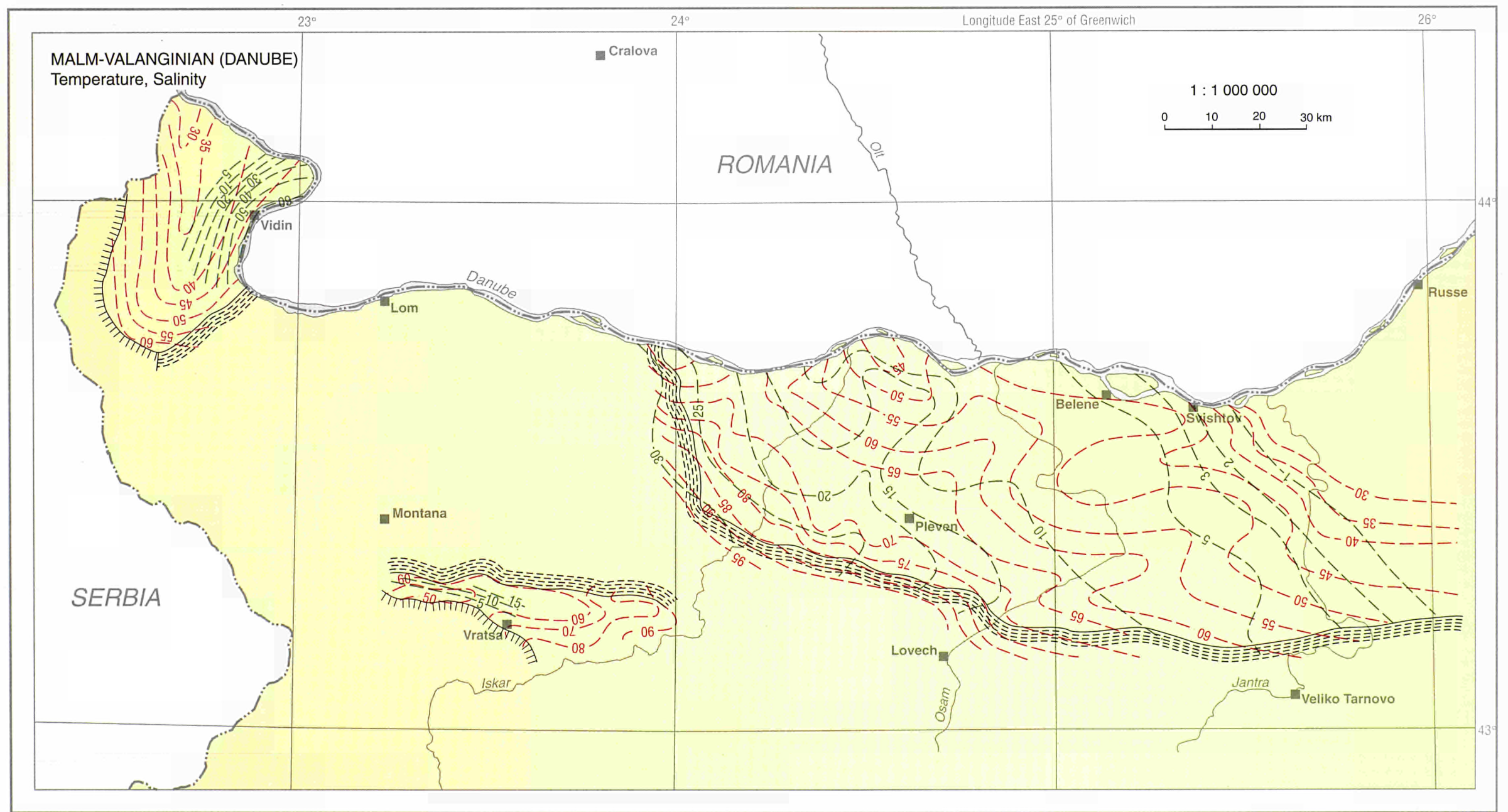
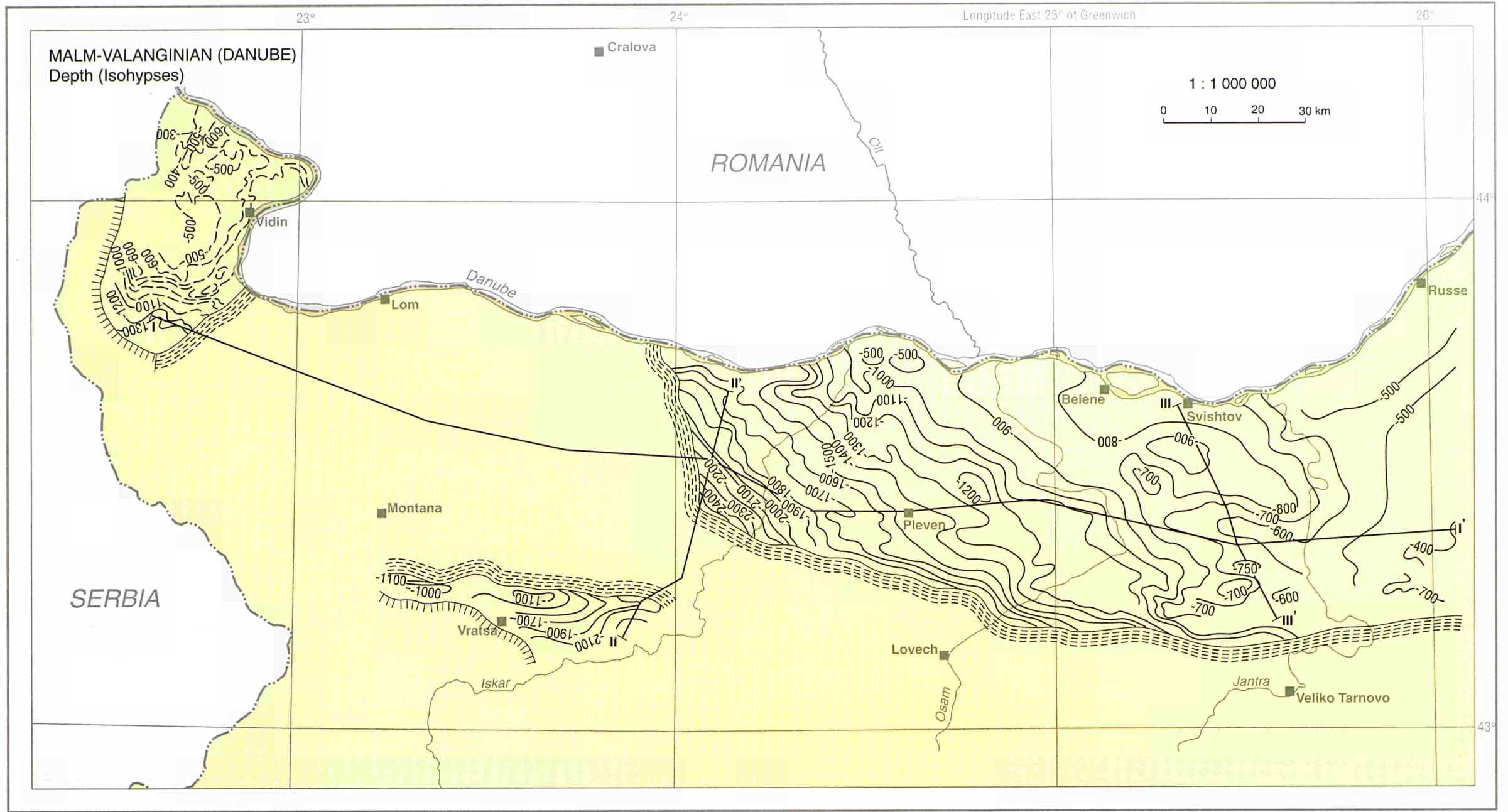
- D_M - C_{10u} (Givetian - Tournaisian) | 2000 - 5000 (6000) m depth; saline thermal waters and brines; 50 - 150 °C; 5 - 25 (30) GJ/m²
 - Tr_{M-L} (Middle - Late Triassic) | 1500 - 4000 m depth; thermal brines; 40 - 140 °C; 1-10 GJ/m²
 - J₁ - K_eval (Malm-Valanginian reservoir) | 800 - 2500 (3000) m depth; **a** - low mineralized meteoric waters; 25 - 65 °C; constant recharge and reproduction; **b** - saline waters and brines; 40 - 90 (100) °C; 0.5 - 20 GJ/m²
- 2.5- H₁(GJ/m²) of the Malm-Valanginian reservoir

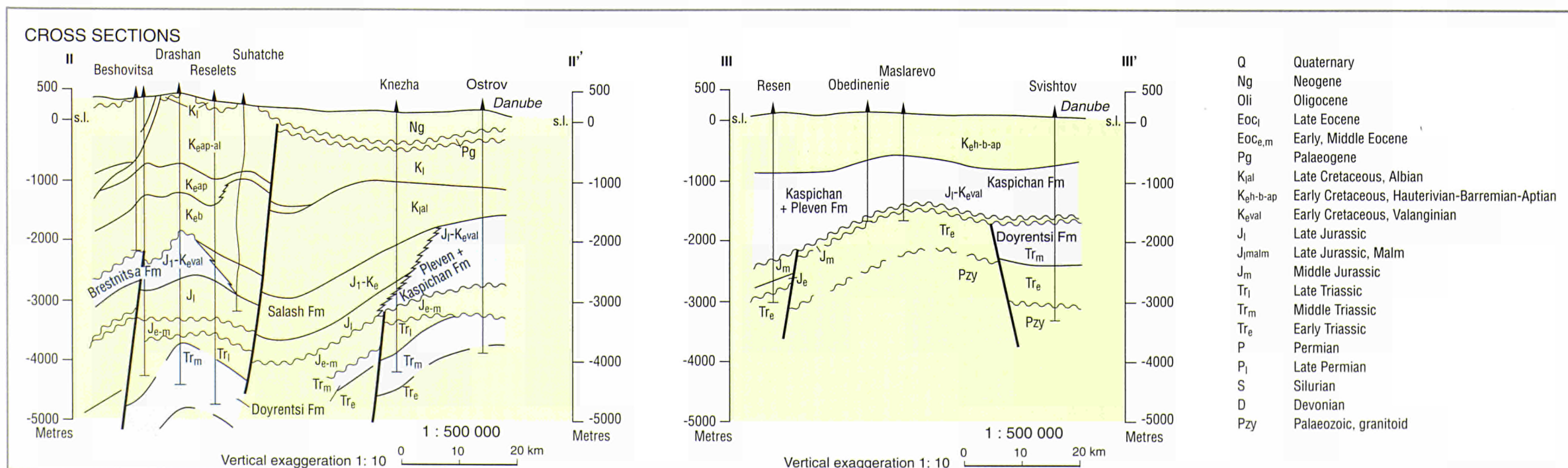
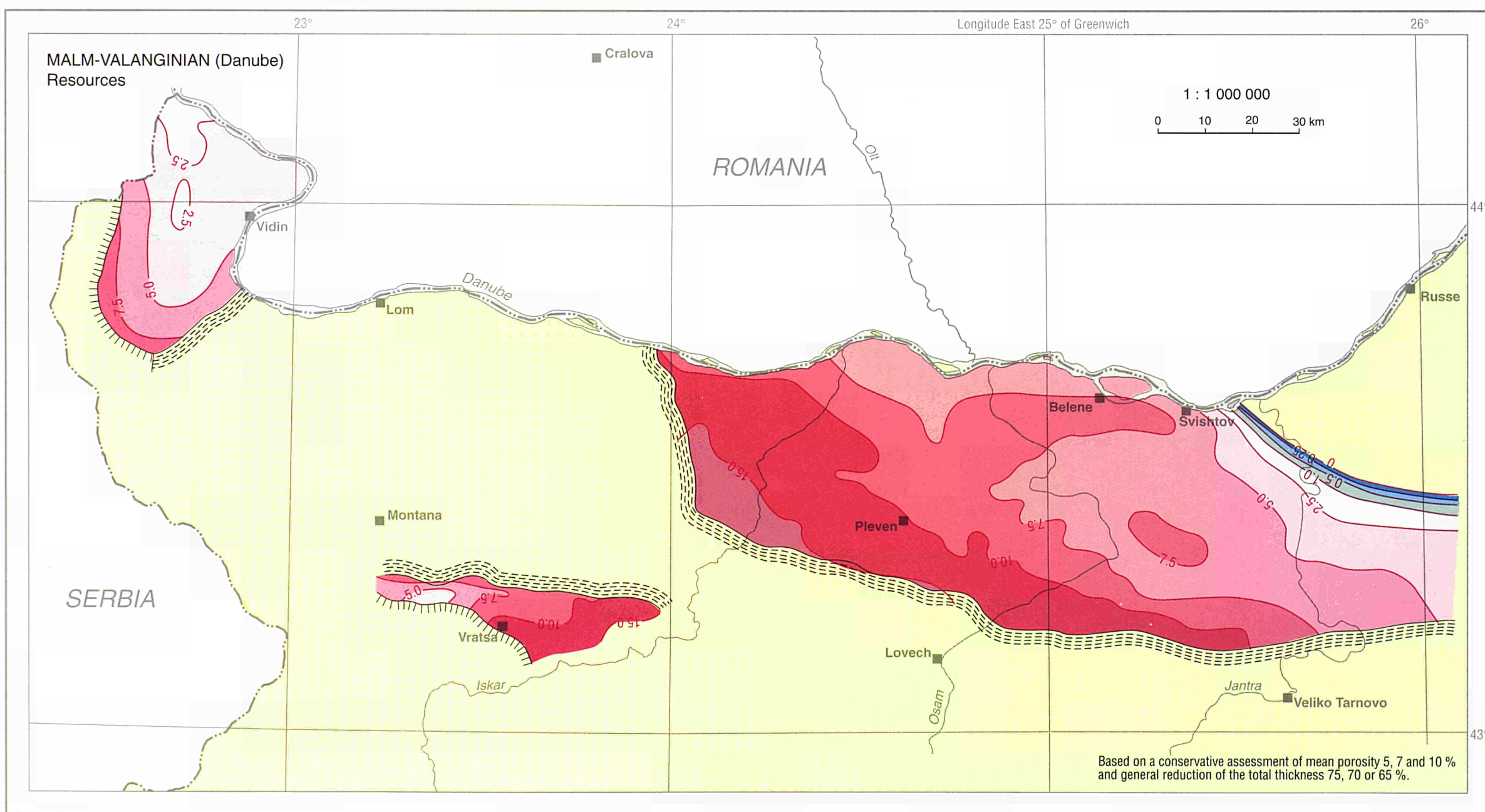
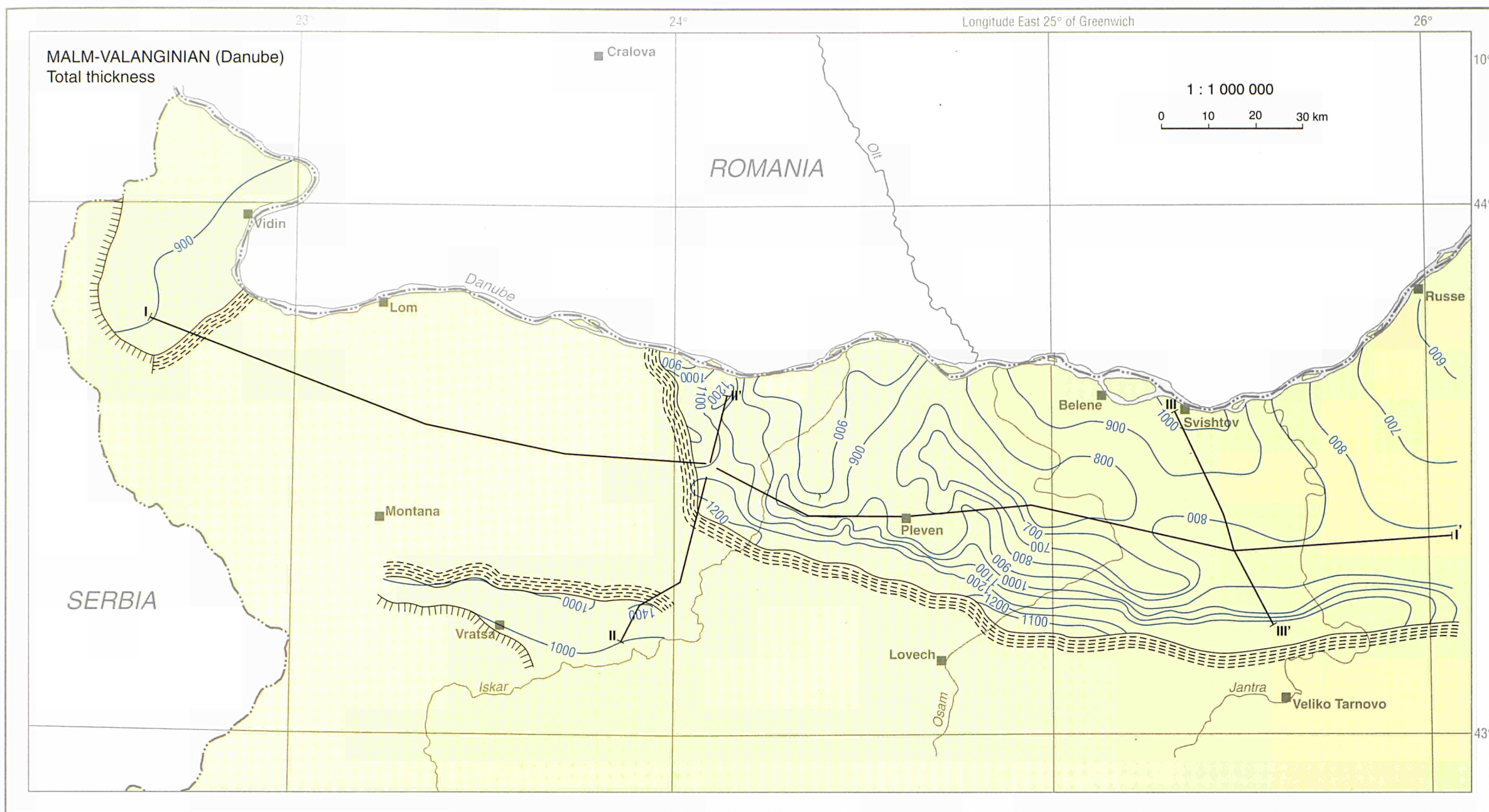
Hydrothermal systems with meteoric waters

- Mesozoic carbonate bodies and Rhodope marbles; 25 - 80 °C
 - Terrigenous - clastic aquifers of Tertiary grabens; 25 - 65 °C
 - Granites, schists and gneisses
 - In volcanic and volcano-sedimentary formations: **a** - Late Cretaceous; **b** - Palaeogene
 - Discharge areas of some non-stratified hydrothermal systems
- Fractured with mean yield per 1km²: 0.2 l/s thermal waters (30/120 °C) and 45 kW_t geothermal energy

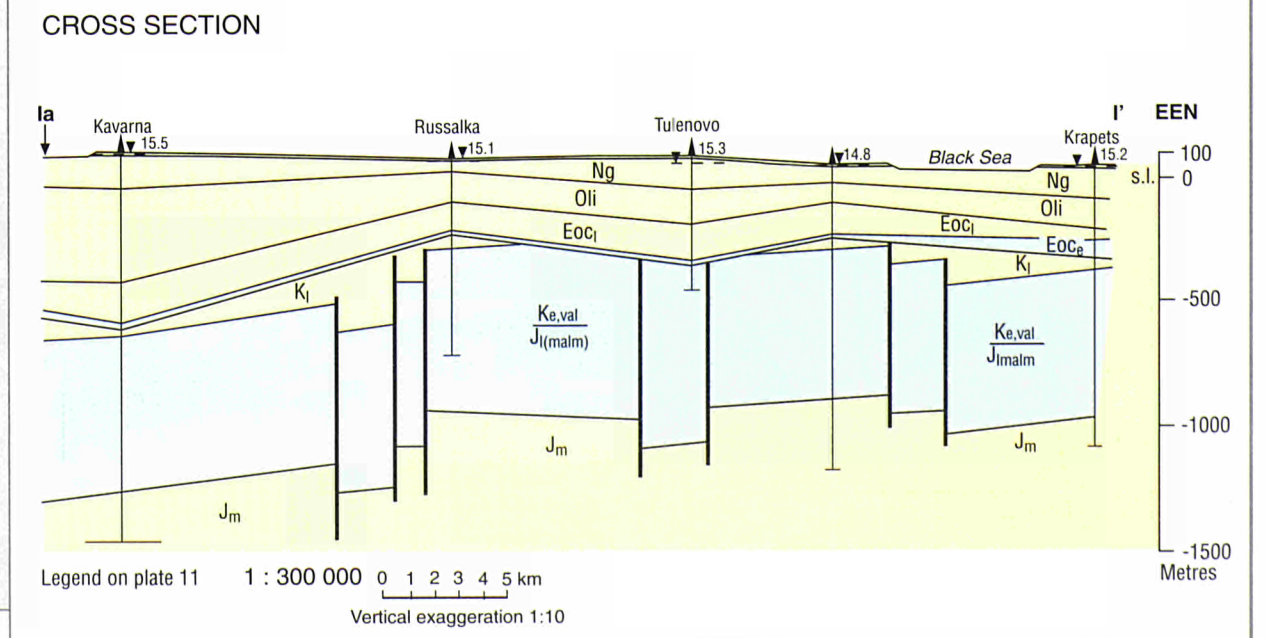
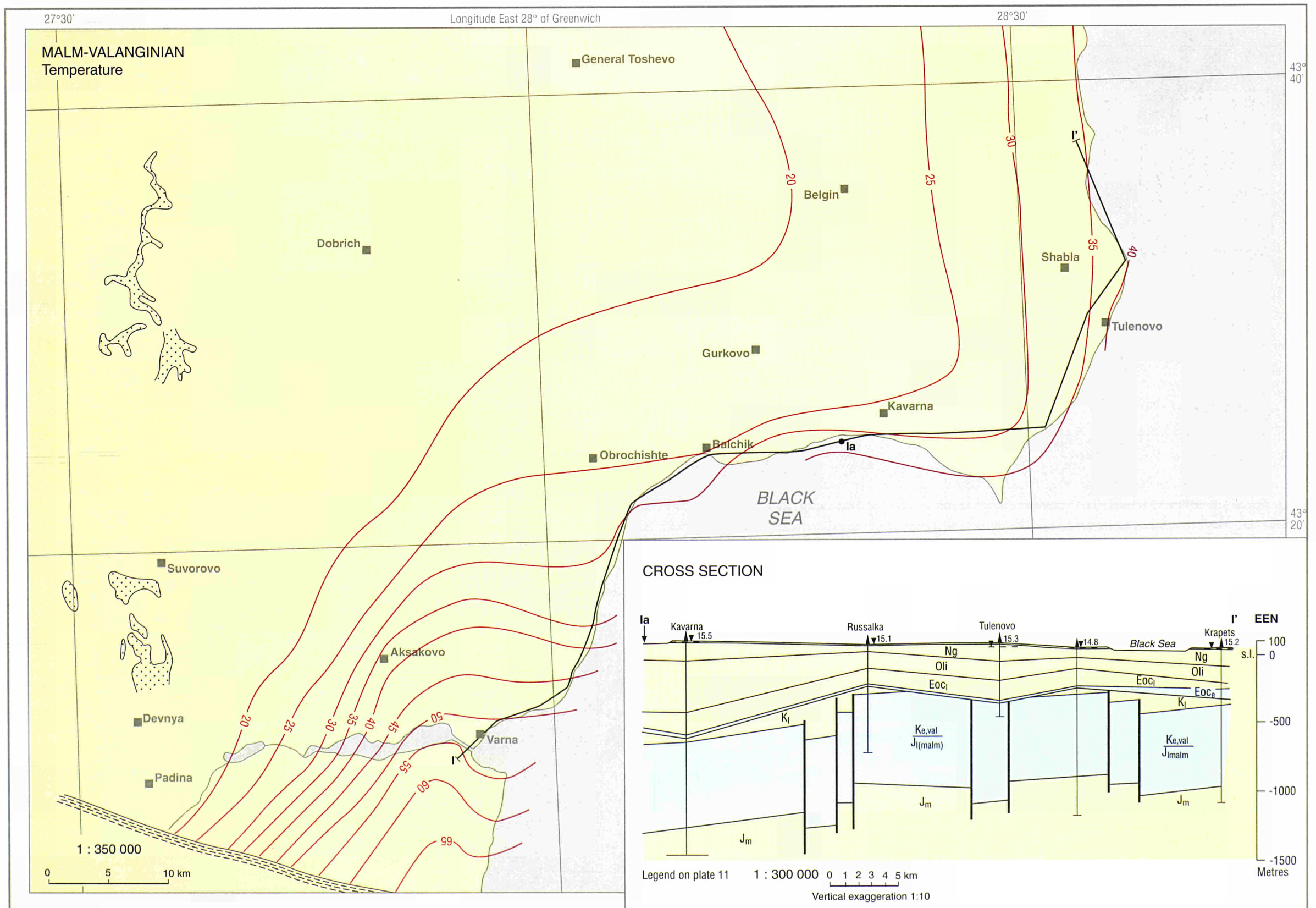
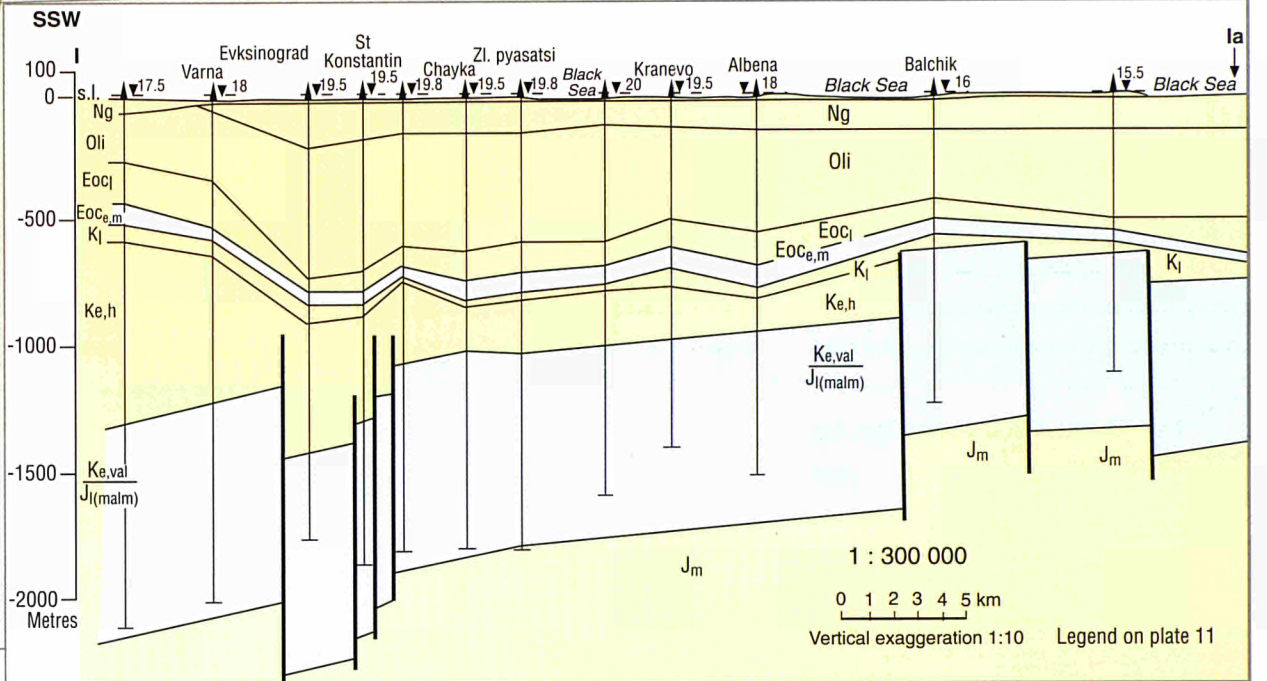
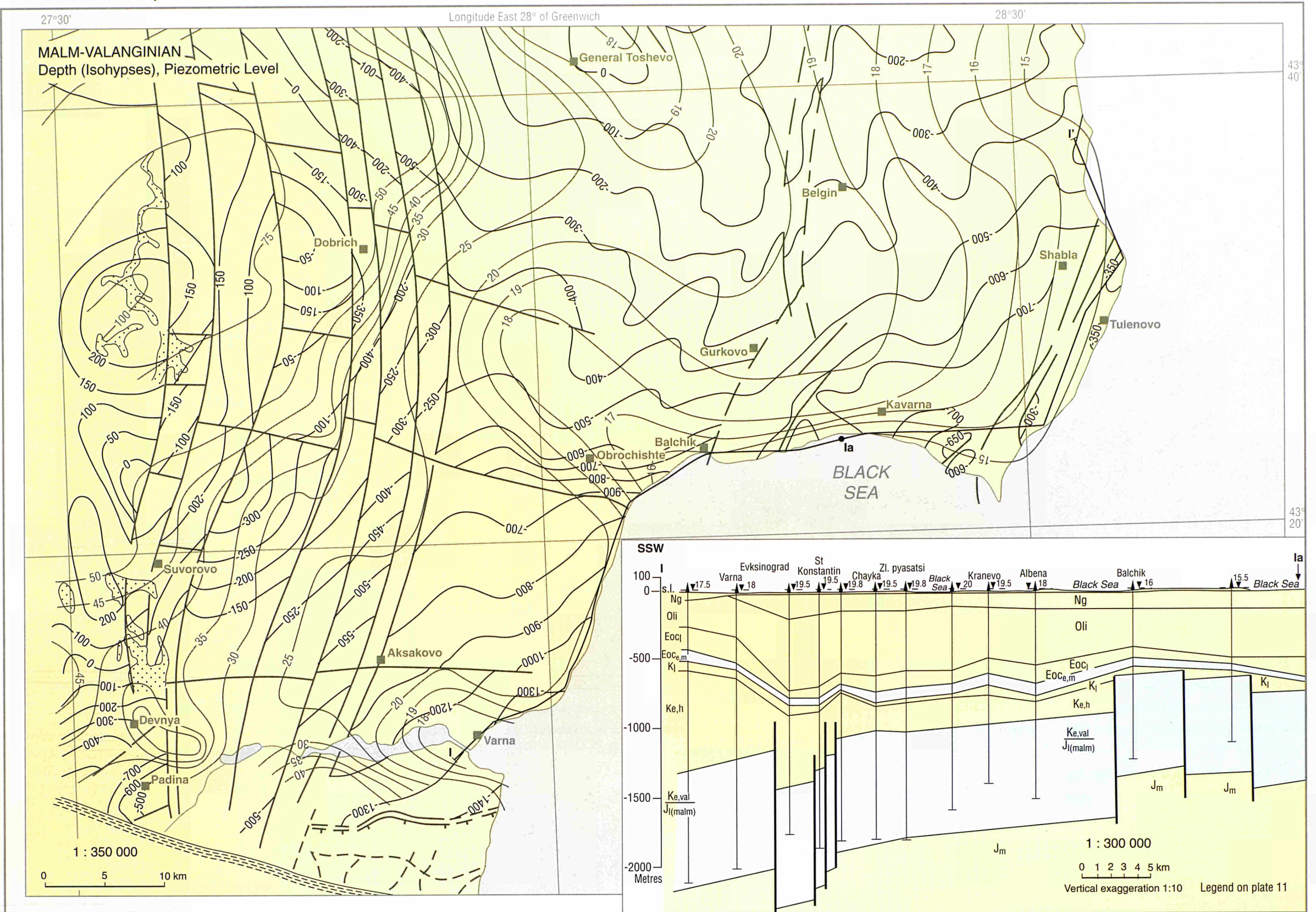


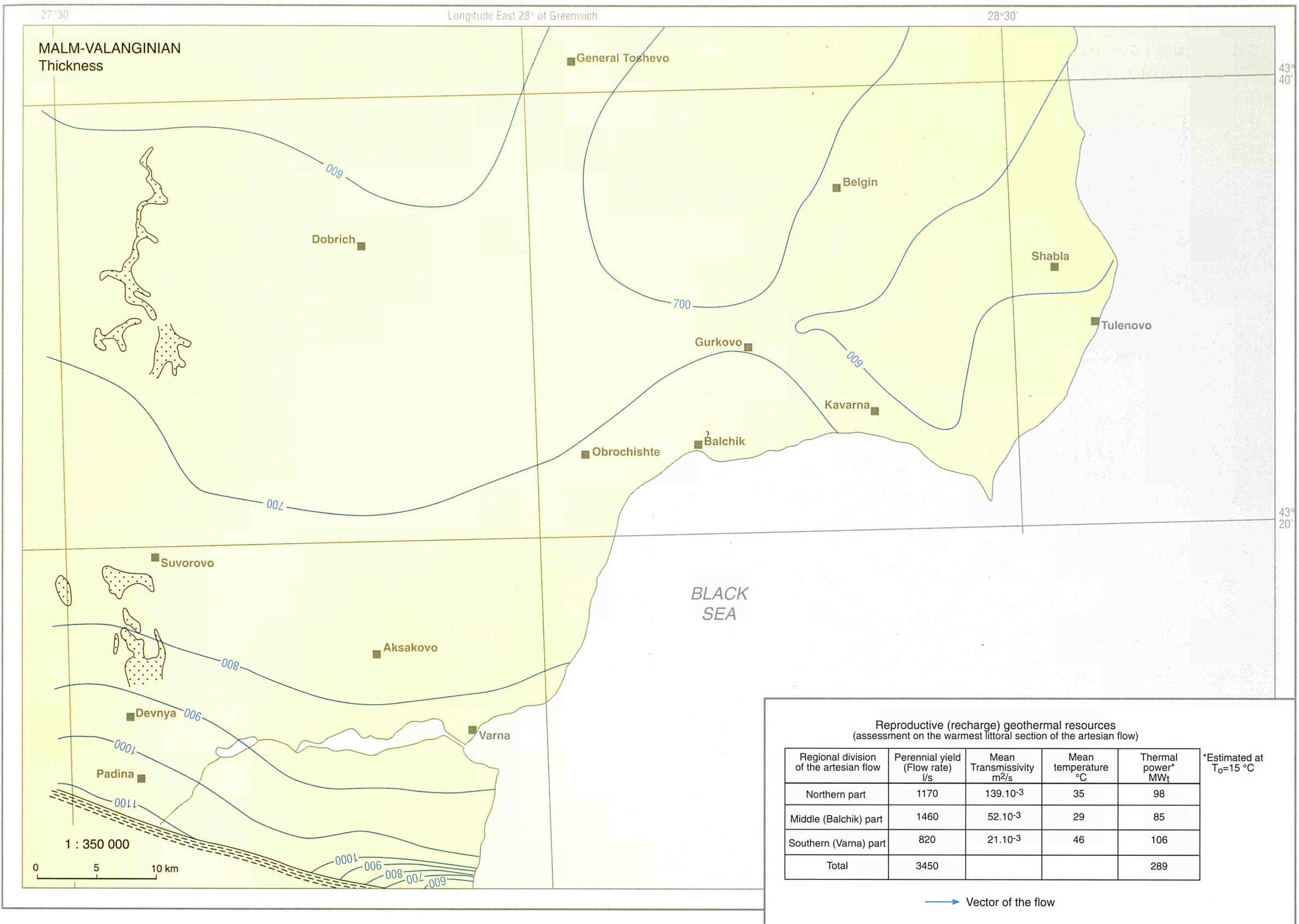
BULGARIA





BULGARIA, Black Sea

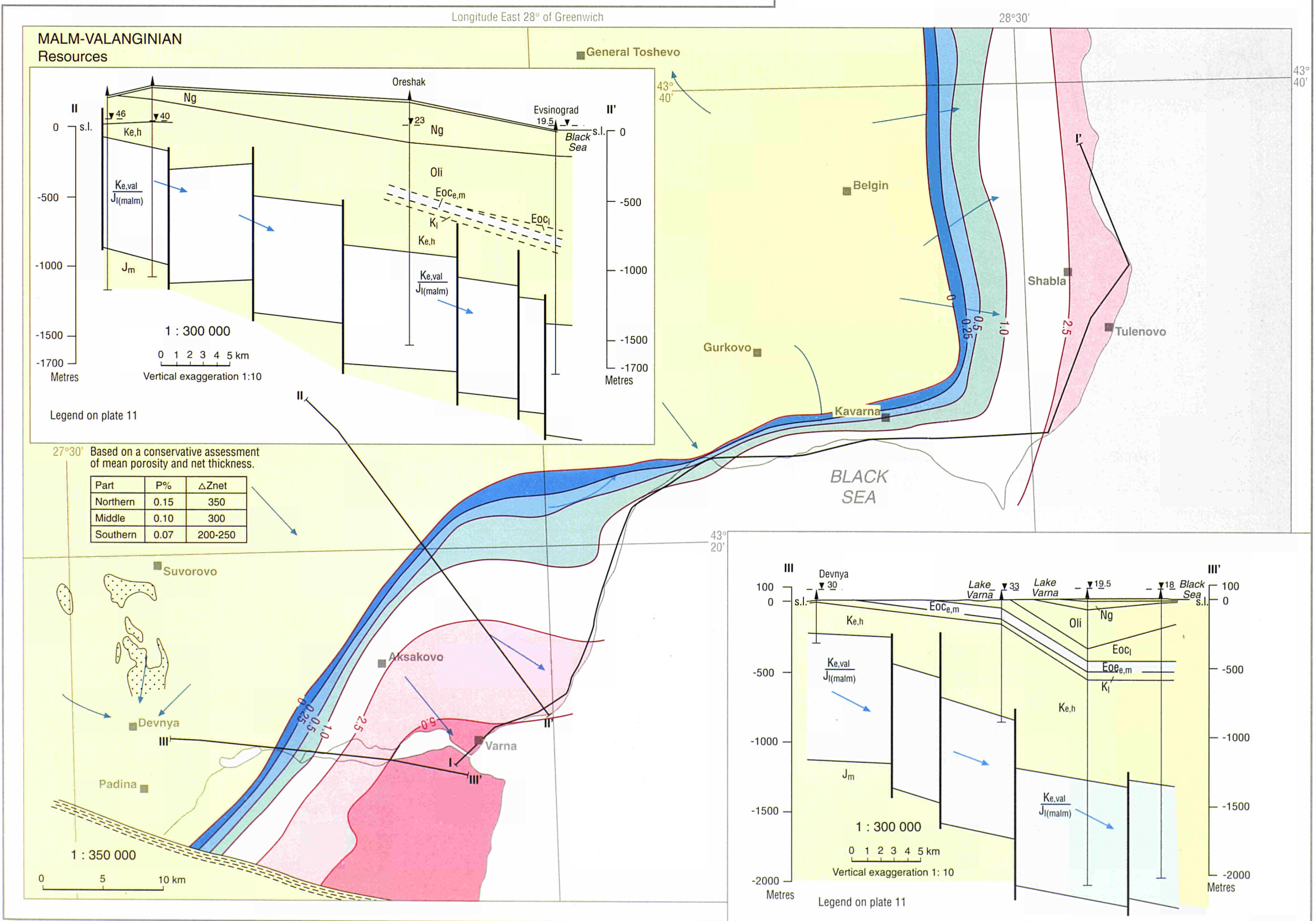




Reproductive (recharge) geothermal resources
(assessment on the warmest littoral section of the artesian flow)

Regional division of the artesian flow	Perennial yield (Flow rate) l/s	Mean Transmissivity m ² /s	Mean temperature °C	Thermal power* MW _t	*Estimated at T ₀ =15 °C
Northern part	1170	139.10 ⁻³	35	98	
Middle (Balchik) part	1460	52.10 ⁻³	29	85	
Southern (Varna) part	820	21.10 ⁻³	46	106	
Total	3450			289	

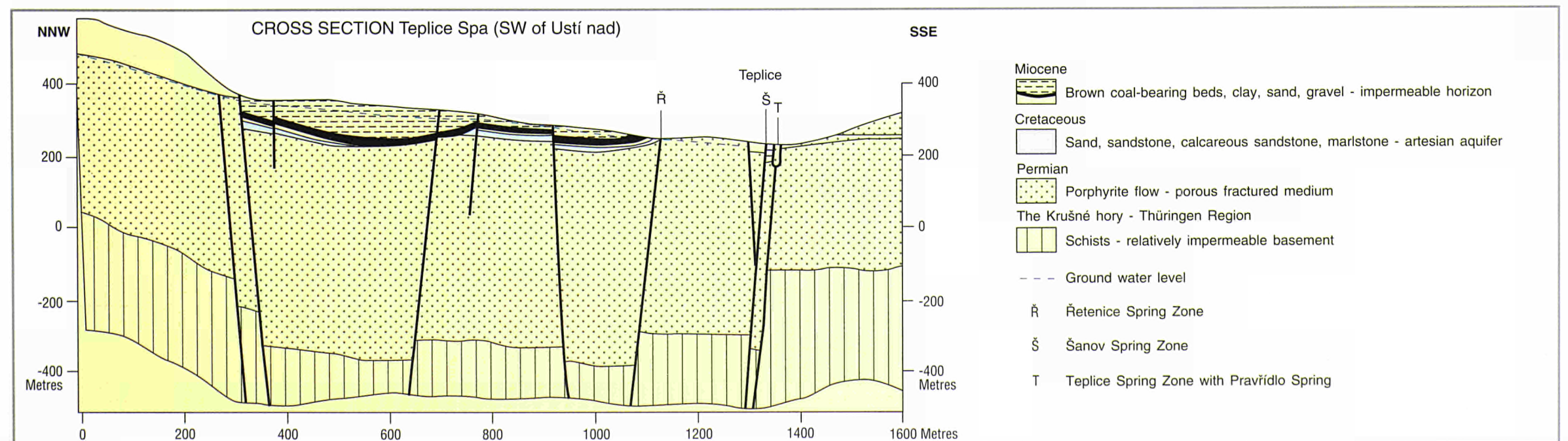
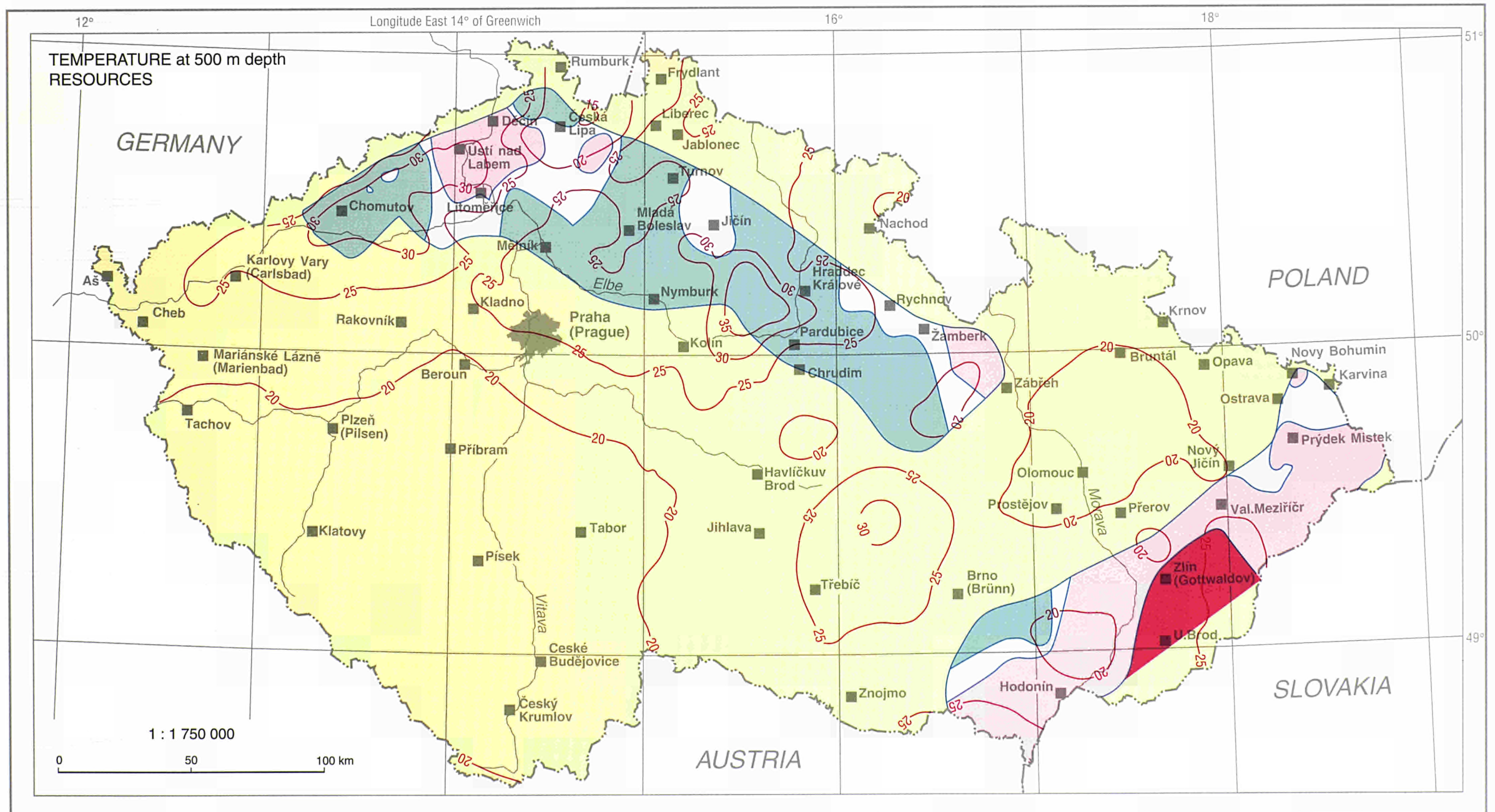
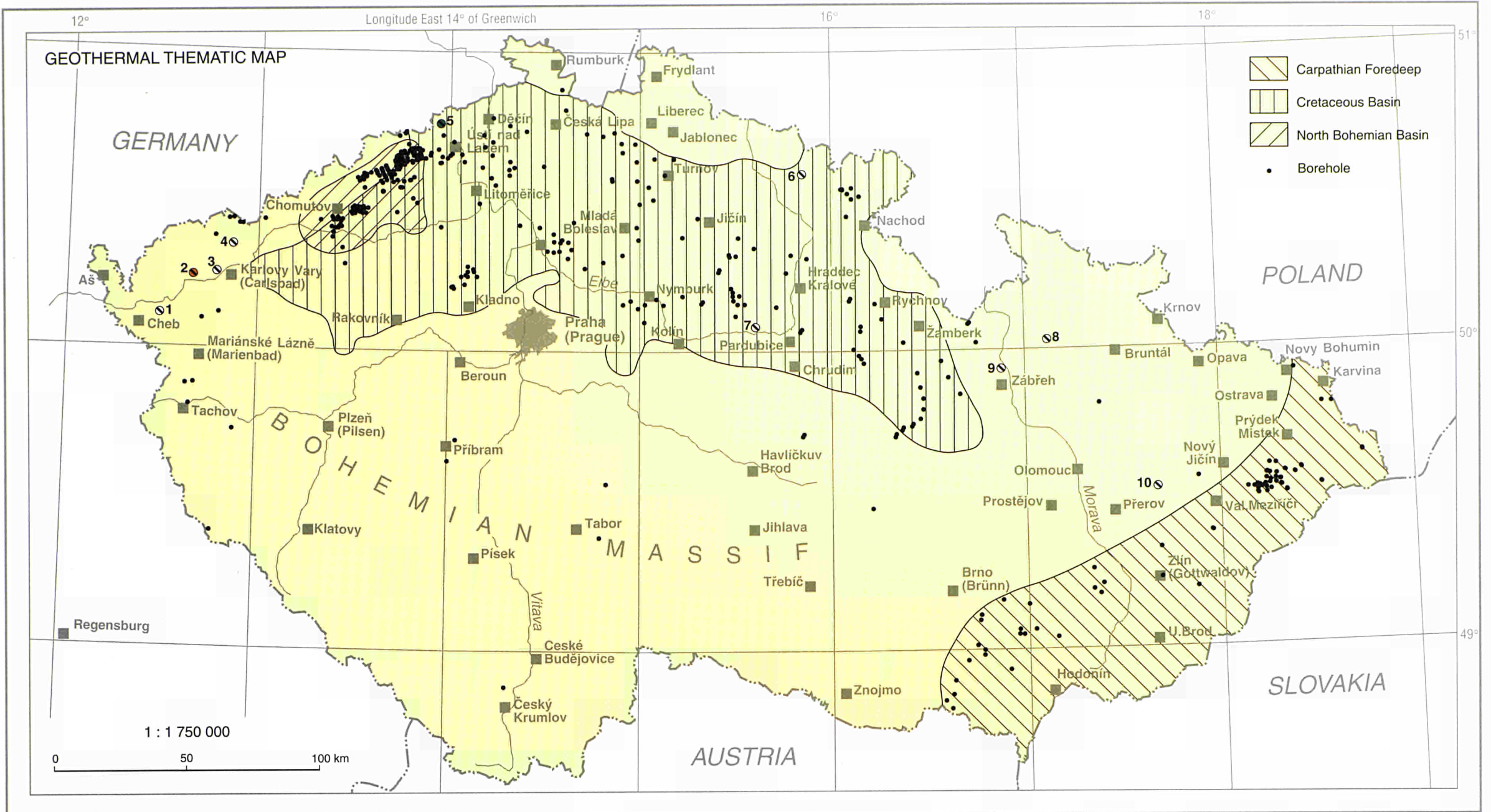
→ Vector of the flow



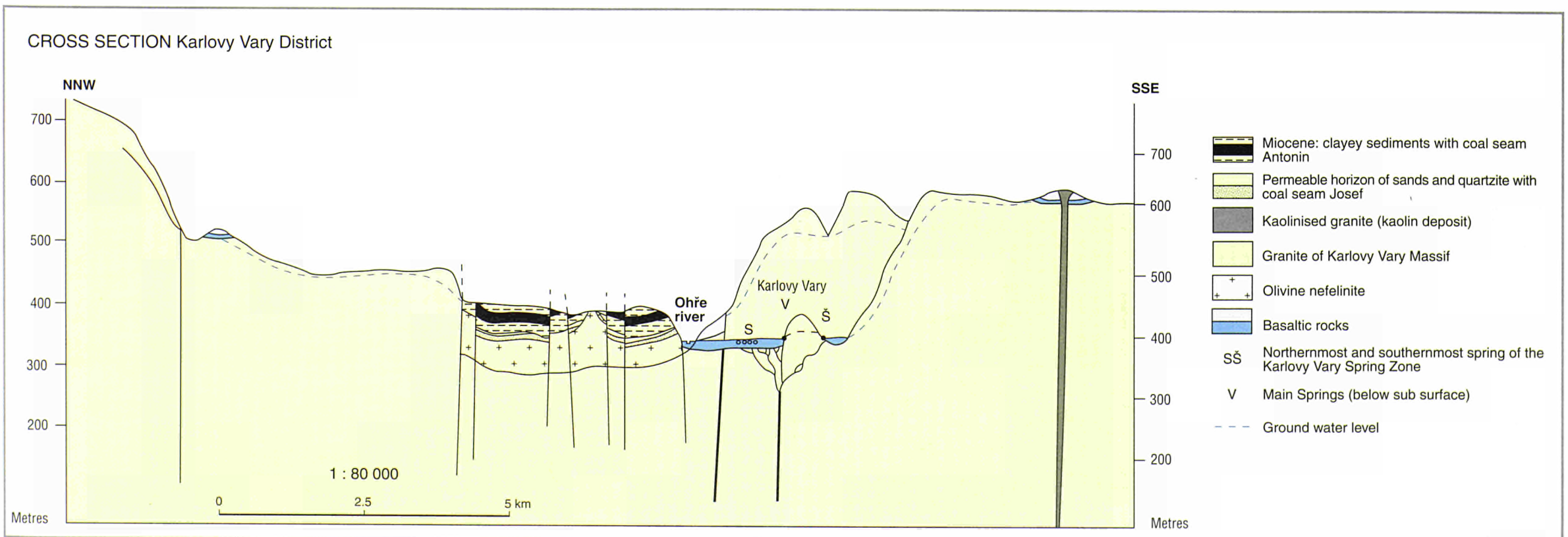
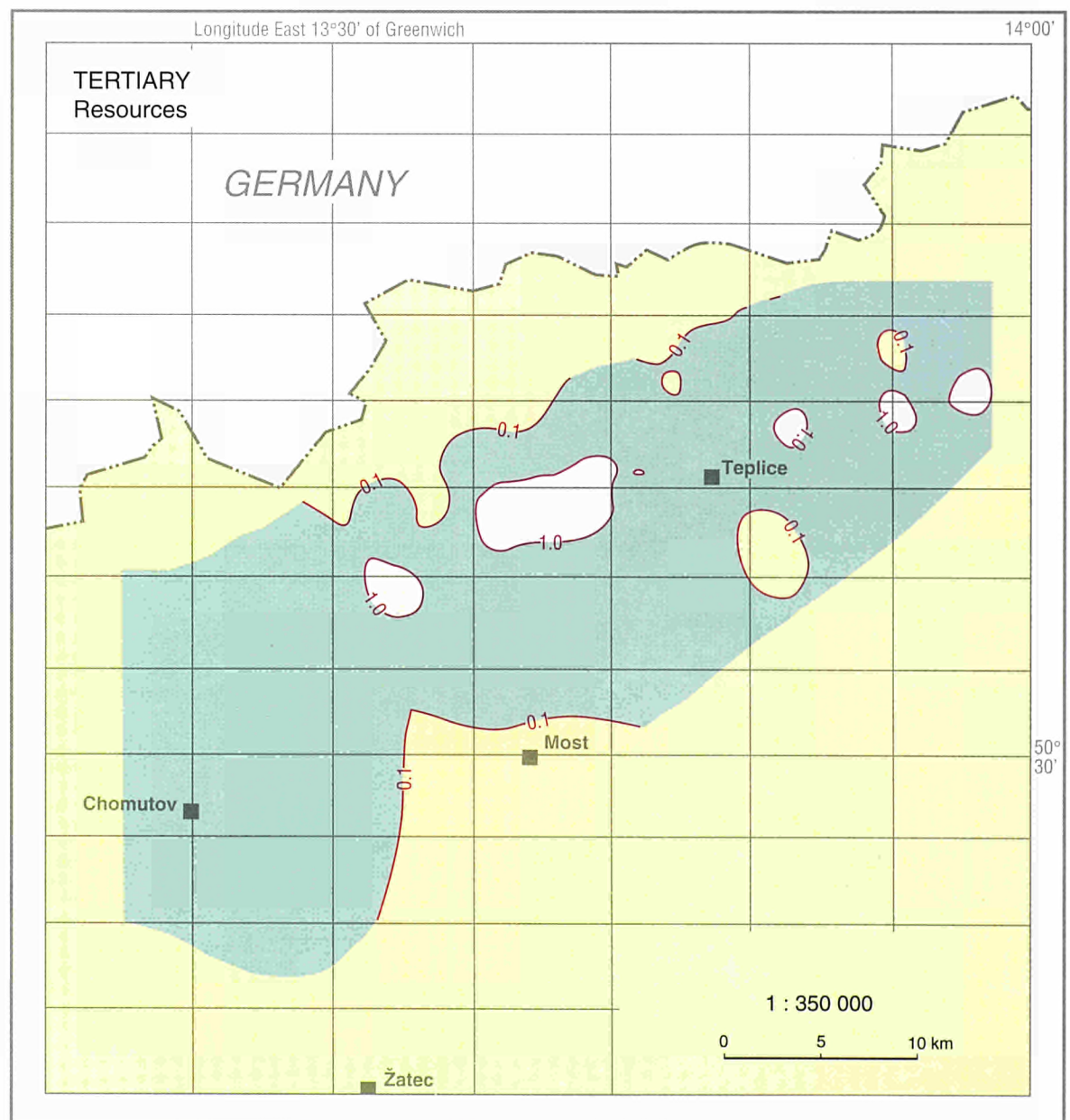
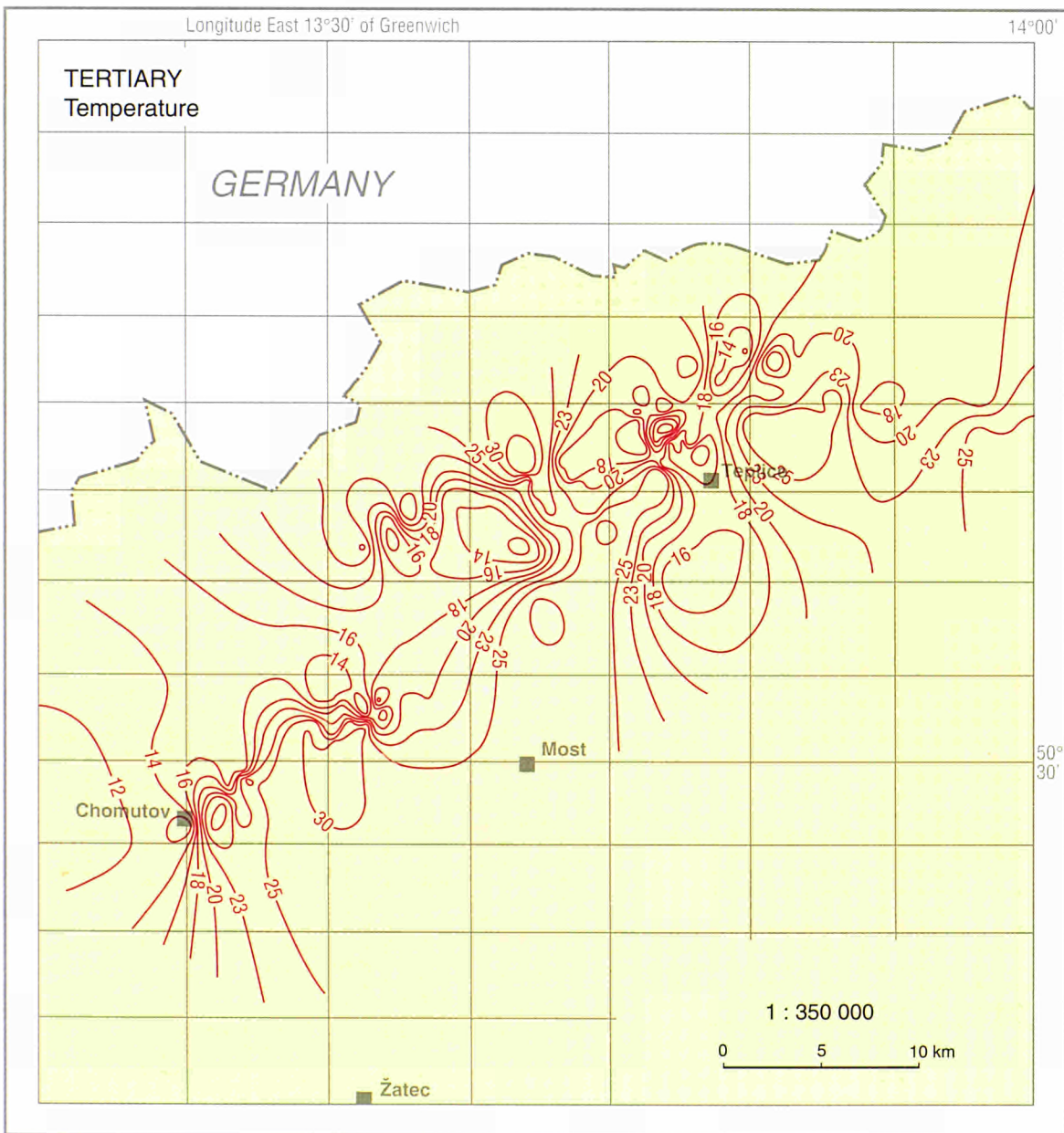
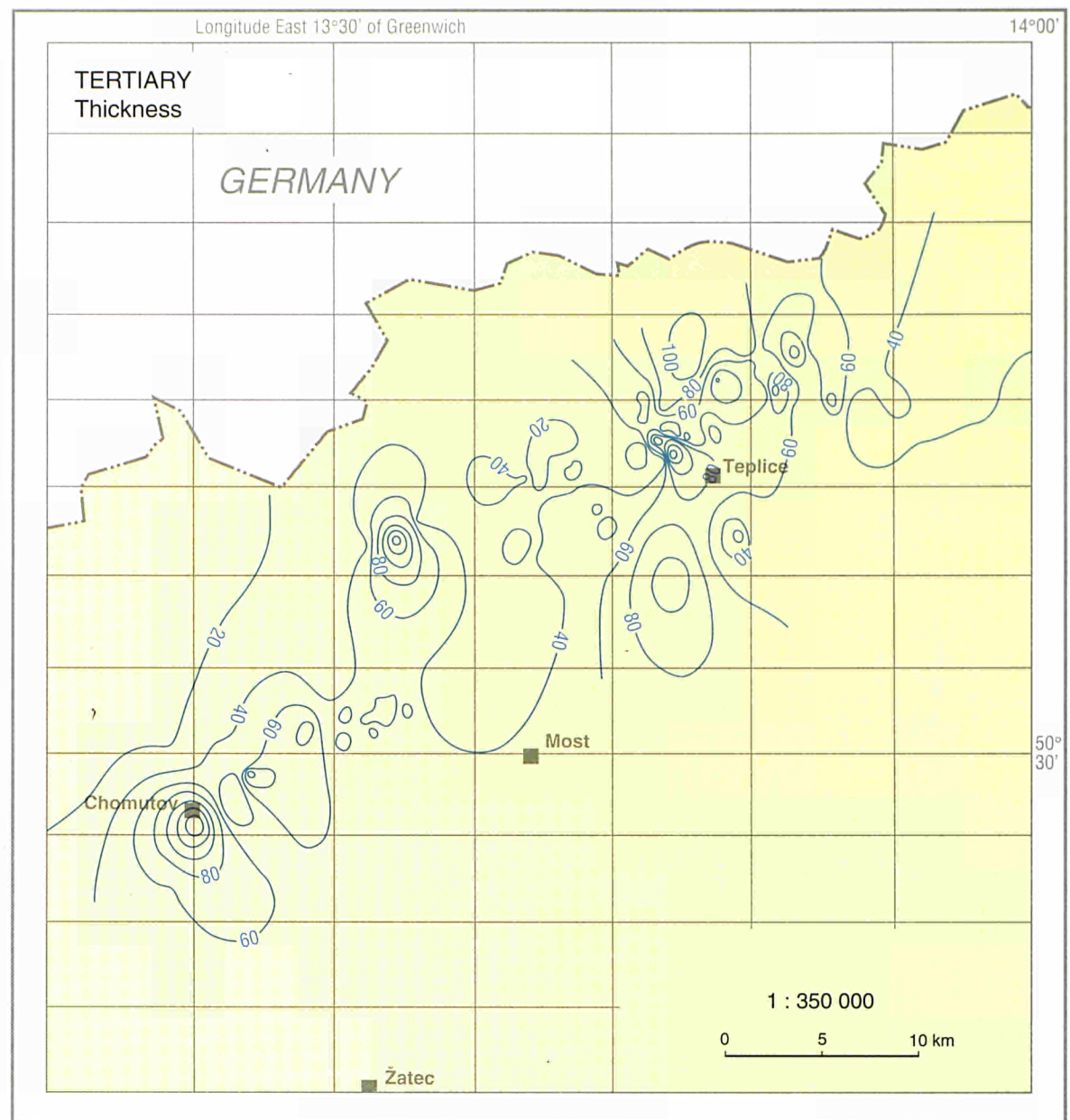
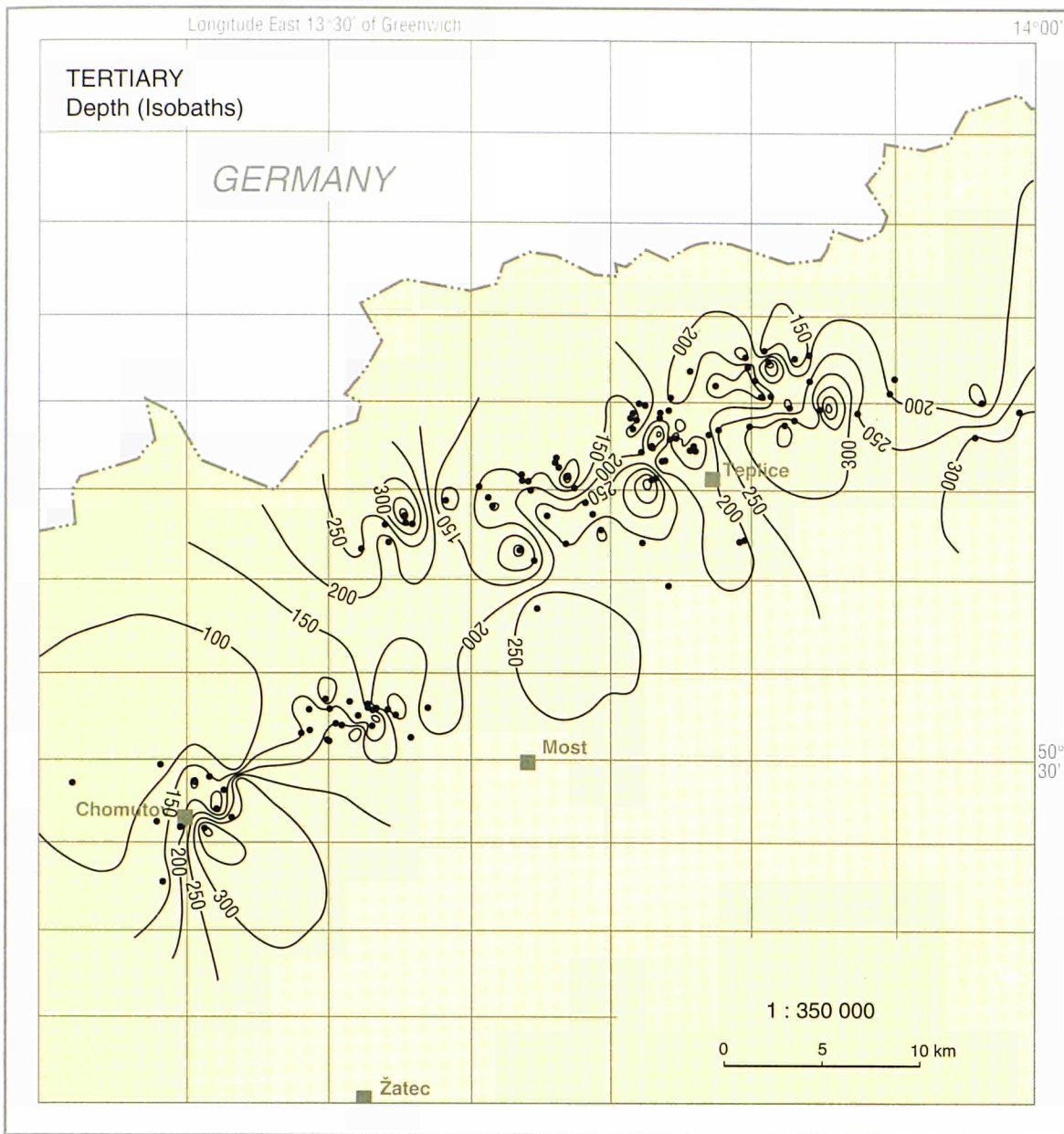
Based on a conservative assessment of mean porosity and net thickness.

Part	P%	ΔZnet
Northern	0.15	350
Middle	0.10	300
Southern	0.07	200-250

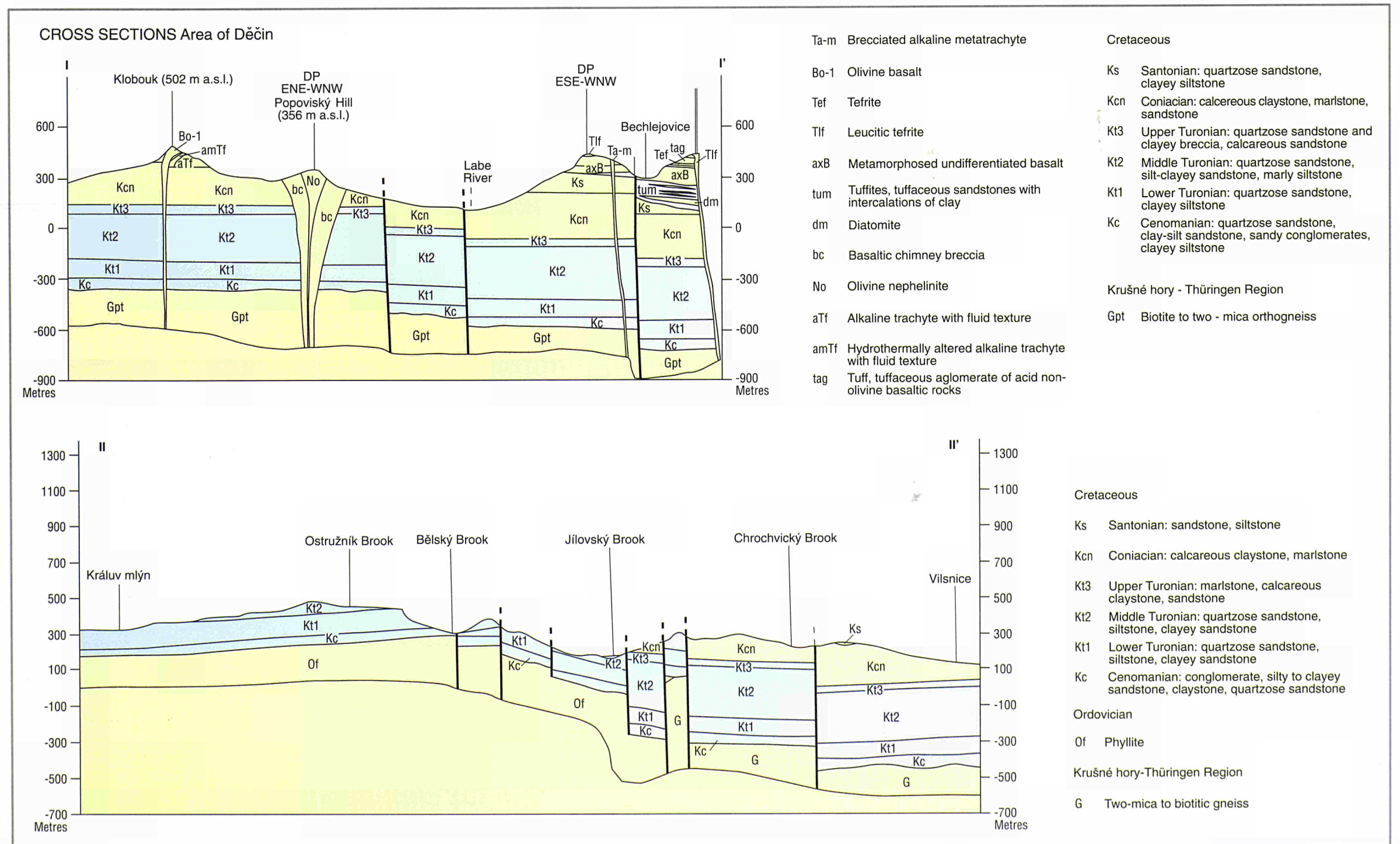
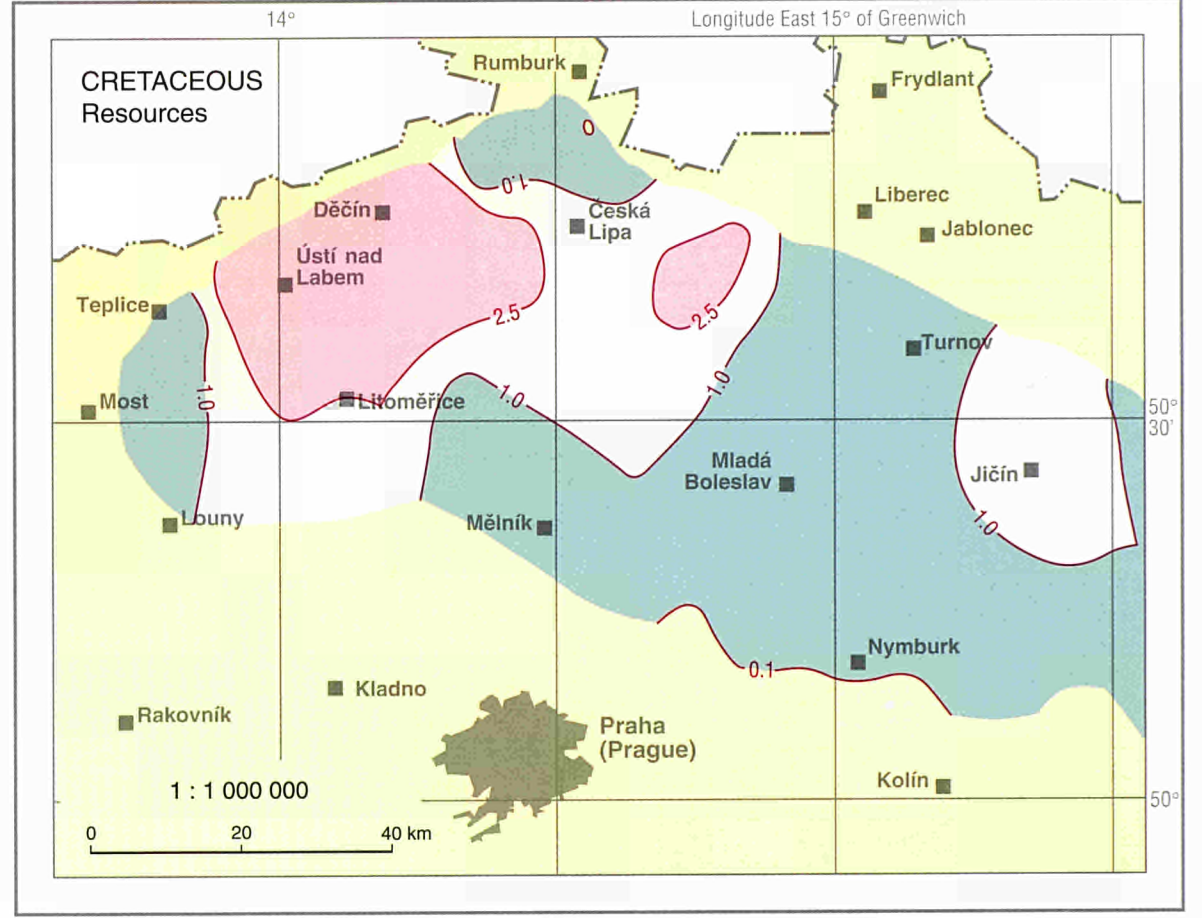
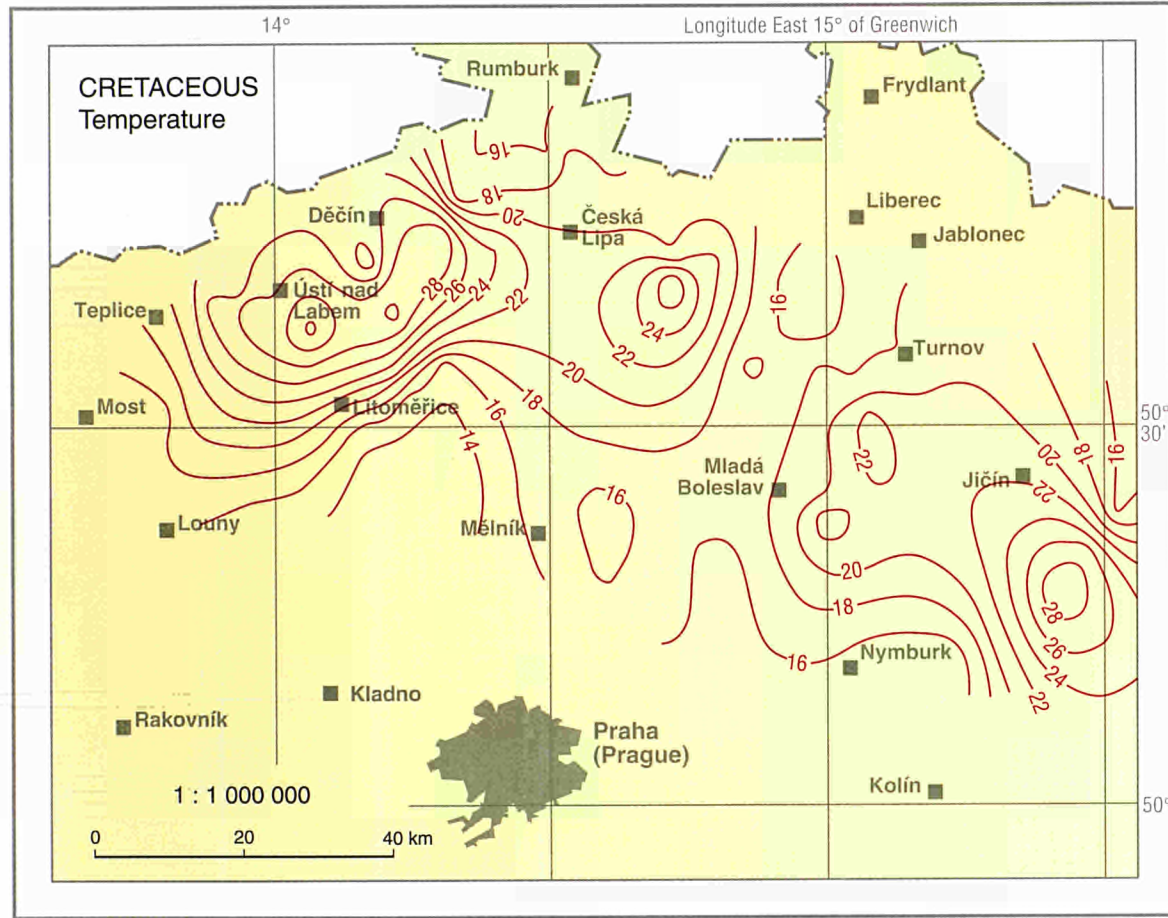
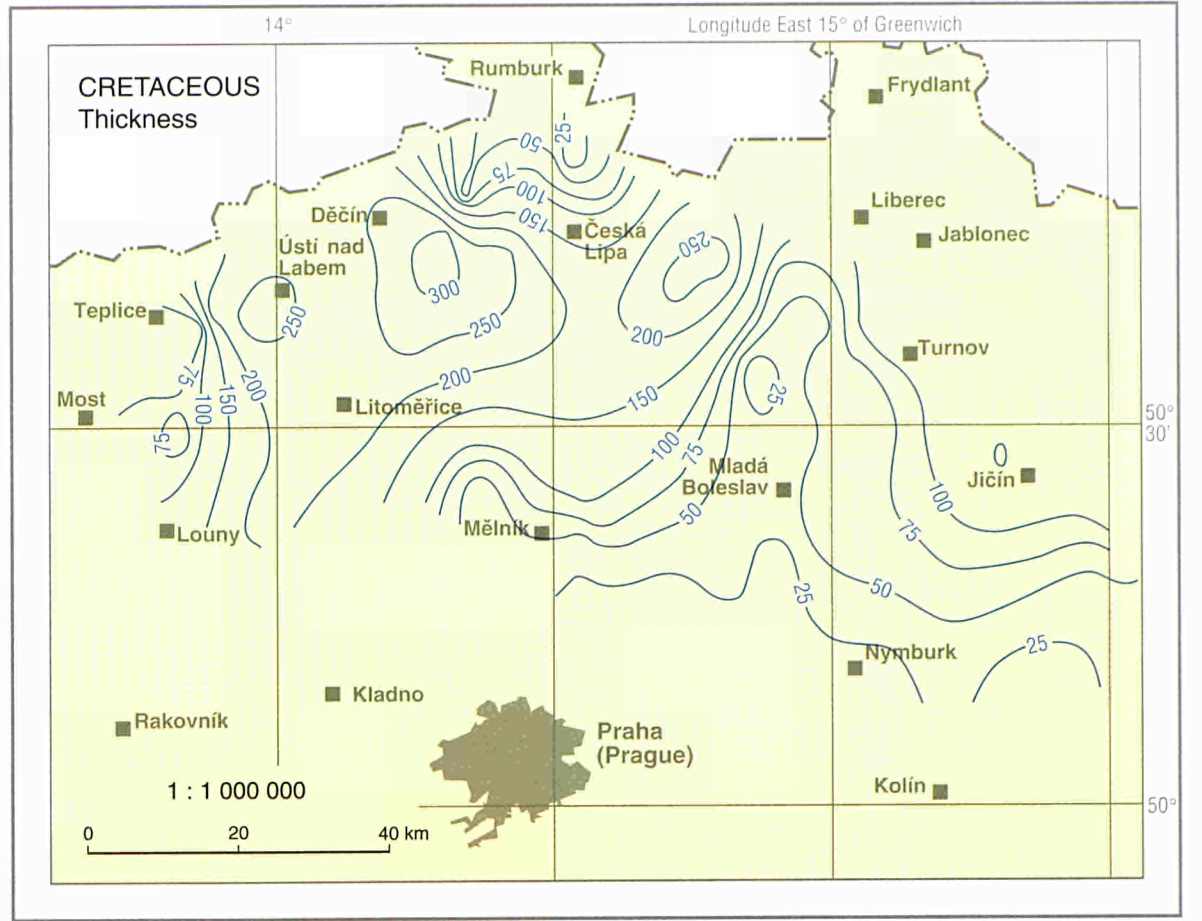
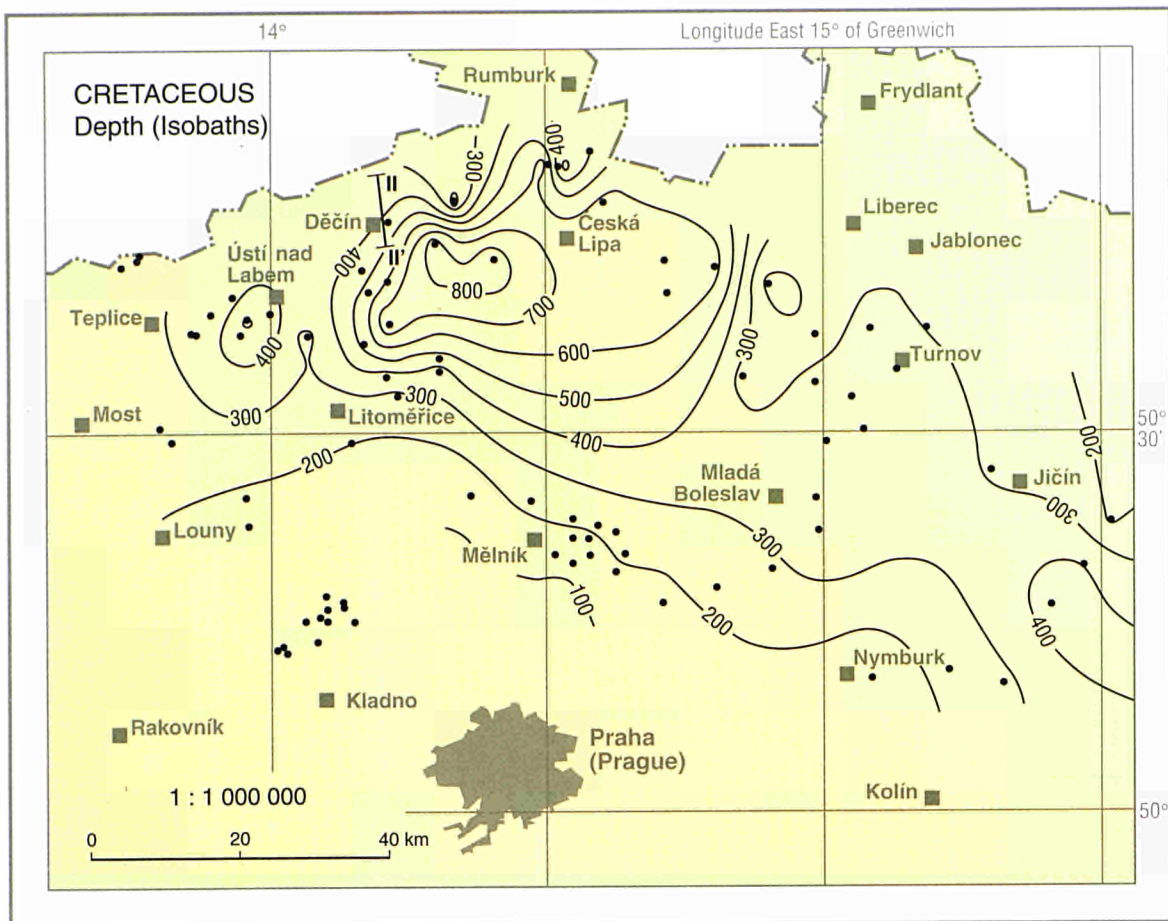
CZECH REPUBLIC

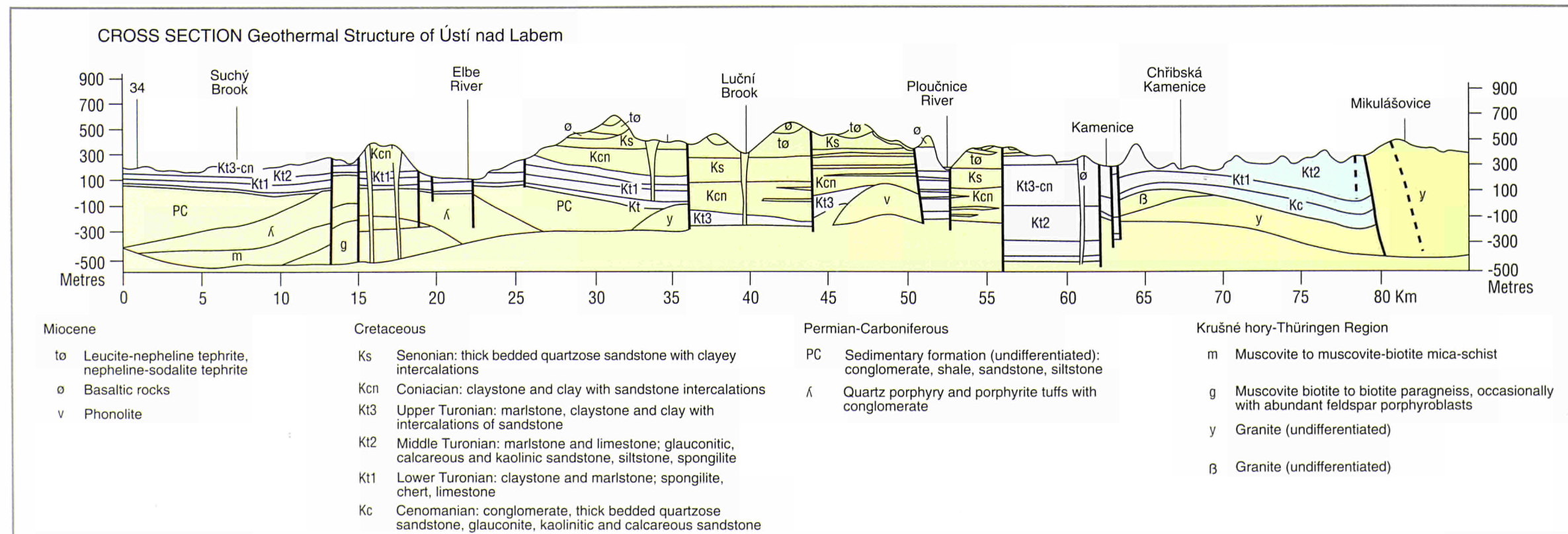
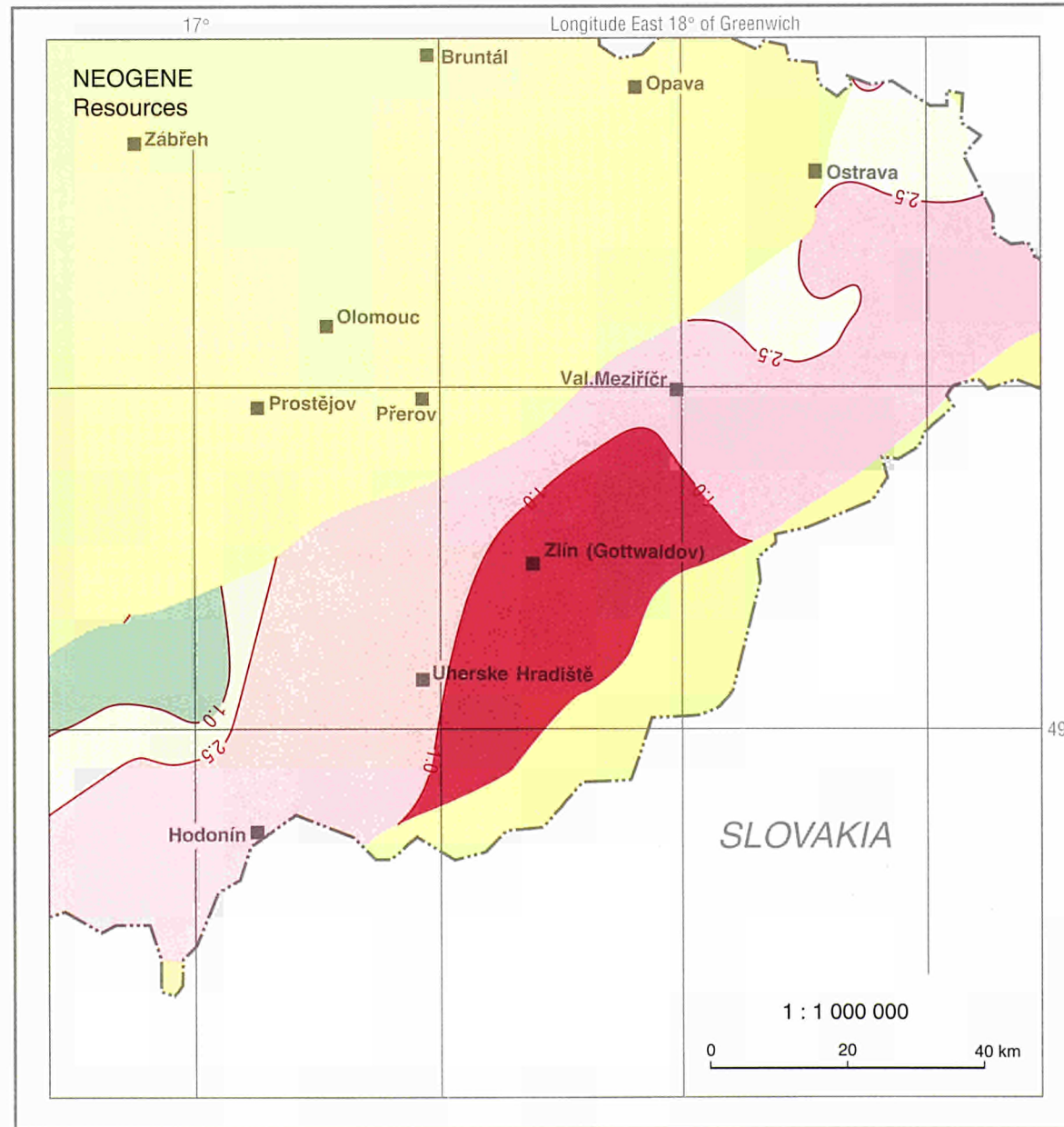
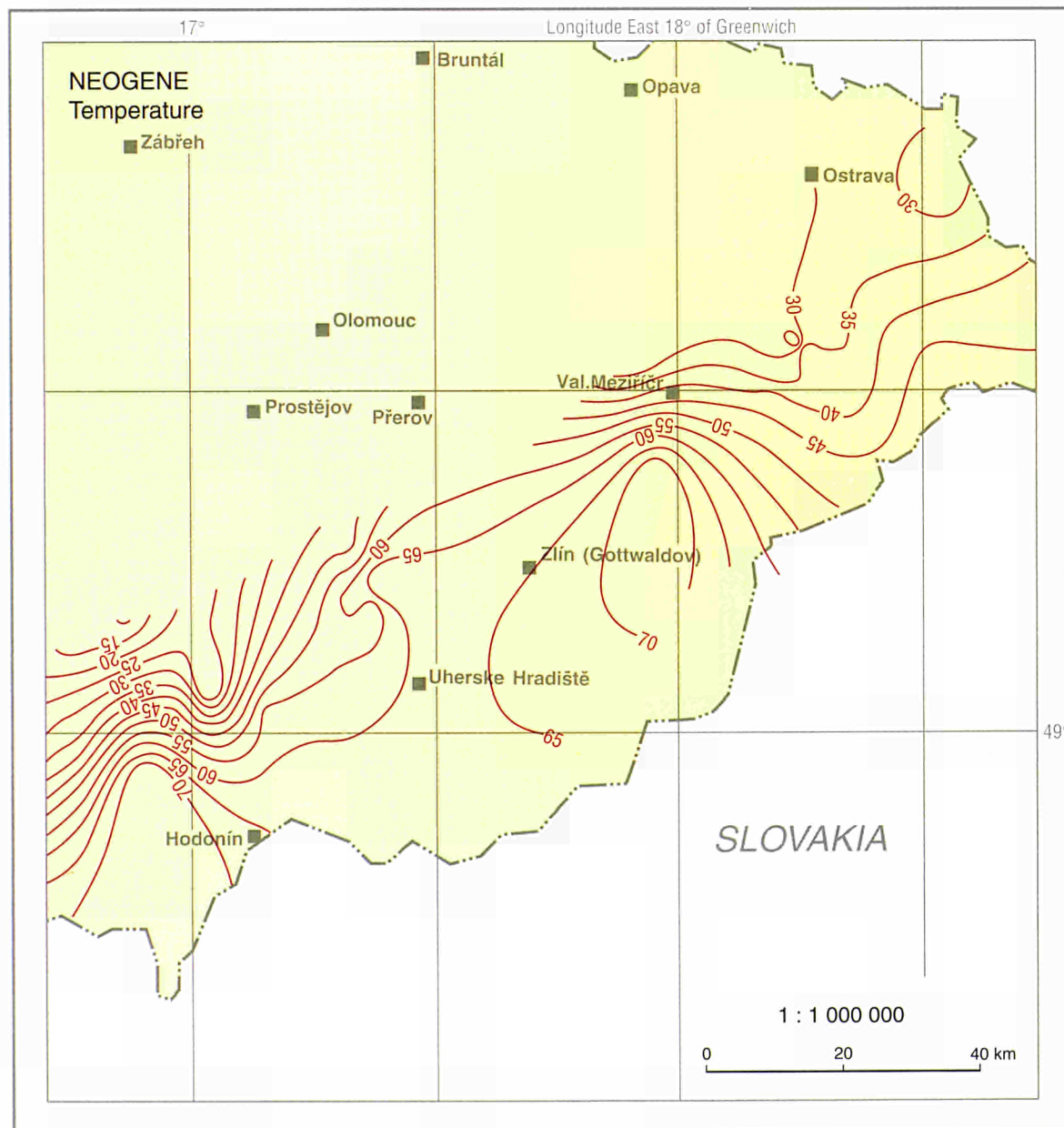
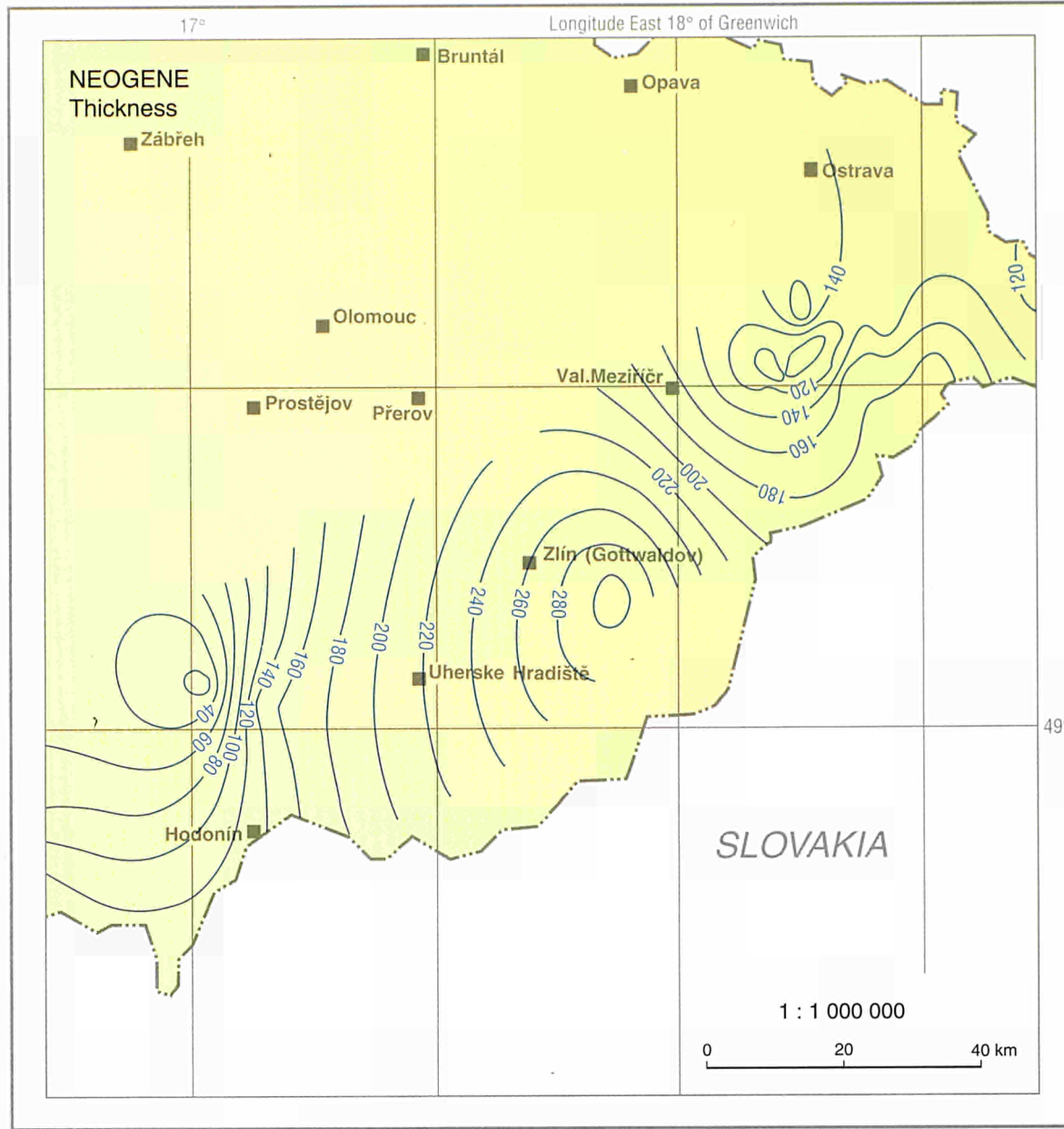
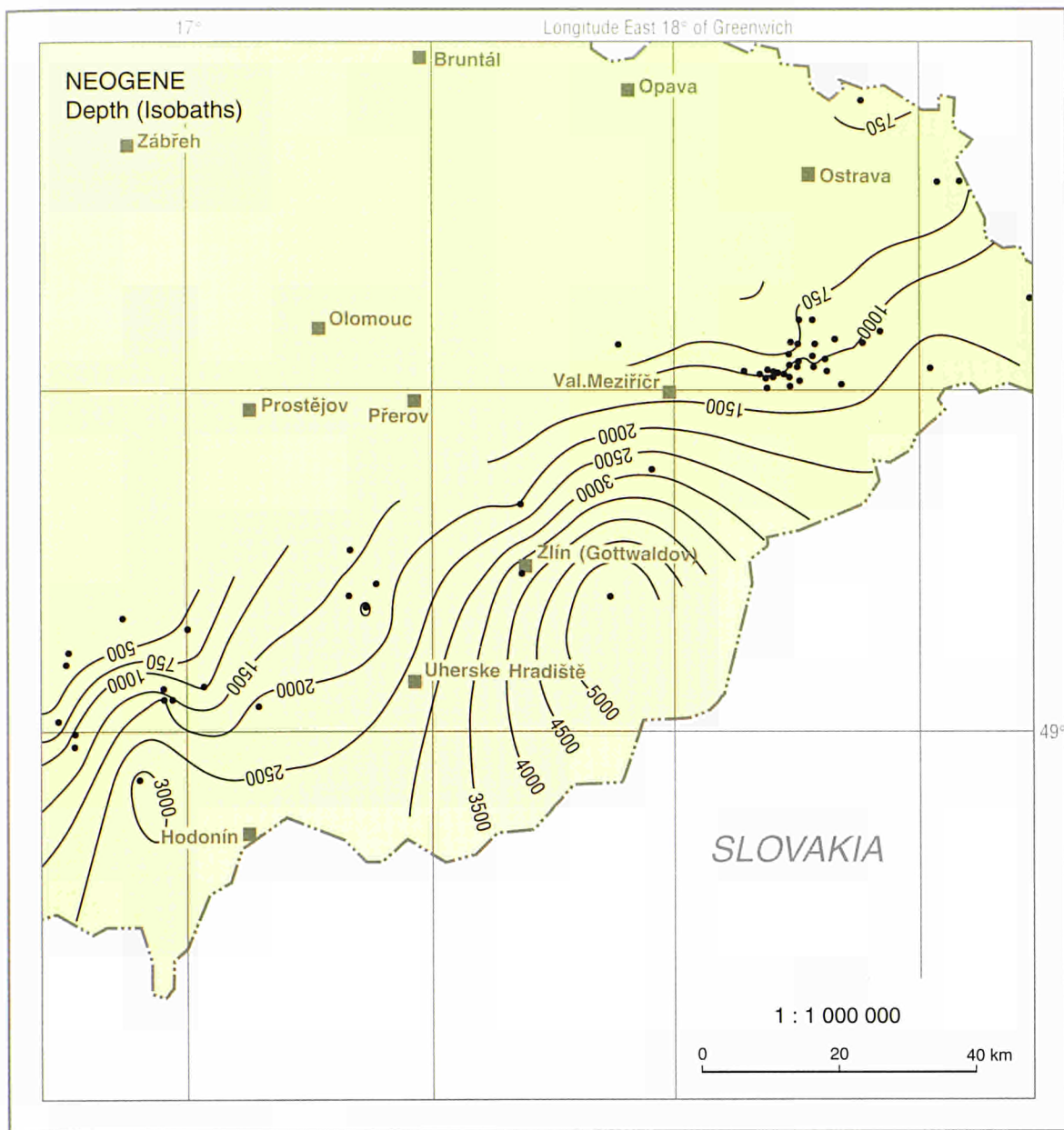


North Bohemian Basin, CZECH REPUBLIC

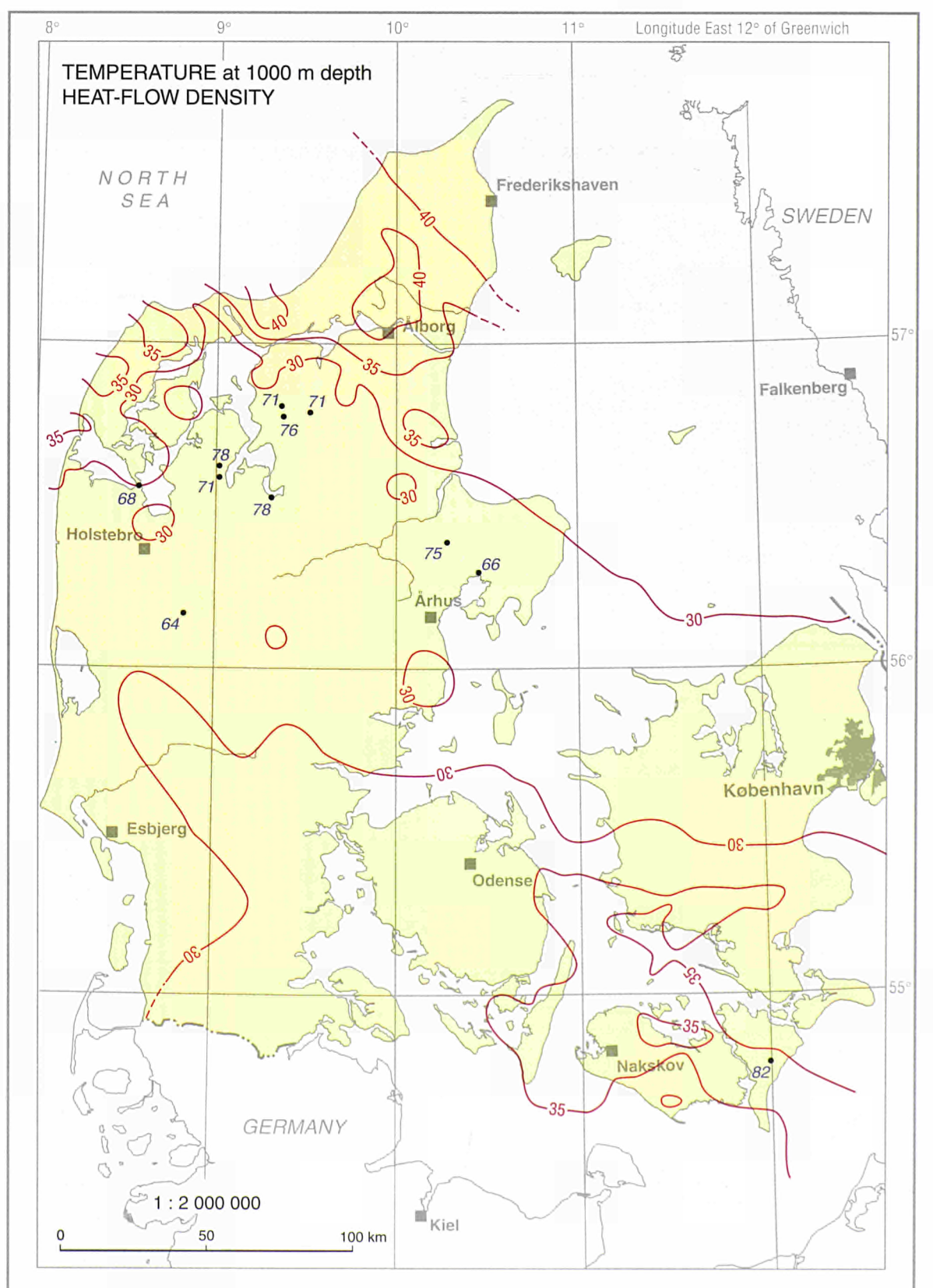
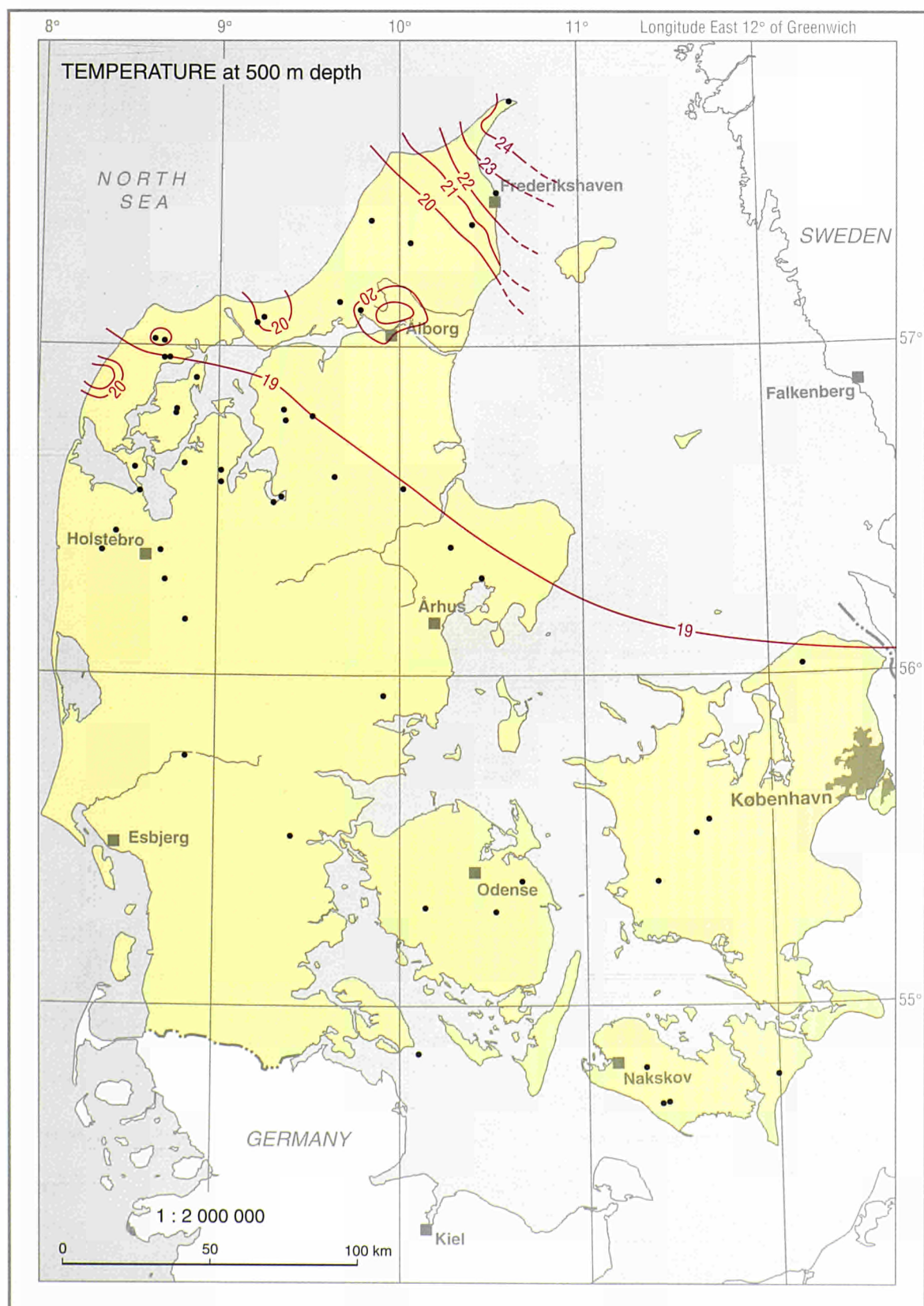
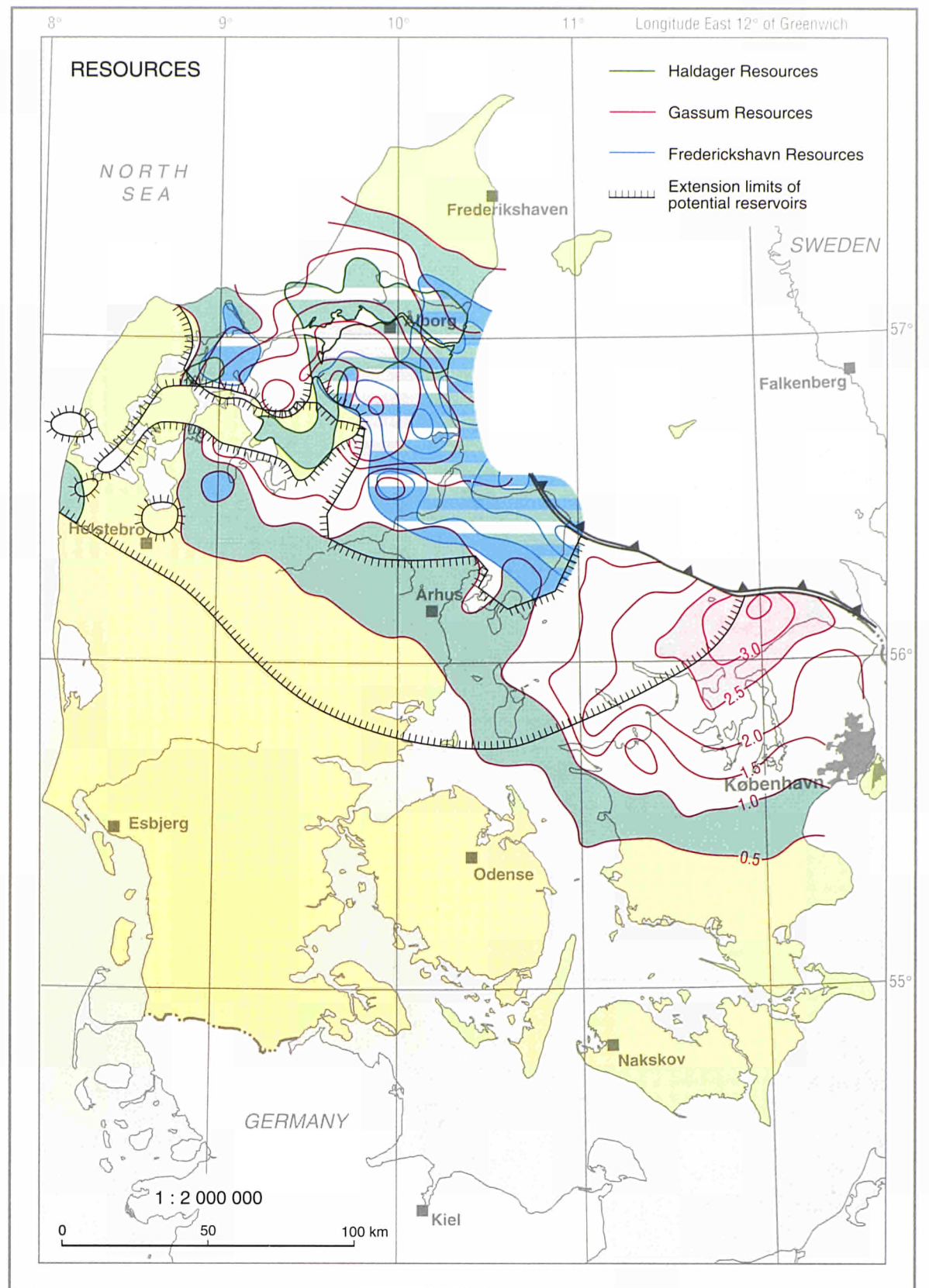
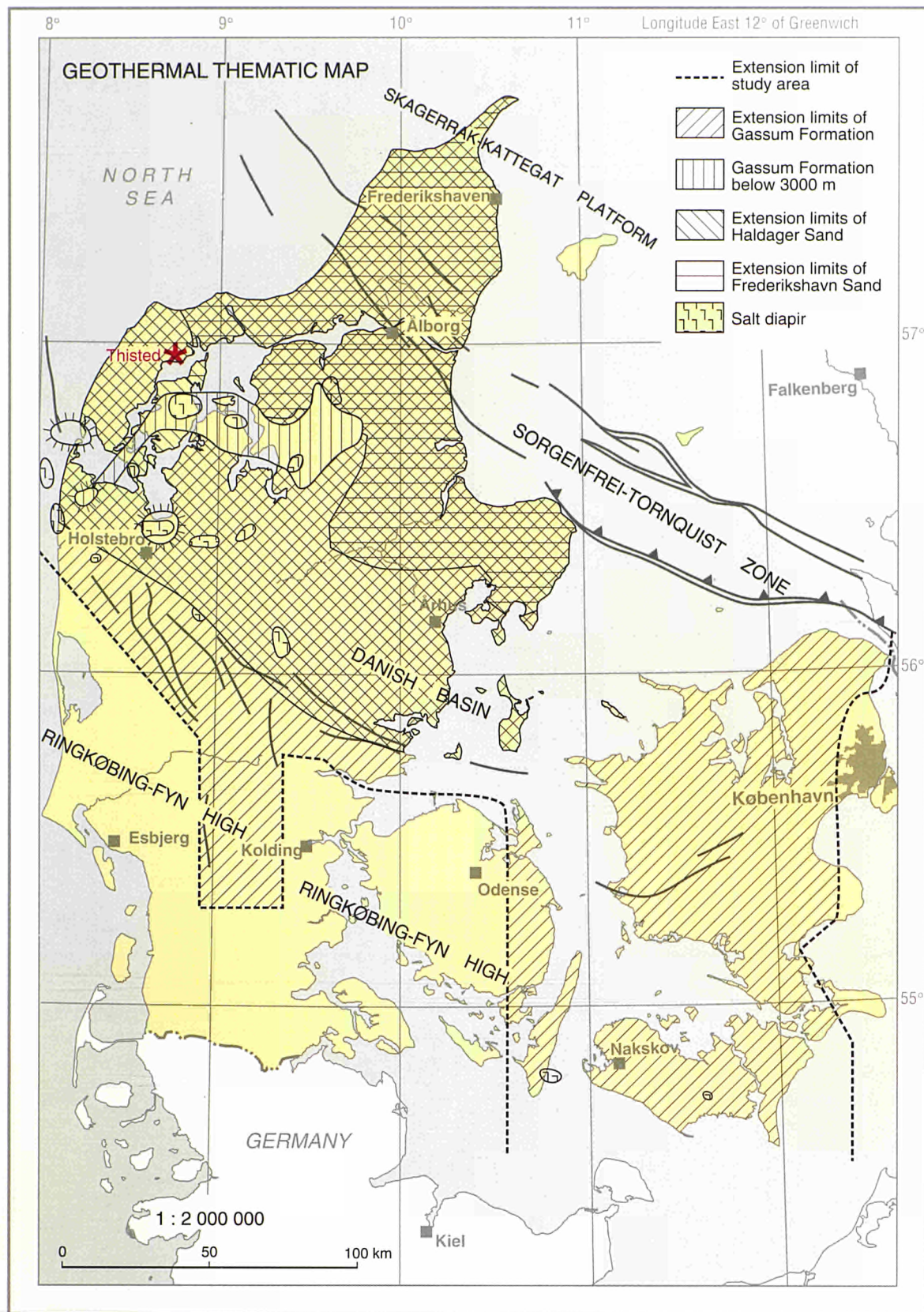


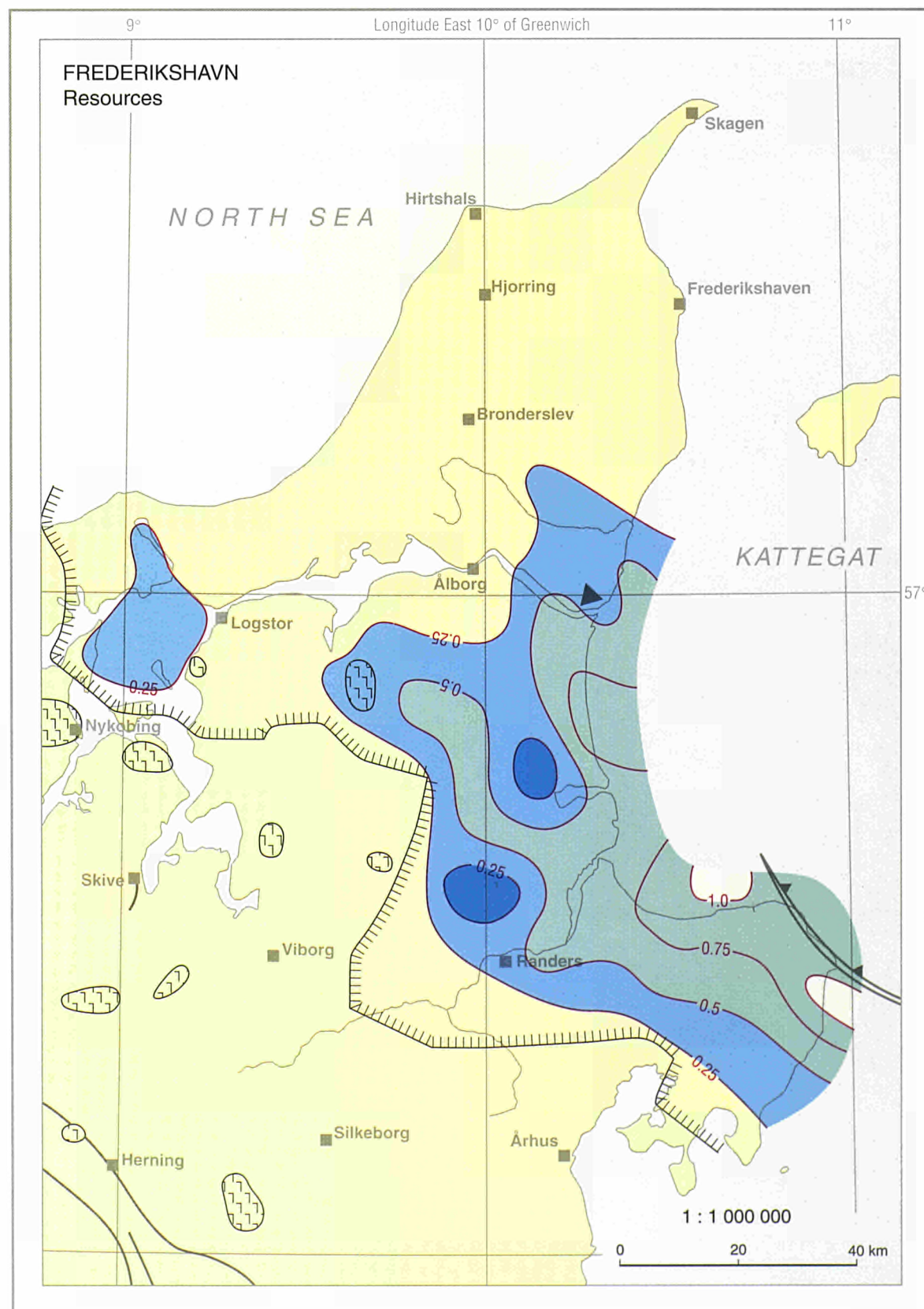
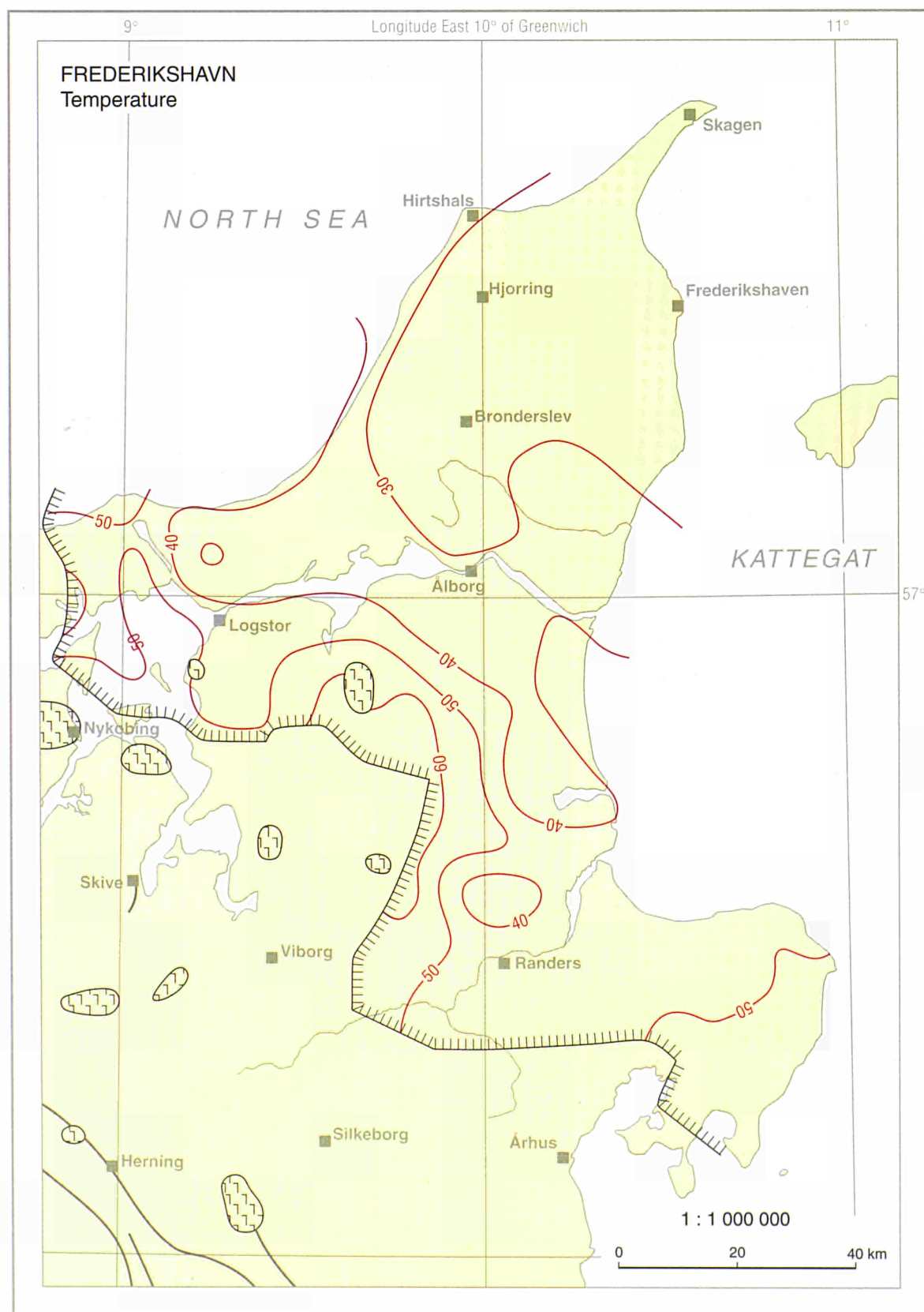
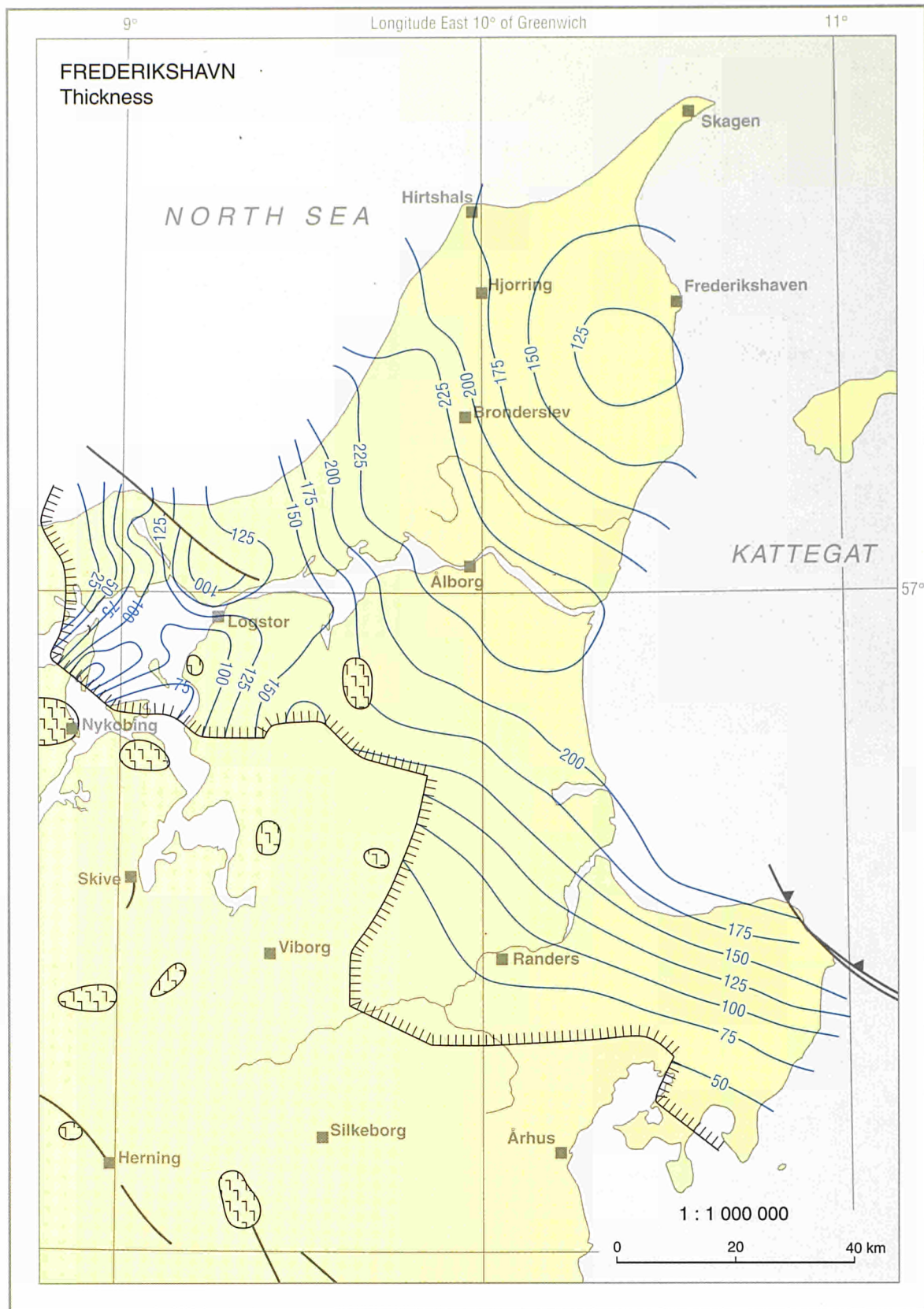
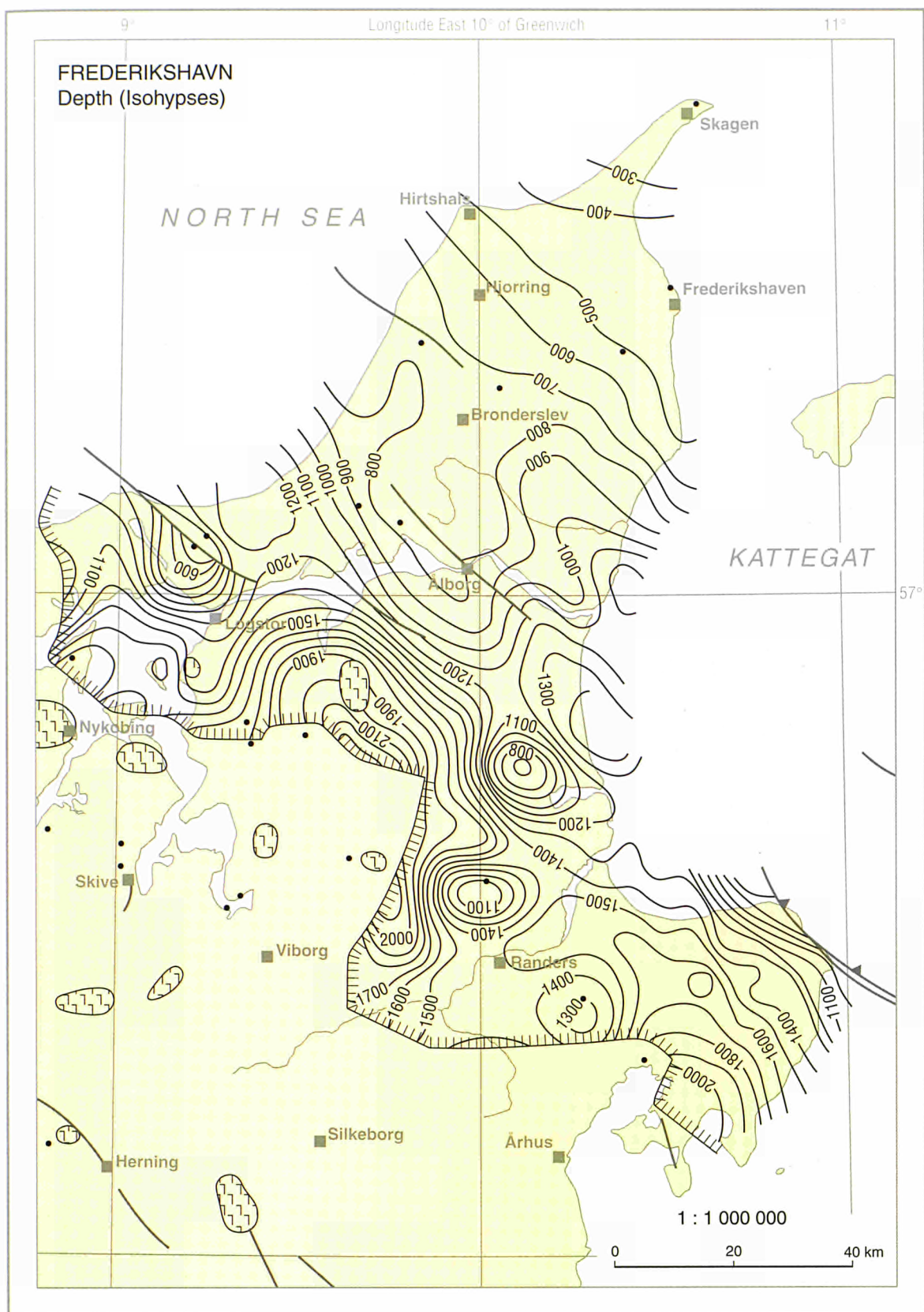
CZECH REPUBLIC



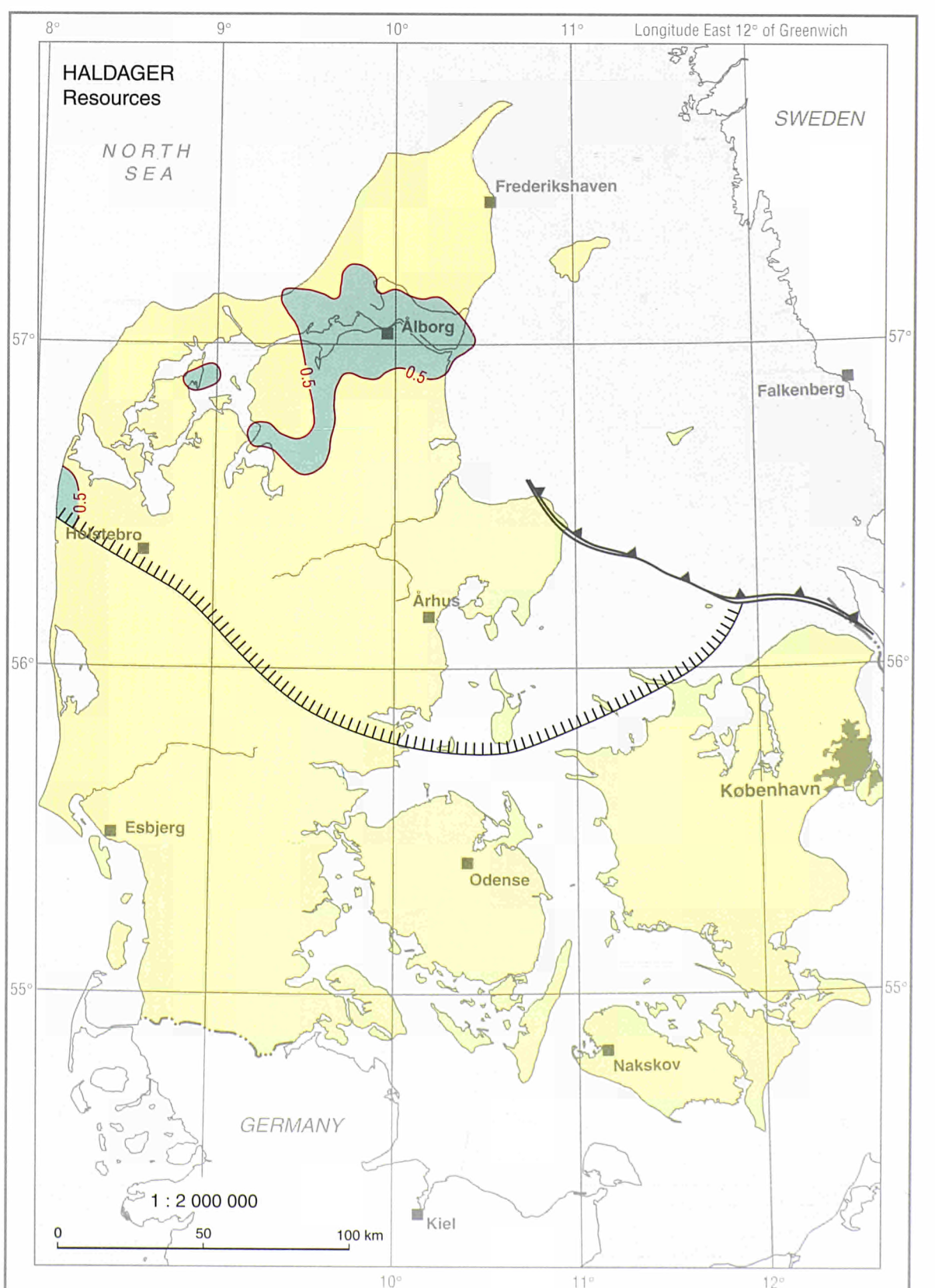
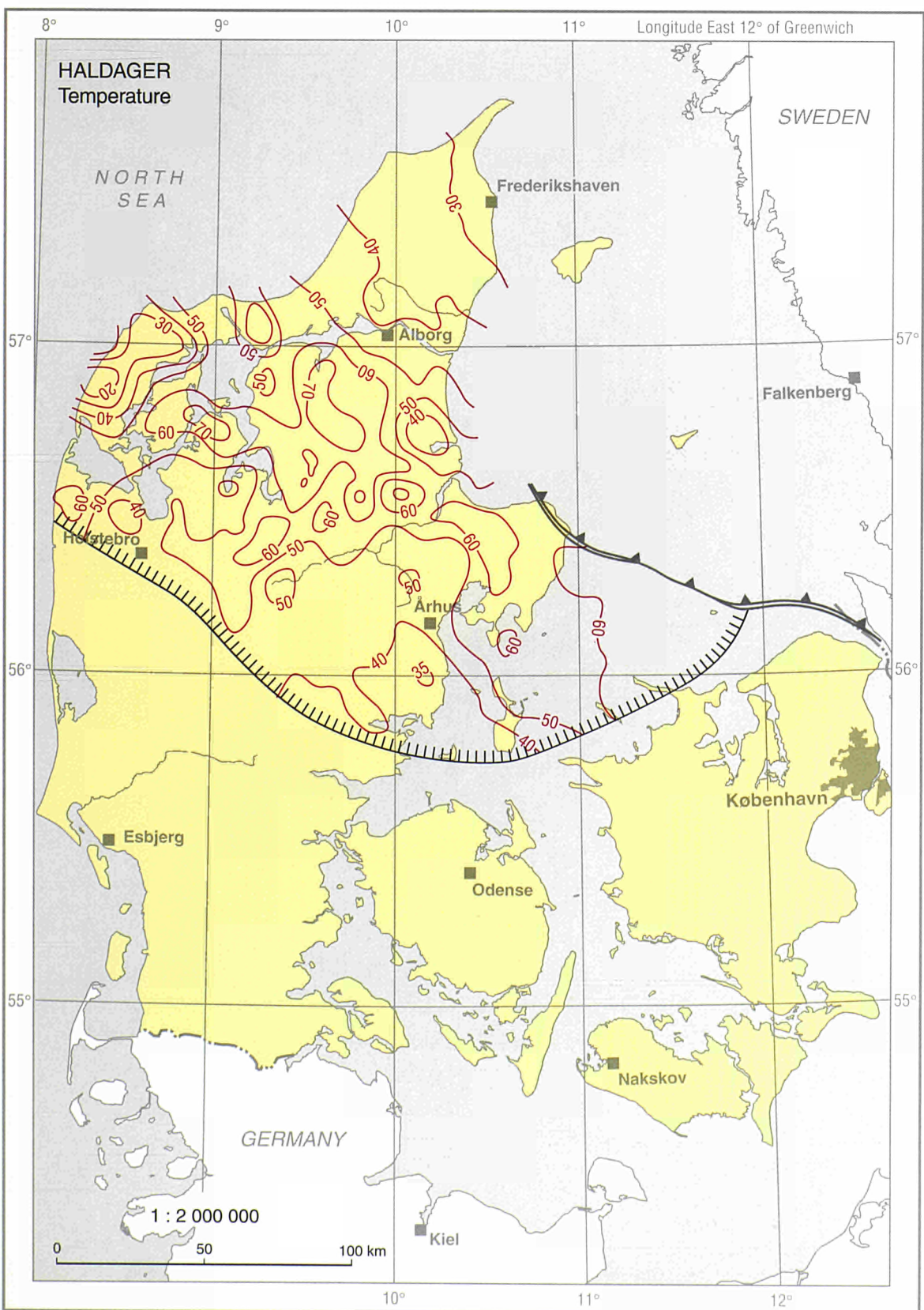
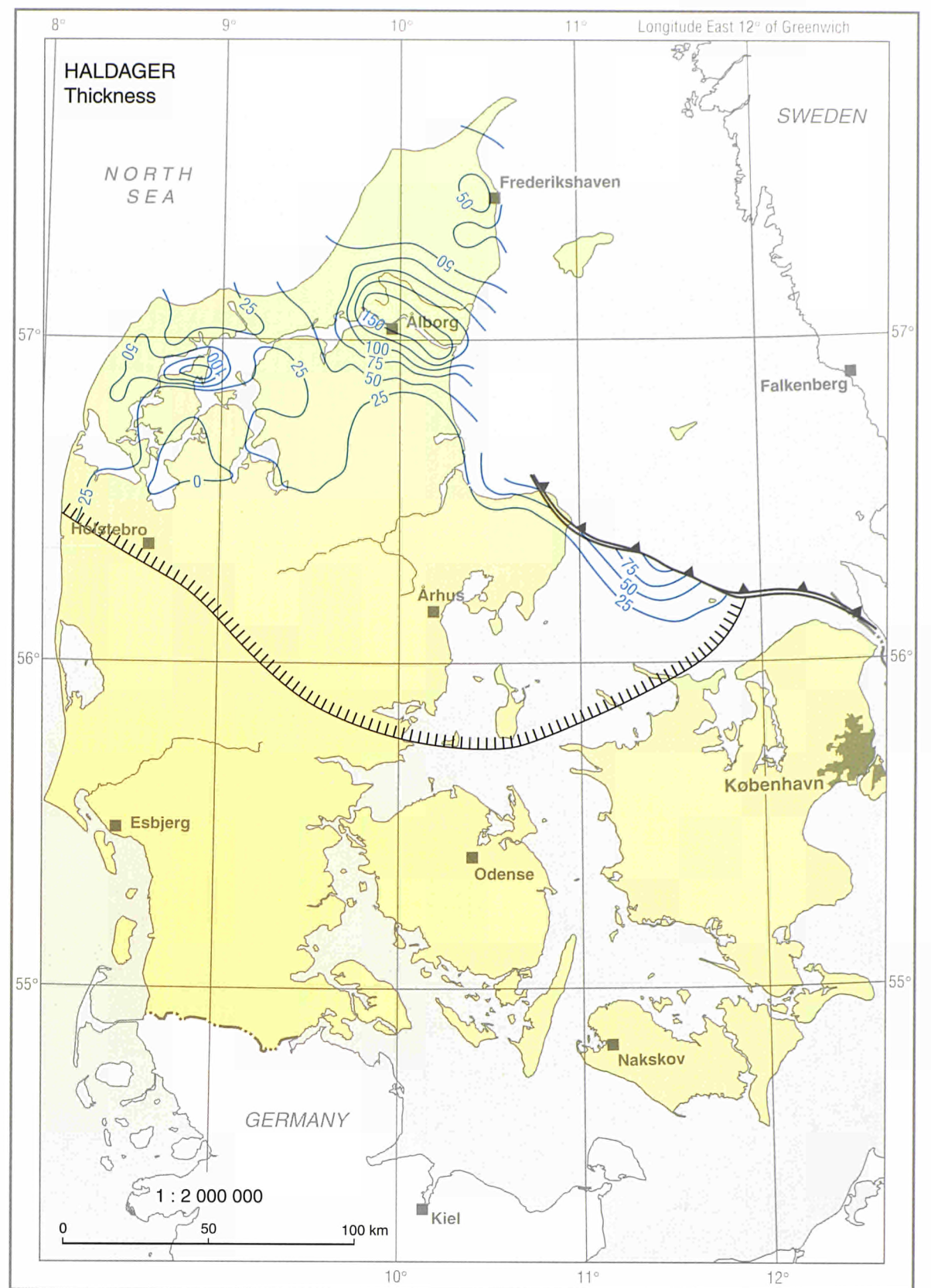
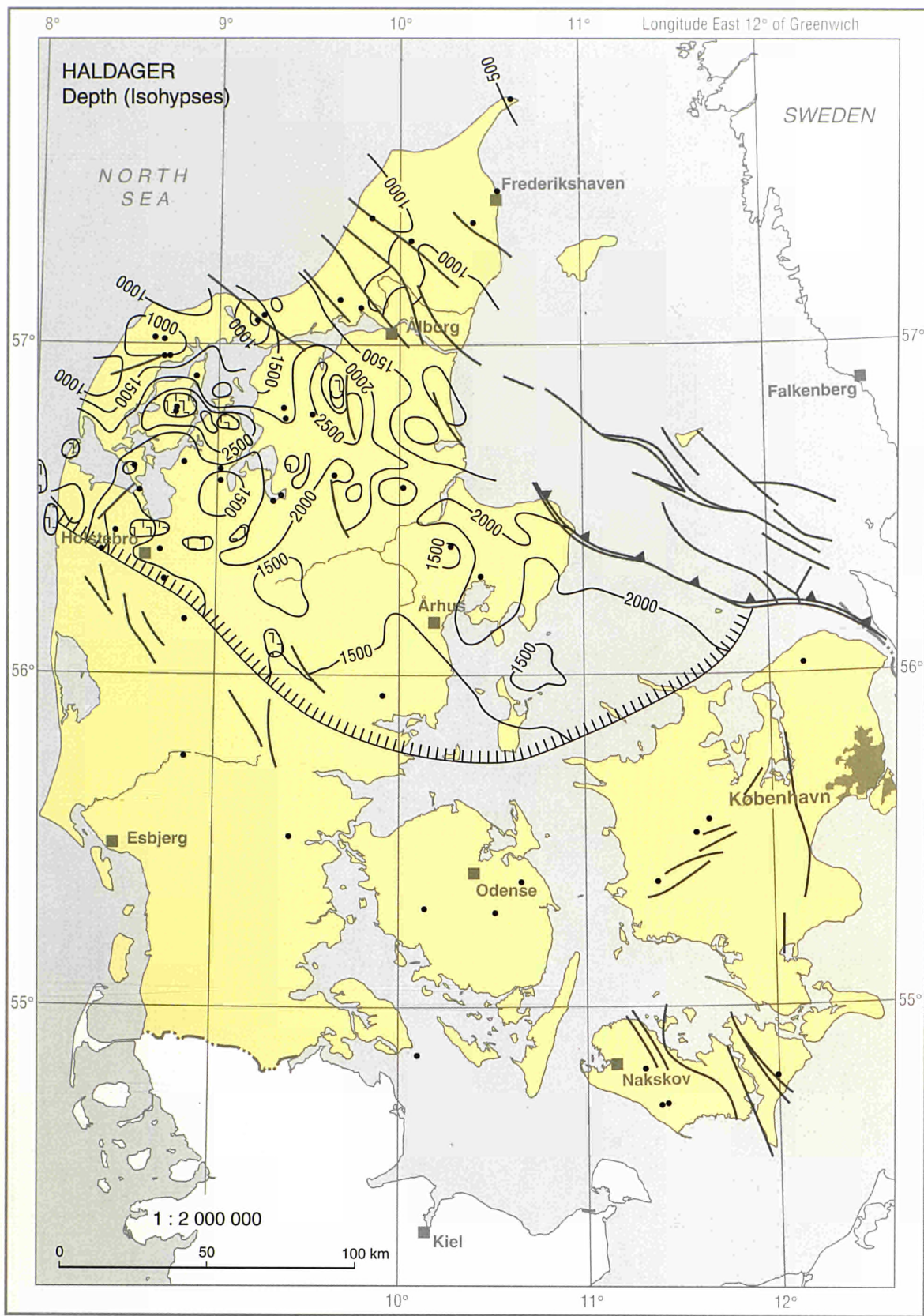


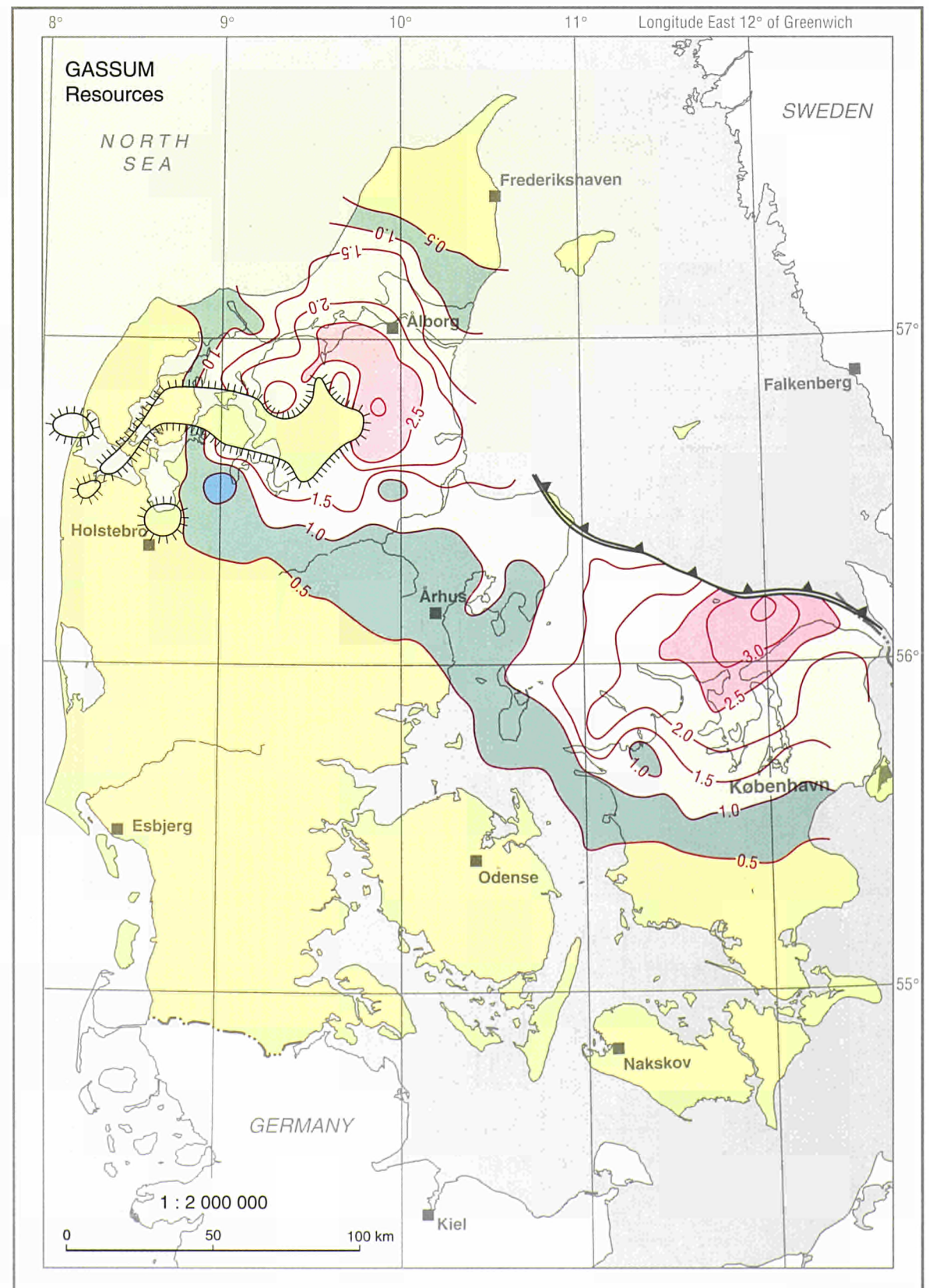
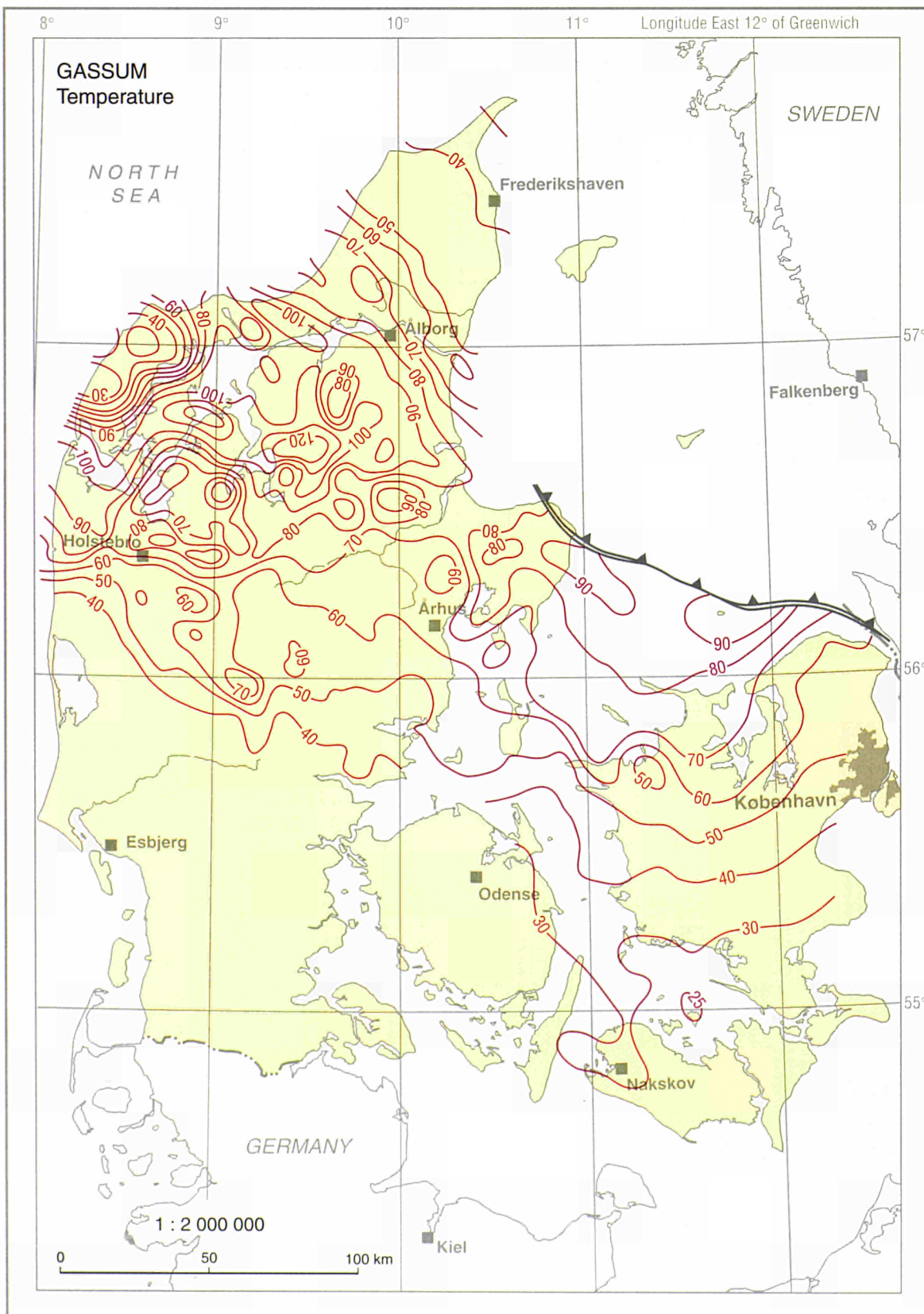
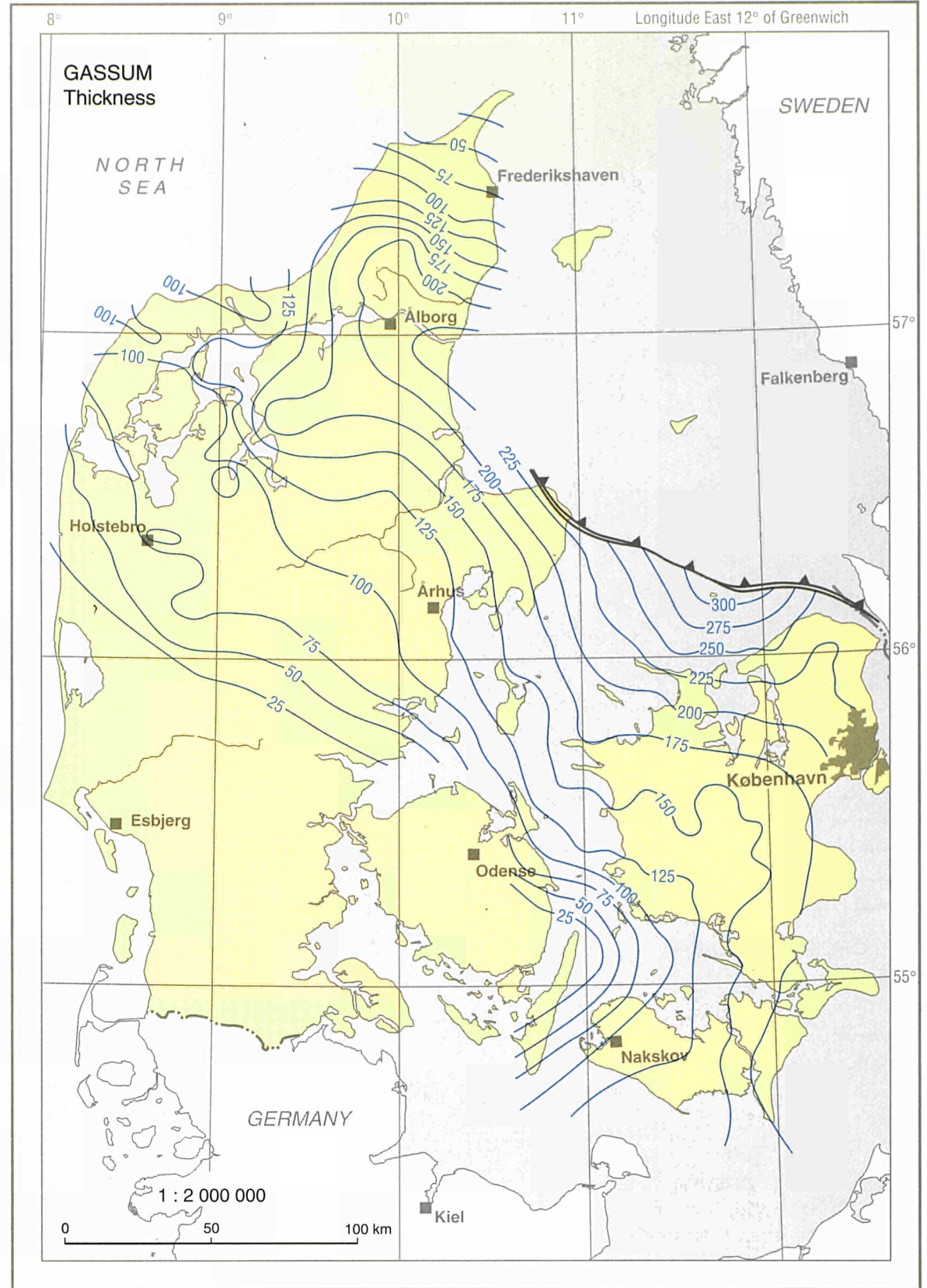
DENMARK



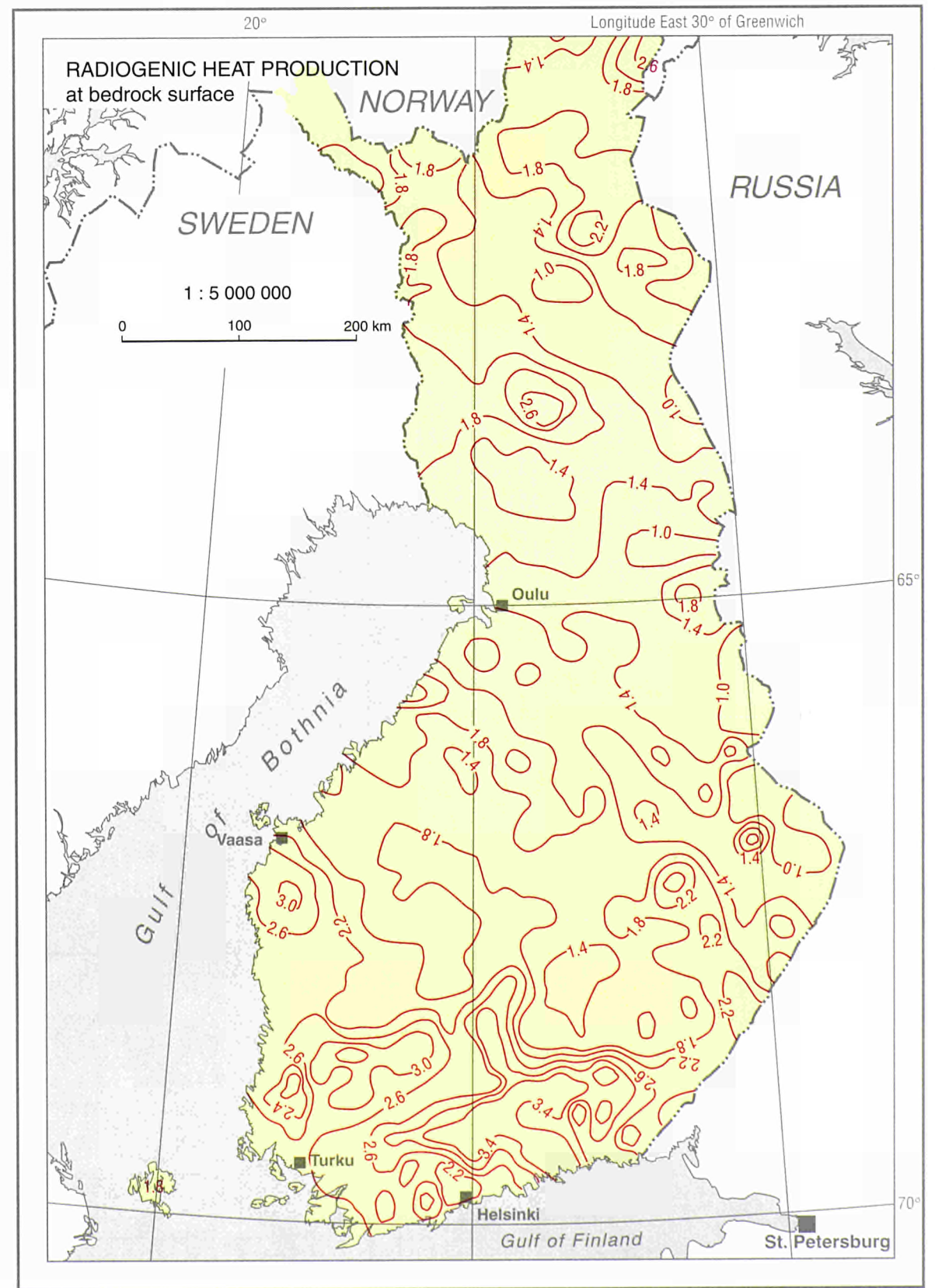
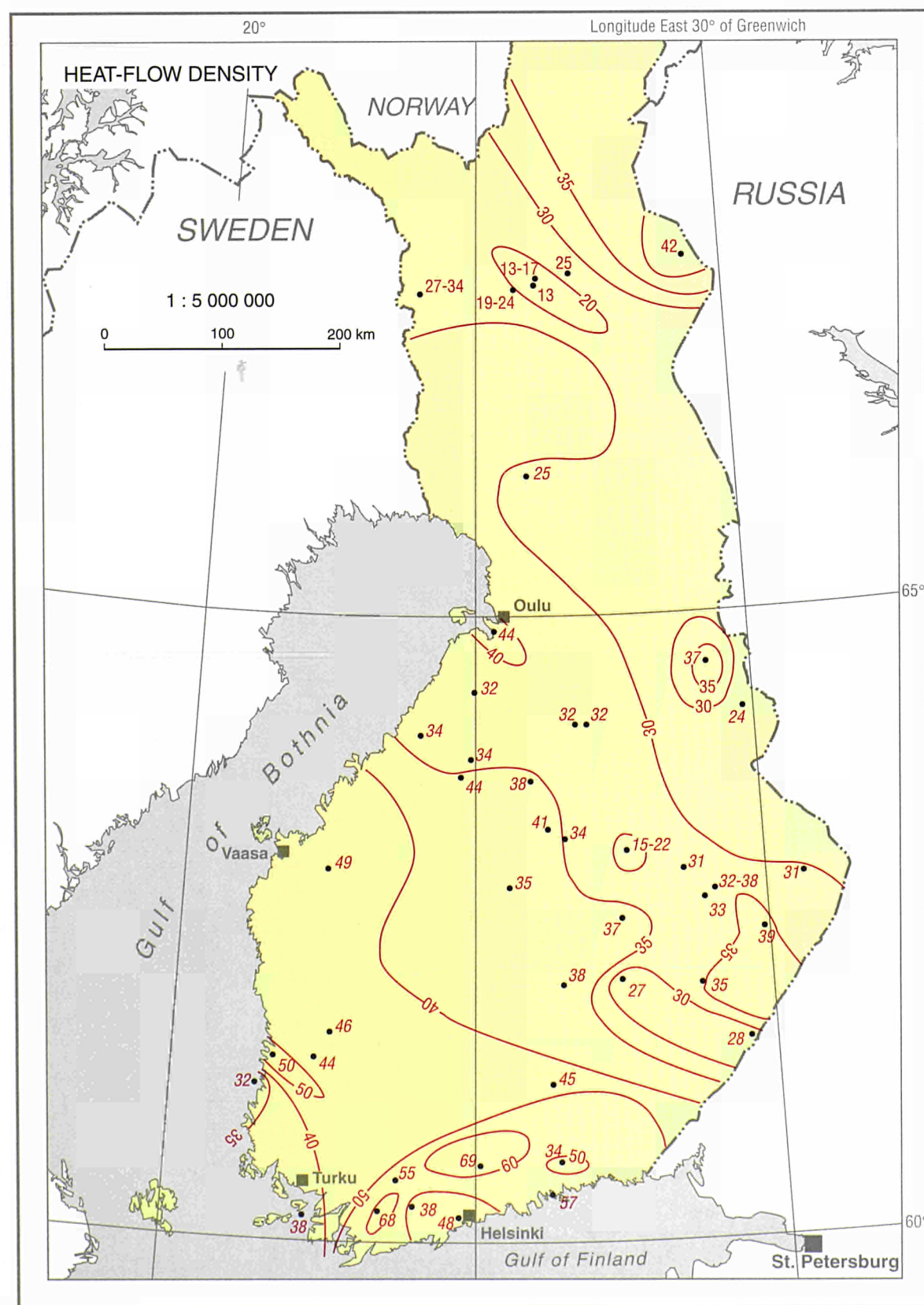
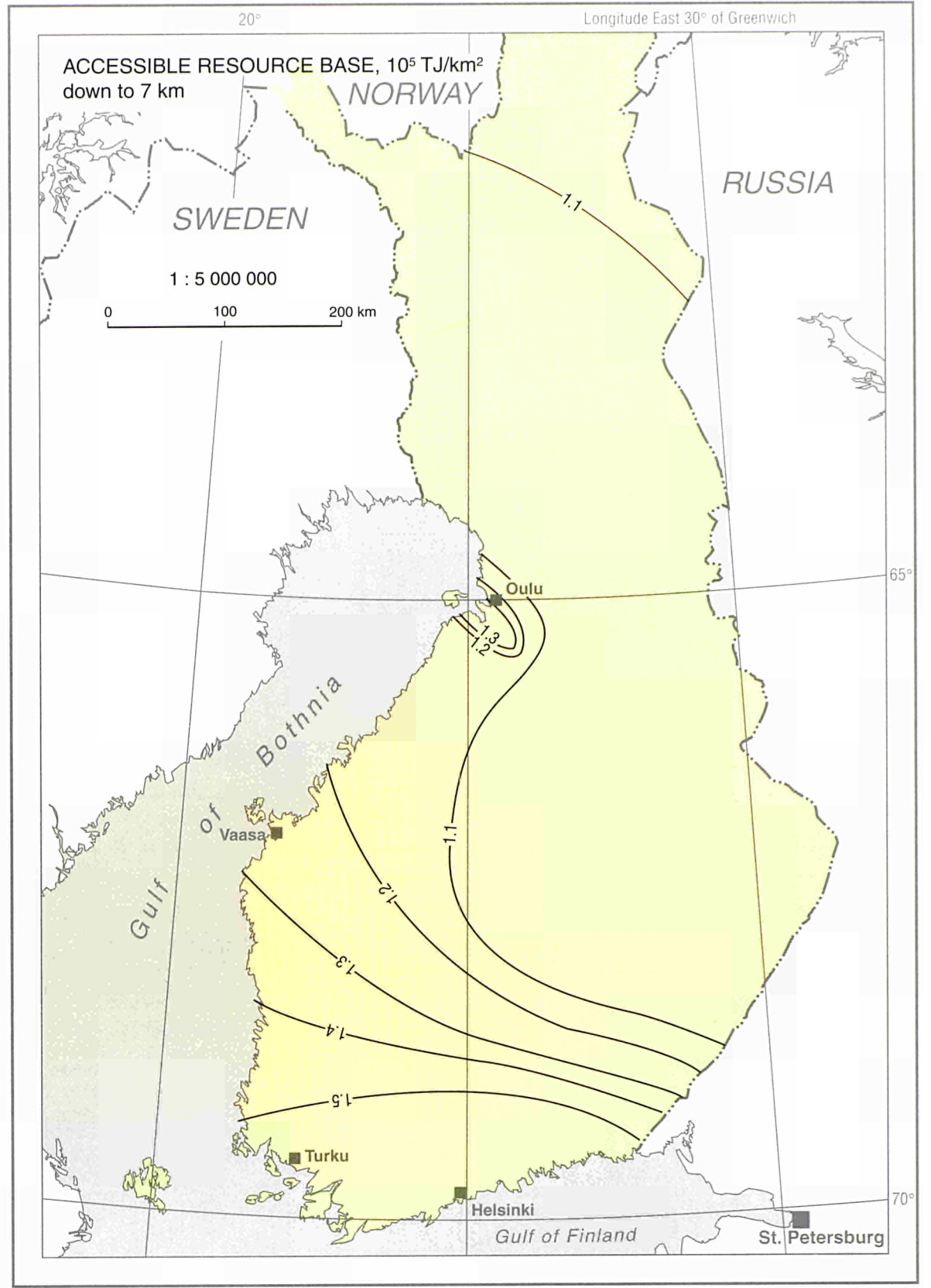
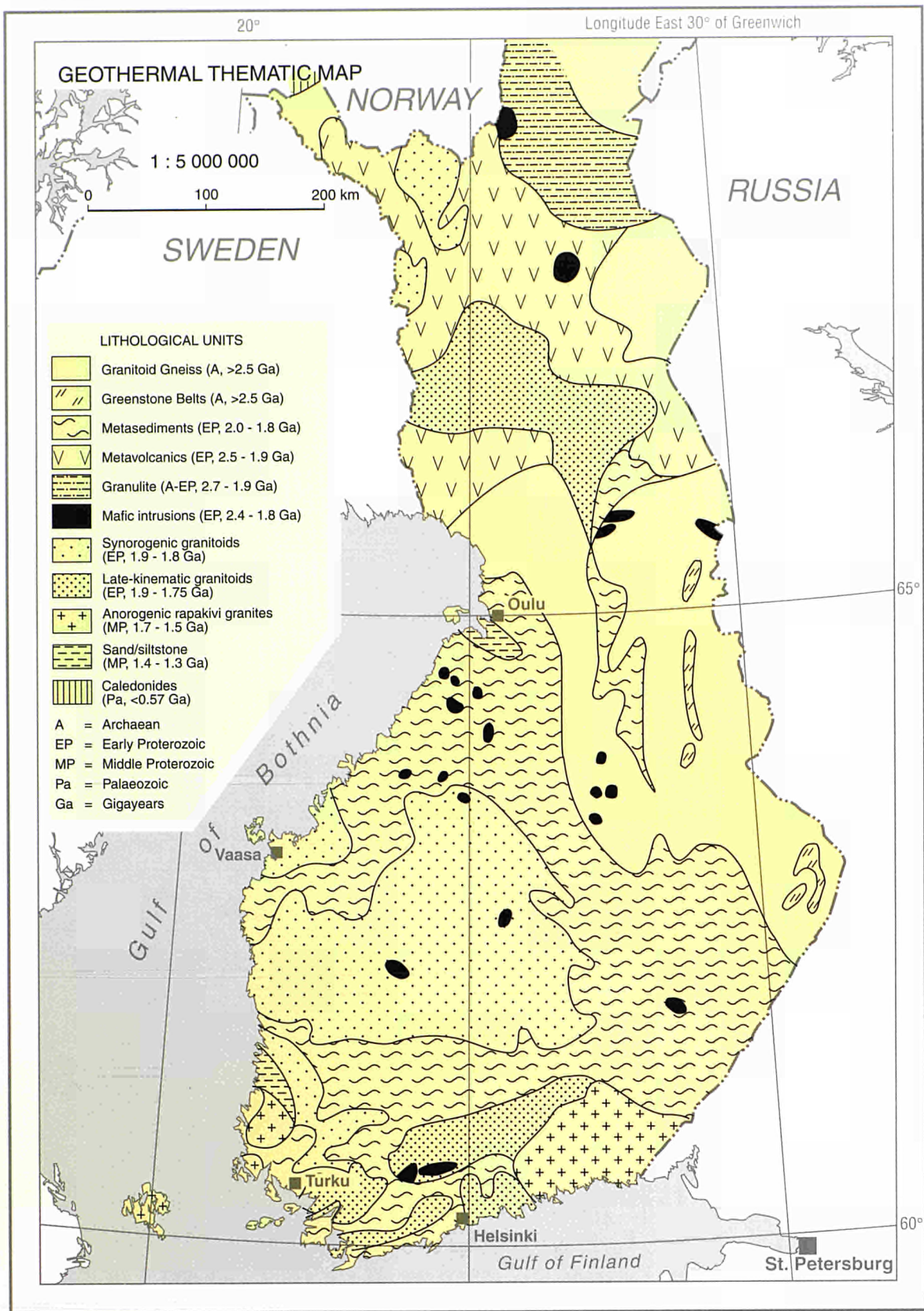


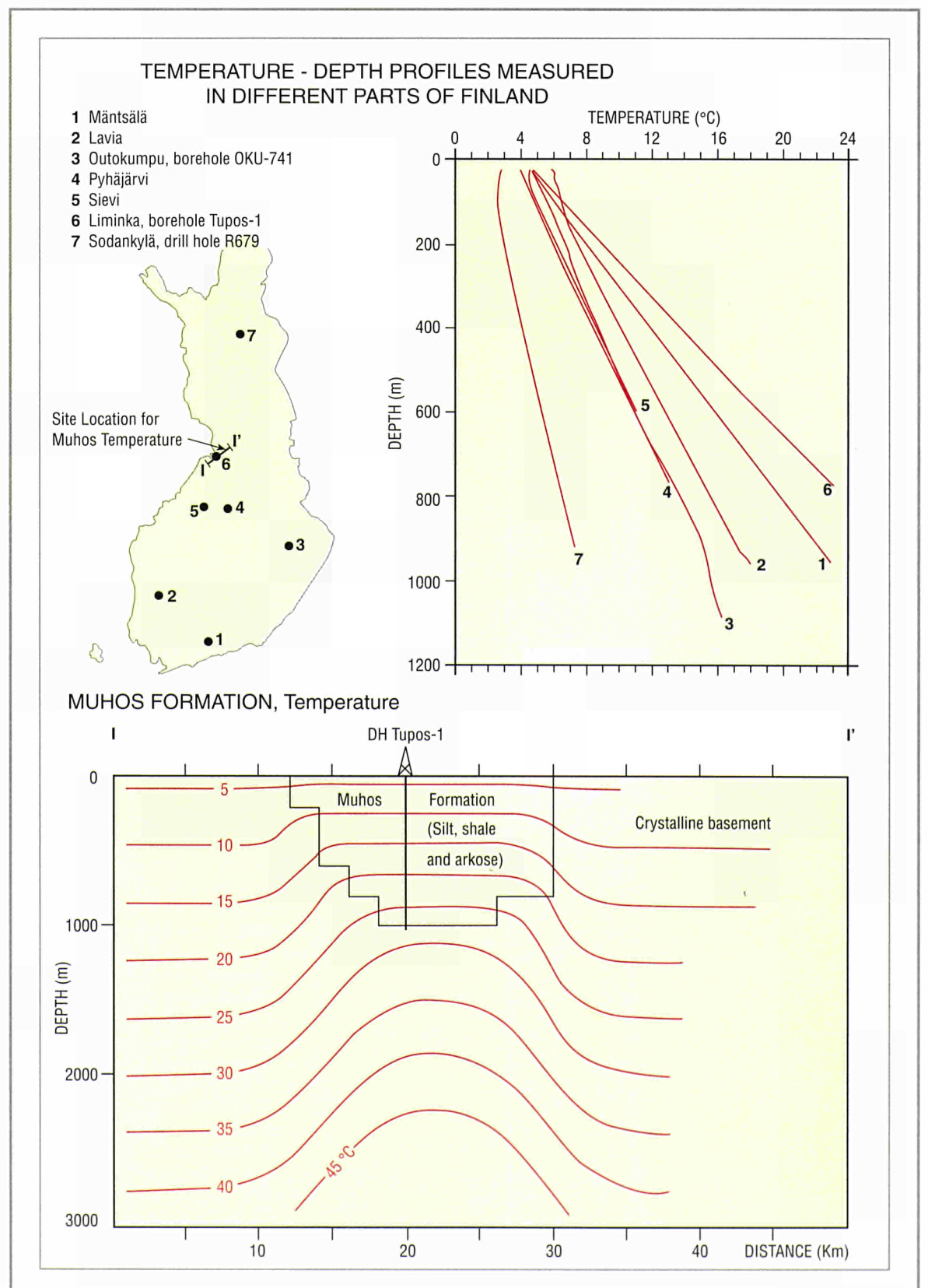
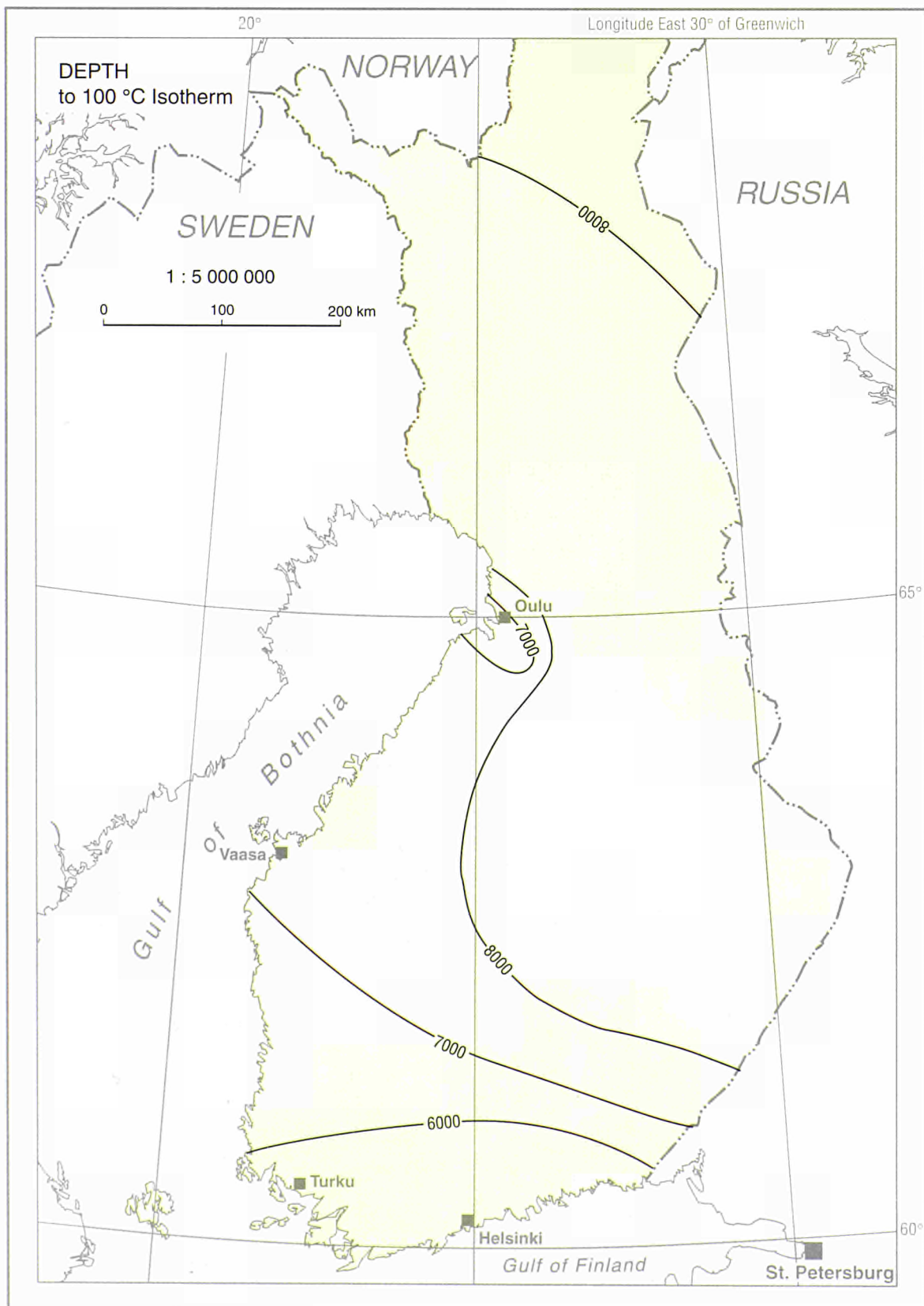
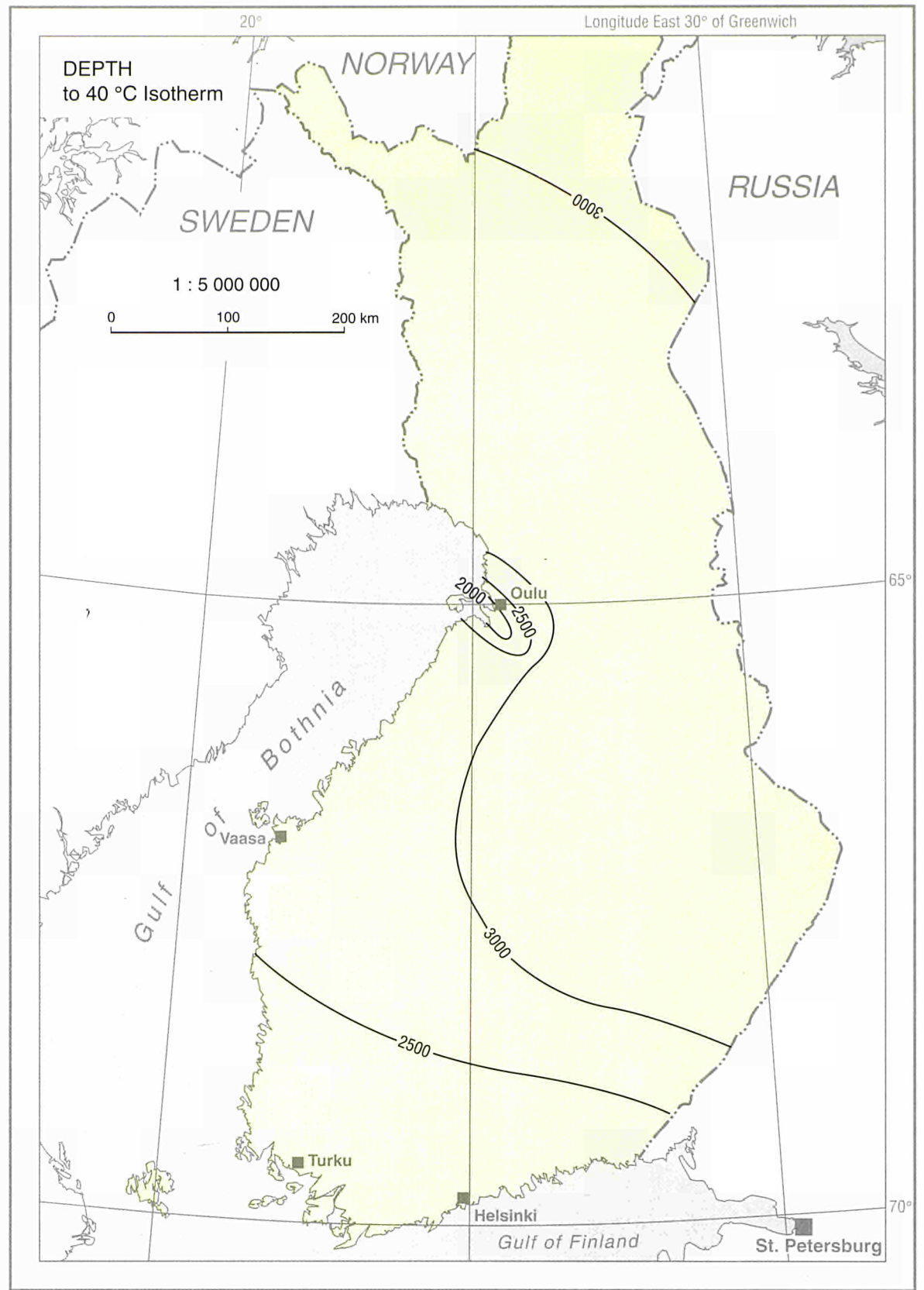
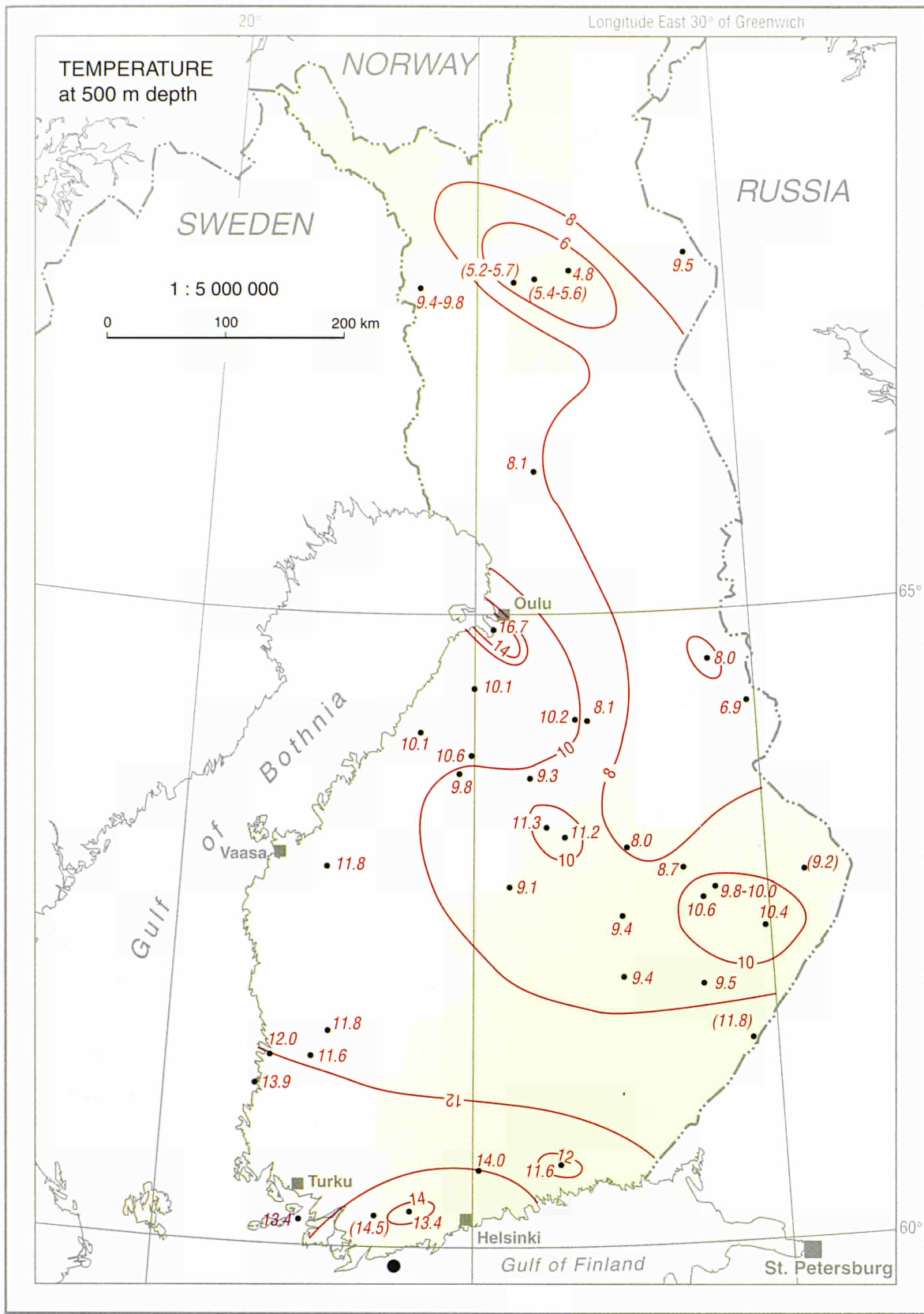
DENMARK



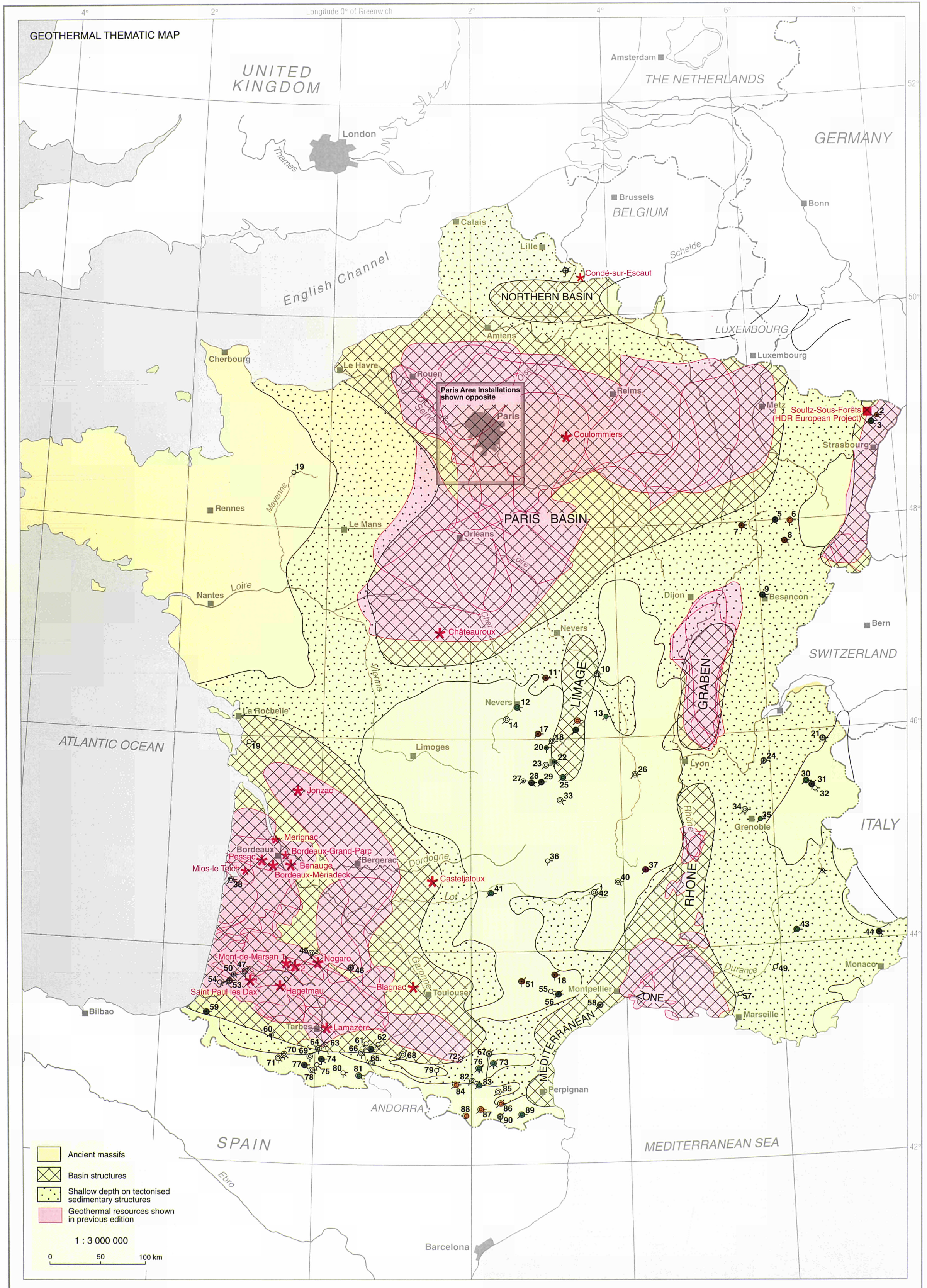


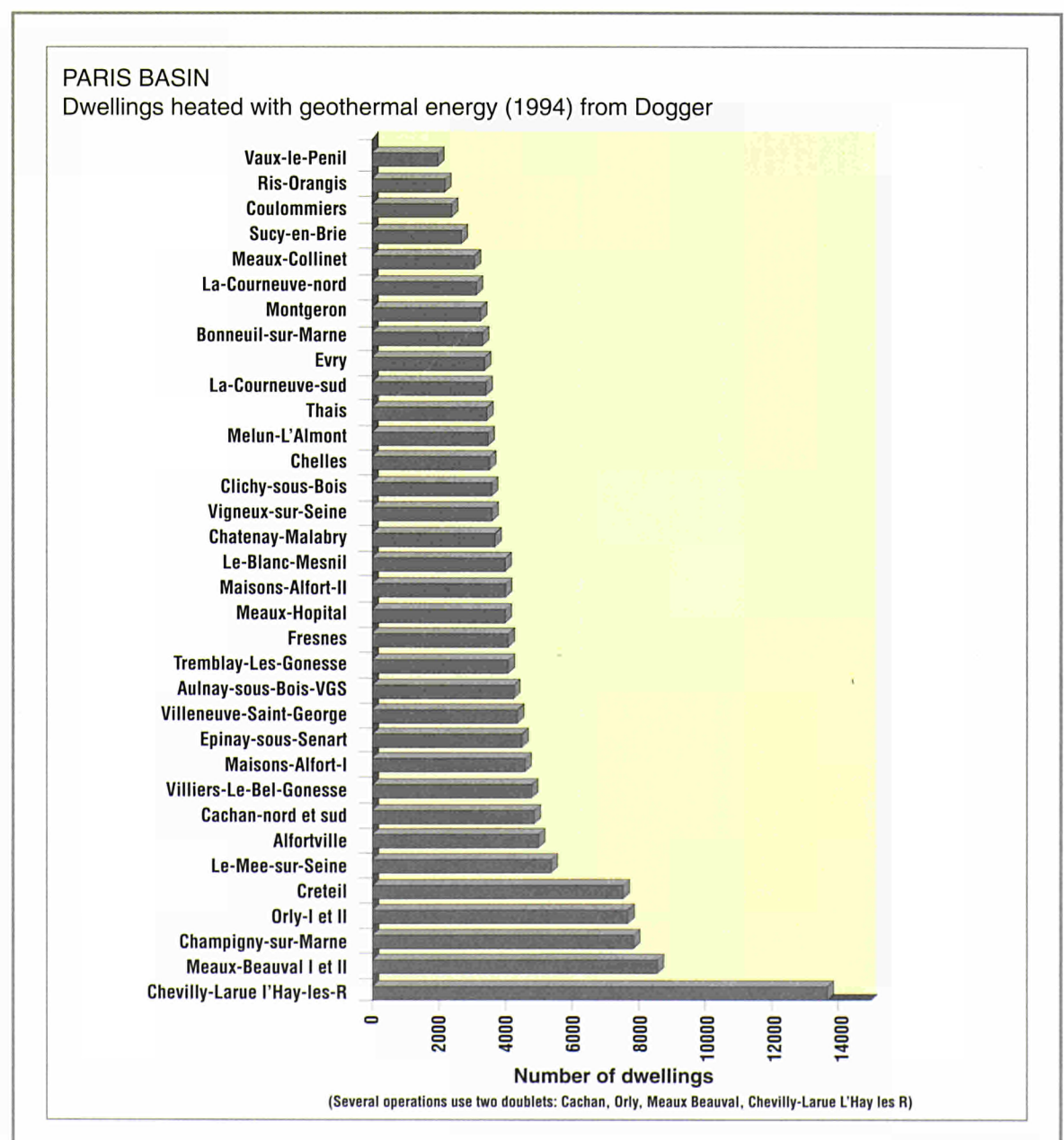
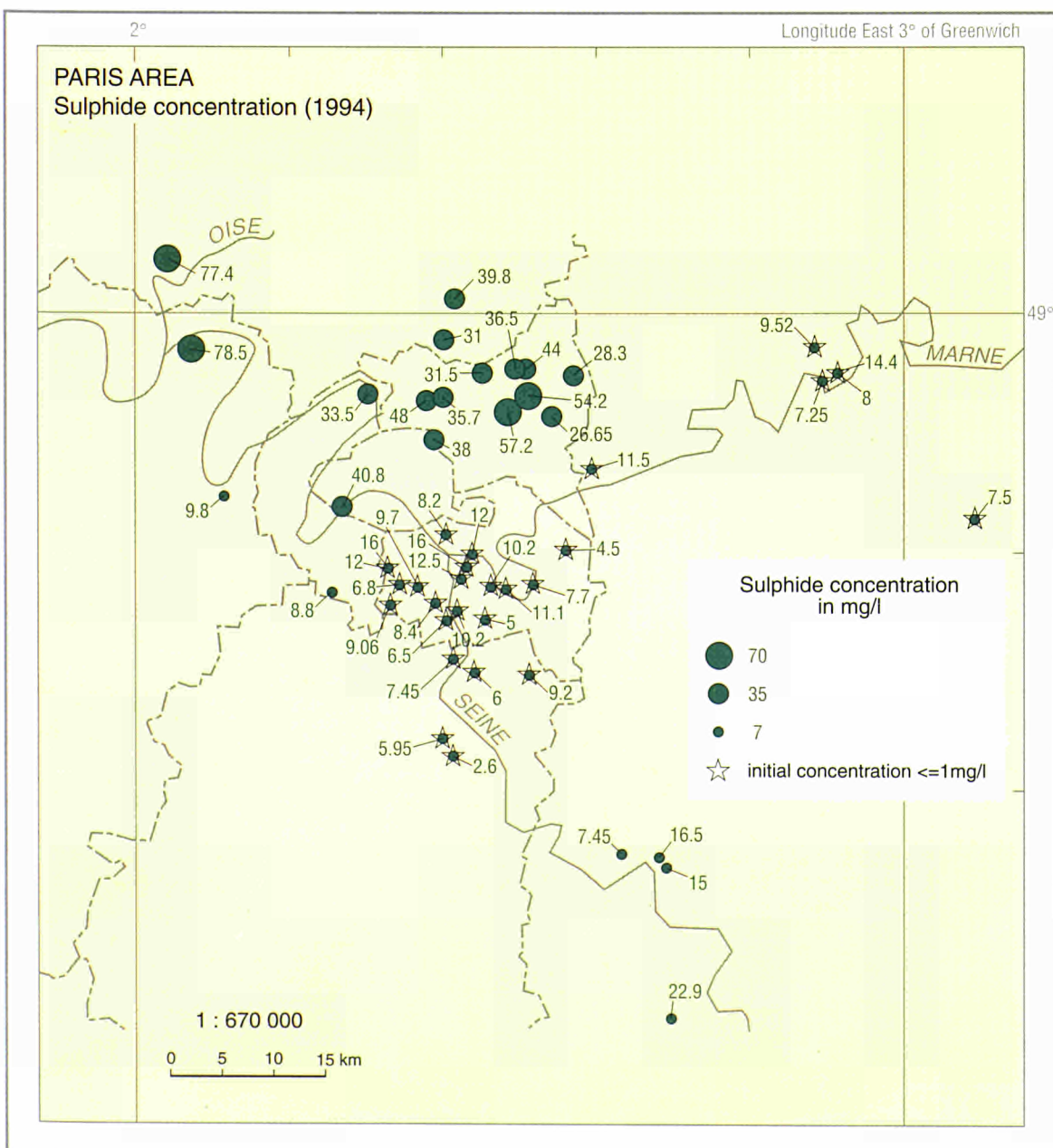
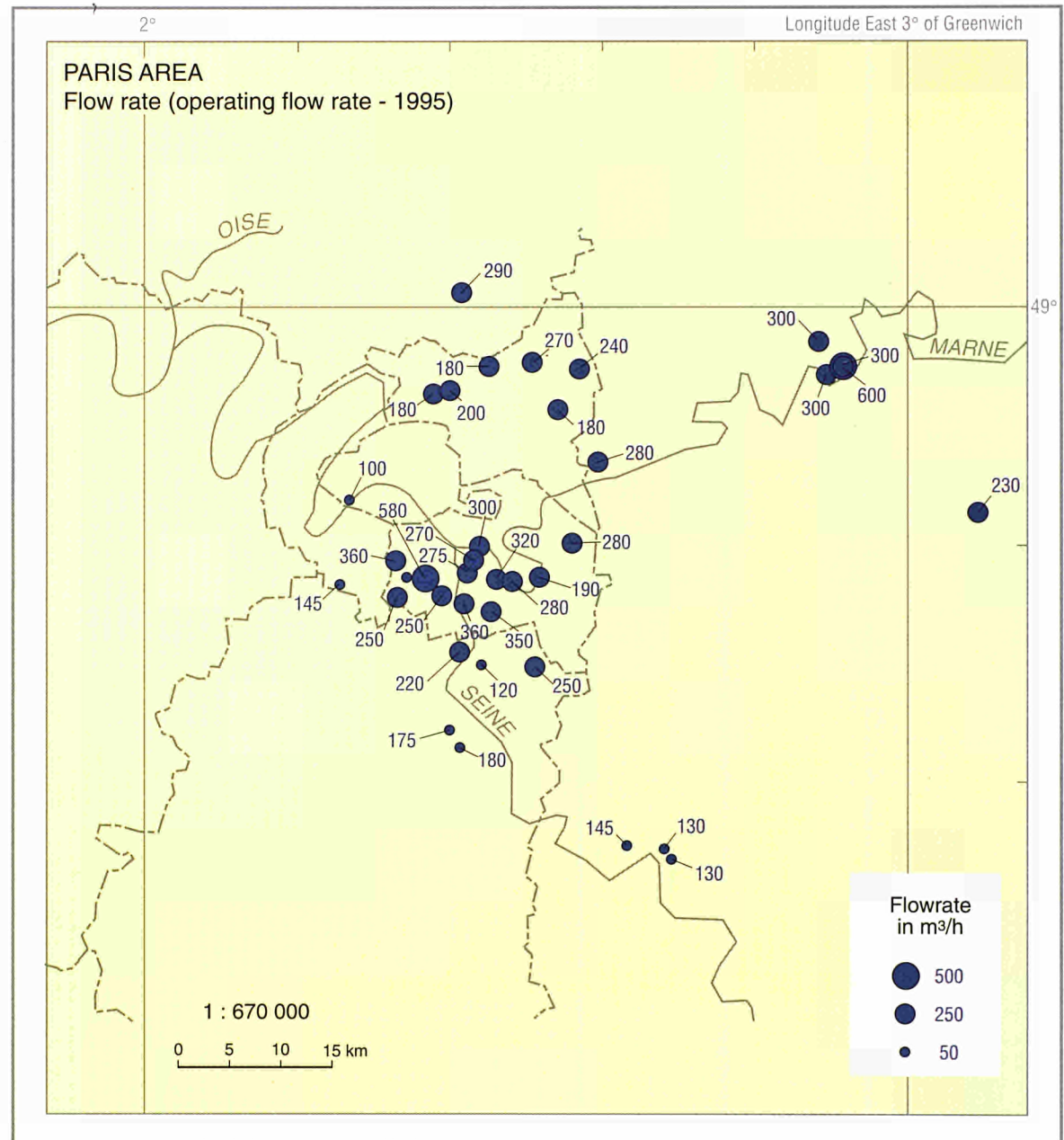
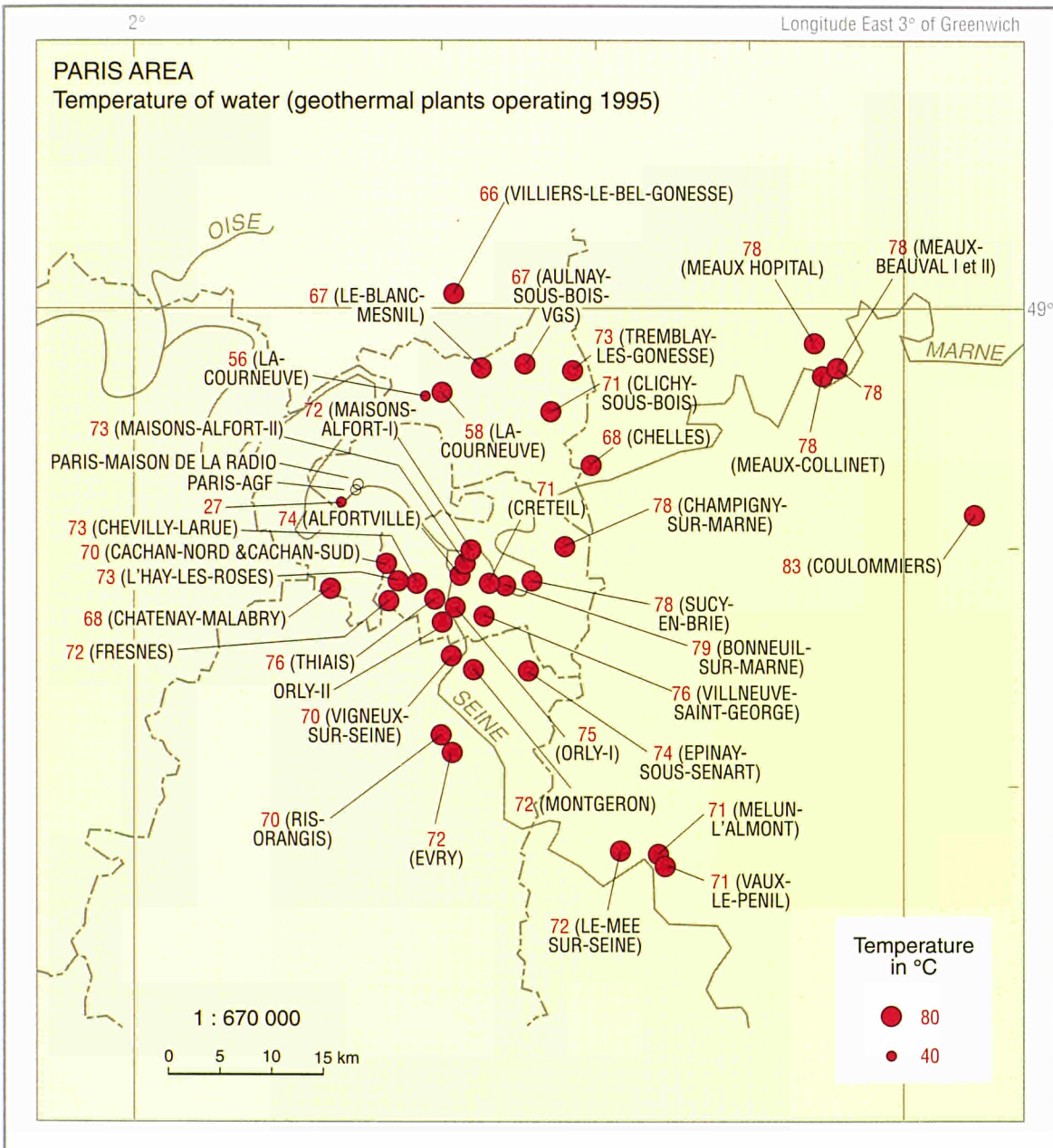
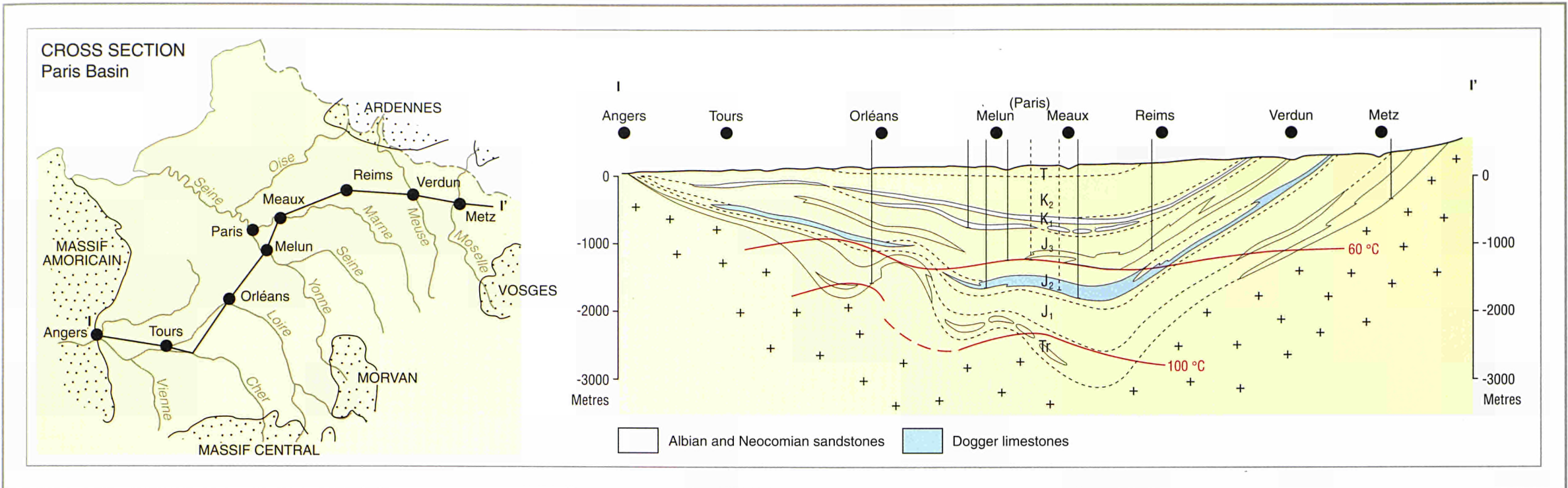
FINLAND





FRANCE

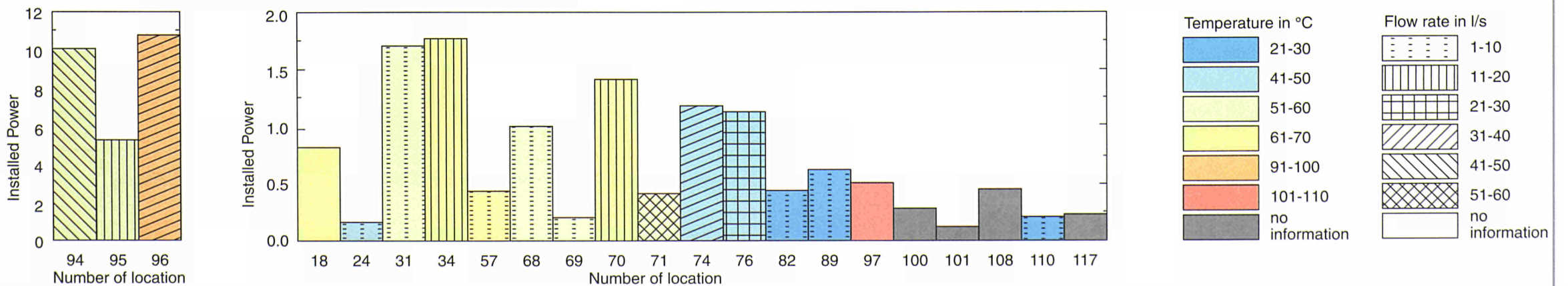


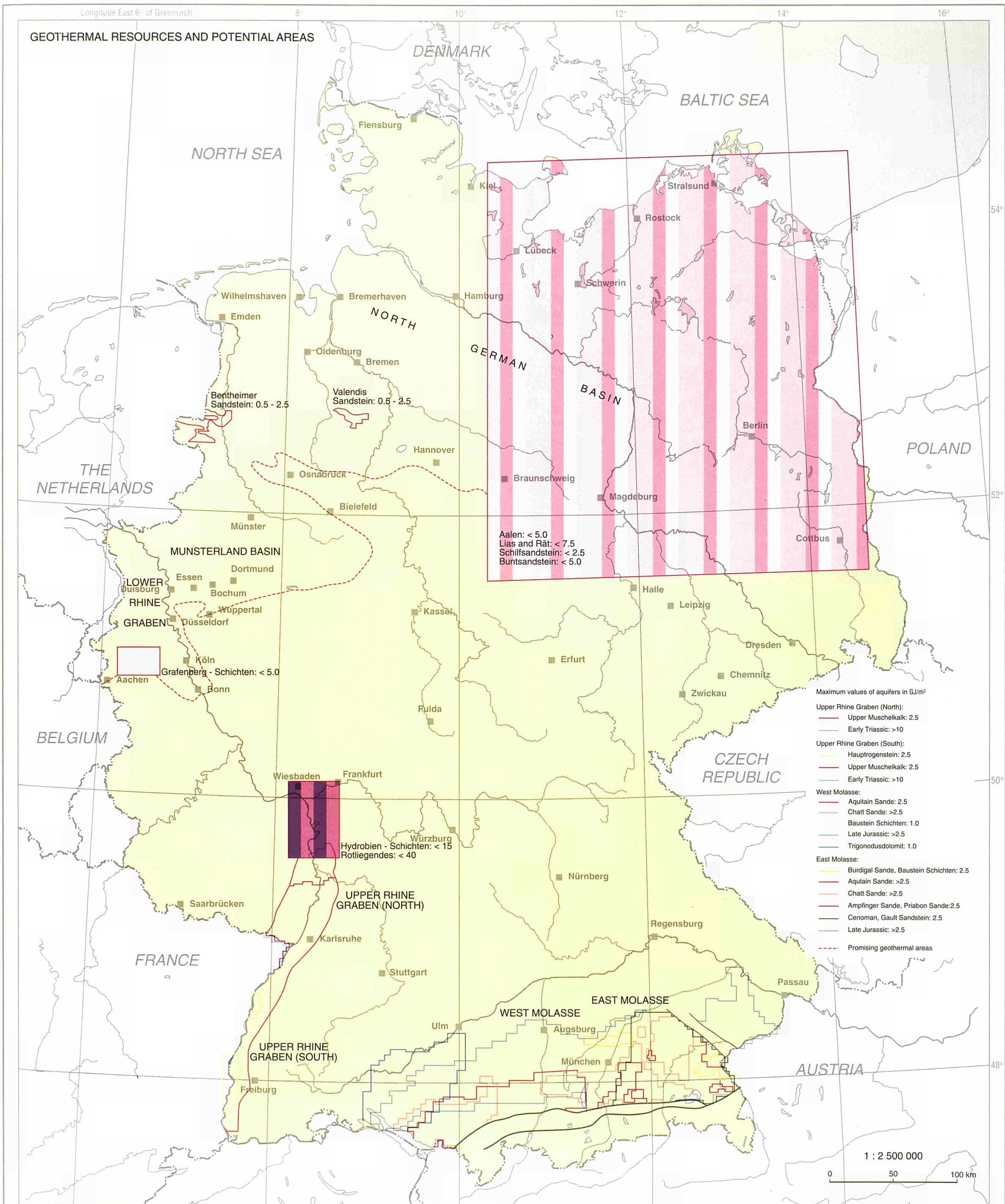


GERMANY

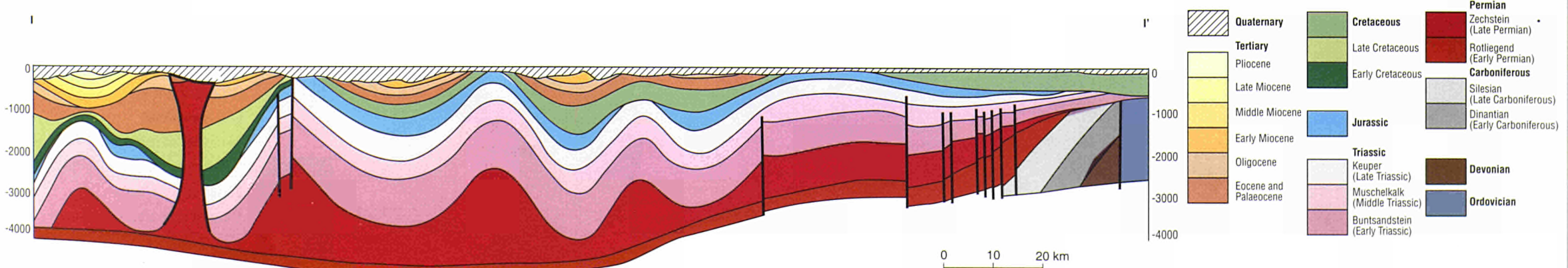


MAIN CHARACTERISTICS OF GEOTHERMAL INSTALLATIONS

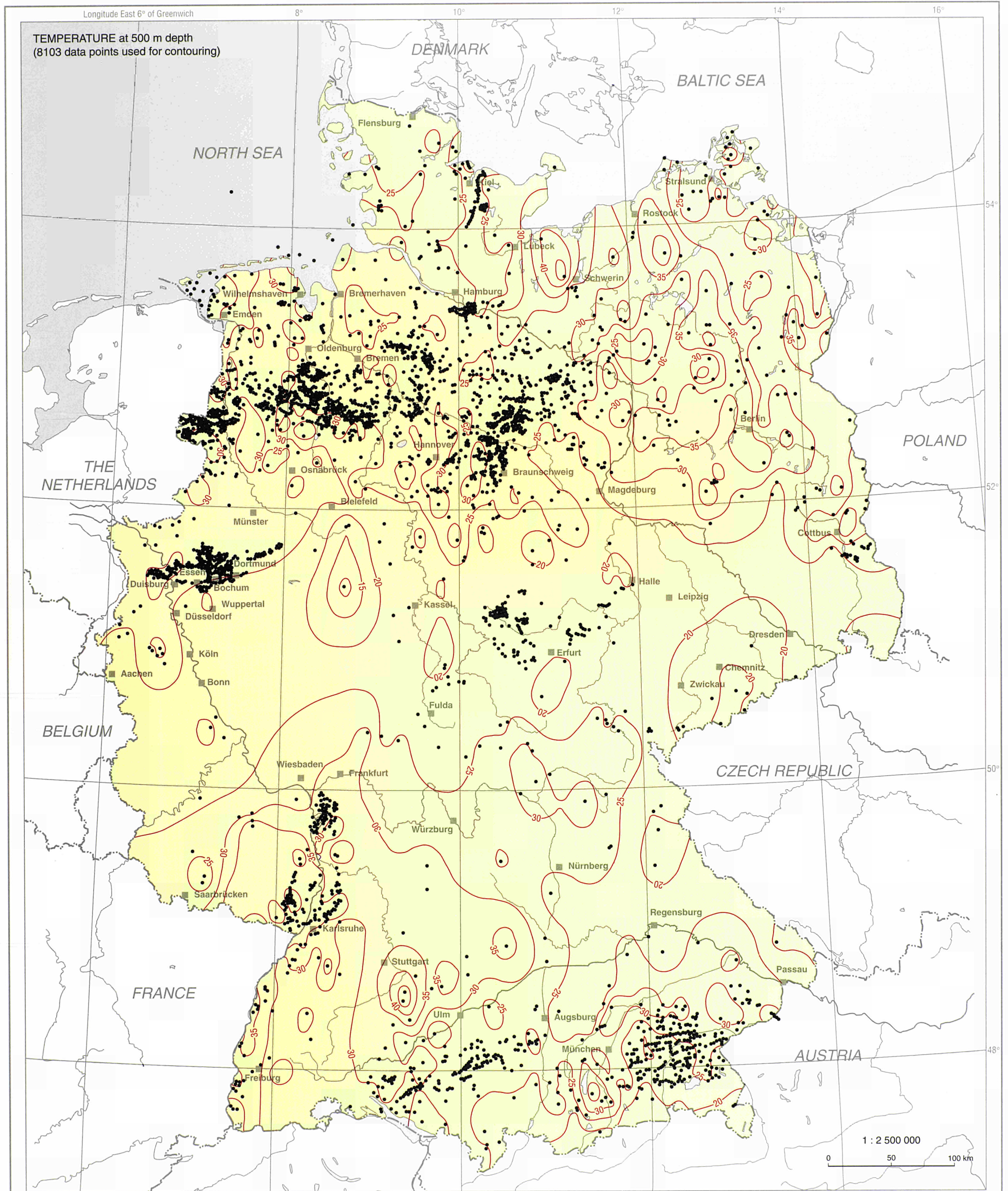




CROSS SECTION

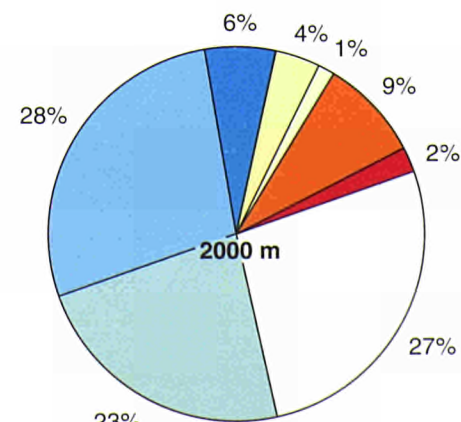
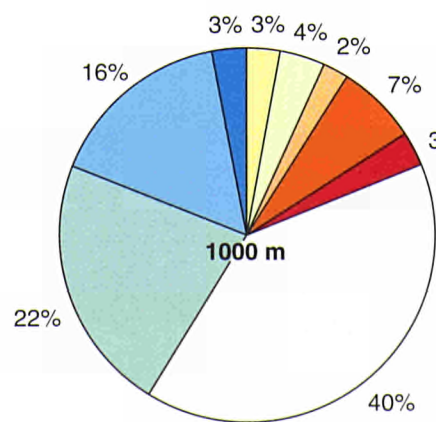
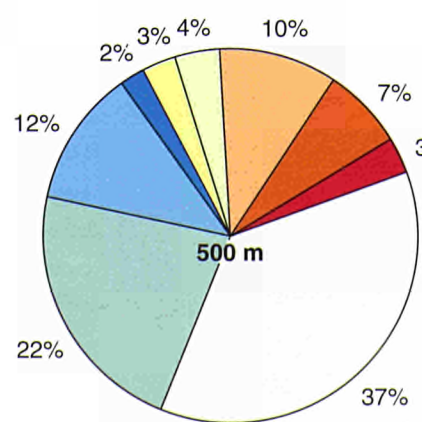


GERMANY

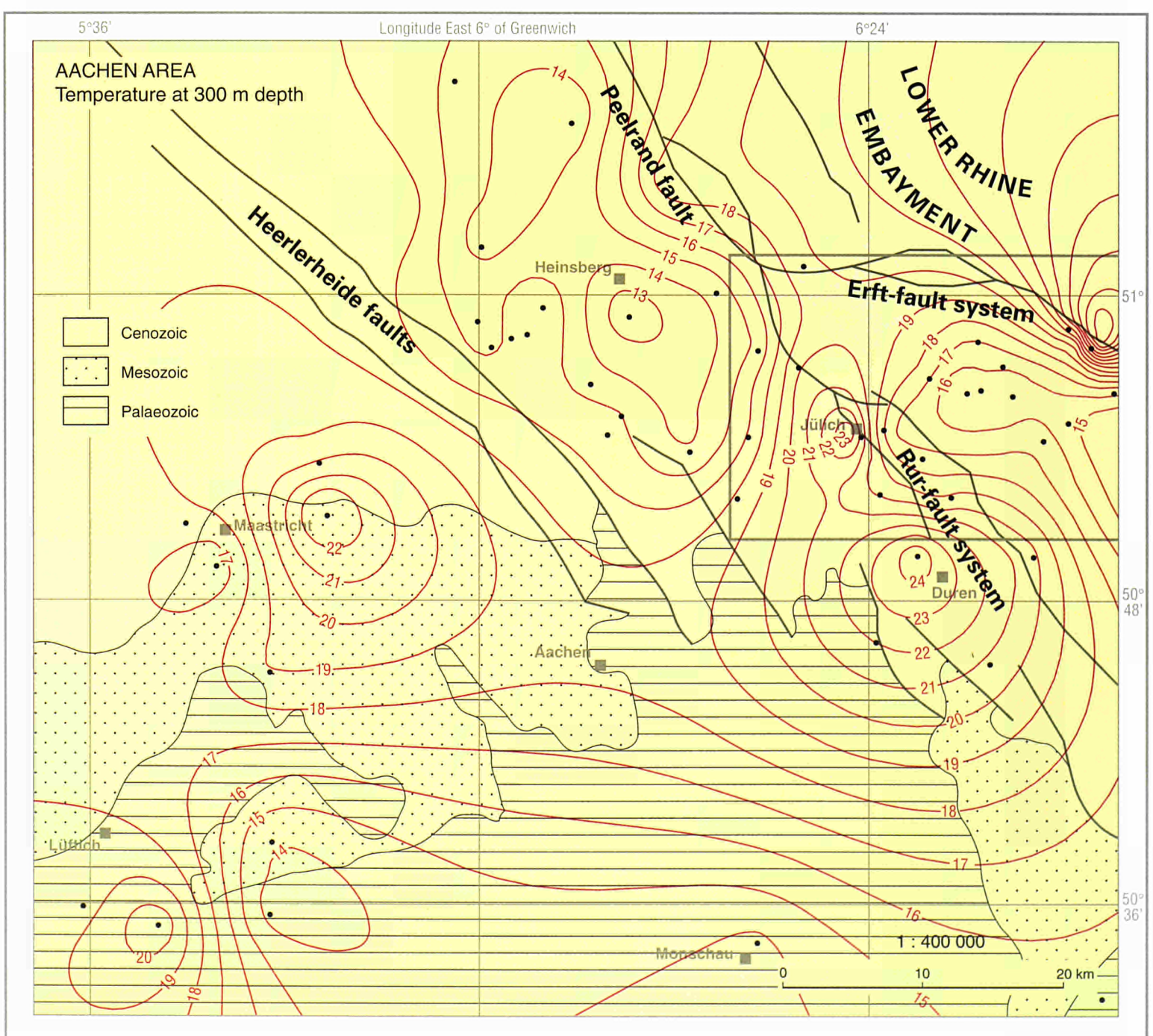
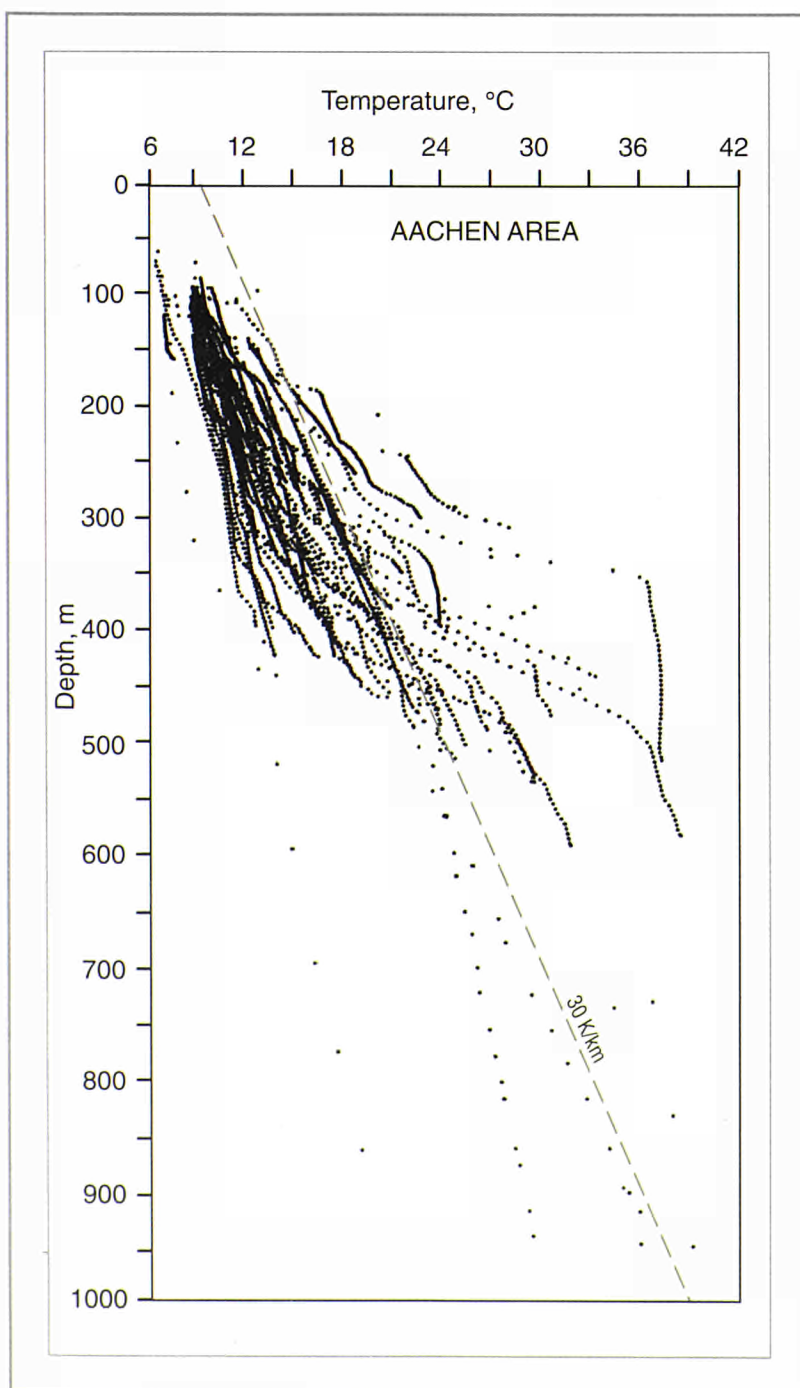
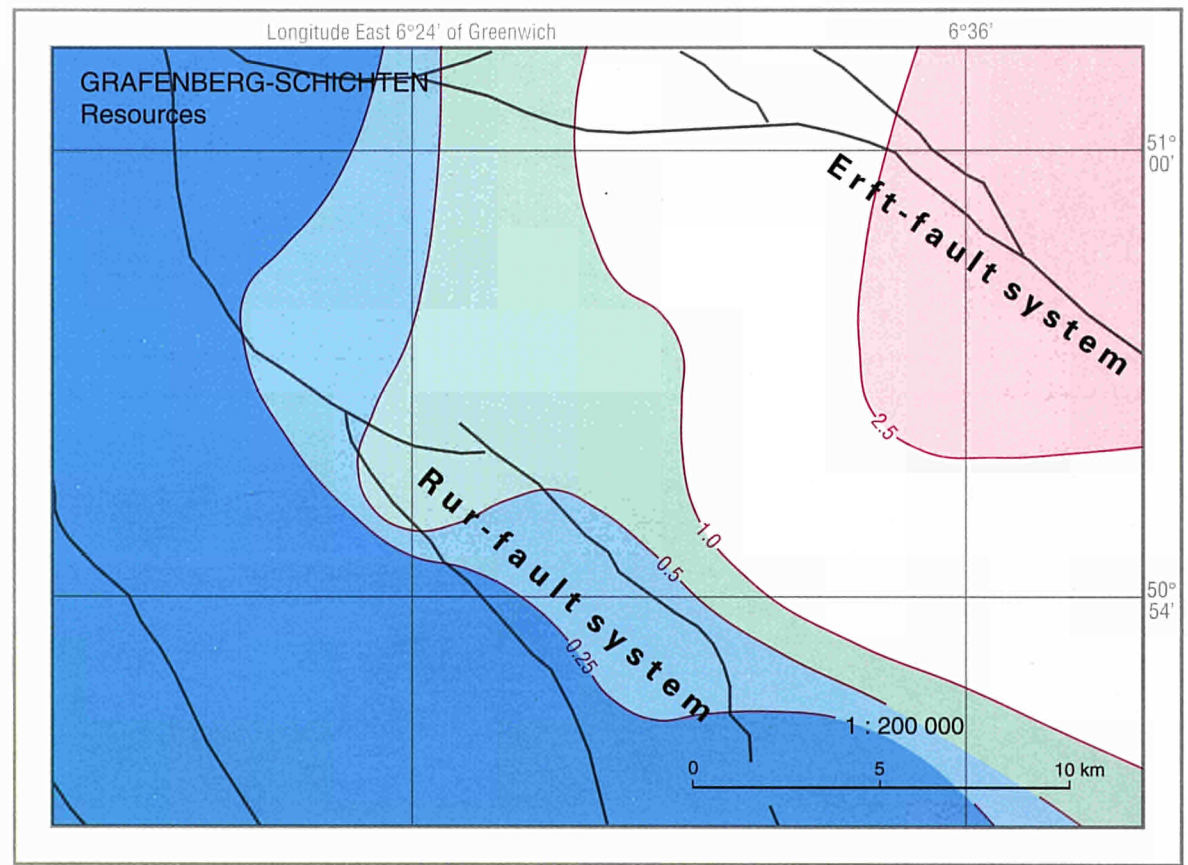
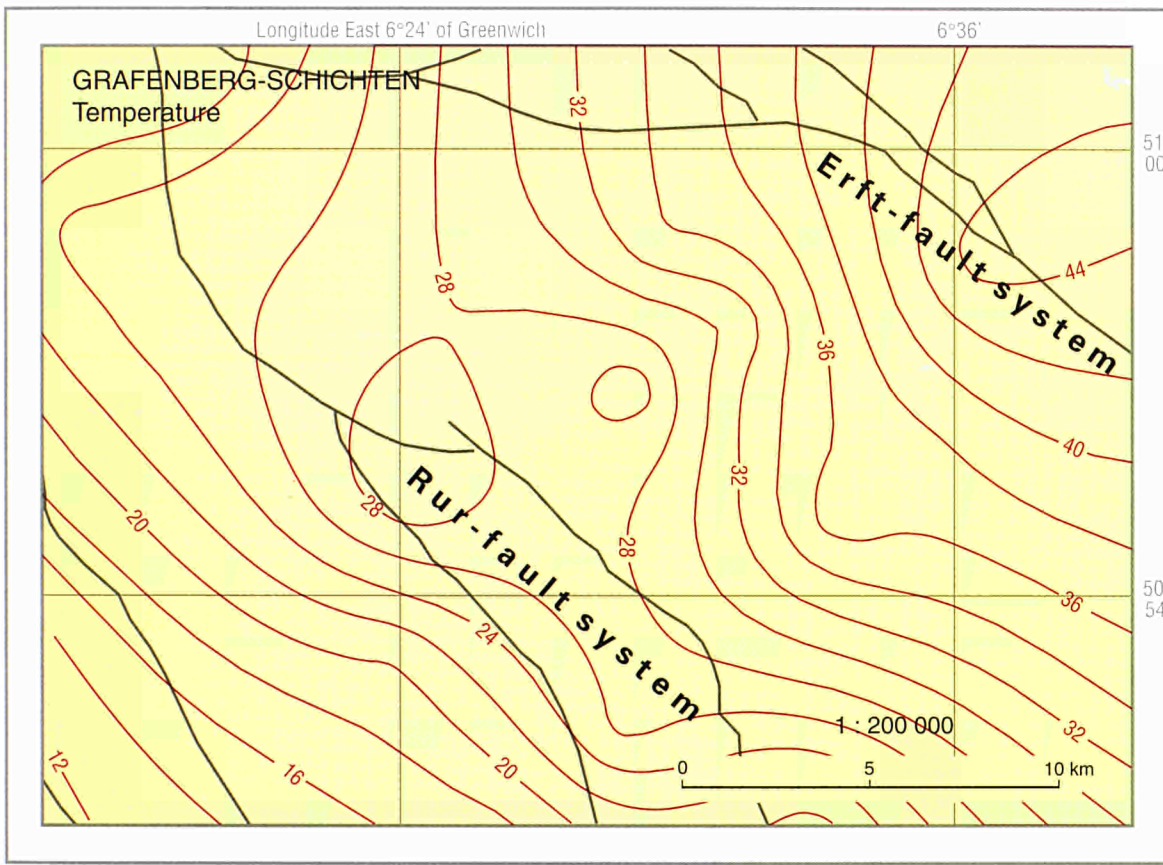
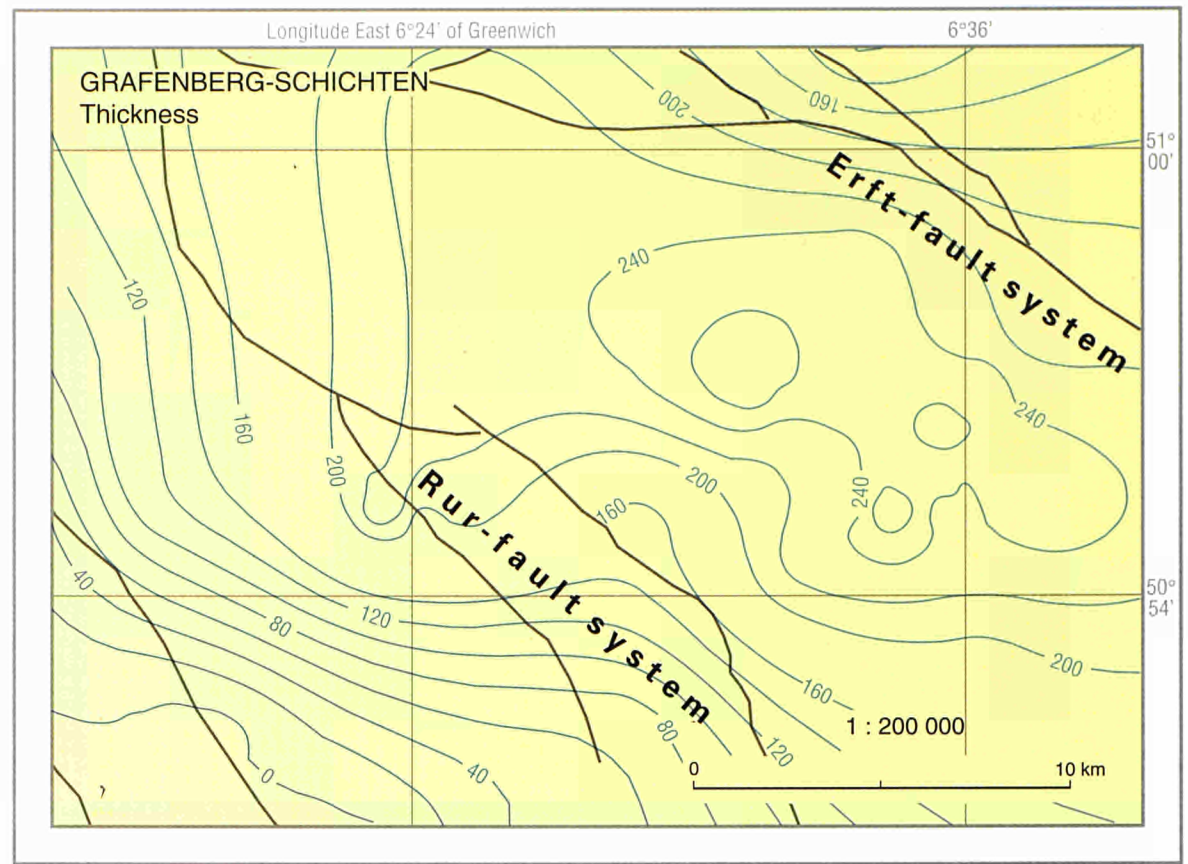
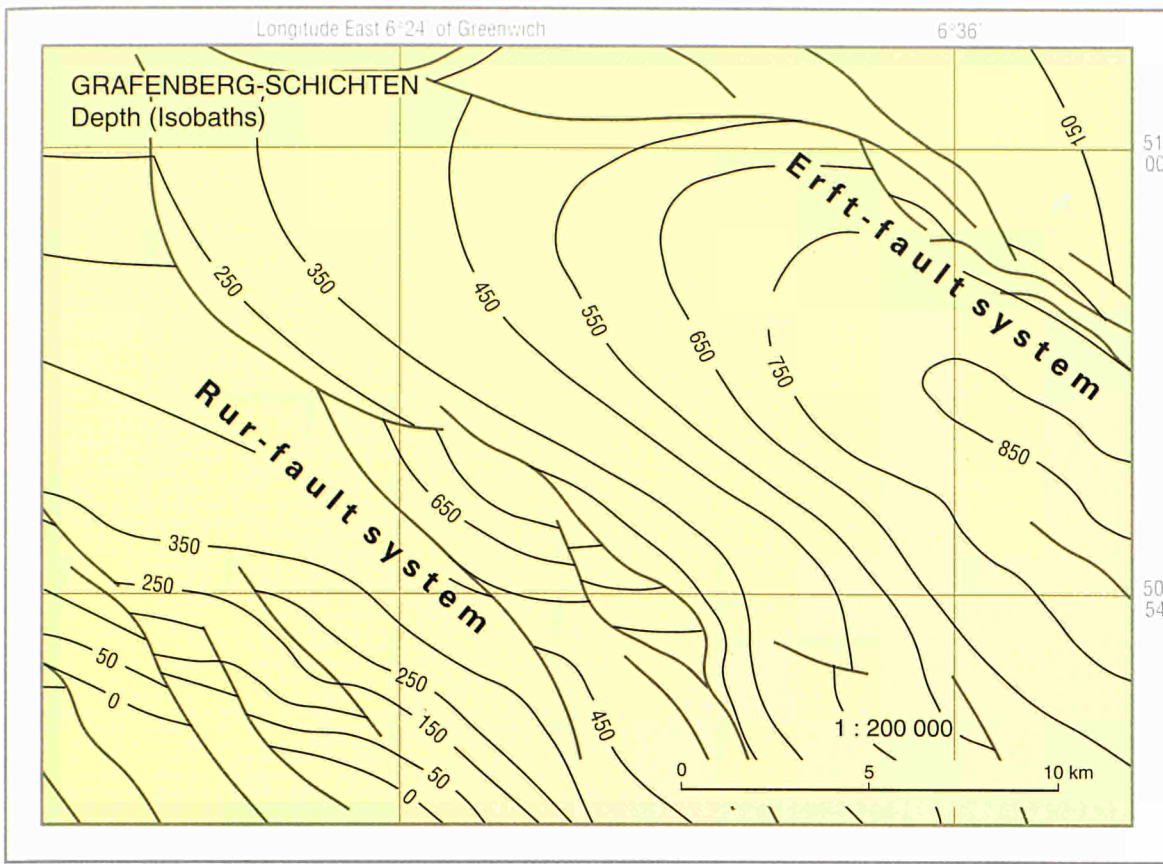


Characteristics of the temperature data

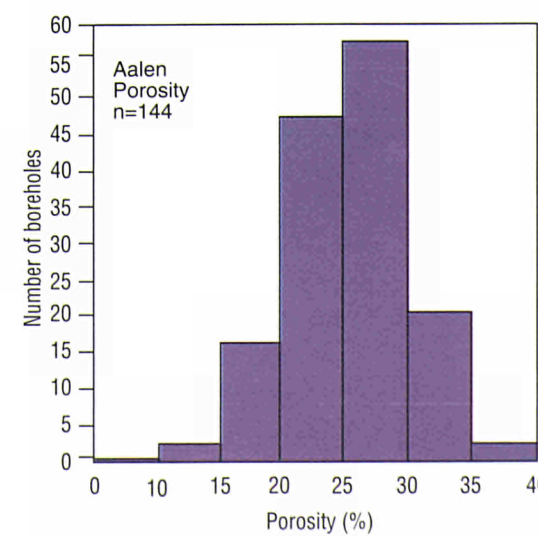
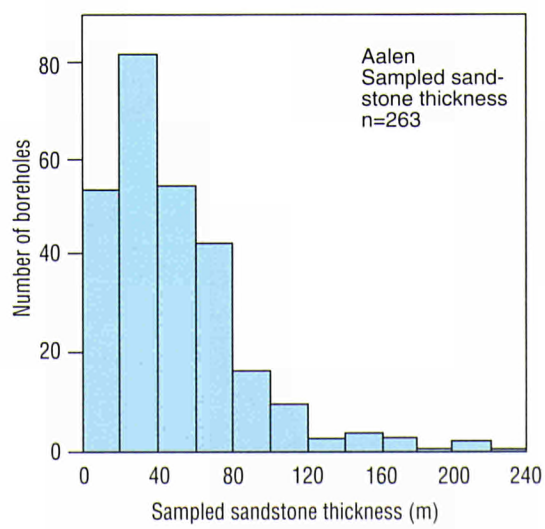
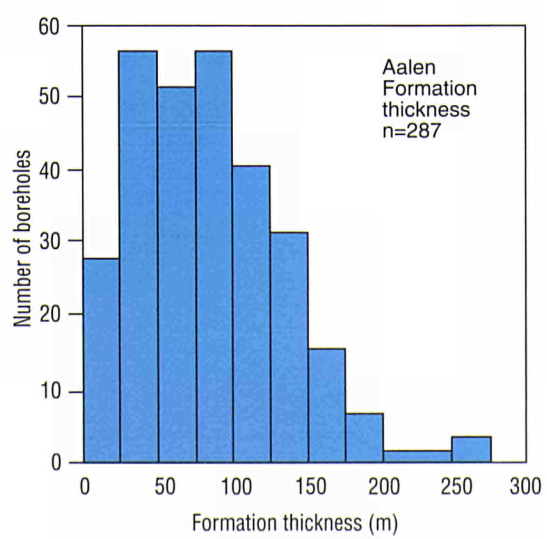
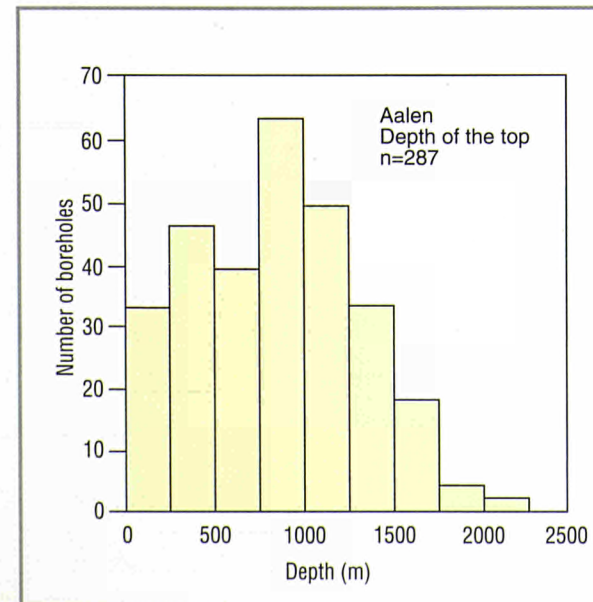
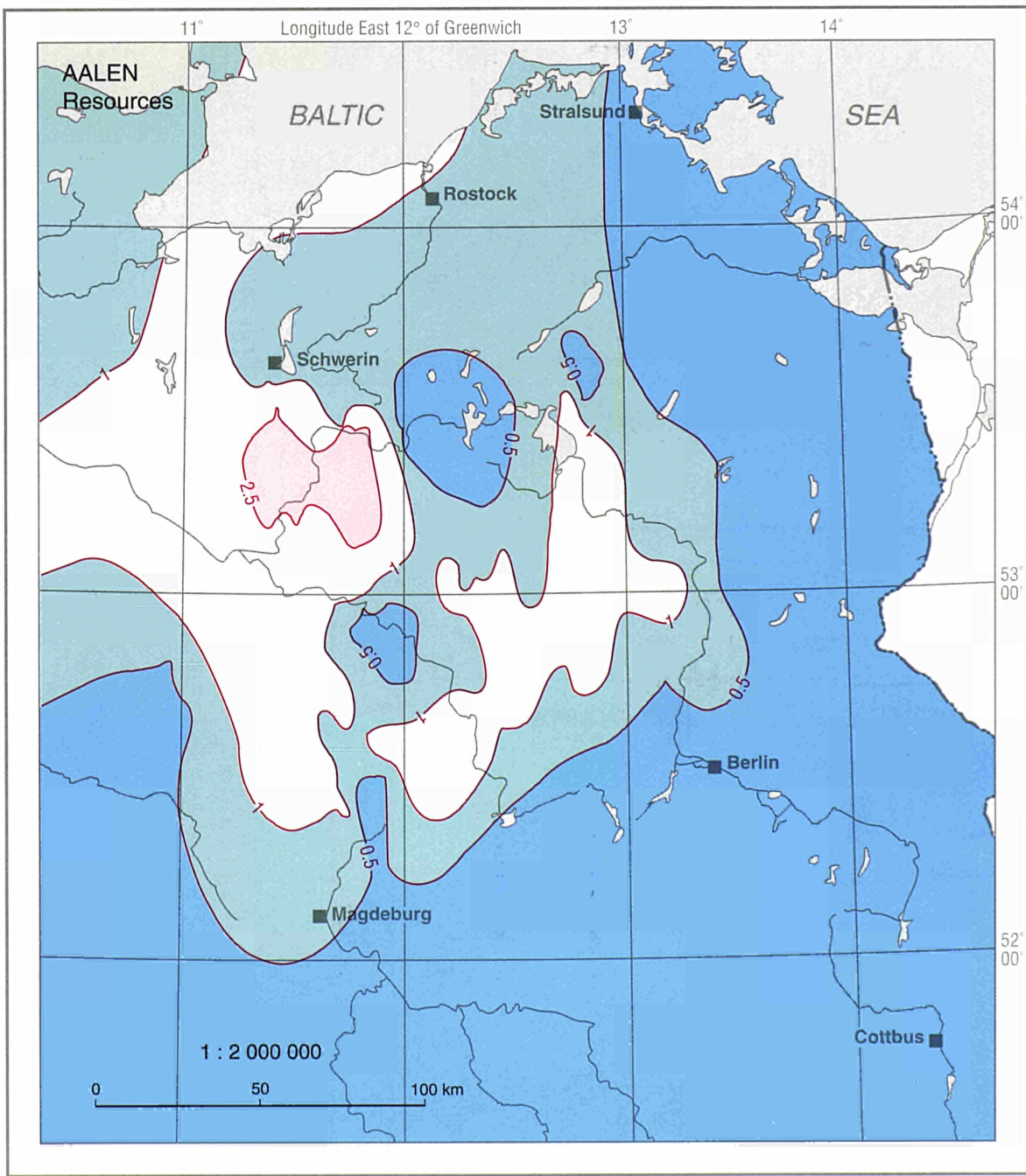
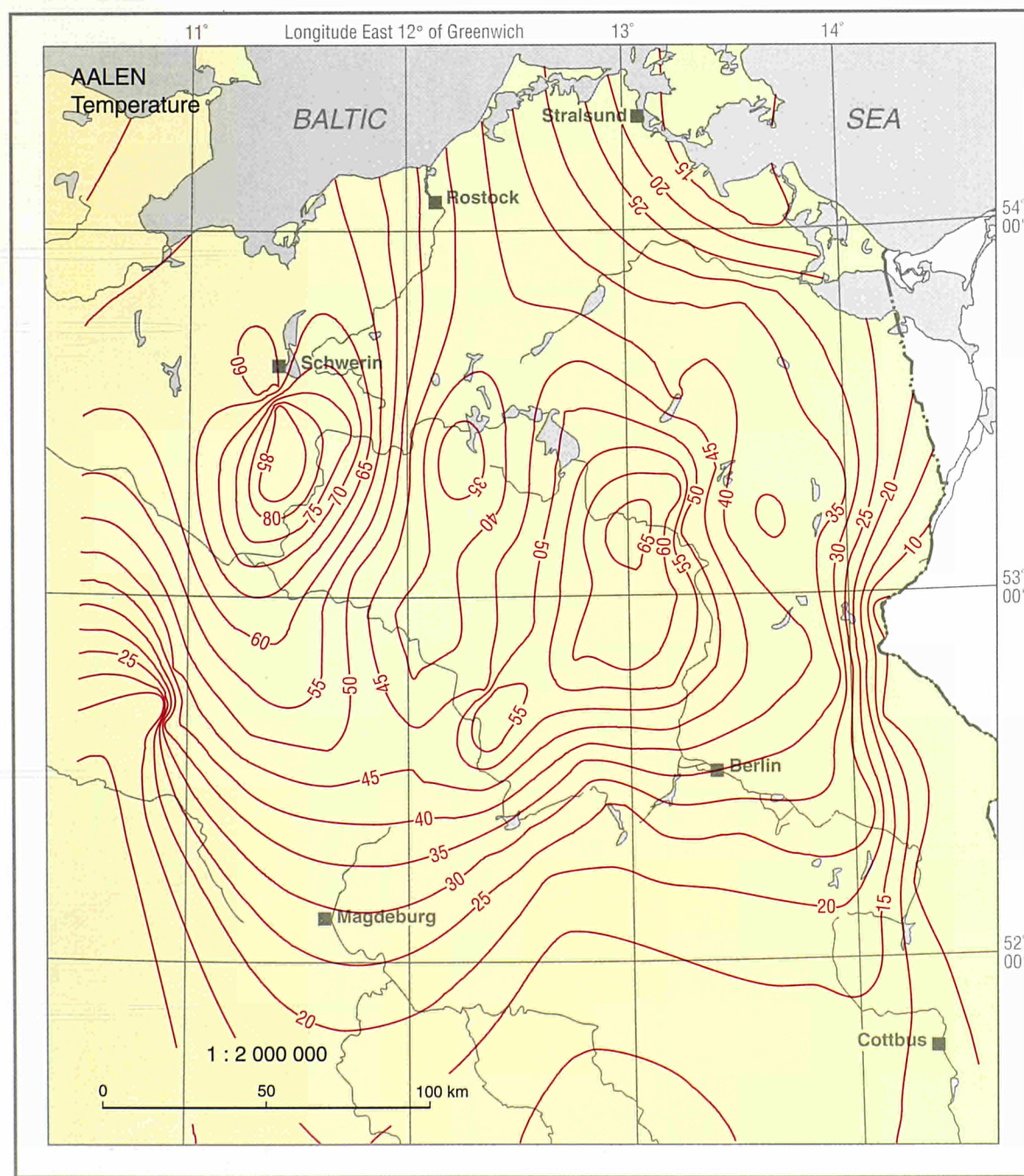
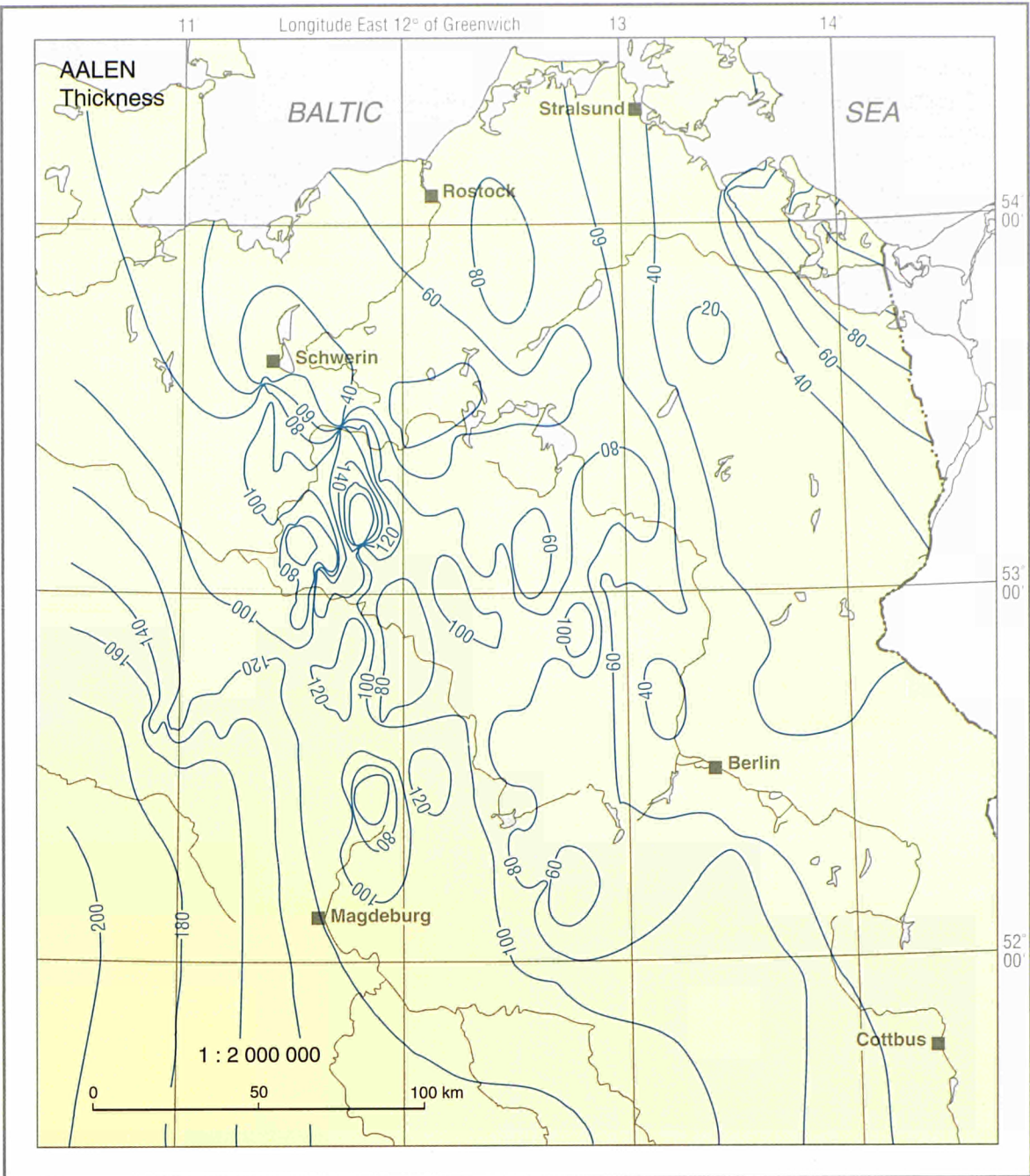
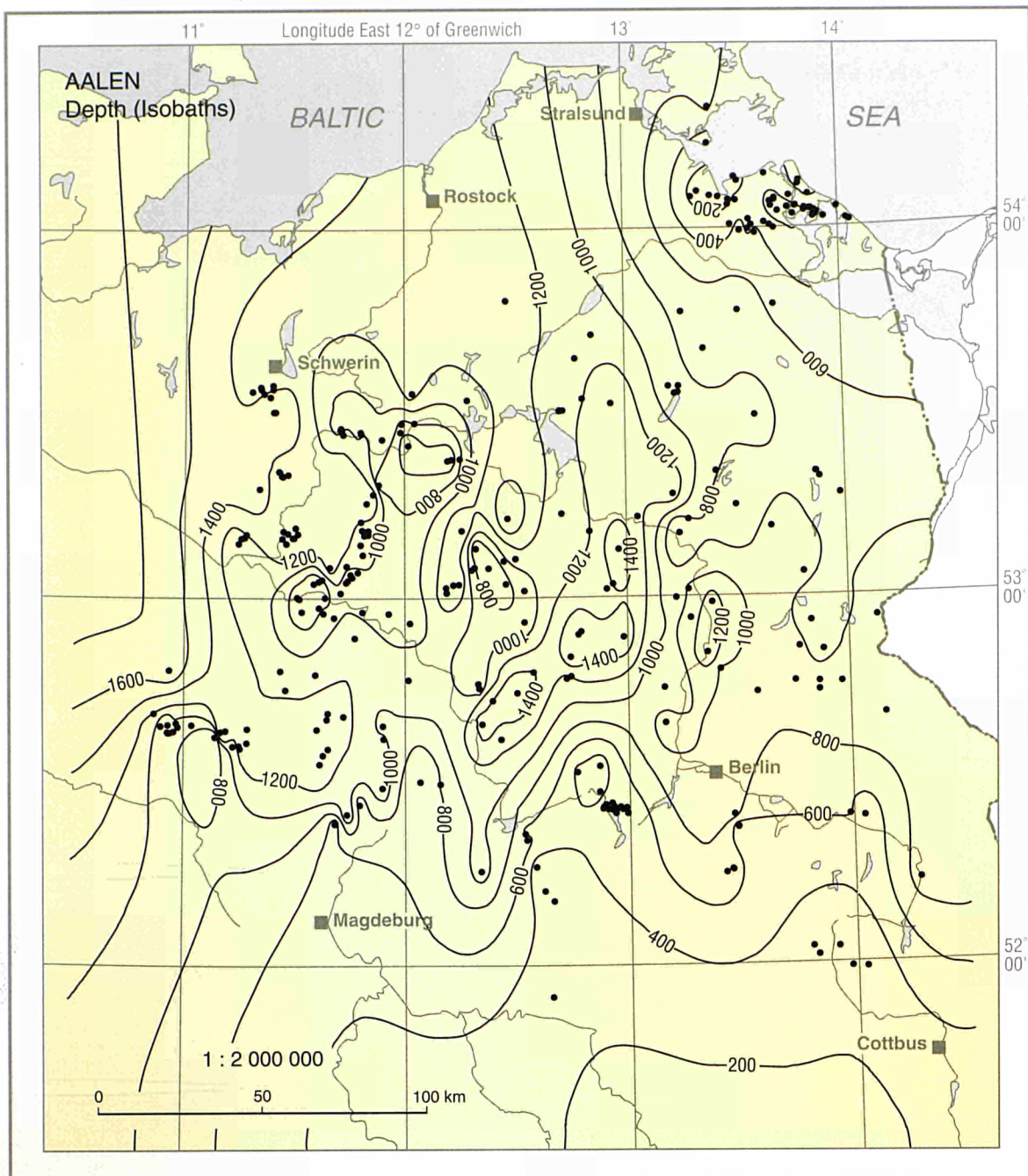
Depth (m)	Number of boreholes
500	8050
1000	5430
2000	1870



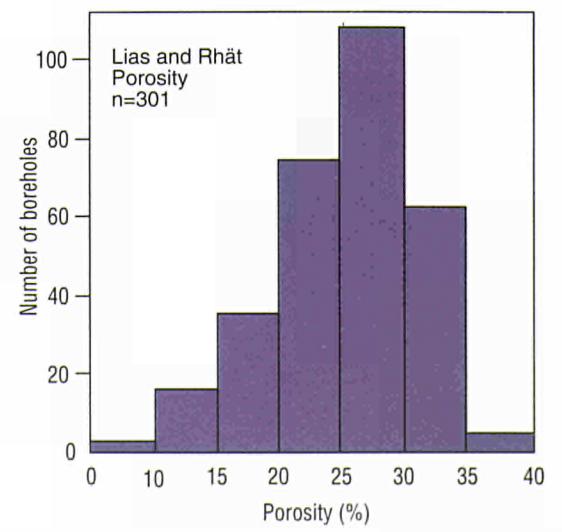
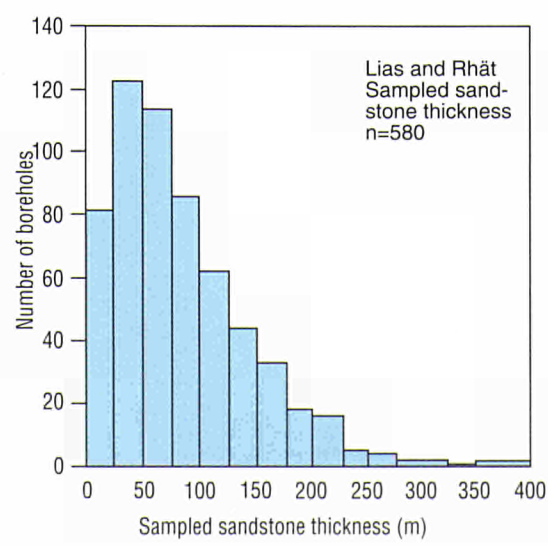
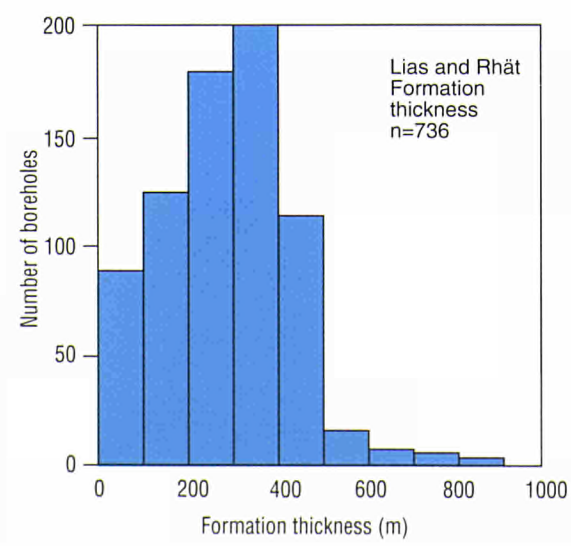
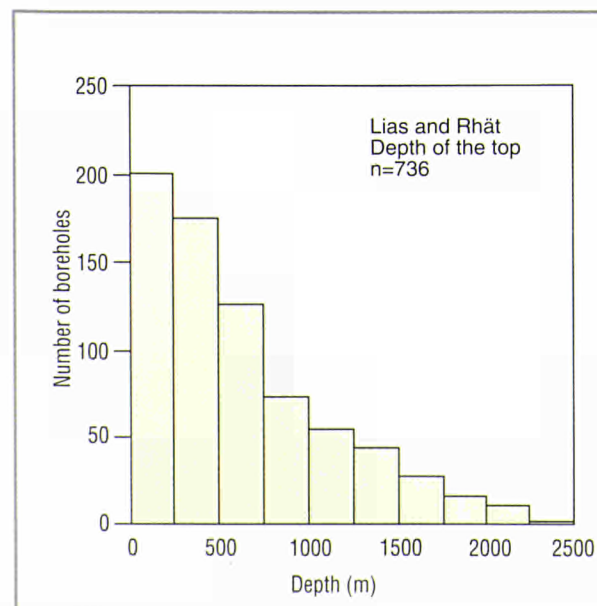
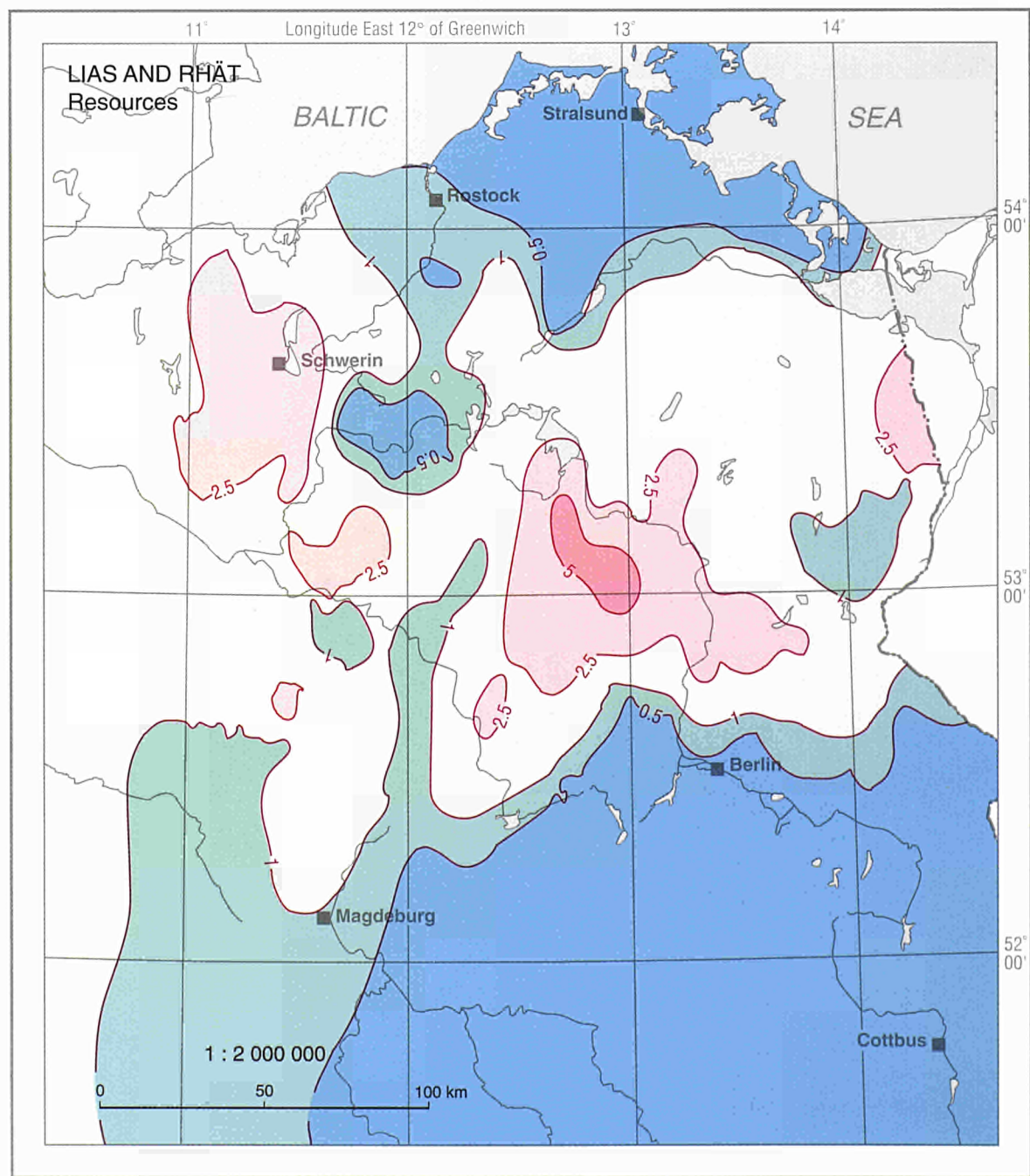
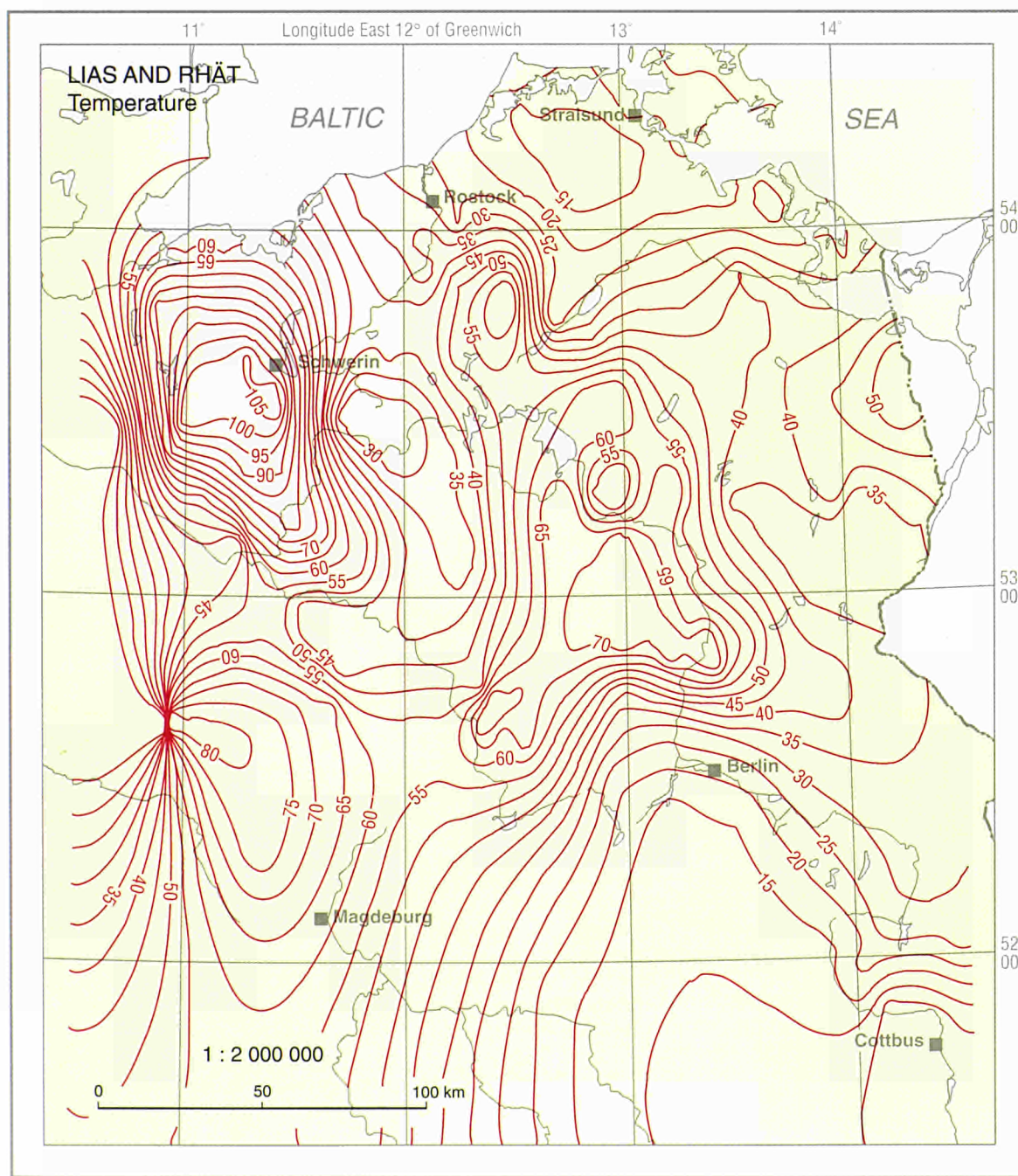
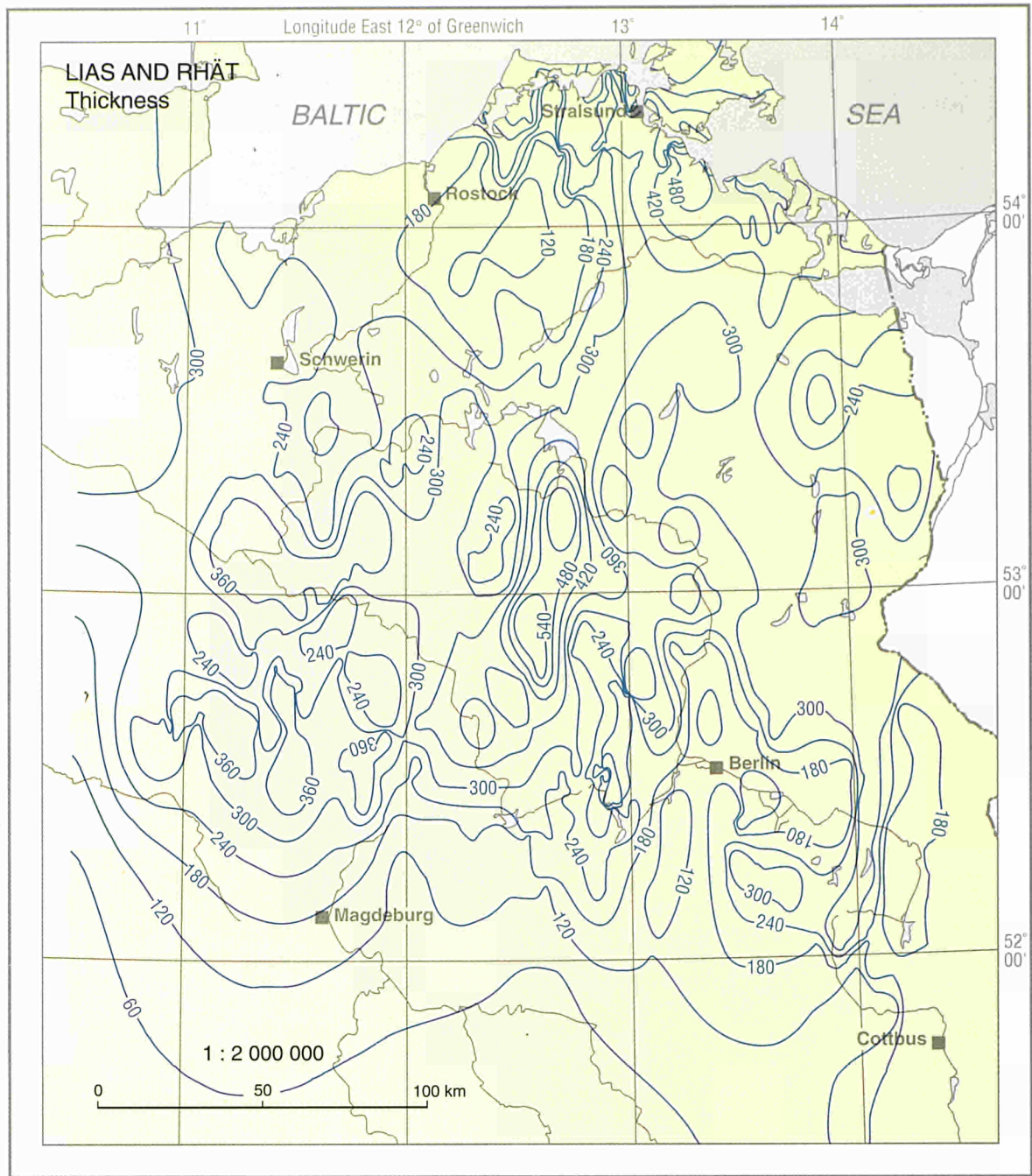
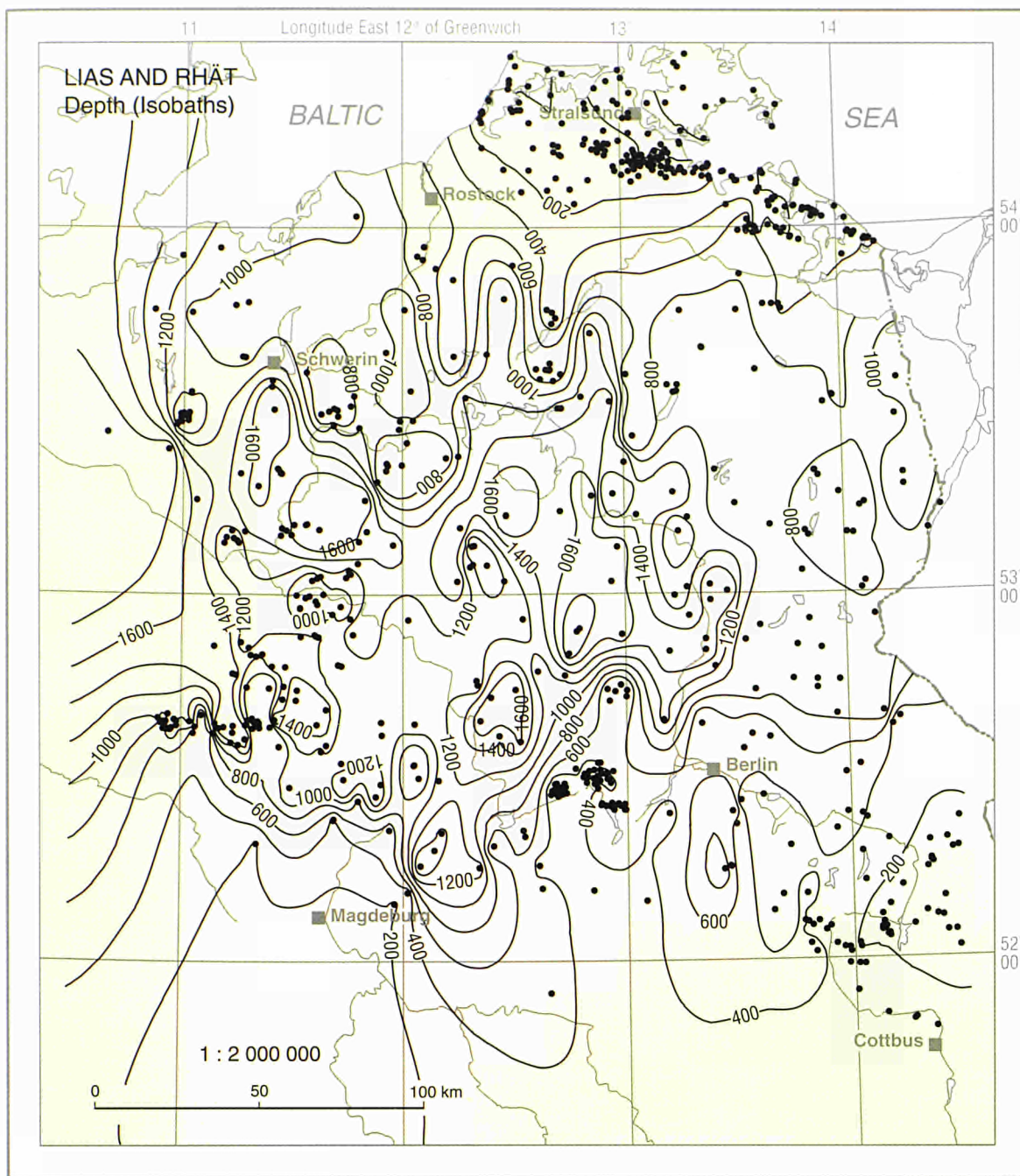
- Equilibrium logs
- Non-equilibrium logs
- Temperature mines
- Production tests
- Drill stem tests
- BHT Measurements:
 - >2 values
 - 2 values
 - 1 value and shut-down time
 - 1 value without time information



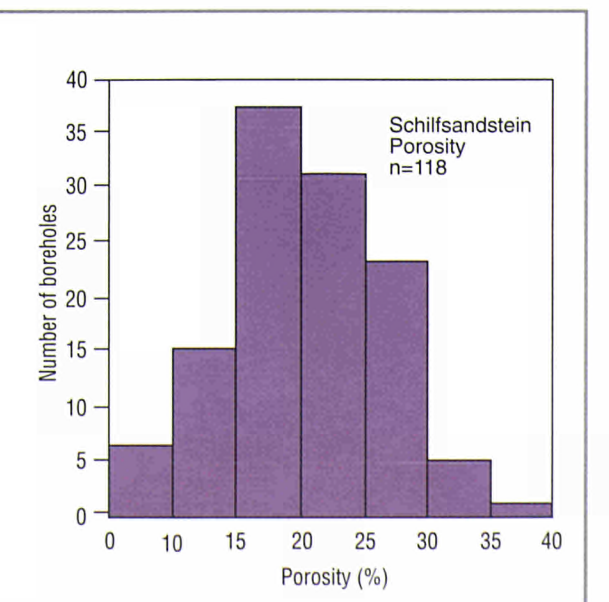
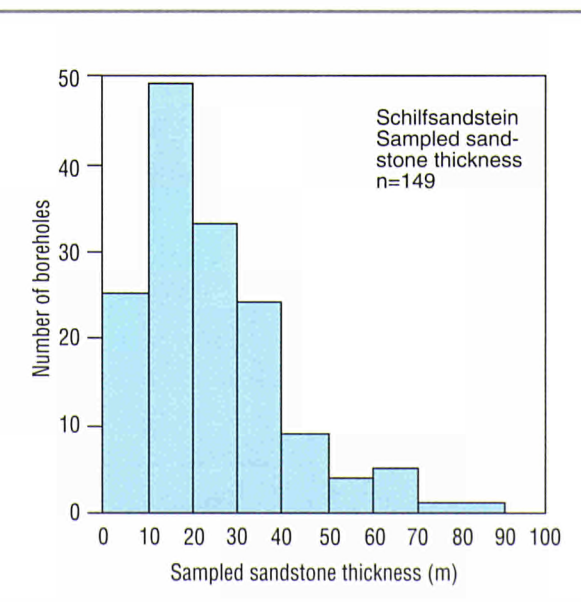
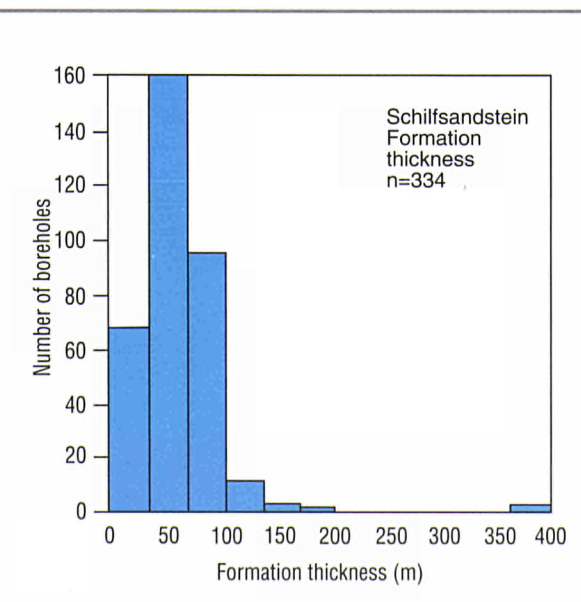
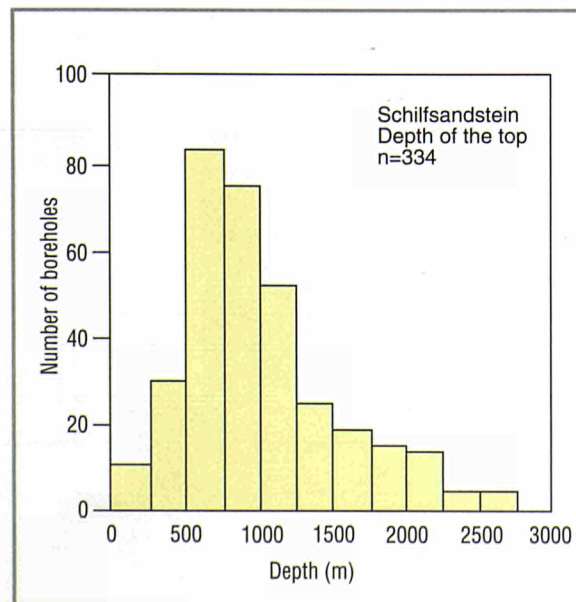
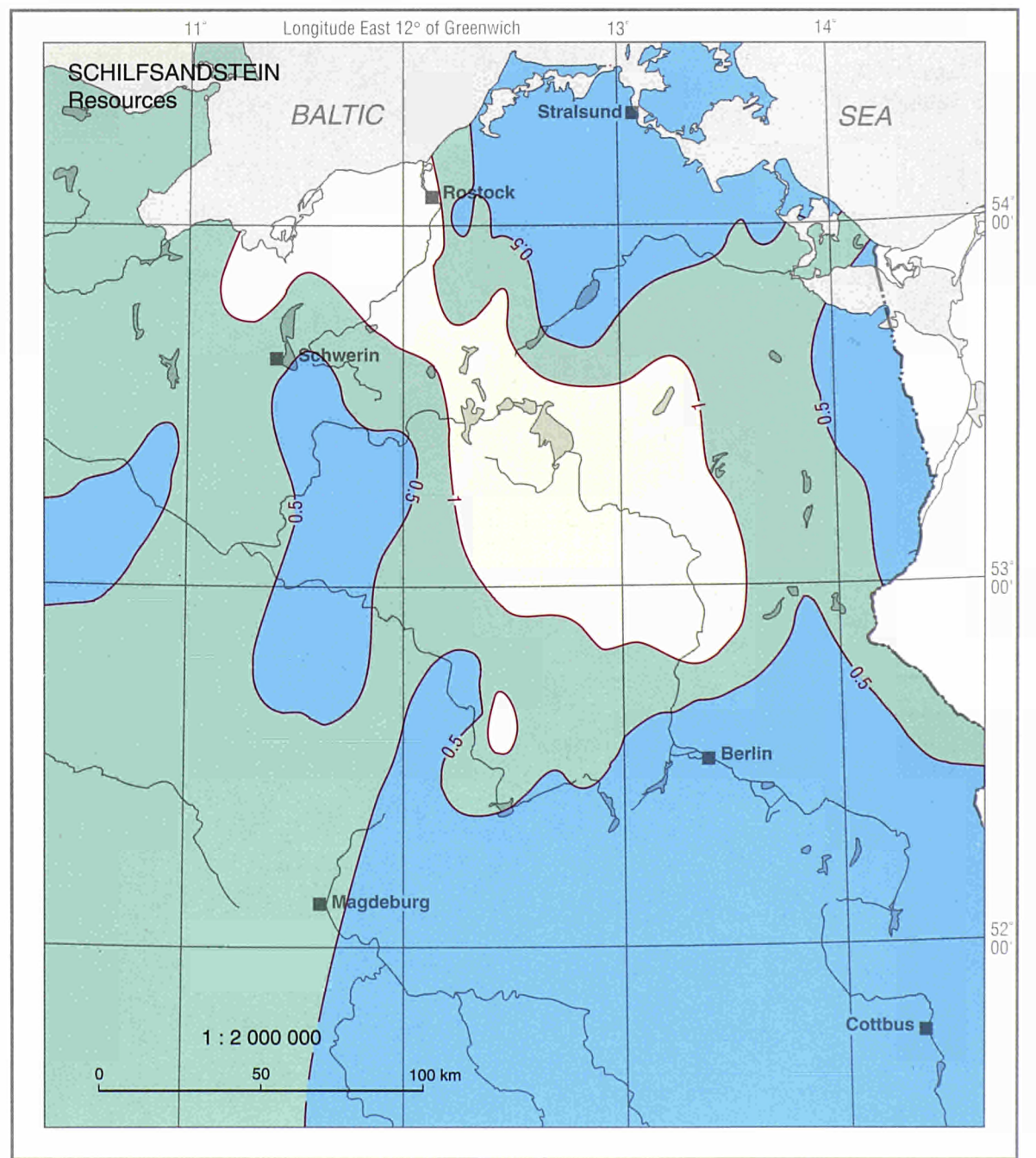
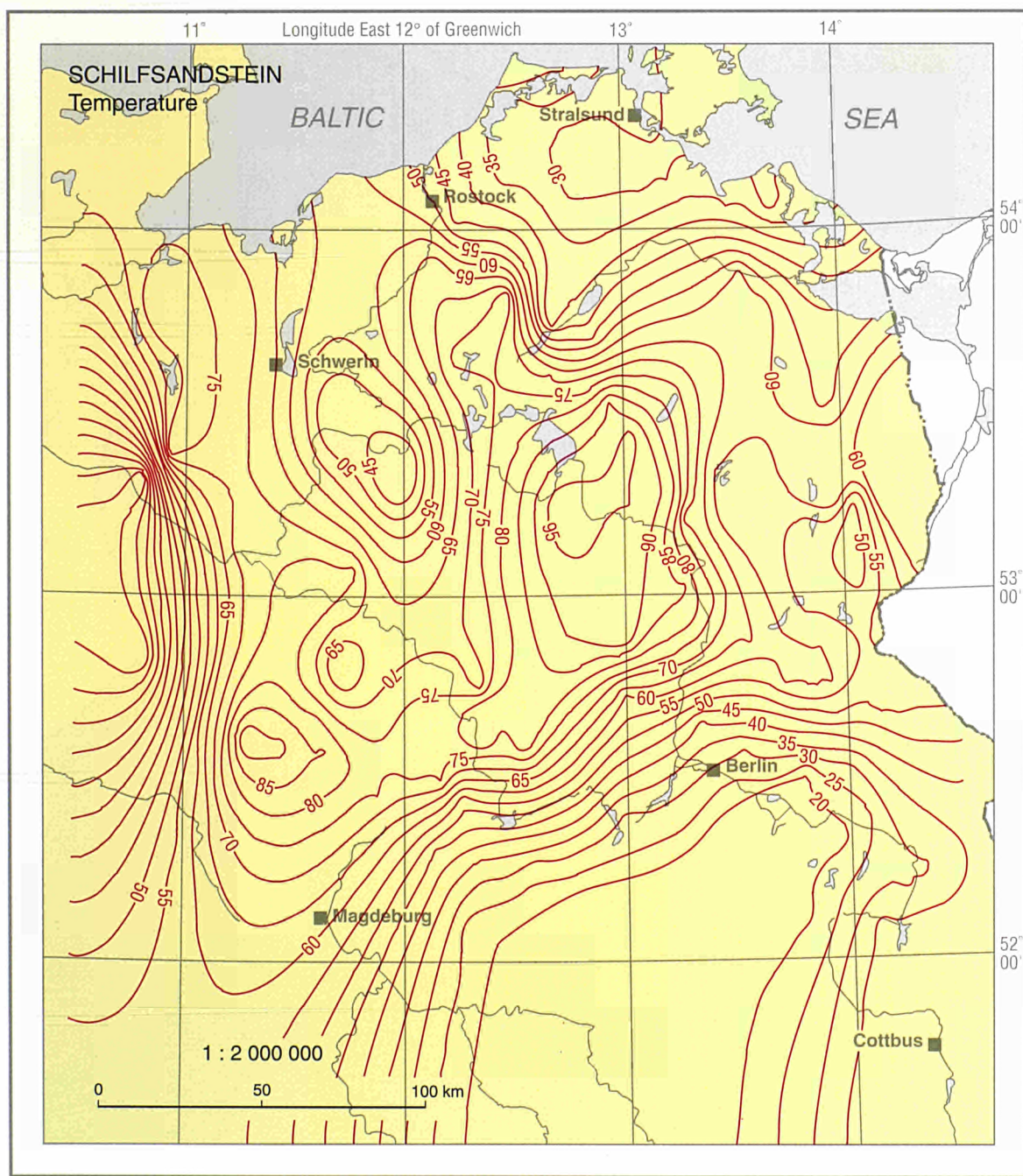
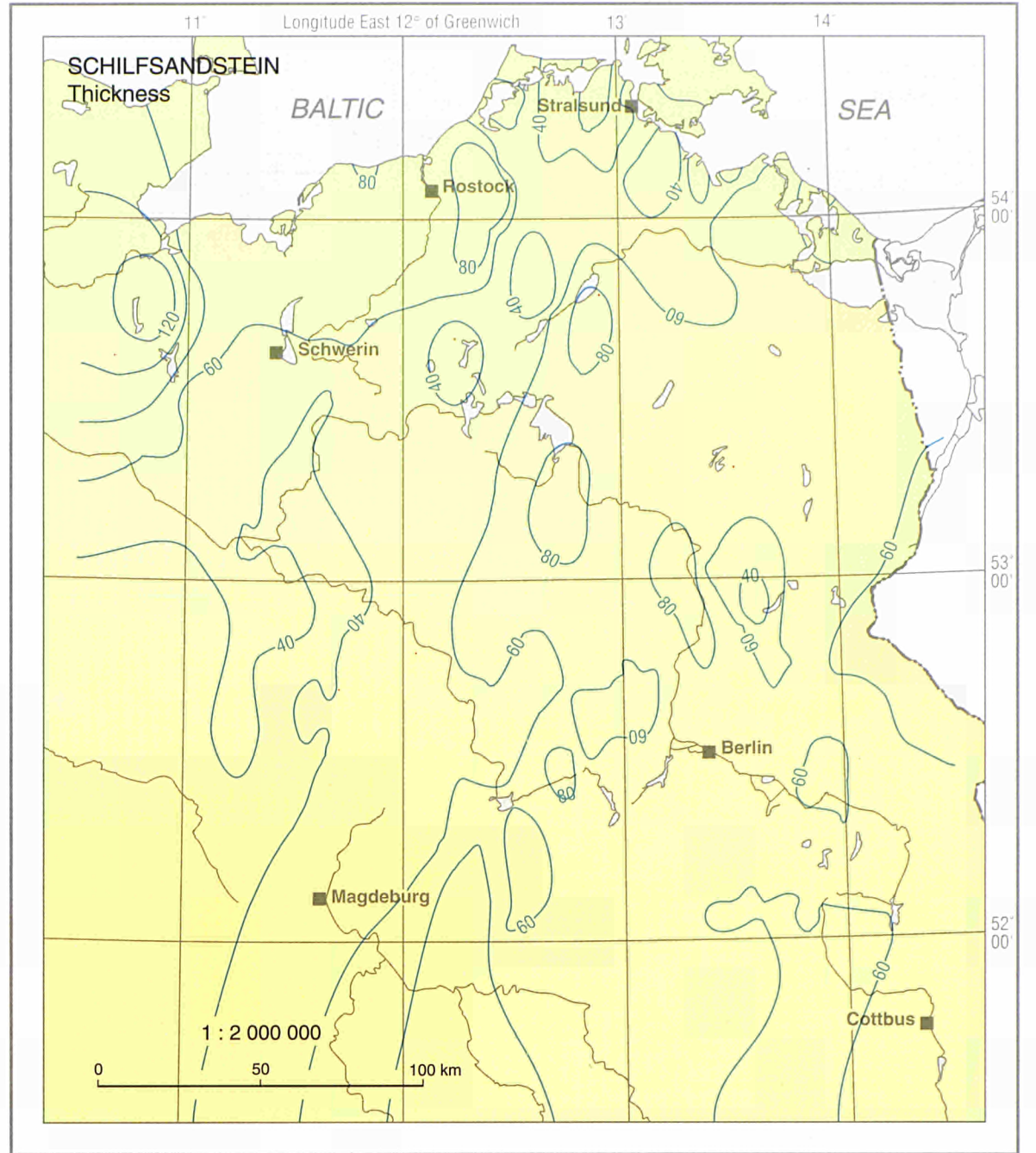
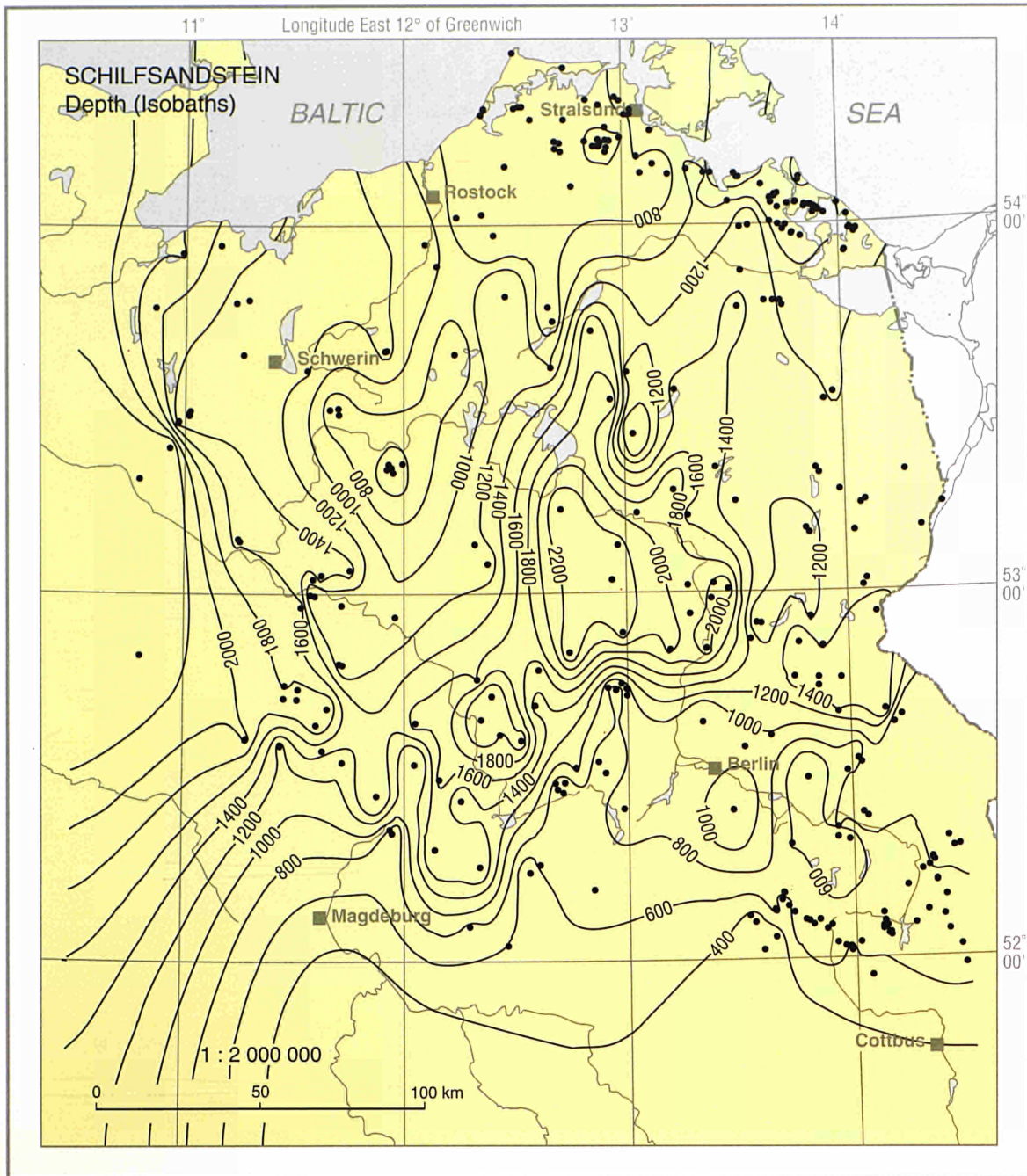
GERMANY, Eastern North German Basin



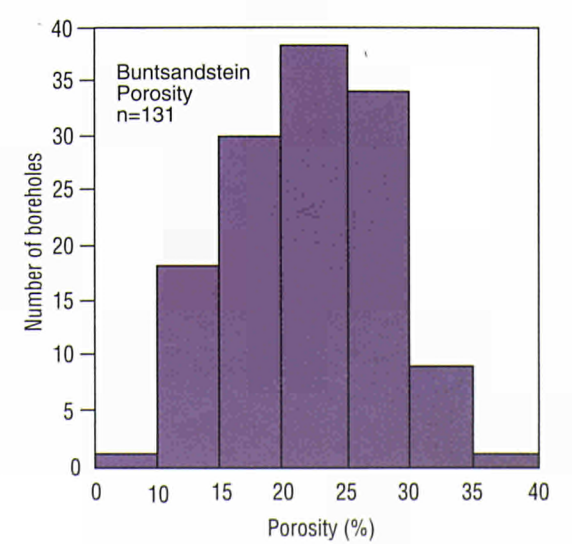
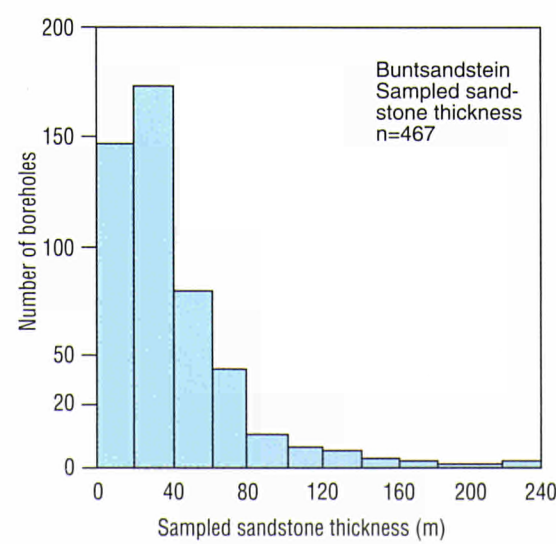
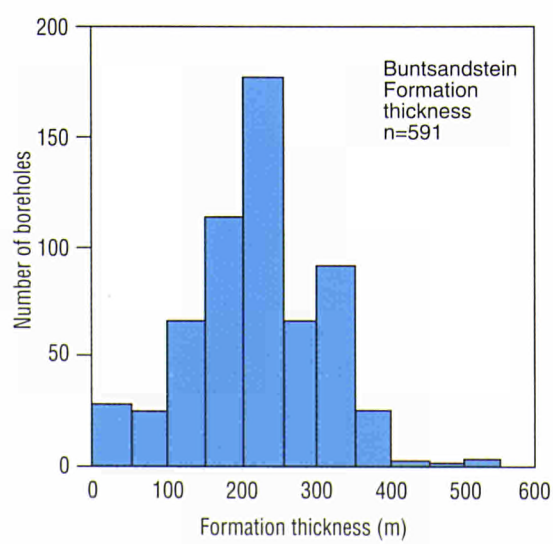
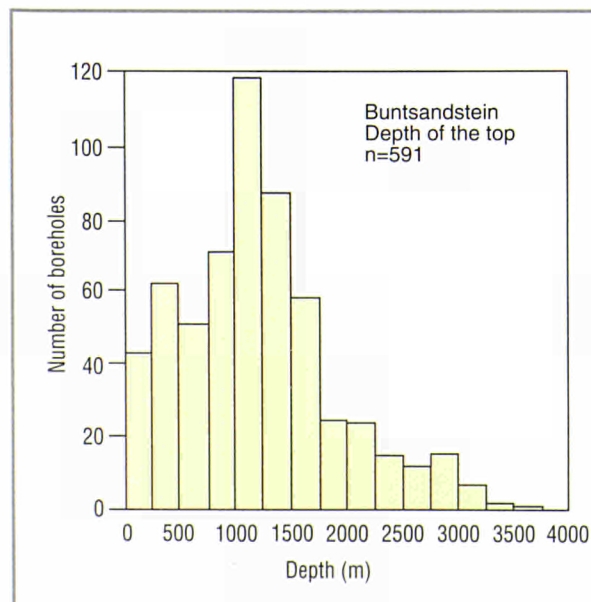
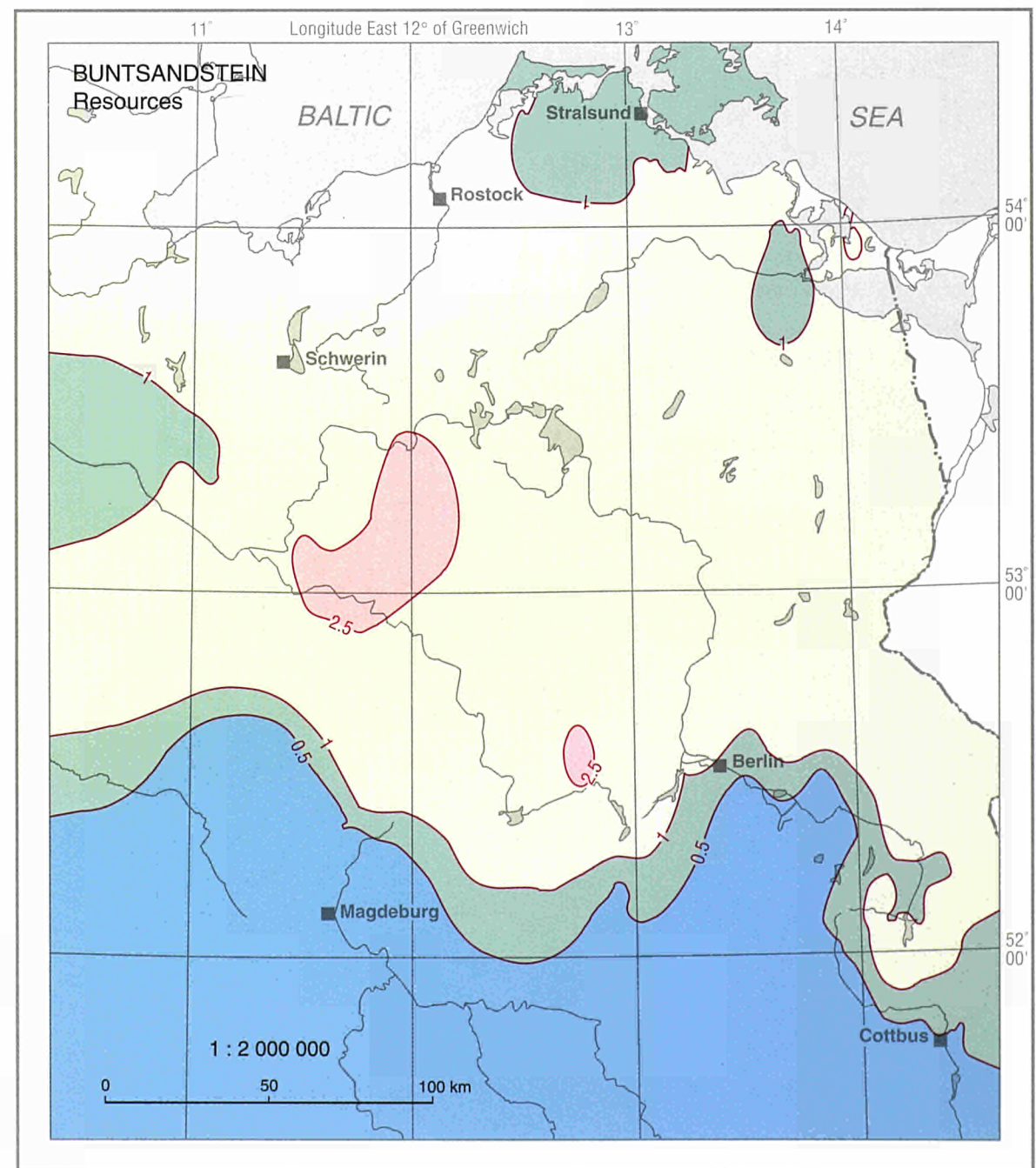
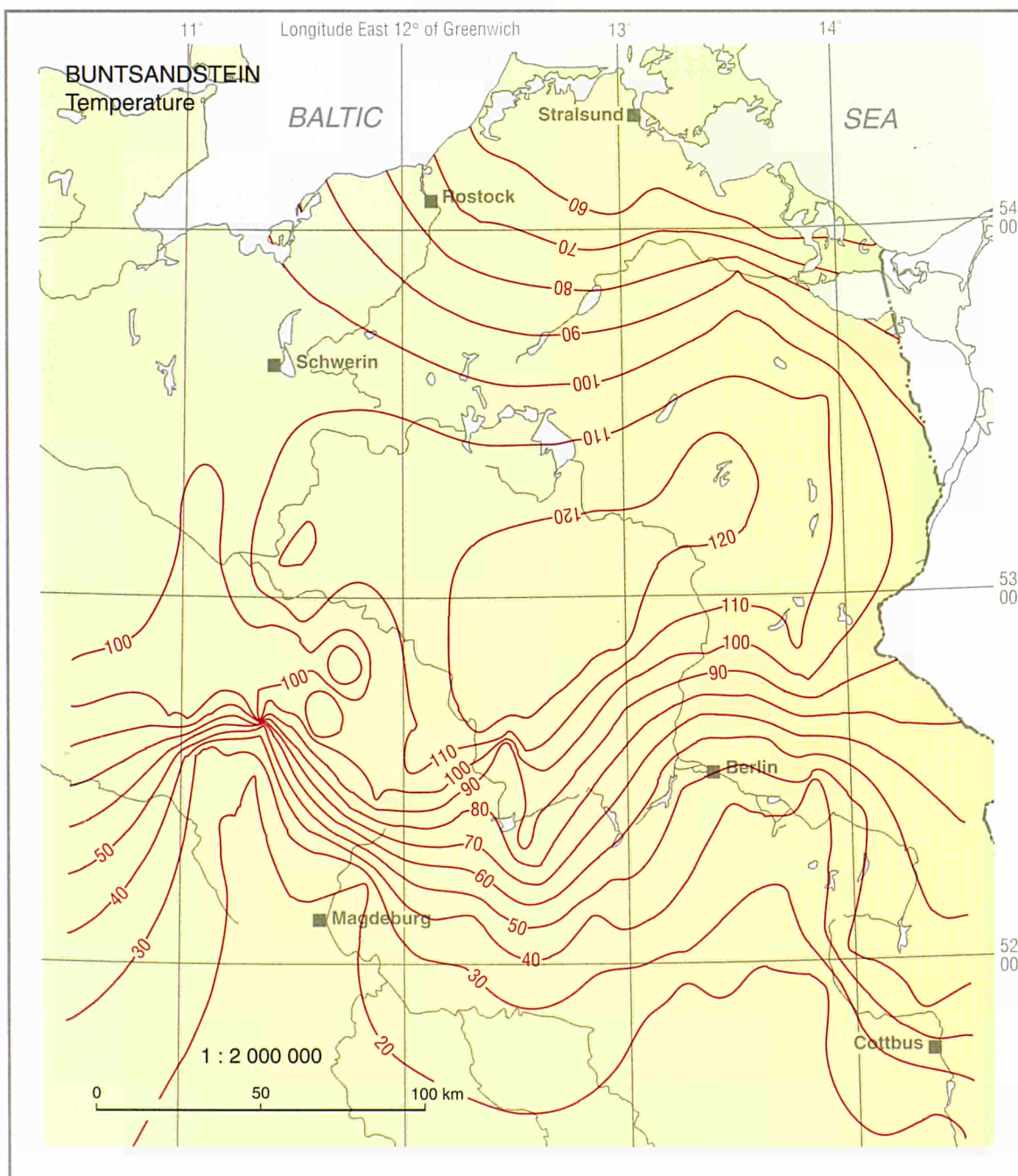
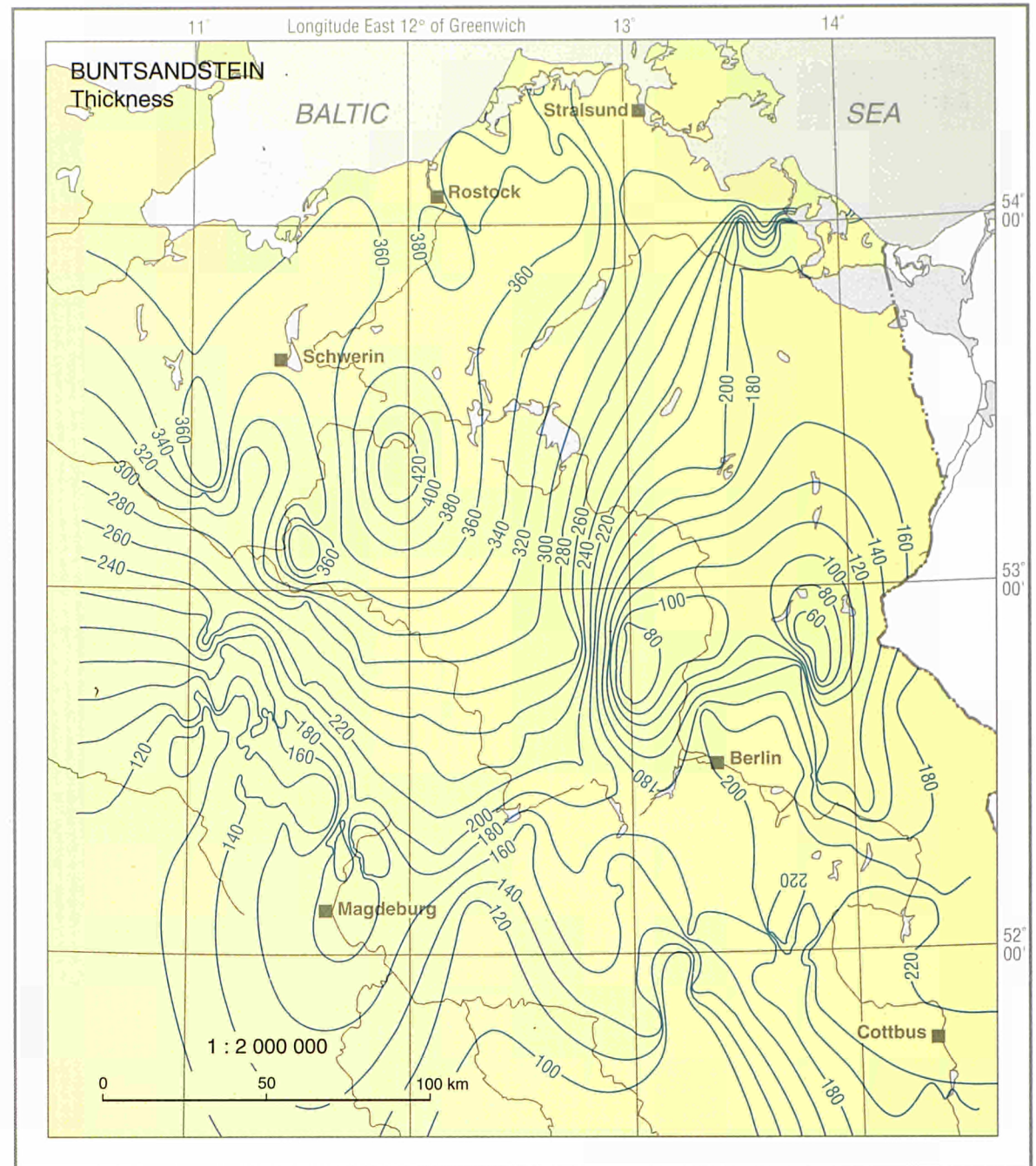
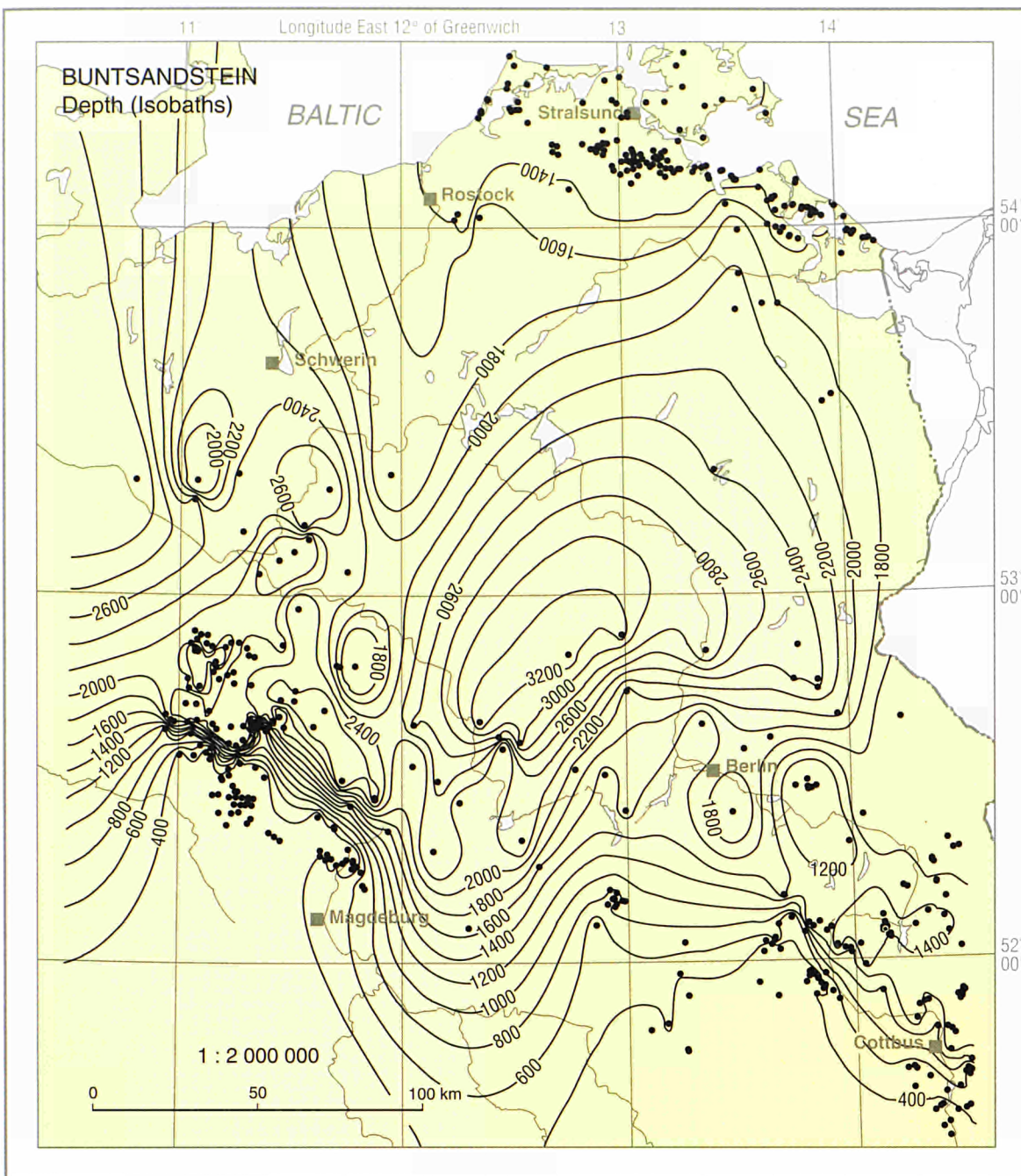
Eastern North German Basin, GERMANY



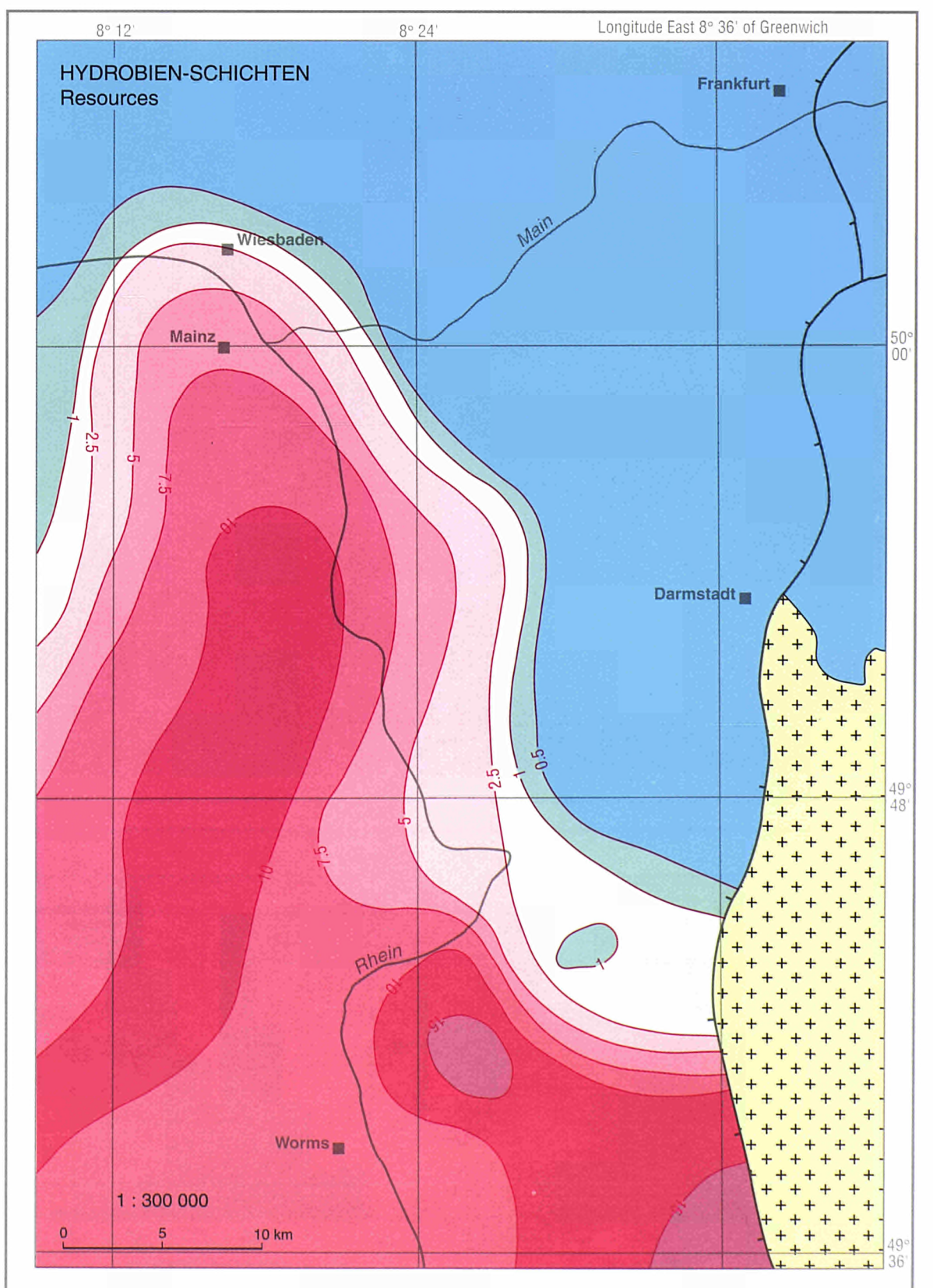
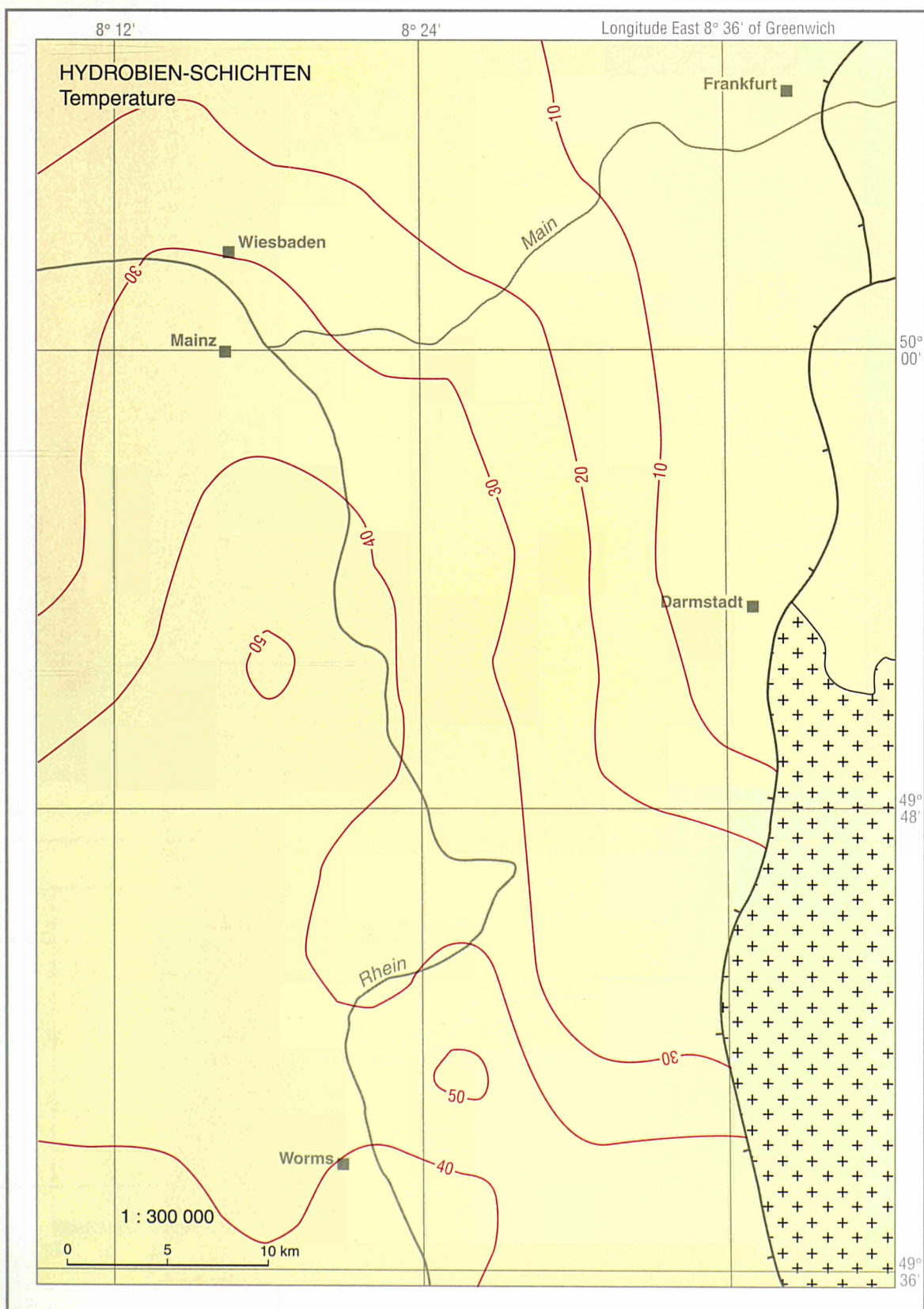
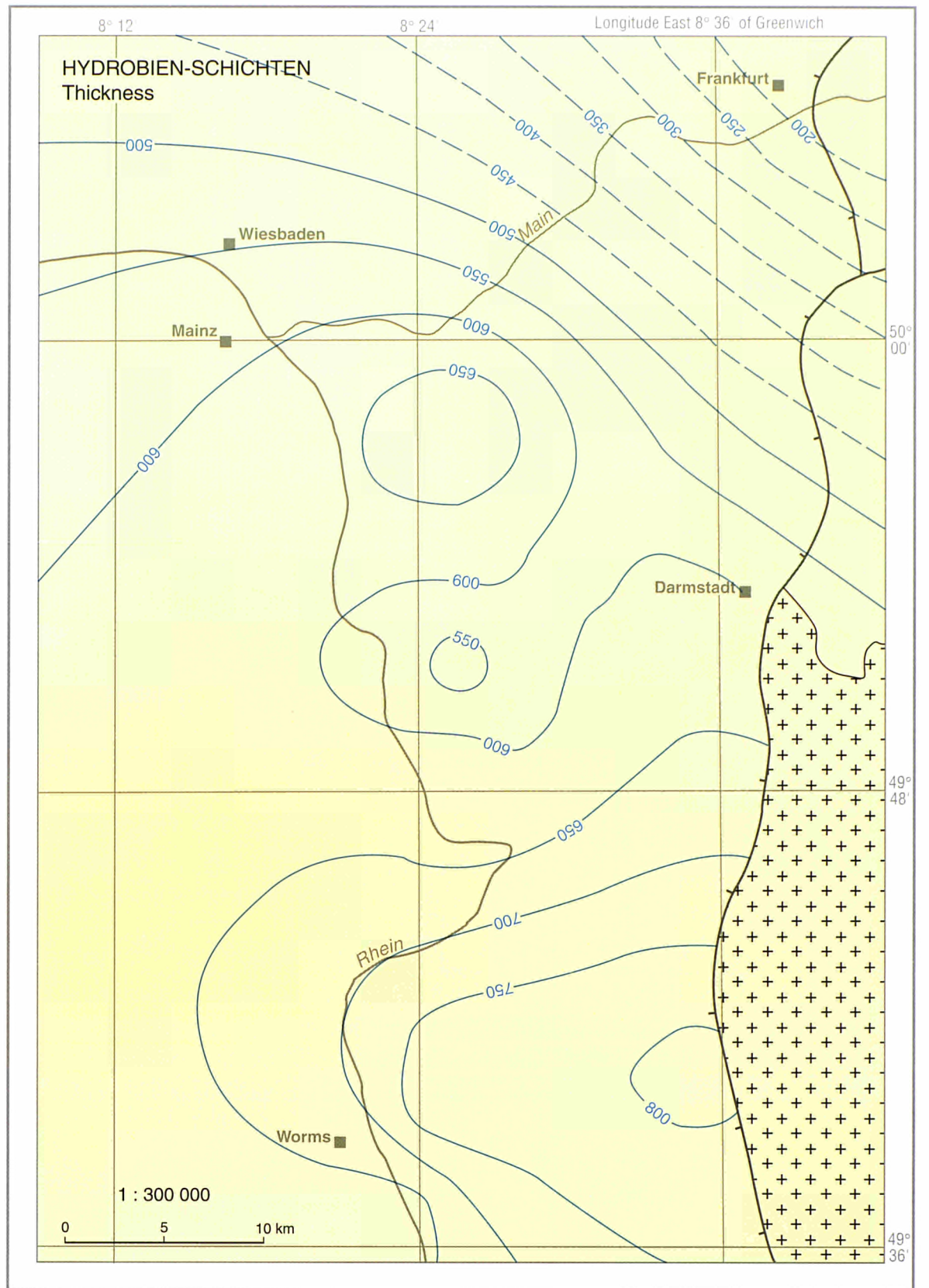
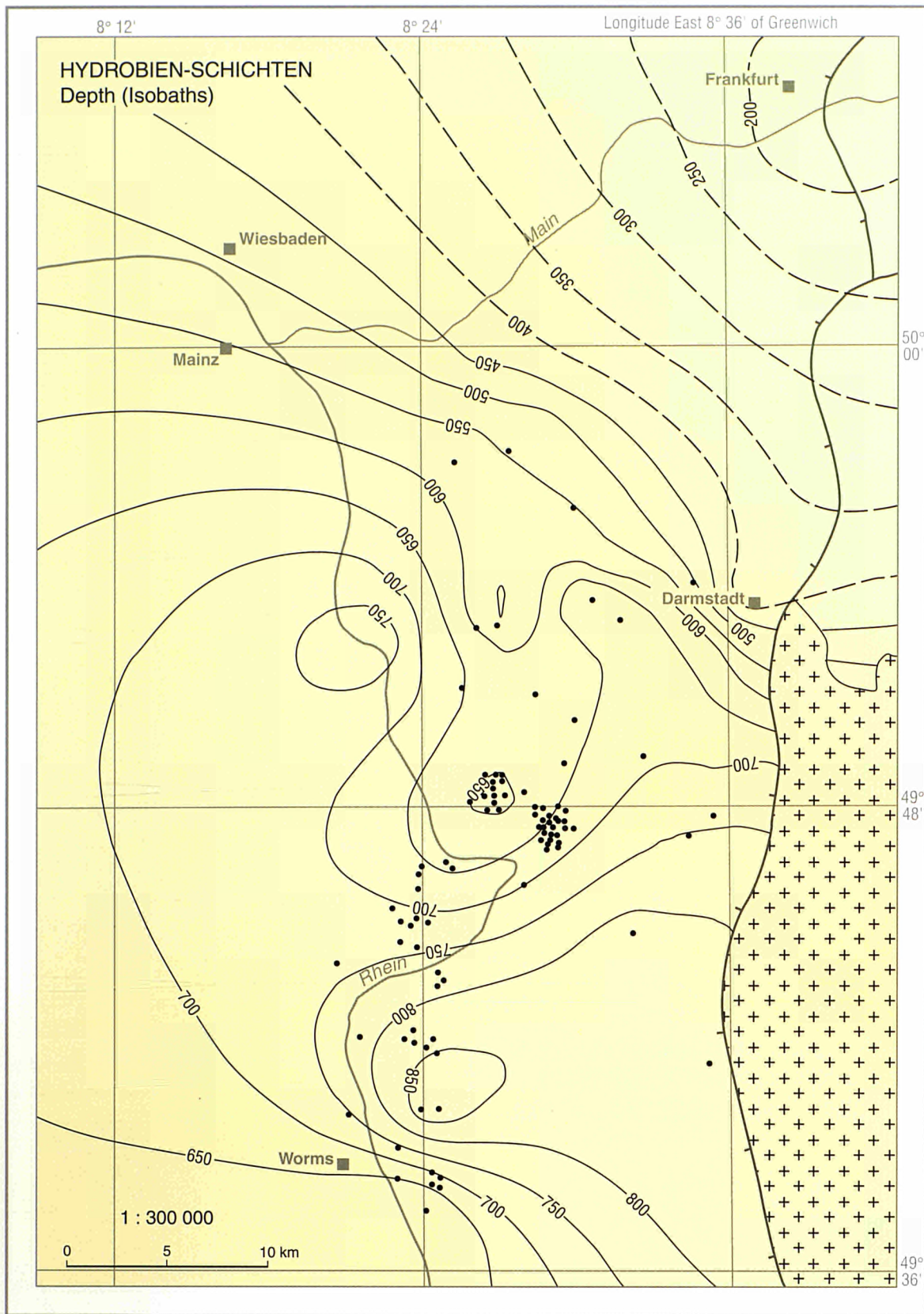
GERMANY, Eastern North German Basin



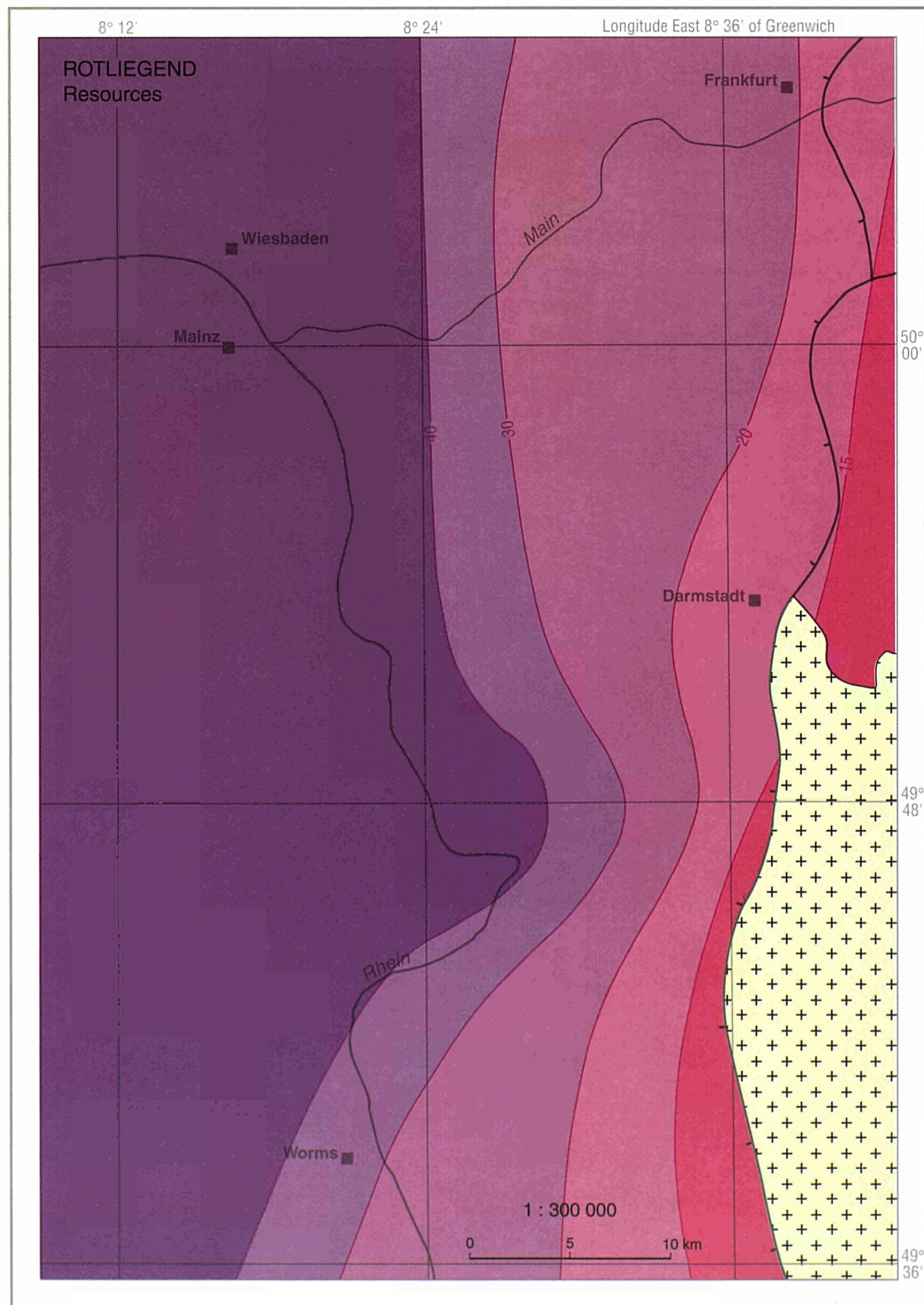
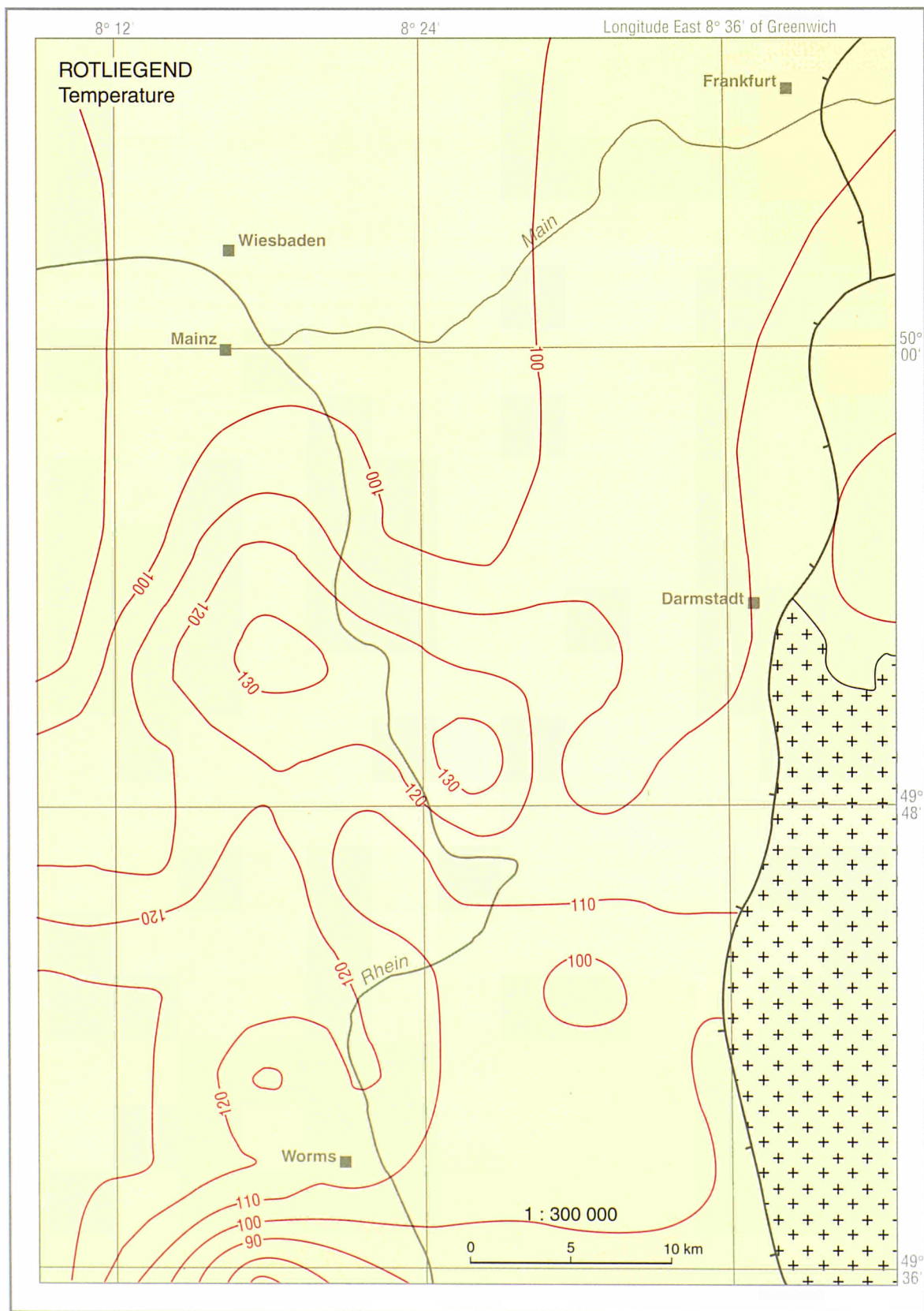
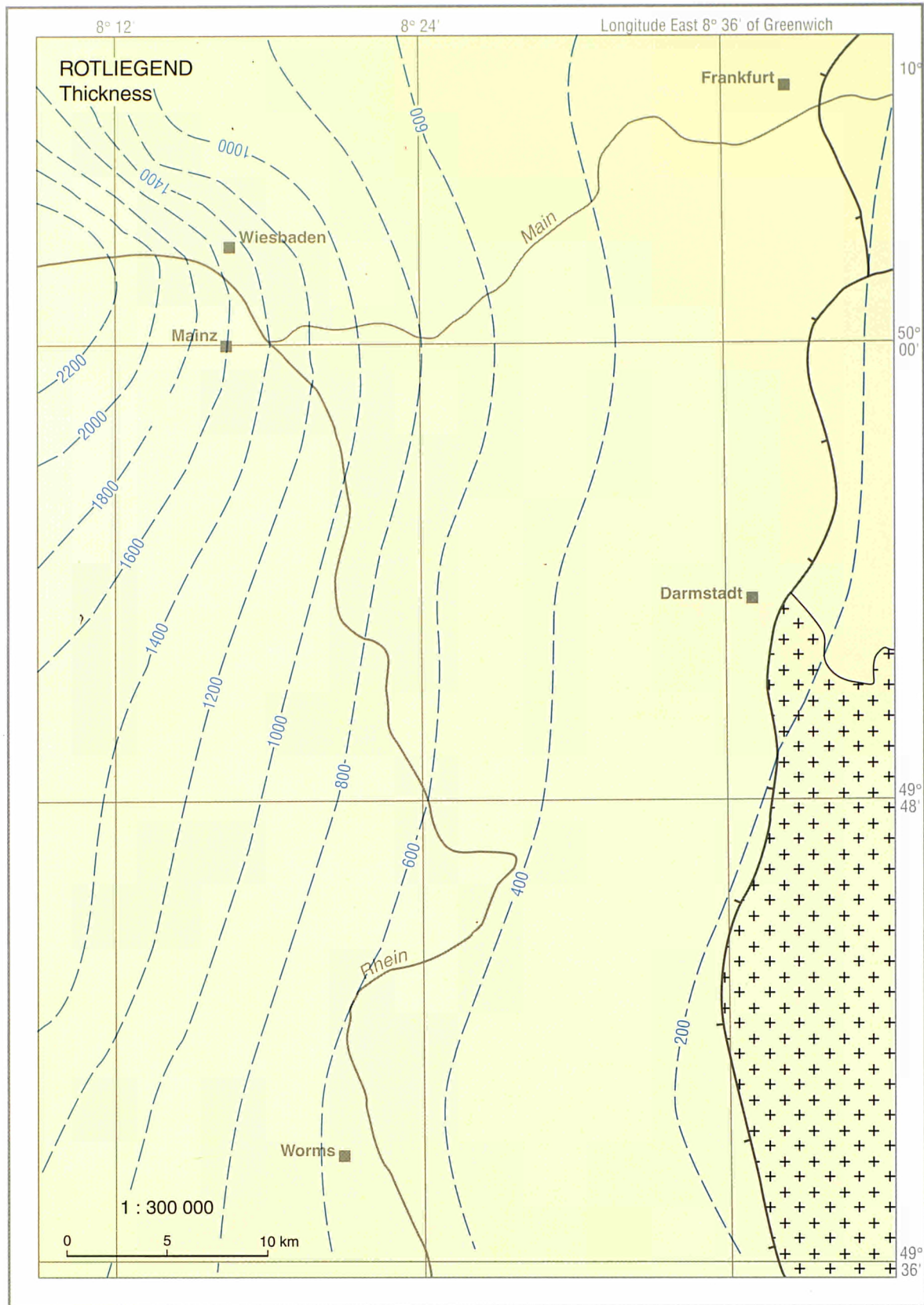
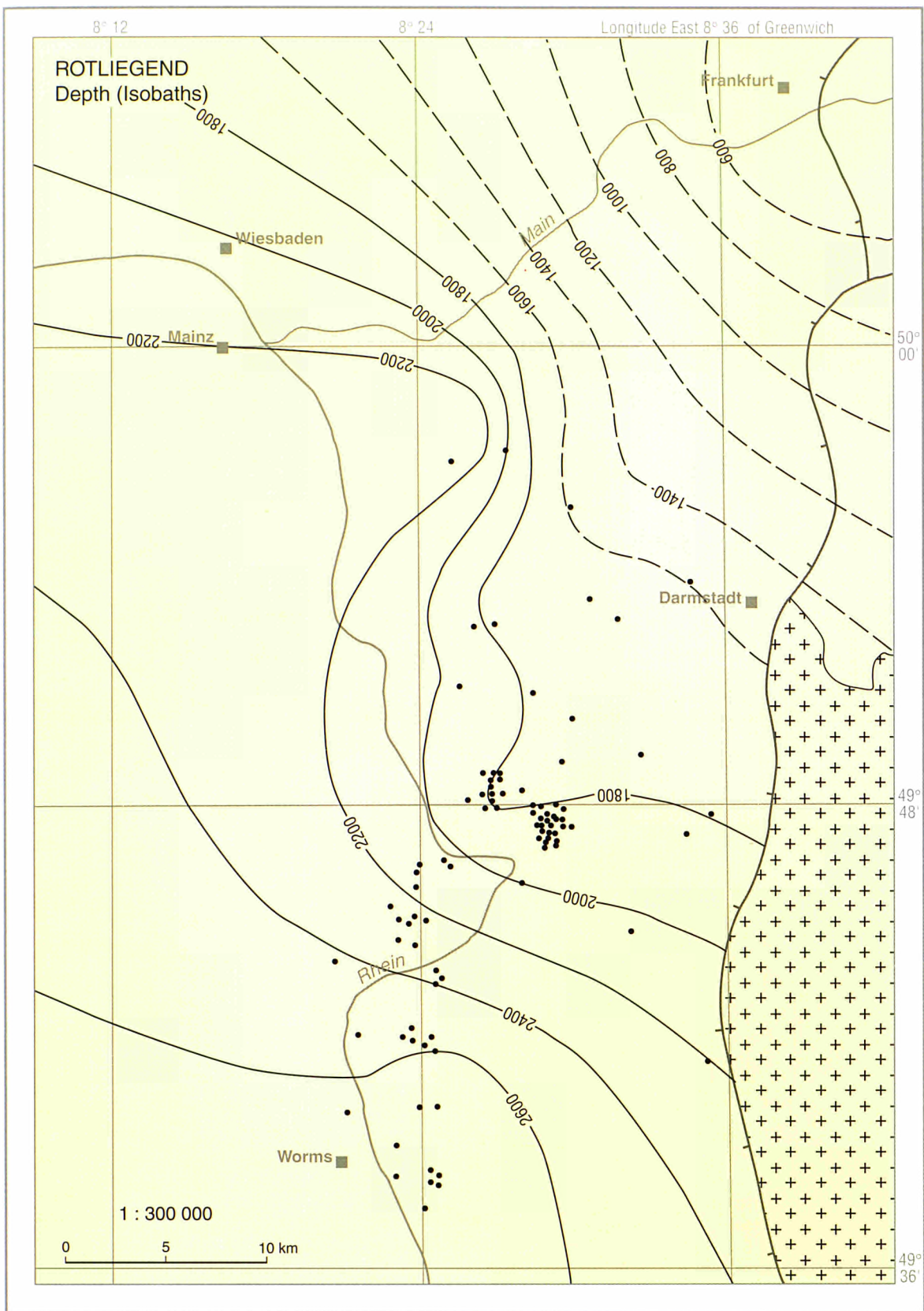
Eastern North German Basin, GERMANY



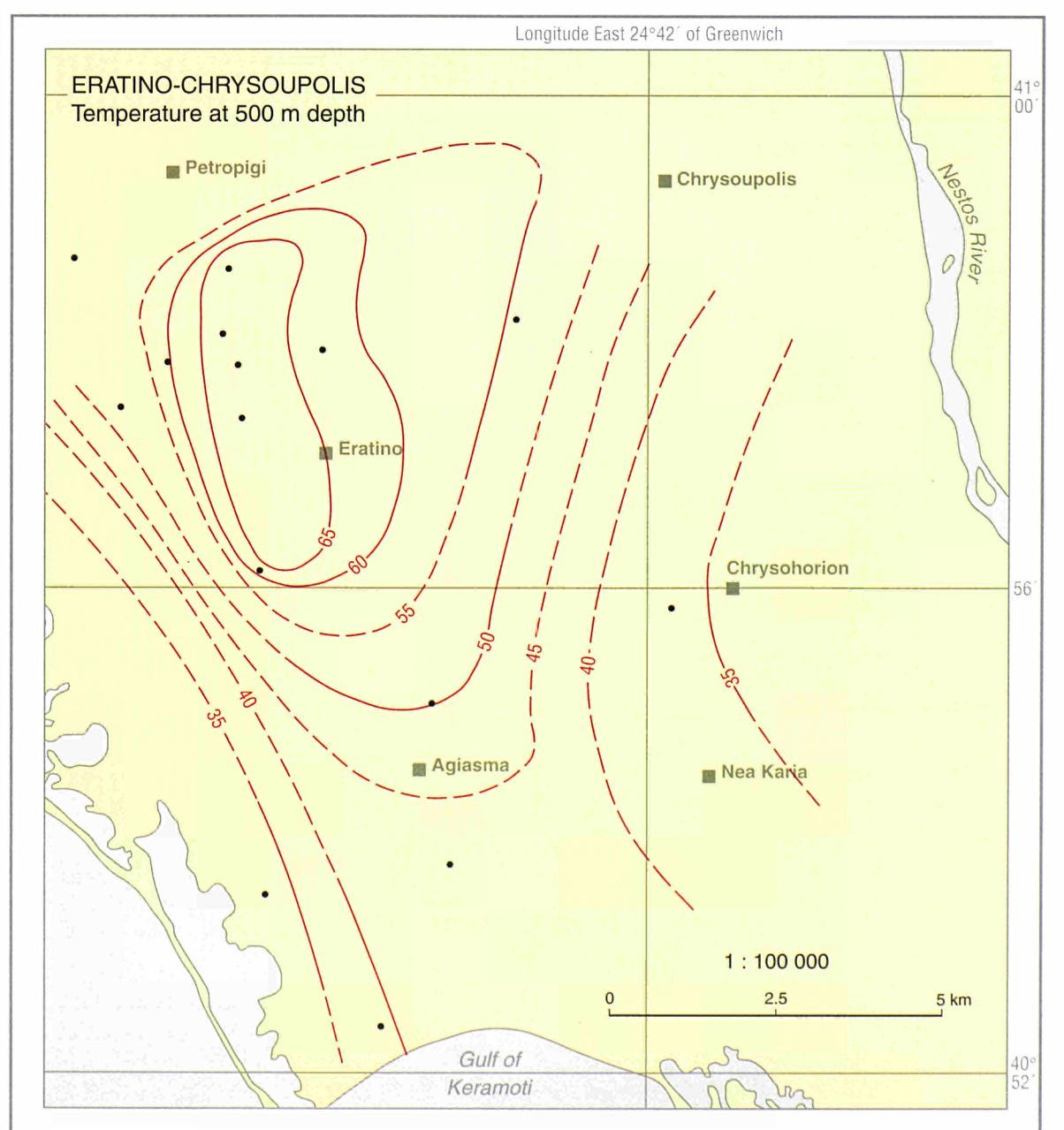
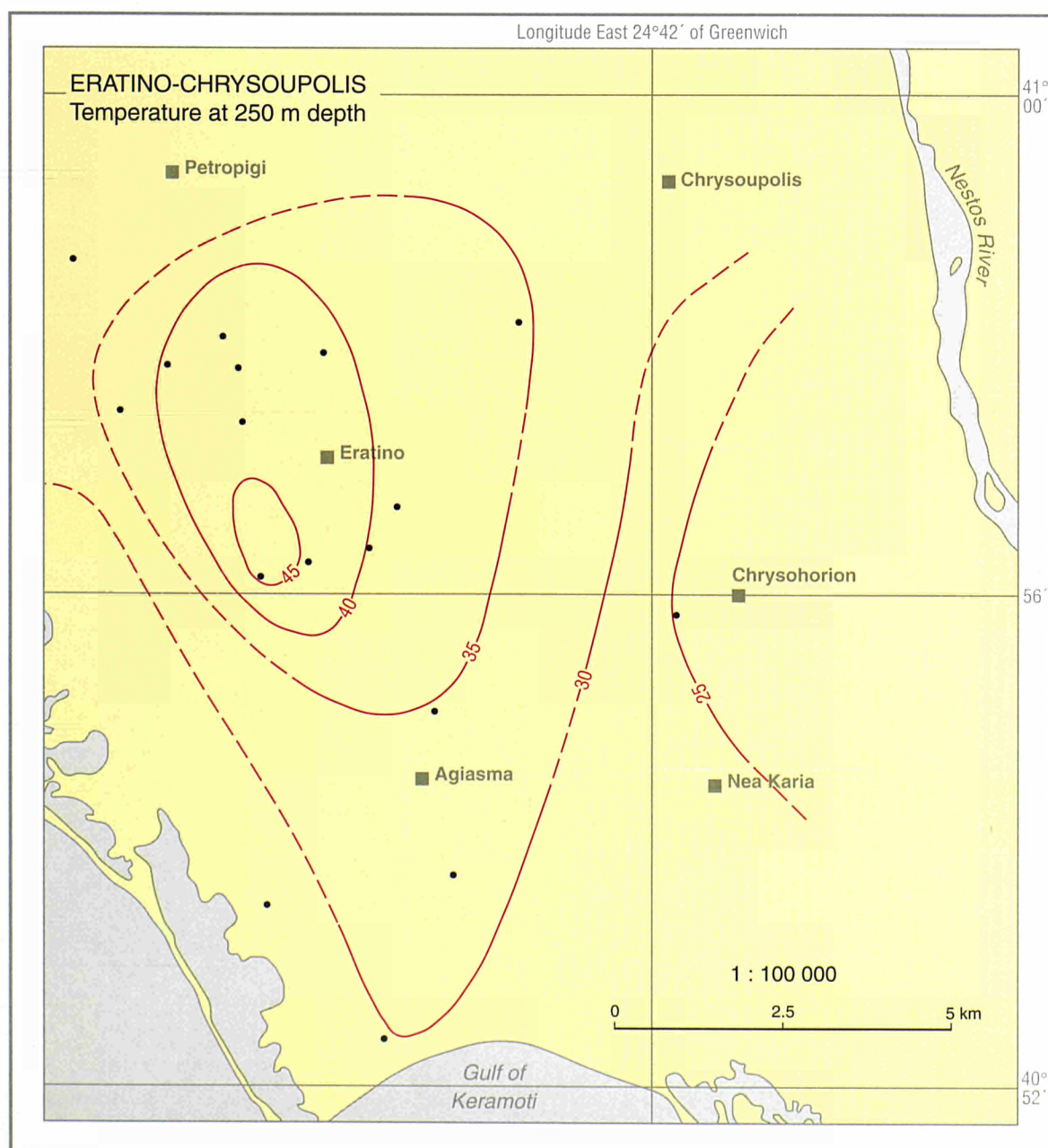
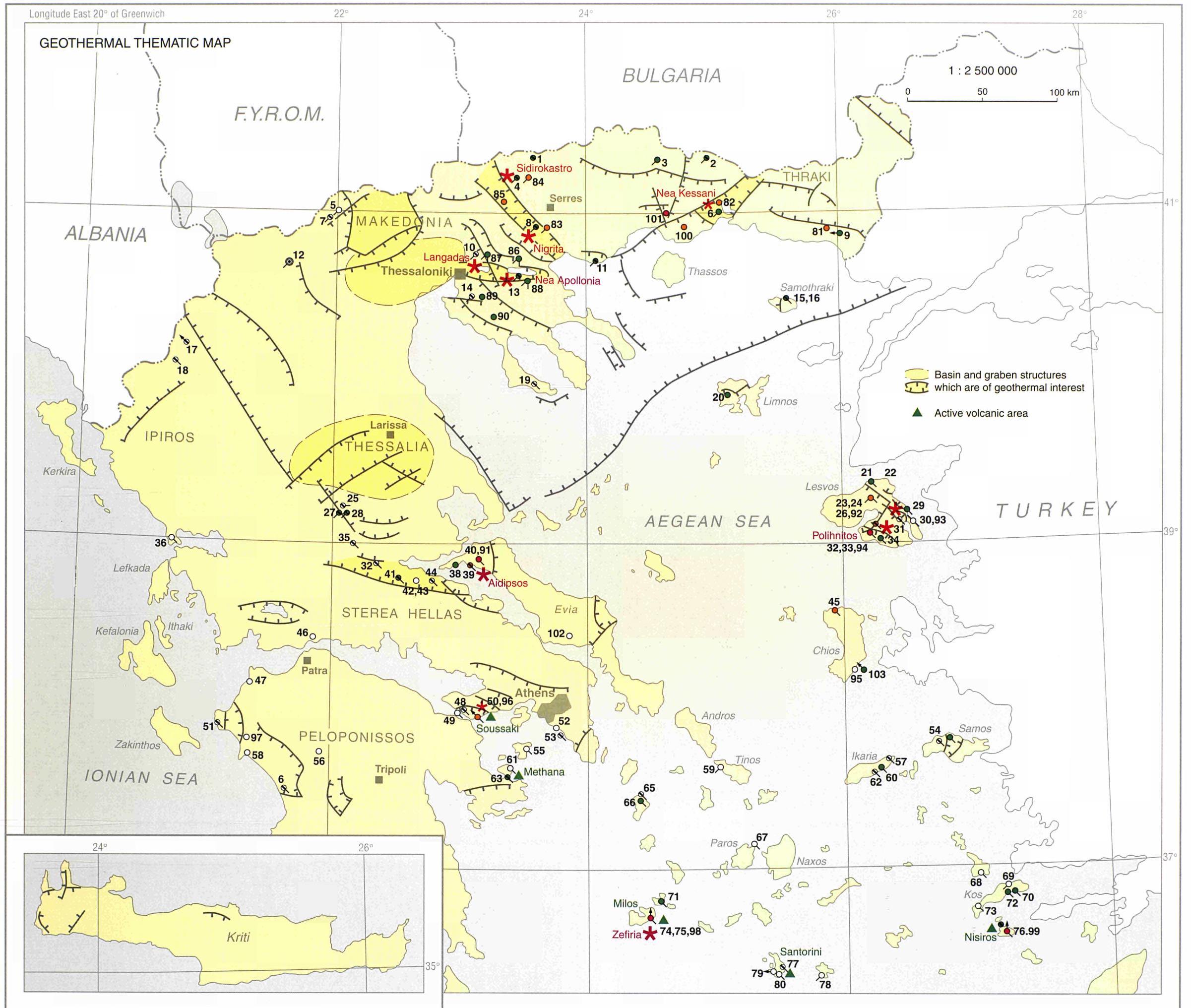
GERMANY, Northern Upper Rhine Graben

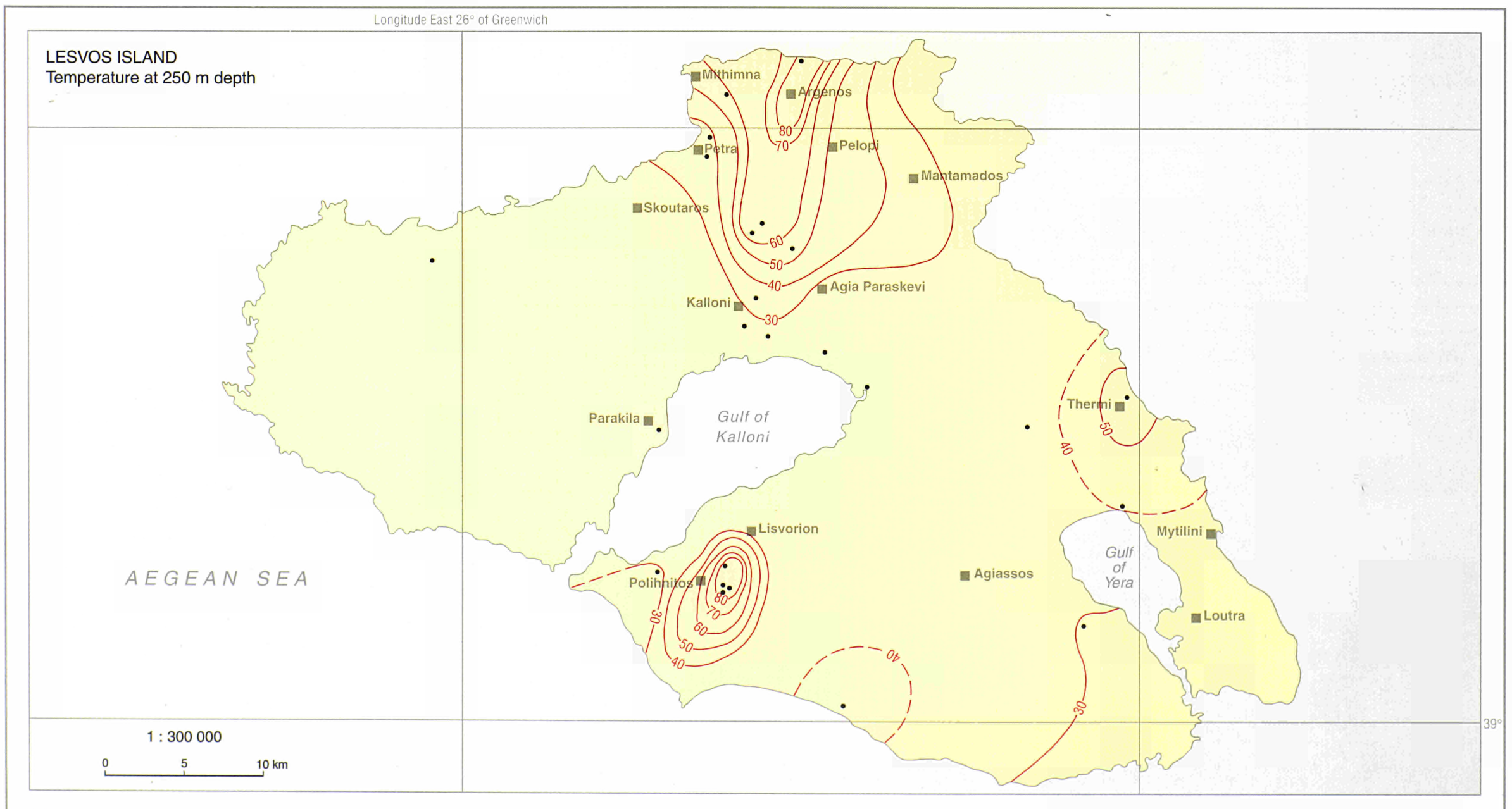
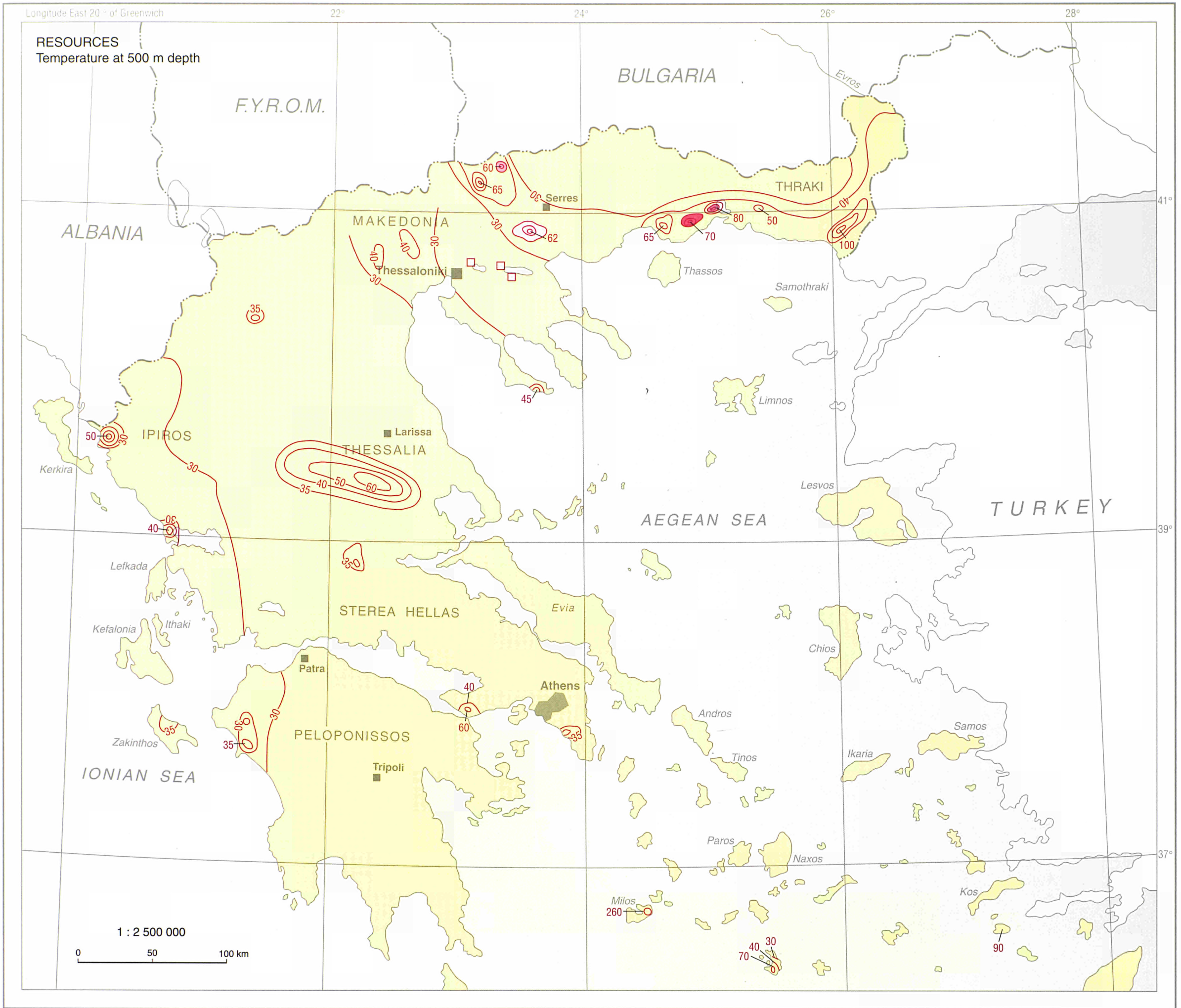


GERMANY, Northern Upper Rhine Graben

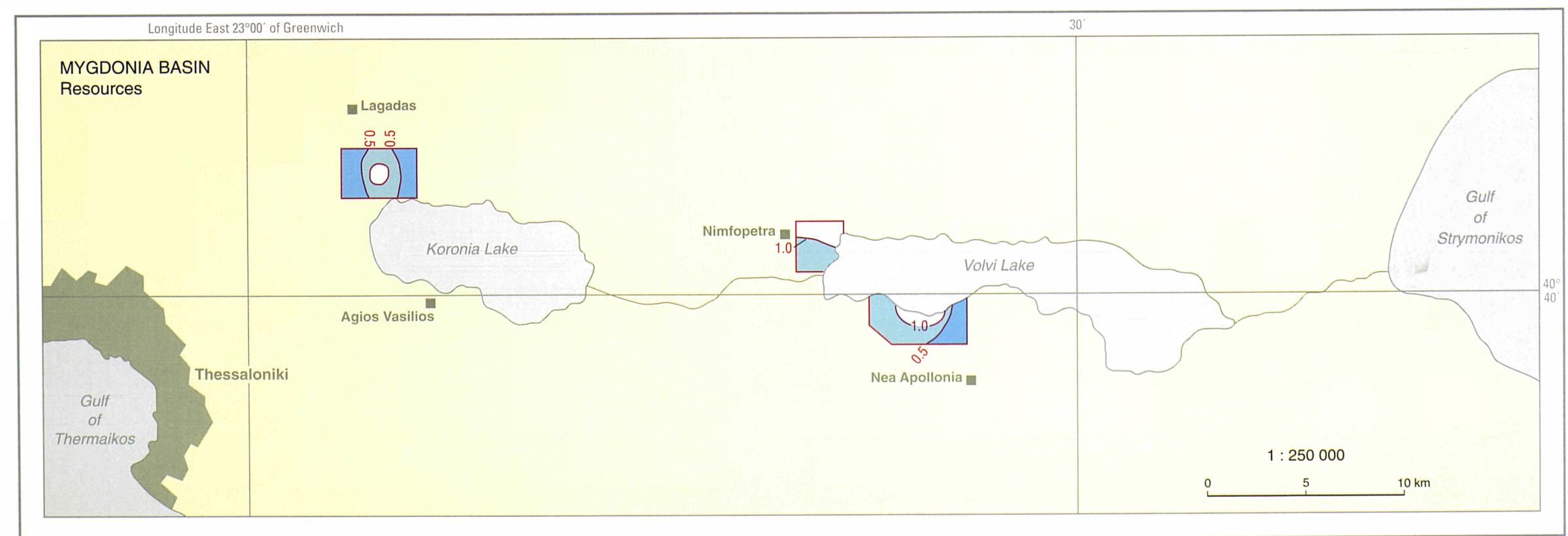
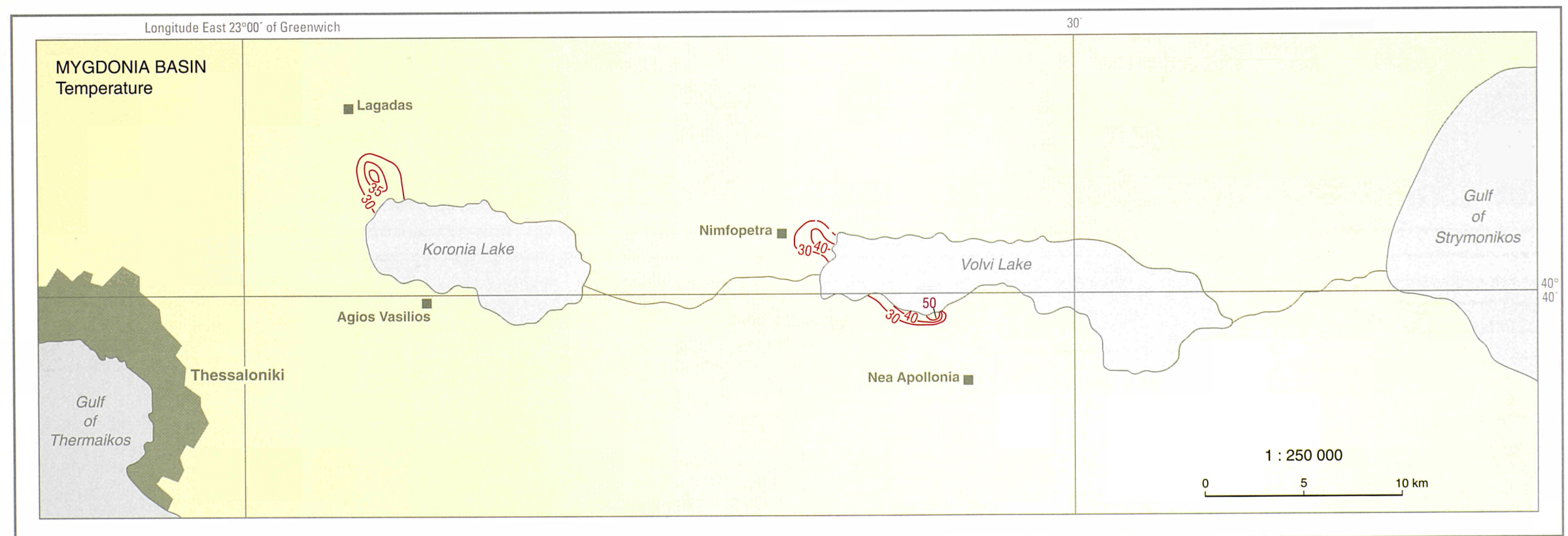
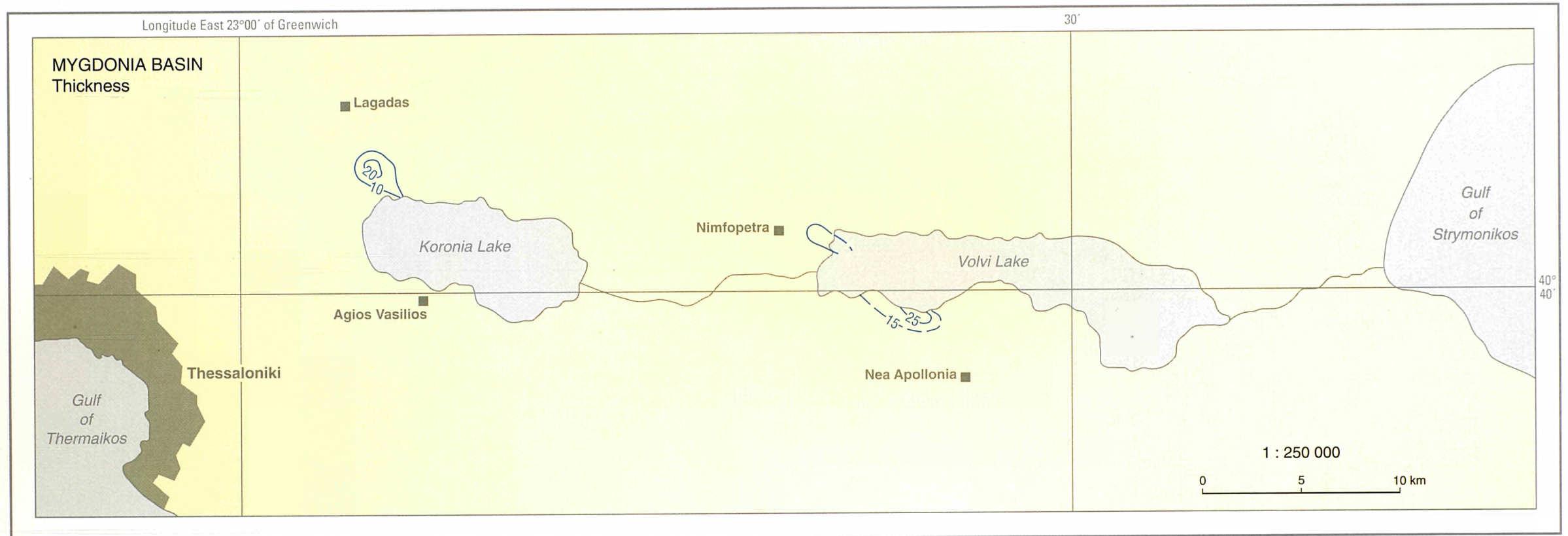
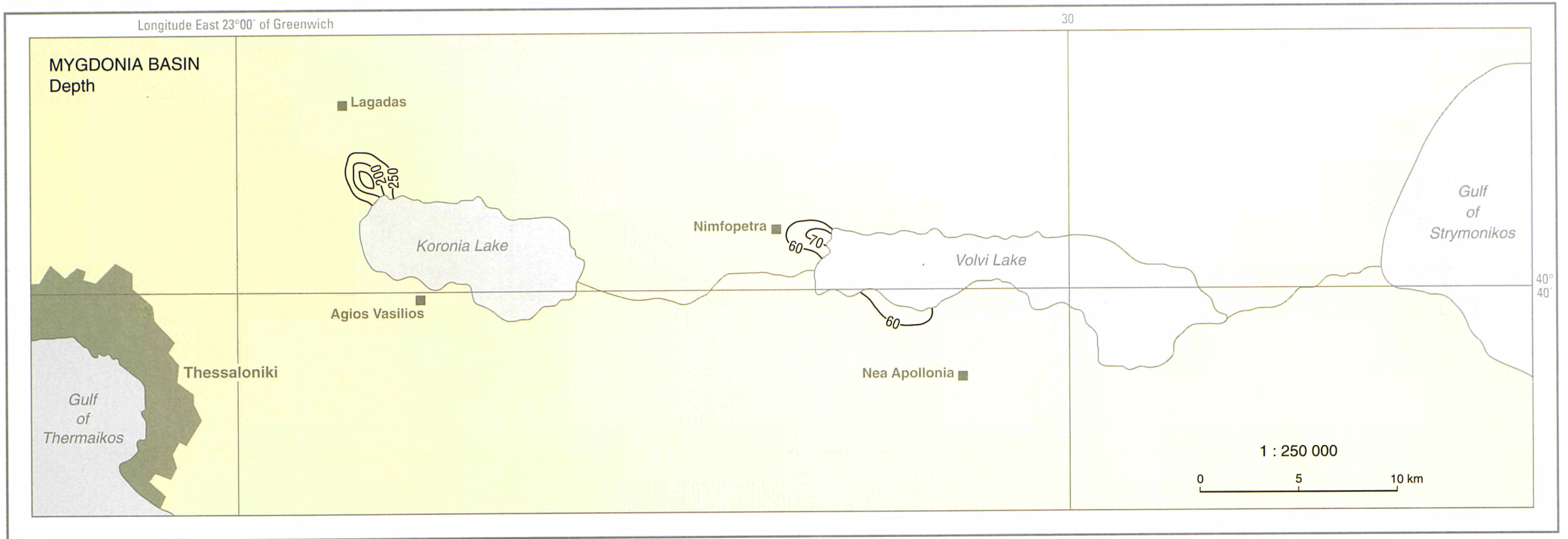


GREECE

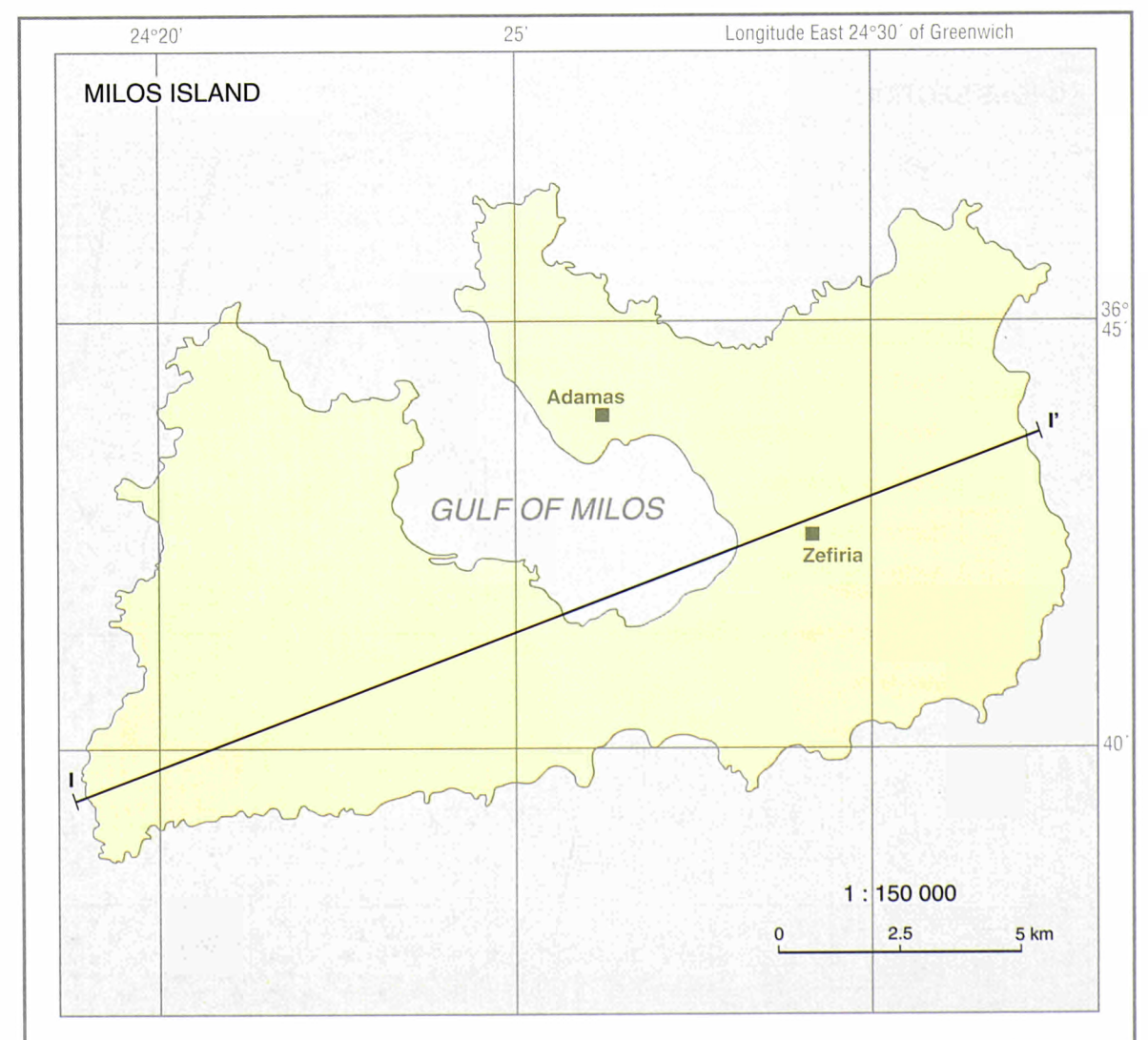
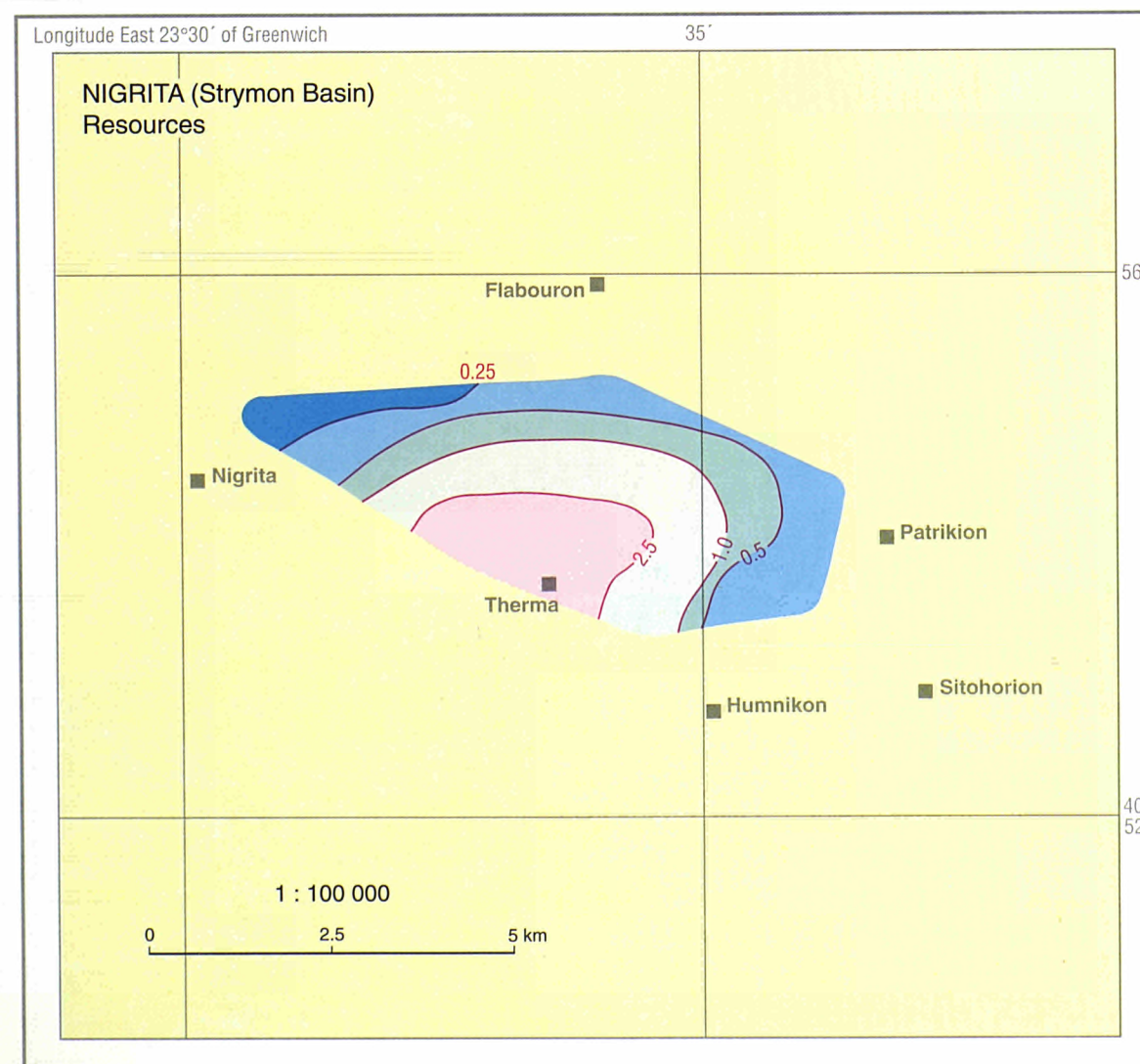
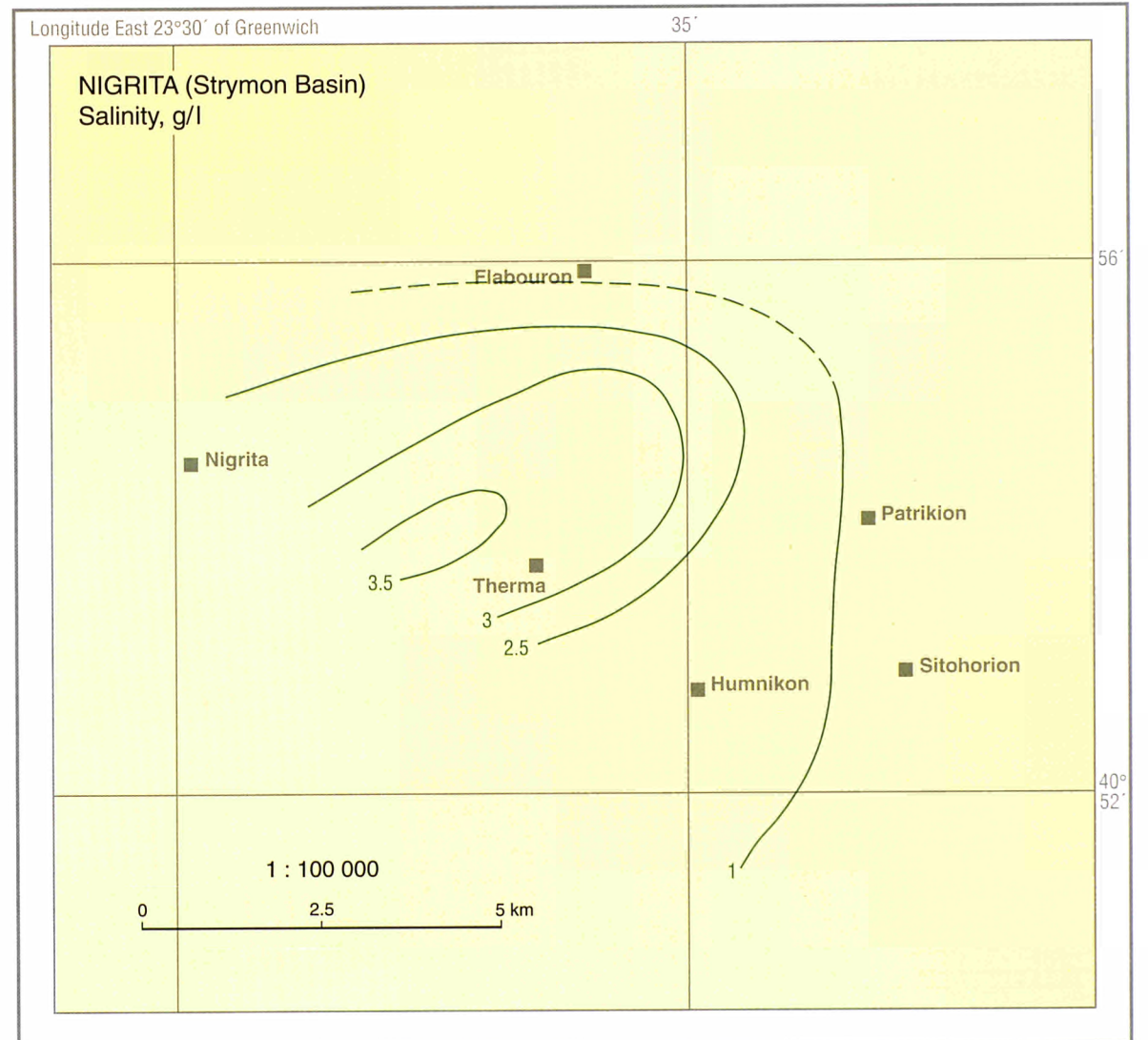
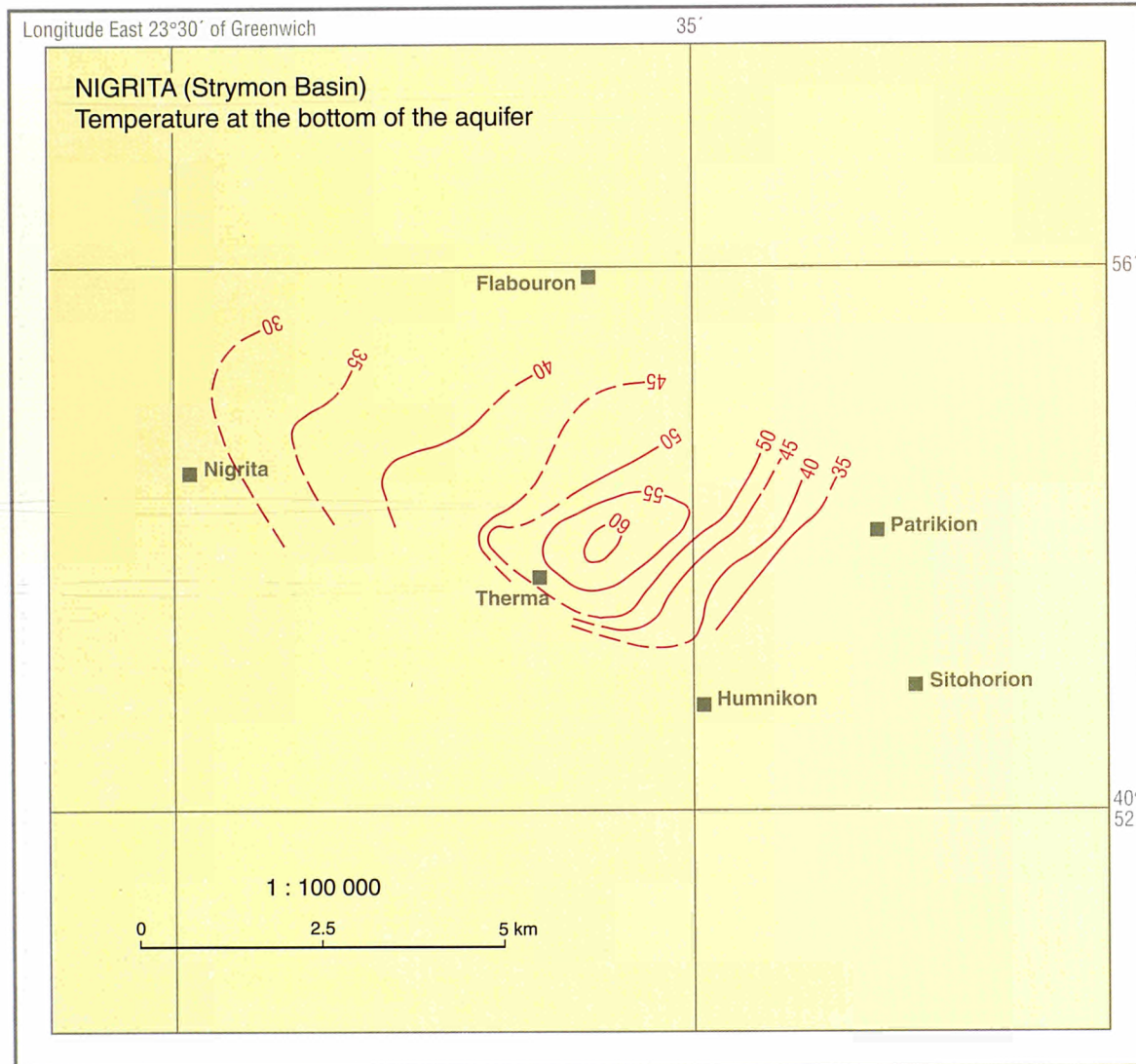
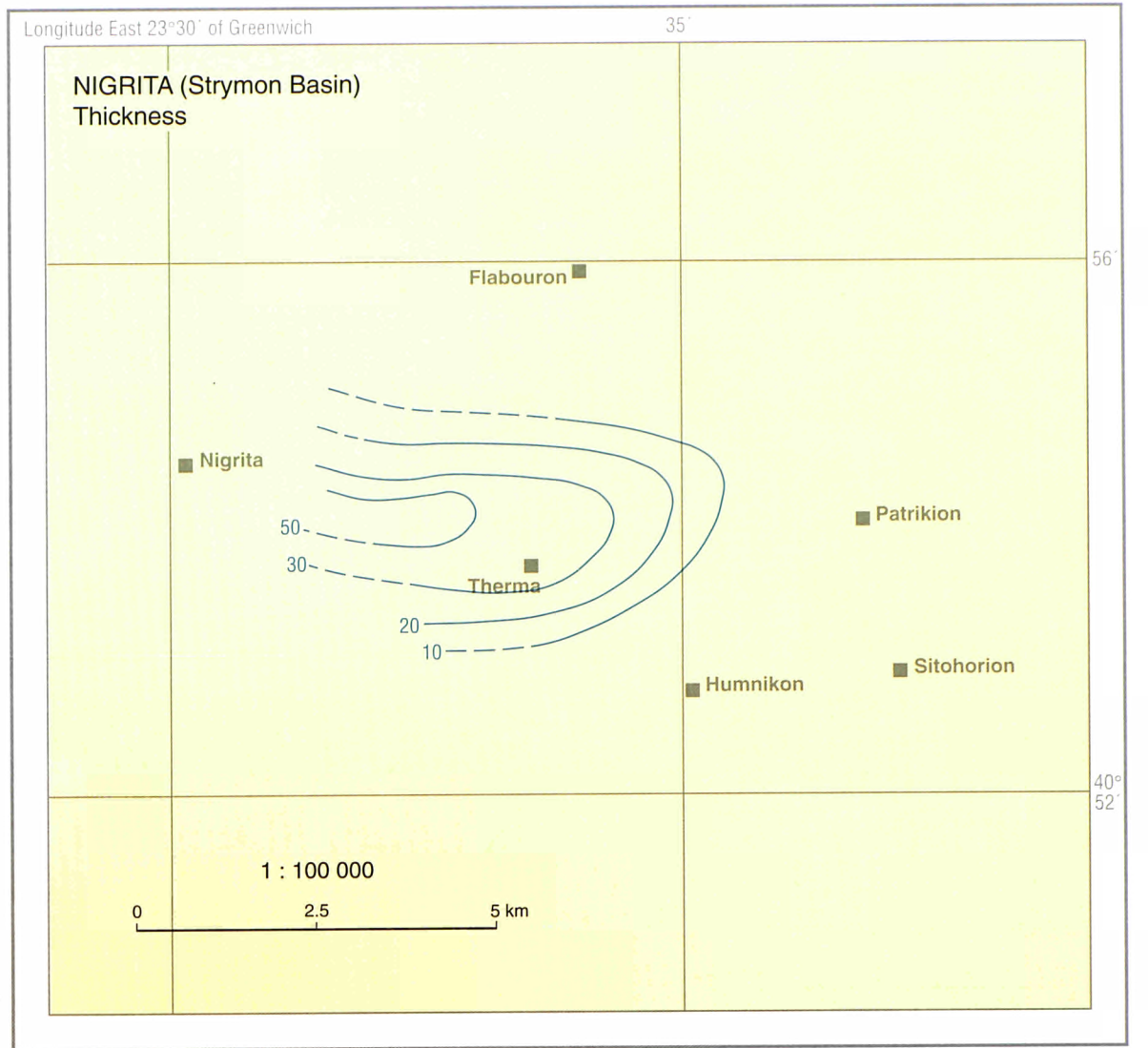
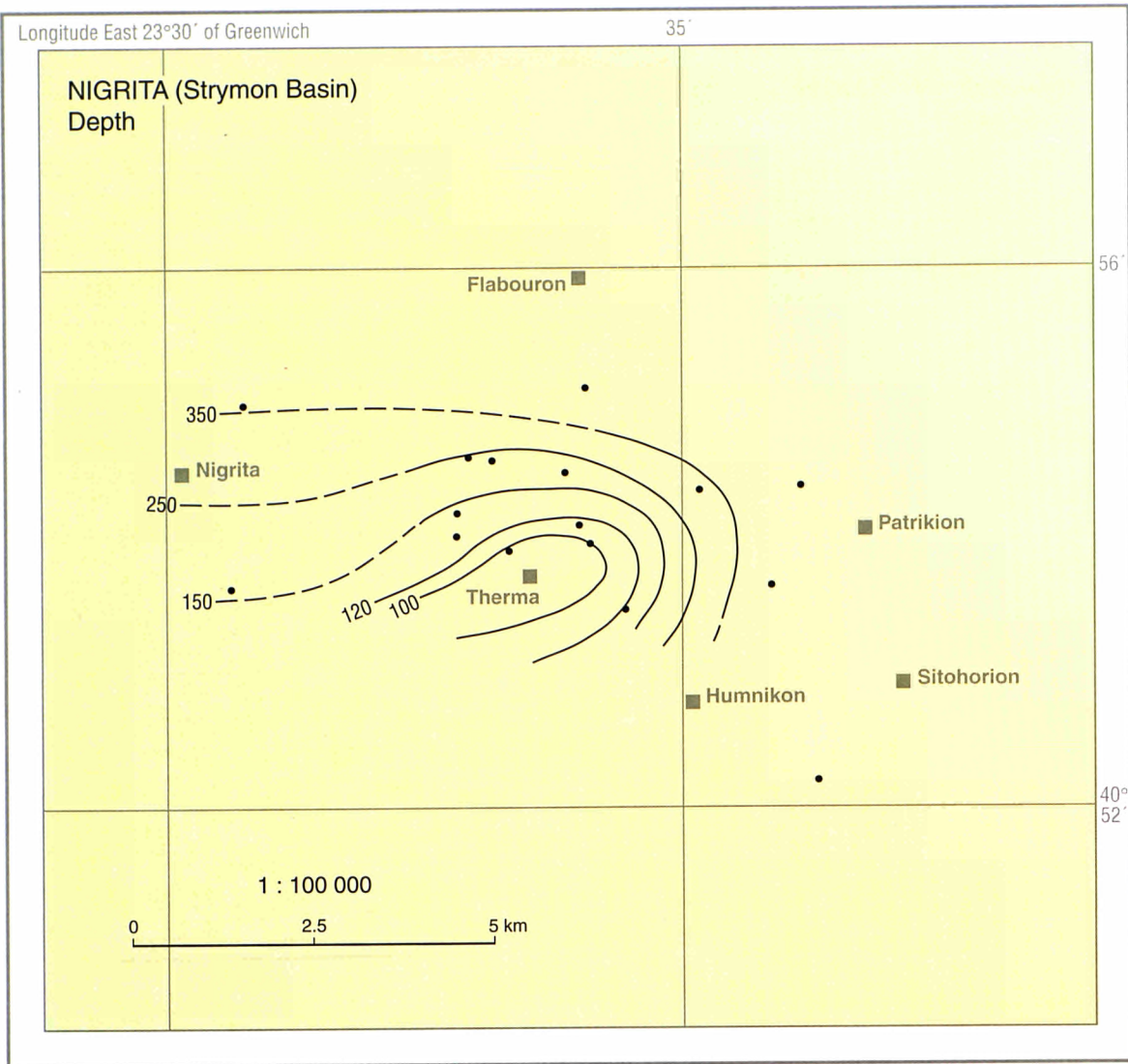


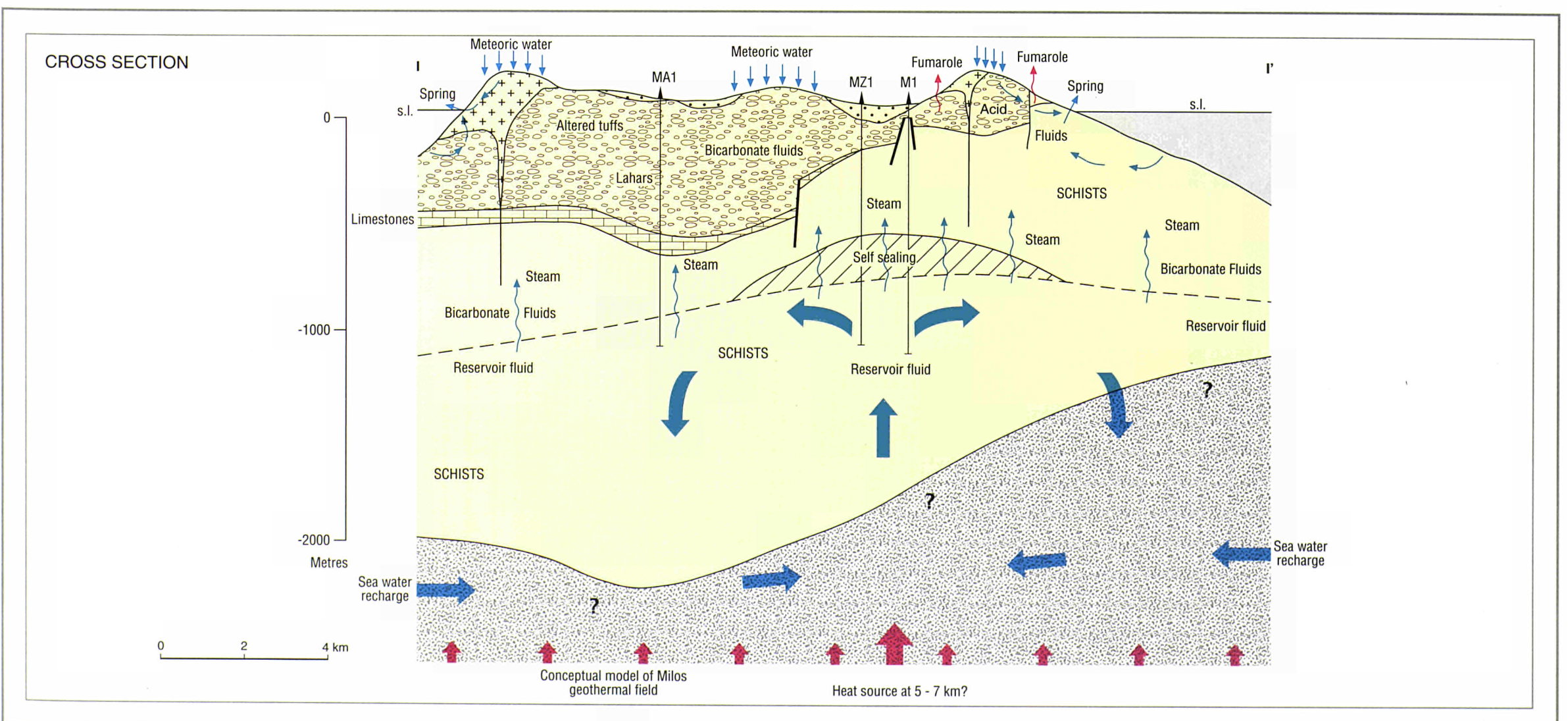
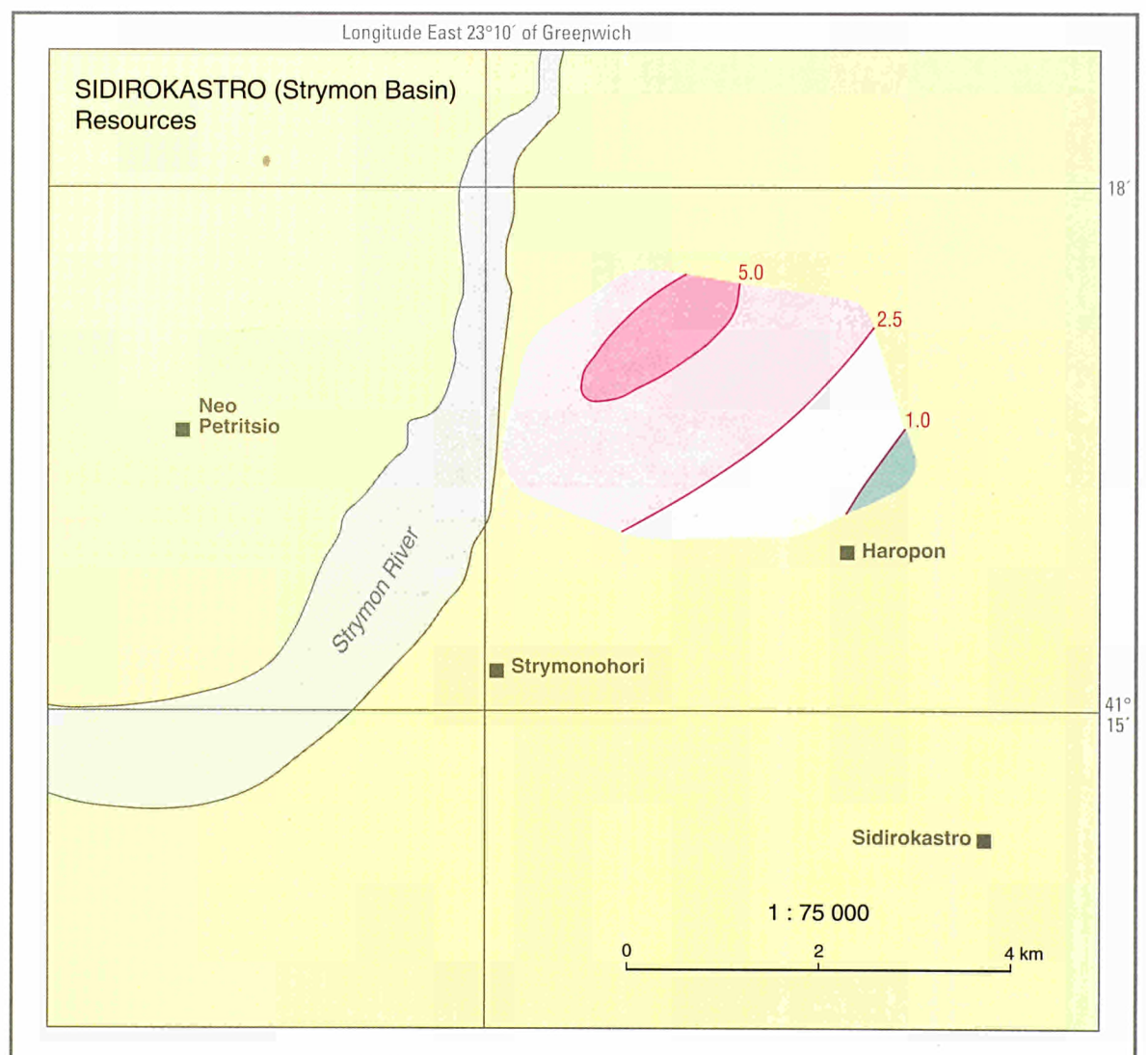
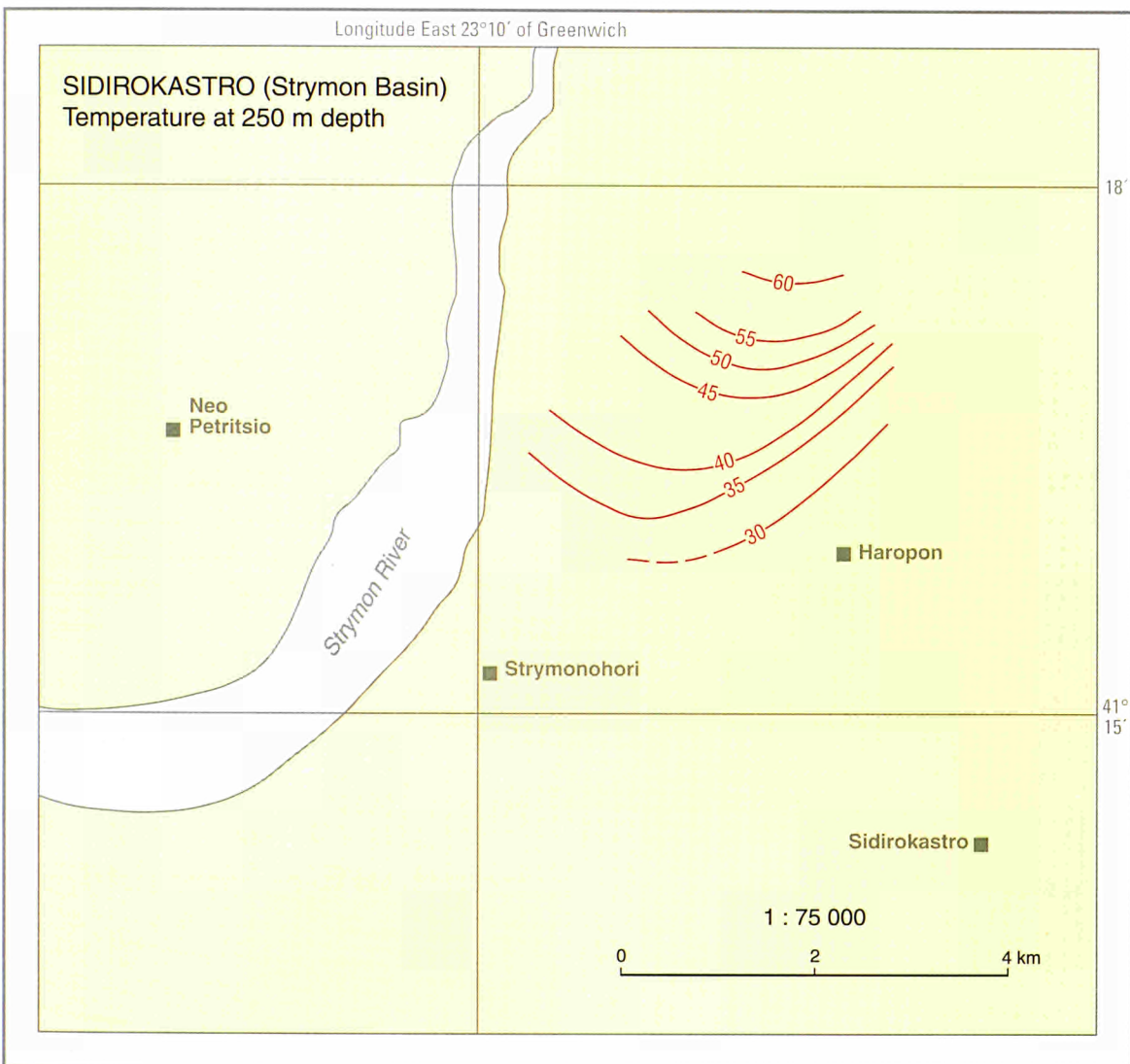
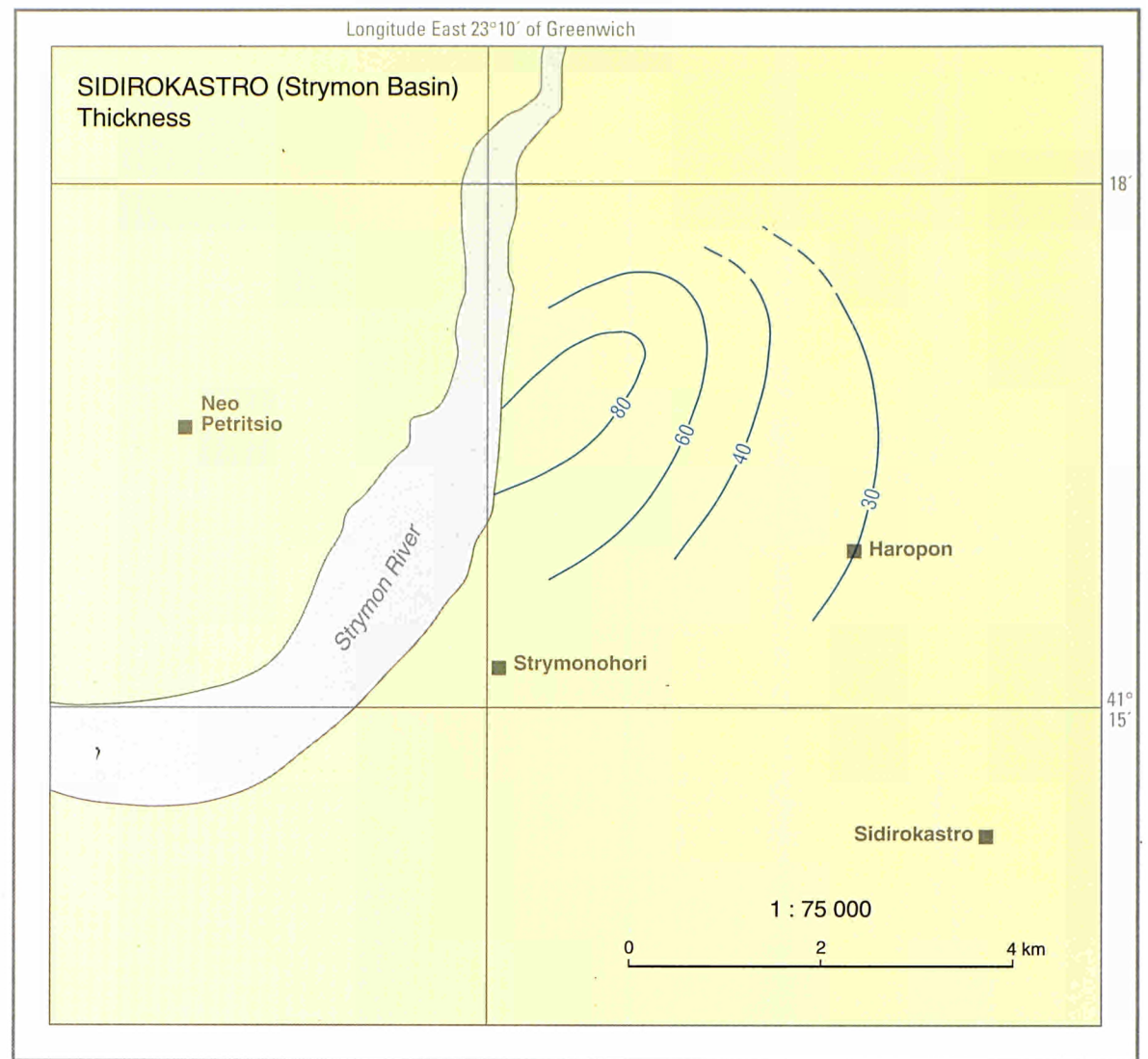
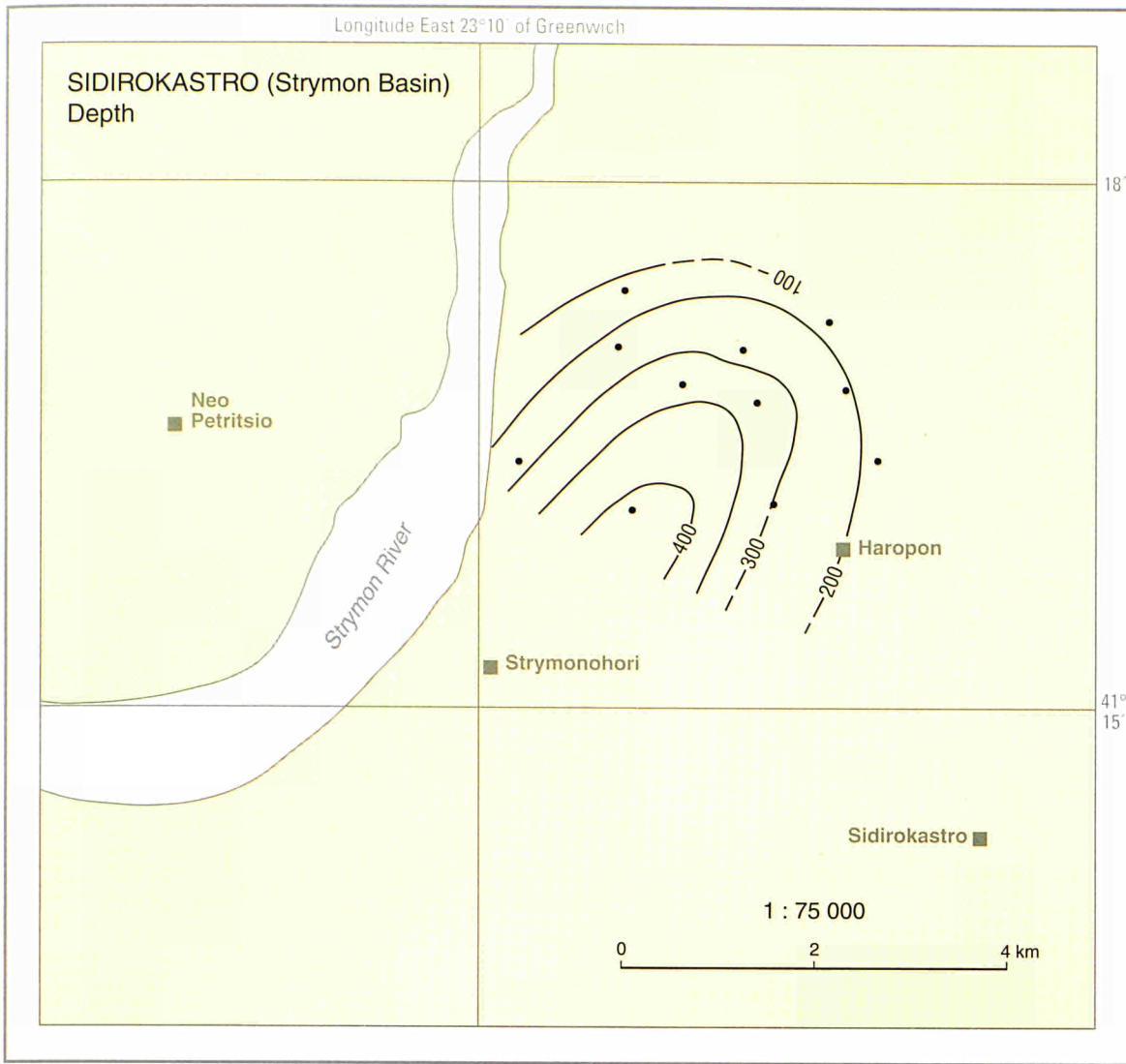


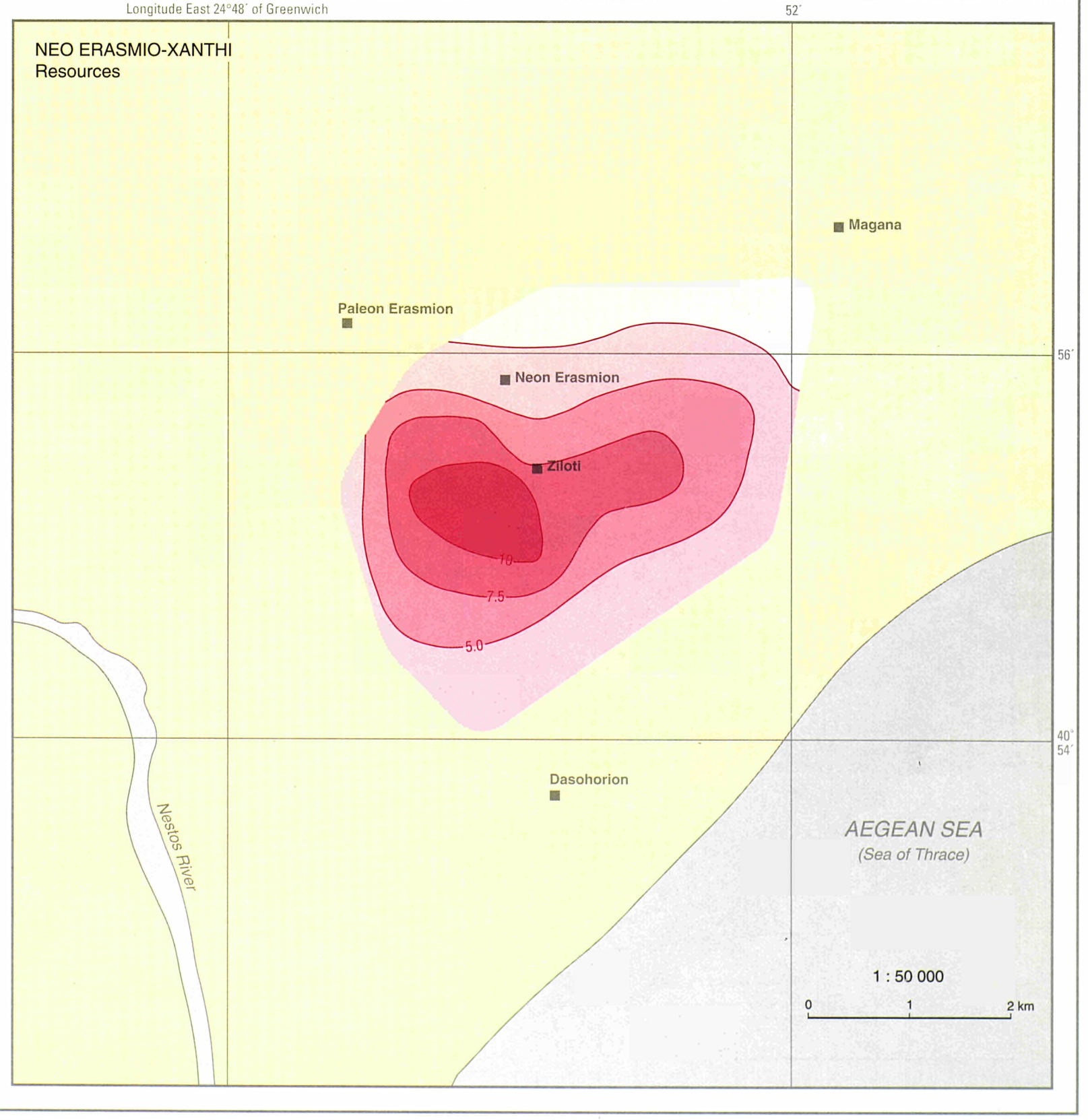
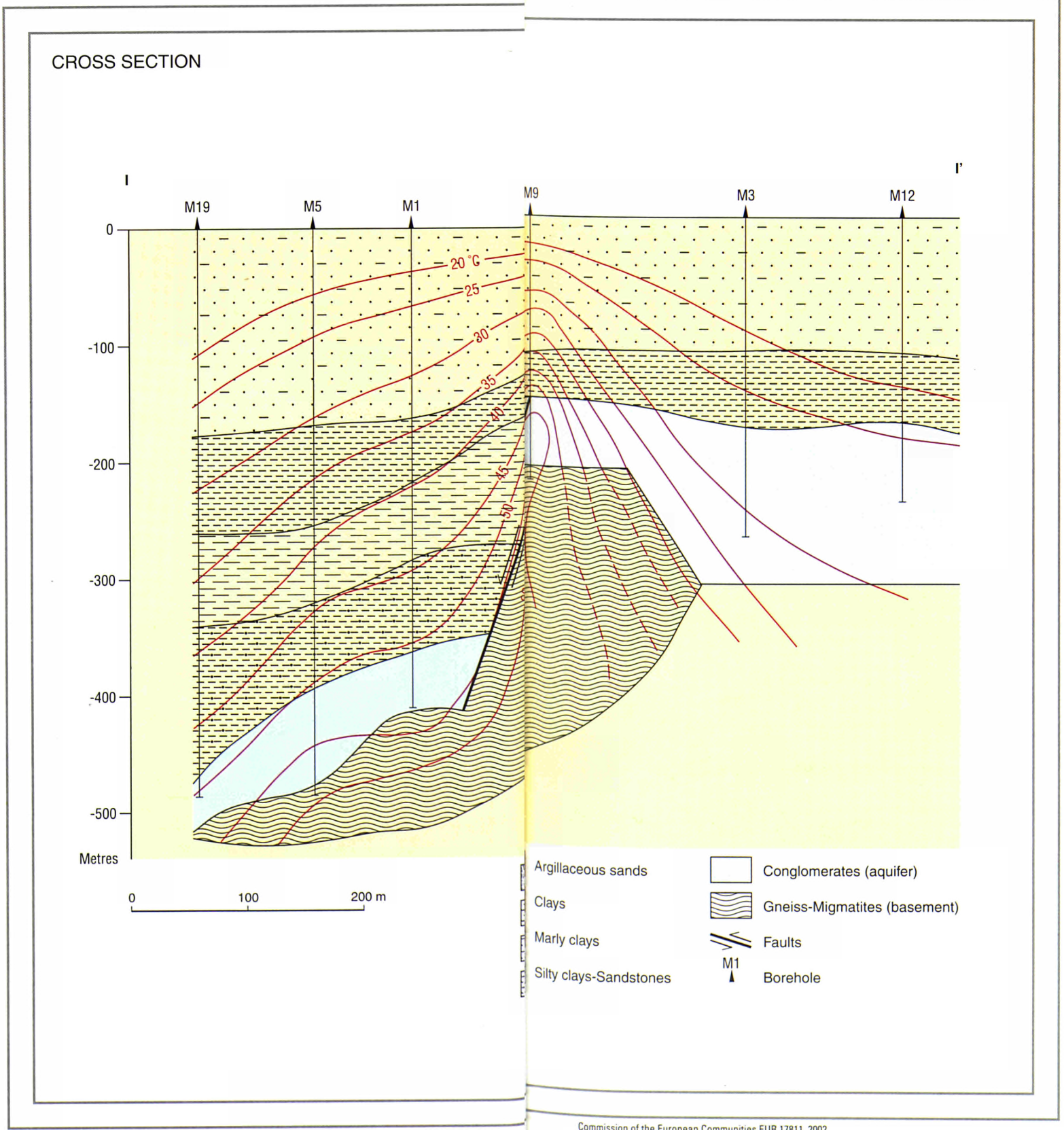
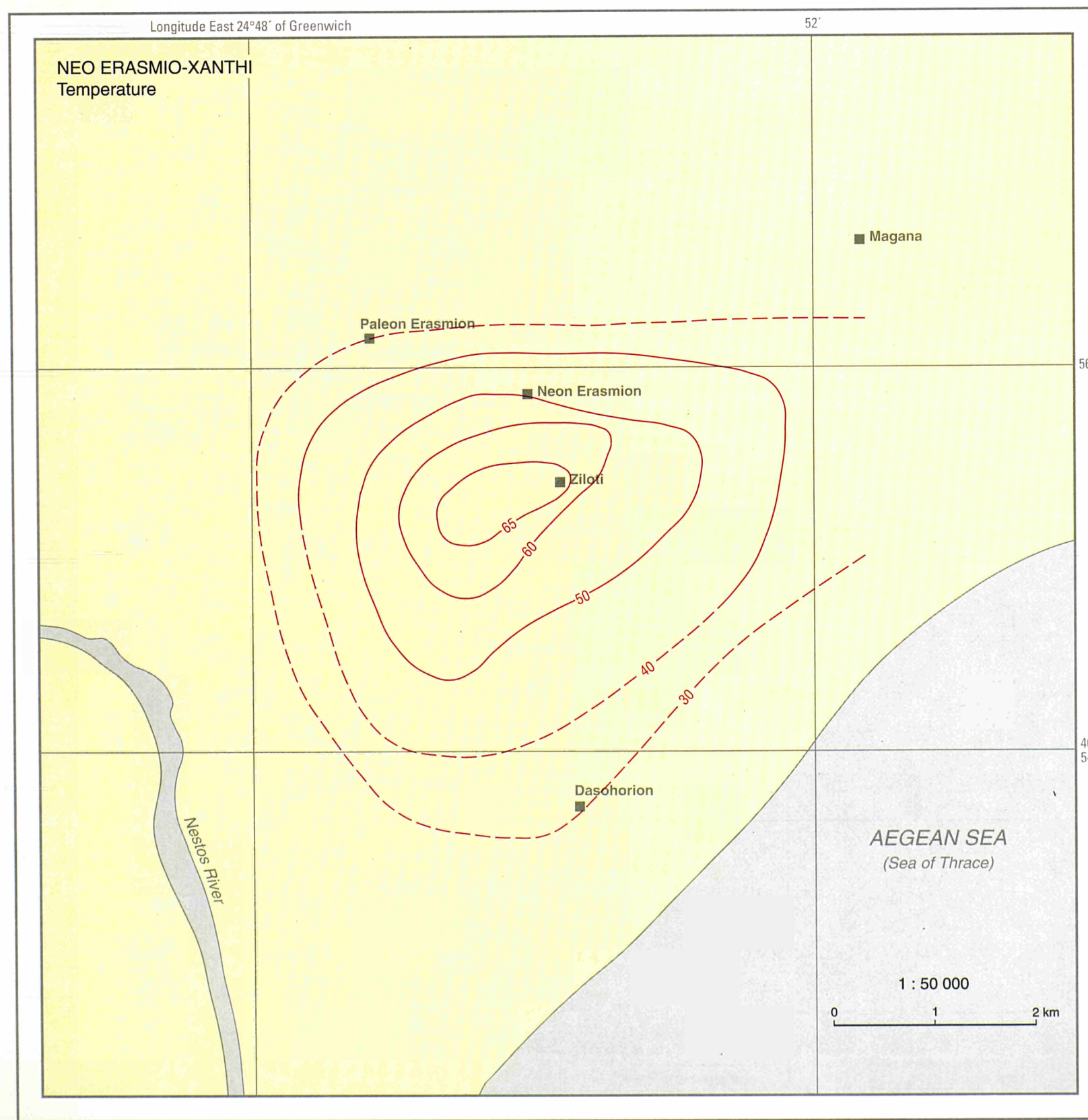
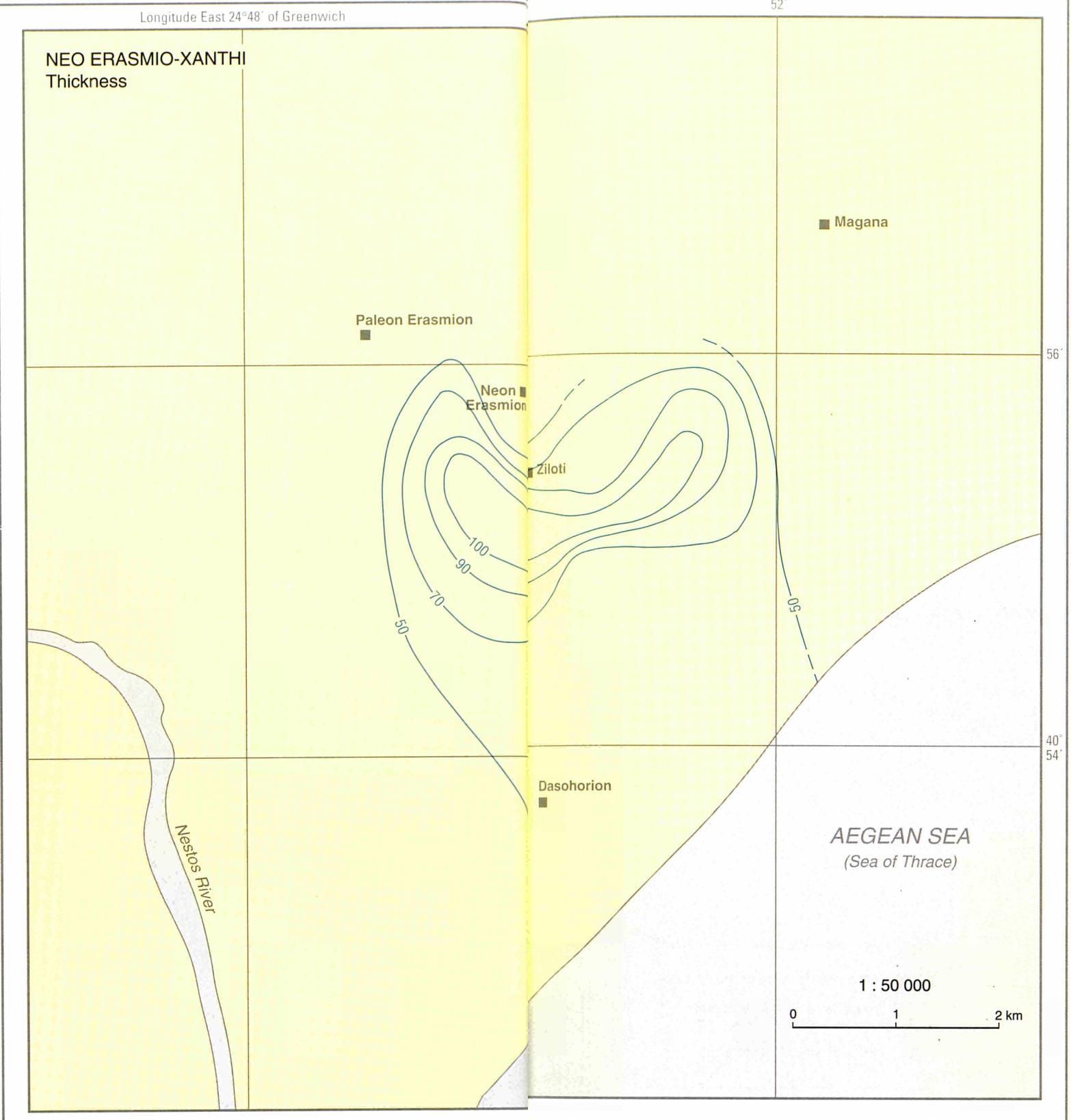
GREECE



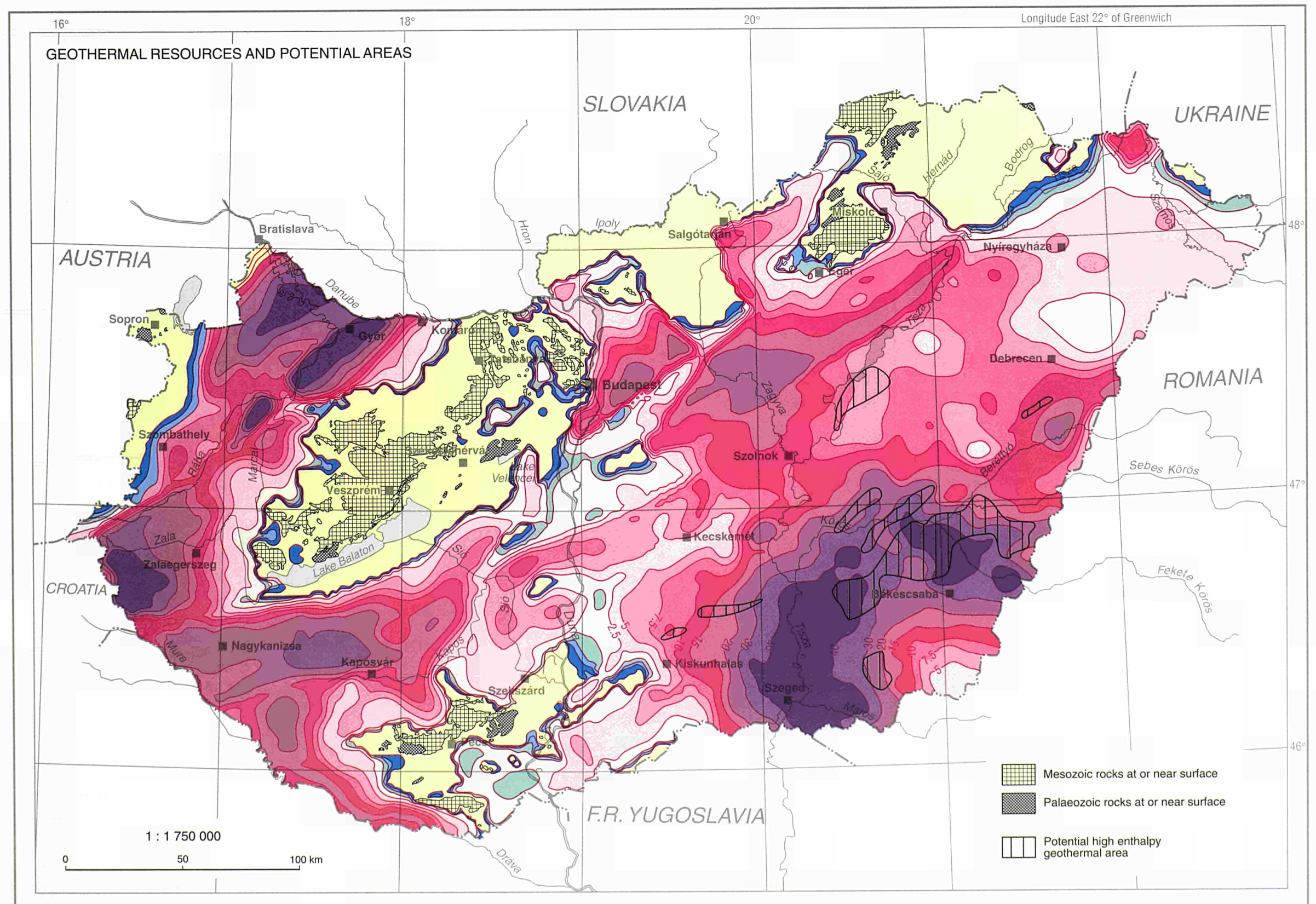
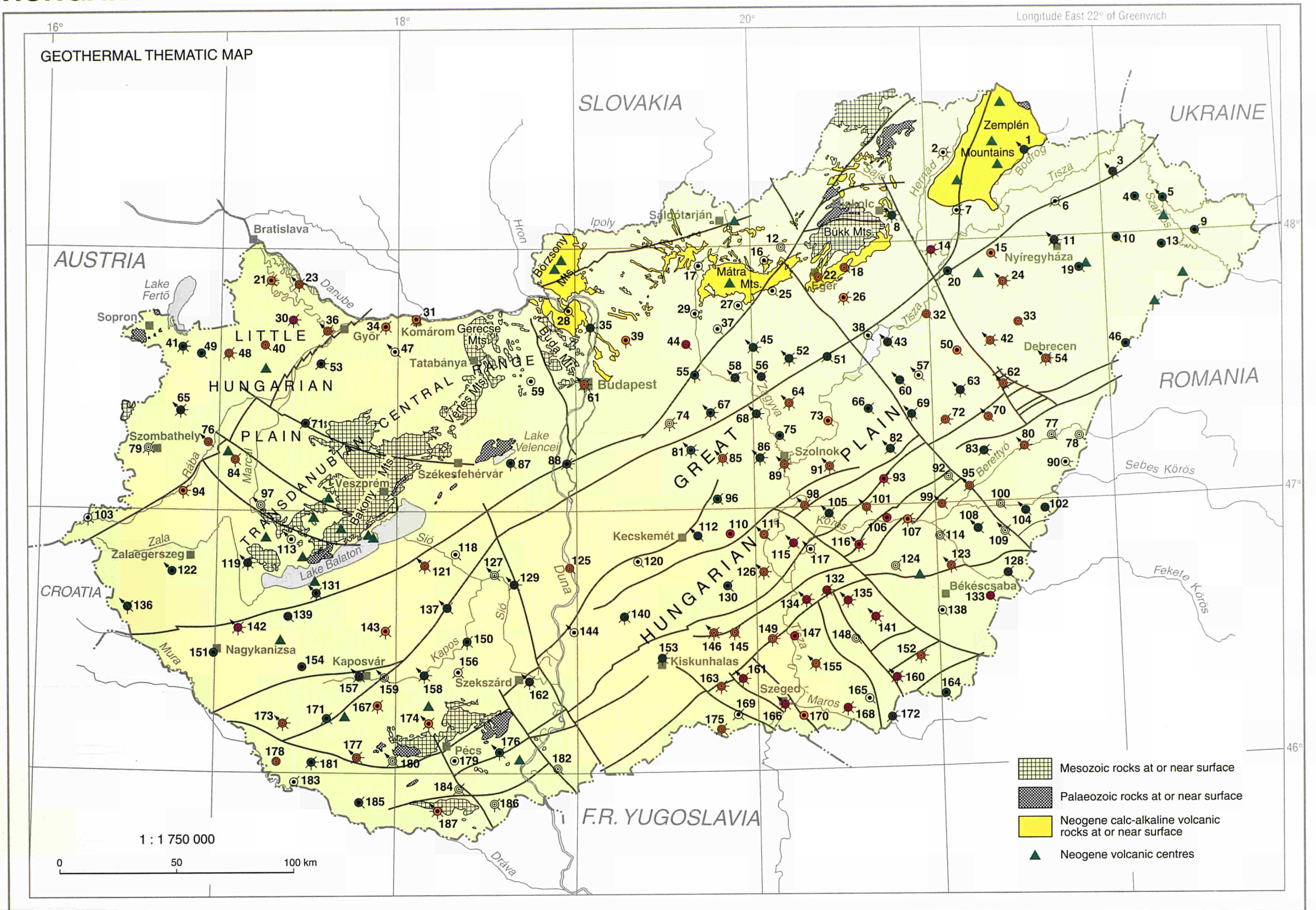
GREECE

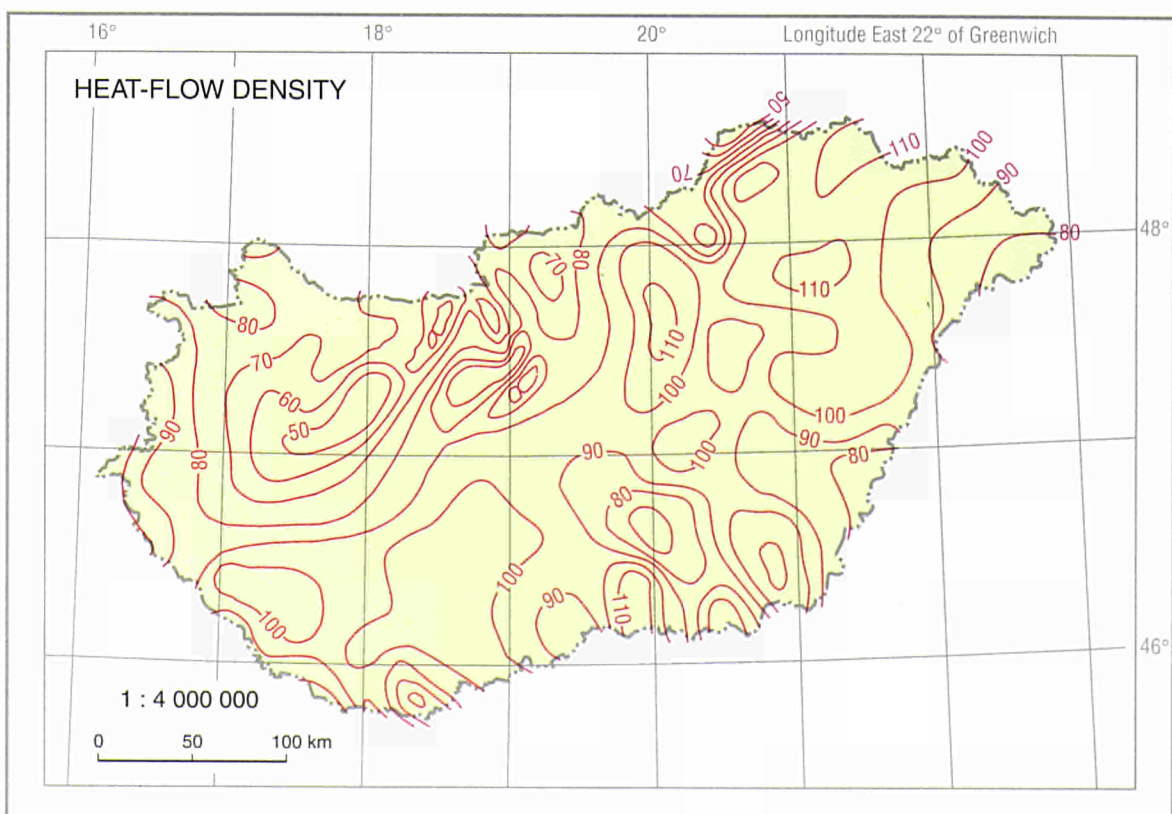
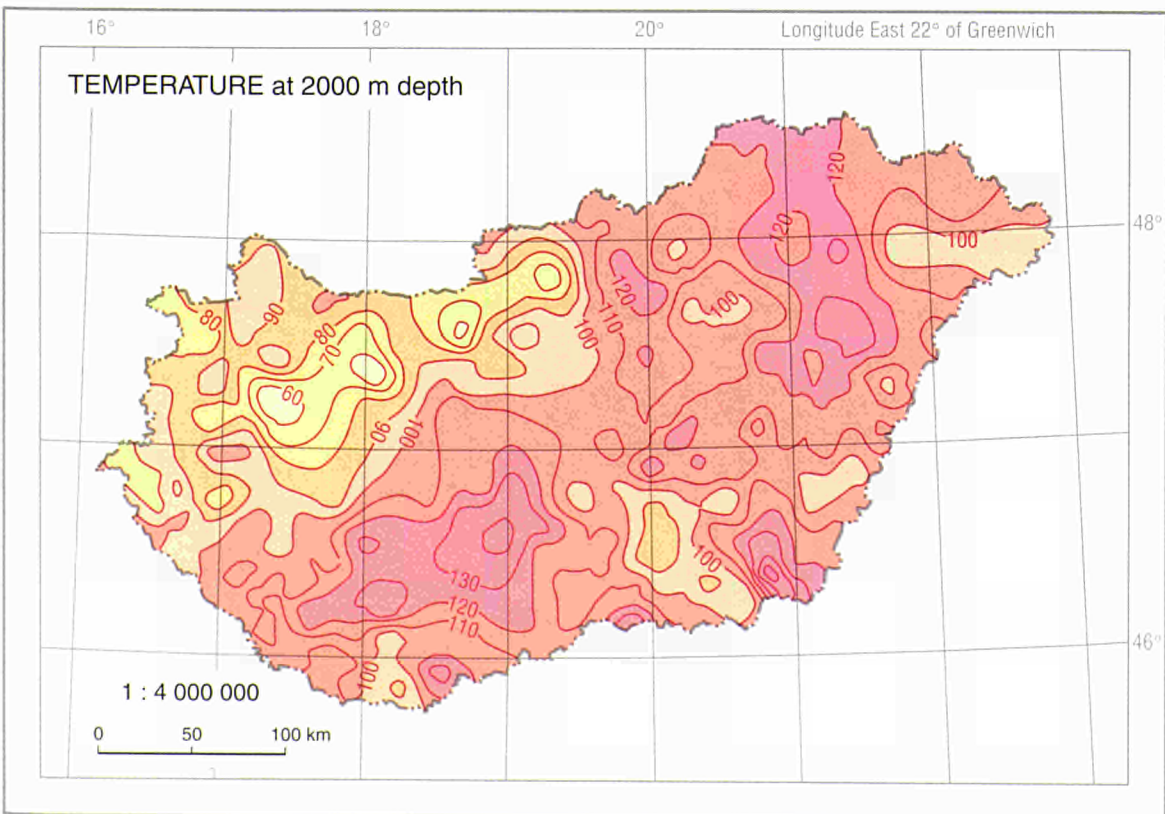
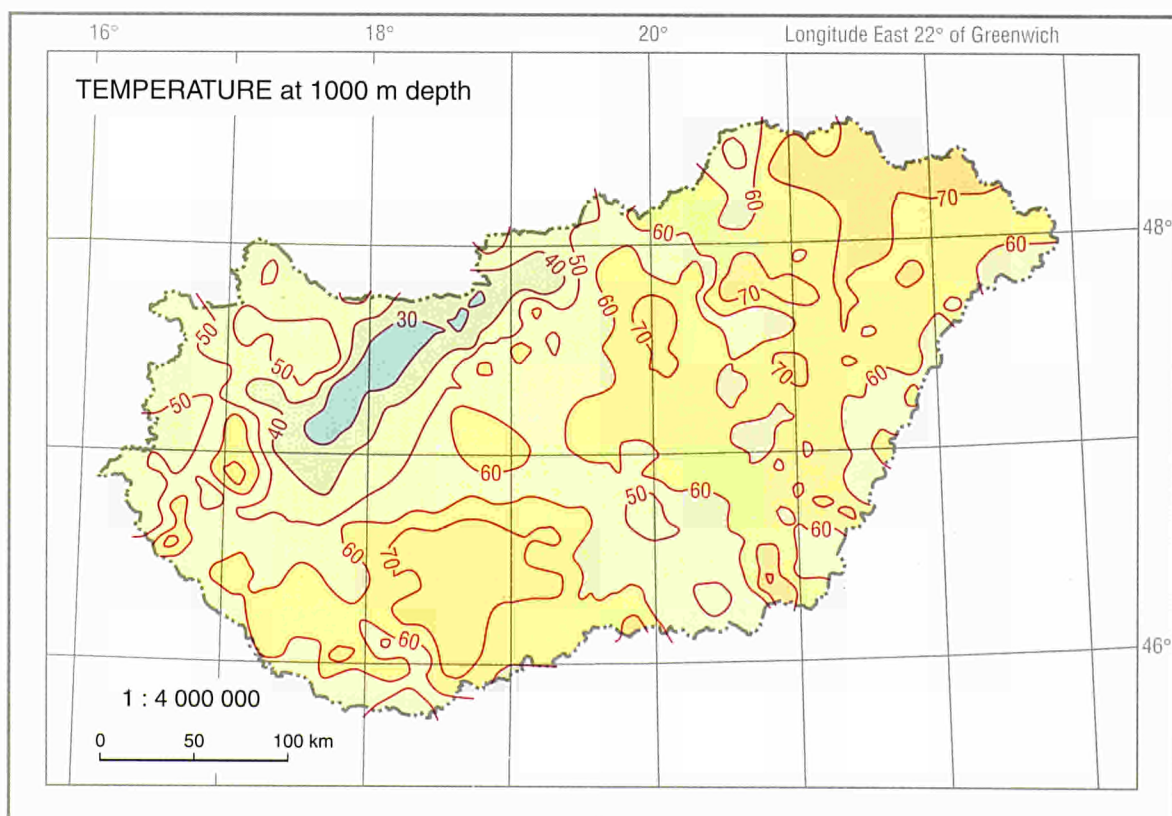
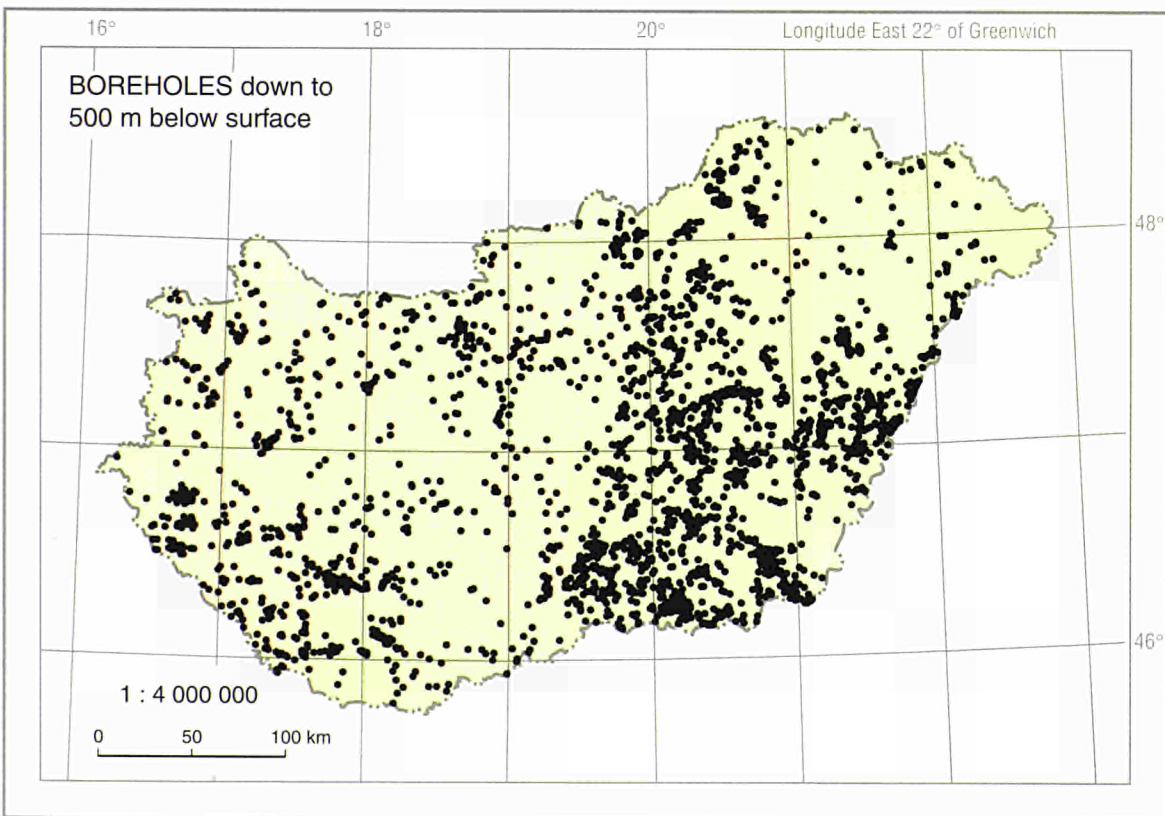
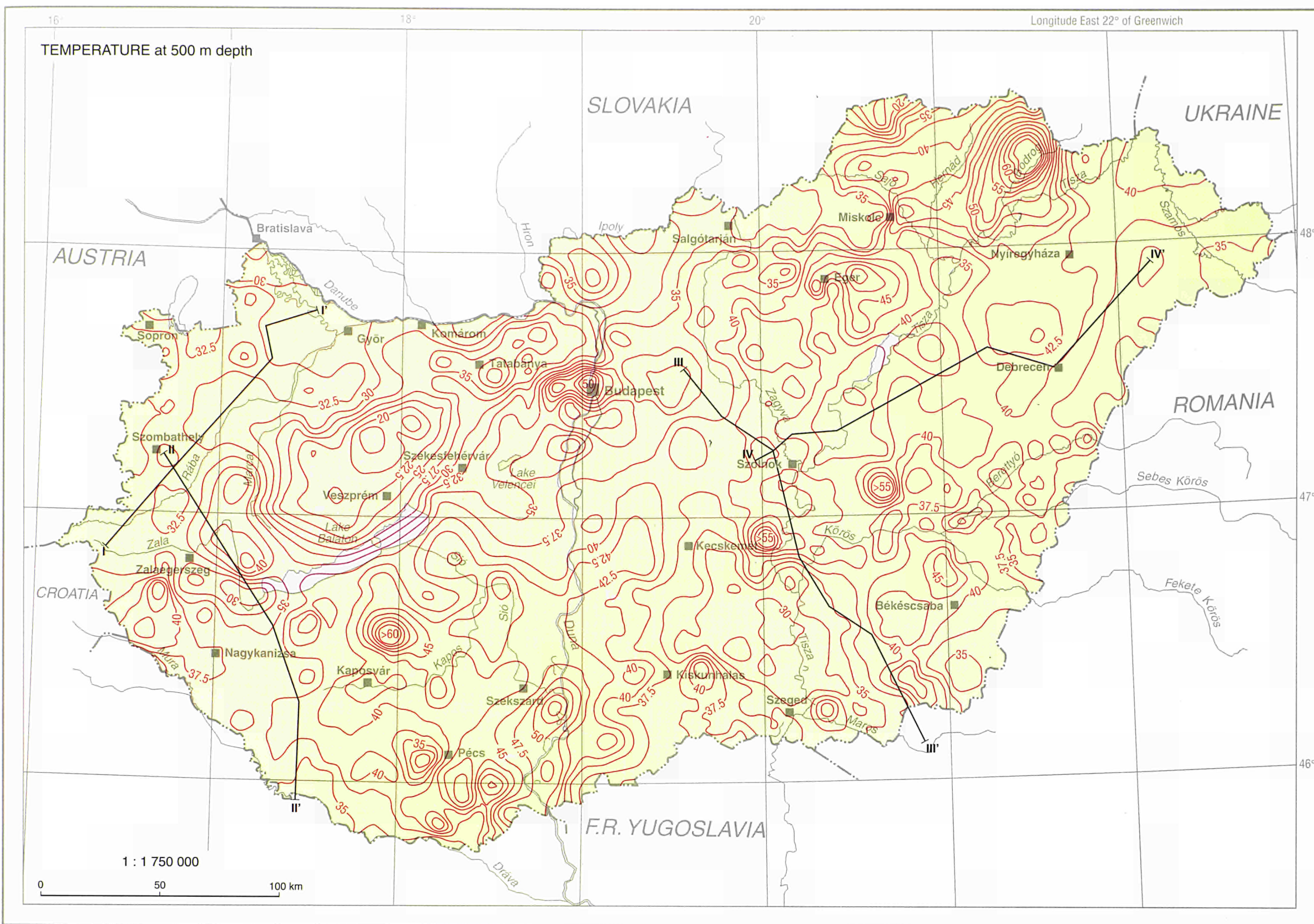




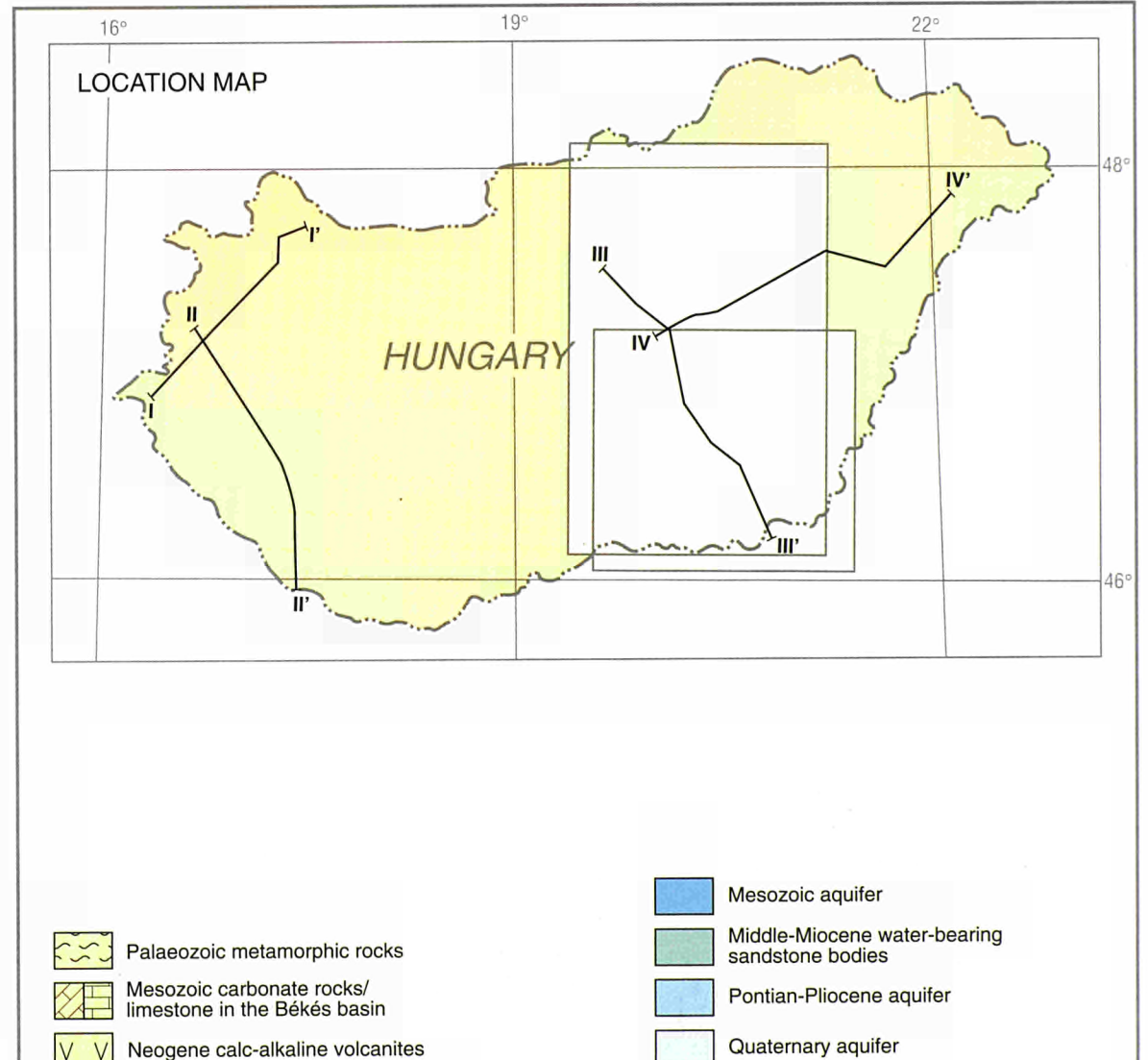
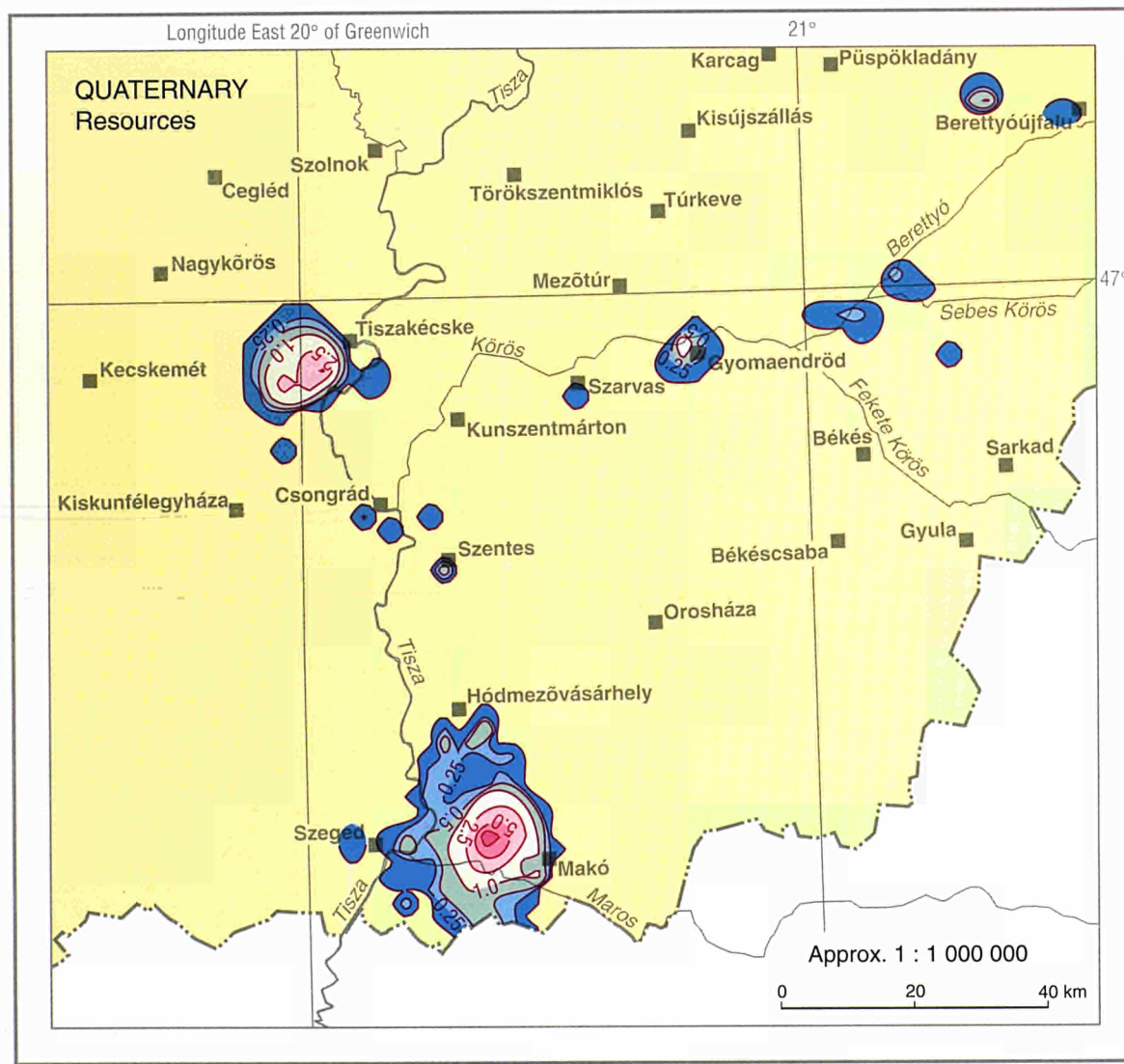
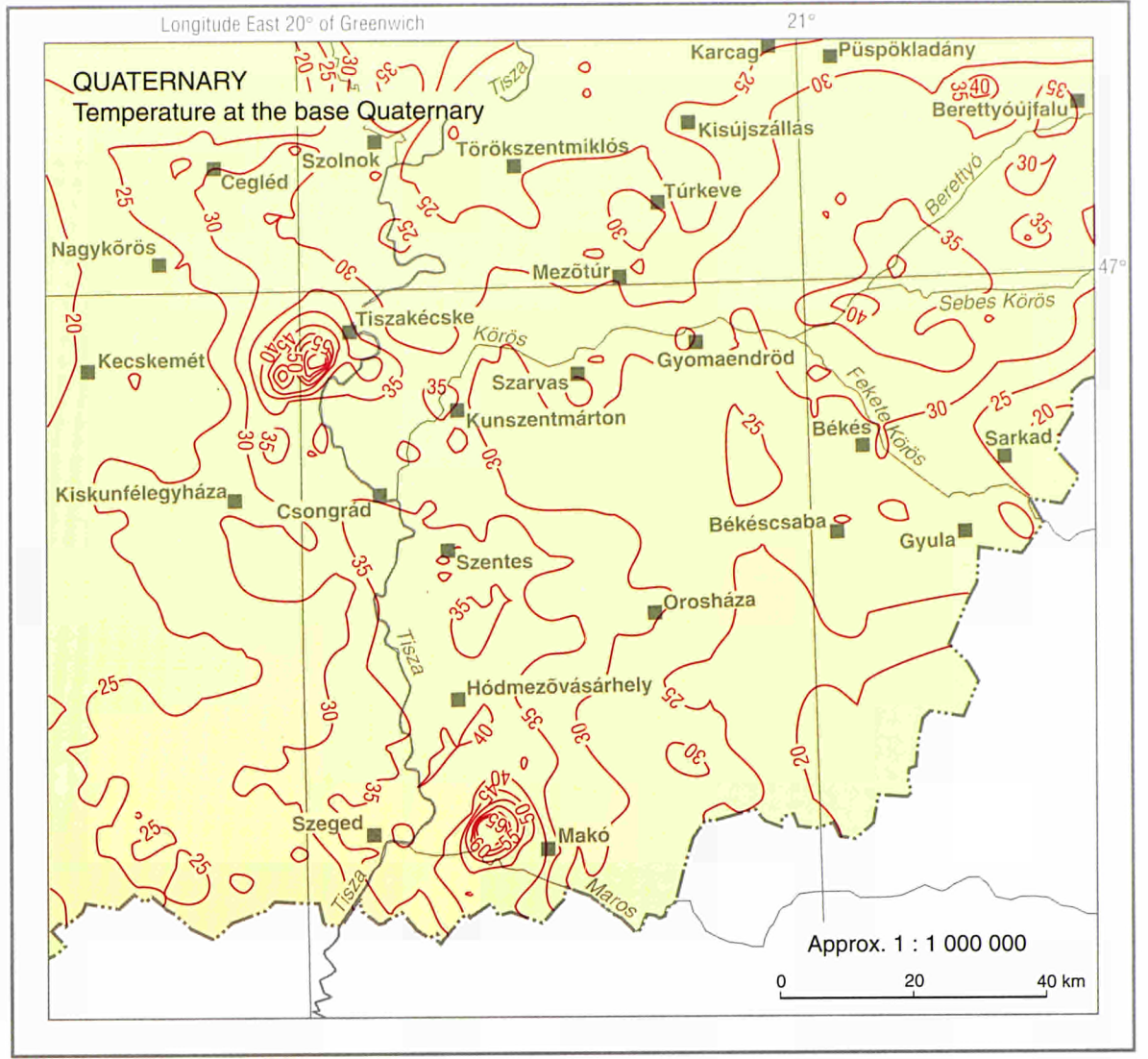
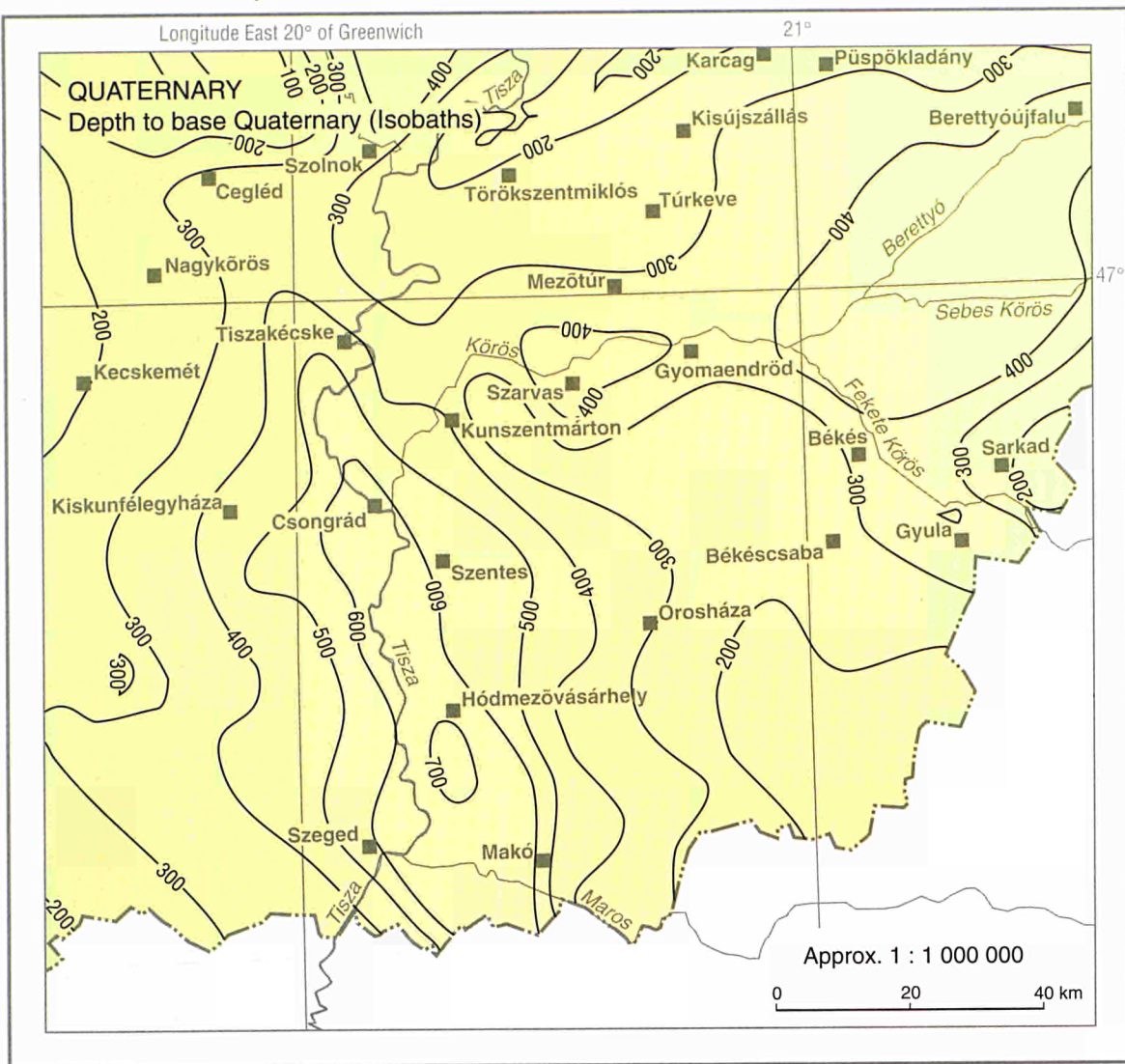


HUNGARY

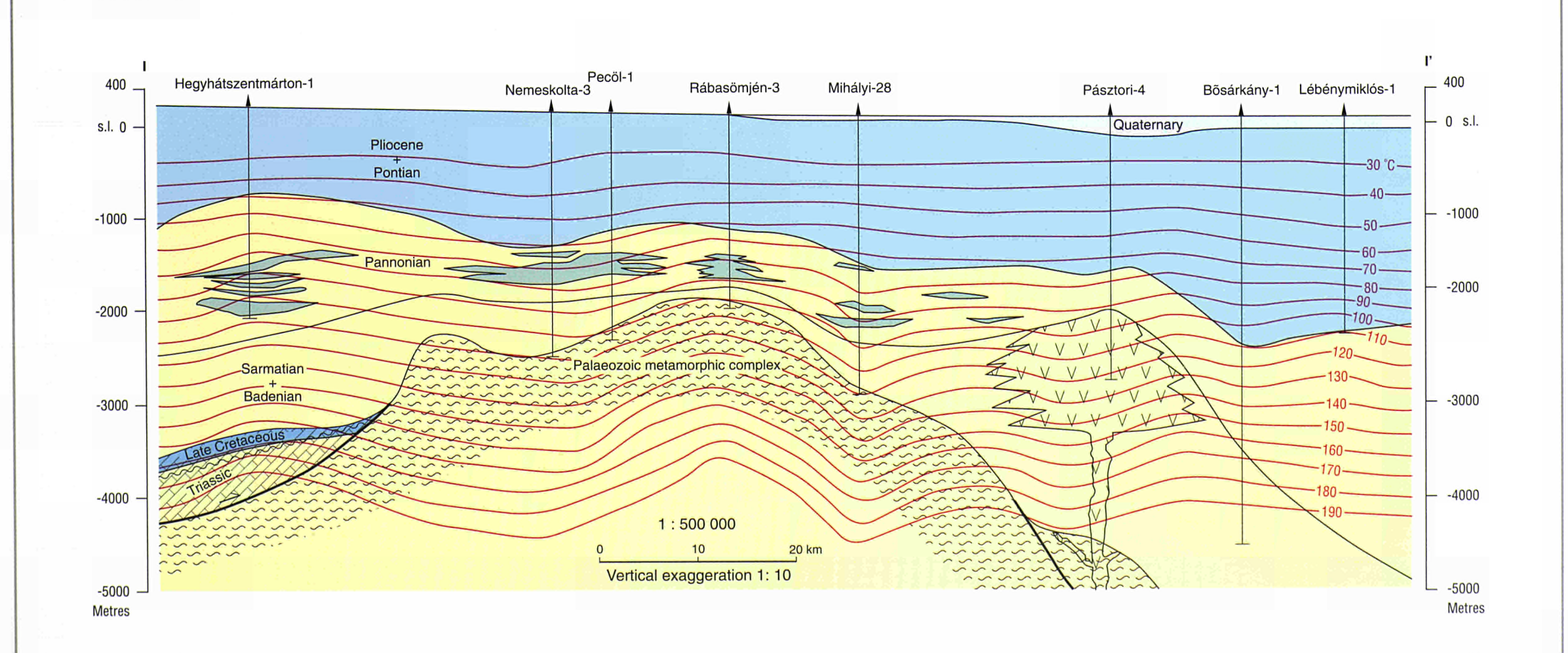


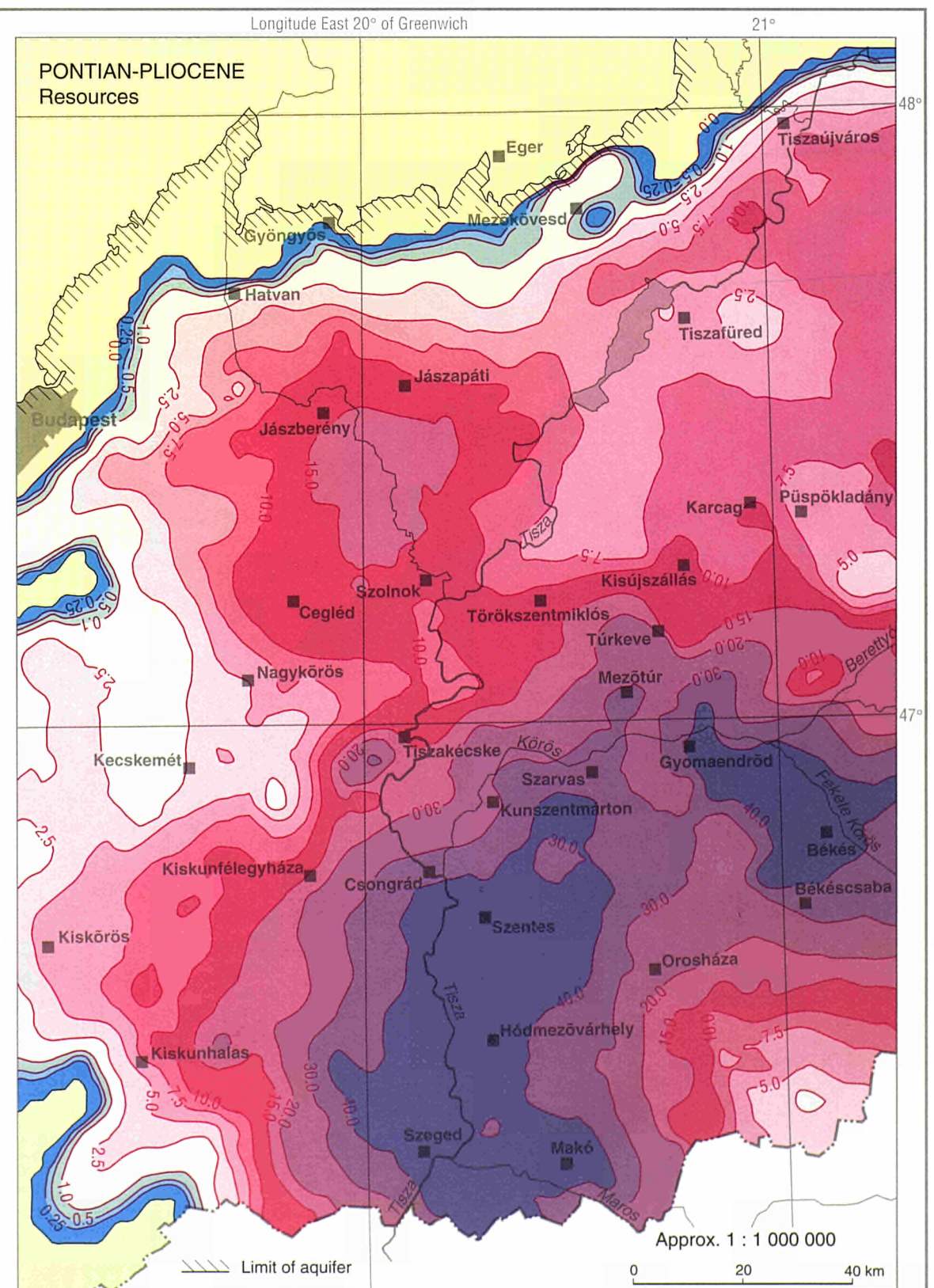
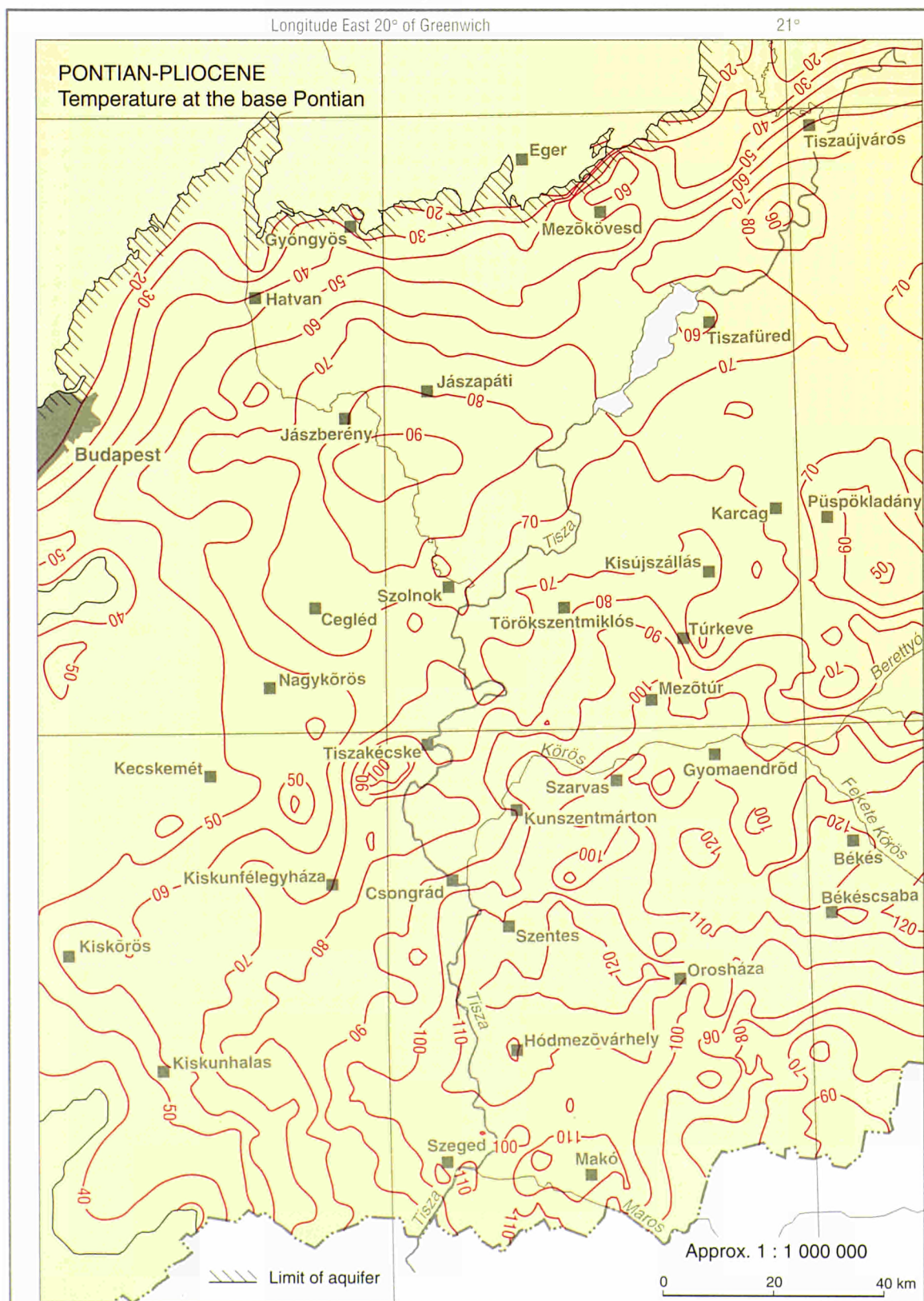
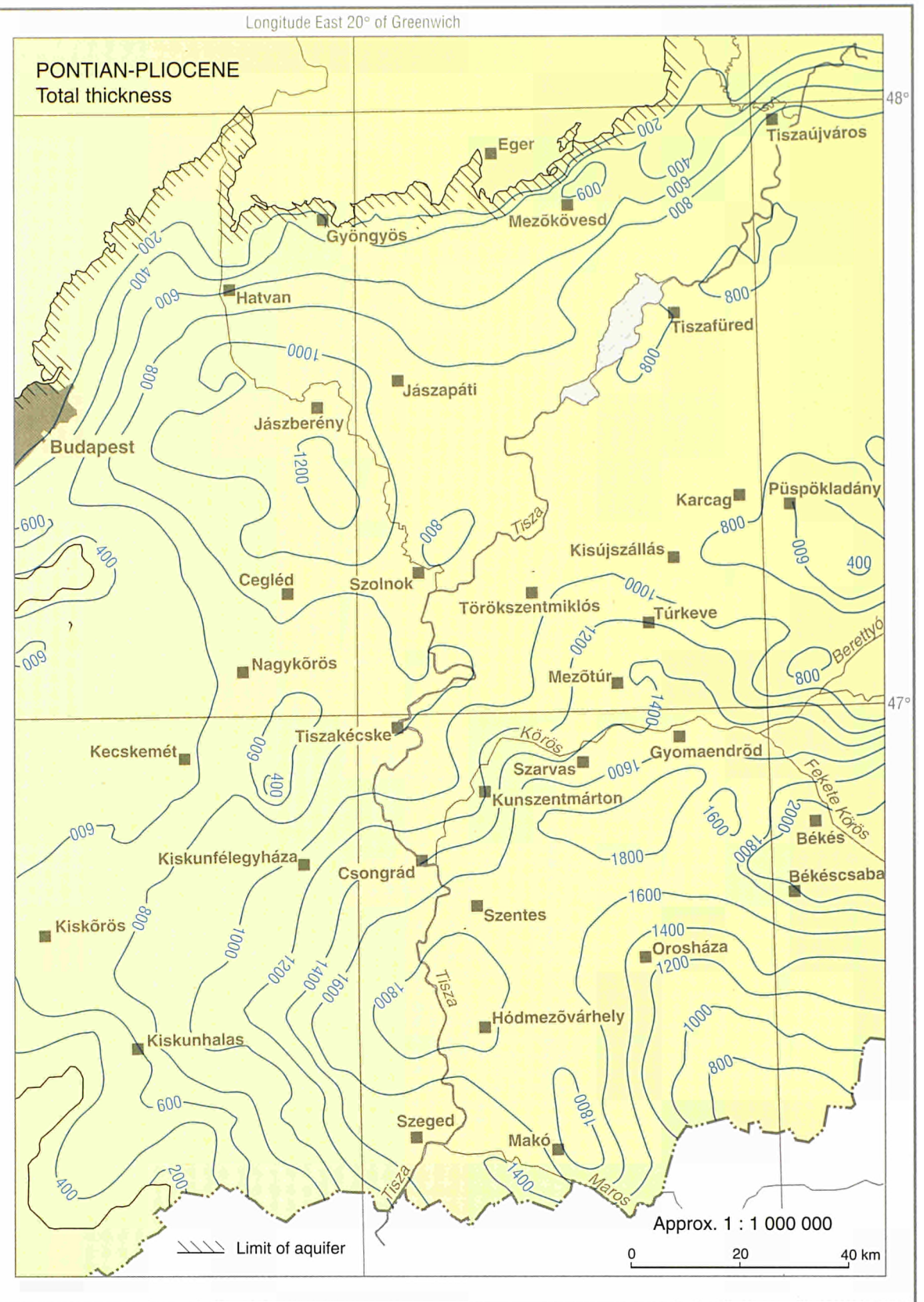
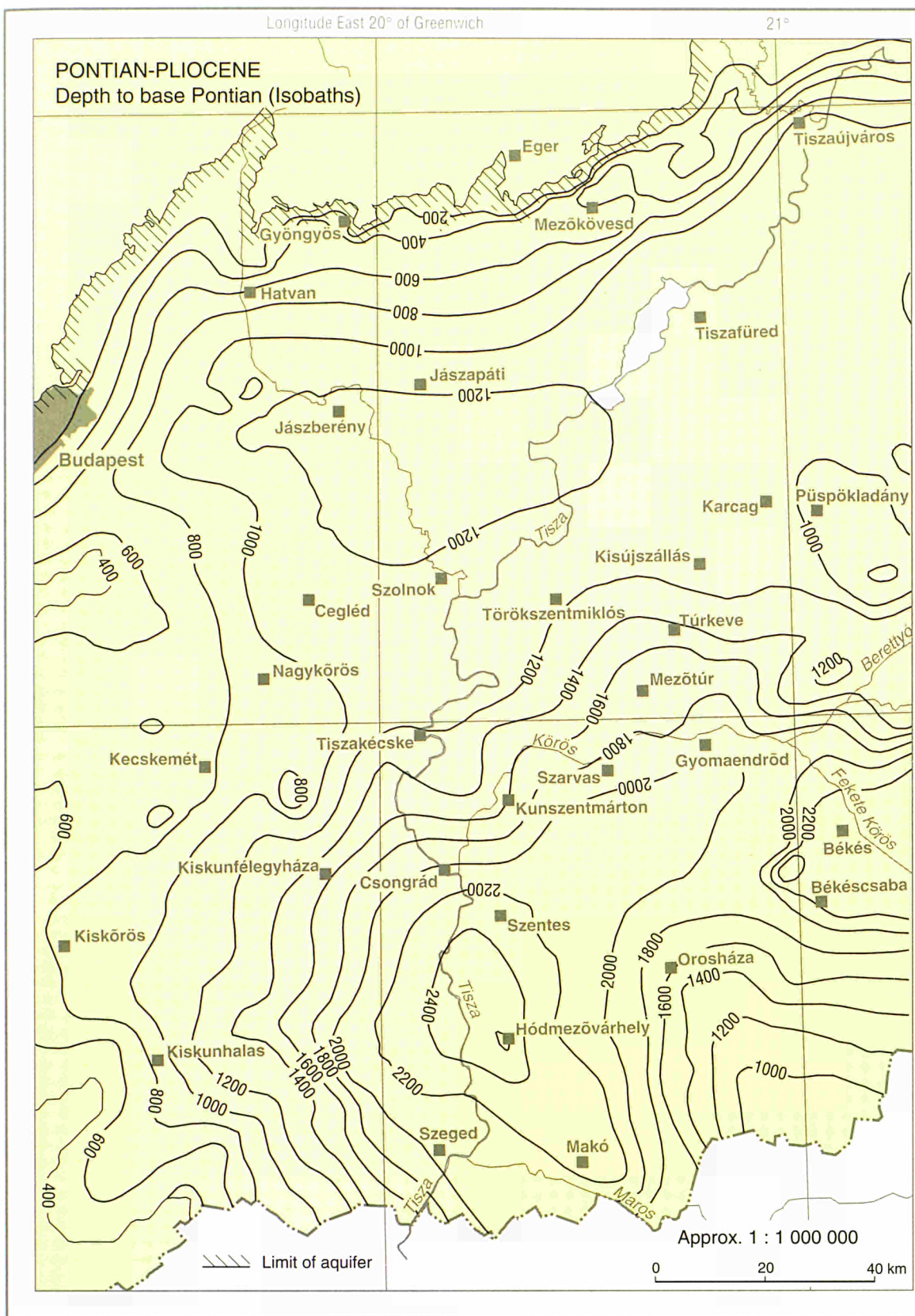


HUNGARY, Great Plain

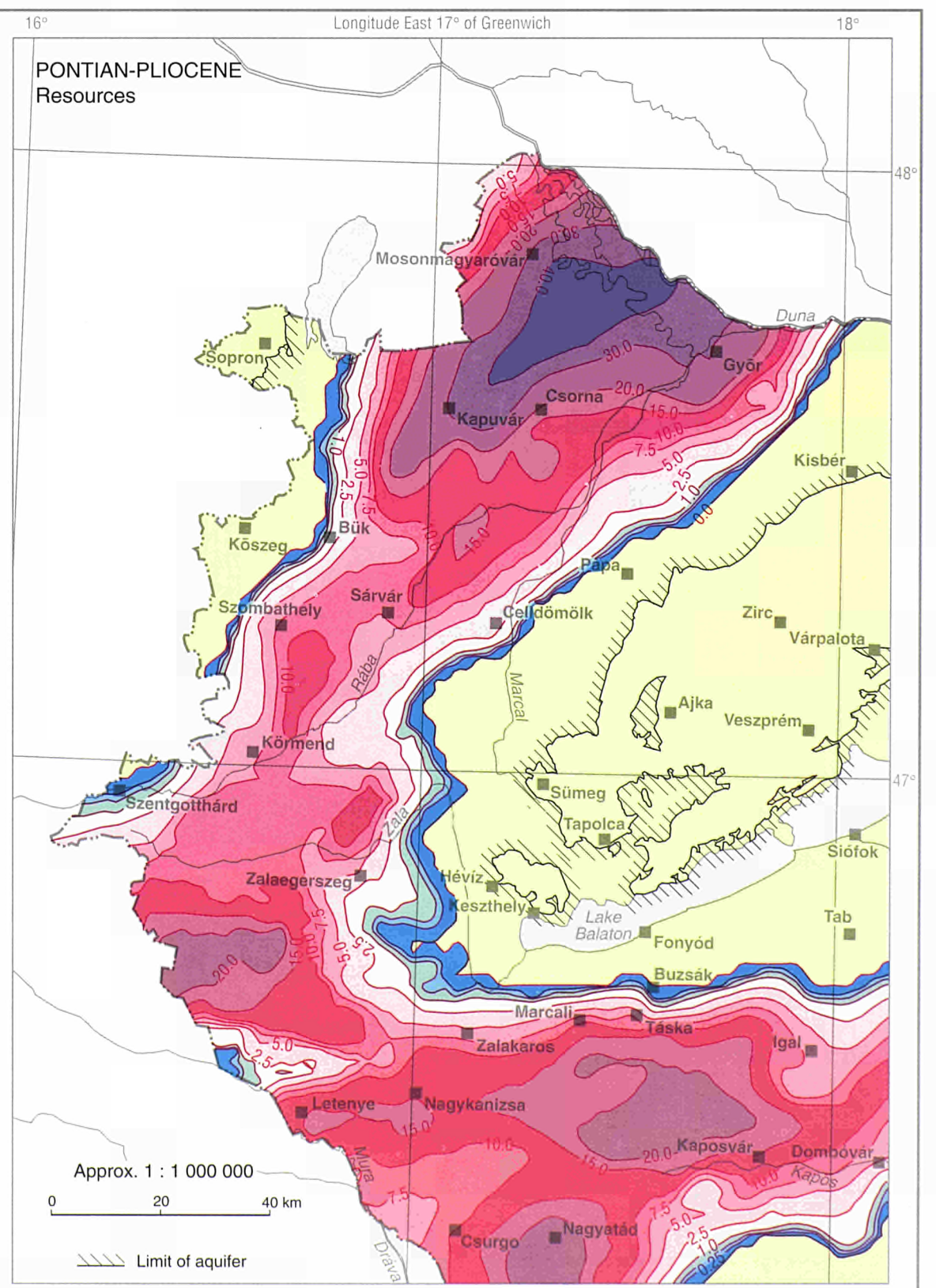
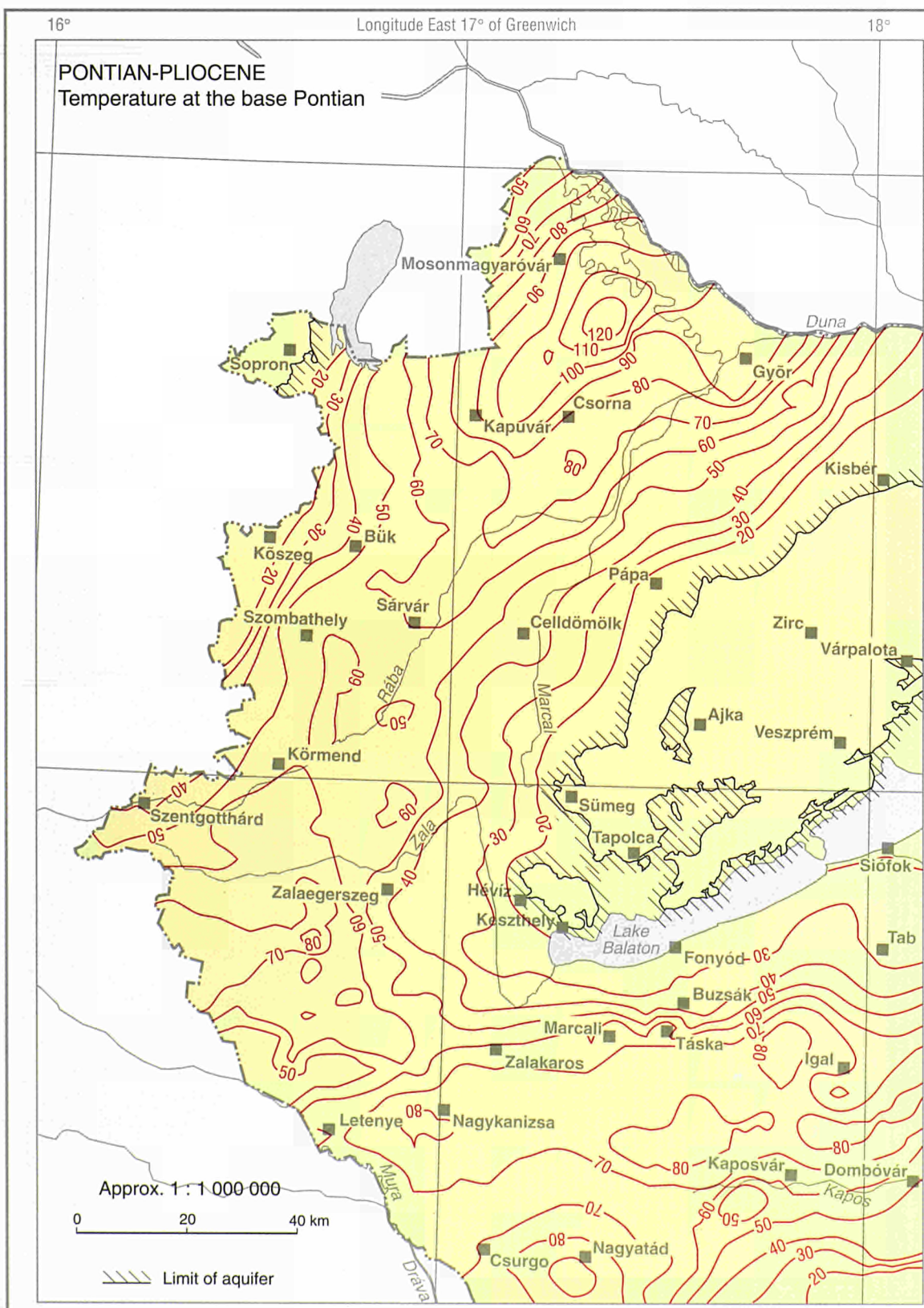
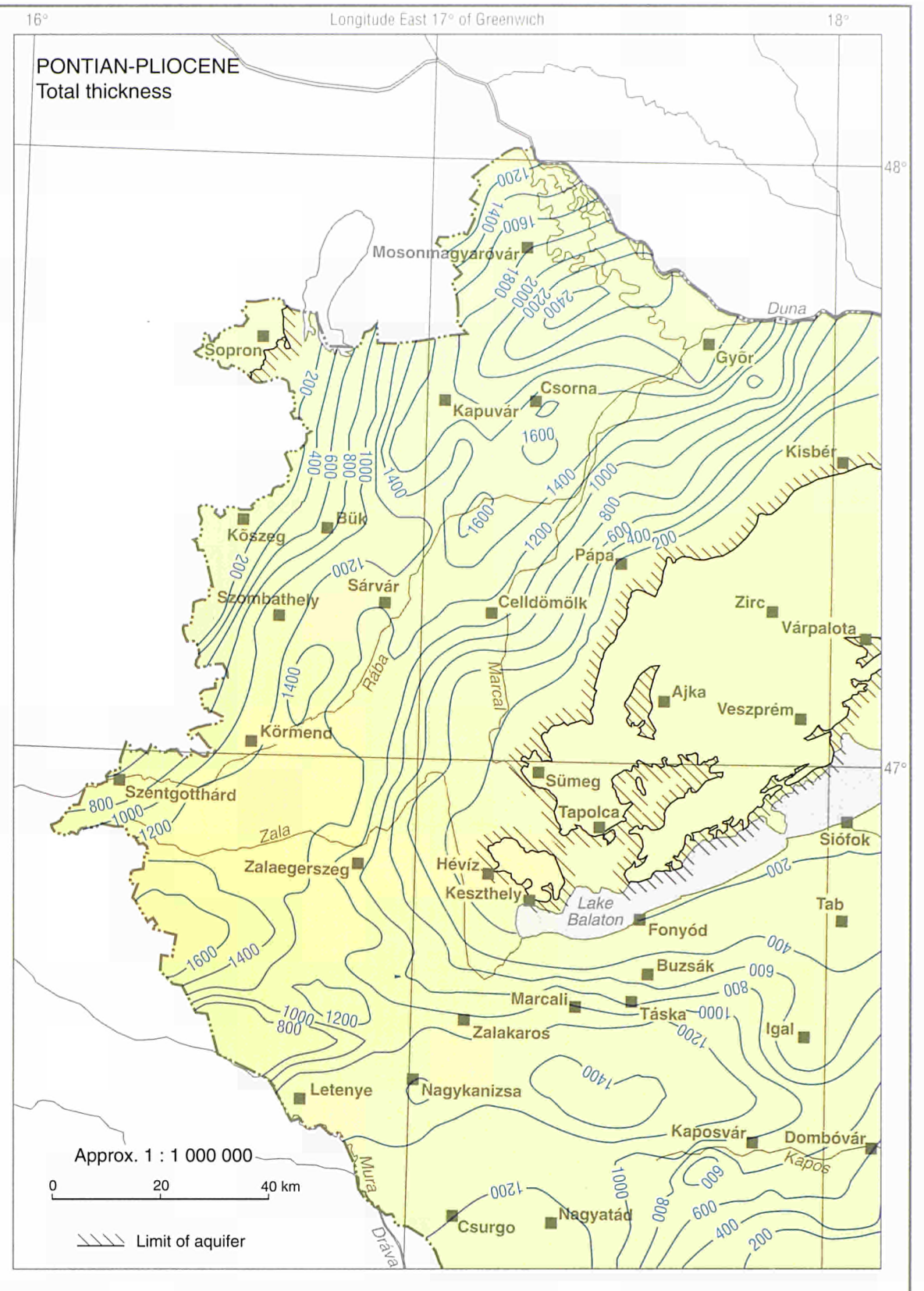
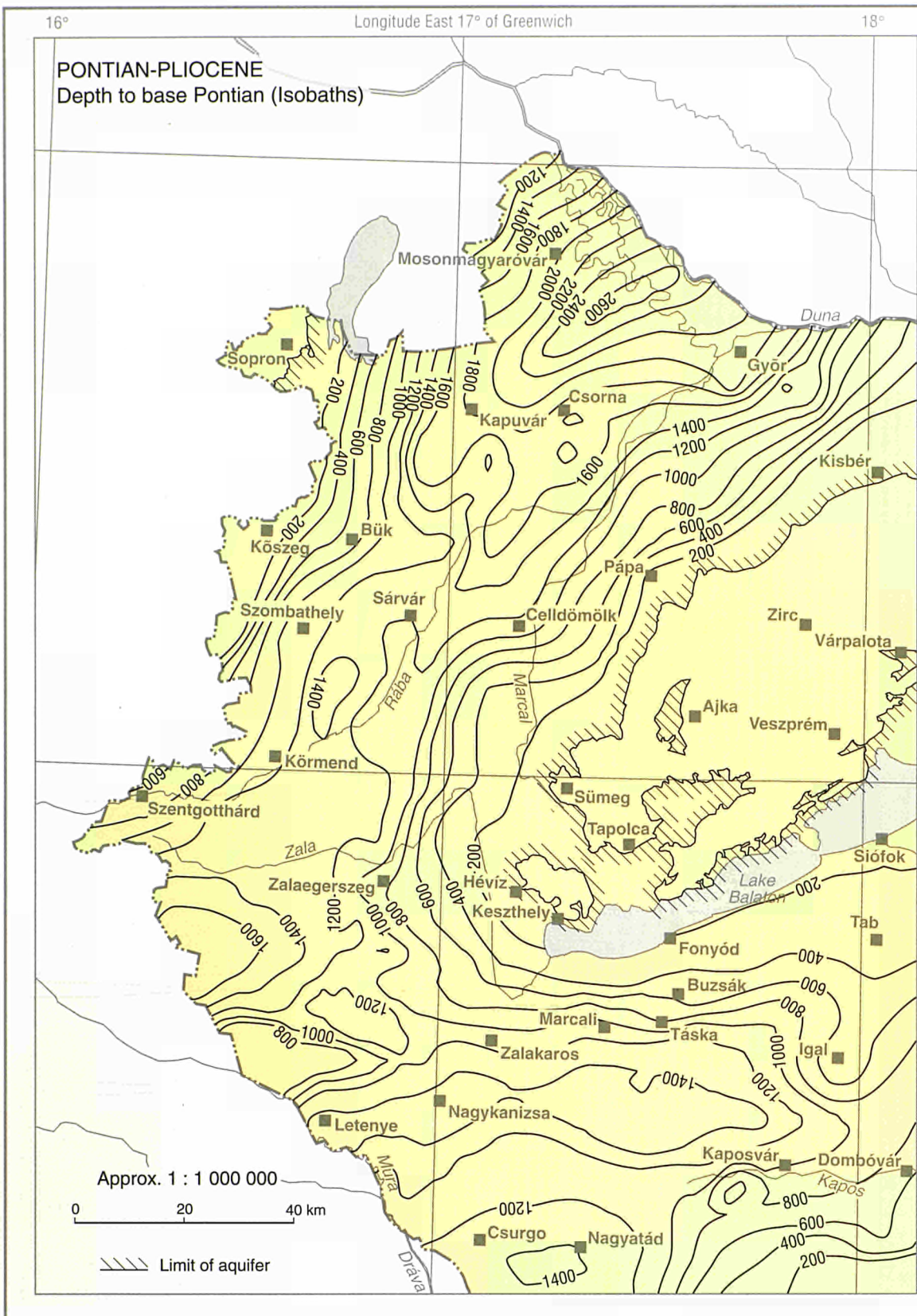


CROSS SECTION

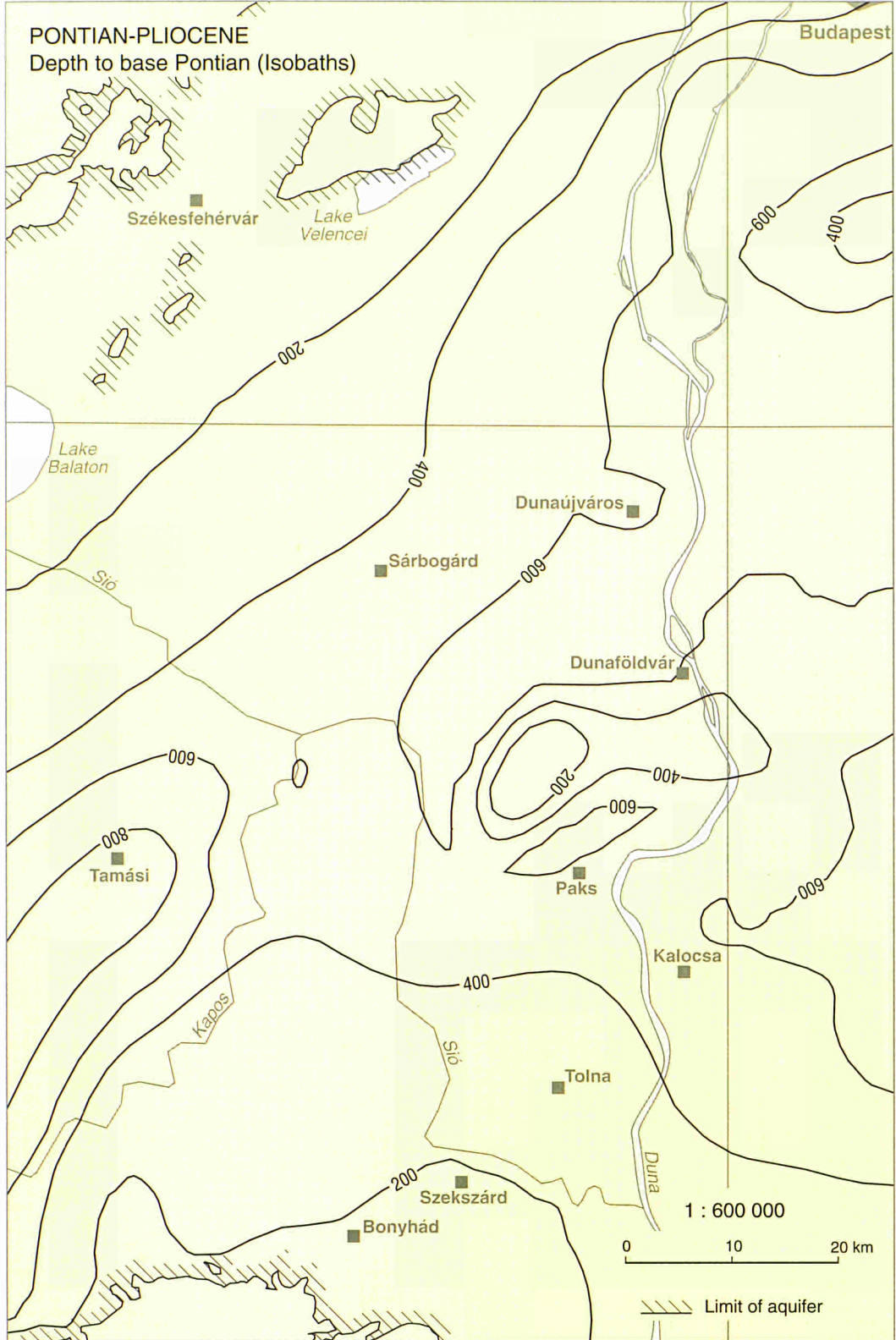




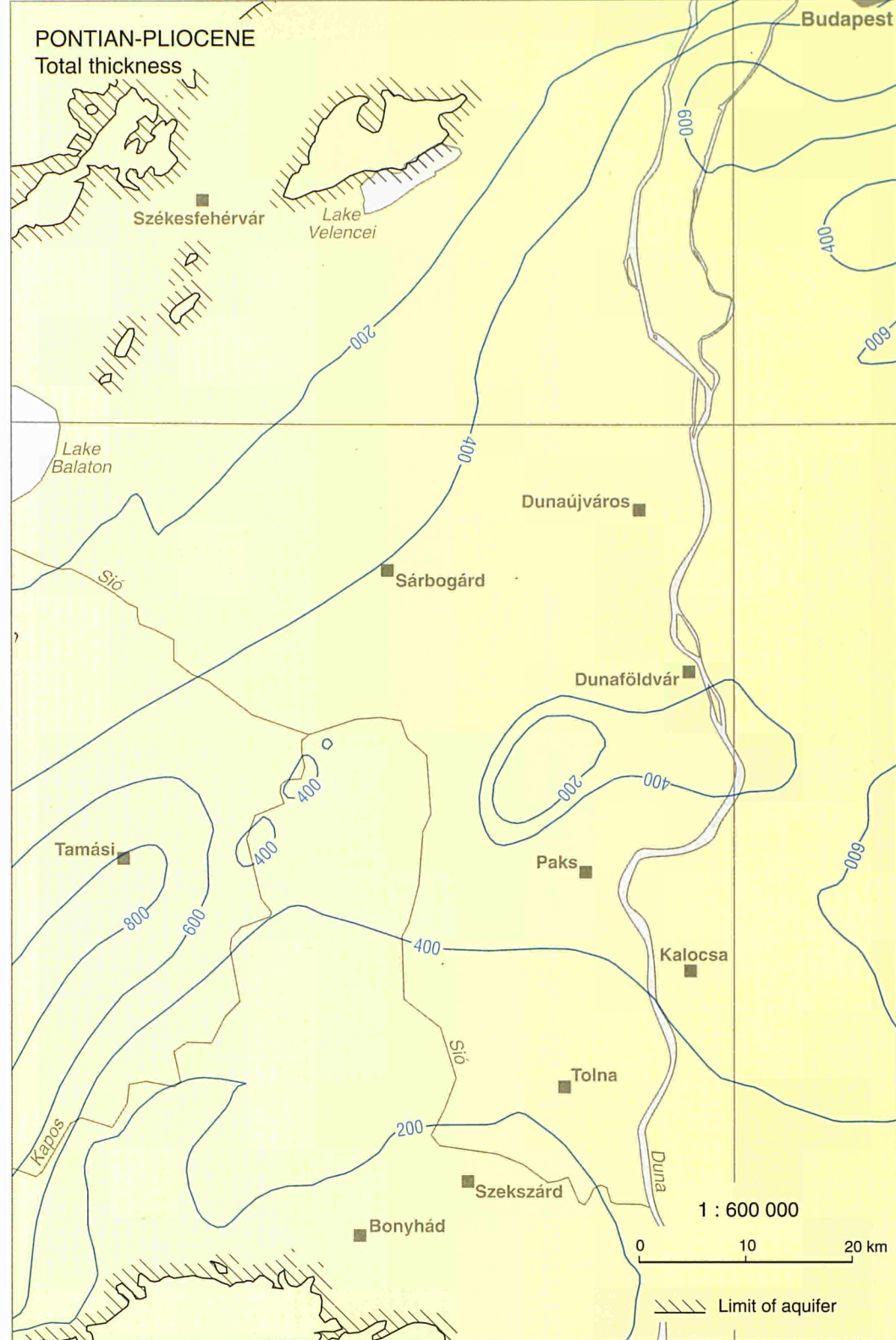
HUNGARY



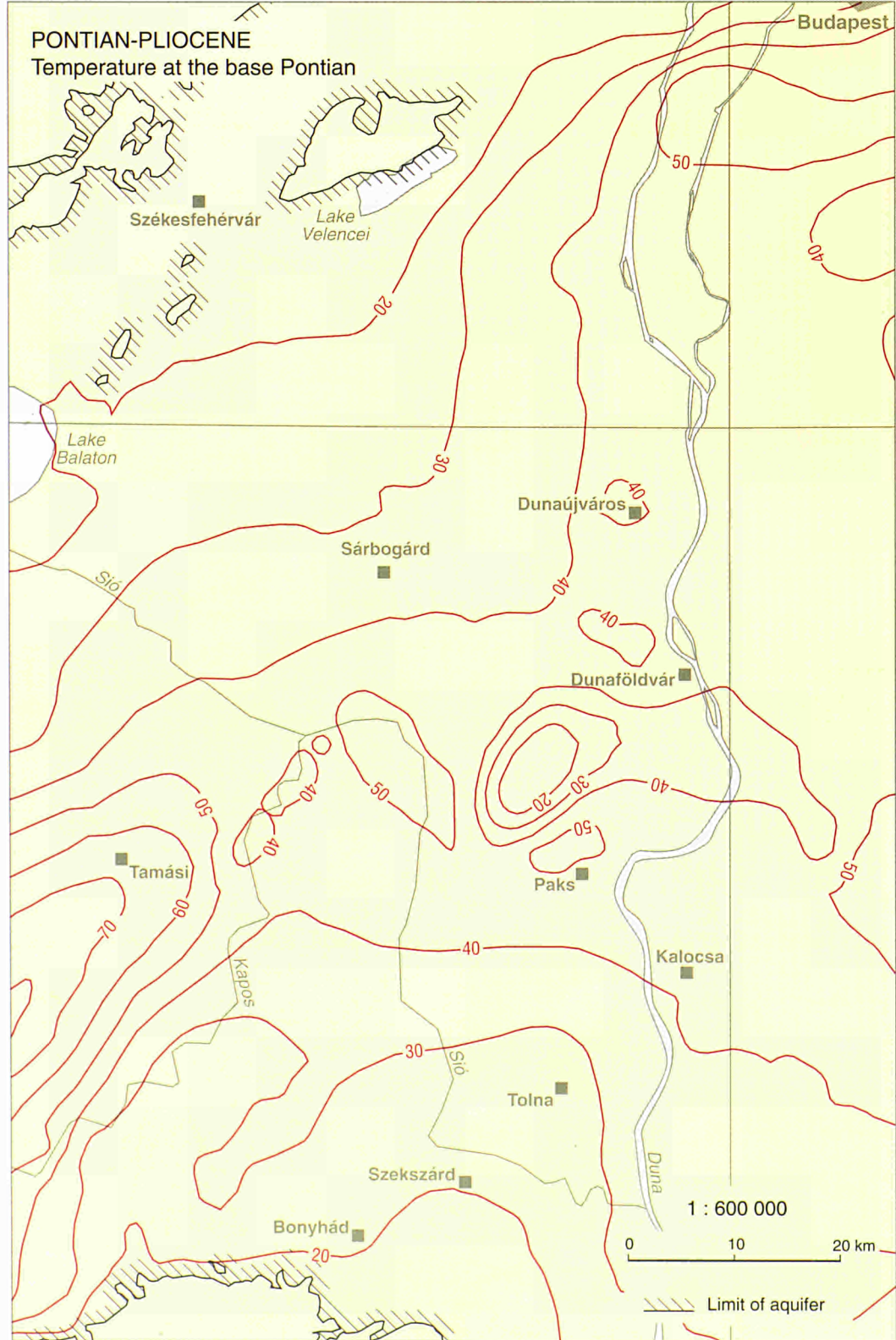
Longitude East 19° of Greenwich



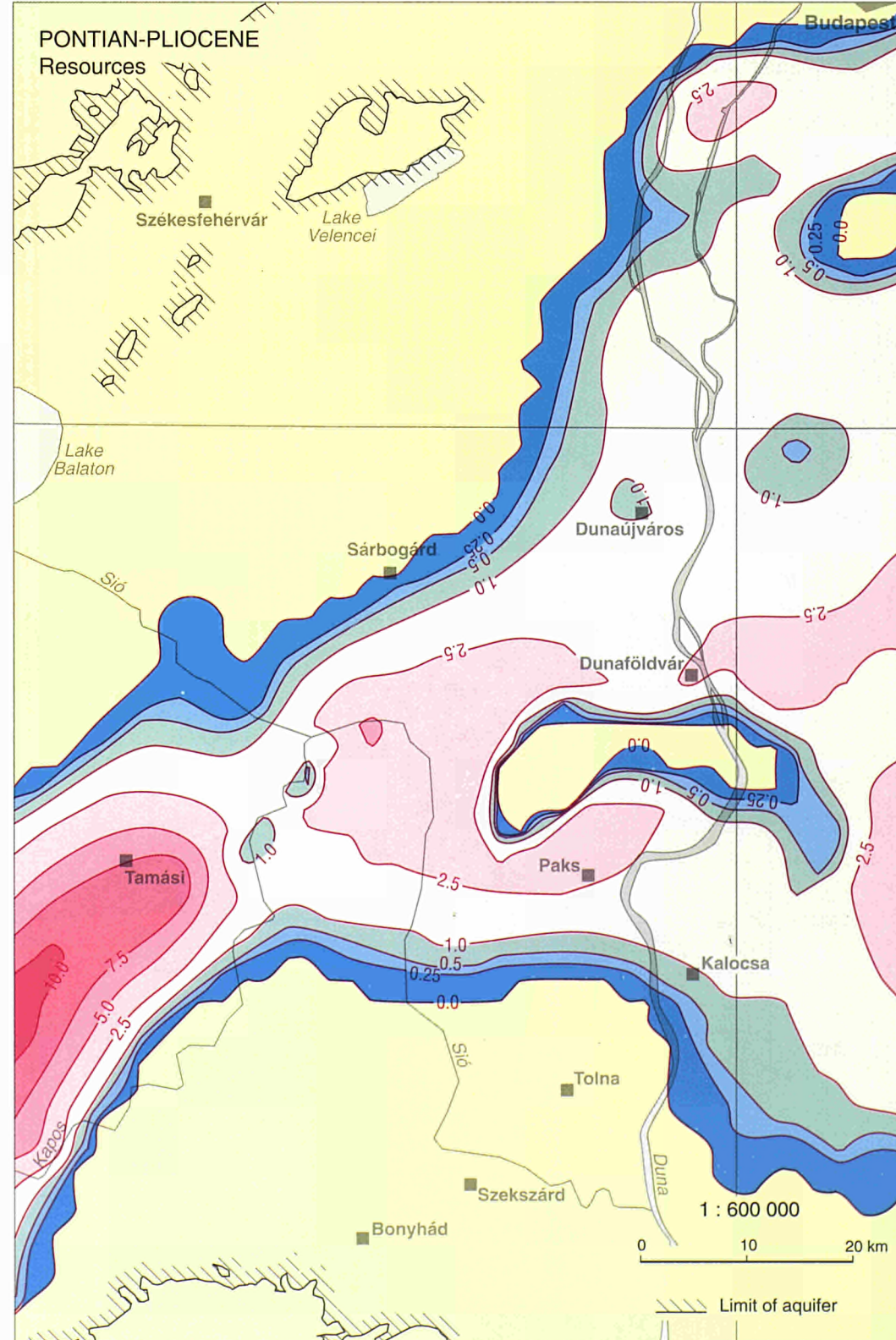
Longitude East 19° of Greenwich

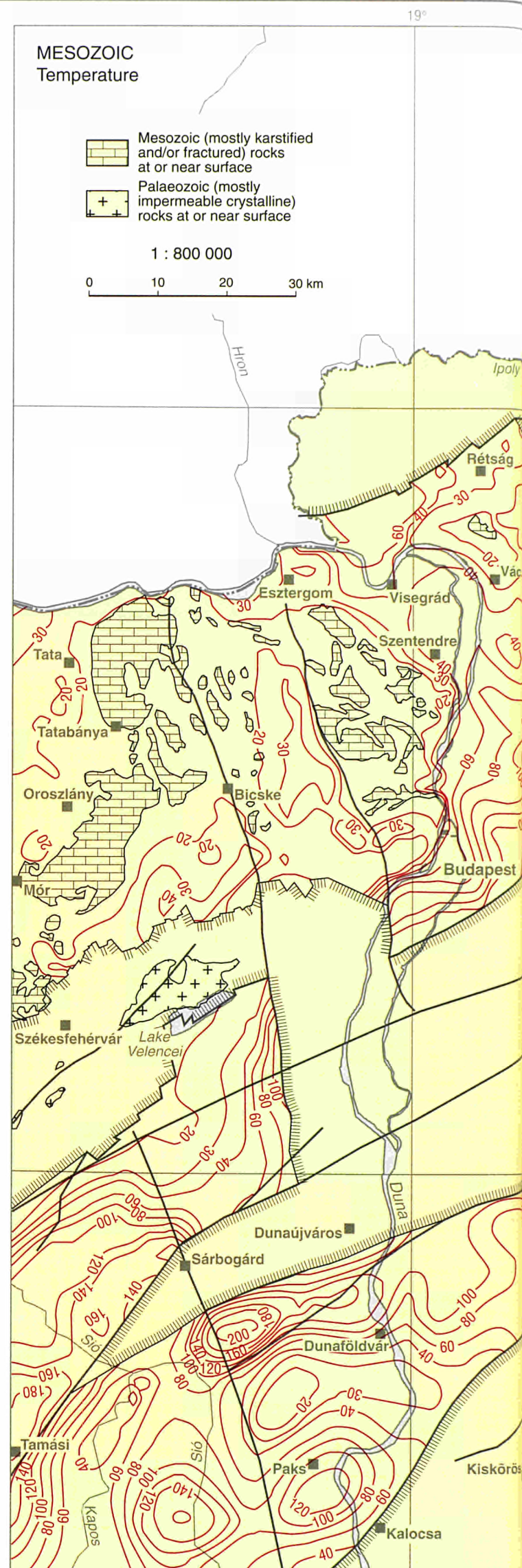
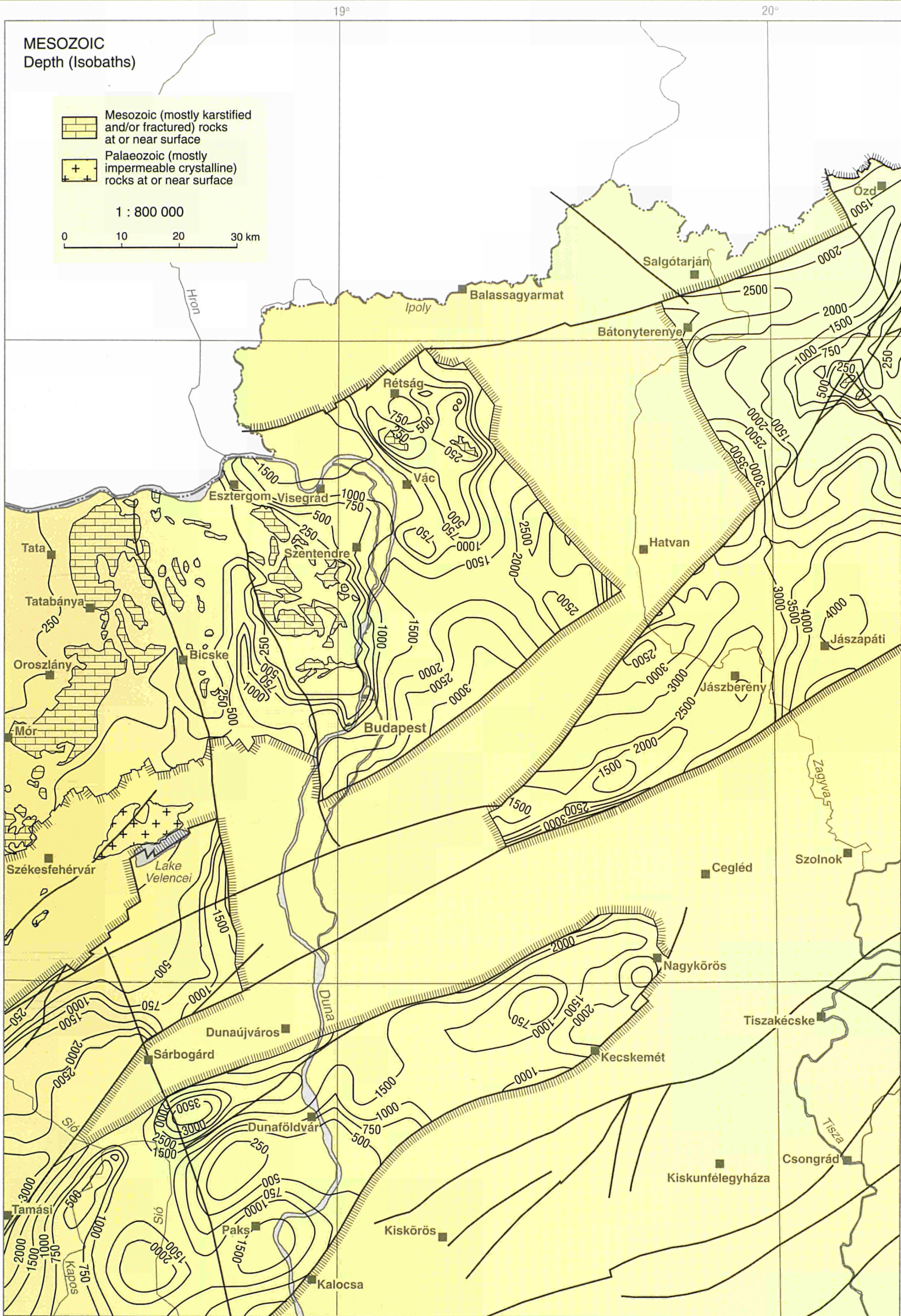


Longitude East 19° of Greenwich

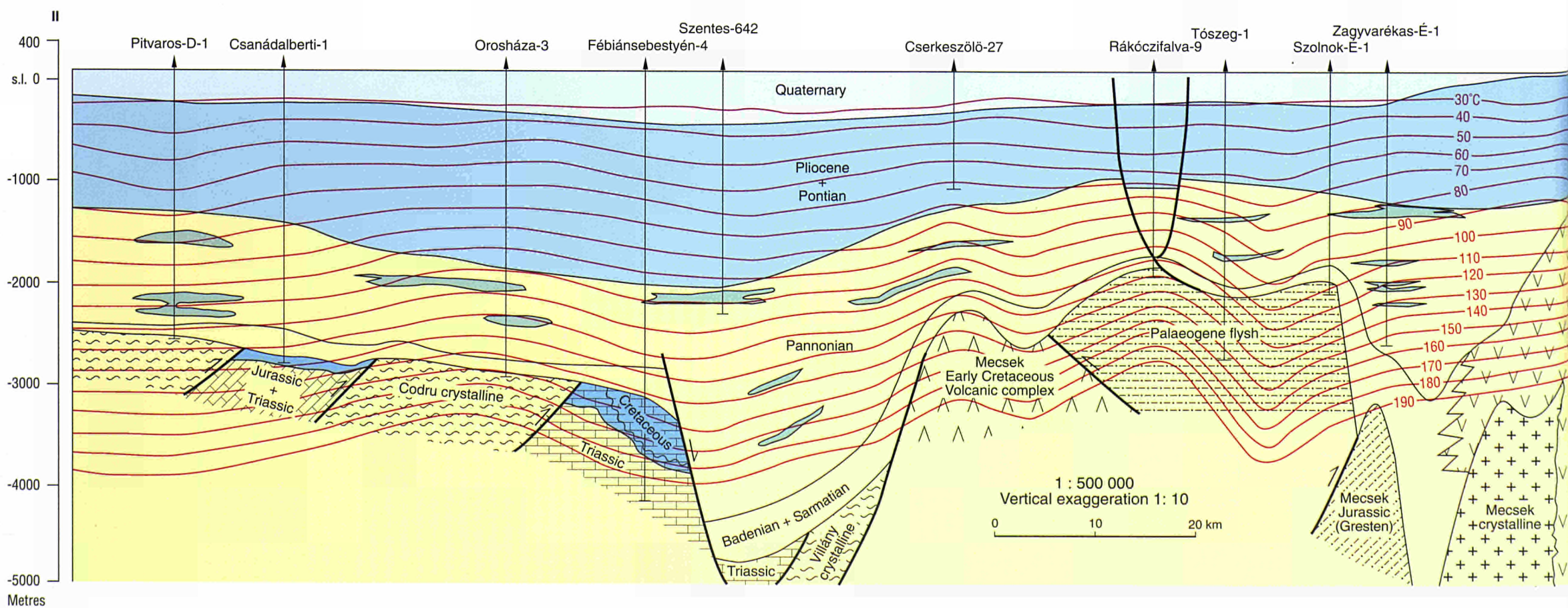


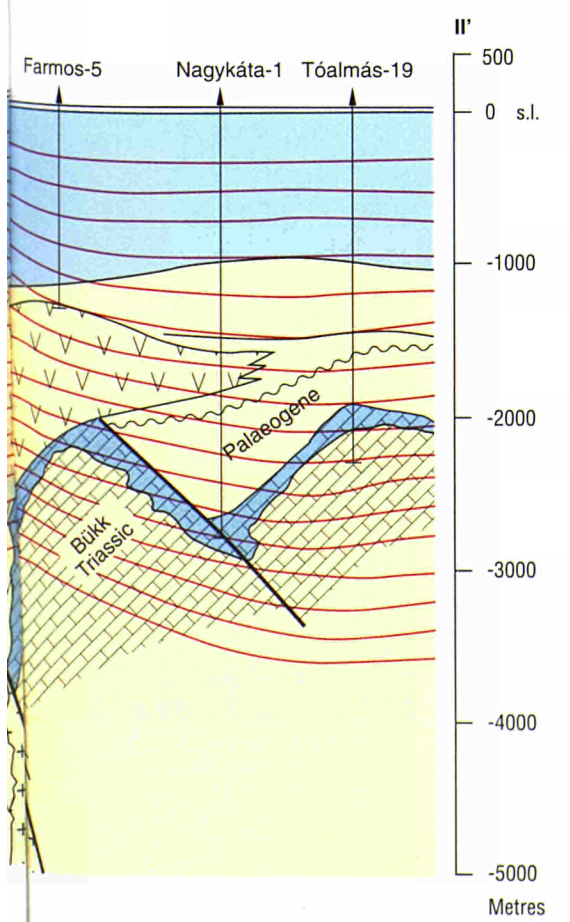
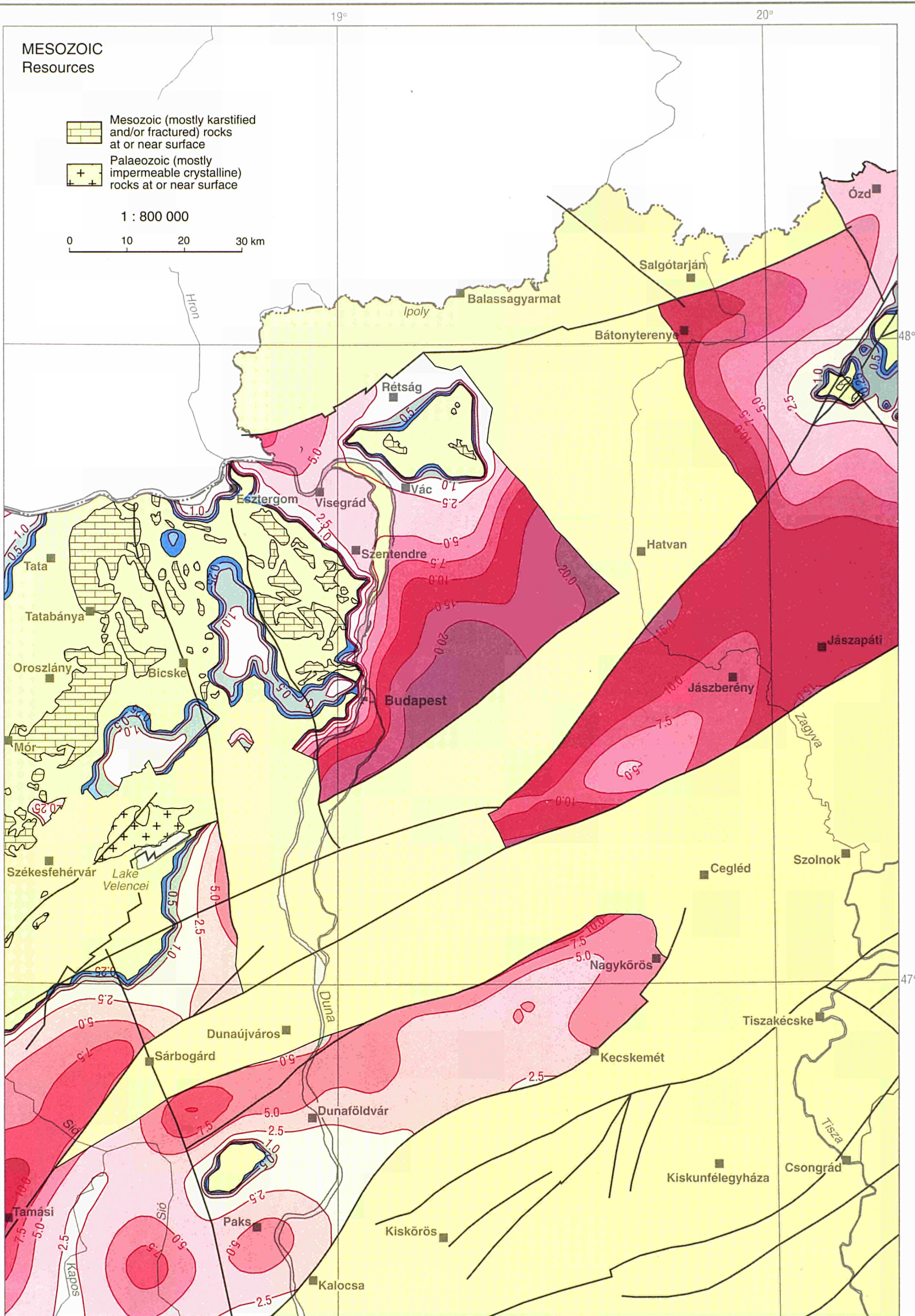
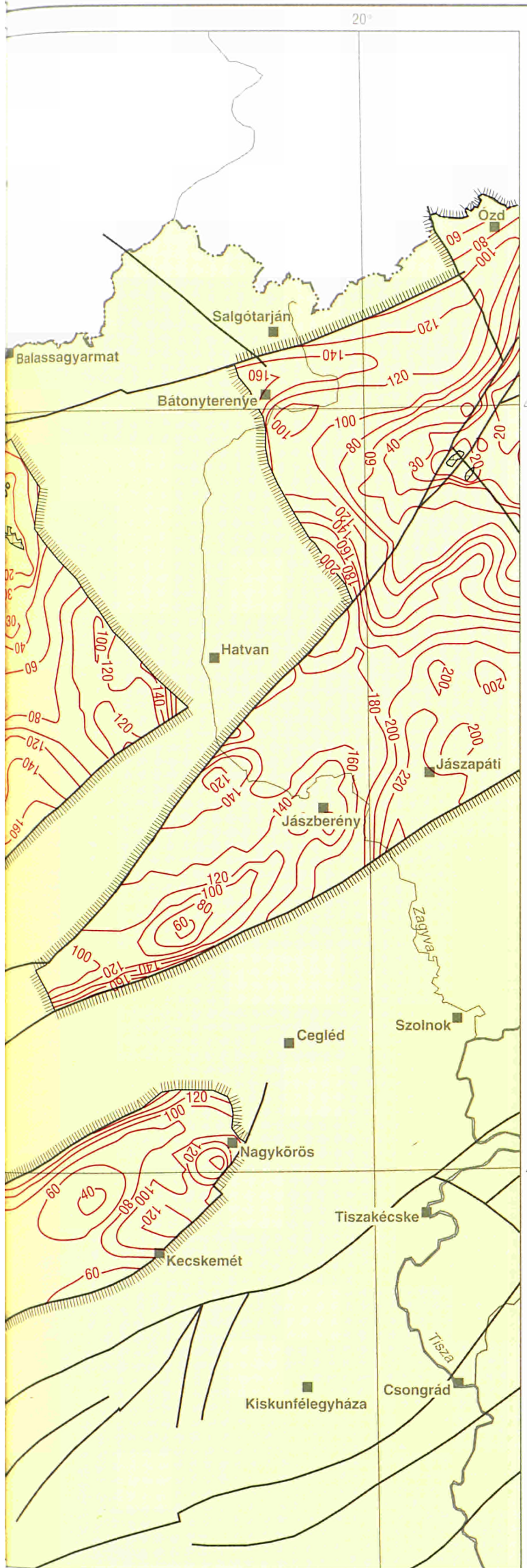
Longitude East 19° of Greenwich





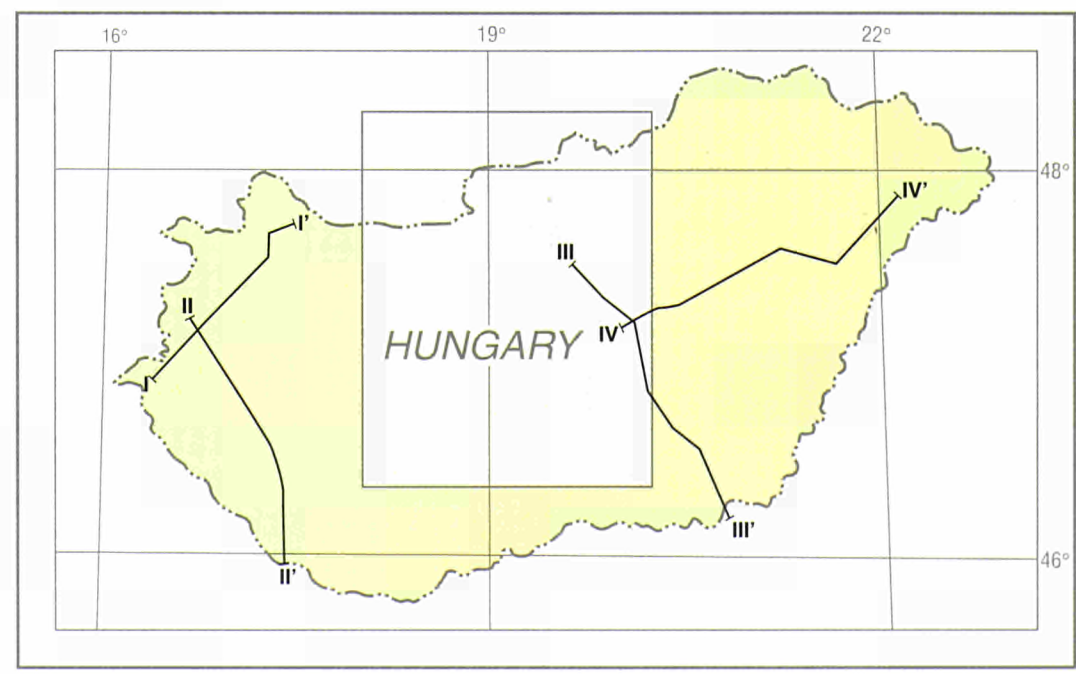
CROSS SECTION



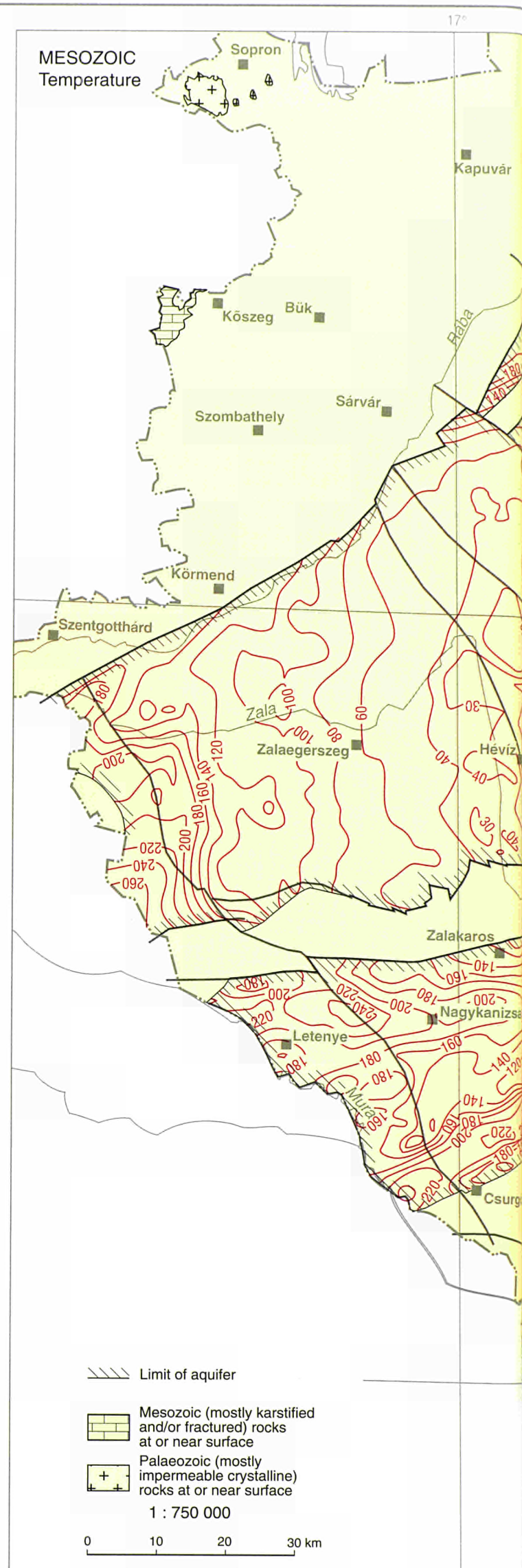
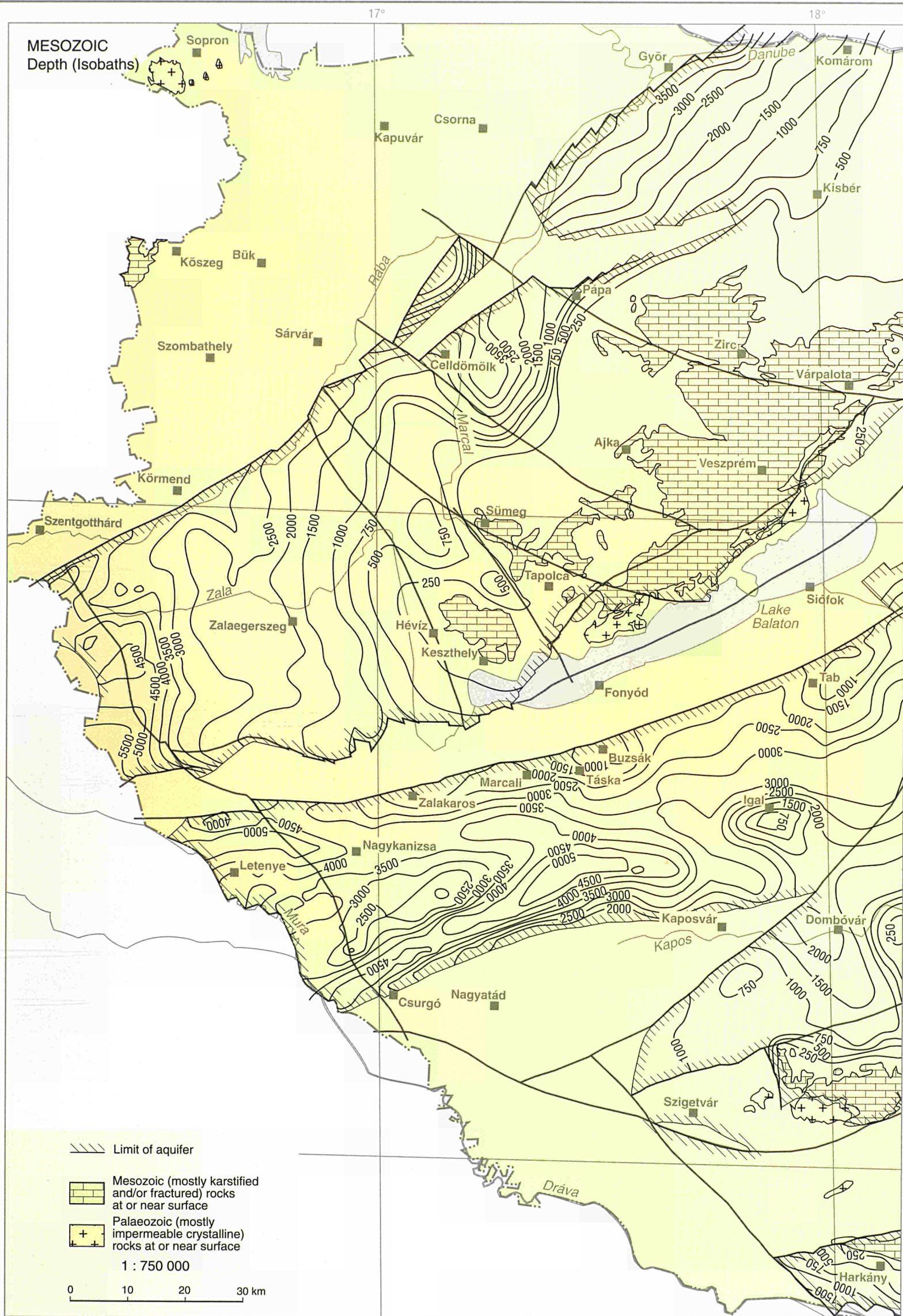


- Palaeozoic metamorphic rocks
- Palaeozoic granitoids
- Mesozoic carbonate rocks/limestone in the Békés basin
- Early Jurassic clastic sediments
- Early Cretaceous mafic magmatites
- Palaeogene flysch
- Neogene calc-alkaline volcanites
- Mesozoic aquifer
- Middle-Miocene water-bearing sandstone bodies
- Pontian-Pliocene aquifer
- Quaternary aquifer

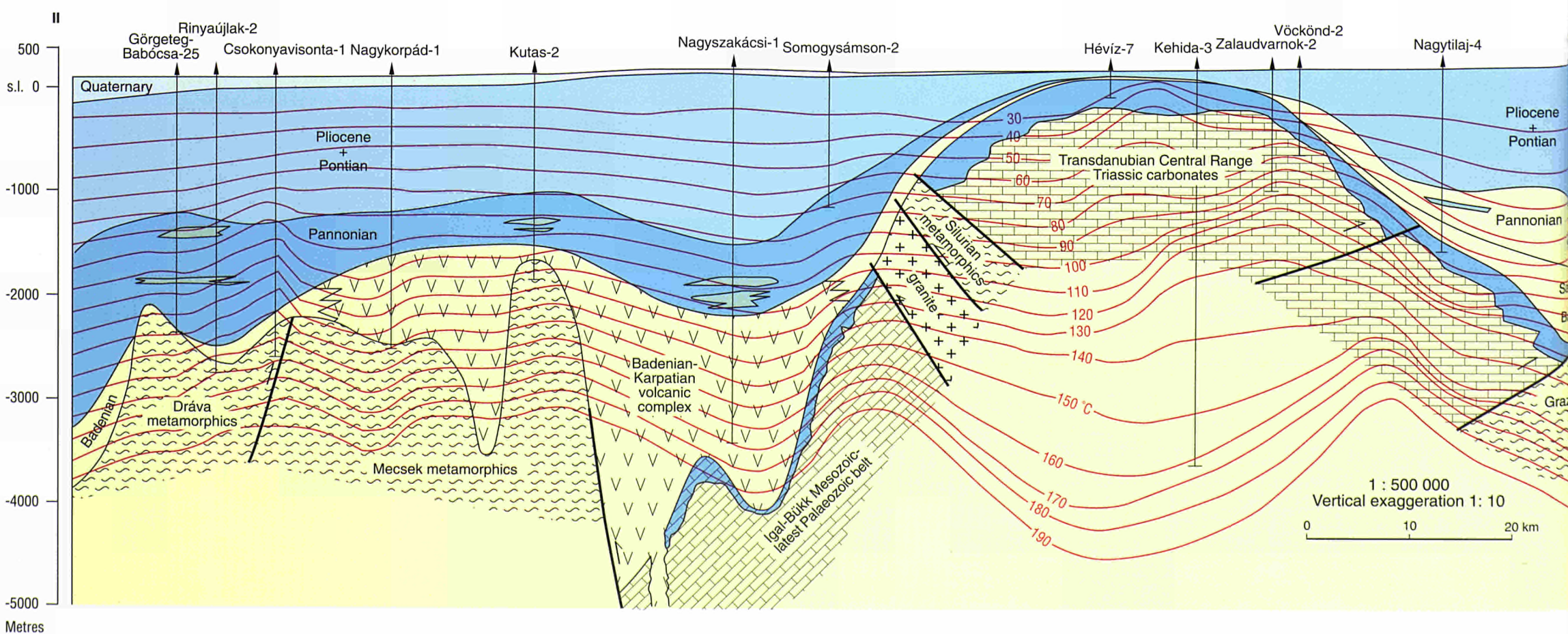
LOCATION MAP

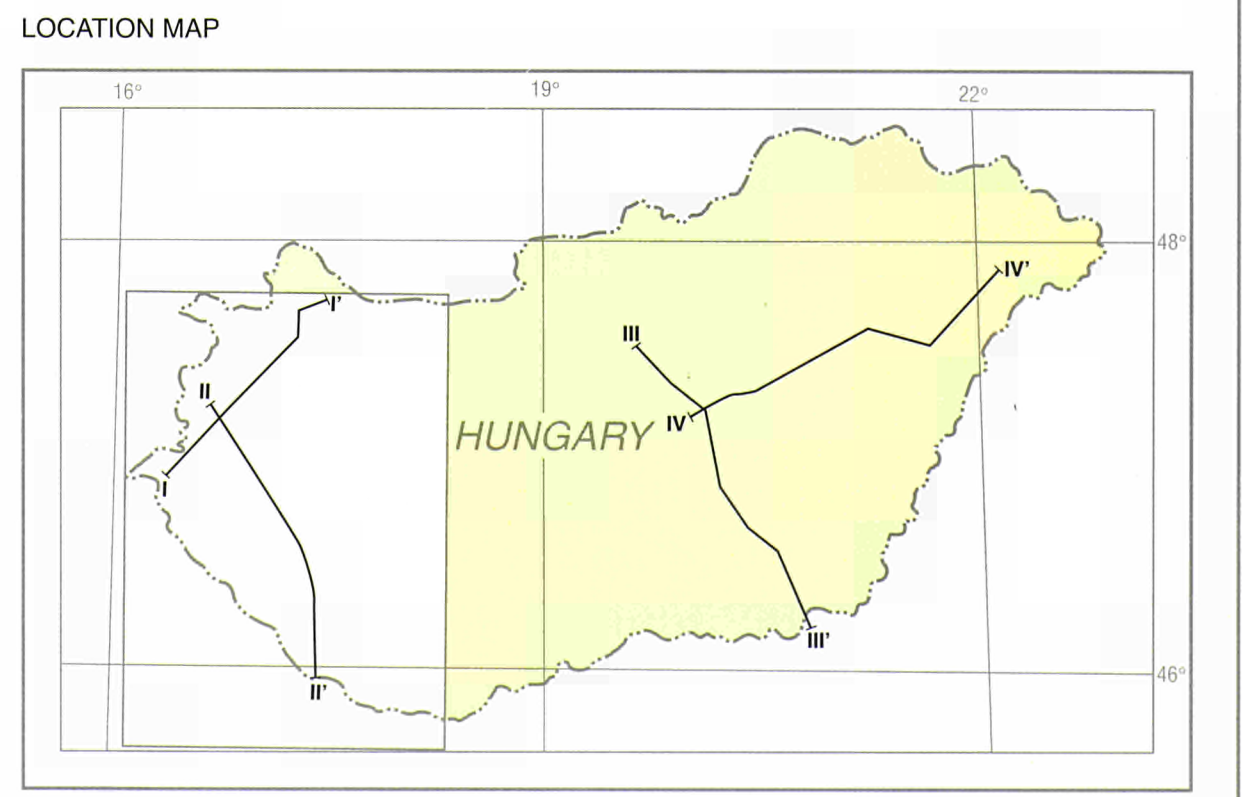
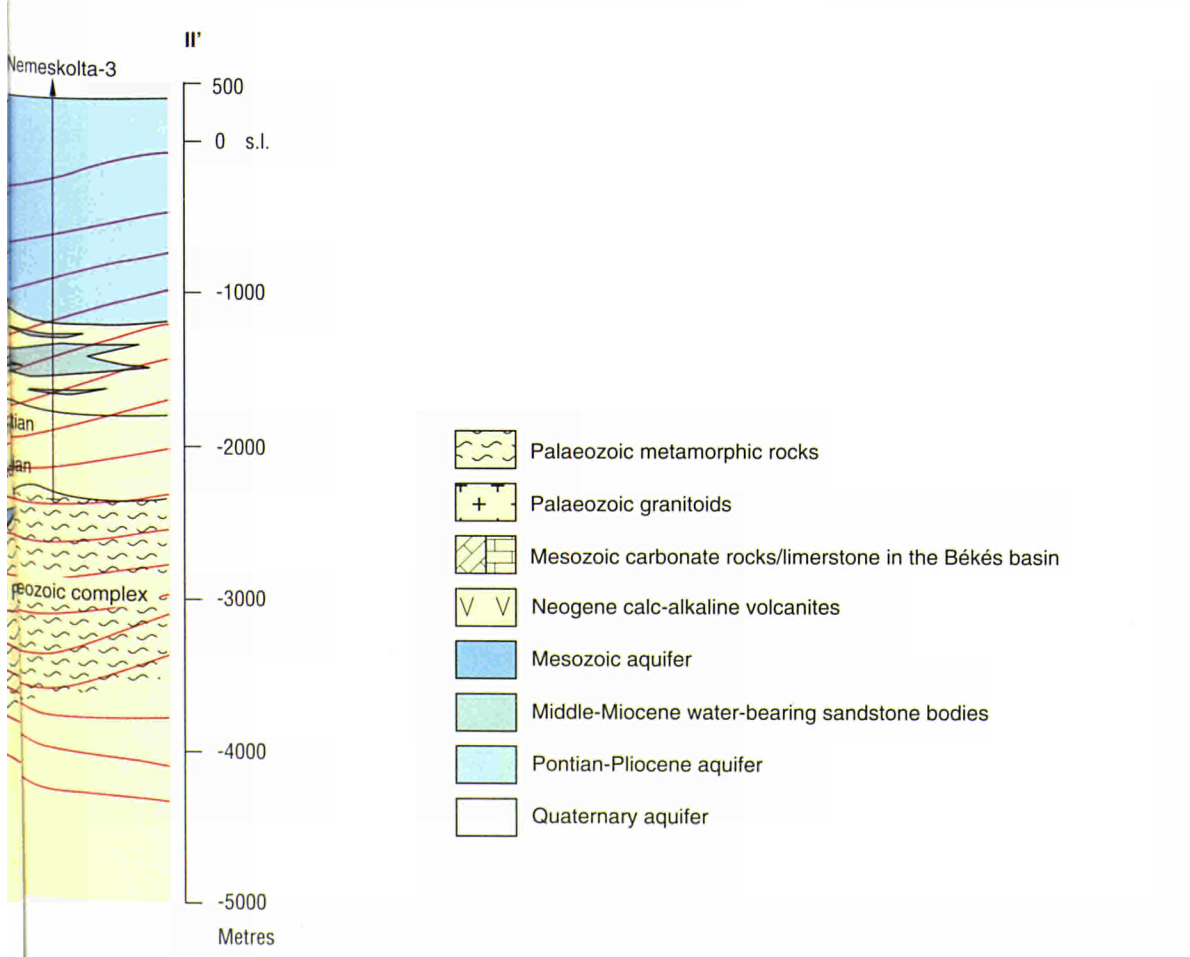
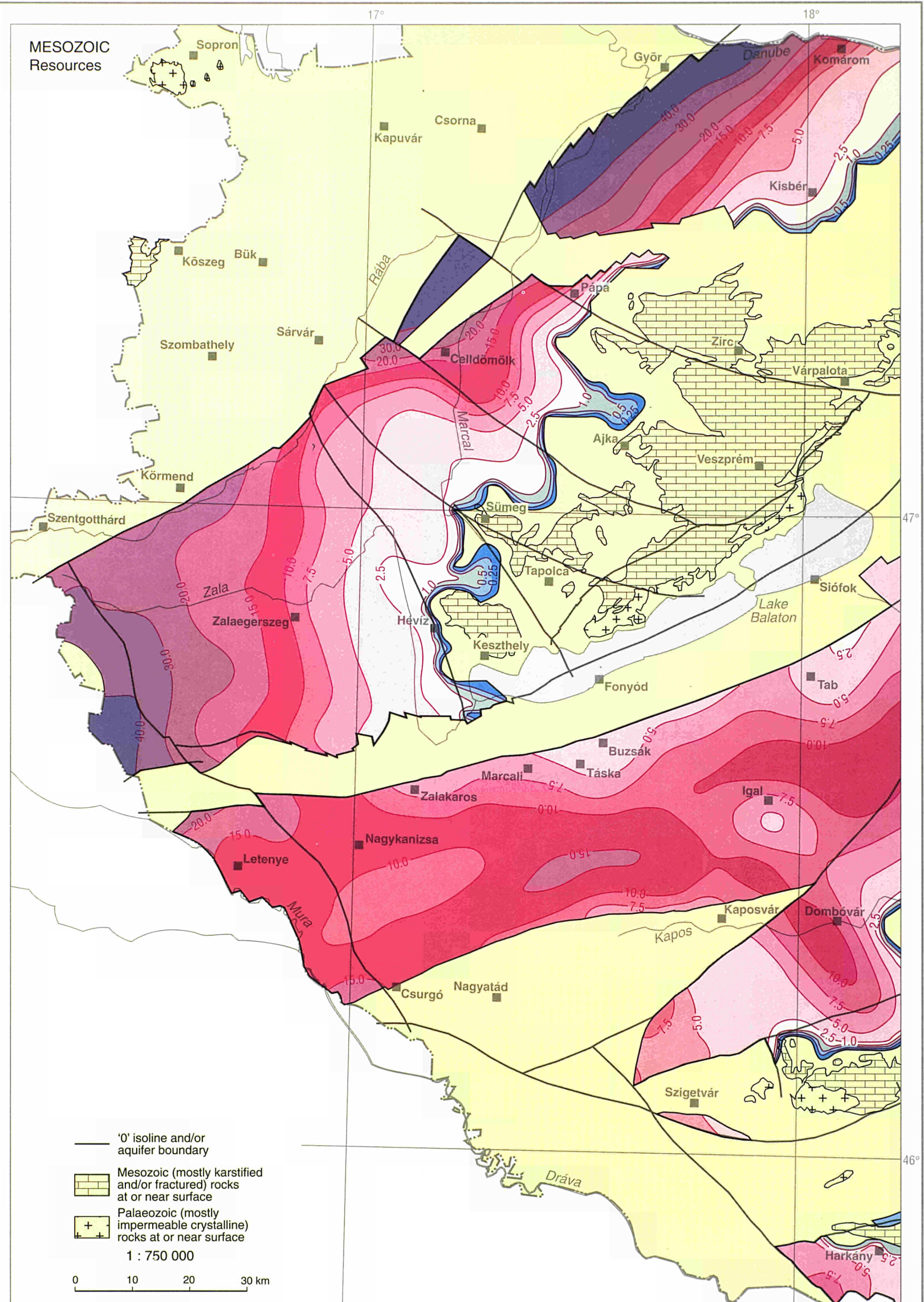
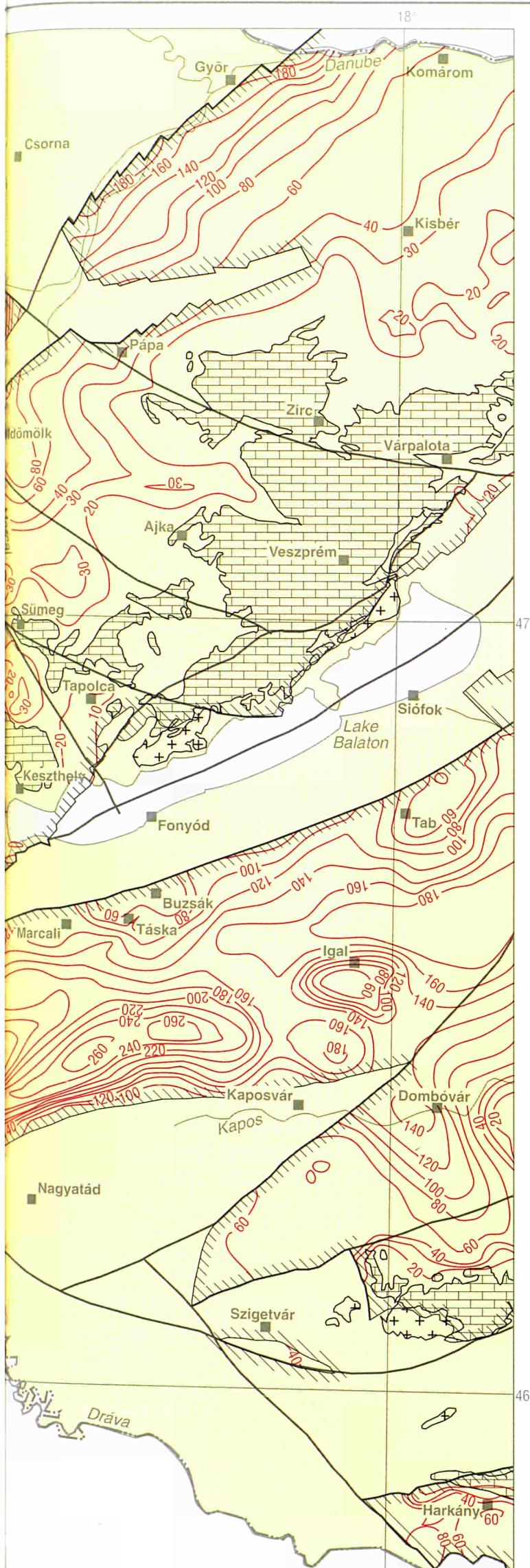


HUNGARY

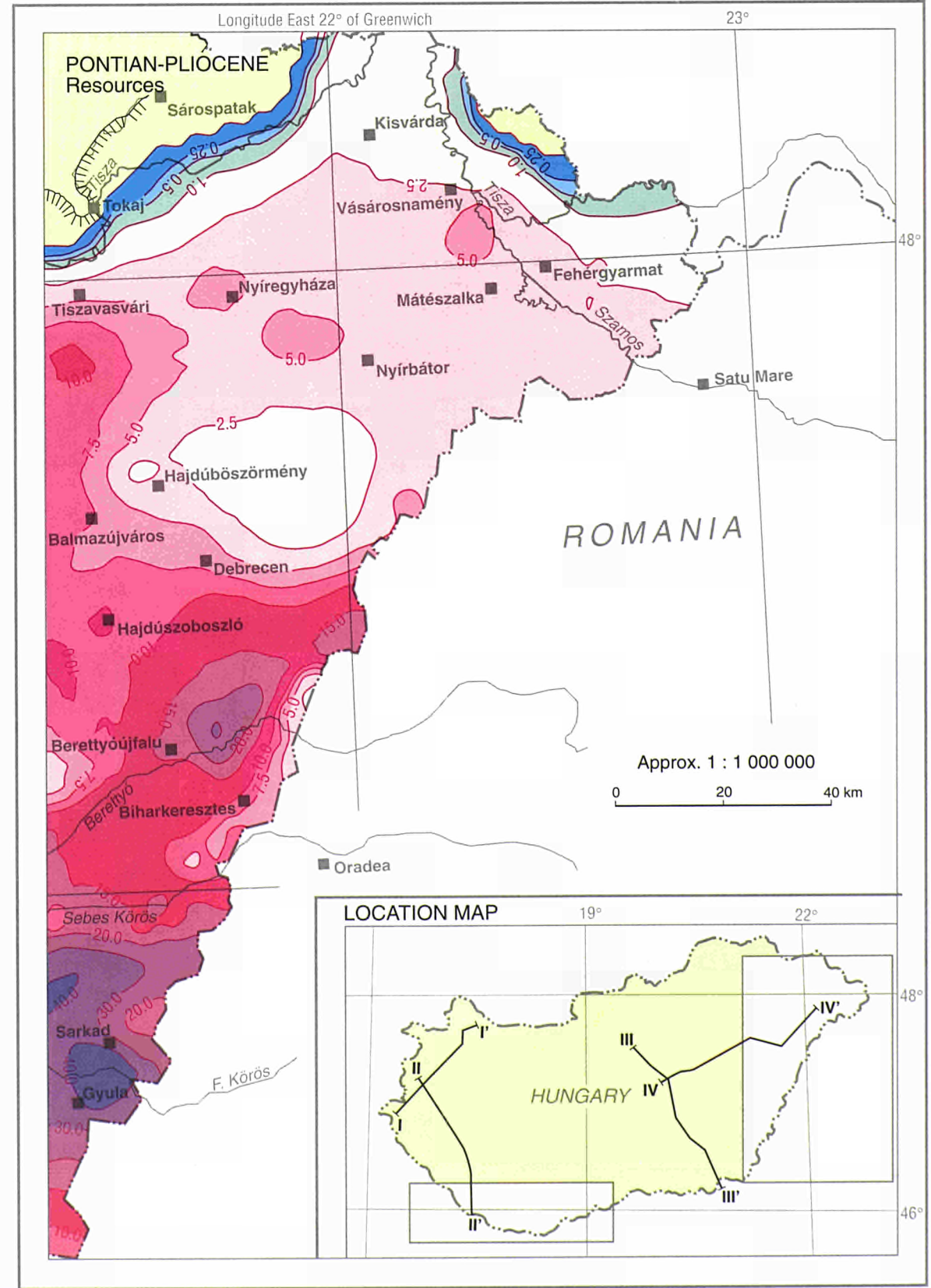
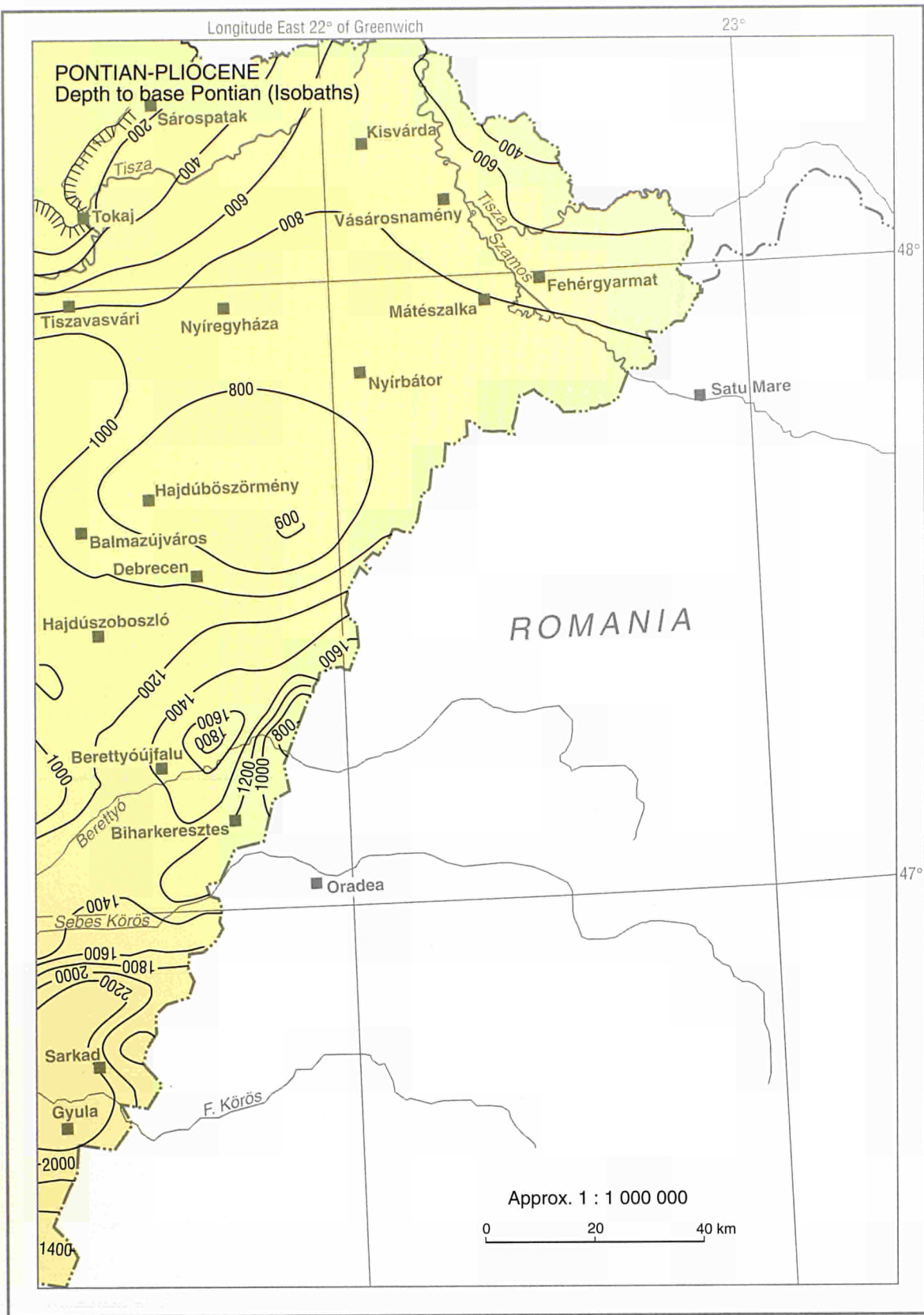


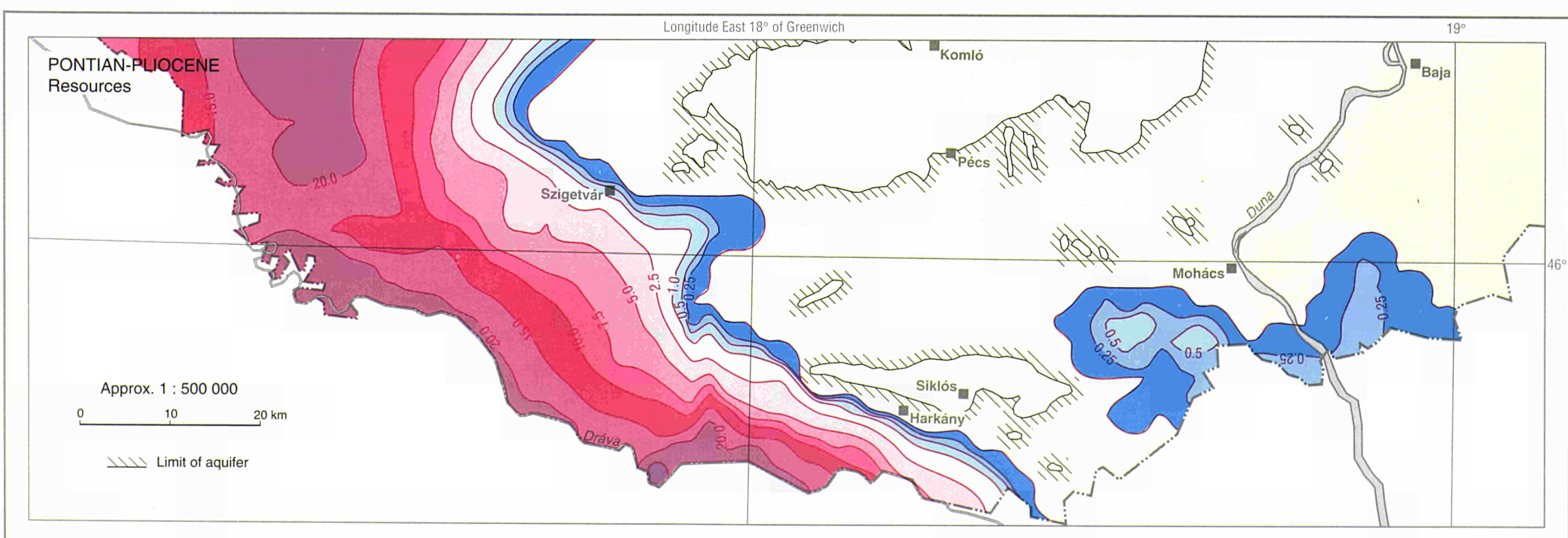
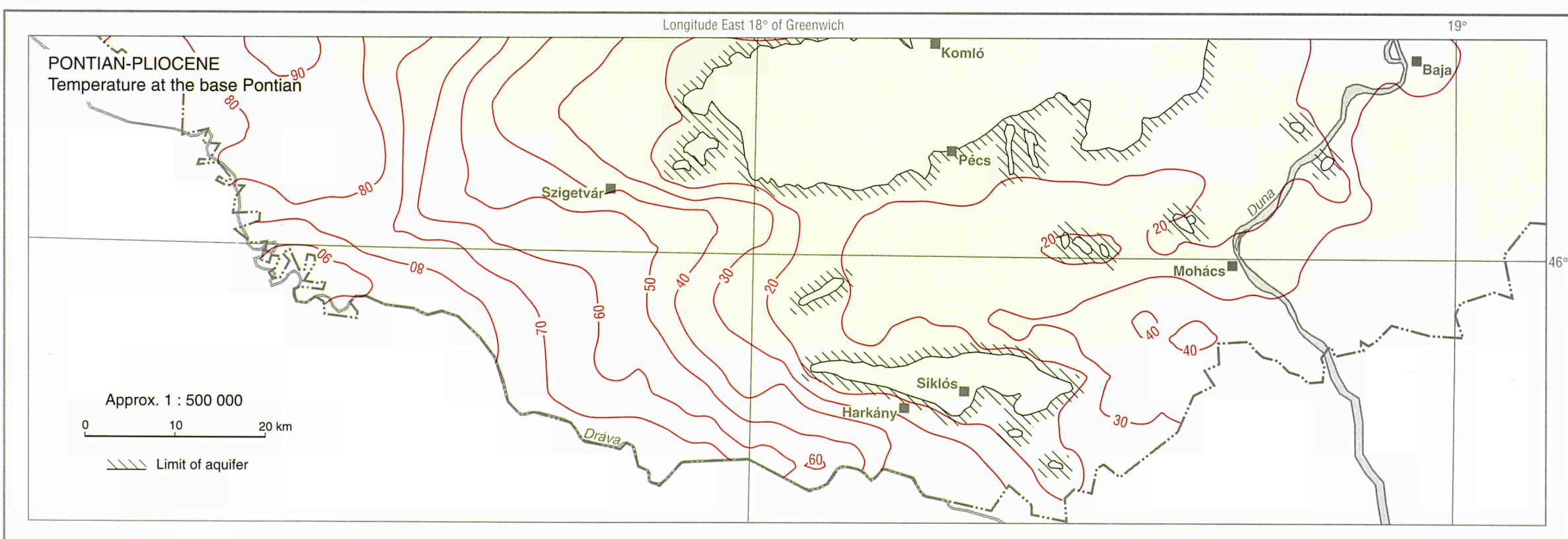
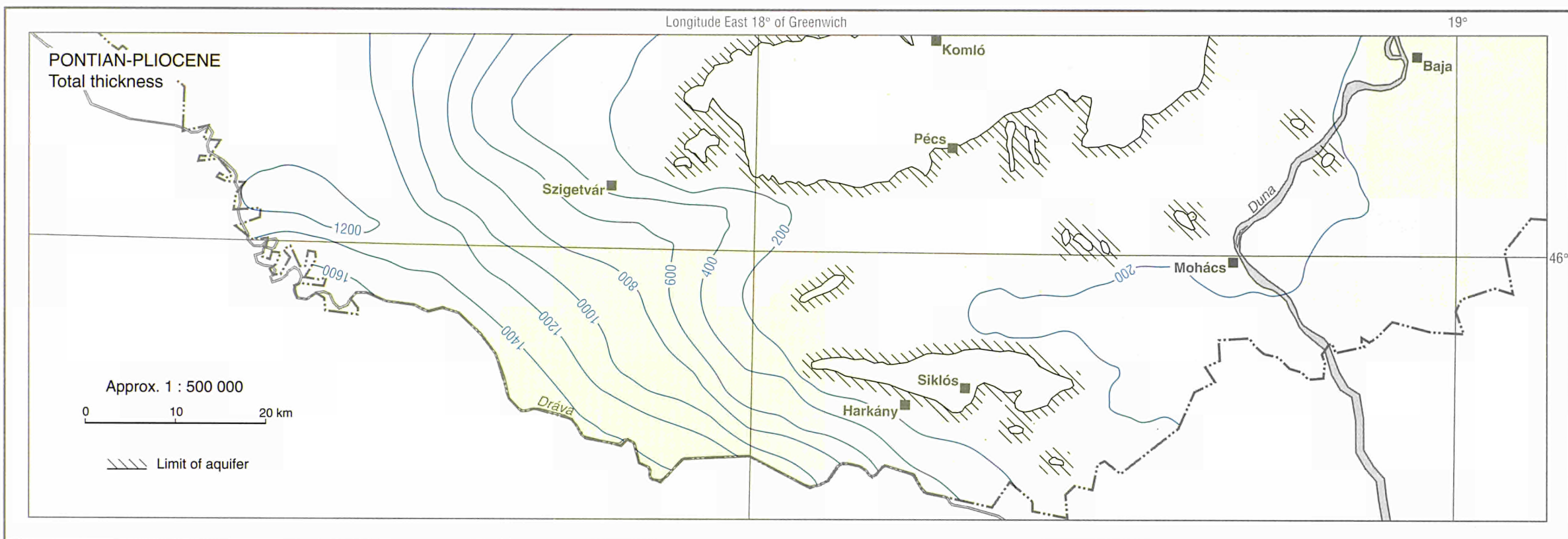
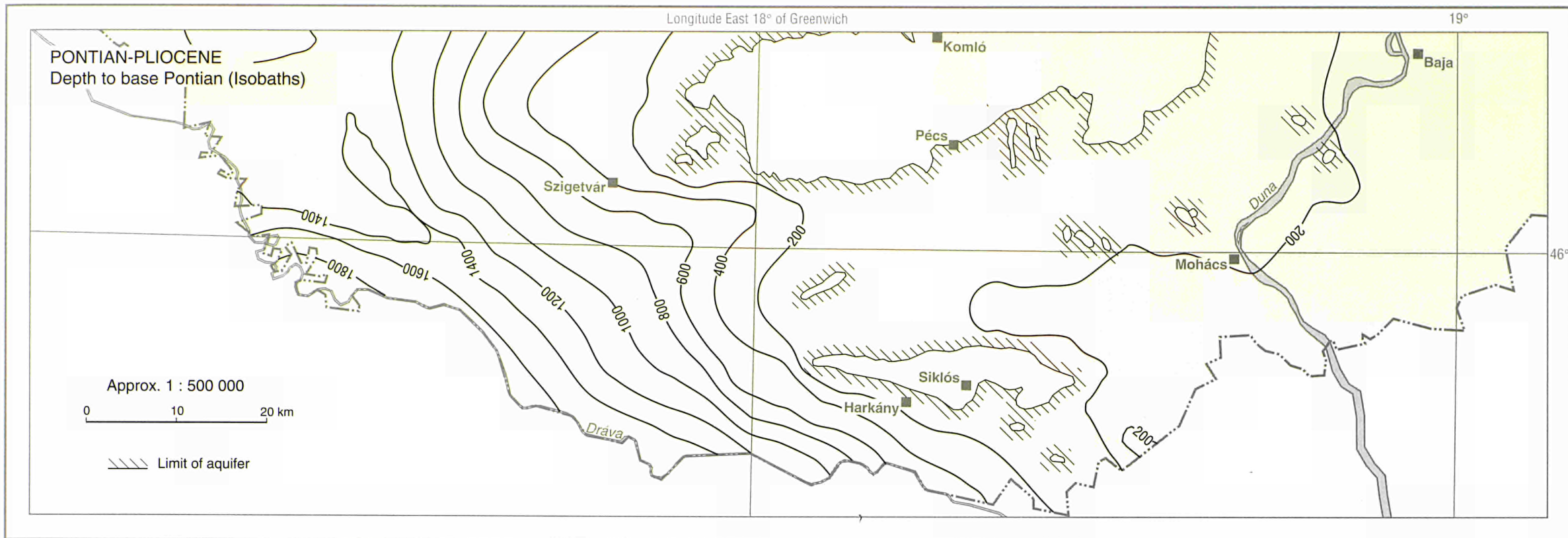
CROSS SECTION

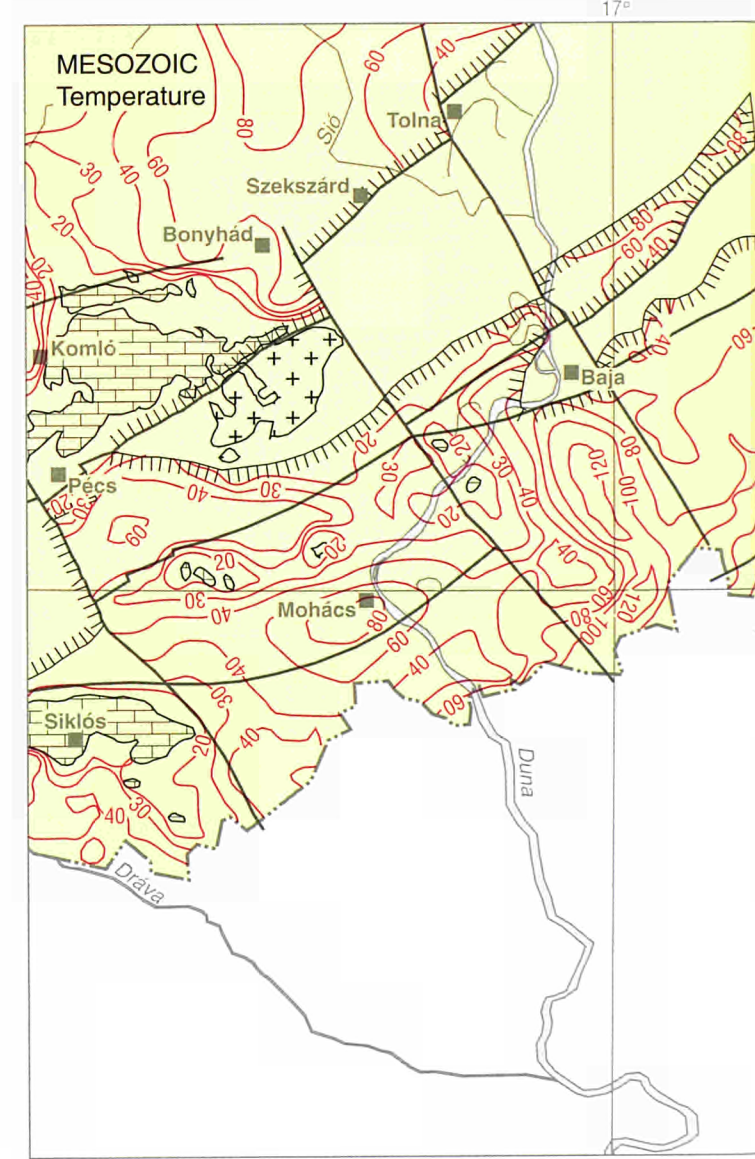
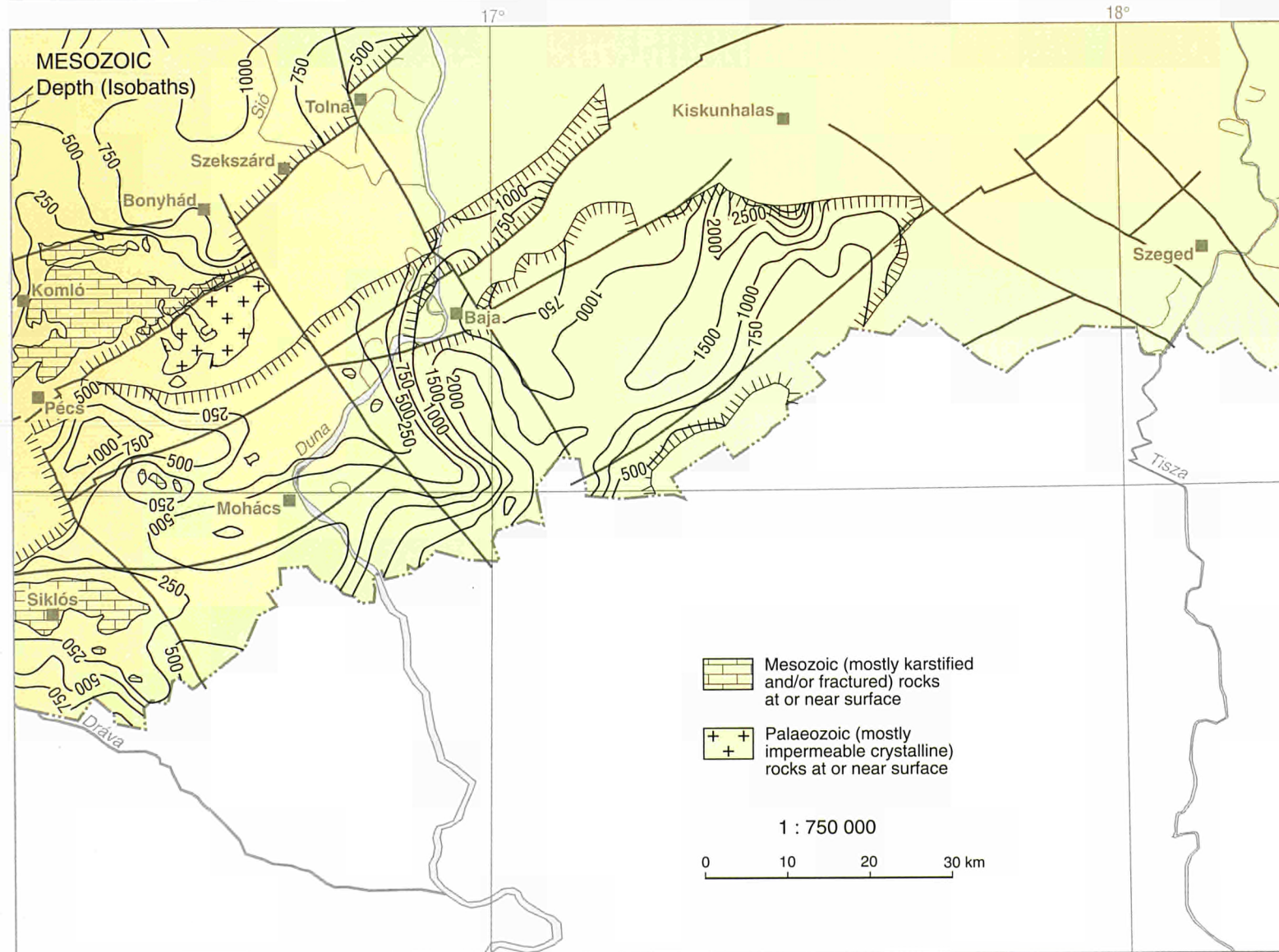
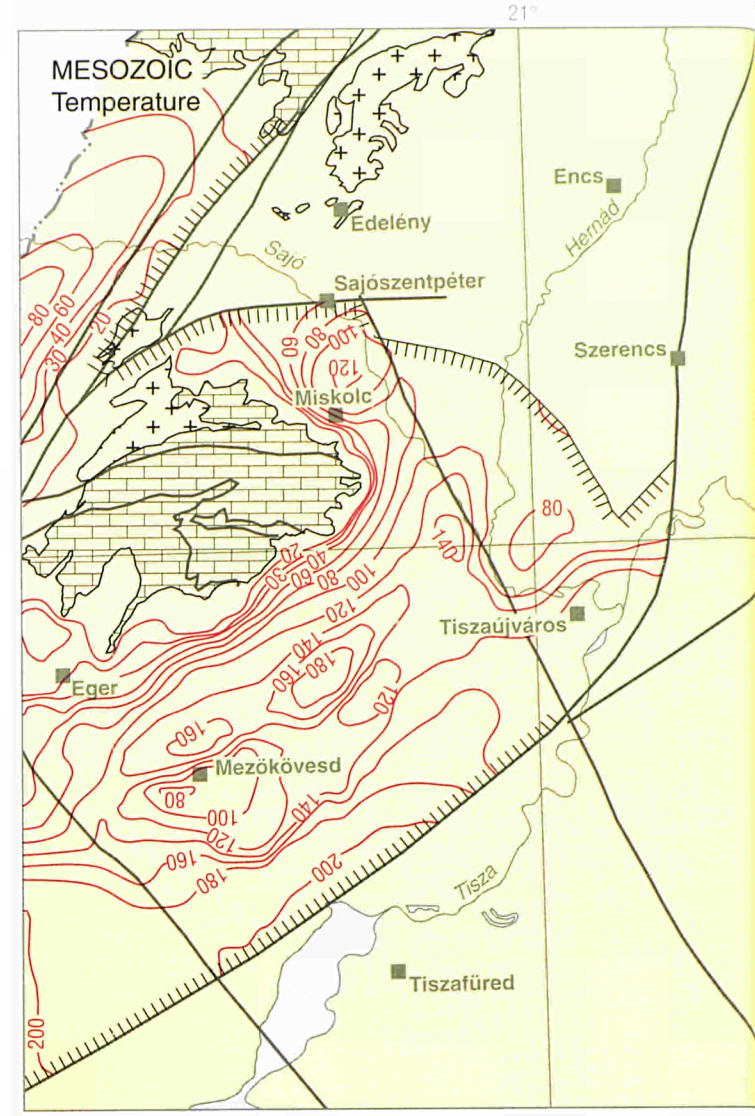
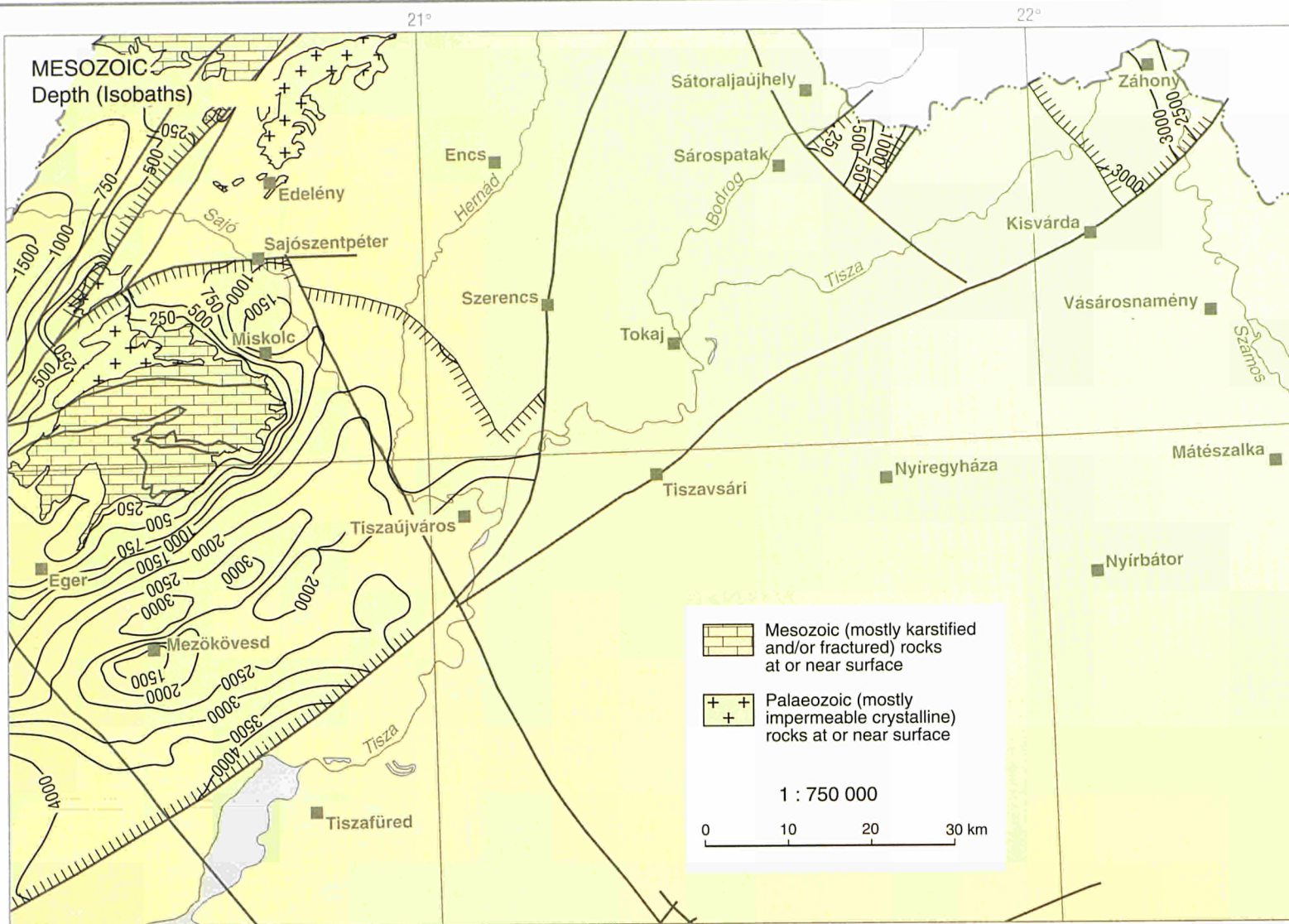




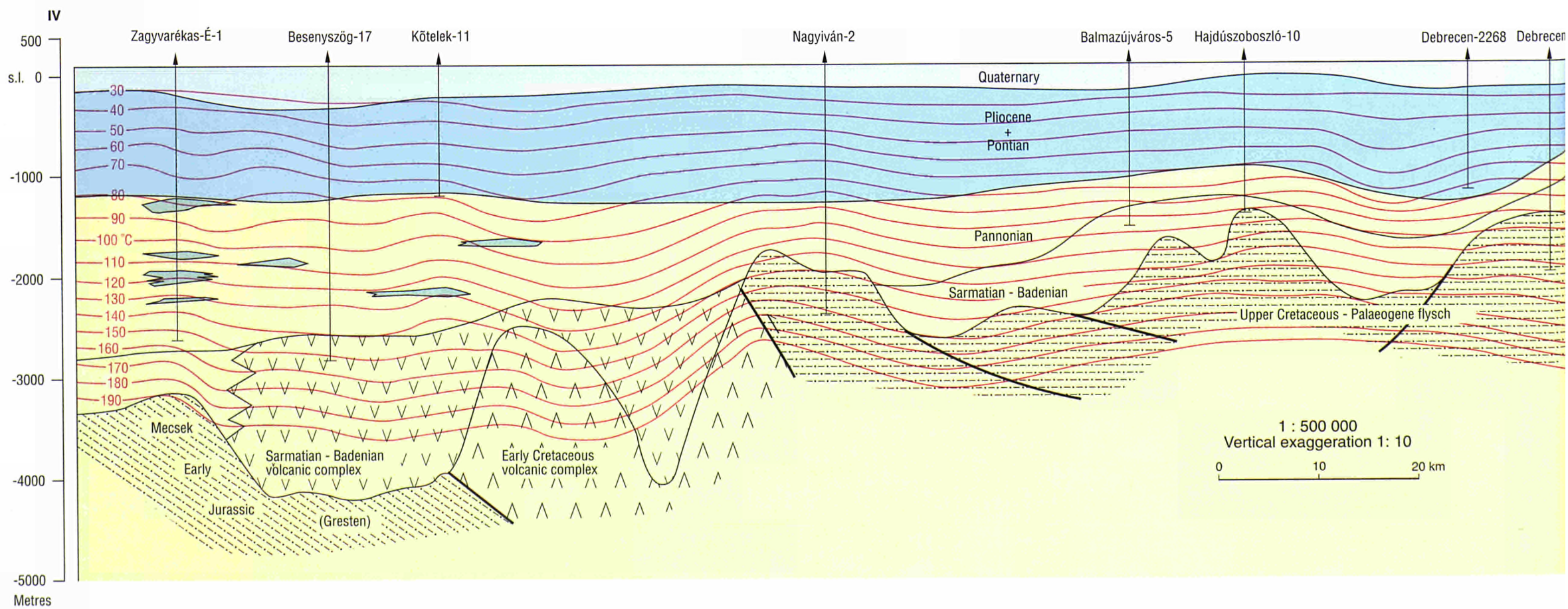
HUNGARY

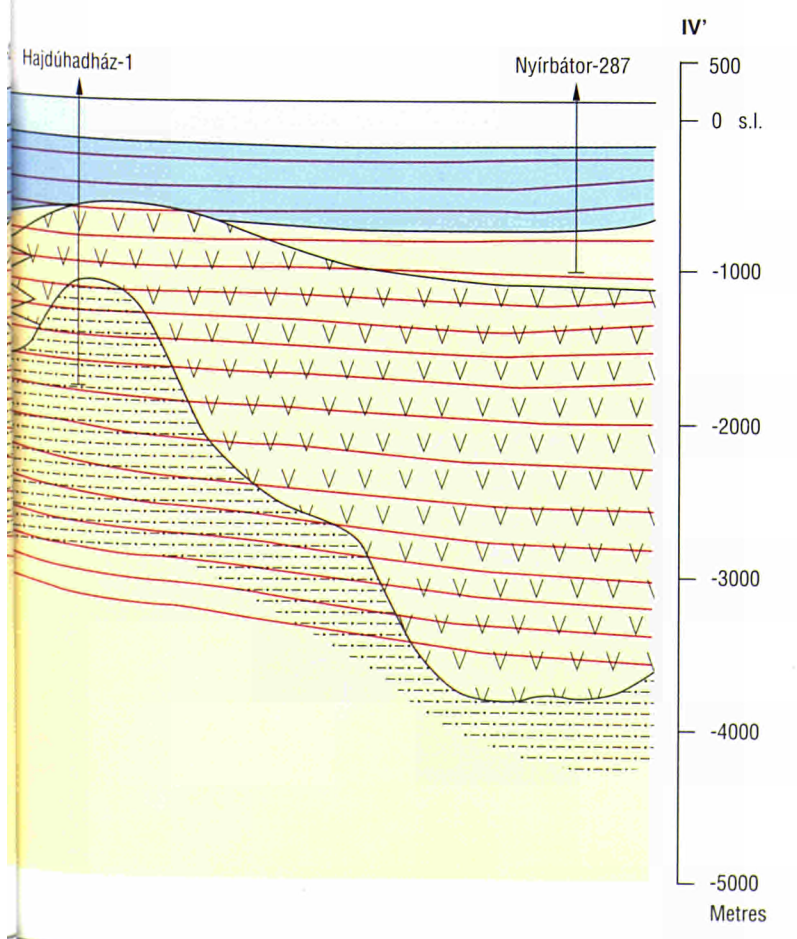
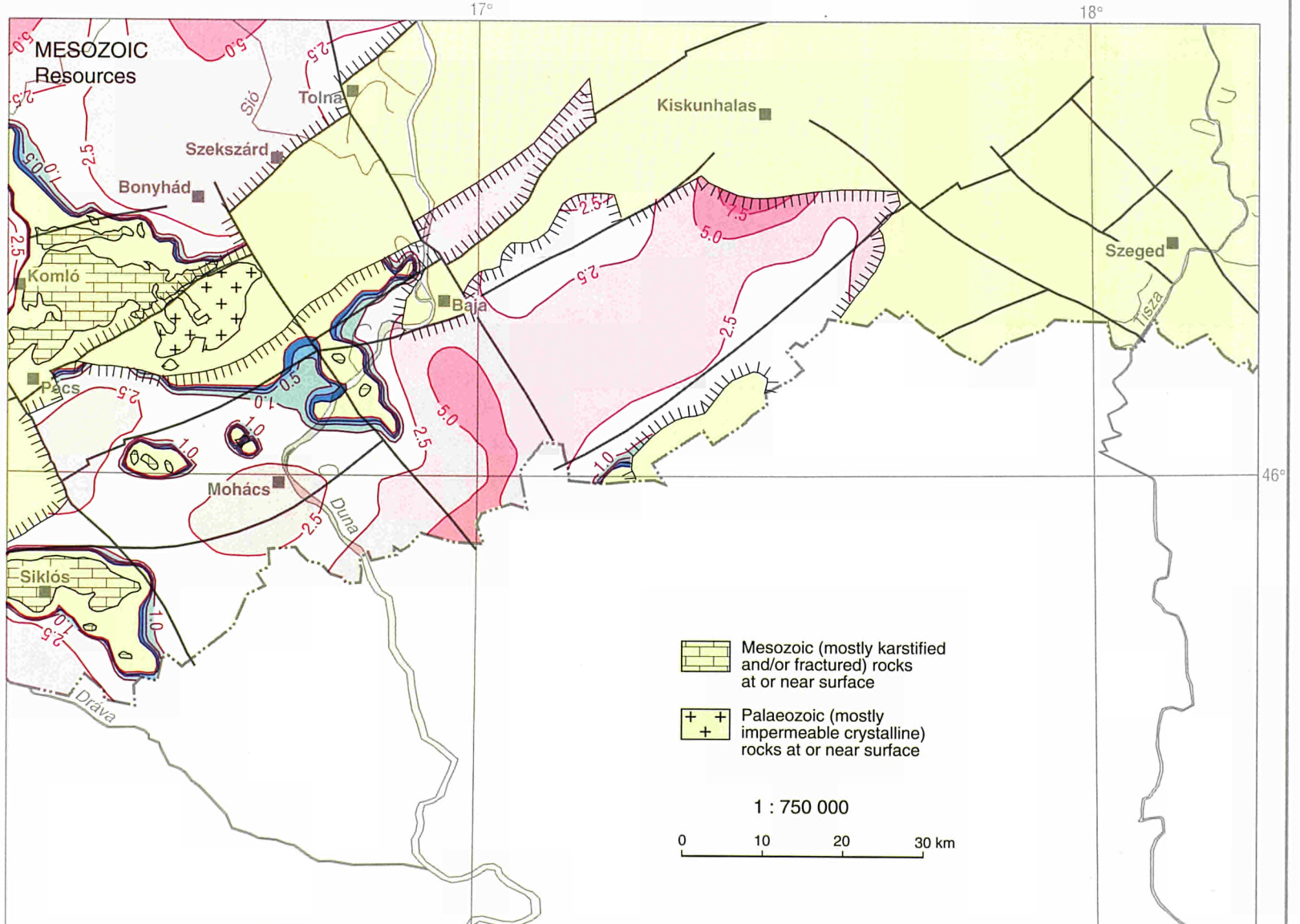
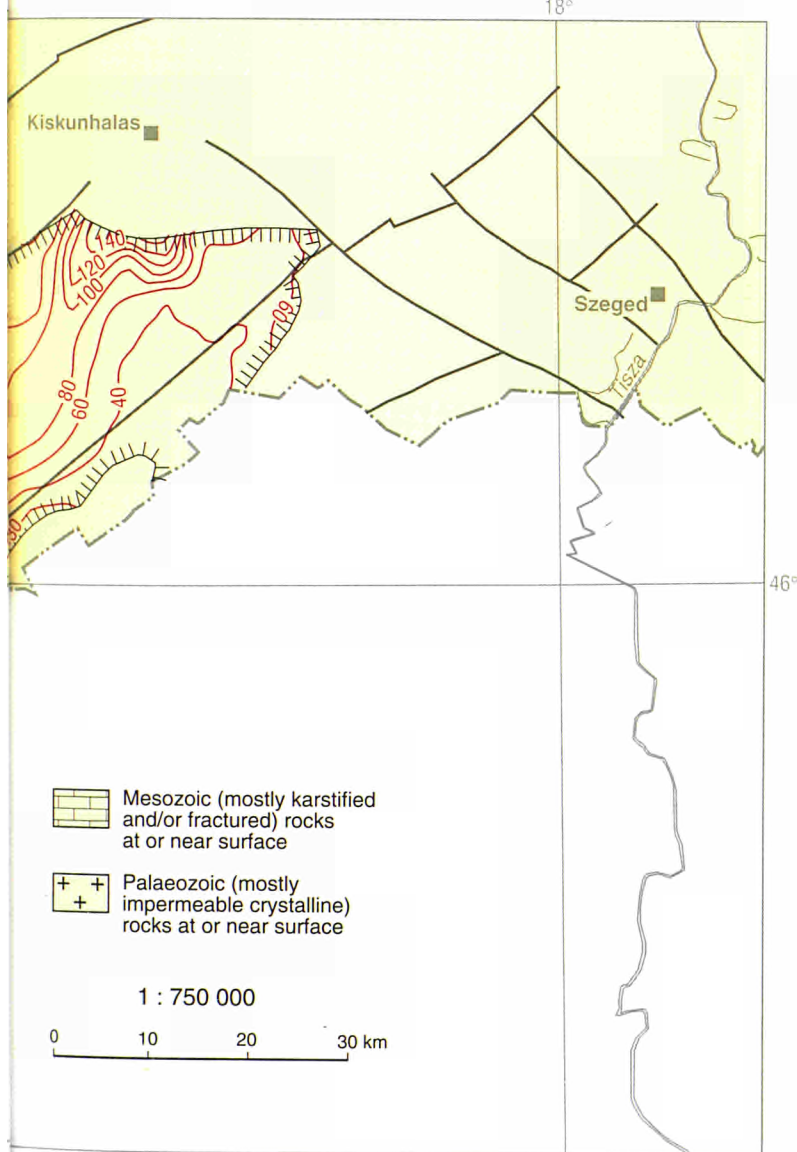
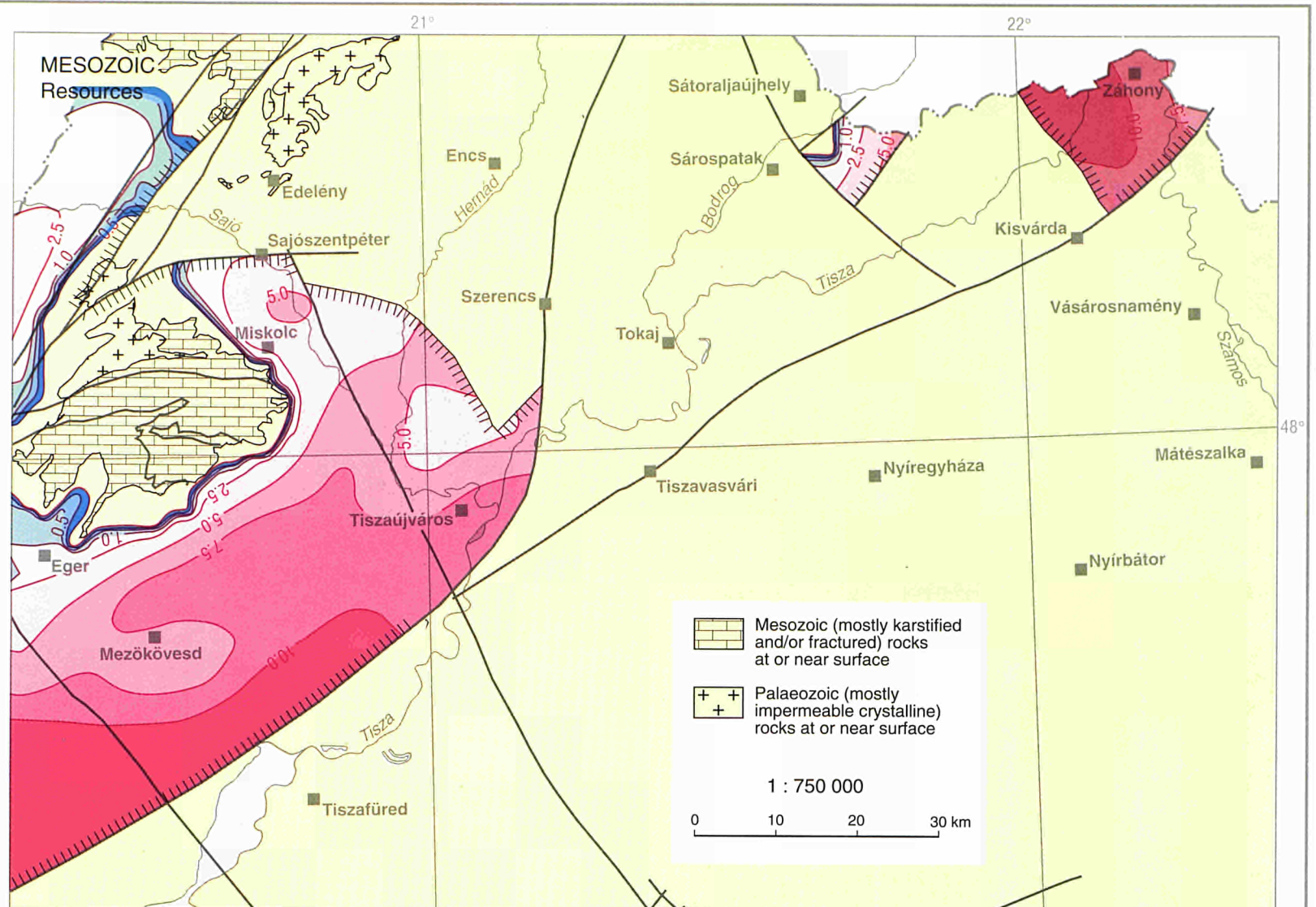
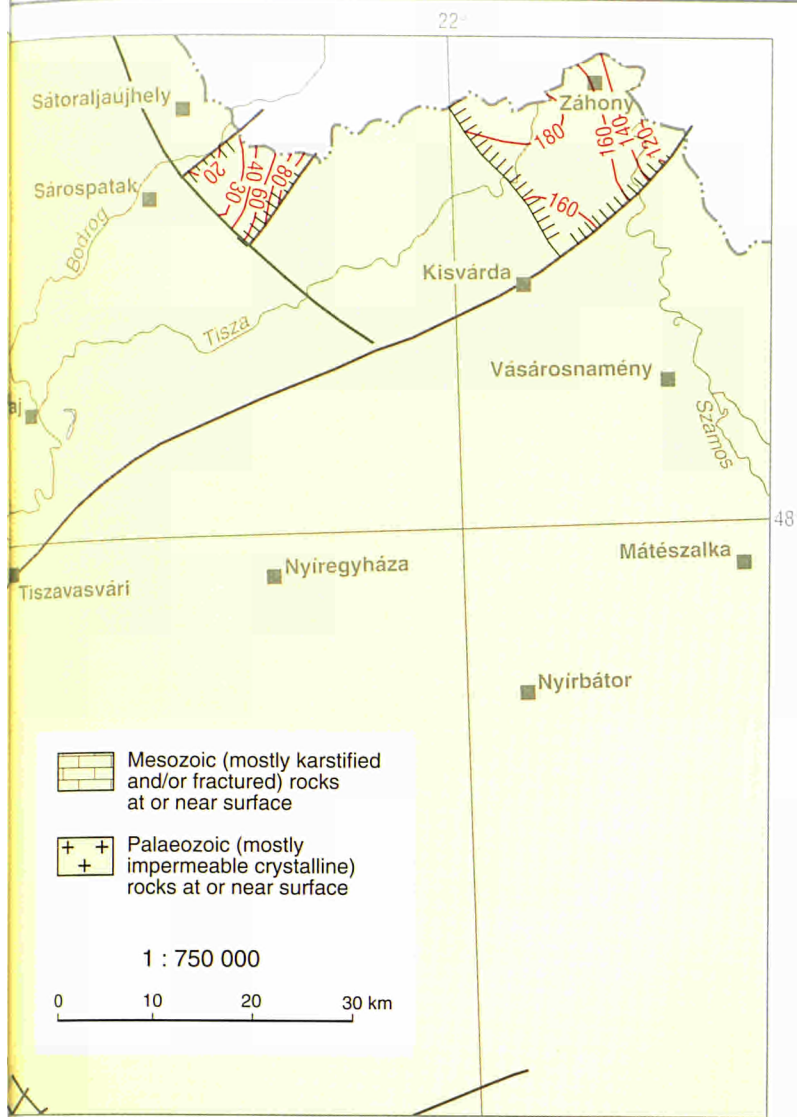




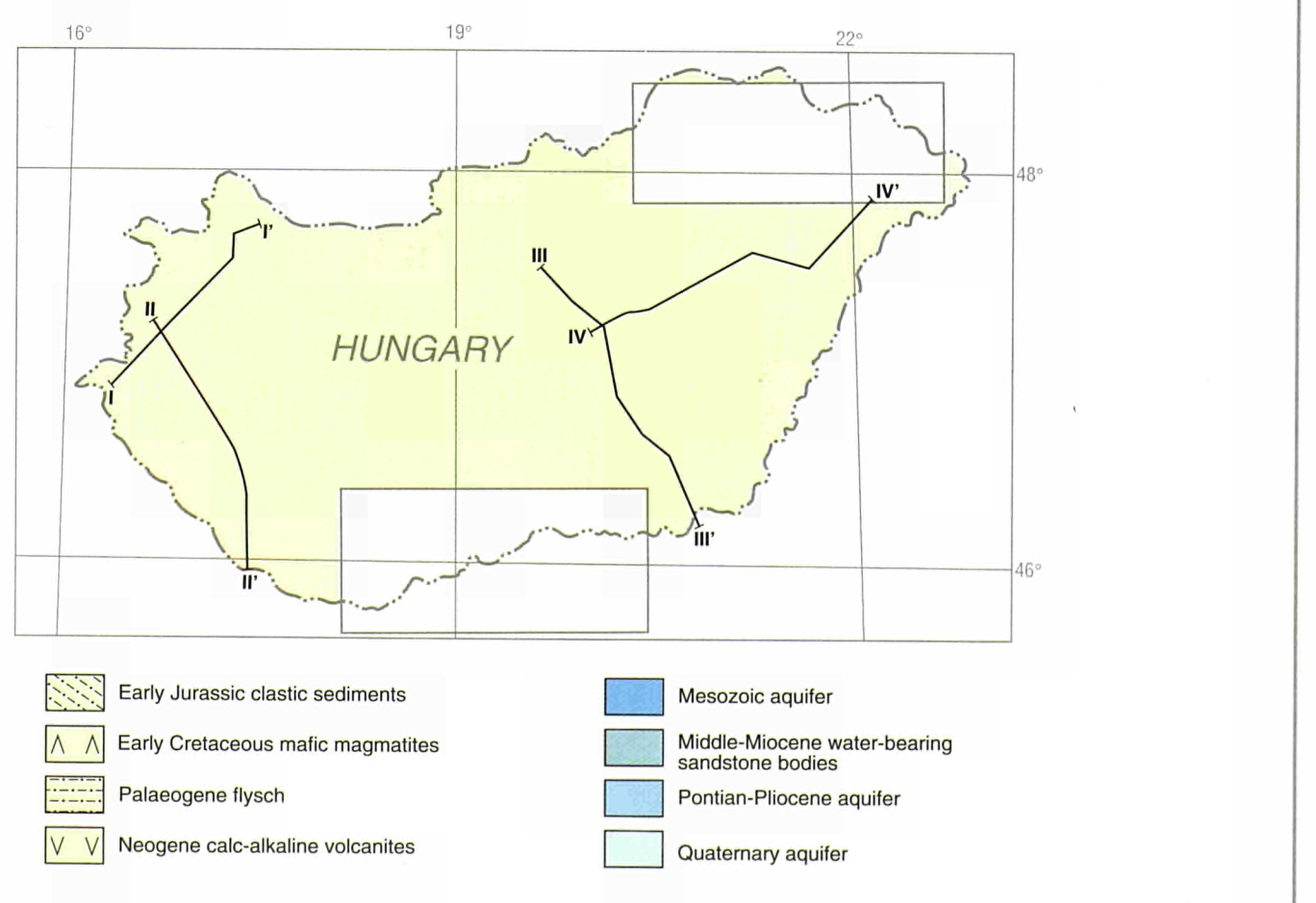


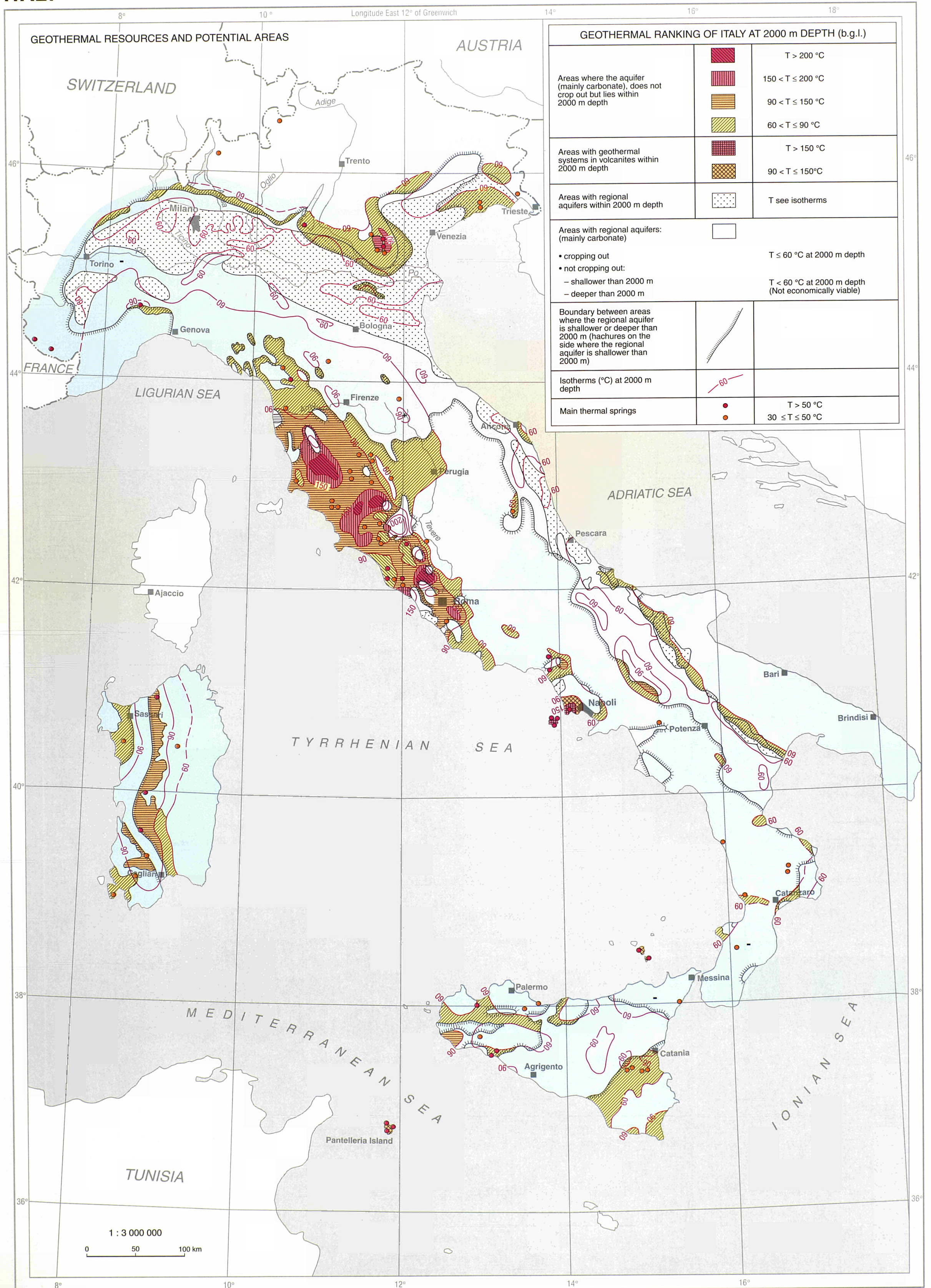
CROSS SECTION

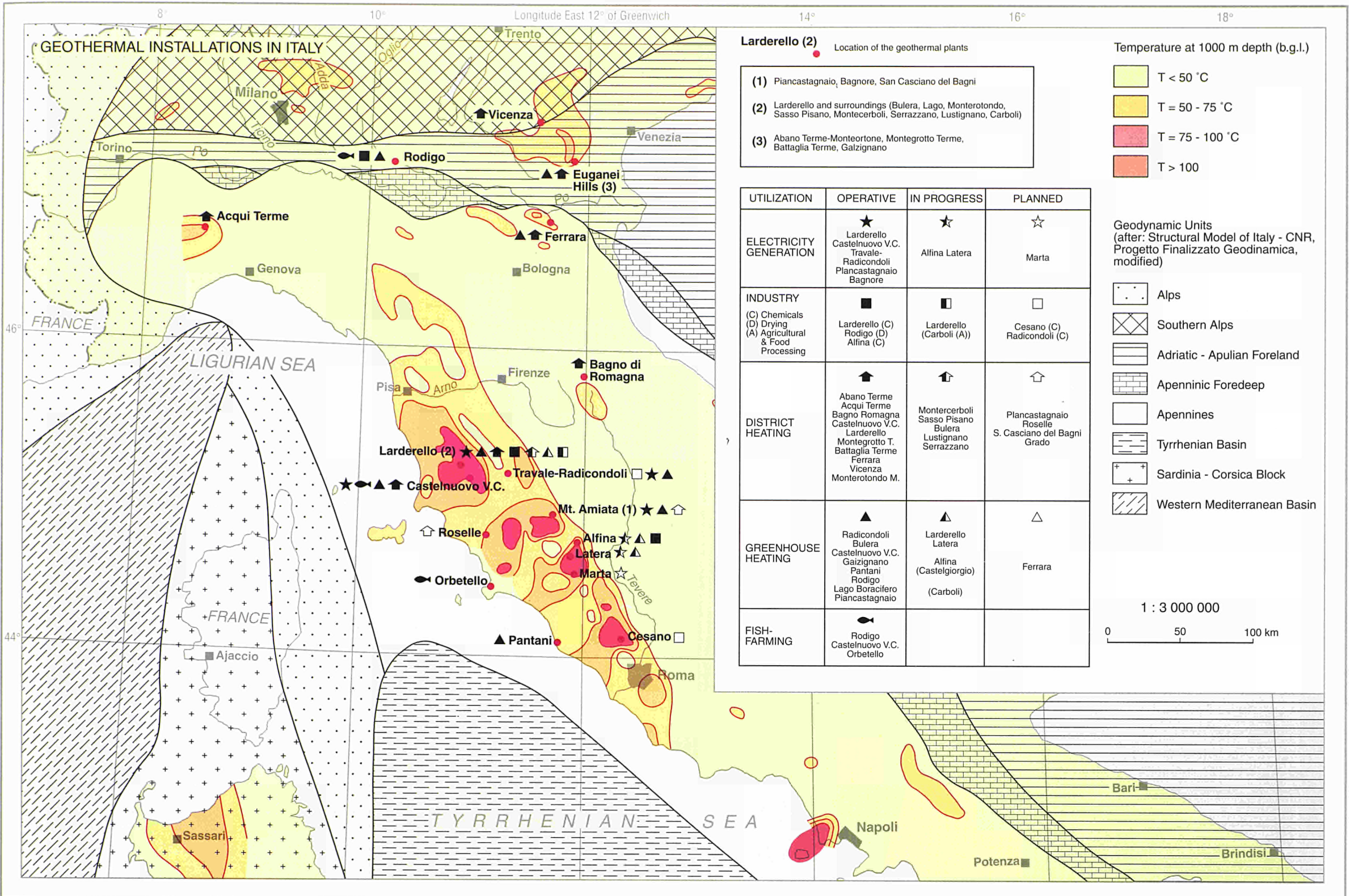




LOCATION MAP







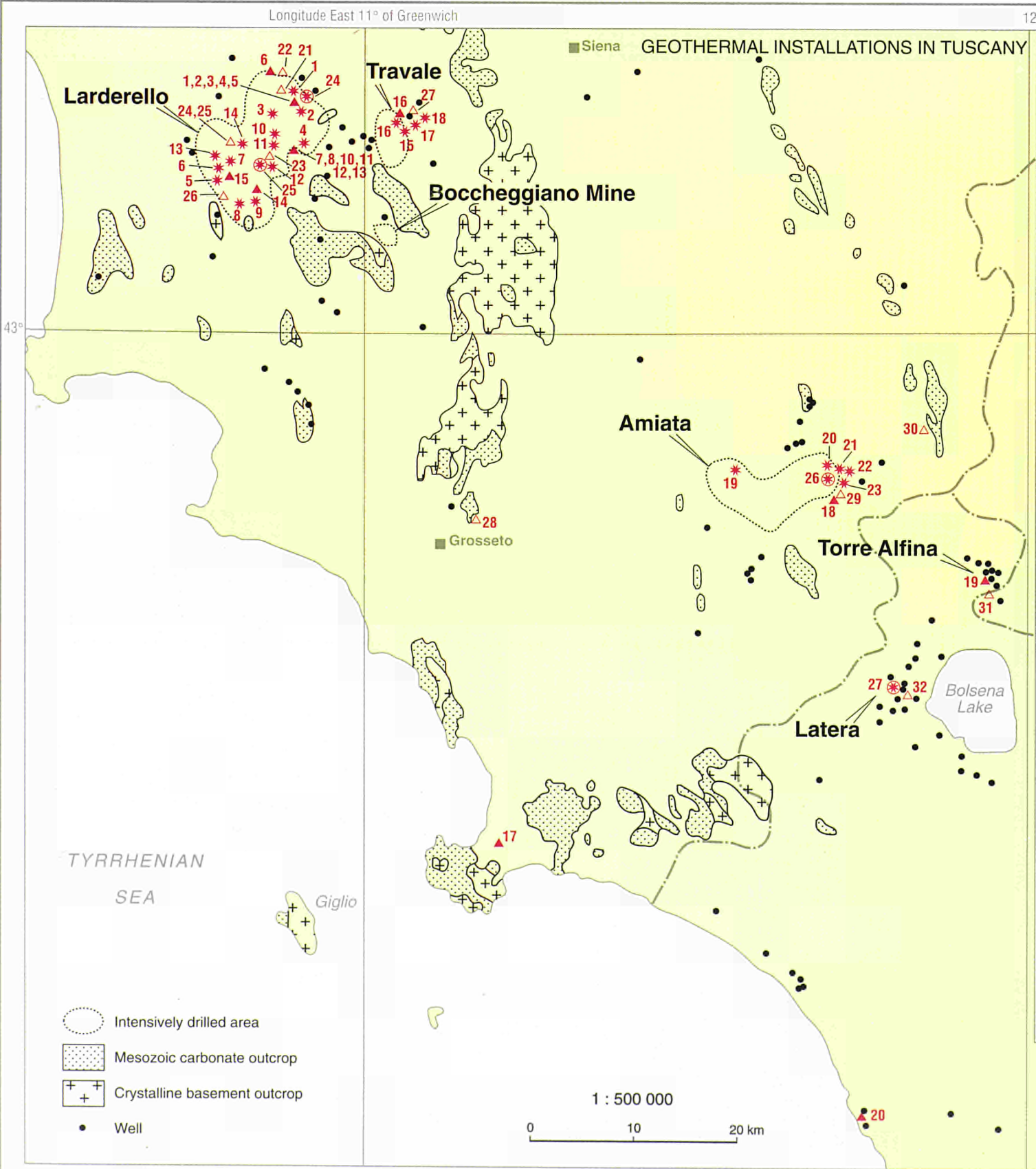
- Larderello (2)** Location of the geothermal plants
- (1) Piancastagnaio, Bagnore, San Casciano del Bagni
 - (2) Larderello and surroundings (Bulera, Lago, Monterotondo, Sasso Pisano, Montecerboli, Serrazzano, Lustignano, Carboli)
 - (3) Abano Terme-Monterotone, Montegrotto Terme, Battaglia Terme, Galzignano

UTILIZATION	OPERATIVE	IN PROGRESS	PLANNED
ELECTRICITY GENERATION	★ Larderello Castelnuovo V.C. Travale- Radicondoli Piancastagnaio Bagnore	★ Alfina Latera	★ Marta
INDUSTRY (C) Chemicals (D) Drying (A) Agricultural & Food Processing	■ Larderello (C) Rodigo (D) Alfina (C)	■ Larderello (Carboli (A))	□ Cesano (C) Radicondoli (C)
DISTRICT HEATING	▲ Abano Terme Acqui Terme Bagno Romagna Castelnuovo V.C. Larderello Montegrotto T. Battaglia Terme Ferrara Vicenza Monterotondo M.	▲ Montercerboli Sasso Pisano Bulera Lustignano Serrazzano	▲ Piancastagnaio Roselle S. Casciano del Bagni Grado
GREENHOUSE HEATING	▲ Radicondoli Bulera Castelnuovo V.C. Galzignano Pantani Rodigo Lago Boracifero Piancastagnaio	▲ Larderello Latera (Castelgiorgio) (Carboli)	▲ Ferrara
FISH-FARMING	● Rodigo Castelnuovo V.C. Orbetello		

- Temperature at 1000 m depth (b.g.l.)
- T < 50 °C
 - T = 50 - 75 °C
 - T = 75 - 100 °C
 - T > 100

- Geodynamic Units (after: Structural Model of Italy - CNR, Progetto Finalizzato Geodinamica, modified)
- Alps
 - Southern Alps
 - Adriatic - Apulian Foreland
 - Apenninic Foredeep
 - Apennines
 - Tyrrhenian Basin
 - Sardinia - Corsica Block
 - Western Mediterranean Basin

1 : 3 000 000
0 50 100 km



POWER PLANTS * (JANUARY 1995)

N°	NAME	LOCALITY	PROVINCE	INSTALLED CAPACITY (MW)
1	GABRO	LARDERELLO	PISA	15
2	LARDERELLO 3	LARDERELLO	PISA	98
3	VALLE SECOLO	LARDERELLO	PISA	120
4	CASTELNUOVO	CASTELNUOVO	PISA	22
5	LAGO	LAGO	GROSSETO	33.5
6	CORNIA 1	CORNIA	PISA	20
7	CORNIA 2	CORNIA	PISA	20
8	SAN MARTINO	MONTEROTONDO	GROSSETO	40
9	MONTEROTONDO	MONTEROTONDO	GROSSETO	12.5
10	MOLINETTO	SASSO PISANO	PISA	8
11	LECCIA	SASSO PISANO	PISA	8
12	SASSO PISANO	SASSO PISANO	PISA	15.7
13	LAGONI ROSSI	LAGONI ROSSI	PISA	8
14	SERRAZZANO	SERRAZZANO	PISA	40
15	RADICONDOLI	RADICONDOLI/TRAVALE	SIENA	30
16	PIANACCE	RADICONDOLI/TRAVALE	SIENA	20
17	RANCIA 1	RADICONDOLI/TRAVALE	SIENA	20
18	RANCIA 2	RADICONDOLI/TRAVALE	SIENA	20
19	BAGNORE 2	BAGNORE	GROSSETO	3.5
20	PIANCASTAGNAIO 2	PIANCASTAGNAIO	SIENA	8
21	BELLA VISTA	PIANCASTAGNAIO	SIENA	20
22	PIANCASTAGNAIO 3	PIANCASTAGNAIO	SIENA	20
23	PIANCASTAGNAIO 4	PIANCASTAGNAIO	SIENA	20

POWER PLANTS UNDER CONSTRUCTION *

N°	NAME	LOCALITY	PROVINCE	INSTALLED CAPACITY (MW)
24	FARINELLO	LARDERELLO	PISA	60
25	NUOVO SASSO	SASSO PISANO	PISA	20
26	PIANCASTAGNAIO 5	PIANCASTAGNAIO	SIENA	20
27	LATERA	LATERA	VITERBO	44

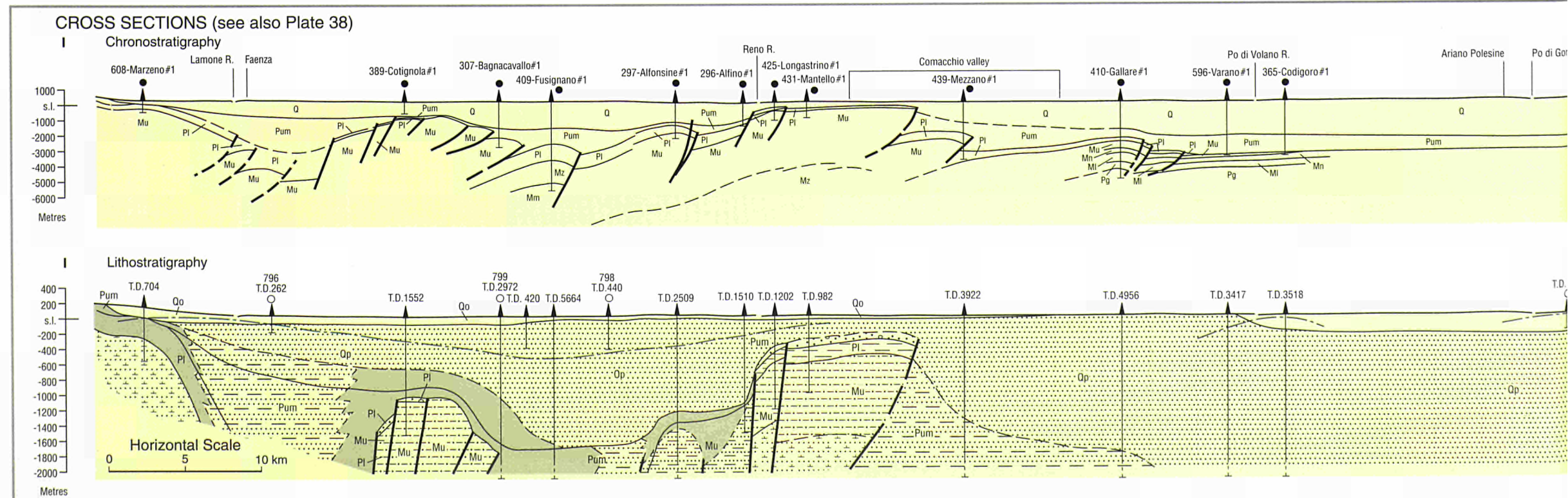
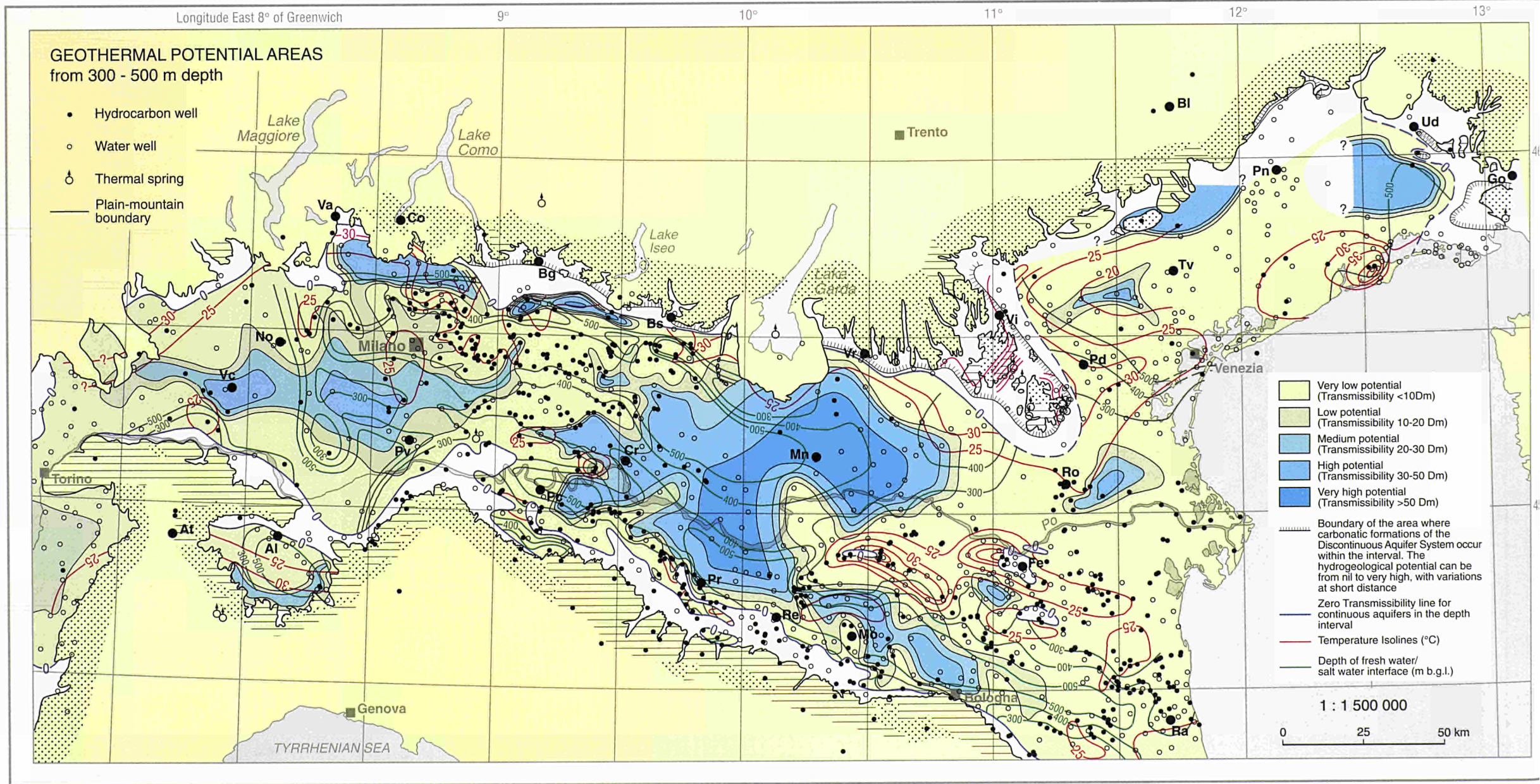
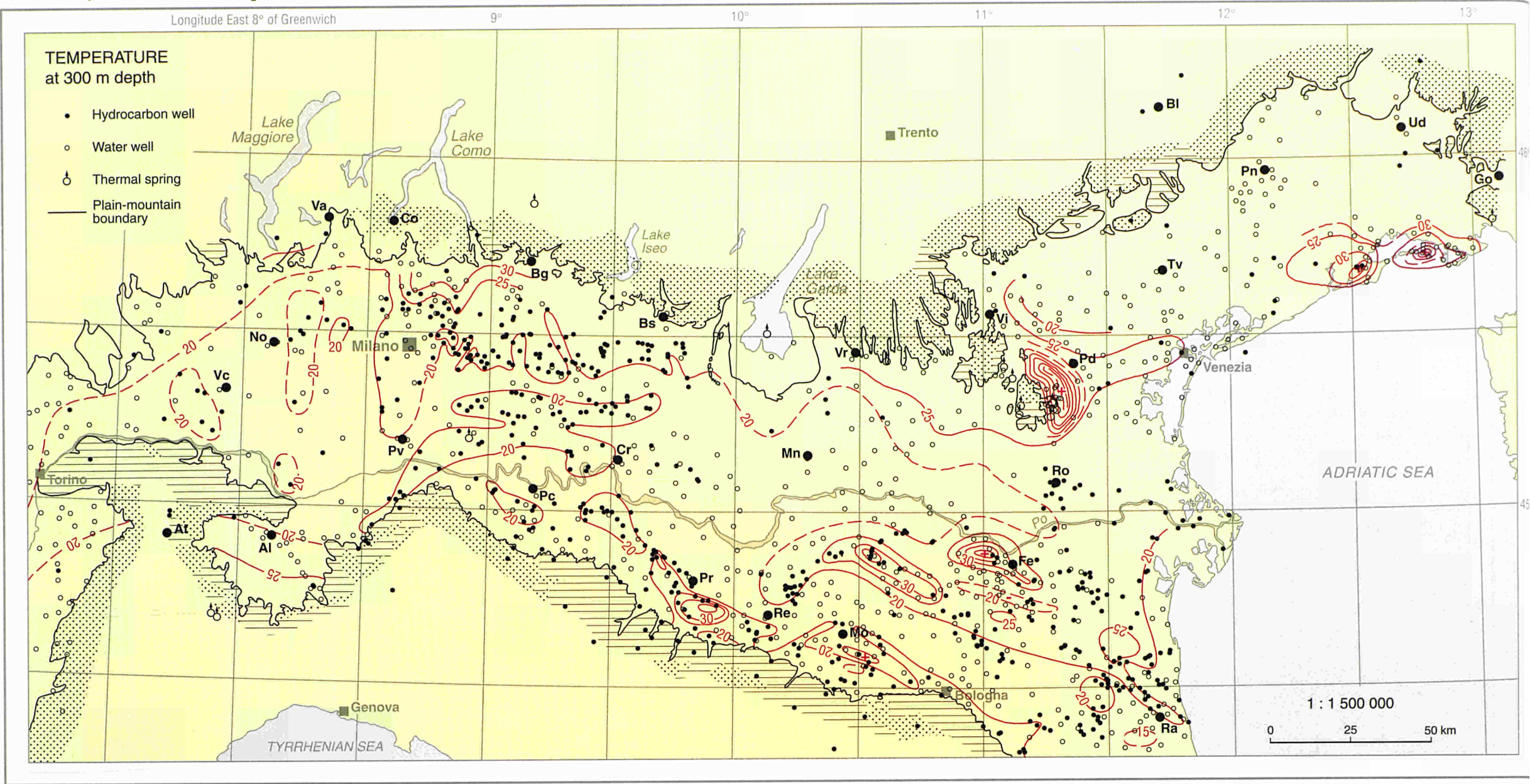
THERMAL PLANTS FOR HEATING AND INDUSTRIAL PURPOSES (JANUARY 1995)

N°	LOCALITY	PROVINCE	USE	ENERGY USE PER YEAR (TJ)	
				INLET TEMP (°C)	PER YEAR (TJ)
1	LARDERELLO	PISA	DISTRICT HEATING	180	6.11
2	LARDERELLO	PISA	DISTRICT HEATING	160	141.8
3	LARDERELLO	PISA	DISTRICT HEATING	160	41.85
4	LARDERELLO	PISA	SWIMMING POOL HEATING	78	4.18
5	LARDERELLO	PISA	INDUSTRIAL PROCESS	200	238.27
6	BULERA	PISA	GREENHOUSE HEATING	120	18.71
7	CASTELNUOVO	PISA	DISTRICT HEATING	117	0.37
8	CASTELNUOVO	PISA	DISTRICT HEATING	160	0.21
9	CASTELNUOVO	PISA	DISTRICT HEATING	105	50.24
10	CASTELNUOVO	PISA	GREENHOUSE HEATING	105	14.64
11	CANALINO	PISA	GREENHOUSE HEATING	70	7.11
12	CASTELNUOVO	PISA	GREENHOUSE HEATING	70	0.41
13	CASTELNUOVO	PISA	FISH FARMING	105	7.55
14	MONTEROTONDO	GROSSETO	DISTRICT HEATING	95	16.91
15	LAGO BORACIFERO	GROSSETO	GREENHOUSE HEATING	125	12.55
16	RADICONDOLI	SIENA	GREENHOUSE HEATING	120	96.25
17	ORBETELLO	GROSSETO	FISH FARMING	22-25	-
18	PIANCASTAGNAIO	SIENA	GREENHOUSE HEATING	97	434.24
19	TORRE ALFINA	VITERBO	CO2 SUPPLY	-	(4t/h)
20	PANTANI	ROMA	GREENHOUSE HEATING	50	147

UNDER CONSTRUCTION OR PLANNED △

N°	LOCALITY	PROVINCE	USE	INLET TEMP (°C)	ENERGY USE PER YEAR (TJ)
21	MONTECERBOLI	PISA	DISTRICT HEATING	200	29.9
22	BULERA	PISA	DISTRICT AND GREENHOUSE HEATING	148	14.64
23	SASSO PISANO	PISA	DISTRICT HEATING	105	12.5
24	SERRAZZANO	PISA	DISTRICT HEATING	180	15
25	LUSTIGNANO	PISA	DISTRICT HEATING	180	5
26	CARBOLI	GROSSETO	AGRICULTURAL/FOOD PROCESSING AND GREENHOUSE HEATING	180	157
27	RADICONDOLI	SIENA	CO2 SUPPLY	-	(4t/h)
28	ROSELLE	GROSSETO	DISTRICT HEATING	42	-
29	PIANCASTAGNAIO	SIENA	DISTRICT HEATING	95	167
30	SAN CASCIANO DEI BAGNI	SIENA	DISTRICT HEATING	40	-
31	CASTELGIORGIO (TORRE ALFINA)	TERNI	GREENHOUSE HEATING	80	27.2
32	LATERA	VITERBO	GREENHOUSE HEATING	85	138.1
33	CESANO	ROMA	SALT EXTRACTION	-	(50000 t/y)

ITALY, Po River plain

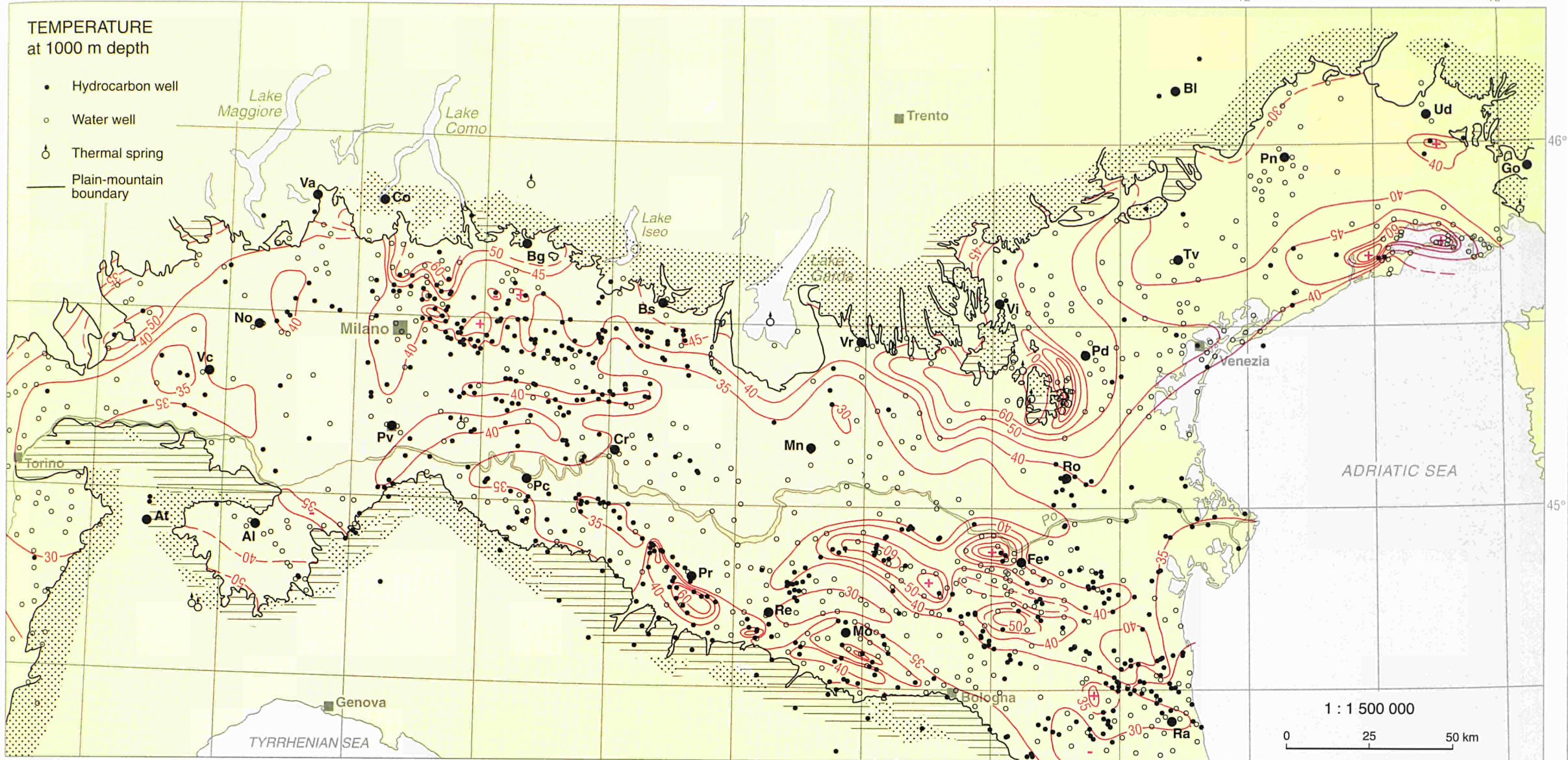


Po River plain, ITALY

Longitude East 8° of Greenwich 9° 10° 11° 12° 13°

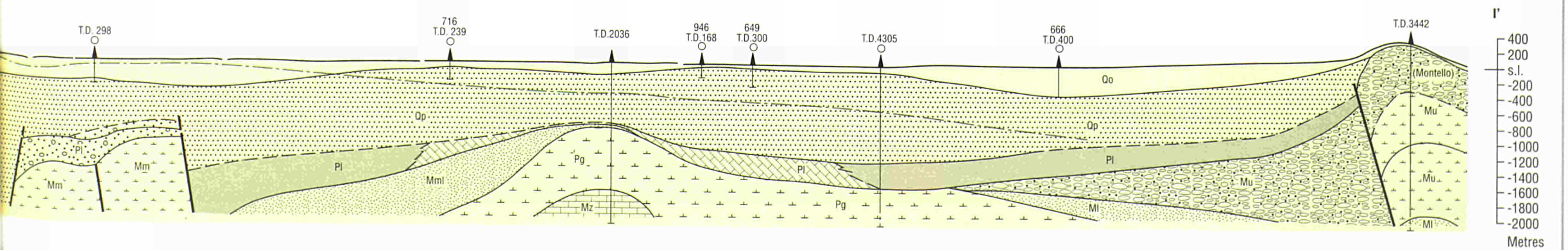
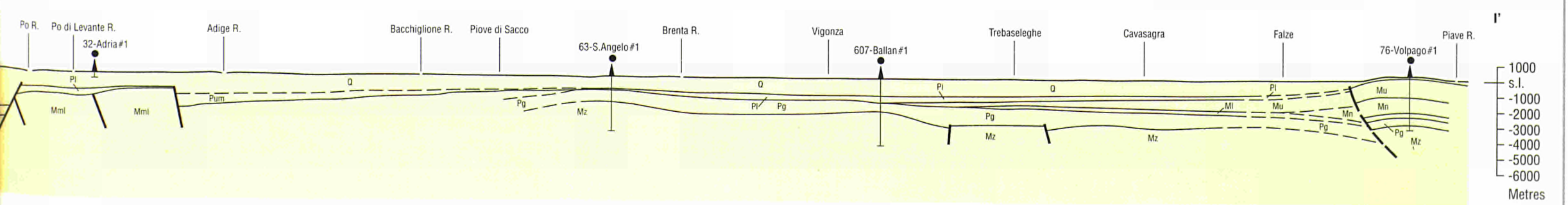
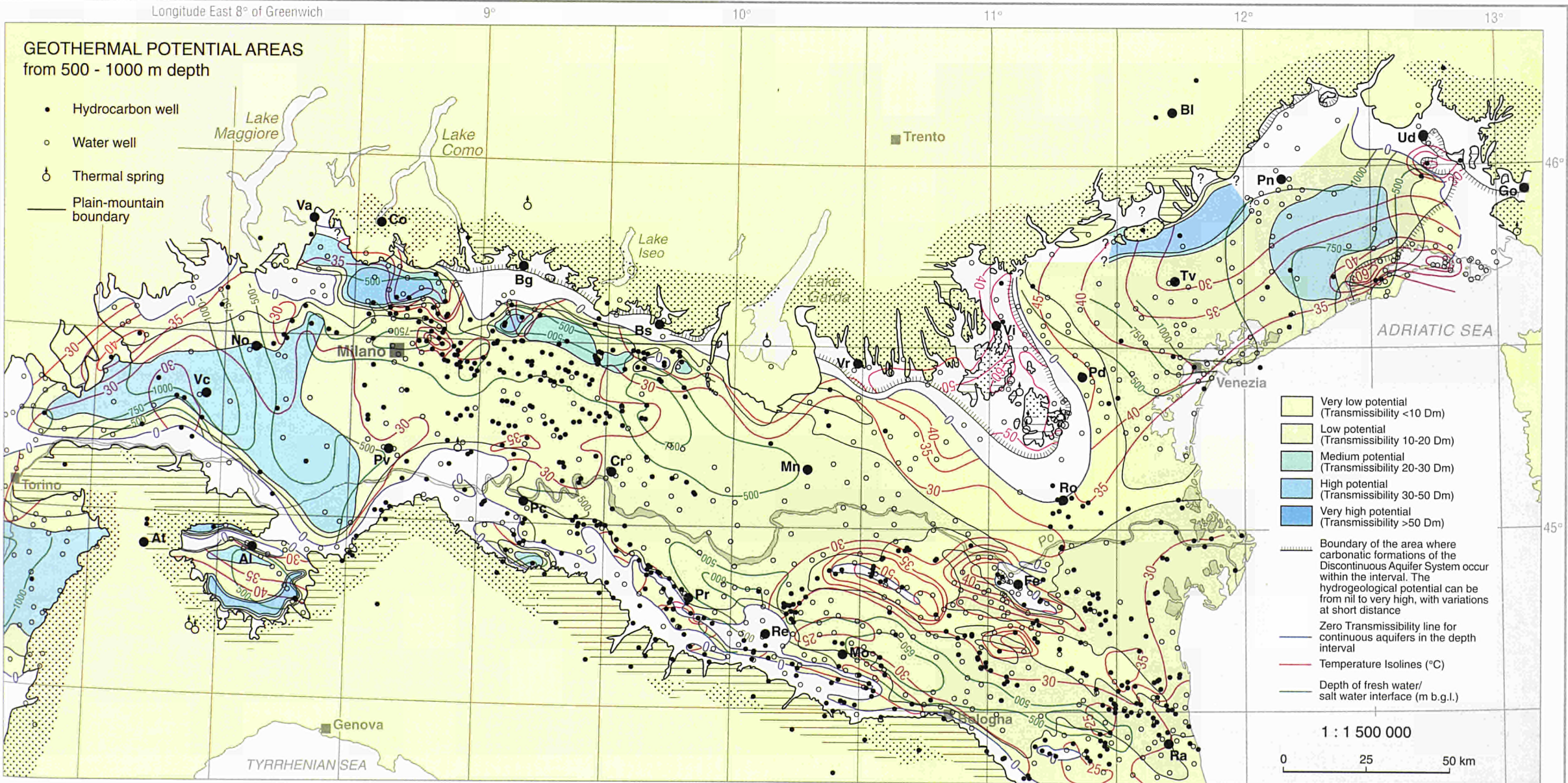
TEMPERATURE at 1000 m depth

- Hydrocarbon well
- Water well
- ⊙ Thermal spring
- Plain-mountain boundary

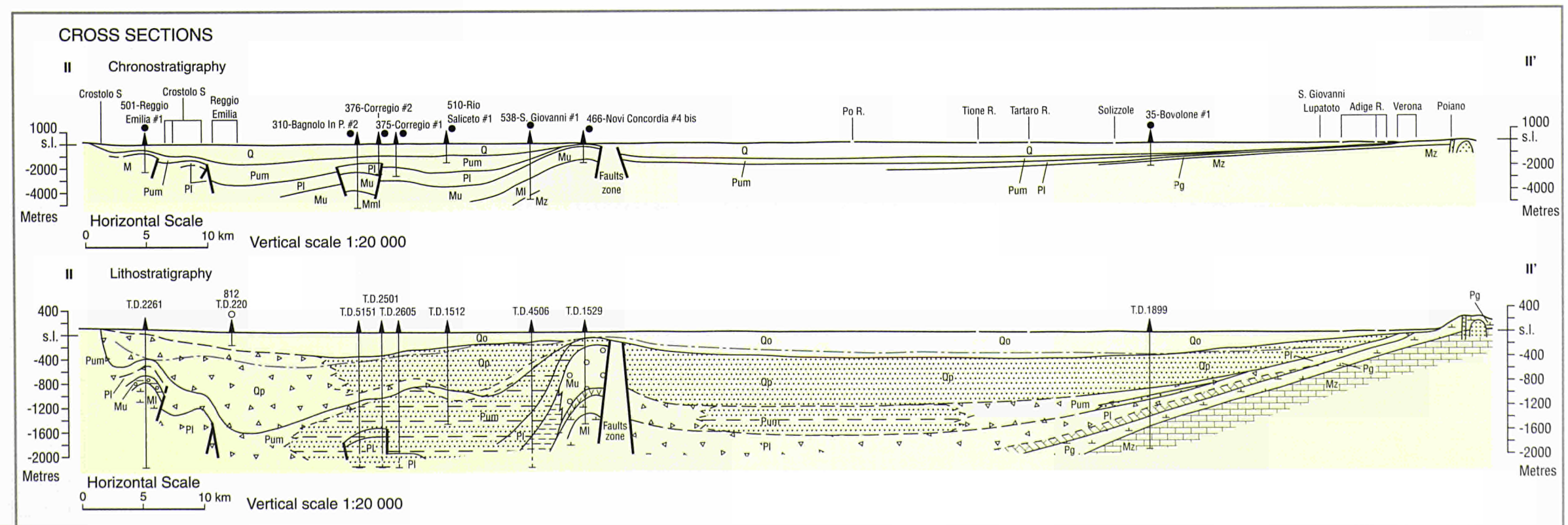
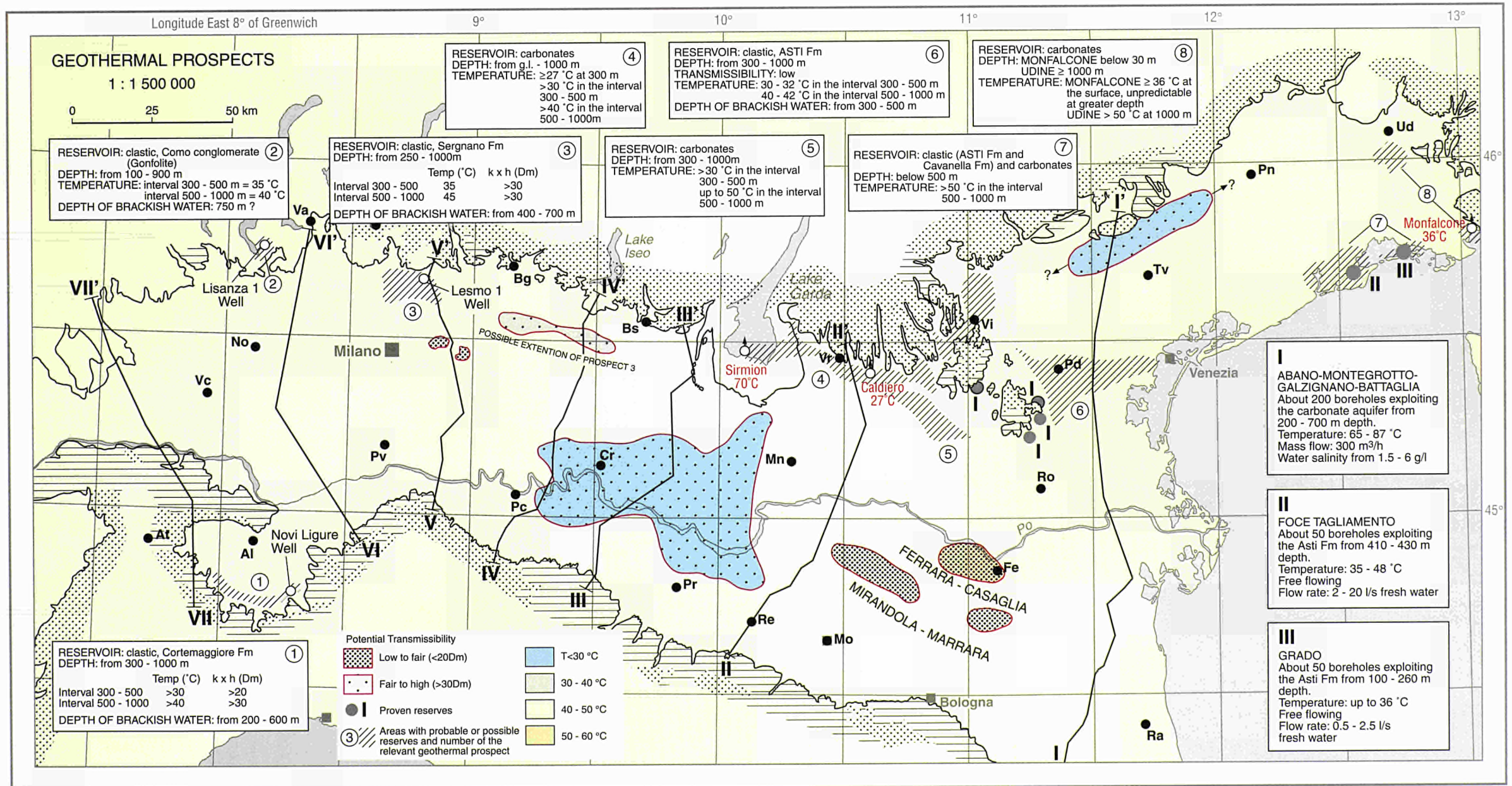
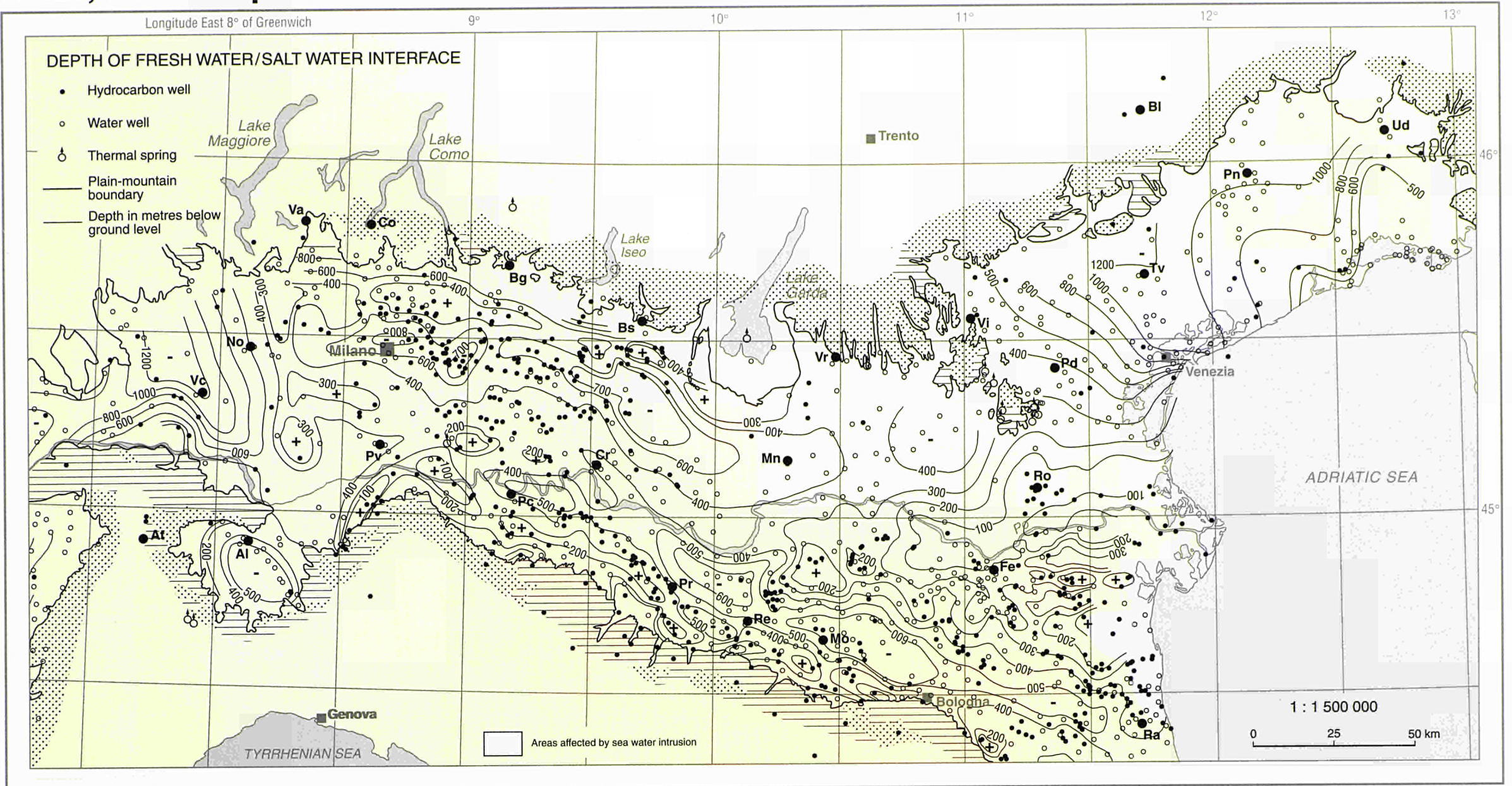


GEOHERMAL POTENTIAL AREAS from 500 - 1000 m depth

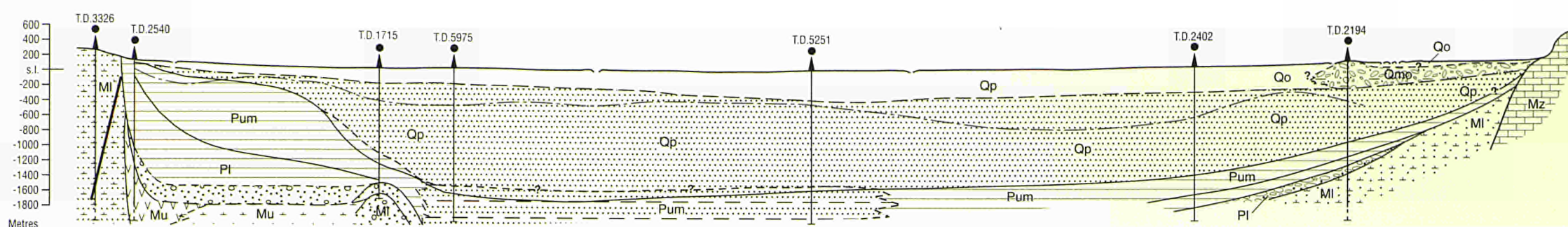
- Hydrocarbon well
- Water well
- ⊙ Thermal spring
- Plain-mountain boundary



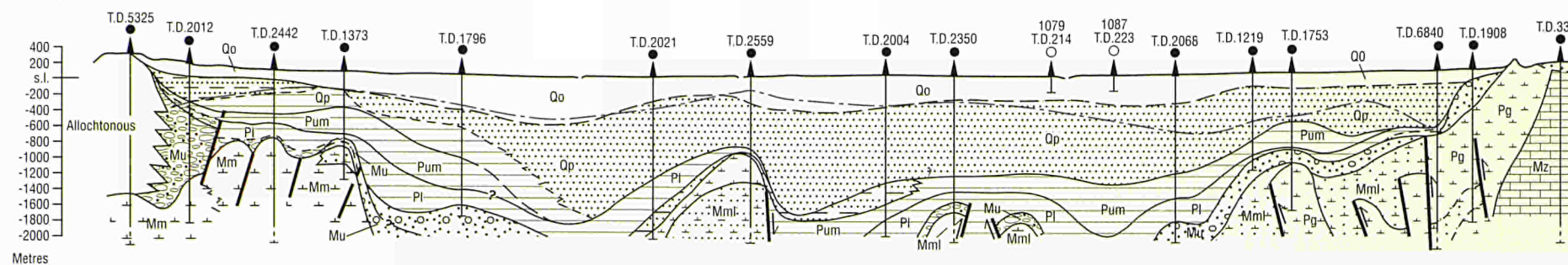
ITALY, Po River plain



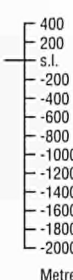
III CROSS SECTIONS



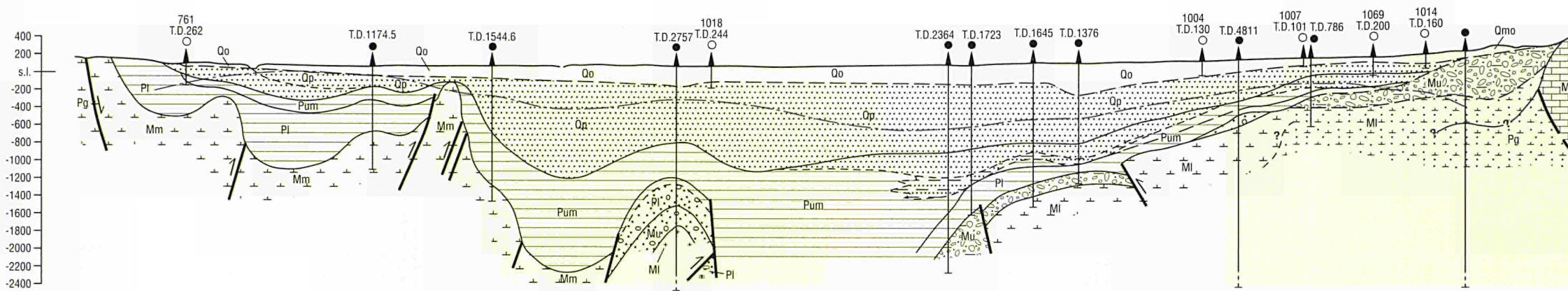
IV



IV'



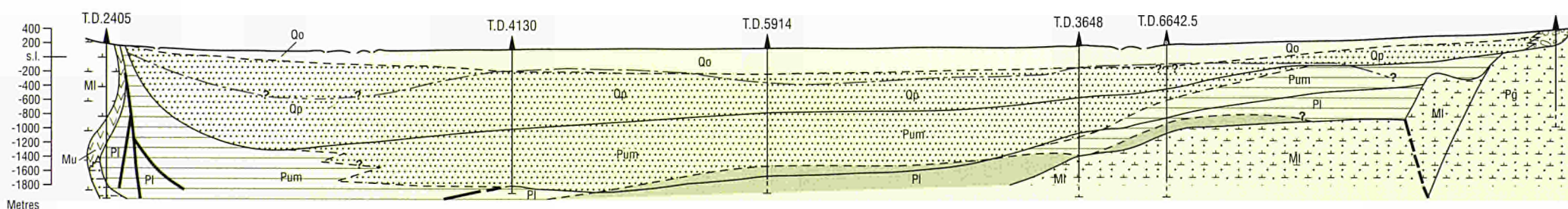
V



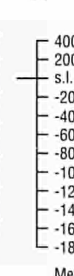
V'



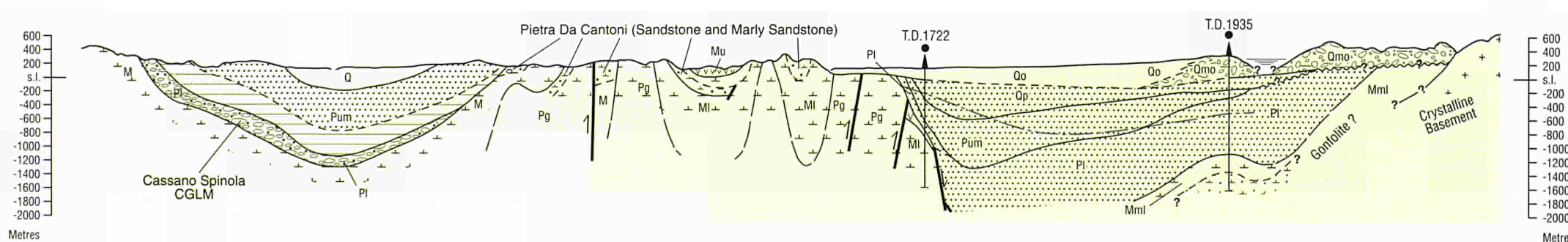
VI



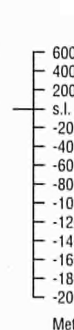
VI'



VII



VII'



LEGEND TO CROSS SECTIONS

- Fornace#1 Hydrocarbon well
- Thermal spring
- T.D. Total Depth in m
- Fault
- Contact between chronostratigraphical units
- - - Contact between formations (when not corresponding to a geochrone line)
- - - Fresh water-salt water interface

CHRONOSTATIGRAPHIC UNITS

- Q Undifferentiated Quaternary
 - Qo Olocene (Continental Quaternary)
 - Qp Pleistocene (Marine Quaternary)
- P Undifferentiated Pliocene
 - Pum Late-middle Pliocene (late-middle)
 - Pl Early Pliocene (early)
- M Undifferentiated Miocene
 - Mu Late Miocene
 - Mm Middle Miocene
 - MI Early Miocene
- Pg Undifferentiated Palaeogene
 - O Oligocene
 - E Eocene
- Mz Undifferentiated Mesozoic

LITHOSTRATIGRAPHIC AND HYDROGEOLOGICAL UNITS (Lower part of cross-sections)

AQUIFER UNITS

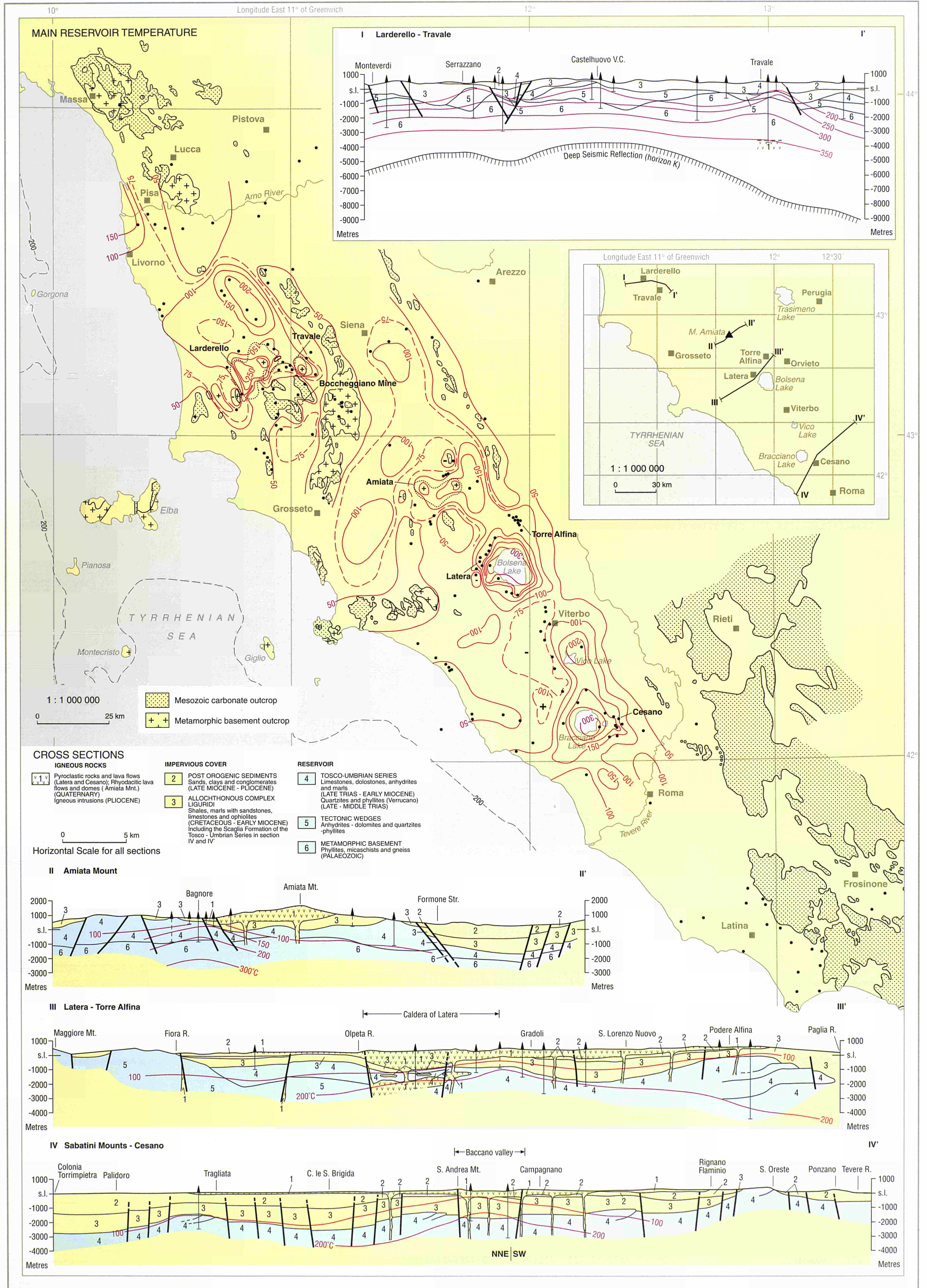
- Qo Continental Quaternary
- SA Asti sand
- PG Porto Garibaldi sand
- Pd Pandino sand
- DE Desana sand
- PC Porto Corsini sand
- M Magnago sand
- E Eraclea sand
- CT Cortemaggiore sand and gravel
- SC Caviaga sand
- FU Fusignano sandstone
- SR Sartirana sandstone
- SE Sergnano gravel
- GC Cavarella glauconitic sandstone
- MA Marnoso-arenacea
- G Gonfolite
- Ls Undifferentiated carbonic formations

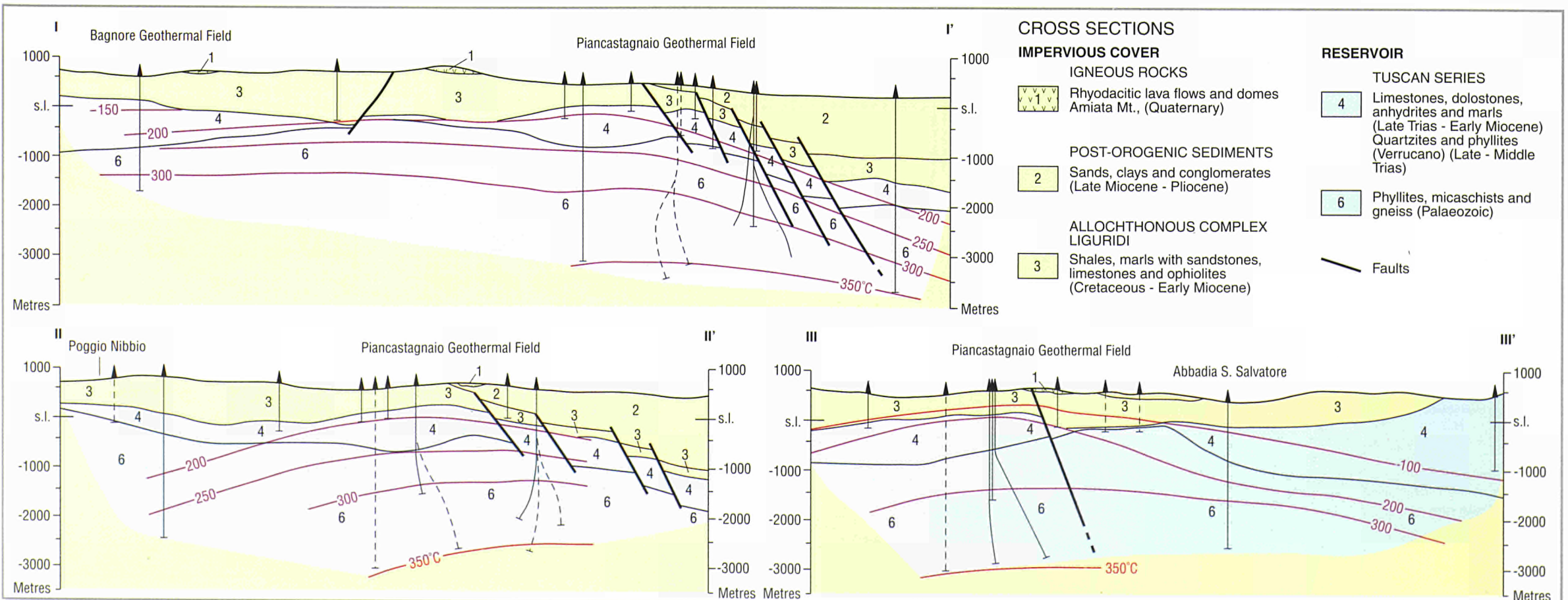
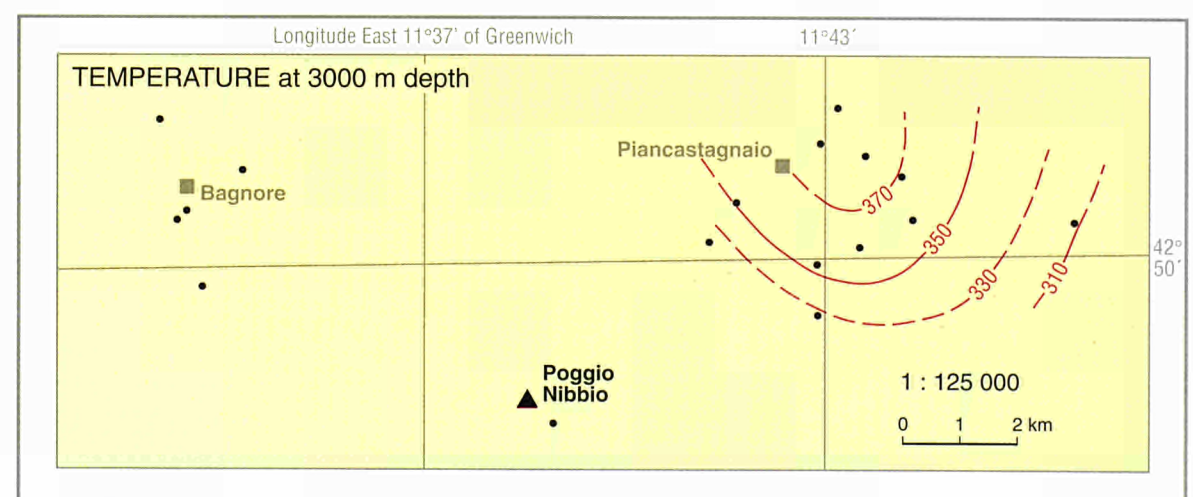
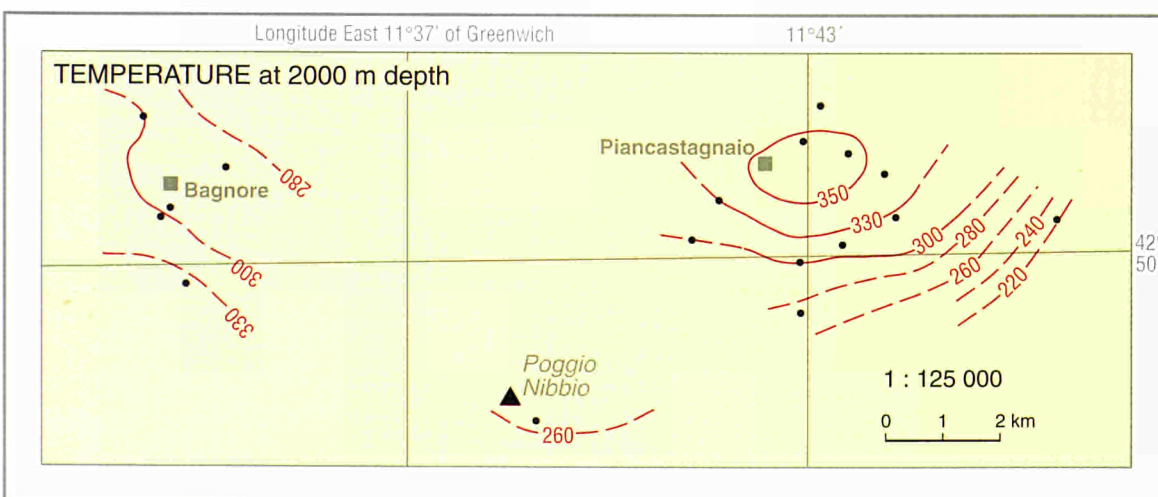
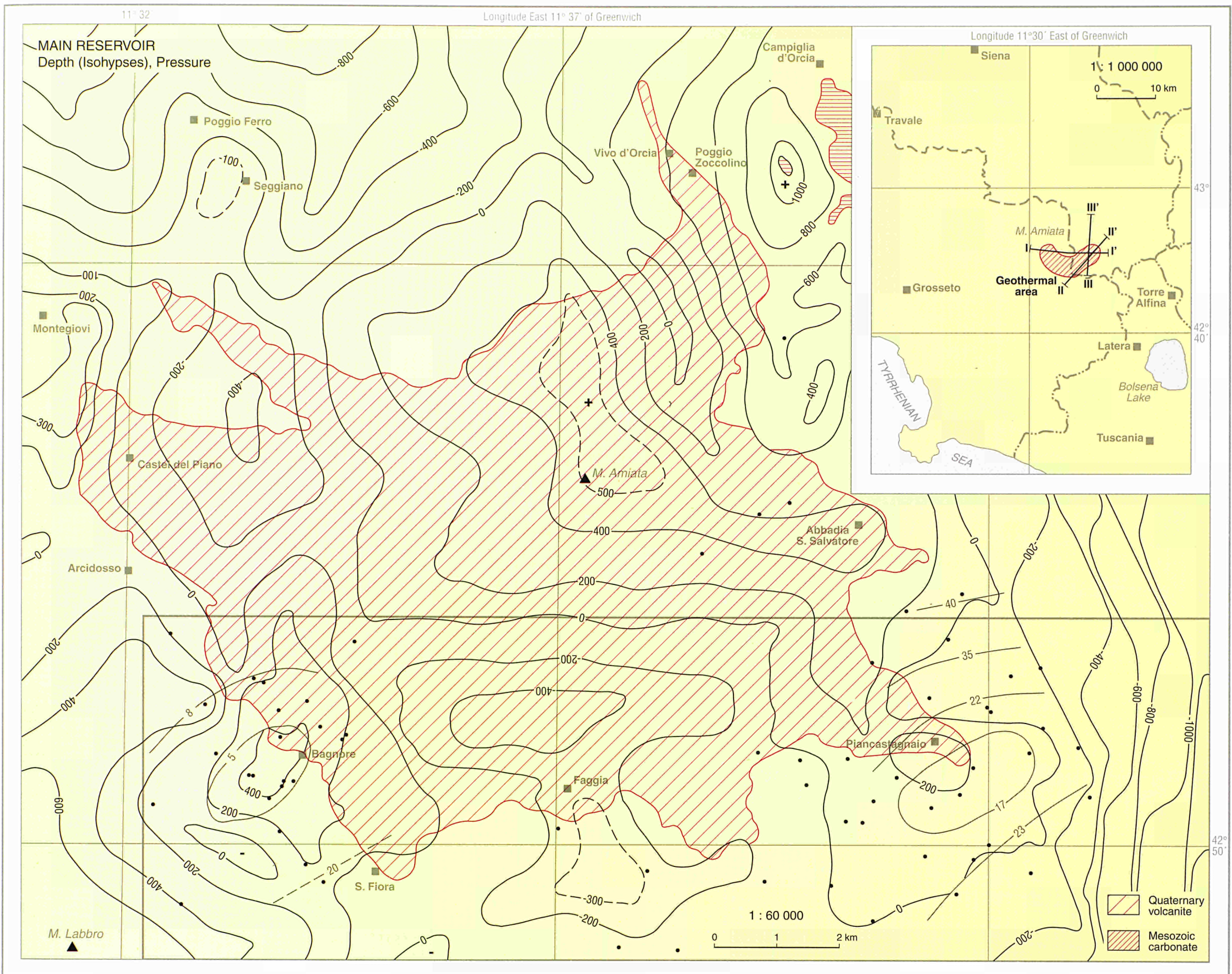
AQUICLUDE UNITS

- Qmo Morainic
- AS Santerno clay
- CO Colombacci clay
- GS Gessoso-solfifera and gypsum arenites
- SD S. Donā marl
- MG Gallare marl
- V Volcanic or crystalline basement

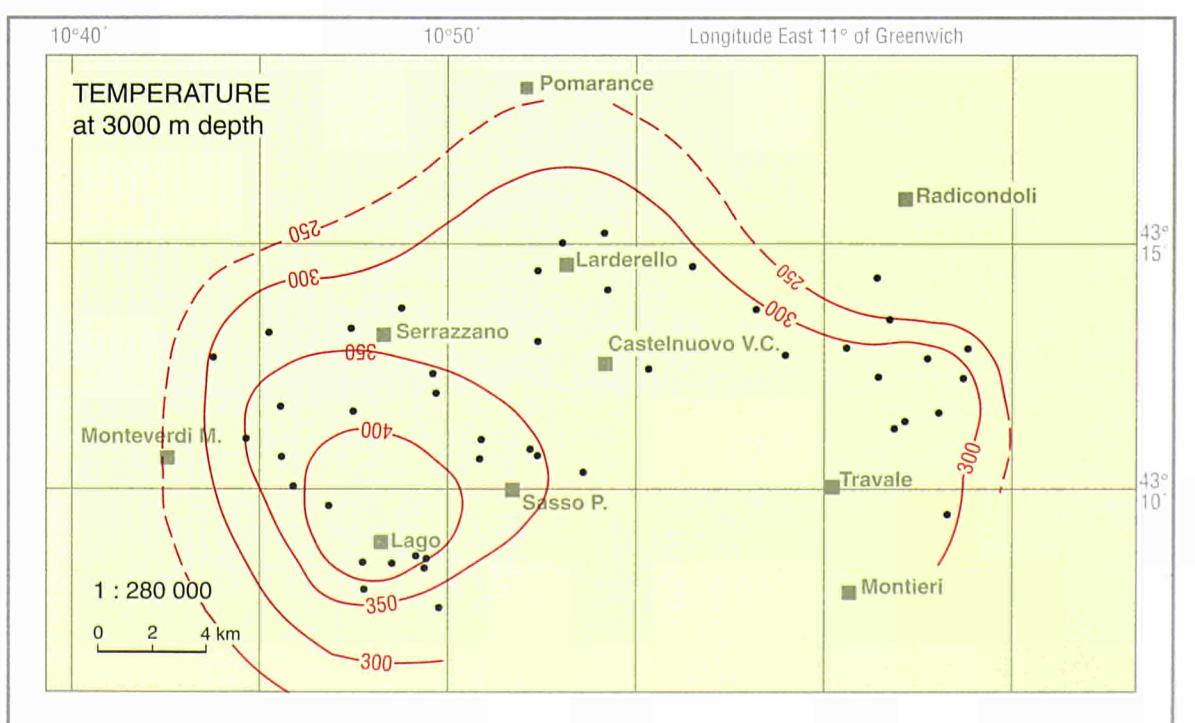
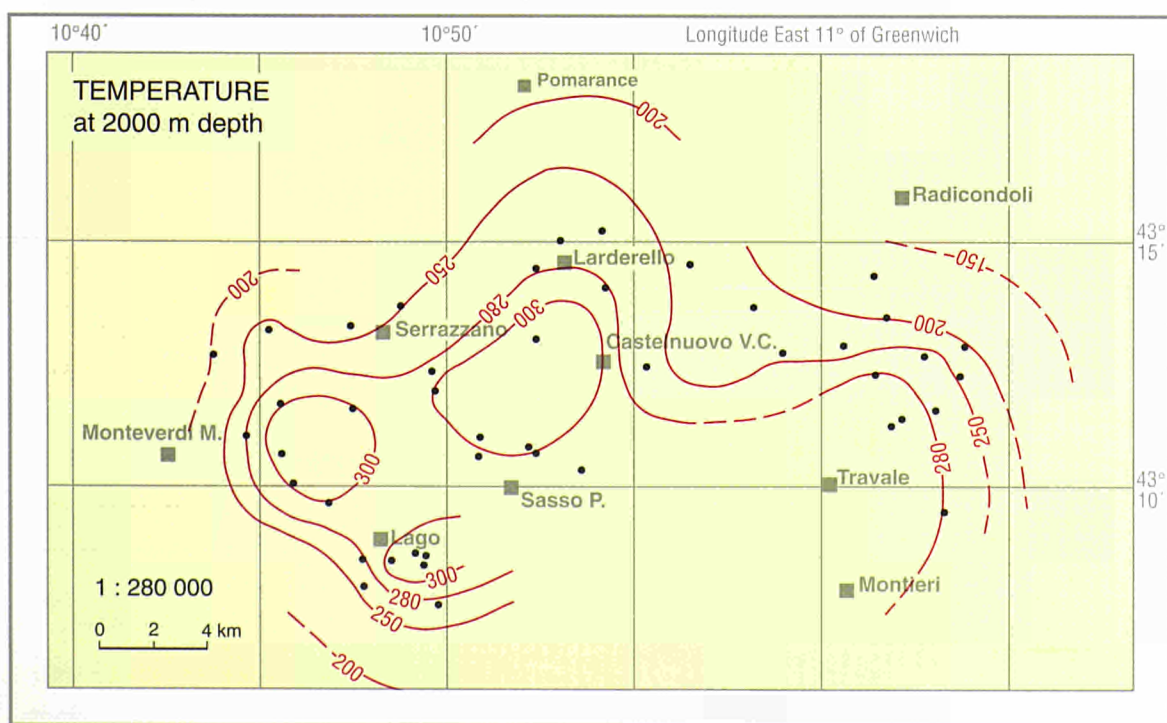
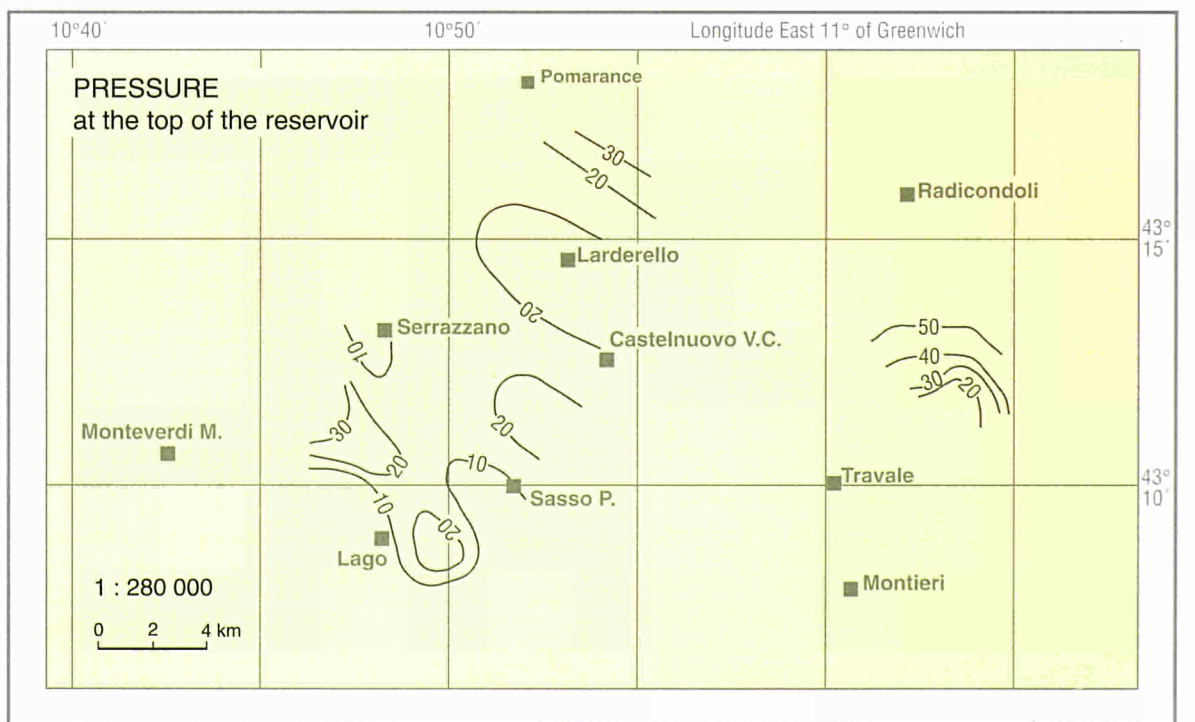
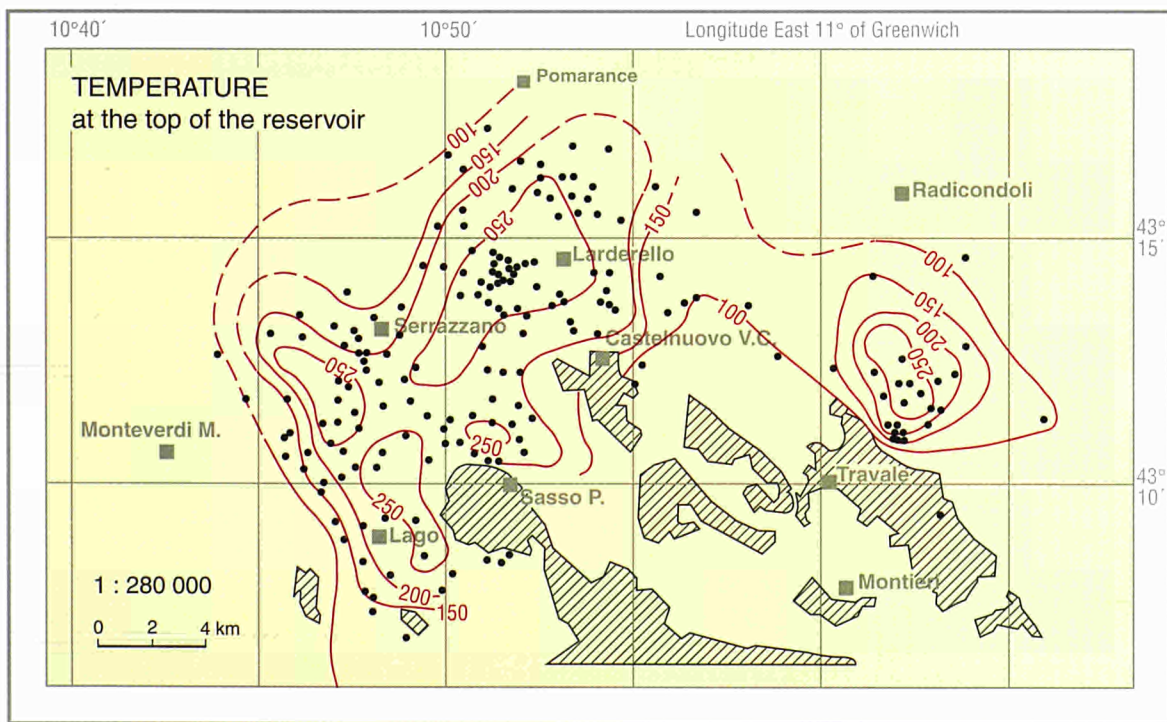
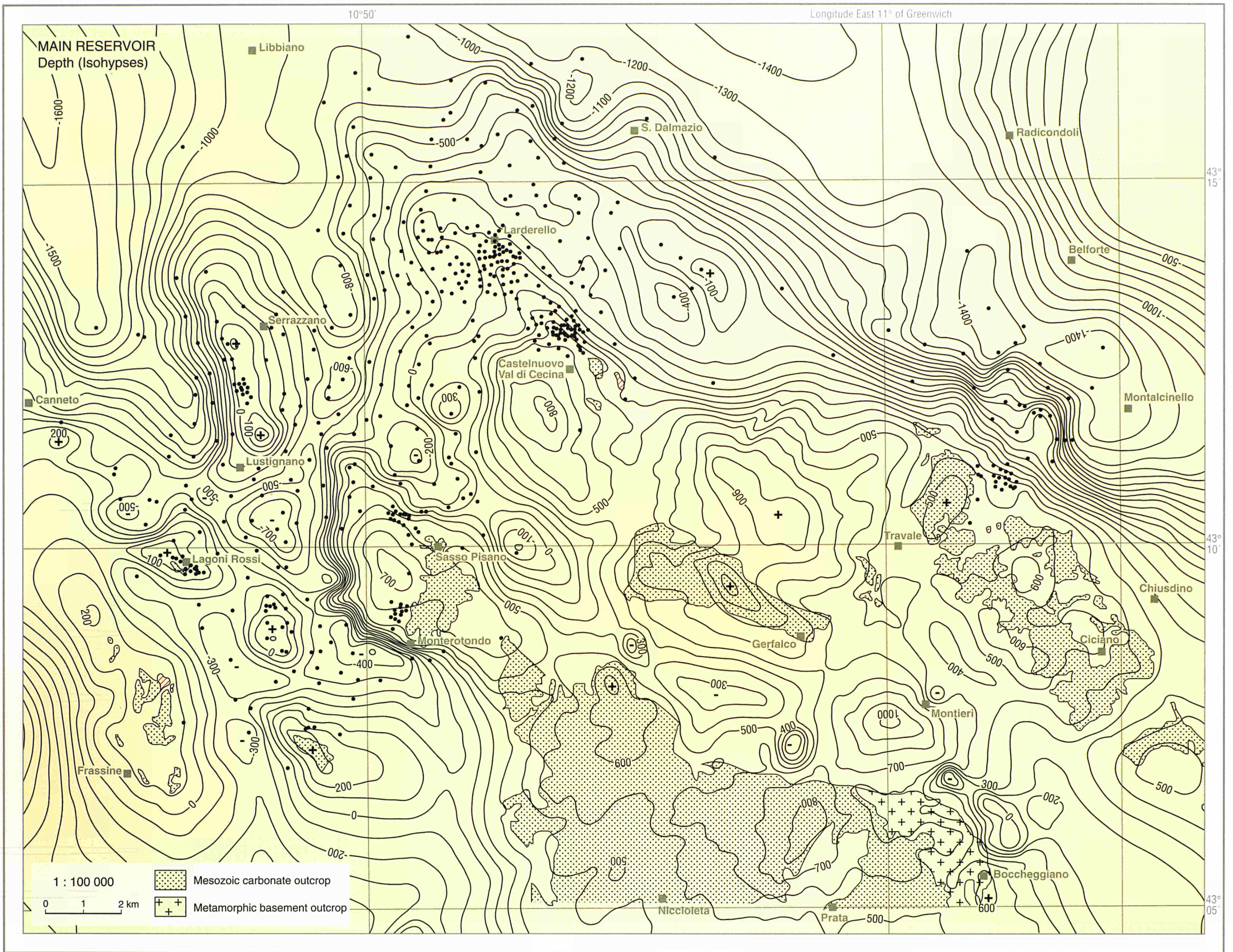
0 5 10 km
Horizontal Scale for all sections

REMARK: The lithostratigraphic units reported in the legend are only those occurring in the cross-section

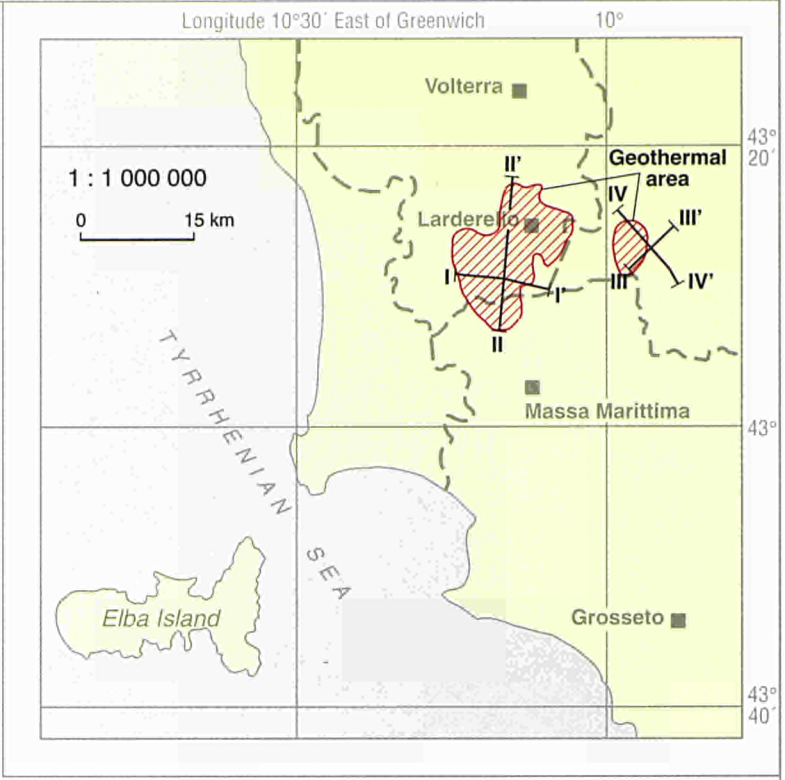
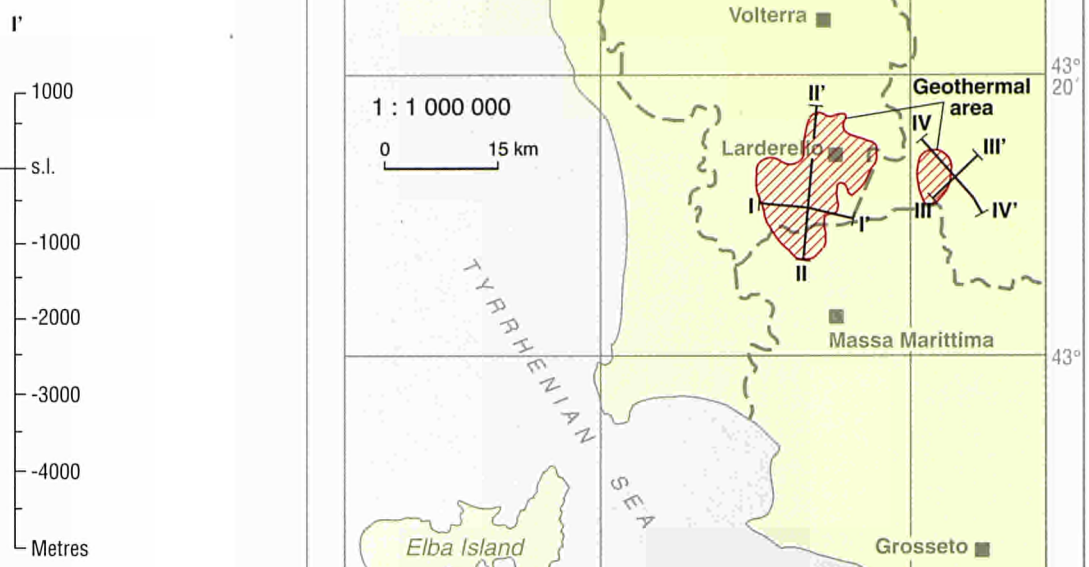
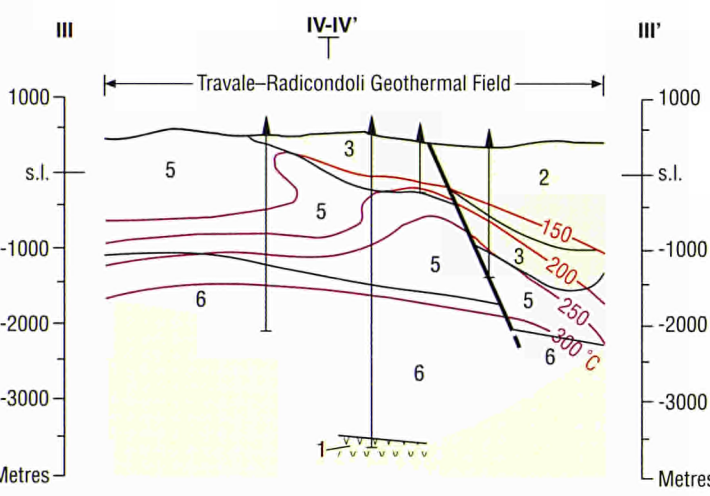
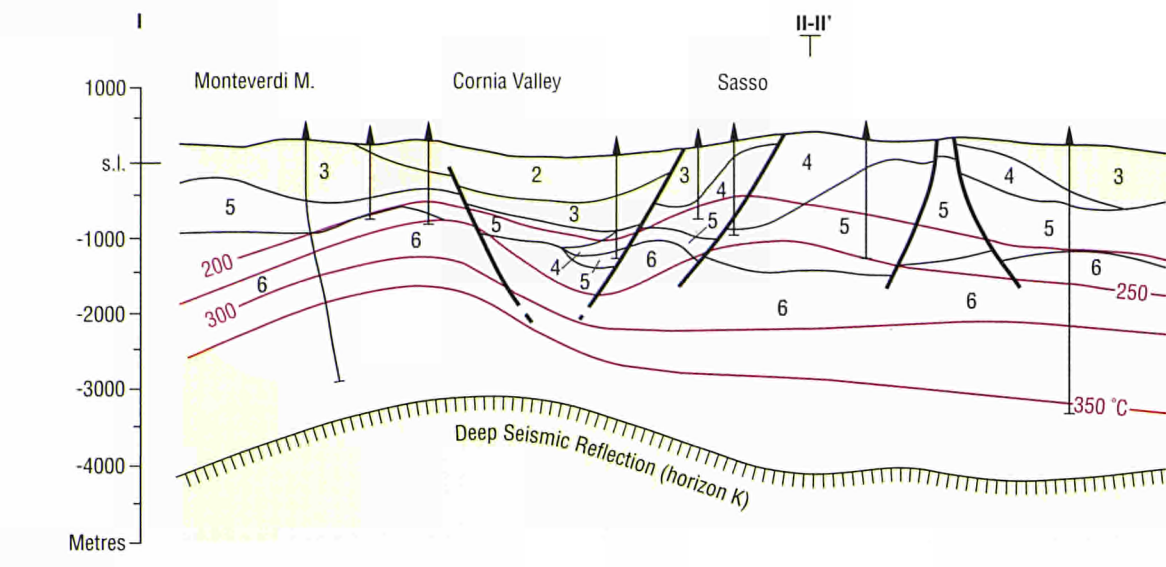




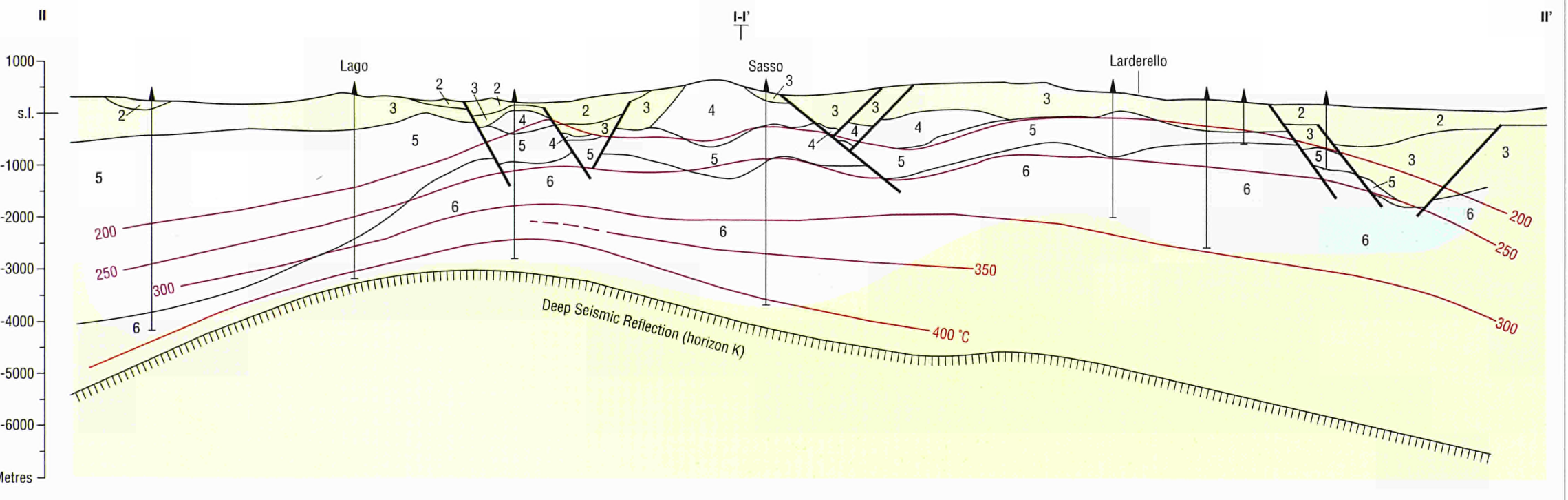
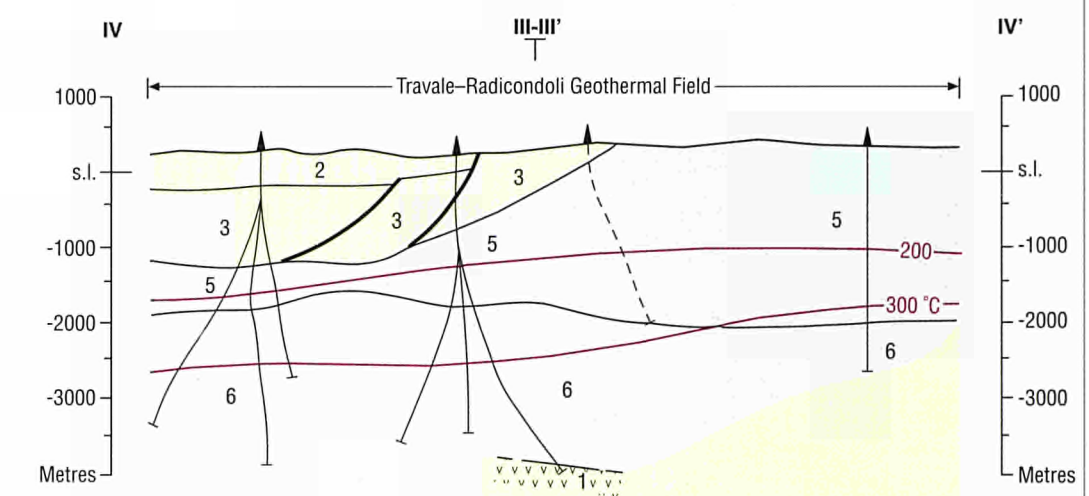
ITALY, Larderello and Travale-Radicondoli



CROSS SECTIONS

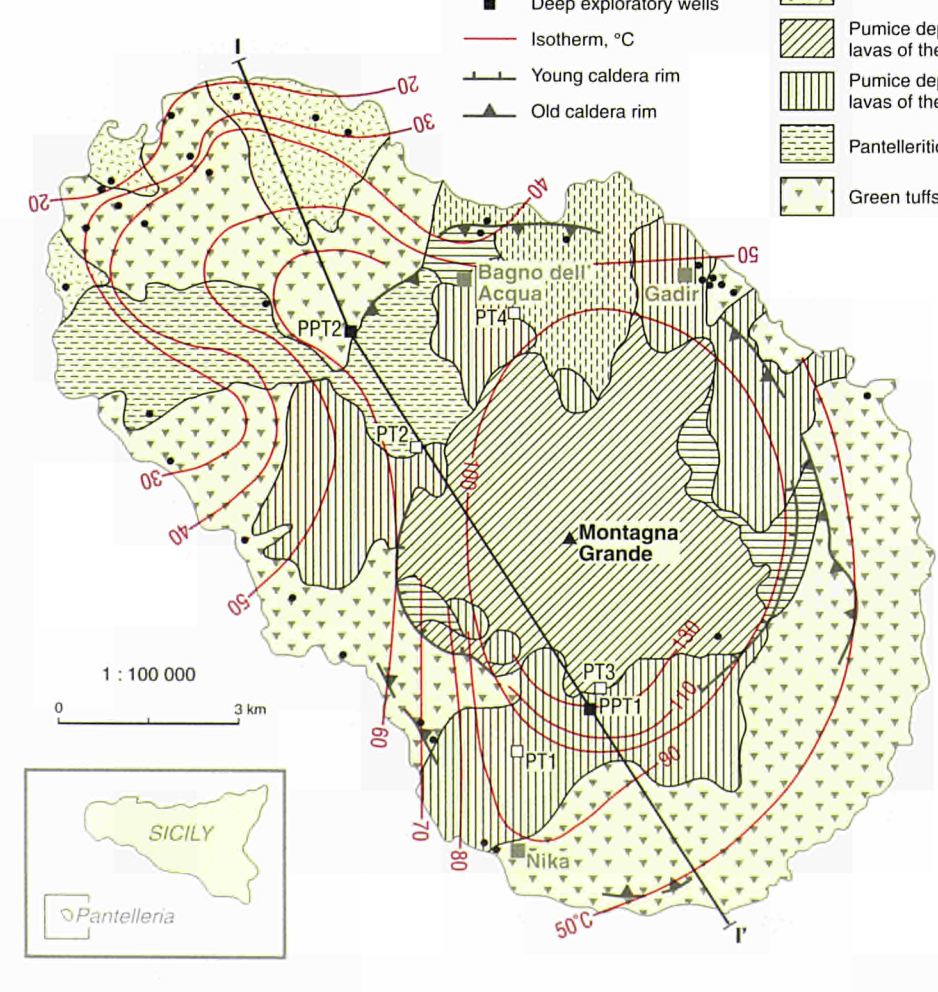


- IGNEOUS ROCKS**
- Igneous intrusions (PLIOCENE)
- IMPERVIOUS COVER**
- 2 POST OROGENIC SEDIMENTS
Sands, clays and conglomerates (LATE MIOCENE - PLIOCENE)
 - 3 ALLOCTHONOUS COMPLEX LIGURIDI
Shales, marls with sandstones, limestones and ophiolites (CRETACEOUS - EARLY MIOCENE)
- RESERVOIR**
- 4 TUSCAN SERIES
Limestones, dolostones, anhydrites and marls (LATE TRIAS - EARLY MIOCENE)
Quartzites and phyllites (Verrucano) (LATE - MIDDLE TRIAS)
 - 5 TECTONIC WEDGES
Anhydrites - dolomites and quartzites - phyllites
 - 6 METAMORPHIC BASEMENT
Phyllites, micaschists and gneiss (PALAEOZOIC)



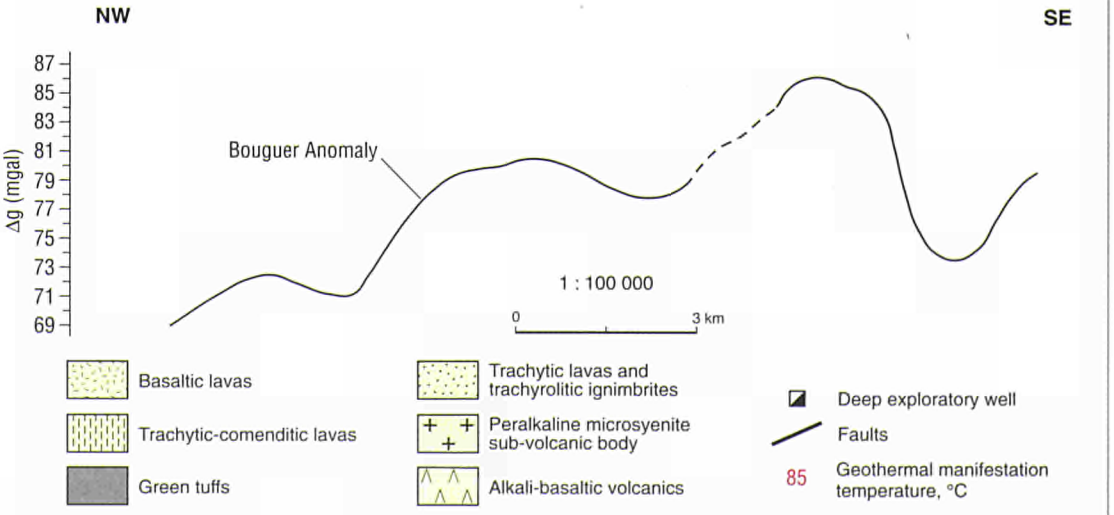
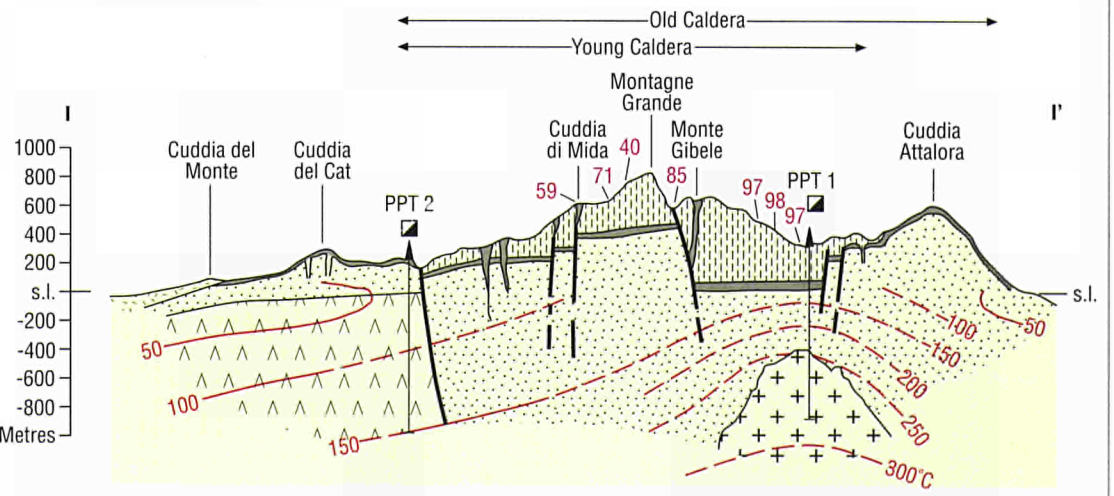
PANTELLERIA ISLAND

Temperature at sea level

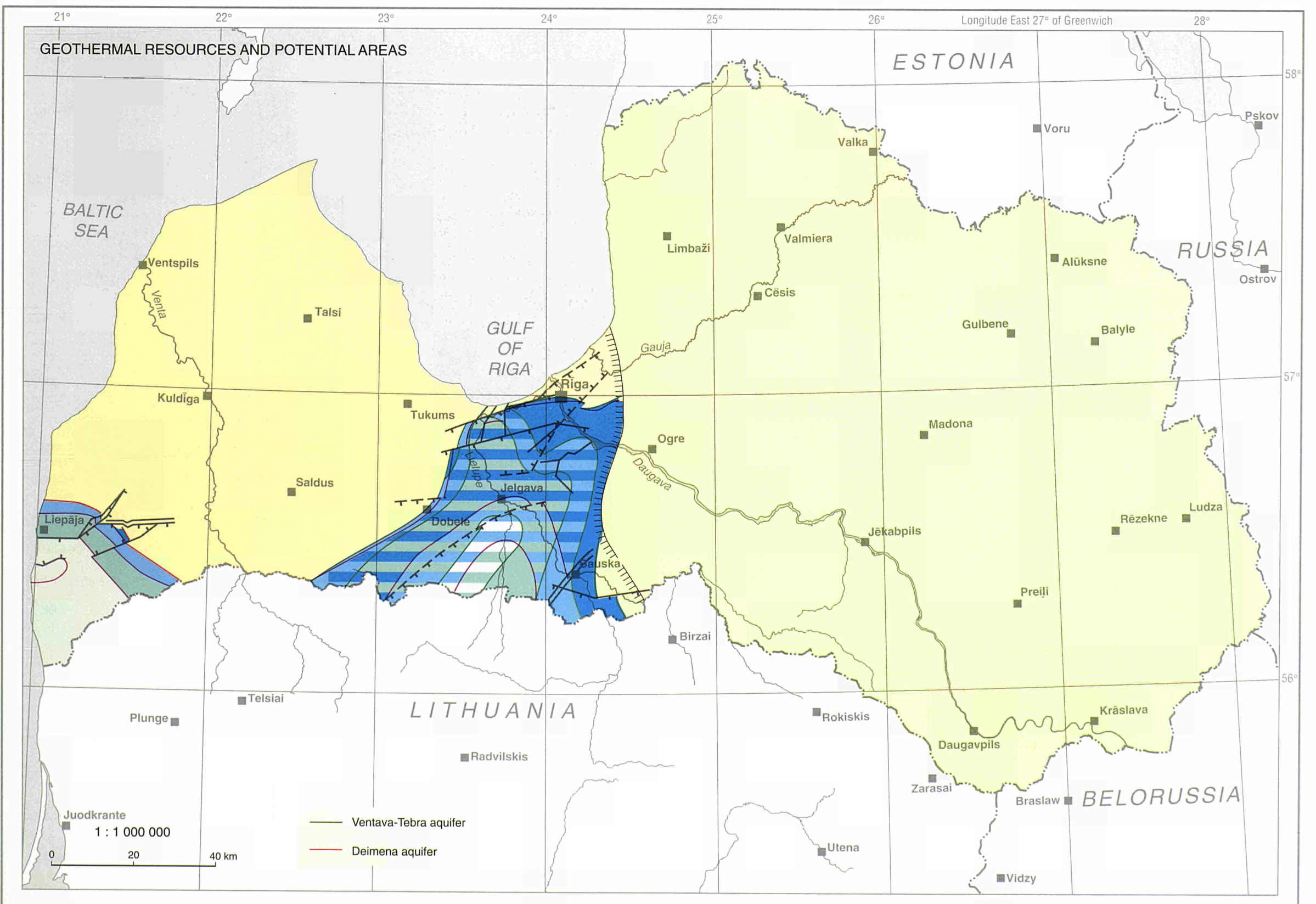
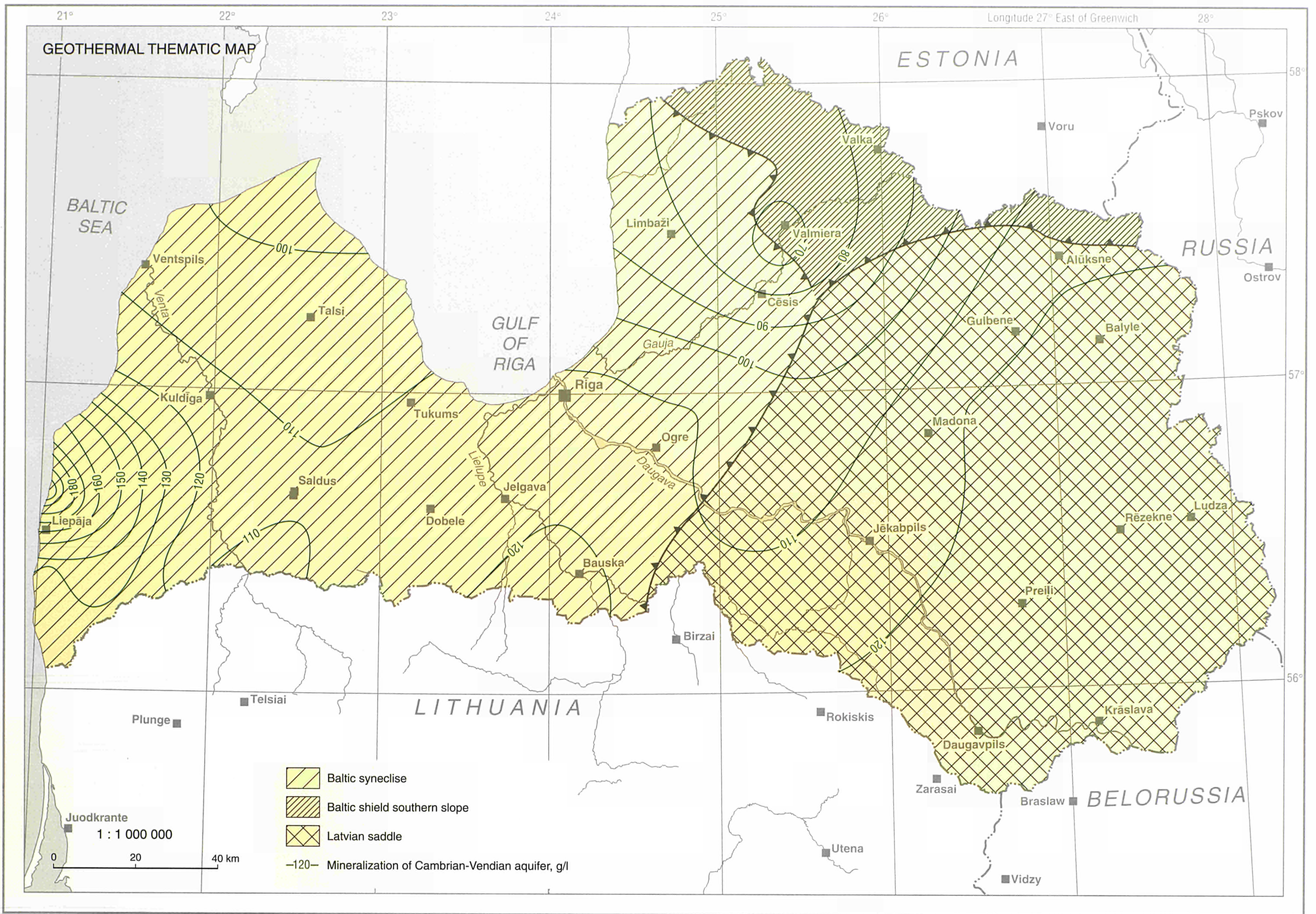


- Water-wells and springs
- Shallow exploratory well
- Deep exploratory wells
- Isotherm, °C
- Young caldera rim
- Old caldera rim
- Sedimentary terrains
- Basaltic lavas
- Pumice deposits and pantelleritic lavas of the II and III cycle
- Pumice deposits and pantelleritic lavas of the IV cycle
- Pantelleritic domes
- Green tufts

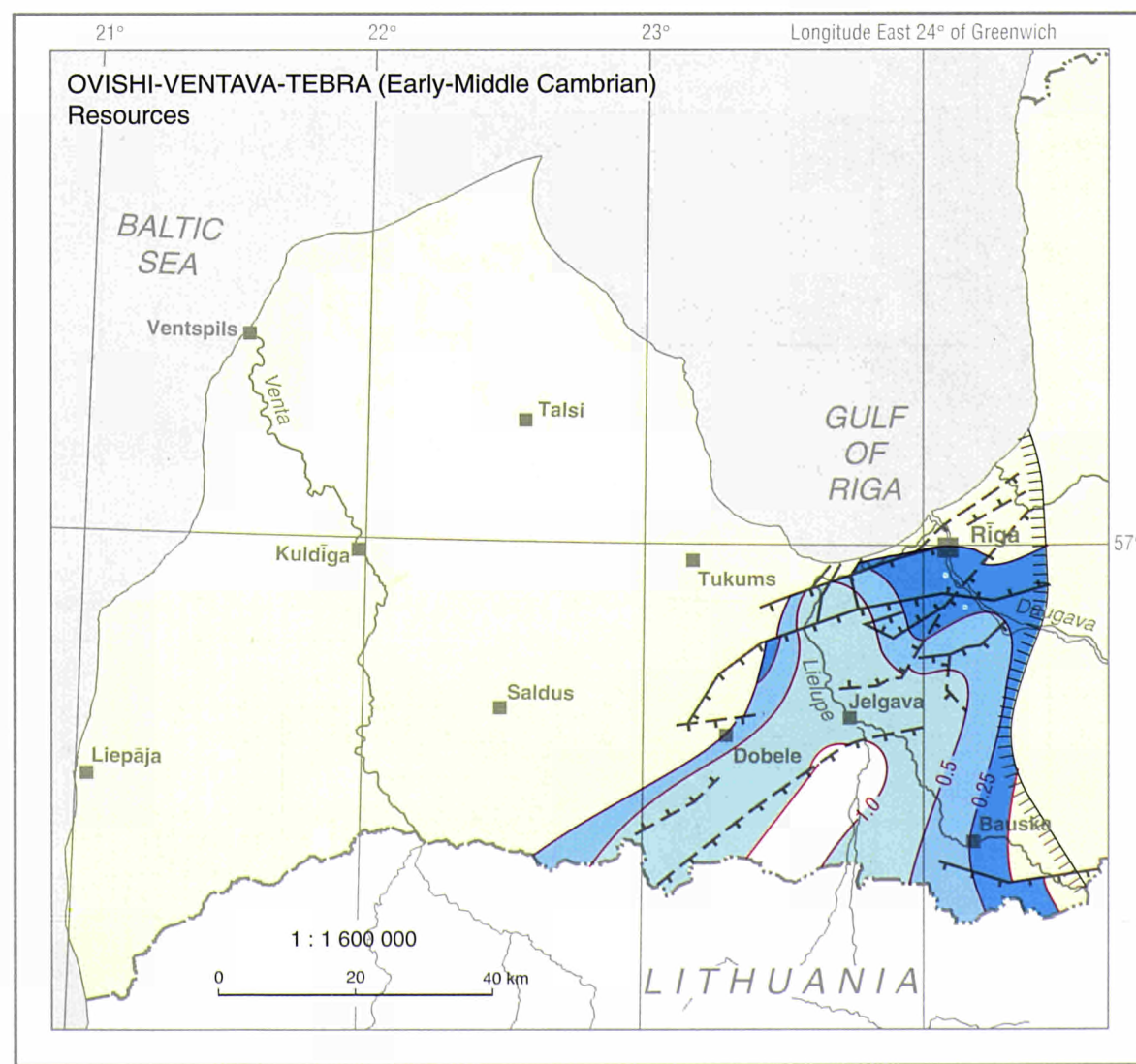
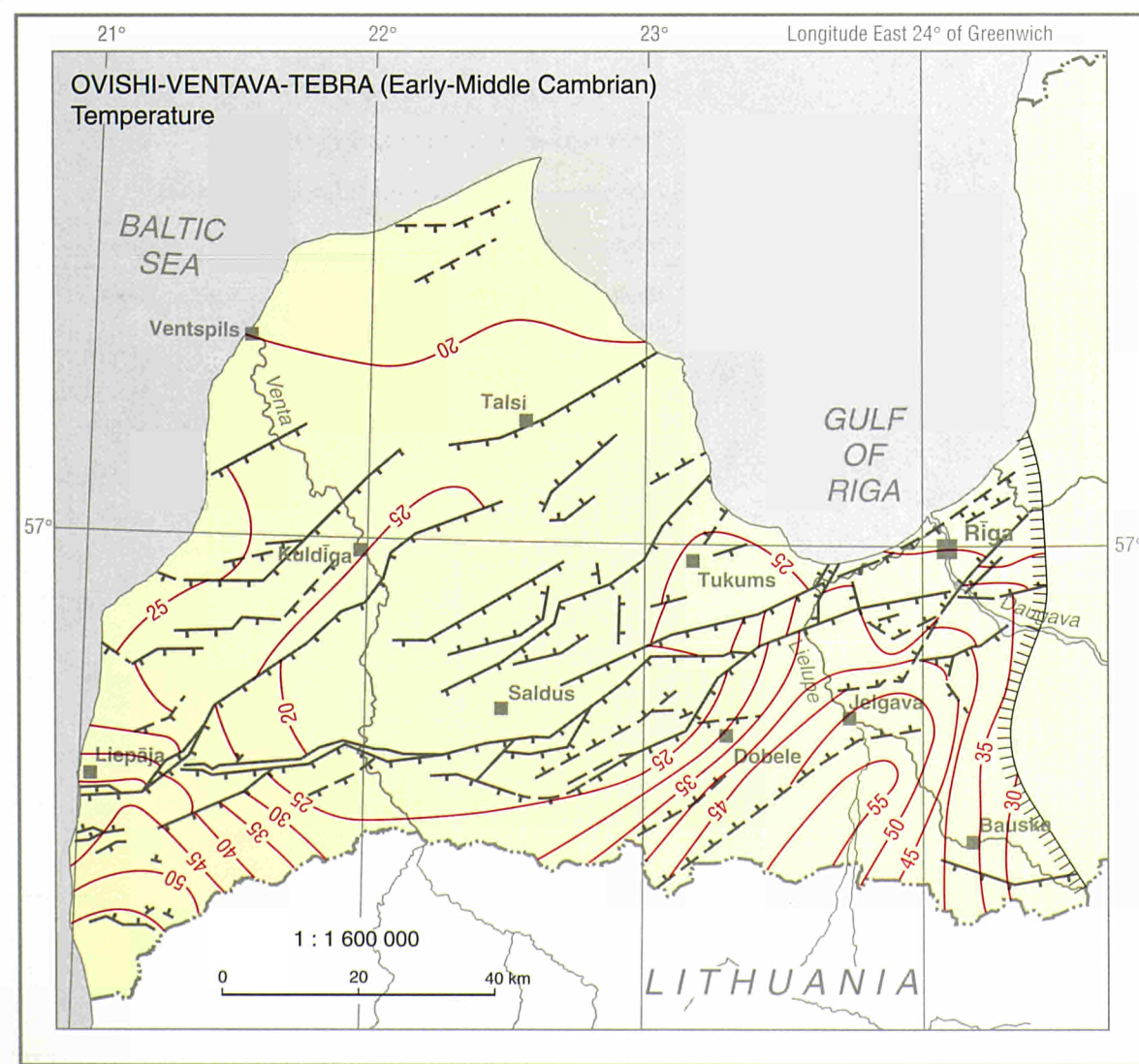
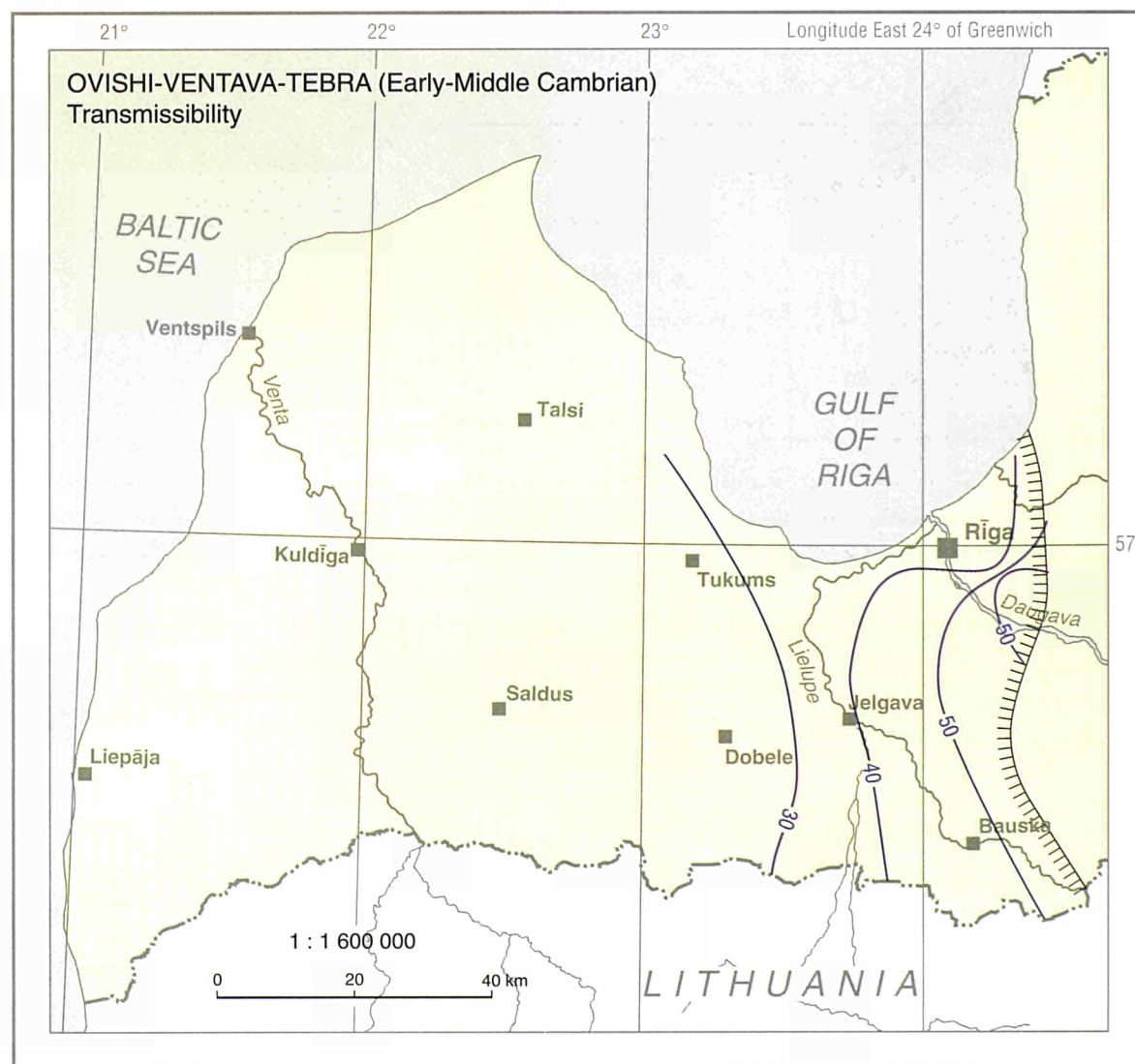
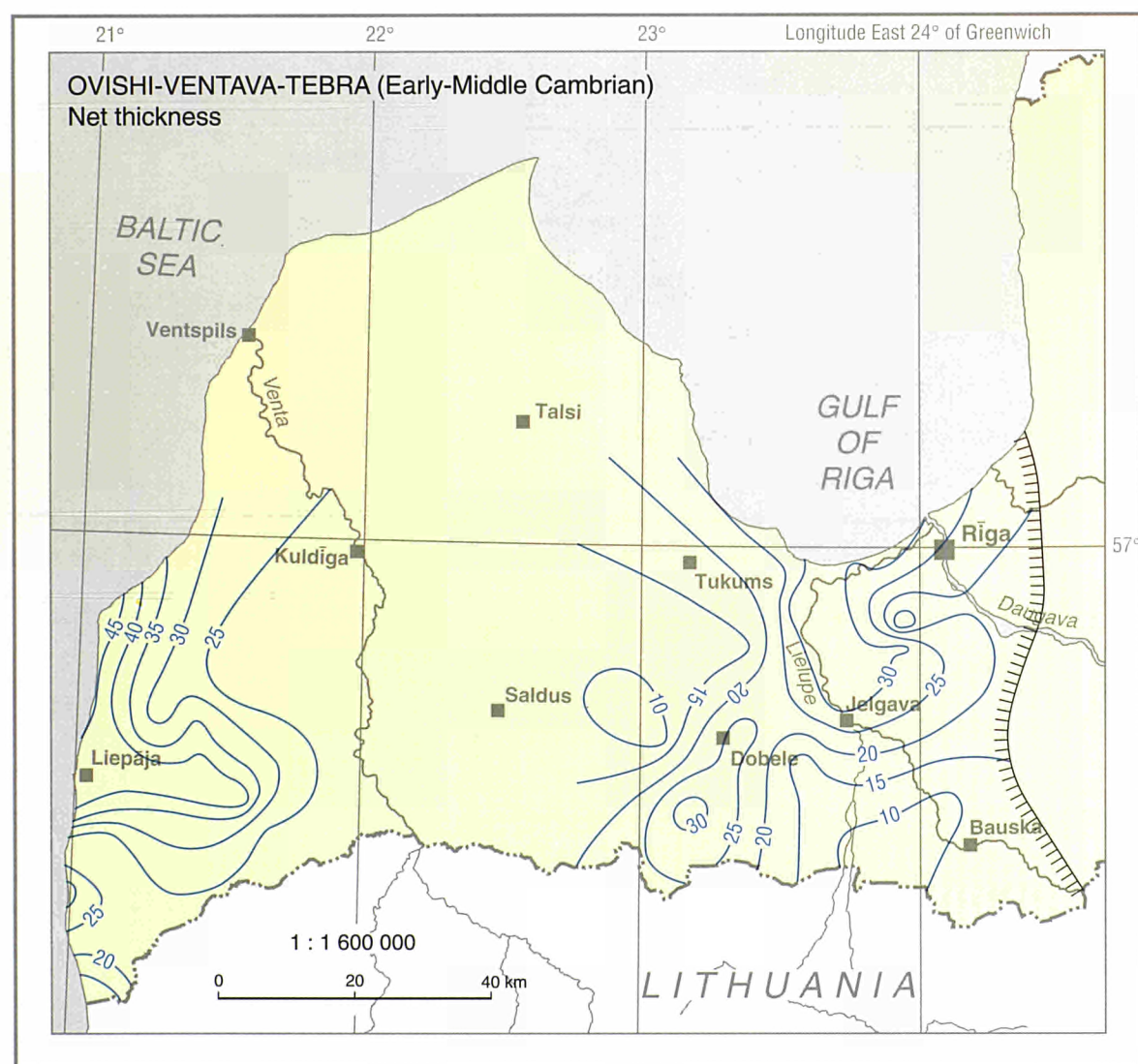
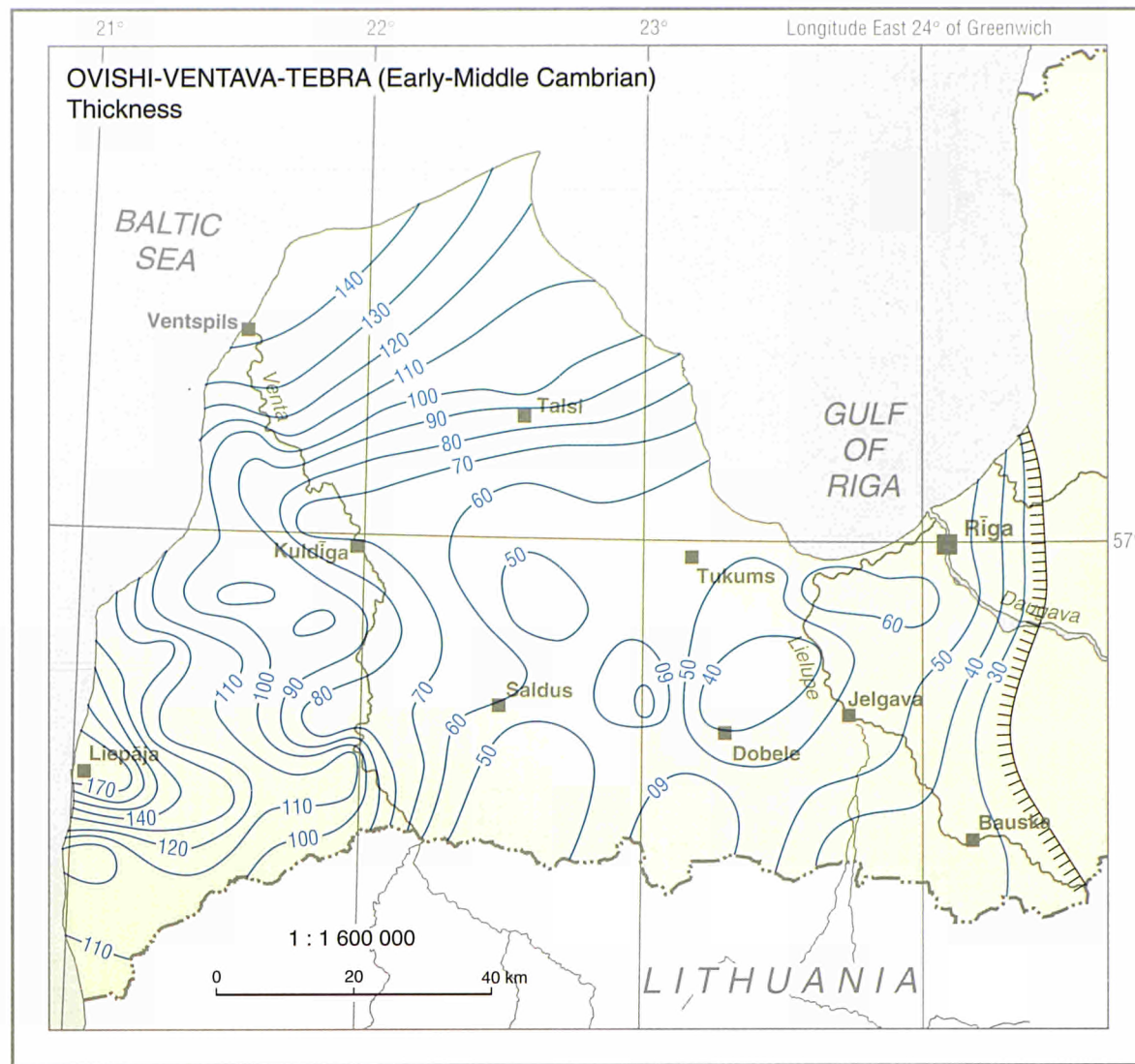
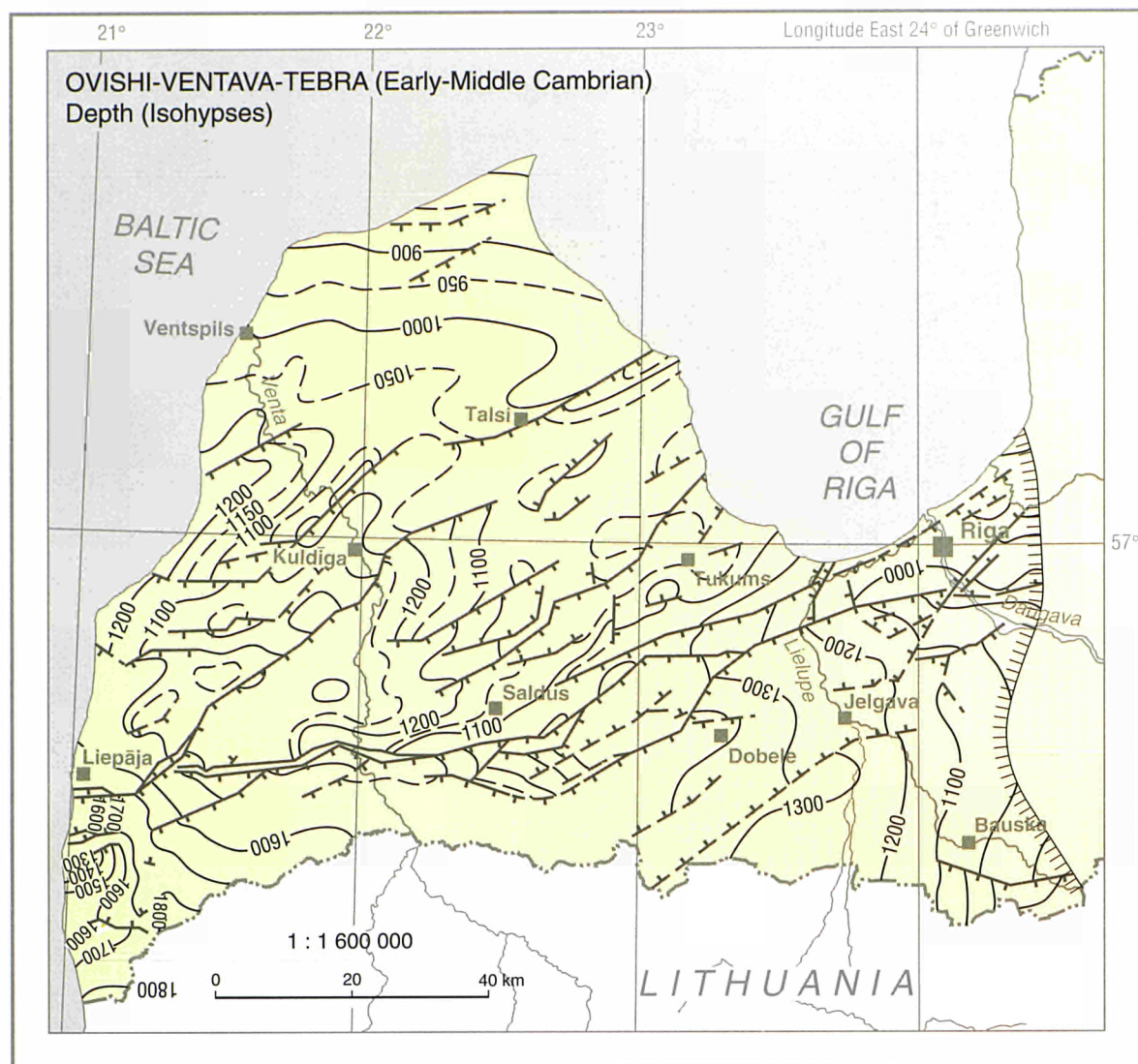
CROSS SECTION

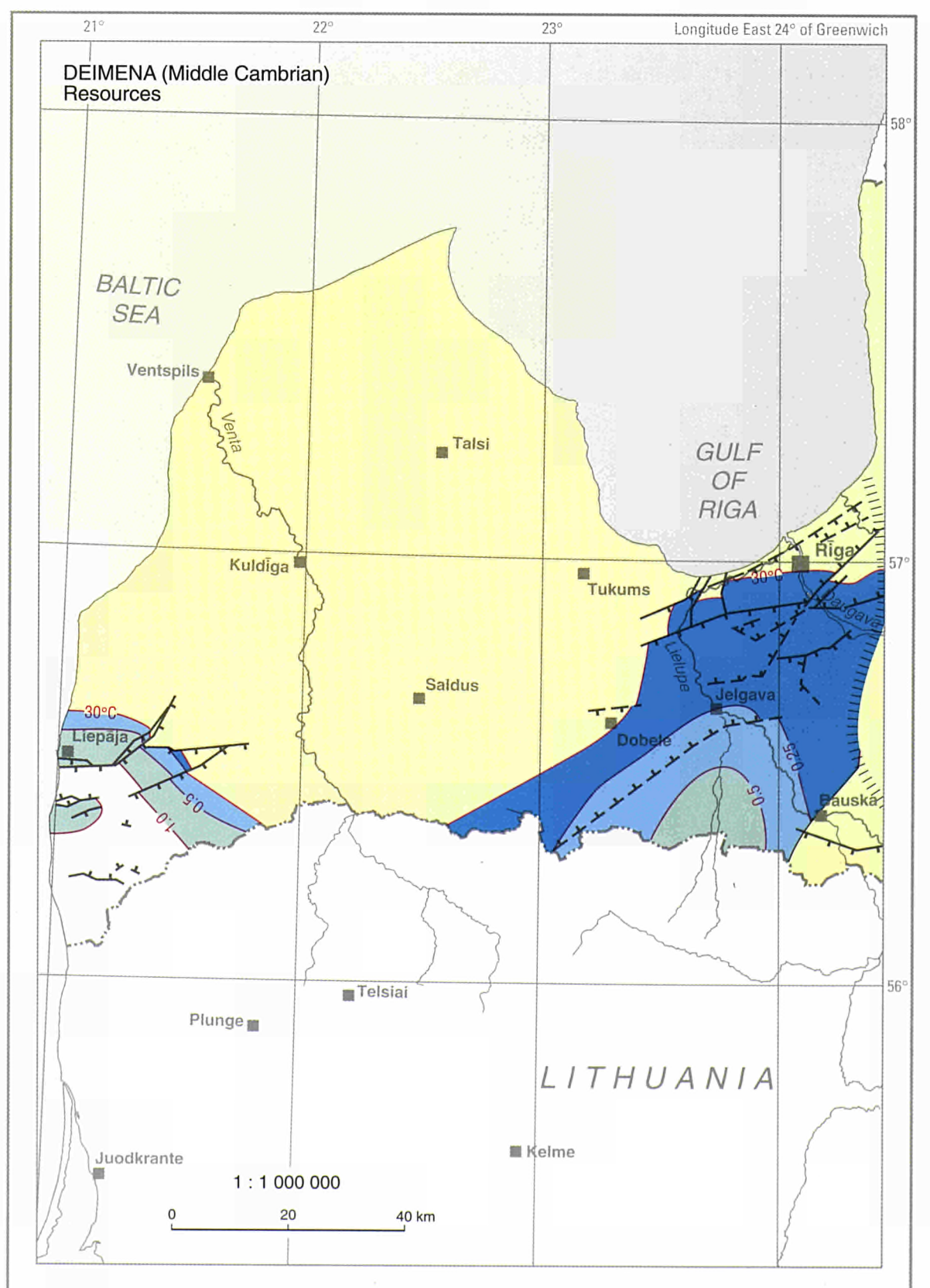
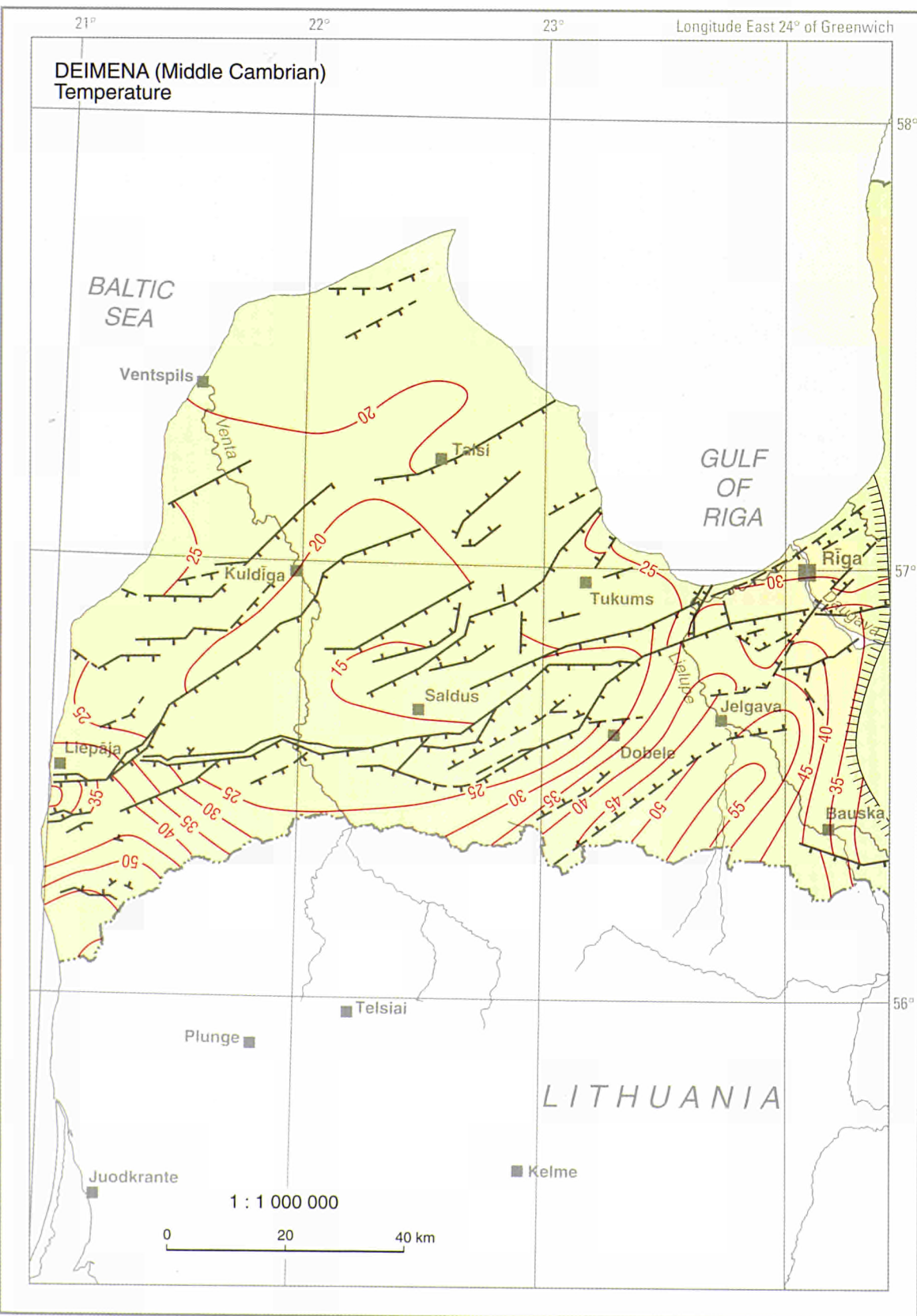
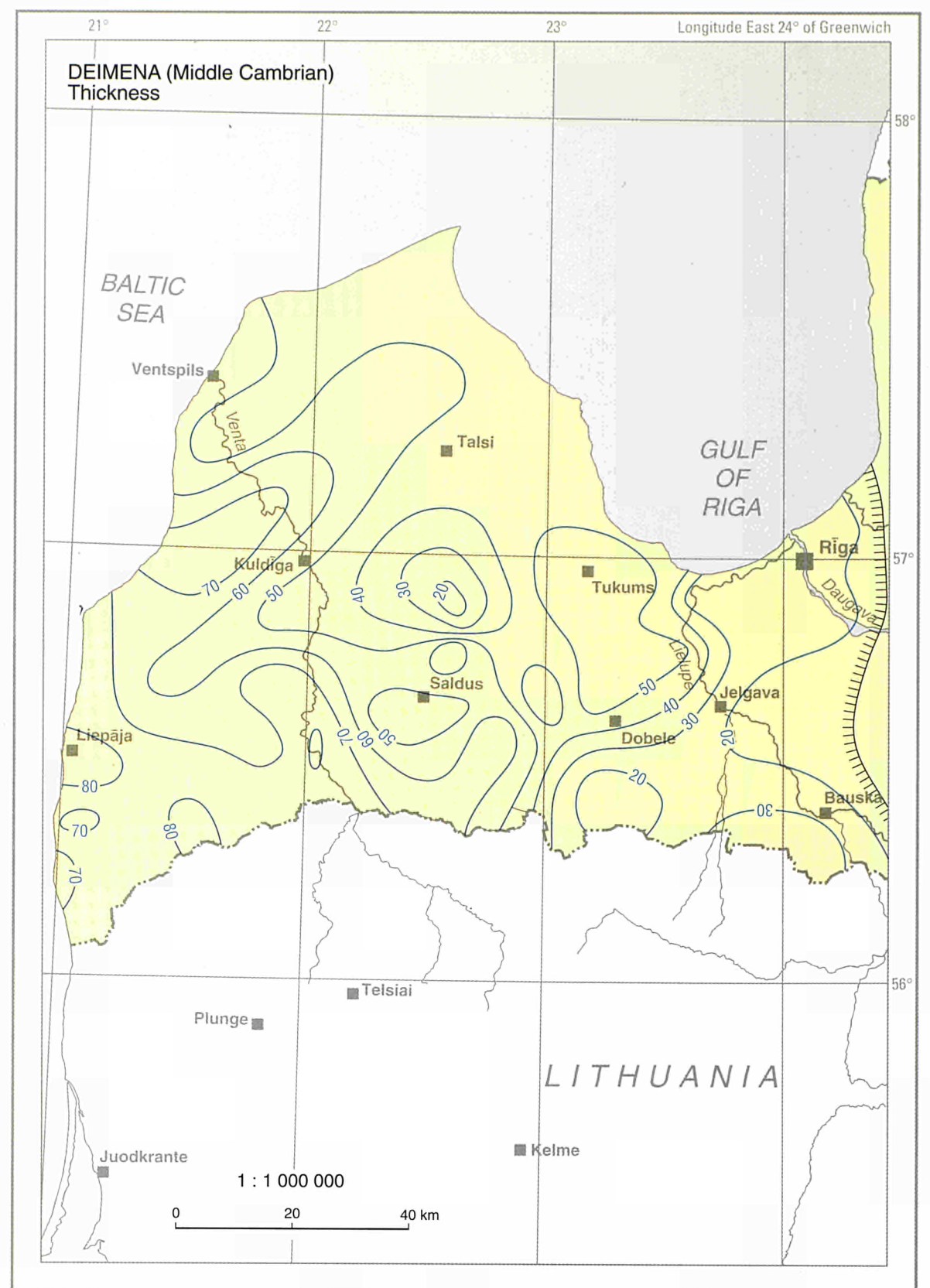


LATVIA

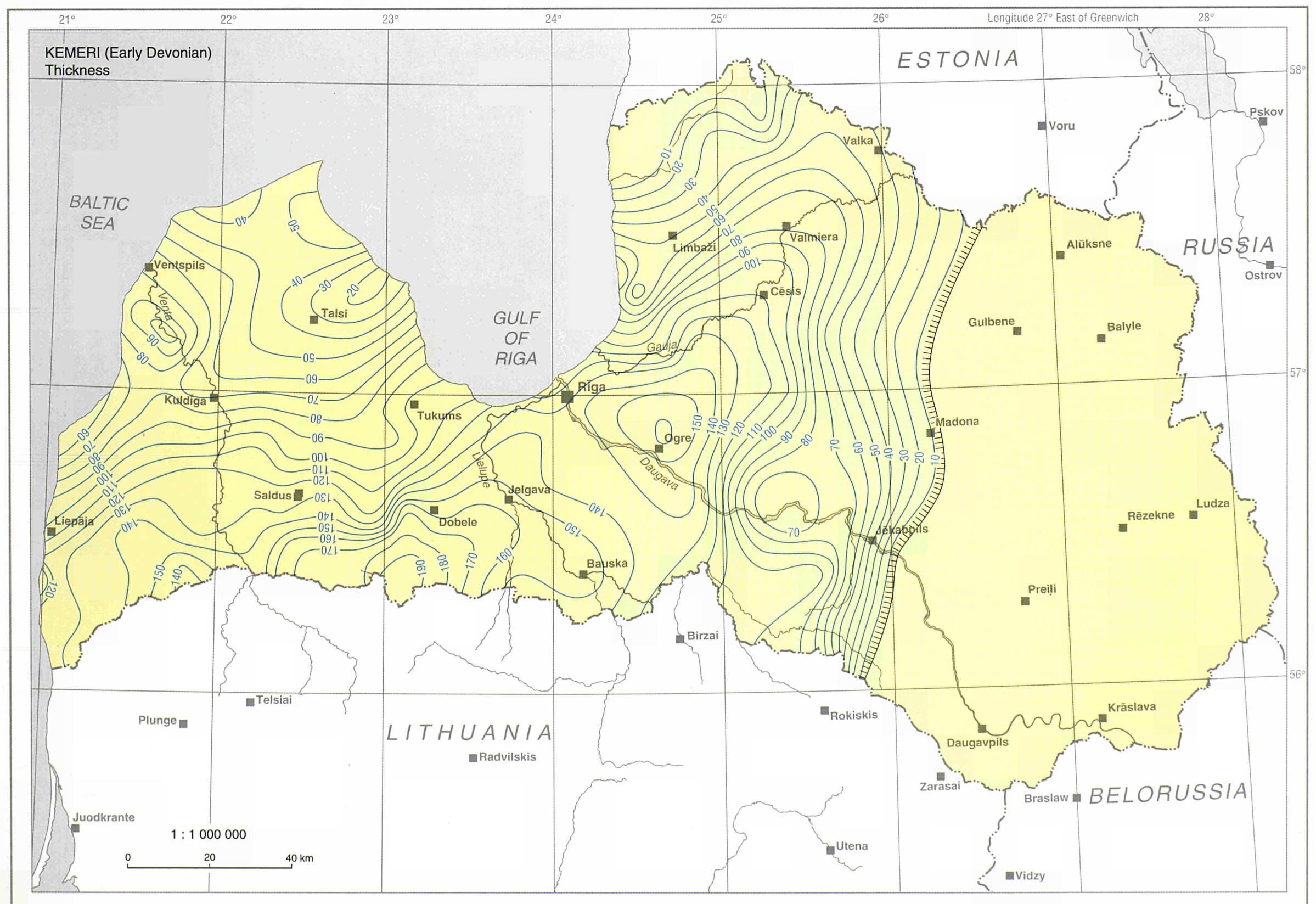
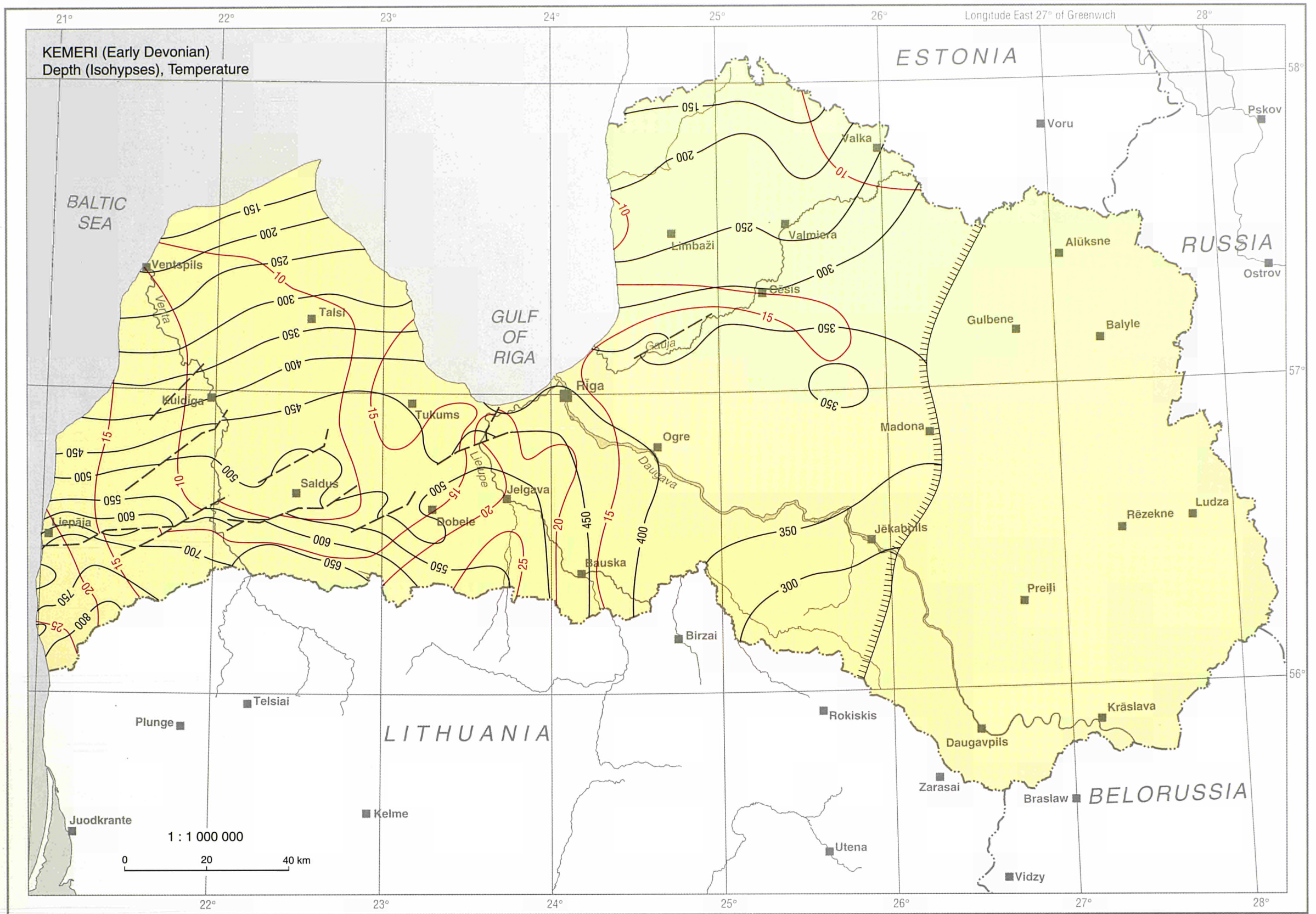


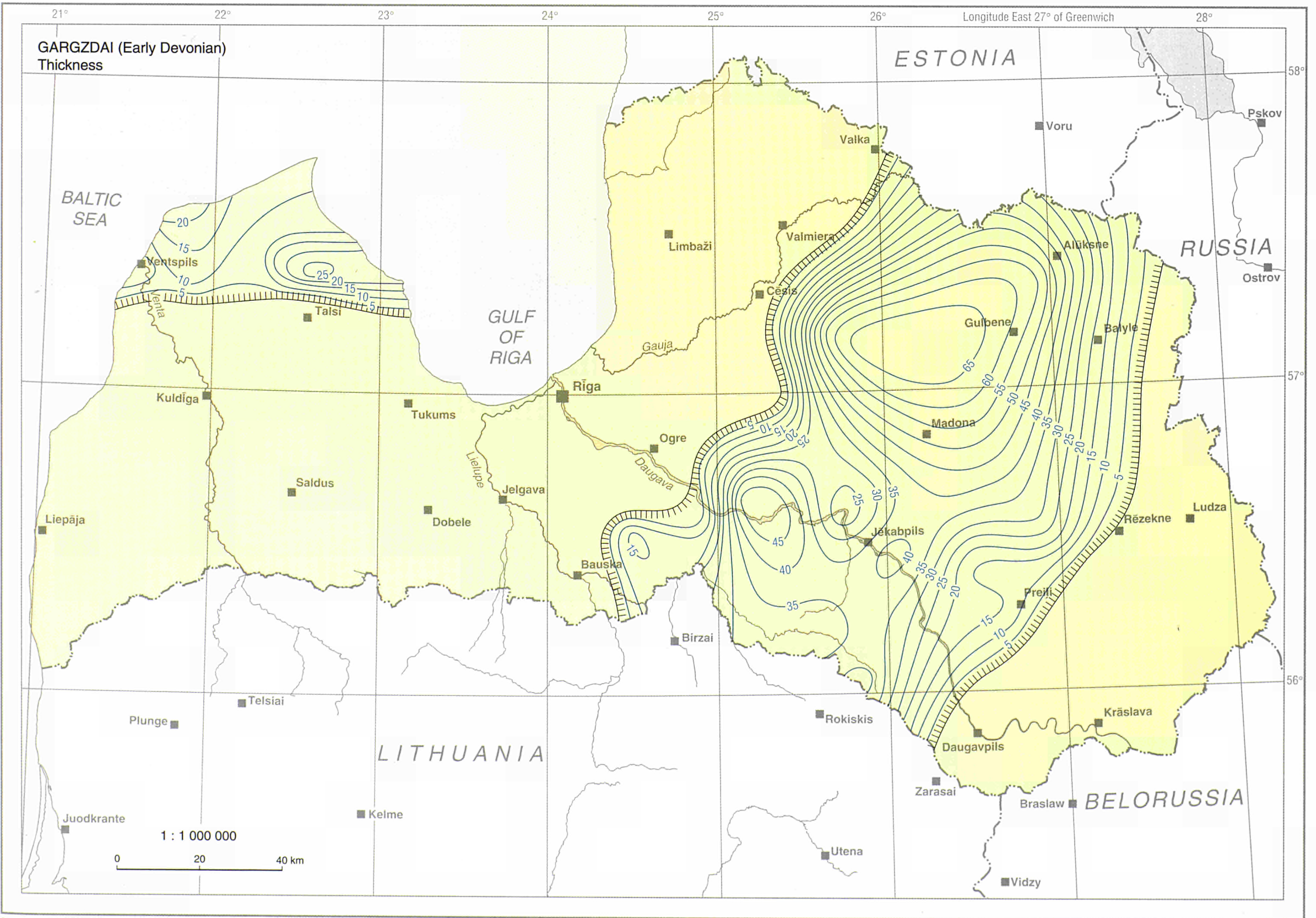
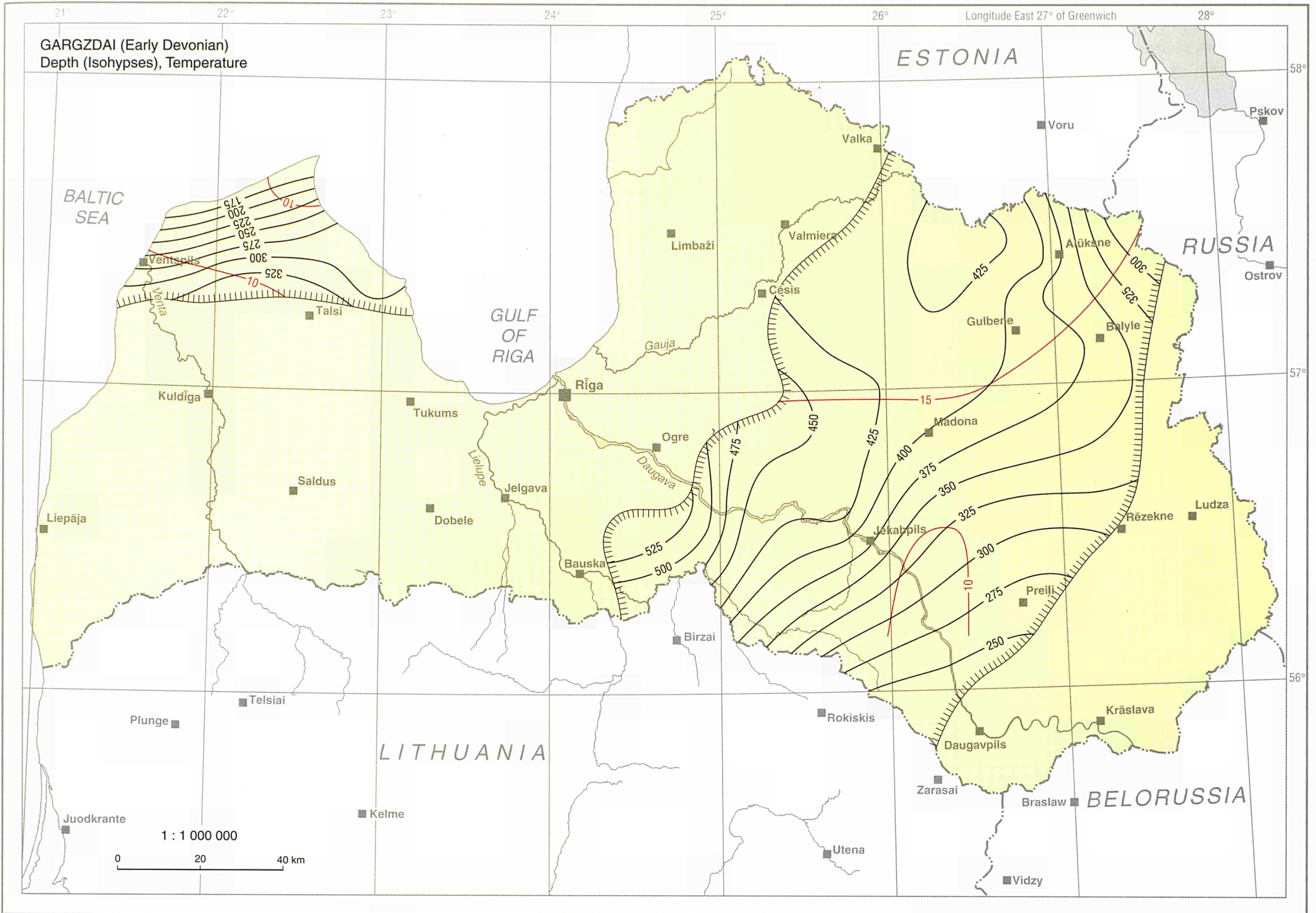
LATVIA



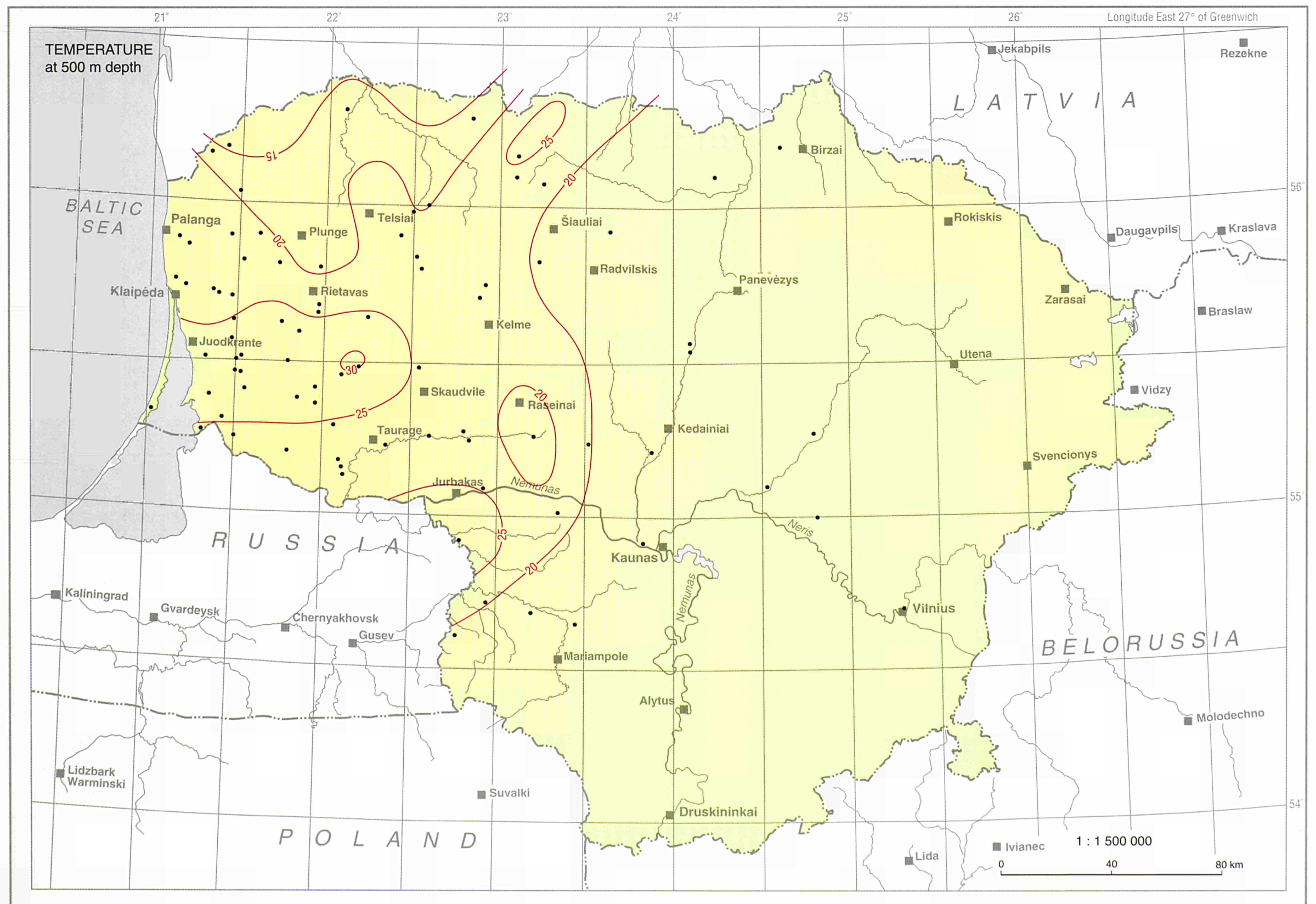
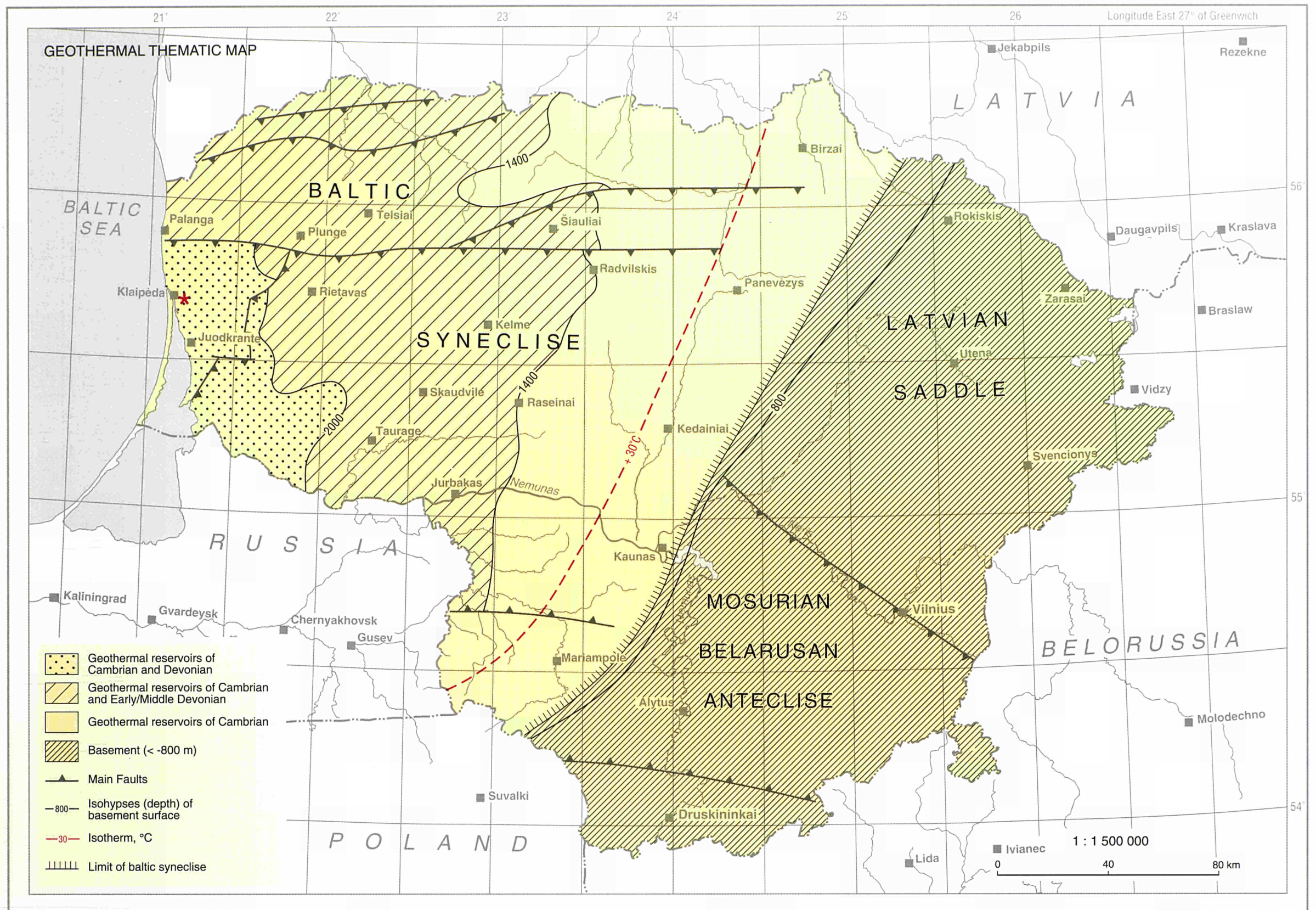


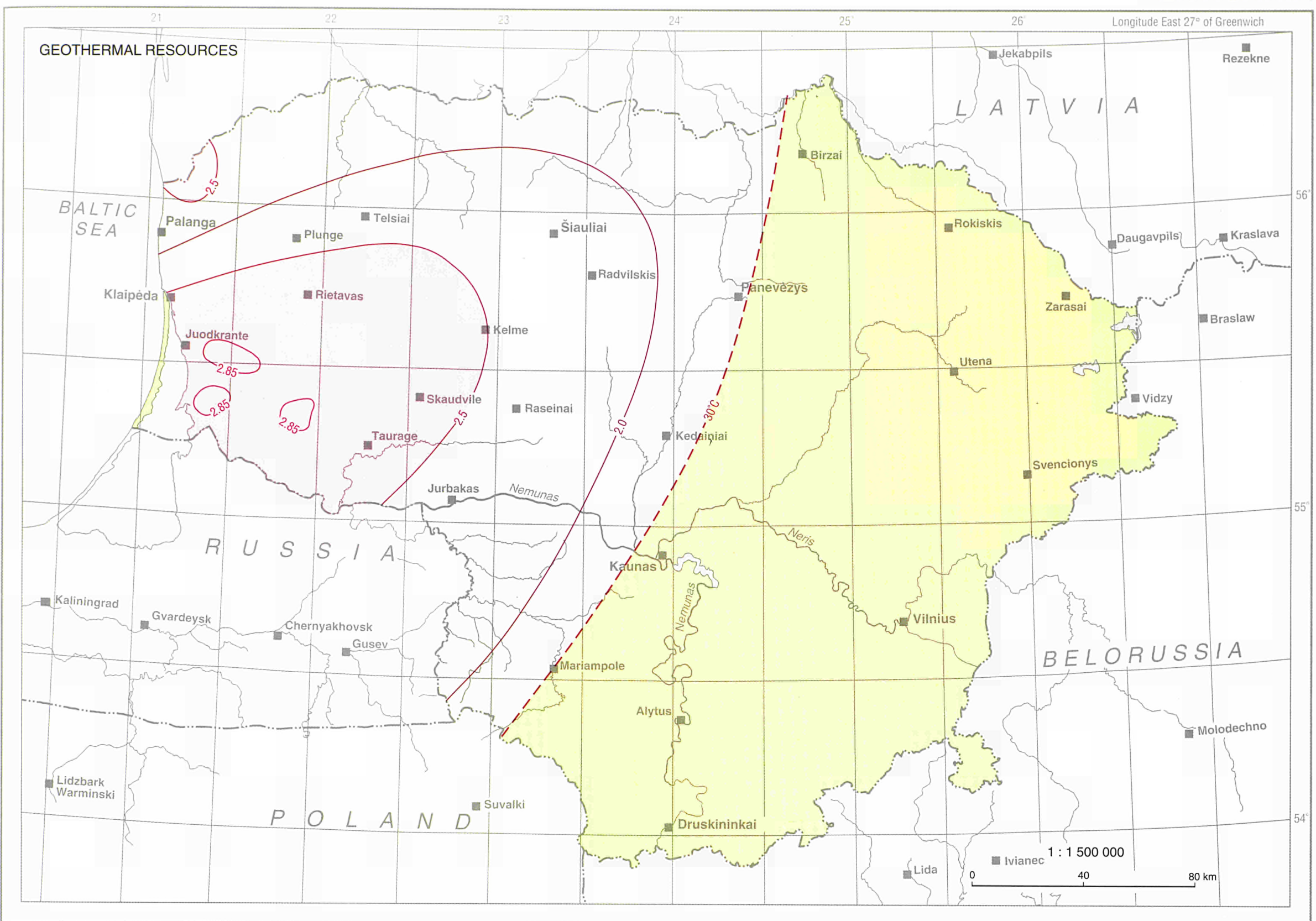
LATVIA



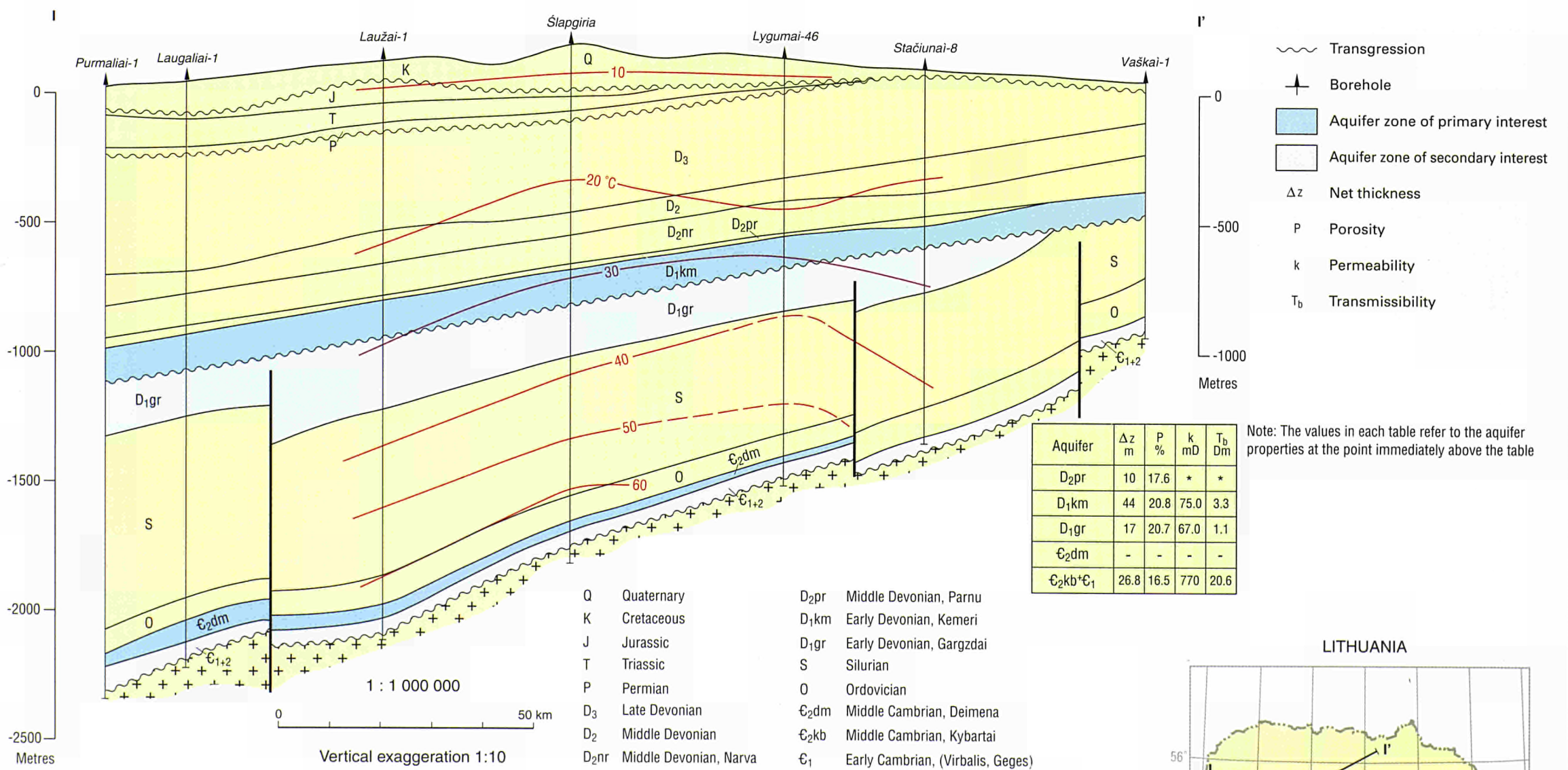


LITHUANIA





CROSS SECTION



Aquifer	Δz m	P %	k mD	T _b Dm
D _{2pr}	5	11.6	*	*
D _{1km}	81.6	25.4	320	26.1
D _{1gr}	31	15.2	12.0	3.4
E _{2dm}	46.4	7.06	1.2	0.06
E _{2kb} *E ₁	2.1	6.3	0.7	0.00

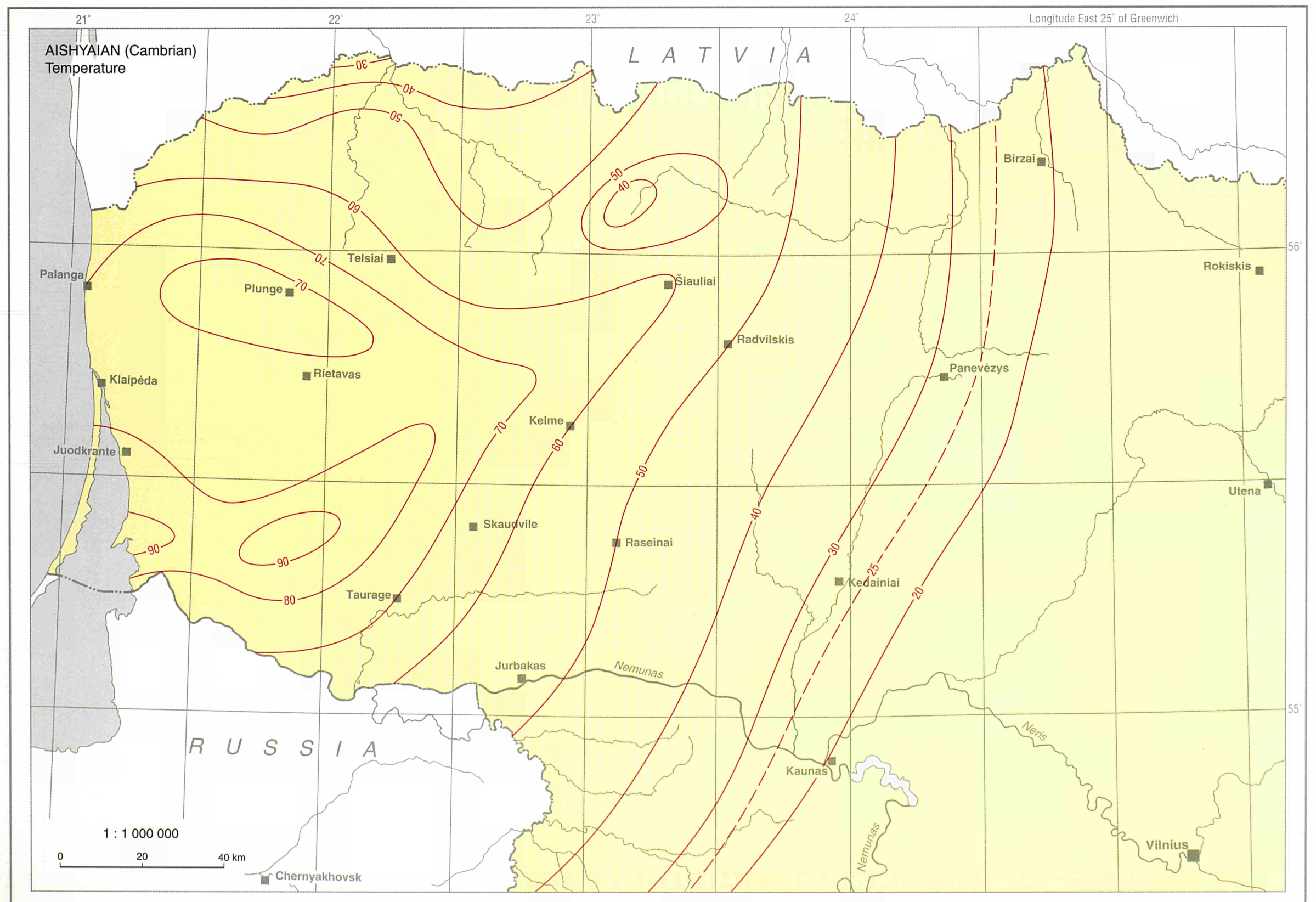
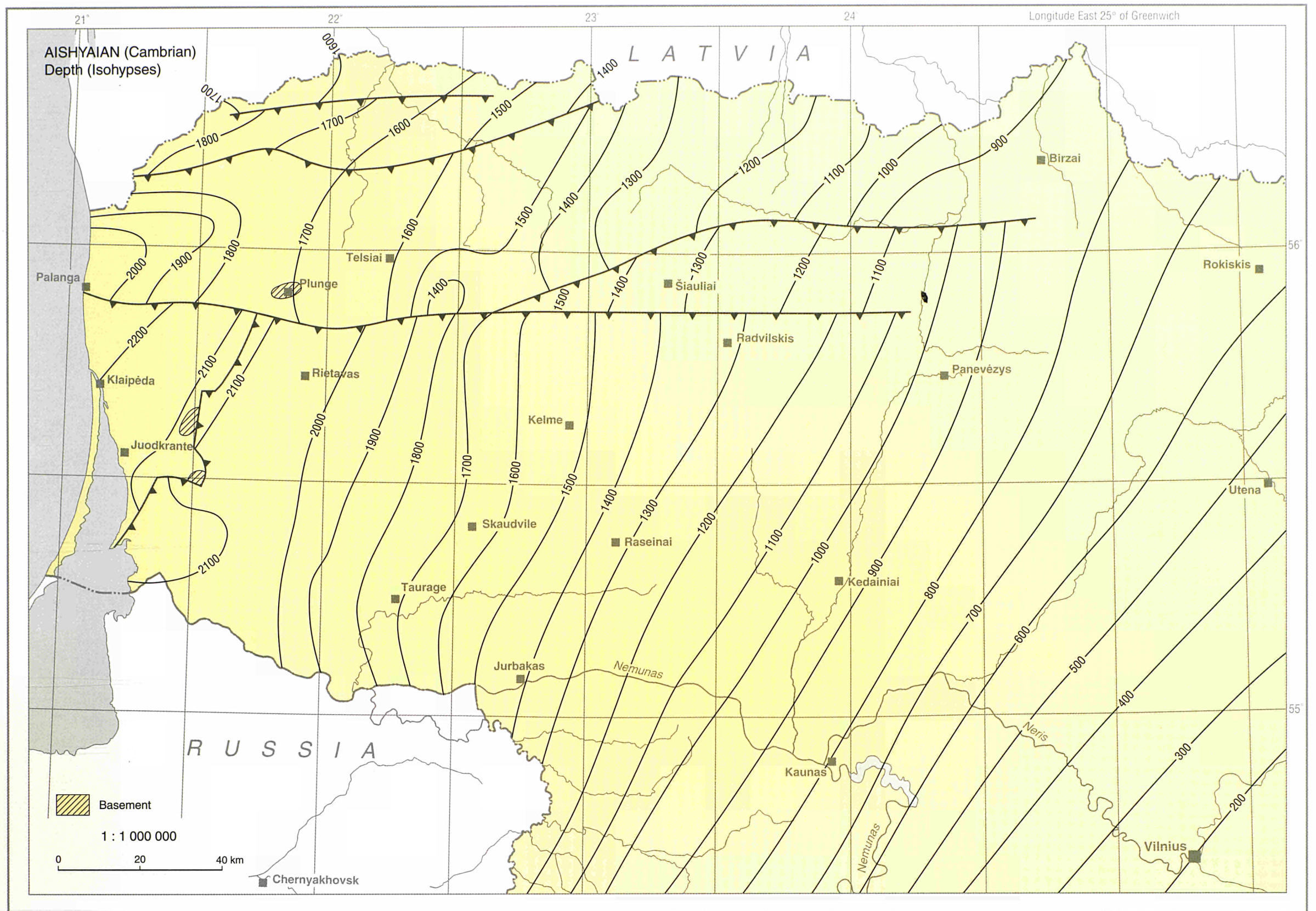
Δz m	P %	k mD	T _b Dm
3	8.1	*	*
98.3	39.8	1500	147.5
42.1	19.2	43	1.8
38.7	8.5	3.2	0.10
5	9.22	5.0	0.02

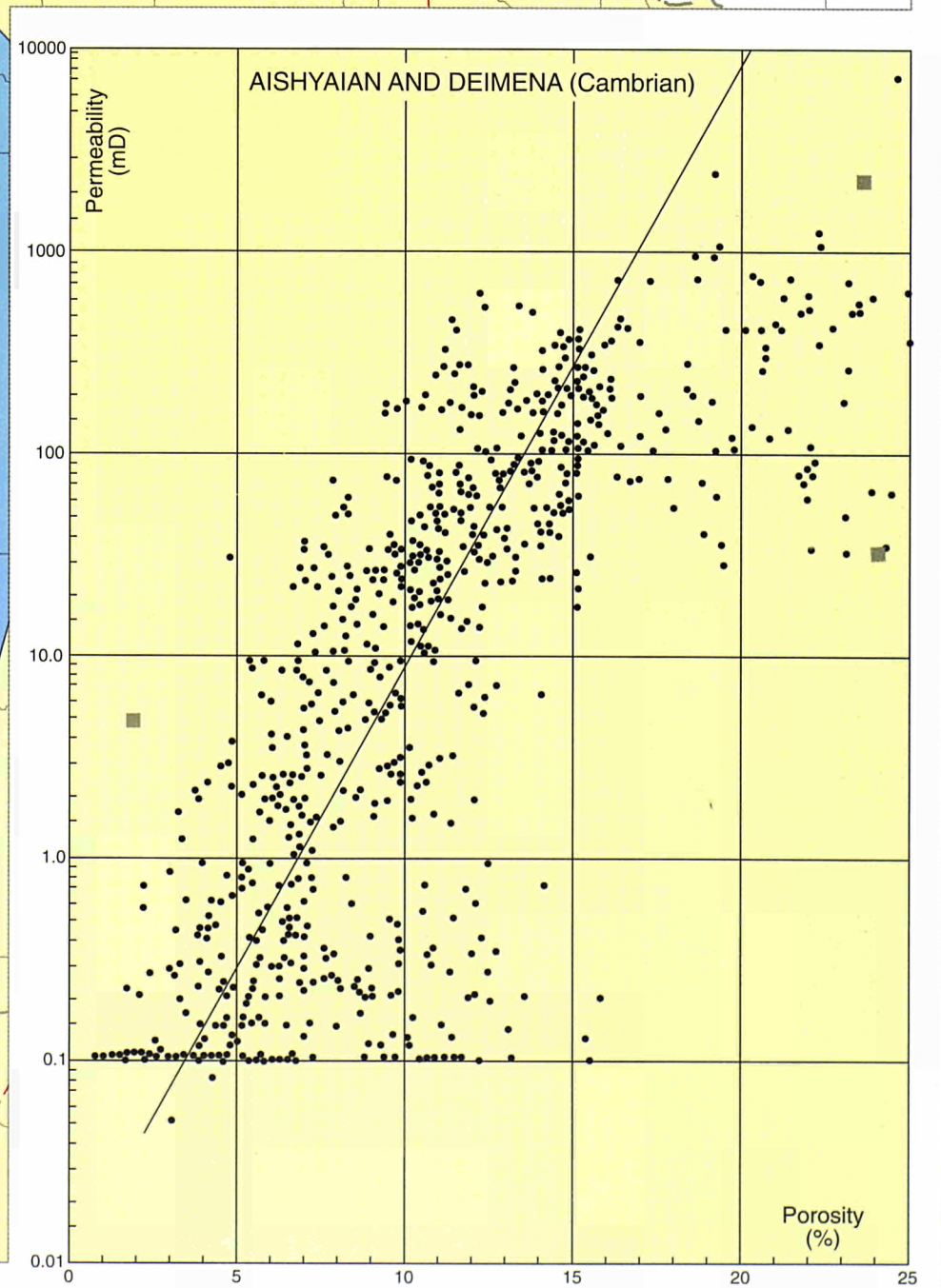
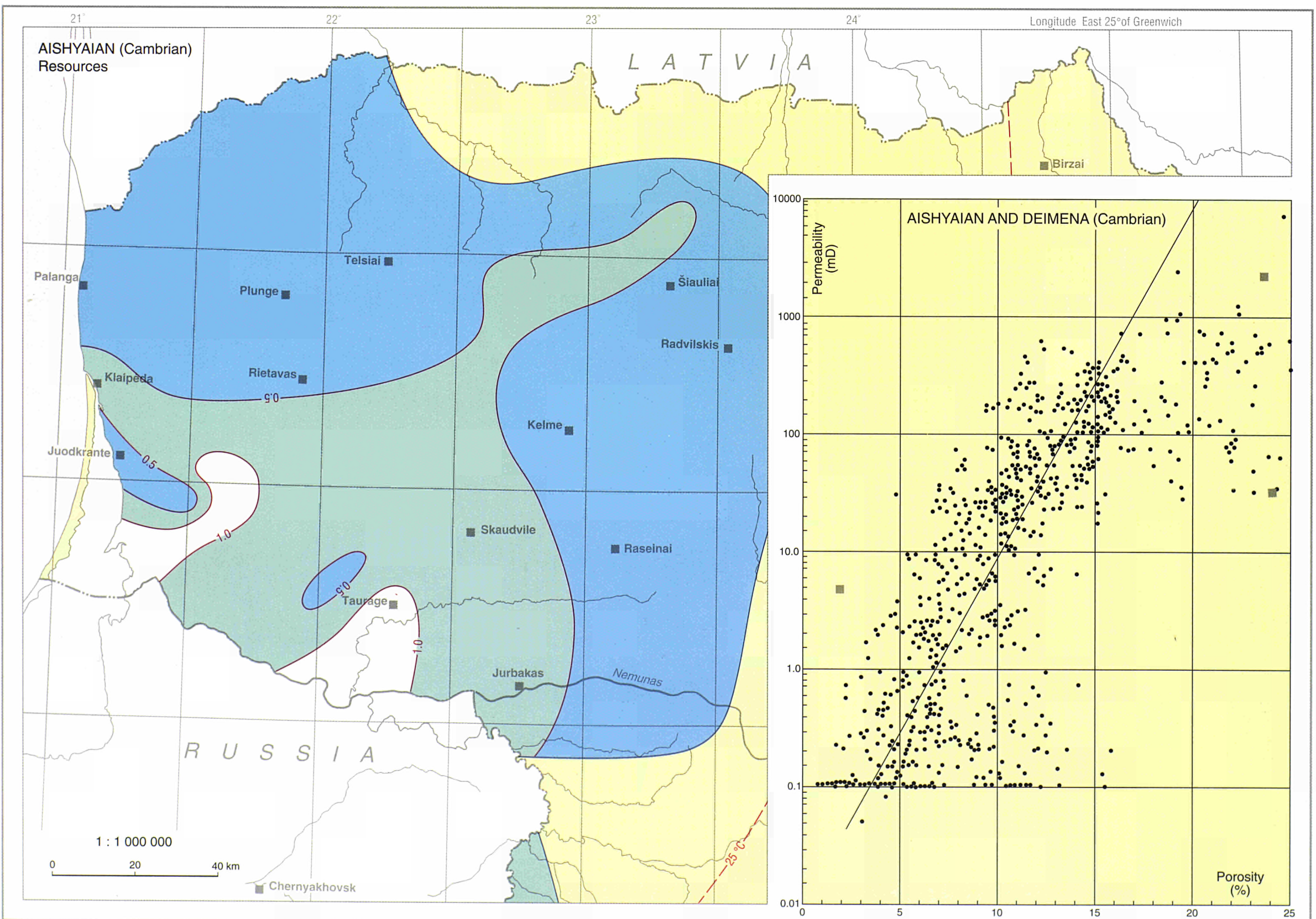
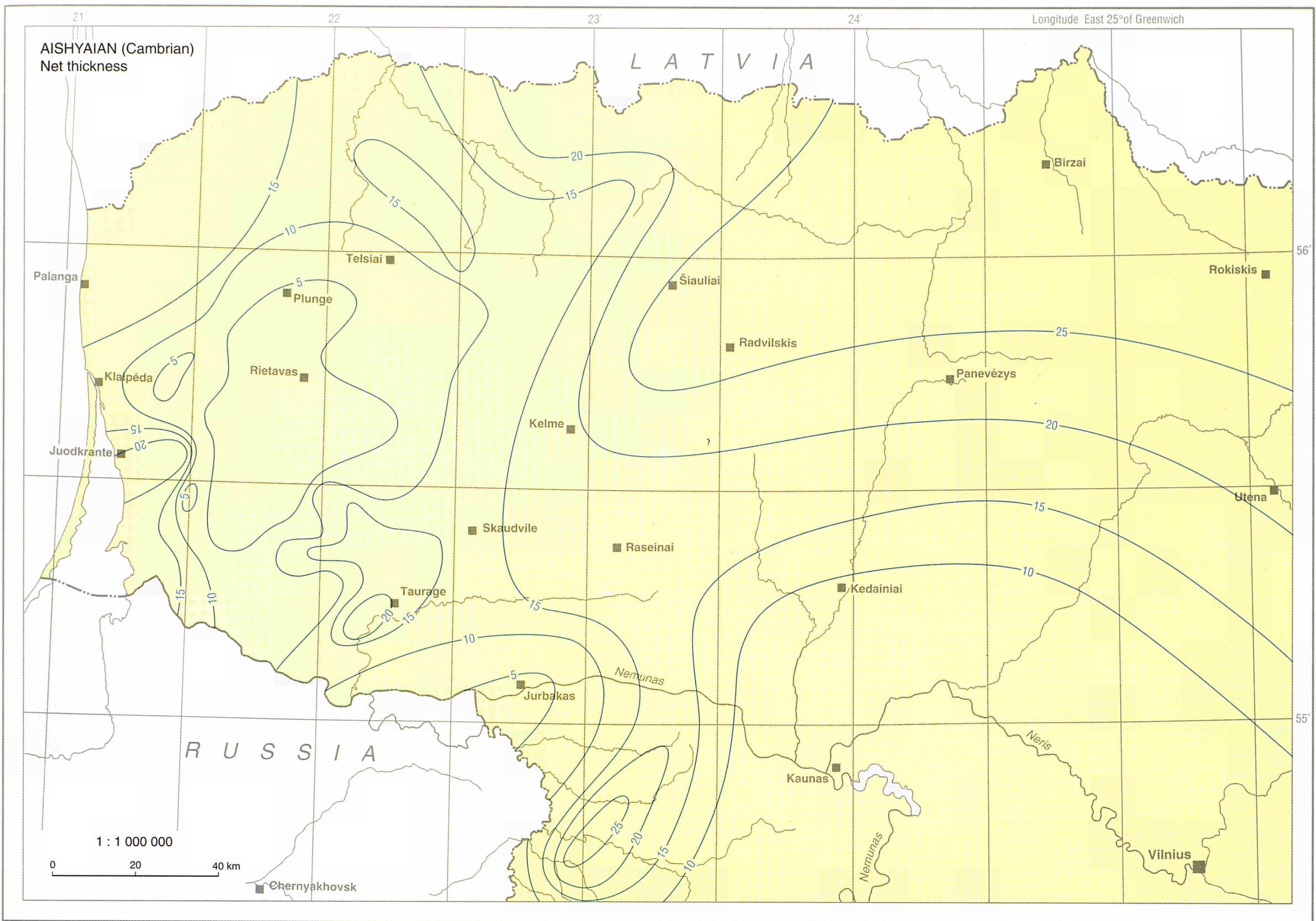
Δz m	P %	k mD	T _b Dm
5.5	6.8	*	*
64.5	21.1	800	52.7
220	22.0	100	2.2
38.0	11.7	29.0	1.1
10.7	8.5	3.1	0.03

Δz m	P %	k mD	T _b Dm
21.2	12.7	*	*
59.0	24.2	210	12.4
22.3	13.6	7.8	0.2
-	-	-	-
-	-	-	-

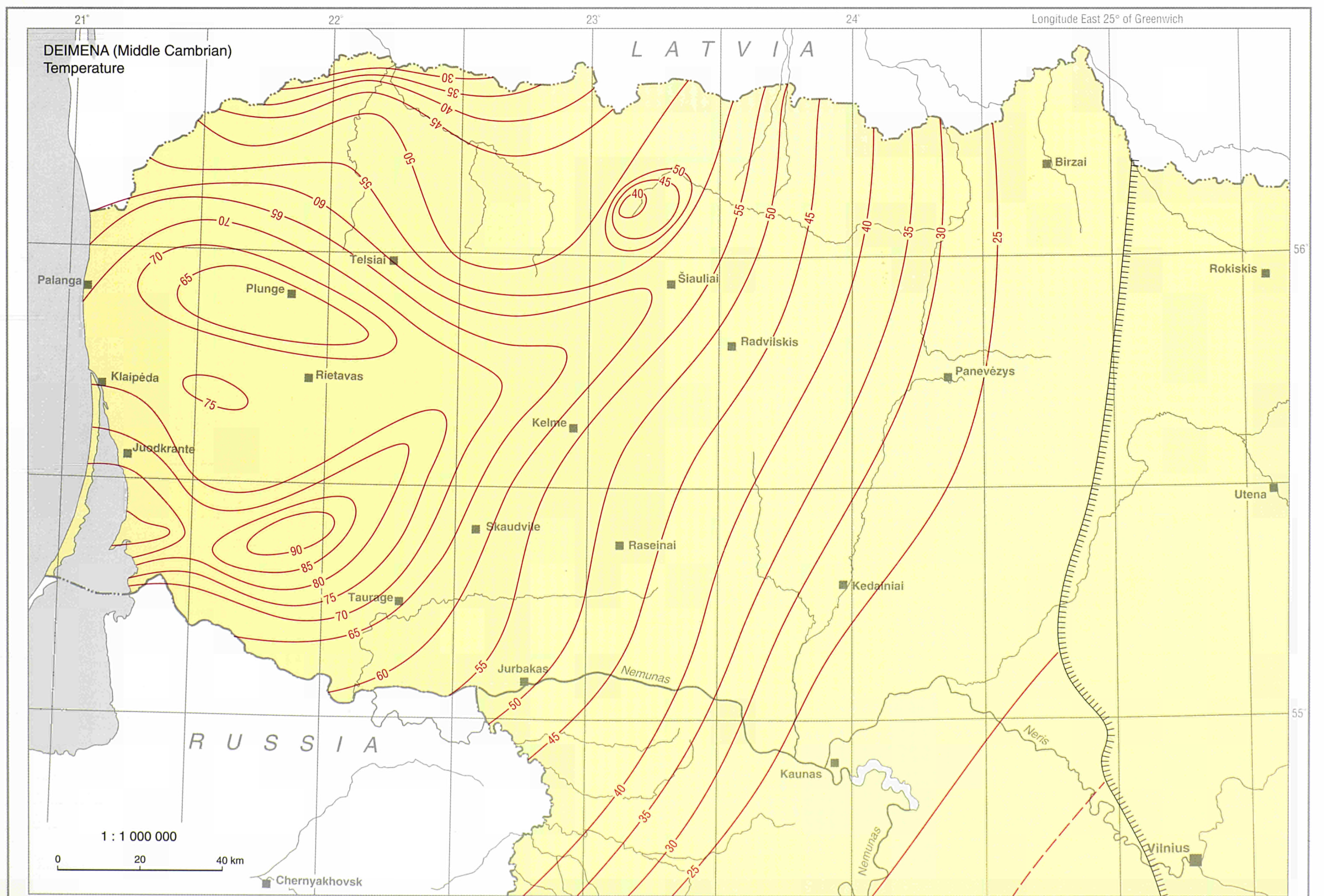
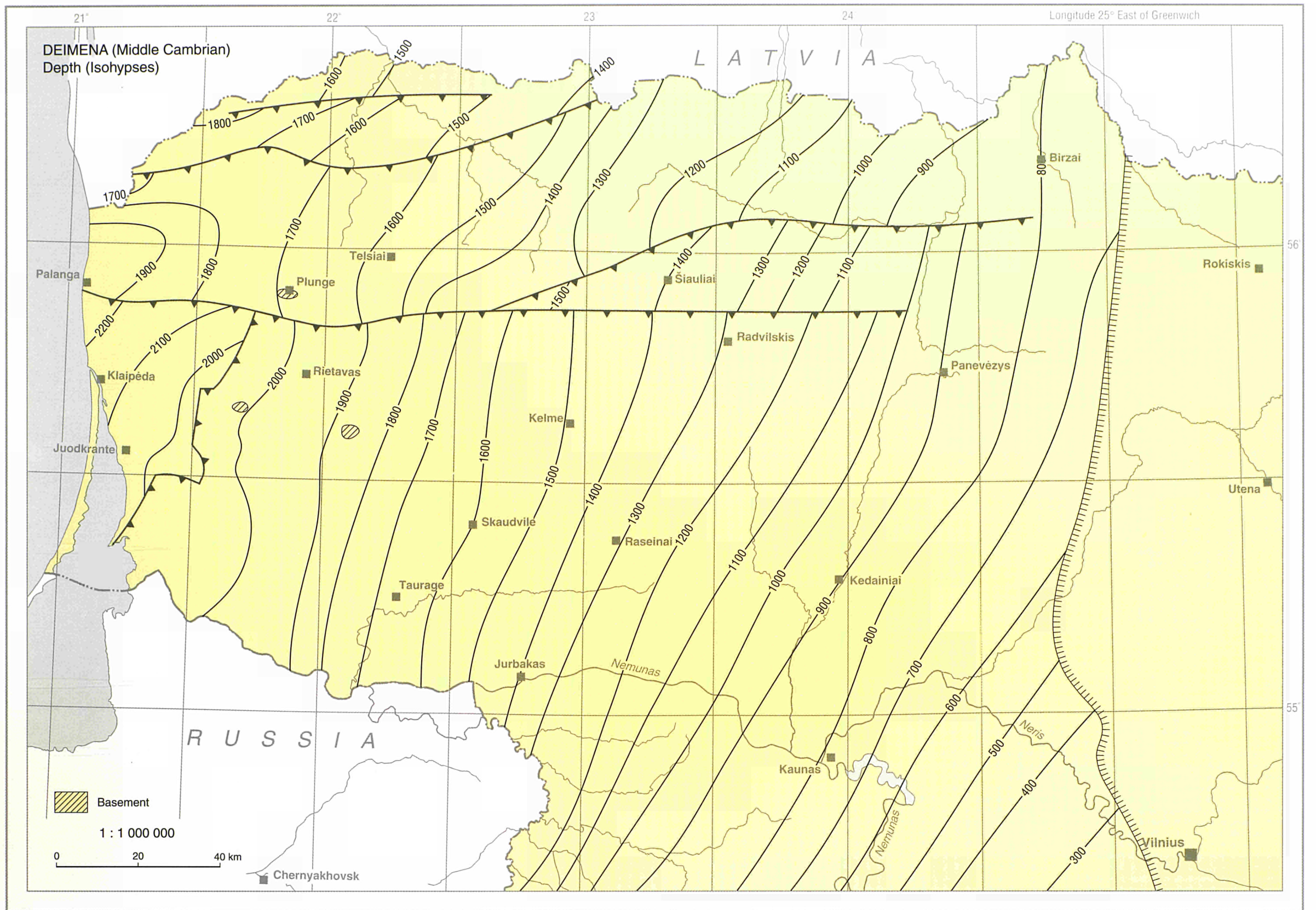


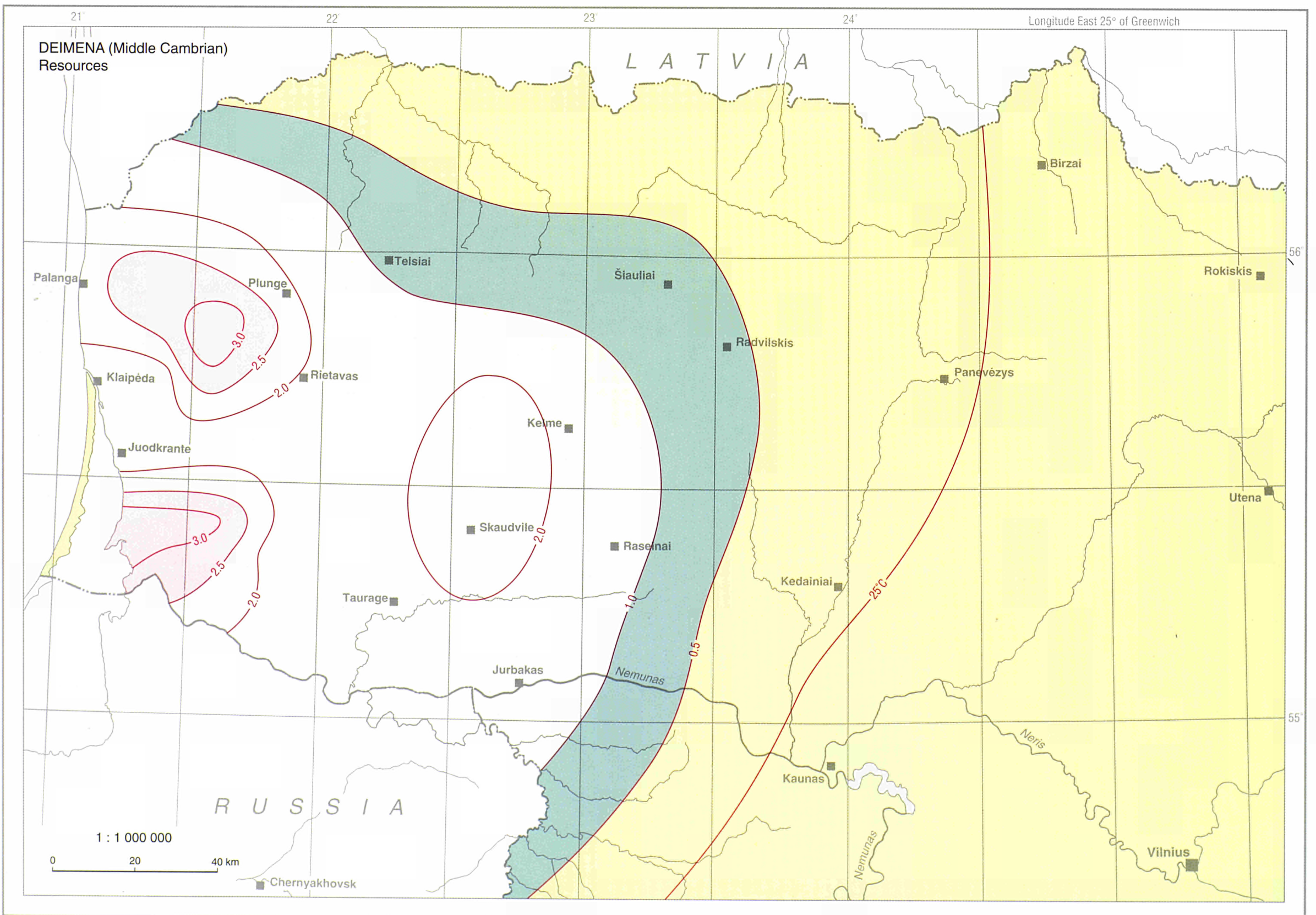
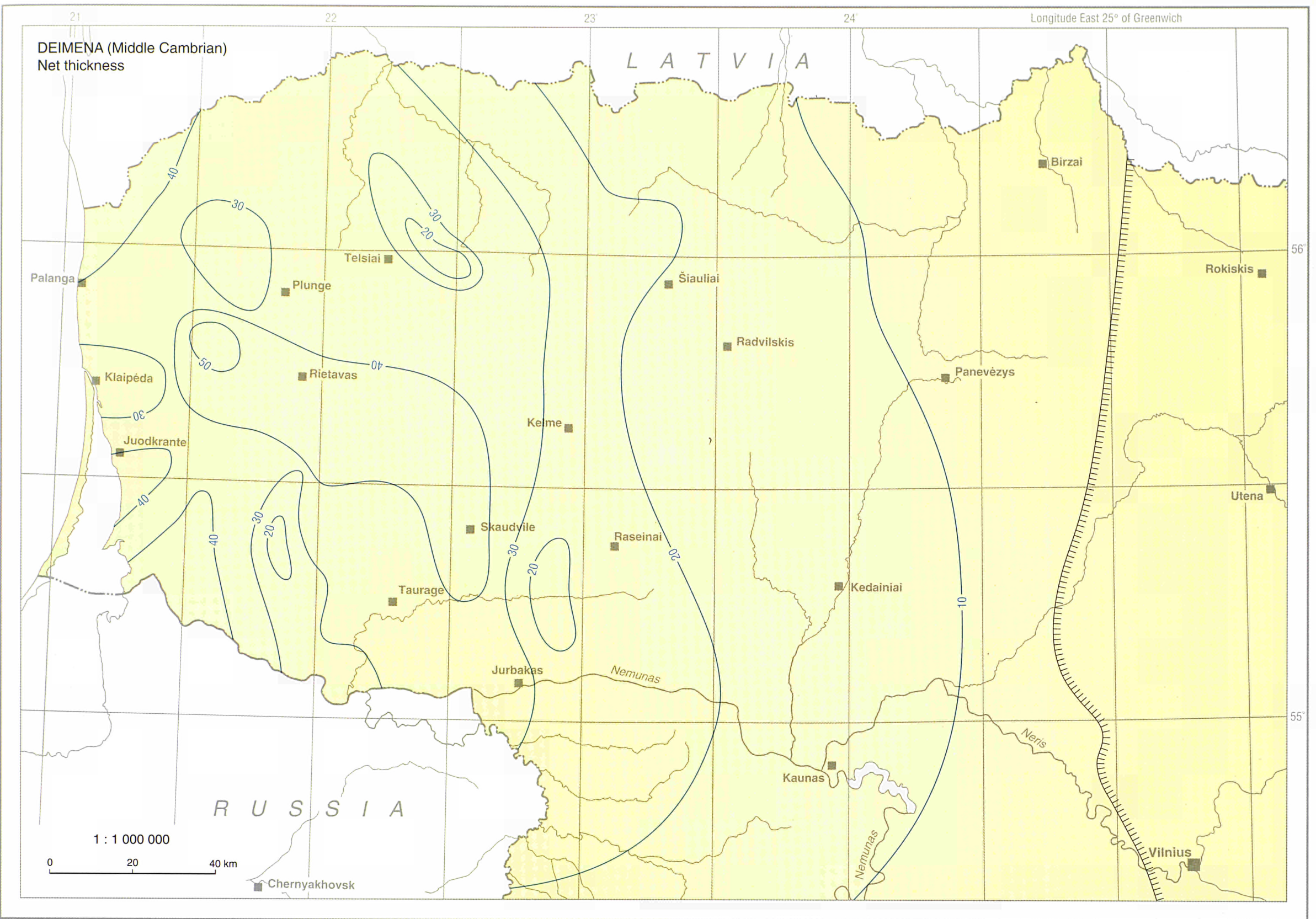
LITHUANIA



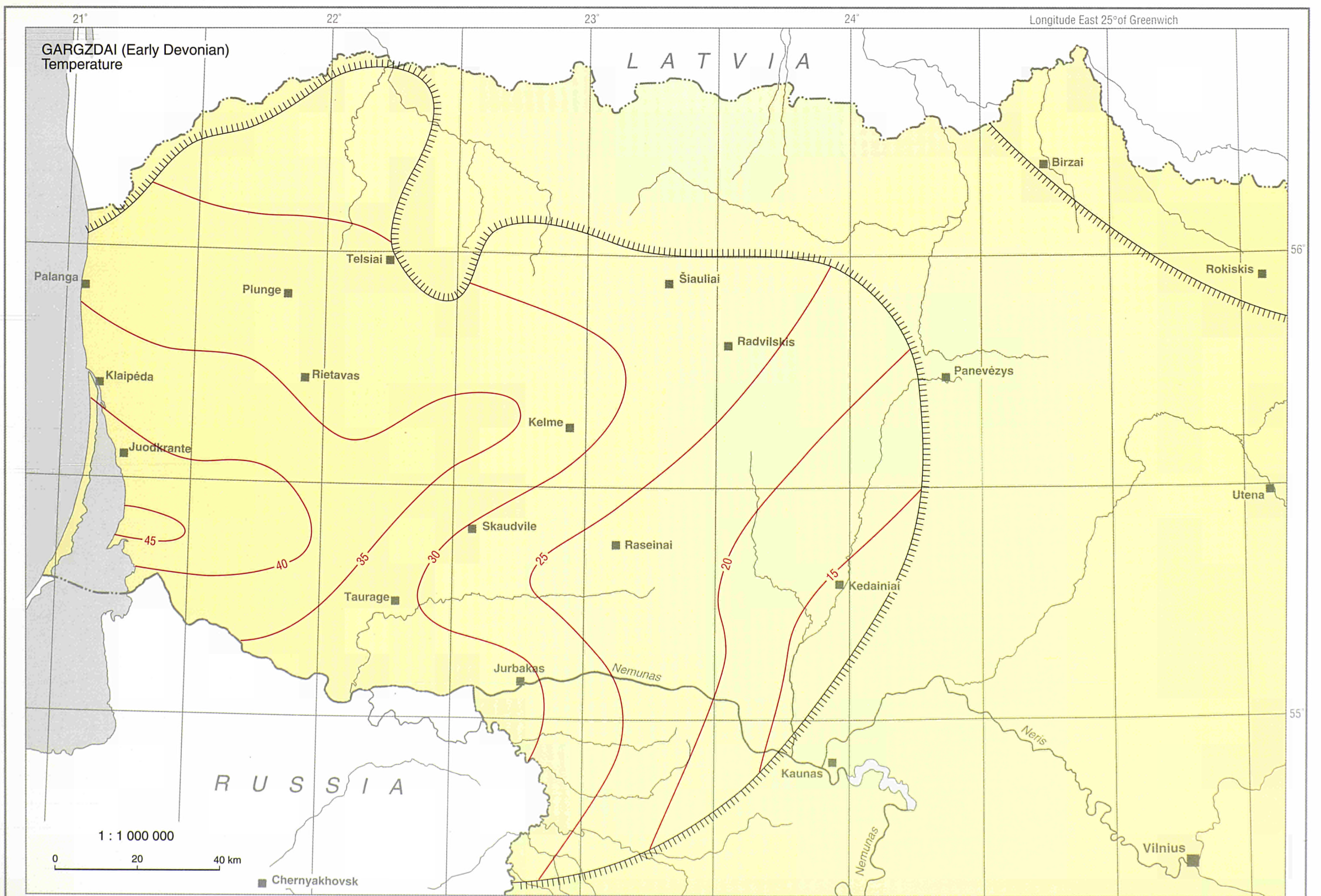
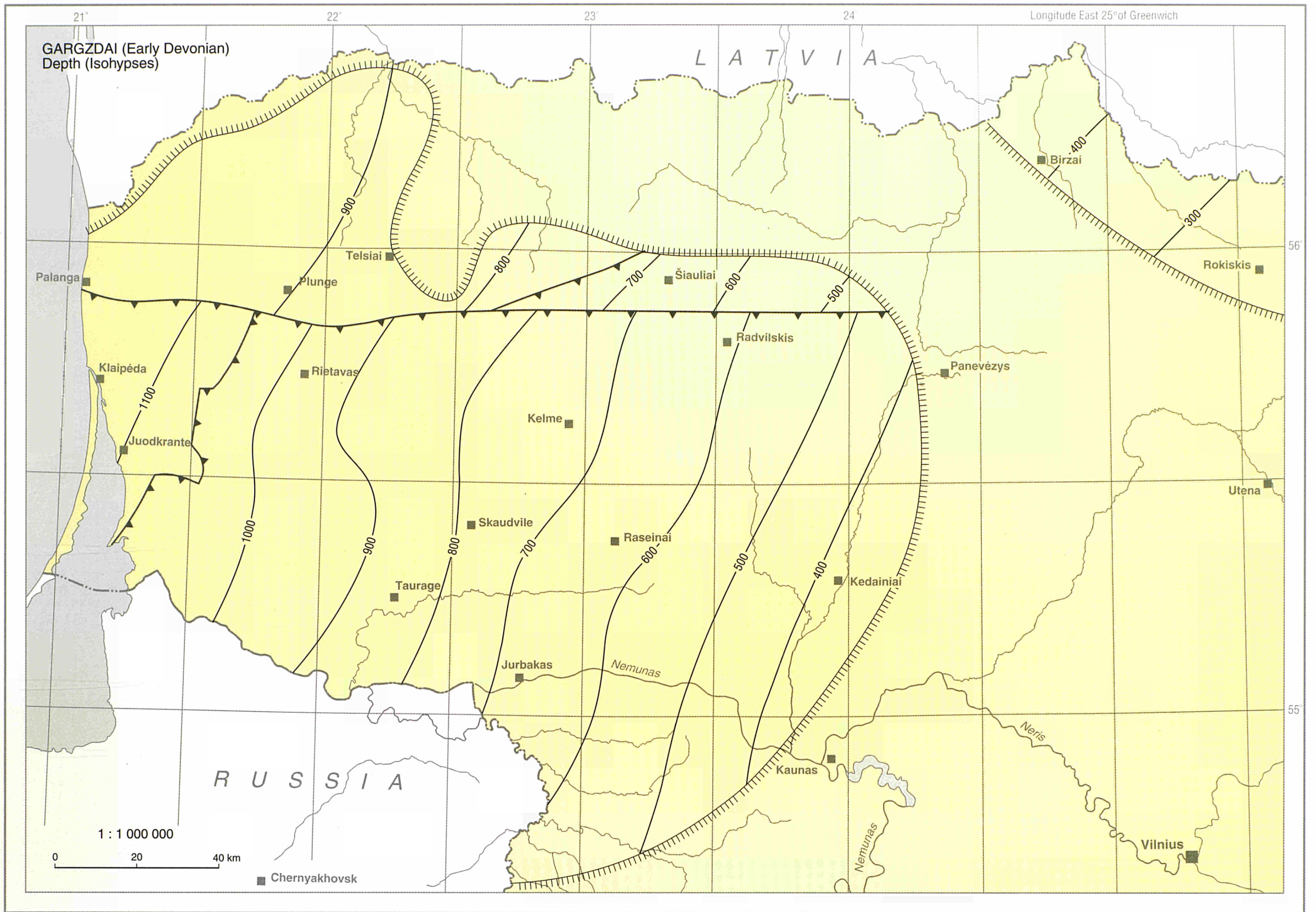


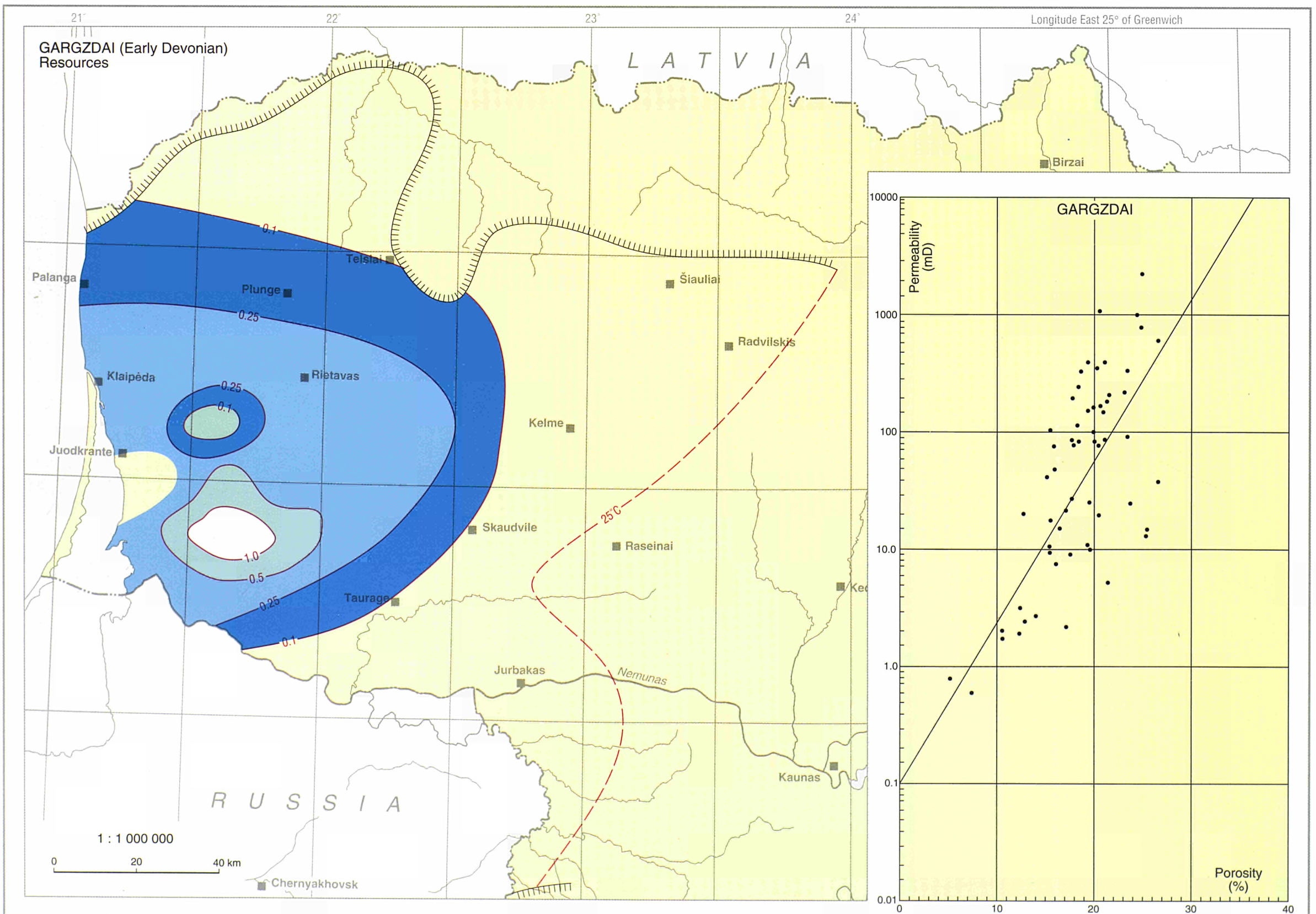
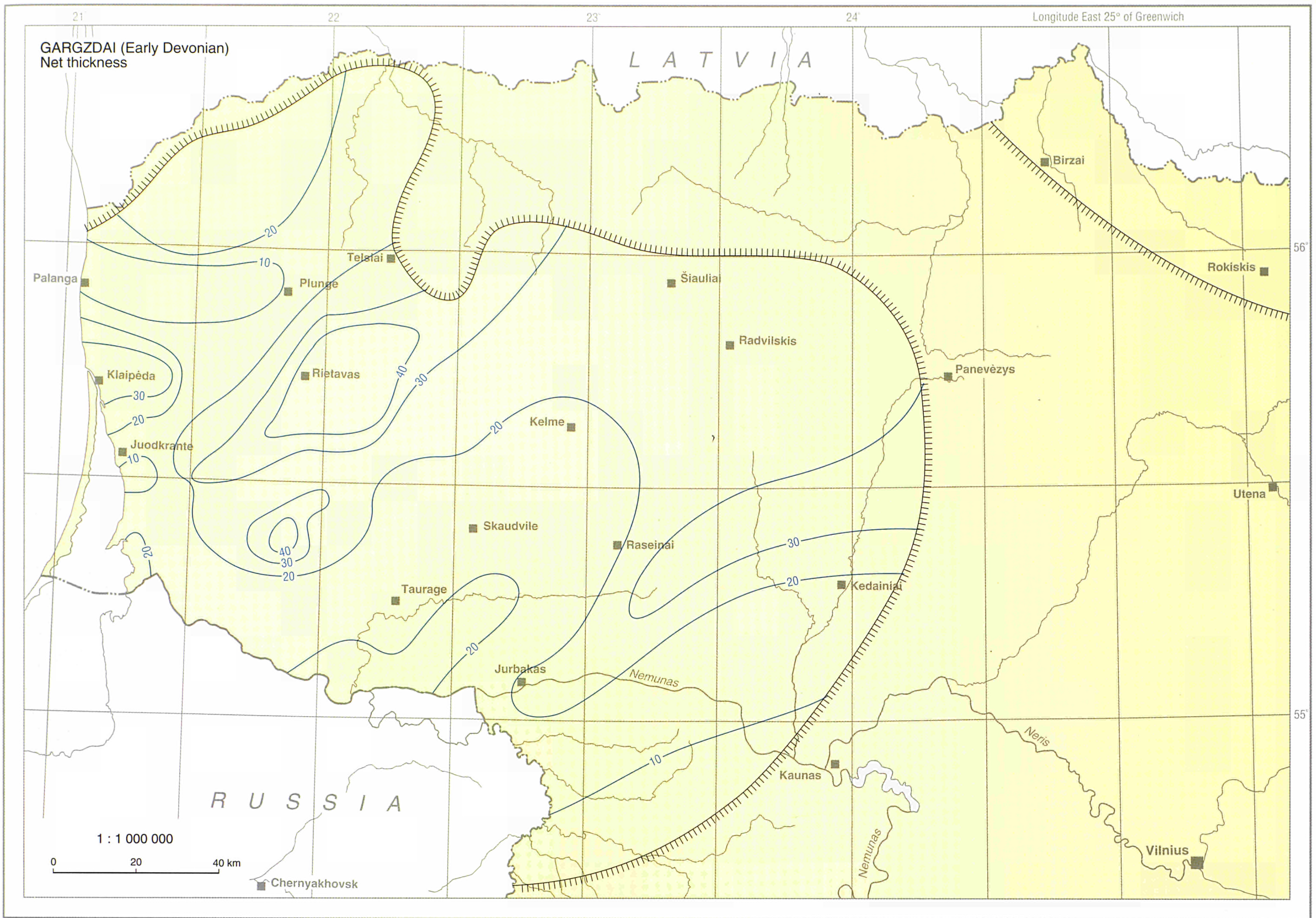
LITHUANIA



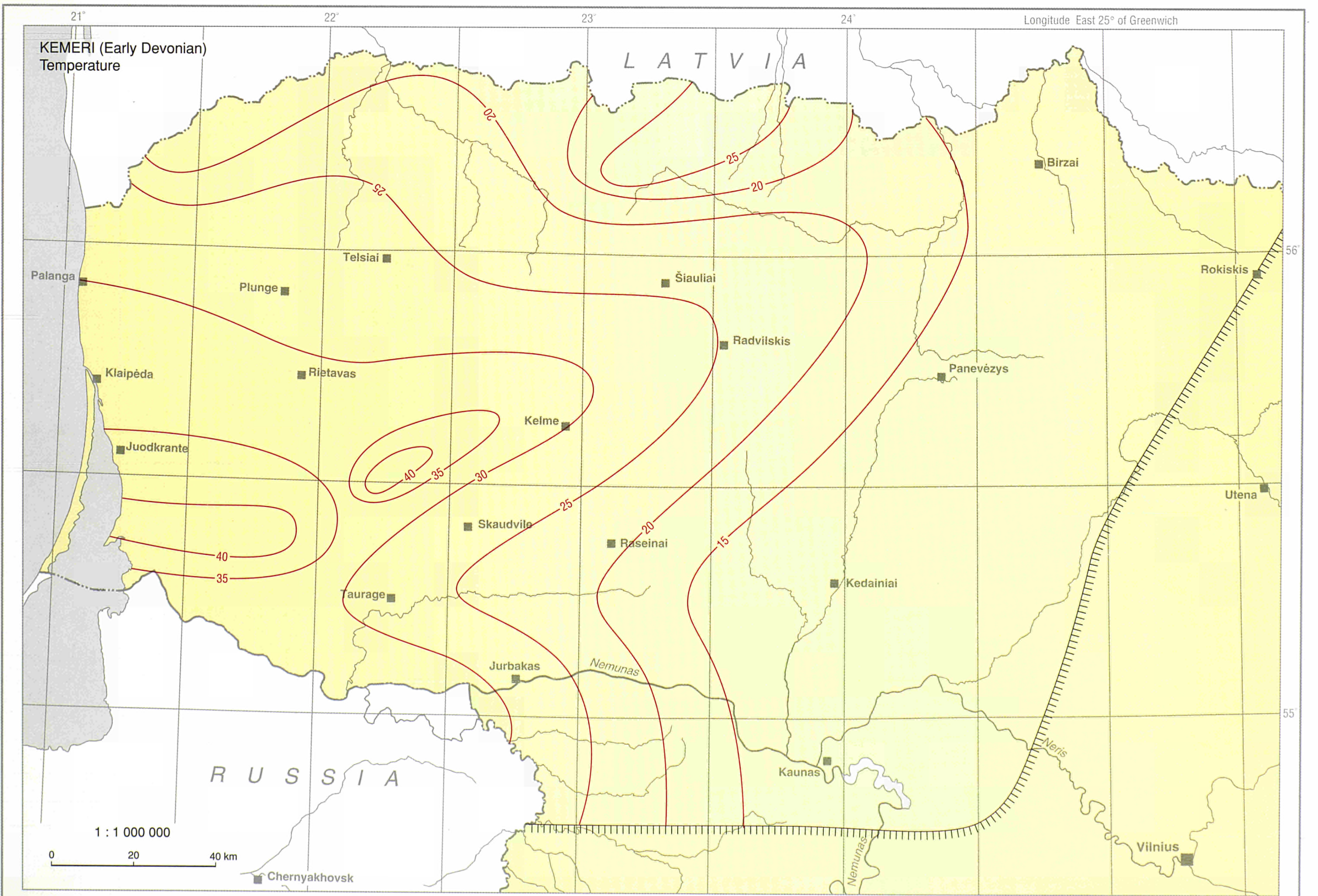
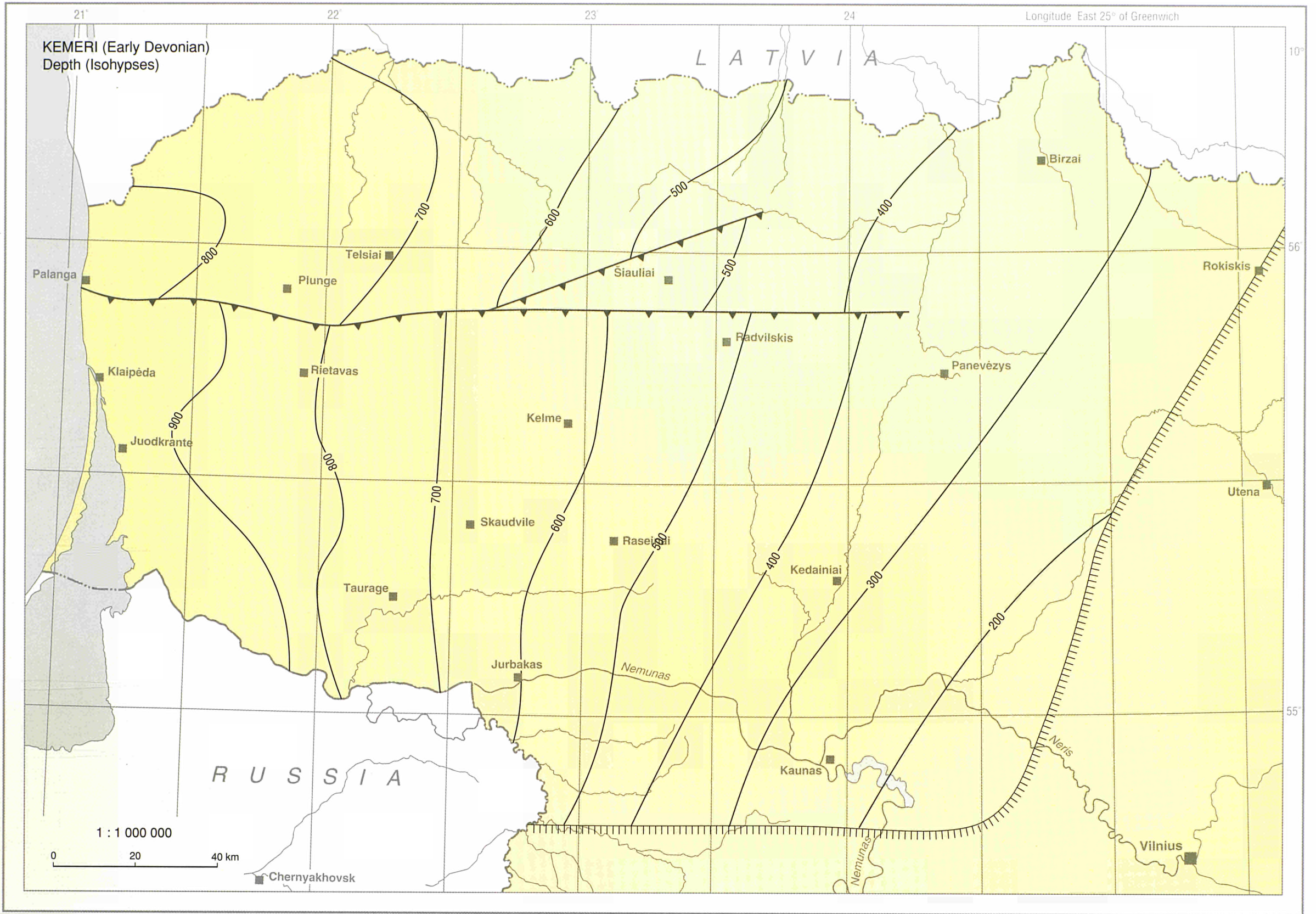


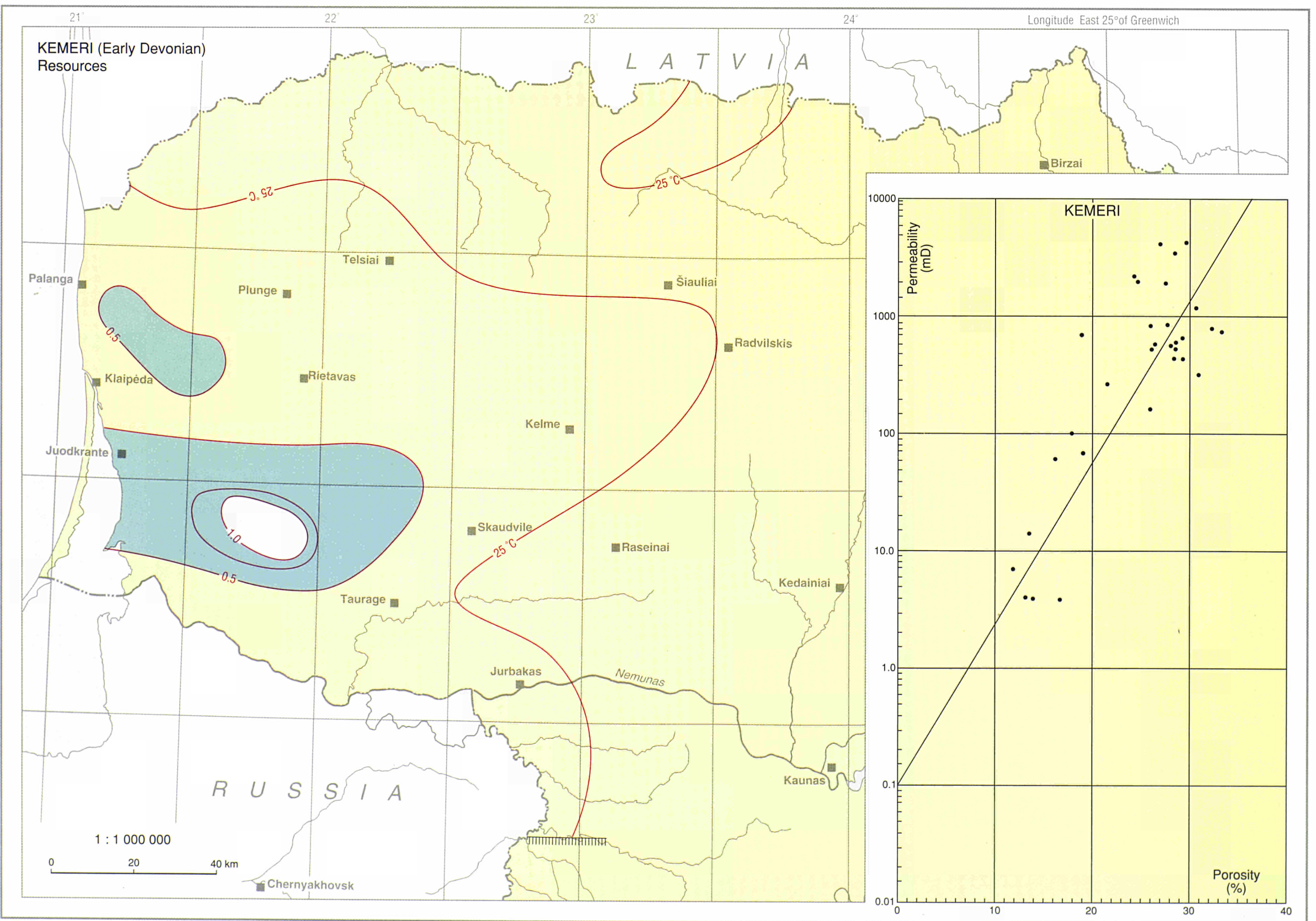
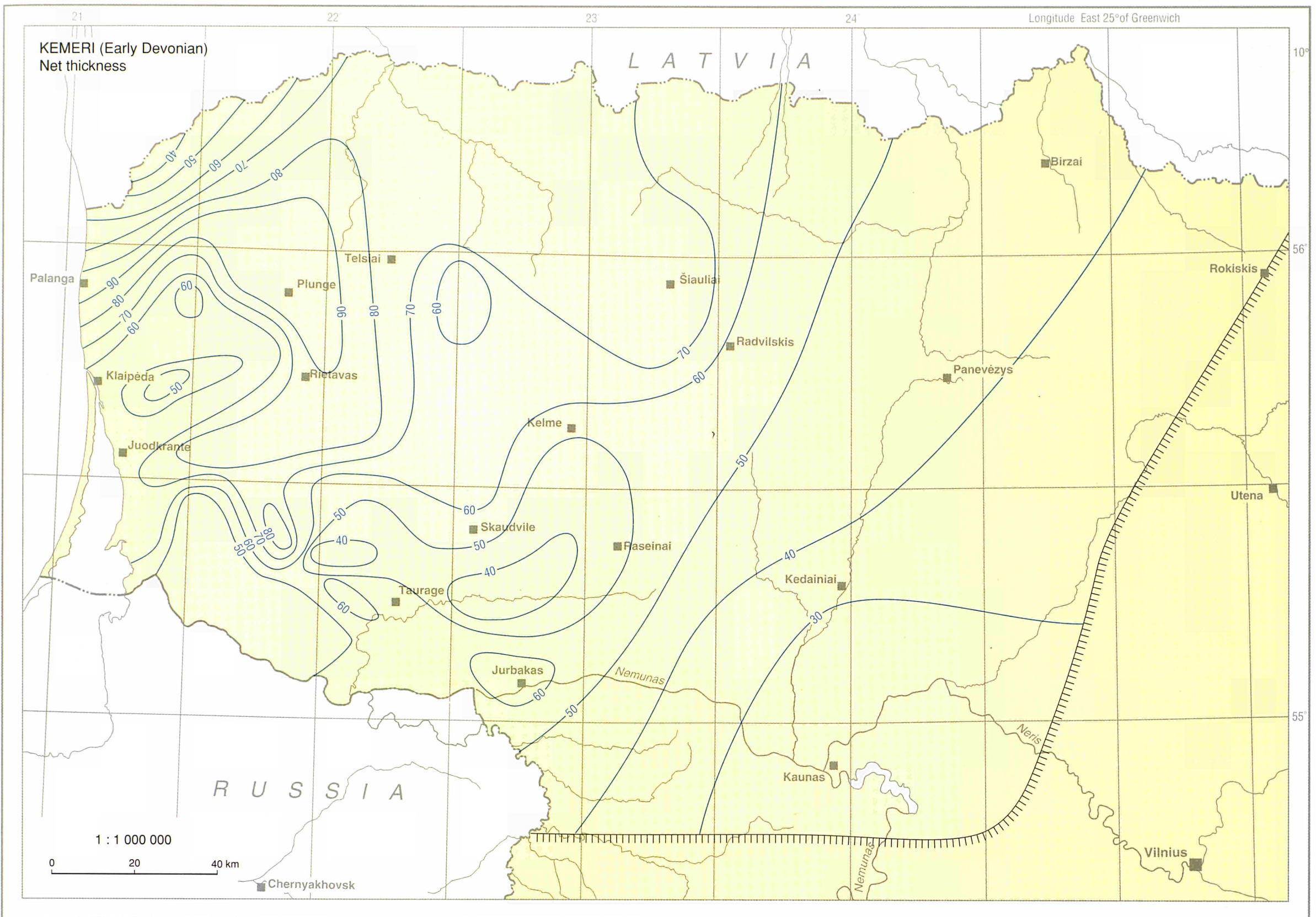
LITHUANIA



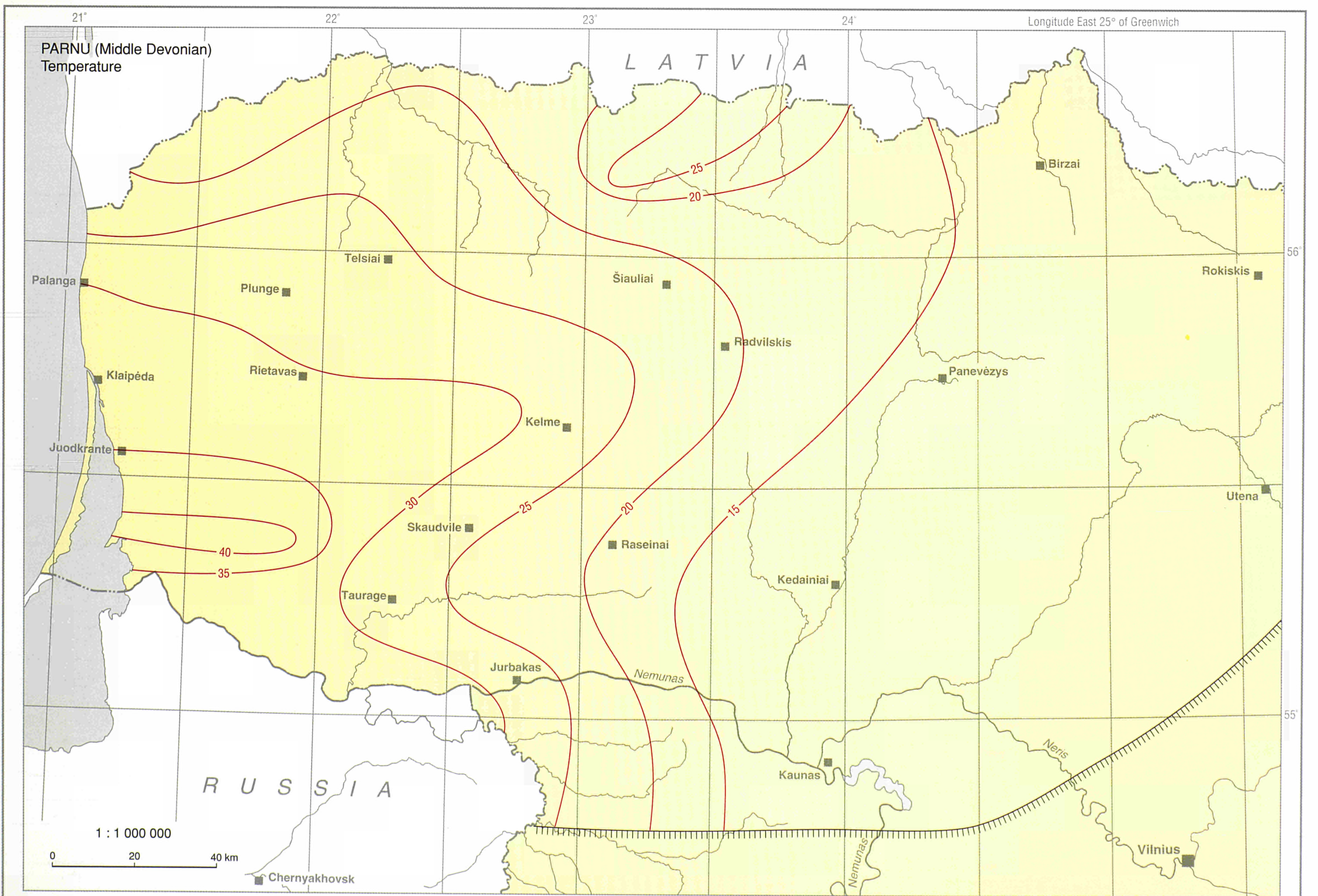
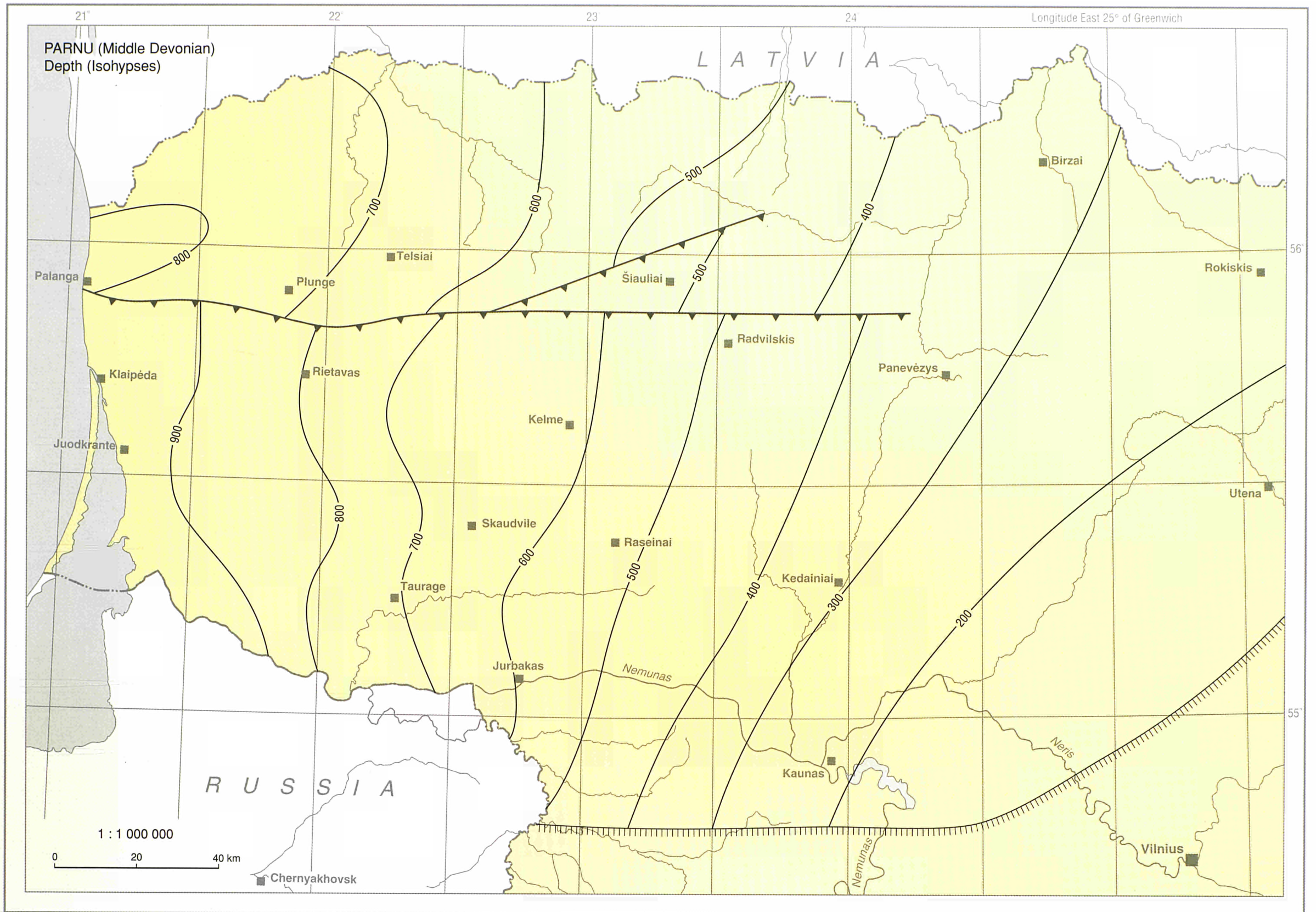


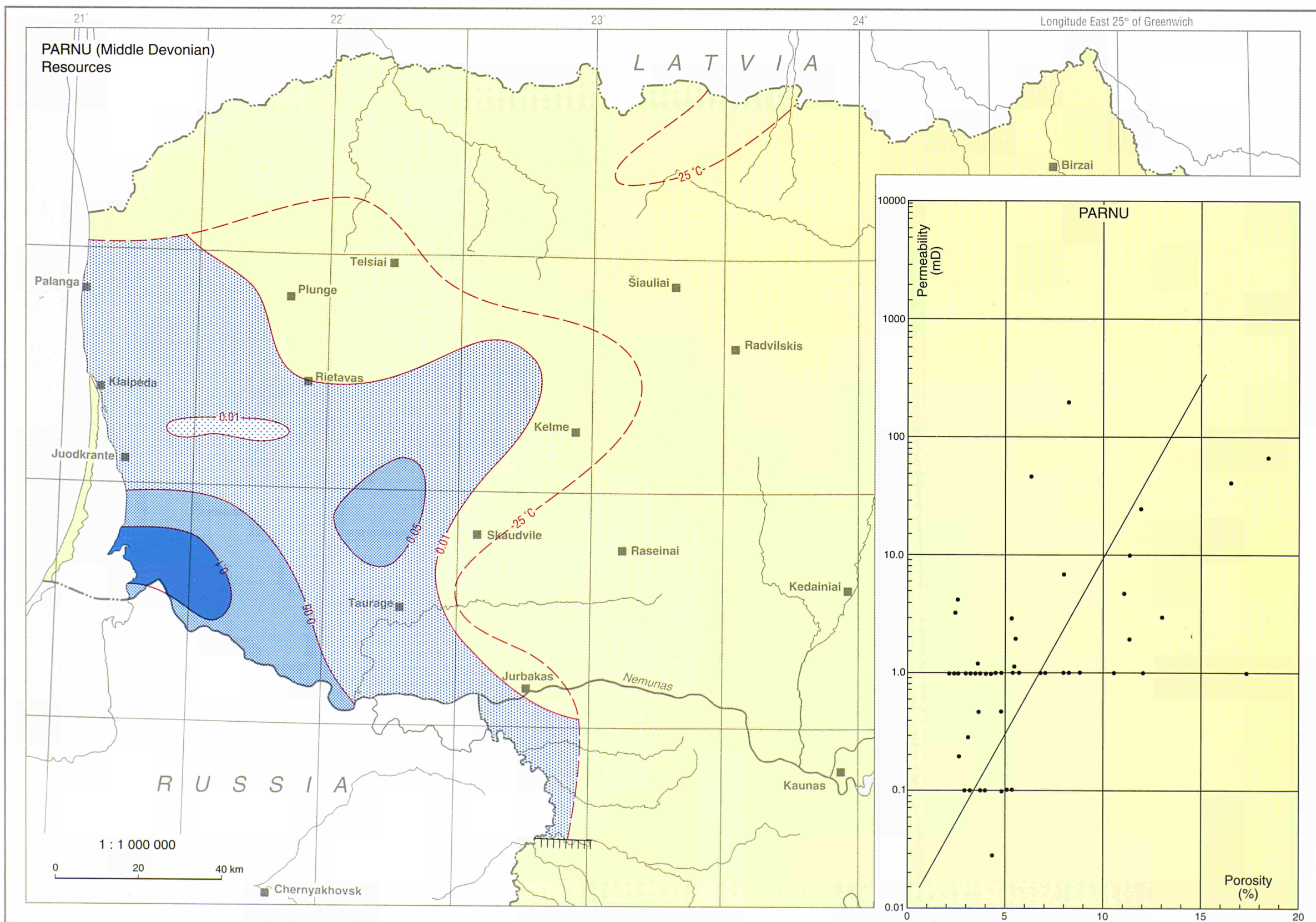
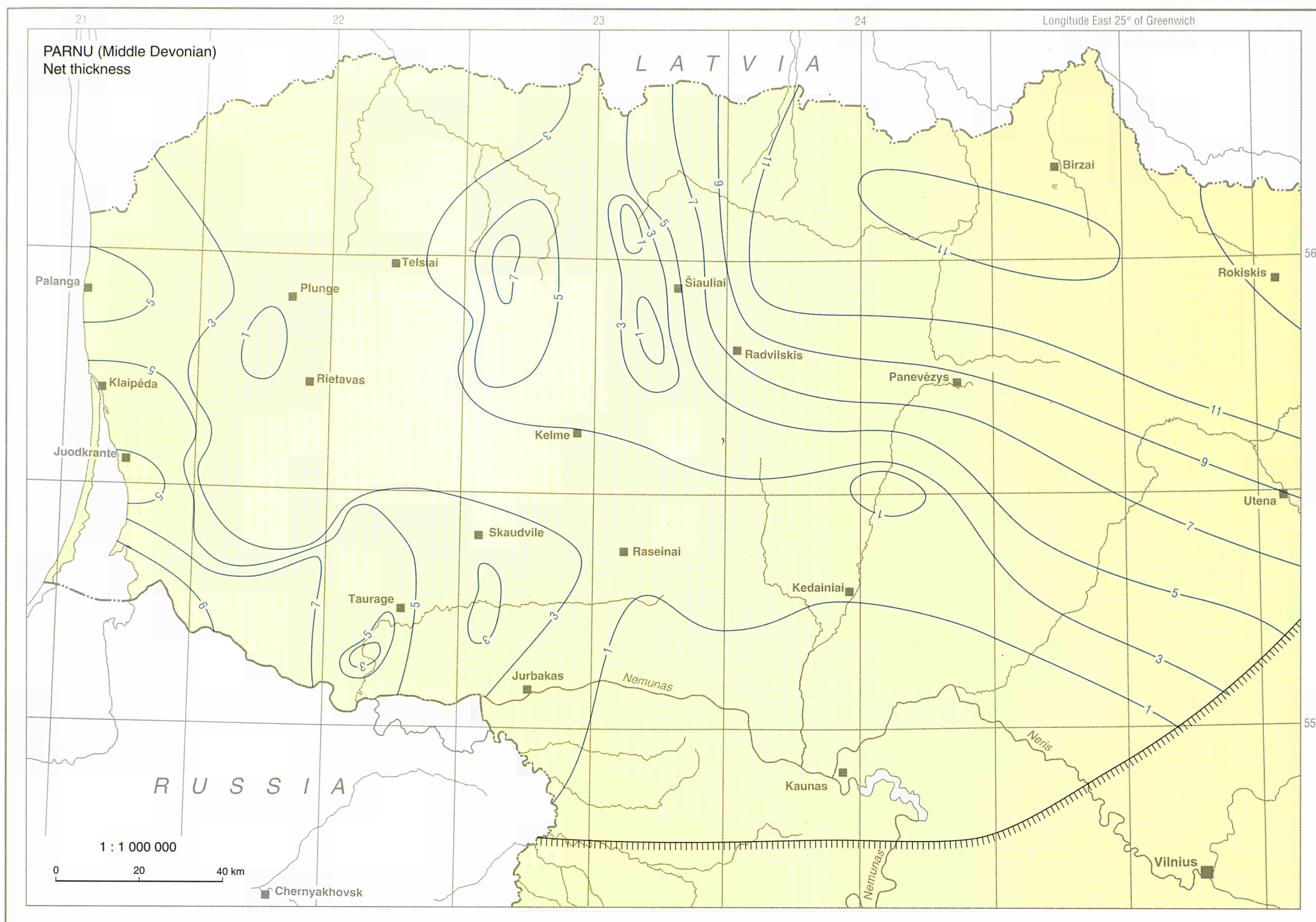
LITHUANIA



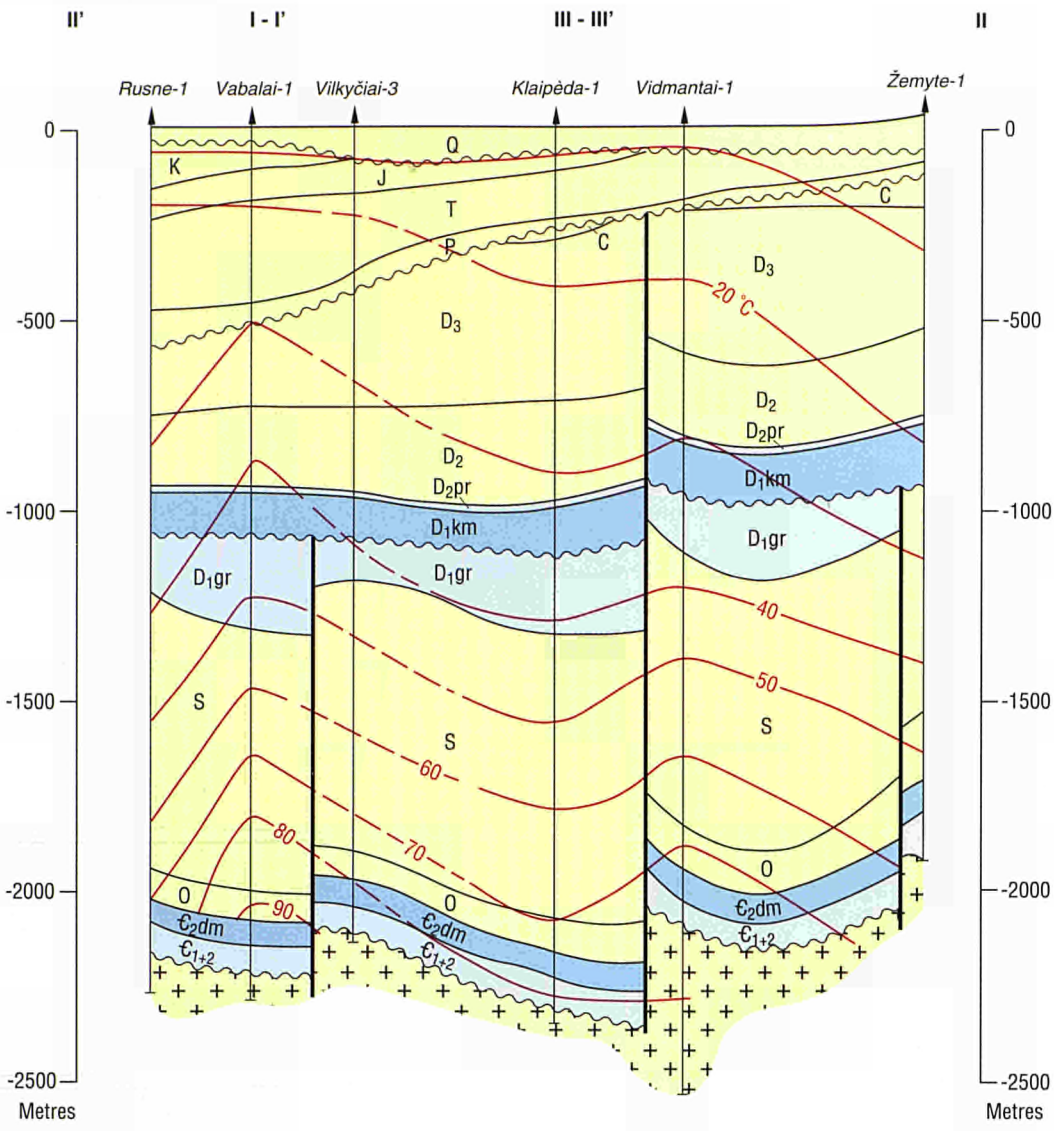


LITHUANIA





CROSS SECTION



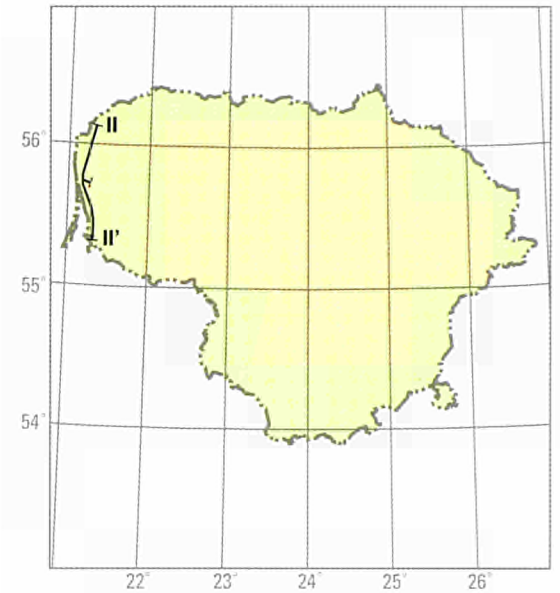
- Δz Net thickness
- P Porosity
- k Permeability
- T_b Transmissibility
- * No values can be given
- Transgression
- Borehole
- Aquifer zone of primary interest
- Aquifer zone of secondary interest

1 : 1 000 000
0 50 km

Vertical exaggeration 1:10

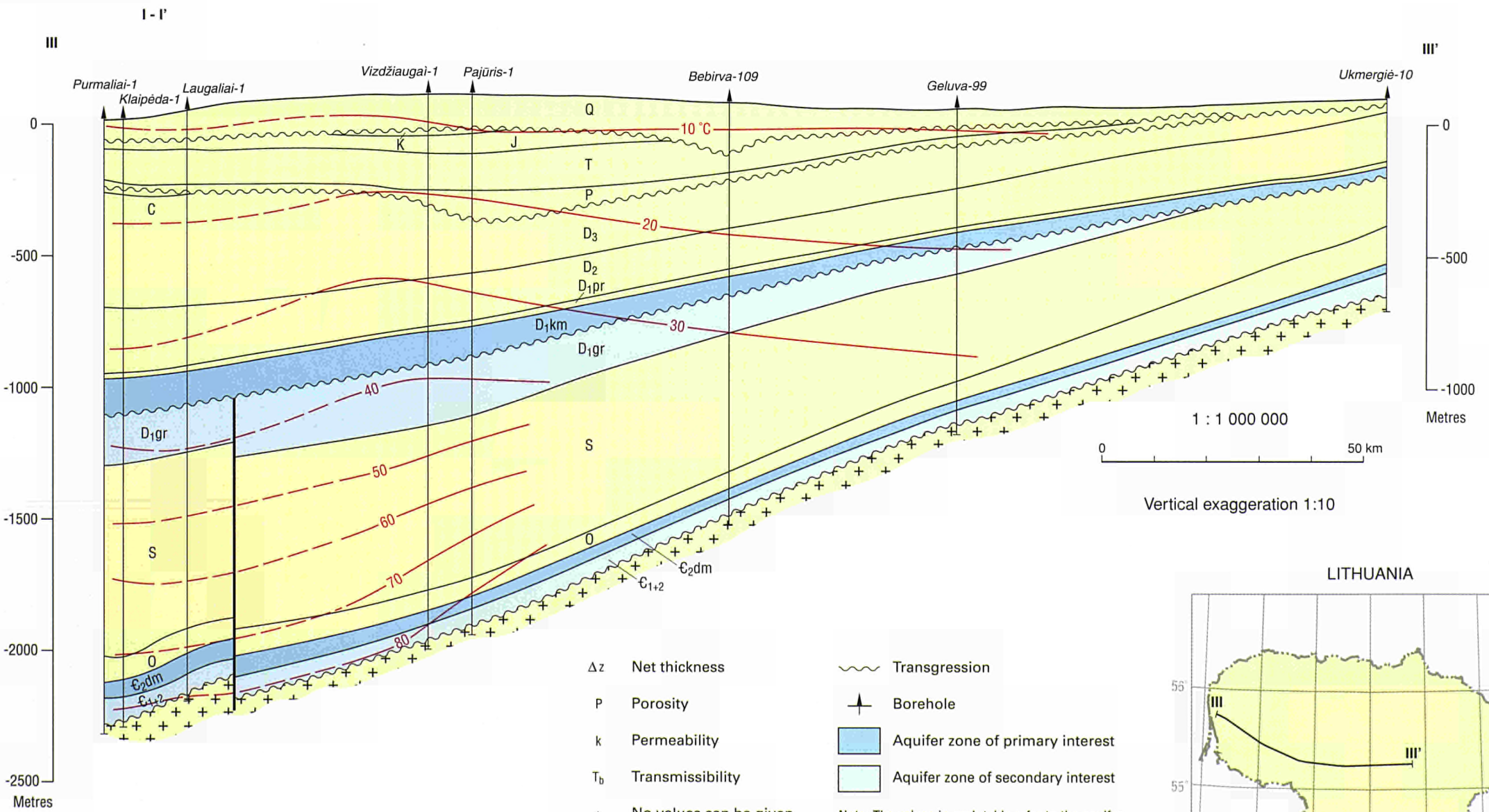
- Q Quaternary
- K Cretaceous
- J Jurassic
- T Triassic
- P Permian
- D₃ Late Devonian
- D₂ Middle Devonian
- D_{2nr} Middle Devonian, Narva
- D_{2pr} Middle Devonian, Parnu
- D_{1km} Early Devonian, Kemeru
- S Silurian
- D_{1gr} Early Devonian, Gargzdai
- O Ordovician
- Є_{2dm} Middle Cambrian, Deimena
- Є_{2kb} Middle Cambrian, Kybartai
- Є₁ Early Cambrian, (Virbalis, Gėges)

LITHUANIA



Well	Rusne-1				Vabalai-1				Vilkyčiai-3				Klaipėda - 1				Vidmantai-1				Žemlyte-1			
Aquifer	Δz m	P %	k mD	T_b Dm	Δz m	P %	k mD	T_b Dm	Δz m	P %	k mD	T_b Dm	Δz m	P %	k mD	T_b Dm	Δz m	P %	k mD	T_b Dm	Δz m	P %	k mD	T_b Dm
D _{2pr}	9.5	7.4	*	*	*	*	*	*	2.5	5.9	0.3	0.00	2.7	8	*	*	*	*	*	*	*	*	*	*
D _{1km}	54.2	25.9	380	20.6	60	24.1	200	12.0	48.3	26.3	750	36.2	63.7	3.0	18.0	11.5	92.7	20.4	6.5	6.0	88.8	22.8	140	12.4
D _{1gr}	22.5	18.4	34	0.8	19.3	20.2	60.0	1.2	29.4	25.2	570	519	32.2	20.5	70	2.3	17.3	18.1	32.0	0.6	-	-	-	-
Є _{2dm}	45.0	8.2	2.5	0.1	37.3	7.27	1.3	0.05	5.0	4.9	2.83	0.00	26.5	7.7	1.8	0.05	39.2	9.0	4.4	0.2	51.2	13.4	95.0	4.9
Є _{2kb} +Є ₁	13.0	7.6	1.69	0.02	14.5	14.8	140	2.0					12	7.6	1.7	0.02	2.8	6.2	0.7	0.00	5.2	13.8	120	0.06

CROSS SECTION

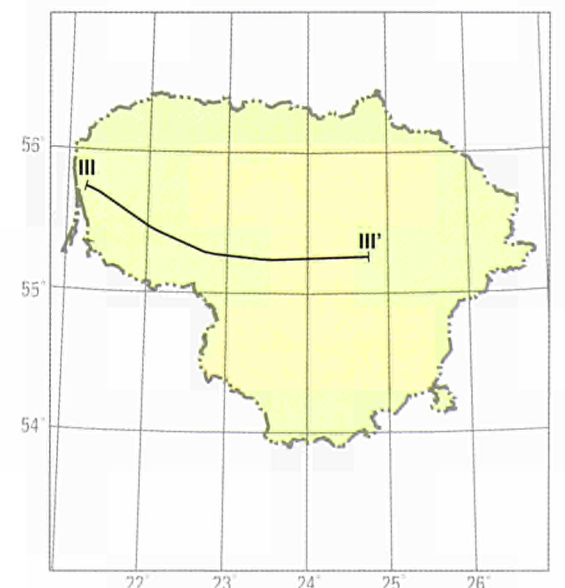


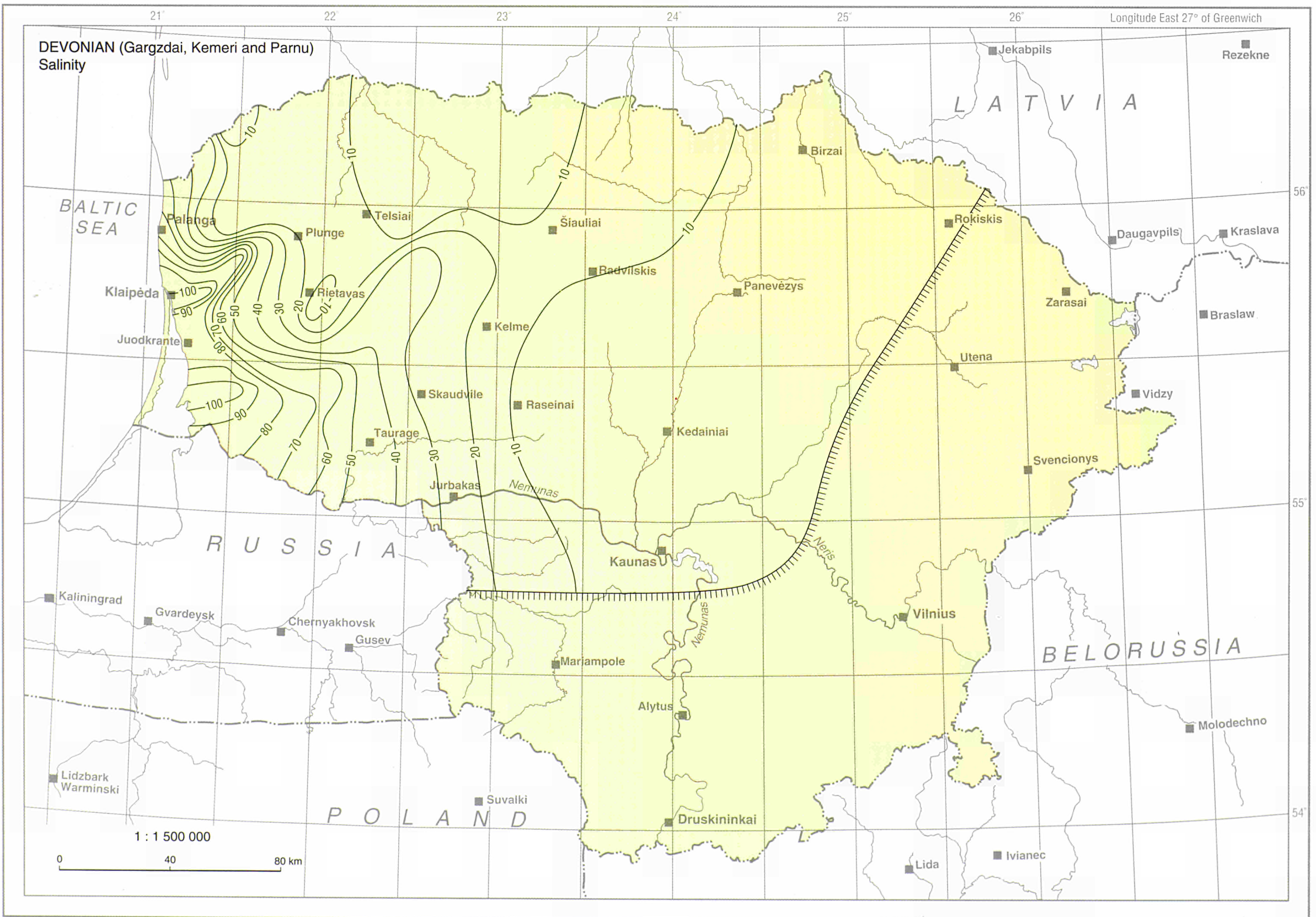
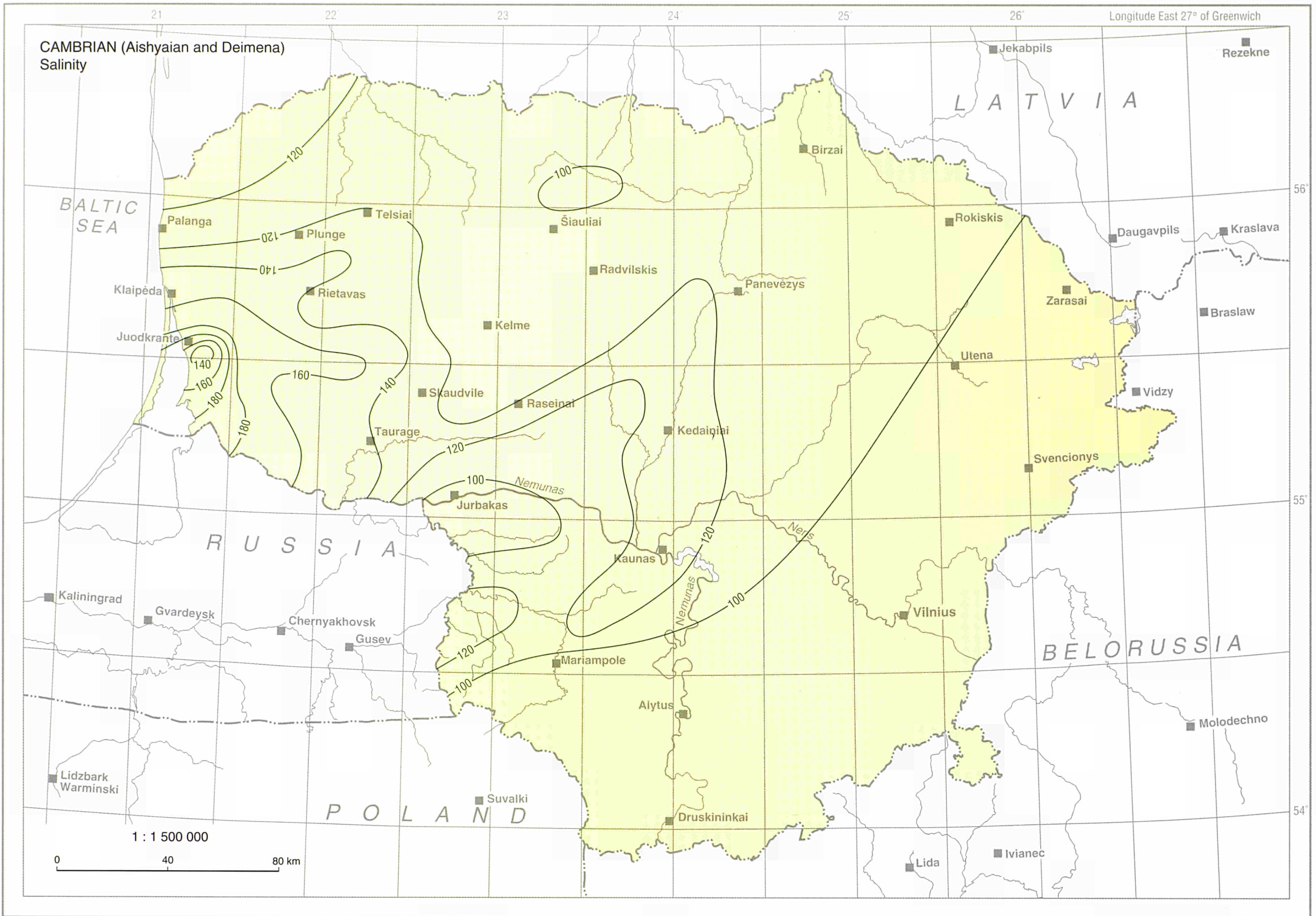
- Δz Net thickness
- P Porosity
- k Permeability
- T_b Transmissibility
- * No values can be given
- Transgression
- Borehole
- Aquifer zone of primary interest
- Aquifer zone of secondary interest

Note: The values in each table refer to the aquifer properties at the point immediately above the table

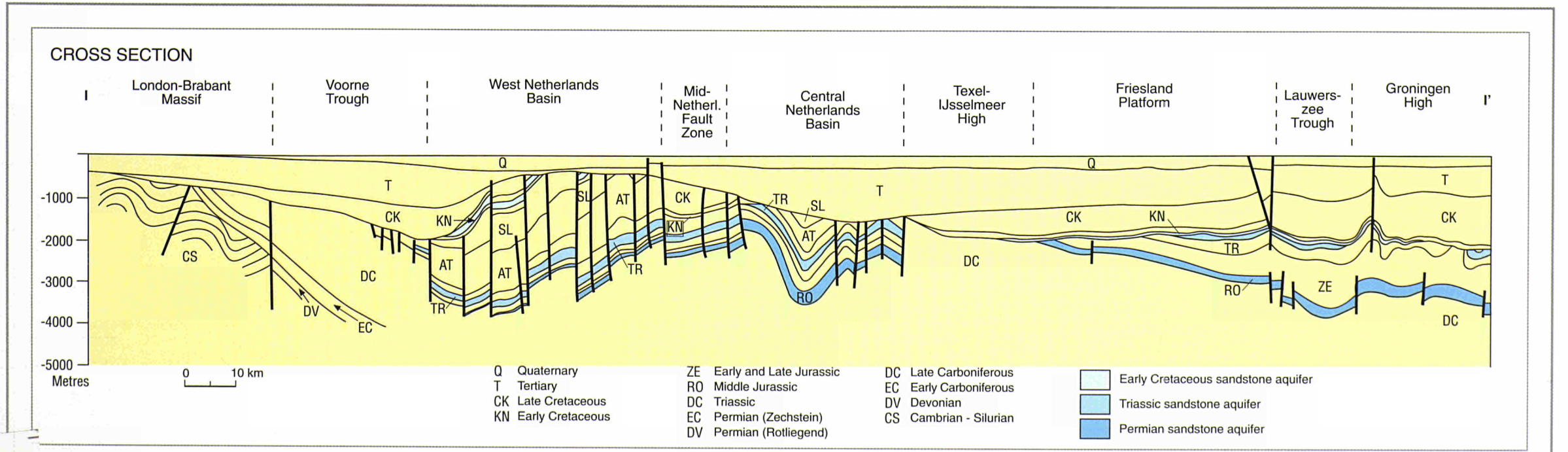
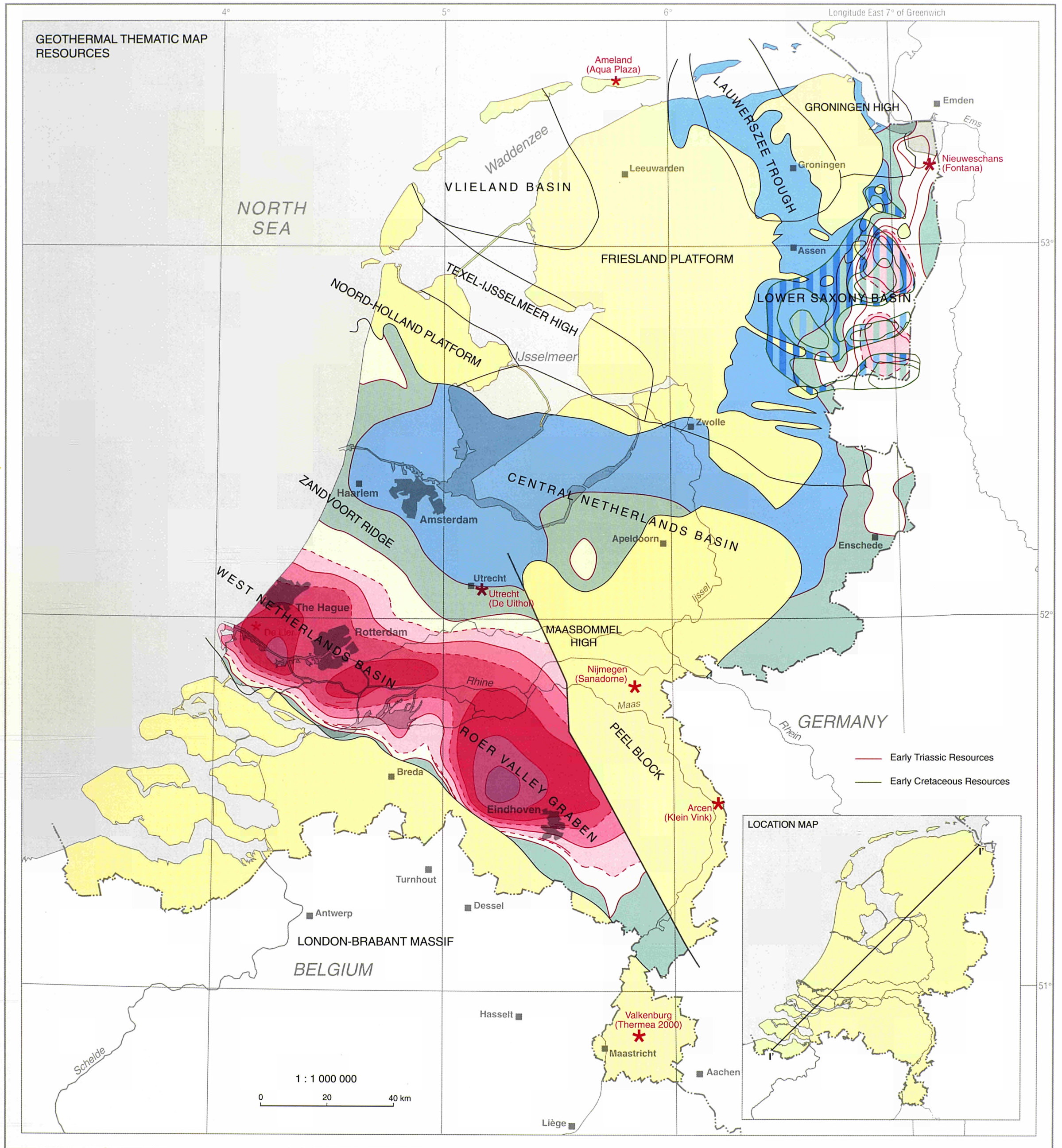
Aquifer	Δz m	P %	k mD	T_b Dm	Δz m	P %	k mD	T_b Dm	Δz m	P %	k mD	T_b Dm	Δz m	P %	k mD	T_b Dm	Δz m	P %	k mD	T_b Dm
D _{2pr}	2.5	5.9	0.3	1.00	5	8.8	*	*	5	20.5	-	-	3.0	20.0	-	-	3.0	20.0	-	-
D _{1km}	63.7	23.8	180	11.5	46.9	24.9	280	13.1	51.6	25.0	280	14.4	39.3	21.84	80	3.1	35.5	27.73	965.1	34.3
D _{1gr}	32.2	20.5	70	23.0	33.4	15.2	13.0	0.4	29.4	17.0	22.0	0.7	14.8	19.35	45	0.7	16.0	22.29	120.0	1.9
Є _{2dm}	26.5	7.7	1.8	0.05	26.7	6.9	1.1	0.03	25.0	6.89	1.1	0.03	14.0	15.8	500.2	7.0	18.5	18.47	300	59.5
Є _{2kb} +Є ₁	12	7.6	1.7	0.02	3.9	7.6	1.7	0.01	12.4	6.58	0.9	0.01	17.8	14.6	230	4.1	11.7	15.53	400	4.7

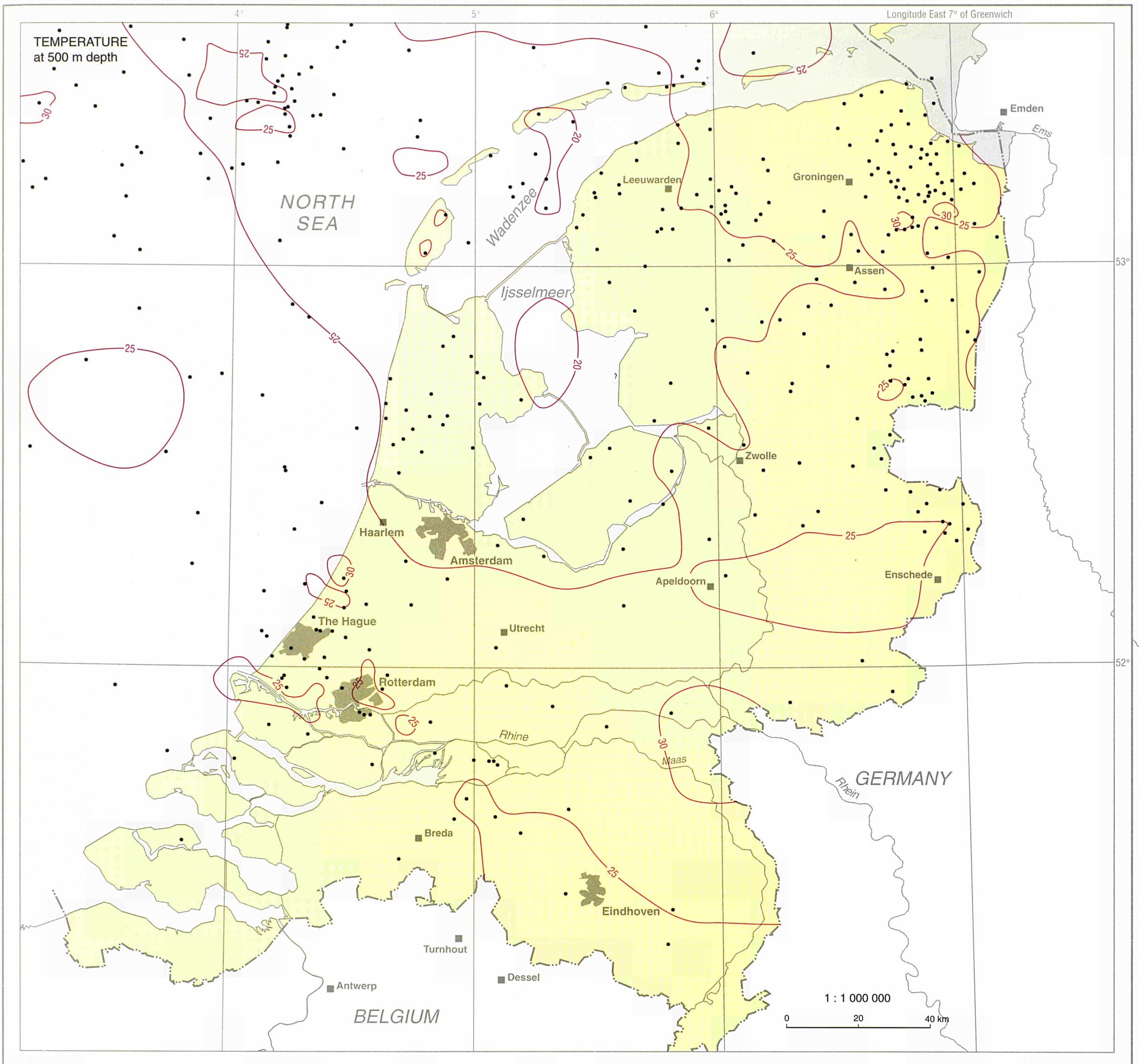
LITHUANIA



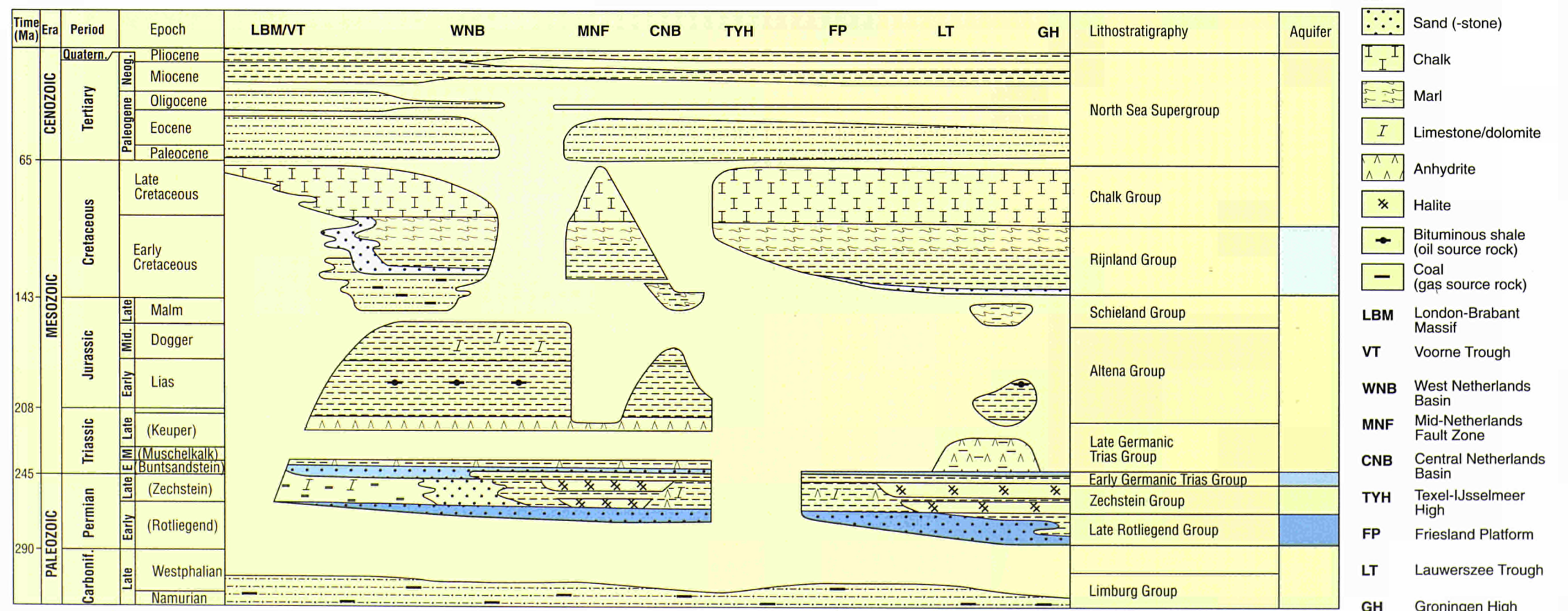


THE NETHERLANDS



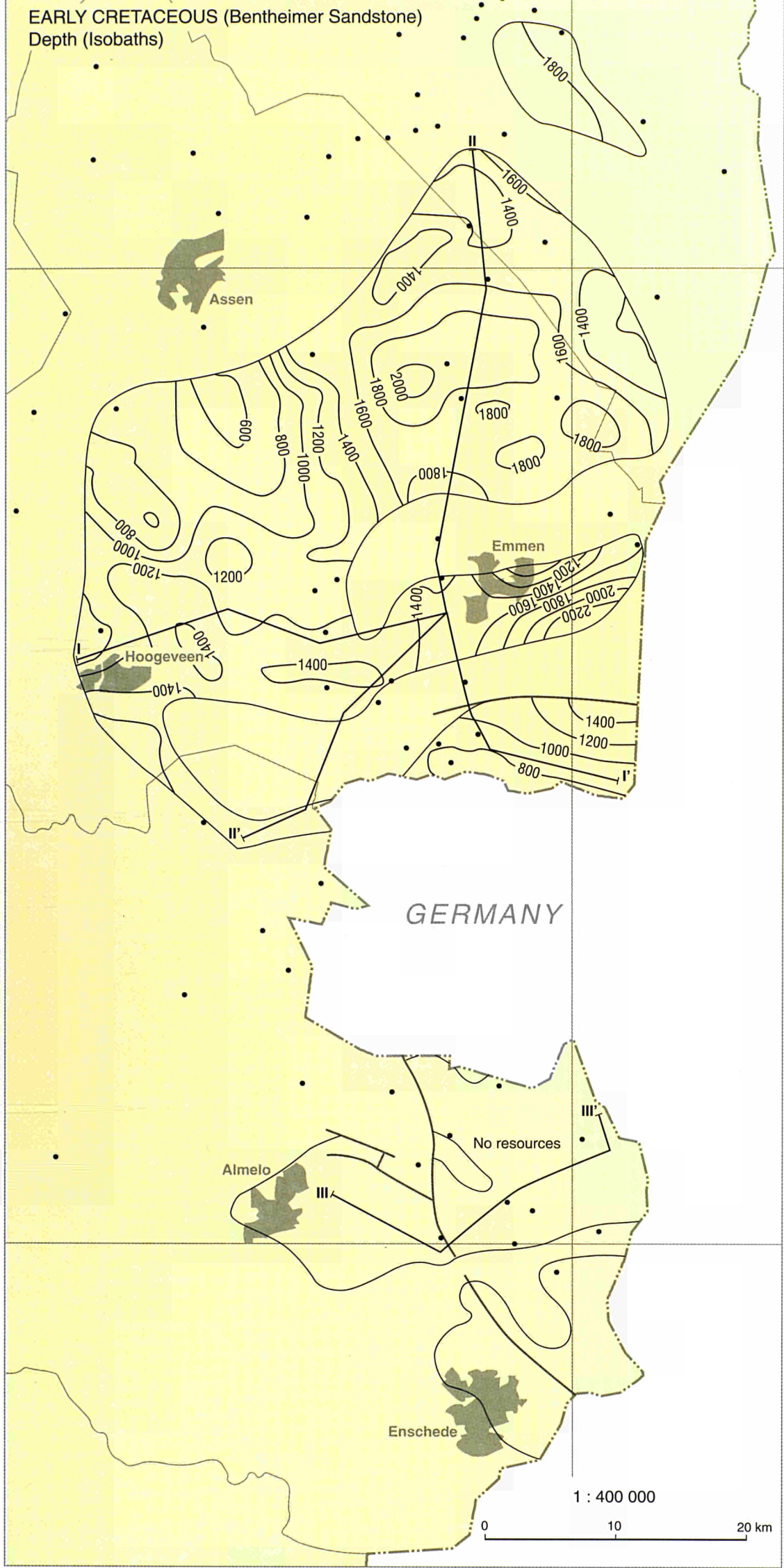


LITHOSTRATIGRAPHIC OVERVIEW OF THE NETHERLANDS

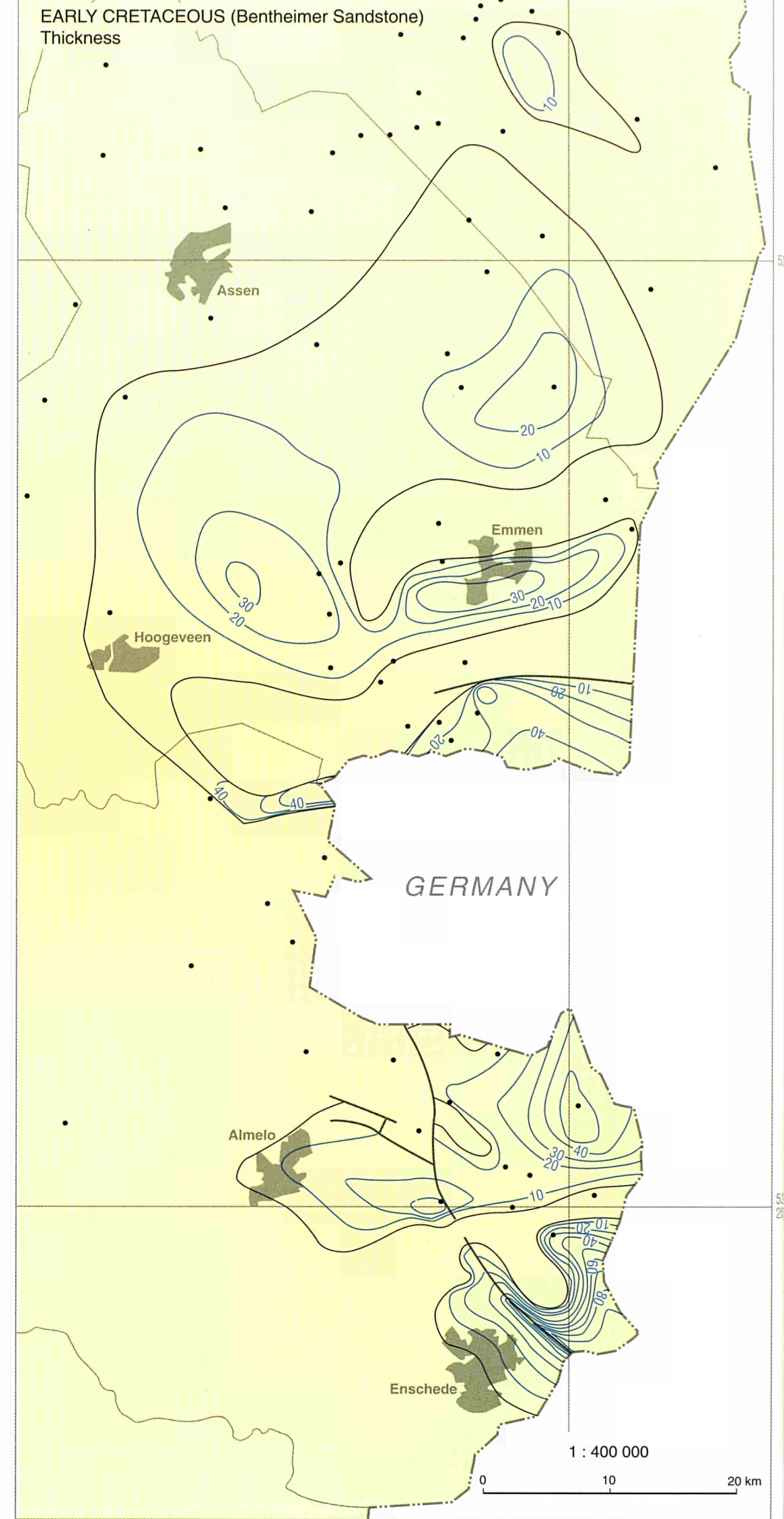


THE NETHERLANDS

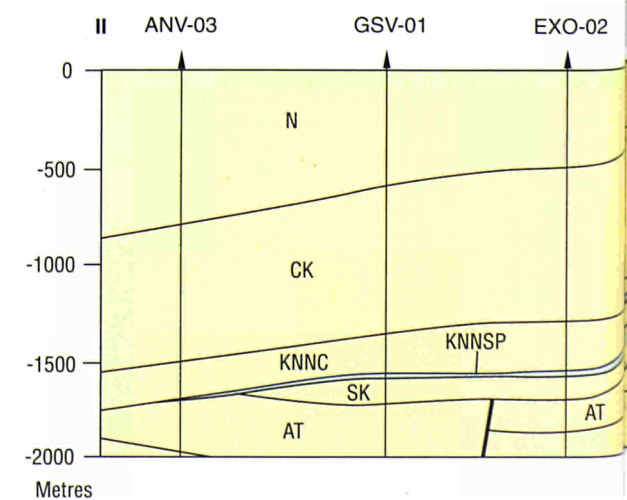
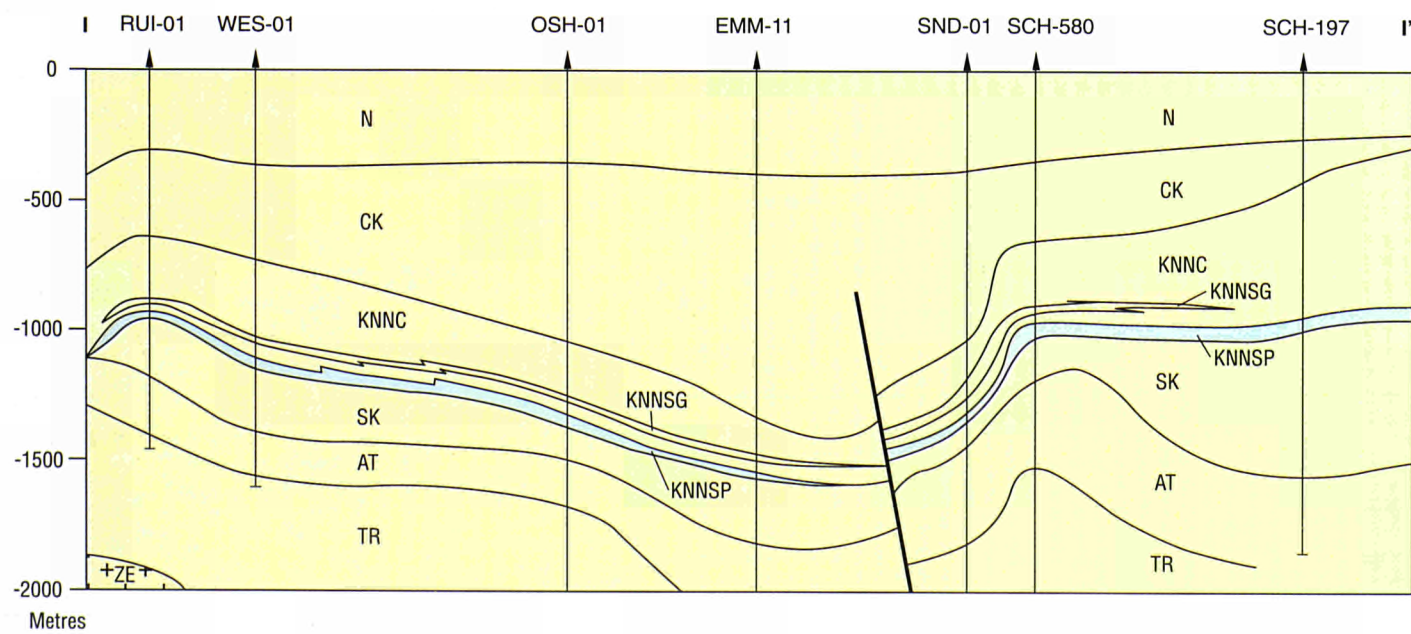
Longitude East 7° of Greenwich



Longitude East 7° of Greenwich

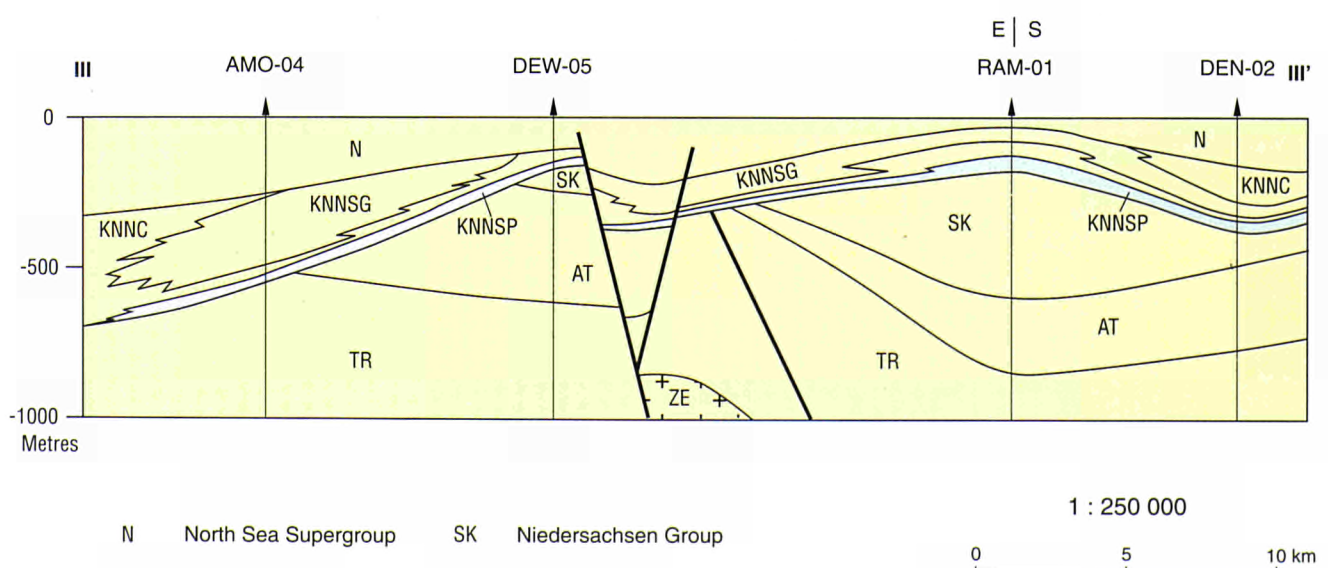
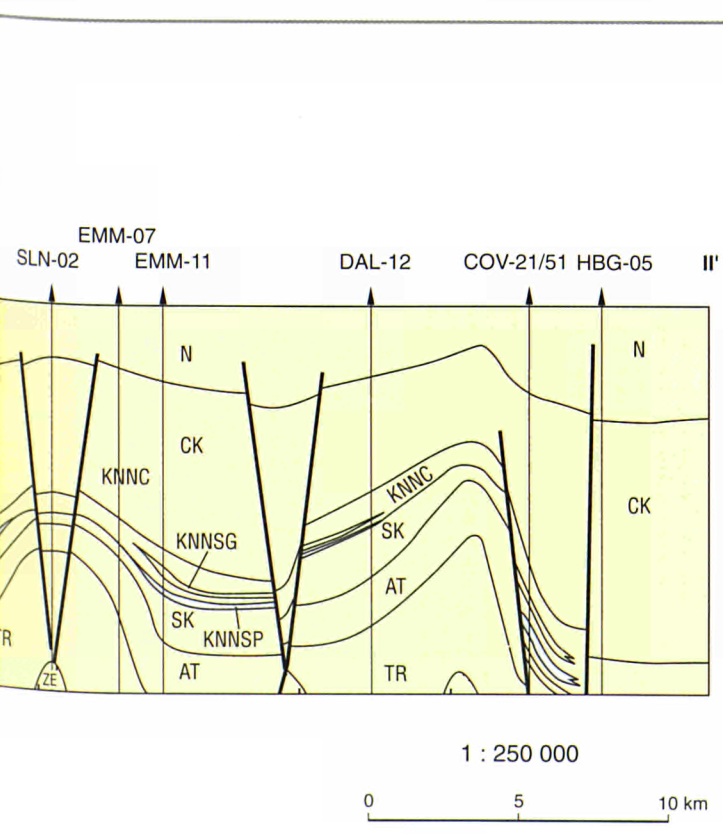
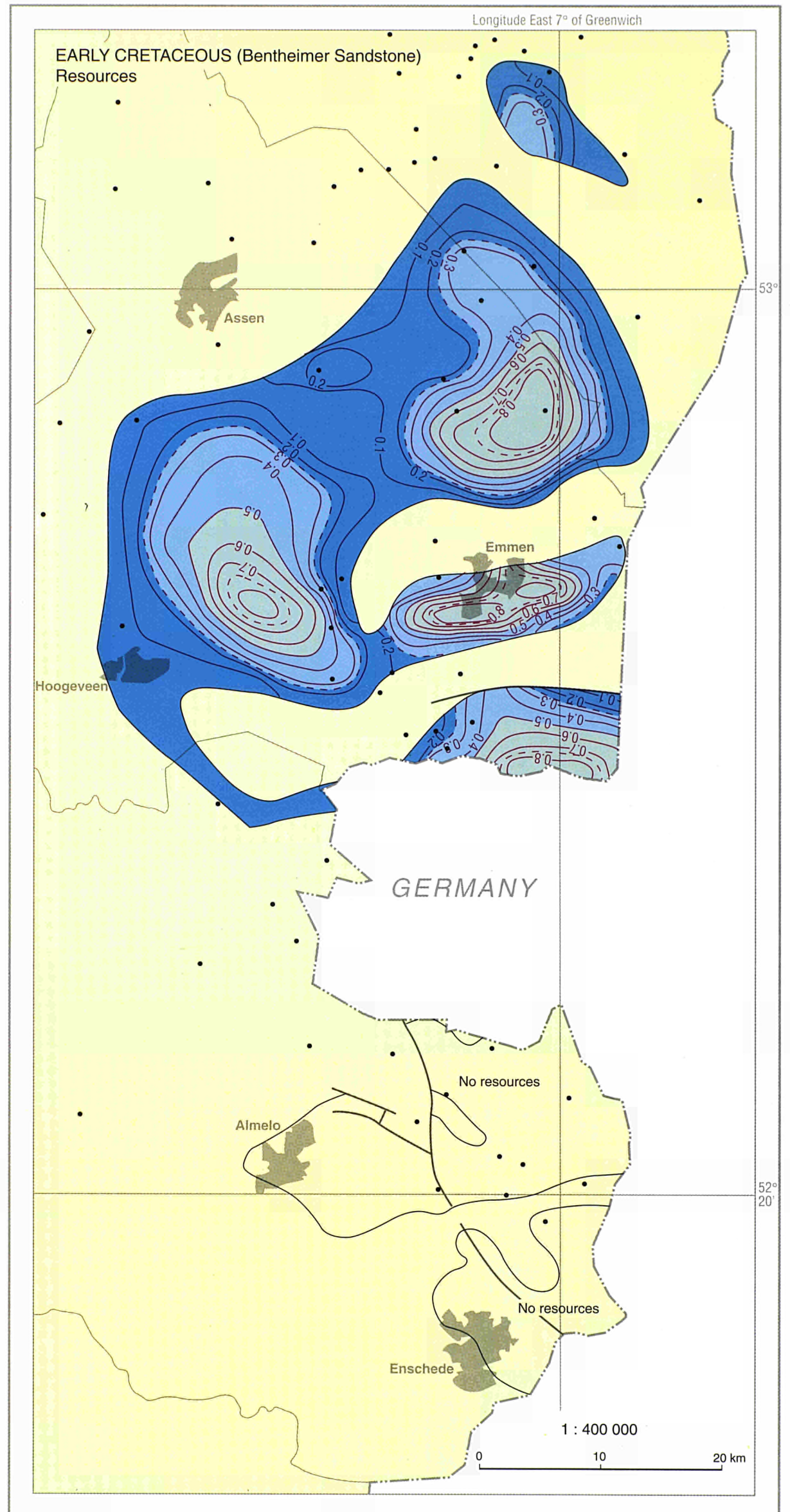
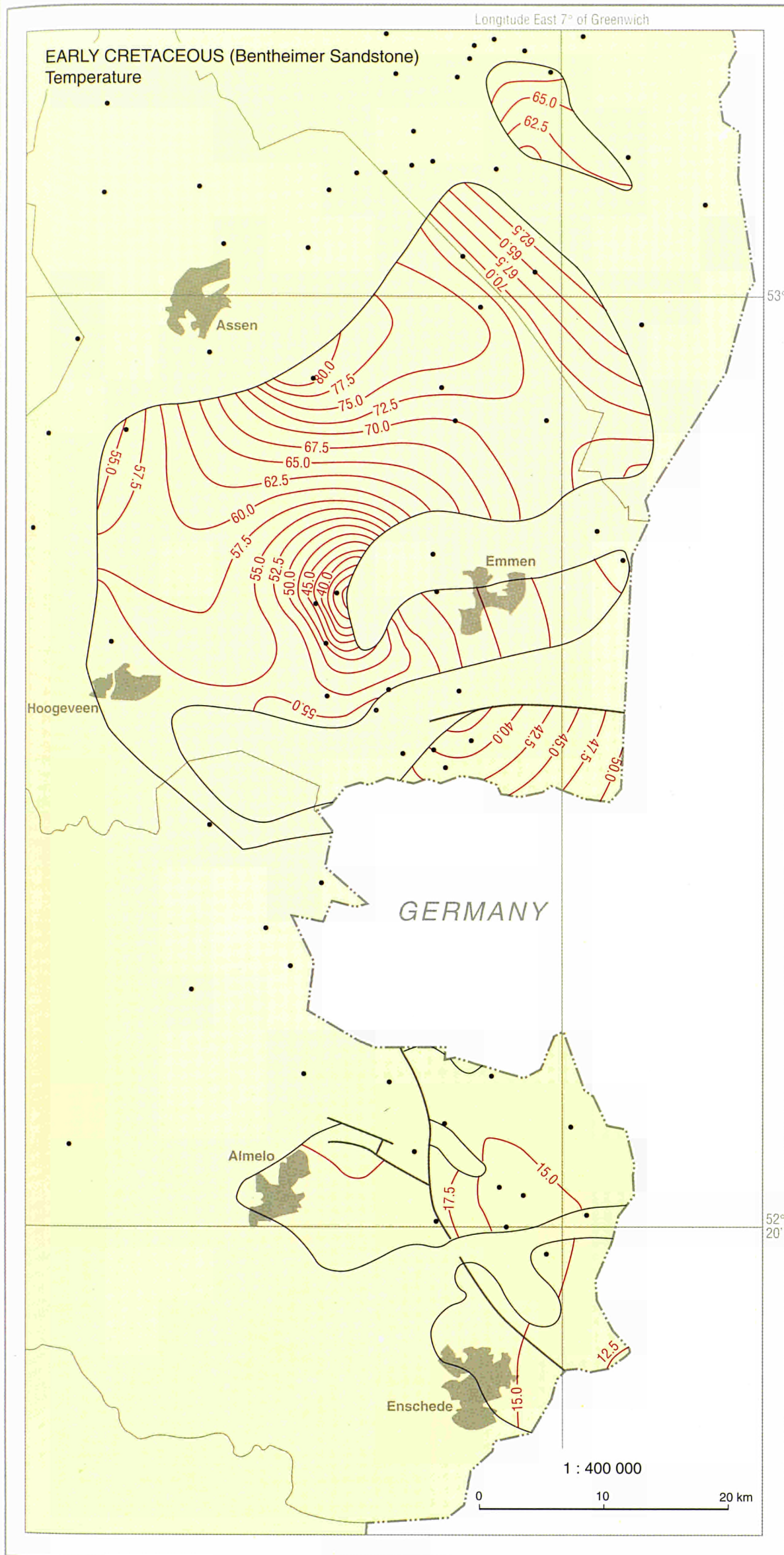


CROSS SECTIONS



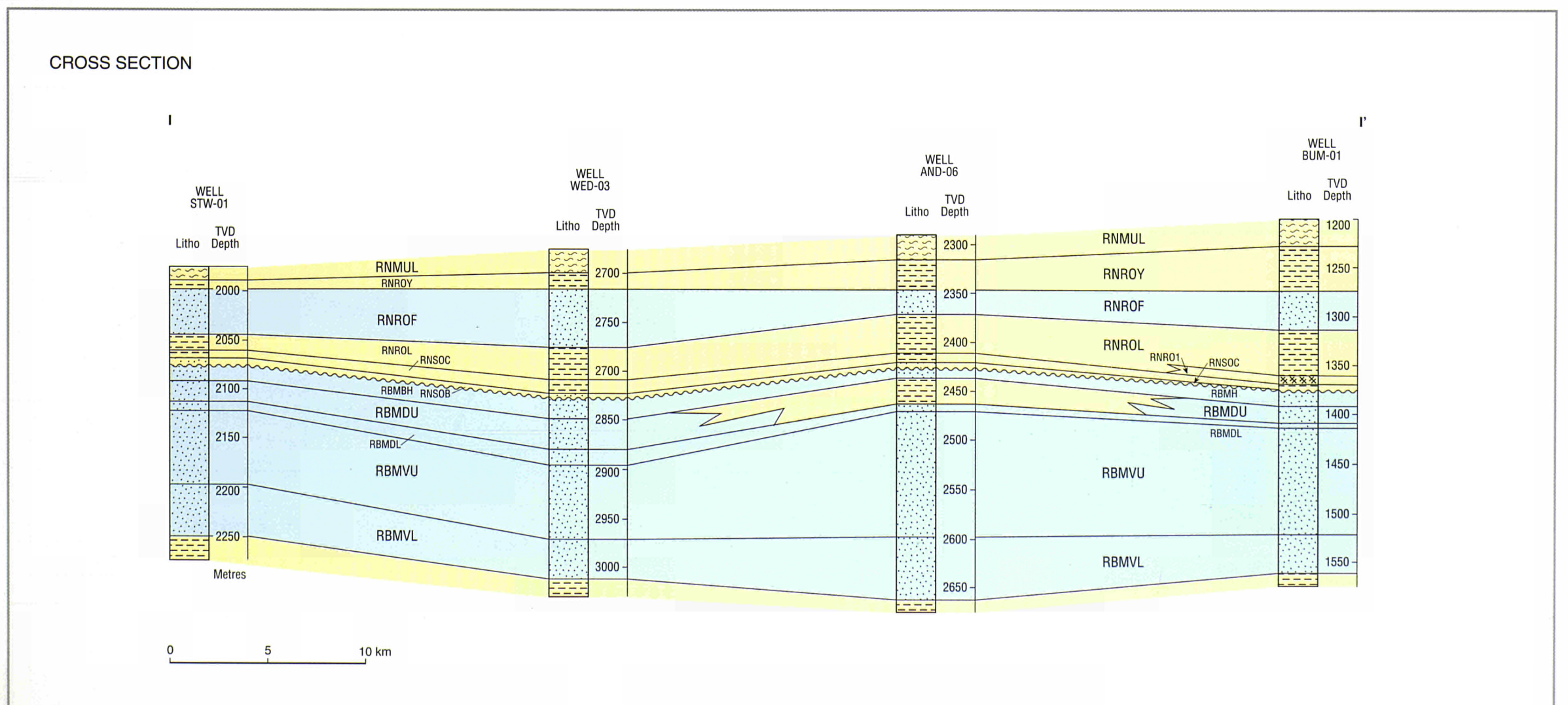
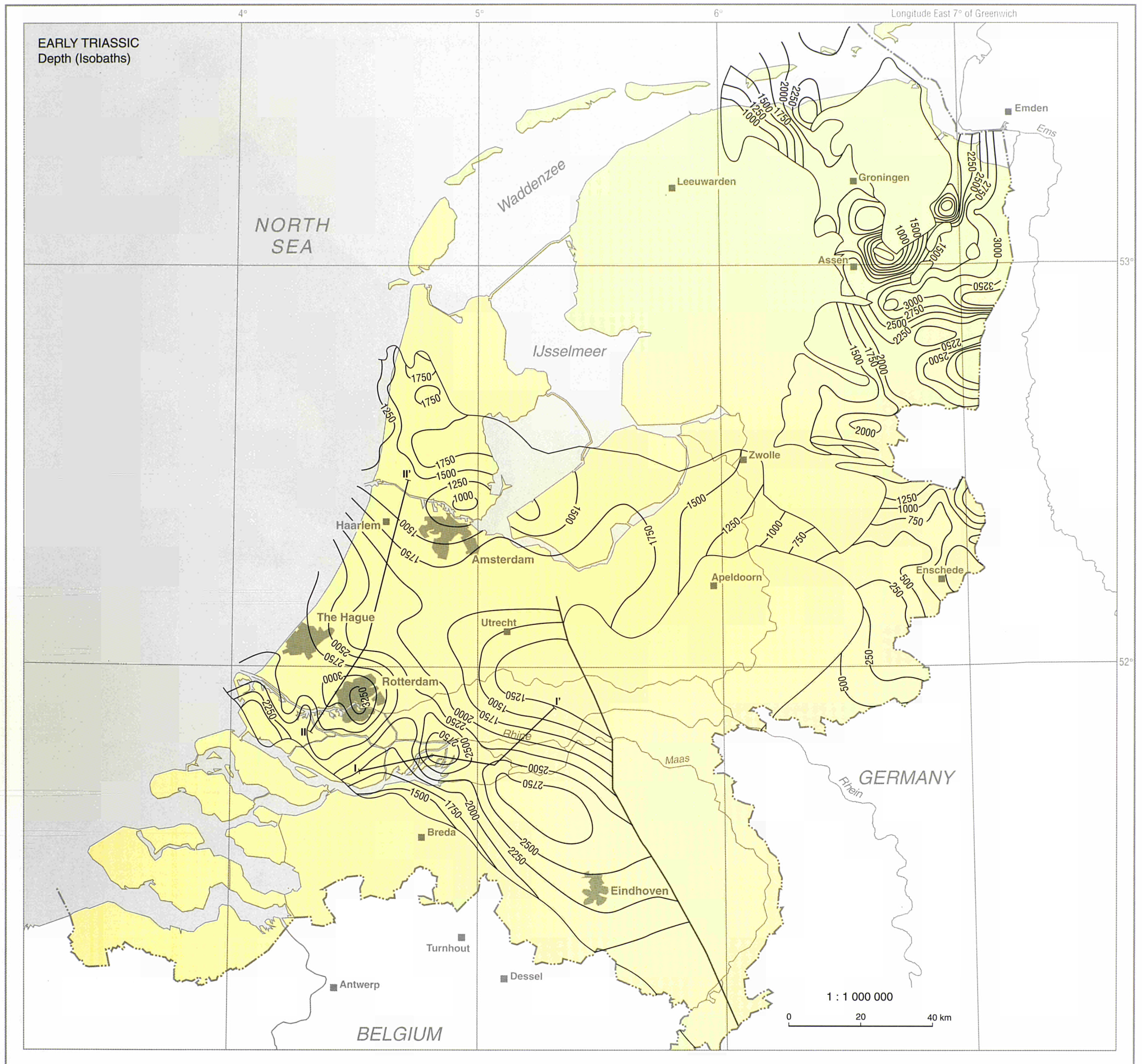
1 : 250 000

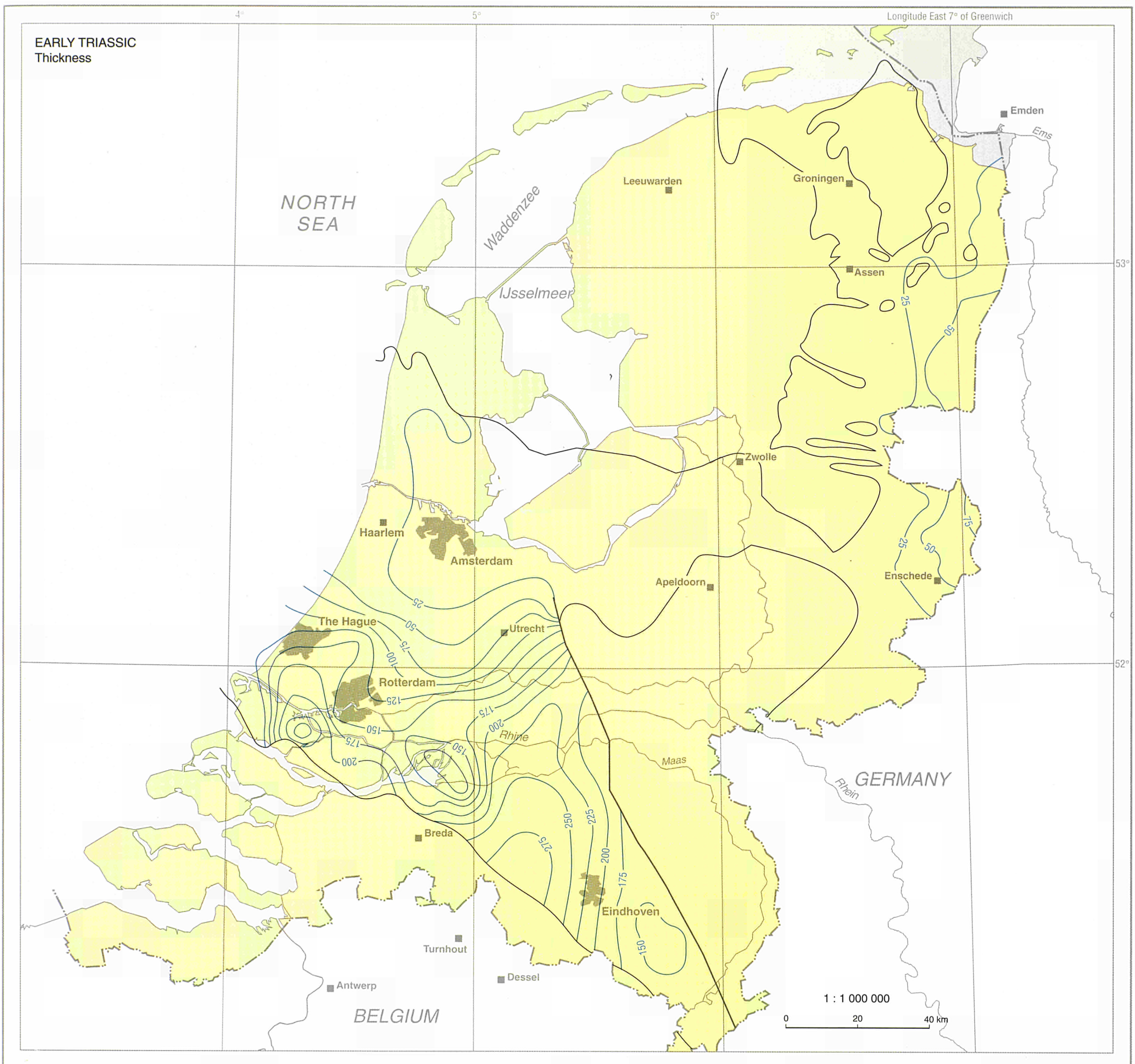
0 5 10 km



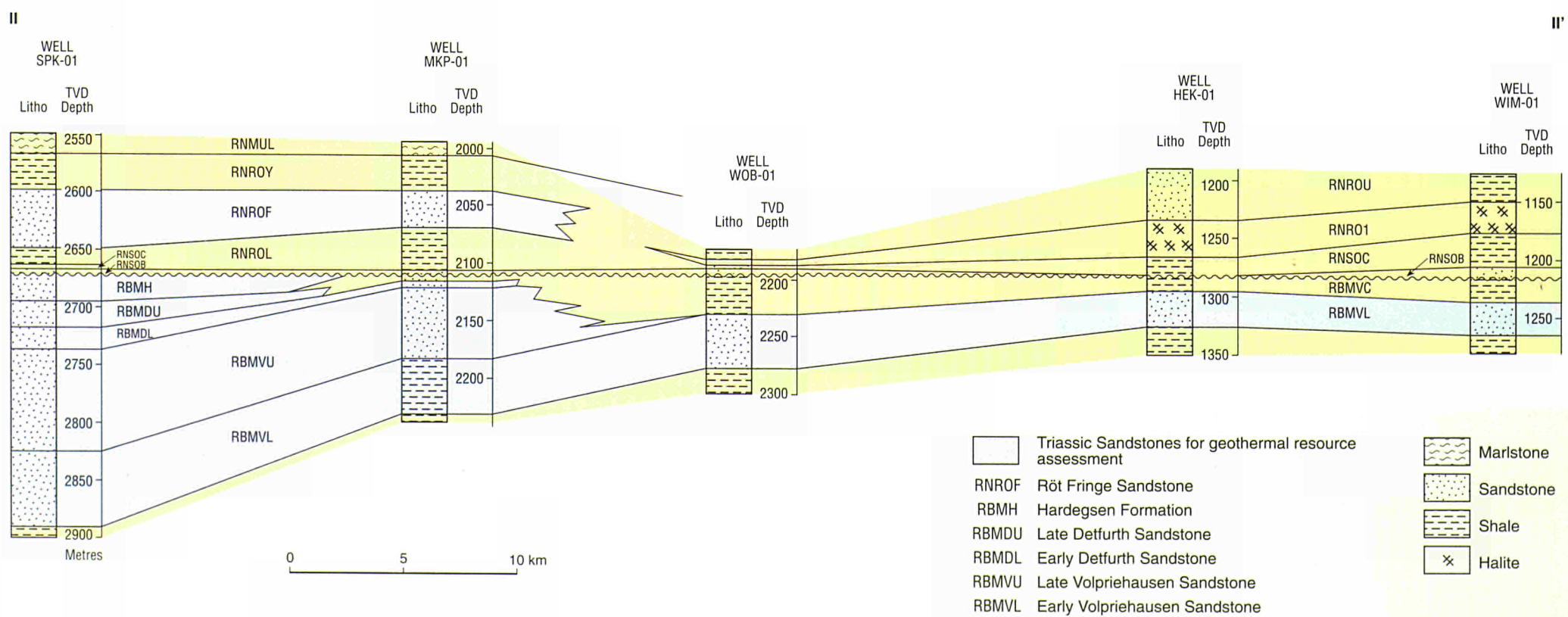
- | | | | |
|-------|----------------------|----|--------------------------------------|
| N | North Sea Supergroup | SK | Niedersachsen Group |
| CK | Chalk Group | AT | Altena Group |
| KNNC | Vlieland Claystone | TR | Late and Early Germanic Trias Groups |
| KNNSG | Gildehaus Sandstone | ZE | Zechstein Group |
| KNNSP | Bentheim Sandstone | | |

THE NETHERLANDS

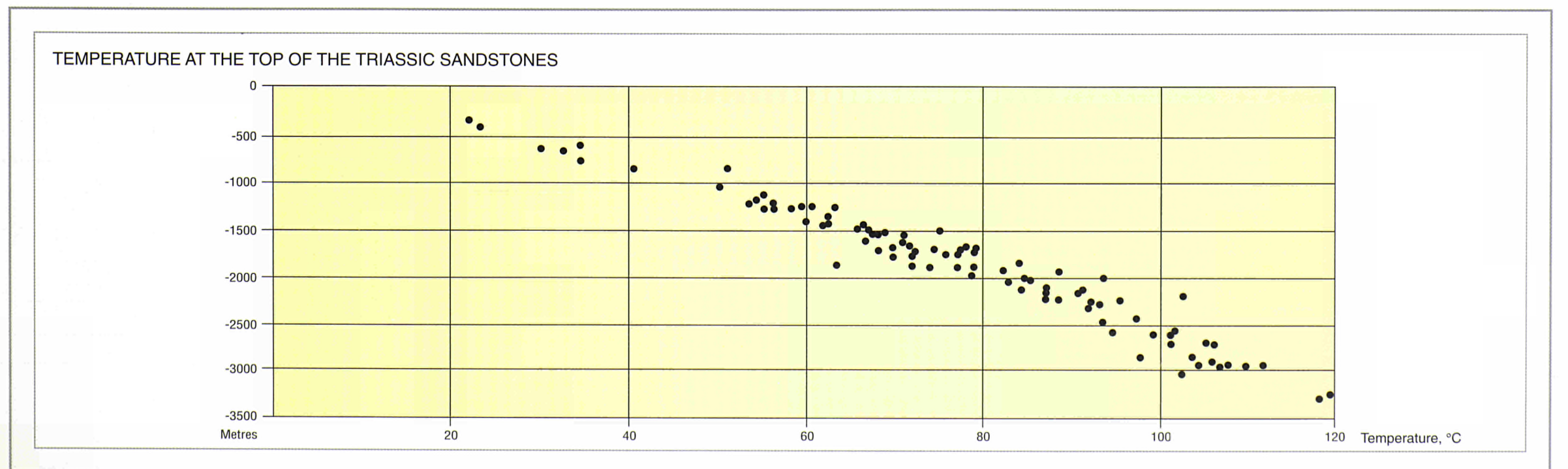




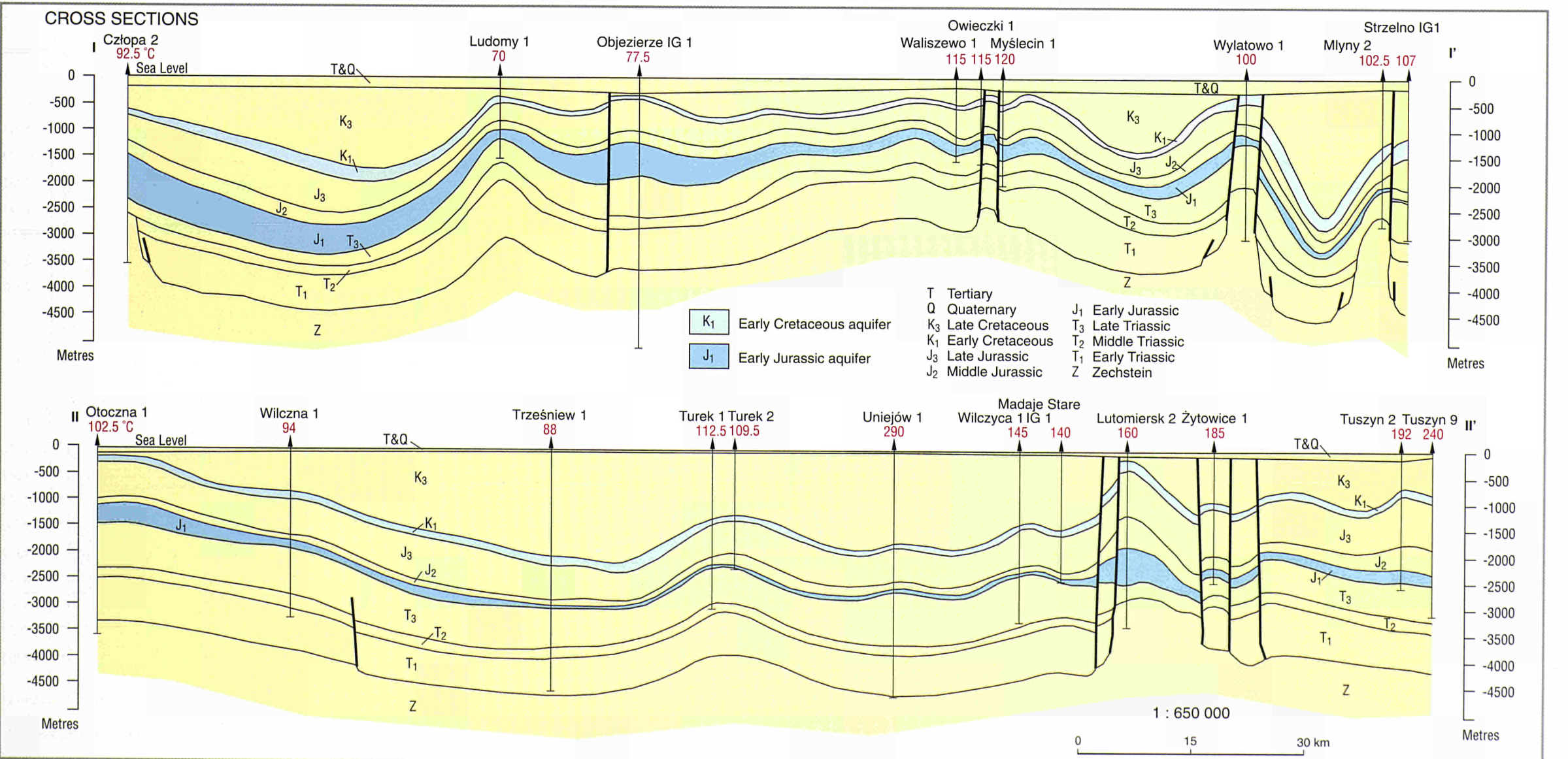
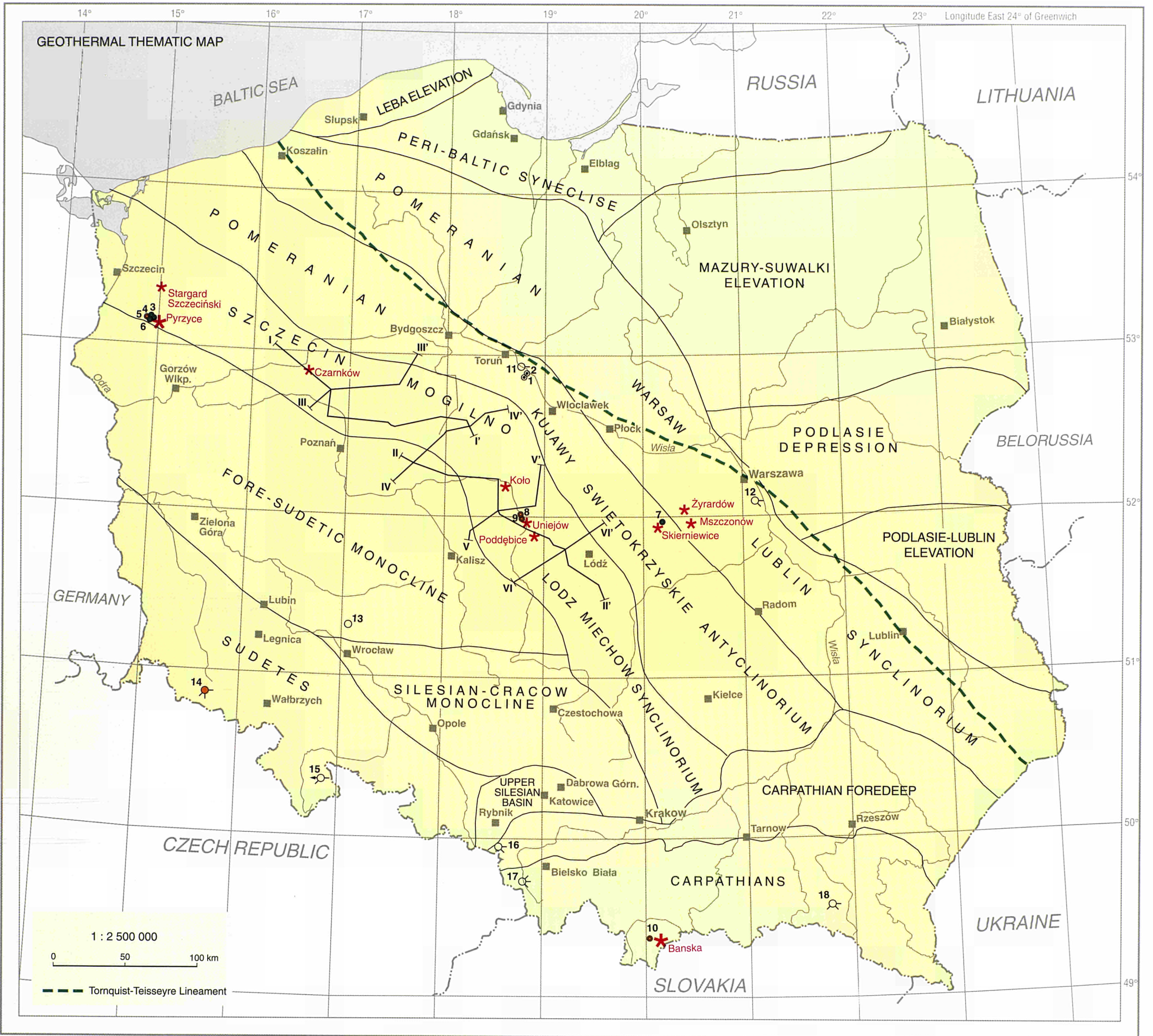
CROSS SECTION

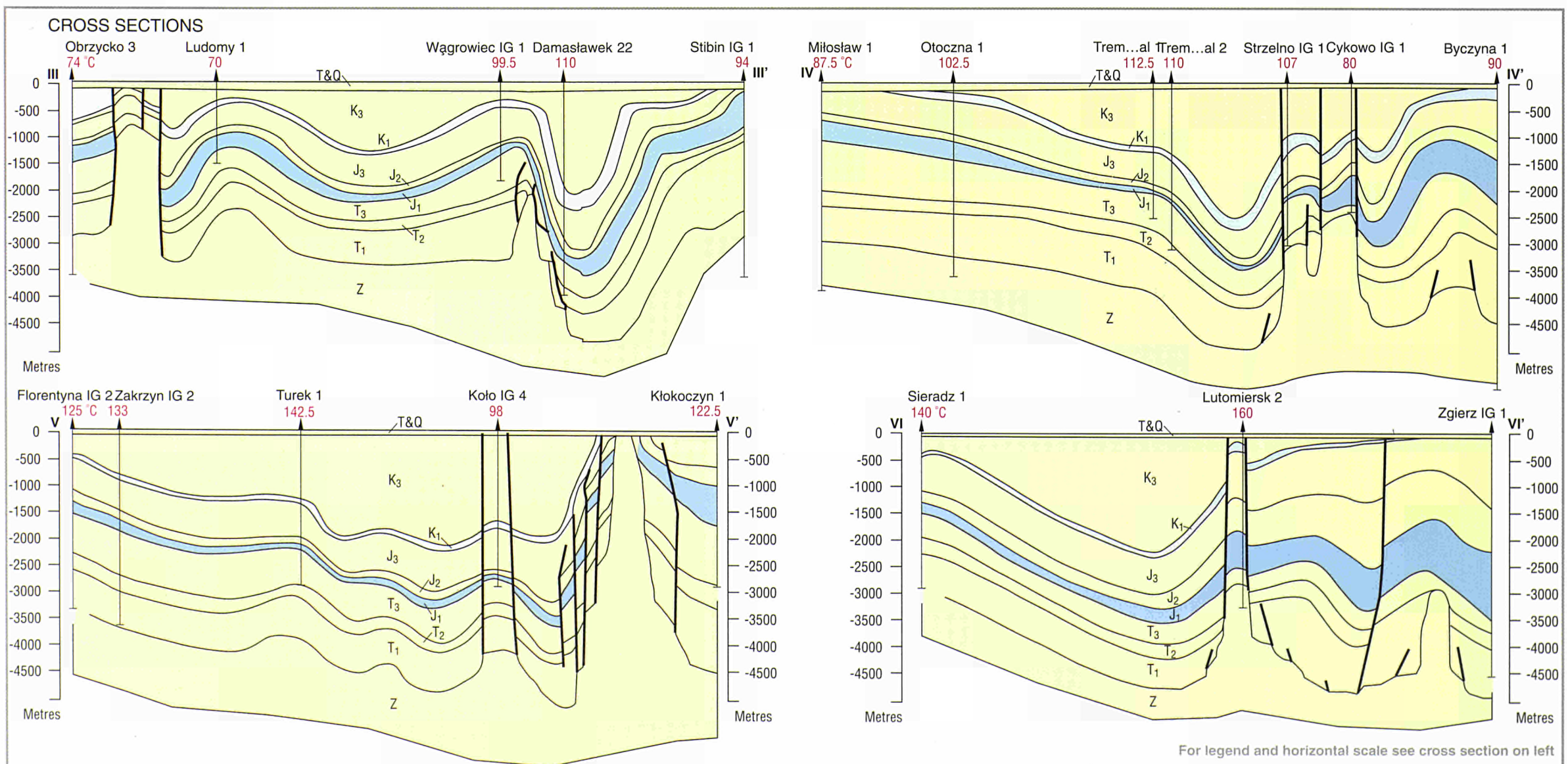
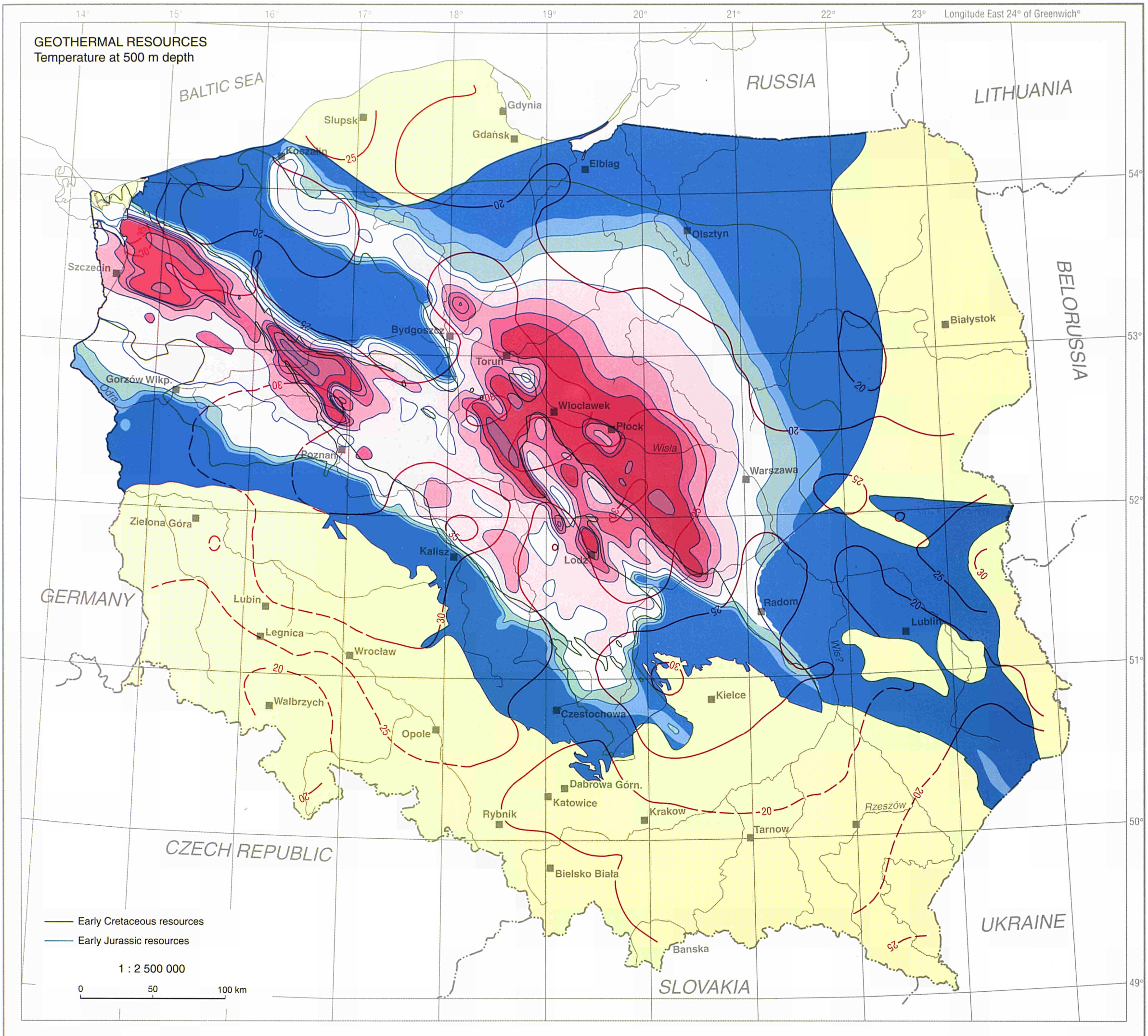


THE NETHERLANDS

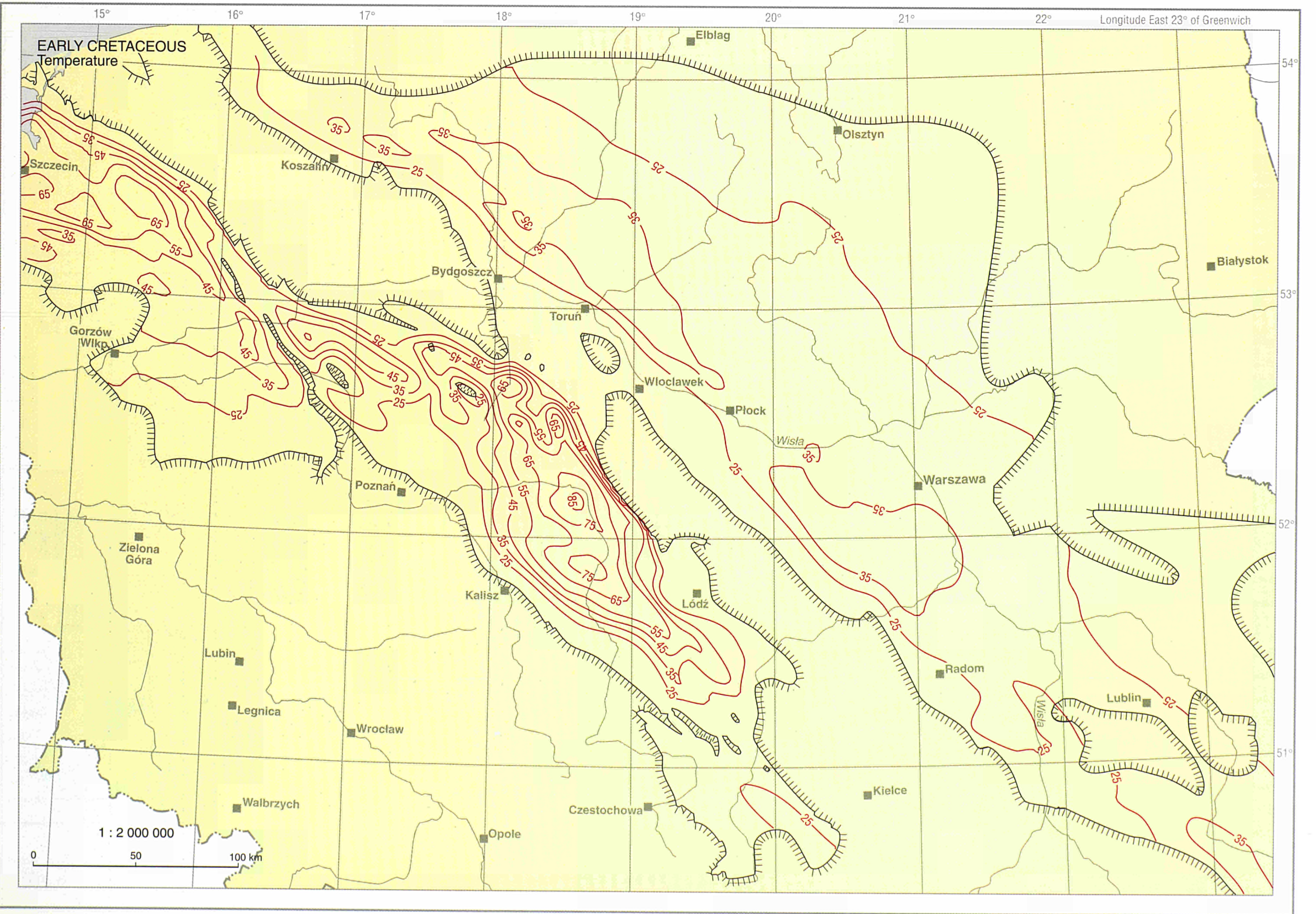
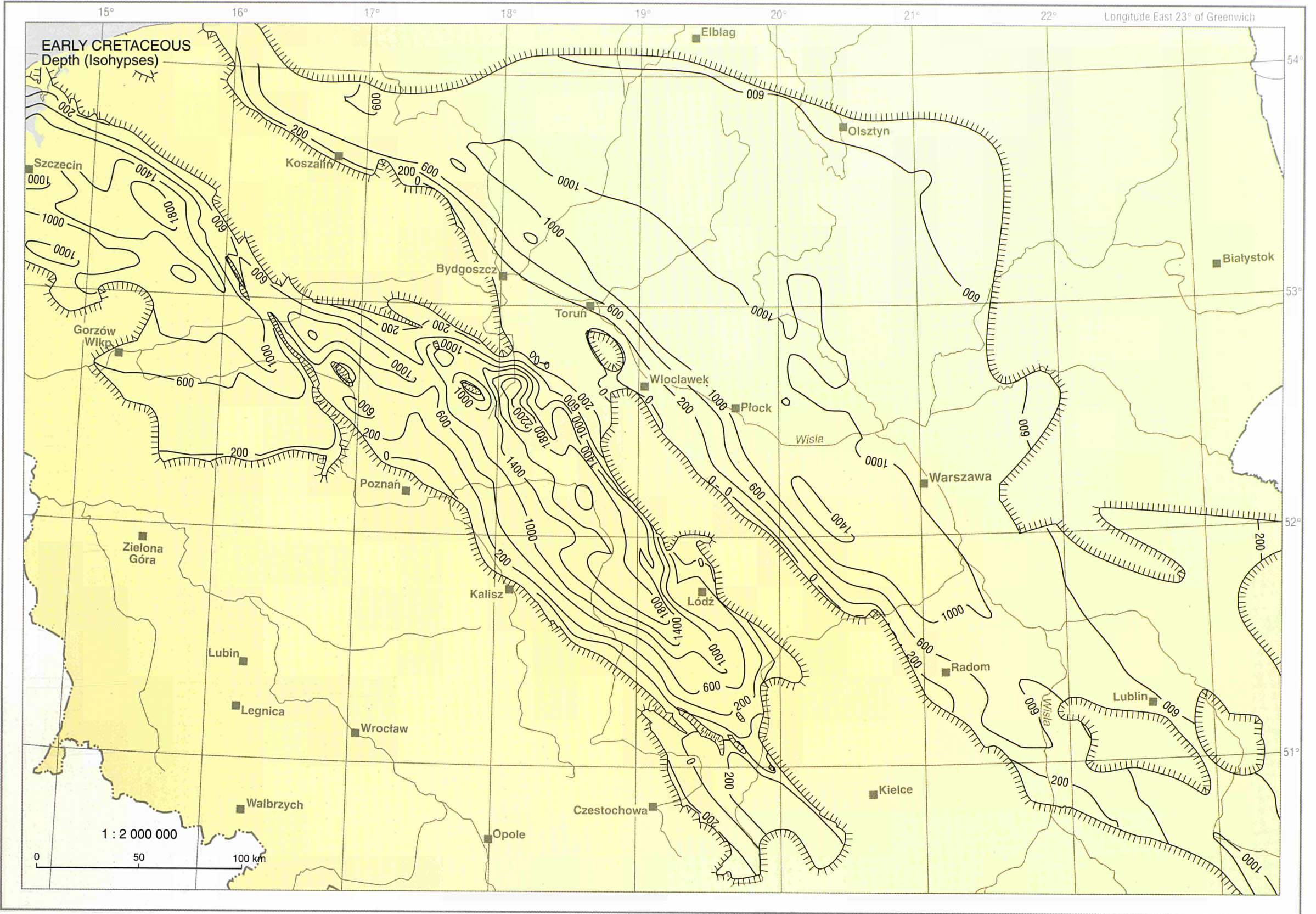


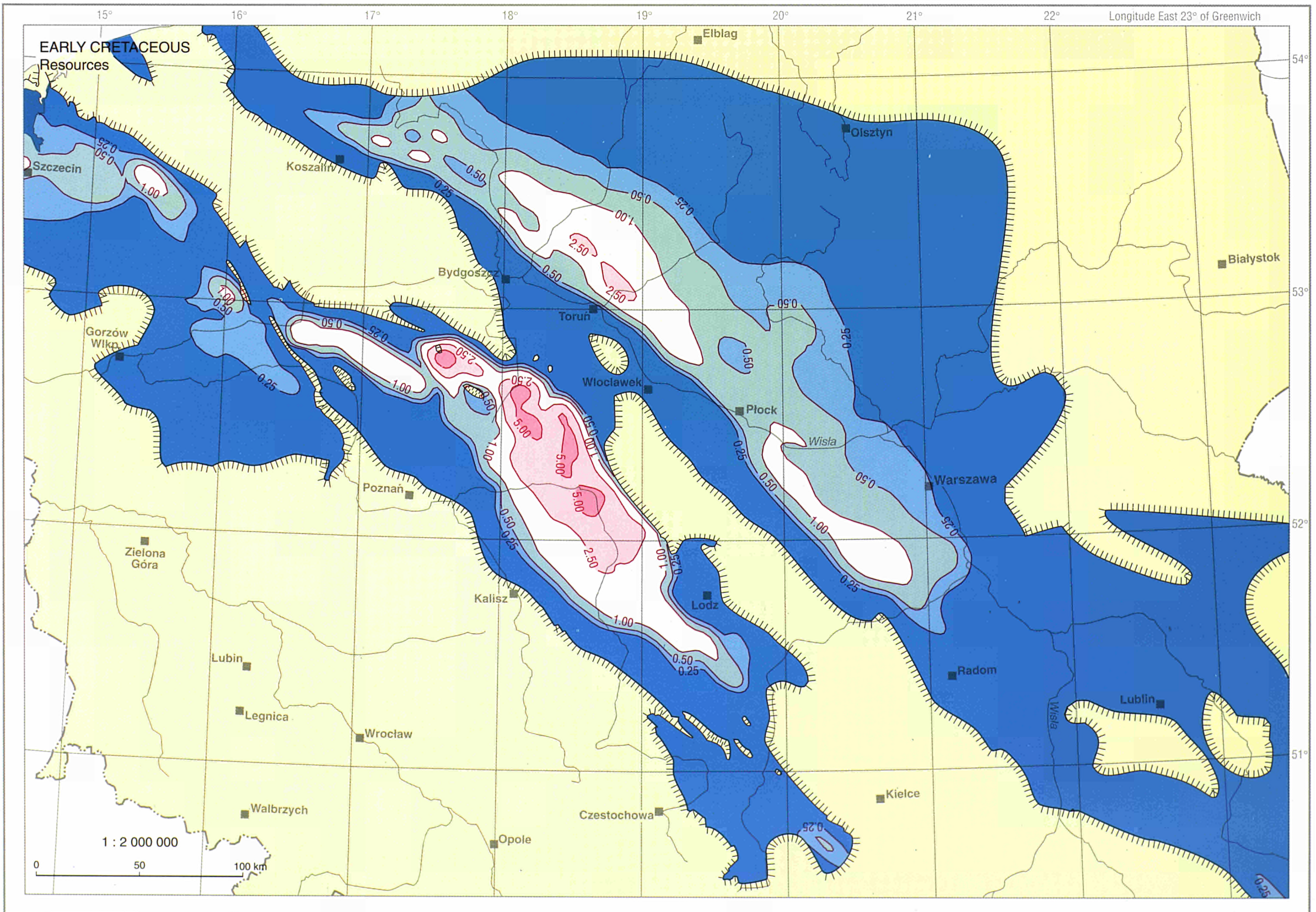
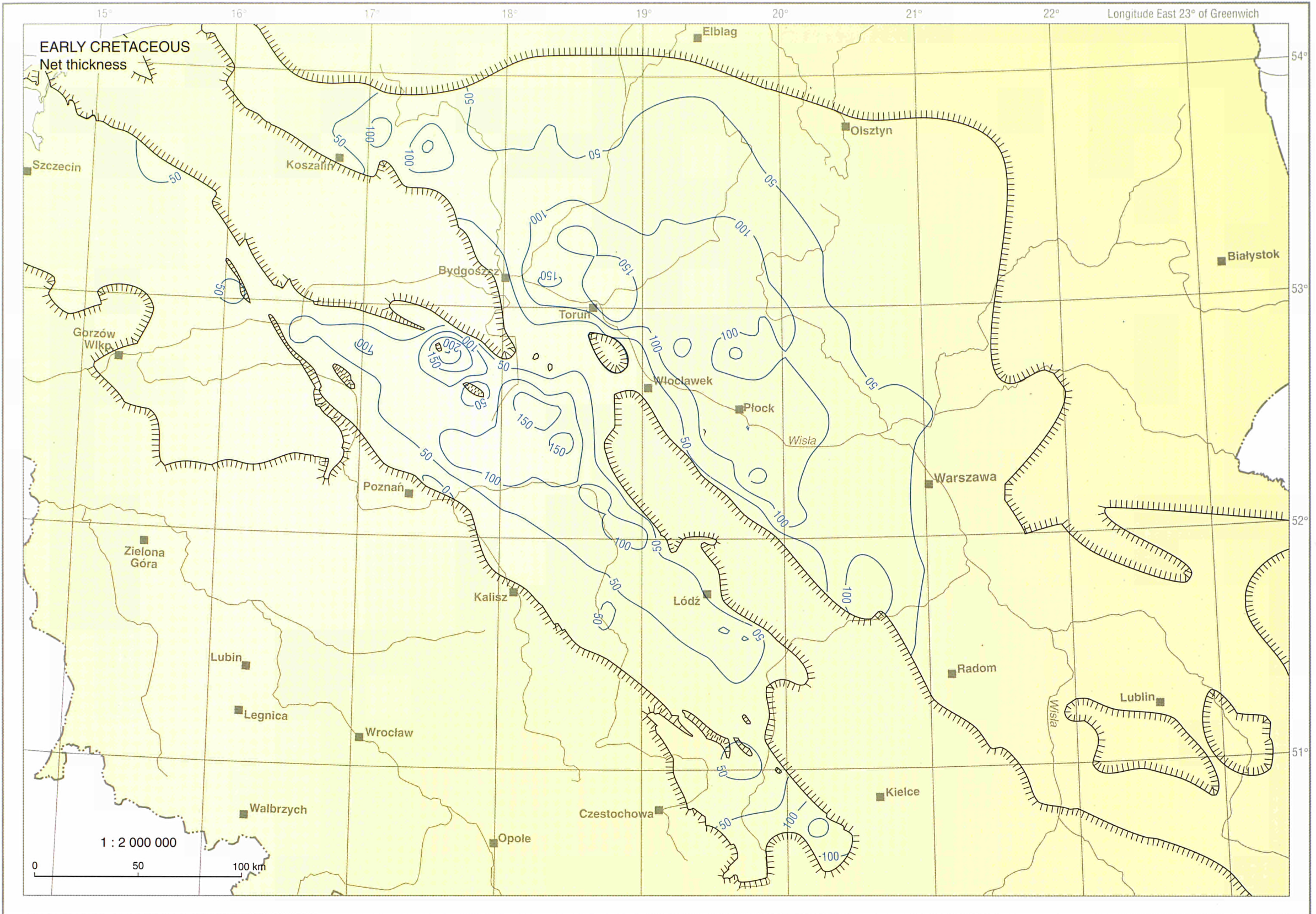
POLAND



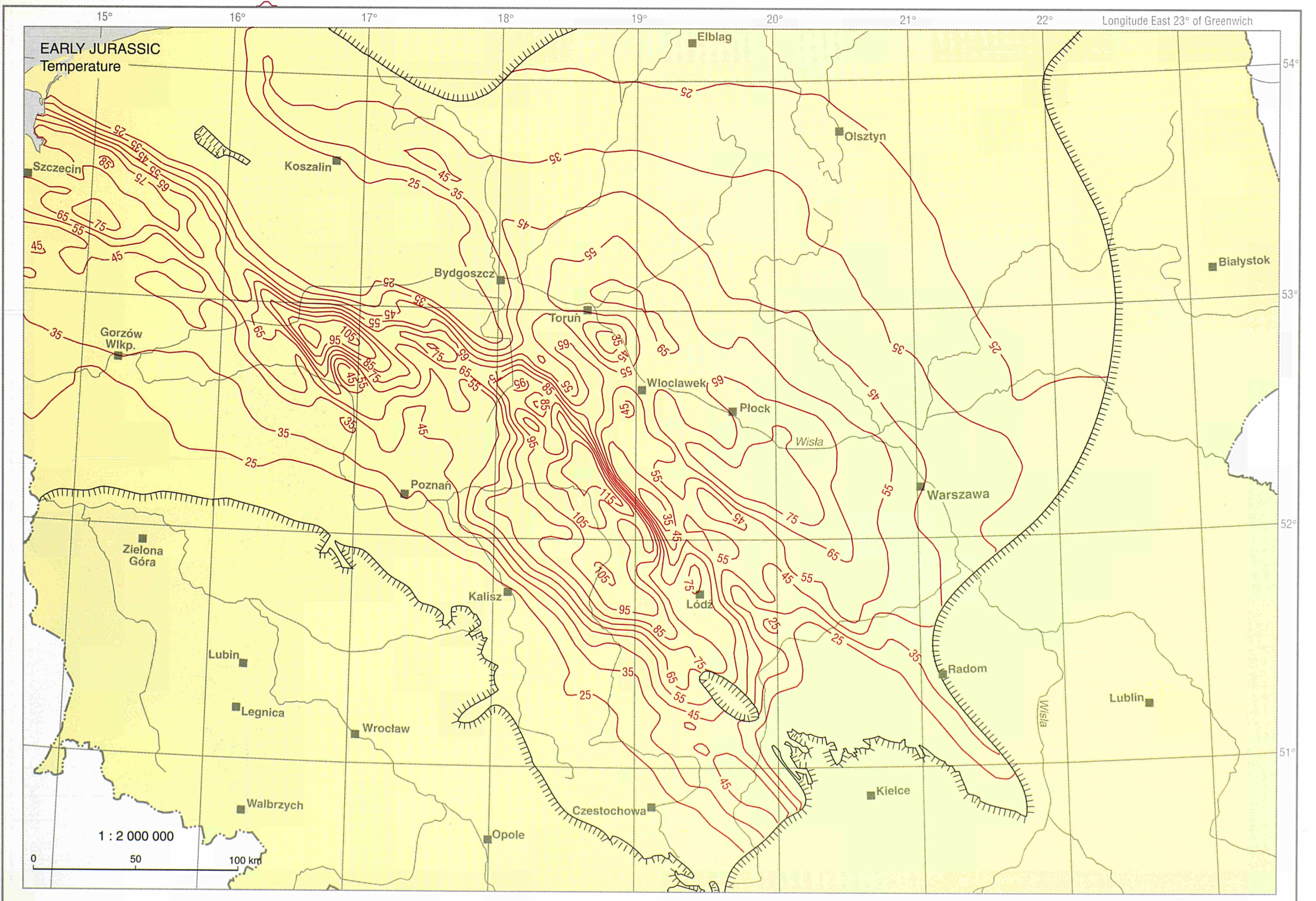
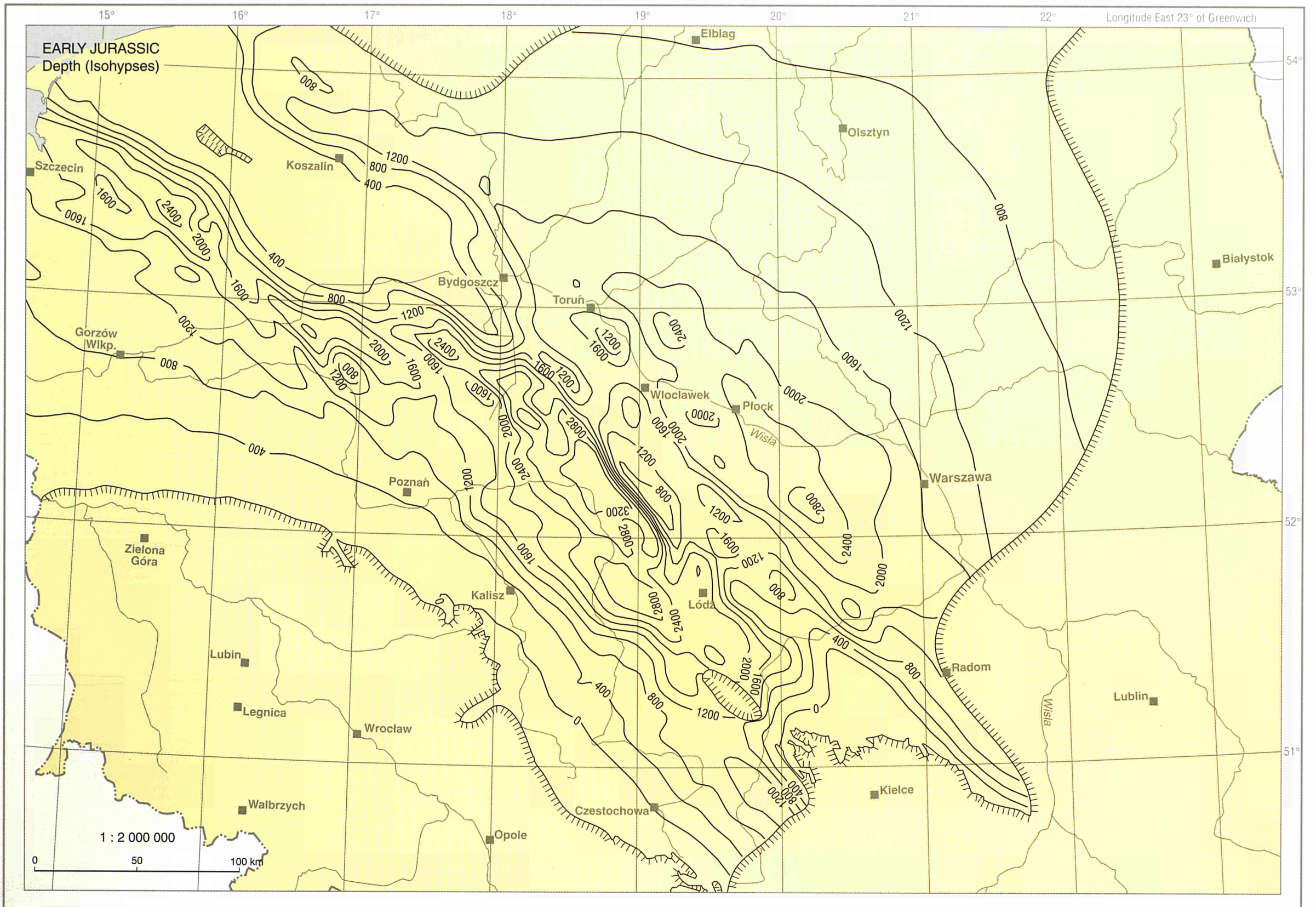


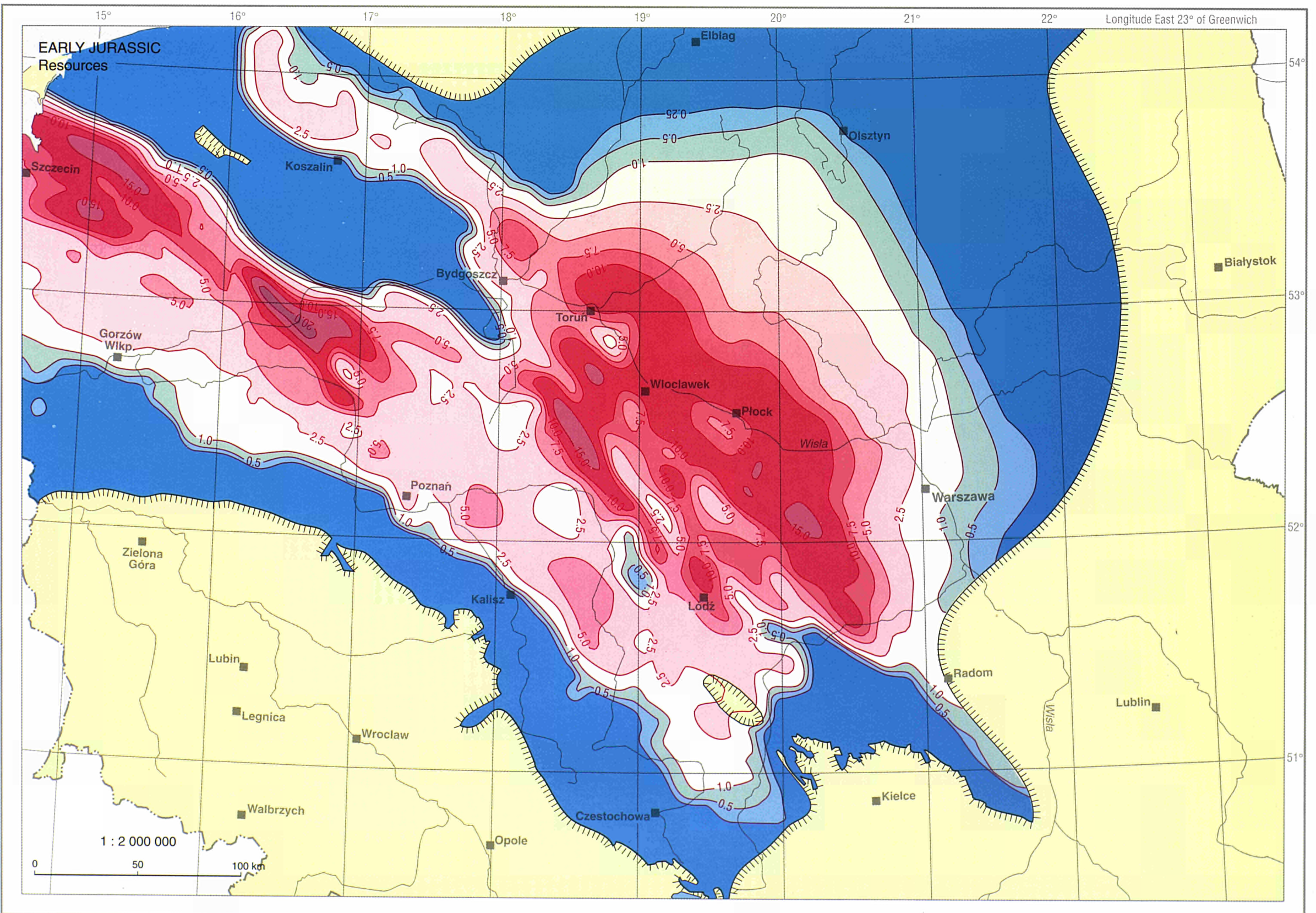
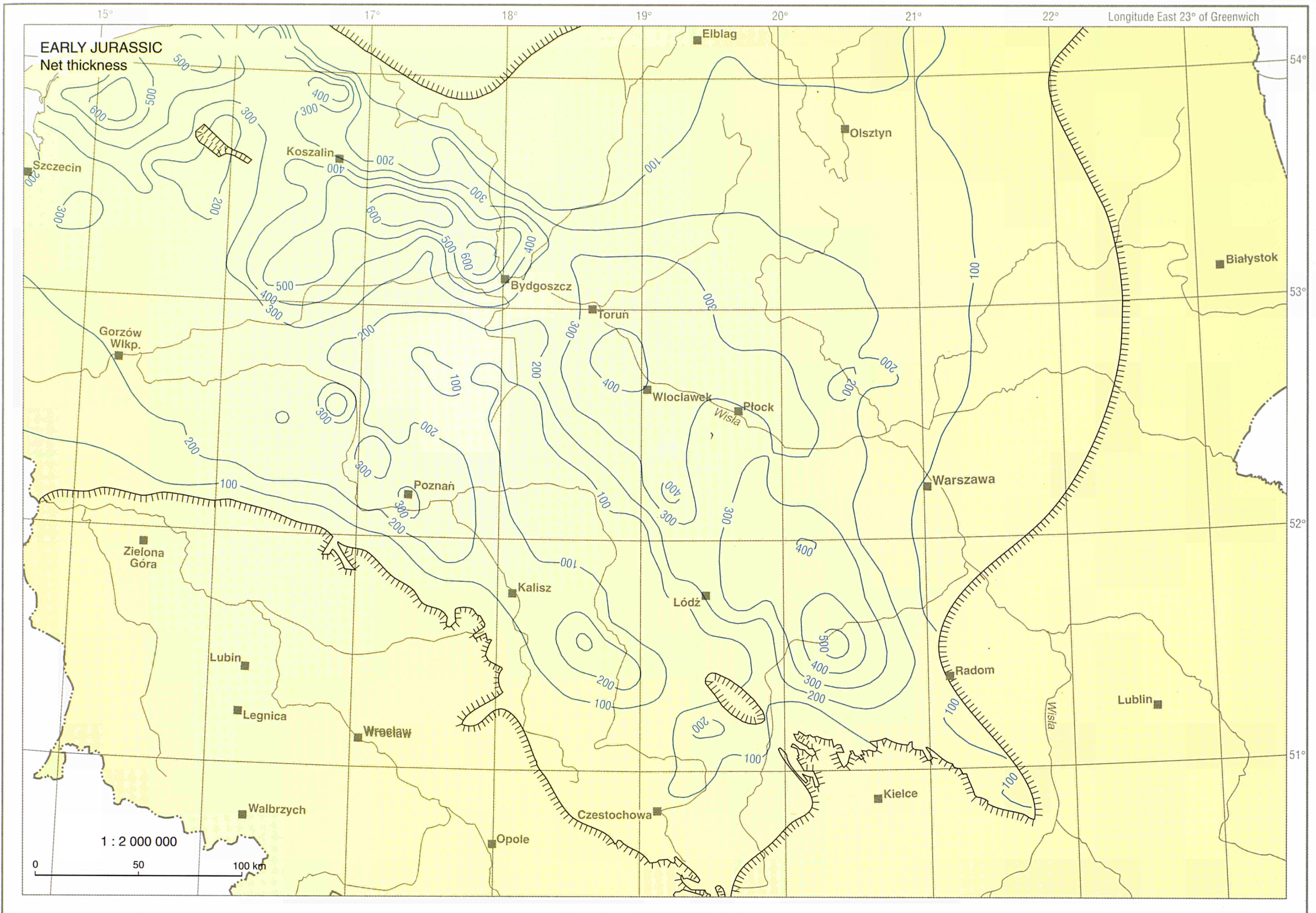
POLAND



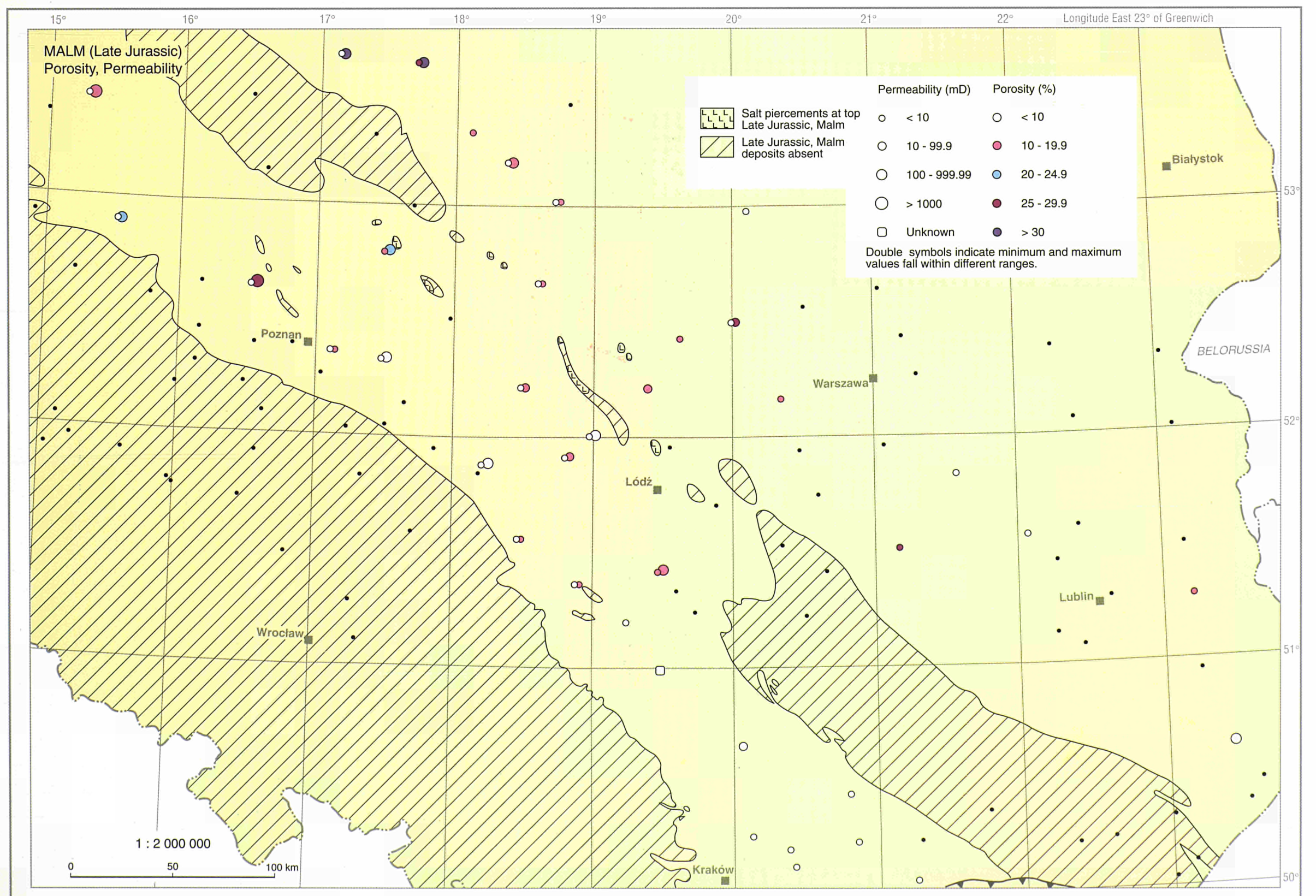
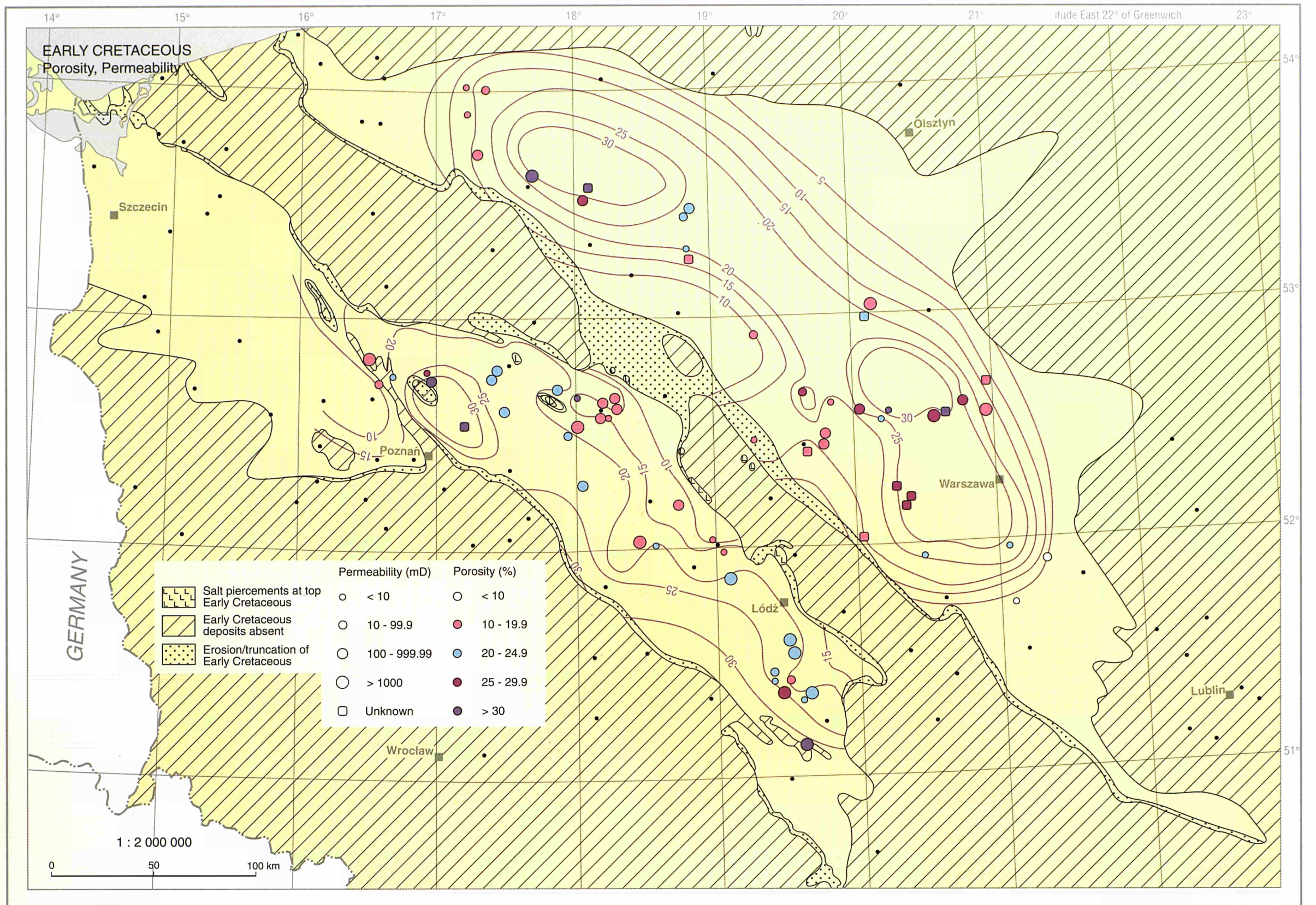


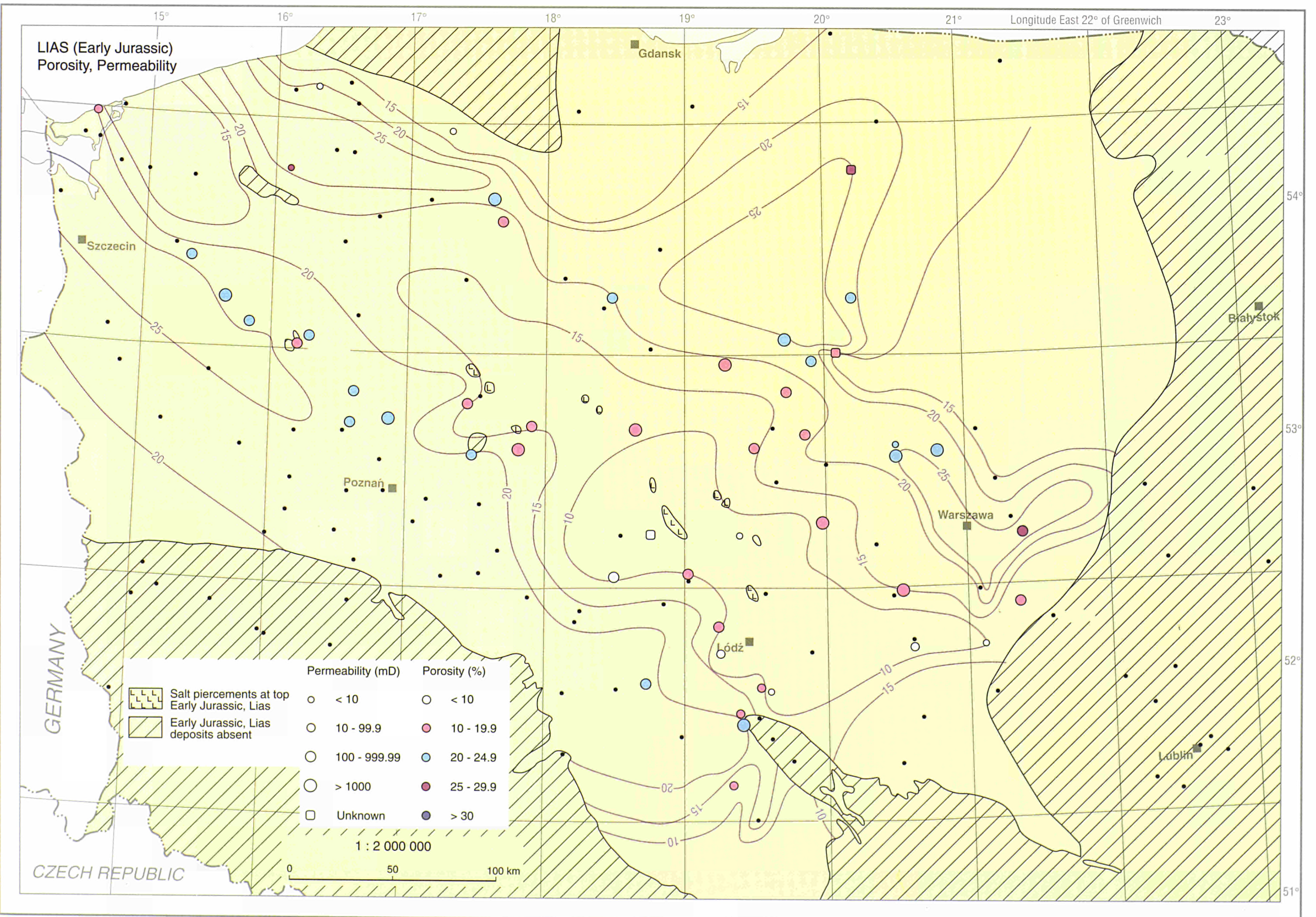
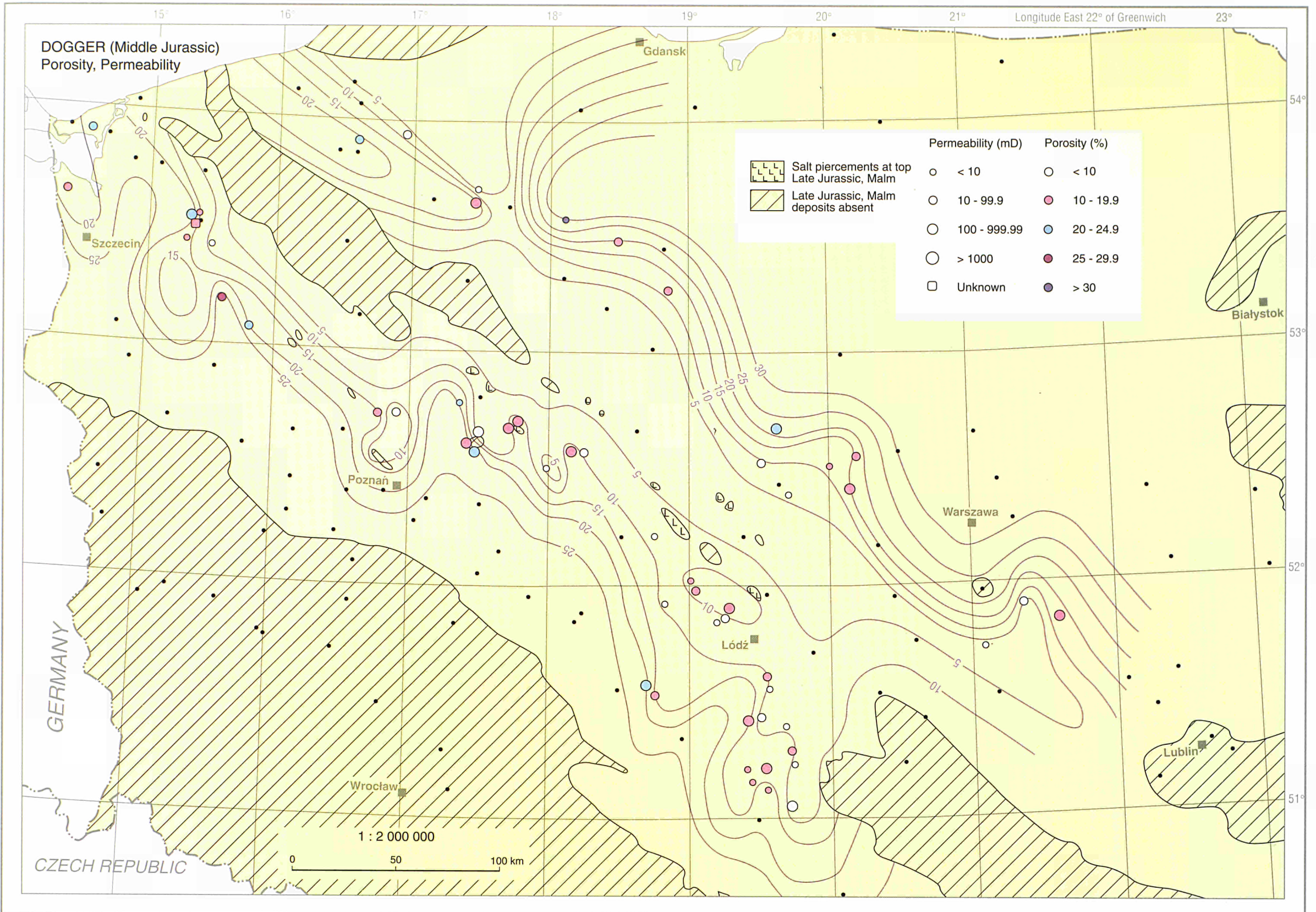
POLAND



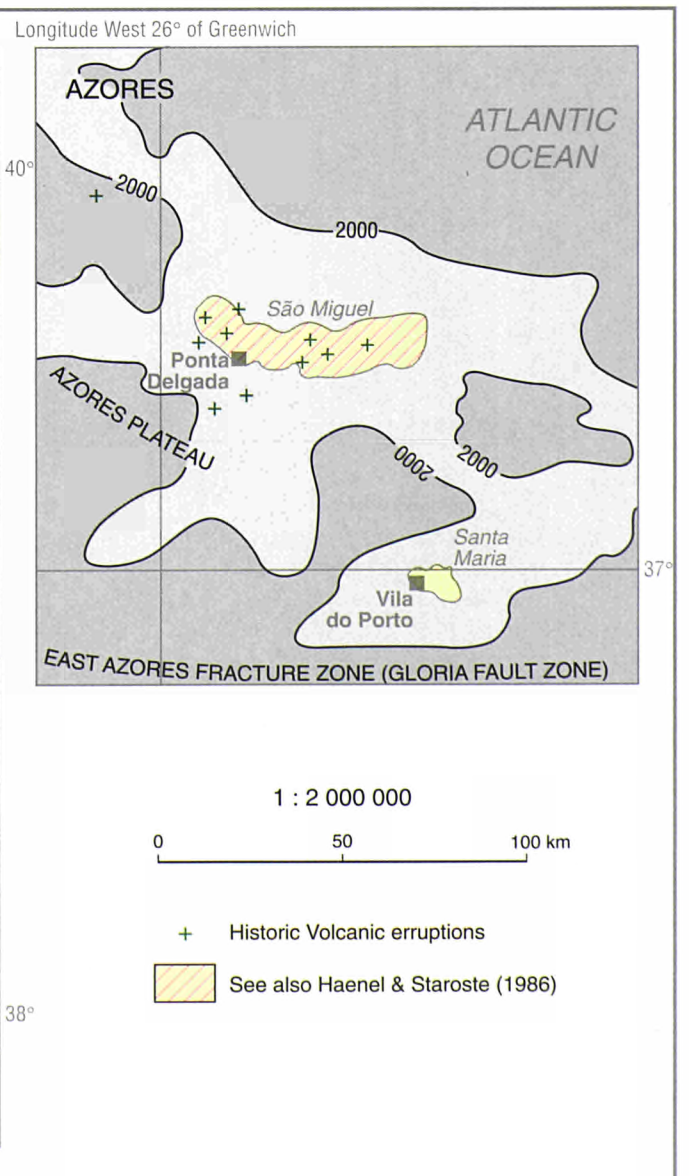
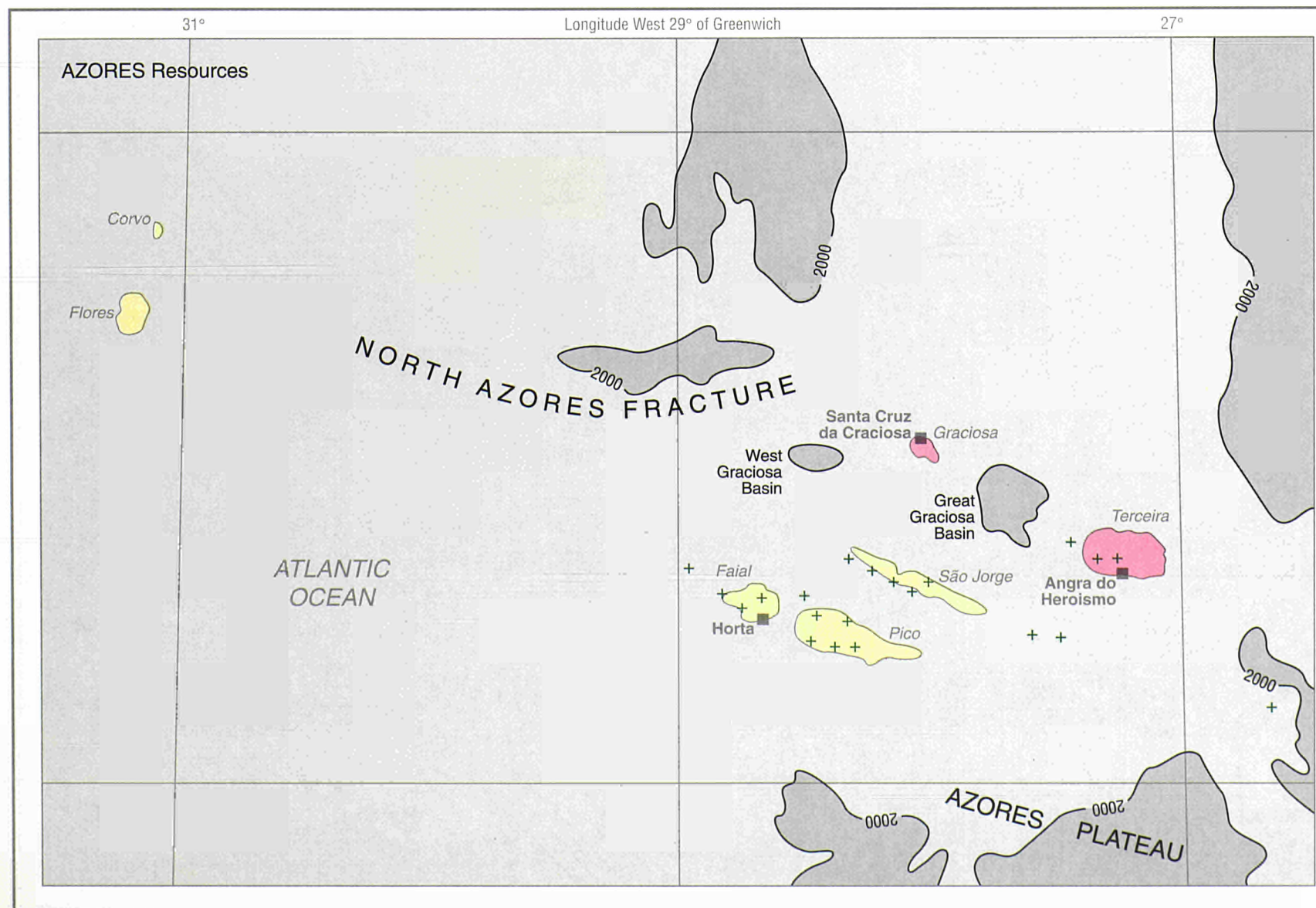
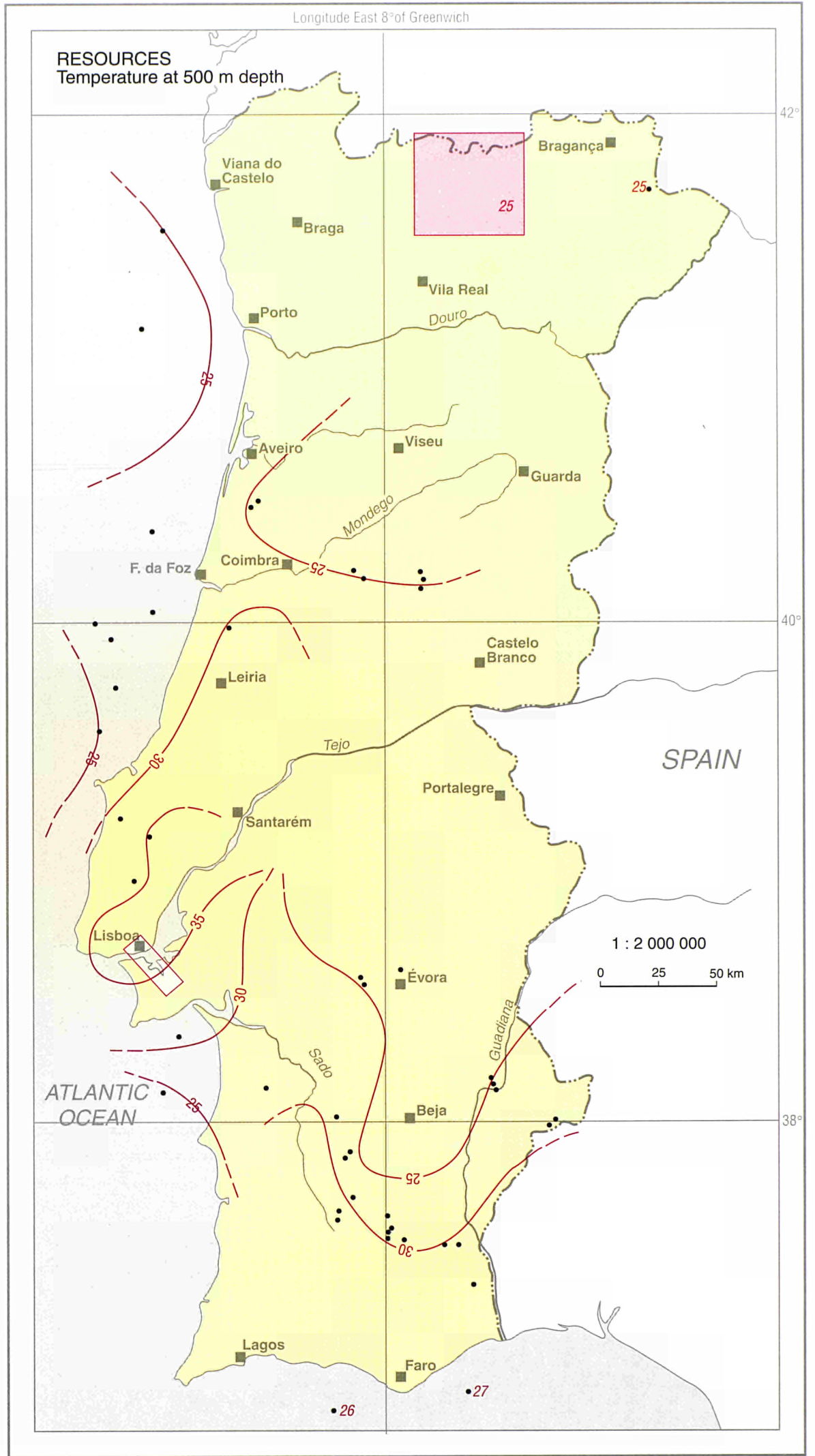
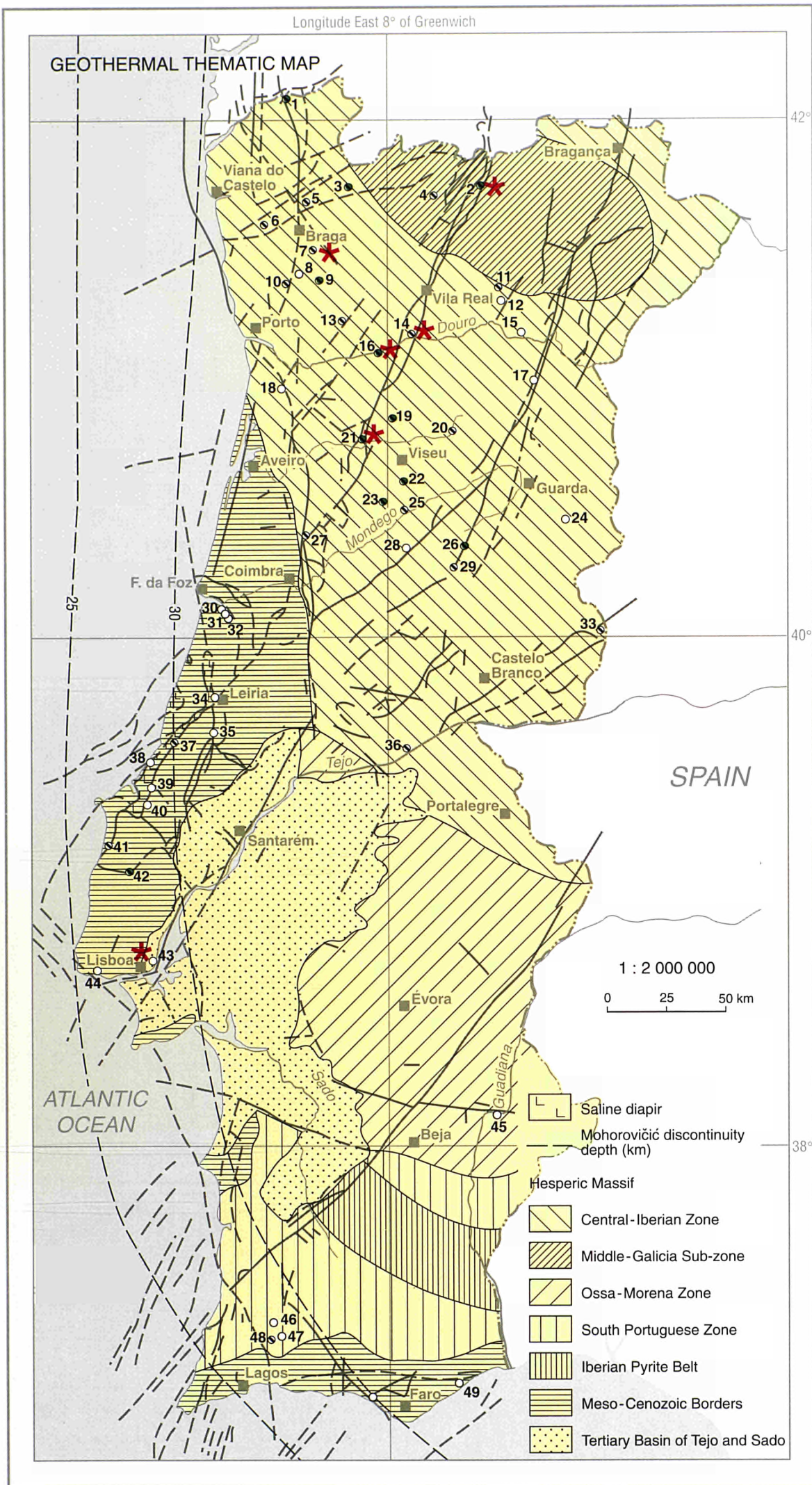


POLAND

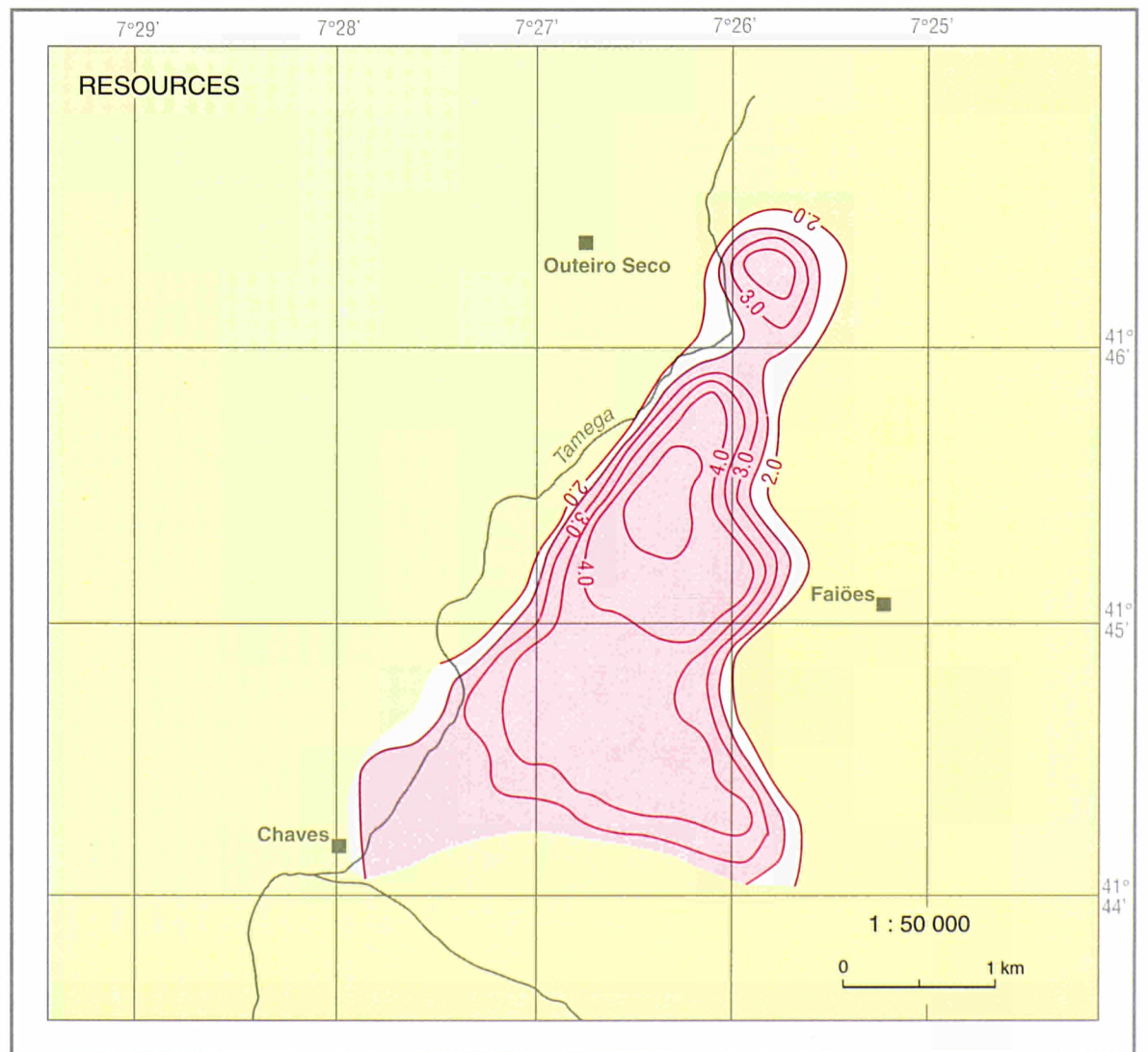
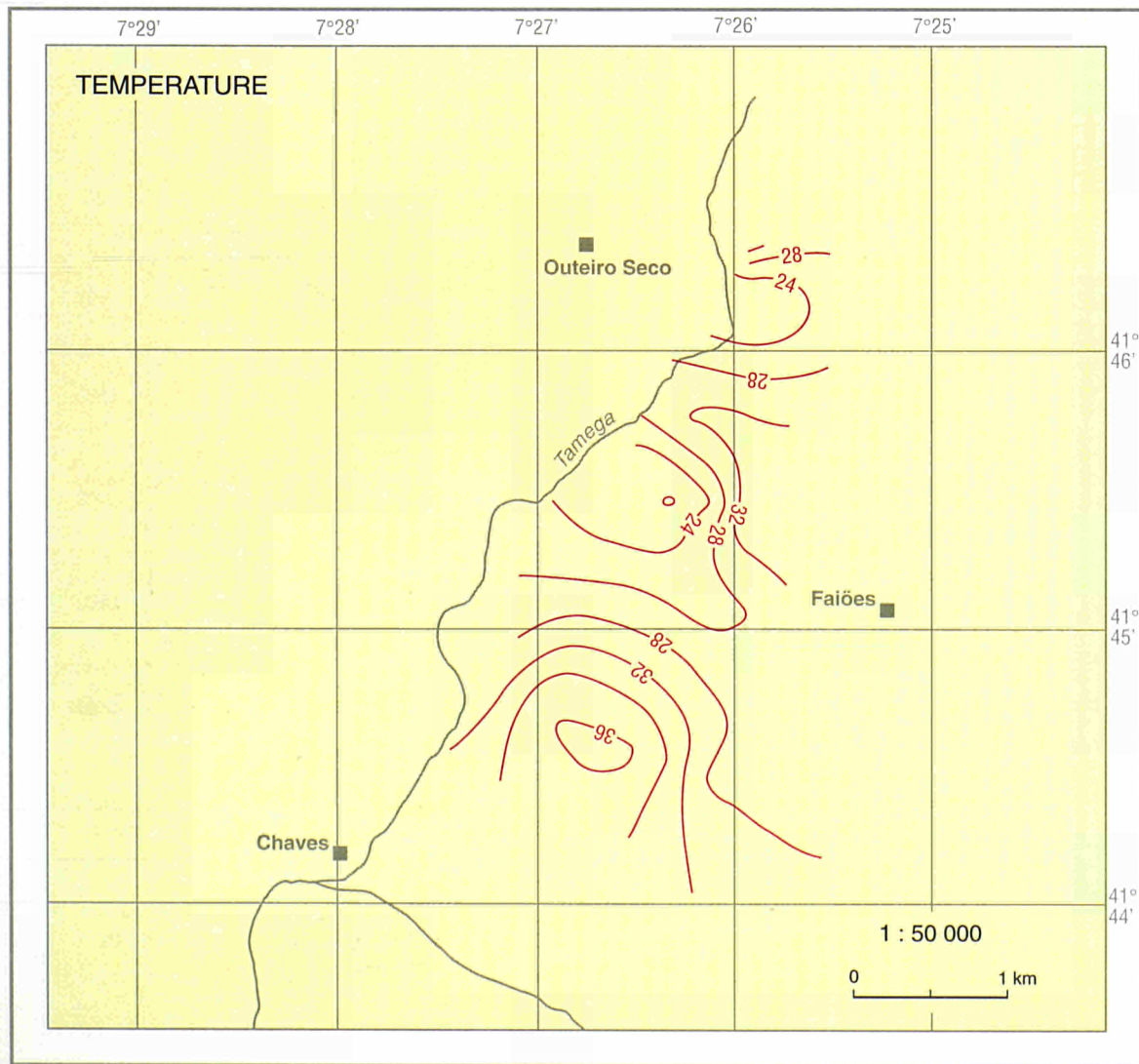
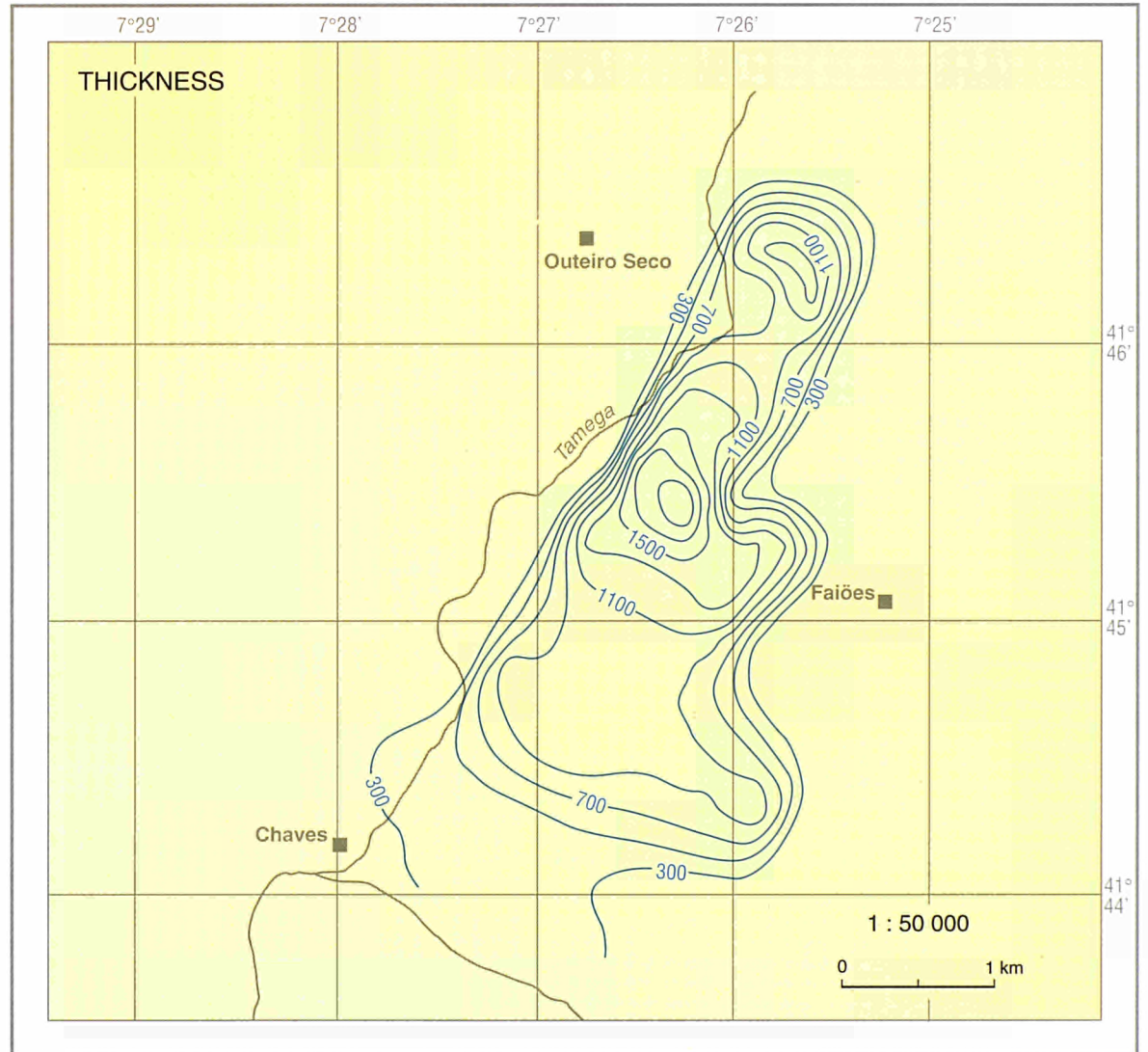
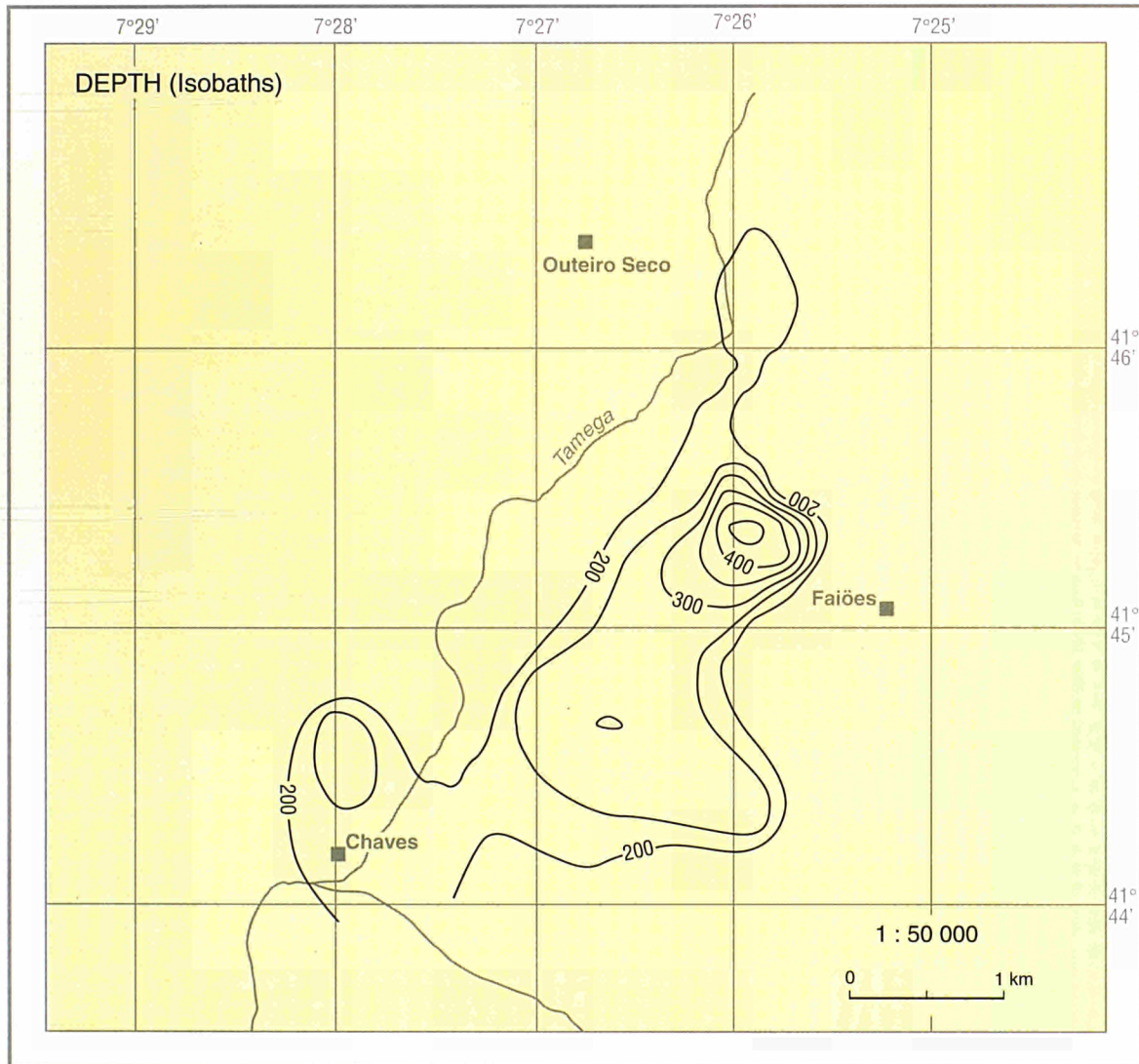
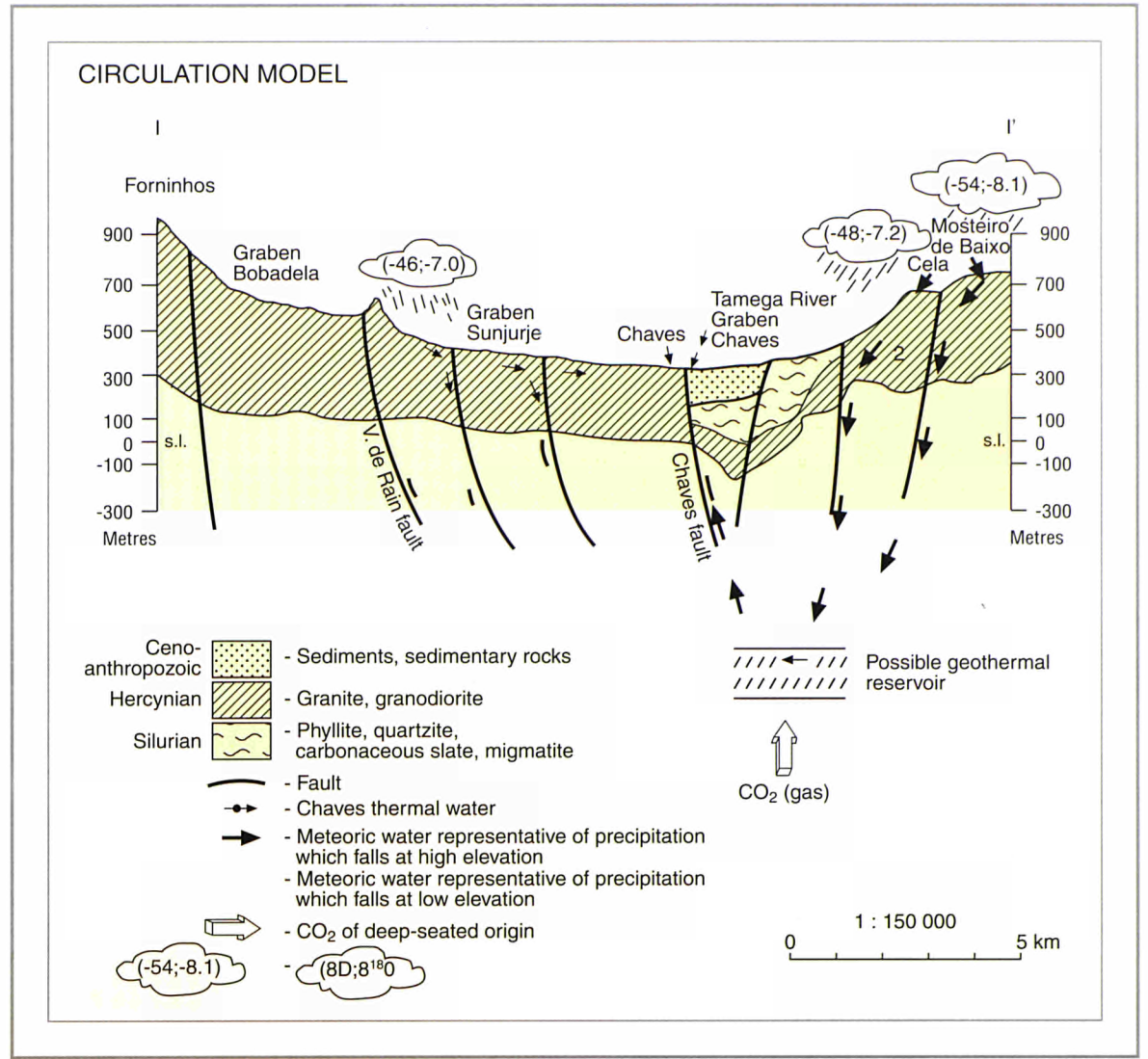
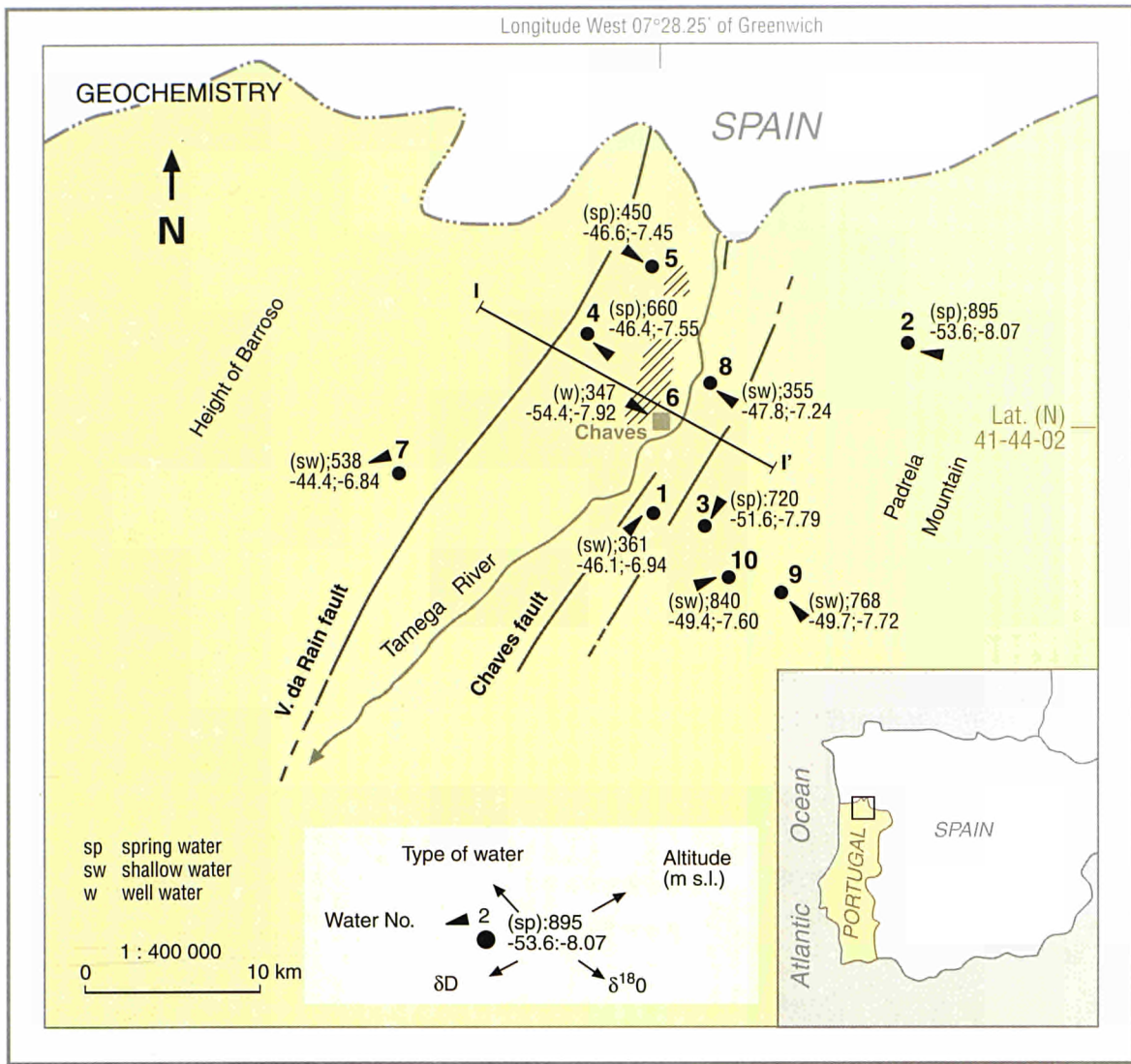




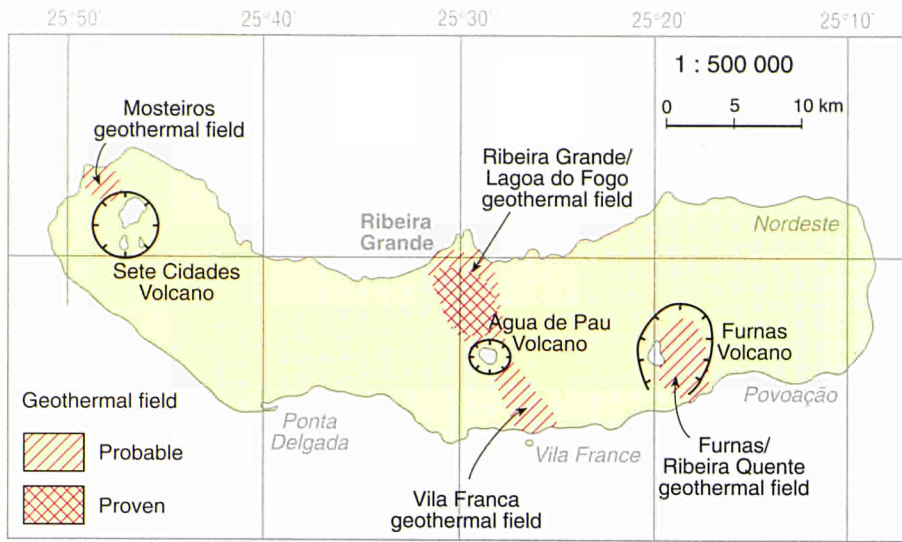
PORTUGAL



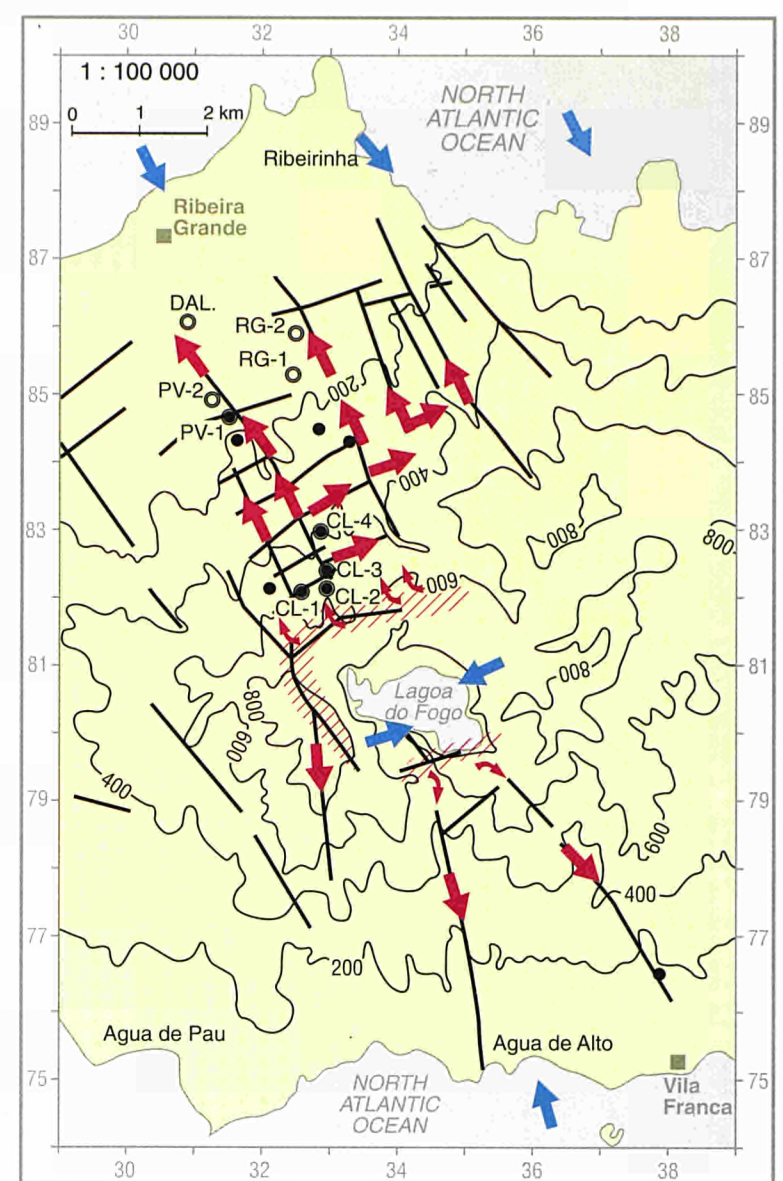
PORTUGAL, Chaves



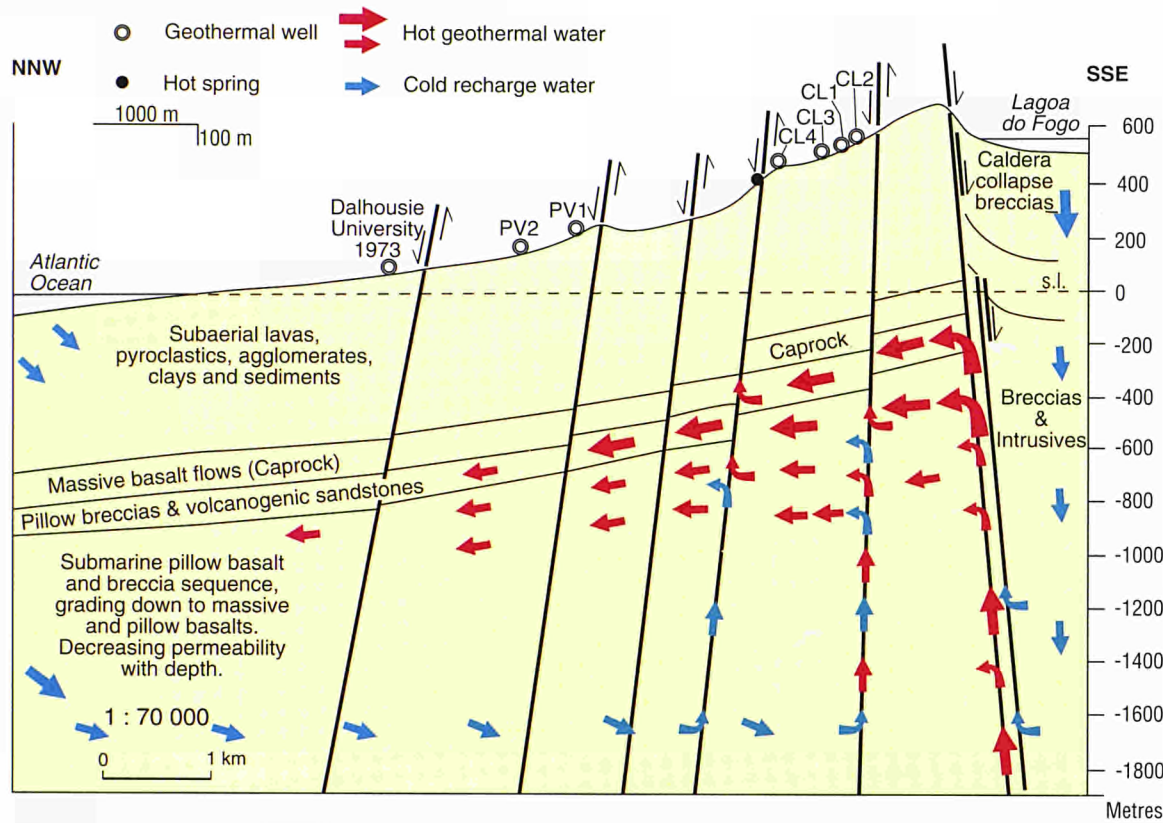
SÃO MIGUEL Geothermal fields



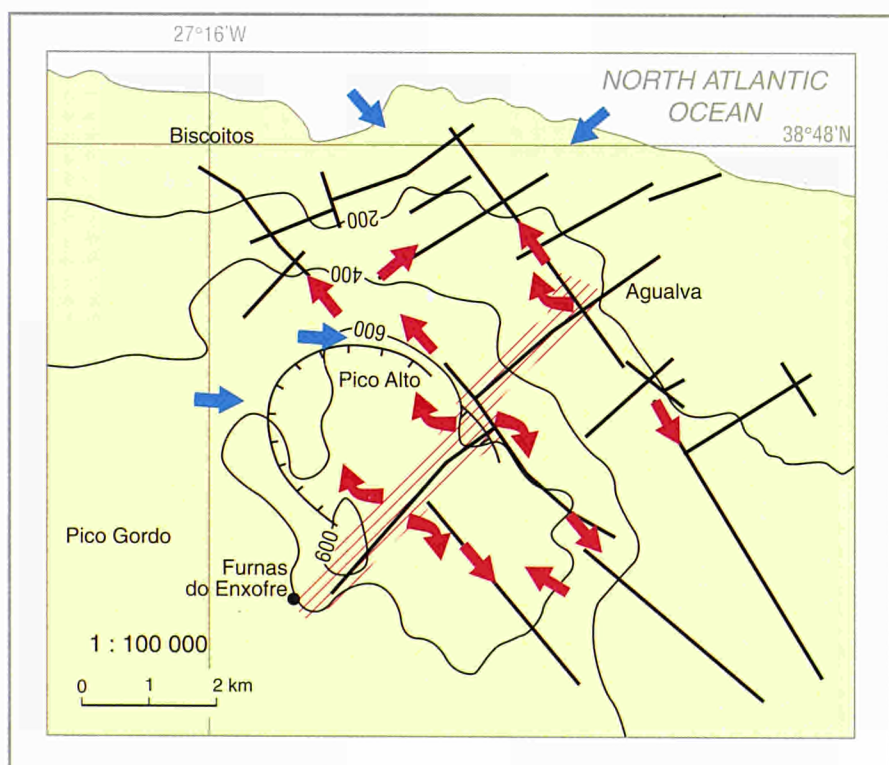
SÃO MIGUEL (Ribeira Grande) Potential areas



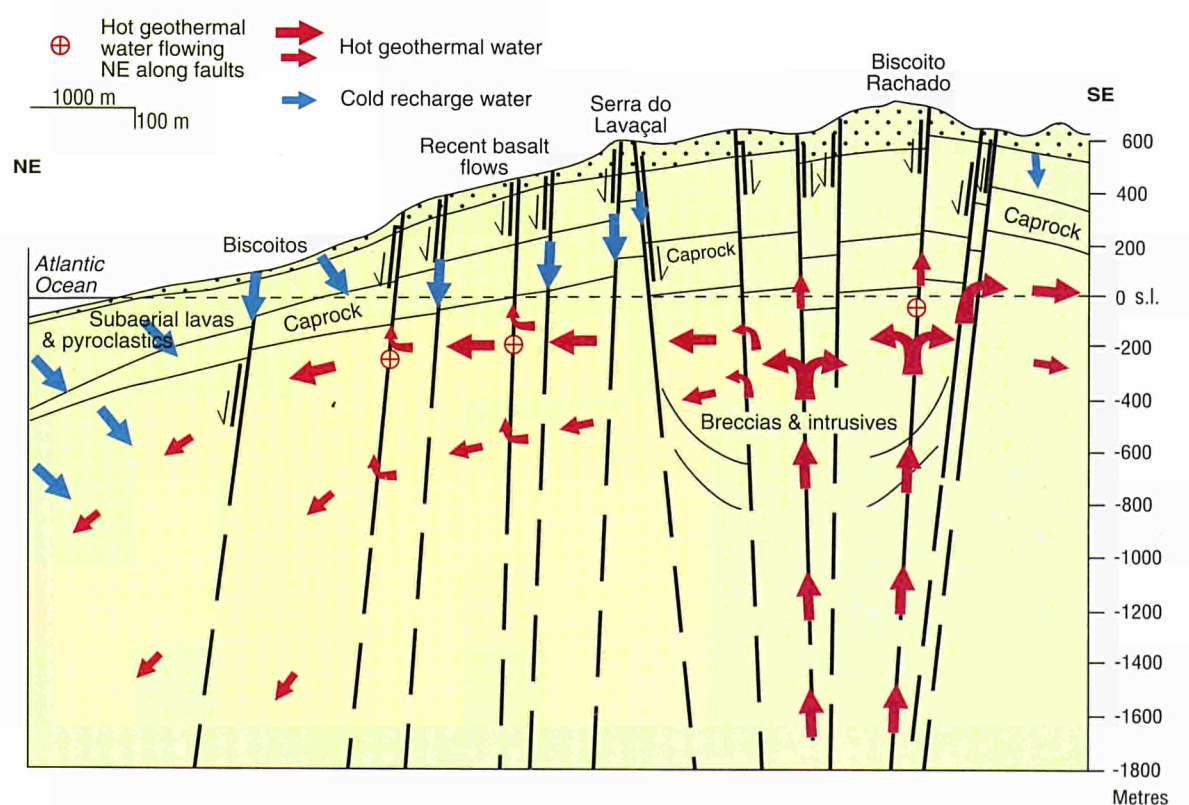
SÃO MIGUEL (Ribeira Grande) Circulation model



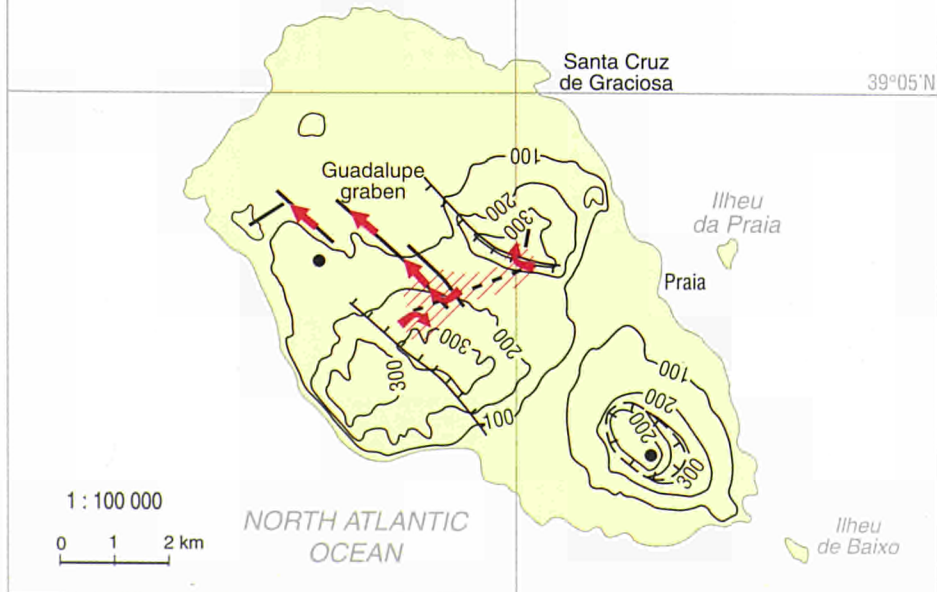
TERCEIRA (Pico Alto) Potential areas



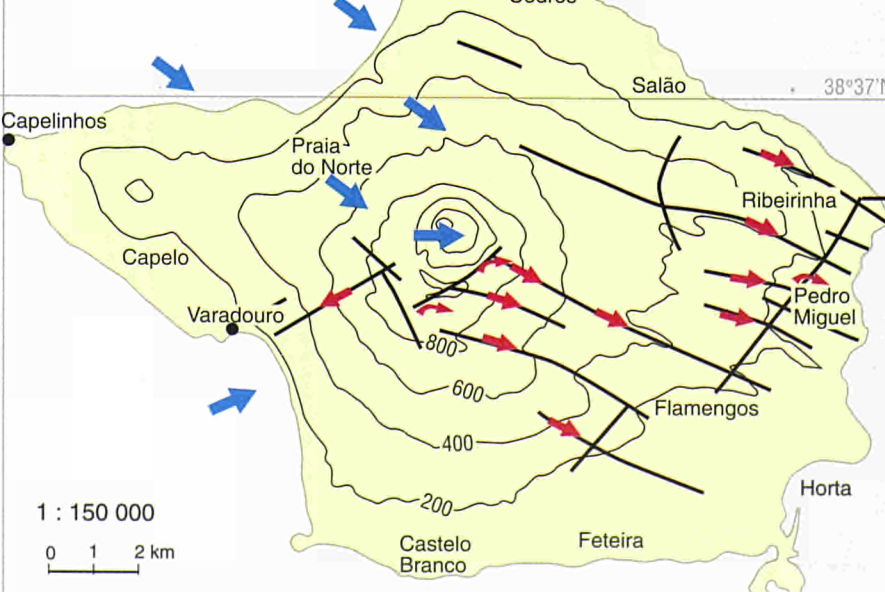
TERCEIRA (Pico Alto) Circulation model



GRACIOSA Potential areas

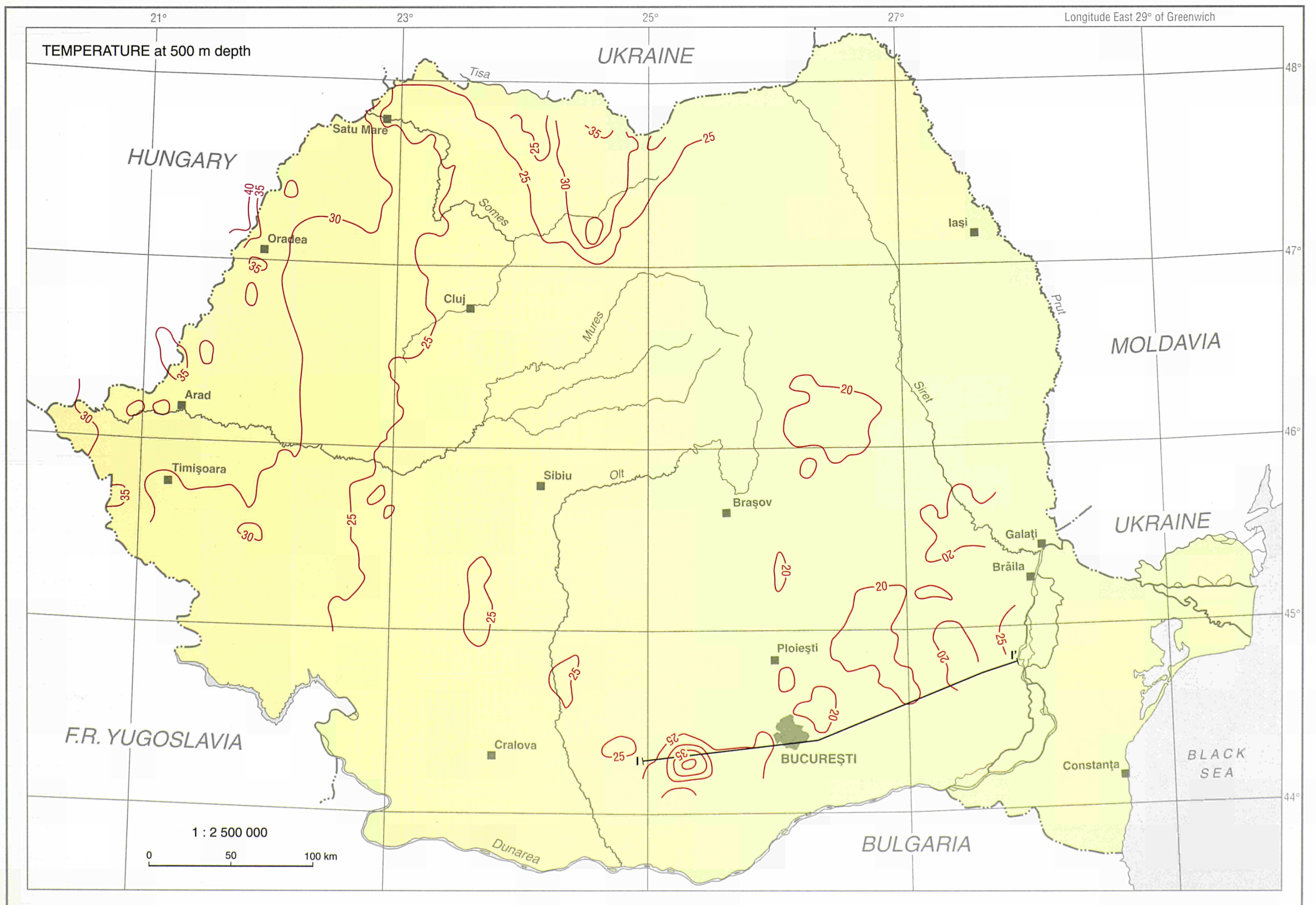
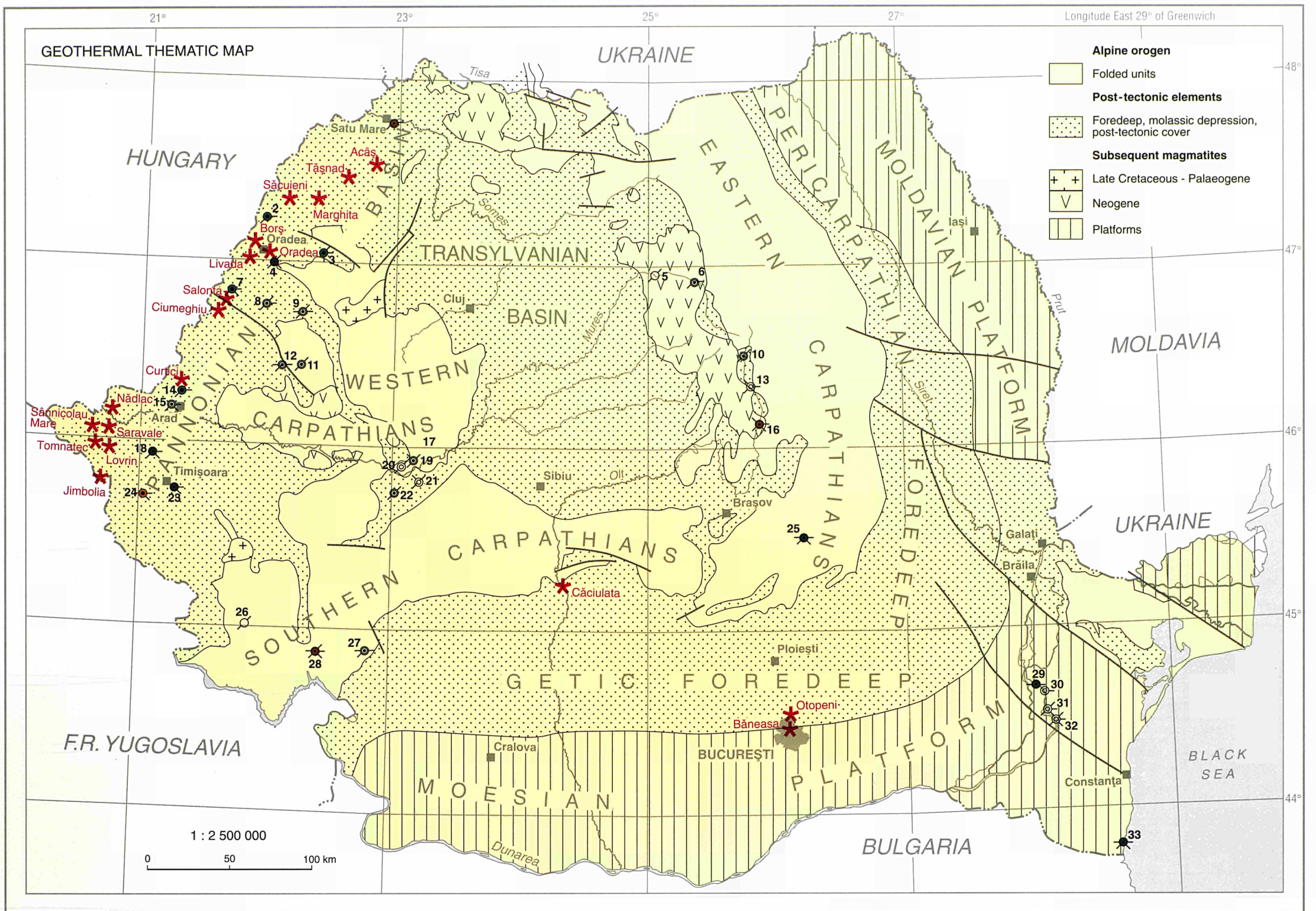


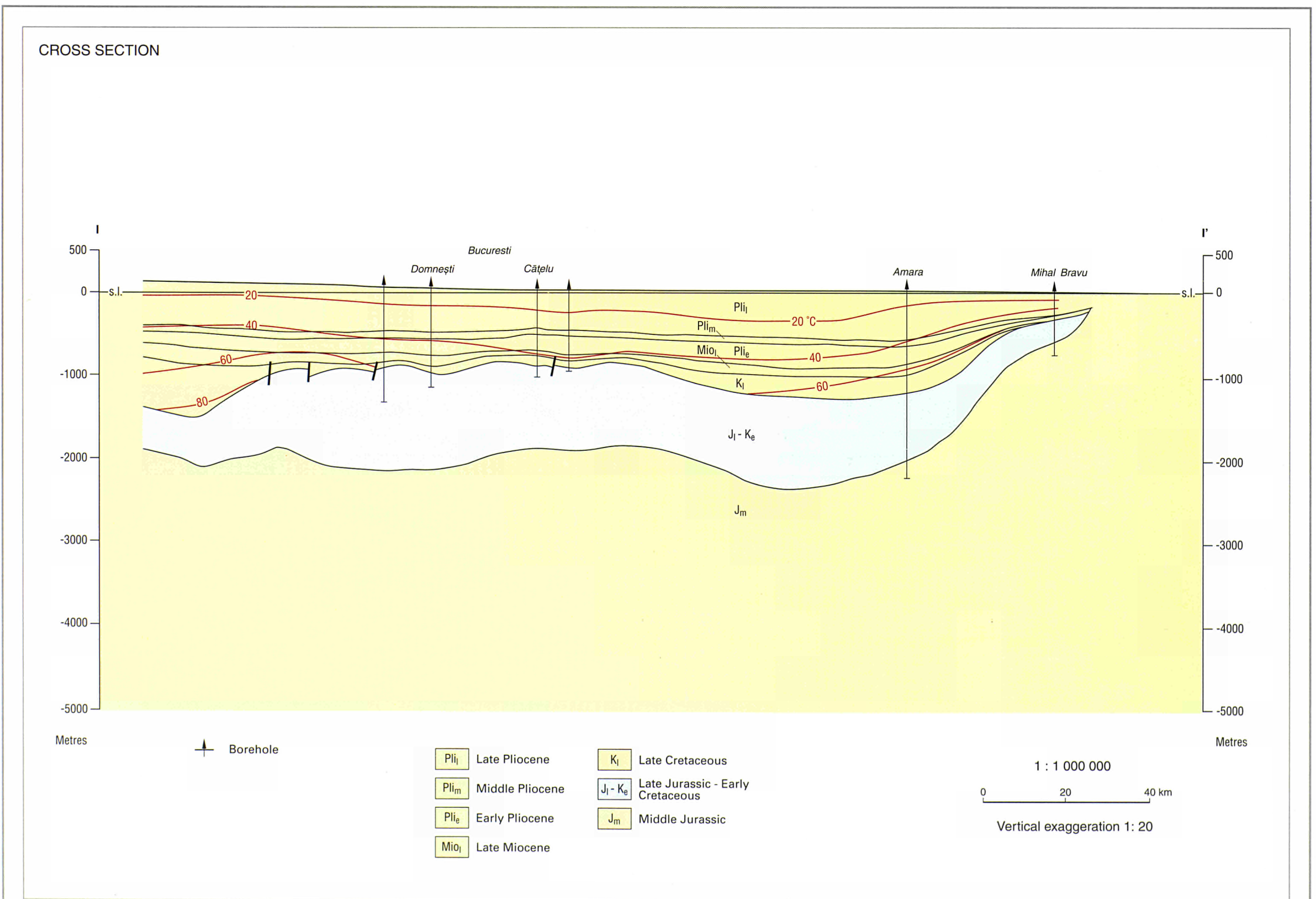
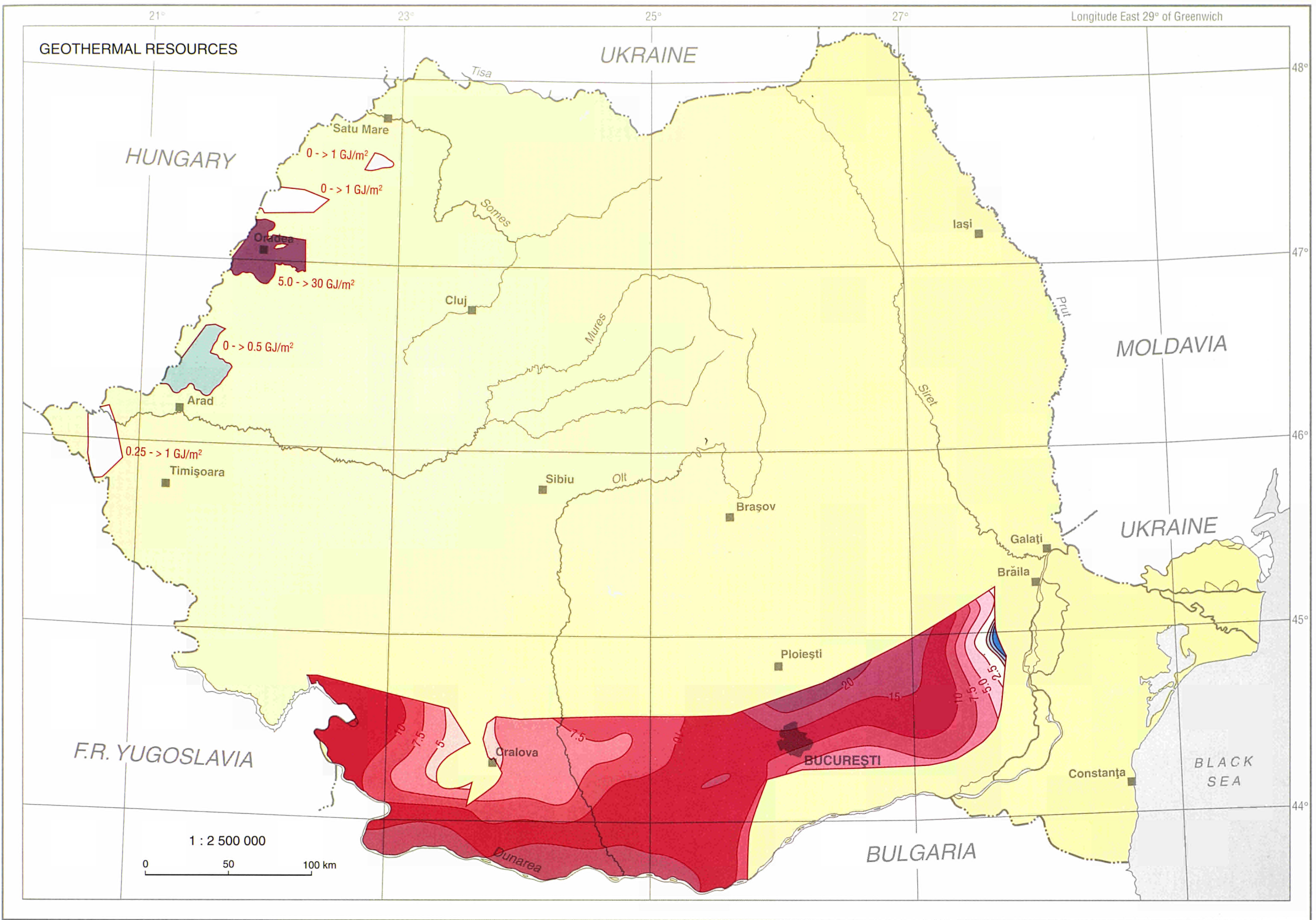
FAIAL Potential areas



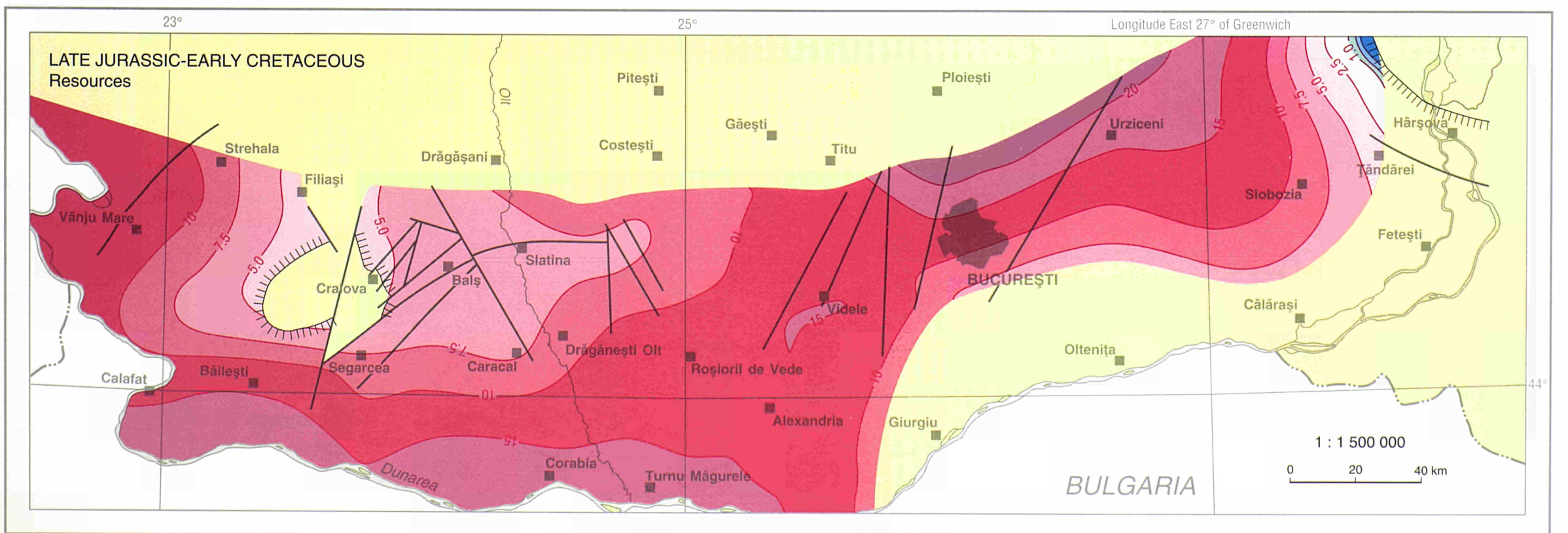
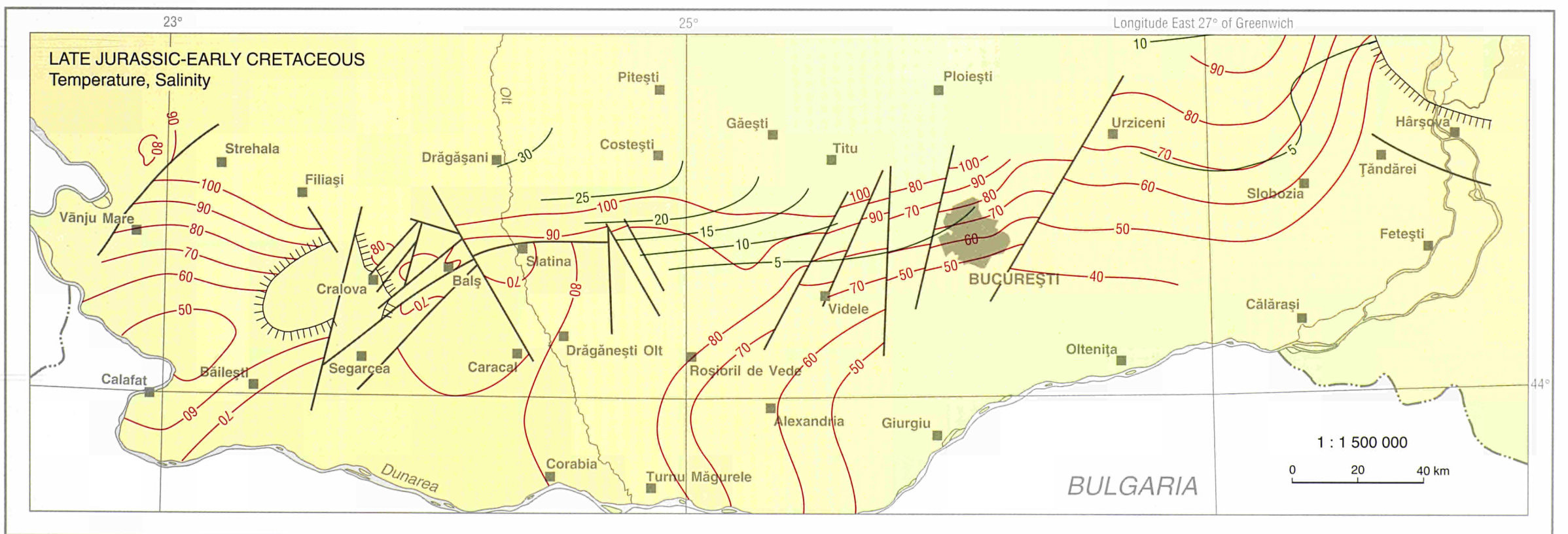
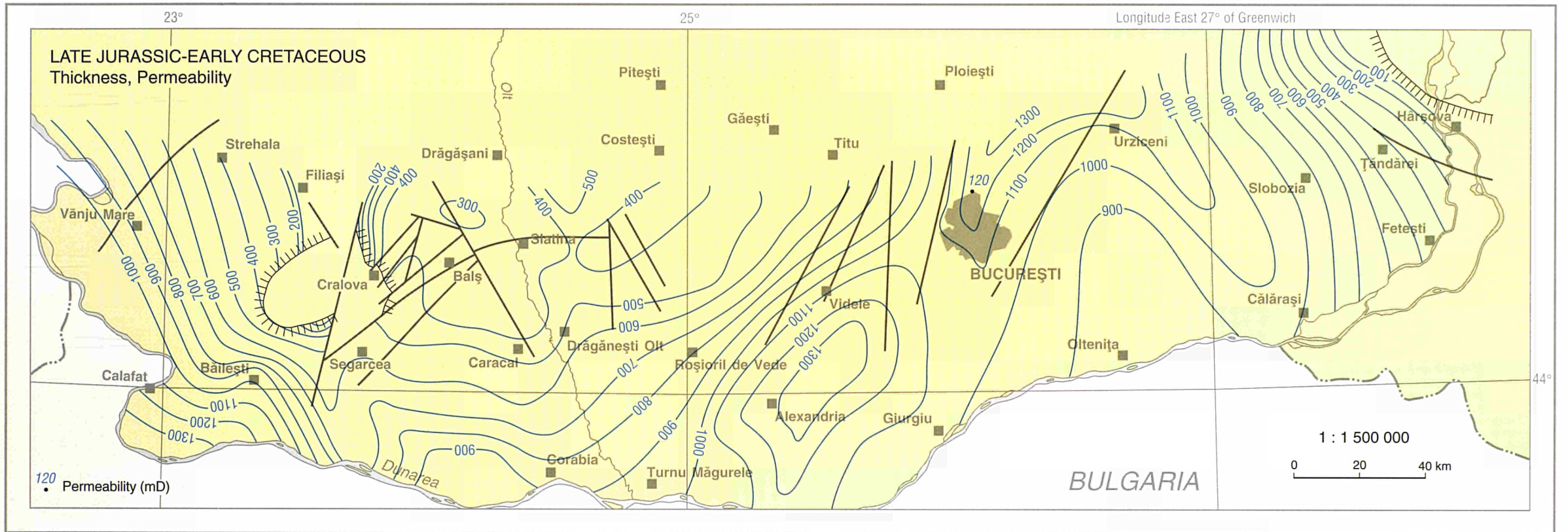
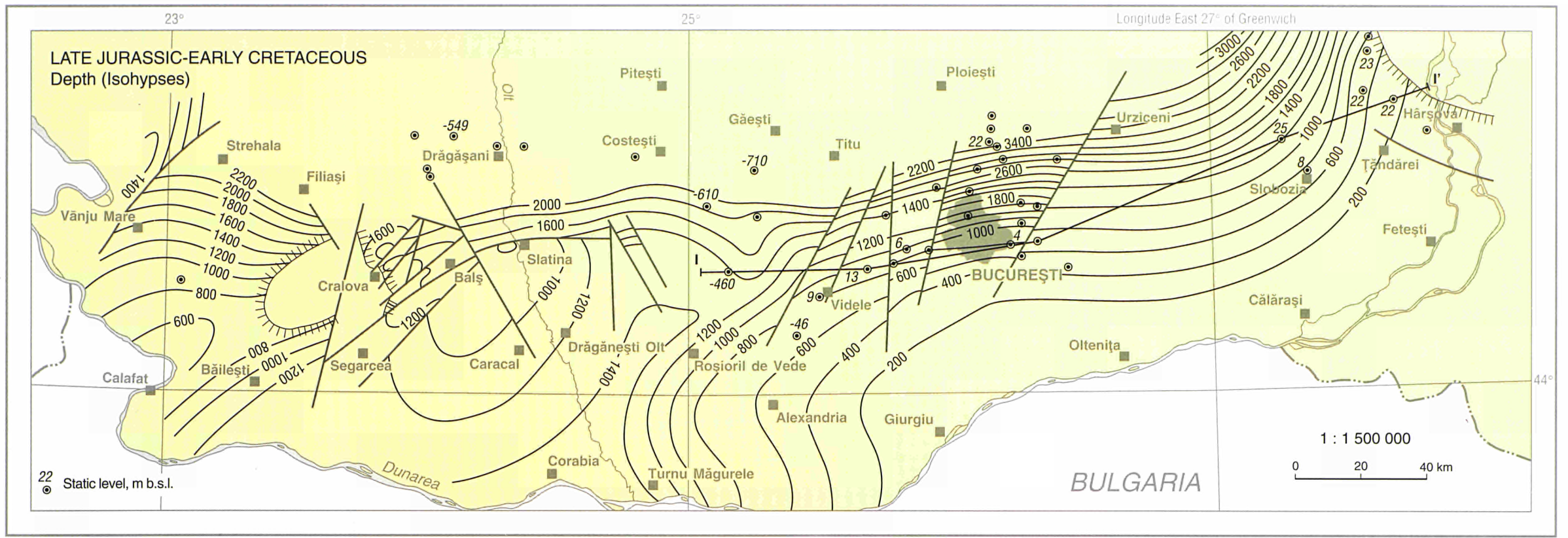
- Geothermally active faults
- Hot spring/fumarole
- ↻ Direction of convection loop
- Fluid outflow from feeder fault zone
- ↔ Suspected path of cold water invasion and descending branches of convection cell

ROMANIA

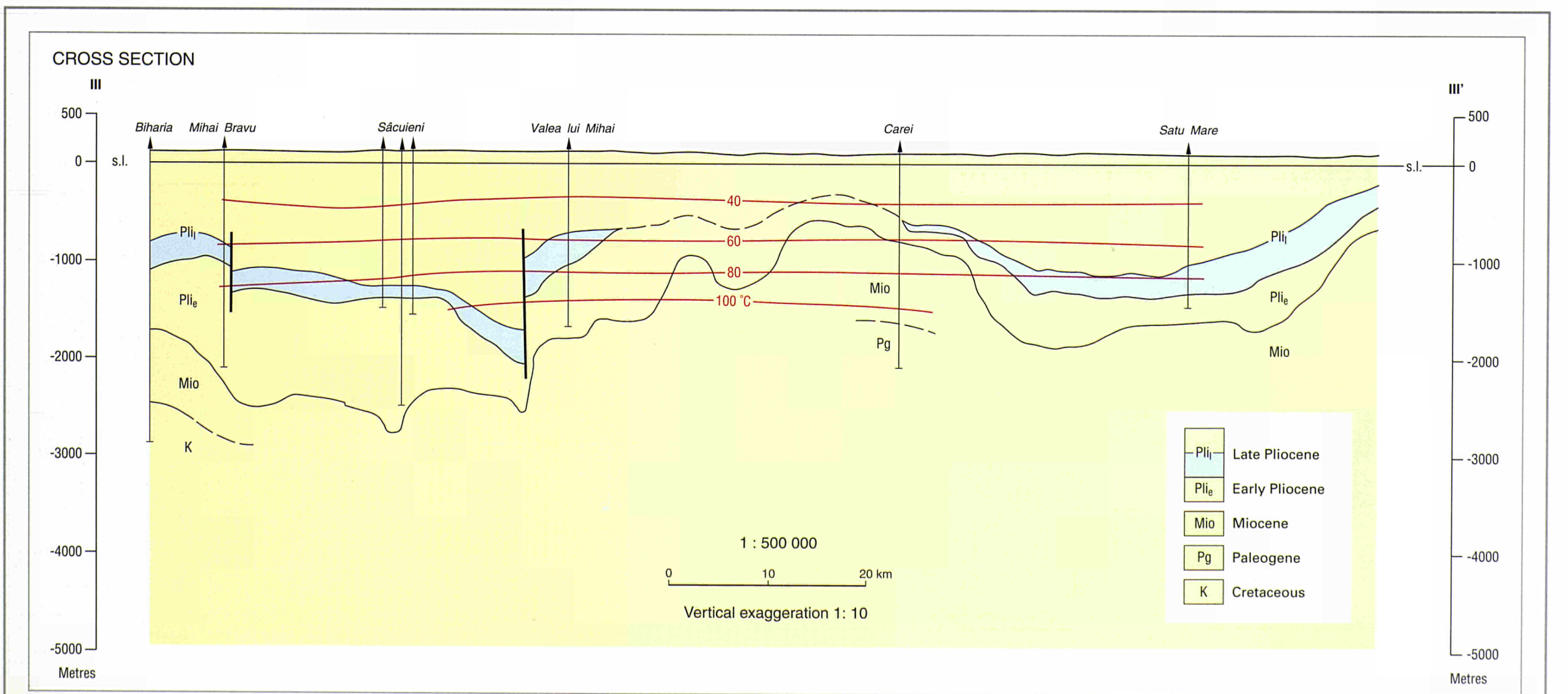
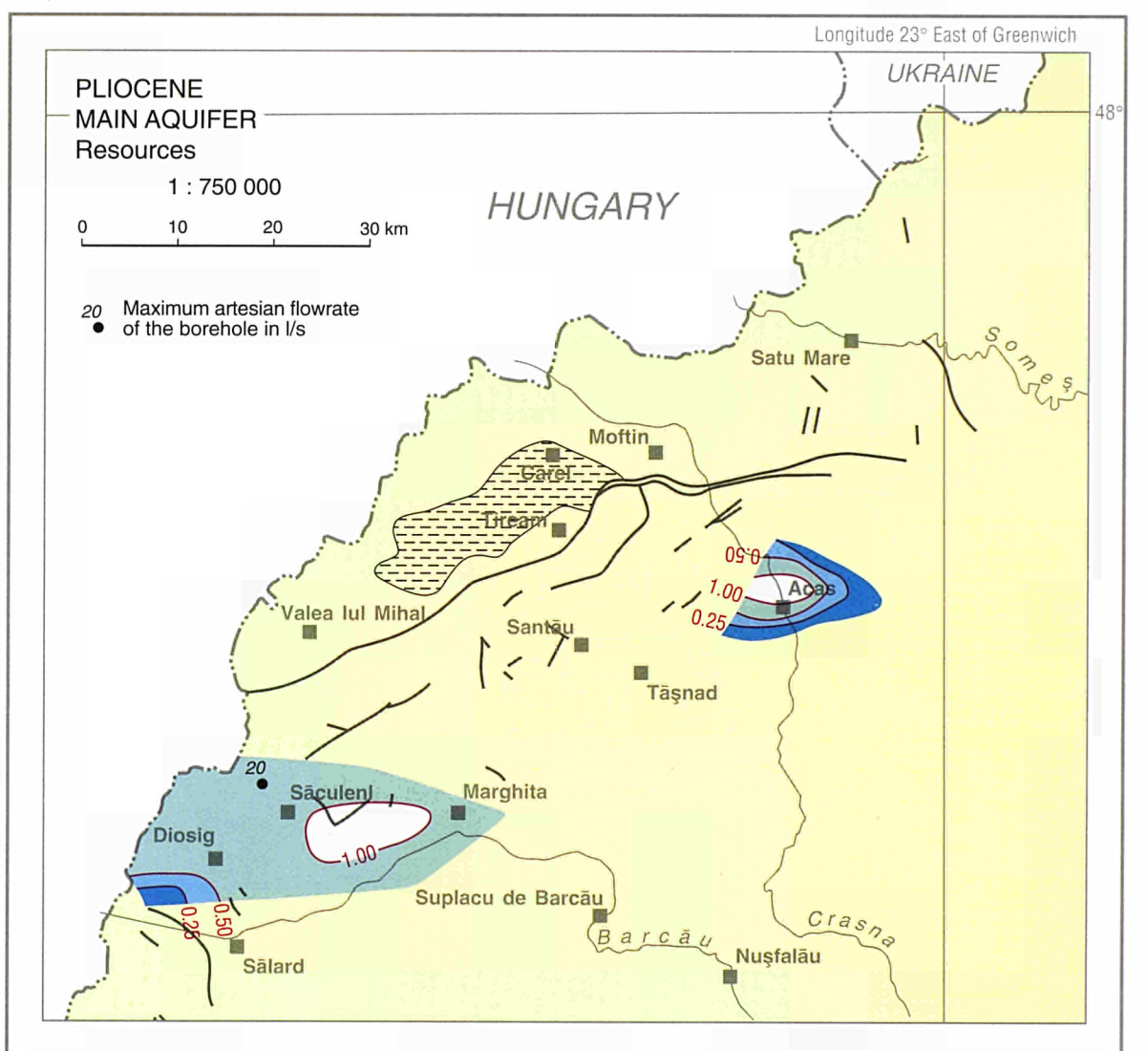
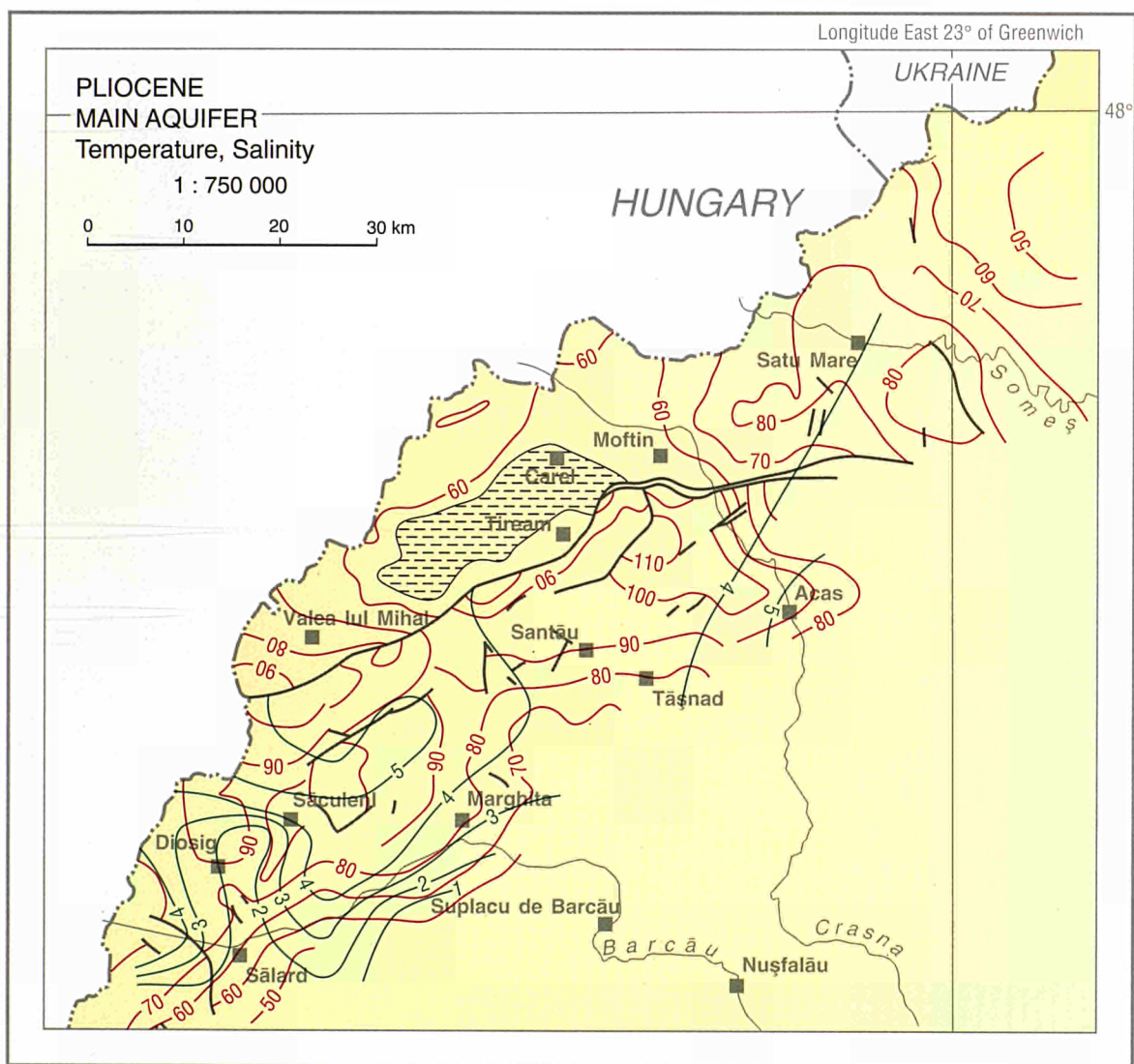
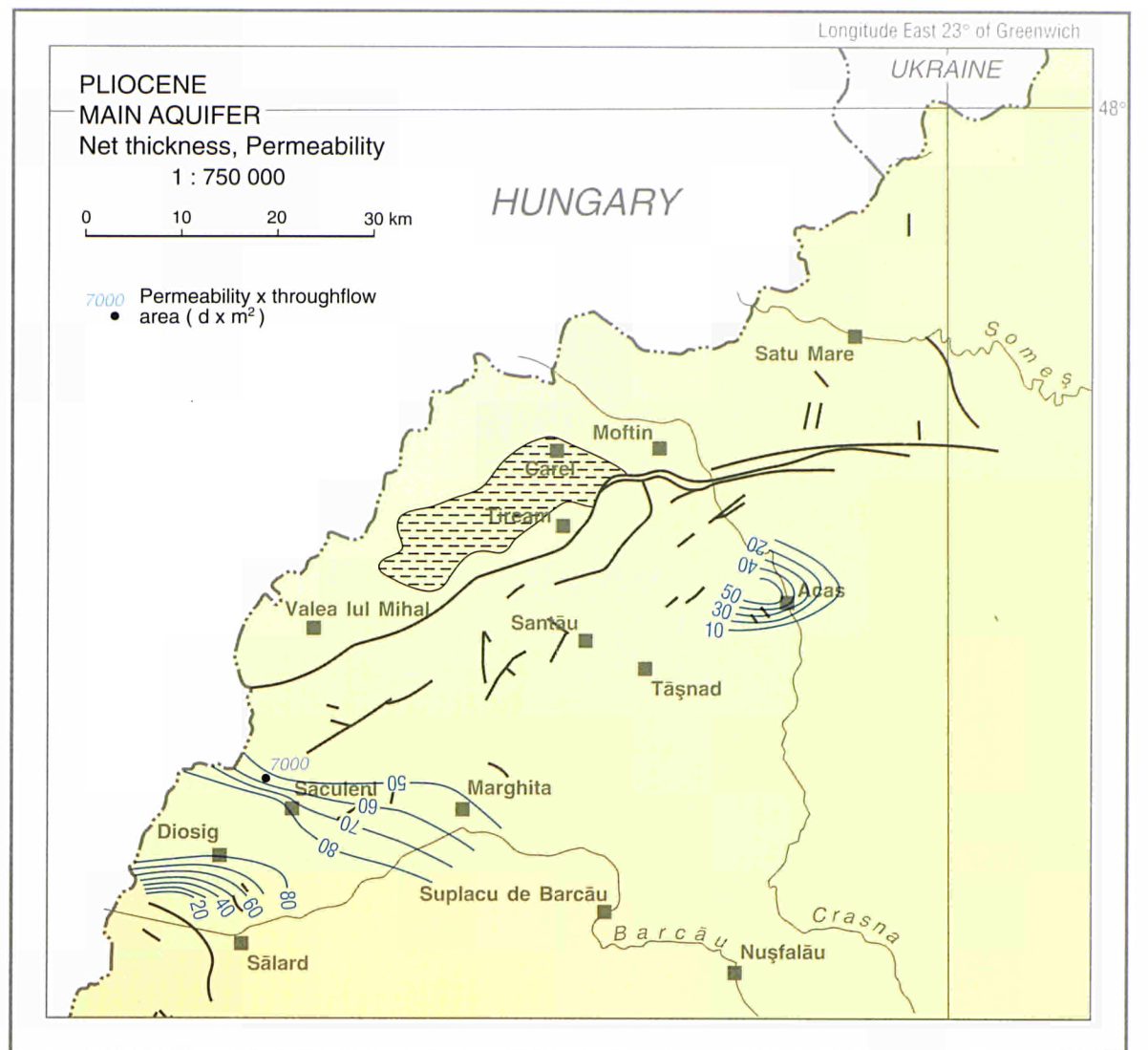
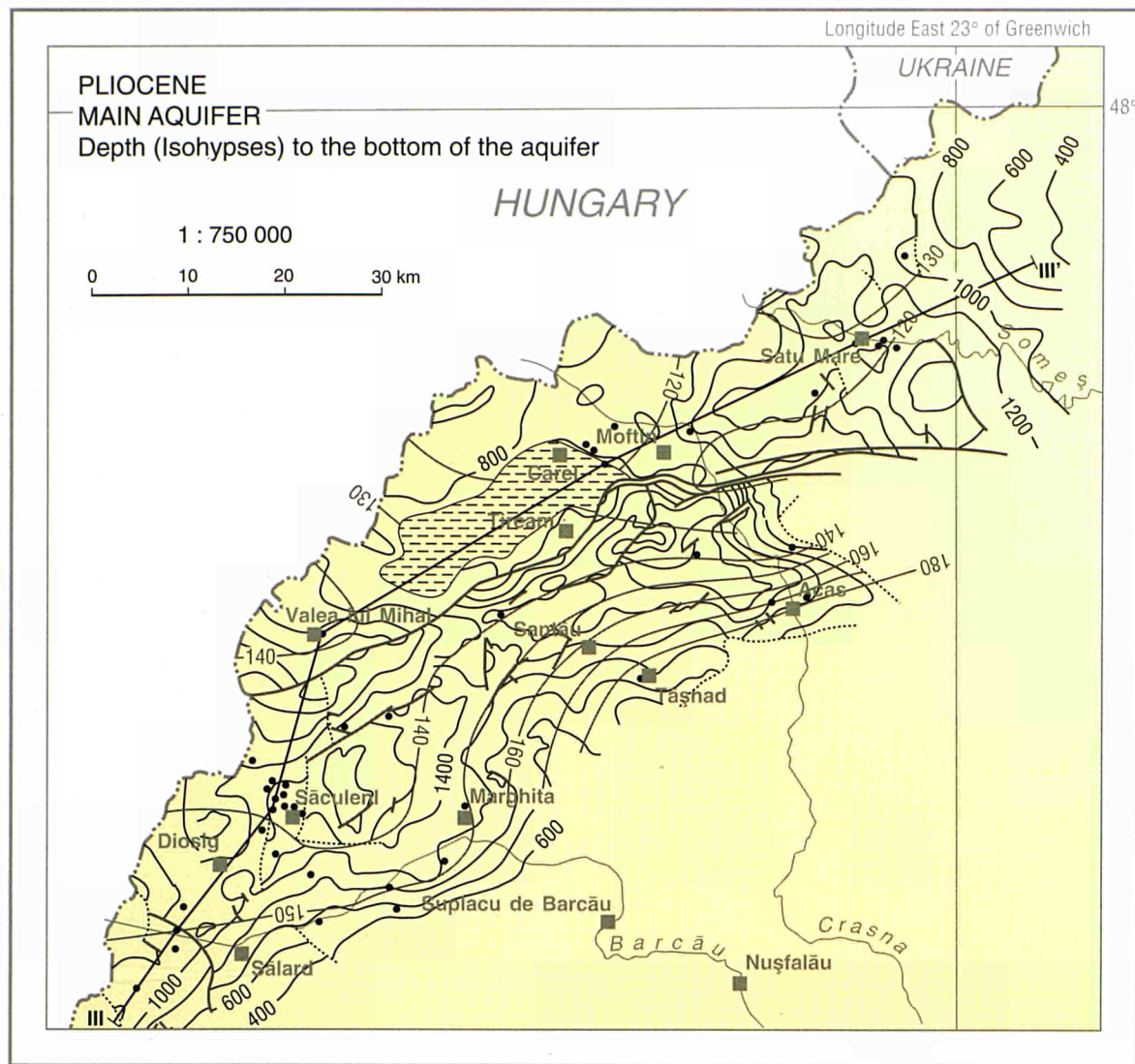




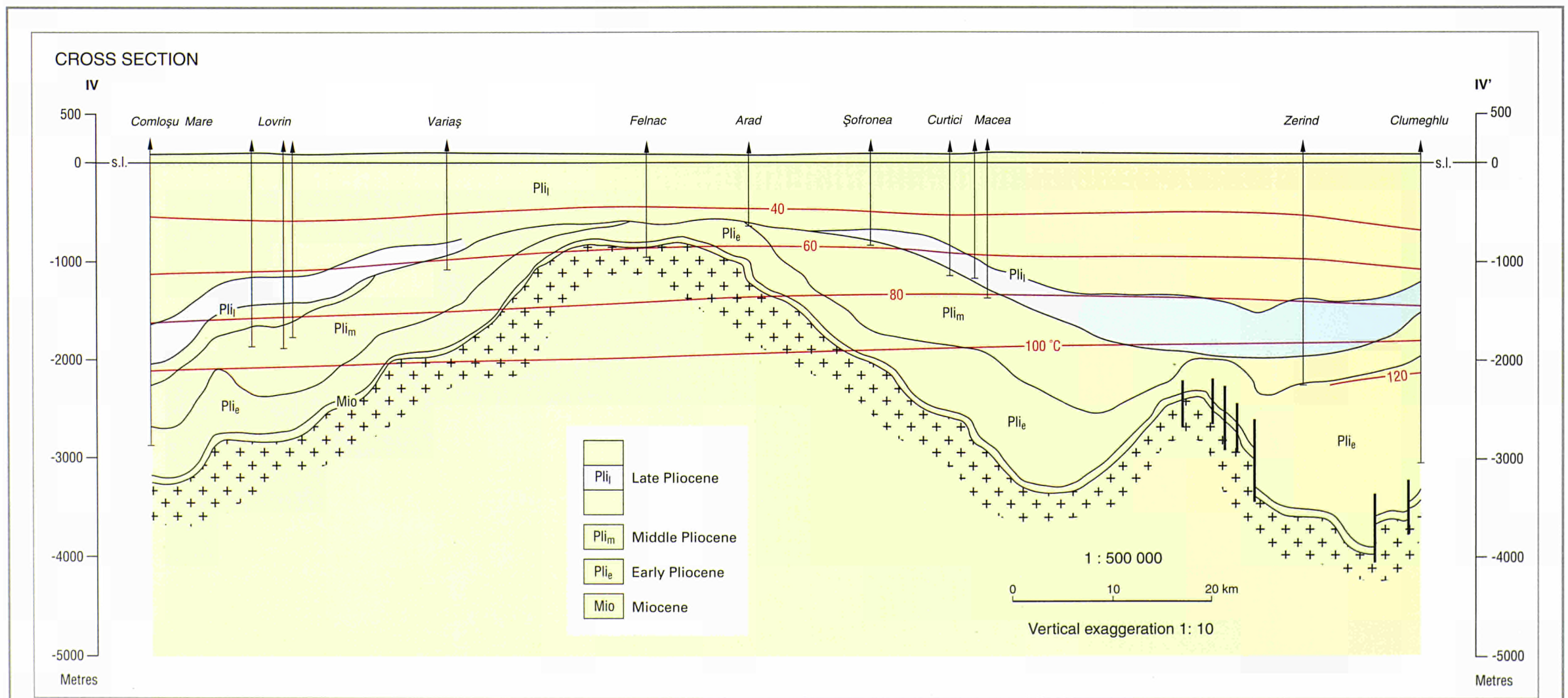
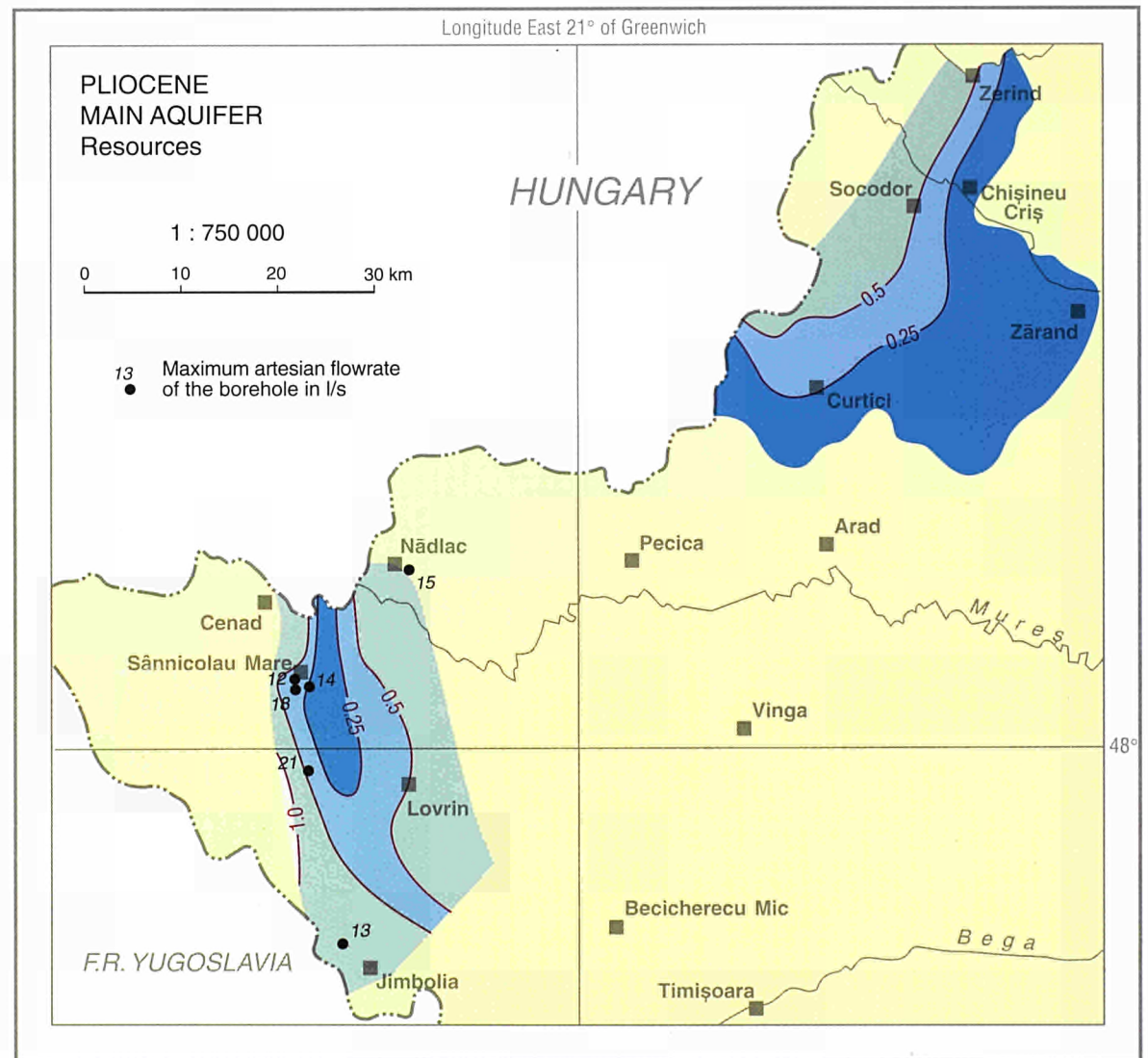
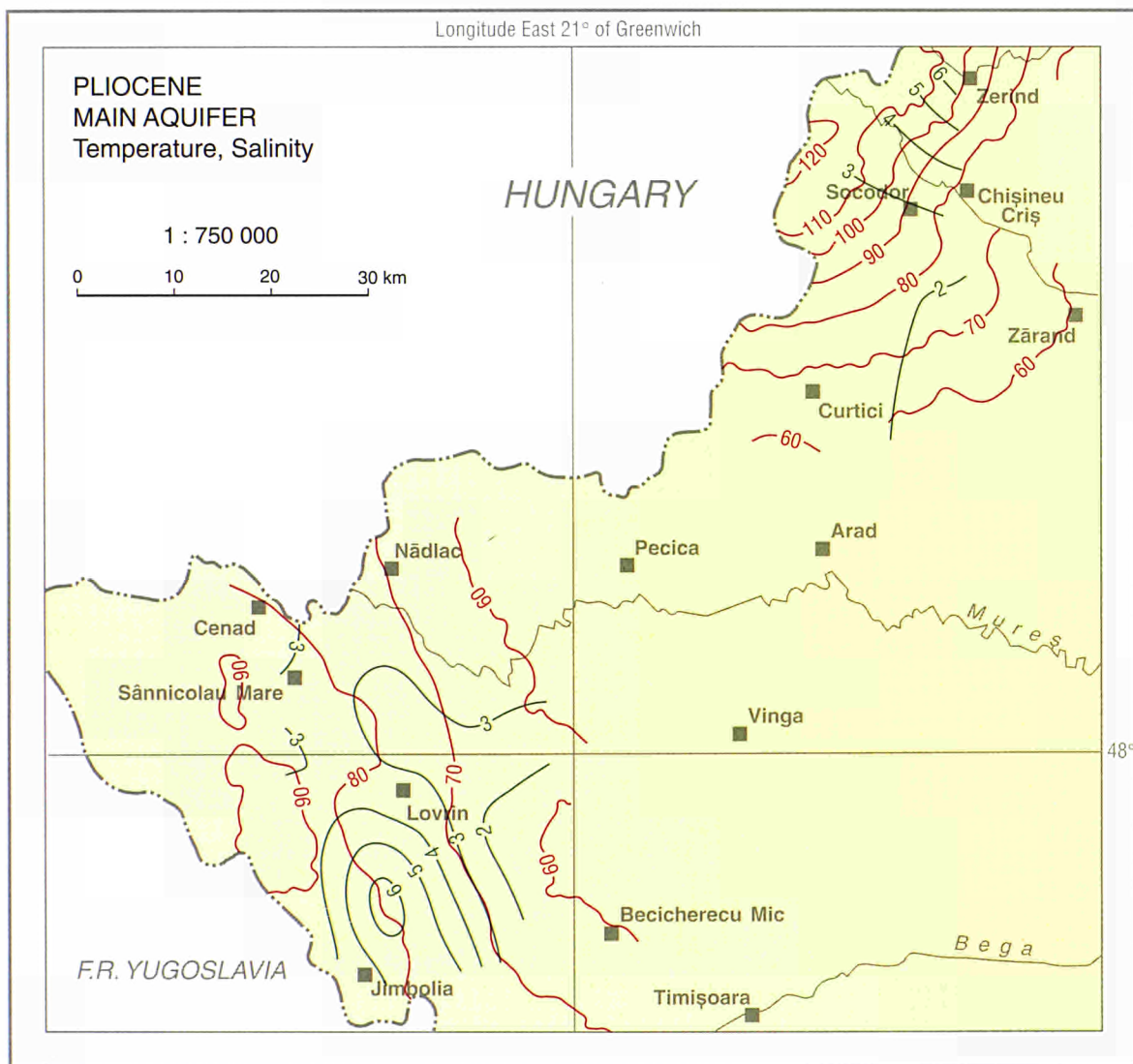
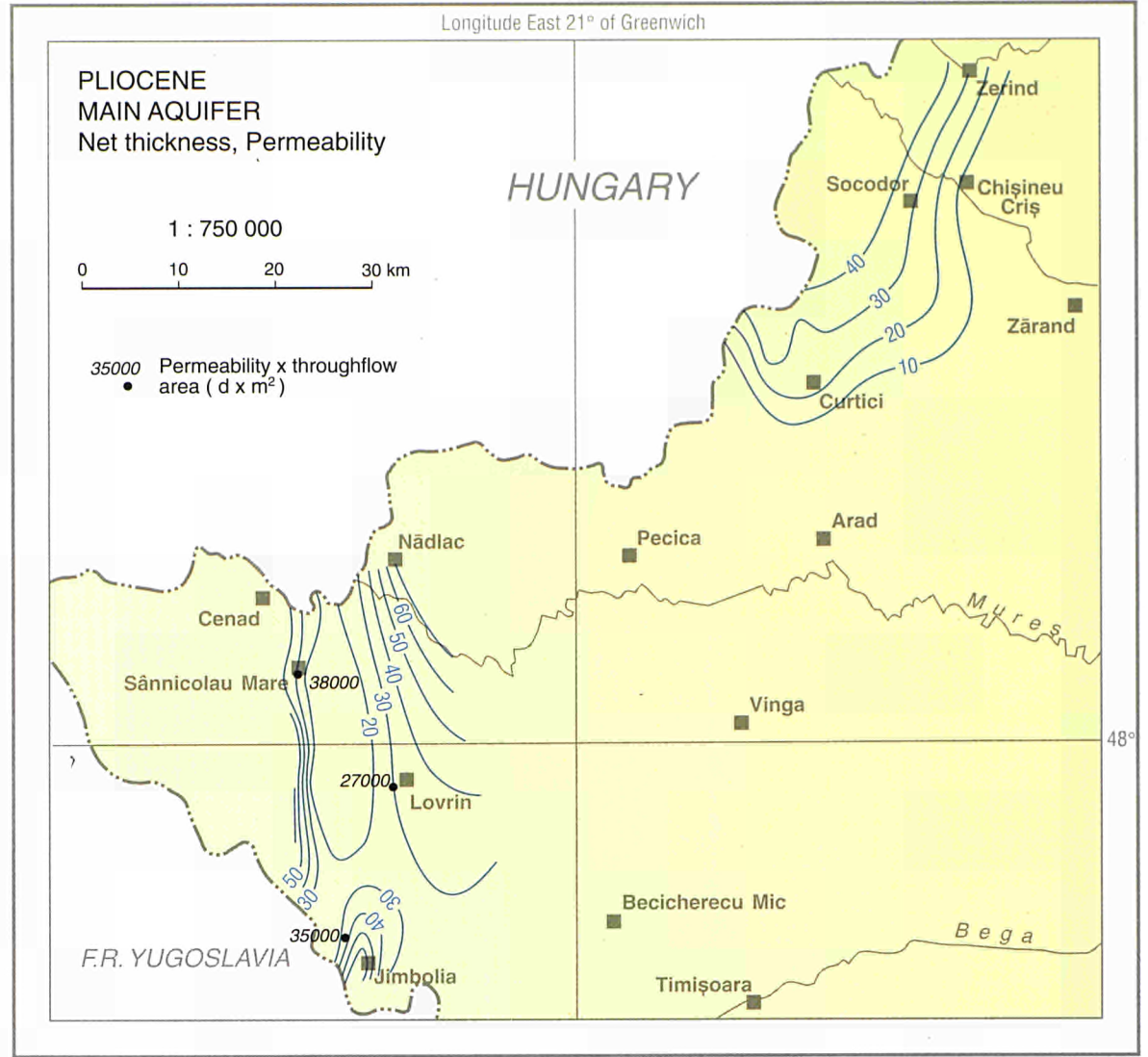
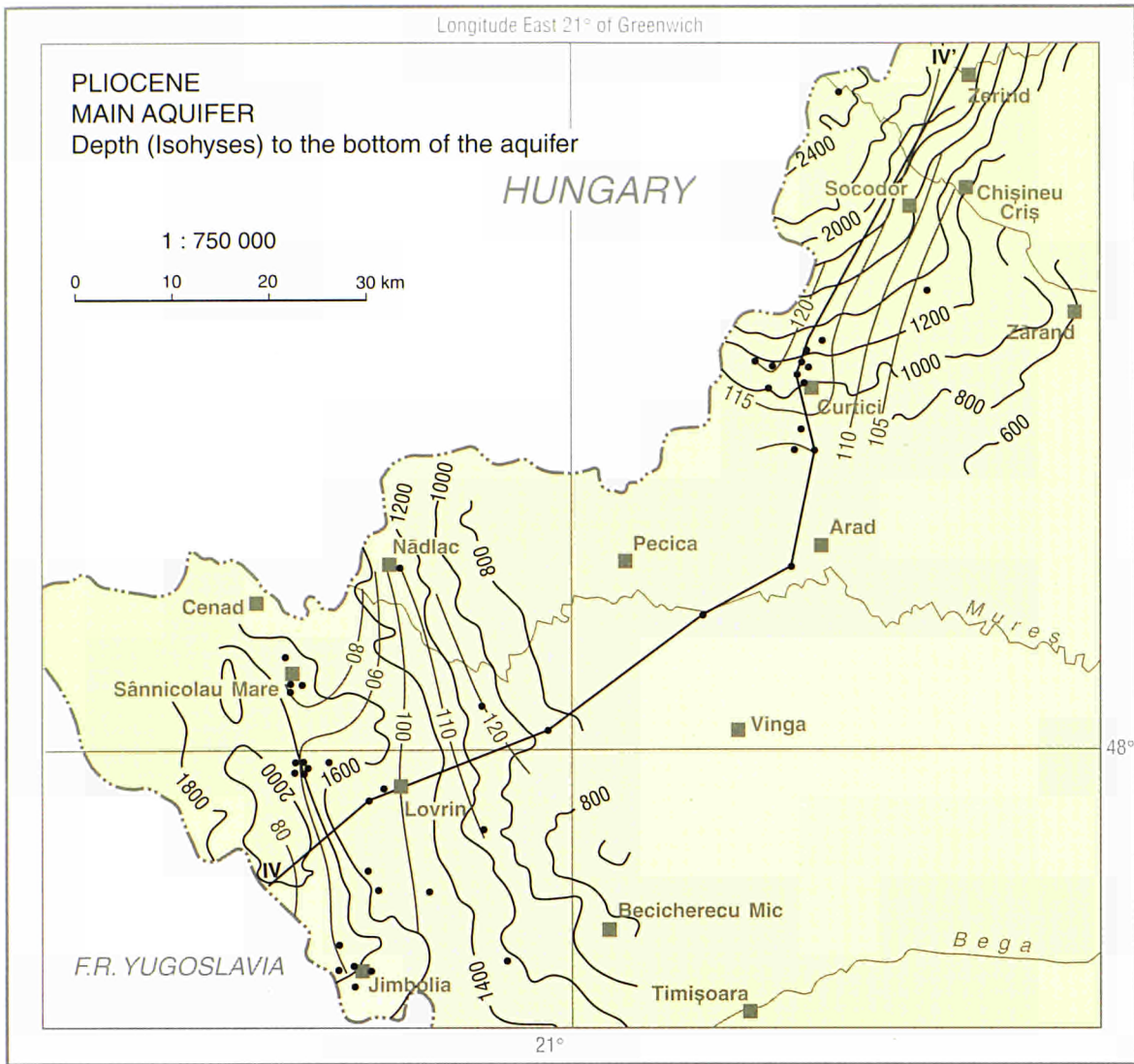
ROMANIA, Moesian Platform



North ROMANIA, Pannonian Depression



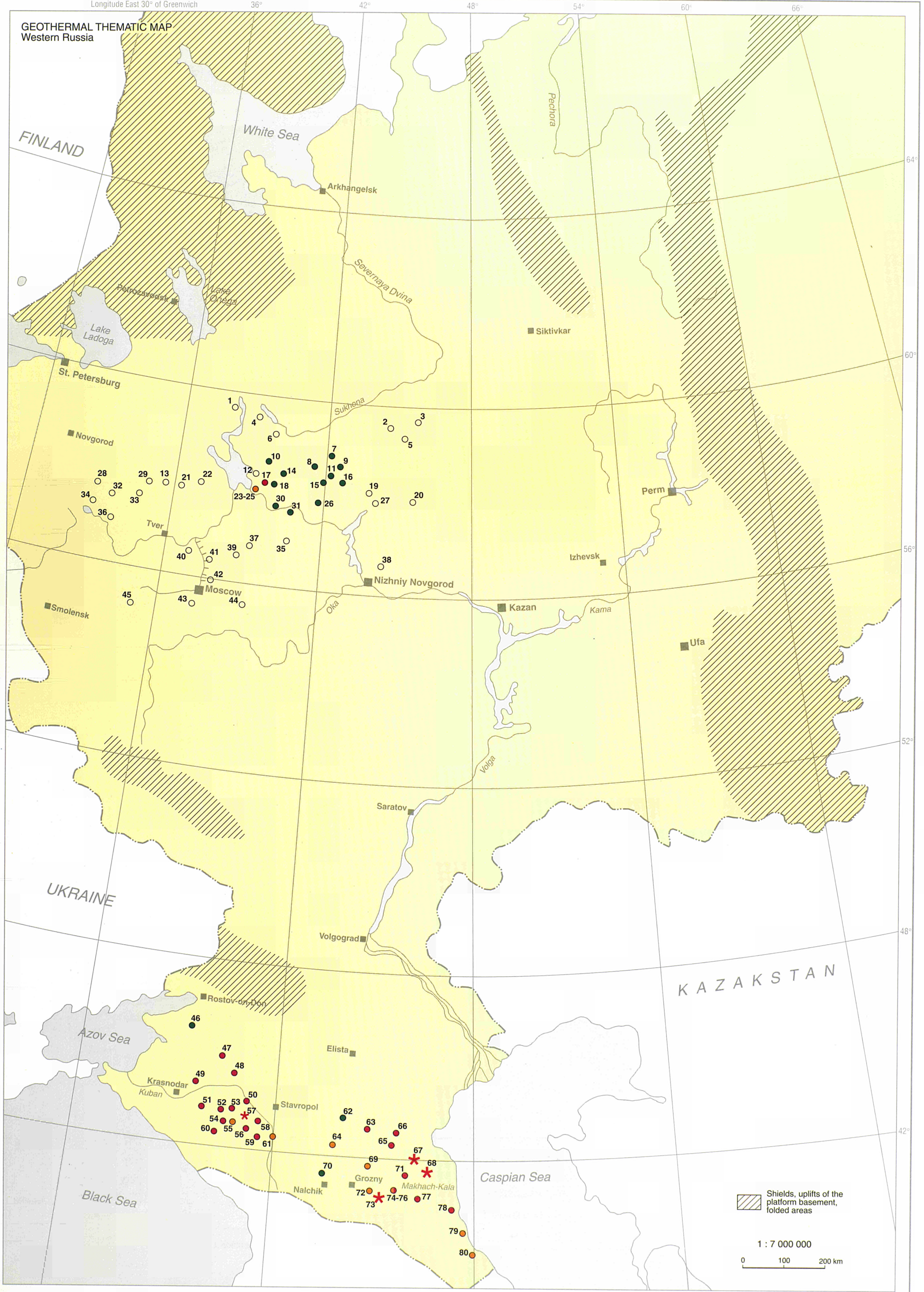
Pannonian Depression, South ROMANIA



RUSSIA

Longitude East 30° of Greenwich 36° 42° 48° 54° 60° 66°

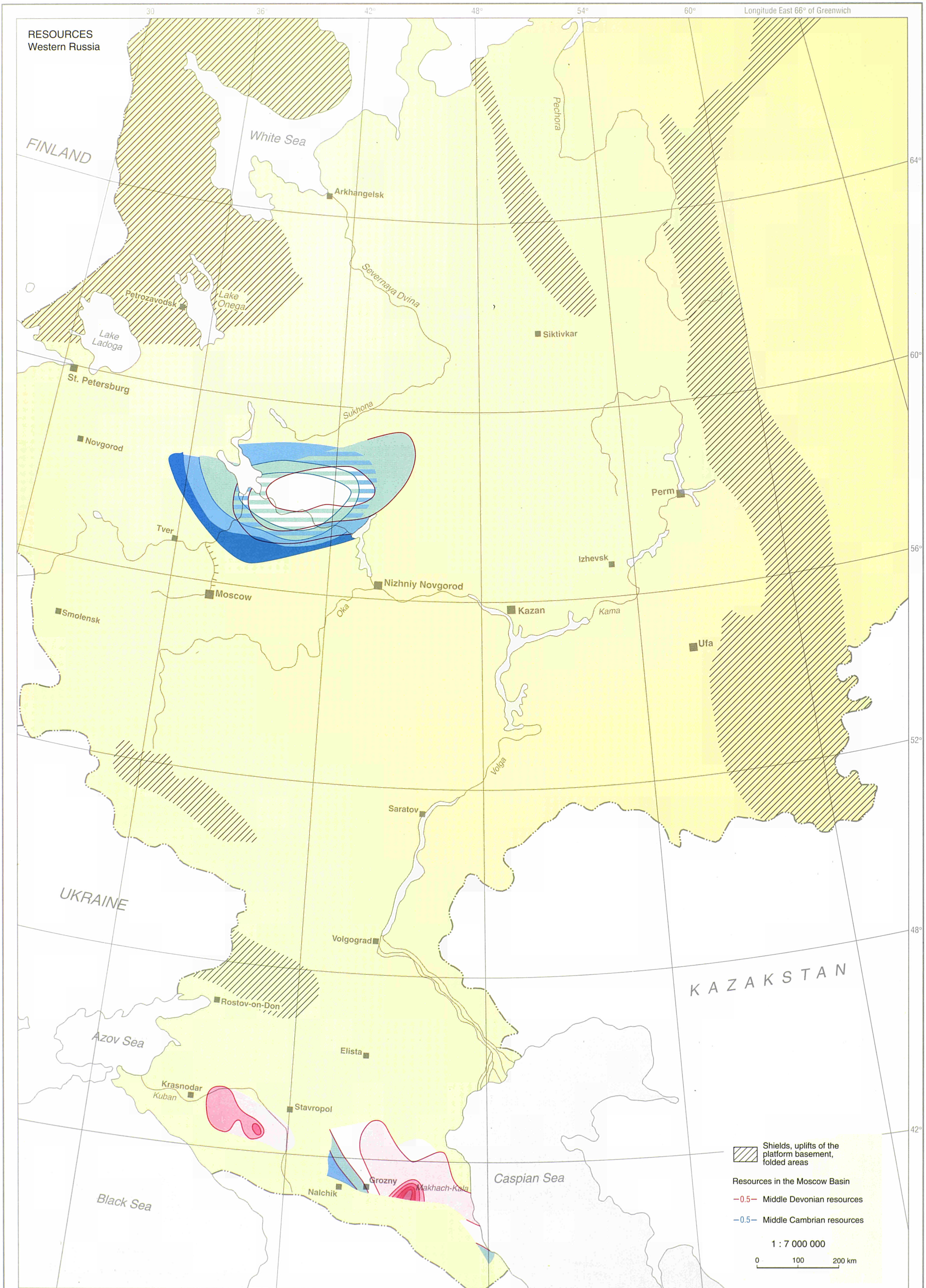
GEOTHERMAL THEMATIC MAP
Western Russia



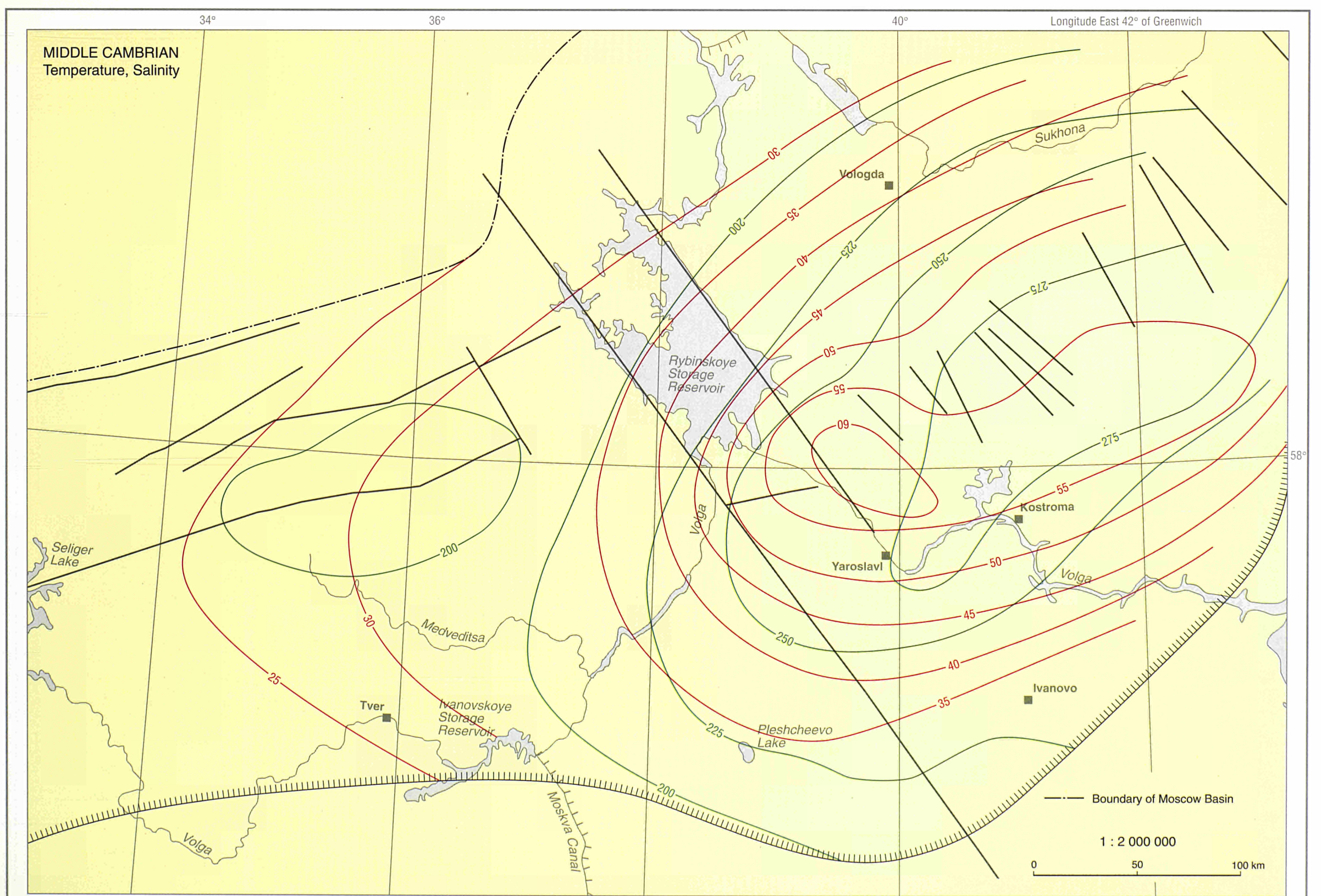
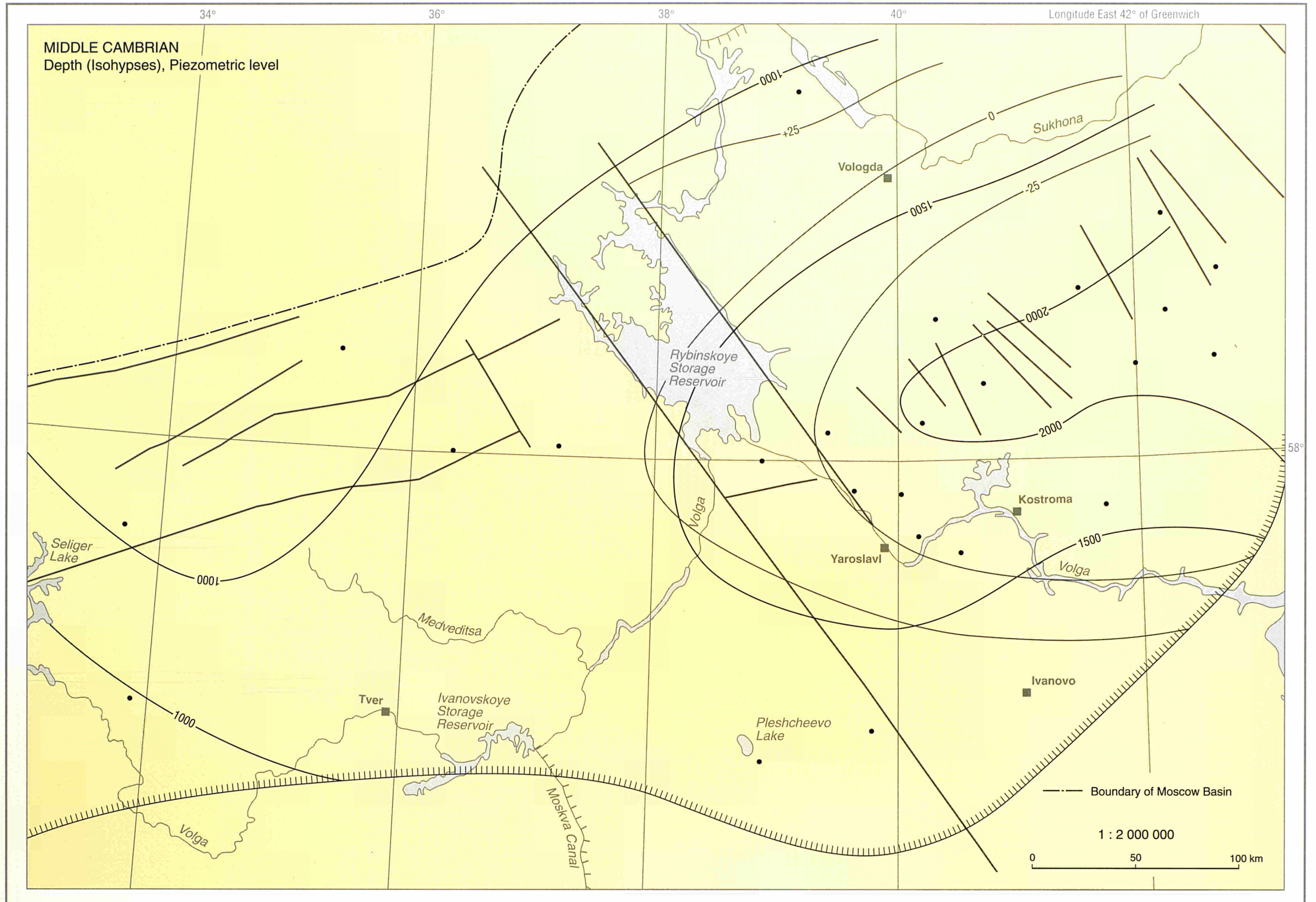
Shields, uplifts of the platform basement, folded areas

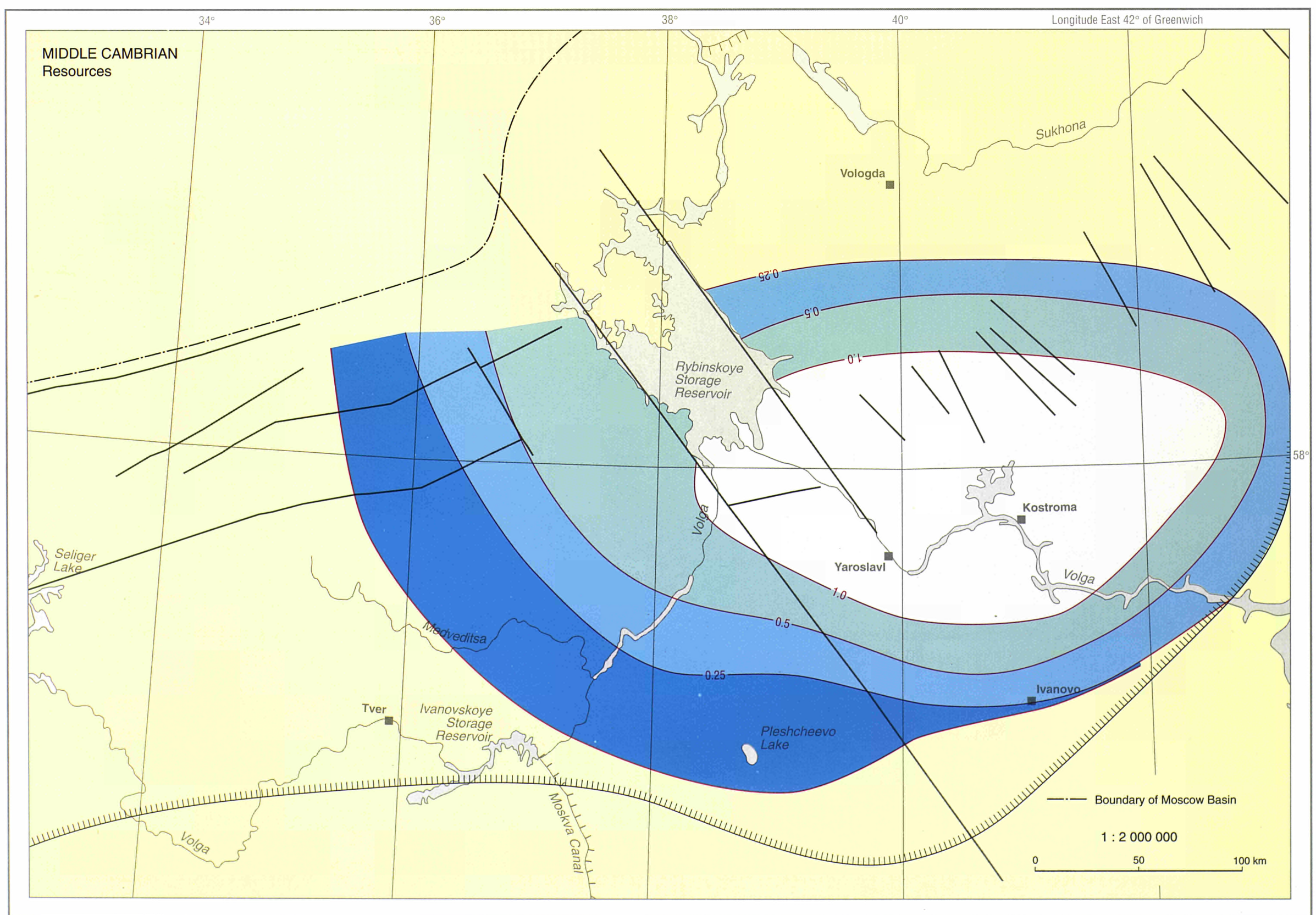
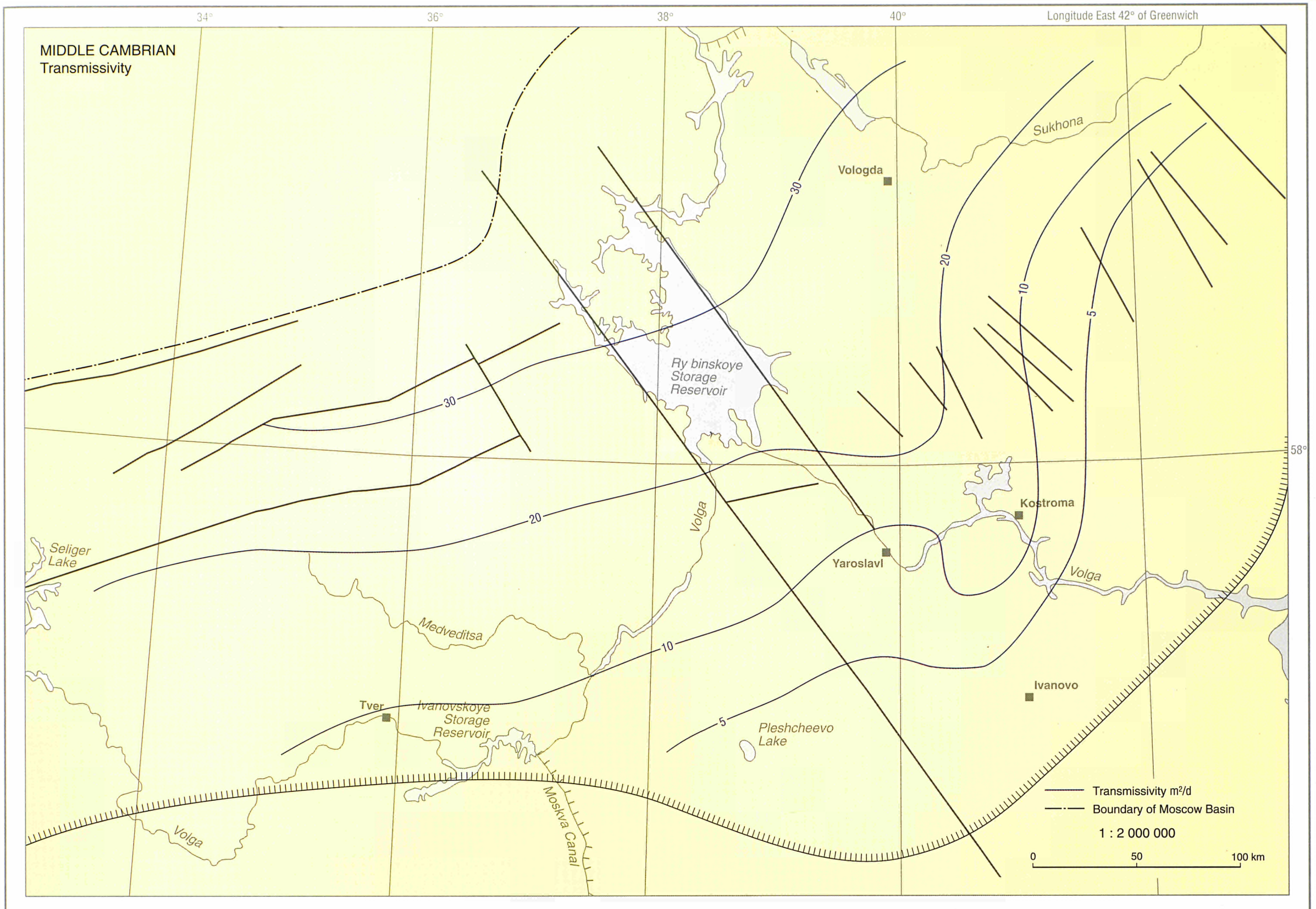
1 : 7 000 000

0 100 200 km

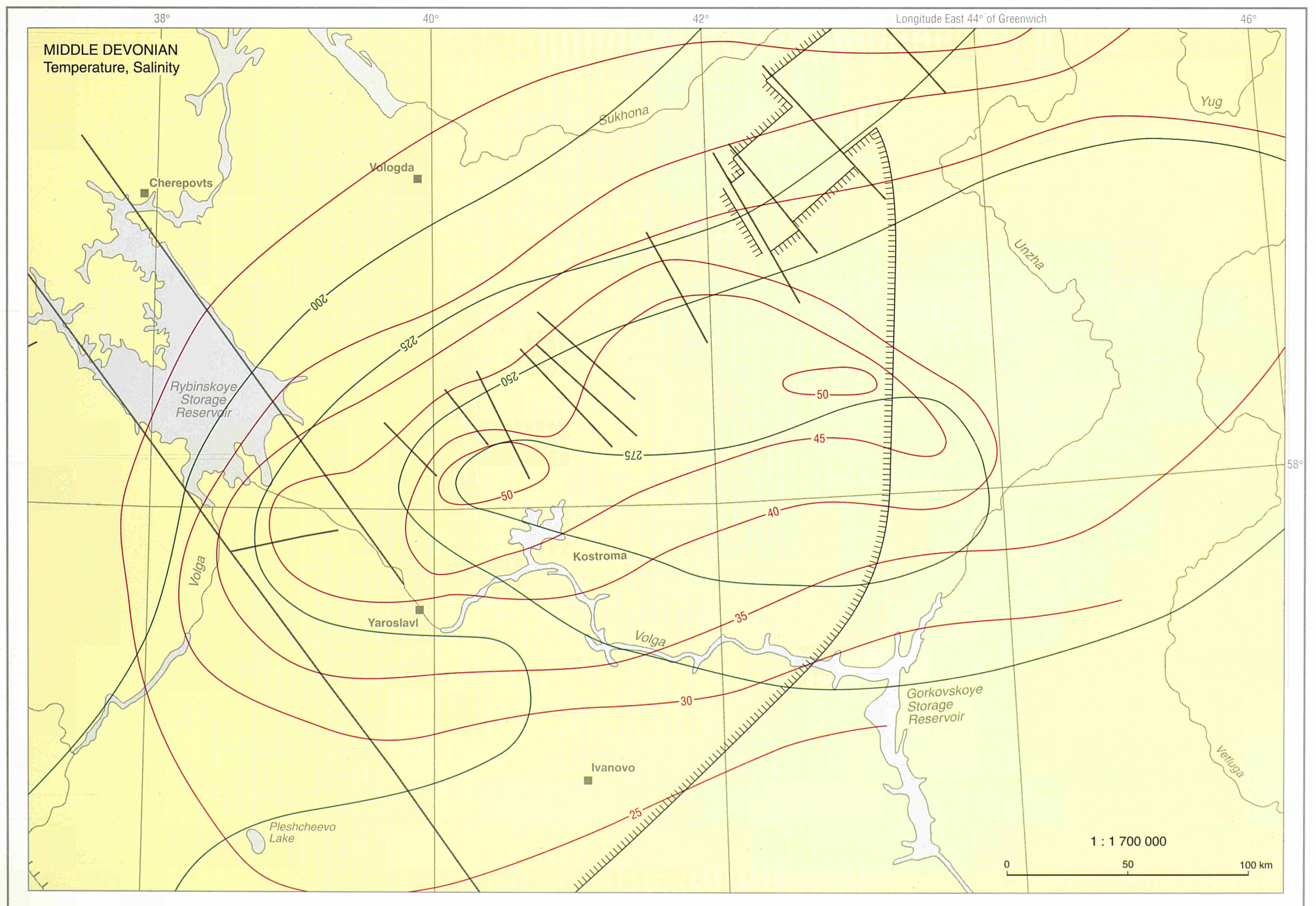
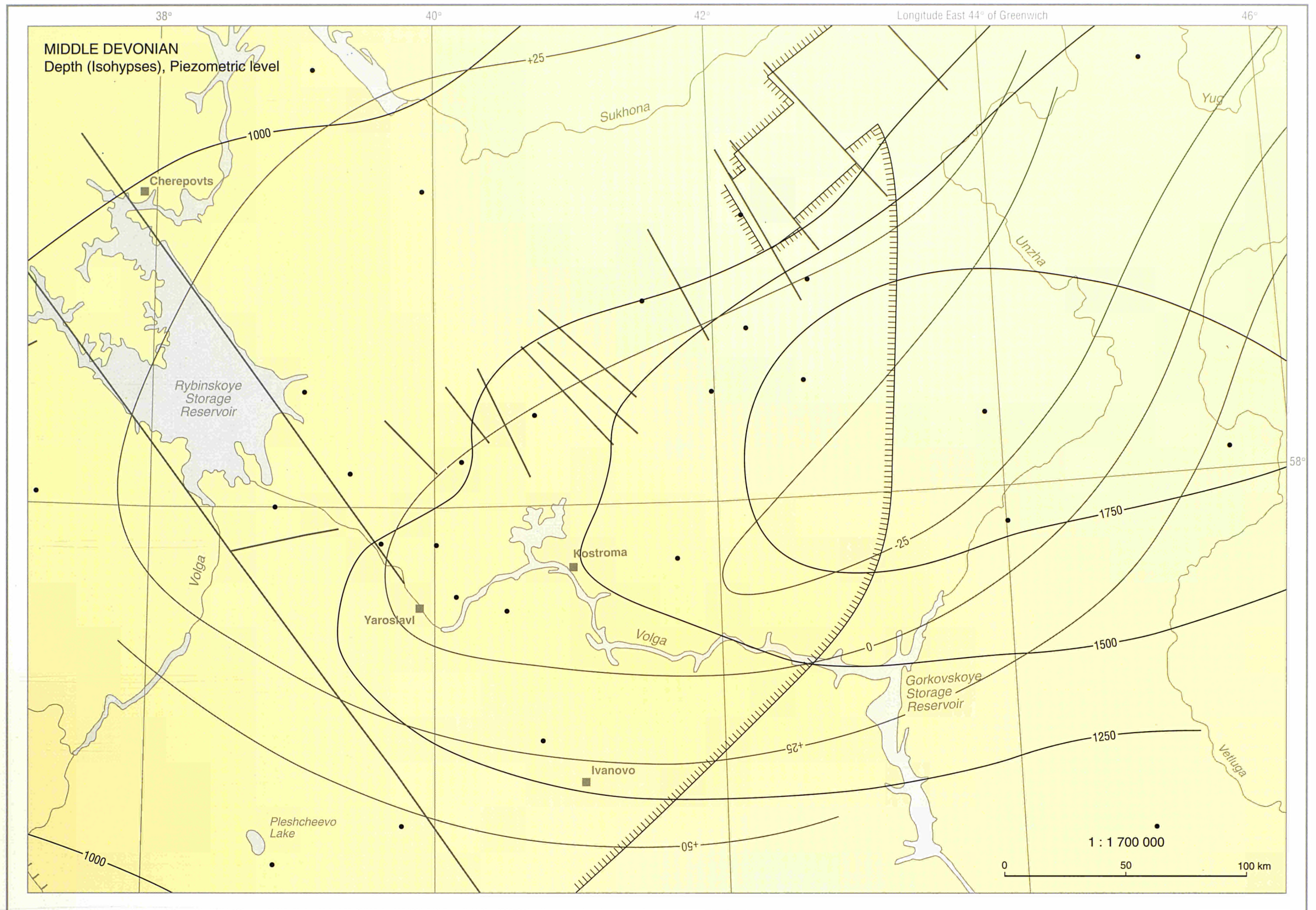


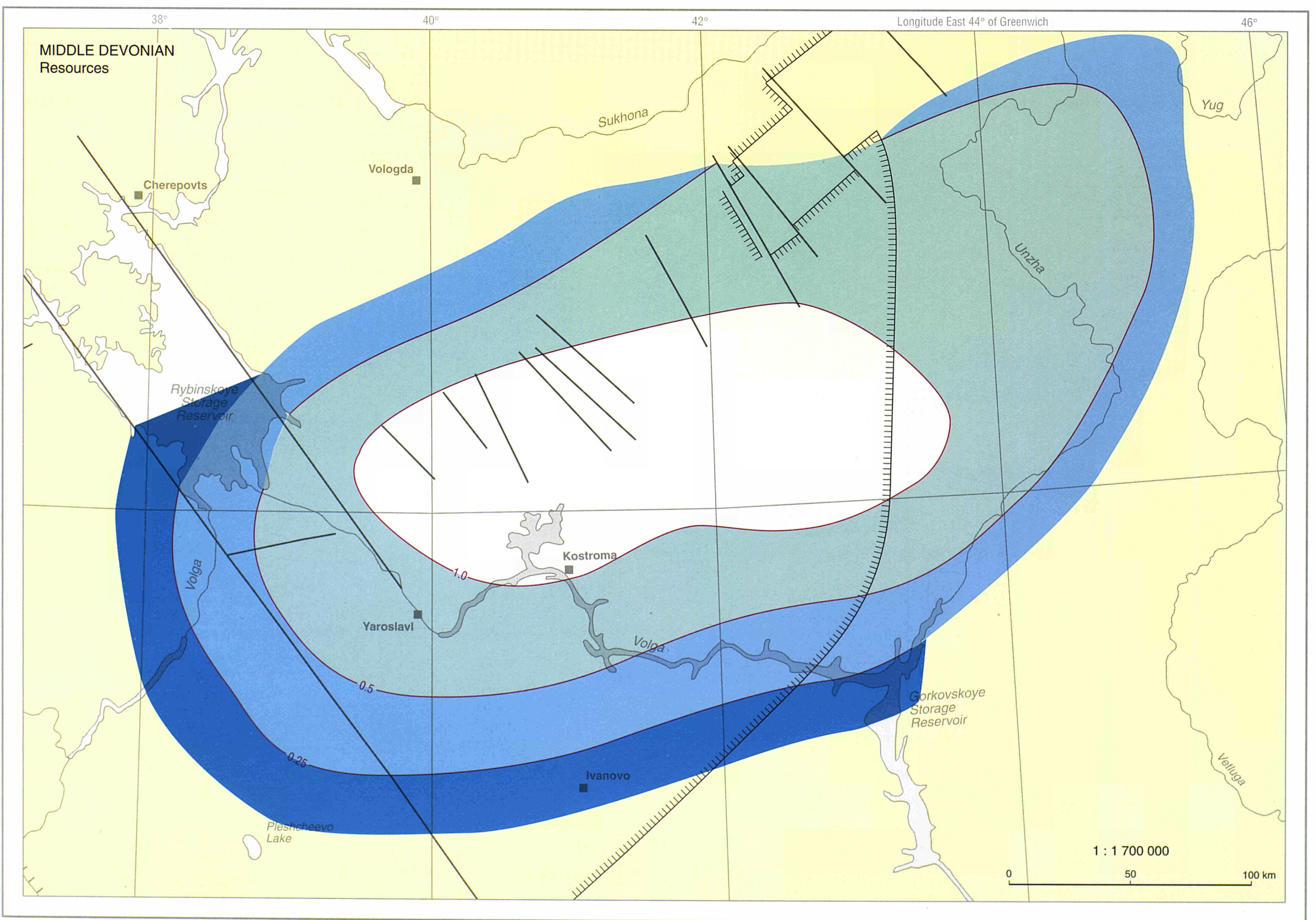
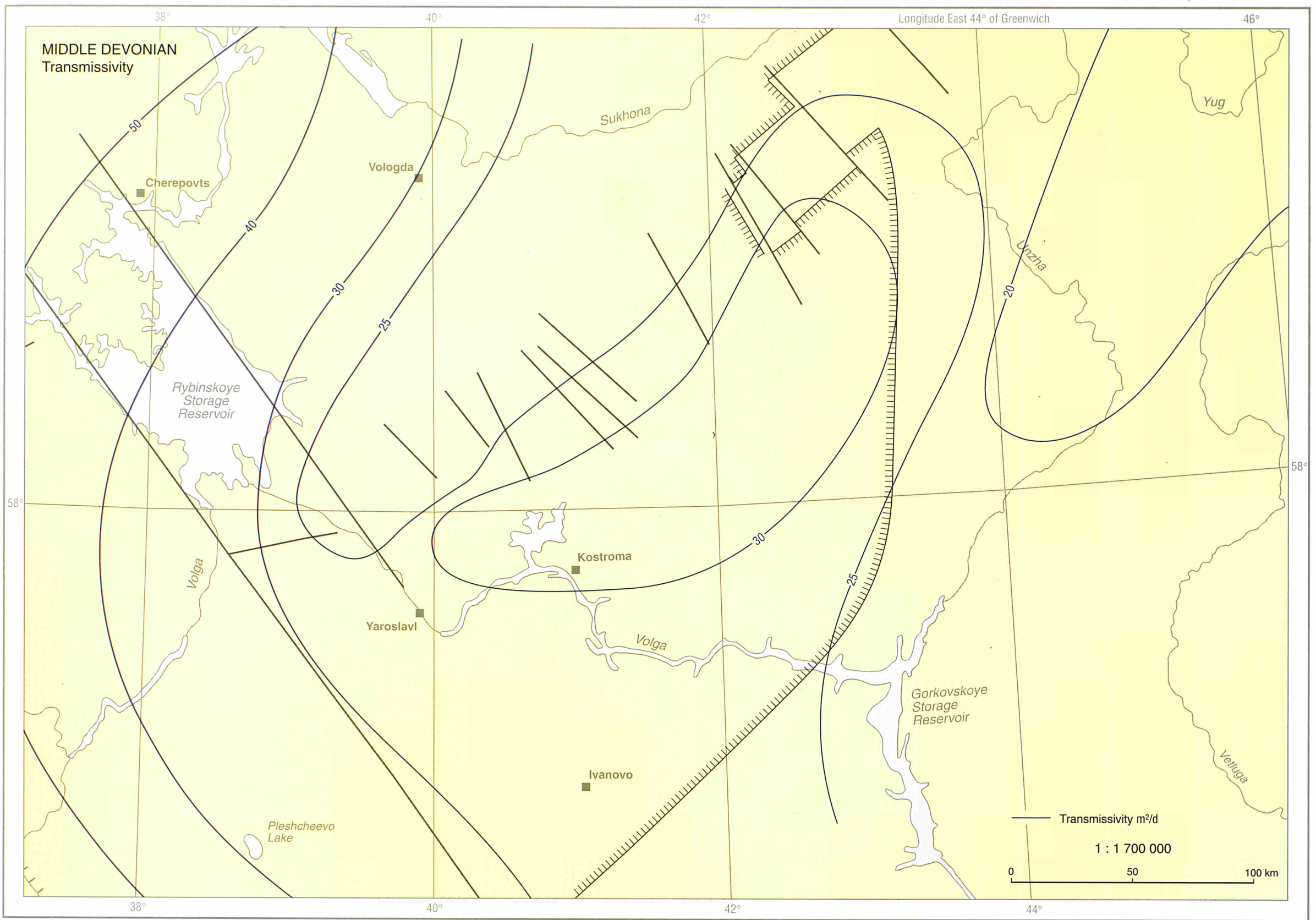
RUSSIA, Moscow Basin



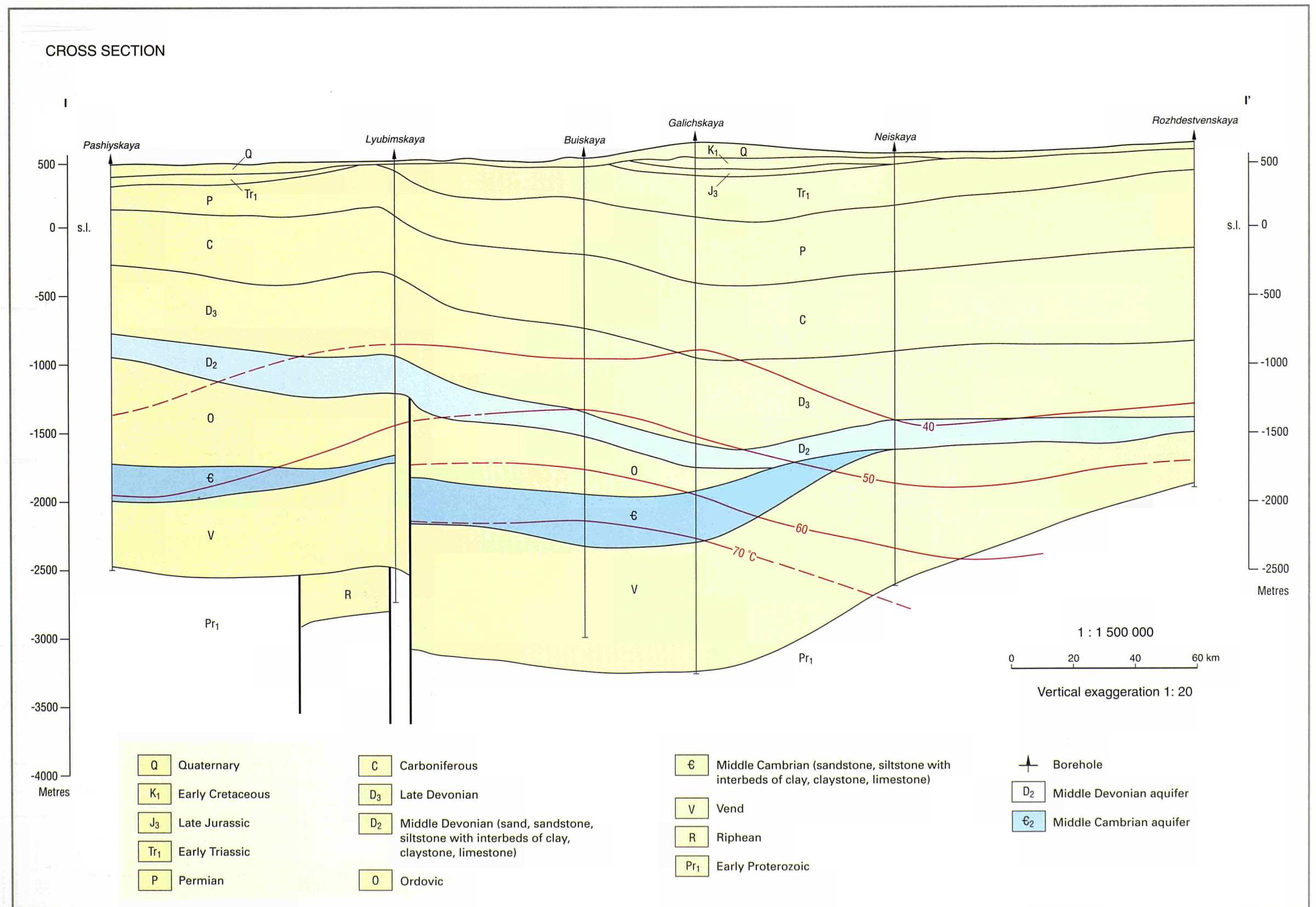
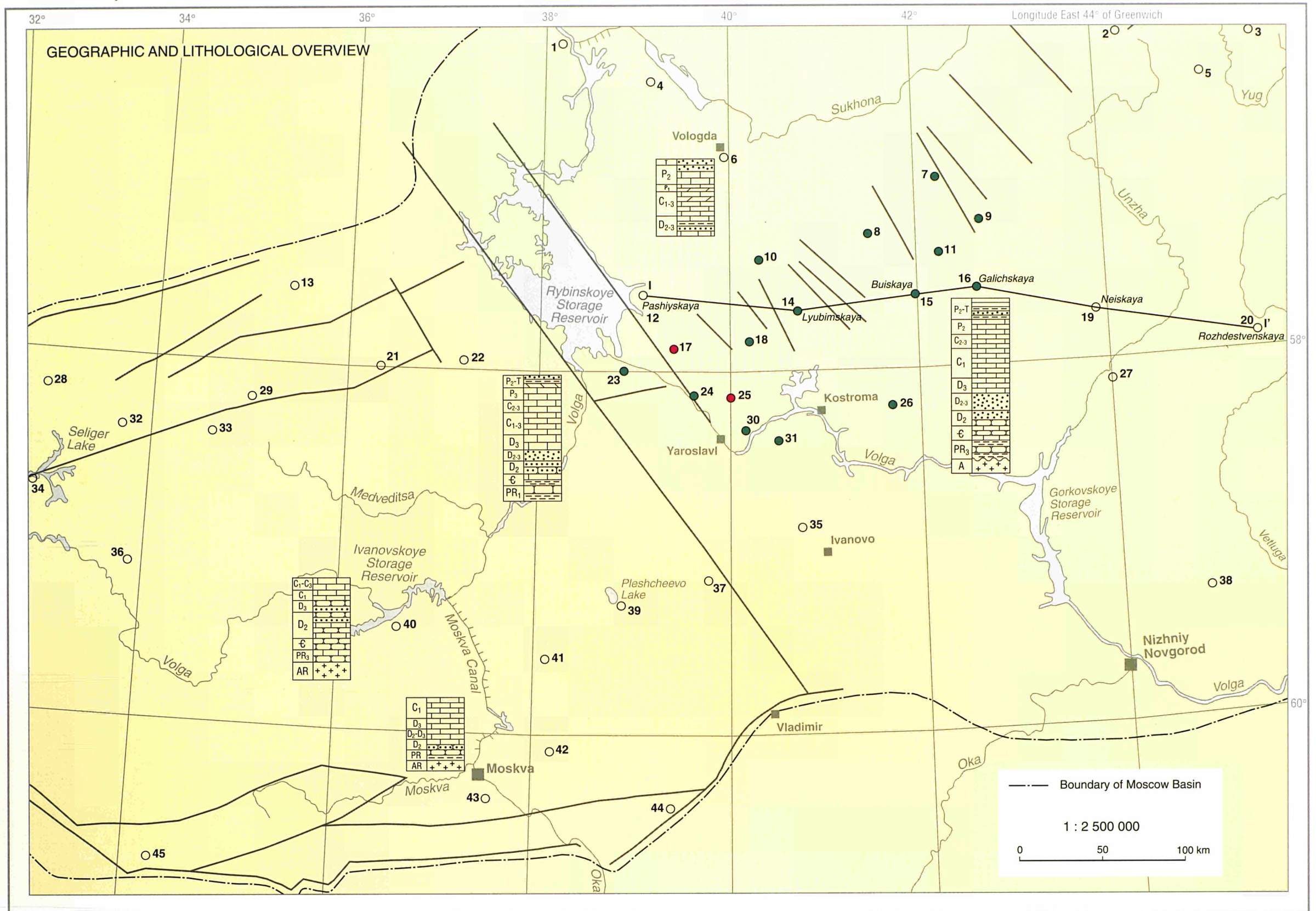


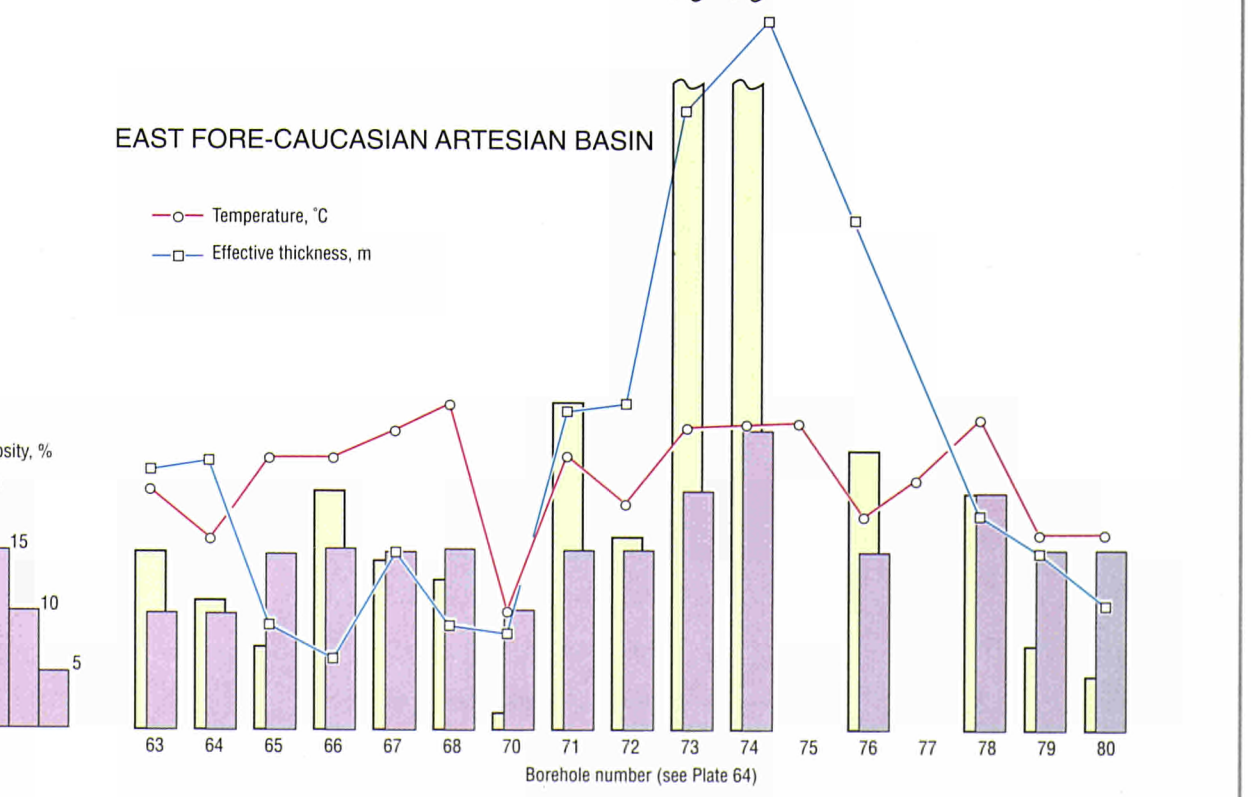
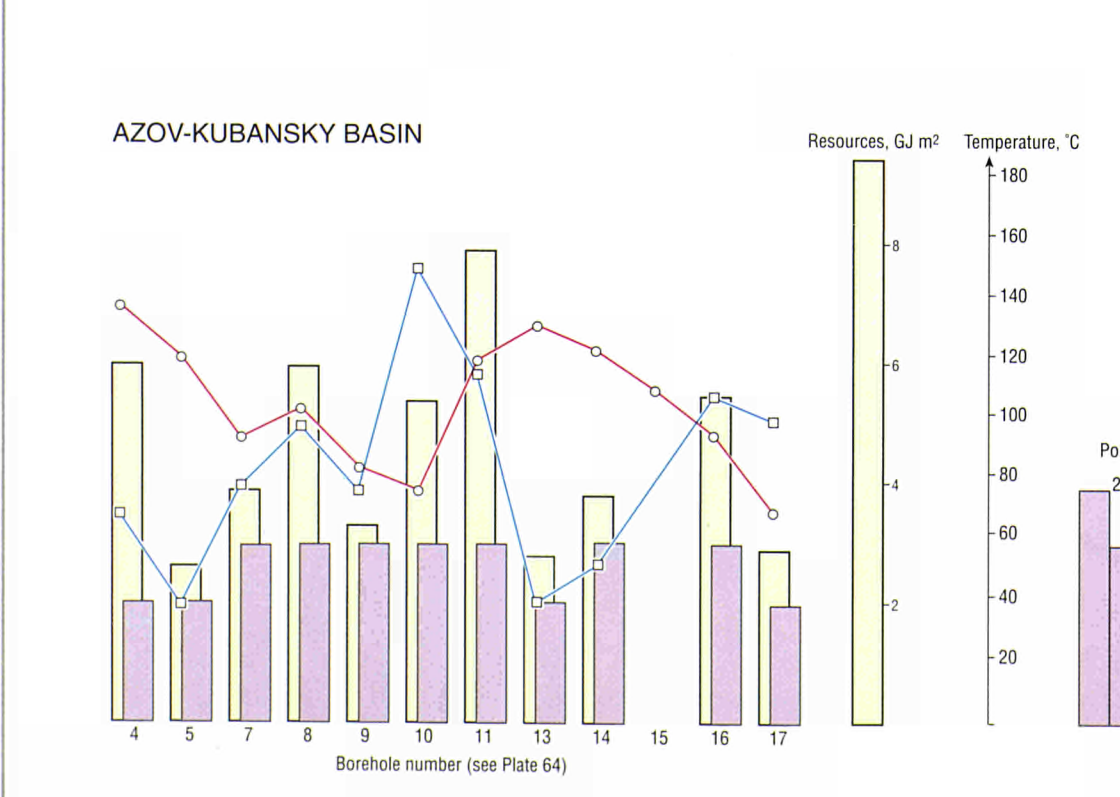
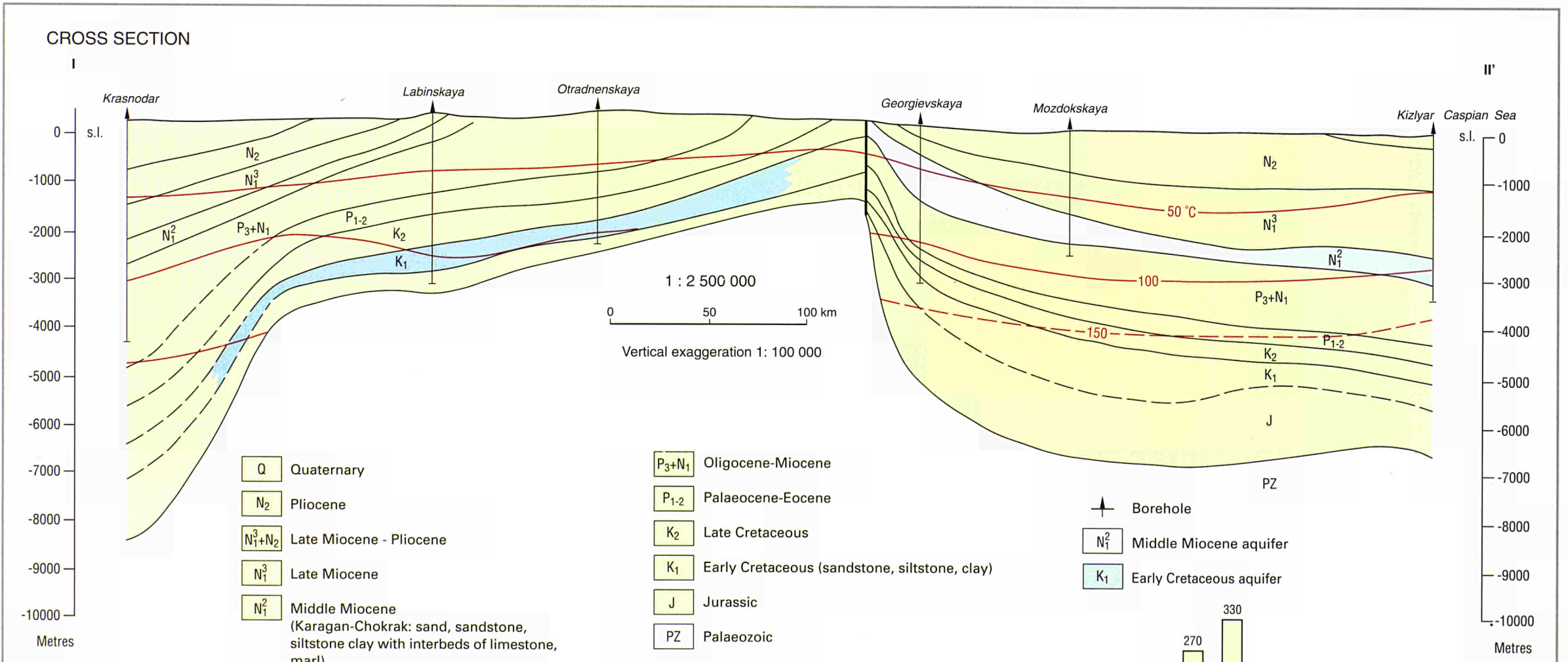
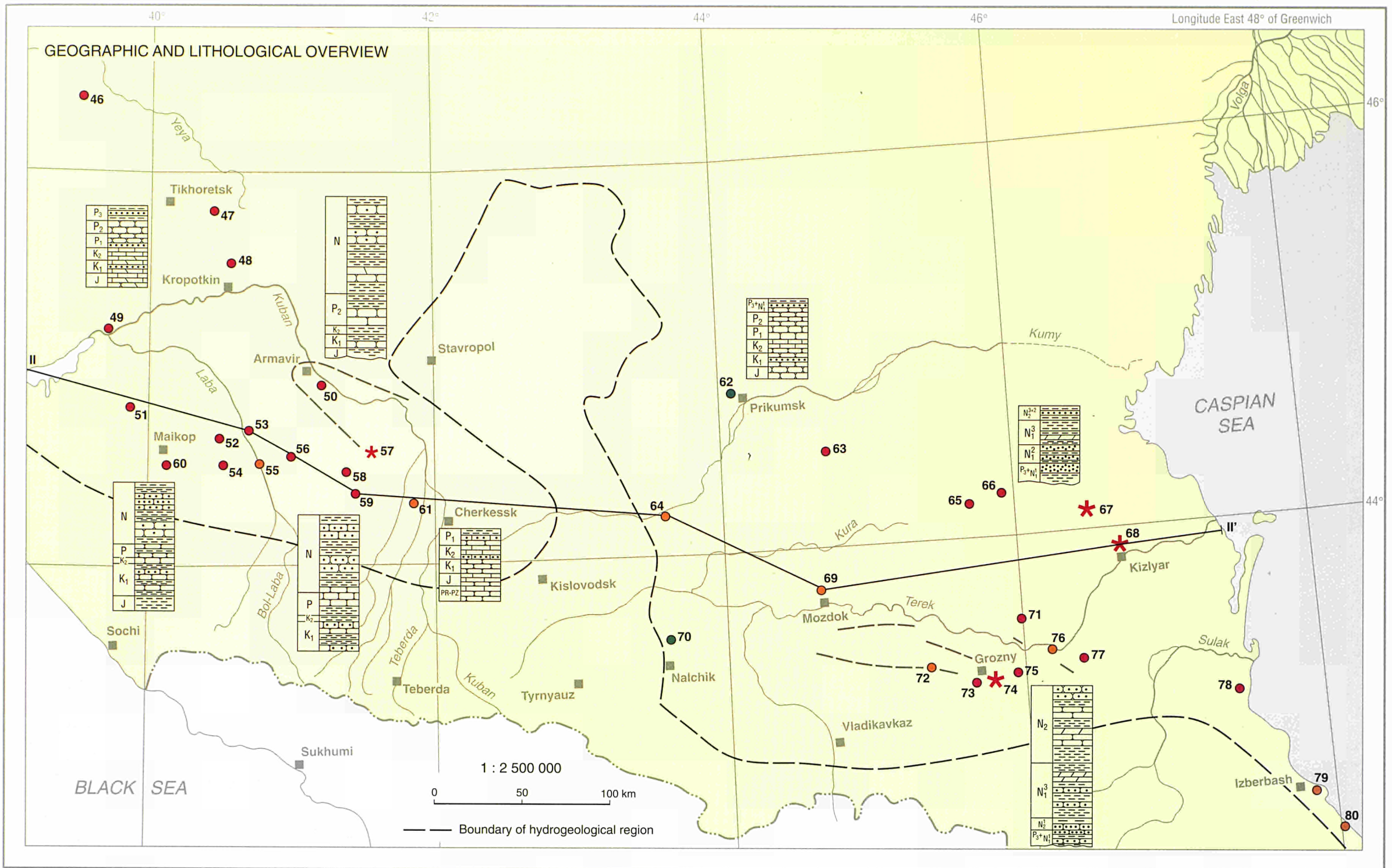
RUSSIA, Moscow Basin



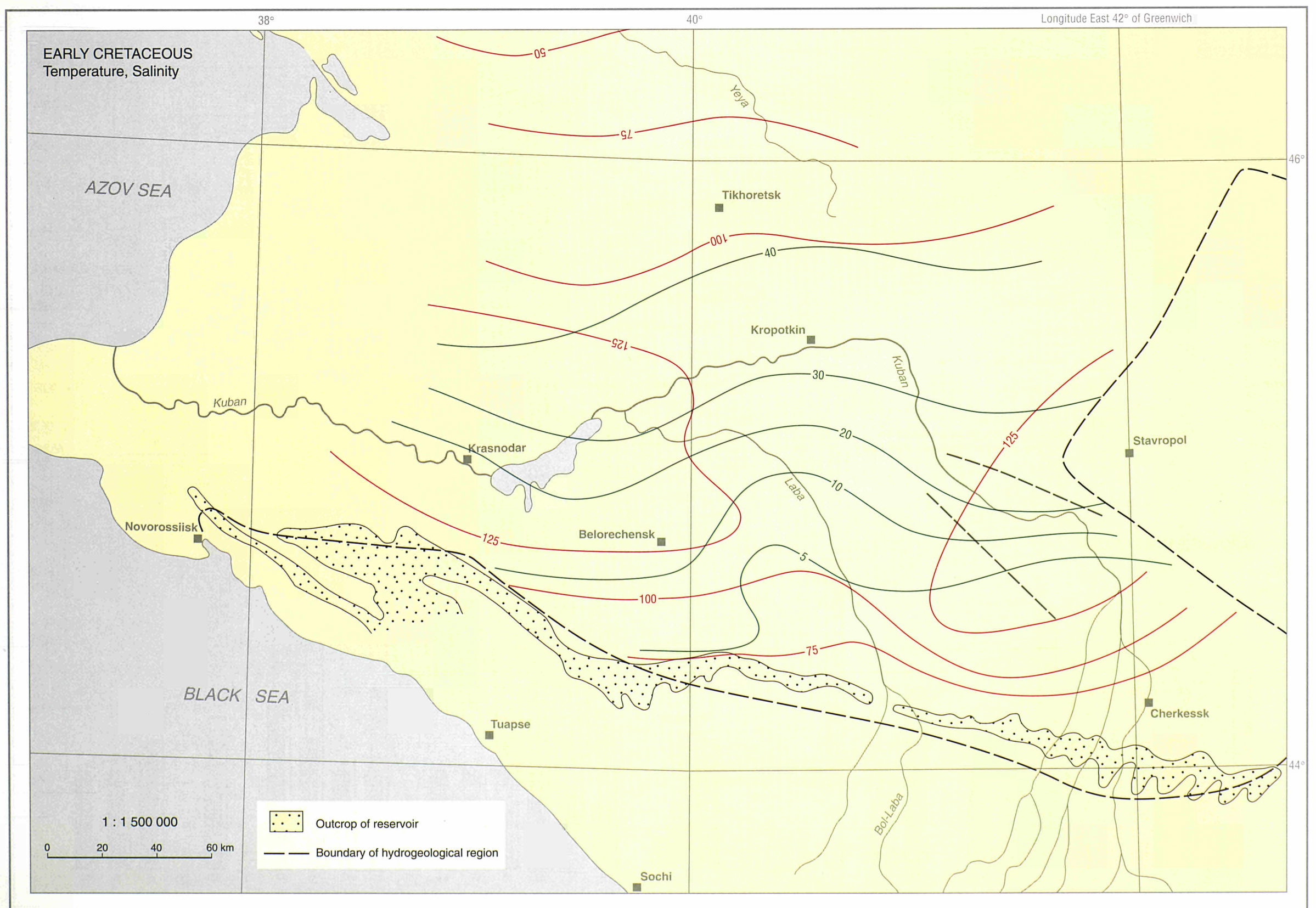
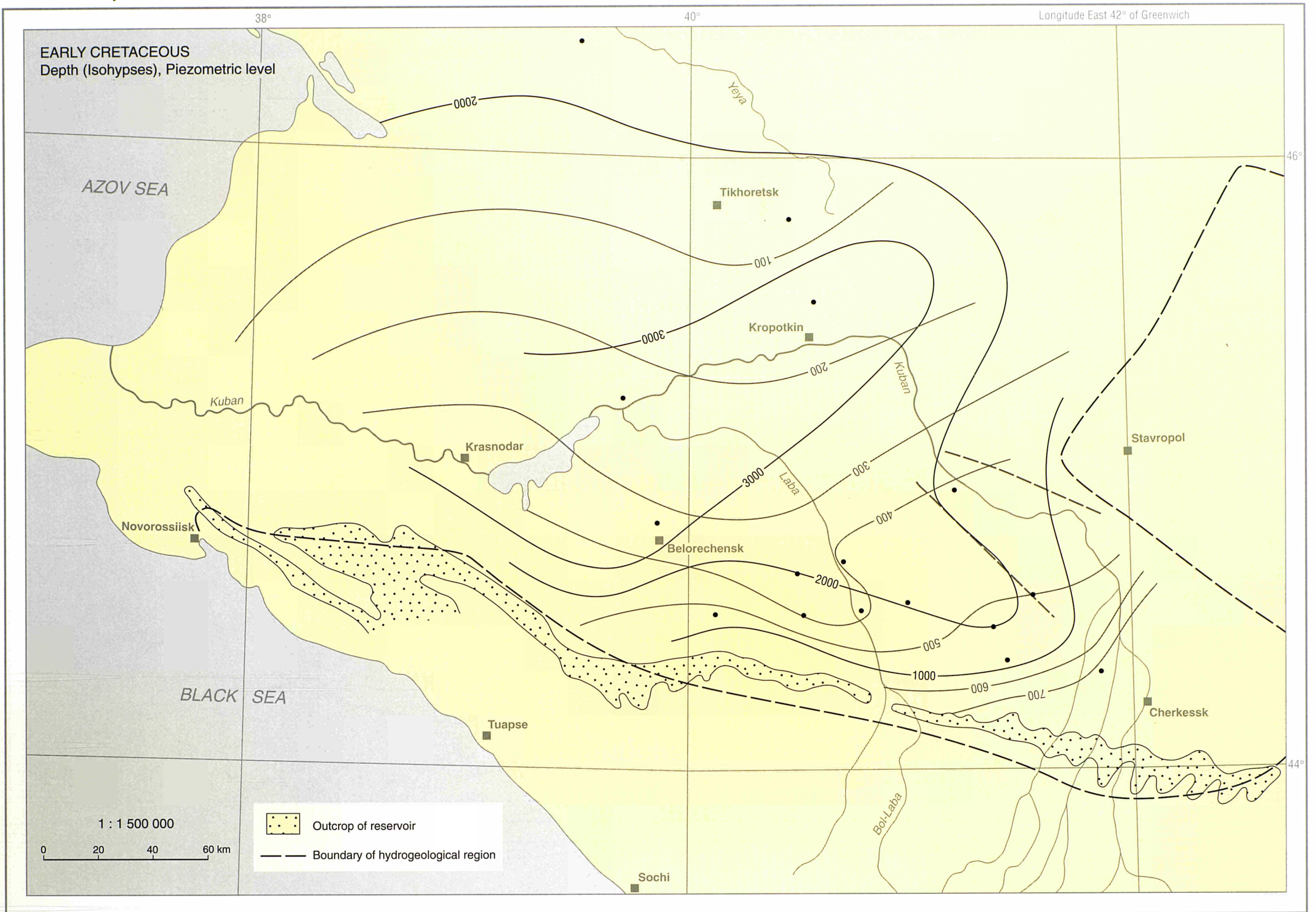


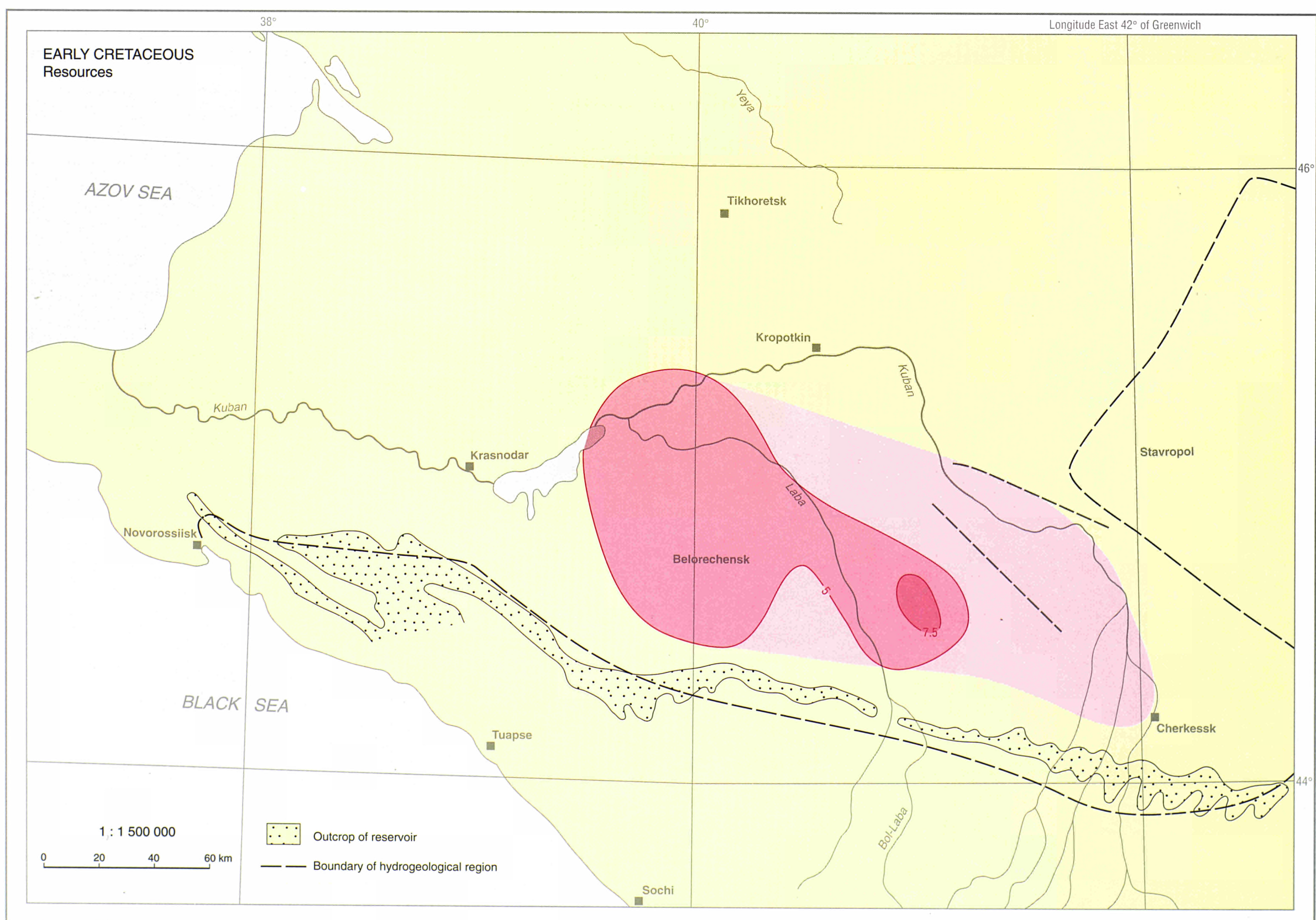
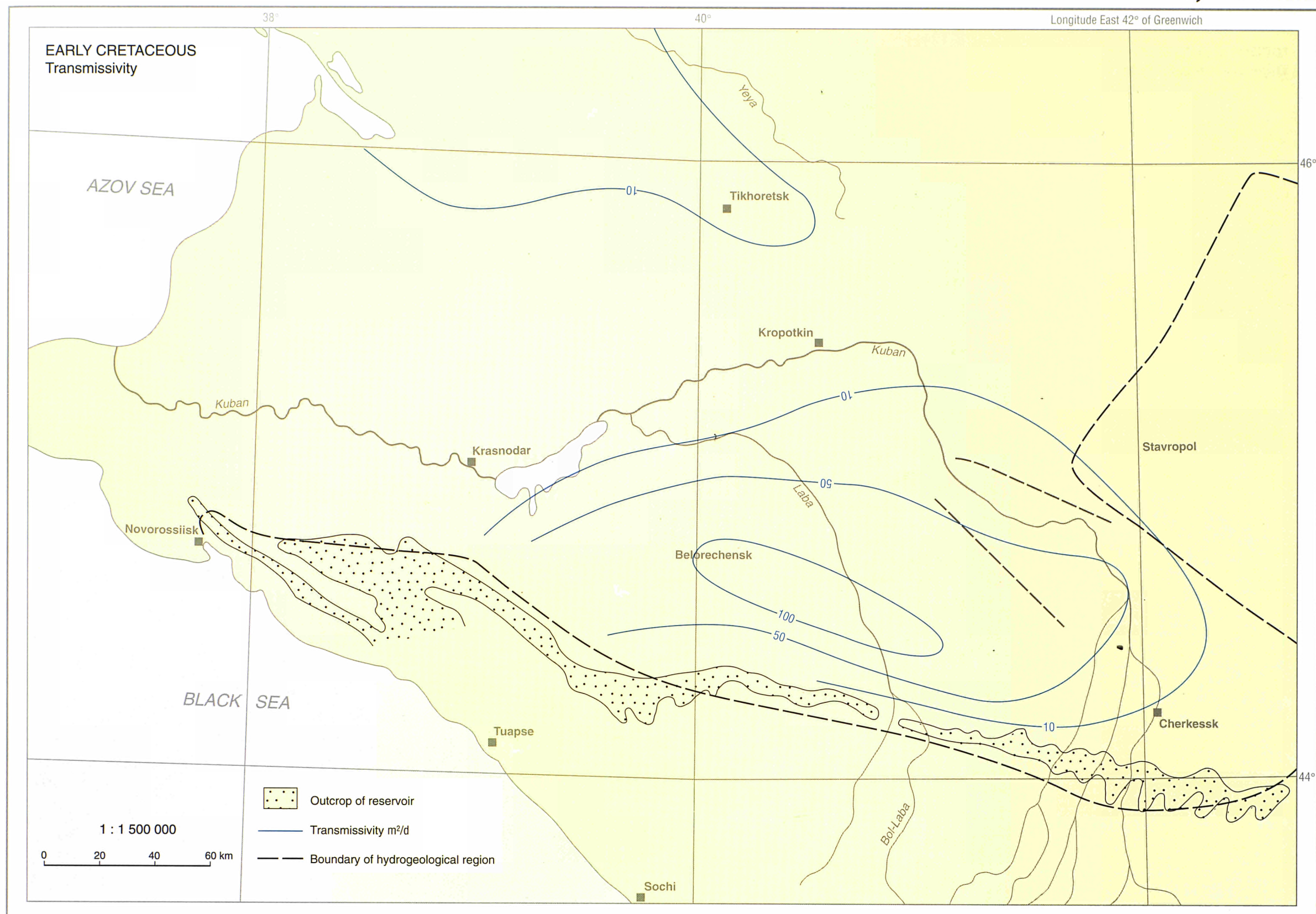
RUSSIA, Moscow Basin



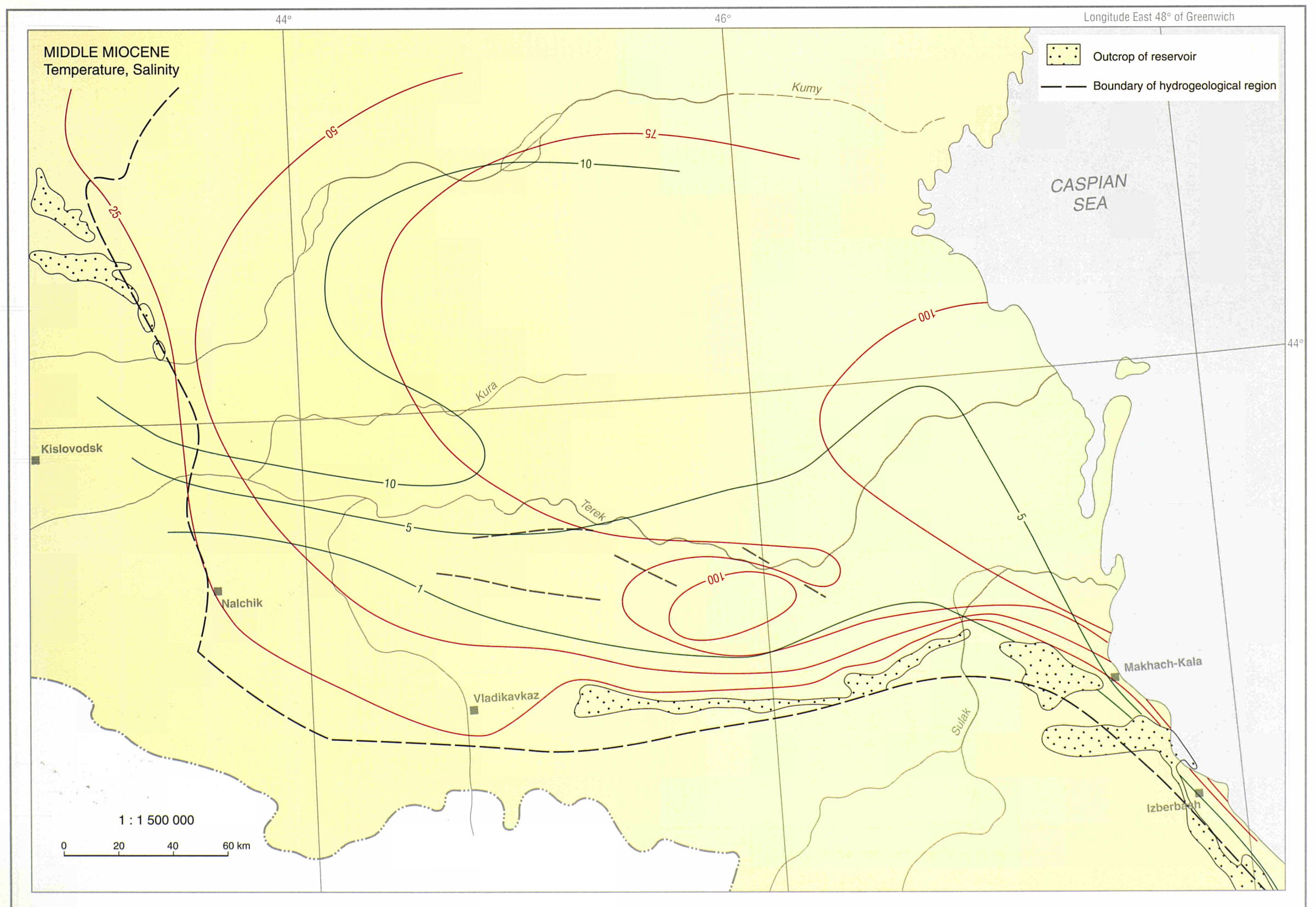
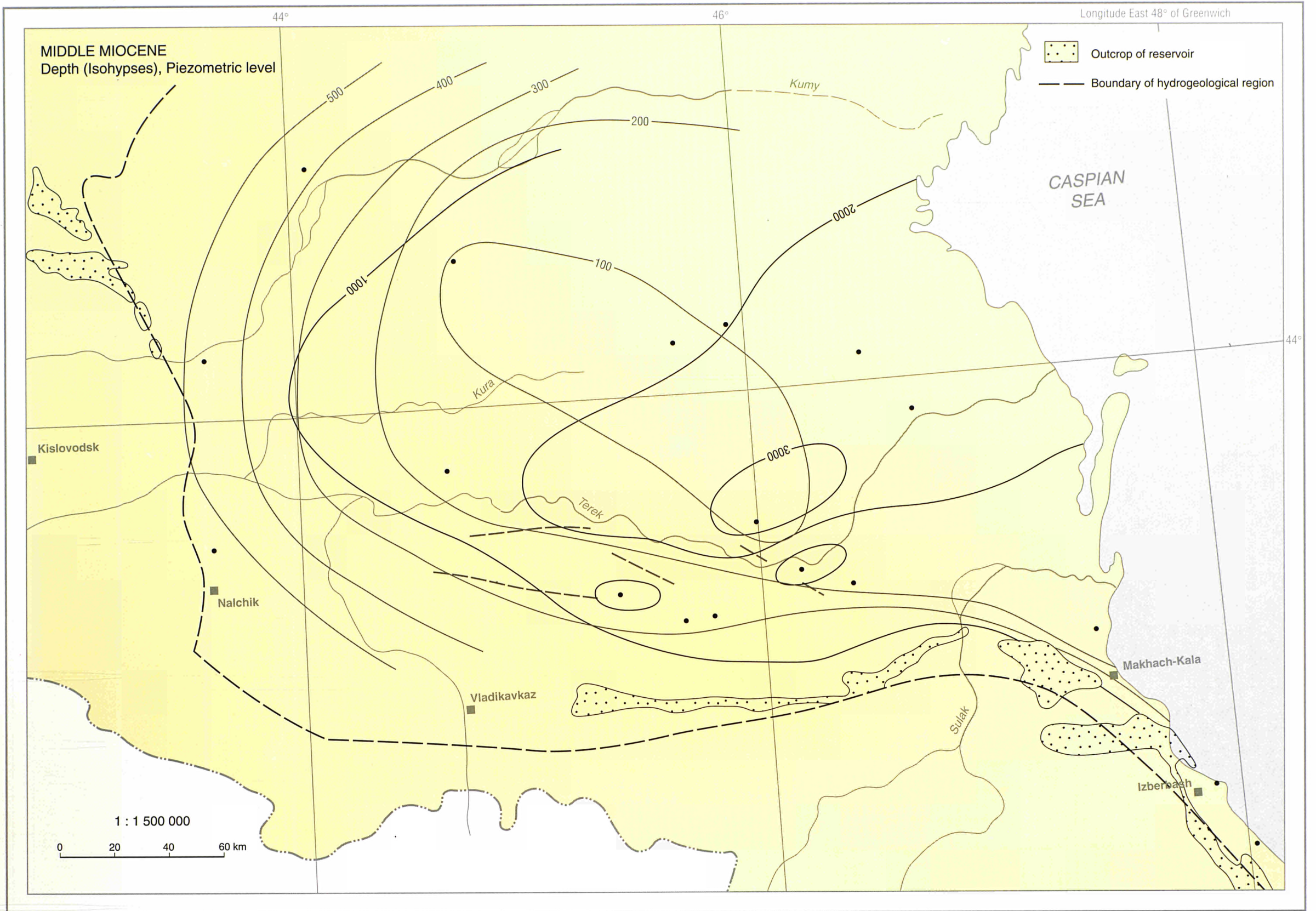


RUSSIA, North Caucasus

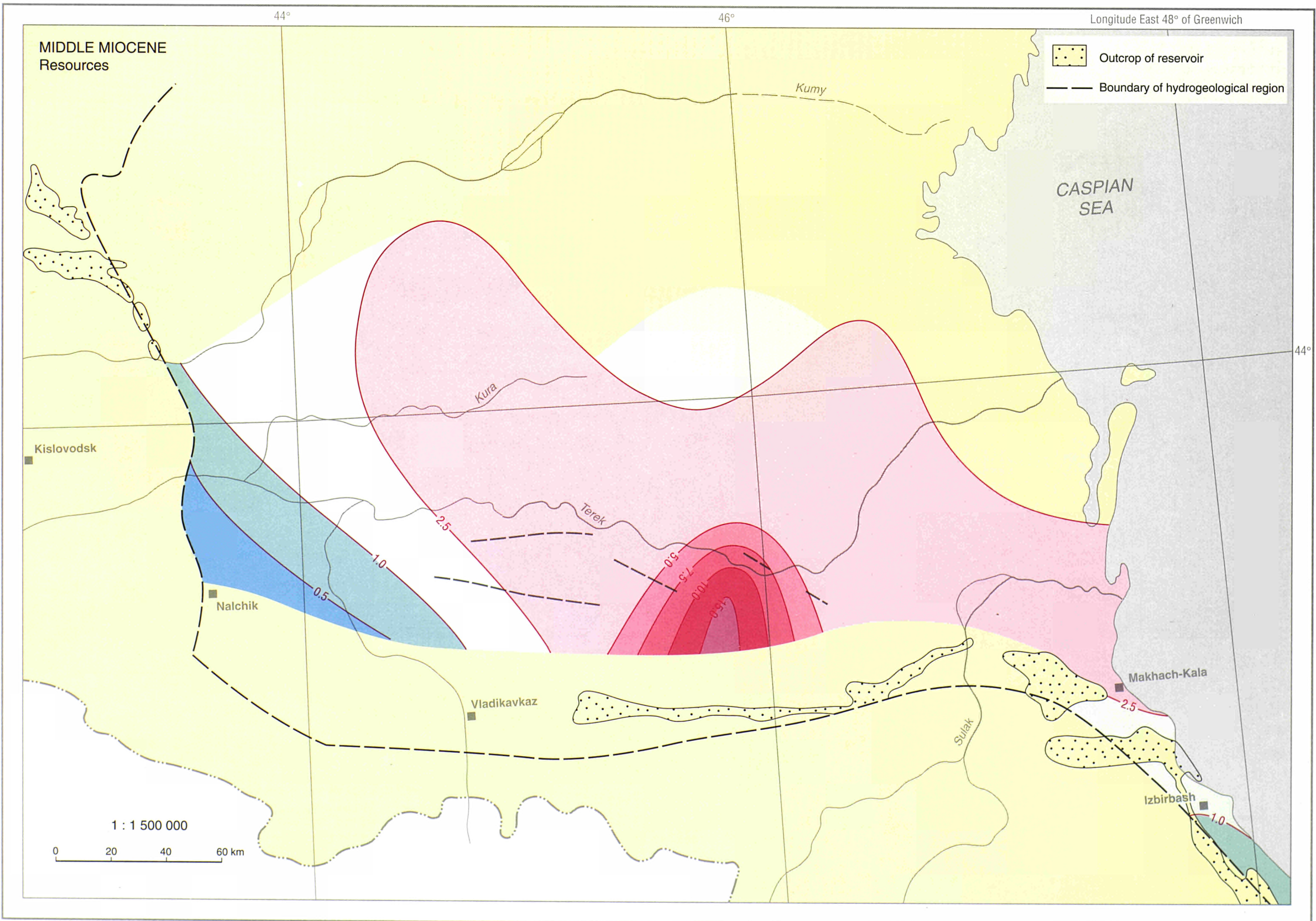
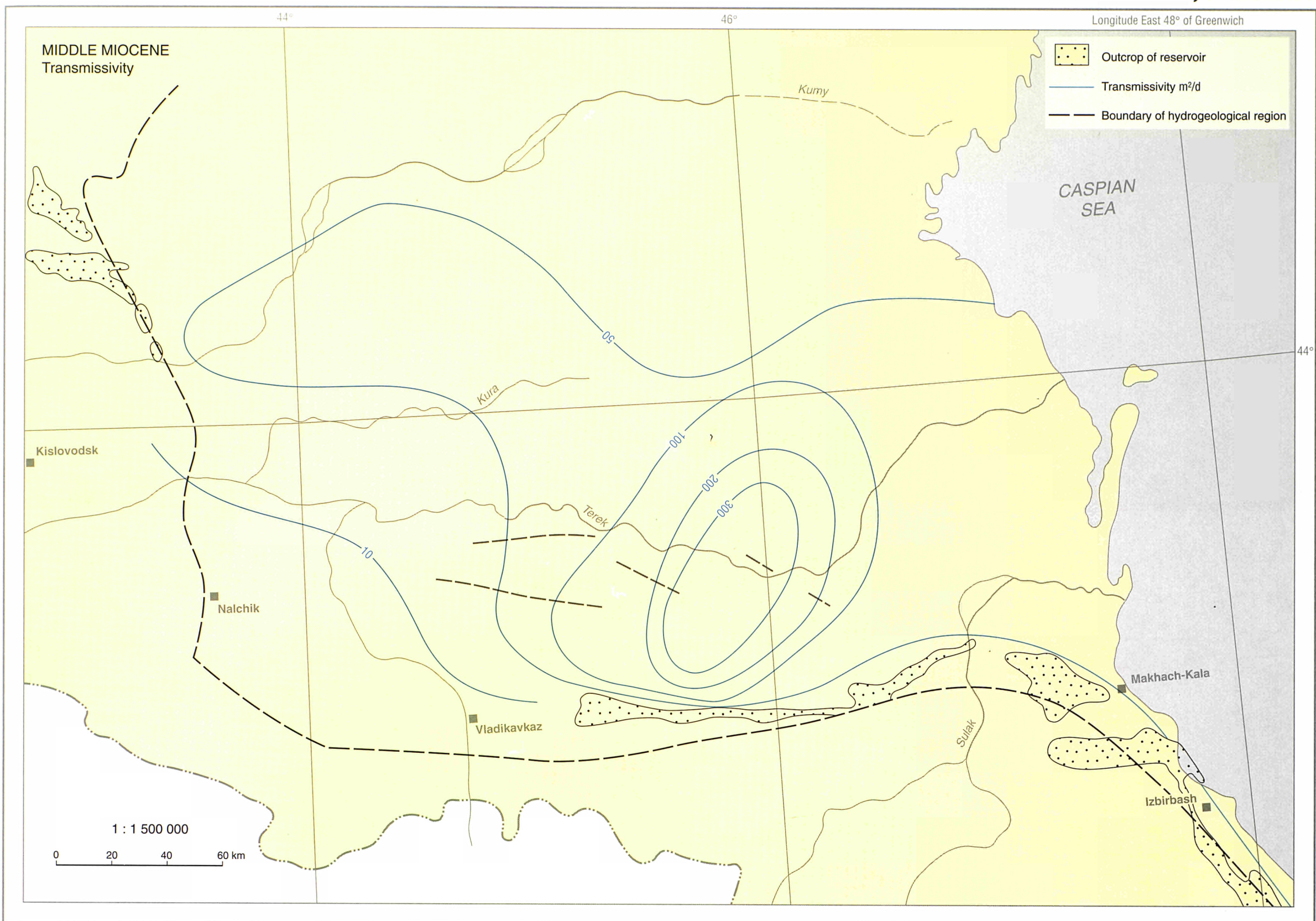




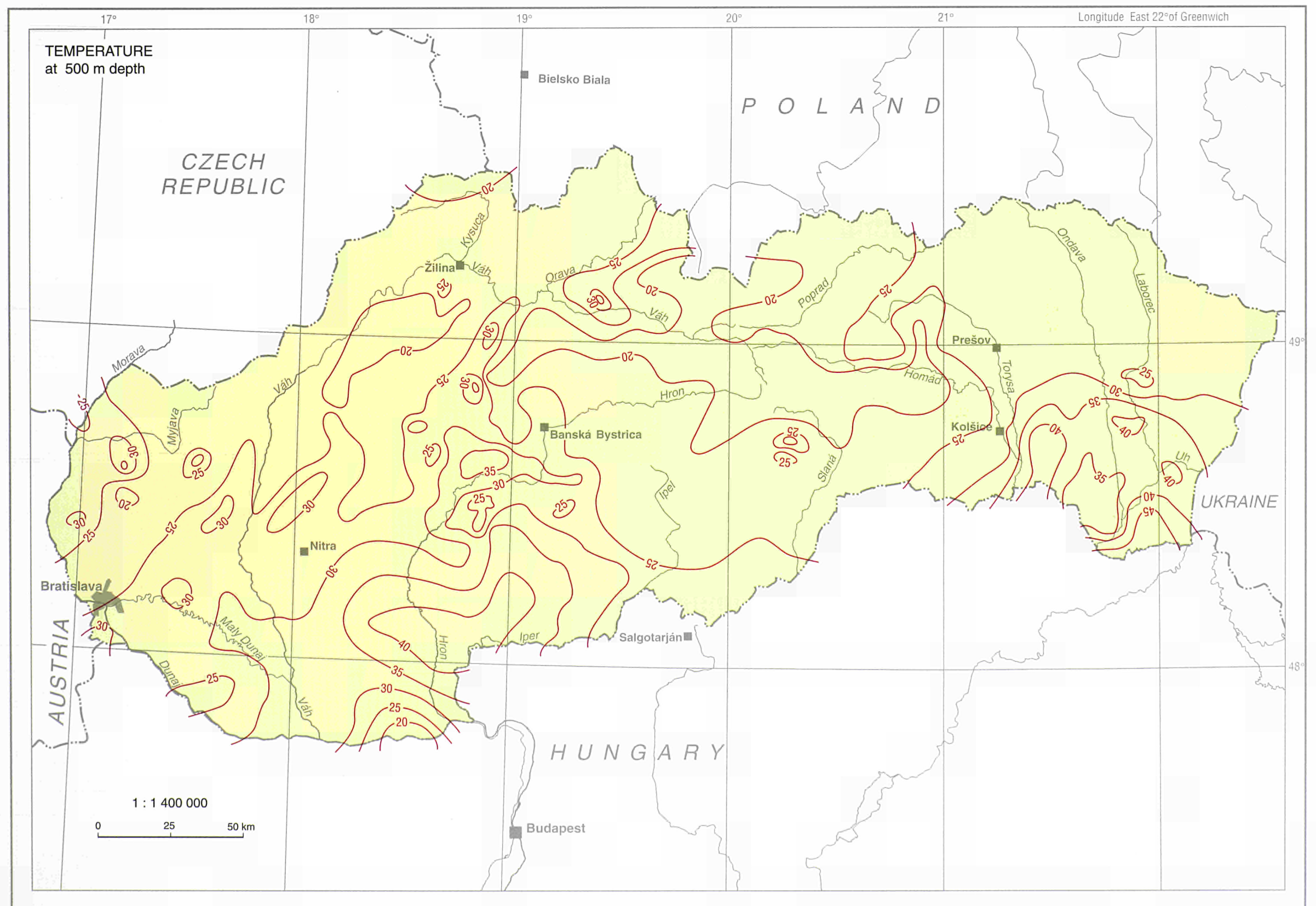
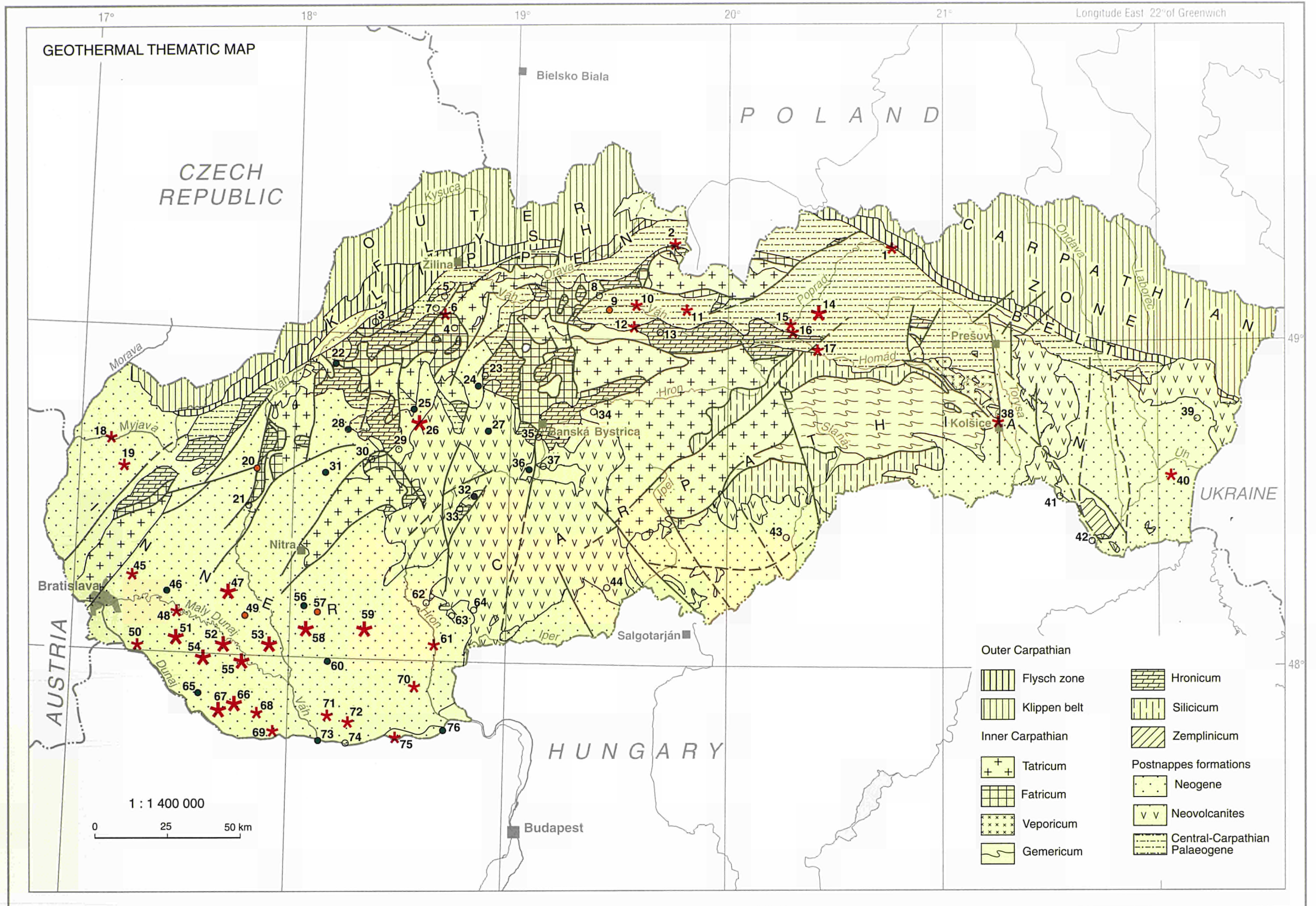
RUSSIA, East Fore-Caucasian Basin

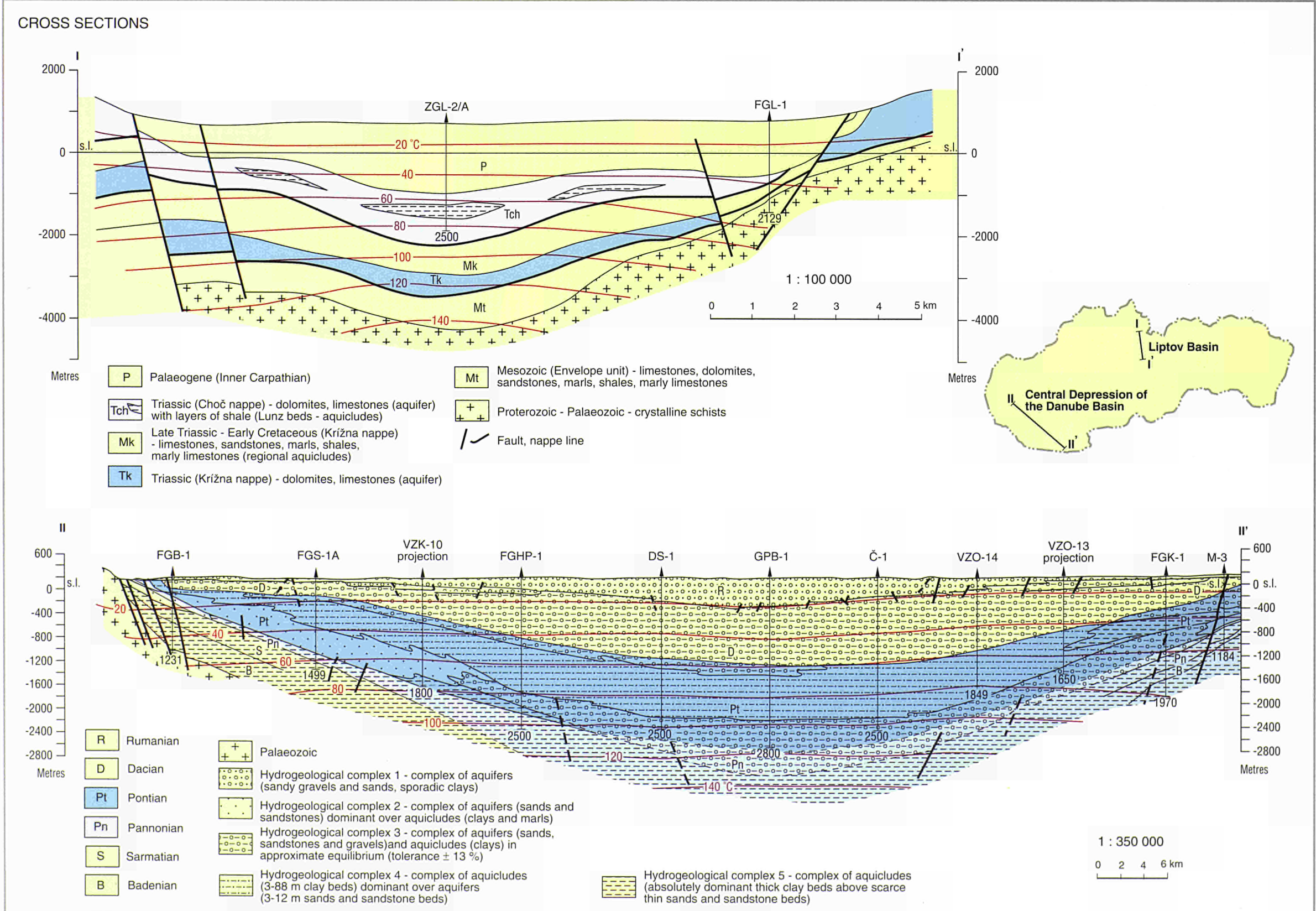
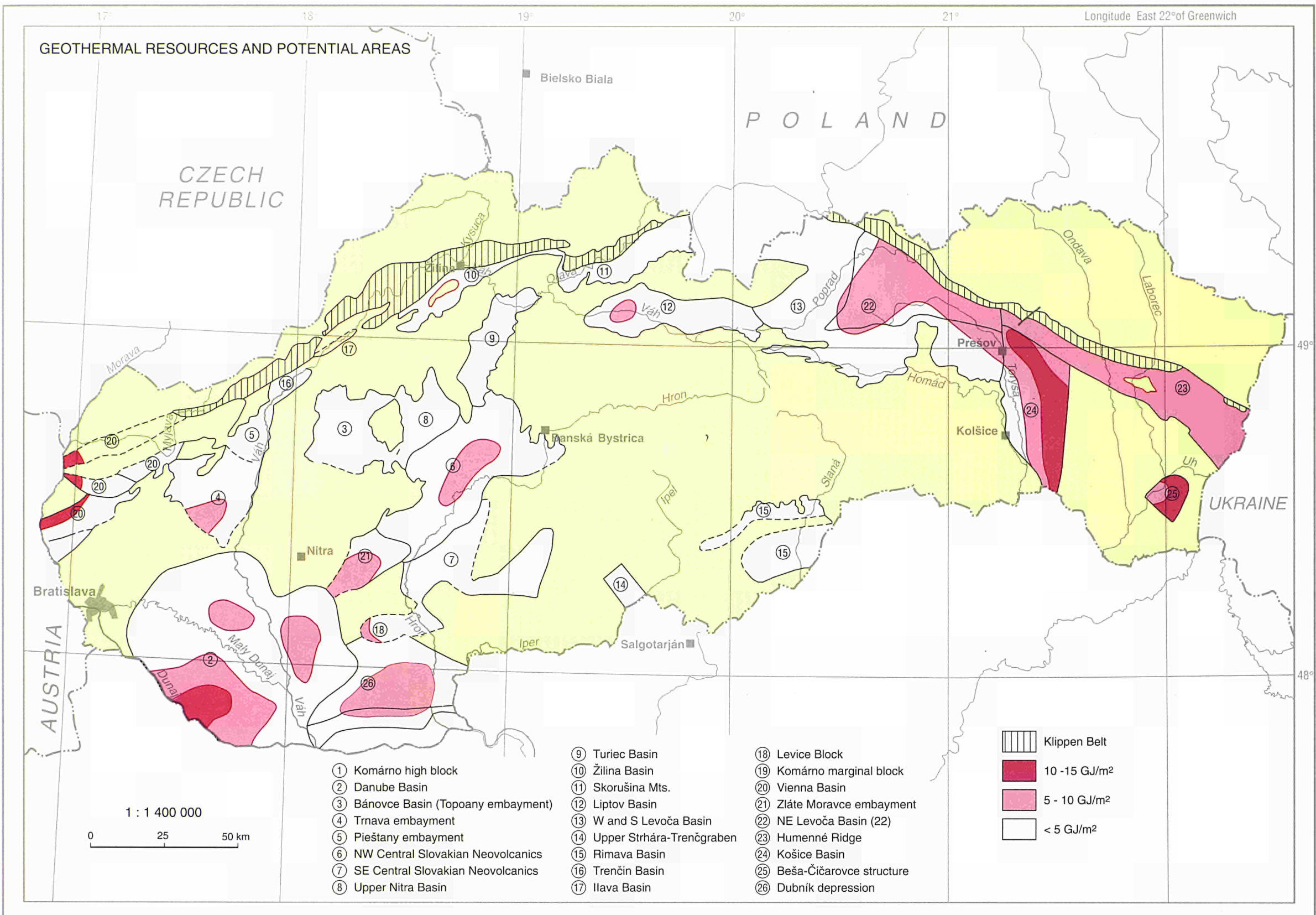


East Fore-Caucasian Basin, RUSSIA

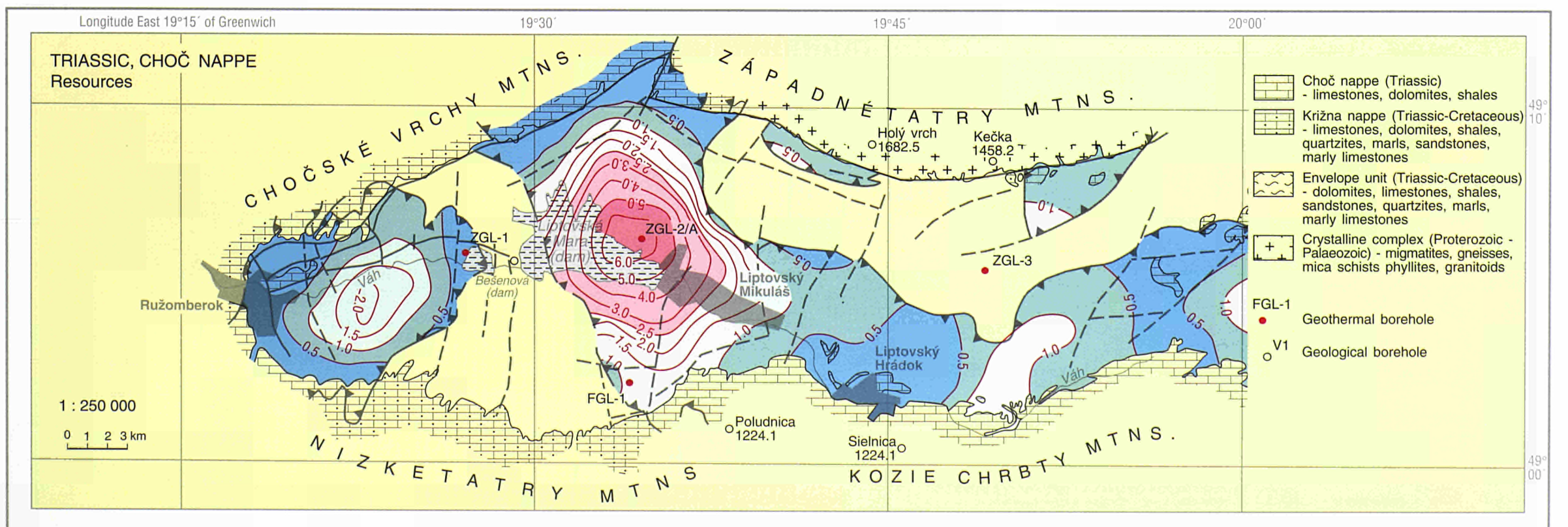
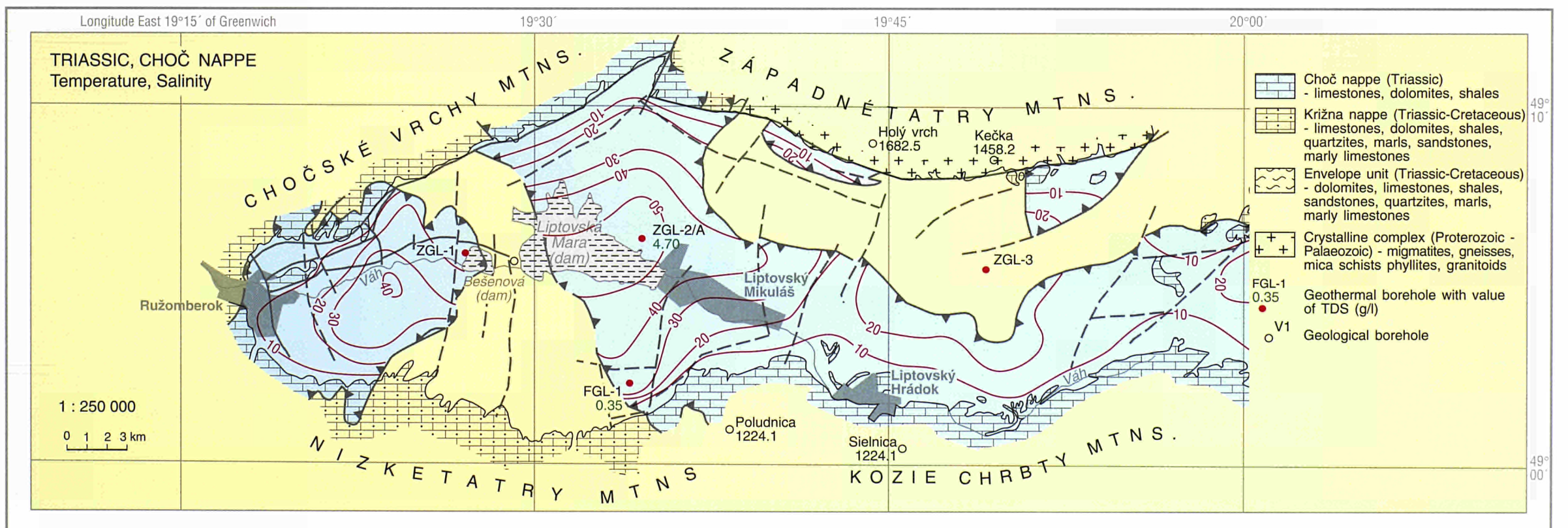
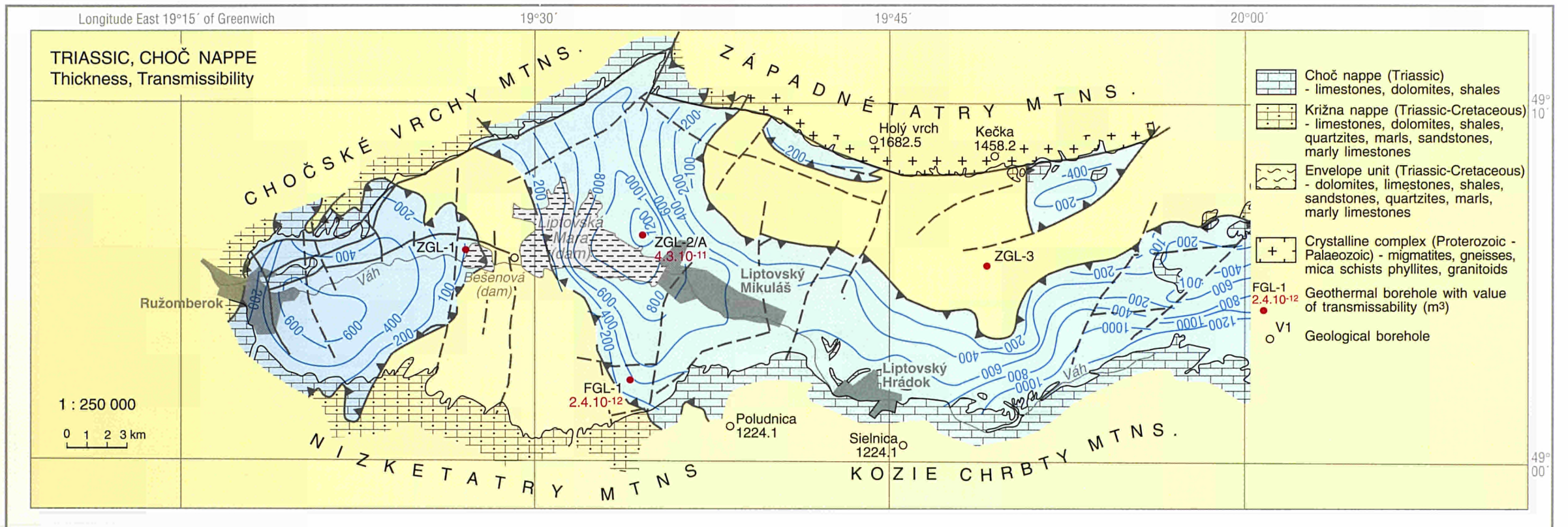
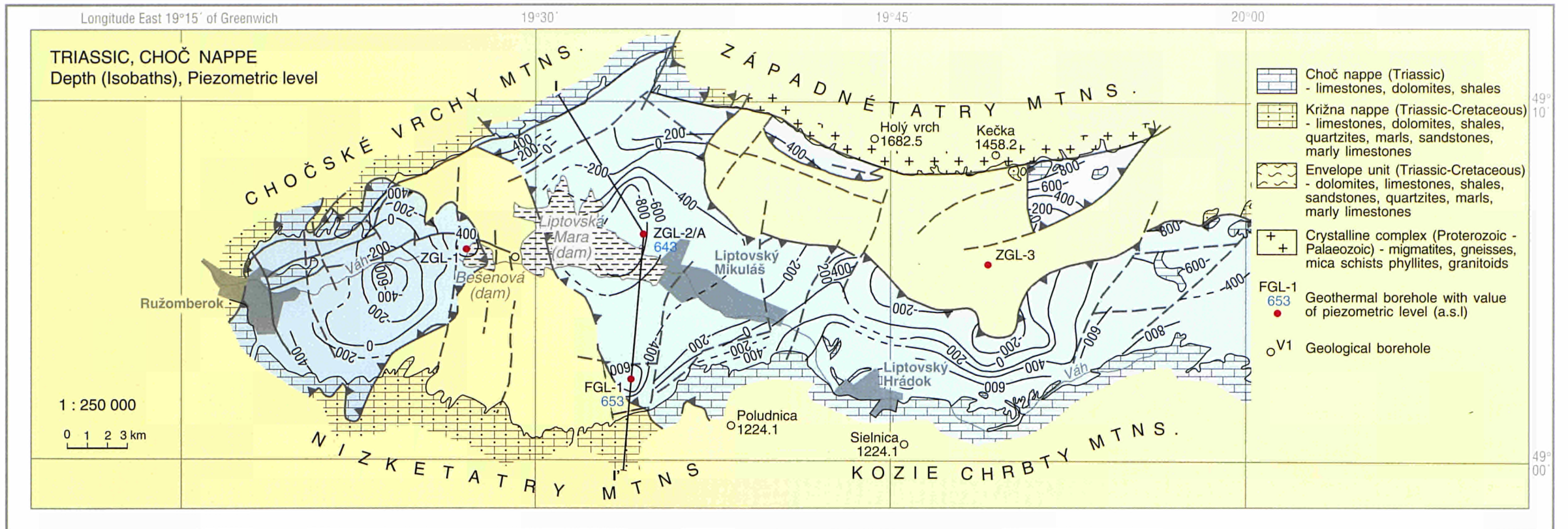


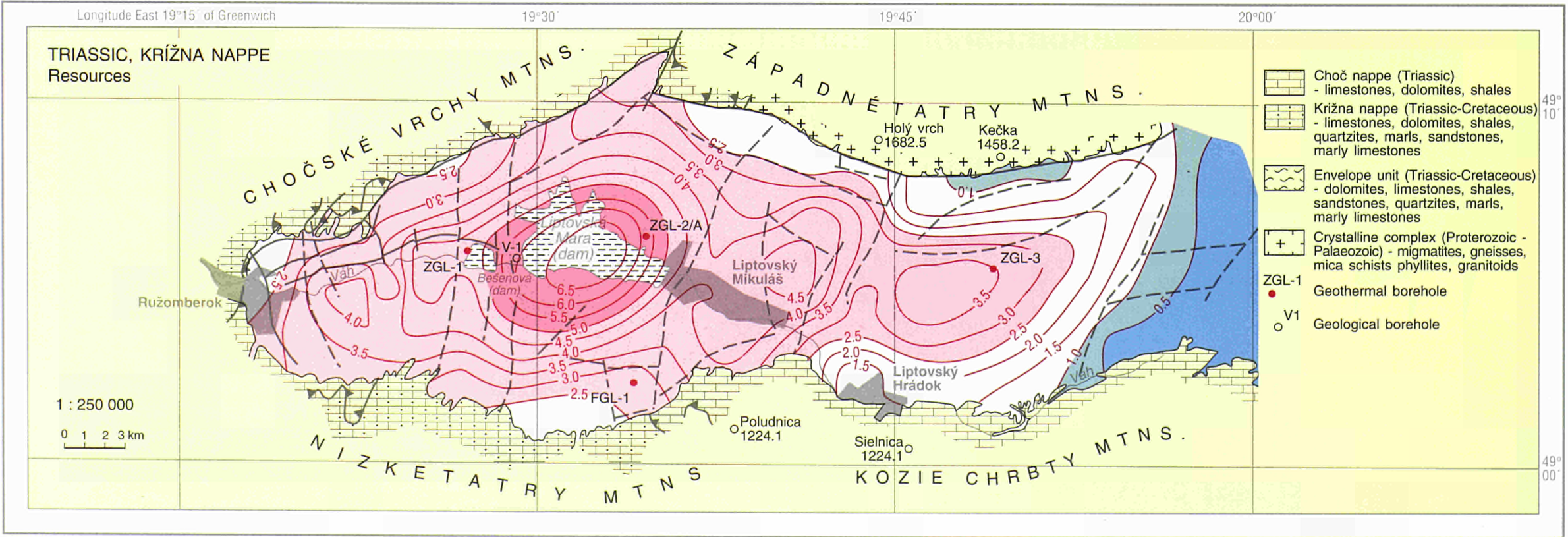
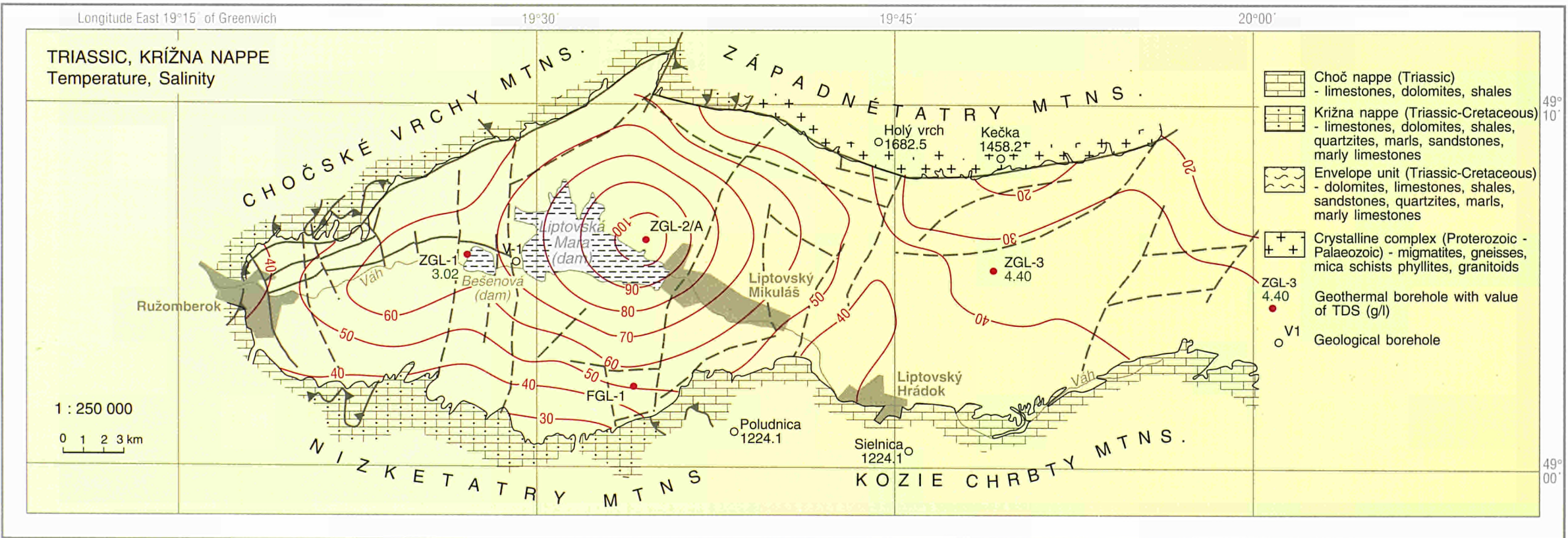
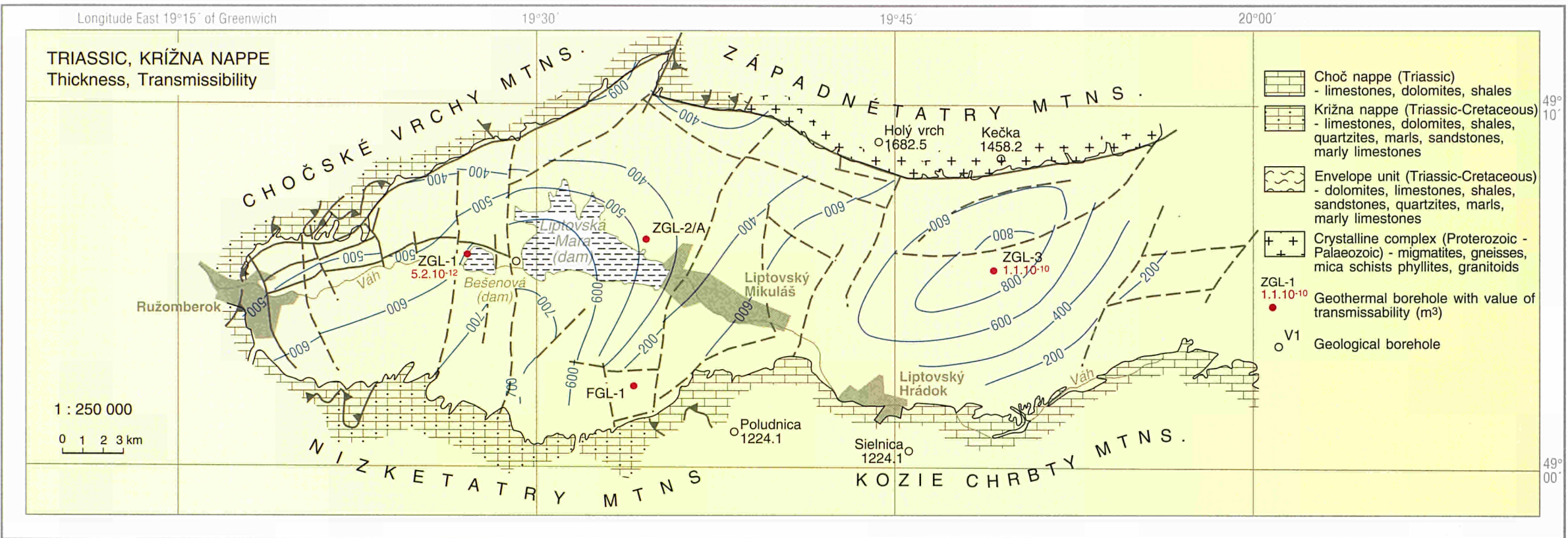
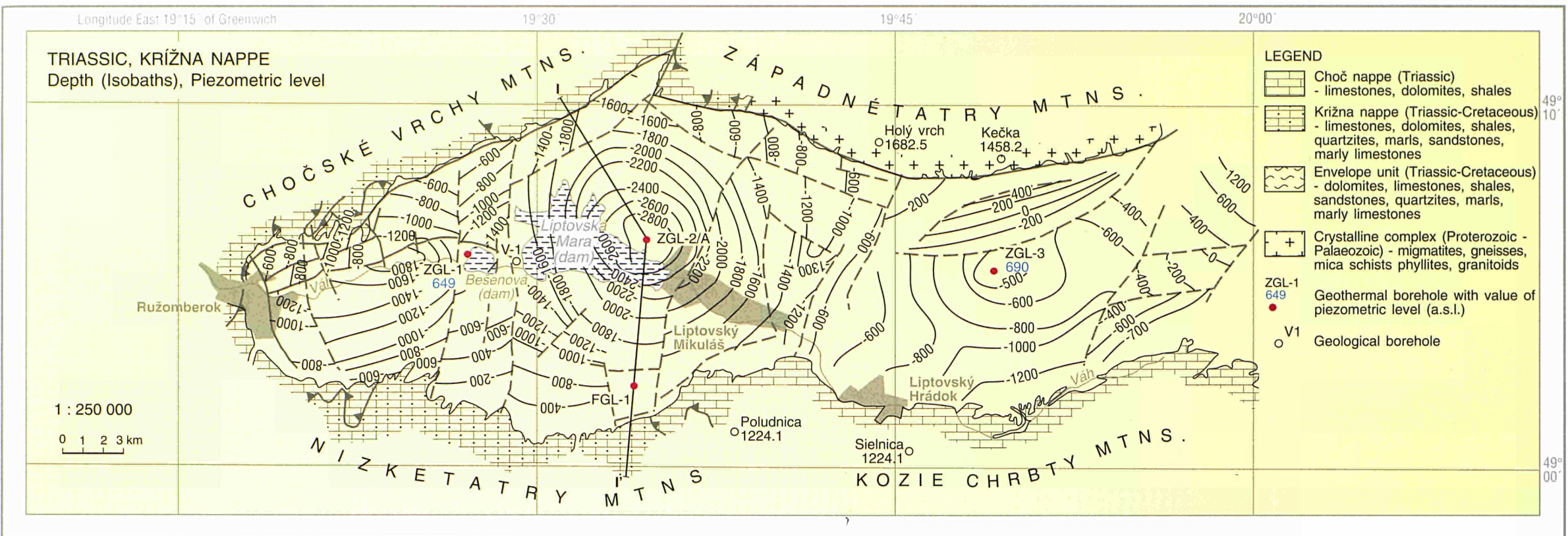
SLOVAKIA



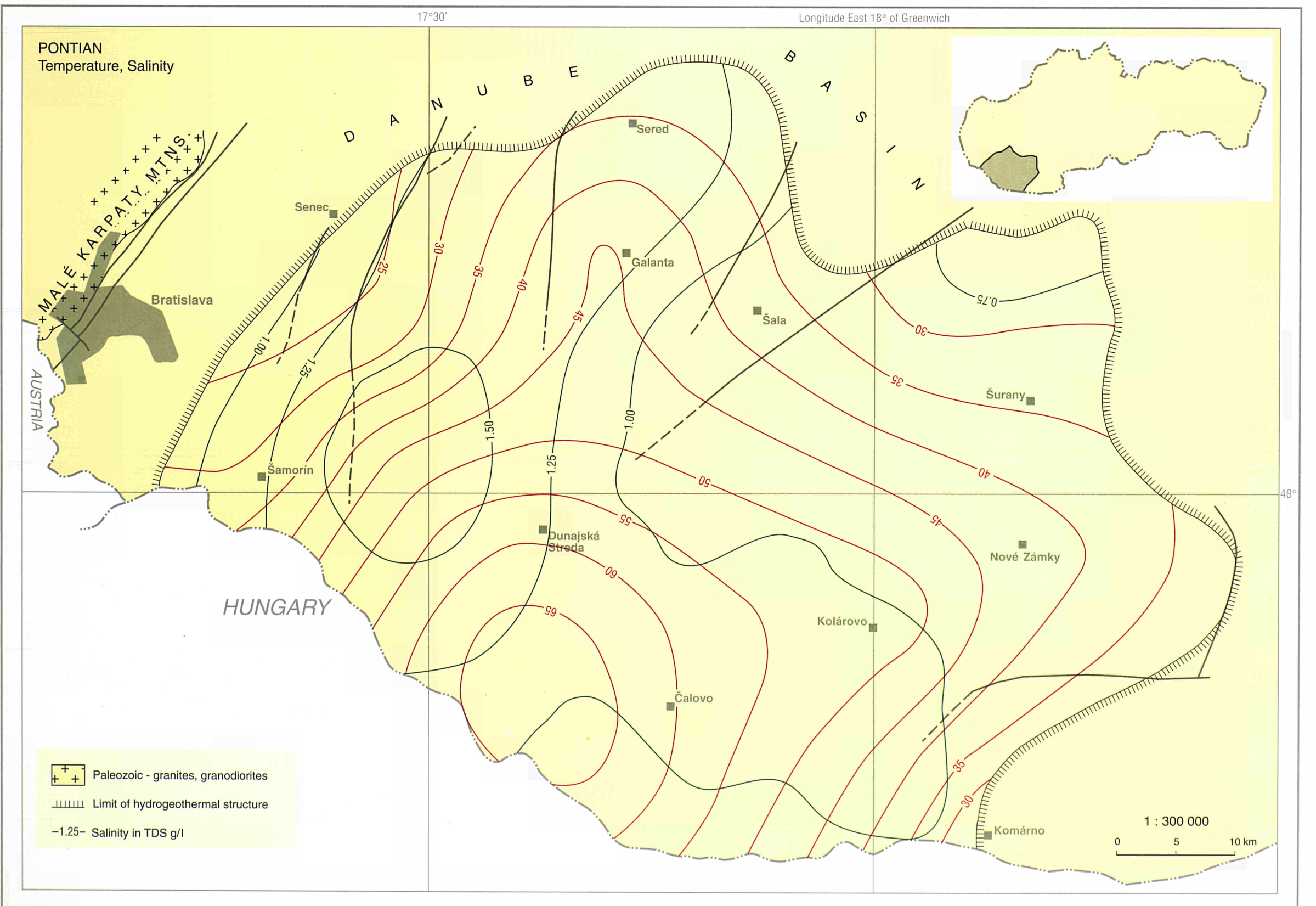
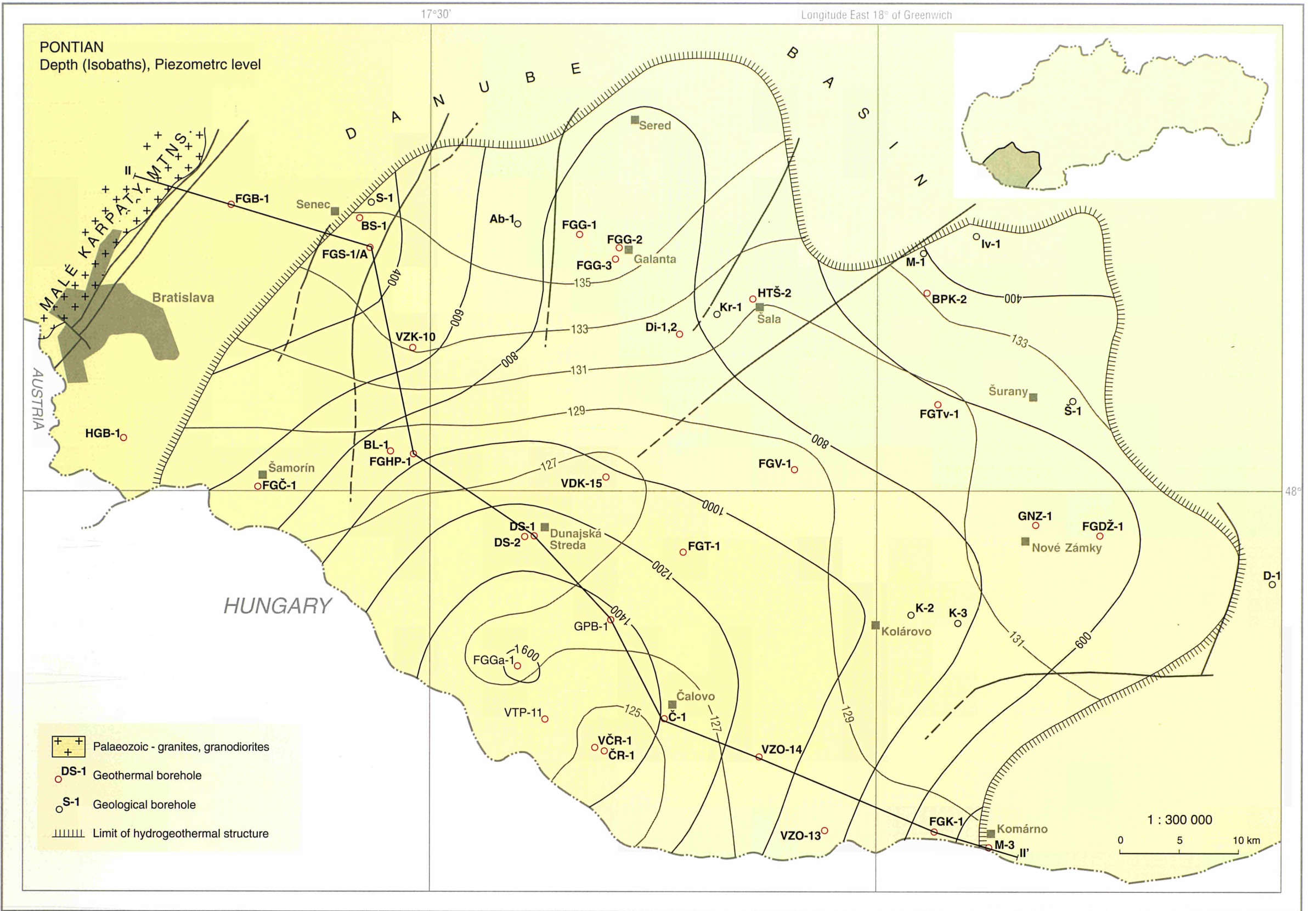


SLOVAKIA





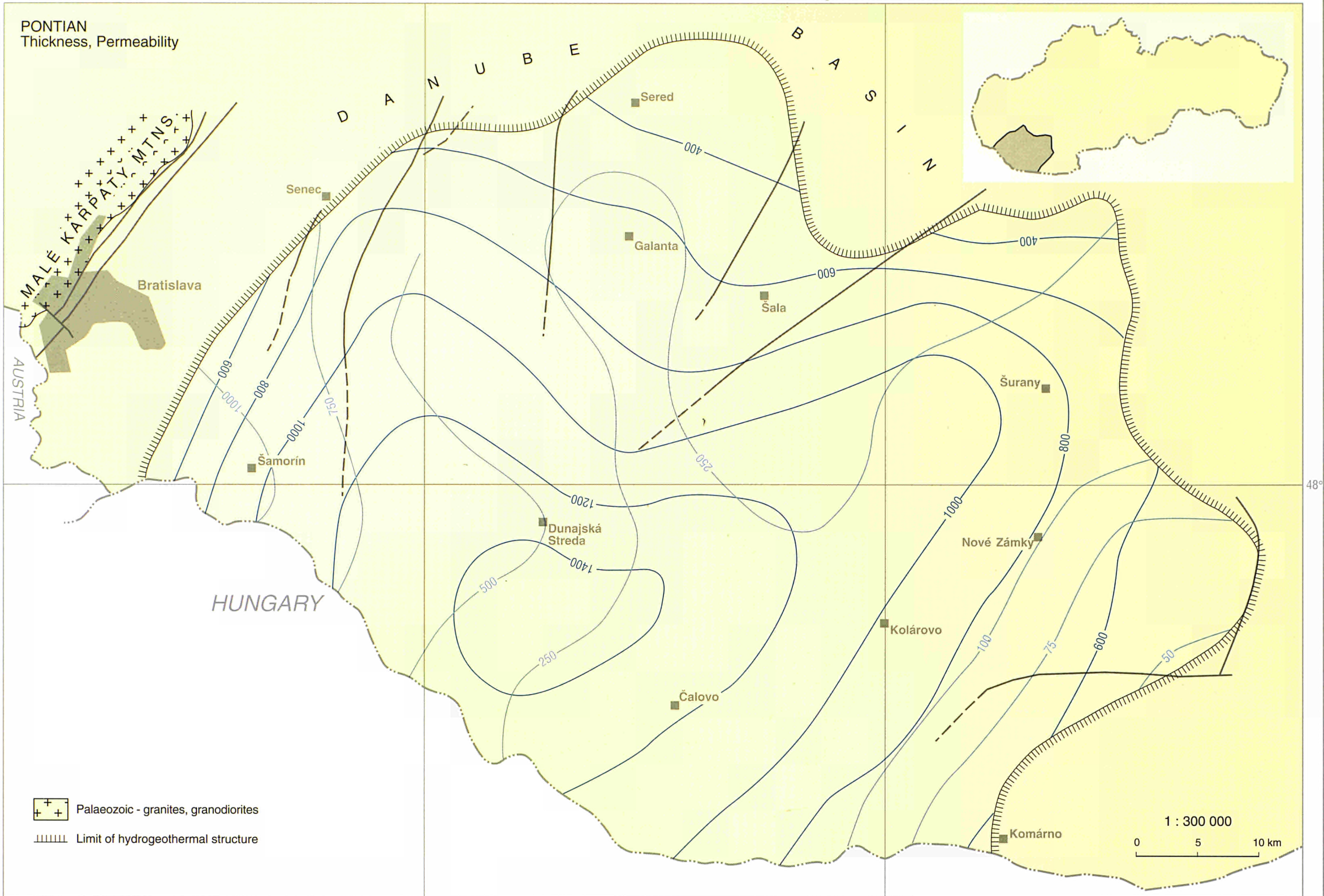
SLOVAKIA



17°30'

Longitude East 18° of Greenwich

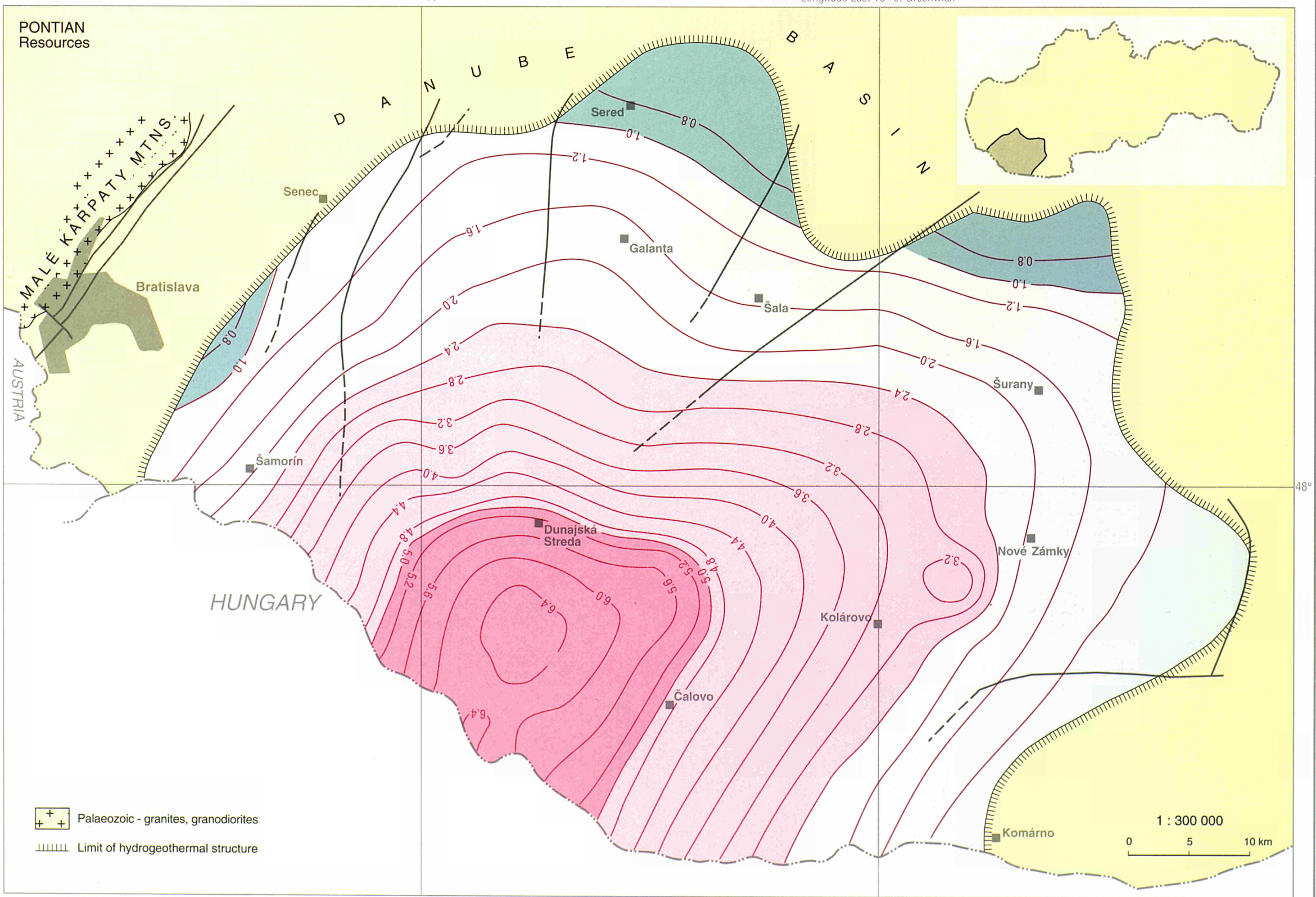
PONTIAN
Thickness, Permeability



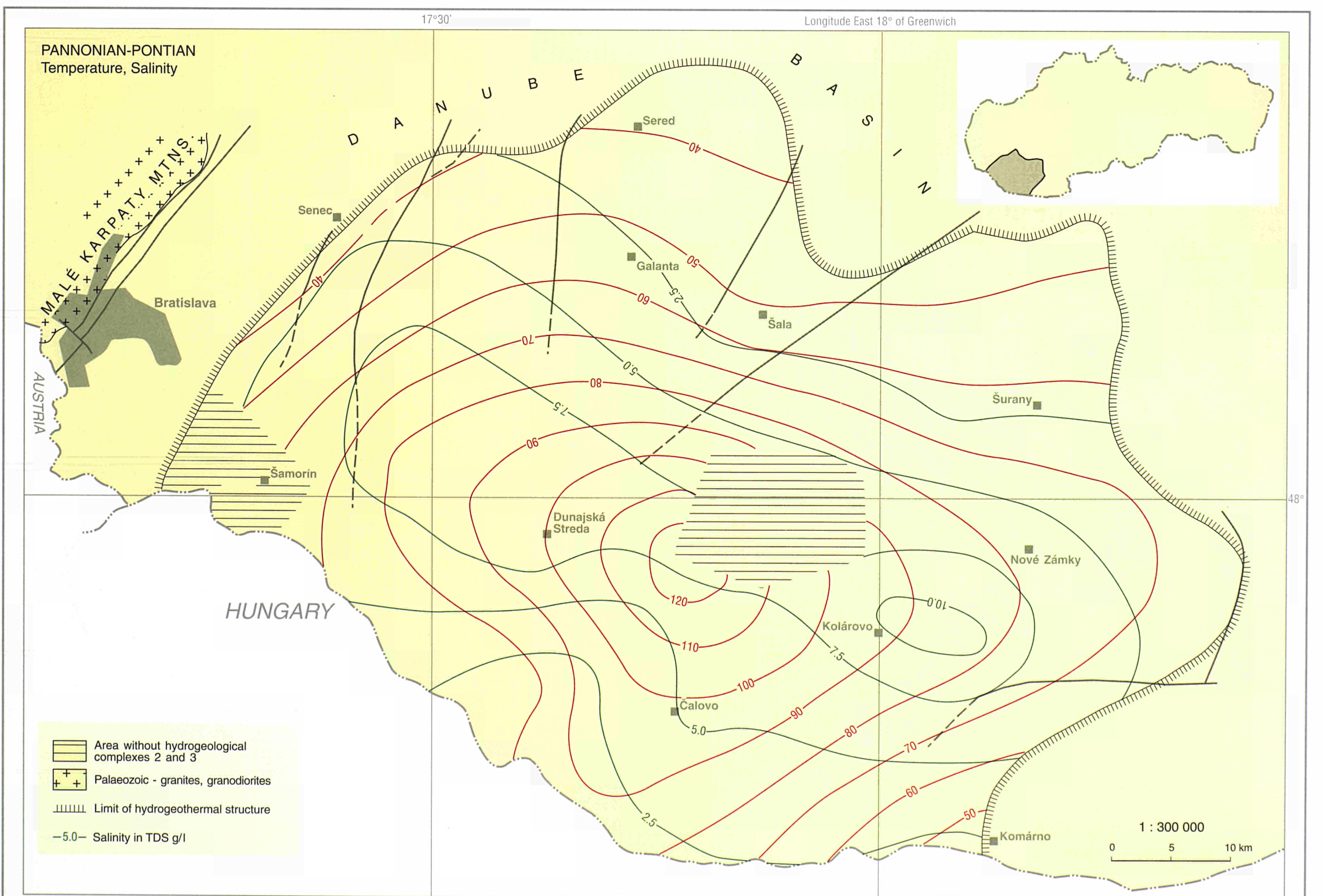
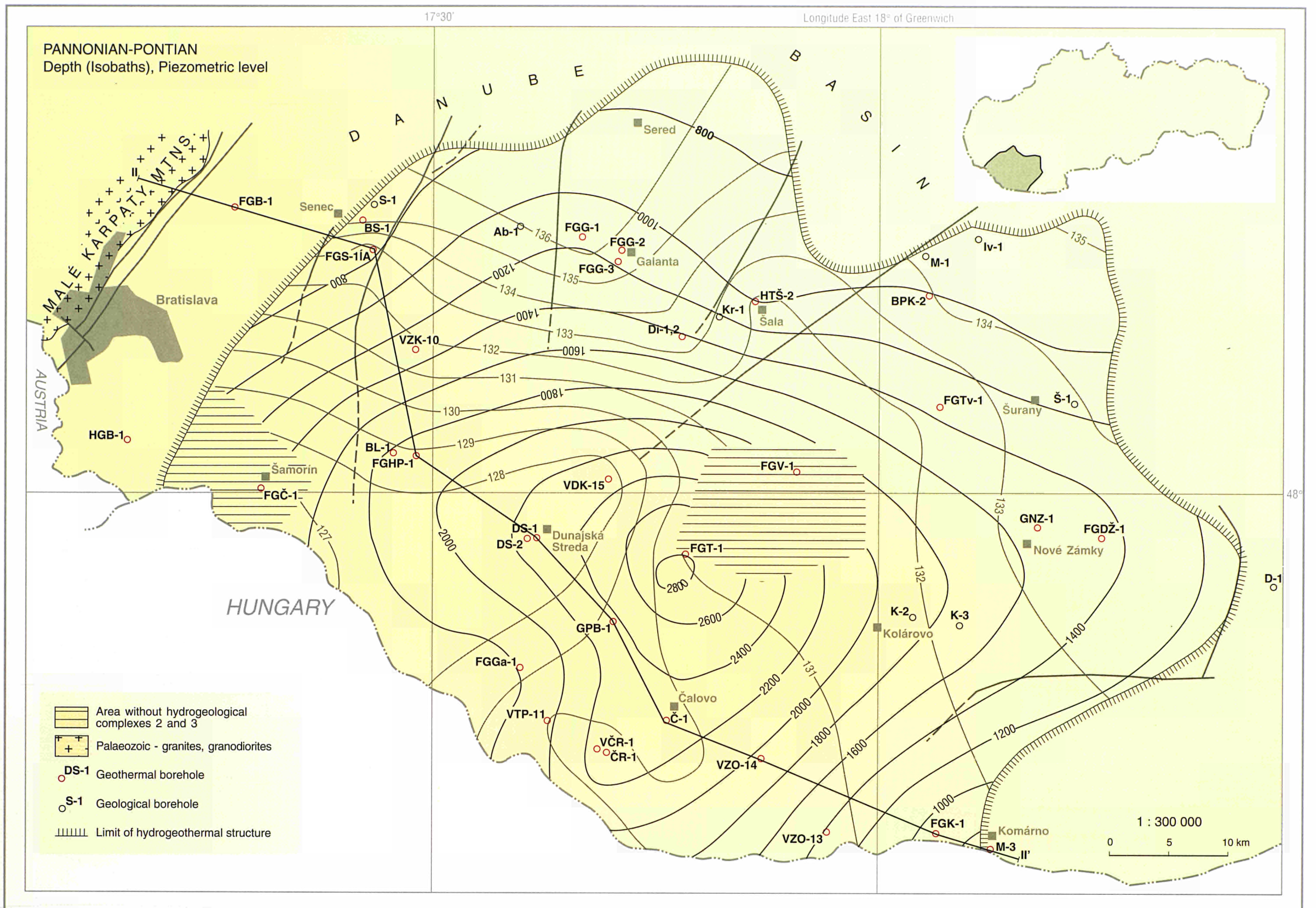
17°30'

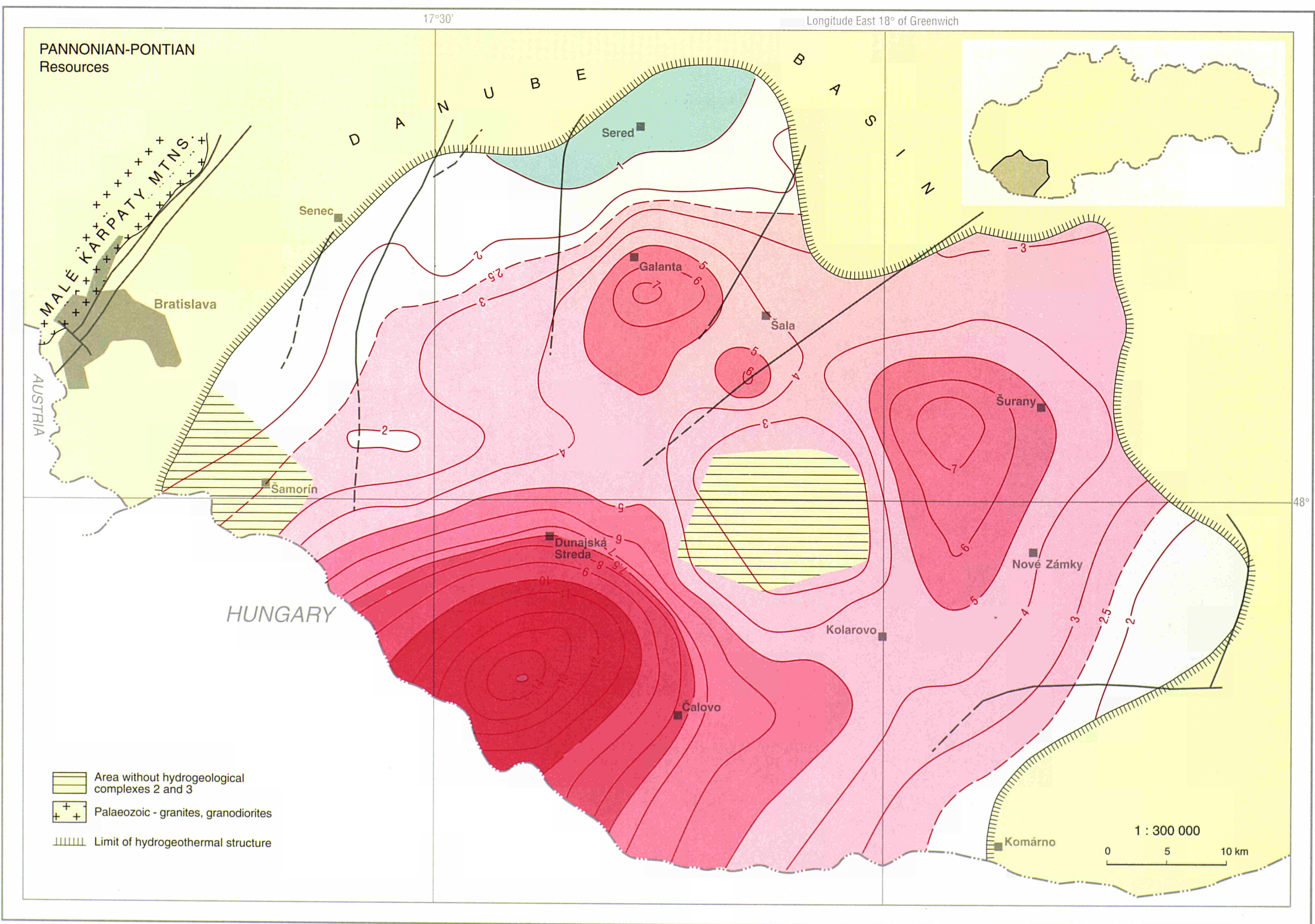
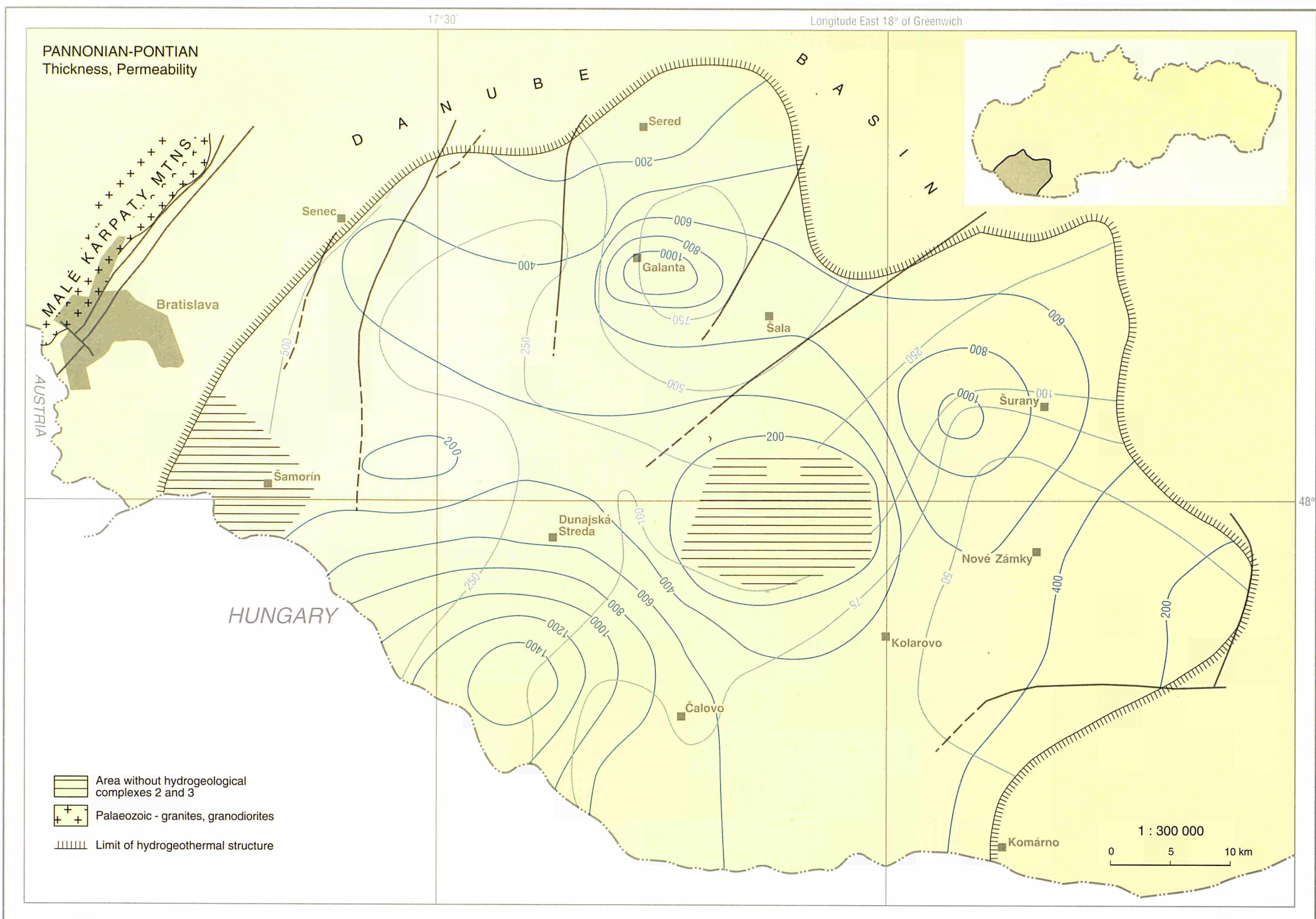
Longitude East 18° of Greenwich

PONTIAN
Resources

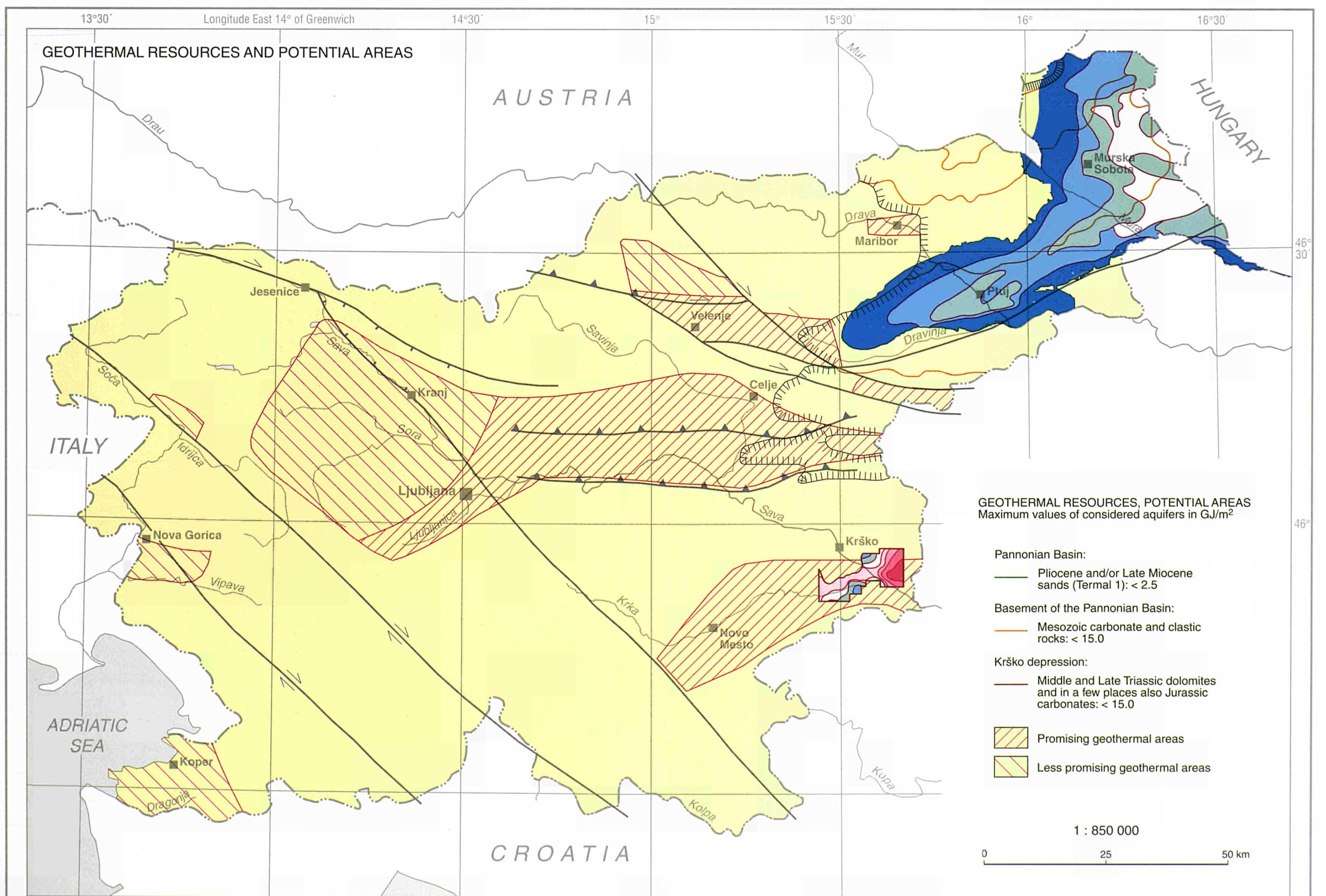
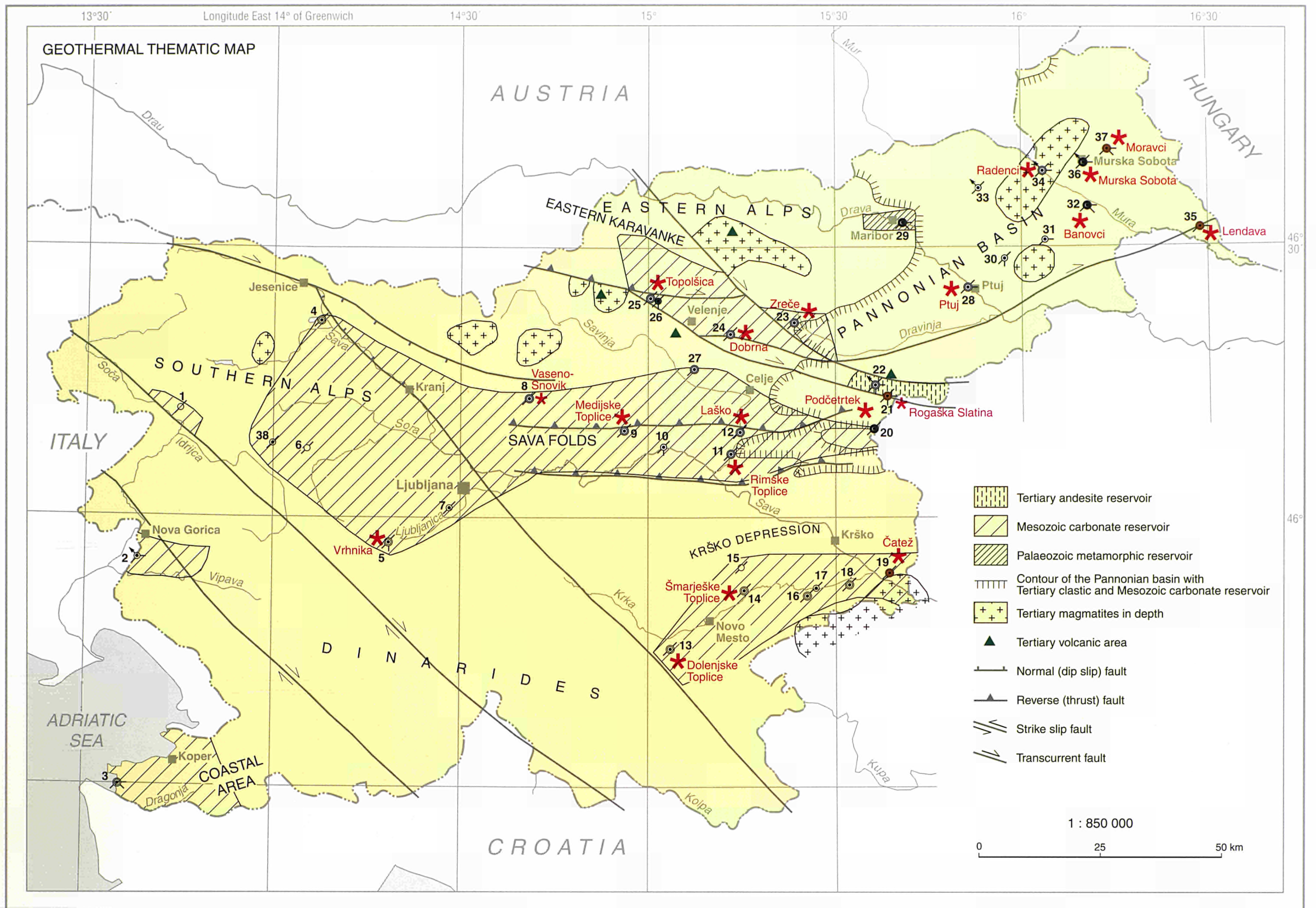


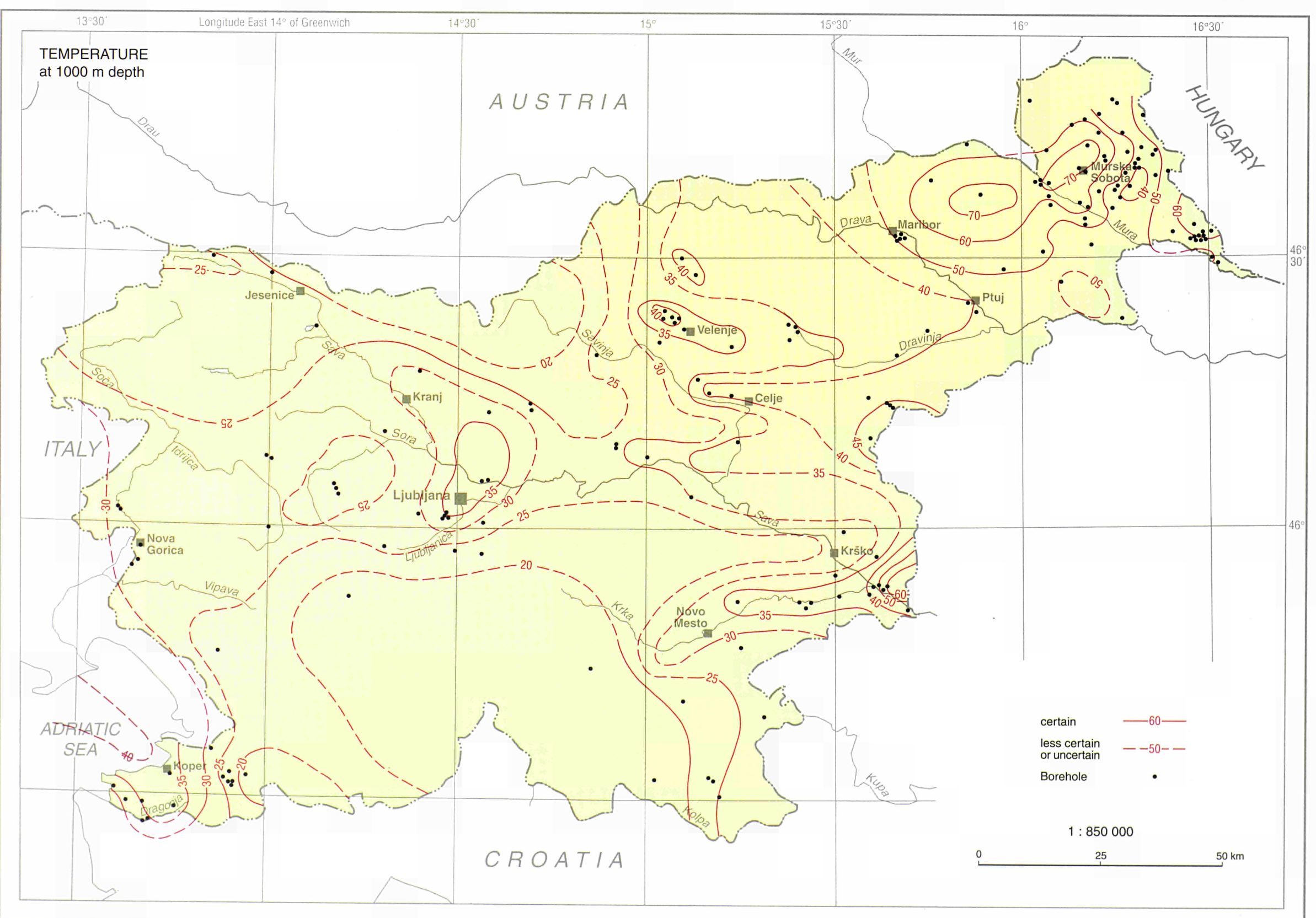
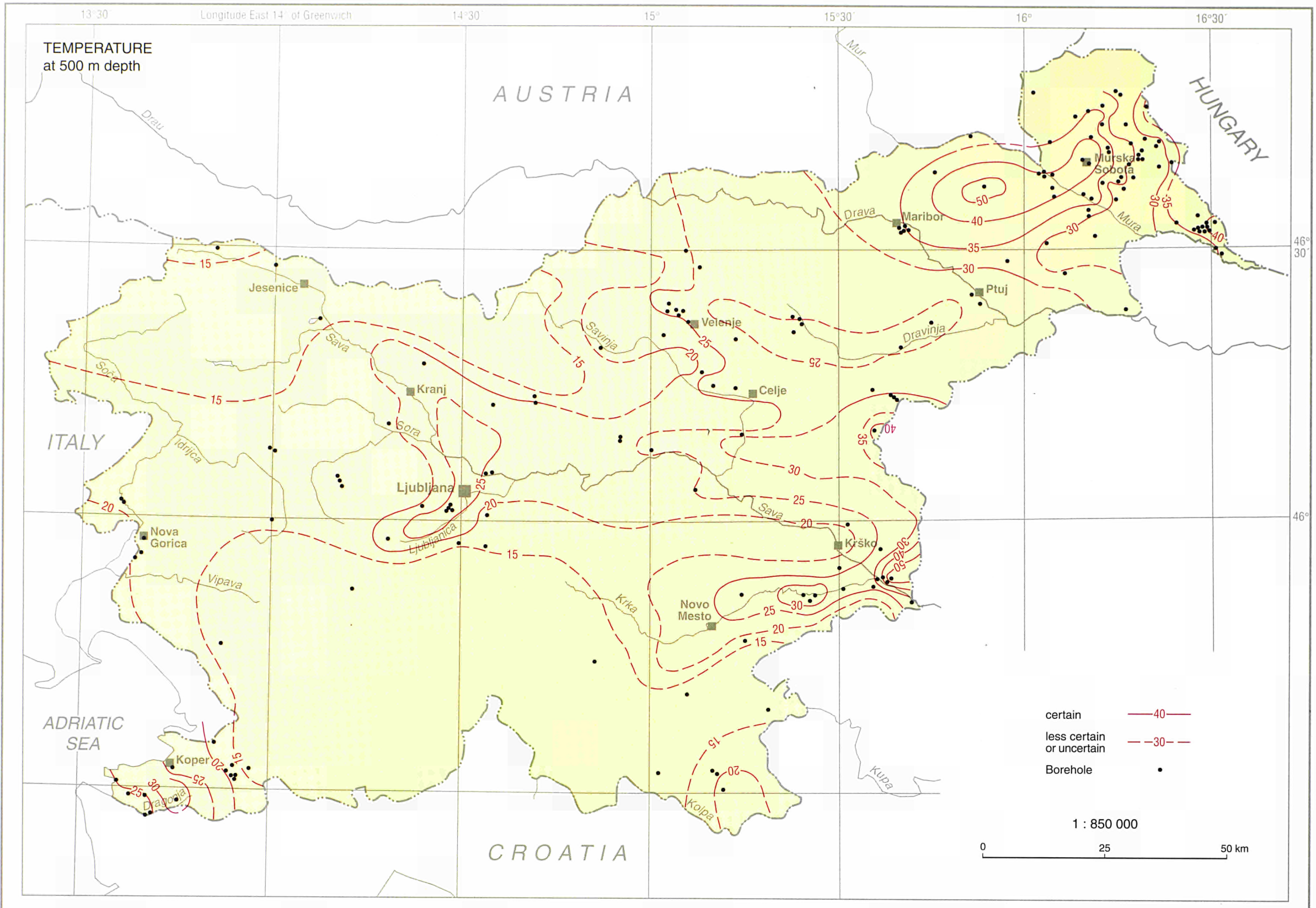
SLOVAKIA





SLOVENIA





SLOVENIA

Longitude 16° East of Greenwich

16°30'

PLIOCENE and/or LATE MIOCENE SANDS Depth (Isobaths)

- Borehole with at least one BHT or DST measurement and/or continuous temperature logging
- ▲ Oil, gasfield

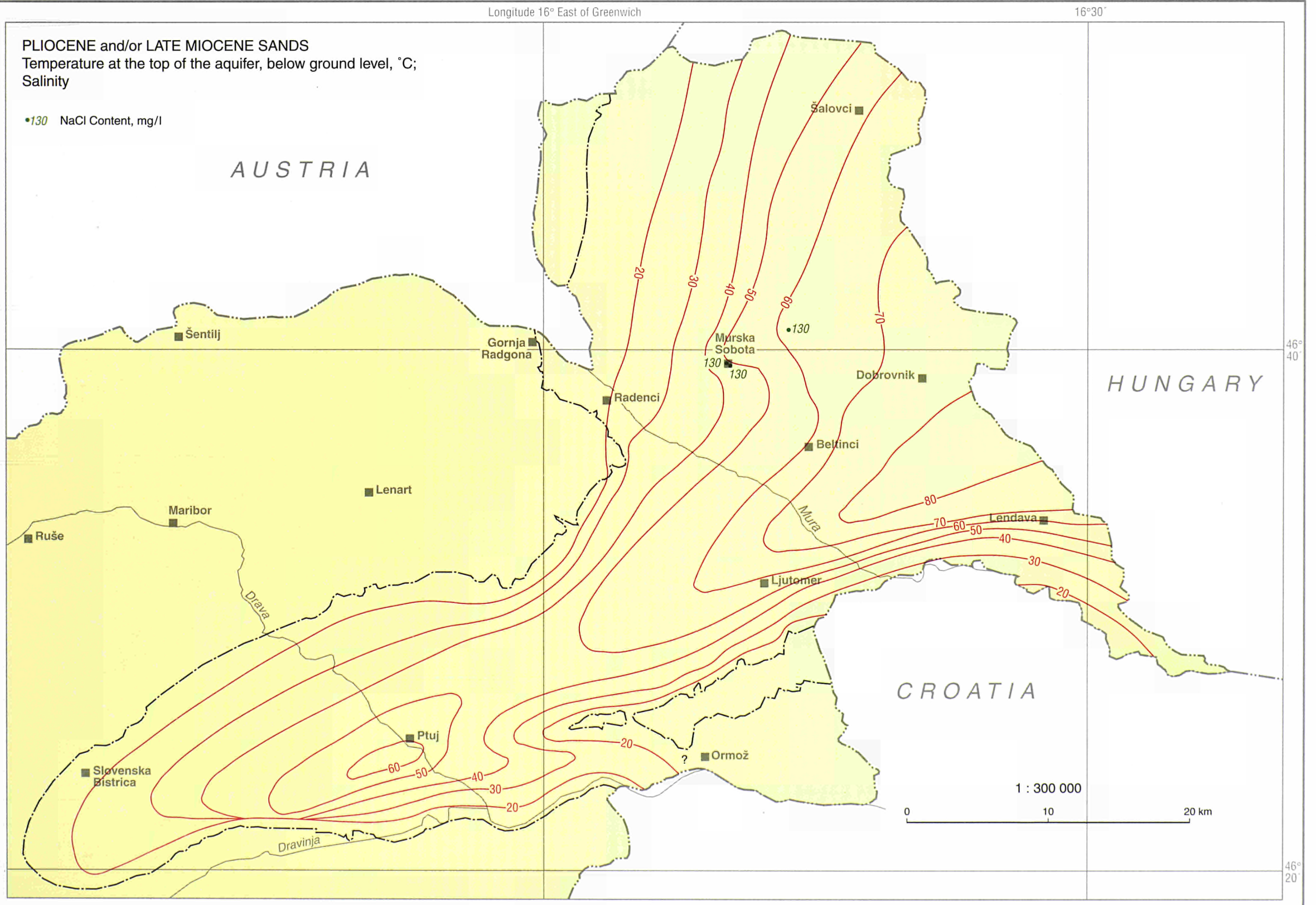


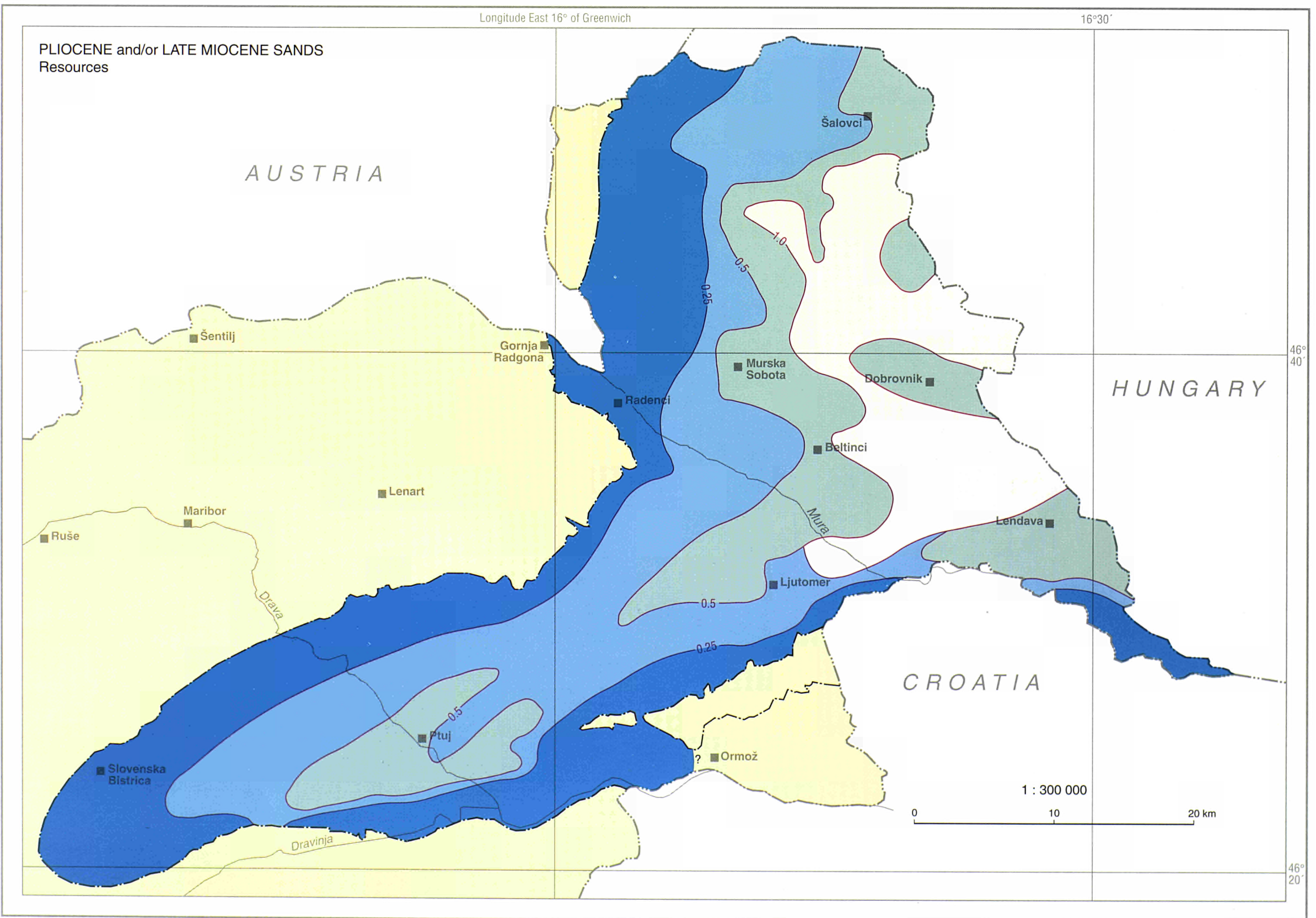
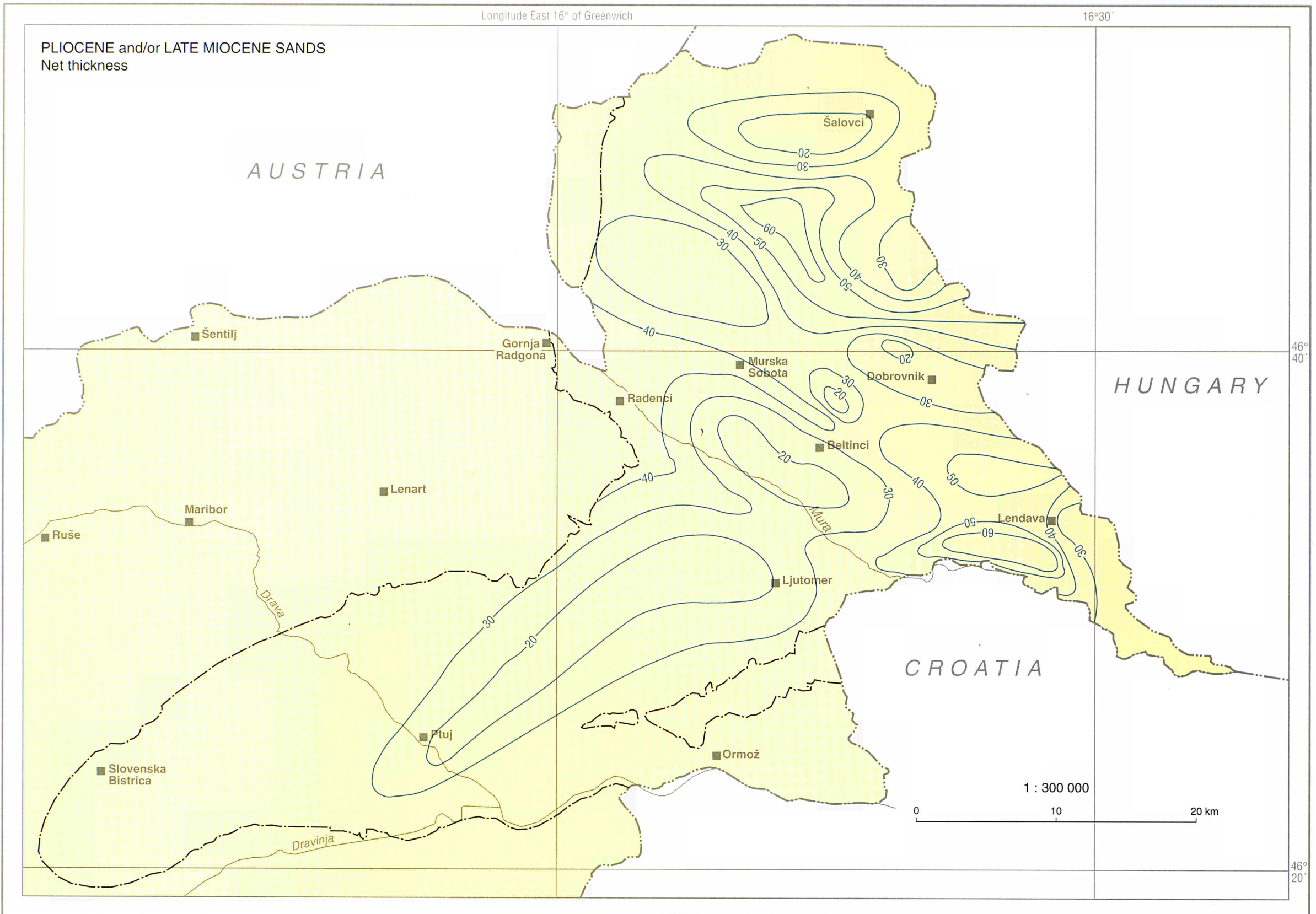
Longitude 16° East of Greenwich

16°30'

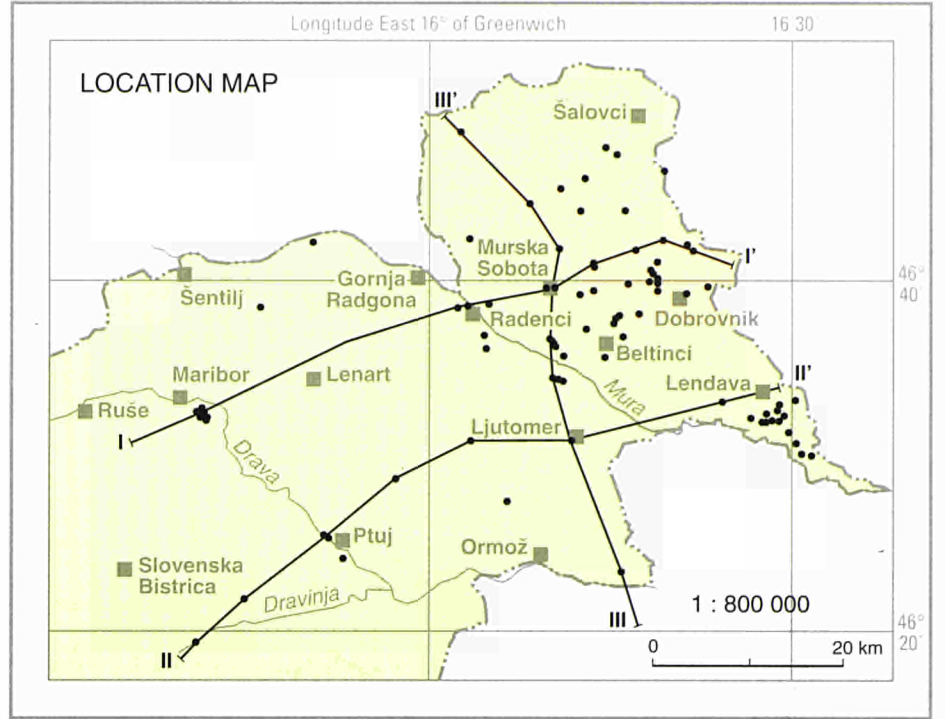
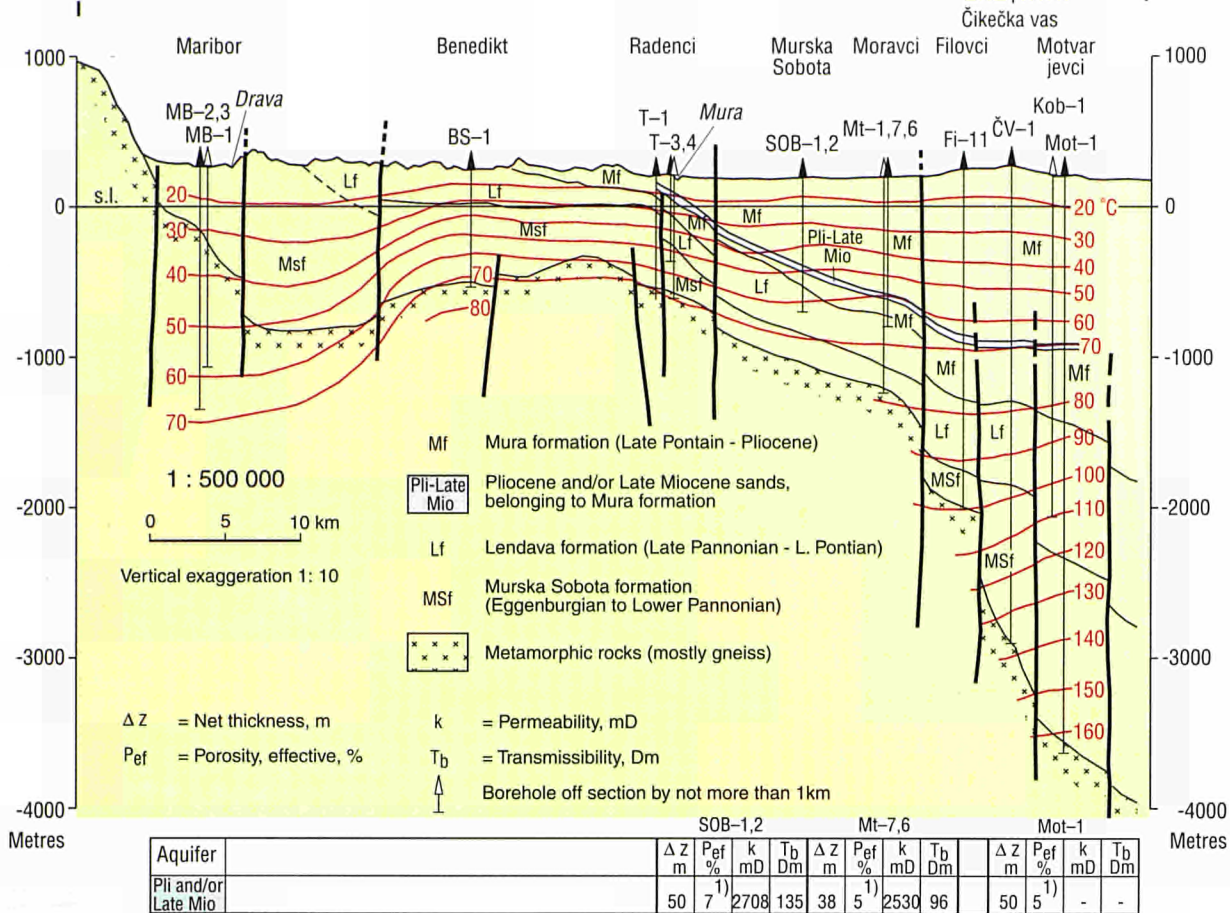
PLIOCENE and/or LATE MIOCENE SANDS Temperature at the top of the aquifer, below ground level, °C; Salinity

- 130 NaCl Content, mg/l

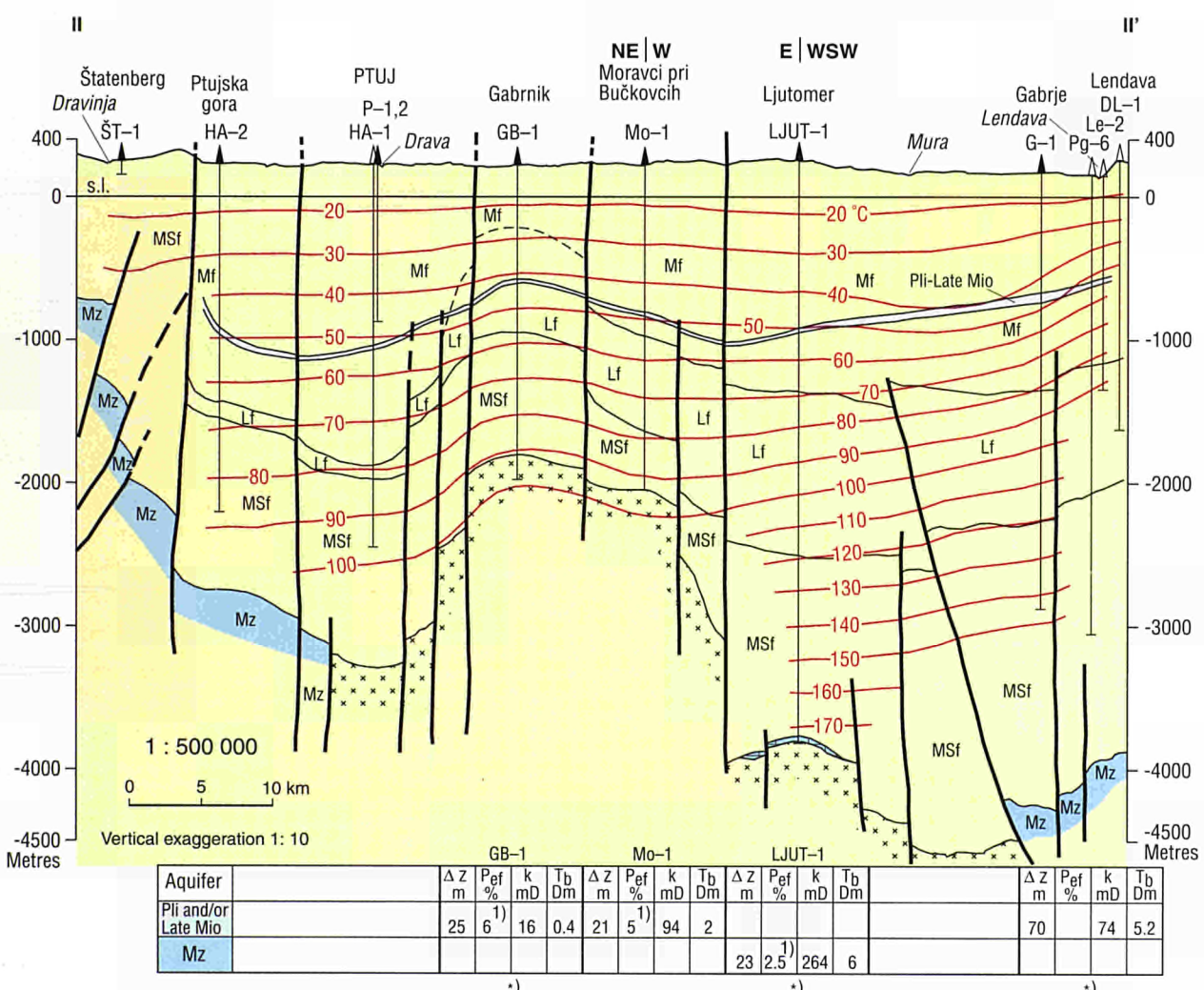
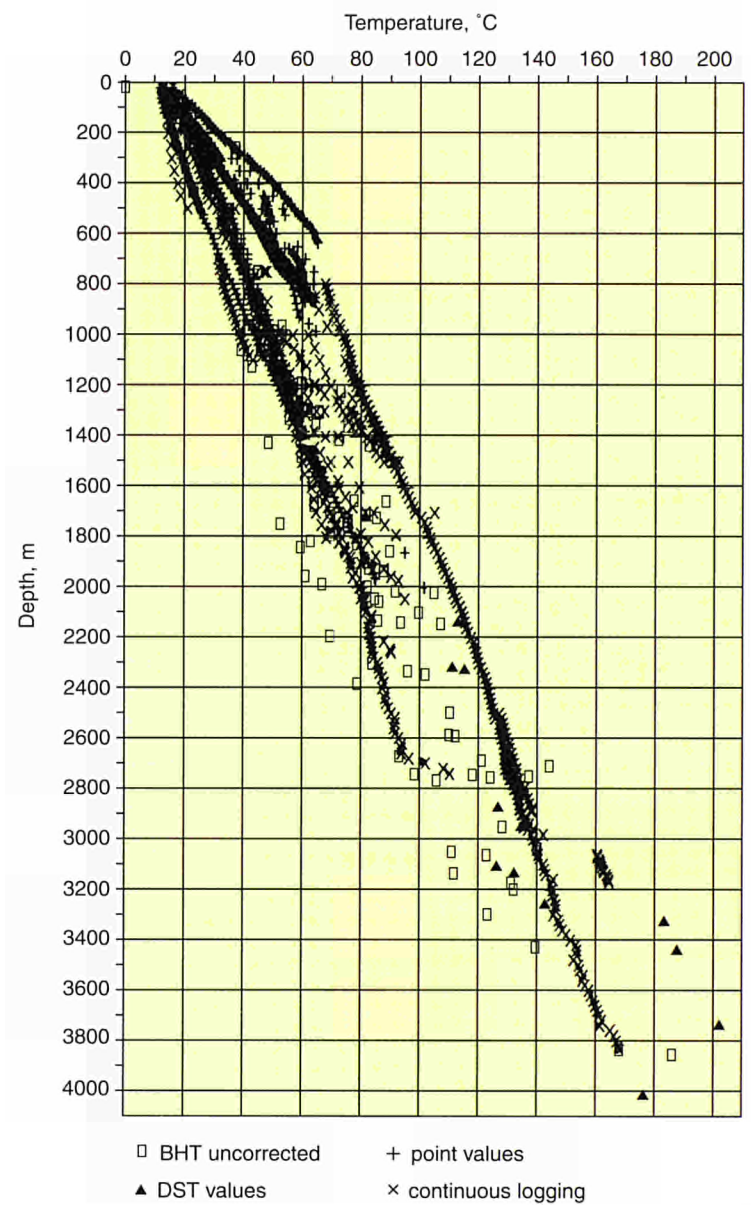




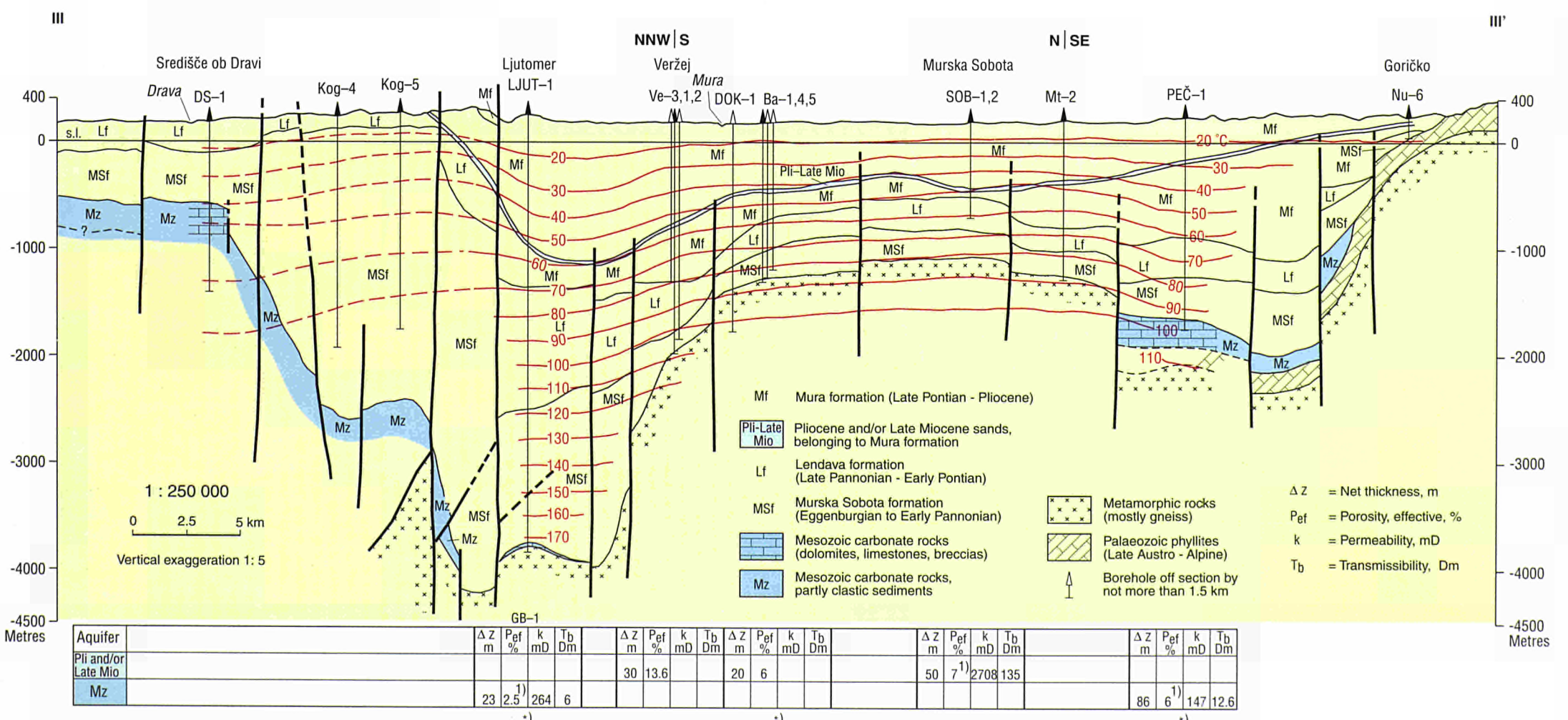
CROSS SECTIONS



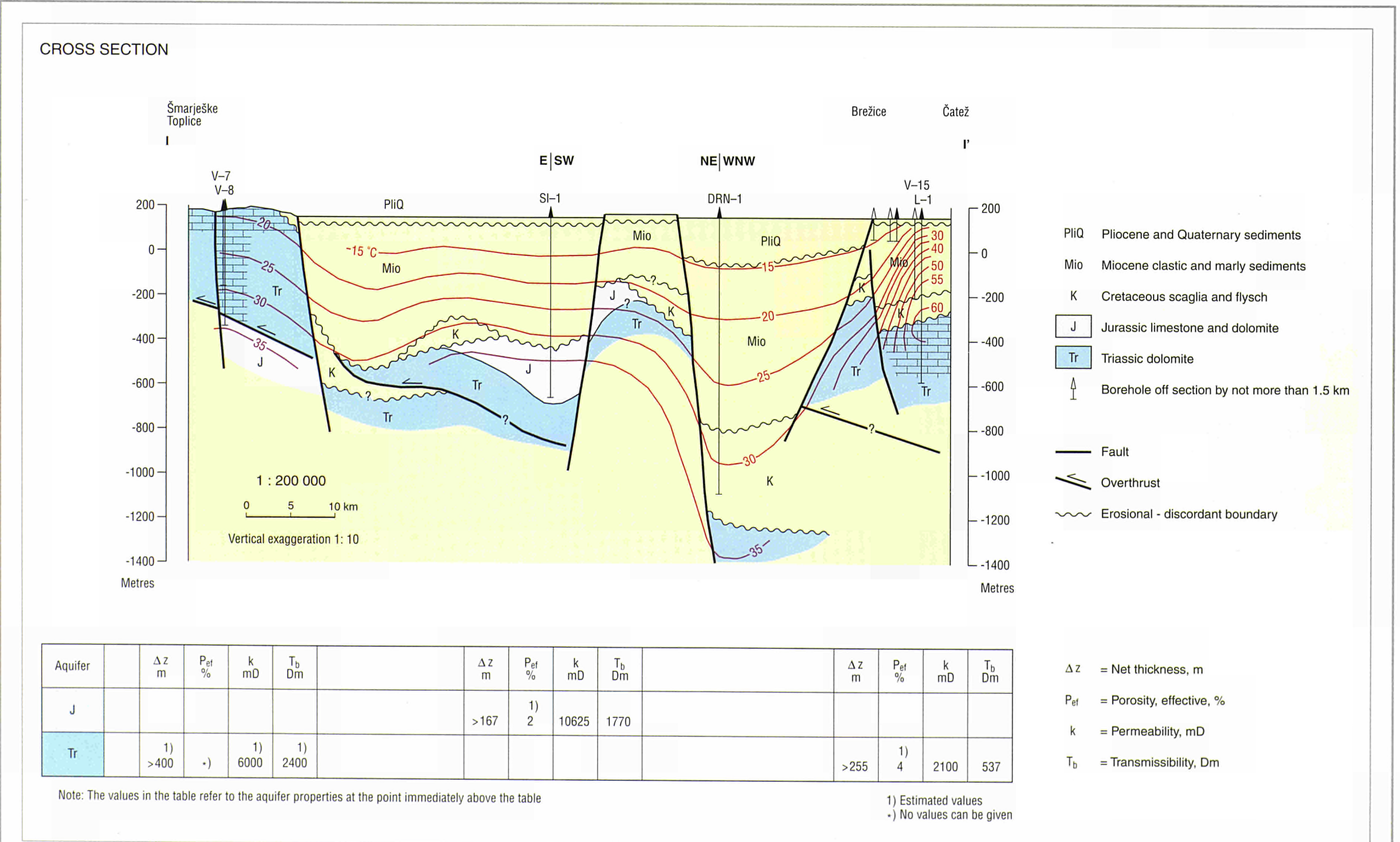
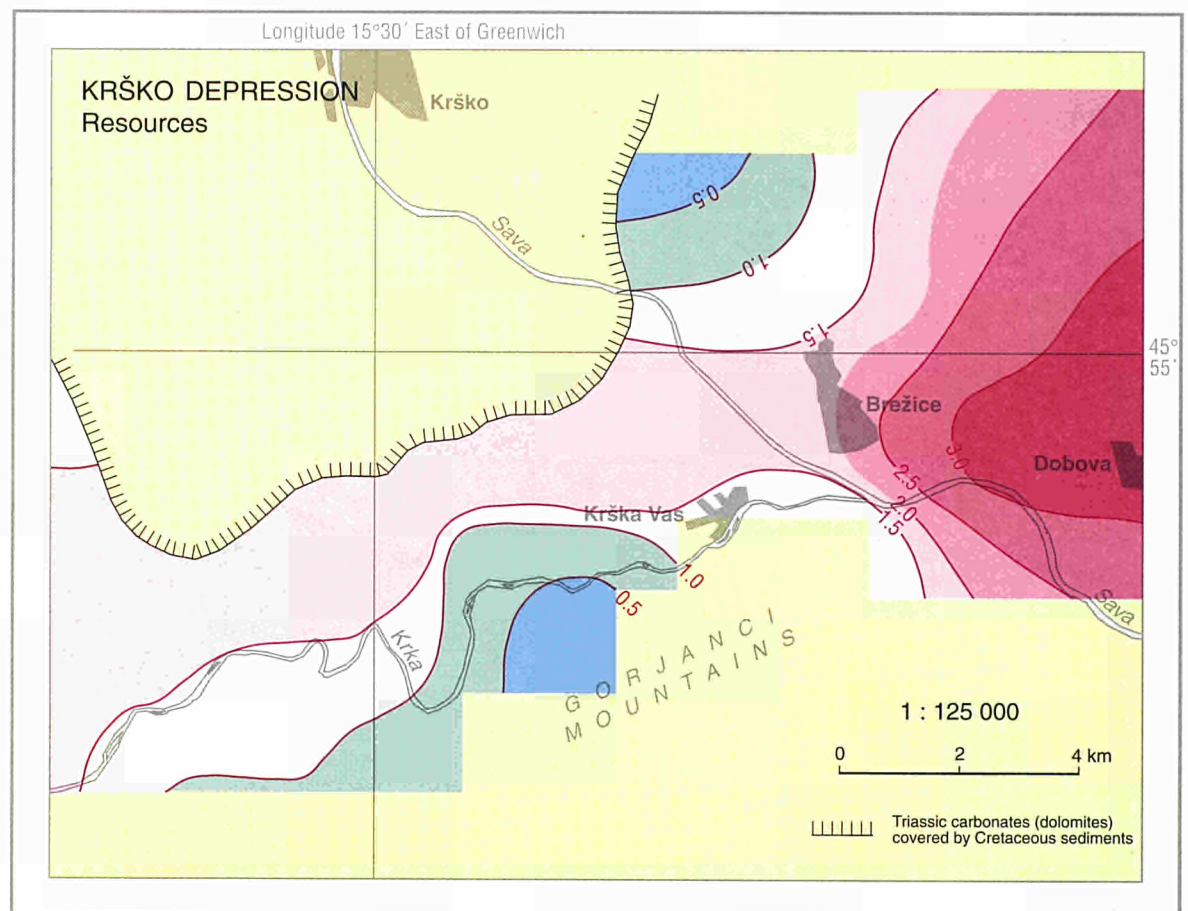
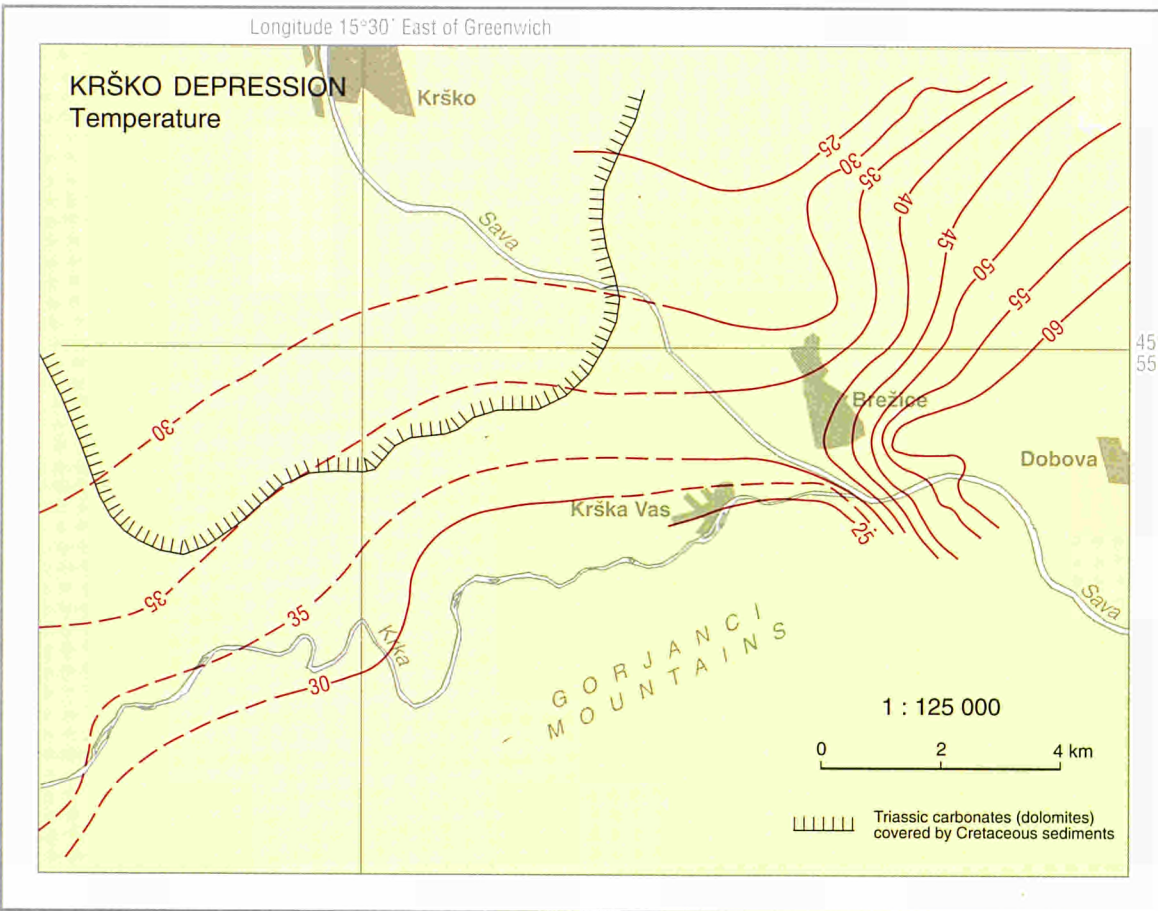
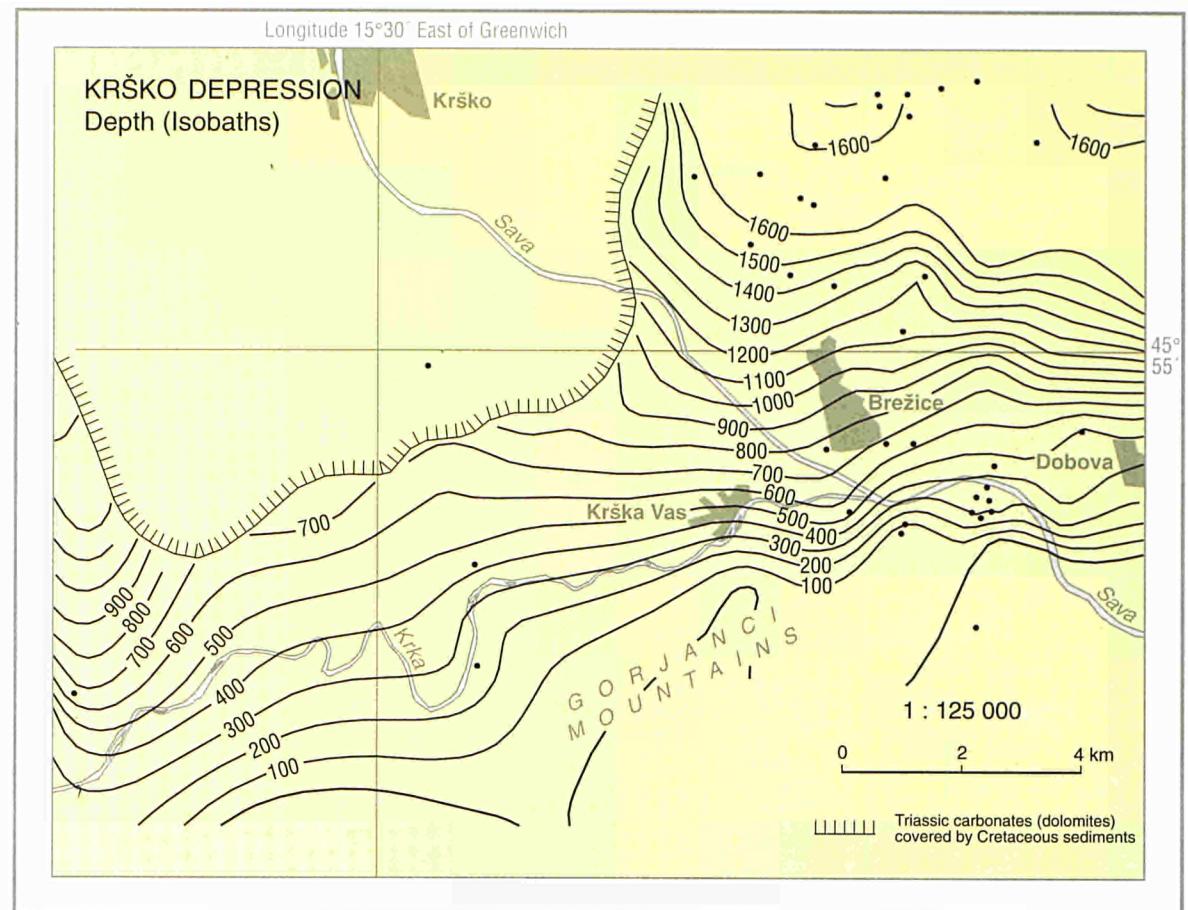
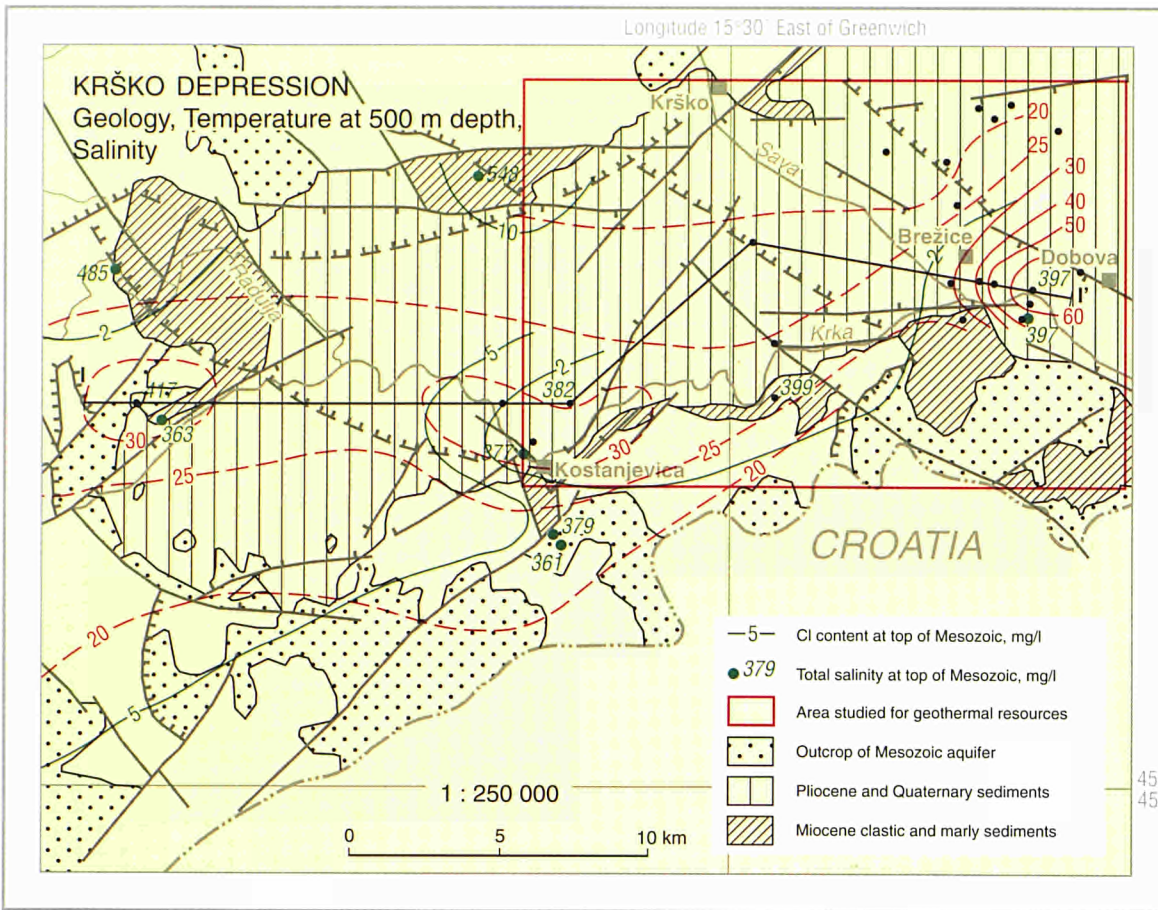
TEMPERATURES IN WATER AND OIL BOREHOLES

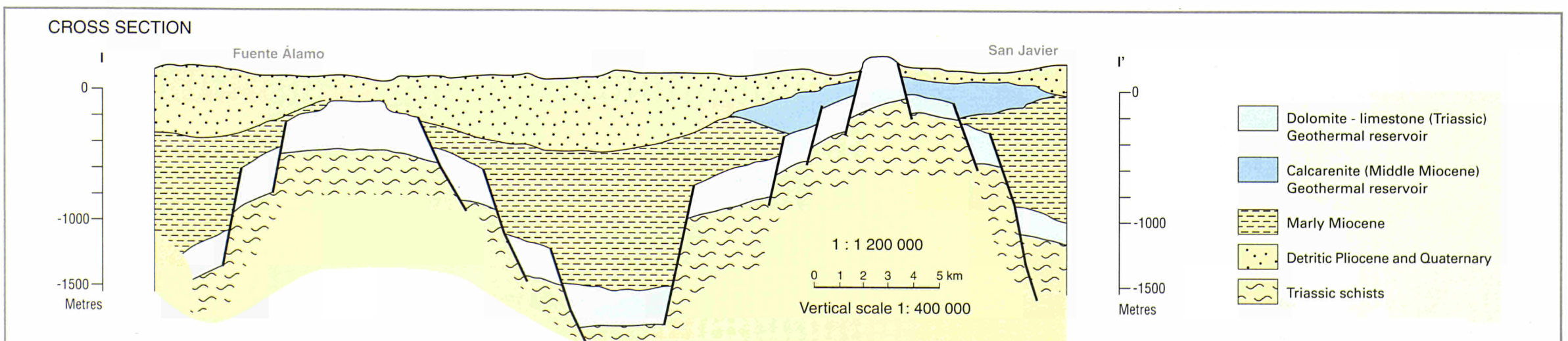
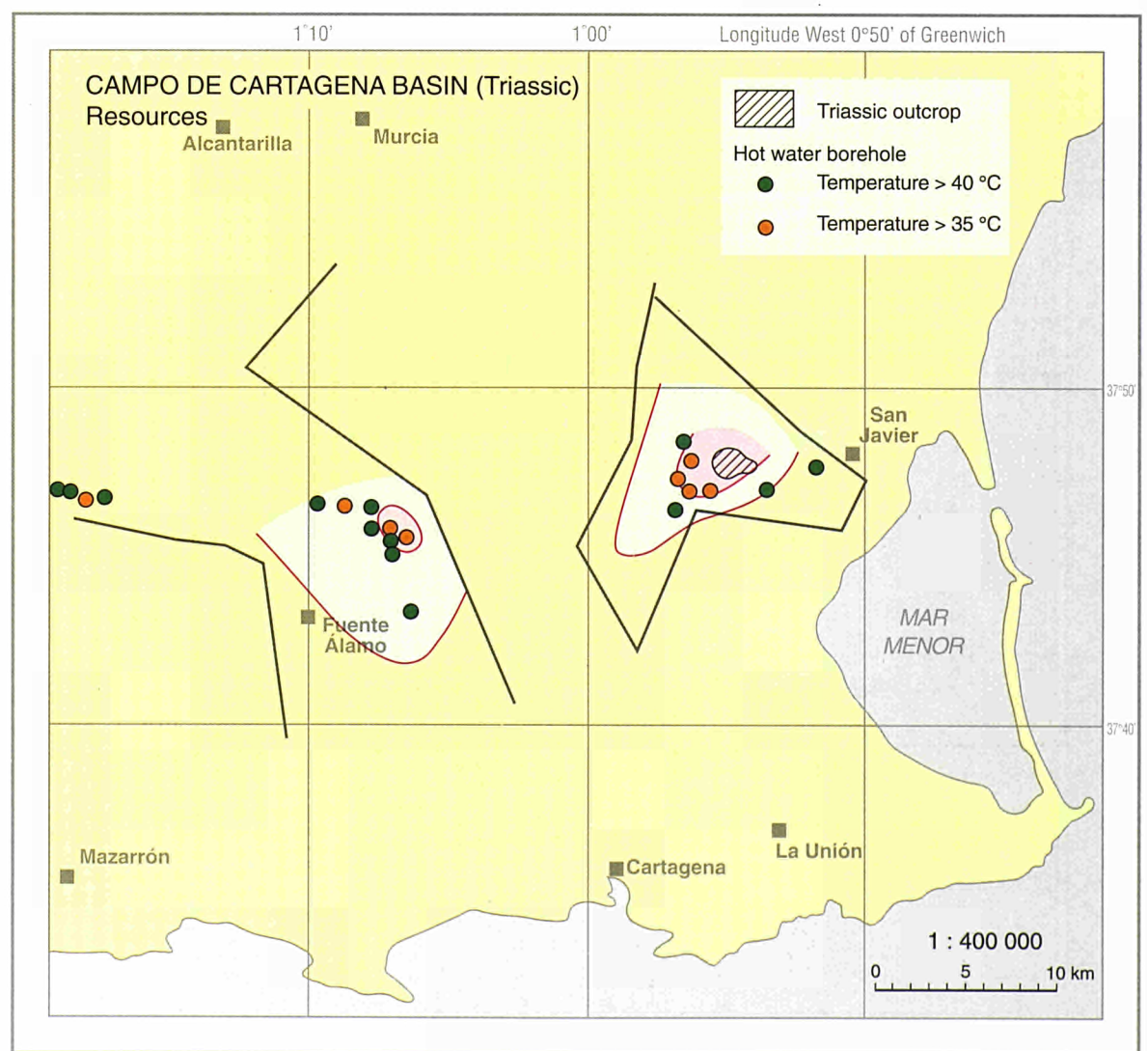
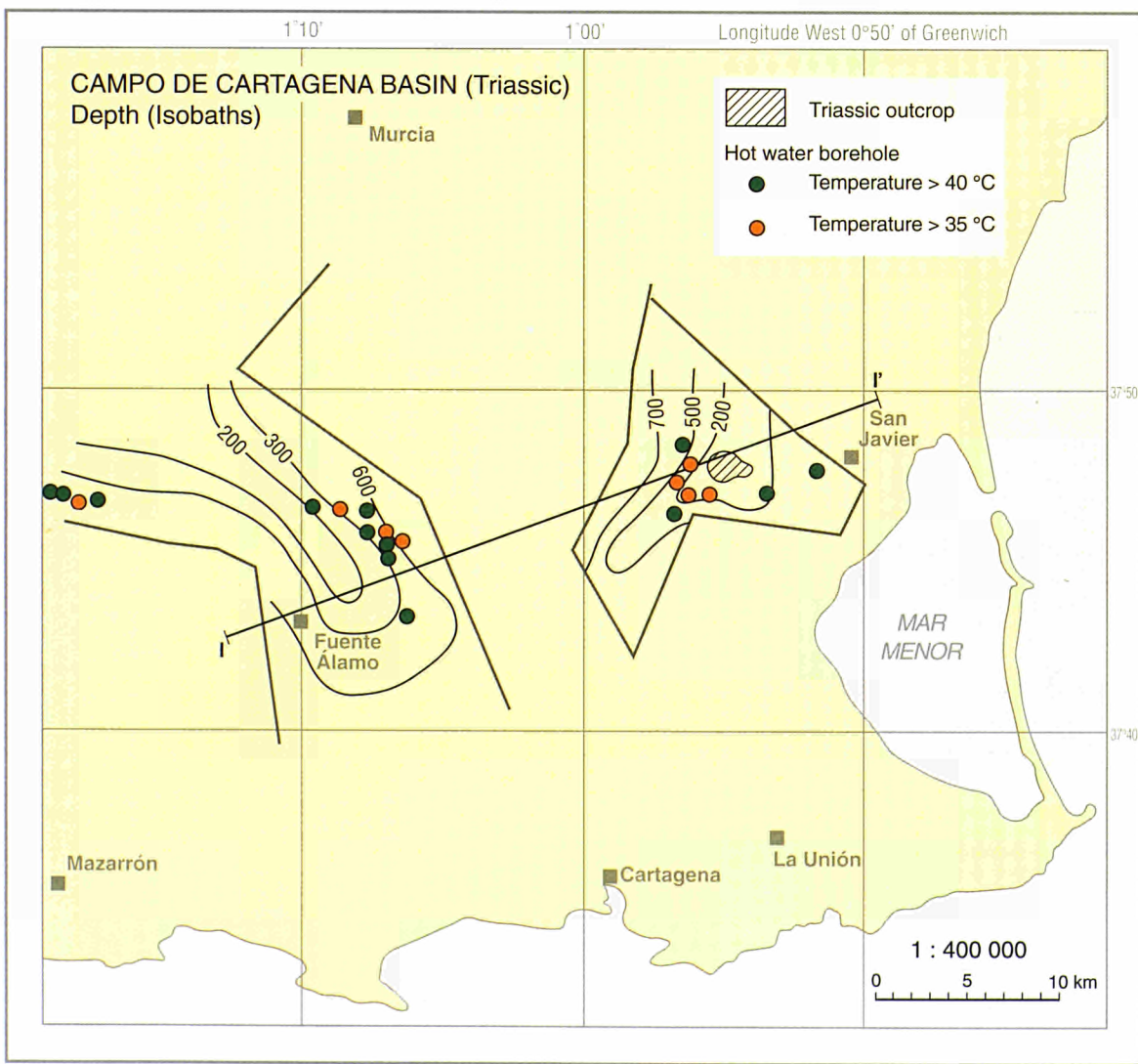
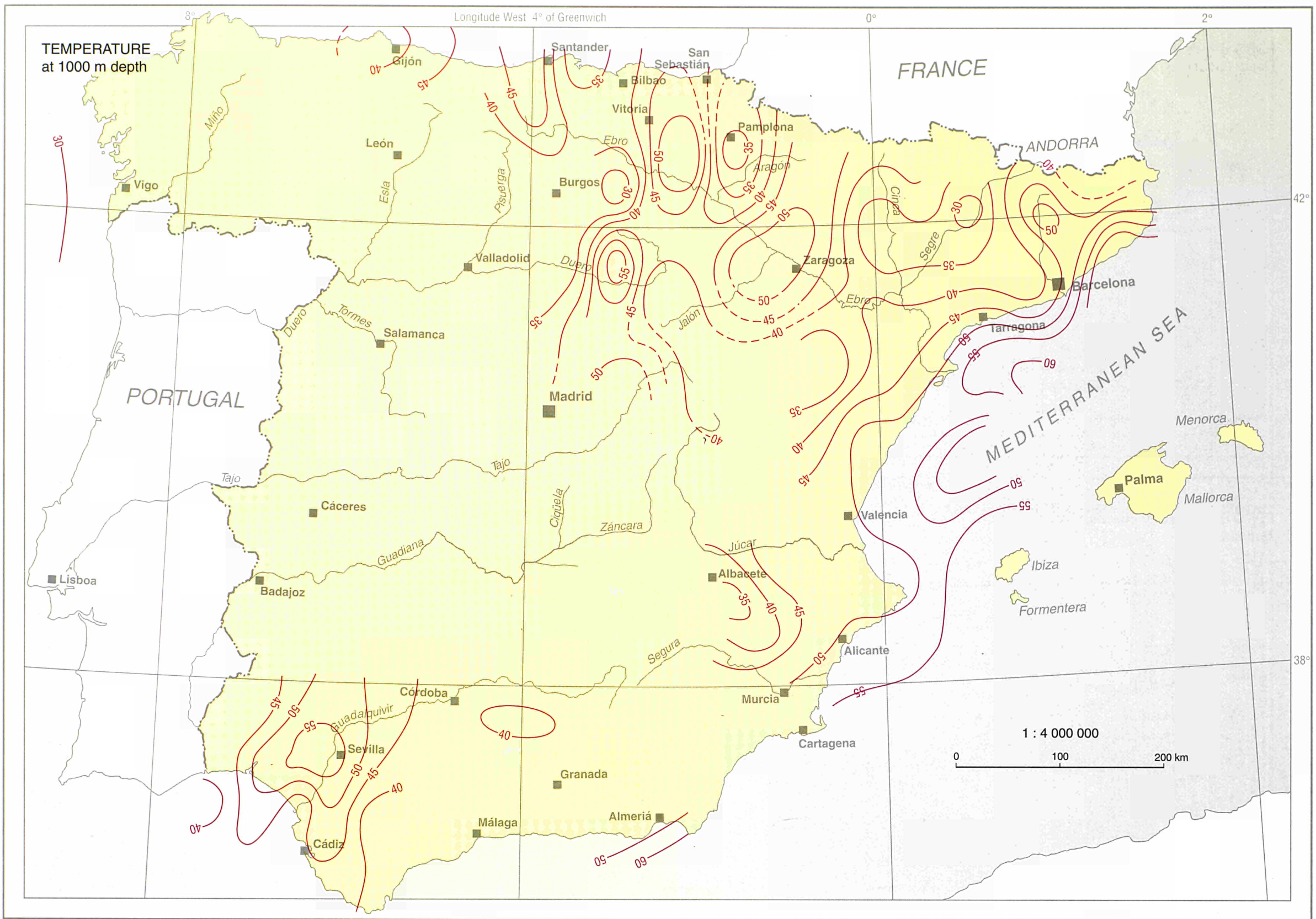


Note: The values in the table refer to the aquifer properties at the point immediately above the table
 -) Data obtained during hydrocarbon investigation
 1) Estimated values

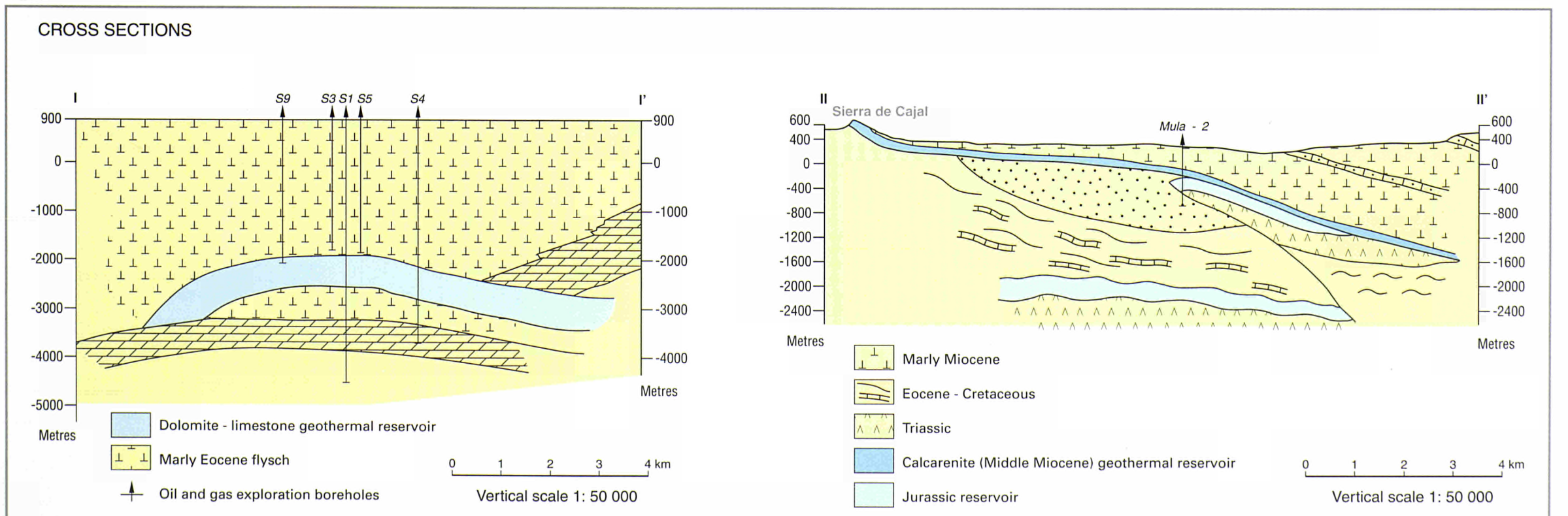
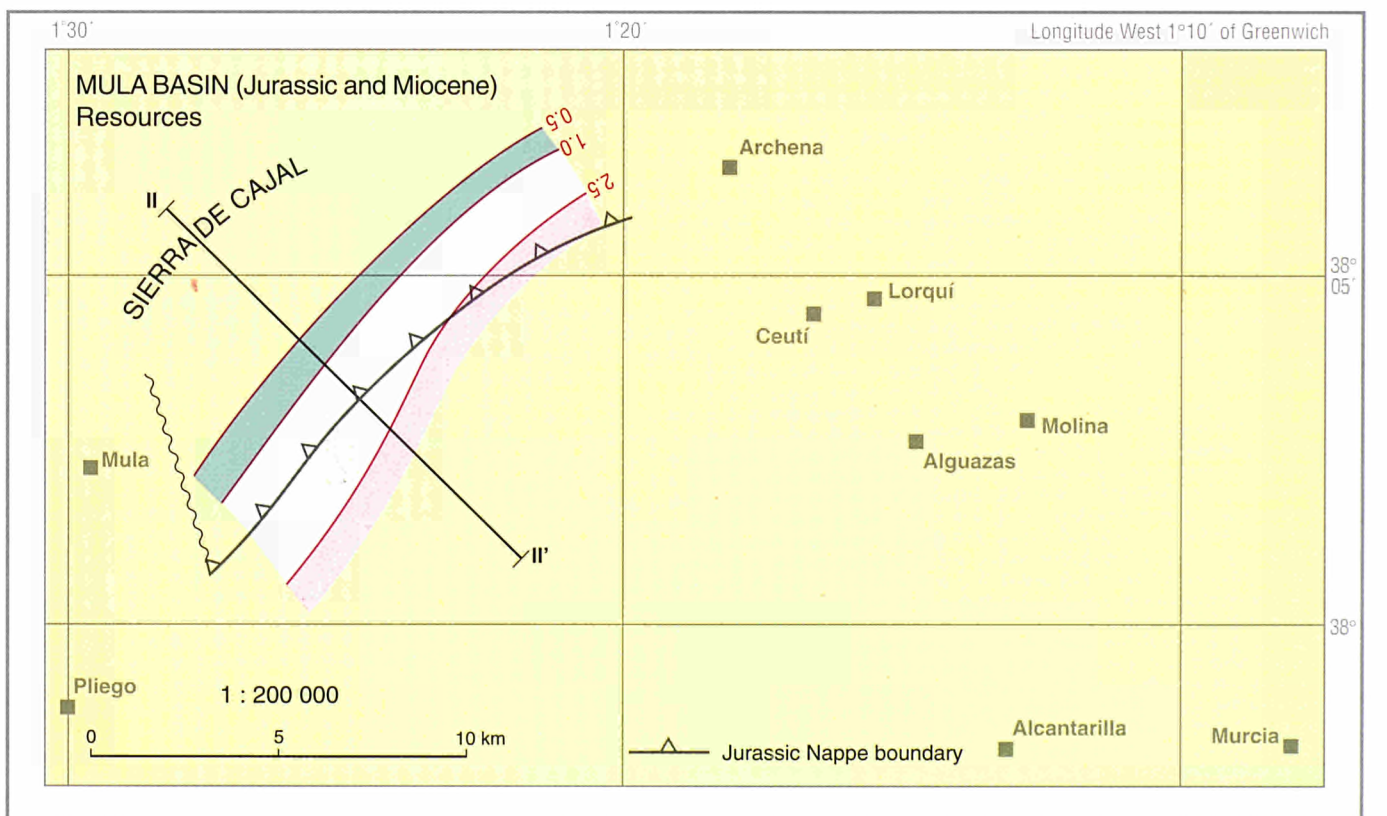
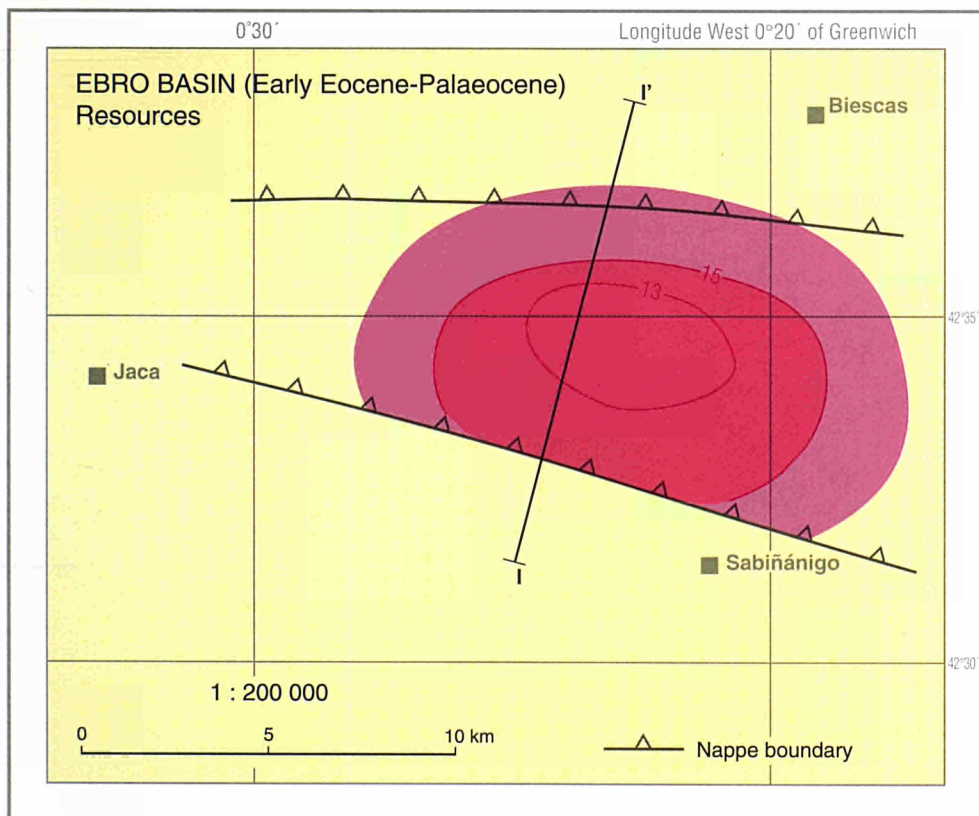
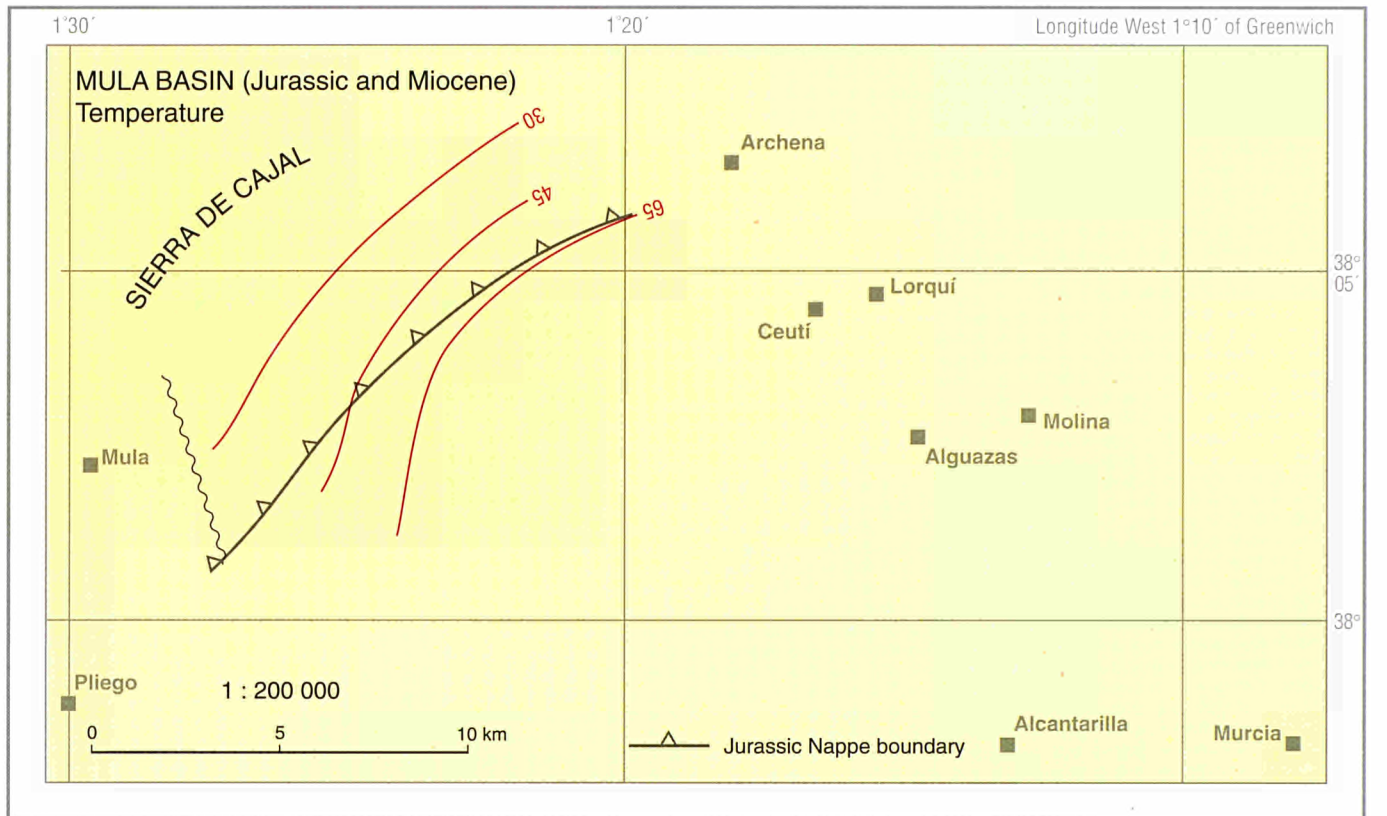
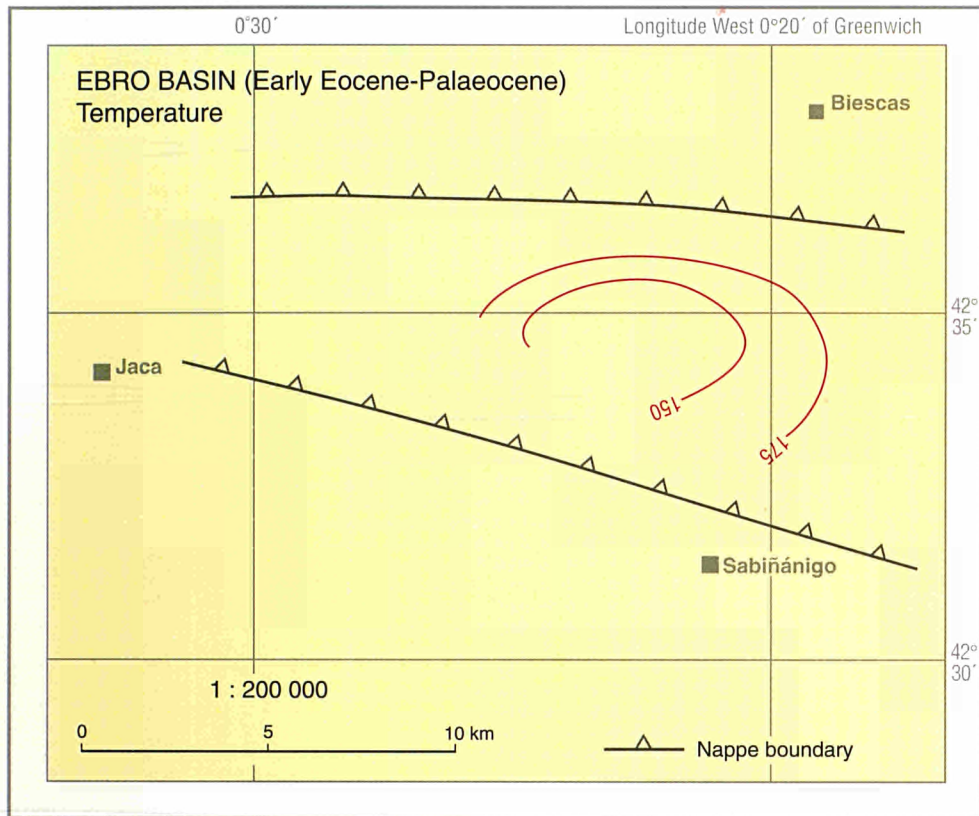
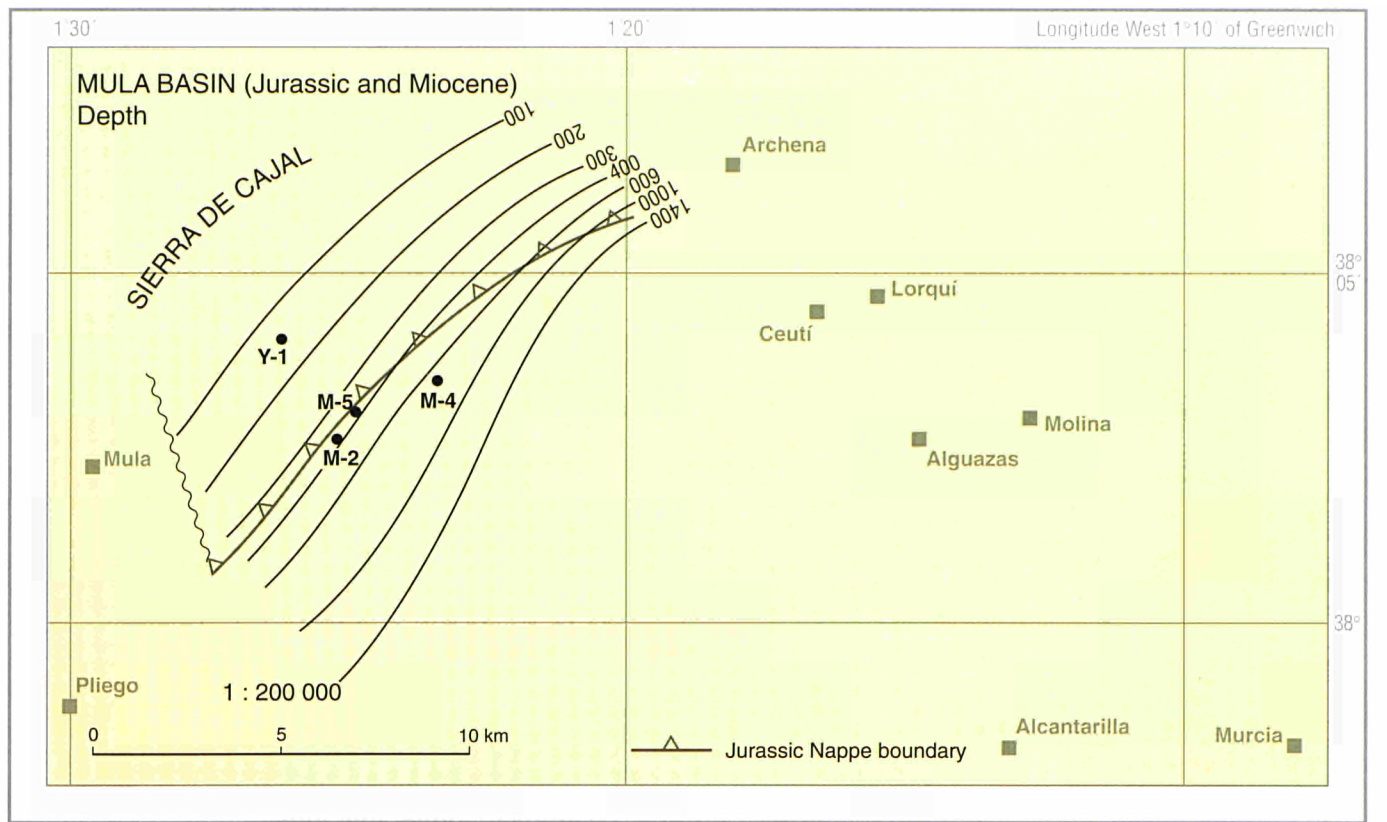
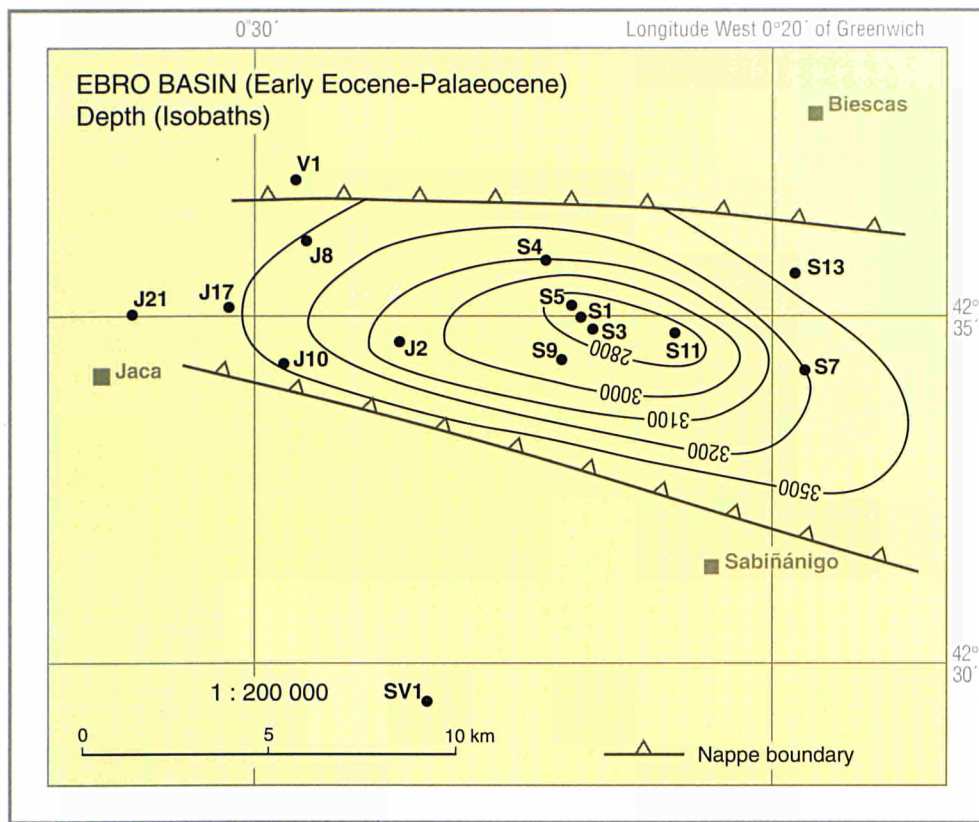


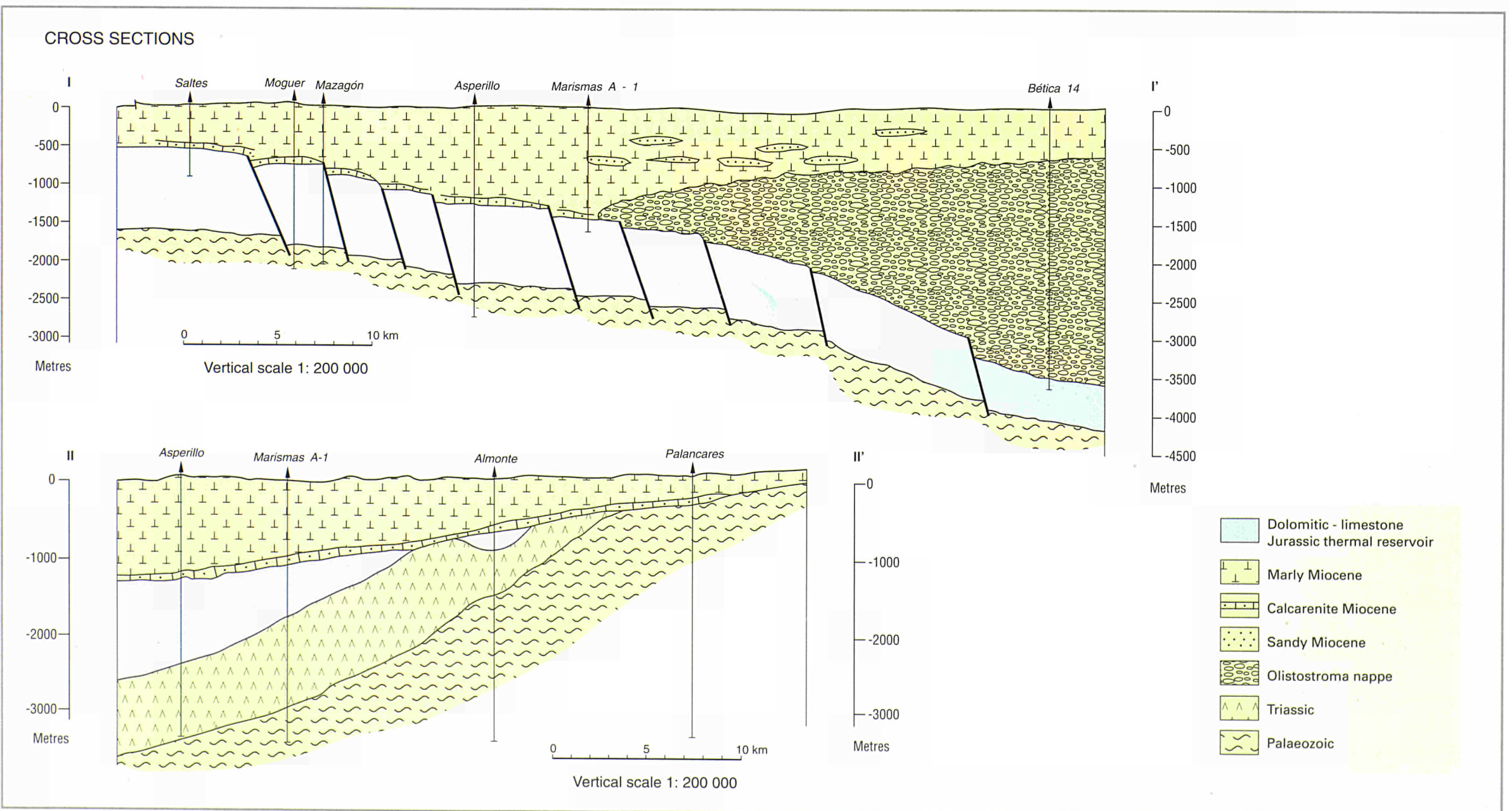
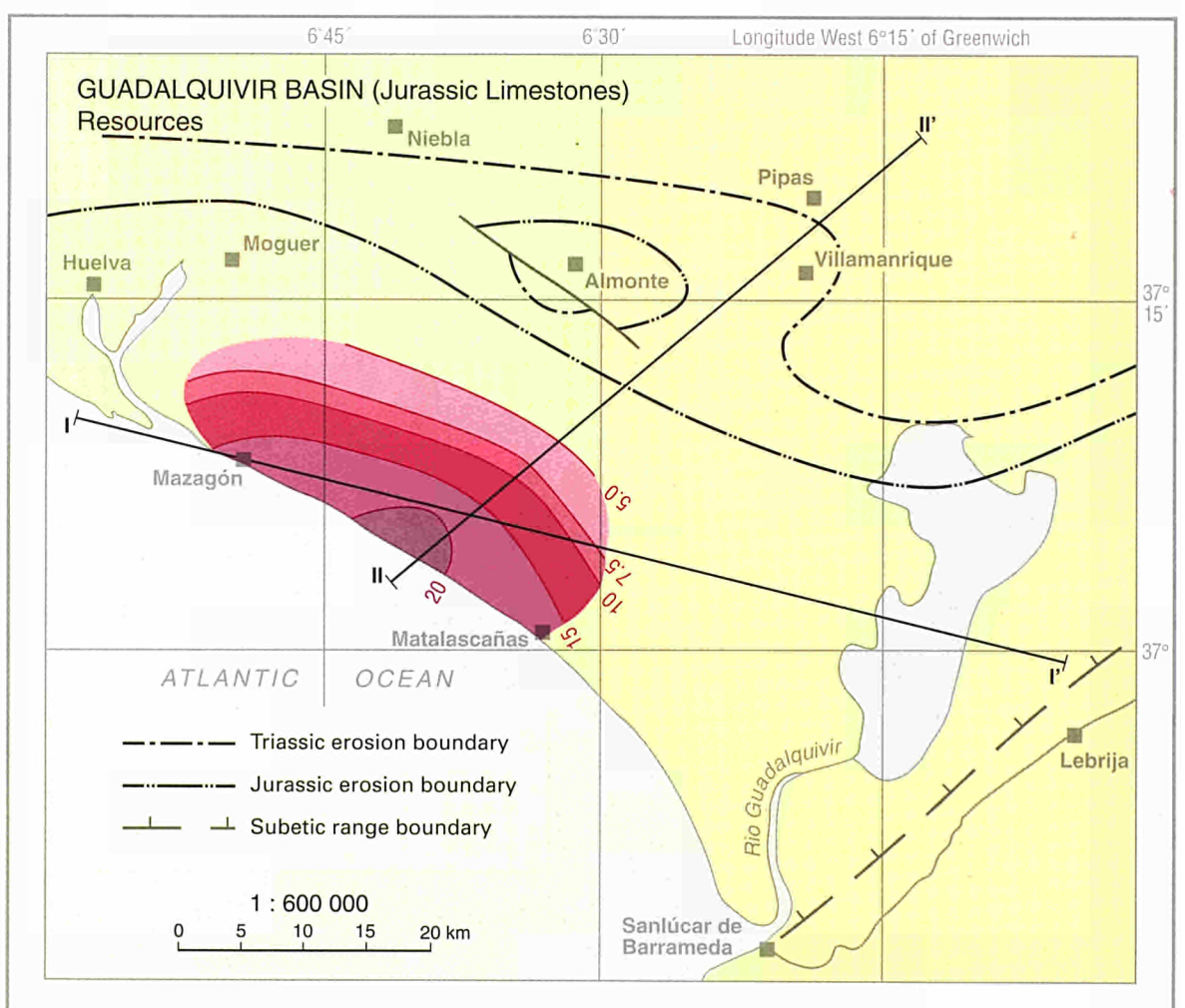
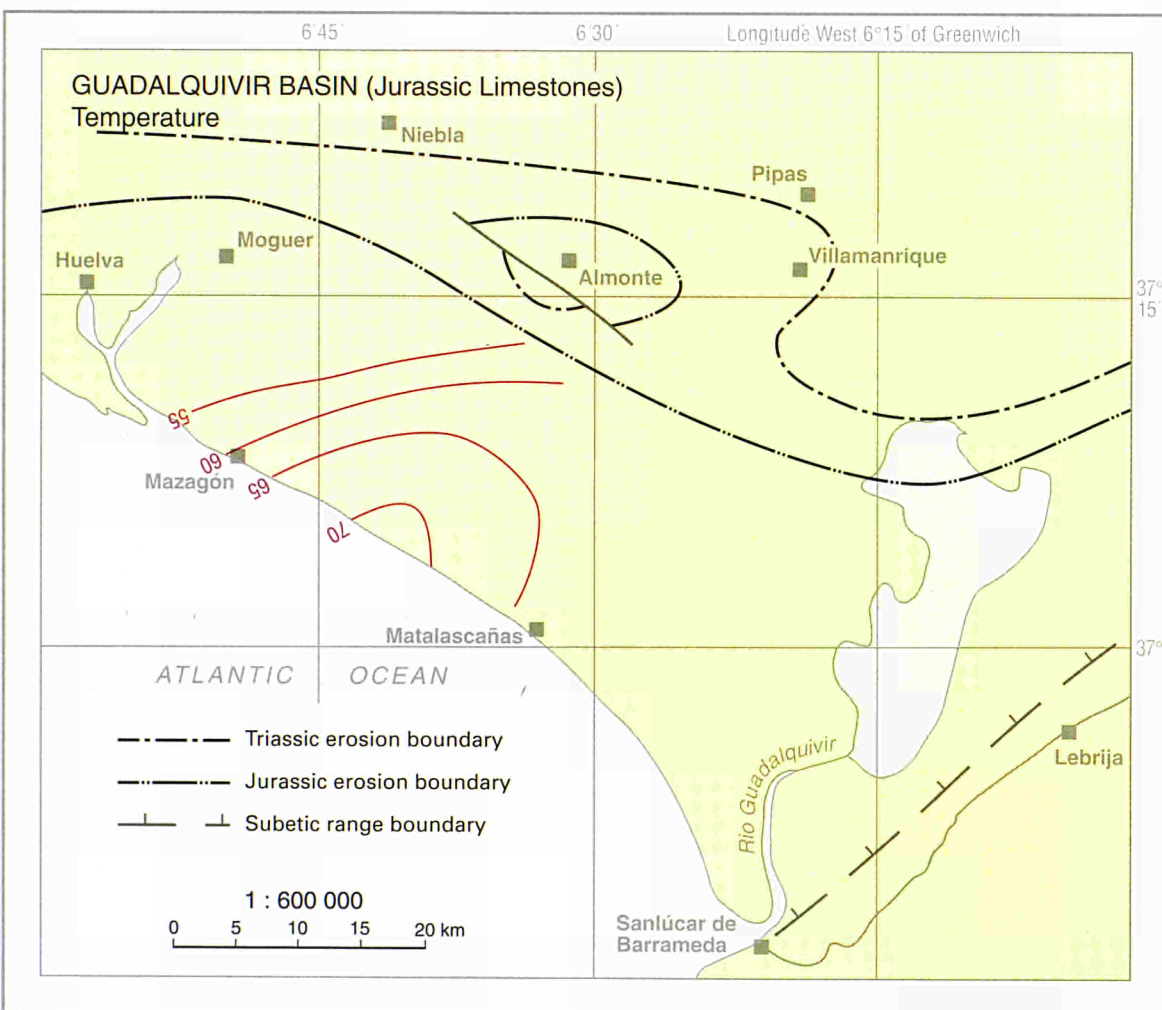
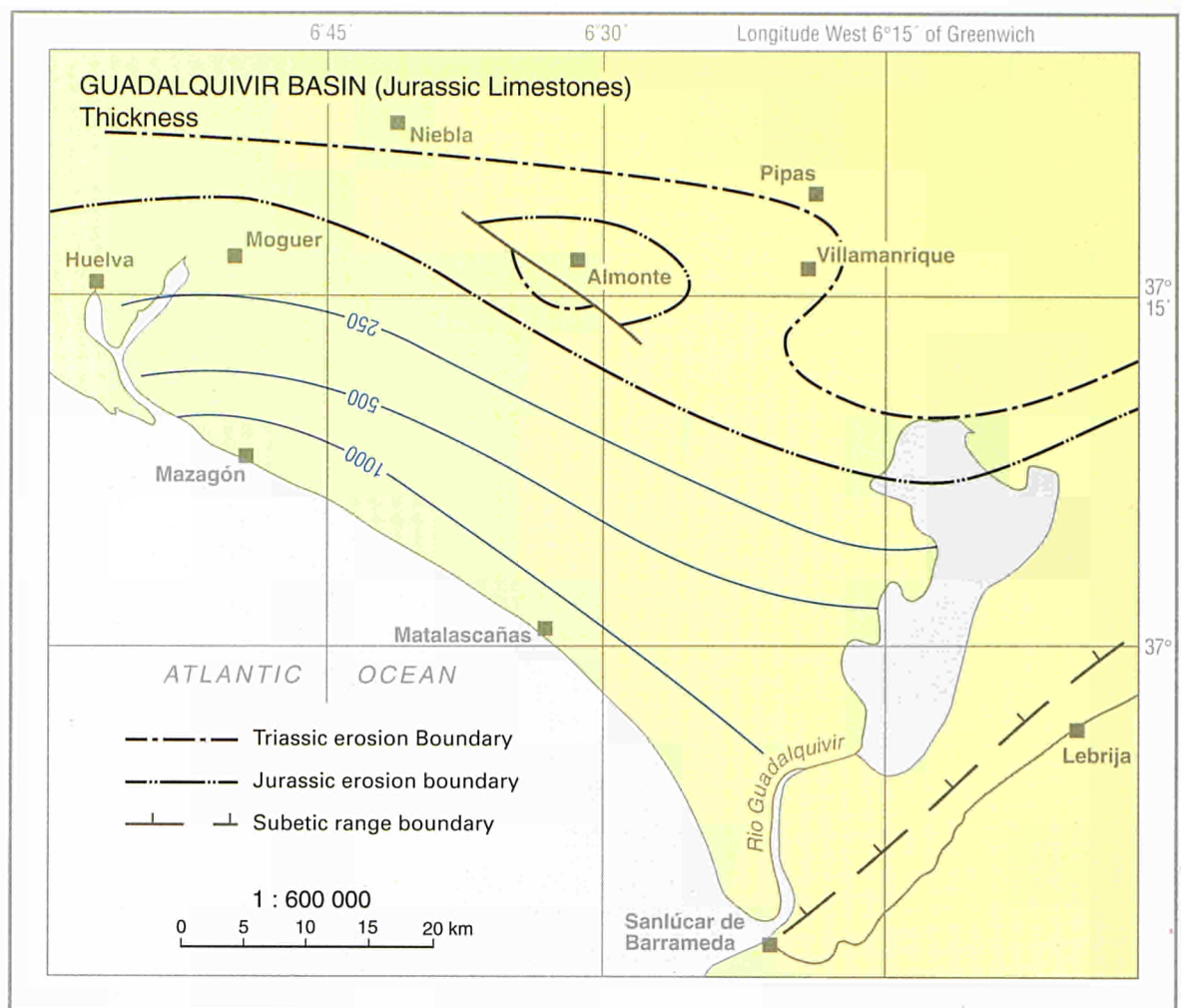
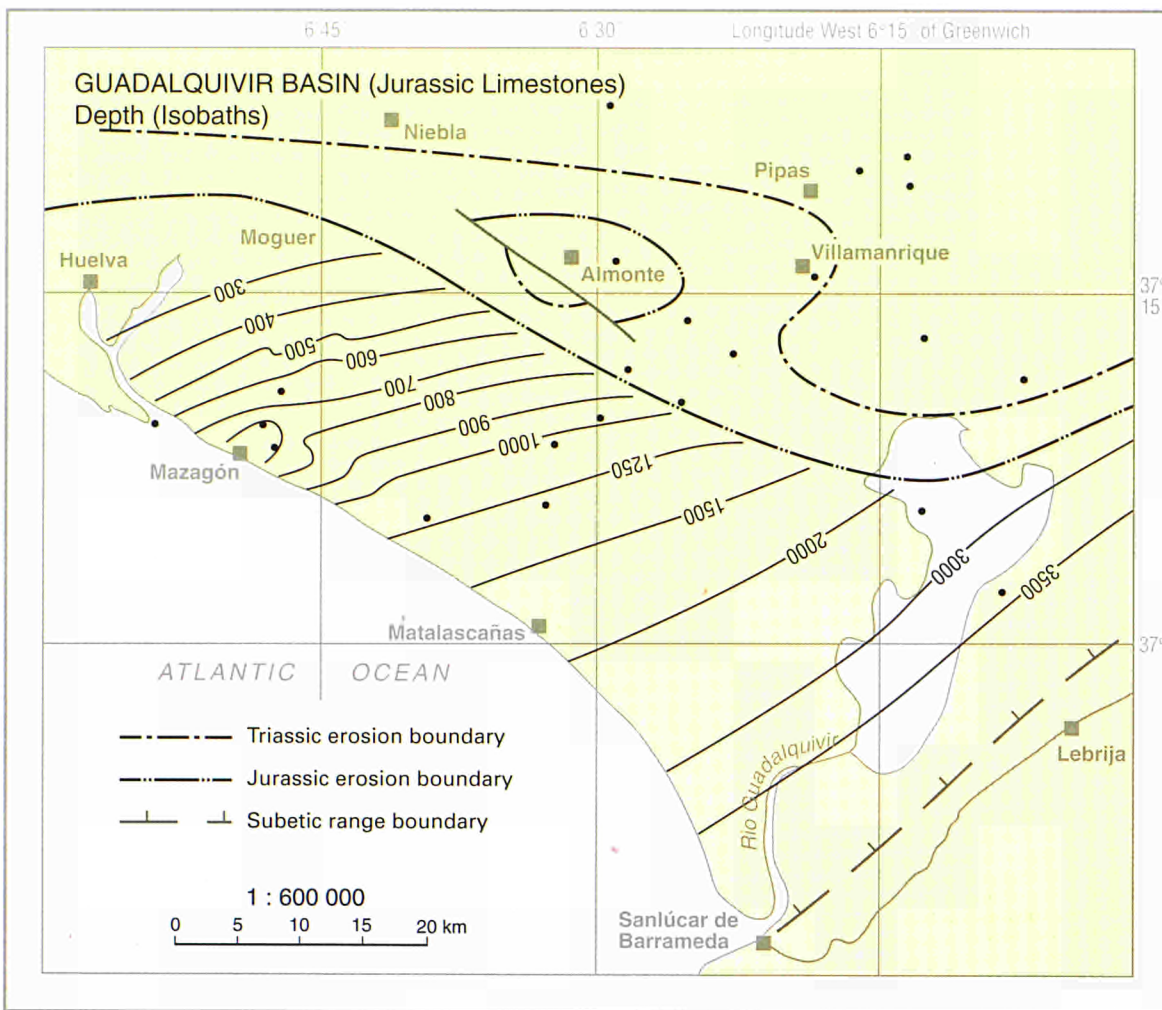
Note: The values in the table refer to the aquifer properties at the point immediately above the table
 -) Data obtained during hydrocarbon investigation
 1) Estimated values



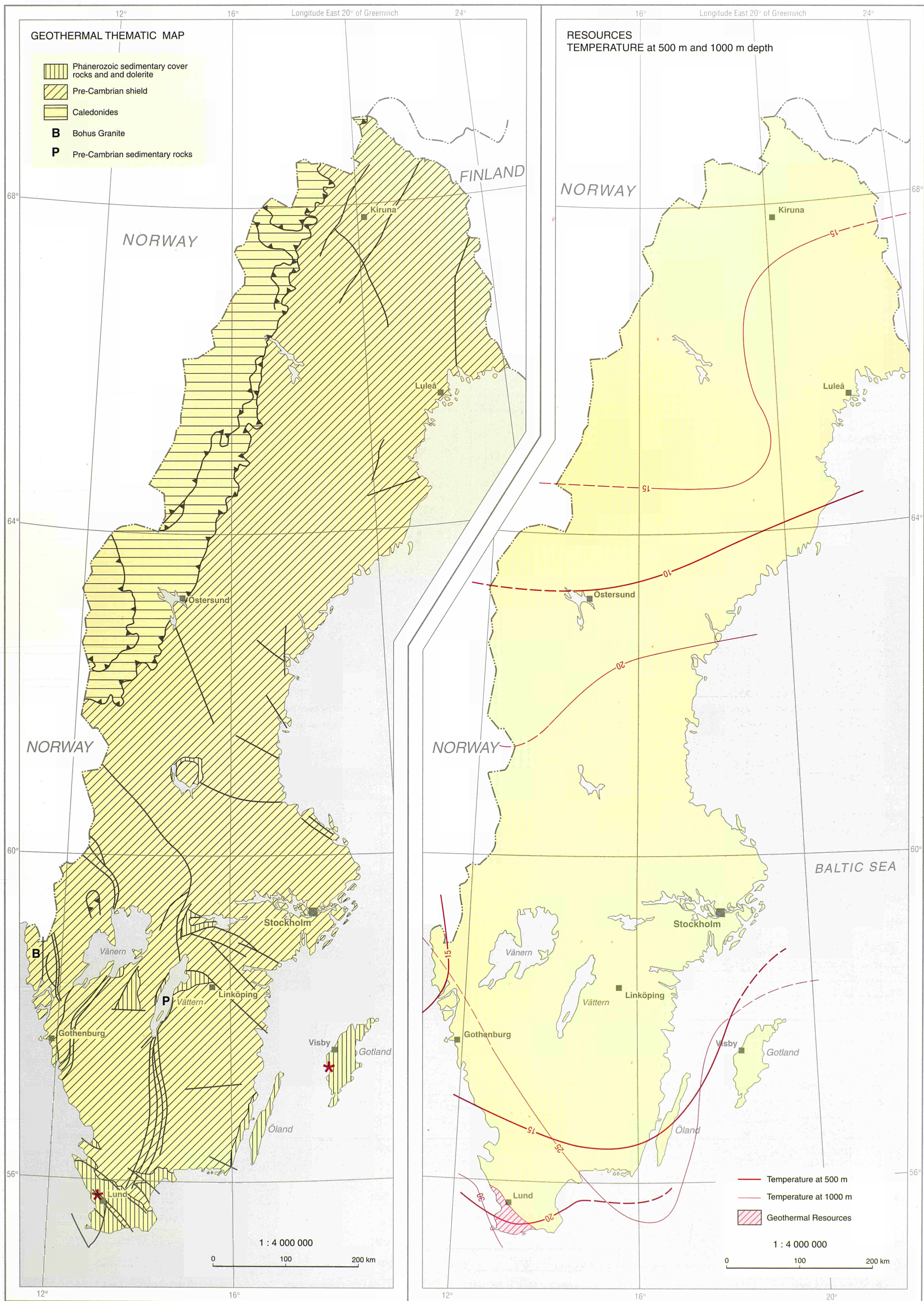


SPAIN





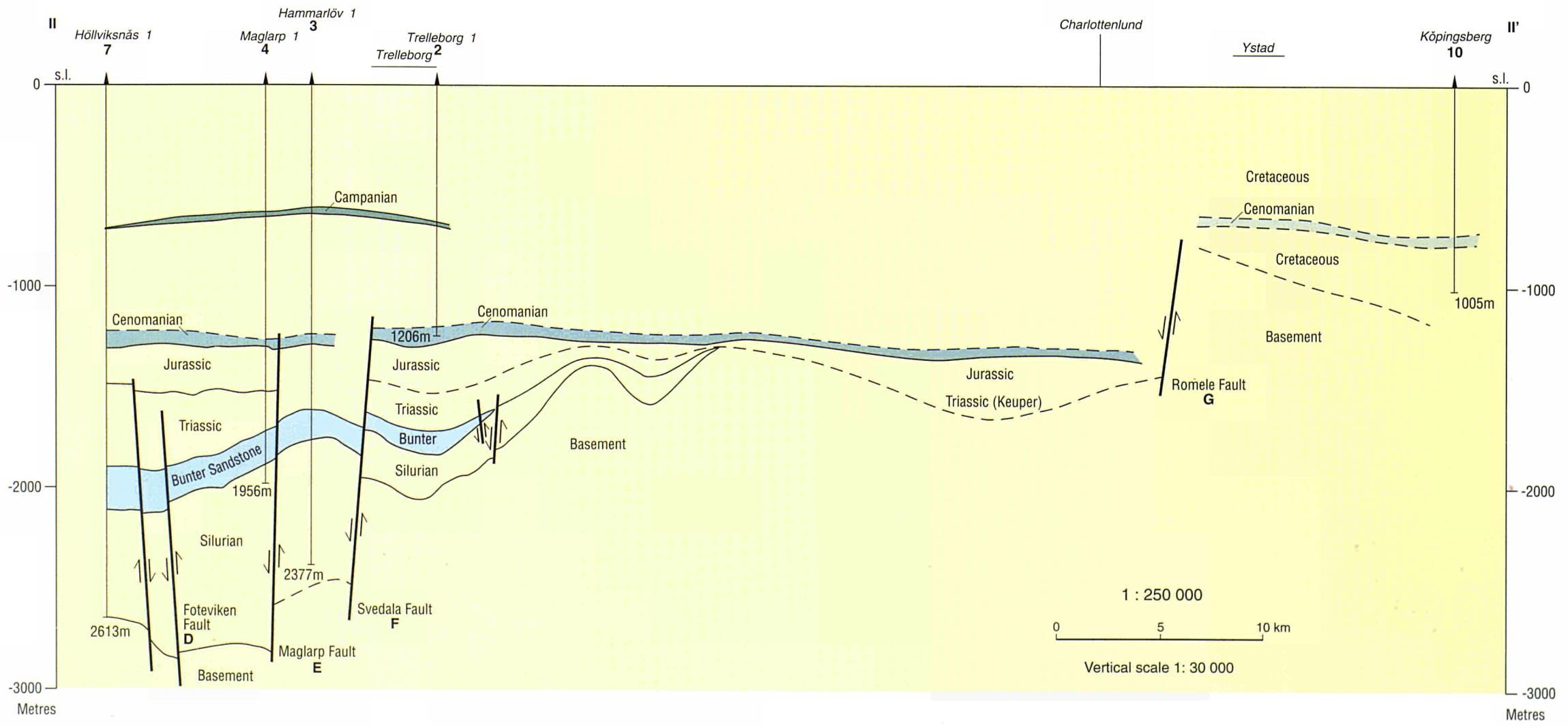
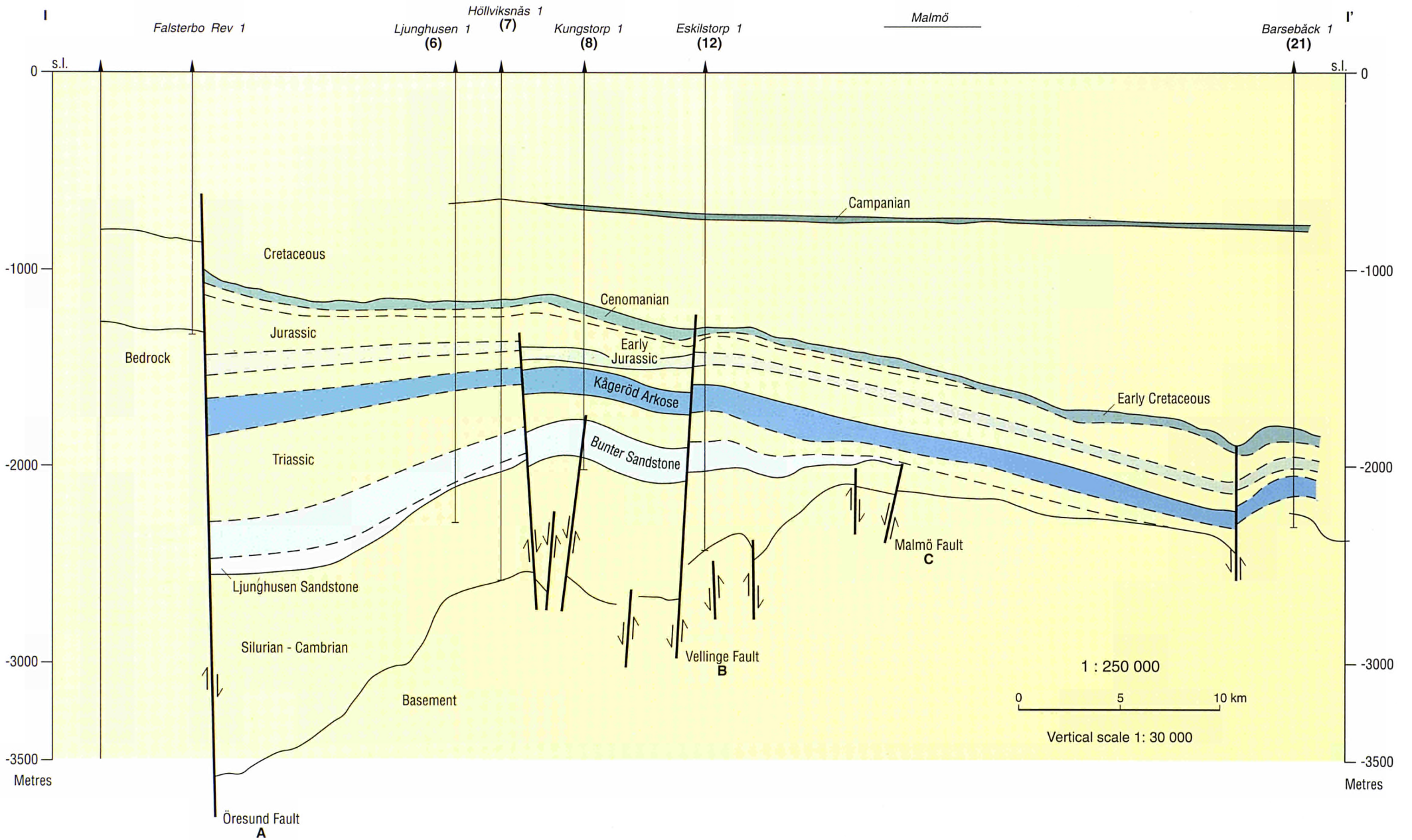
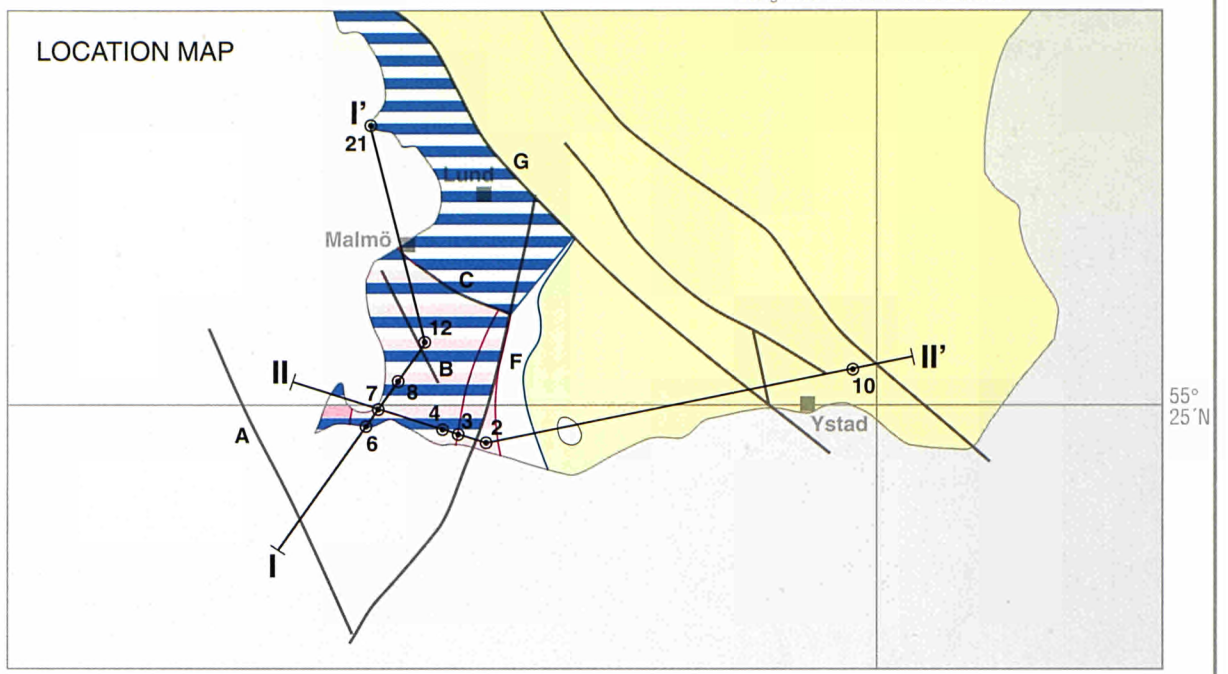
SWEDEN



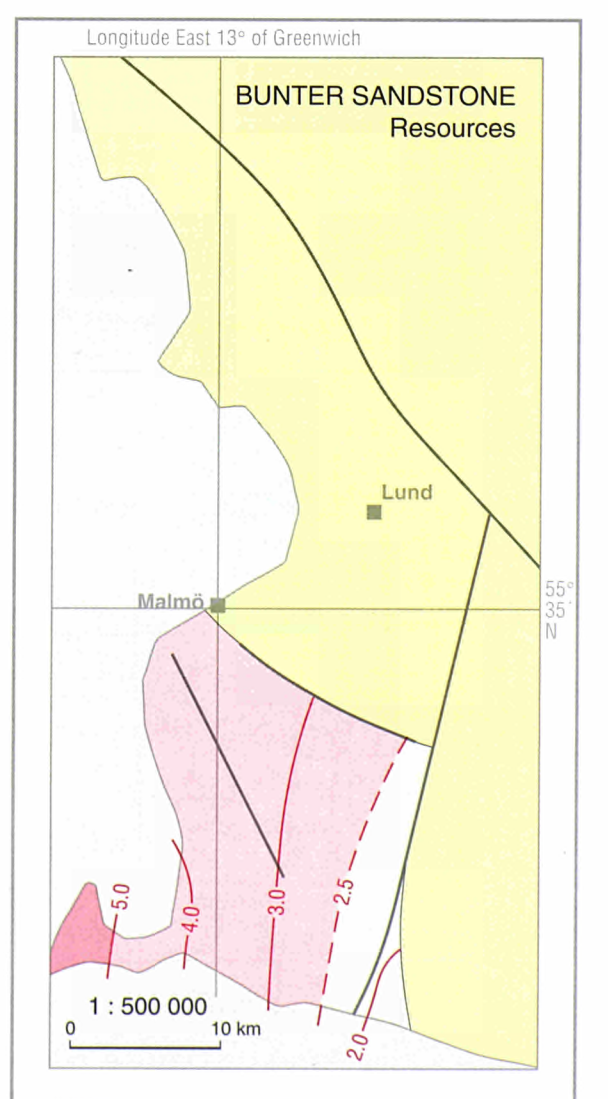
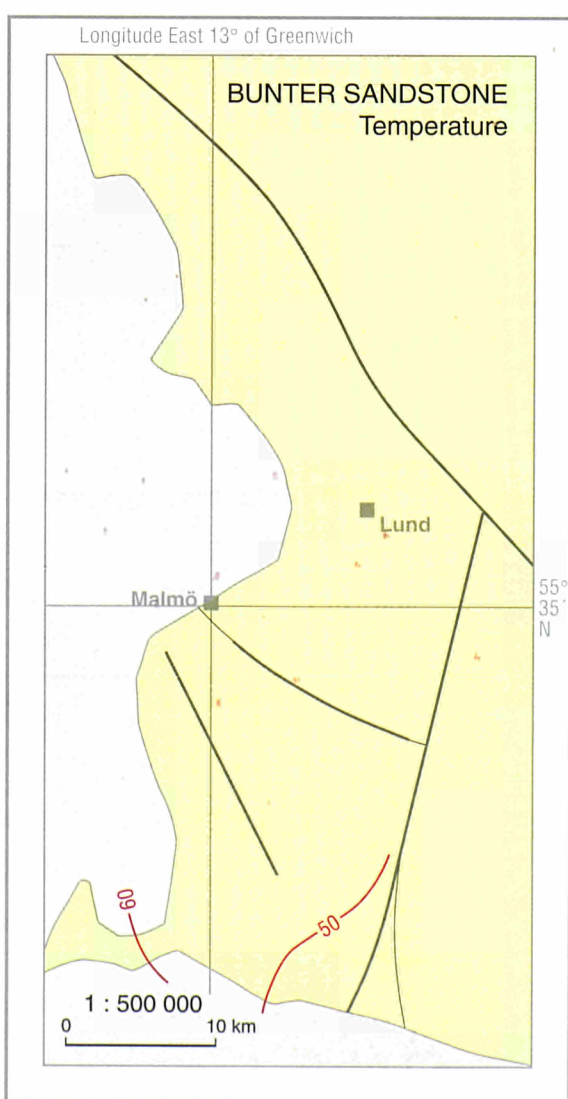
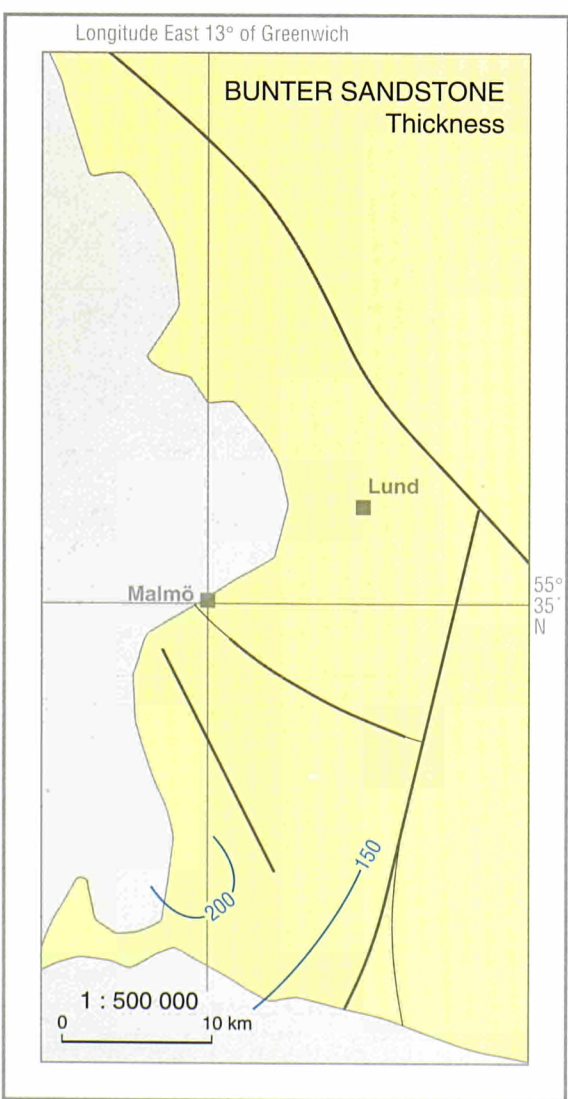
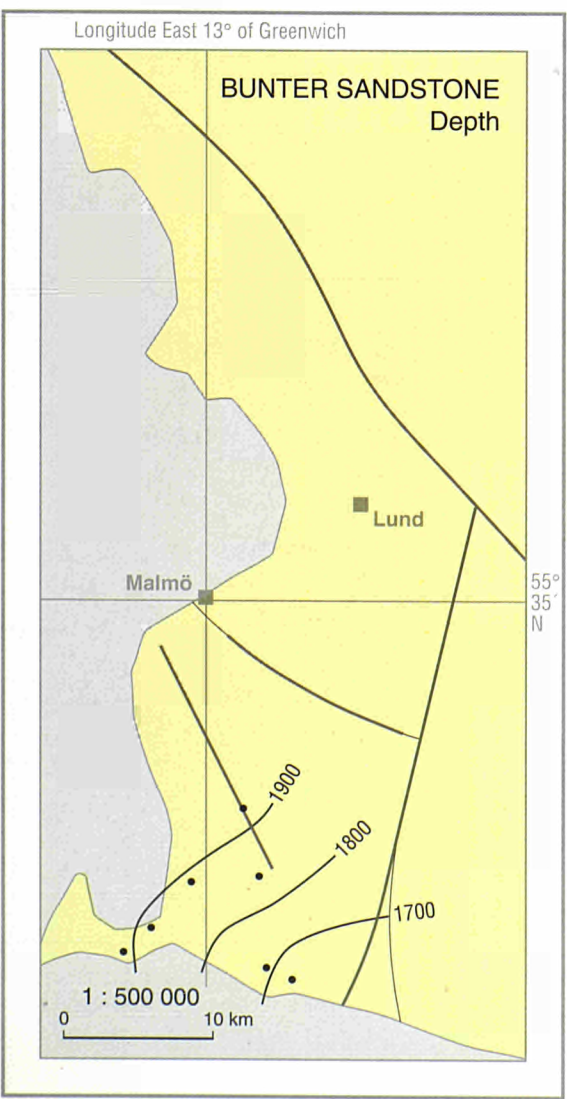
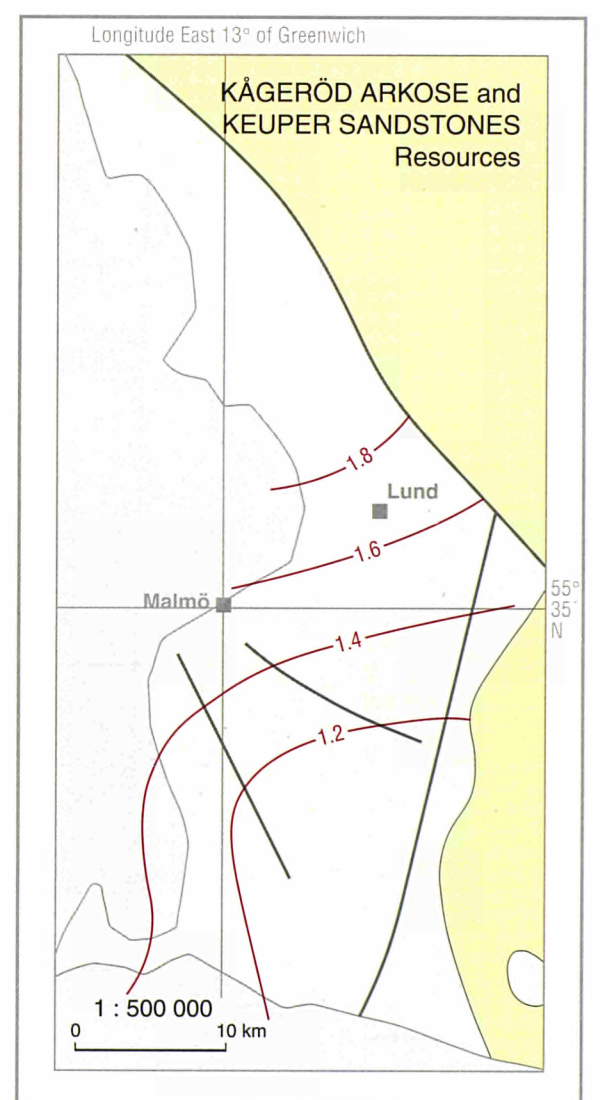
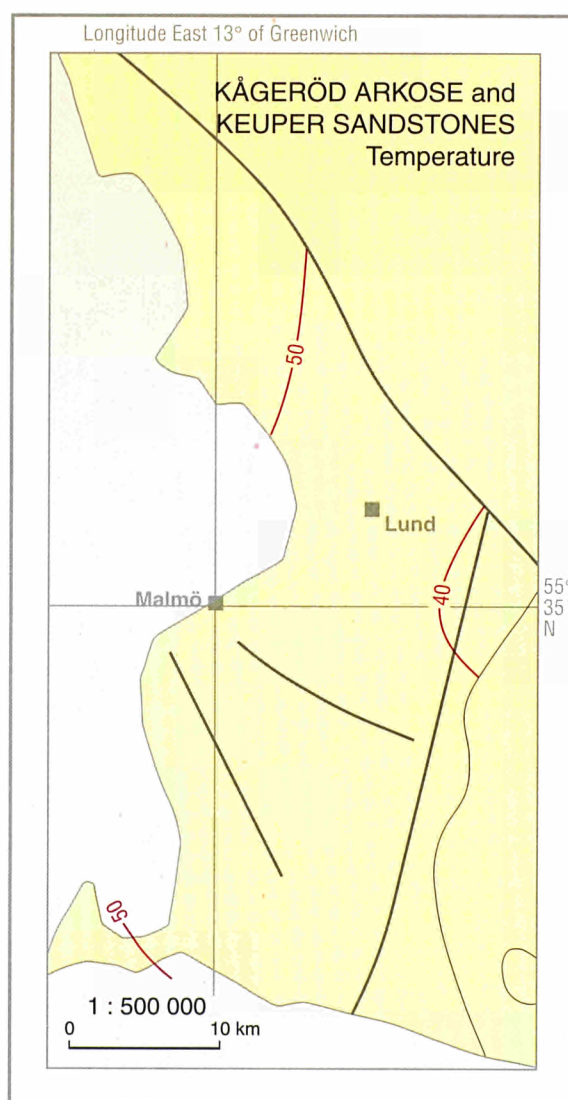
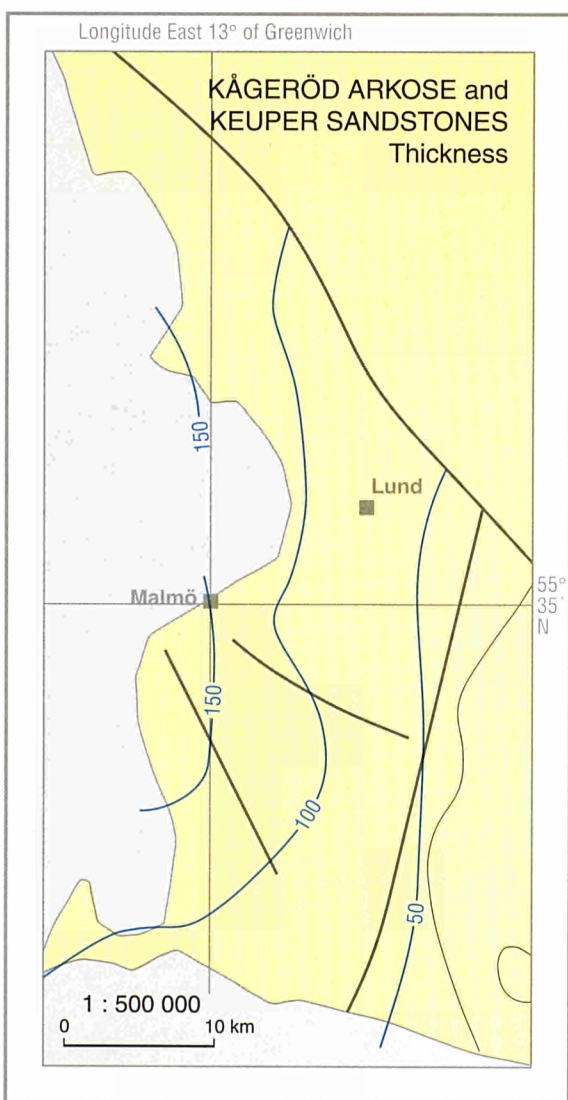
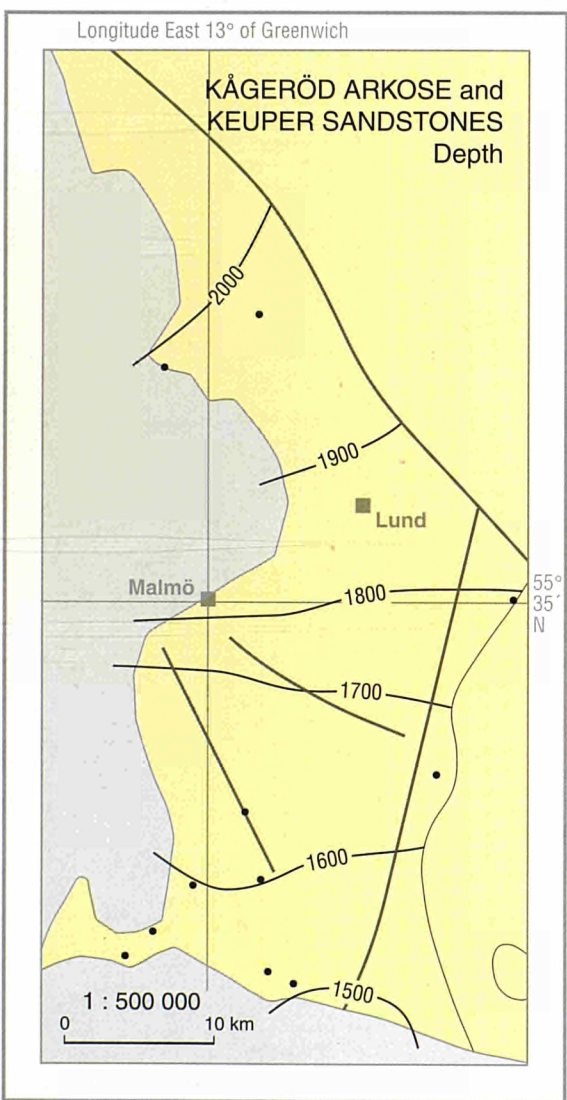
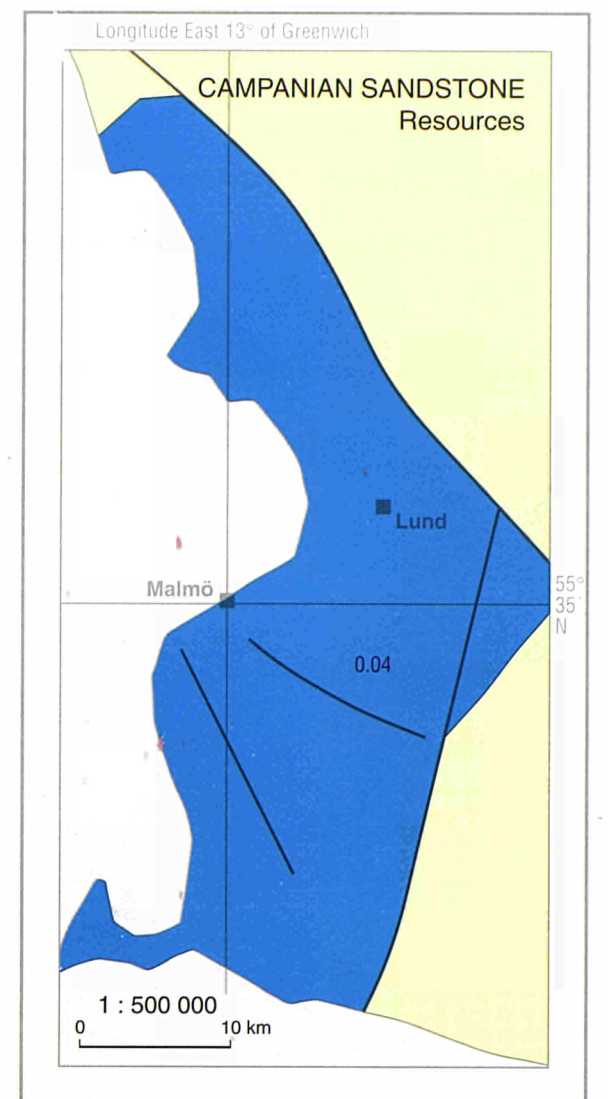
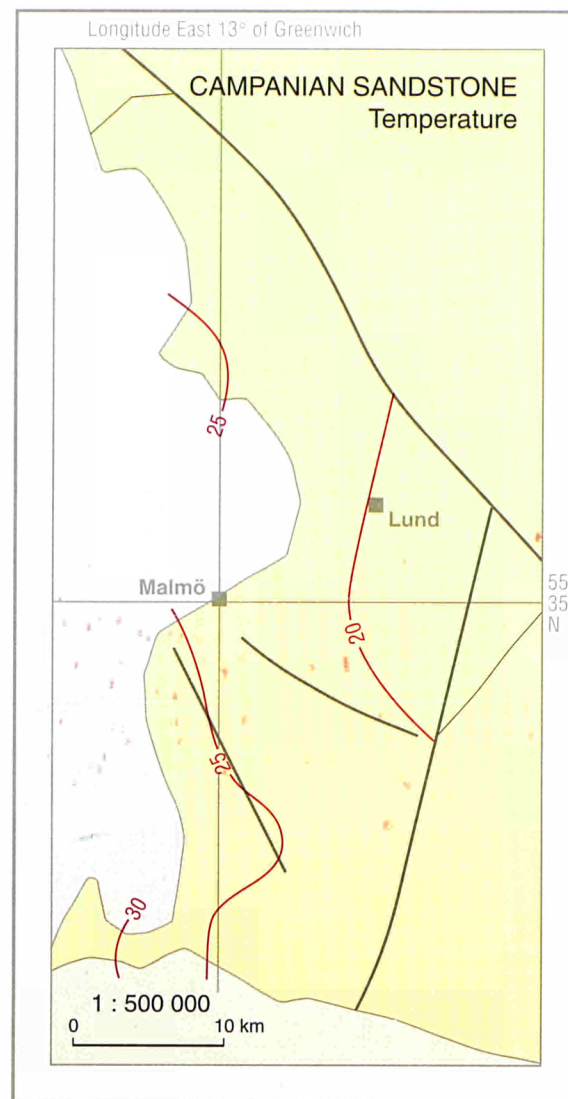
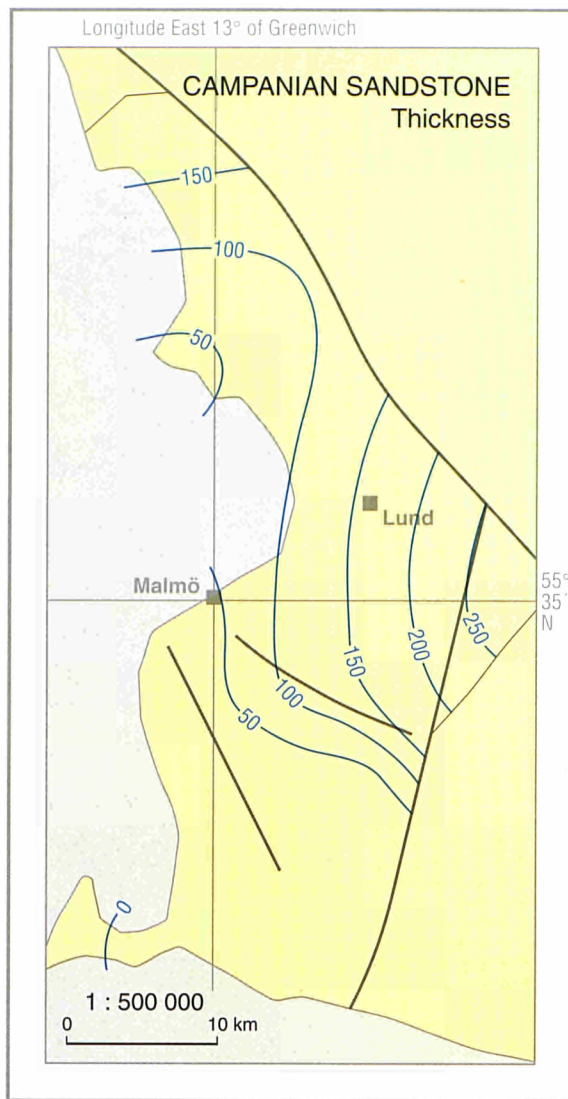
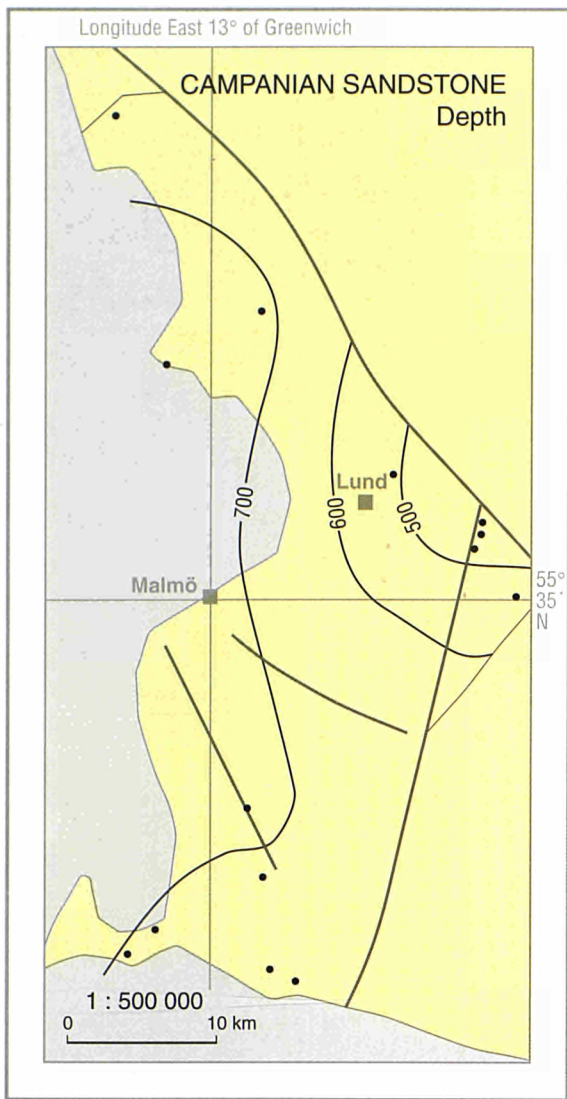
CROSS SECTIONS

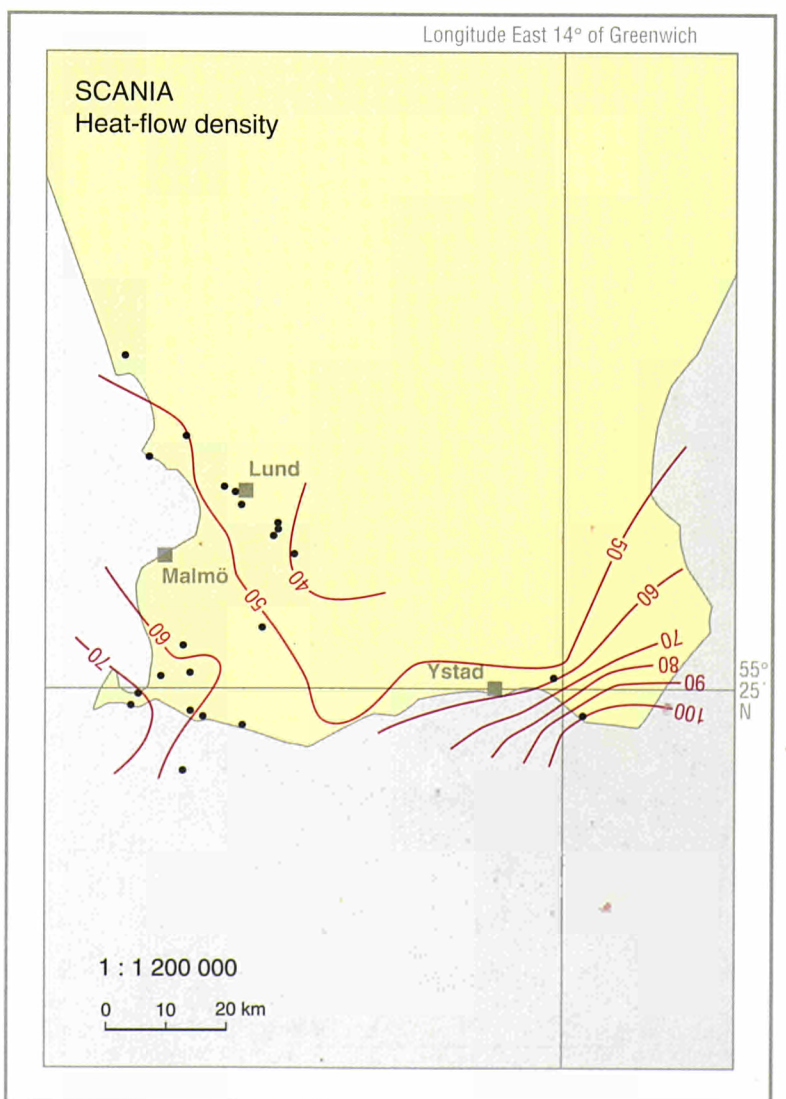
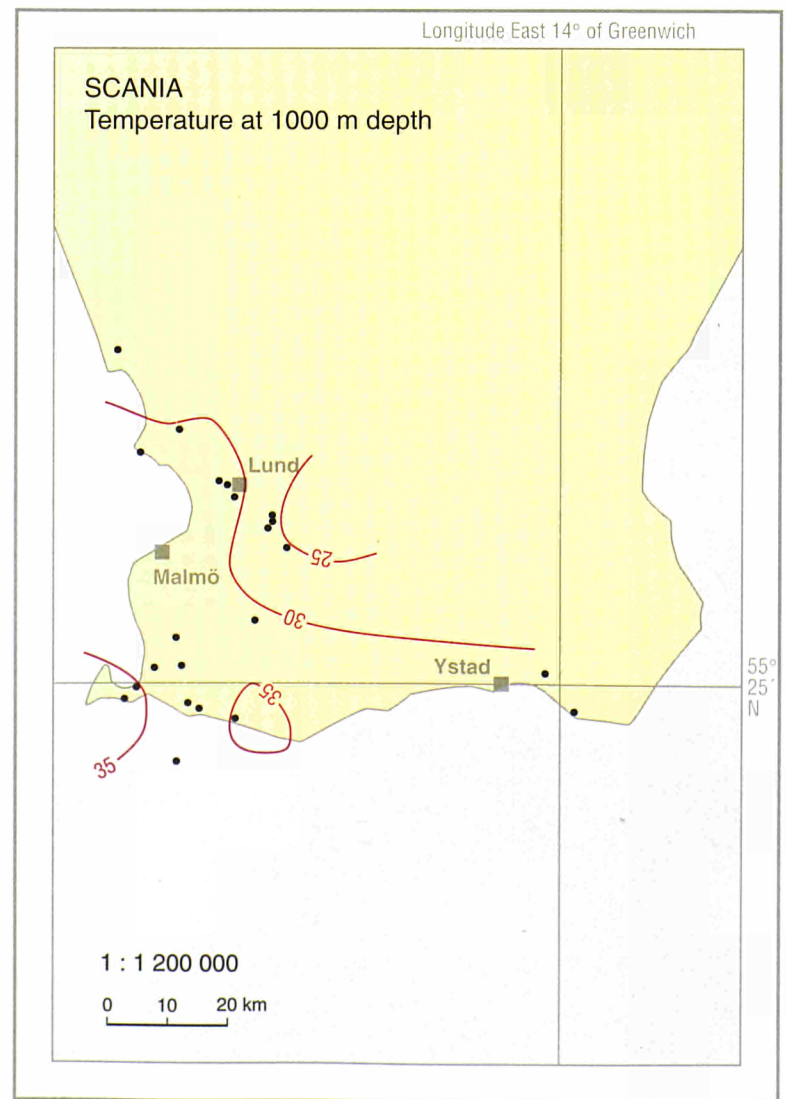
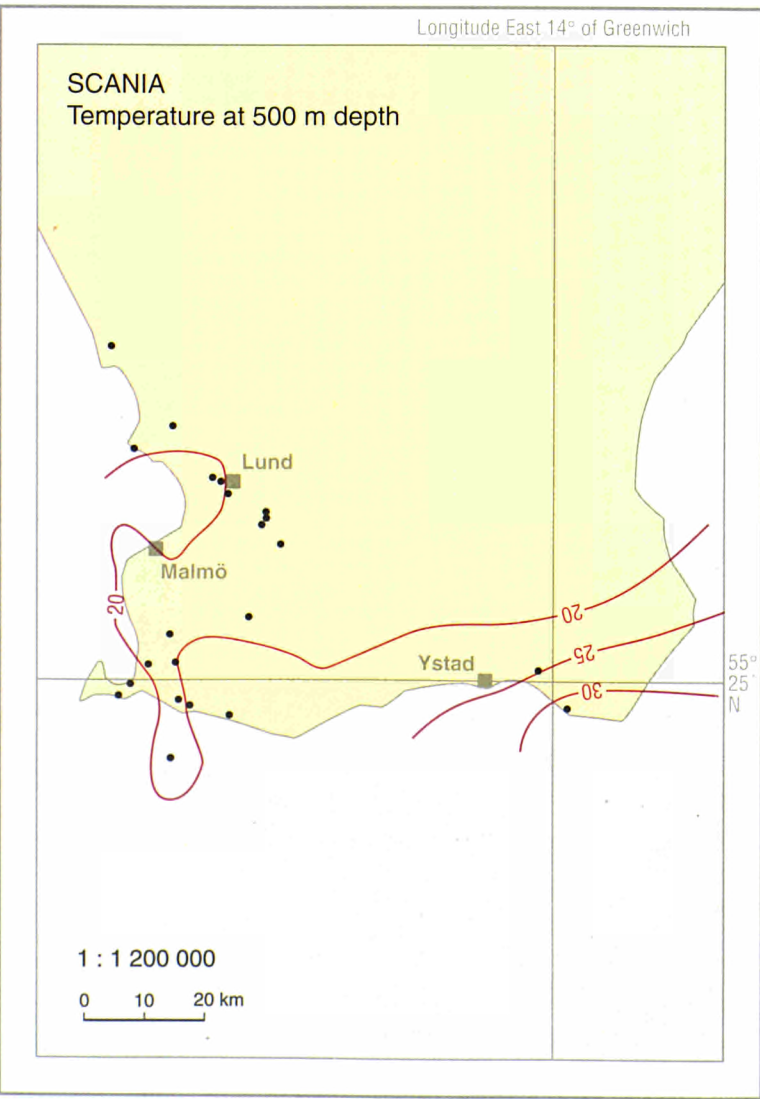
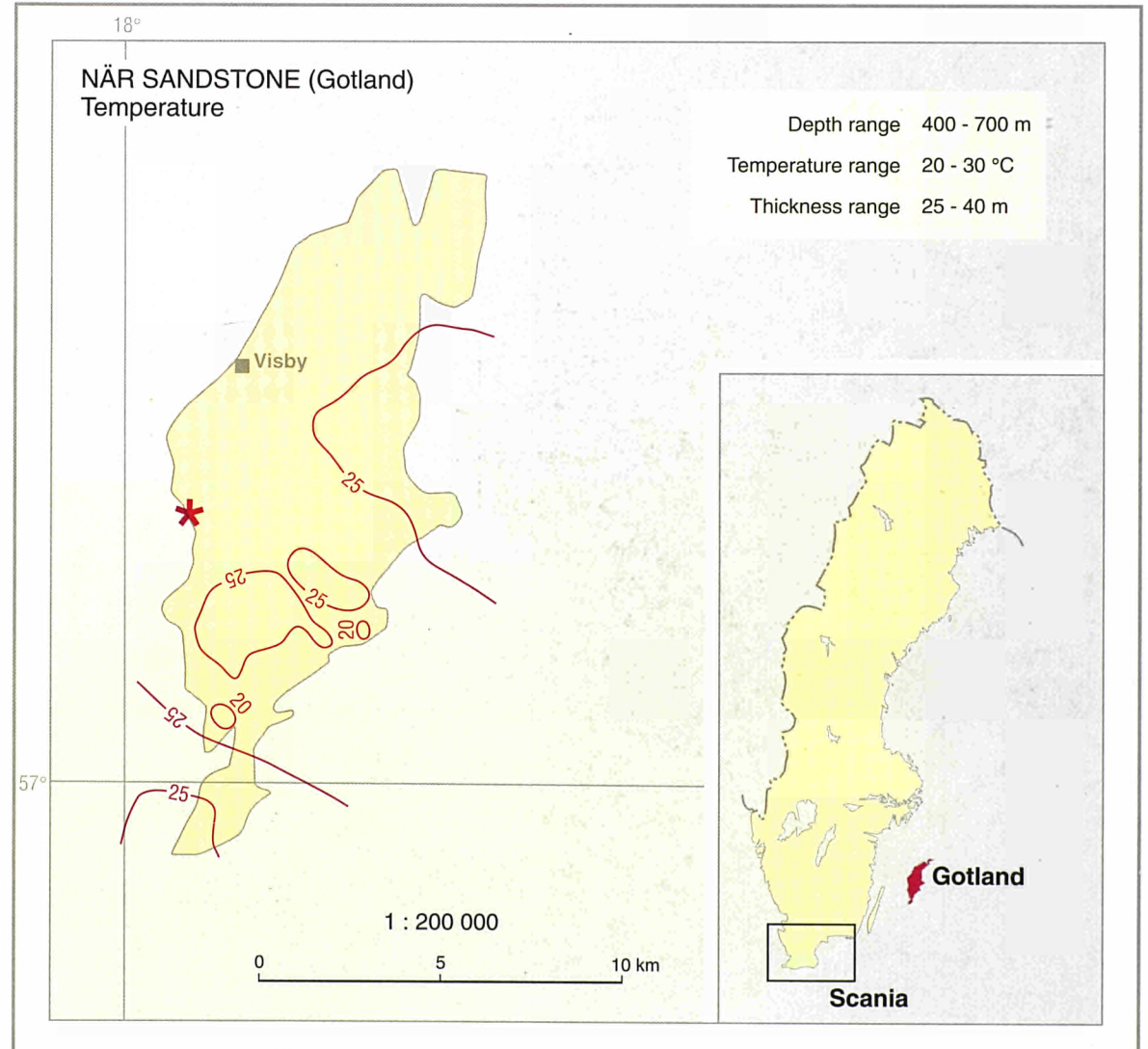
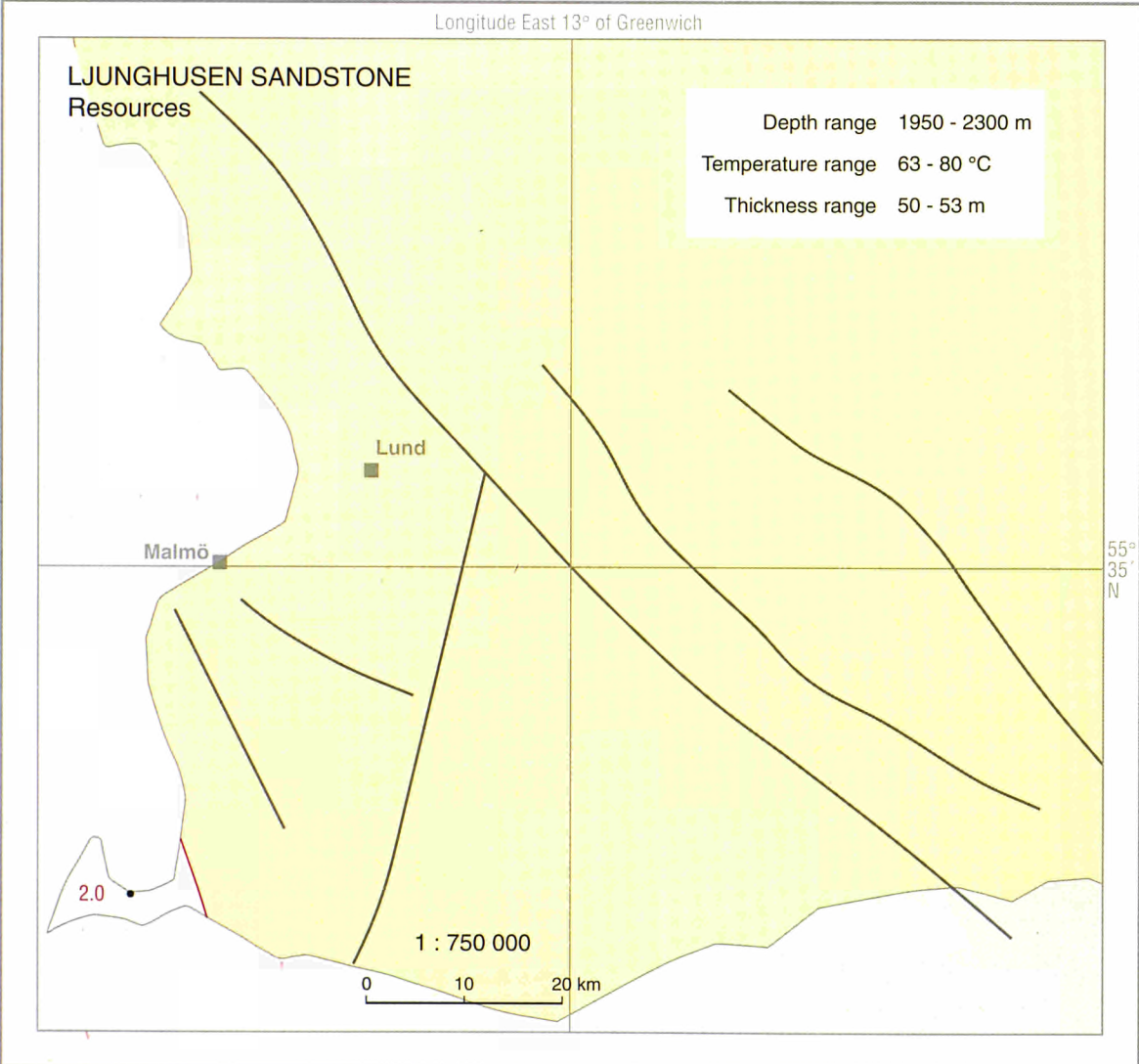
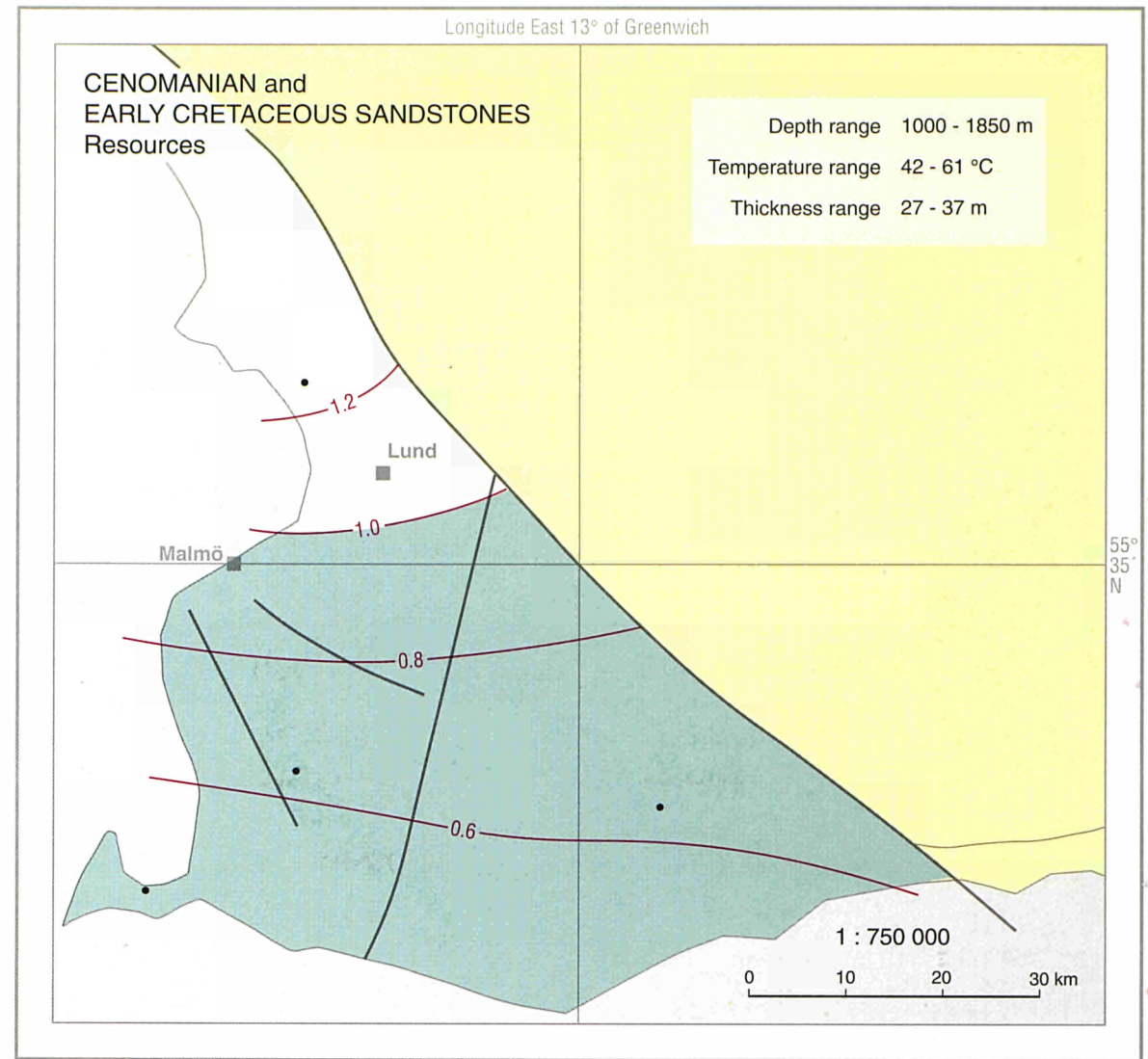
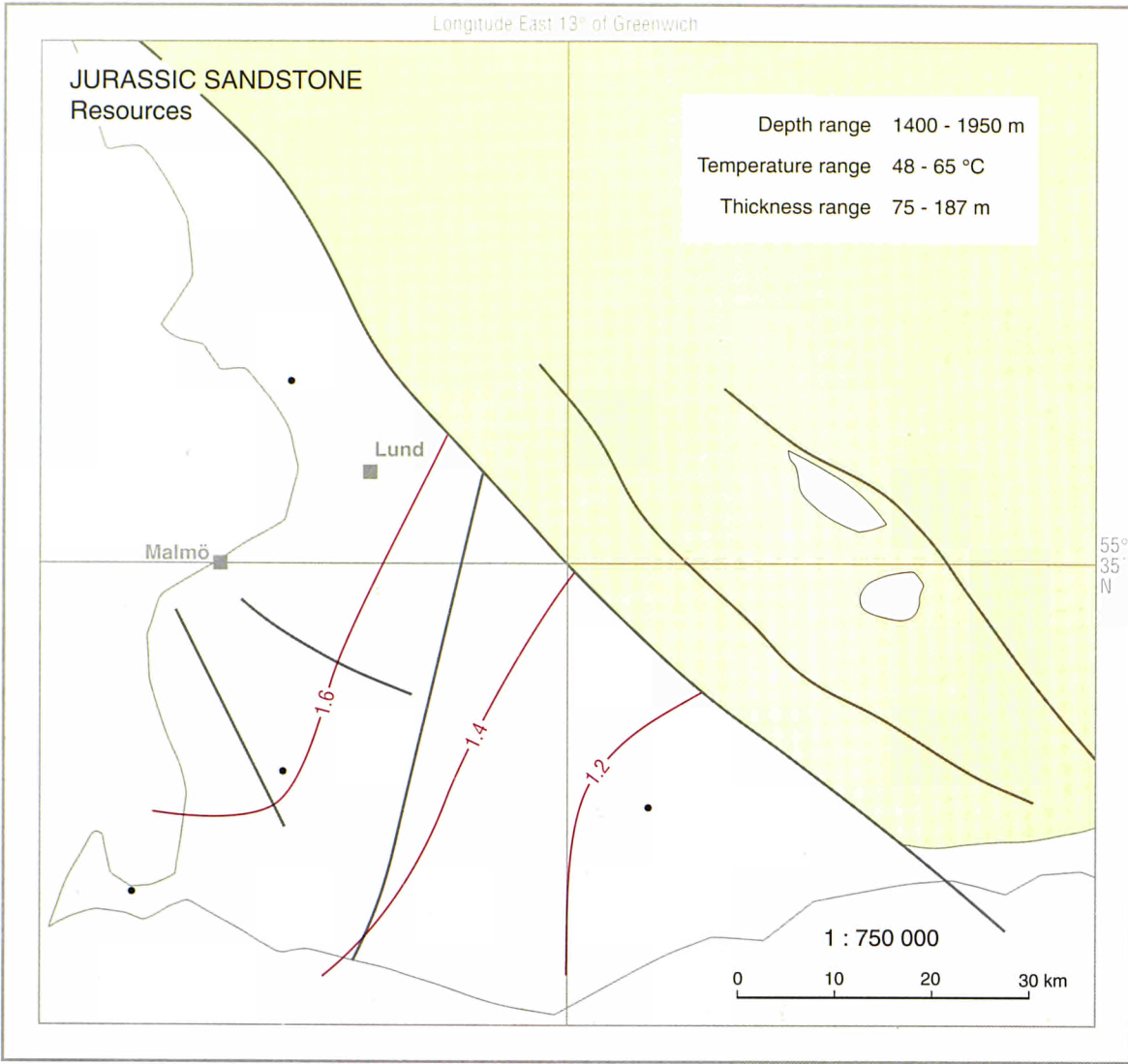
- Campanian Sandstone
- Cenomanian / Early Cretaceous Sandstone
- Jurassic Sandstone
- Kågeröd Arkose / Keuper Sandstone
- Bunter Sandstone
- Ljunghusen Sandstone
- Boreholes
- Fault

LOCATION MAP

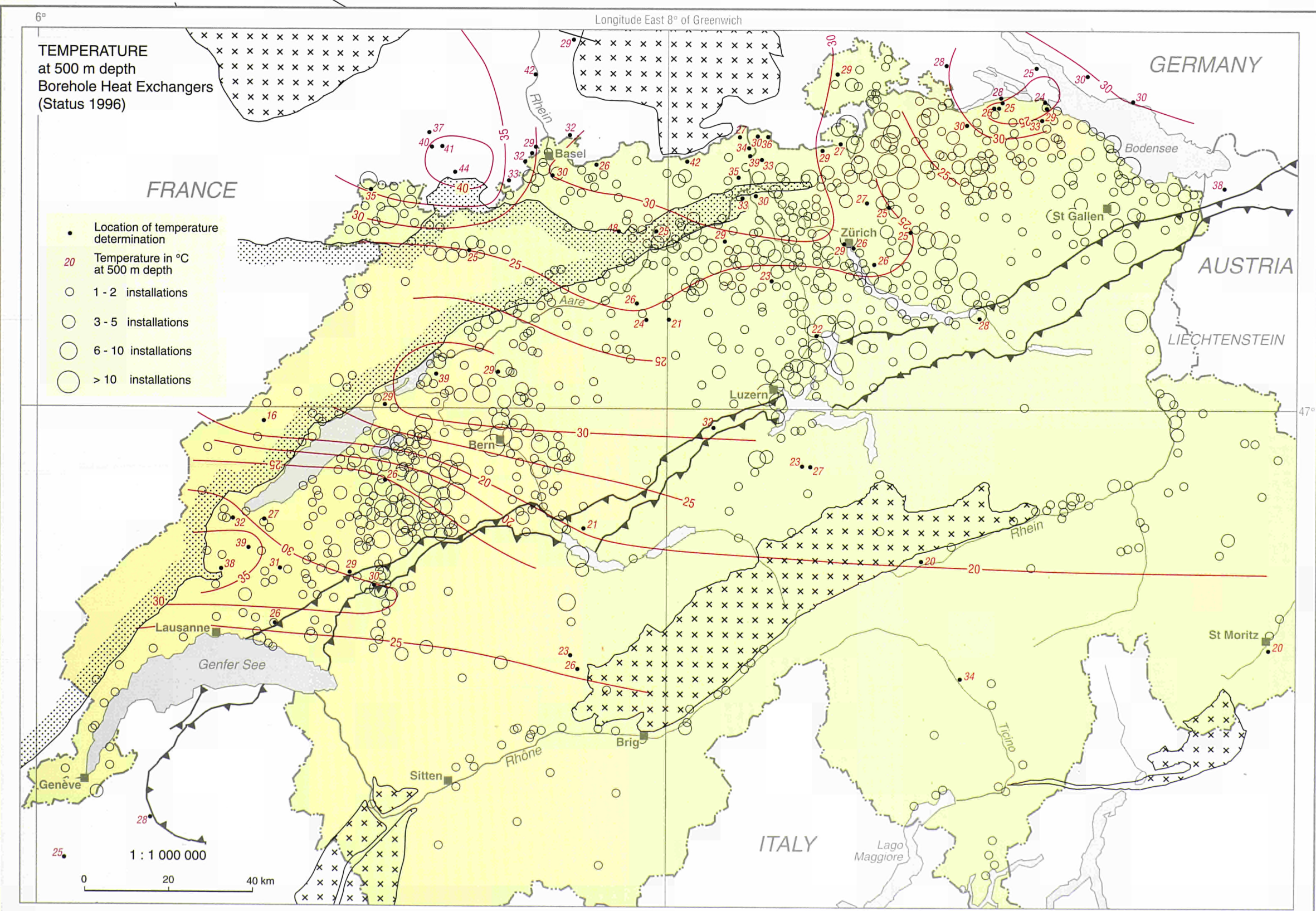
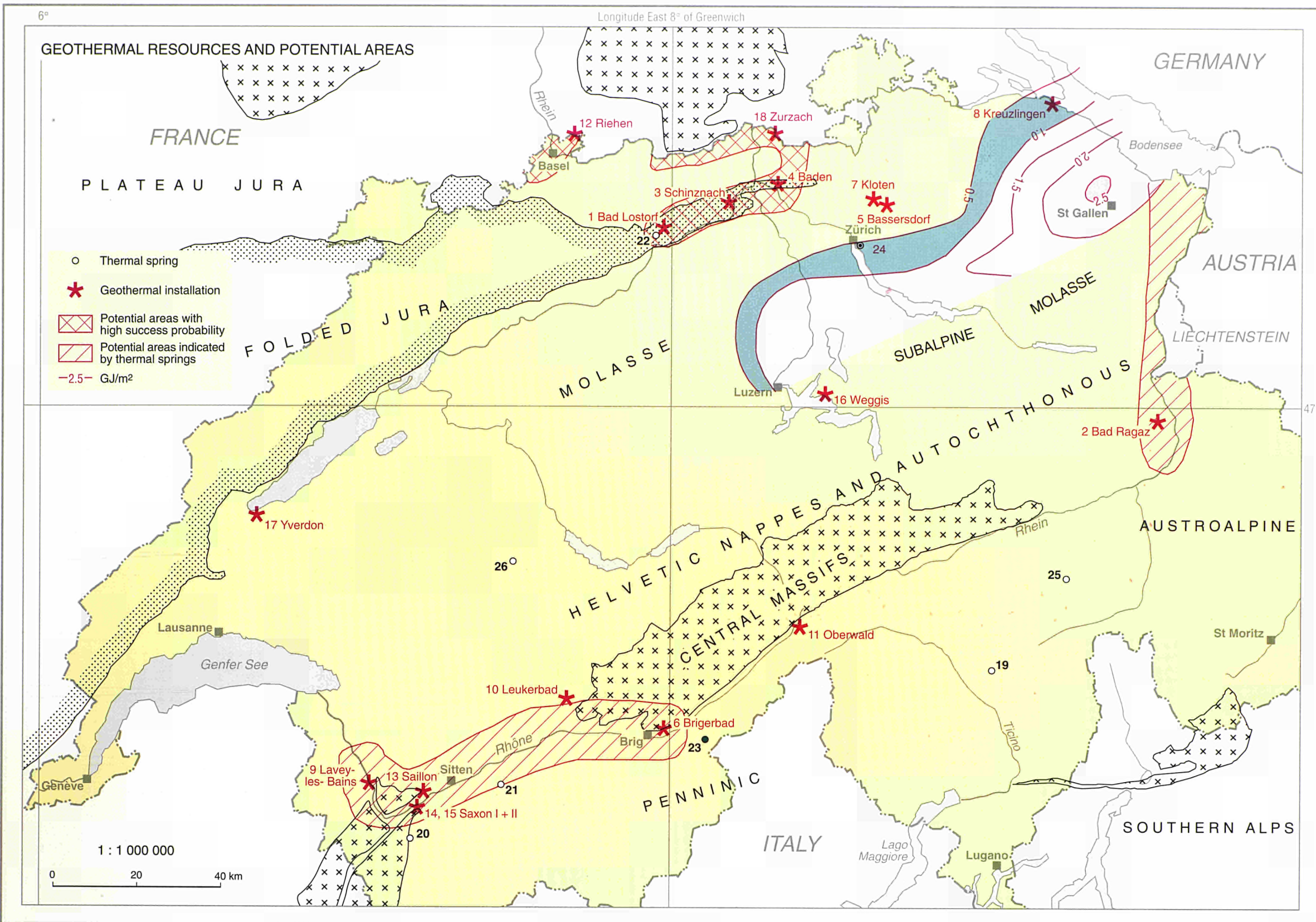


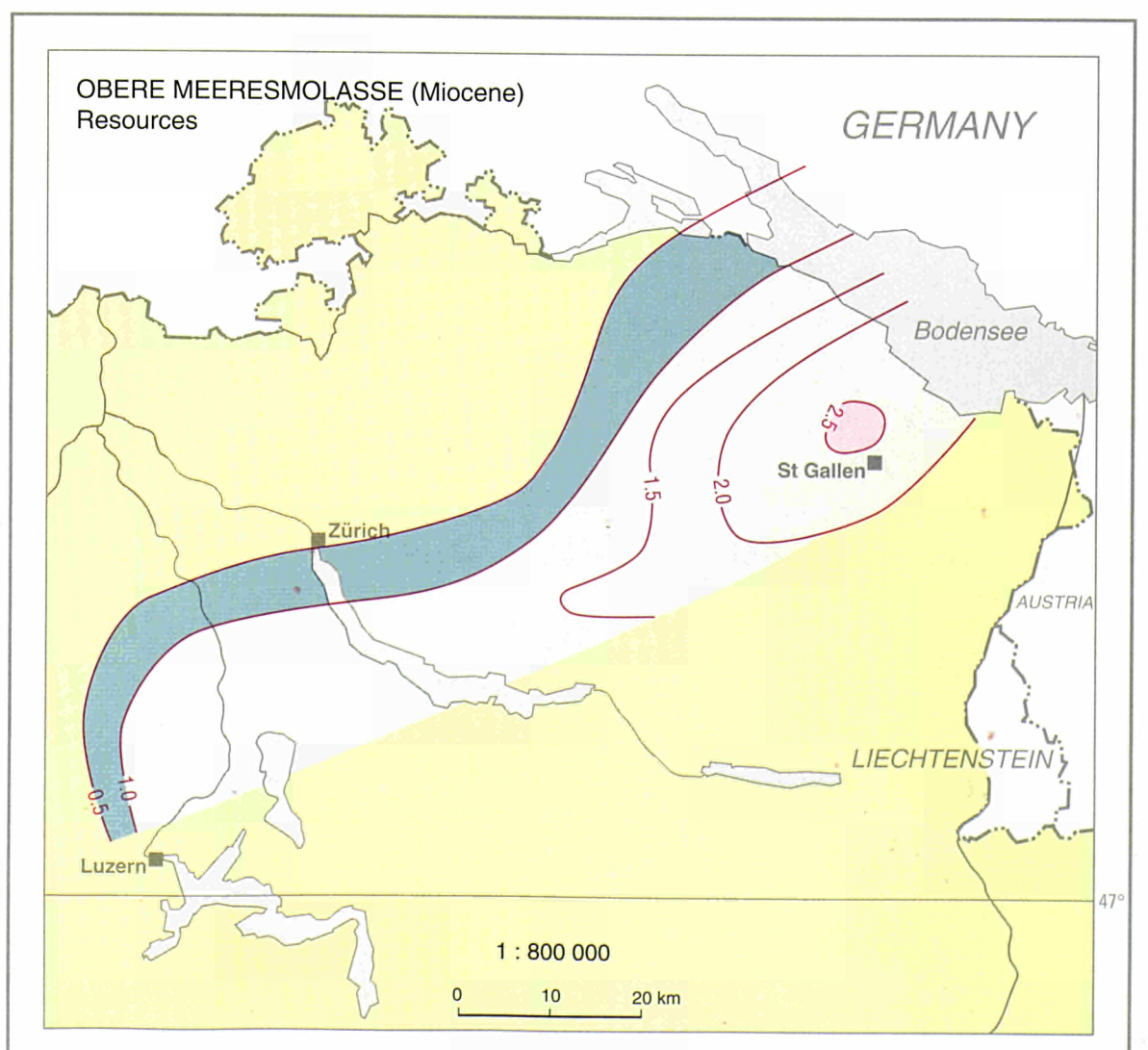
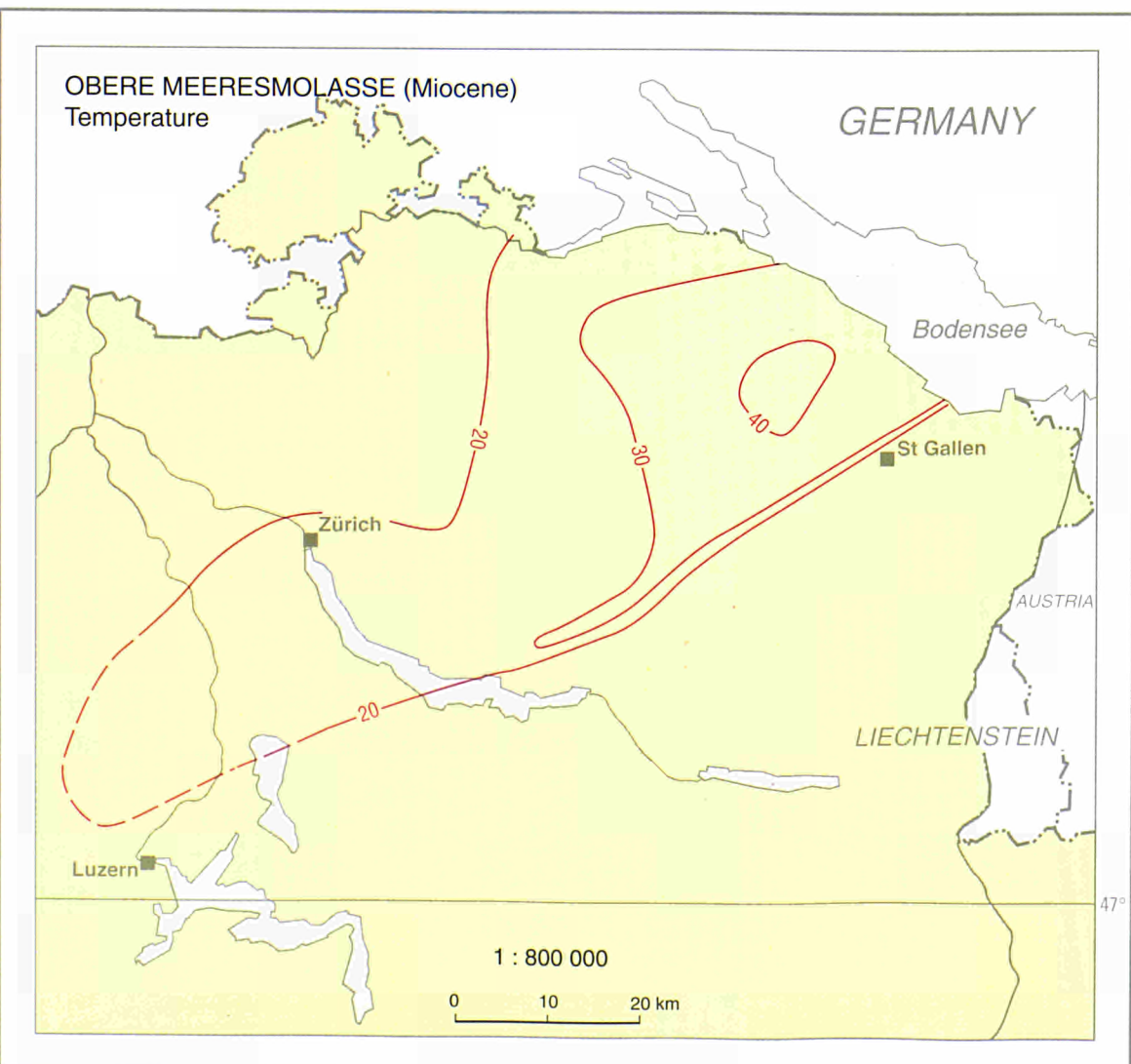
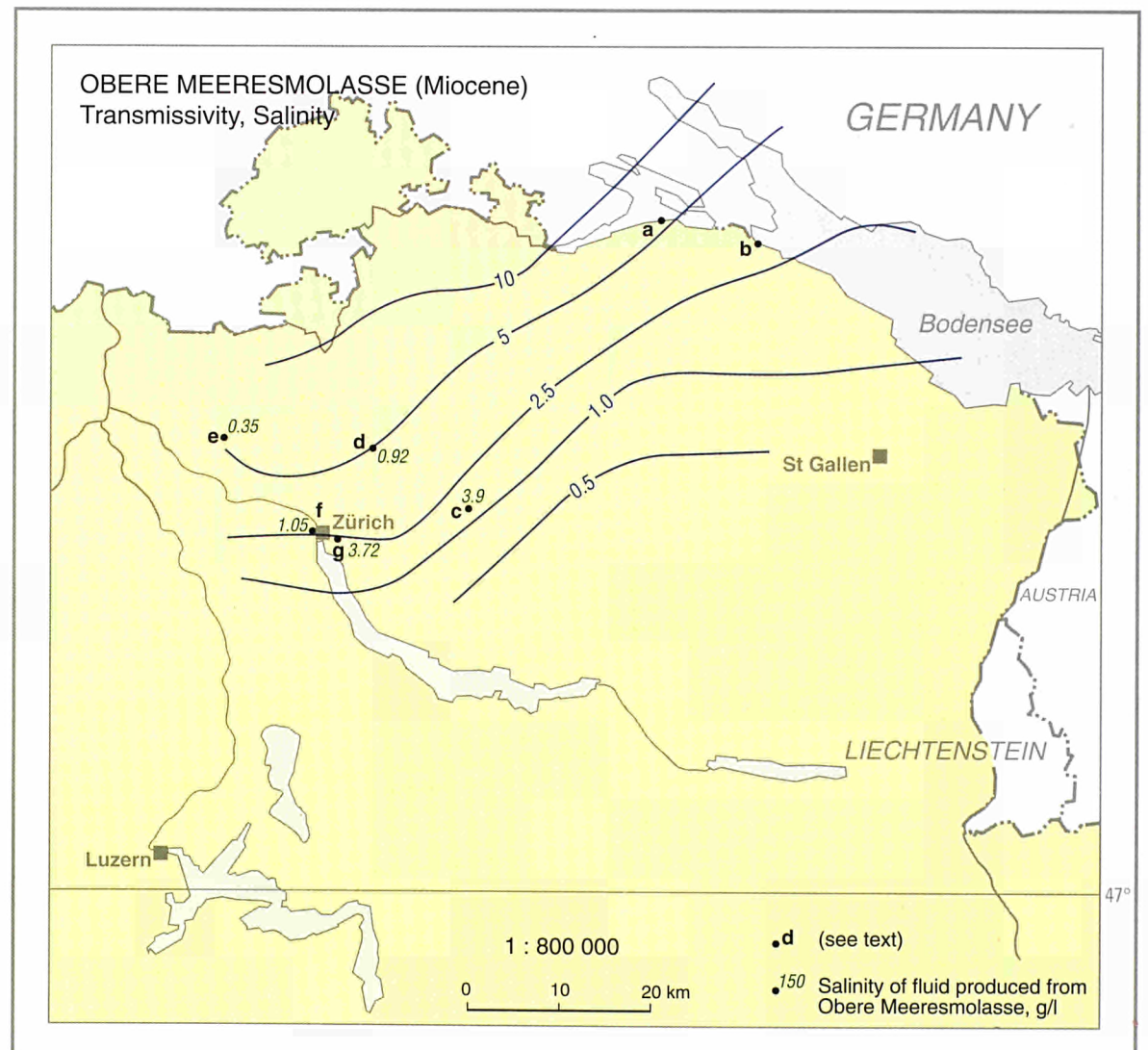
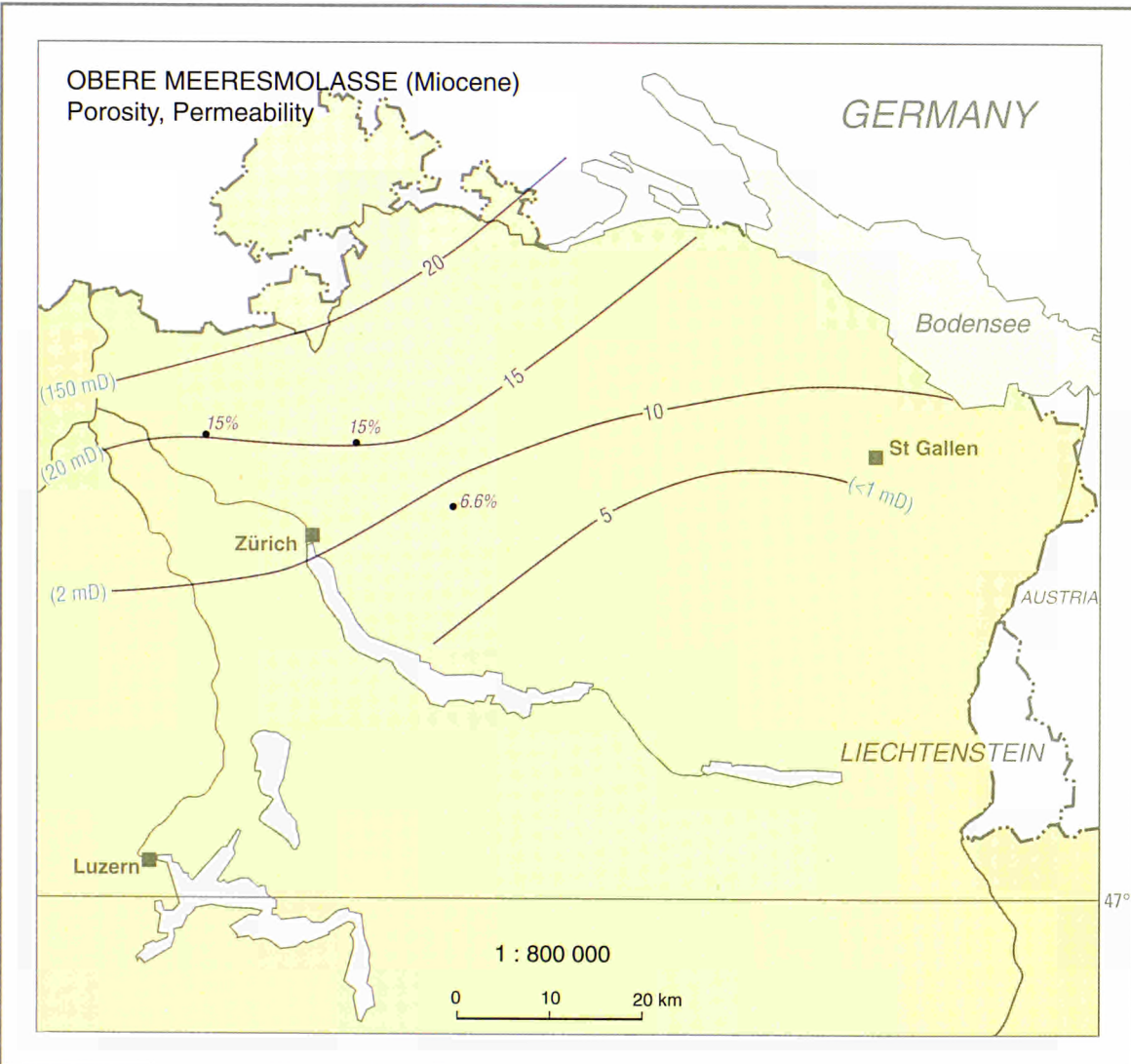
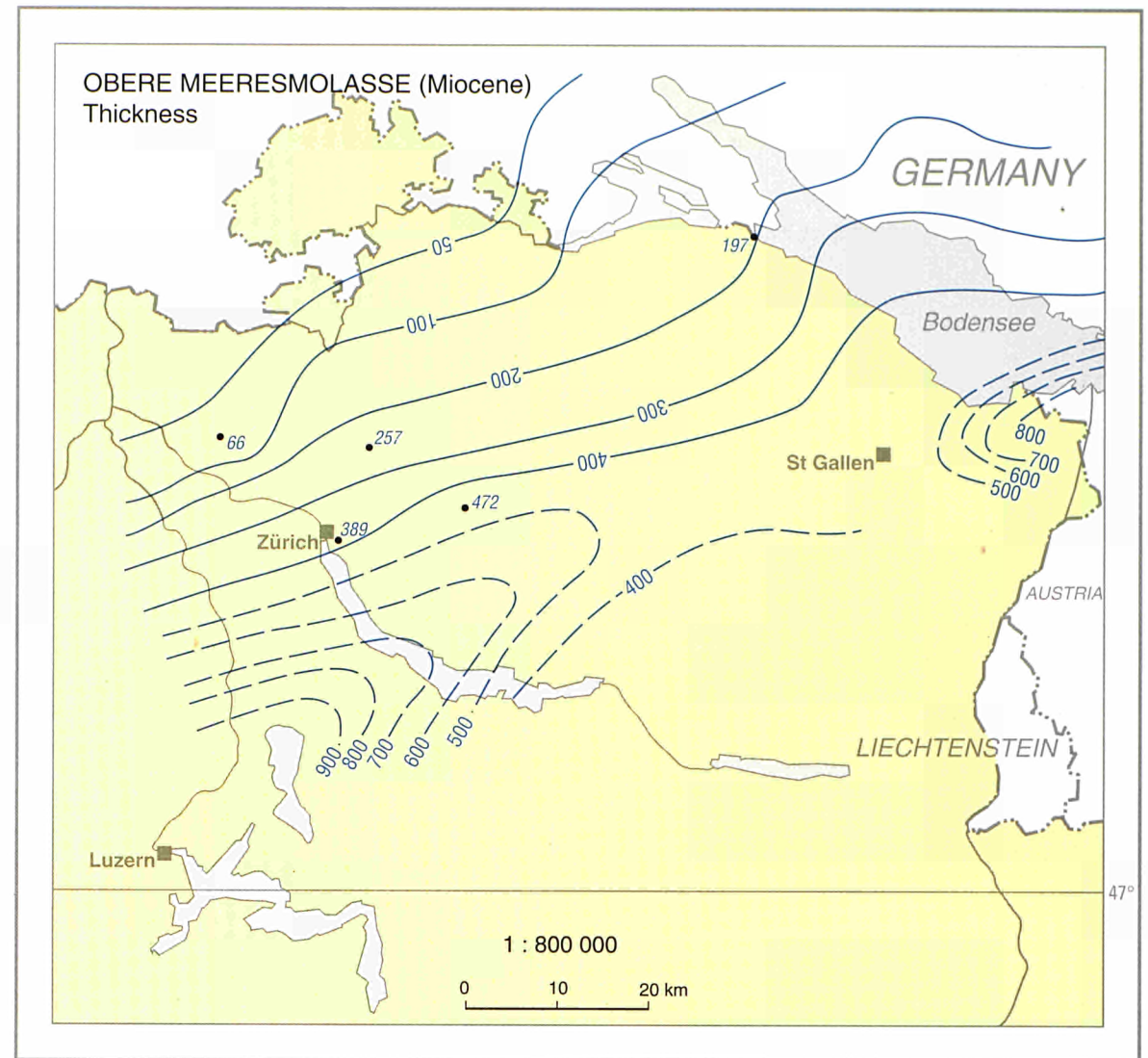
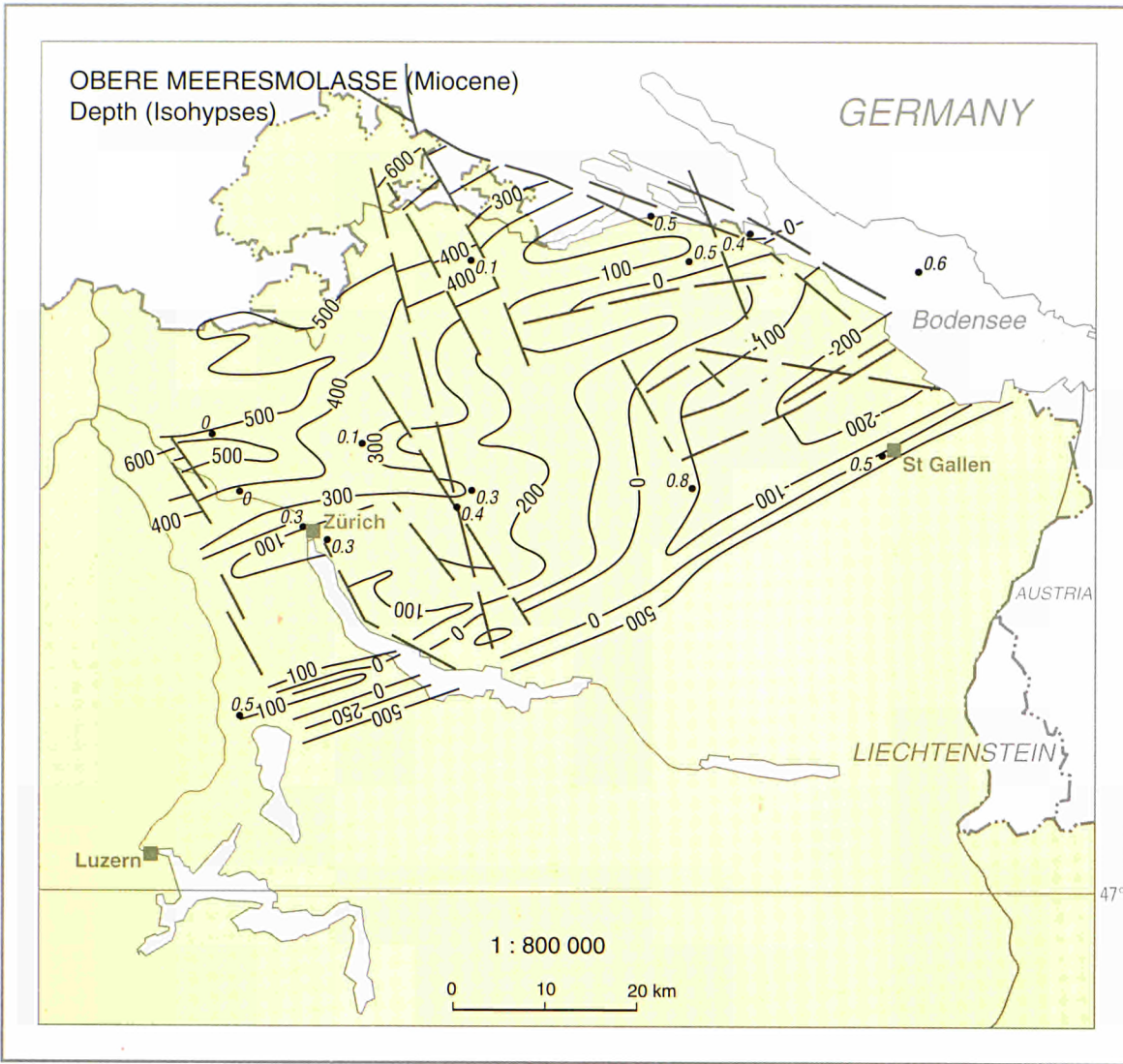
SWEDEN, Scania



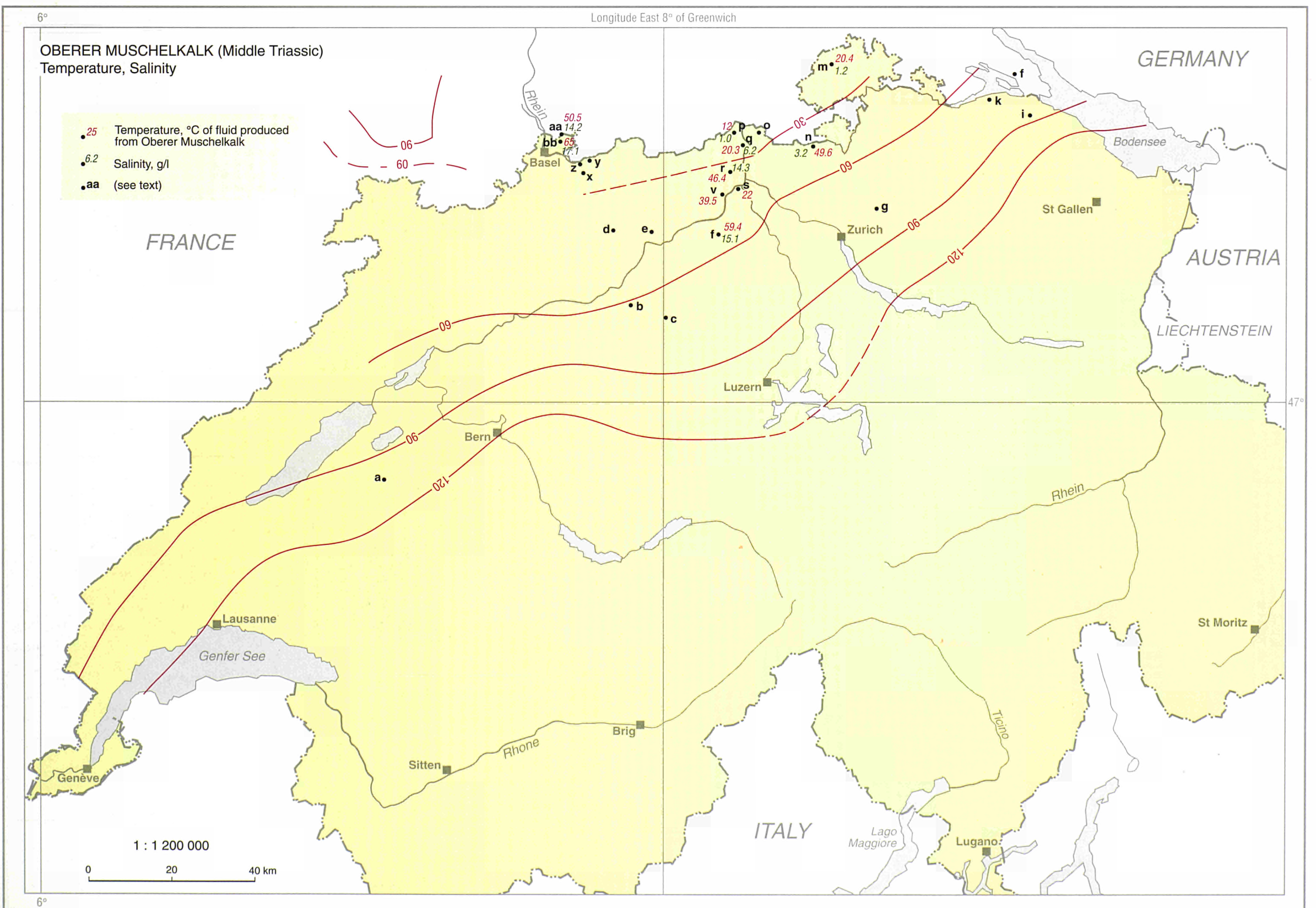
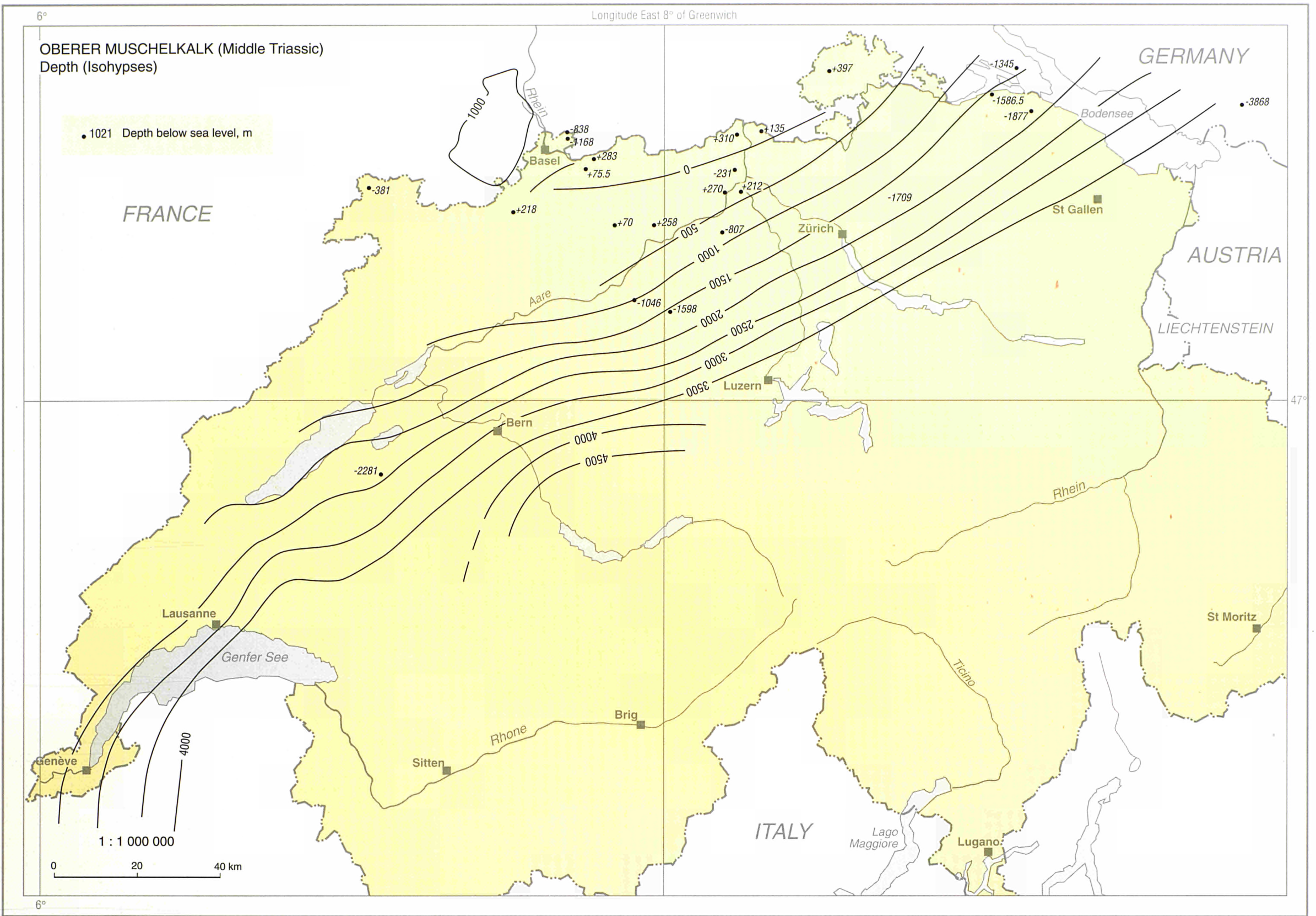


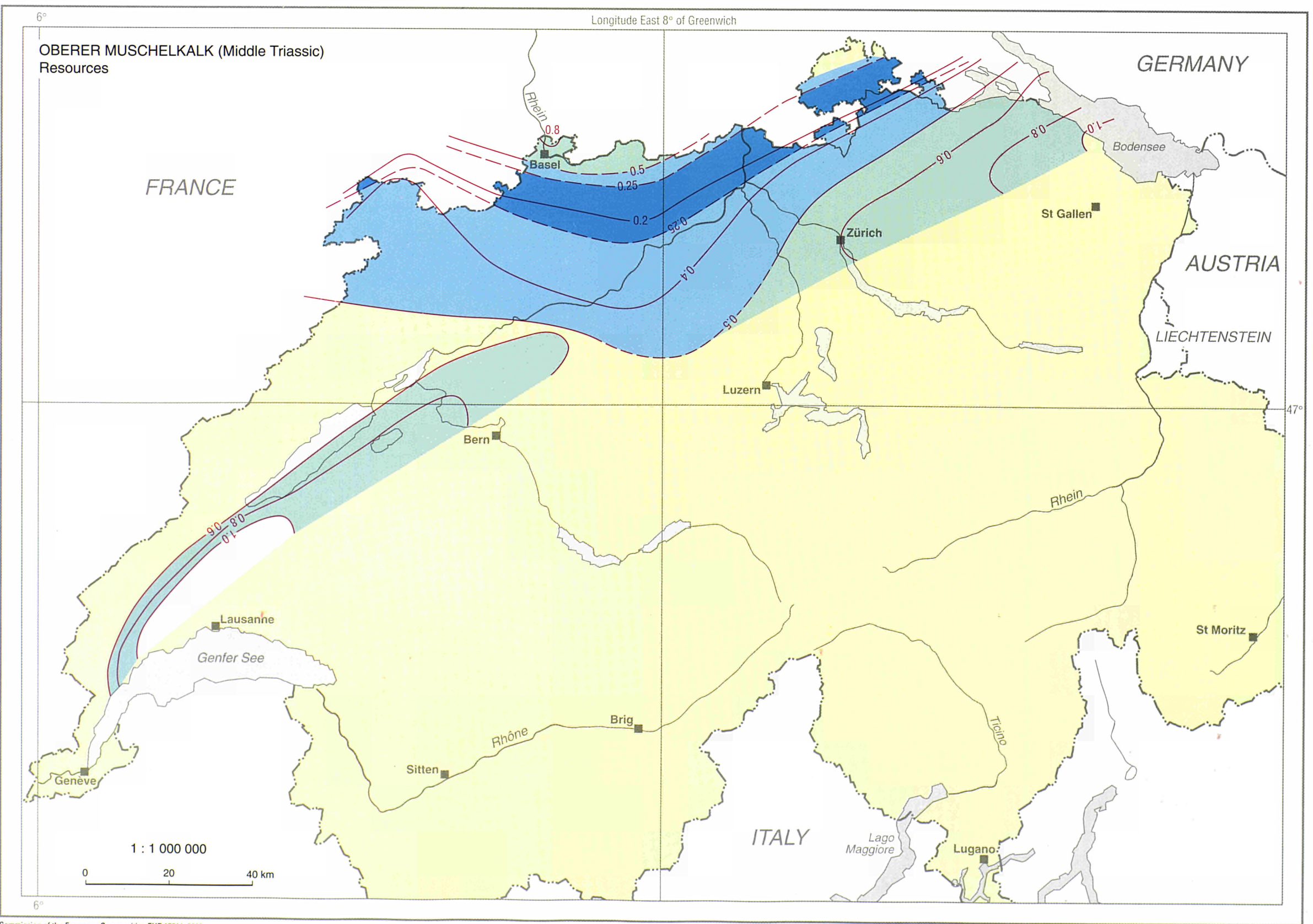
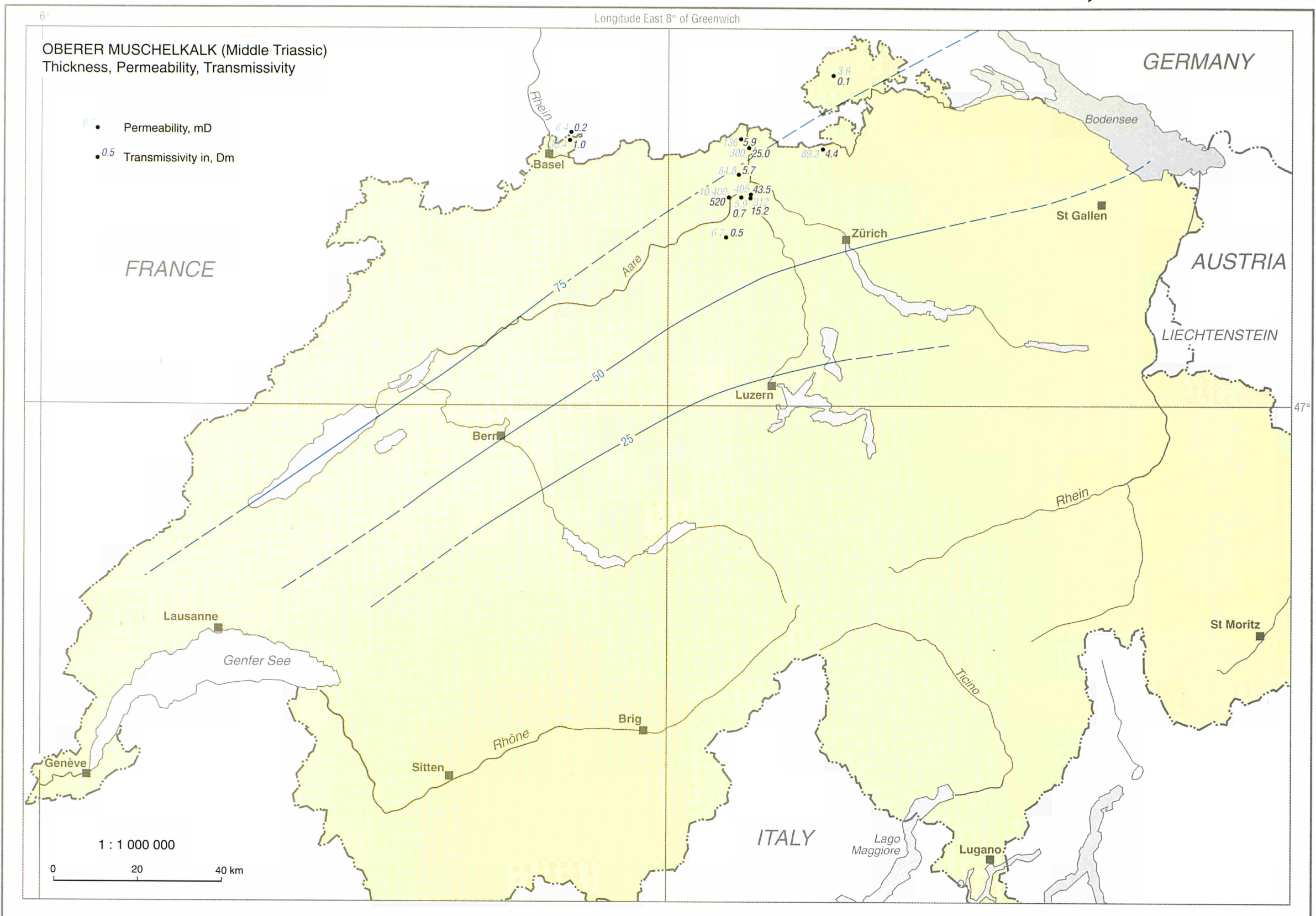
SWITZERLAND





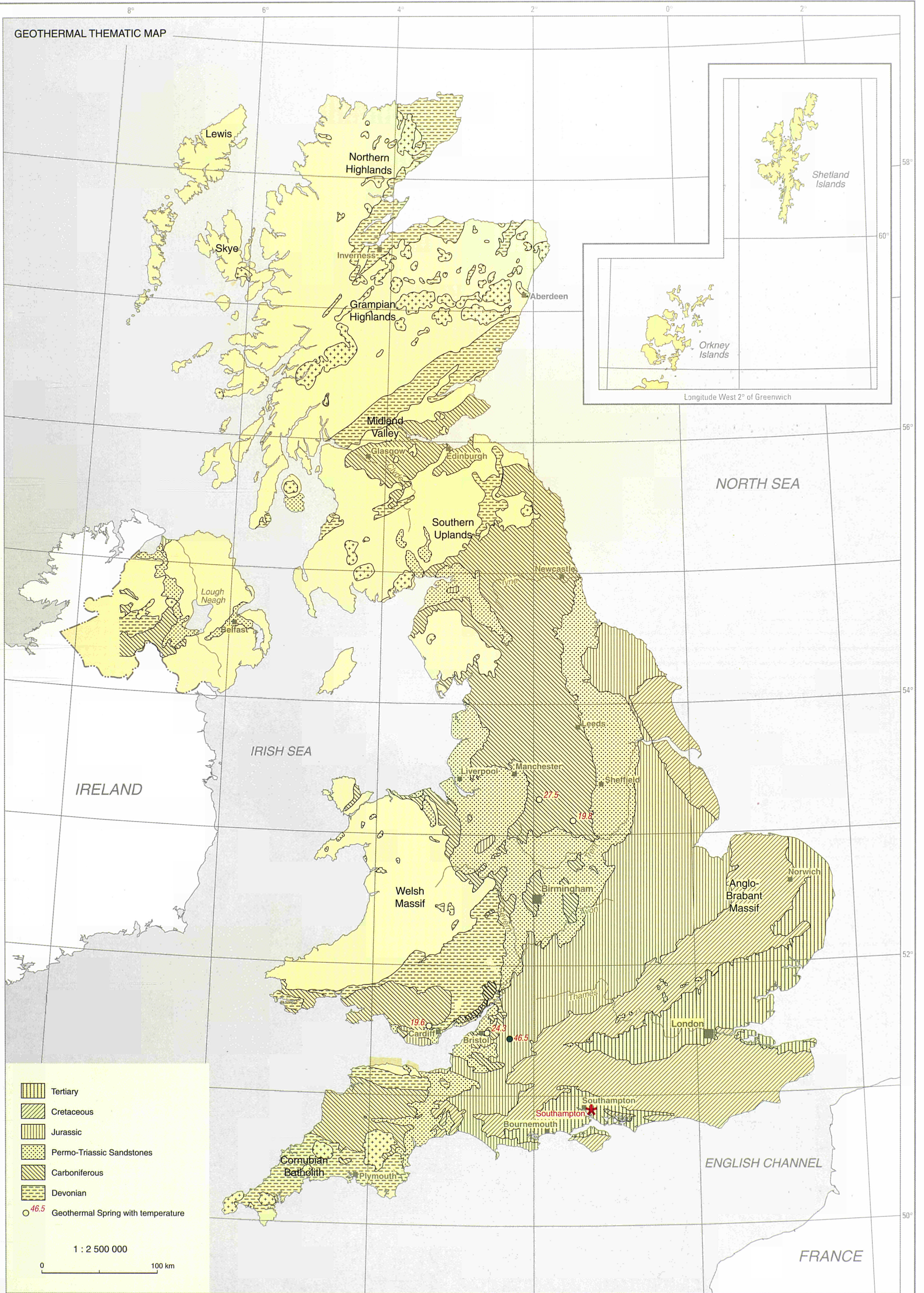
SWITZERLAND, Jura

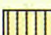


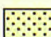

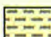





UNITED KINGDOM

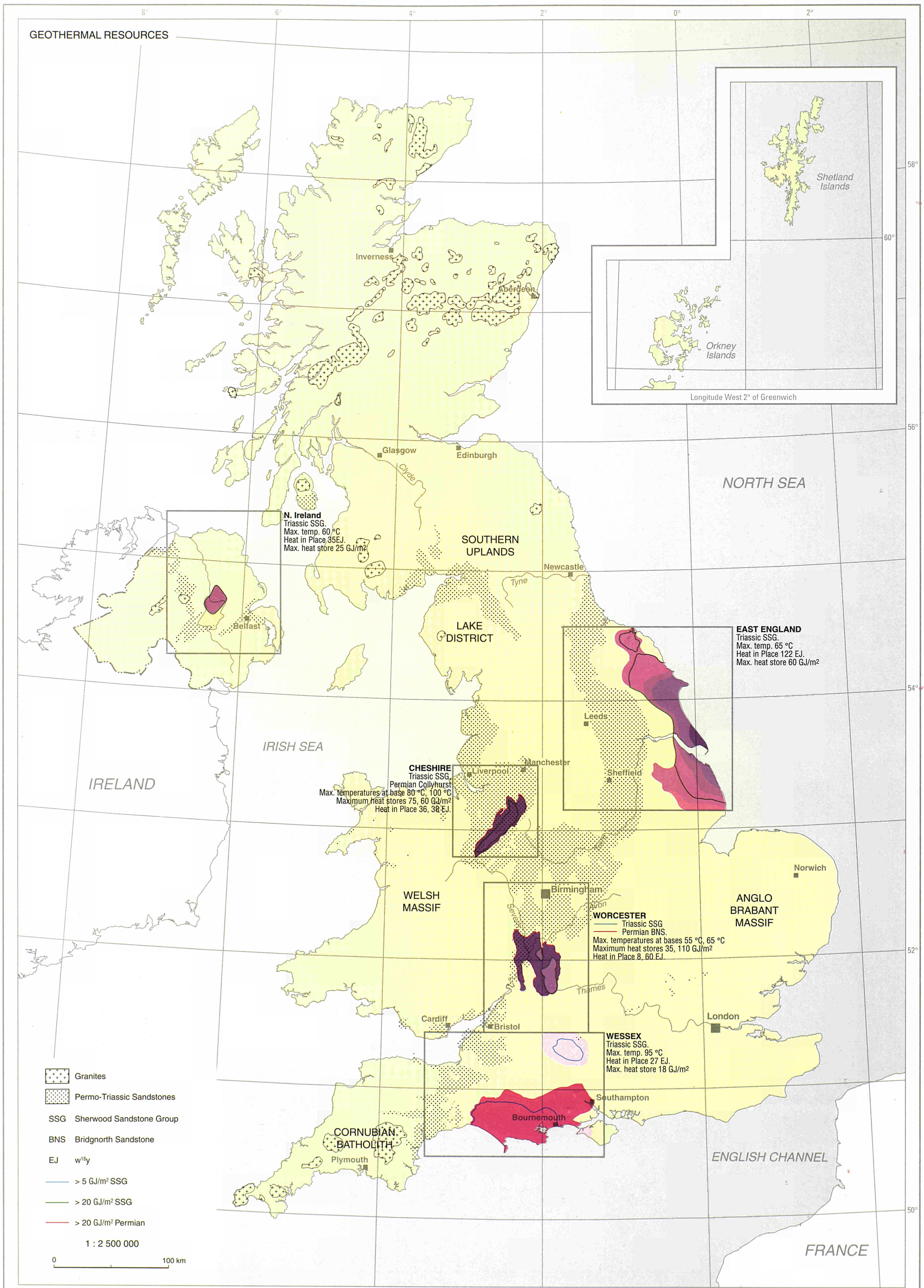
GEOTHERMAL THEMATIC MAP



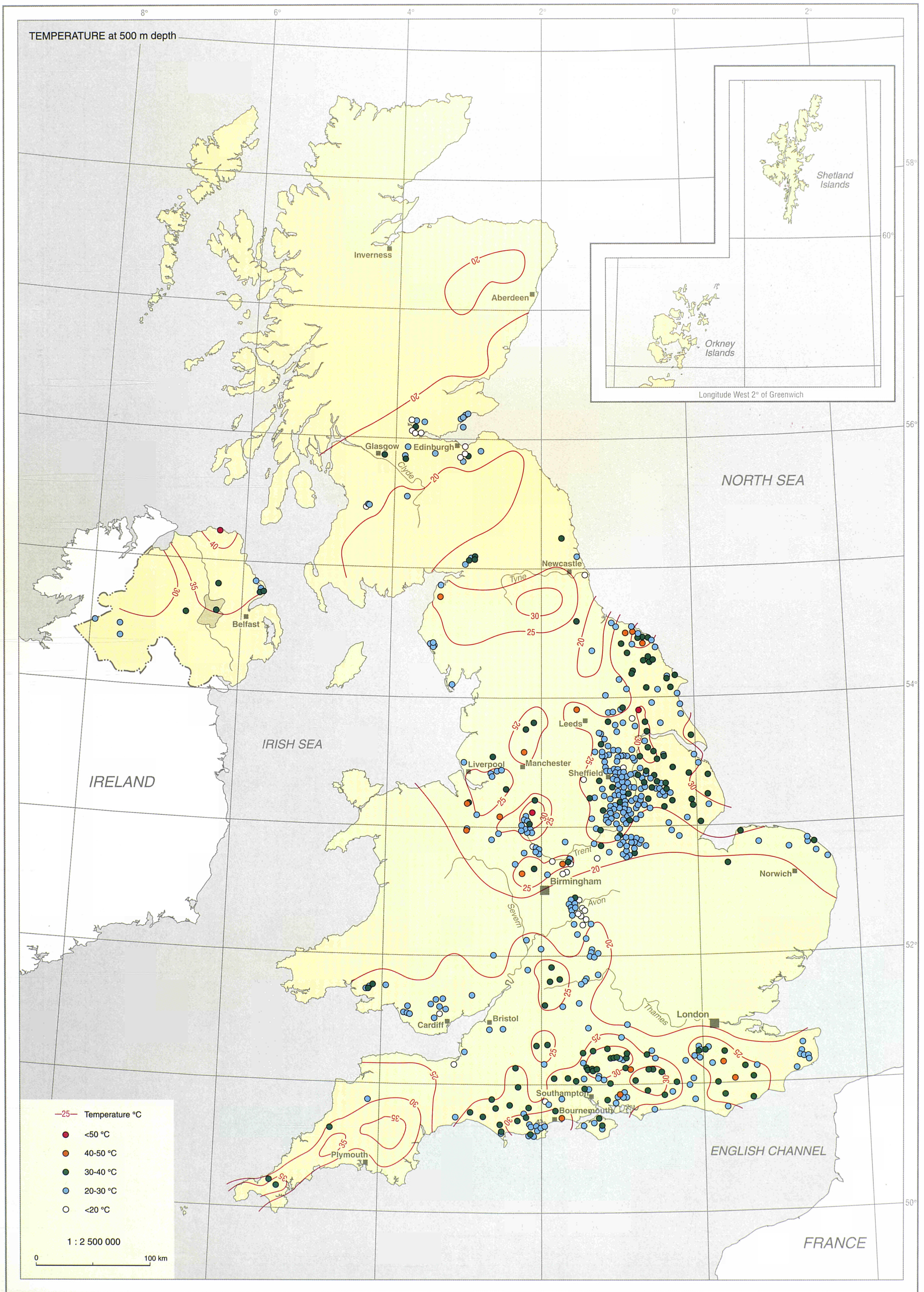
-  Tertiary
-  Cretaceous
-  Jurassic
-  Permo-Triassic Sandstones
-  Carboniferous
-  Devonian
-  46.5 Geothermal Spring with temperature

1 : 2 500 000

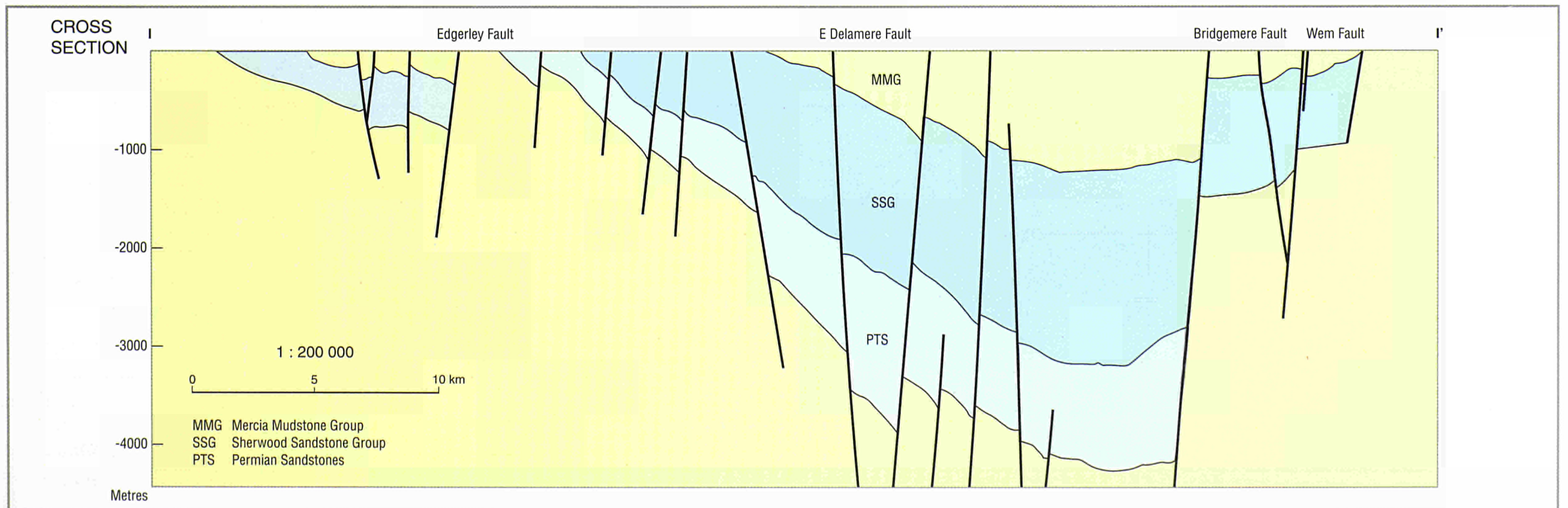
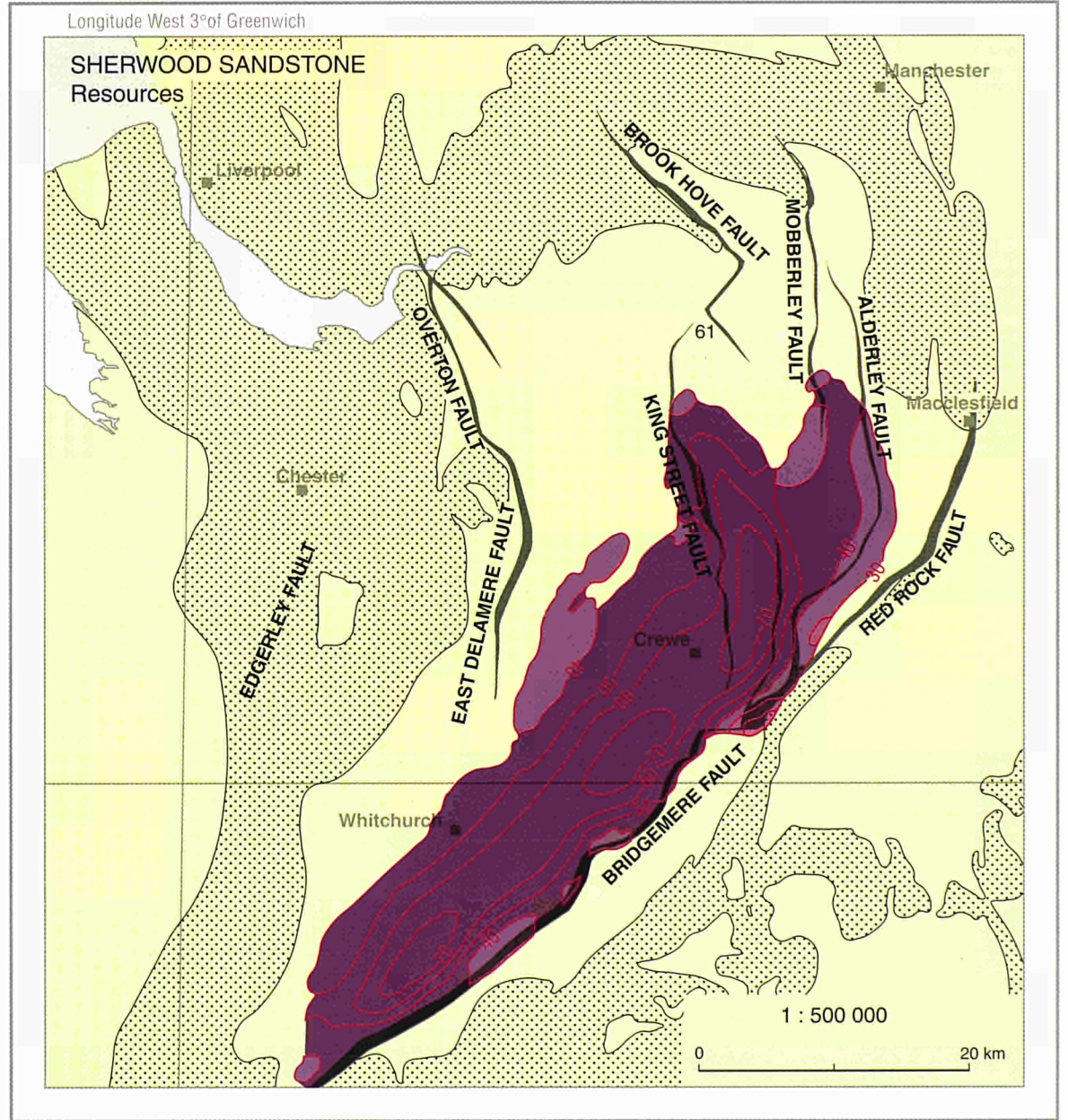
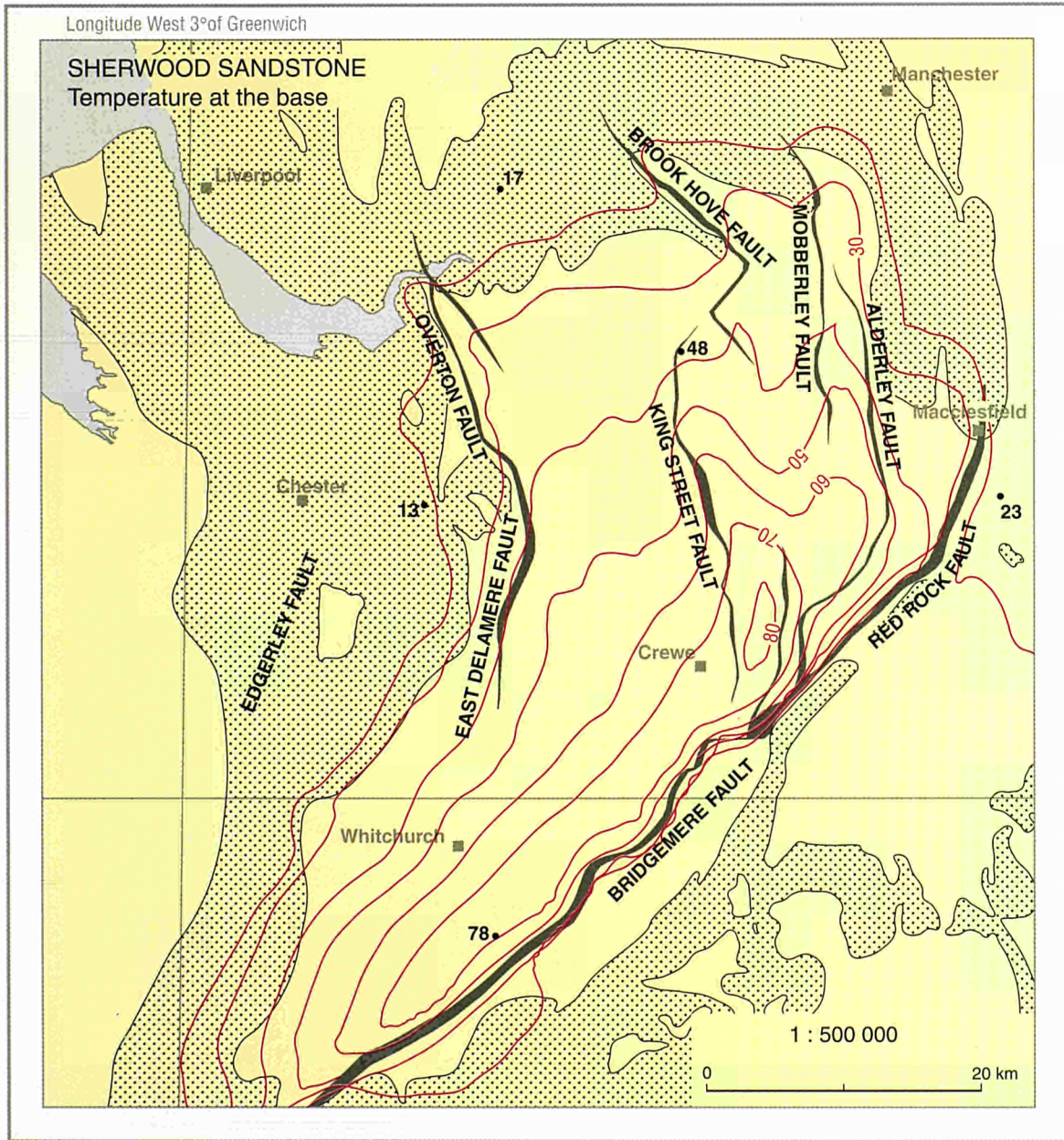
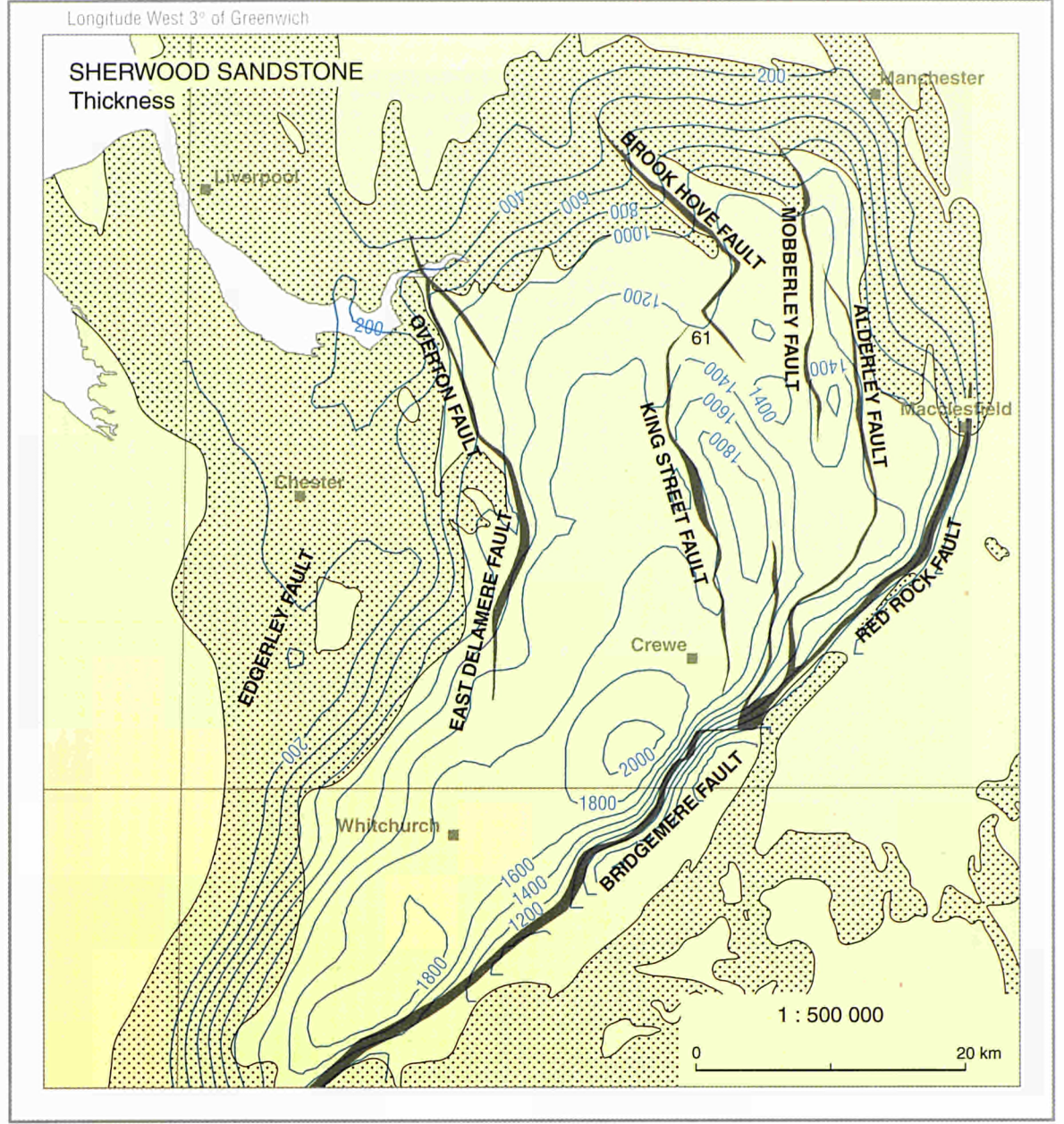
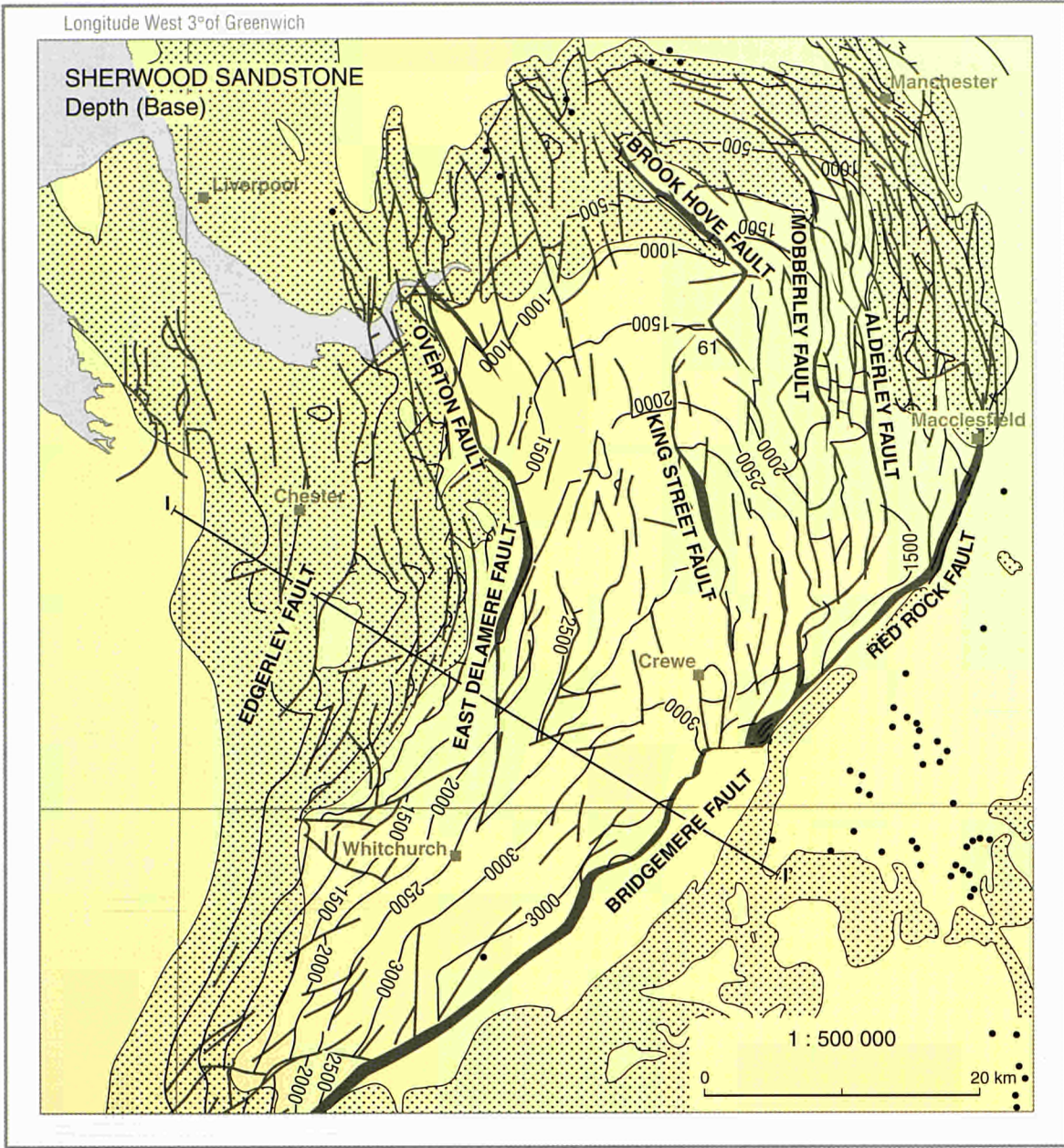
0 100 km

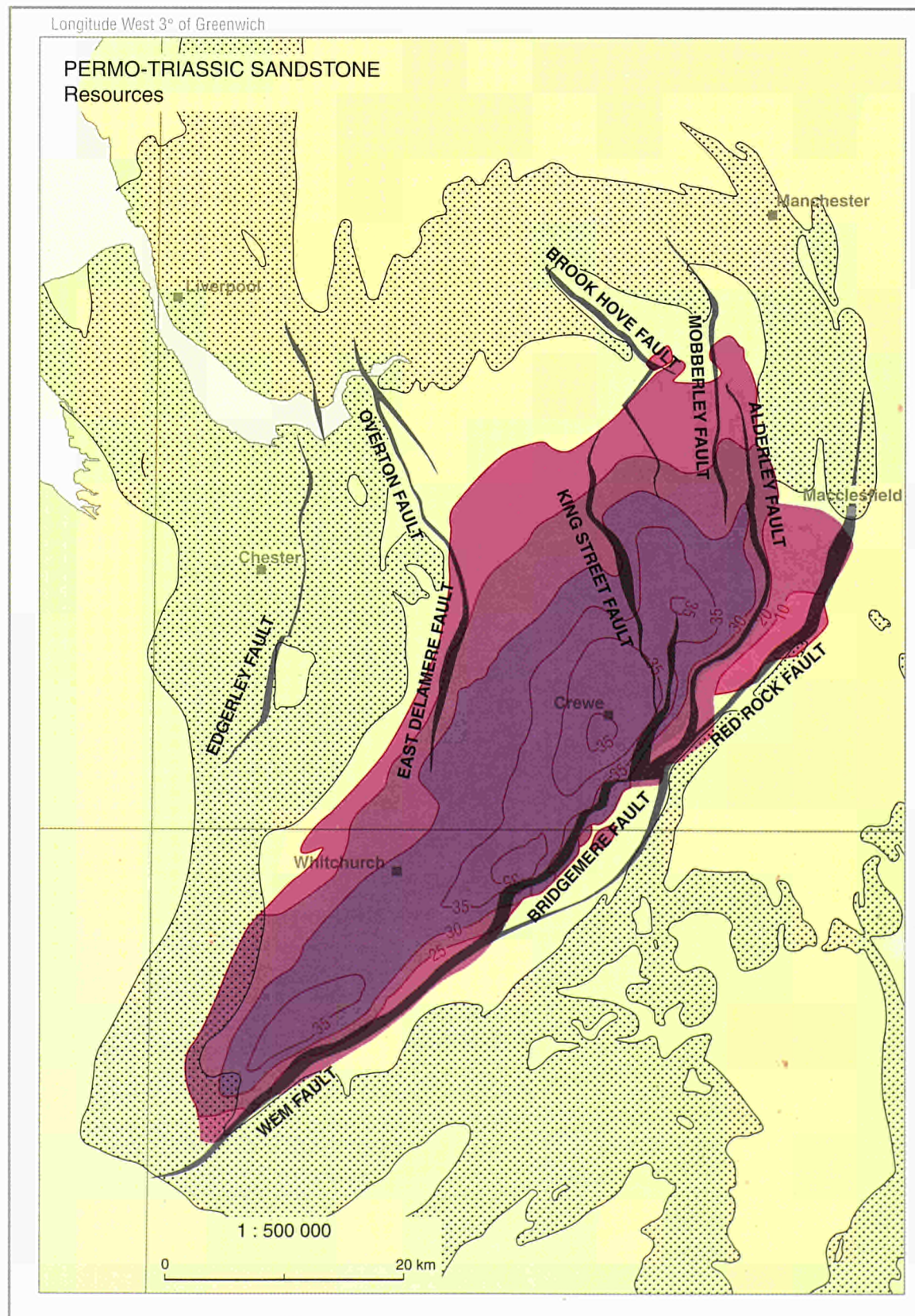
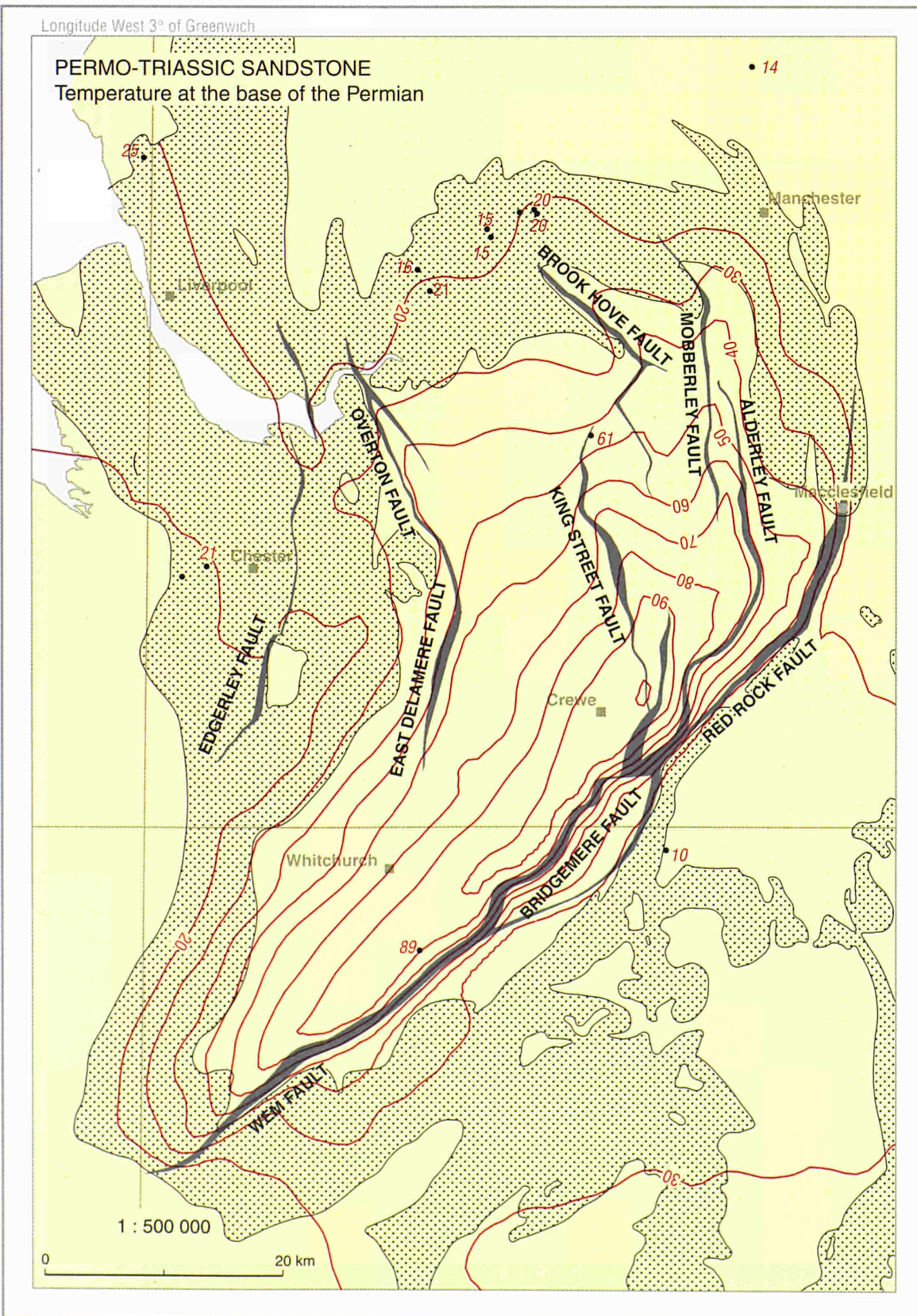
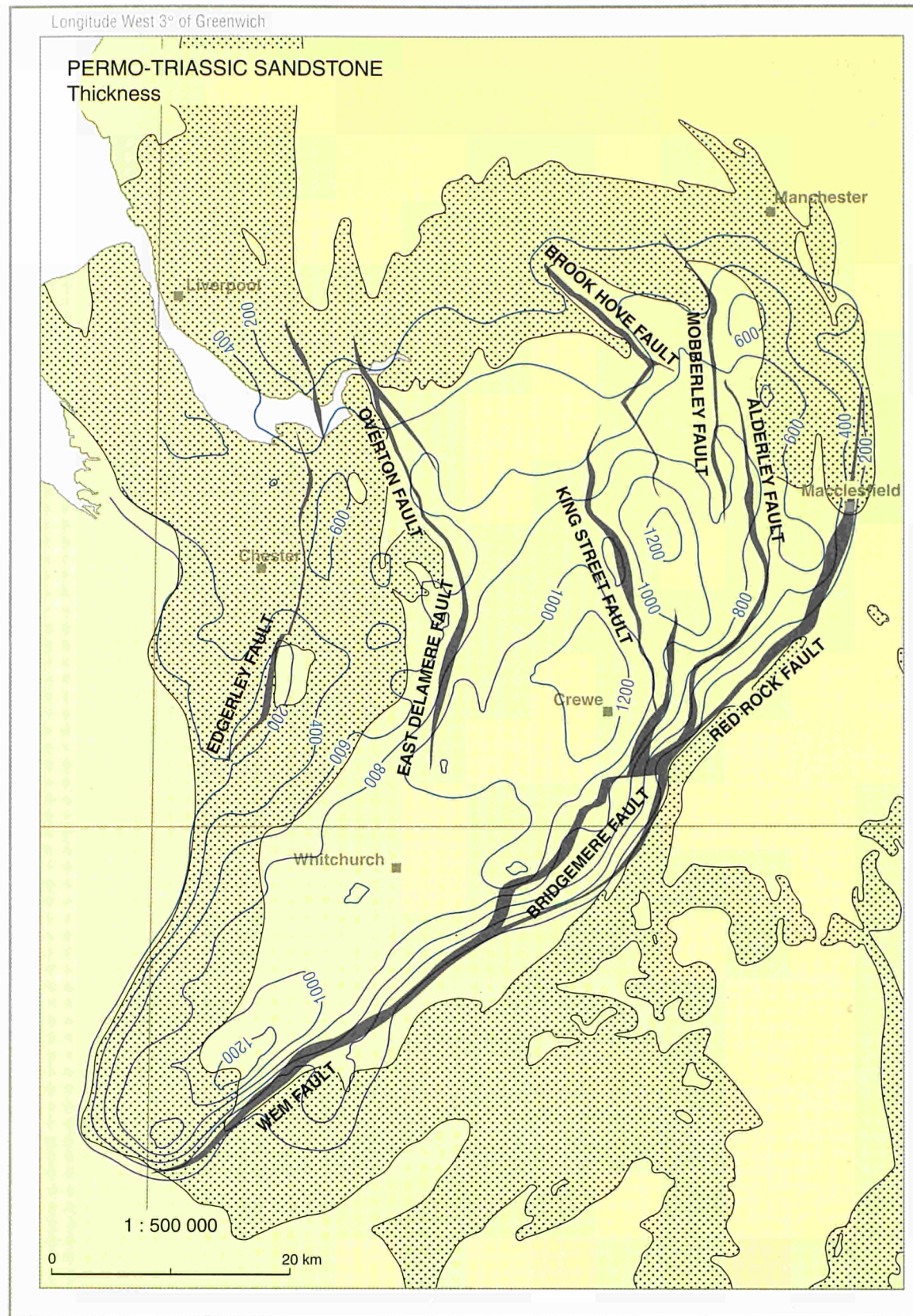
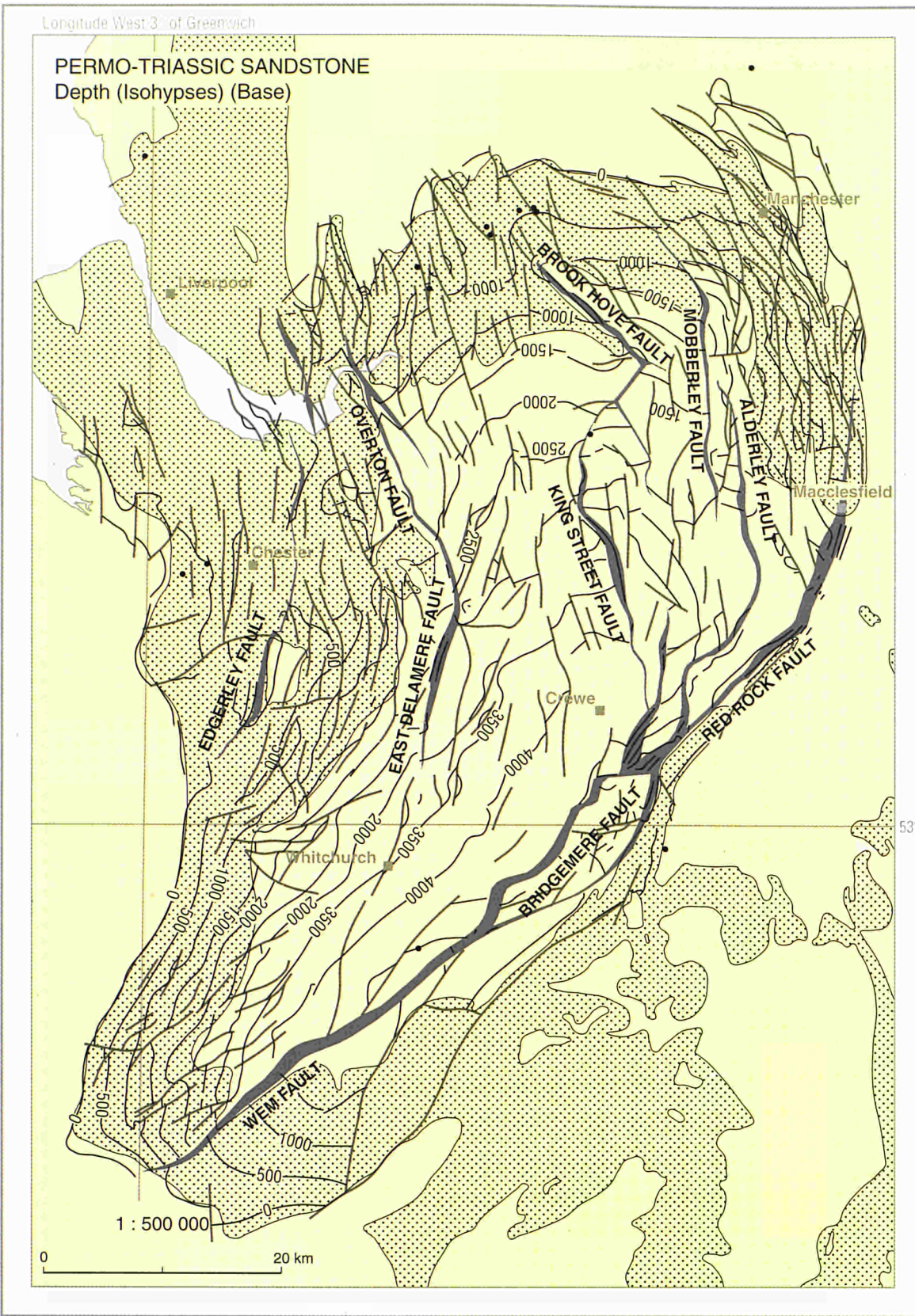


UNITED KINGDOM

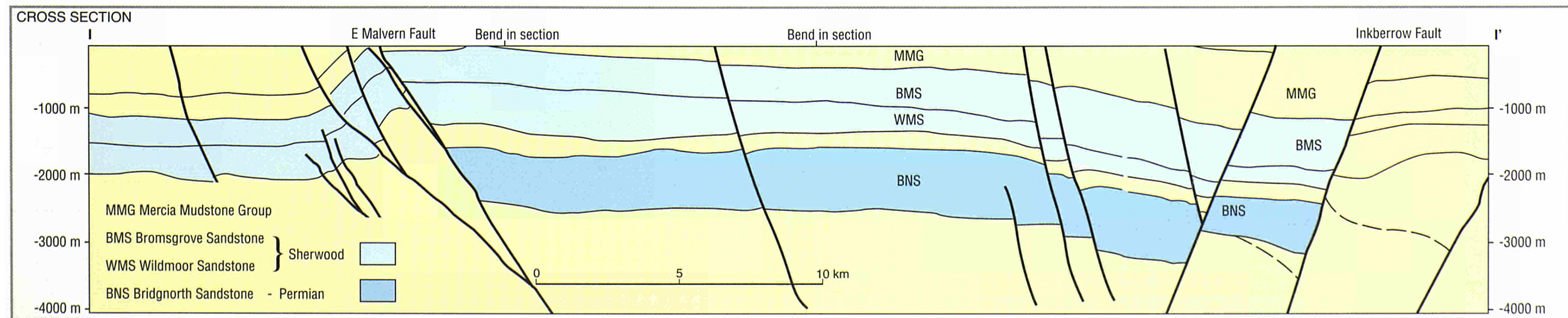
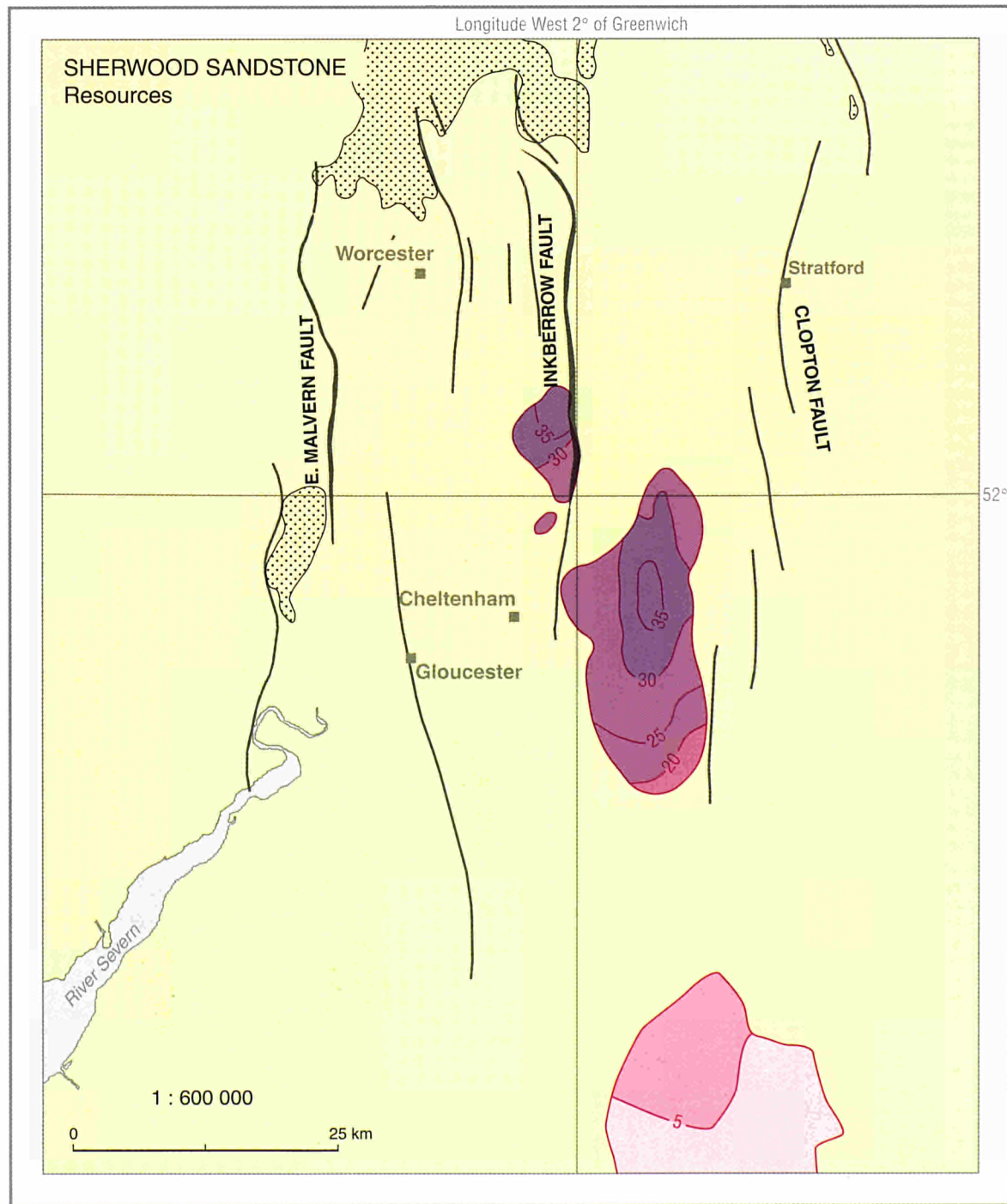
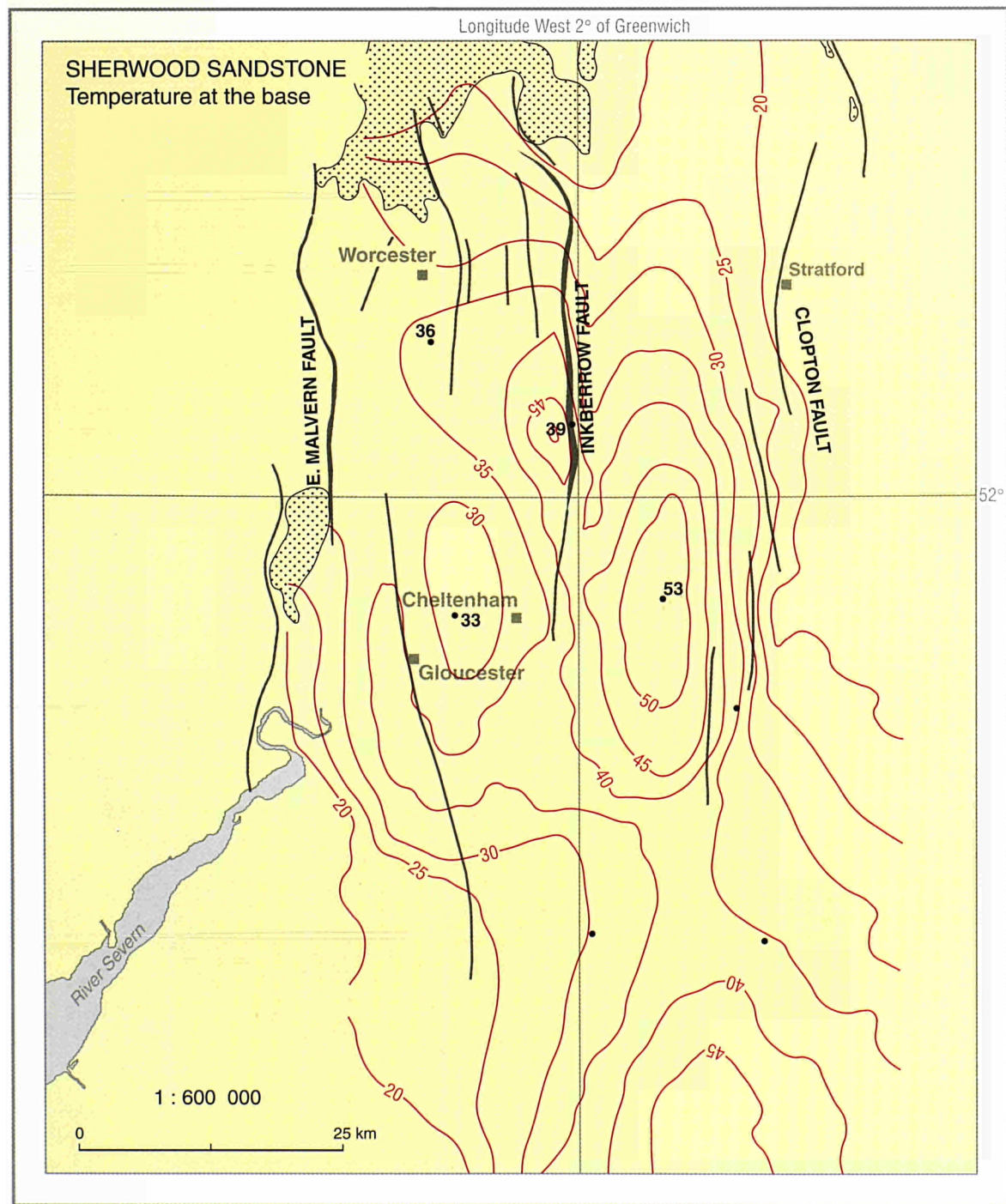
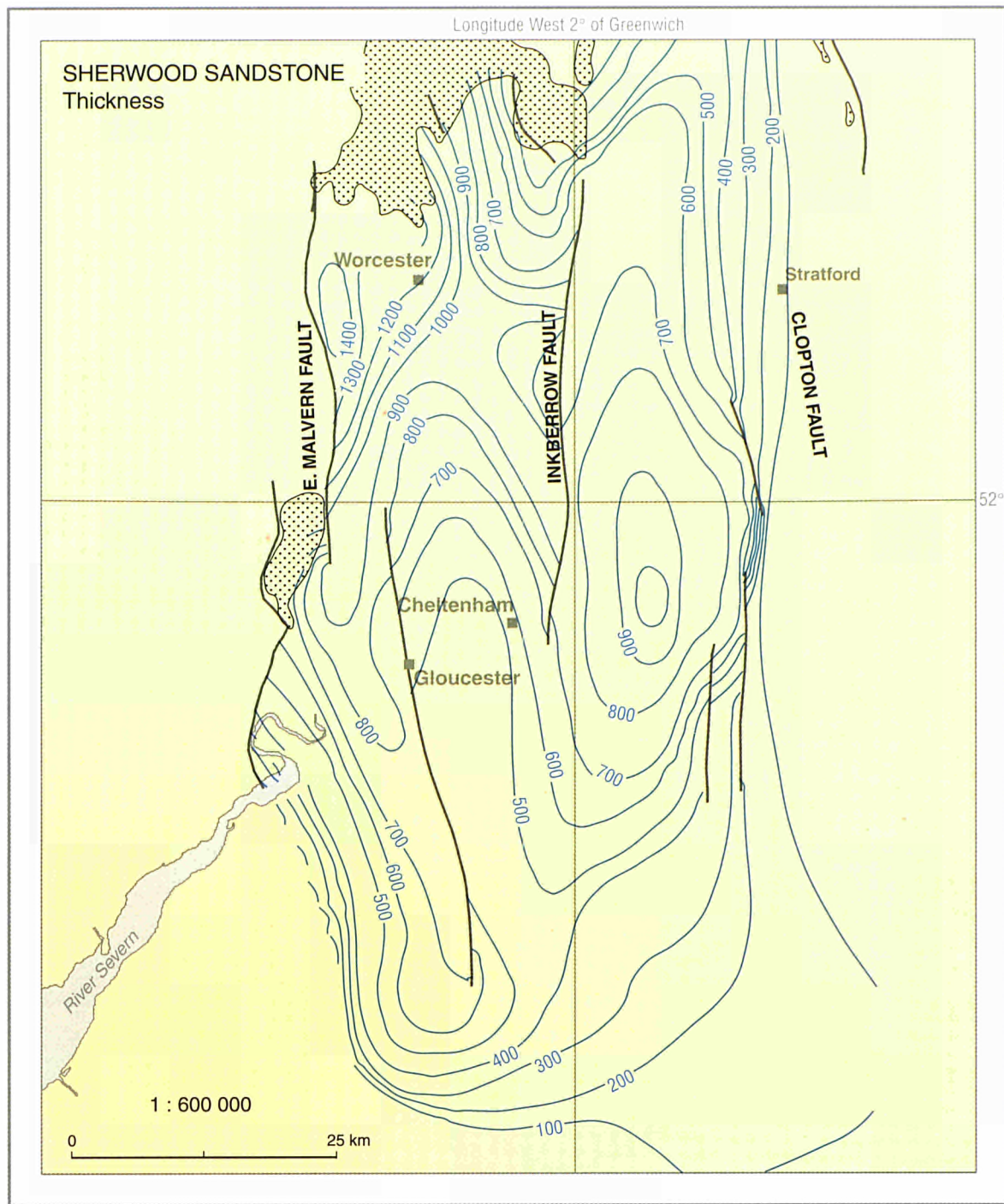
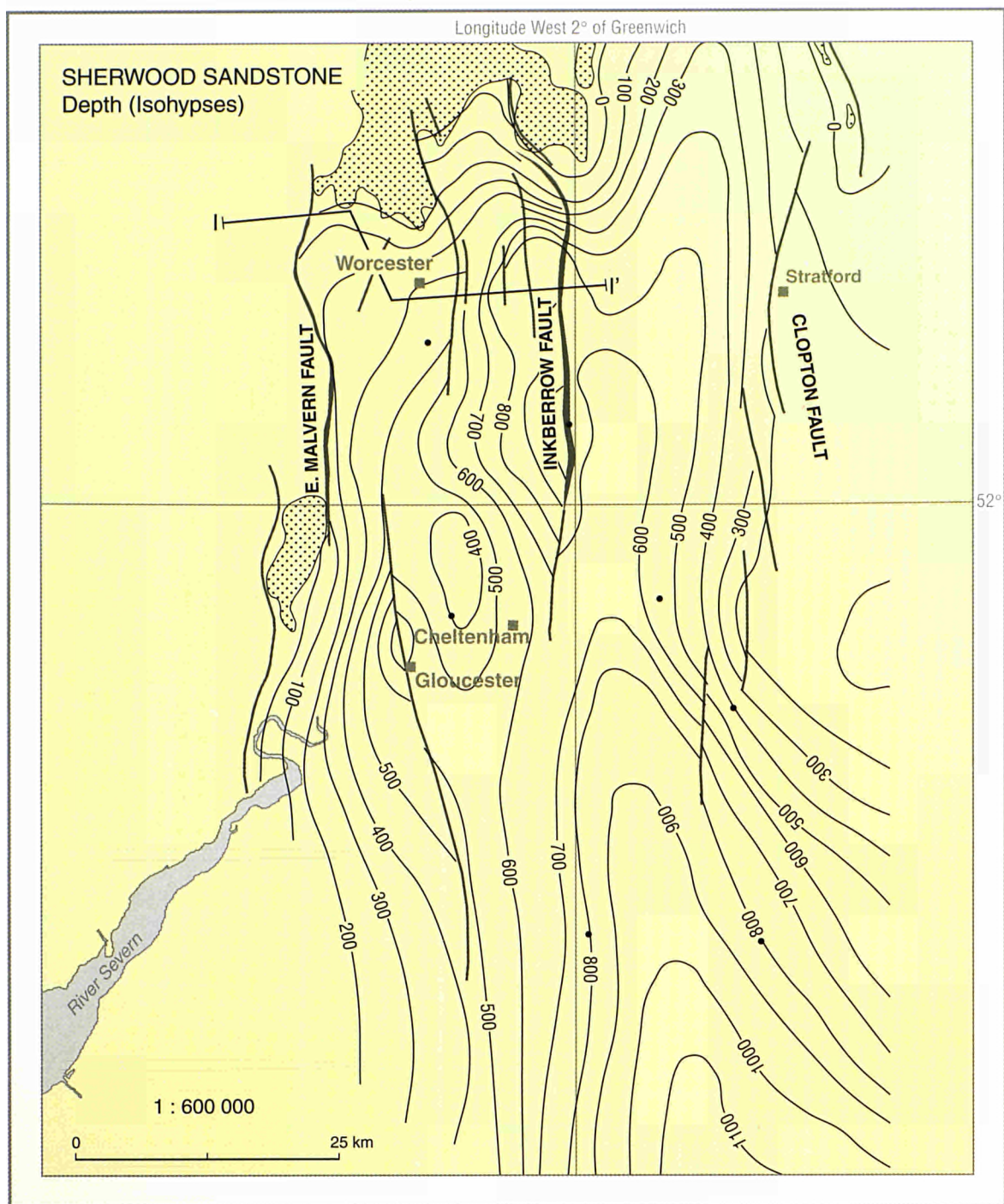


UNITED KINGDOM, Cheshire Basin

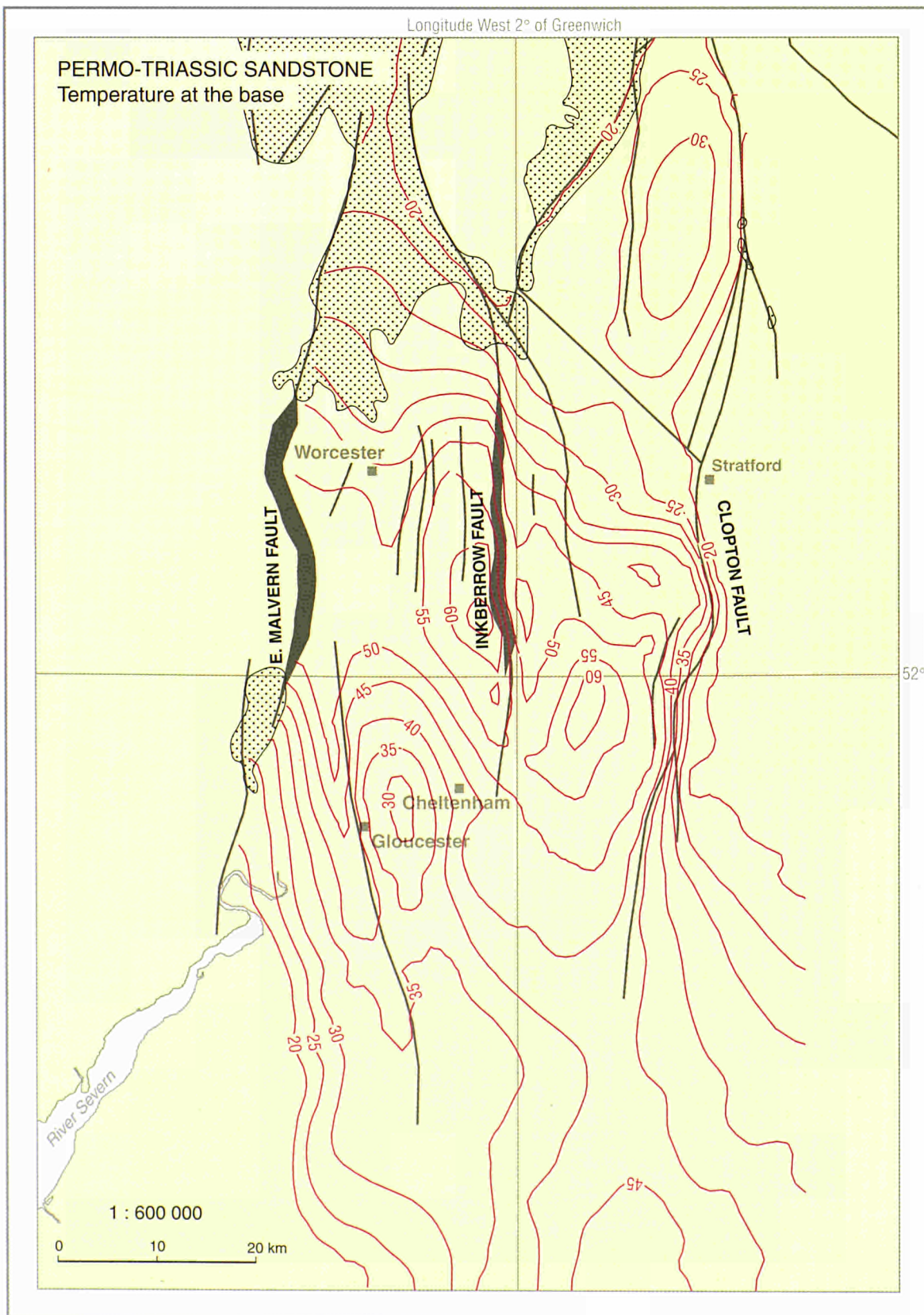
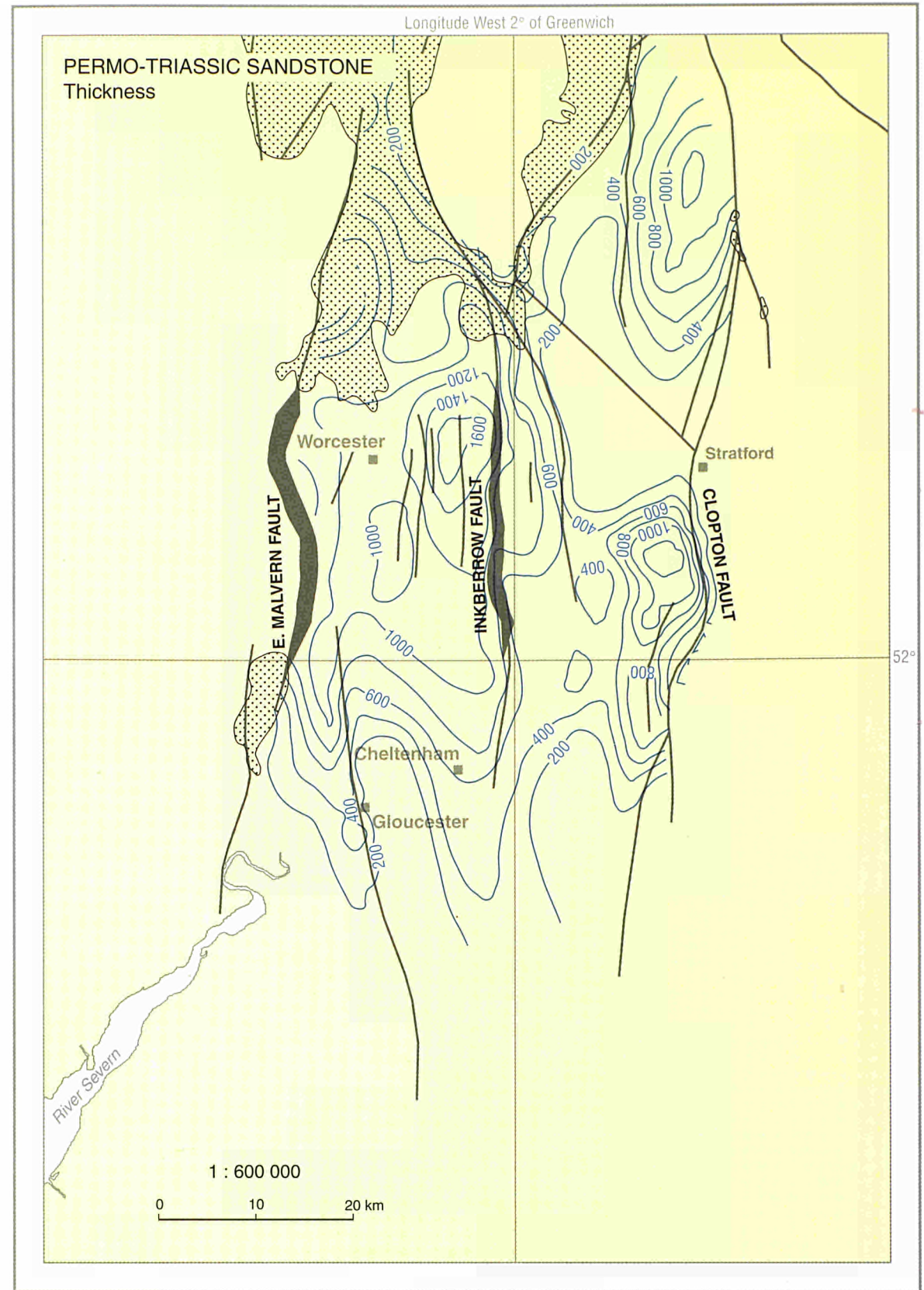
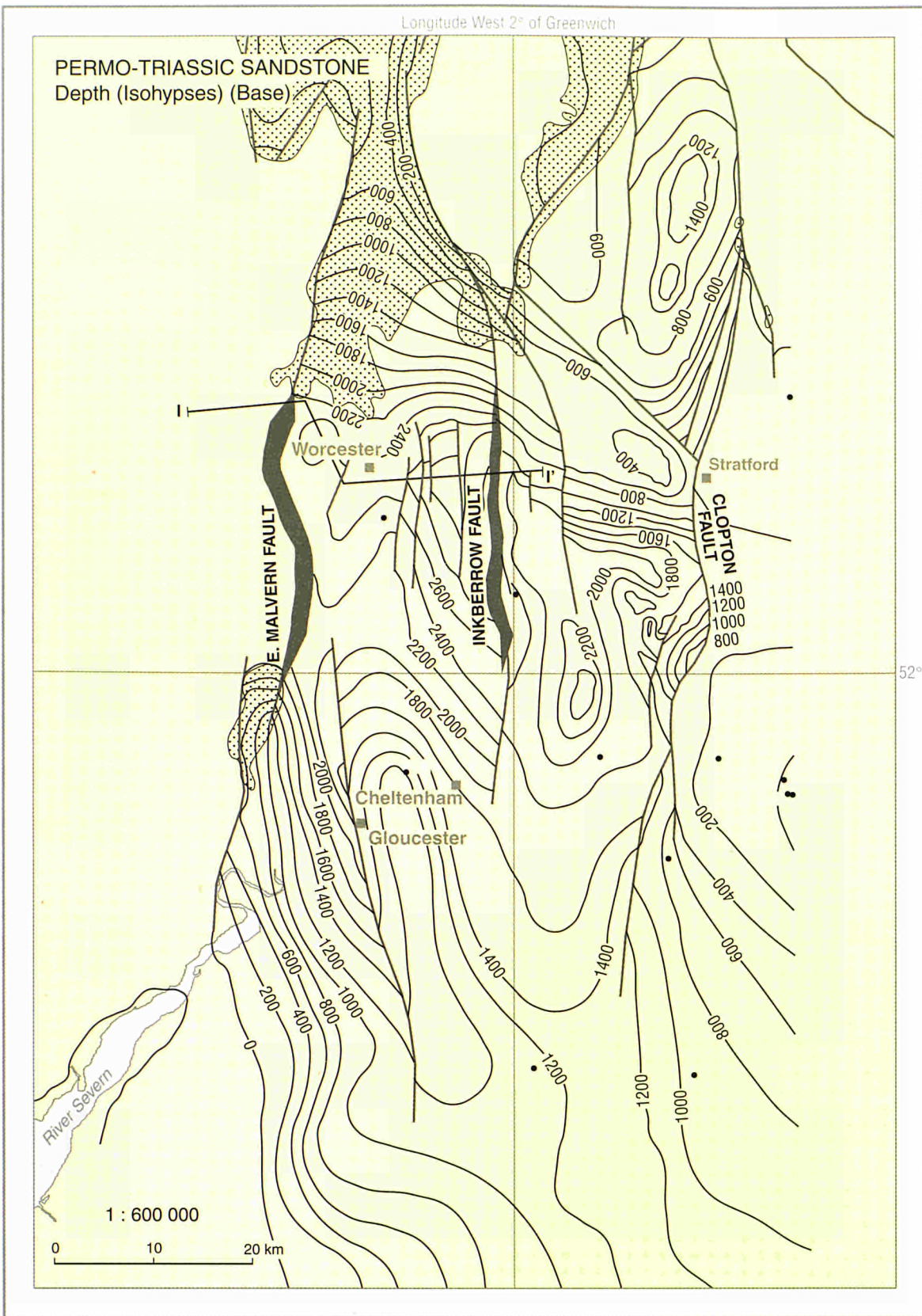




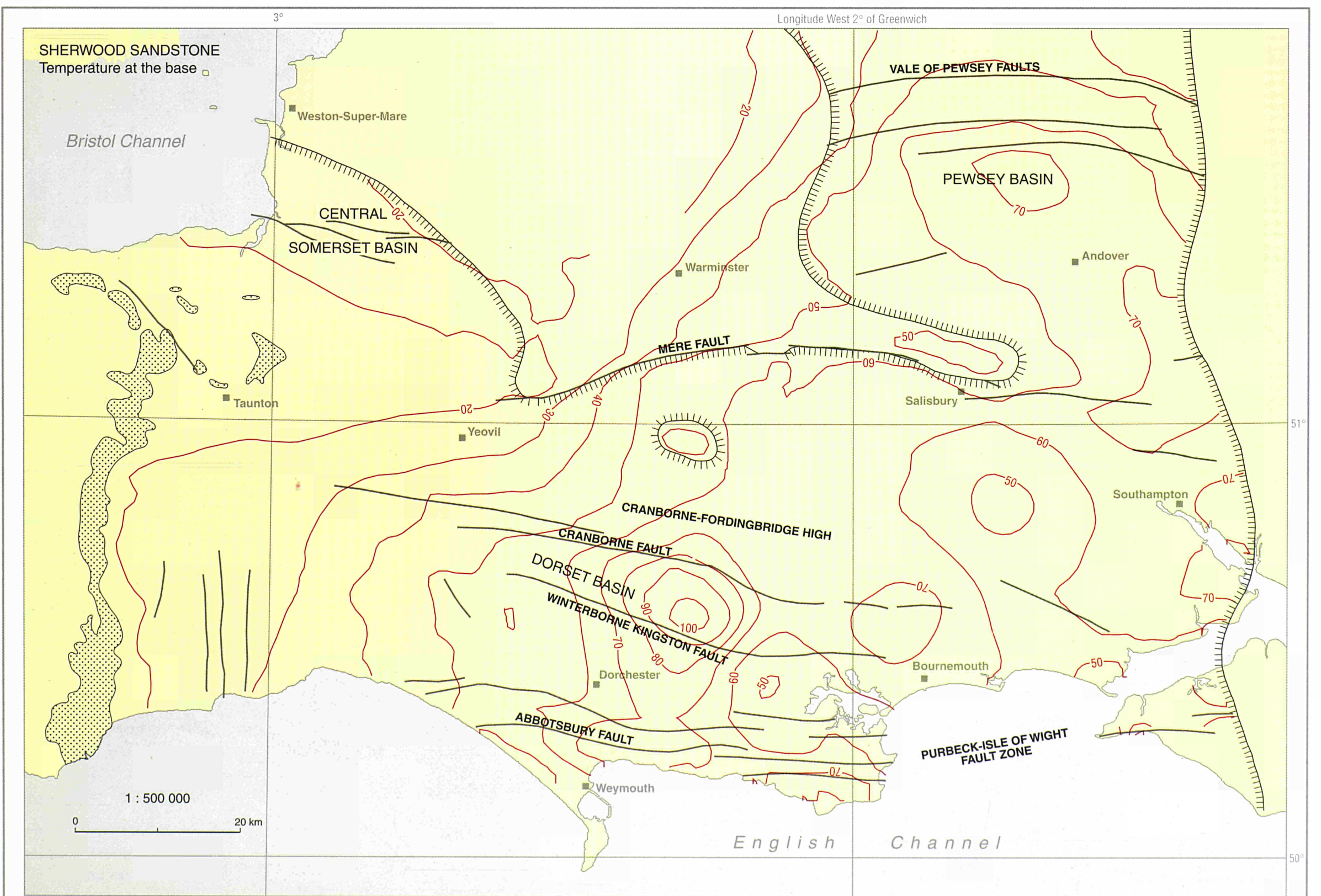
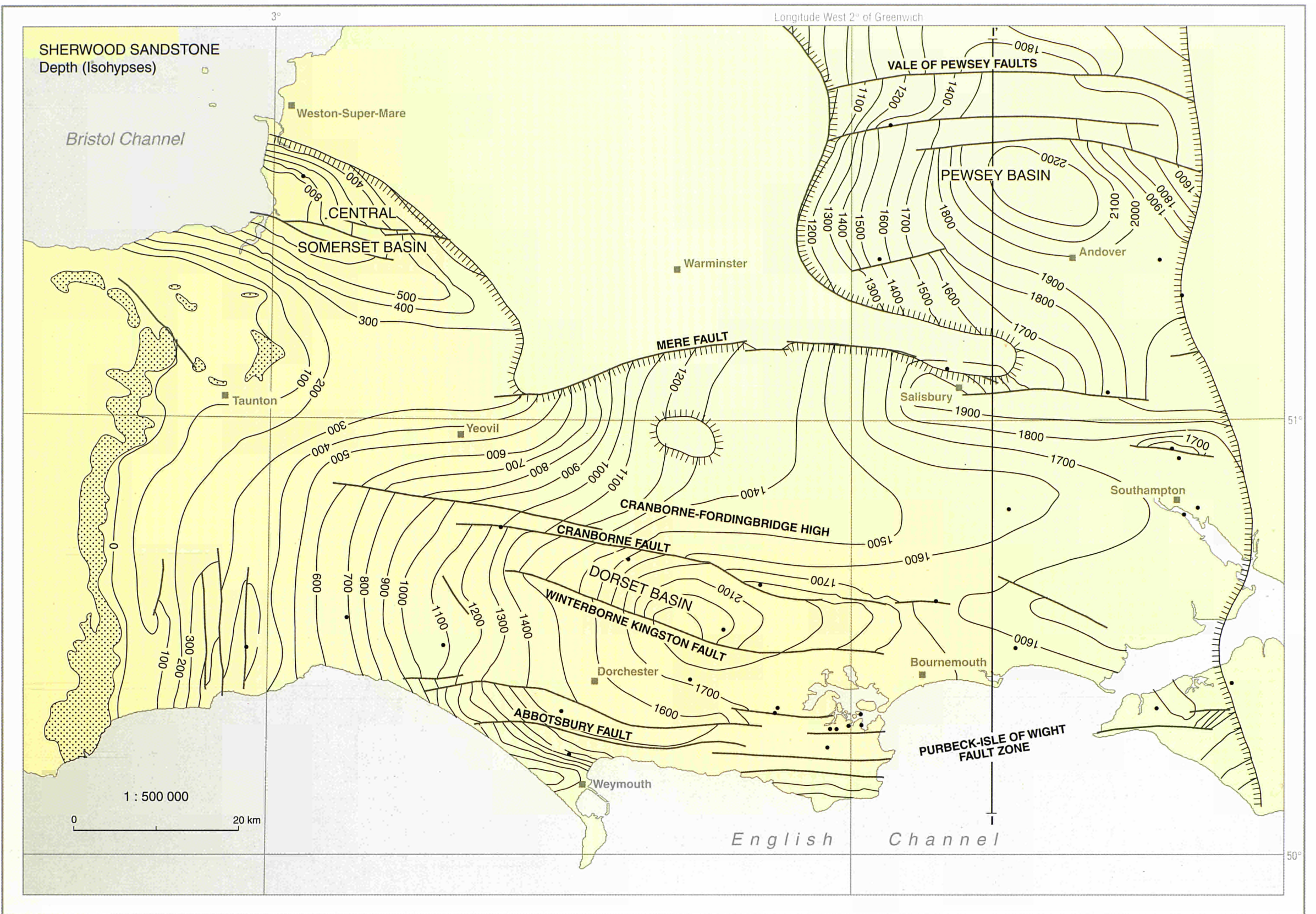
UNITED KINGDOM, Worcester Basin

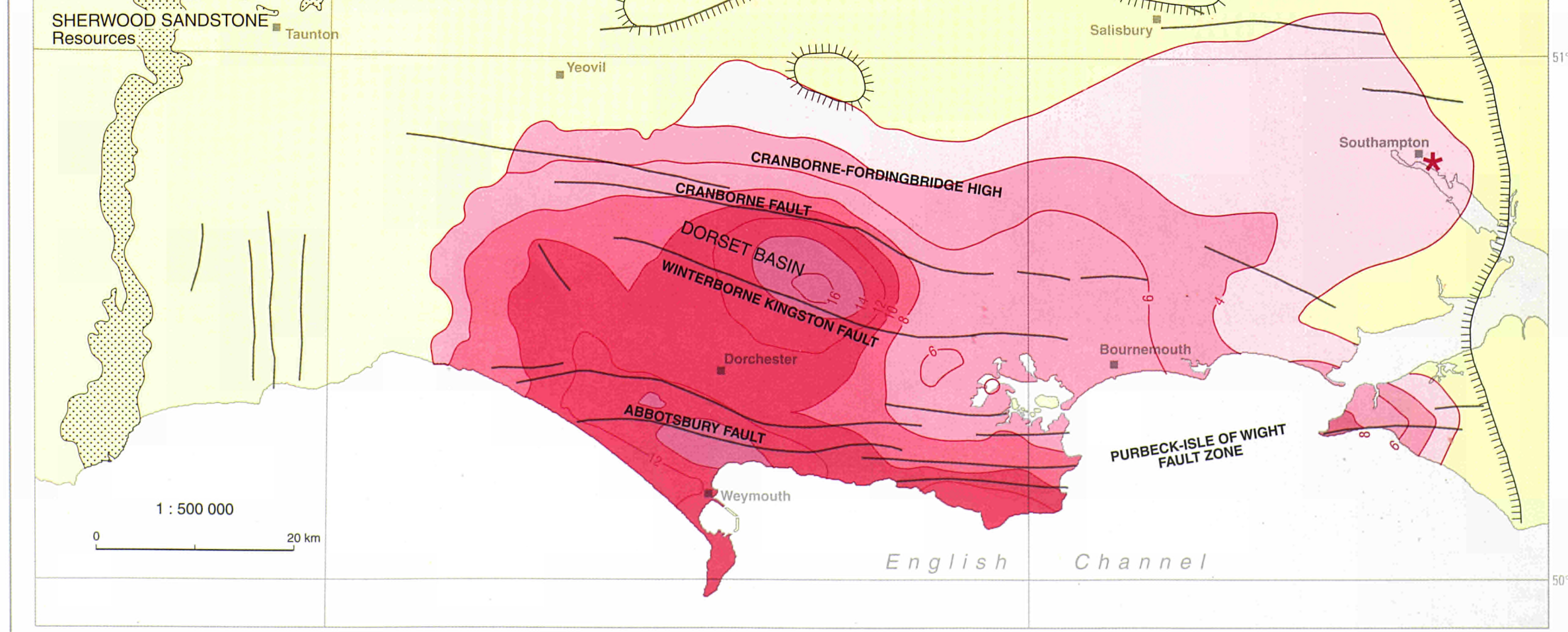
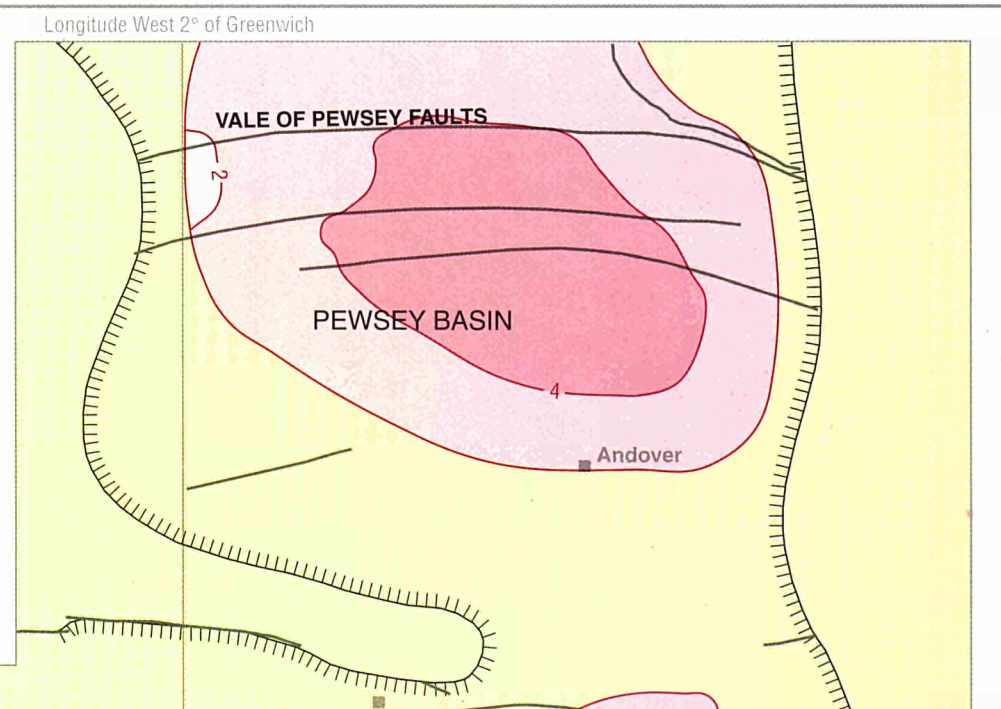
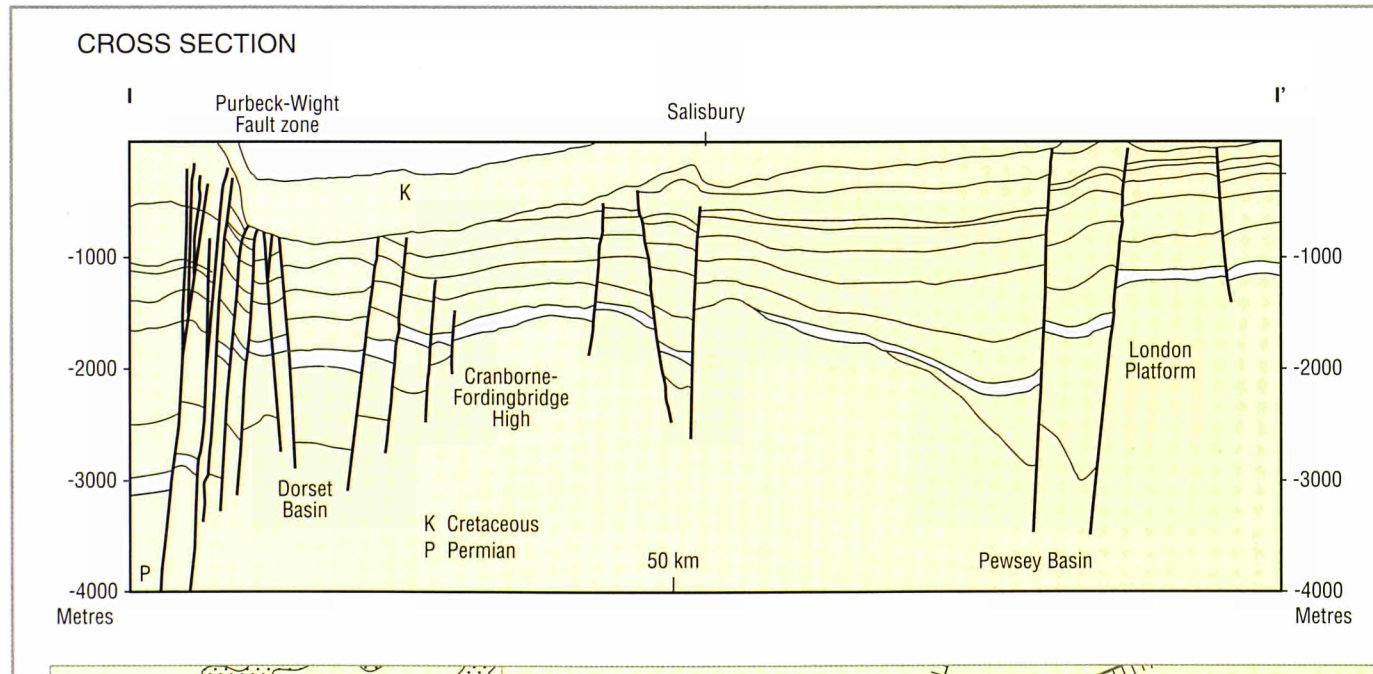
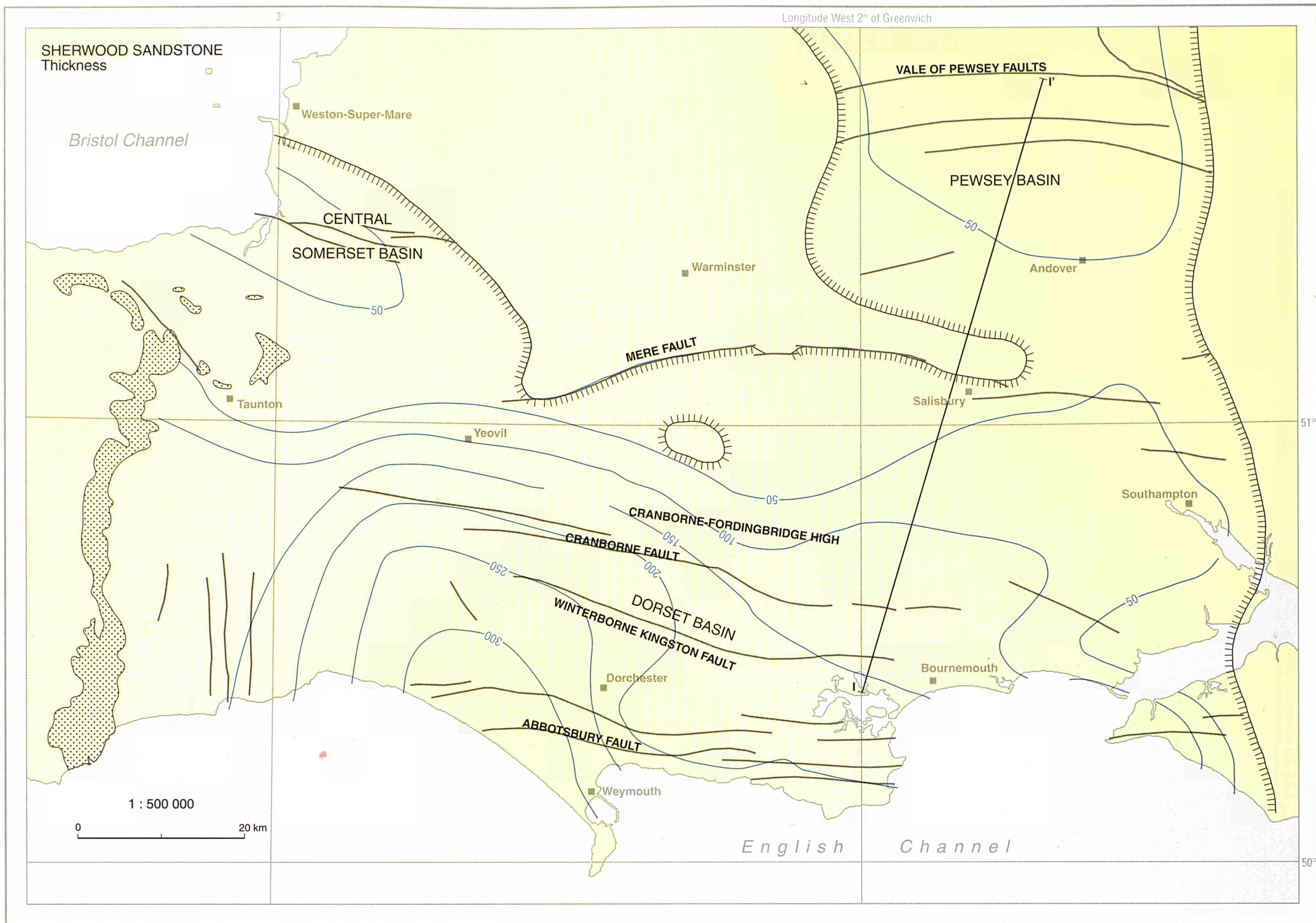


Worcester Basin, UNITED KINGDOM



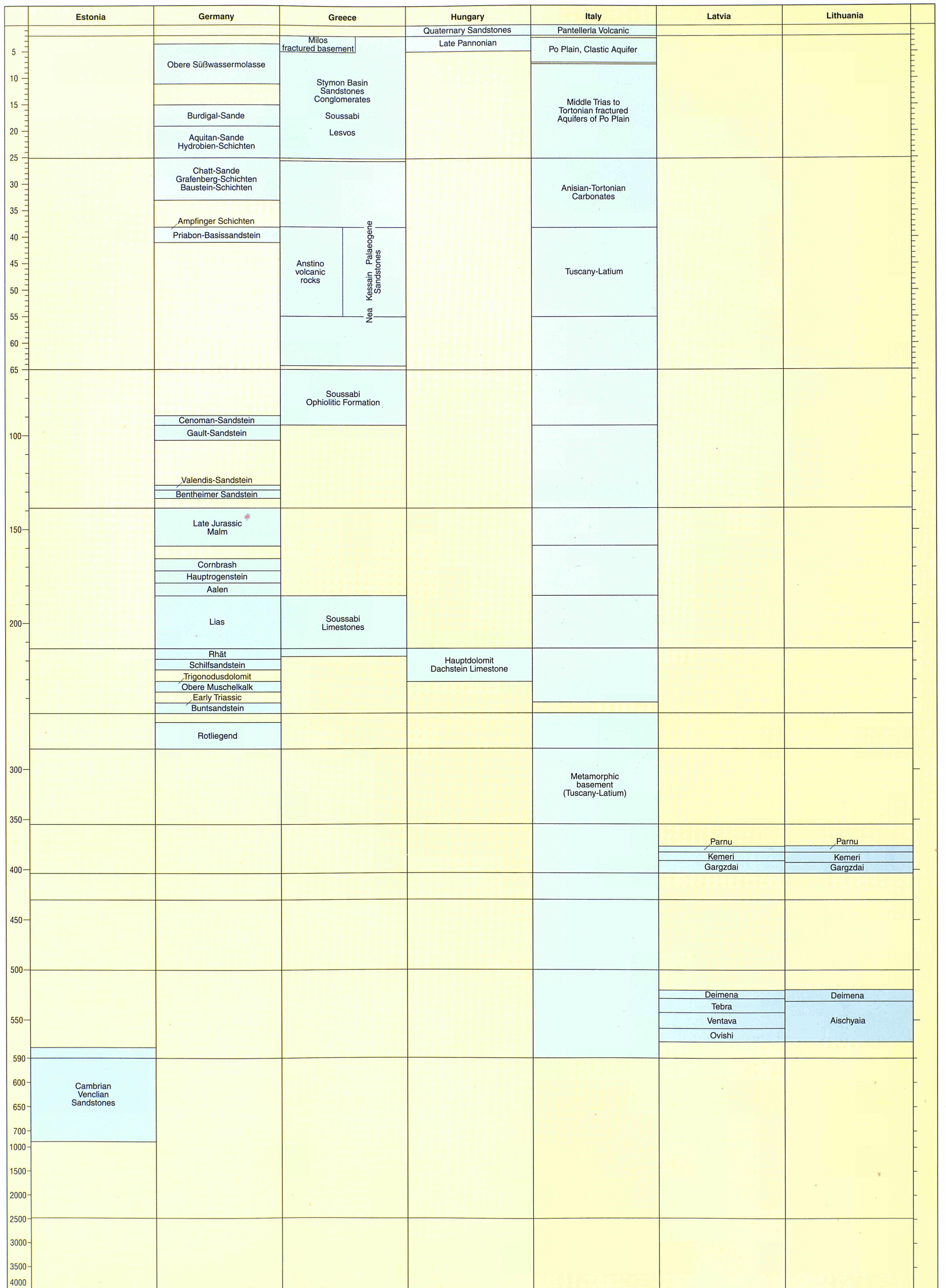
UNITED KINGDOM, Wessex Basin





LOCAL AQUIFER NAMES IN RELATION TO THE GEOLOGICAL TIME SCALE

AGE IN MA	ERA SUB-ERA	PERIOD	EPOCH	AGE	Albania	Belgium	Bulgaria	Czech Republic	Denmark			
5 10 15 20 25 30 35 40 45 50 55 60 65	CENOZOIC TERTIARY	NEOGENE	Pliocene	Pli	Piacenzian							
				Ze	Zanclean							
			Miocene	L	Messinian		Sandstones (Ardenica)		Katuntsi-Sandanski, Gnilyane-Terrigenous, and Ahmatovo Formations			
					Tortonian							
				M	Serravallian							
					Langhian							
				E	Burdigalian					North Bohemian Basin Sandstones		
					Aquitanian					West Carpathian Foredeep		
				Ng	Mio							
		PALAEOGENE	Oligocene	L	Chattian							
				E	Rupelian							
			Oli	L	Priabonian							
					Bartonian							
			Eocene	M	Lutetian							
				E	Ypresian				Beloslav-Avnen Formations			
			Eoc	L	Thanetian		Limestones (Kruja)					
				E	Danian							
			Palaeocene	Pal								
		65 100 150 200 250 300 350 400 450 500 550 600 650 700 750 800 850 900 950	MESOZOIC	CRETACEOUS	L	Senonian	Maastrichtian					
						Campanian						
					K2	Santonian						
						Coniacian						
					E	Cenomanian						Bohemian Cretaceous Basin Sandstone
Albian												
Neocomian	Aptian											
	Barremian											
K1	Hauterivian											
	Valanginian								Valanginian			
Berriasian												
	Tithonian								Frederikshavn Formation			
J3	Malm			Kimmeidgian				Malm				
				Oxfordian								
J2	Dogger			Callovian								
				Bathonian					Haldager Sand Formation			
J1	Lias			Bajocian								
				Aalenian								
E	Lias			Toarcian								
				Pliensbachian								
Hettangian												
	Rhaetian								Gassum Formation			
Norian												
	Carnian											
Ladinian												
	Anisian					Doirentsi Formation						
Scythian												
	Buntsandstein						Bunter Sandstone Formation					
PERMIAN	P2	Changxingian										
		Loupian										
P1	Wartanian											
	Wordian											
Asselian					Salt Diapir at Peshkopia (Korabi)							
CARBONIFEROUS	Gze	Gzelian										
		Kasimovian										
Mos												
	Bashkirian											
Serpukhovian												
	Spk											
Visean	Vis											
		Dinantian Limestones										
Tournaisian	Tou											
		Tournaisian										
DEVONIAN	D3	Famennian										
		Frasnian										
D2	Givetian											
	Eifelian											
D1	Emsian											
	Pragian											
Lochkovian												
SILURIAN	Prd	Pridoli										
		Ludlow										
Wenlock	Wen											
		Llandovery										
ASHGILL	Ash											
CARADOC	Crd											
LIANDILO	Lio											
LIANVIRN	Liv											
ARENIG	Arg											
TREMADOC	Tre											
MERIONETH	Mer											
ST. DAVID'S	St D											
CAERFAI	Crf											
		Tommotian										
590 600 650 700 1000 1500 2000 2500 3000 3500 4000	PRECAMBRIAN	PROTEROZOIC	Neo-proterozoic									
			Meso-proterozoic									
			Palaeo-proterozoic									
ARCHAEAN	Ar											



LOCAL AQUIFER NAMES IN RELATION TO THE GEOLOGICAL TIME SCALE

AGE IN MA	ERA SUB-ERA	PERIOD	EPOCH	AGE	Netherlands	Poland	Portugal	Romania	Russia			
5 10 15 20 25 30 35 40 45 50 55 60 65	CENOZOIC TERTIARY	NEOGENE	Pliocene	Ple			Azores volcanic Aquifers Chaves Graben Deposits	Sandstones (Pannonian Basin)	Early Pliocene			
				Pli	Piacenzian							
				F	Zanclian							
			Miocene	L	Messinian							
					Tortonian							
				M	Serravallian							
					Langhian							
					Burdigalian					Middle Miocene (Karagan-Chokrak) Sandstones, Carbonates		
				E	Aquitanian							
				PALAEOGENE	Oligocene	L				Chattian		
		E	Rupelian									
		Eocene	L		Priabonian							
					Bartonian							
			M		Lutetian							
					Ypresian							
					E							
			Eoc		L	Thanetian						
					E	Danian						
			MESOZOIC		CRETACEOUS	K	Palaeocene	Pal				
		Senonian		Maastrichtian								
		L		Campanian								
				Santonian								
				Coniacian								
		K2		Cenomanian								
				Turonian								
JURASSIC	J	K1		Neocomian			Albian			Almargem Sandstone	Carbonates (Moesian Platform)	Early Cretaceous Conglomerates, Sandstones
							Aptian					
							Barremian					
			Hauterivian									
			Valanginian		Bentheim Sandstone	Early Cretaceous	Valanginian Sandstone					
			Berriasian									
			Tithonian									
			Kimmeidgian			Malm						
			Oxfordian									
			Callovian			Dogger						
Bathonian												
Bajocian												
Aalenian												
Toarcian												
Pliensbachian		Lias										
Sinemurian												
Hettangian												
PALAEOZOIC	TRIASSIC	Tr	Mz	L								
				Norian								
				Carnian								
				Ladinian								
				Anisian	Röt Formation		Carbonates (Pannonian Basin)					
				Scythian	Main Buntsandstein							
				Changxingian = Tatarian								
				Loupian								
				Capitanian								
				Wordian								
Ulian												
Asselian	Slochteren Sandstone											
PALAEOZOIC	PERMIAN	P	Mz	Gzelian								
				Kasimovian								
				Moscovian								
				Bashkirian								
				Serpukhovian								
				Visian								
				Tournaisian								
				Famennian								
				Frasnian								
				Givetian								
Fifelian												
Pragian												
Lochkovian												
PALAEOZOIC	DEVONIAN	D	Mz	L								
				M								
				E								
				Pridoli								
				Ludlow								
				Wenlock								
				Llandovery								
				Ashgill								
				Caradoc								
				Llandello								
Llanvirn												
Arenig												
Tremadoc												
PALAEOZOIC	SILURIAN	S	Mz	Merioneth								
				St. David's								
				Caerfai								
				Tommotian								
				Neo-proterozoic								
				Meso-proterozoic								
				Palaeo-proterozoic								
				PRECAMBRIAN	ARCHAEAN	Ar	Pz					



The first part of the document discusses the importance of maintaining accurate records of all transactions. It emphasizes that every entry, no matter how small, should be recorded to ensure the integrity of the financial data. This includes not only sales and purchases but also expenses and income. The document provides a detailed list of items that should be tracked, such as inventory levels, accounts payable, and accounts receivable. It also outlines the procedures for recording these transactions, including the use of double-entry bookkeeping to ensure that the books balance.

The second part of the document focuses on the analysis of the financial data. It explains how to calculate key financial ratios and metrics, such as the gross profit margin, operating profit margin, and return on investment. These calculations are essential for understanding the company's financial performance and identifying areas for improvement. The document also discusses the importance of comparing the company's performance to industry benchmarks and providing a clear explanation of the reasons for any variances.

The final part of the document covers the preparation of financial statements. It provides a step-by-step guide to creating the income statement, balance sheet, and cash flow statement. It also discusses the importance of auditing the financial statements to ensure their accuracy and reliability. The document concludes with a summary of the key findings and recommendations for the future, emphasizing the need for continued monitoring and reporting of financial performance.